Table of Contents of Presentations

KEY:
GT = Papers in ***Global Trade Session***
EC = Papers in ***Energy and Carbon Session***
BAF = Papers in ***Bamboo and Agri Fibers Session***
SRF = Papers in ***Sustainable Resources for the Future Session***
AP1 = Papers in ***Advanced Processing I Session***
AP2 = Papers in ***Advanced Processing II Session***
WAFC= Papers in ***Wood and Agri Fiber Culture Session***
PS = Papers in ***Poster Session***
SP= Papers in ***Student Poster Competition Session***

Papers from Global Trade—China's Impact on Global Forest Products Trade Session

Papers from Carbon and Energy Issues Session

Papers From Development and Research in Bamboo and Other Agri Fibers Session

Papers From Sustainable Resources for the Future Session

Papers From Advanced Wood Processing I Session

Papers From Advanced Wood Processing II Session

Papers From Wood and Agri Fiber Culture Session

Papers From Poster Session

Papers From Student Poster Competition Session

Proceedings Edited by:

Victoria L. Herian, Executive Director
SWST
P.O. Box 6155
Monona, WI 53716-6155
608-577-1342
vicki@swst.org

ISBN: 978-0-9817876-3-3

Chinese Policy on Forest Products Trade and Its Global Impacts

Zhang Yanhong

（Deputy-Director-General，Department of Development Planning and Assets Management，State Forestry Administration, P. R. China，yanhongg@yahoo.com.cn）

Abstract： In the Twelfth Five-year Plan period, China will face greater opportunities and challenges in forest products trade. Therefore, accelerating the change in the mode of forest product foreign trade is the indispensable option for China to achieve the change from a big country to a strong power in forest product trade. The paper analyzed the characteristics of China's forest product foreign trade in the Eleventh Five-year Plan period, and pointed out that China has grown into a big country in the production, consumption and import/export trade of forest products with the constant increase in forest product production and trade, the diversified modes of forest product foreign trade, diversity in investment entities, large progress in foreign capitals utilization by forestry sector and increasing overseas investment in forestry. But some problems should not be ignored in the meanwhile. Therefore, we should realize 3 shifts in the development mode of forest product foreign trade: (1) Changing the reliance on traditional comparative advantages as labor force, raw material and land, to competitive advantages as technology, brand, quality, and service; (2) Changing from scale extension to quality and efficiency improvement;(3) Changing from passive complier to active participant of international trading rules and standards.
Keywords: forest products trade, policy

Currently, China is facing more complicated external environment in the development, as the economic globalization and cooperation continue to progress, and the influences of international financial crisis still exist in deep layers. In front of increasingly serious challenges worldwide as climate change, ecological deterioration, energy resource security, food security and significant natural disasters, effectively dealing with the challenges faced by global development and realizing joint growth have become major issues concerned by international society. Therefore, it is urgently needed to accelerate the transformation of foreign trade development, as well as to create new advantages in international cooperation and competition.

1. Trend Of The World's Forest Products Trade Development And Current Situation Faced By China's Forest Products Trade

1.1 Trend of the world's forest products trade development

For more than 10 years, the world's forest products trade has experienced rapid development. According to FAO data, the forest products exports worldwide surged to 236.8 billion USD in 2008 from 129 billion USD in 1998, although the figure dropped to 188.8 billion USD in 2009 due to the setback arisen from the financial crisis. Europe, Asia and North America took 80% of the international forest products trade.

1.1.1 The globalization in forestry sector has been accelerated, as cooperation and interdependence among different countries increasingly went deeper.

At present, global economic structure is going to be reorganized, while the international competitions on market, resource, talent, technology and standard are tending to be increasingly fierce. In face of the new trend, the internationalization of forestry sector will be further accelerated. It is helpful to create a win-win situation in international cooperation of forest products trade, to realize optional allocation of global forest resources, as well as to establish a safe, stable, economic and diversified forest resource security system; It is beneficial for all the countries to build the capacity of independent development through introducing in capital, technology, talent and management experience, as well as to enlarge space for development through extending international economic and trading cooperation in terms of range and depth; Also, it provides an extensive platform for all the countries to participate in the formulation of international regulations, obtain louder voice in the world and protect their own interests.

However, as forestry sector is becoming increasingly internationalized, together with forestry industry and forest products market are experiencing more and more specific international division of labor, many internationally important issues, including ecological security, climate change and energy shortage, relating to forestry lead to greater sensitivity. Forest-related issues and international forest products trade became hot topics globally and will directly determine a state's rights and interests, and future development.

1.1.2 International forest products trade emphasizes more on environmental protection and sustainable development, and takes measures against illegal logging and related trade.

As people's awareness of environmental protection had been awakened, the thinking of sustainable development was included in trade development strategy. The changes in people's consumption ideology and values also facilitated the development towards environmental-friendly forest products.

However, as illegal logging and related trade emerged globally, international forest products trade was significantly distorted. Currently, illegal logging has become an important topic in important political and diplomatic events as APEC, and a hot issue widely concerned by the international society. Superficially, illegal logging falls into the forestry sector. Intrinsically, it involves sustainable development, competition over resources and interests, and re-allocation of forest resources between developed and developing countries. The main causes leading to illegal logging and relevant trading include unreasonable international economic order, enterprises' being driven by interests, poverty of forestry communities, as well as poor law enforcement and forest management in timber producer countries. Therefore, fighting against illegal logging shall be a joint action taken by all timber producer countries, importer countries and consumer countries, and a common responsibility shared by all stakeholders.

Currently, international society emphasizes environmental protection, and each country has carried out some policies or measures to fight against illegal logging and relevant trading. However, some rules or regulations reflected trade protectionism, which will only increase suppliers', buyers', importers' and exporters' costs, and further reduce the convenience of trade.

1.1.3 Forest certification becomes an important means to promote sustainable management and utilization of forest, together with legal trading.

Forest certification does not have a long history, but it has significantly influenced forestry, forest products industry and forest products trade. Up to March 2012, more than 390 million hectares of forests in over 80 countries in the world have been certified, taking nearly 10% of global forests. FSC and PEFC, as 2 different systems, have preliminarily formed the competitive and opposite relationship worldwide, in addition to more than 30 forest certification systems developed by other countries. Forest certification socially, environmentally and economically influenced forest management, improved environmental service of forest, eliminated contradictions between forest managers and surrounding communities, enhanced products' market access, improved enterprise image, facilitated cooperation among private sectors, governmental and non-governmental organizations, as well as stimulated responsible forestry and forest products trade.

However, forest certification also face the problems in credibility, validity, equality, mutual acceptability, especially cost effectiveness and market development, all of which are exerting a serious challenge to developing countries.

1.2 Current situation faced by Chinese forest products trade development

For years, China has been providing policy support for forestry sector's development in foreign trade, enabling its survival from international financial crisis and favorable growth. In 2005, total forest products' imports and exports accumulated to over 40 billion USD. Until 2011, the figure has increased to 120.5 billion USD. With total forest products' imports and exports ranking second in the world, China has become a big producer and trader country in the world. As forestry sectors' foreign trades increased rapidly, the industry attracted more

and more private and foreign capital investments; Meanwhile, China accelerated the implementation of "outbound" strategy in forestry sector. Chinese enterprises have launched more than 130 overseas joint investment programs in forest logging and processing in over 20 countries, which relieved the problem of more demand and less supply of timber, and improved enterprises' international competitiveness.

Overall, forestry sector's foreign trade will maintain stable development, but will face some difficulties and challenges, such as complicated and severe global economic situation, continuously decreasing overseas demand, trade protectionism, increased prices of production factors including labor force price, higher ecological and environmental protection costs, fluctuation of RMB exchange rate and difficult financing.

Therefore, the model featuring excessive dependence on export to drive industrial develop is no longer sustainable. It is urgently necessary to change industrial structure, expand domestic demand and stabilize export, optimize the structure of forest products trade, as well as extend domestic and overseas markets. It is imperative to develop low-carbon economy, circular economy and green economy, promote transformation of forestry sector's economic development, as well as accelerate the reform of forestry sector's foreign trade development.

2. Making Significant Change To The Mode Of Forestry Sector's Foreign Trade

2.1 Changing the reliance on traditional comparative advantages as labor force, raw material and land, to competitive advantages as technology, brand, quality, and service

As economic globalization and trade freedom further progressed, currently some developing countries with even lower labor cost, including Vietnam and Philippine, are striving to develop labor-intensive timber processing industry and have become powerful competitors of Chinese timber processing industry. If Chinese forest products trade failed to change its traditional development model, China would be deprived of traditional advantage in competition. Therefore, from long-term perspective, we shall change our development strategy to realize development based on competitive advantage in technology, brand, quality, and service, step to medium- and high-end international division of labor from low-end, strengthen scientific and technological innovation, improve product quality, intensify brand building, promote industrial image, extend industrial territory, stimulate the momentum of foreign trade development and increase China's international competitiveness in forest products trade.

2.2 Changing from scale extension to quality and efficiency improvement

We will optimize the structure of forestry sector's foreign trade market to stabilize traditional market, develop new market, cultivate surrounding markets, exploit potential market and actively establish multi-lateral trade system. Meanwhile, we will optimize the mode of trading to extend industrial chain, increase export of high-value-added products, develop service trade, increase export of traditional services, including forestry project contracting, labor export, investigation planning, design consultation, information service and forest tourism, and to steadily improve the quality and efficiency of forestry sector's foreign trade.

2.3 Changing from passive complier to active participant of international trading rules and standards

We will try to get a louder voice in formulating technical standard and trading rules for international forest products trade, further intensify the cooperation among governmental authorities, industrial associations, research institutions and enterprises, improve the "three-in-one" coping mechanism, as well as settle down trade disputes through intergovernmental negotiation, counterargument and industrial cooperation in different ways to protect our own rights and interests.

3. Foreign Trade Policy For Chinese Forestry Sector

To improve the policy promotion system for forestry sector's foreign trade development, to increase its status in national public fiscal system, to clarify the guiding role of finance and taxation policy, to intensify the catalyst function of finance and to enhance balanced and coordinative development of forestry sector's foreign trade.

3.1 Optimize foreign trade structure and build new competitive advantage in export.

We will accelerate the transformation and upgrade of processing trade, and strive to develop service trade. Through implementing the strategy of driving up export with forestry techniques, brand, marketing and service, we will facilitate the change of export from traditional cost advantage to new competitive advantage, as well as the leap forward from "made in China" to "created in China" and "served by China." We will set up and complete forestry trade policy system to encourage technically intensive forest products and emerging industries to develop international market. In addition, we will cultivate our export brands, support enterprises to establish overseas forest products marketing network, increase the added value of exported products and particularly emphasize the development of forestry's foreign trade of service.

As for policy, we will consolidate and improve promotion policy for forest products' import and export, and establish long-acting mechanism of preferential policies for forest products trade. Based on stable and continuous implementation of existing export tax rebate policy for forest products, we will intensify our support for deeply processed timber products with high added value, and increase the threshold of export tax rebate. Also, we will launch encouraging policy for green procurement to encourage and support legal timber and timber products, work out green products list for governmental procurement, as well as to create green products logo, in order to ensure the legal source of timber and timber products procured by government.

3.2 Implement diversified international trade strategy for forest products and facilitated stable increase of product export.

We will work out encouraging policy, actively expand trading partner countries and consolidate emerging products market. The underdeveloped countries and newly emerging developing countries in Africa and Asia with increasing demand for forest products are the key markets of Chinese forest products. We will shift part of the previous trade shares of forest products for developed countries to those countries, and will set up early warning benchmark for export shares to developed countries. (In 2010, forest products singly took 35.6% of total exports to U.S. and Japan.)

3.3 Actively deal with international forest products trade barrier and establish complete coping mechanism.

We will further intensify the cooperation among stakeholders, as well as improve the mechanism to deal with trade barriers and to break through the limitations caused by international trade barrier. Also, we will accelerate the setup of pre-alert system of foreign trade barrier, further complete laws, regulations and policy frameworks counteracting dumping, subsidy, industrial damage and technical trade barrier, as well as establish foreign trade relief system in accordance with international conventions. In addition, we will raise enterprises' awareness on legally protecting their own rights and effectively preventing risks, encouraging them adopt applicable rules, collect relevant evidences, as well as actively deal with unfair treatment and unreasonable requirement through negotiation or legal means, so as to protect their own legal rights.

3.4 Promote overseas investment and cooperation, and improve overseas investment quality.

3.4.1 Support capable enterprises to carry out overseas forestry investment and cooperation, innovated cooperation and development model of forestry's processing trade, and improve the level of forestry's investment cooperation. We will encourage enterprises to establish overseas demonstration park of forest resource cooperation integrating production, processing, scientific research and trade in countries and regions with rich forest resource, favorable foundation for timber processing and utilization, relatively standard market and better investment environment mainly in Russia, Southeast Asia, Pacific, Africa, North America and South America, so as to accelerate industrial structure upgrade and improve the level of overseas forest resource cooperation.

3.4.2 Improve forestry's strength to "step out," cultivate internationally competitive multi-national corporations, improve their operation and management, and gradually establish internationally famous and influential multi-national corporations. We will encourage forestry enterprises and nationally powerful public or private enterprises to jointly establish forestry group with scale benefit, strong anti-risk capacity and integrated functions in logging, processing, trading and scientific research. Meanwhile, we will encourage and support Chinese enterprises and foreign forestry enterprises to establish strategic alliance, in order to realize mutual complementation, and carry out cooperation through direct investment, purchase of property rights and power of management. In particular, we will fully develop the advantages of medium- and small-scale enterprises, together with private enterprises, as well as support medium- and small-scale enterprises to accelerate the development of overseas industrial clusters.

We will study on and work out national promotion policy for overseas forestry investment and cooperation, and intensify financial support. We will fully exploit the driving force of financial service policy, in order to stimulate commercial trade financing through policy trade financing, and commercial export credit insurance through policy-driven export credit insurance. We will encourage insurance companies to develop policy and commercial insurance products specifically for forest products import and export on the basis of market needs, in order to help enterprises counteract external risks. In addition, we will encourage different credit guarantee institutions to carry out financing guarantee business for forest products trade.

3.5 Set up foreign trade service platform for forestry

3.5.1 Intensify public information service, improve foreign trade warning information

distribution mechanism in forestry, as well as instantly publish major changes in partner countries' laws and regulations, economic, market and forestry policies, so as to facilitate Chinese enterprises in correspondingly adjust their production, operation and trading activities.

3.5.2 Study and analyze forestry development strategy of resource countries, instantly and accurately feel their market orientation, cooperative mode and development trend in forest resource development and utilization, so as to provide Chinese enterprises with overseas forestry investment services in investment and financing, market and risk evaluation, improve their decision-making level and reduce investment risk.

3.5.3 Set up cooperation and communication mechanism for governmental department, industrial association, scientific research institution, international organization and enterprise. Refer to general operational model of industrial association in developed countries, and make full use of the organizing, coordinating and service functions of forestry industrial association to help enterprises reduce trading risk and loss from trade conflict. Truly develop the function of industrial association as the bridge between the government and enterprise, provide guidance and instruction to avoid disordered competition, participate in formulation of standard and popularization of relevant knowledge, actively take part in trade negotiation and act as the spokesman for enterprises. Regularly hold training and service consultation meeting on foreign trade and investment policy to discuss the problems in foreign trade.

3.5.4 Provide scientific instruction and strengthen supervision. Continue to promote publicity, training and pilot implementation of Guidance on Sustainable Management and Utilization of Chinese Enterprises' Overseas Forest and Guidance on Sustainable Management of Chinese Enterprises' Overseas Forest. Based on their actual situation, we will provide instructions and code of conduct on overseas forest resource cooperation, so as to guide and standardize their overseas forest resource cooperation and establish favorable enterprise image.

3.6 Intensify international communication and cooperation, and strengthen publicity and propaganda

We will further promote bi-lateral, multi-lateral communication, negotiation and cooperation, and actively participate in formulating international rules and standards. Also, we will increase negotiations and cooperation on forestry-related issues under the frameworks as Sino-US Strategic and Economic Dialogues, Sino-U.S. Joint Commission on Commerce and Trade, Japan-China High-Level Economic Dialogue, Sino-Russian and Sino-European Bilateral Mechanism, and Forum on China-Africa Cooperation, and increase China's international say. Meanwhile, we will publicize Chinese forest policy in different circumstances, including Chinese position, viewpoint and main actions on climate, forest and forest products trade issues, to protect enterprise interests and state image.

In a word, in the stage featuring accelerated global economic integration, intensified international contacts, and prosperous development of international forest products trade, China needs to join hands with the world to actively promote the opening of forestry sector. We expect this conference will provide opportunity for communication, understanding and cooperation, as well as facilitate common efforts in promoting sustainable development and green growth of forest products trade.

Proceedings of the 55th International Convention of Society of Wood Science and Technology
August 27-31, 2012 - Beijing, CHINA

Reducing Illegal Wood Trade: the European Union Forest Law Enforcement, Governance and Trade Action Plan Developments

Ed K. Pepke [1]

[1] Senior Timber Trade Analyst, EU FLEGT Facility, European Forest Institute, Joensuu, Finland
Ed.Pepke@efi.int

Abstract

The European Union (EU) established the Forest, Law Enforcement, Governance and Trade (FLEGT) Action Plan in 2003. It has the intention of changing the international trade of wood, in order to ensure legality. The Plan also attacks the causes of illegal logging through improving governance in the forest sector, and enforcement of laws. The EU has established Voluntary Partnership Agreements (VPAs) with six tropical timber producing countries, and is in the process of negotiating VPAs with other countries. These Agreements are intended to assist countries to evaluate their forest sectors through an inclusive stakeholder process. The wood products exports from VPA countries will carry a FLEGT license, which will facilitate their export to the EU. In 2013 a new EU Timber Regulation comes into effect, which will require importers to have proof of legality of their imports. EU imports of FLEGT- and CITES-licensed timber will be considered legal, while other imports will need different assurances of legality. The Regulation applies equally to timber traded between EU countries. All wood and paper traders and processers will need to establish a due diligence system to minimize the risk of illegal timber products. Thus, the FLEGT Action Plan is establishing a new trade regime, which will have important implications for all exporters to the EU, as well as the entire timber trade within the EU.

***Keywords*:** Forest, Law Enforcement, Governance and Trade; FLEGT; illegal logging; illegal timber; illegal timber trade; EU Timber Regulation.

Introduction

Illegal logging came into international attention 20 years ago at the first Rio Earth Summit, and was again a subject of negotiation in the Rio +20 this year in 2012. Illegal logging consists of harvesting without government permits or in violation of those permits, against laws governing the harvests, transport, processing and trade of timber. It includes the evasion and underpayment of taxes and fees. Illegal logging can involve removals of protected species and sizes, harvesting in protected areas or locations without proper authorization and by illegal practices (not fully following management plans, not conducting social and economic impact assessments, not reforesting, etc.).

Part of illegal harvests is exported which accounts for a significant portion of the billions of dollars lost per year. It affects the legal trade in many ways, including reducing revenues for the forest sector, undermining prices and profits, negating sustainable forest management and creating consumer confusion about using wood and paper products. The value of the latter is unmeasured, but may total more than all others in lost markets. The opportunity cost, when architects, specifiers and buyers do not choose wood and paper products devalues the productive function of forests.

New legislation aimed at curbing illegal logging attacks the problems from many fronts, and most importantly for this session of the SWST Convention, by prohibiting the trade of illegal wood and paper products. These include European Union (EU) FLEGT Action Plan initiated in 2003, the United States Lacey Act Amendment of 2008, the Australian Illegal Logging Prohibition Bill of 2011, New Zealand's Voluntary Code of Practice of 2010 and Japan's Green Purchasing Policy of 2006. This paper focuses on developments of the EU FLEGT Action Plan and the EU Timber Regulation.

Evolution of the FLEGT Action Plan

At the G8 in 1998, world leaders crafted the G8 Forestry Action Programme, of which one action area was against illegal logging. This was a first step for countries to produce their own legislation to reduce illegal harvests in their countries, and to protect themselves from illegal timber trade (figure 1). Later the EU Forest Law Enforcement and Governance (FLEG) was established, but soon it was found that without a "T" for trade, the policies lacked sufficient strength. Hence, FLEGT gained momentum, especially when the EU's FLEGT Action Plan published in 2003 spawned the FLEGT Regulation in 2005. In 2007 the FLEGT Implementing Regulation came into force, and the same year the EU FLEGT Facility was set up at the European Forest Institute (EFI). The EU FLEGT Facility works together with the European Commission and EU Member States to implement the FLEGT Action Plan.

Figure 1. Developments against illegal logging and trade

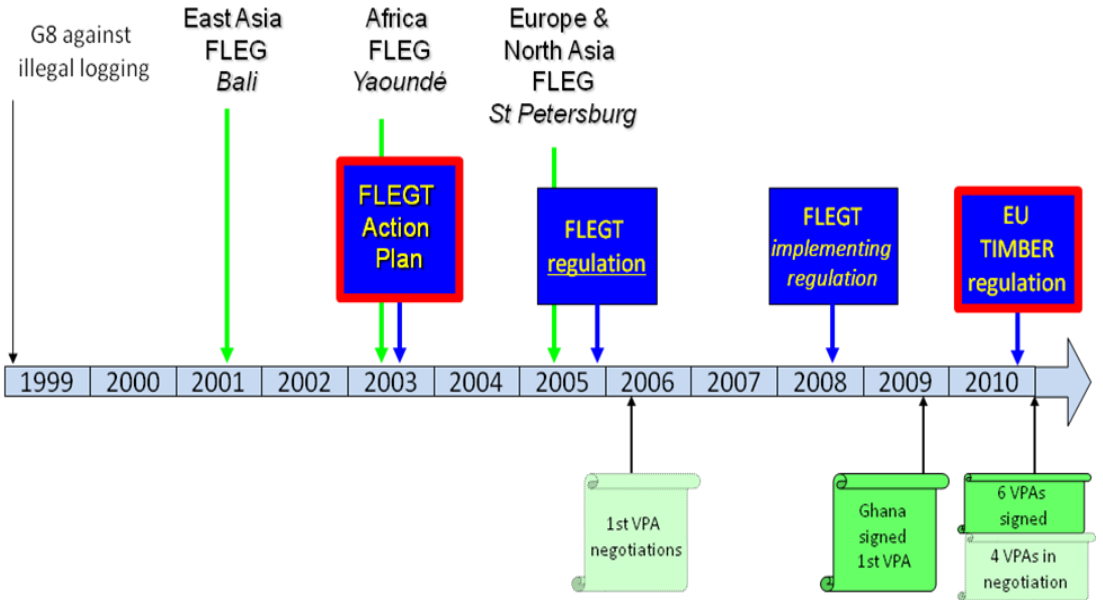

Source: Viitanen, 2012.

Why Europe, where almost all harvesting is legal? While harvesting in the EU is tightly controlled by the twenty-seven individual member states, the EU is the major importer of forest products. The first source is from within the EU, i.e. country-to-country trade, for example from France to Germany and back to France. But the EU imports a significant volume and value of wood and paper products from outside its borders. The EU accounted for over one-third of global primary wood products imports in 2010, down from 43% in 2007 before the global economic crisis (includes trade within Europe) (FAO, 2012). Tropical primary-processed imports (industrial roundwood, sawnwood, panels and veneer) in 2010 made up 11.4% of the total imports, and were valued at $20.4 billion, down from twice that in 2007.

Tropical timber is losing market share to temperate timber in Europe, in part because of concerns about unsustainable and illegal harvesting in the tropics by consumers, retailers, processors and importers (figure 2). The WWF claims that 16-19% of the EU's timber imports (from outside of Europe) are derived from illegal or suspicious resources, and WWF cites mainly the Russian Federation (WWF, 2008). Today our SWST Convention is in China, and WWF notes the EU's growing imports from China, and claims that wood used for those products comes from high-risk regions, specifically the far east of Russia, Southeast Asia and Africa. How can purchasers of tropical timber in the EU be assured of its legality?

Figure 2. Tropical versus temperate timber imports in the EU

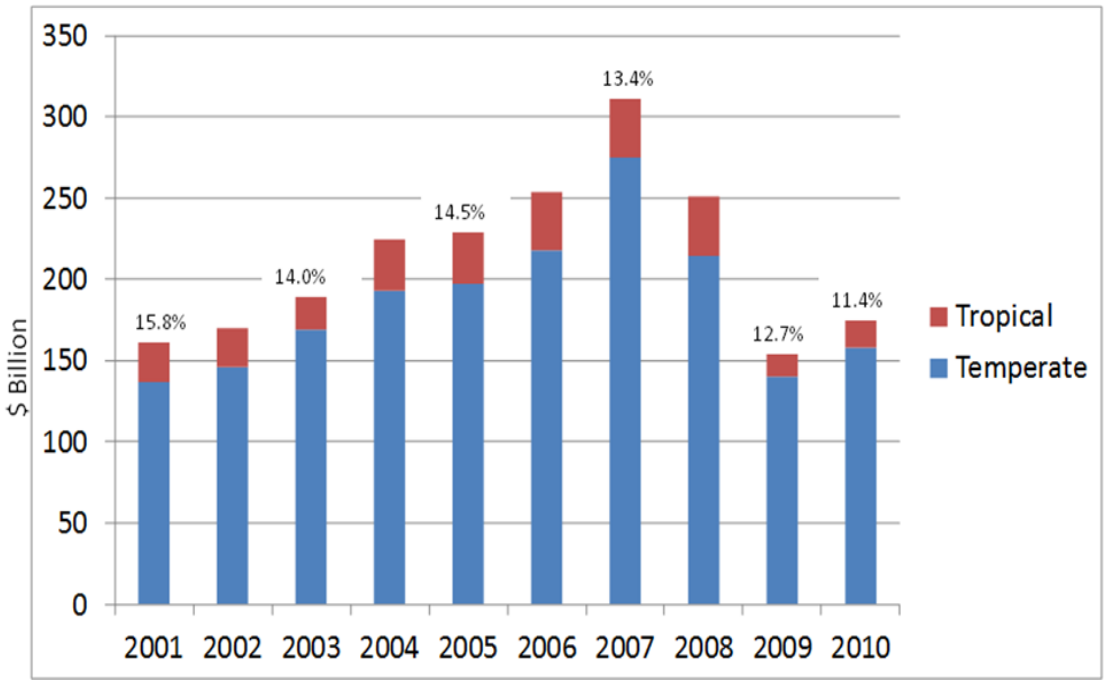

Note: Primary-processed products only. Specifically, industrial roundwood, sawnwood, plywood and veneer.
Source: ITTO, 2012.

To accomplish the FLEGT objectives, including establishing forest sector legislation and governance, and enforcing it, by mid-2012, VPAs have been signed by the EU with 6 countries in Africa and Asia. A number of other countries are conducting negotiations for a VPA (figure 3). In some other important timber trading countries, e.g. China, the EU is conducting a high-level dialogue on forest issues including illegal logging and trade. Once a VPA is signed, countries introduce new measures of governance and enforcement in their forest sector.

Figure 3. Voluntary Partnership Agreements, as of mid-2012

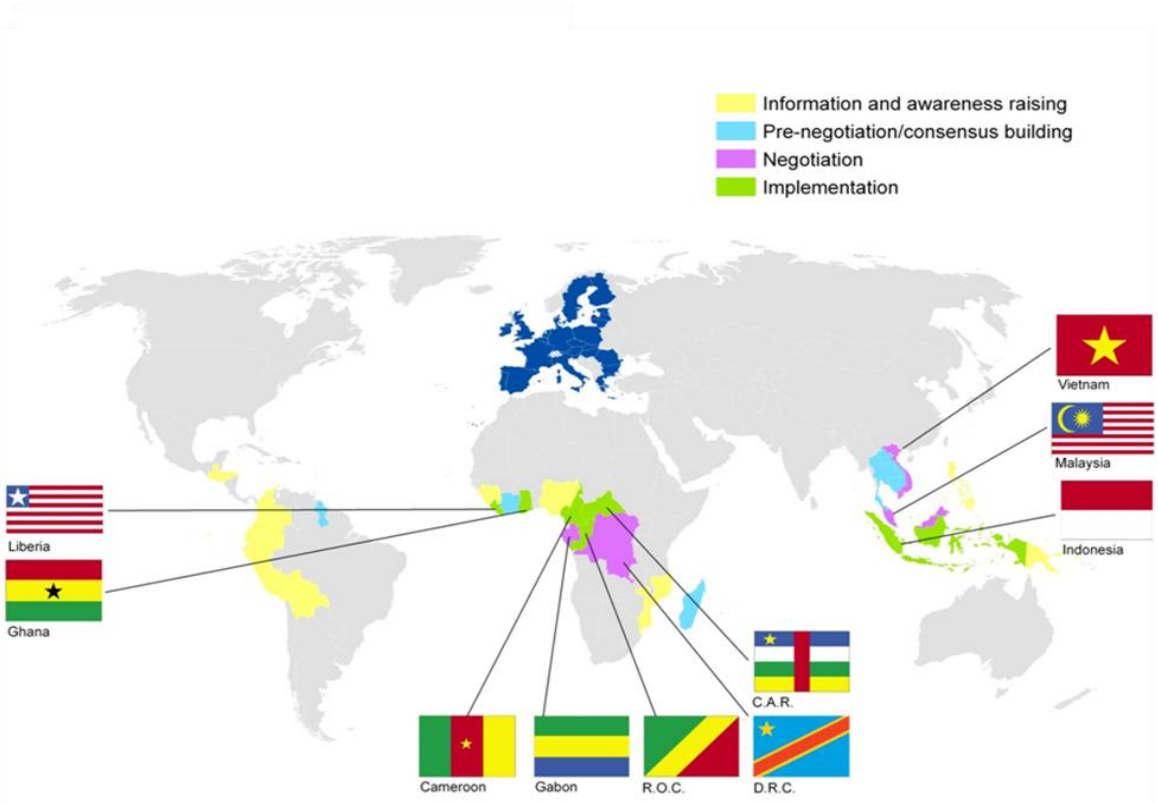

Source: EU FLEGT Facility, 2012.

Of specific interest for this paper is the establishment of a FLEGT licensing scheme which includes a set of procedures and requirements aimed at verifying that timber products are produced and exported legally. After which the country will be able to export FLEGT-licensed timber and timber products to the EU. To ensure legality, Legality Assurance Systems are established to control and independently audit the harvest, production and supply chain to the port of export. Eventually an Independent Market Monitoring system will be established to collect trade, policy and other information to analyze how the trade and markets are evolving, and simultaneously to provide evidence for the functioning of the FLEGT Action Plan.

The strength of the FLEGT approach lies in the combination of various elements and the linkages between them:

1. Bilaterally negotiated trade agreements with a focus on legality and forest governance as a means to enter into an open discussion with timber producing and processing countries based on their own legal framework

2. A reliance on changes taking place in the EU market for timber and timber products that exerts leverage over individual timber suppliers and processors

3. A reinforcement of these market changes with i) new EU legislation against the trade in illegally harvested timber products; ii) mandatory due diligence systems for timber traders; and iii) public and private purchasing policies

4. A focus on strengthening forest sector governance through a negotiating process based on stakeholder participation, broad in-country ownership, transparency and accountability

5. Development of concrete supply chain controls, verification and licensing systems relying on independent third party monitoring.

Regardless of the onset of FLEGT-licensed timber flowing to the EU, one of the successes of the process is bringing all the stakeholders together to craft a VPA. The EU and partner countries' governments have brought together the different government agencies at federal and local levels, the harvesting and processing industry, timber trade associations, non-governmental organizations and others that have an interest in the VPA.

Causes Of Illegal Logging And The Trade Of Illegal Wood

Poor governance and enforcement of national legislation, often combined with corruption, enable illegal logging and the trade of illegal timber. As mentioned above, the FLEGT Action Plan aims to address these problems. Through the VPA process legislation is to be strengthened and laws are to be enforced. Measures are built in to monitor the process in the EU's VPA partner countries.

The "T" in FLEGT aims to eliminate the demand from abroad for illegally logged timber. In other words, if there was no demand for illegal timber, it would eliminate one of the causes of illegal logging. The foreign trade of illegal wood is often highly organized.

Timber illegally logged is also bought and sold or bartered domestically. A considerable volume of timber is felled, inefficiently processed into sawnwood, and used for local construction and other uses. Rather than high-yield sawmilling, illegal timber is often sawn locally into boards by wide-kerf chainsaws and imprecise pitsaws.

Combating Illegal Logging And The Trade Of Illegal Wood

Bringing awareness of the problems of illegal logging and the trade of illegal wood and paper products is the first step in achieving solutions. However, we need to maintain the demand for wood and paper products to continue to support sustainable forest management and legality. In its 2012 study, the World Bank proposed these policy recommendations (World Bank, 2012):

- Develop an integrated criminal justice strategy for illegal logging that adopts and implements clear and comprehensive policies
    - Improves domestic cooperation

    - Enlists the private sector
    - Engages civil society actors
- Include criminal justice as part of development assistance programs to combat illegal logging.

The World Bank study continues with these operational recommendations:

- Improving international cooperation
- Working together between stakeholders in the forest sector, the criminal justice sector
- Attacking corruption
- Targeting individuals, groups, forests and companies that are vulnerable
- Enforcing anti-money laundering
- Enforcing due diligence requirements.

The FLEGT Action Plan covers much of the above. The next step of the Plan is EU Timber Regulation which will come fully into force in March 2013.

EU Timber Regulation

The EU Timber Regulation (EUTR) was adopted by the European Parliament in 2010, and parts of it have been initiated already, but it will fully take effect as of 3 March 2013 (EUTR, 2010). This new legislation prohibits placing illegally harvested and traded timber on the EU market. It requires operators (timber importers, traders, processors, middlemen, wholesalers and retailers) to carry out due diligence. "Due diligence" was defined in July 2012 in the "Commission Implementing Regulation" (EC, 2012). Each operator's system must be able to account for the scientific name of the timber species and the precise source, down to in high risk regions of the harvest concession and site. In practice operators must minimize the risk of illegal timber by assessing risks and taking mitigation measures. Certification of sustainable forest management and certified chain-of-custody is one measure of risk mitigation, but in itself is not proof of legality. However, major international certification systems are making modifications to be proof of legality too. Appropriate assessment of the risk of illegality, and complementary mitigation measures if necessary, rely on sound and reliable information on legal and illegal timber trade.

The onset of the EUTR will provide significant challenges to the timber trade. Tracing wood products back to their harvest site, and verifying the legality of logging, transport, processing and all allied steps through the export and import will necessitate comprehensive systems. Coordination is required between exporting countries' harvesters, processors and exporters, and importing countries' importers, i.e. the first person placing wood on the EU market. The EU is authorizing official monitoring organizations that companies can engage for these purposes. Monitoring organizations can be a company or an organization that develops a due diligence system for an operator; the monitoring organization can also maintain and manage the system. The EU Member States have designated their individual Competent Authorities that will be responsible for checking the trade, as well as the monitoring organizations. The EU Member States will be responsible for determining fines and penalties.

One key need at this time is communication to operators throughout the EU about the forthcoming EUTR. It is now time for operators to establish their due diligence systems, especially when placing orders in 2012 that could arrive in Europe in 2013.

Another challenge will be for counties that import timber, process it, and export it to the EU. This paper is prepared for the SWST Convention which takes place in 2012 in China. Using China as an example, in order to fulfill their due diligence requirements, EU wood products importers will begin to ask their Chinese exporters for detailed information. It will require new systems in China to know the province of their wood, as well as to have documentation of its legal harvesting, transport, processing, exporting and importing. This information is needed by EU operators for their due diligence systems, and specifically risk mitigation, under the EUTR. Even for domestically produced timber, Chinese manufacturers will need similar assurances. Most of Chinese wood products exports to Europe are value-added products, of which many have composite board products such as MDF. Even for MDF produced from domestically grown species such as populus, the fiber is sourced from a multitude of sites. China is a major exporter of plywood, which is often composed of multiple species for the face and core. In addition to knowing the scientific names of the species, exporters and in turn middlemen and producers will be asked about the legality of the source of the veneer. The EUTR applies equally to timber traded within the EU.

The goals of this legislation are admirable, but its implementation will be challenging for the timber trade. One means to ensure legality and sustainability will be to trade in FLEGT-licensed timber. Initially the supply of licensed timber will be small, but the intention is that over time the supply will increase. Continuing with the example for China, if FLEGT-licensed timber is imported and processed, it would find easy access to the EU. Of course processers would need to keep their supply chains separate, as many do now for certified and non-certified wood.

Conclusion

In order to stem the flow of illegal timber, and thereby reduce illegal, the EU, as well as other countries, have established policies to eliminate imports of illegal wood and paper products. Through the FLEGT Action Plan the EU is setting up VPAs with tropical timber producing and exporting countries. In addition to contributing to the improvement of the legal framework for the governance of the forest sector, and its enforcement, the implementation of the agreements will result, inter alia, in FLEGT-licensed timber. The licensed timber will be easily imported into the EU after the 2013 implementation of the EUTR. For all other timber imported into the EU, operators will need due diligence systems to mitigate risks of illegal timber trade. This new paradigm for timber trade is aimed at reducing illegality in the EU and its trading partners. As more countries establish similar policies, and enforce them, eventually illegal logging will diminish.

References

EFI. 2008. Forest Law Enforcement Governance and Trade – the EU approach. EFI Policy Brief 2. Available at: www.efi.int/files/attachments/publications/efi_policy_brief_2_eng_net.pdf

EFI. 2010. Changing international markets for timber and wood products – Main policy instruments. EFI Policy Brief 5. Available at: www.efi.int/files/attachments/publications/efi_policy_brief_5_eng_net.pdf

European Commission. 2010. Regulation (EU) No 995/2010 of the European Parliament and of the Council. Available at: http://eur-lex.europa.eu/LexUriServ/LexUriServ.do?uri=OJ:L:2010:295:0023:0034:EN:PDF

EC. 2012. Commission implementing regulation (EU) No 607/2012. Available at: http://eur-lex.europa.eu/LexUriServ/LexUriServ.do?uri=OJ:L:2012:177:0016:0018:EN:PDF

EUTR platform. 2012. Available at: http://www.eutr-platform.eu/en

FAO. 2011. Global forest resources assessment 2010. Available at: www.fao.org/forestry/fra/fra2010/en/

FAO. 2012. ForesSTAT. Available at: http://faostat.fao.org/site/626/default.aspx#ancor

ITTO. 2012. ITTO Annual review statistics database. Available at: http://www.itto.int/annual_review_output/

Viitanen, J. 2012. Illegal logging and FLEGT – How a trade agreement can promote governance reform. Available at: https://colloque4.inra.fr/globalforestrycourse

World Bank. 2012. Justice for forests: Improving criminal justice efforts to combat illegal logging. Available via: http://www.illegal-logging.info/item_single.php?it_id=1272&it=document

WWF. 2008. Illegal wood for the European market. Available via: http://www.illegal-logging.info/uploads/WWFeuropeanmarketwood1.pdf

China's Impact On Global Forest Products Trade -- Viewpoint From Abroad

Dr. Ivan Eastin, Professor and Director, Center for International Trade in Forest Products (CINTRAFOR), School of Environmental and Forest Science, University of Washington, Seattle, WA 98195 USA
Dr. Jeff Cao, Researcher, Asian Institute for Energy, Environment and Sustainability (AIEES), Seoul National University, Seoul, South Korea
Dr. Indroneil Ganguly, Research Associate, Center for International Trade in Forest Products (CINTRAFOR), School of Environmental and Forest Science, University of Washington, Seattle, WA 98195 USA
Dr. Miyhun Seol, Research Scientist in Forest Carbon Policy, Center for Forest and Climate Change, Korea Forest Research Institute, Seoul, 130-712, Republic of Korea

Overview

The global economic crisis had a significant impact on the Chinese export-oriented wood products industry and slowed its appetite for raw materials imports. According to trade statistics, China's imports of wood products fell by 9.6% in 2009 to US$7.3 billion from US$8 billion in 2008 and China's wood products exports (excluding wood furniture) dropped from US$9.3 billion in 2008 to US$7.7 billion in 2009 (Global Trade Atlas 2012). Chinese wood furniture exports also declined substantially during the first half of 2009, but quickly bounced back following the government's decision to reinstate the 15% export tax rebate in June 2009. By the end of 2009, Chinese wood furniture exports had registered 11% growth over the previous year, growing from US$6.8 billion in 2008 to US$7.6 billion in 2009. The economic crisis also resulted in high wood material inventories and significant price drops for wood based commodities and subsequently put over 50% of wood-based panel companies (approximately 3,000 enterprises) in severe financial trouble, resulting in many plant closures. Forest products companies located in 6 counties within the provinces of Zhejiang, Shandong, Jiangsu and Hebei reportedly laid off a total 3 million workers (State Forestry Administration, 2009).

However, China has rebounded strongly and still maintains its position as the world's largest manufacturer and consumer of wood-based panels, furniture, flooring and wooden door products. With GDP growth exceeding 9 percent between 2009 and 2011 (and projected to be 8.2% in 2012 and 8.6% in 2013), Chinese domestic demand has become an important growth engine, supported by massive urbanization and continued growth within the housing sector. Planned reforms of pensions, healthcare and education should also support expansion of domestic consumption and broad-based growth in the long-run. Strong domestic stimulus spending on infrastructure, renewable energy and other technology innovations has also been a boost to China's economy and the Chinese government continues to transition to a low-carbon economy through investments in

energy efficient technologies such as high-speed rail, solar power and green building technologies, thereby enhancing long-term competitiveness.

The Chinese government has shown a growing interest in green building products and technologies and China is already the largest manufacturer of solar panels and wind turbines. To expand demand within the domestic market, the government provides generous subsidies to households that install solar panels and energy efficient water heaters. The Chinese Ministry of Housing recently signed a memorandum of mutual understanding with the government in British Columbia, which included a provision to build a six-floor wood-frame apartment building utilizing materials and technologies provided by forest products companies in British Columbia. This program will allow Chinese government officials and local industry to observe the energy and carbon savings, seismic safety, speed of construction and cost comparability of multi-story, multi-family wood frame construction.

The housing industry is becoming an important driver of wood products consumption in China. Following a setback in 2008, home sales jumped by over 43% in 2009 to reach 850 million square meters with total sales of ¥4.4 trillion (Figure 1). In 2011, the value of home sales had reached 5.9 trillion yuan and the area of residential housing sold exceeded 1 billion square meters for the first time ever. According to government statistics, the total floor space of new construction (including both residential and non-residential projects) continued increasing and exceeded 8 billion square meters in 2011, with almost 3 billion square meters of floor space being completed (Figure 2). While the area of completed construction grew at a more modest pace, the area of projects under construction increased much faster, reflecting an increase in investment and the goals of the 12th Five-Year Plan (2011-2016) which calls for the construction of 36 million units of affordable housing.

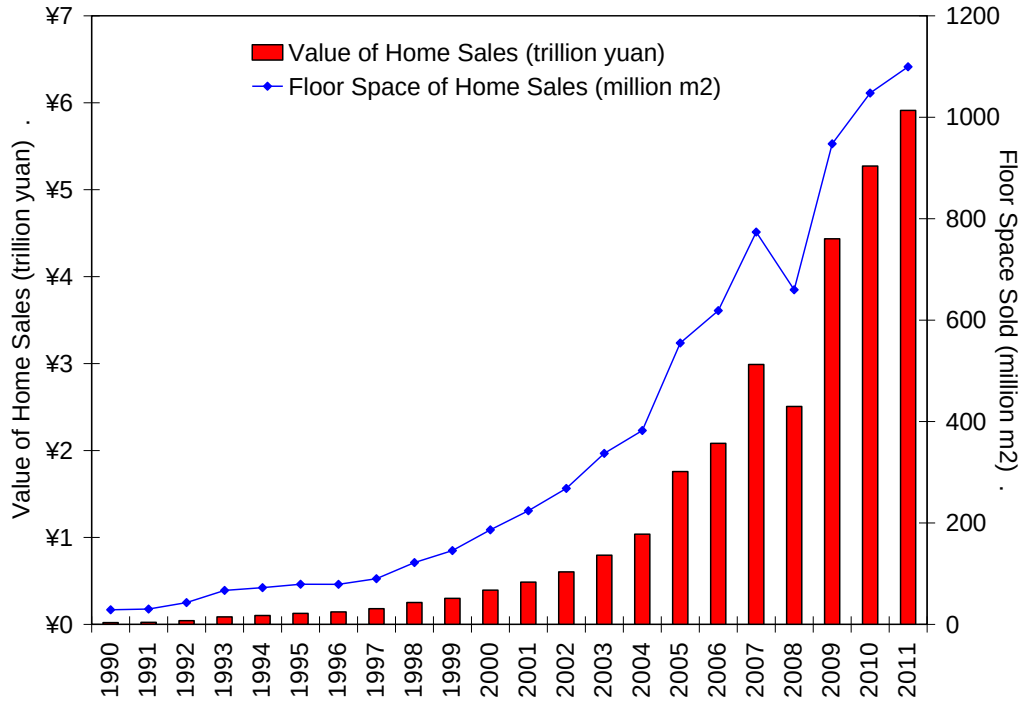

Figure 1. China's Fast-Growing Housing Industry *(Source: China Statistics Bureau 2010; China Index Research Institute 2010)*

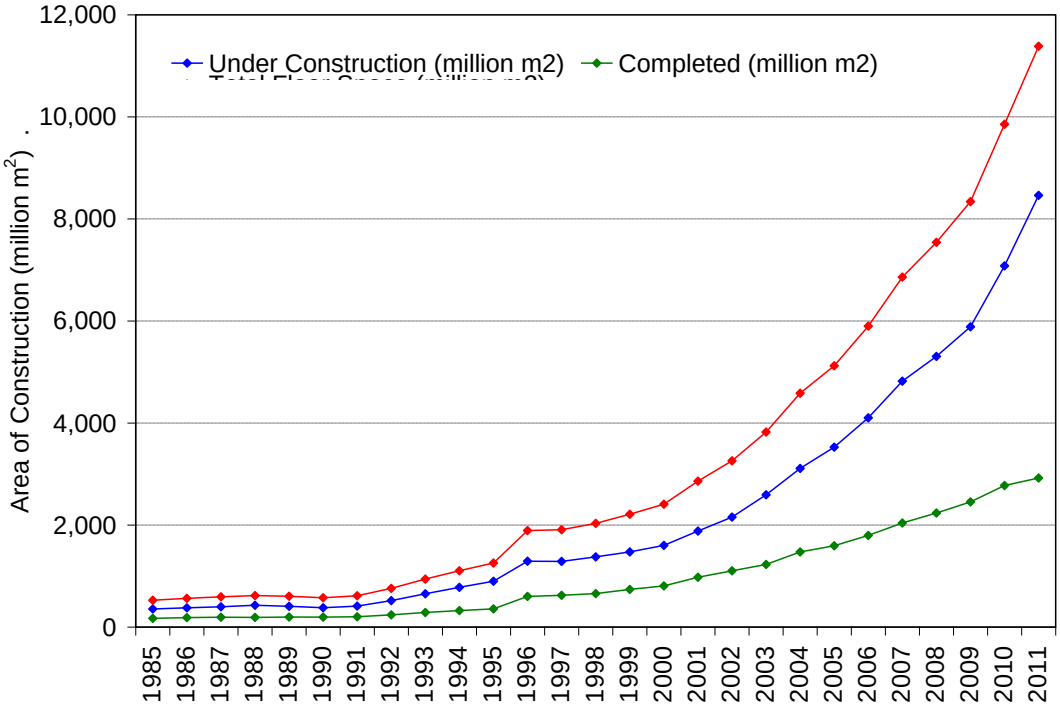

Figure 2. China's Investment in Real Eastate Development 2000-2009 (*Source: China Statistics Bureau, 2010*)

Currently, about 30% (or 12.4 billion square meter) of these residential buildings are located in the urban area. Due to poor construction quality, industry experts estimate that

at least half of the existing urban residential buildings will have to be torn down and rebuilt over the next 15-20 years. According to industry insiders, another 30 billion square meter of new residential buildings will be constructed over the next decade, in addition to the current inventory of 42 billion square meters (as of 2008). Therefore, on-going new home construction, combined with remodeling and expansion projects, will open up tremendous markets for wooden building and home furnishing products.

The wood products industry in China has experienced significant structural changes since 2007. The global financial crisis has slowed Chinese wood products export growth and its zest for capacity expansion. However, it has also provided an opportunity for many companies to readjust their business strategies to increase their focus on the domestic market and the new growth opportunities resulting from increases in household wealth that have occurred over the past ten years and which are expected to accelerate over the next twenty years. With the government's new policy stimulus, many Chinese companies have begun to shift their focus from the export market to domestic market, particularly in smaller third- and fourth-tier cities, as well as rural markets. In addition, a new round of industry consolidation is occurring across all major industry sectors. Companies are vying to build factory-owned brands, develop new products and establish market channels to reach Chinese consumers more directly and efficiently. Leading companies are becoming bigger through M&A with funds from private equity firms and international investment banks.

Looking towards the future, the Chinese government is likely to play a key role in further restructuring and guiding the Chinese forest products industry onto the track of recovery. According to a recently released government strategy entitled "Forest Products Industry Revitalization Plan" (which is supported by 5 key government agencies led by the State Forestry Administration) the Chinese government has set ambitious goals to maintain the industry's position as the world's largest producer and exporter of furniture, wood-based panels, wood flooring, and wood door. The goal of the plan is to grow the industry at an annual rate of 12% and reach ¥2.25 trillion in total output by the end of 2012 (compared to ¥1.44 trillion in 2008). The government will also support the top 100 state-owned forest enterprises in becoming vertically integrated and help establish 10 specialized industry clusters to encourage increased production and marketing efficiencies. Meanwhile, in response to the growing demand for legal and sustainable timber products in international markets (which is widely perceived as a "green trade barrier" or "trade protectionism" by Chinese manufacturers and exporters), the Chinese government is promoting the newly developed Chinese national forest certification standard (CFCC), which is very likely to be endorsed by PEFC in the near future. This new domestic certification program should help Chinese wood products maintain (and potentially increase) access to international markets.

By the end of 2012, employment within the wood products industry is expected to have increased by 27% (from 2008's level) to reach 57 million jobs and remain a leading employer of rural workers. Besides assisting the wood manufacturing sector, promoting eco-tourism and related environmental services is another focus of the Chinese

government during the 2010-2012 period, with this sector expected to provide an additional 16 million jobs.

Over the medium-term we should expect to see demand for imported timber products pick up for several reasons. First, the government will continue to emphasize the export-oriented wood manufacturing sector will continue to be a driver of employment and economic activity. While there will be some consolidation in the industry and geographic dislocation (as some firms move inland in search of lower wage rates), the lack of a mature and high quality timber supply means that China will continue to rely on timber imports for the foreseeable future. Second, continued investment in expanding and improving the transportation infrastructure will support imports of construction grade lumber and wood-based panels. Third, the Twelfth Five-Year plan (2011-2016) called for the construction of 36 million affordable housing units; an increase of seven million housing units in addition to the large number of market rate housing units being built in China. While housing units in China are generally multi-story concrete and brick buildings, interior finishes (including flooring, wall panels, cabinets, mouldings and stair parts) and furniture use a substantial volume of higher quality wood.

Finally, increasing affluence in China and the rapid growth of the Chinese middle-class (Figure 3) will support the import of higher quality interior wood products and provide an opportunity for introducing brand name value-added wood products. A recent report by McKinsey estimates that the share of Chinese households that will move into the

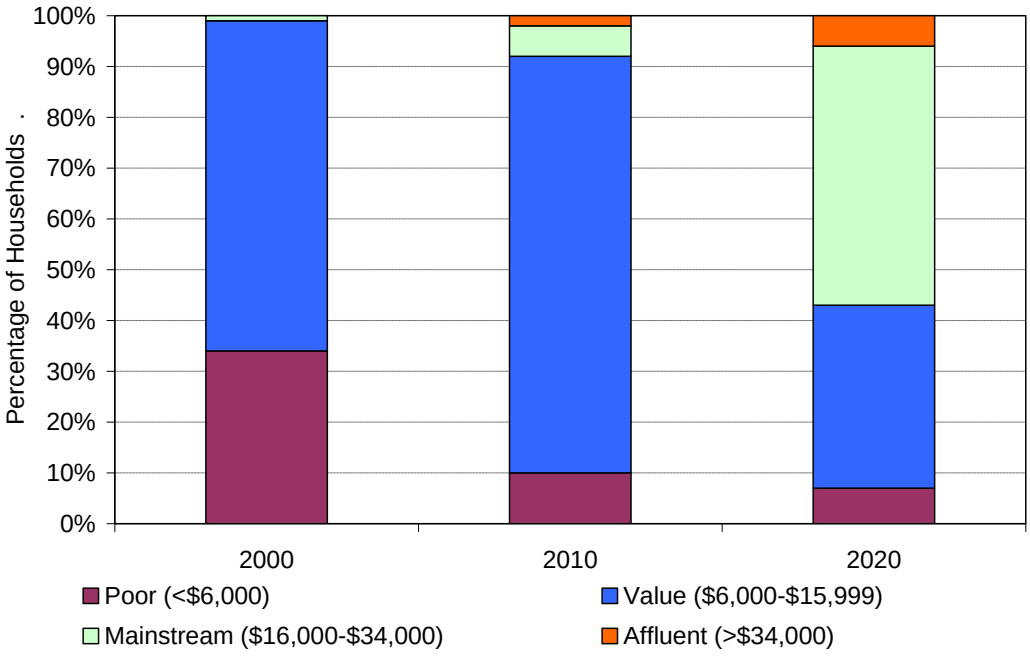

(Source: Meet the 2020 Chinese Consumer. McKinsey & Company 2012)

Figure 3. By 2020, it is expected that over half of Chinese households will have moved into the mainstream consumer segment. (*Source: McKinsey and Company 2012*).

mainstream income level will jump from 6% to 51% between 2000 and 2020, while the total number of households will increase from 226 million to 328 million. This

unprecedented surge in household wealth will have huge implications for wood manufacturers around the world. For example, the combination of increasing affluence and families moving into new housing caused Chinese consumption of wooden furniture to increase from just over $5 billion in 2003 to almost $30 billion in 2011.

The currency exchange policy largely remains an unclear issue at this time. A successful shift to consumption-led growth should allow Chinese policymakers to adopt a more flexible exchange rate policy, which should help correct global economic imbalances and reduce the risk of trade wars and protectionist policies. A stronger Chinese currency would also draw liquidity from the domestic economy and help ease imported inflationary pressures, boosting household purchasing power and consumption. This boost should help domestic demand become a stronger driver of growth and begin to wean the Chinese economy away from excessive dependence on low value-added exports. However, a stronger currency will undoubtedly hurt forest products exporters and slow the industry's recovery. Therefore, it remains to be seen whether or not China's wood industry will be able to maintain strong export growth with a stronger yuan, although it is safe to say that China will continue to be a major importer of wood products during its transition to a consumption-led economy. The following section provides a discussion of China's wood products industry from an environmental and economic perspective.

Economic and Environmental Aspects of China's Wood Products Industry

Over the past two decades China has grown to become the most important player in the global trade of wood products. During this period China emerged as the largest exporter of value added wood products (particularly, wood flooring and furniture), and the largest importer of unprocessed and semi processed wood products. Domestic timber supply constraints mean that future growth in the Chinese wood processing sector will almost certainly have to be sustained by imported logs and lumber. China's wood processing industry follows an 'export oriented processing' trade model, similar to the model employed by Japan in the 1960's. This export strategy, in combination with an undervalued yuan, massive investments in the wood product manufacturing sector and comprehensive fiscal support by the Chinese government (including a variety of subsidies), has resulted in China's emergence as the largest player in the global wood products market.

Raw Material Imports

China's wood products industry is heavily dependent on imported logs and lumber as the raw material input for the furniture and flooring industry. In 2007, China's log imports totaled more than US$ 5.3 billion before dropping to US$ 4.1 billion in 2009, as a result of the global recession (Figure 4). However, log imports have surged since 2009 reaching $US8.3 billion by the end of 2011. During the same period, China's lumber imports continued to exhibit strong growth, jumping from US$1.7 billion in 2007 to over US$ 5.7 billion in 2011, (Figure 5). Chinese lumber imports have grown so rapidly that in 2010 China became the largest importer of lumber in the world, a position traditionally held by the US.

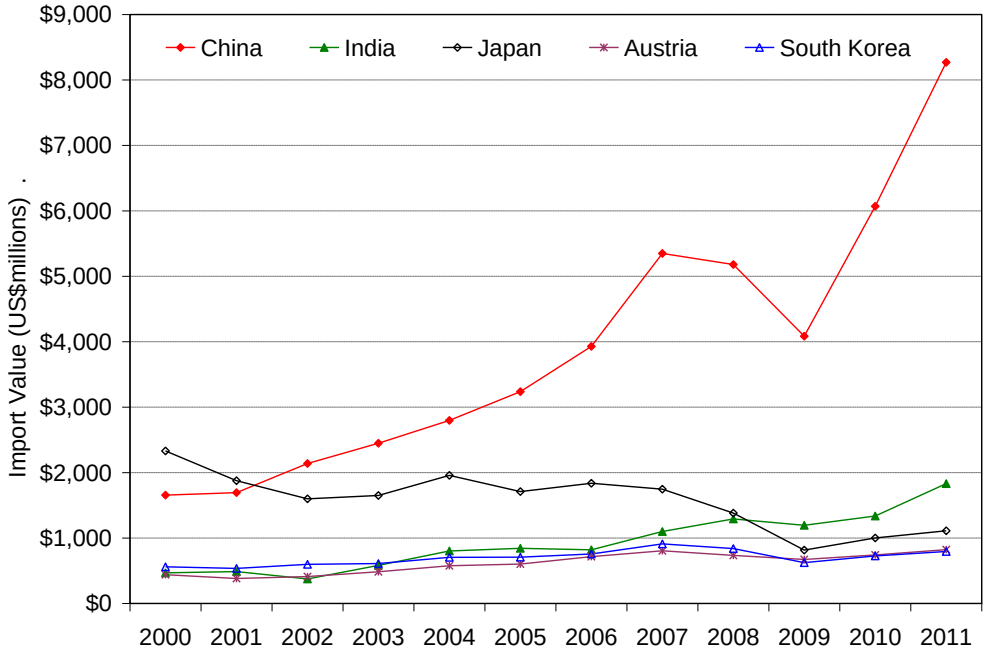

Figure 4. The value of China's log imports actually exceeds the combined log exports of the next fourteen countries combined *(Source: Global Trade Atlas 2010)*

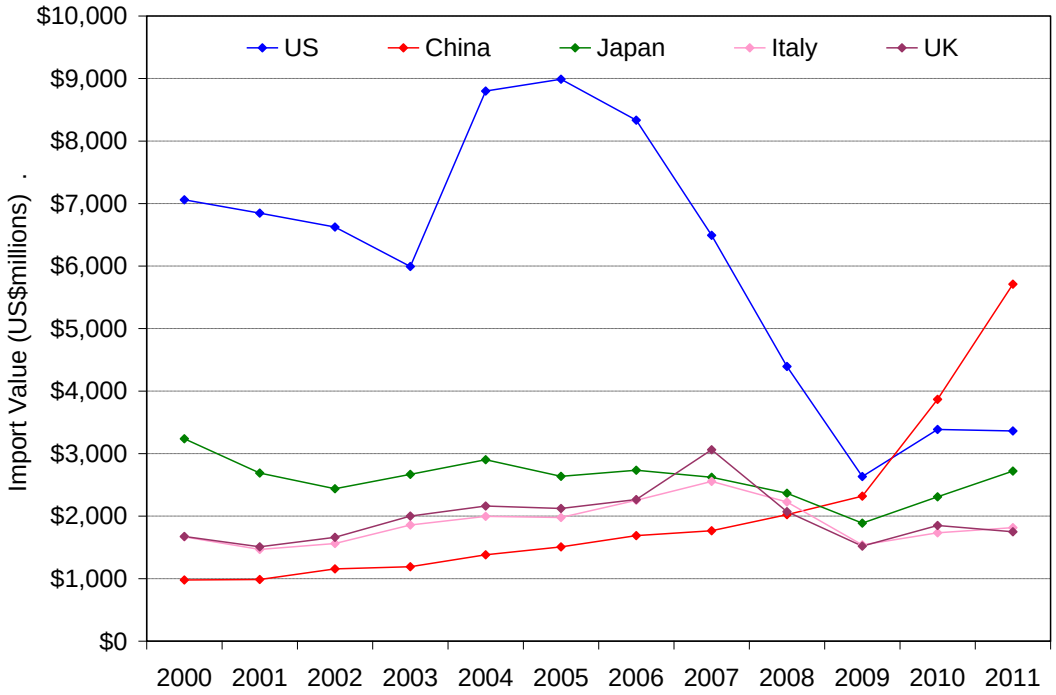

Figure 5: China surpassed the US as the largest lumber importer in 2010. *(Source: Global Trade Atlas 2010)*

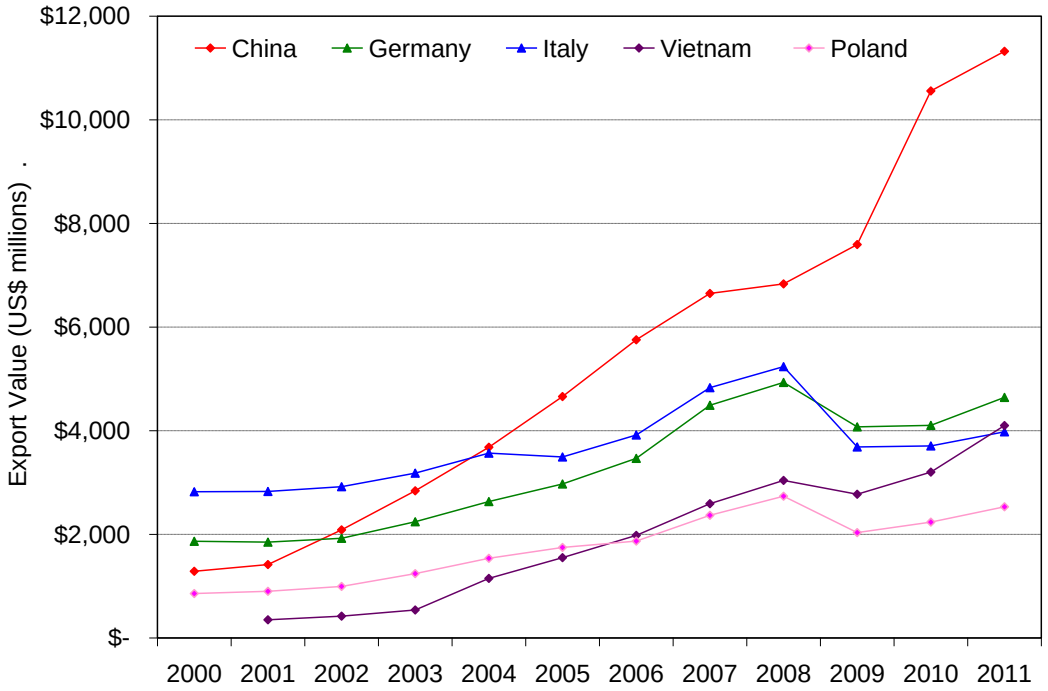

Figure 6. Chinese wooden furniture exports exceed those of the next two countries combined. *(Source: Global Trade Atlas 2010)*

Value Added Good Exports

The Chinese value-added wood products industry has been a tremendous success story, playing a dominant role in global trade. China has been the leading exporter of wooden furniture since 2005, overtaking the traditional European exporters of wooden furniture, Germany and Italy. In 2011 the total value of Chinese wooden furniture exports exceeded $11 billion, more than the exports by Germany and Italy combined (Figure 6). As recently as 2006, over 80% of all Chinese wooden furniture exports were destined for the Unites States. However, in the last few years China has successfully diversified its exports of wooden furniture to include a range of Asian and European countries and in 2011 the US share of Chinese wood furniture exports was just 29.8%.

Over the last decade China has also emerged as the world's largest producer and exporter of plywood. China's exports of plywood recorded phenomenal growth between 2000 and 2007, increasing at an average rate of 60% per annum. During this period, China's plywood exports rose from US$190 million to US$ 3.6 billion, a 19 fold increase since 2000 (Figure 7). At the beginning of this decade Indonesia was the leading exporter of plywood in the world, followed by Malaysia. However, through massive investment in the domestic plywood industry, in combination with a steady supply of local and imported raw material, the Chinese plywood production grew at an unprecedented rate. Given the advantage of low labor rates, Chinese plywood manufacturers initially targeted the domestic market and low-end export markets. However, increased investment in advanced production technology has allowed Chinese manufacturers to produce higher

quality plywood and successfully enter and compete in the US, European and Japanese markets. Since the second quarter of 2008, Chinese plywood production and exports dropped substantially as the global financial crisis affected international demand for plywood. The severe drop in international demand led to a long overdue consolidation within the Chinese plywood industry as small undercapitalized manufacturers dropped out of the industry. The recovery of global demand for plywood began in late 2009 and Chinese exports of plywood reached an all-time high of US$4.3 billion in 2011.

Environmental Challenges For The Chinese Wood Products Industry

China became the biggest exporter of value added wood products in 2010 including wooden furniture, plywood, fiberboard, wood flooring, miscellaneous wood articles, and builders joinery. However, there are a number of issues confronting the Chinese wood products industry that could affect its competitiveness or restrict its access to lucrative developed markets. Some of these issues are associated with the rapid industrialization of the Chinese economy, whereas, others relate to trade regulations targeted to wood products. The rapid increase in Chinese exports of low priced value-added wood products have resulted in a number of anti-dumping complaints from the US, Canada, the EU and other importing nations. Such anti-dumping complaints tend to focus on furniture and plywood exports from China, but are not uncommon for other value added wood products, such as wood flooring.

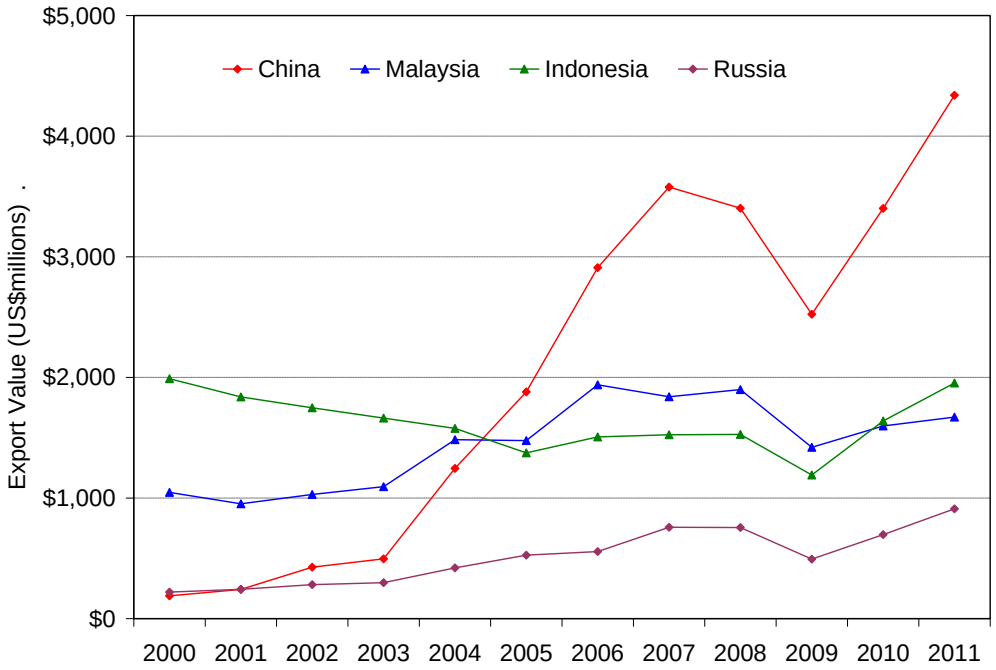

Figure 7. Chinese plywood exports skyrocketed between 2000 and 2007. *(Source: Global Trade Atlas 2010)*

The Chinese wood products industry is also facing steep price competition from other Asian nations (such as Vietnam, Malaysia and Indonesia), who are attracting significant investment in their wood products sectors. For example, Vietnam has experienced substantial growth in furniture exports and has seen their share of the US market jump from 3.1% in 2004 to 14.5% in 2009 and it is projected to be almost 17% in 2011. Despite this competition, China remains the dominant exporter of wood furniture and their global market share increased from 16.7% in 2008 to an estimated 28.8% in 2011. To a large extent, the rise of furniture exports from Asia has come at the expense of the more established furniture producers in Europe. Between 2008 and 2011, Italy saw its share of global exports drop from 13.5% to 10.1%, while Germany's share dropped from 12.6% to 11.8%, and Poland's share dropped from 7.1% to 6.5%. The success of Asian countries such as Vietnam, Malaysia and Indonesia can be attributed to several factors, including rising labor and raw material costs in China. In addition, several large multinational furniture manufacturers have implemented a strategy of diversifying their production capacity across several countries in order to reduce their exposure to production disruptions. In addition, Chinese manufacturers have begun to recognize the potential of the domestic market as incomes and consumer spending increase across China.

China's Timber Procurement and Changes in Procurement Patterns

It is well established that illegal logging is a major contributor to global deforestation. The rapid increase in China's demand for logs, with sawlog imports increase from 4.8 million m^3 in 1998 to 25.3 million m^3 in 2007, put China in the spotlight. The Chinese wood products industry has been harshly criticized for supporting irresponsible procurements practices that have expanded the incidence of illegal logging. According to a report published in 2007 by a UK based environmental organization, China has become the largest importer of illegally harvested logs in the world. For example, the UK report estimates that over 75% of logs harvested illegally in Myanmar, Congo, Equatorial Guinea, Gabon, Papua New Guinea and the Russian Far East end up in China. Since China's wood products industry is predominantly export oriented, the UK report claims that the demand for illegal logs is also supported by the fact that consumers in developed countries either ignore or are unaware of the illegal nature of the timber used to manufacture wood products imported from China.

Table 1: Summary of Chinese log import trends for the period 2000-2007 and 2007-2009. *(Source: Global Trade Atlas 2010)*

Log Imports From	% Change 2000 to 2007	% Change 2009 to 2011
Overall (World)	173% ↑	51% ↑
Russia	328% ↑	• ↓
Malaysia	-34% ↓	-42% ↓
Gabon	1% •	-97% ↓
Papua New Guinea	210% ↑	13% ↑
Mozambique	543% ↑	-2% ↓
Myanmar	23% ↑	59% ↑
New Zealand	213% ↑	39% ↑
Equatorial Guinea	36% ↑	38% ↑
Cameroon	16% ↑	-17% ↓
Solomon Islands	1062% ↑	22% ↑
United States	425% ↑	76% ↑
Australia	4281% ↑	49% ↑
Canada	1,502% ↑	109% ↑
Congo	5,545% ↑	28% ↑

Legend: ↑ imports increased significantly
↓ imports decreased significantly
• imports remained approximately same

Legality Verification Requirements by Importing Nations

In response to the growing trade of wood and wood products sourced from illegally harvested timber, the US and Japan have adopted environmental procurement policies requiring that all imported wood products be sourced from legally harvested wood. The US

Congress recently approved the "Combat Illegal Logging Act of 2007" which amended the Lacey Act to prohibit the trade in illegal plants and plant products (including wood products). The emphasis by the US government on ensuring the legality of imported wood, coupled with a growing awareness of eco-labeled wood, has influenced the Chinese to implement more responsible wood procurement policies. A similar policy requiring legality verification of traded wood products has been approved by the EU parliament and is scheduled to be implemented in March 2013.

A review of the recent trade statistics reveals that there have been significant changes in the composition of log imports by Chinese firms, Table 1. Some of these changes suggest a more responsible raw material procurement policy by Chinese wood importers. Table 1 shows the Chinese log import trends from some of the important trade partners for periods 2000-2007 and 2007-2009. Chinese overall log imports grew by 173% between 2000 and 2007, while they declined by 24% between 2007 and 2009. Much of this can be attributed to the fact that China became increasingly dependent on the steady supply of Russian logs across the border beginning in 1995 when just 13.8% of log imports came from Russia. By 2007, 69% of all logs imported by China came from Russia,. However, the gradual imposition of a log export tariff by the Russian government in 2007 increased log prices and forced Chinese wood manufacturers to look for other, more reliable sources of supply and resulted in the substitution of lumber for logs within the raw material mix. The decline in Chinese log imports was further exacerbated by the global financial crisis which occurred in 2008 and significantly reduced global demand for wood products in the developed countries. During the 2000-2007 period, Chinese imports of logs from countries with a high incidence of illegal logging (such as Myanmar, Congo, Equatorial Guinea, Indonesia and Russia) increased at an extremely high rate. However, the post-2007 period saw a significant decline in Chinese log imports from most of these countries, whereas log imports from developed countries where illegal logging was not a concern (such as New Zealand, Australia, Canada and United States) increased substantially after 2007. This trend in the sourcing of log import suggests a more responsible approach to sourcing logs by the Chinese wood products industry.

Role of Forest Certification Programs and Eco-Labeling

The success of sustainable forest management is inextricably linked to the development of markets for 'environmentally certified wood products' (ECWPs). An increase in the awareness and demand for legal and sustainably managed wood products in developed nations resulted in significant interest among Chinese wood products manufacturers to adopt chain-of-custody certification. The major internationally recognized certification programs being used in China include the Forest Stewardship Council (FSC) and the Program for Endorsement of Forest Certification (PEFC) programs. Fundamentally, these environmental certification programs promote both sustainable forest management practices by forest managers (Forest Management 'FM' certification), and responsible procurement policies by manufacturers of wood products (Chain-of-Custody 'CoC' certification).

CoC certification programs in China: The appeal of the chain-of-custody programs is strong among Asian producers and exporters of wood products. However, the rate at

which Chinese manufacturers of wood products have adopted CoC certification, primarily through the FSC program, is truly impressive. The FSC CoC program was introduced in China in 1998. Between 2000 and 2011, the number of companies in China that have obtained FSC-CoC certification jumped from 12 to 1,867, as of January 2012 (Figure 8). Though this is positive trend, given the total size of the Chinese wood manufacturing sector these numbers constitute a small proportion (less than 4%) of all wood manufacturing firms in China. In addition, only an extremely small fraction of the wood products manufactured by these CoC certified firms use certified wood. The PEFC-CoC certification, which was introduced in China in 2006, has also experienced significant growth over the last four years. Despite this, the total number of wood product manufacturers in China certified under the PEFC-CoC program is only 167 as of January 2011. Since the PEFC program is relatively new in China, one of the major challenges PEFC is facing in China is low brand awareness among wood products manufacturers.

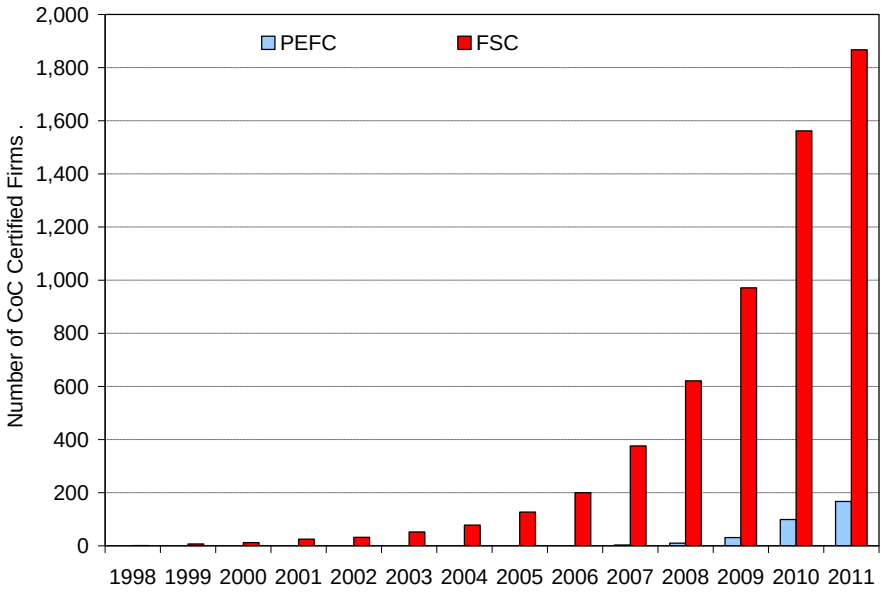

Figure 8. Chinese wood manufacturers have rapidly adopted chain-of-custody certification to maintain access to developed country markets. *(Sources: www.FSC.org; www.pefcchina.org)*

FM certification programs in China: The lack of availability of FSC certified wood, both from domestic and international sources, has been cited as the major reason why such a low percentage of manufactured wood products are produced from certified wood in China. The adoption of FSC-Forest Management certification in China has been slower than CoC certification, primarily due to the fact that virtually all forests in China are state-owned. A recent report published by FSC in February 2012, found that 47 forests with a total area of 2.7 million hectares have been certified under the FSC's forest management program in China. Most of these certified forests are integrated with state-owned wood manufacturing operations that have also received CoC certification. Hence, most of the supply of FSC certified logs from these forests are routed into the supply

chain and are not sold into the market, substantially constraining the supply of FSC logs available in China. Moreover, for those logs that are available to be sold into the general market, there is a logistical mismatch between the location of the log supply and the demand for the certified wood. For example, most of the domestic supply of FSC certified logs is located in the northeastern region of the country, whereas the primary demand for certified wood is located in the southeastern region of the country. The long distance between the certified forests in the northeast and the wood products manufacturers in the southeast makes supply chain logistics very difficult. Hence, most of the FSC-CoC certified manufacturing operations in China are dependent on imported FSC certified logs and lumber.

While the PEFC certification program has certified the largest area of forests in the world, it does not have any certified forests in China. The PEFC program has evolved to become an international umbrella organization that provides mutual recognition of other regional/national certification programs upon ensuring that their standards meet those of the PEFC program. Upon receiving mutual recognition by PEFC, the approved certification program can either adopt the PEFC brand logo for their products (such as PEFC-Italy or PEFC-France) or the program can retain their existing name and simply ally with the PEFC program (such as the Sustainable Forestry Initiative and the American Tree Farm System in the US). In the absence of a regional or national forest certification program in China, PEFC has not been able to introduce their forest certification program within the country. Hence, all of the PEFC-CoC certified companies in China are currently dependent on imported certified logs.

However, this situation is expected to change soon with the recent introduction of a Chinese national forest certification system that incorporates most FSC and PEFC certification criterion. Under the aegis of the State Forestry Administration (SFA) the China Forest Certification Council (CFCC) has developed the necessary guidelines to implement the national forest certification program. As per the SFA website, pilot projects involving the Chinese National Forest Certification (CNFC) program will be introduced in state-owned forests in China, by 2015. After 2020, the program will be extended to non-state owned collective forests as well. The CNFC will also offer a chain-of-custody certification program for export-oriented wood products manufacturers. The SFA website also indicates that upon establishment of the CNFC, China will seek international recognition for the program. Most likely they will look to PEFC for mutual recognition although Chinese officials have informally expressed interest in gaining mutual recognition from FSC as well.

Impact of the Lacey Act: The US Congress approved the "Combat Illegal Logging Act of 2007" which amended the Lacey Act to prohibit the trade in illegal wood products. As a result of this amendment, all US wood products importers are required to provide some documentation about the wood used in the products being imported. This information includes a description of the product, value, scientific name of the wood used (genus and species), country of harvest, amount of material and unit of measure. Recent interviews in China by CINTRAFOR researchers found that all the parties interviewed were aware of the Lacey Act amendment, although none expressed a clear understanding of the

amendment or how it would be implemented. The FSC and PEFC representatives indicated their dissatisfaction with the fact that CoC certification under their programs were not considered to be a sufficient condition for demonstrating the legality of wood under Lacey Act. Certification agencies, certifying bodies and industry managers were of the opinion that since the eco-labeling process ensures the legality of the wood used in the product, CoC certification should be considered a sufficient condition for proving legality of the wood.

Though US importers are required to provide sufficient documentation to demonstrate the legality of an imported wood product, this documentation is generally supplied to the US importer by the foreign exporter. Hence, US importers are highly reliant on their foreign partners to provide them with accurate documentation. However, the apparent lack of information and understanding of the documentation requirements for legality verification among some Chinese wood manufacturers suggests the need for an on-going outreach program designed to inform and update Chinese manufacturers and exporters. Some of the managers we talked with indicated that because of their uncertainty regarding the documentation requirements imposed by the Lacey Act, they have stopped exporting to the US and are now focusing on the European and Asian markets. However, they noted that the adoption of similar regulations in the EU meant that they would need to become familiar with these regulations sooner rather than later.

Concluding Remarks

As the largest importer of wood products and the largest exporter of value-added wood products in the world, China has emerged as the most important player in the global wood products industry. The level of processing technology within the Chinese wood products industry varies from traditional small-scale operations with a high labor input to highly automated and highly efficient large-scale production facilities. Traditionally, the Chinese wood products industry has been viewed as an industry reliant on high inputs of low cost labor and of an OEM supplier for foreign companies. Over the last decade, many Chinese manufacturers have made significant investments in order to transition to becoming highly efficient manufacturers of high end furniture and flooring products, many with Chinese brand names. Chinese wooden furniture manufacturers are successfully competing with their Italian and German counterparts in the global market and gaining market share at the European's expense. Though a large segment of the Chinese wood products industry continues to produce low cost commodity products, the industry has made significant process towards manufacturing high quality, innovative wood products.

Being the global leader in the wood products industry also comes with significant environmental responsibilities. Over the years the Chinese wood products industry has been blamed for its irresponsible procurement practices that drive illegal logging in developing regions around the world. A number of environmental organizations have identified the Chinese wood products industry as the primary user of illegally harvested wood. Because products manufactured with illegally harvested logs are exported from China into markets around the world, the developed nations have begun to require that

importers in their countries provide verification of legality for all wood products imports. Such measures have created significant awareness among wood manufacturers in China. Recent Chinese import statistics reveal a shift in log imports from countries known to have large scale illegal logging to countries where illegal logging does not pose a significant problem. Given the size and fragmented nature of the Chinese wood products industry, a complete change in the procurement policy may take some time. Based on our interviews with industry managers, and a review of Chinese import data, it is clear that the Chinese wood products industry is transitioning towards more responsible procurement practices.

The increased awareness and interest in chain-of-custody certification is a further indication of the Chinese wood products industry's changing environmental orientation. The chain-of-custody production process ensures that Chinese companies are sourcing wood that has been legally harvested. However, the rapid increase in the number of CoC certified manufacturers has not translated into a corresponding increase in the manufacture of eco-labeled wood products. Since the eco-labeling process is essentially a market driven approach, it is clear that its acceptance and success will depend on consumers across the globe being willing to pay a price premium for eco-labeled products. Moreover, the lack of a reliable supply of FSC certified logs and lumber as well as a lack of awareness of the PEFC certification program have created bottlenecks for the expansion production of eco-labeled wood products and held back the adoption of these programs in China.

In summary, China's wood products industry is transitioning from being a low cost producer of commodity exports to manufacturing high quality, differentiated products for both the export market as well as the growing domestic market. As the Chinese wood products industry matures, it is increasingly integrating globally accepted environmental procurement policies within its manufacturing sector. While the Chinese wood products industry has already established itself as a world leader in manufacturing value-added wood products, only time will tell if it can establish itself as a world leader in environmentally responsible procurement practices. This transition, in conjunction with supply constraints in Russia and Canada, will provide US forest products exporter's with unequalled opportunities in China over the next decade.

Literature Cited

Cao, Jeff., X. Sun and I. Eastin. 2012. Chapter 8. The Chinese Era, in: Global Forest Products Trends: Trends, Management and Sustainability. Taylor and Francis Group, LLC. ***(in press)***.

Cao, Jeff. 2012. Does it Pay to be Green? An Integrated View of Environmental Marketing with Evidence from the Forest Products Industry in China. CINTRAFOR Working Paper 124. University of Washington. 107 pages.

Eastin, I.L., D. Sasatani, I. Ganguly, J. Cao and M. Seol. 2011. The Impact of Green Building Programs on the Japanese and Chinese Residential Construction Industries and the Market for Imported Wooden Building Materials. CINTRAFOR Working Paper 121. University of Washington. 74 pages.

Forest Stewardship Council. 2012. http://info.fsc.org/
Global Trade Atlas. 2012. http://www.gtis.com/gta/
Programme for the Endorsement of Forest Certification. 2012. http://www.pefcregs.info/search1.asp
Robbins, Alicia. 2012. China's Forest Sector in the Reform Era. CINTRAFOR News. pp: 1, 3-6.
Robbins, Alicia. 2012. China's Forest Sector: Essays on Propduction Efficiency, Foreign Investment and Trade and Illegal Logging. CINTRAFOR Working Paper 122. University of Washington. 100 pages. ***(in press)***
Seol, Mihyun. 2012. Factors Causing Firms to Adopt Forest Certifications: Chinese Manufacturer's Perspective. CINTRAFOR Working Paper 125. University of Washington. 103 pages.
Yuan, Yuan and I.L. Eastin. 2007. Forest Certification and It's Influence on the Forest Products Industry in China. CINTRAFOR Working Paper 110. University of Washington. 69 pages.

Acknowledgements:

This research was made possible by a USDA NIFA-ISE competitive grant (no: 2009-51160-05463). Travel and logistical support for the research is provided by the Softwood Export Council (SEC). The researchers also acknowledge the support provided by Dr. Jeff Cao, Mr. Xu Fang (SEC Director, China Office), and Ms. Melody Ren (SEC Program Manager, China Office) in organizing the interviews.

Building Supply Chain for Sustainable Future: Perspectives and Learning from the Chinese Forest Sector

Xiaozhi (Jeff) Cao [1] – Eric Hansen[2] – Jeff Morrell[3]*

[1] Researcher, Asian Institute for Energy, Environment and Sustainability (AIEES), Seoul National University, 599 Gwanak-ro, Gwanak-gu, Seoul 151-921, REPUBLIC OF KOREA
* *Corresponding author*
caoxz@snu.ac.kr
[2] Professor, Department of Wood Science and Engineering, College of Forestry, Oregon State University, Corvallis, OR 97331, USA.
Eric.Hansen2@oregonstate.edu
[3] Professor, Department of Wood Science and Engineering, College of Forestry, Oregon State University, Corvallis, OR 97331, USA.
Jeff.Morrell@oregonstate.edu

Abstract

The forest sector in China has undergone tremendous growth over the past three decades. At the same time, the regulatory and business environment has changed and Chinese forest products companies are faced with serious issues related to global trade in protected wood species and illegal logging. A series of in-depth interviews were conducted with corporate executives, NGO leaders, and scholars in 2011 to examine how Chinese forest products companies were developing supply chain strategies to respond to the fast-changing environment as countries increasingly collaborate with each other to combat illegal logging and promote responsible forestry and trade on an international scale.

Our findings suggest that some pioneering companies are leading the way by "greening up" their supply chains to achieve a competitive advantage or reduce potential risks. Non-governmental organizations (NGOs) are playing an important role by advocating for sustainable industrial development and connecting policies with corporate practices. However, most forest products company supply chains seem to be poorly equipped to cope with this changing regulatory environment. Most are engineered to manage high-volume commodity sales that capitalize on low-cost production opportunities available in places with easy access to inexpensive labor, land and raw materials. Many of these advantages are disappearing as the economy grows. Increasing market demand for "legal" and "responsibly produced" forest products, driven in part by the need to meet trade regulations such as those promulgated by the EU through EU timber regulations or in the U.S. through the amended Lacey Act may leave many traditional forest products

companies dangerously exposed. Our interviews show near unanimity concerning the need for effective public-private partnerships to improve market-based mechanisms to advance sustainability in the supply chain.

***Keywords*:** China, forest, supply chain, sustainability, legality

Introduction

After twenty years since the Rio Earth Summit proposed the concept of sustainable development, an increasing number of policy directives, sourcing initiatives and market-based voluntary standards have been developed by the global community for the forest sector.

As the world's largest wood processing hub, China is a key link in many company supply chains. Between 1995 and 2011, China's total wood products exports (including wooden furniture) increased by an average of 16% per year, from US$1.8 billion to US$22.7 billion [1]. Meanwhile, China's wood products imports (including wooden furniture) grew by nearly 15% annually from $1.6 billion to $16.3 billion over the same period. It is estimated that wood imports have accounted for at least 70% of China's annual timber consumption since the early 2000s. In 2010, China's timber supply deficit was estimated to be 160-180 million cubic meters and the gap is projected to increase to 300 million cubic meters by 2015, when Chinese plantations and natural forests are expected to reach full production [2].

The changes witnessed over the past few decades have important implications for the Chinese forest industry. First, low cost production, which is a major competitive advantage for Chinese forest products in global markets, is disappearing, if not already gone. Secondly, global trade is subject to increasingly stringent laws and regulations. The Lacey Act Amendments in the United States, the European Union's Timber Regulation and Indonesia's timber legality assurance system are all examples of the recent strengthening of policy signals designed to promote sustainable timber production and transparent trade. China is now developing its own national timber legality verification system as well. An important component of these international timber legality regulations is the due diligence or due care system to assure consumers of the legality of the products. Last but not the least, China's growing domestic market is providing growing opportunities for "green" products, driven by China's public procurement policy directives and green building programs, as well as growing consumer demand for environmental and healthy products [3].

A "traditional" supply chain in the forest sector consists of a group of organizations and people (as well as information and technologies) that are involved in value-adding activities that transform logs and lumber into finished products such as furniture and floors that are delivered to the end customer. Most company supply chains in China are engineered to manage high-volume commodity production by capitalizing on low-cost production opportunities available in places with easy access to inexpensive labor, relatively loose environmental and social regulations and favorable taxation policies for foreign investment, however, these factors are fading.

By comparison, a "sustainable" supply chain is more complex and requires a high degree of sourcing capacity and governance. Sustainability in the supply chain cannot be achieved by private sector efforts alone, it needs concerted efforts and support by

multiple stakeholders including government agencies, industry associations, NGOs, standards development and monitoring organizations, as well as consumers. Building a sustainable supply chain is not a pure business decision, but also incorporates facets of social, environmental, and embedded governance issues. Hence, the concept of "sustainable supply chain" is complex, and can vary by industry and country settings. In this paper, we deliberately take a narrow approach to explore this complex concept and confine our discussion to the Chinese forest sector which is experiencing a changing regulatory and business environment after more than three decades of reform that opened the sector to global market forces.

Methodology and Data

A series of interviews were conducted between April and September, 2011, with executive-level managers and experts from organizations active in the forest sector in China and beyond (Table 1). These interviews were conducted under various topics and published in the Rainforest Alliance's "Responsible Markets Communication" newsletters (http://www.cfcn.cn/cmc4/resources.asp). Two key questions of interest were:

1) What does sustainable supply chain mean to the Chinese forest industry?
2) What it takes to building a sustainable supply chain in response to a changing regulatory and business environment?

Table 1 Organizations Interviewed

Industry Association	*China Wood Products and Timber Distribution Association;*
International Development Agency	*USAID's Responsible Asia Forestry and Trade (RAFT) Program;*
NGOs	*The Forest Trust (TFT);* *The Nature Conservancy (TNC);* *Rainforest Alliance;* *WWF/GFTN-China;*
Private Companies	*B&Q;* *China Wood International;* *Haworth;* *IKEA;*
Research Institutes	*European Forest Institute's FLEGT Asia Program;* *Northland College;* *Yale University;*

Results

What does sustainable supply chain mean to Chinese forest industry?

Our analysis of these interviews indicated that building a sustainable supply chain is viewed strategically as means of delivering long-term environmental, social and economic benefits by securing reliable raw material supply, reducing impact on forests,

mitigating business risks and improving supply chain relationships. Specifically, a sustainable supply chain can help Chinese forest industry achieve:

1) Social and environmental benefits: Industry and the society at large will gain benefits by keeping valuable forests in-tact, as opposed to being converted to other types of land uses which often happens when timber is devalued on the export market because of legality concerns. Lowering the environmental and social costs of production and consumption can be achieved by increasing the use of legal wood as part of production within the complete supply chain of wood based products for ultimate consumption in primary export markets with new legality regulations. Over the long term, securing reliable raw material sources will be particularly important for the Chinese forest industry.
2) Risk mitigation: International markets are putting pressure on Chinese suppliers and global buyers to comply with ever tightening regulations such as EU Timber Regulations and the amended US Lacey Act. Businesses need to monitor compliance to prevent illegally sourced or unsustainable raw materials from entering their supply chain.
3) Enhanced corporate image and buyer-seller relationships: being green is one aspect of becoming a more dependable supplier or business partner. Many international buyers such as IKEA are looking for long-term supply chain partners, for mutual business growth.

What does it take to build a sustainable supply chain?

According to the interviews, key enabling factors for building sustainable supply chains include transparency, monitoring, selecting right partners, outreach/capacity building, and market-based governance. These factors will require simultaneous collective actions by the global community.

1) Transparency: companies need to establish clear and transparent mechanisms for tracking raw materials back to the forest source. This is particularly important for companies to maintain/gain market access to environmentally sensitive markets such as the EU and the US. Transparency can also help companies efficiently assess the environmental impact of production processes.
2) Monitoring: illegal timber can come from both import and domestic sources. Respondents suggested that the risk tends to be much higher for timber from countries or regions such as Russia, Indonesia, the Amazon, and the Congo basin. Collecting legality documents only from these countries or regions is not enough. Export and import documentation may be good evidence that the trade was not associated with smuggling, but does not necessarily mean that the timber was legally harvested and traded. In this regard, many companies employ independent, third-party verification of legality and/or certification as one of the effective method of due diligence or due care practices for timber sourced from tropical forests or where illegal logging is a common practice.
3) Selecting the right supply chain partners: Sharing the same business philosophy and vision with partners is important. Many global buyers such as IKEA want to

work with suppliers who operate sustainably. Suppliers that cannot make this commitment in the beginning, will find it increasingly difficult to do so later. Hence, it is important to choose the right supplier from the beginning.

4) Outreach/capacity building: Successfully implementing a corporate responsible purchasing policy down the value chain, requires significant efforts to communicate with business partners, provide support to them for compliance, train staff involved in purchasing and receiving, and perform baseline analysis of sources. They also need tp constantly monitor the implementation and progress against policy goals. In this regard, the public sector and NGOs can work together to provide support to help the industry, particularly those companies who have limited resources or expertise in meeting these standards.
5) Strengthen market-based governance: governance and markets are often inter-twined. Market-based governance works best when there are clear signals to business that adopting sustainable practices will render a competitive advantage, versus a competitive disadvantage. The Chinese forest industry is largely depending on exports even though the domestic market has been growing quickly. Regulations and standards required by export markets in this "export-driven" commodity supply chain have created significant pressure on Chinese exporters and also imposed significant costs for complying with these regulations and standards. This has created some urgency for the global community to work together to improve market mechanisms to ensure that sustainable practices will be rewarded and that competitive incentives exist.

Conclusion

Supply chain management will become increasingly important in the forest products industry. "Being sustainable" isn't only a nice thing to do but is a "must do" in a global economy with constrained natural resources. Companies must take a sustainable and strategic view of all their business behaviors and investments. Building a sustainable supply chain can eventually bring improvements to the bottom line through efficiency gains in the supply chain, enhanced buyer-supplier relationships and increased trust.

Building sustainable supply chains in the Chinese forest sector will be a long-term process because the majority of forest products, particularly small and medium-sized companies, are still weak in supply chain management and have difficulties meeting international and national standards. Significant financial investments and capacity-building efforts will be required upfront to help the industry develop the infrastructure and improve market-based governance to encourage companies to take a relatively progressive approach to becoming greener. Our interviews show near unanimity concerning the need for effective public-private partnerships to advance sustainability in the supply chain. Open dialogue and collaboration among government agencies, business, NGOs, standards development organizations and other stakeholders will be needed in order to identify effective and efficient solutions to improve supply chain competence and environmental and social performance.

Reference

1 GTA. 2012. *Global Trade Atlas.* Columbia, SC : Global Trade Atlas.
2 Flynn, R. 2008. *China Timber Supply Outlook 2008-2012.* Boston: RISI, Inc.
3 Cao, X., Sun, X. and I. Eastin. 2013. *The Chinese Era. "Global Forest Products: Trends, Management, and Sustainability*". Edited by: Hansen, E. Vlosky, R and R Panwar. Publisher: Taylor and Francis, Philadelphia, PA. USA. (upcoming);

The Effects of International Trade Show Marketing Strategies on Trade Show Performance: A Preliminary Analysis

Wenping Shi [1] – Paul M. Smith[2] - Shuangbao Zhang[3]*
[1] Graduate Research Assistant, Dept. of Agricultural and Biological Engineering,
The Pennsylvania State University, University Park PA, USA
** Corresponding author*
wxs191@psu.edu
[2] Professor, Dept. of Agricultural and Biological Engineering, The Pennsylvania State University, University Park PA, USA
pms6@psu.edu
[3] Professor, College of Material Science and Technology,
Beijing Forestry University, Beijing, China
shuangbaozhang@tom.com

Abstract

International trade shows are important venues where international marketing opportunities occur. Exhibiting at an international trade show is increasingly being viewed by firms as a cost-effective and efficient way to improve export performance and penetrate global markets. This study targets exhibitors at the largest international furniture supply trade show in China to examine their trade show strategies and trade show performance. A four-dimension framework of trade show performance is presented relevant to this particular market setting (i.e., sales-relational, psychological-related, market-exploring, and competitive-intelligence). And the differential effects of six trade show marketing strategies (i.e., visitor-attraction techniques, number of exhibited product, booth size, booth staff number, booth staff training, and follow-up contacts) on these four performance dimensions is examined. Marketing executives tasked with trade show planning, in particular, from furniture supplying industries and are considering exhibiting in China, may use the results from this study to more effectively implement trade show strategies to enhance specific dimension(s) of trade show performance.

***Keywords*:** International trade show, trade show marketing strategies, trade shows performance, China, furniture supply trade show

Introduction

Companies who conduct their marketing activities must decide where to best apply their resources for these business elements. In terms of marketing efforts, trade shows (TSs) are growing in importance as viable promotional and selling strategies (Smith et al. 2003). With the acceleration of globalization, international trade shows (ITSs) have increasingly represented a cost efficient and quick way to promote exports and to gain valuable information for market entry (Shoham 1999, Motwani et al. 1992, Rice 1992). These venues require a considerable expenditure for participants. TSs represent a significant line item in the business marketing budget, accounting for 10-15 percent of the business marketing communications budgets of U.S. firms (Dekimpe et al. 1997, Smith et al. 2003, Harriette et al. 2010), and more than 20 percent of the budget for European firms (Skallerud 2010, Sandler 1994).

To rationalize high TS exhibitor expenditures, researchers have focused on understanding the TS strategic factors (e.g., visitor-attraction techniques, booth size, booth staff number, and booth staff training) affecting TS performance to help TS practitioners develop effective strategies for successful TS exhibits (Li 2008, Smith et al. 2004, Dekimpe et al. 1997, Gopalakrishna et al. 1995, Li 2007). However, many of these studies examined the effects of TS strategies on single performance measures, such as booth-attraction effectiveness (Dekimpe et al. 1997), sales leads generated during the show (Gopalakrishna and Lilien 1995), and Return On Trade Show Investment (ROTSI) (Smith et al. 1999). Recent studies have reached a consensus that TSs represent a multi-dimensional marketing tool (Tafesse and Korneliussen 2011, Lee and Kim 2008, Hansen 2004) and exhibitors tend to have multiple TS objectives. Thus, a better understanding of specific TS strategy factors on each dimension of TS performance can aid marketing executives tasked with TS planning of effective implementation of TS strategies.

Opportunities in Emerging Markets

The global TS industry has grown dramatically. China's TS exhibition industry has experienced rapid advancement with the boom of the country's economy over the past several decades (Jin et al. 2010). According to the Global Association of the Exhibition Industry (UFI), China's indoor exhibition space totaled approximately 4.7 million square meters in 2011, accounting for 15% of the world's total after the U.S. with share of 21% (UFI 2011).

Within the forest products industry, one type of typical horizontal TSs, "International Furniture Supply Trade Shows" (IFS-TSs), feature furniture supplying industries such as wood raw materials, woodworking machinery, hardware and other furniture accessories. These IFS-TSs have long served as an important venue for suppliers in these industries to communicate with target customers worldwide. As a result of Chinese market liberation and the subsequent rapid growth of the Chinese furniture industry, IFS-TSs in China have grown in international importance and prestige, attracting increasing numbers of exhibitors and attendees from around the world. The top 3 major IFS-TSs identified by Shi and Smith (2011) attracted approximate 116,000 attendees and 2,270 exhibitors

worldwide in 2010, and these numbers are still growing annually. This indicates how suppliers in this industry value TSs as an important marketing and selling strategy.

Despite the increasing popularity of TSs in China, inquiry into the dimensionality of TS performance and the affecting TS strategies in this market is lacking. Although there are a few limited research efforts in emerging markets (Tafesse and Korneliussen 2011, Li 2008), none of these studies examine the different effects of TS strategies on multi-dimensional TS performance. Several researchers have noted that TS strategies and TS performance evaluation may differ across countries and/or industries (Dekimpe et al. 1997, Hansen 2004, Tafesse and Korneliussen 2011). These differences imply that TS performance dimensions and the relationship between TS strategy and TS performance developed in the extant literature may not be generalizable to other TS contexts.

Therefore, this study contributes to the limited emerging market research by investigating the multi-dimensionality of TS performance through an ITS-FS venue in China. Further, this study extends research on the effects of TS strategies on relevant TS performance dimensions to IFS-TSs; thus providing additional empirical evidence regarding these relationships.

Study framework

TS performance has typically been evaluated based on exhibiting firm's ability to enhance key TS activities set by senior marketing managers such as lead generation, customer relations-building, competitor intelligence gathering, image building, and sales team training (Bonoma 1983, Bello 1992, Kijewski et al. 1993, Hansen 2004, Kerin and Cron 1987). This study applied the sixteen TS activities validated in previous literature to measure exhibitors' TS performance; and the six TS marketing strategies from earlier studies to examine their effects on exhibiting firms' TS performance. The framework is presented in Fig. 1.

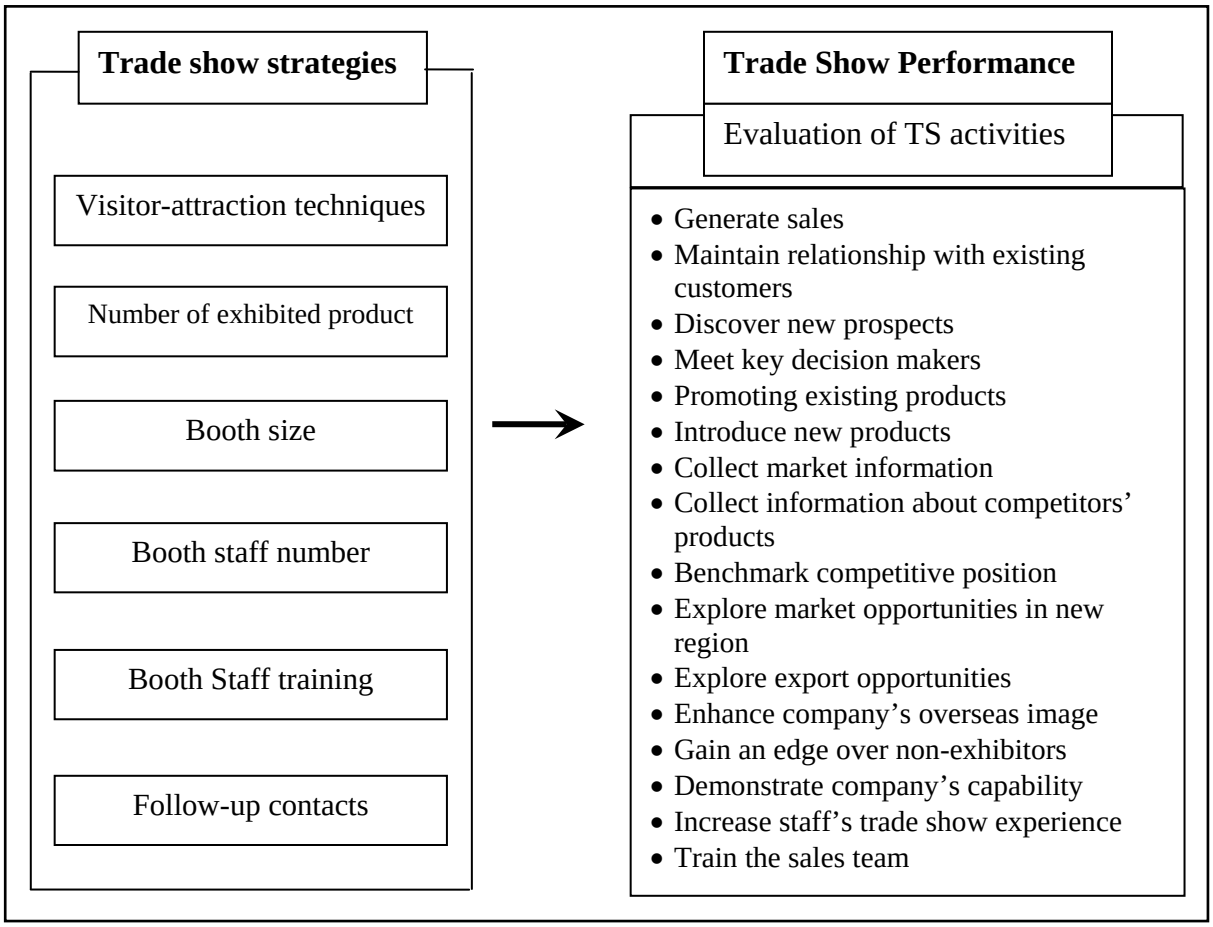

Figure 1. Framework of Trade Show Strategies and Trade Show Performance

Research Methodology

Data collection

This study defines the population as all exhibiting firms at the largest IFS-TS in China, the Chinese International Woodworking Machinery and Furniture Raw Material Fair in 2011 (CIFM'11). The official directory of exhibitors through the CIFM exhibition organizer, Koelnmesse Co., Ltd. was used as sample frame and a census was conducted to ensure adequate responses for further analysis and inferences. Online surveys were developed in two languages (English and Chinese) using SurveyMonkey. To establish translation equivalence, the original English-version instrument was translated into Chinese by a bilingual person and re-checked by another bilingual person. Observed discrepancies were addressed and resolved.

Before administering the survey, pretesting was performed with both an expert panel and an industry panel drawn from the database of exhibitors at CIFM'11 to assess the applicability of the online instrument and the precision of language translation and interpretation. The finalized surveys were sent to all exhibitors at CIFM'11 (n=970) with a customized message. Delivery failures and/or bounced email addresses reduced the total population to 940. After one week, a second survey was sent to non-respondents.

Two weeks after the initial online surveys, a systematic random sample of 160 non-respondents received follow-up phone calls, which further increased the number of respondents by 61 while also providing an opportunity to examine non-response bias.

A total of 300 responses were obtained, of which 267 respondents completed all questionnaire items related to trade show strategies and performance. Non-response bias check was performed on key demographic variables and selected TS performance and strategy variables resulting in no significant differences (at the p=.05 level) between respondents and non-respondents. Characteristics of respondents were categorized according to nationality of exhibitor (international/domestic), industry sector, and size of company (number of employees) (Table 1).

Table 1. Respondent Profile

Category	N	%
Nationality		
International	99	33.0
Domestic	201	67.0
Industry sector		
Woodworking machinery	57	19.0
Raw material and components	168	56.0
Hardware and other	75	25.0
Number of employees		
1-99	99	33.0
100-299	156	52.0
300-599	34	11.3
Over 600	11	3.7

Measurements

TS strategy variables from previous studies were used and included visitor-attraction techniques, number of exhibited products, follow-up contacts, booth size, number of booth staff, and booth staff training (Table 2). TS performance was measured via a 7-point scale on the 16 trade show activities validated in earlier studies.

Table 2. Description of measurement variable used in this study

Measure	Scale description	Source
Trade Show Strategy		
Visitor-attraction techniques	Total number of techniques used	Seringhaus and Rosson (2001)
Number of exhibited products	Number of displayed product at the booth	Kerin and Cron (1987)
Booth size	Booth space used in square meter	Dekimpe et al. (1997)
Booth staff number	Number of booth staff used	Gopalakrishna and Lilien (1995)
Booth staff training	Degree of systematic training received (5-point scale)	Gopalakrishna and Lilien (1995)

Follow-up contacts	Total number of contact tools used	Seringhaus and Rosson (2001)
Trade show performance	Performance on 16 identified international trade show activities (7-point scale)	Kerion and Cron (1987); Hansen (2004); Lee and Kim (2008); Tafesse and Korneliussen (2011)

Research Results

Multi-Dimensions of Trade Show Performance

To develop the multi-dimensional constructs of TS performance evaluated by TS activities, principal component analysis (PCA) was performed on the identified 16 TS activities using SPSS 20.0. PCA is a multivariate technique which determines the structure of measured variables by specifying condensed sets of dimensions with minimal loss of information (Fabrigar et al. 1999, Hair et al. 2010). The factorability of the performance variables was tested by using Kaiser-Meyer-Olkin (KMO) test to measure sampling adequacy and Bartlett's test for sphericity. A KMO value of 0.743 and significant (0.000) for Bartlett's test ensures the adequacy.

PCA analysis resulted in a reduction of the 16 TS activities into four components, suggesting the multi-dimensionality of TS performance. The four components explained 66 percent of the total variance in the data. The variability of the components was evaluated using Cronbach's alpha coefficient. Each component attained Cronbach's alpha greater than 0.7 (0.815, 0.842, 0.832, and 0.92) indicating satisfactory level of reliability. Based on the previous studies and the nature of the 16 TS activities in this study, we assigned these labels to the four components from PCA as our four TS performance dimensions: sales-relational, psychological-related, market-exploring, and competitive-intelligence[1].

Multiple Regression Analysis Results

Effects of TS Strategies on Sales-Relational Dimension

Visitor-attraction techniques, booth size, booth staff number and follow-up contacts were found to have a significant positive effect on the sales-relational performance dimension (Table 3). Unlike results from previous studies (Gopalakrishna and Lilien 1995, Li 2007, Lee and Kim 2008), booth staff training was not found to be significantly related to sales-relational performance dimension. Our study measured booth staff training by asking exhibitors to evaluate the level of systematic TS training booth staff received in preparation for CIFM'11, without asking for information on the detailed content of the actual training and ignoring the possibilities that the booth staff could be well-trained and experience prior to this particular show. Therefore, future studies may consider a better design of this variable for clearer interpretation.

[1] Due to the page limit, the PCA results are not presented in this paper.

Compared to visitor-attraction techniques, follow-up contacts were found to have a strong influence on sales-relational performance (beta coefficient: 0.254 vs. 0.134). At TSs, the interaction and buying process are often complex and may require months to complete. Sales leads generated at these shows may lead to actual contracts through follow-up contact activities. This could explain the strong impact of follow-up contacts on sales-relationship performance.

Table 3. Multiple Regression Analysis of TS Strategies Effects on TS Performance Dimensions

Independent variables	**Trade show performance dimensions**			
	Sales-Relational	Psychological-Related	Market-Exploring	Competitive-Intelligence
	----------Standardized regression coefficient (beta) [1]----------			
Visitor-attraction techniques	0.134*[2]	0.083	0.058	0.024
Number of exhibited products	0.041	0.091	-0.174**	-0.045
Booth size	0.253***	0.112*	-0.014	0.022
Booth staff number	0.179***	0.187**	0.136**	0.2**
Booth staff training	0.096	0.075	0.377***	0.238**
Follow-up contacts	0.254***	0.178**	0.12*	0.039
R square [3]	0.350	0.165	0.345	0.166
Adjust R square [4]	0.335	0.145	0.330	0.146

1. Standardized regression coefficient (beta) refers to how many standard deviations a dependent variable will change, per standard deviation increase in the independent variable, while controlling for other independent variables;
2. This is 2-tailed p-values associated with testing whether a given beta coefficient is significantly different from zero. * Significant at 0.10 level; ** significant at 0.05 level; *** significant at 0.001 level;
3. R square tells the proportion of variance in the dependent variable (TS performance dimension) which can be explained by the independent variables (TS strategies);
4. Adjust R square is intended to control for overestimates of the R square resulting from small samples, high collinearity or small subject/variable ratio.

Effects of TS Strategies on Psychological-Related Dimension

Booth size, booth staff number and follow-up contacts were found to be significantly positively related to psychological-related performance. This is in line with existing literature. A sizable booth and sufficient booth staff numbers attract more attendees to the booth so that booth staff has a greater chance to communicate directly with attendees. And the more booth staff engages in follow-up contacts, the more opportunities they have to interact with existing and/or potential customers. Through these communications and interactions, booth staff may enhance the corporate image and gain more experience.

Effects of TS Strategies on Market-Exploring Dimension

Booth staff number, booth staff training and follow-up contacts were found to have a significant positive impact on the market-exploring dimension. The number of exhibited products was found to be significantly negatively related to exhibiting firm's market-exploring performance. Since the CIFM'11 is a horizontal show, how exhibitors from different industry sectors interpret the number of exhibited products might be different.

For instance, hardwood lumber exhibitors may view the number of exhibited products as one for lumber instead of counting different species. Therefore, the interpretation of these results should be taken with caution.

Booth staff training was found to have a stronger influence on market-exploring performance than other variables (beta coefficient 0.377). It has been shown that better-trained booth staff can make more contacts with attendees and interact with prospects in an efficient way (Gopalakrishna and Lilien 1995, Li 2008). In this international TS venue (CIFM'11), well-trained booth staff were found to be more important to help a company identify prospective markets and evaluate threats and opportunities in these markets.

Effects of TS Strategies on Competitive-Intelligence Dimension

Booth staff number and booth staff training were found to have a significant positive impact on competitive-intelligence performance. Booth staffs are the personnel who identify potential prospects' needs and collect information on competitors' products, prices and strategies. Sufficient trained booth staff may help exhibiting company to collect, synthesize, and analyze competition and external environment that can affect company's plans, decisions and operations. These competitive-intelligence gathered by booth staff could lead to more insightful market-based actions.

Implications and Future Activities

China is the largest furniture producer and exporter in the world and demand for various raw materials, components, and hardware (furniture supplies) has grown dramatically. Chinese IFS-TSs provide a great opportunity for furniture supplying firms to sell products, network with hard to reach customers, build their reputation, collect foreign market information, and perform a variety of important sales and promotional activities in a cost-effective venue. This preliminary analysis of the effects of different TS strategies on each dimension of TS performance could help marketing executives tasked with TS planning decisions such as booth staffing practices, and appropriate follow-up contacts. Booth staffing may include sufficient and well-trained personnel to strengthen market research and competitive intelligence gathering. Follow-up efforts may be designed to improve relational and psychological-related performance (i.e., image building and experience gaining).

More analysis on how different TS strategies impact each dimension of TS performance will be carried out in future work to provide additional marketing insights and applications for TS decision markers and, in particular, those from furniture supplying industries.

Literature Cited

Bello, D. C. 1992. Industrial Buyer Behavior at Trade Shows. Journal of Business Research, (25): 59-80.

Bonoma, T. V. 1983. Get More Out of Your Trade Shows. Harvard Business Review, Jaunuary-February: 75-83.

Dekimpe, M. G., François, P., Gopalakrishna, S., Lilien, G. L., and Bulte, C. v. d. 1997. Generalizing about Trade Show Effectiveness: A Cross-National Comparison. Journal of Marketing, 61(4): 55-64.

Fabrigar, L. R., Wegener, D. T., MacCallum, R. C., and Strahan, E. J. 1999. Evaluating the Use of Exploratory Factor Analysis in Psychological Research. Psychological Methods, 4(3): 272-99.

Gopalakrishna, S. and Lilien, G. L. 1995. A three-stage model of industrial trade show performance. Marketing Science, 14(1): 22-43.

Gopalakrishna, S., Lilien, G. L., Williams, J. D., and Sequeira, I. K. 1995. Do Trade Shows Pay Off? Journal of Marketing, 59(July 1995): 75-83.

Hair, J. F., Black, B., Babin, B. J., and Anderson, R. E. 2010. Multivariate Data Analysis: A Global Perspective. Uper Saddle River, NJ: Prentice Hall.

Hansen, K. 2004. Measuring Performance at Trade Shows Scale Developement and Validation. Journal of Business Research, 57(1): 1-13.

Harriette, B.-O., Cromartie, J. S., Johnston, W. J., and Borders, A. L. 2010. The Return on Trade Show Information (RTSI): A Conceptual Analysis Journal of Business & Industrial Marketing, 25(4): 268-71.

Jin, X., Weber, K., and Bauer, T. 2010. The State of the Exhibition Industry in China. Journal of Convention & Event Tourism, 11(1): 2-17.

Kerin, R. A. and Cron, W. L. 1987. Assessing trade show functions and performance: an exploratory study. The Journal of Marketing, 51(3): 87-94.

Kijewski, V., Yoon, E., and Young, G. 1993. How exhibitors select trade shows. Industrial Marketing Management, 22(4): 287-98.

Lee, C. H. and Kim, S. Y. 2008. Differential Effects of Determinants on Multi-dimensions of Trade Shows Performance: By Three Stages of Pre-show, At-show, and Post-show activities. Industrial Marketing Management, 37(7): 784-96.

Li, L.-y. 2007. Marketing Resources and Performance of Exhibitor Firms in Trade Shows: A Contigent Resource Perspective. Industrial Marketing Management, 36: 360-70.

--- 2008. The effects of firm resources on trade show performance: how do trade show marketing processes matter? Journal of Business & Industrial Marketing, 23(1): 35-47.

Motwani, J., Rice, G., and Mahmoud, E. 1992. Promoting Exports Through International Trade Shows:A Dual Perspective. Review of Business, 13(4): 38-42.

Rice, G. 1992. Using the interaction approach to understand international trade shows. International Marketing Review, 9(4): 32-45.

Sandler, G. 1994. "Fair Dealing". The Journal of European Business, 4(Mar/Apr): 46-48, 52.

Seringhaus, F. H. R. and Rosson, P. J. 2001. Firm Experience and International Trade Fairs. Journal of Marketing Management, 17: 877-901.

Shi, W. and Smith, P. M. 2011. Exploring opportunities for U.S. hardwoods via international furniture supply trade shows in China. Presentation on International Scientific Conference on Hardwood Processing, October 16-18, 2011 Blacksburg, VA.

Shoham, A. 1999. Performance in Trade Shows and Exhibitions:A Synthesis and Directions for Future Research. Journal of Global Marketing, 12(3): 41-57.

Skallerud, K. 2010. Structure, Strategy and Performance of Exhibitors at Individual Booths versus Joint Booths. Journal of Business & Industrial Marketing, 25(4): 259-67.

Smith, T. M., Gopalakrishna, S., and Smith, P. M. 1999. 'Trade Show Synergy: Enhancing Sales Force Efficiency.' in Trade Show Synergy: Enhancing Sales Force Efficiency, 1-38. University Park, PA: Institute for the Study of Business Markets, The Pennsylvania State University.

--- 2004. The complementary effect of trade shows on personal selling. International Journal of Research in Marketing, 21(1): 61-76.

Smith, T. M., Hama, K., and Smith, P. M. 2003. The effect of successful trade show attendance on future show interest: exploring Japanese attendee perspectives of domestic and offshore international events. Journal of Business & Industrial Marketing, 18(4/5): 403-18.

Tafesse, W. and Korneliussen, T. 2011. The Dimensionality of Trade Show Performance in an Emerging Market. International Journal of Emerging Markets, 6(1): 38-49.

UFI 2011. Global exhibition industry statistics. Global Association of the Exhibition Industry: 31.

Assessment of China's Green Public Procurement Policy for Forest Products

Prof. Dr. LI Zhi-yong

International Center for Bamboo and Rattan，Beijing, 100102, P. R. China, zyli@inbar.int

Dr. HE You-jun

Research Institute of Forestry Policy and Information, Chinese Academy of Forestry，Beijing, 100091, P. R. China, hyjun163@163.com

Dr. SU Hai-ying

Research Institute of Forestry Policy and Information, Chinese Academy of Forestry，Beijing, 100091, P. R. China, suhaiying0724@163.com

Abstract

How to effectively meet the globally increasing demands for forest products and meanwhile put forest resources and eco-environment under better protection for achieving the balance between protection and growth is a long-term challenge in face of the international community. China is the largest country in forest products import/export in the world. In such sense, the realistic state and future orientation of China's forest product procurement policy will impose considerable impact on and play a significant role in forestry industry development in China as well as the global sustainable forestry development. In view of the state and trend of forest product procurement by Chinese enterprises, the paper analyzed the problems and challenges facing China's forest product green procurement based on the results of field survey carried out for different types of forest product processors, including customers' weak awareness of green consumption, deficient green procurement resources of forest products, high prices of green procurement products, limited green procurement list of forest products, lack of laws and regulations for green public procurement and lack of policy support and green market planning. At the same time, by comparing and learning the experiences and lessons of the UK, Japan, France, Netherland and other countries in green public procurement of forest products, the paper, in line with the national and forest conditions in China, proposed some policy recommendations, e.g. strengthening dissemination and education for raising green consumption awareness, updating laws and regulations for government green procurement, adopting marketing means to encourage green enterprises development, upgrading green product lists to incorporate more green procurement enterprises into government green procurement program, establishing monitoring and execution mechanism for green procurement and enhancing the oversight of green procurement, with the aim to facilitate China's green procurement process of forest products and quicken China's pace of green socioeconomic transition.

Keywords: green public procurement, forest product, policy

Promoting transitional development to a green economy is the focus and direction of China's future strategy for sustainable development. Green public procurement is one of green development policy. The active facilitation of environmentally responsible green procurement actions and their integration into government procurement program are the vital measures to promote green transition. In 2006, the Ministry of Finance and State Environment Protection Administration of China officially released Opinion on Implementing Government Procurement of Environment Labeling Products and the first batch of Government Procurement List of Environment Labeling Products, explicitly defining the scope of green procurement, the list of green product and the time table for implementation. This marks that Chinese government officially subsumes environment criteria into its procurement pattern. The formation of green development concept, the upgrading of green development policy and the sustained demand for green products by international and national markets put Chinese forest product enterprises under market pressure and transition opportunities for green development and accelerate their shift towards green production, green consumption and green procurement.

1. Policy analysis on requirements of green public procurement of China's forest product

China is the world's largest forest product importer and exporter. China Customs Statistics indicates that in 2011 China's total import-export value of forest products amounted to US$ 120.45 billion, while the export was valued at US$ 55.08 billion, up 18.3%, and the import at US$ 65.37 billion, an increase of 37.5%, with the trade deficit of US$ 10.29 billion. In general, China's forest products trade is still dominated by the trade of wooden forest products. China mainly imports logs, sawn-timber and pulp and exports furniture, paper, paper board, paper products, wood-based panel and profile. China's forest product procurement policy has important impact on the domestic forest industry development and the world's sustainable forestry development. Especially in recent years, the international society lists the combating of illegal logging and associated trade as the hot issue in world sustainable development, and attempt to employs legal means, such as the USA's Lacey Act and EU Timber Regulations, to minimize the risk of illegal timber. How to effectively meet the increasing global and domestic demand for forest products while effectively protecting forest resources and achieving the protection-development balance are the long-term challenge facing the international and national society.

1.1 Meeting the requirement to protect fragile resources and environment on the earth

So far, human society development has brought significant consequences to ecological environment due to human activities and their means to survive on the earth, leading to irreversible change of environment. Since the United Unions Conference on Environment and Development in 1992, the connections between green economy, food security, ecological health and social equality have attracted wide concerns. In the Rio+20 Summit held in 2012, participants felt delighted to see the advancements in eco-environment protection during the past 20 years, and however, also worried about ecological environment issues such as climate change,

desertification control, biodiversity conservation and water resources crisis. On 6th June, 2012, the UNEP launched the fifth report of Global Environment Outlook. The report assessed 90 of most important environment goals and objectives, but found that little or no progress had been made in 24 goals and objectives, including climate change mitigation, fish resources protection and combating desertification and draught. The report also pointed out that if the current policies and strategies were altered and big-scale measures could be taken, it would be possible to realize a range of ambitious goals and objectives of sustainable development at the middle of this century.

As for forest state, the data in the Global Forest Resources Assessment (2010) illustrates that forest logging and natural loss still rose at an astonishing rate, but with a slowdown in the overall trend. Most forest loss occurs to tropical countries and regions, while most increases in forest area are observed in temperate and cold temperate areas as well as in some emerging economies （FRA. 2010）. China has made a progressive advance in forest protection. The 7th National Forest Resources Inventory results show that nationally, the forest area is 195.4522 million ha, the forest coverage is 20.36%, the standing stock volume is totally 14.915 billion m^3 and the forest stock volume is 13.721 billion m^3. In nearly 30 years, the forest area and the stock volume in China have undergone a constant growth and the national forest coverage has risen steadily (Fig. 1-1). However, the forest coverage in China is only equivalent to 2/3 of the world average level, ranking the world 139th (State Forestry Administration, 2010). The supply of forest resources distances amazingly itself either from the ecological demand or from the demand for forest products, especially for wood. The main forestry indicators in China are now far behind the level of developed countries, and also lower than the world average level. Overall, China is one of countries with deficient forest resources in the world (SFA, 2009).

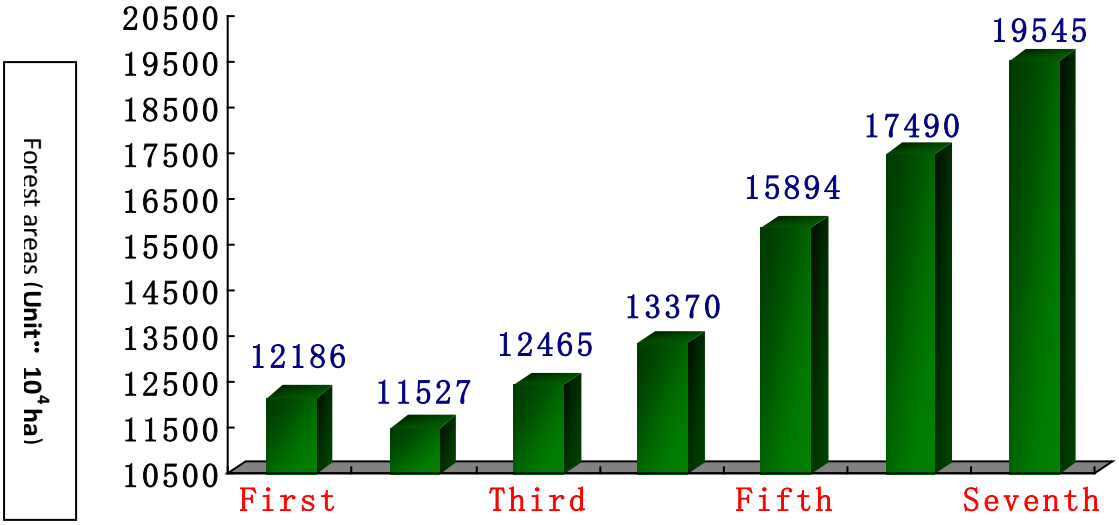

Fig. 1-1 Trend of the change in forest resources in China

Data source： SFA, 2010

In face of the ecological challenges in the globe, it is supposed to be proactive and useful to adopt green public procurement of forest products for protecting forest and improving eco-environment on the earth with joint efforts from governments, enterprises and consumers.

1.2 Meeting the requirement of international green trade

In recent years, the international community has placed the illegal timber logging and associated trade issue as the hotspot in world sustainable development, and employed legislative means in attempt to minimize the risk to use illegal timber, such as the USA Lacey Act amendments and the EU Timber Regulation. In order to crack down on illegal logging and associated trade in a more effective way, some developed countries have embarked on developing public procurement policy, and required government agencies to preferably buy the legal and sustainable timber, i.e. the implementation of government green procurement policy for forest products (Li Xiaoyong et al 2008, 2009).

China is a big country in forest product trade, which has progressed at a drastic rate (Fig. 1-2). In such sense, China is a significant participant of international green trade. The statistics from China Customs indicates that the forest product import-export trade was valued at 120.45 billion USD; the export was 55.08 billion USD in value, an increase of 18.3%, while the import value was 65.37 billion USD, up 37.5%, with the trade deficit amounting to 10.29 billion USD. Generally, Chinese forest product trade is still dominated by wood-based forest products. The imported wood-based forest products mainly consist of logs, sawn-timber, pulp, etc., while the exports are predominantly furniture, paper, paperboard, paper product, wood-based panel, plywood, etc. The differences in comparative advantage and international division make world forest product production and trade pattern take shape, in which Russia and some African countries are the material suppliers, North American countries and the Europe are the importers and consumers while China is the processor at the middle part of the chain.

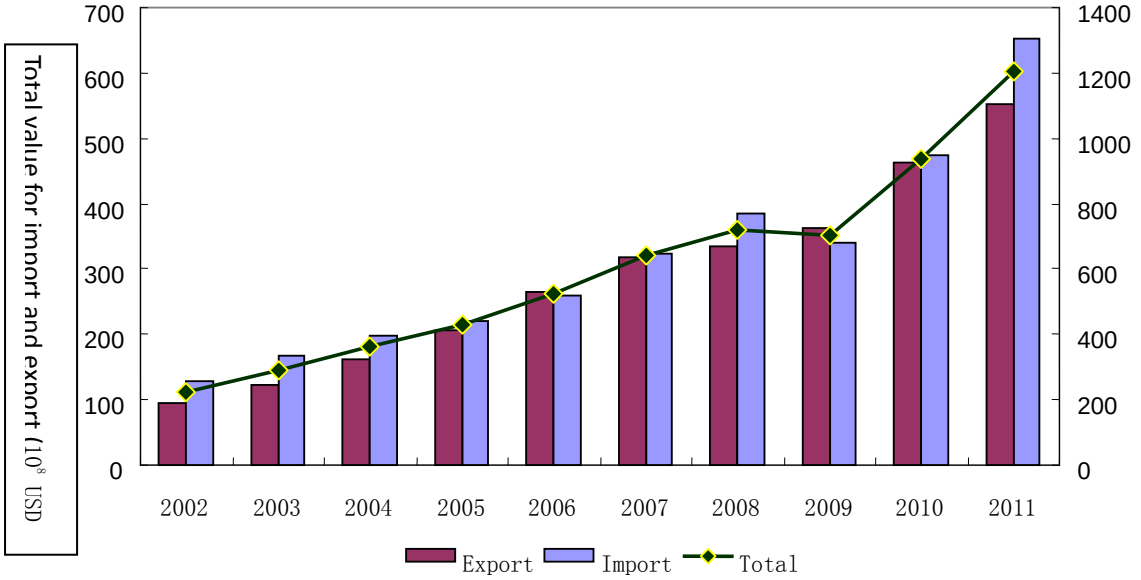

Fig. 1-2 Total value of forest product import- export trade in 2002-2011 (10^8 USD)
Data source： SFA，2011

As a world center for forest product processing and trading, China is subject to the policies developed by the upstream and downstream countries. Chinese Government is also aware of the necessity to put in place sustainable forest management, and consider it indispensable to work together with other big timber consumers and timber producers to jointly solve the problems such as illegal logging and deforestation. Therefore, some measures, such as the research on China Timber Legality Verification System and related pilot work, have been taken to encourage people to use legal and sustainable timber. These measures lay a foundation for green procurement of forest products and provide some protections to shrinking forest resources due to illegal logging.

1.3 Meeting the requirement to promote green and transitional development of China

Green trade develops on the basis of green development. During the reform and opening up lasting for more than 30 years, China has gone over a rapid socioeconomic development, and the GDP has long kept a high growth (Fig. 1-3). Promoting green and transitional development with an eye on the future is the keynote and direction of future sustainable development strategies in China.

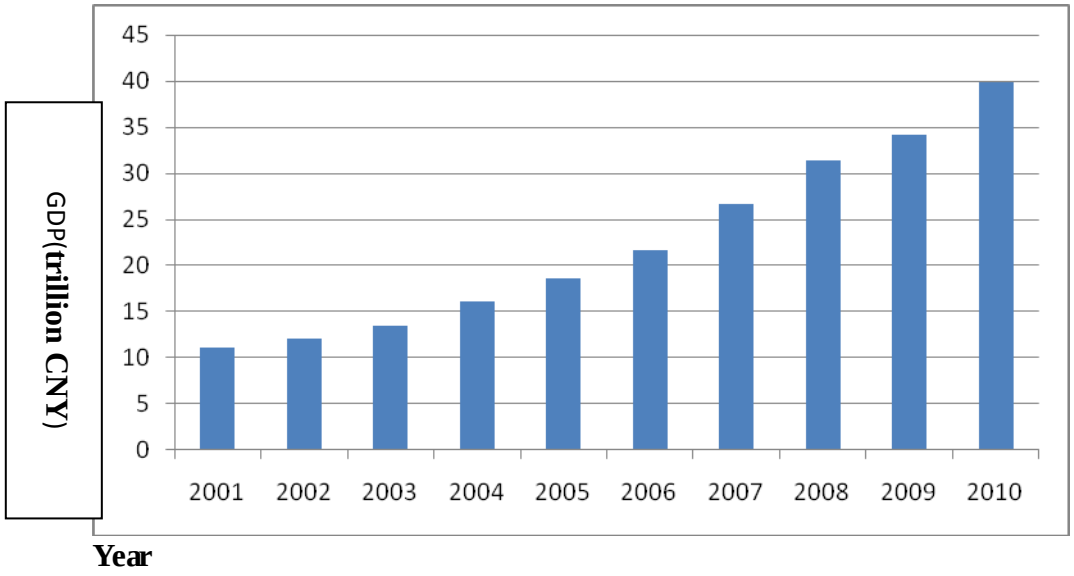

Fig. 1-3 GDP growth trend in China in 2001-2010

Green public procurement is a component of green development policy. The progressive initiatives of environmentally responsible green procurement actions and the inclusion of the actions into government procurement plans are the important measures to promote green transition. In 2006, the Ministry of Finance of China and the State Environment Protection Administration officially issued the *Opinions on Implementing Government Procurement of Environment Label Products* and the first *Government Procurement List of Environment Label Products*, which explicitly provide the scope of green procurement, the list of green products and the implementation timelines. This indicates that Chinese Government has formally included environment codes into its procurement model. The green development conception, the implementation of green development policy and the increased demand for green products from international and national markets put Chinese forest product enterprises under the market pressure for green development and also bring them opportunities for transitional development (Fig. 1-4). This also precipitates forest product processor moving towards green production, green consumption and green procurement.

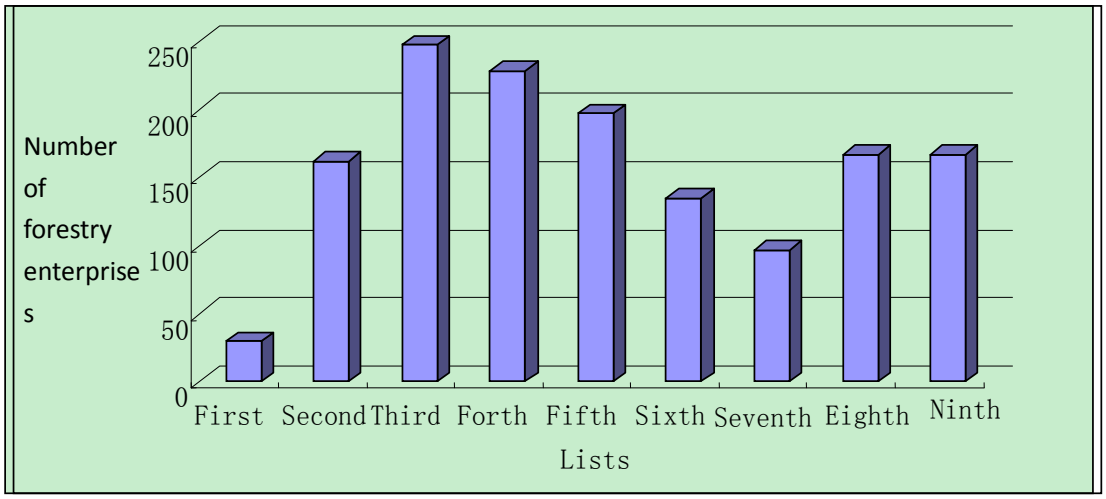

Fig. 1-4 Statistic of the number of forestry enterprises in government

procurement lists (1-9) for environment label products

2. Policy assessment on the problems of green public procurement of China's forest product

With the view to better analyzing and researching the current state and trend of green forest product procurement by Chinese enterprises, the national soft science project of China Green Public Procurement Policy for Promoting the Market Development for Environmentally Friendly Tropical Forest Products was launched in 2009, and aimed to carry out research on China's green procurement policy. The project team from the Chinese Academy of Forestry carried out the field investigations on forest product processors manufacturing logs, flooring and plywood. The results show that green forest product procurement in China is still challenged by many problems, such as people's weak awareness in green consumption, lack of laws and regulations relative to green public procurement, short of green procurement sources, limited scope covered by green procurement list of forest products, and high prices of green procured products.

2.1 Weak social awareness in green consumption

Engel's Coefficient is an important index internationally used to measure citizens' livelihood level and household consumption orientation, which generally drops with the rising household income and livelihood level. Since the reform and opening up, Engel's Coefficient of urban and rural households in China has retreated from 57.5% and 67.7% in 1978 to 35.7% and 41.1% in 2010 (Fig. 2-1). Judged by the Engel's Coefficient and livelihood standard set out by the United Nations, China is at the stage of fast development and relative wealth. This means that people's consumption level and quality are overall improved but there is a room to improve in terms of consumption value and ecological view. The green consumption awareness that is an indication of high literacy is still rather weak.

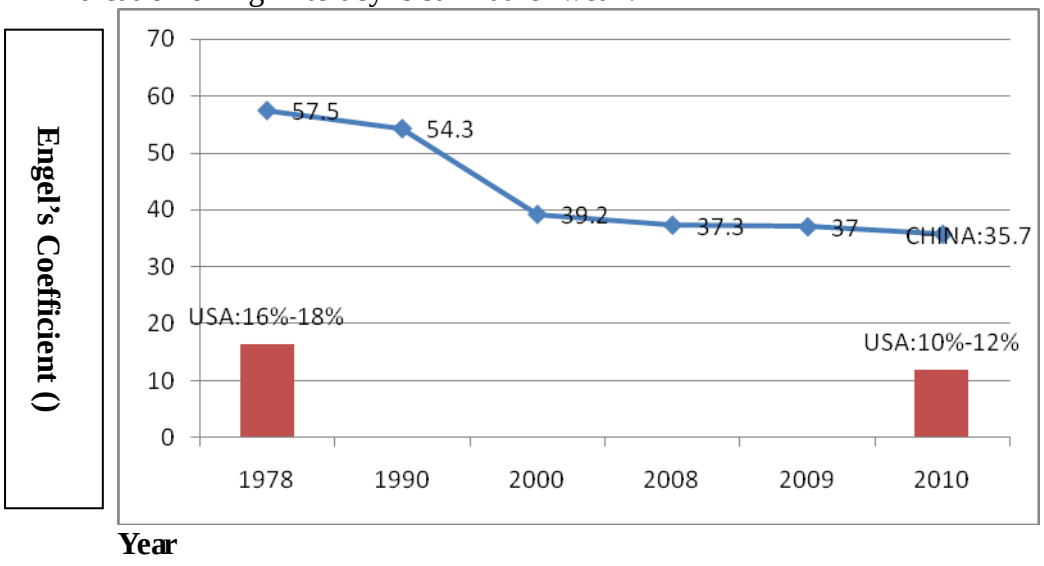

Fig. 2-1 Engel's Coefficient development trend for urban citizens in China in 1978-2010

Green procurement is a critical means to facilitate green consumption. The

investigation carried out by the above mentioned project shows that the real green consumers currently account for only one quarter in China, non-green consumers are approaching one third, while the quasi-green consumers represent nearly one second. A large number of people have little awareness of green consumption. The investigation conducted at the Nature Flooring Company indicates that Chinese consumers have fair recognitions towards green timber products, but they have deficient knowledge of green consumption in terms of energy saving, environment protection, health and low carbon. Obviously, only when material suppliers, producers and end users uphold and put green consumption conception into practices, can green development of forestry industry be really realized.

2.2 Uncompleted legislative system for green public procurement

The practices at domestic and abroad show us that legislation provides important guarantee to promote green public procurement. The world main forest products trading countries, especially developed countries, all formulate laws to implement green forest product procurement policy. For example, the forest product procurement policy put into effect by France in June 2003 is a part of national sustainable development strategy. Denmark published Tropical Timber Procurement: Environment Guidelines in June 2003, and also developed a series of guidance documents and tool package for government green procurement. In addition, Japan, the UK, Dutch, the USA and the more developed and implemented laws and regulations in relation to green forest product procurement（Bao Yingshuang et al.2010; Araya Akihiko 2010; Wang Xiuzhen et al.2011; Japan Legal Timber Website. http://goho-wood.jp/world/ch.html）.

At present, China also developed some laws and regulations relative to green public procurement for progressively promoting environmentally friendly and resources-saving consumption, and executed environment labeling, environment certification and government green procurement (Table 2-1). But these laws and regulations are comparatively uncompleted. The Chinese legislative framework for government procurement only provides the summary and guiding requirement to related aspects, lack of explicit statement of green procurement and implementation bylaw. The existing laws cannot embody the requirement and connotation of green procurement. For instance, though setting out the environment protection objectives of government procurement, *Government Procurement Law of China* provides no detailed stipulations and descriptions in respect to implementation regulations and bylaws for government green procurement, and makes no statement on detail issues such as how to embody the objective of environment protection and how to balance the weight of environmental products in a specific procurement. In such sense, the Law fails to provide explicit and detailed systematic restraints and policy guidance for government to implement green procurement. The *Management Measures for Government Procurement and Ordering of Independent Innovation Products* developed by the Ministry of Finance also fails to propose explicitly the management measures and requirements for government green procurement. In the Measures, there are no detailed descriptions of related system and short of operational provisions and implementation mechanisms.

Table 2-1 Catalog of laws and regulations relative to green procurement in China

No.	Laws and policies	Time to issue or put into effect
1	*Government Procurement Law*	2003
2	*Decisions of the State Council on Fulfilling Scientific Development Conception and Strengthening Environment Protection*	2005
3	*Several Opinions of the State Councils on Accelerating Recycling Economy Development*	2005
4	*Opinions on Implementing Government Procurement of Environment Label Products, Government Procurement List of Environment Label Product*	2006
5	*Recycling Economy Promotion Law*	2009

2.3 Short of green procurement sources of forest product

Presently, China's forest products are mainly sourced from Malaysia, Indonesia, Carbon, Laos, Vietnam and some African countries (Fig. 2-2). Some areas in these countries are predominantly haunted by illegal logging, which induces the questioning on the legality of forest products from these countries or regions. For example, in 2001-2010, China's imports of tropical log presented a dropping trend in amount, but a rising trend in the import value (Figure 2-3), while the log which cannot be proved as from legal and sustainable sources occupied a rather large share in markets. The strict requirements on legal source narrows the scope of wood available for forest products production, and bring large limits on government public procurement. The narrowing selection scope will result in supply bottlenecks to some extent.

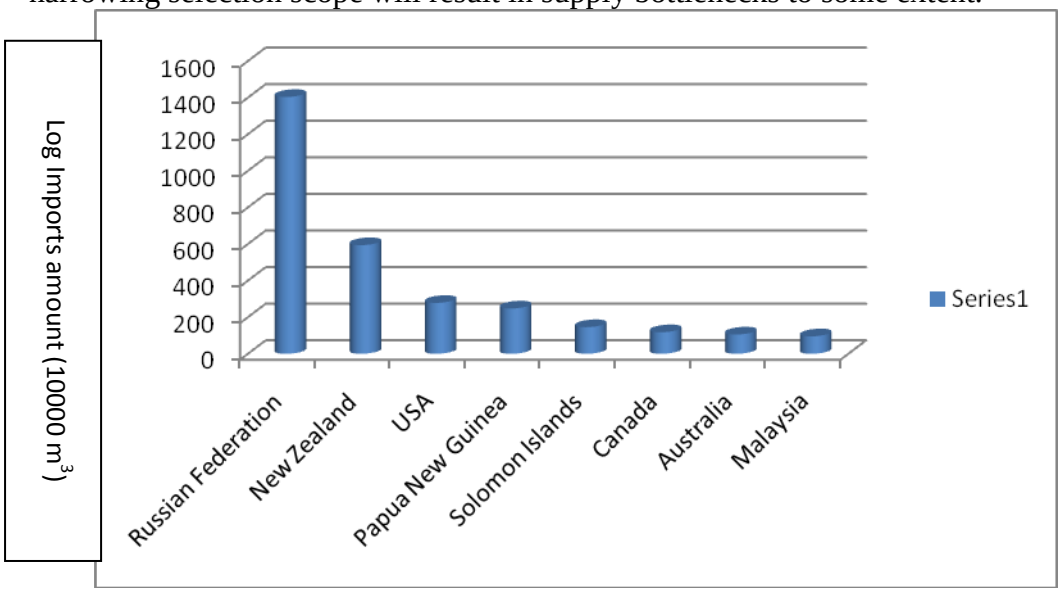

Fig.2-2 Sources of China log imports in 2010

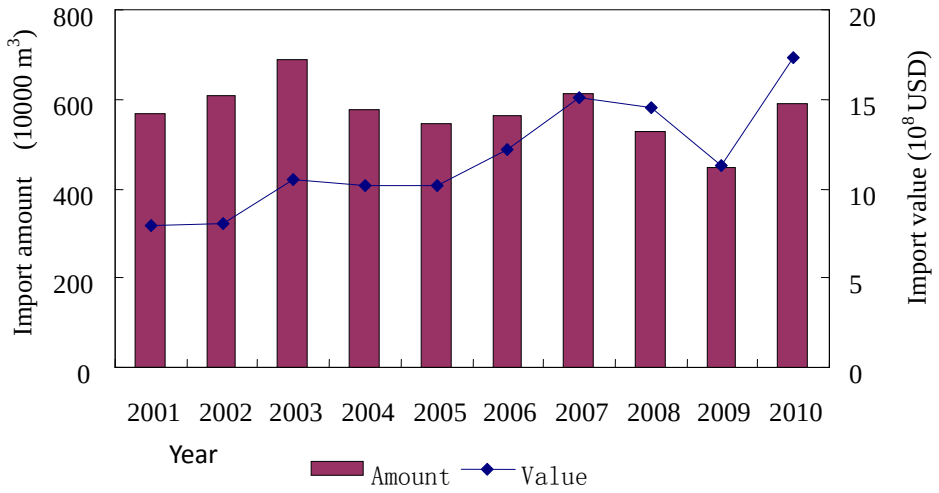

Fig.2-3 Changes in China tropical log imports, 2001-2010
Note: Data are sourced from China Customs.

After carrying out the investigation on Jiansu Suntian Lihua Wood (Industry and Trading) Co., Ltd. that specifically engages in plywood production and trade, the project team got the finding that in the international trade, the documents or evidence issued by China covering logging permit and transport permit to demonstrate the legality of timber cannot get full accreditation of the EU and the North America as well as related bodies, and these markets require other certifications. This caused some difficulties to the production and sale of green forest products from China. In the meanwhile, the stringent supply and rising prices of certified material haunt the markets as China has a small amount of forest achieving FSC certification.

2.4 Limited scope of tropic forest products in Green Procurement List

The EU and the North America are the main destinations of China's tropic forest products. China has a small number of tropical timber processors which pass forest certification or have proof to demonstrate the legal source of timber. These certified or verified enterprises export products mostly to the European and North American markets based on make-to-ordered production. Domestically, green procurement is still in a static state, giving less impetus to these enterprises to produce green products. This also limits the scope of government green procurement and increases the difficulties for procurers.

But, in general, the number of forestry enterprises in the government procurement lists of environment label products presented a climbing trend in 2010-2012 (Fig. 2-4). Among the categories, the number of furniture manufacturers remains a surging trend, the number of wood-based panel and wooden flooring processors began to fall in the third lists, while the number of light wall form manufacturers remains stable without great change (Fig. 2-5).

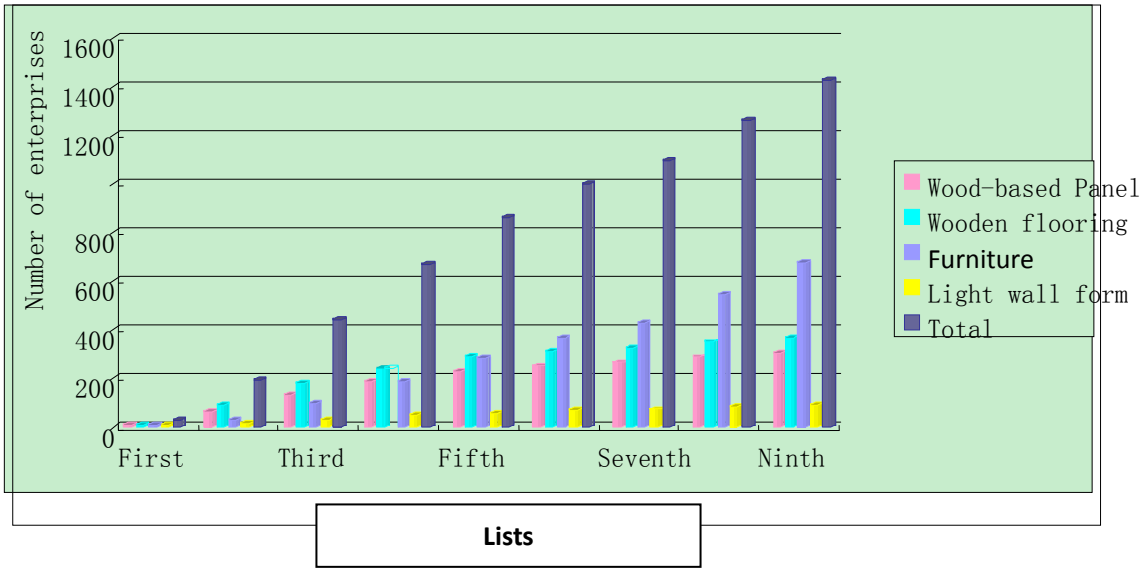

Fig.2-4 Total number of forestry enterprises in 1-9 government procurement lists of environment label products

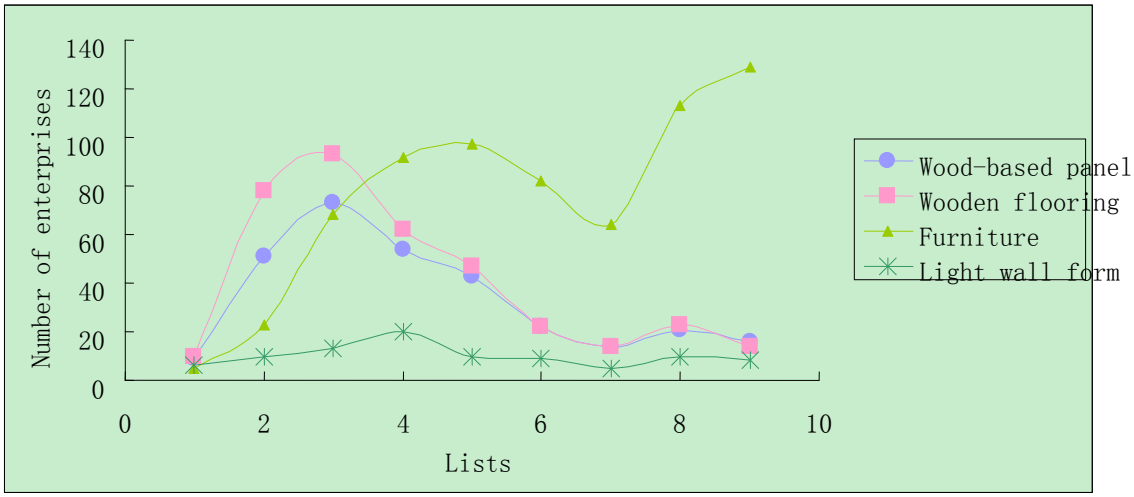

Fig. 2-5 Statistics of the number of forestry enterprises in the 1-9 government procurement lists of environment label products

It should be noted that processors to supply green forest products need to purchase certified timber or the timber with evidences to demonstrate the legal sources. The products made from these certified timber cost more than average products. According to statistics, the cost of certified forest products will increase by 20%-30%, which will create some pressure on enterprises. In China, public

procurements are mostly carried out in a form of bidding and tendering, in which price is an important reference indicator. In such sense, green products are hard to win bids. As a result, the conflicts between procurement policy and actual practices arise.

3. Policy design on green public procurement of China's forest product in the future

With an eye to China's national and forest conditions, international experiences and lessons in terms of green procurement are compared and learned. It is supposed to innovate and update policies, raise green consumption awareness by bolstering education and dissemination and upgrade the legislative system for government green procurement. It is expected to promote China's green forest product procurement process and precipitate the pace of green socioeconomic transition in China, by encouraging green enterprises to develop by virtue of market means, updating green product lists to cover more green procurement enterprises, putting in place green procurement monitoring and implementation mechanisms and strengthening policy design and execution in relation to green procurement supervision.

3.1 Upgrade legislations relative to green forest products procurement

From the experiences of developed countries in green forest product procurement policy, it can be seen that mandatory implementation of green forest product procurement policy through legislations is the most effective approach. It is feeble to rely on private environment forces, corporate social ethics and the self-disciplinary actions of timber exporting countries to implement green forest product procurement. It is a must to promote the green procurement through legislations at national level and to push forwards green forest product procurement with national will and law authority. It is needed to pin down the procedure, process, technical norms and standards of procurement in mandatory law documents and include them into environment requirements through developing a series of guiding documents and tool packages.

3.2 Set up green procurement standard for forest products

The development of green procurement standards is the centerpiece of government green procurement. The guidelines for products under government green procurement should be developed on the basis of environment label products, which require government to buy environment label products. Hence, it is needed to connect environment label products with products under government green procurement at the time of preparing green procurement standards for forest products. Moreover, the standards should be further extended at a faster speed to provide a good environment for the growth of green products and green industry, which also benefits government to conduct green procurement in a more regulated and more operational way.

Taking the national soft scientific research project of China's Green Public Procurement Policy for Promoting the Market Development for Environmentally Friendly Tropical Forest Products（2009GXS5B081） executed by the Research Institute of Forestry Policy and Information under the Chinese Academy of Forestry

as an example, the project team studied and formulated the code of action with regard to the procurement relation between Chinese consumers and tropical forest product suppliers, which is translated into the Green Public Procurement Guidelines on Tropical Forest Products in China (GPGT). The Guidelines provide a detailed description of green procurement standards for tropical forest products in terms of consumers' requirements on quality system (pertinent to consumers), requirements for tropical forest product supply (pertinent to suppliers), legal procurement (pertinent to consumers and suppliers), environment assessment (pertinent to suppliers and consumers), social responsibility (pertinent to supplier and consumers), risk assessment (pertinent to consumers and suppliers), validation procedure (pertinent to consumers and suppliers), sales of procured products (pertinent to traders) and control of procurement cost (pertinent to consumers and suppliers). The Guidelines will provide guidance to all parties in their compliance with various procurement requirements in relation to tropical forest products and therefore promote the green procurement process.

3.3 Step-wise implementation of green procurement process

The rapid economic growth in China imposes increasing consumption demands for timber. At present, China is the second big timber importing country and the big consuming country in the world, and China's timber imports account for approximately 35% of the total supply amount. China can set the phased objectives and resort to step-wise implementation for gradually achieving green procurement. For example, state-owned and responsible large enterprises should take the lead in the implementation to guide forest product import on the track of green procurement, and thus lead related agencies, departments and other enterprises gradually on the road of green procurement.

3.4 Enhance the capacity building for green forest product procurement

Authority third party certification need to be introduced to verify whether the timber used comes from sustainably managed forest or whether the forest products procured come from legal sources. Therefore, it is important to establish national certification system and bodies. The setup of specific organizations in charge of green forest product procurement and green procurement network, the publication of detailed guiding manual on forest product procurement and hiring full-time employees will help the full use of information from all sources and therefore save resources. It is pleased to see that the SFA has embarked on relative work. After researches, experts from the Chinese Academy of Forestry came up with the China Timber Legality Verification System, and related policy evaluation and pilot work will be carried out when conditions grow mature.

3.5 Release preferential policy for enterprises to procure green forest products

In order to provide preferential conditions for enterprises implementing green procurement policy in terms of import duty and value-added tax, the form of subsidy is adopted to reduce the costs of enterprises in timber import, with the aim at providing assistance in finished product development and enterprises' fund-raising. At

the same time, government agencies should give precedence to forest products produced by enterprises implementing green procurement policy when they procure, thus stimulating enterprises to actively participate in green procurement, facilitate green production and consumption and forward the management of forest ecosystems, green economy and inclusive society

References

Araya Akihiko. Countermeasures against illegal logging and green procurement law in Japan. China Wood-based Panel, 2010，（2）： 35-37

Bao Yingshuang, Su Haiying, He Youjun. Green forest products procurement policy and its practice in Dutch. World Forestry Research, 2010，23（5）：64-6.
FRA. 2010. http://www.fao.org/forestry/fra/fra2010/en/

http://www.cpet.org.uk/international-context/international-policies-1/france
Japan Legal Timber Website. http://goho-wood.jp/world/ch.html

Li Xiaoyong, Chen Xiaoqian, Hou Fangmiao. Evaluation of government green procurement policy for forest products. Journal of Beijing Forestry University (Social Science Edition), 2009，8（4) :134-138

Li Xiaoyong, Hou Fangmiao, Wen Yali, et al. Emergence and development trend of government green procurement of forest products in developed countries. Forestry Economics, 2008 (8) :78-80

SFA,2009.http://www.forestry.gov.cn/ZhuantiAction.do?dispatch=index&name=slzyqc7

Wang Xiuzhen, Chen Jie, HE Youjun (corresponding author). Impact analysis of green procurement policy for forest products in France and its reference. Chinese Forestry Science and Technology, 2011, 11(3): 24-30

Japan Legal Timber Website. http://goho-wood.jp/world/ch.html

CPET, WWF, TTF. Where does your timber come from? 2009

CPET, The UK Government Timber Procurement Policy, 2009

Timber Trade Federation, The Responsible Purchasing Policy Annual Report, 2010

CPET. Government procurement of timber in France. 2011-7-8.
http://www.cpet.org.uk/international-context/international-policies-1/france

Developments of Wood Markets – Resizing of Timber Industry

Marius C. BARBU
Professor of Faculty for Wood Engineering, University ”Transilvania” Braşov
Address: Str. Colina Universitatii Nr.1, 500068 Braşov, România
E-mail: *cmbarbu@unitbv.ro*

Abstract

The forecasts for the next decades point out new centers of economic development far away from current ones, which will confirm the changed balance of today's situation. The unprecedented demographic growth in Asia and the aging of the European and North American population will also result in the occurrence of controversial scenarios for the whole region in terms of economic evolution. China became the world leader also for wood products and furniture manufacturing, respectively in raw material import. Wood markets and trade worldwide are changing rapidly because of the booming production capacities of the last decades, dramatic reduction of North American consumption, the new energy policy based on wood biomass, the increased demand of wood as raw materials especially in Asia and Central Europe and, of course, the continuing current economic crisis. The new development related to energy production from wood biomass hardly starts to compete with the raw material market for European and soon the North American wood based panel producers. High productivity may be obtained by means of new wood working technologies with low raw material input and reduced power consumption. The new requirements for low emission panel products increased the competition between the European producers. Also the top 10 of the world and European wood based panels producers start to close their aging capacity and reduce production figures. The last of which consists of more than half of the panel production capacity and control a fifth of world production. Also the environmental issues continue to differ from one country to another and even within different regions in the same country and involve different levels of investment and production costs having an immediate impact on market competitiveness.

Key words: forest figures, wood markets, wood based panel developments

1. SOCIAL AND ECONOMIC SITUATION

Population distribution and its welfare still contrast strongly from one country to another. In 2011 according to UNO the world population is already 7 bill., mainly concentrated in Asia (60%), as follows: 20% in China (1.34 bill.), 17% in India (1.19 bill.), 3.4% in Indonesia (238 mill.), 2.5% in Pakistan and Bangladesh each (170 mill.), 14% on the African continent (2.3% in Nigeria) only 11% in Europe (731 mill.), 8% in North America (514 mill.) and 5% in South America (371 mill.). The actual projection is 8 bill. by 2025. The population of the world in 1960 was about 3 bill.

According to UNO statistics the population growth forecast for the following four decades is further in favour of the Asian, African and South American continents. The population of the North American continent will slowly continue to grow by designed emigration; the European population will dramatically diminish if no immediate emigration policy is provided by the Commission. In the next 40 years, according to the best case scenario of UN the African population could increase twofold (1.9 bill.), and India, with 1.6 bill., will surpass China (1,4 bill.). In addition to the fact that the populations of the today's advanced countries will significantly decrease and will grow old. In accordance with the present moderate forecasts, the world population will reach 9 bill. inhabitants before the year 2050.

The world gross product (WGP) according IMF was about 78,950 bill. USD in 2011. It is to be pointed out that USA and European Union, with less than 20% of the world population, contribute more than 50% of WGP. Also contrasting is the fact that Africa and the Indian Peninsula contribute only 4% of WGP, although possessing considerable natural riches and having about 40% of the world population. The hierarchy of the industrialized countries is now substantially modified by the fast growing countries (e.g. China, Brazil, India, Mexico) ranking among the top 10 with respect to gross national product.

2. FOREST AND LOG PROCESSING

About 31% of the land area of the world is covered by forests, which means 4 bill. ha, out of which more than two thirds belong to underdeveloped or developing countries. Of the world’s total forested area 20% belongs to Russia, 17.5 % to North America (half by Canada), 13% to Brazil and less than 4% to EU27.

Inside the EU27, the main area covered by forest represents 41% (177.8 mill. ha). Only 132.6 mill. ha (75%) are suitable for roundwood production. The main area of forest for the wood supply is owned by Sweden and Finland (each 15%), followed by France and Spain (each 11%), Germany (with 8%), and Poland and Italy 6% each). The forest ratio per capita of EU27 is 0.35 ha but Scandinavian countries are the leaders: Finland 4.5 ha, Sweden 3.5 ha compared to Spain 0.6 ha/ and France 0.3 ha.

The growing stock of the world in 2010 was above 500 bill. m³, from which Brazil accounts for one quarter, followed by Russia and North America (each 16%) while the EU27 has less than 5%. The growing stock of EU27 is approximated at 21.75 bill. m³ at an yearly increment of 768 mill. m³. Between countries, Germany has 3.47 bill. m³ (16%), Sweden 2.65 bill. m³ (12%), France 2.45 bill. m³ (11%), Poland and Finland over 2 bill. m³ (each 9%).

The roundwood density (over bark) are reaching the maximum in Brazil (243 m³/ha),

followed by USA and EU27 (each about 160 m³/ha), Canada and Russia (each above 100 m³/ha) compared to China and India with only 80 and 70 m³/ha. respectively. Inside the EU27 Austria, Slovenia and Germany have the highest roundwood density in their forest (approx. 330 m³/ha) followed by Slovakia, Belgium and Poland (over 245 m³/ha) and Romania, Estonia and Lithuania (over 200 m³/ha each). France and Italy have approx. 160 m³/ha each and Sweden only 129 m³/ha.

The share of coniferous growing stock in the world is two thirds (same like in EU27) compared to three quarters in North America and Russia.

The annual average removal of roundwood in the world in 2009 was 3.28 bill. m³ (of which 57% as fuel) shared by the EU27 (12%), USA and India (each 10%), China and Brazil (each 9%), Russia (5%) and Canada and Indonesia (above 3%). The difference between these world top 10 countries is the way to use the removed roundwood: processing over 90% in North America, over 80% for EU27, over 70% for Russia and less than 50% for Brazil vs. less than 10% in India and China. The production of roundwood in the EU reached an all-time high in 2007, peaking at 458 million m³ - also because of additional removals attributable to the large number of trees damaged in storms. Industrial roundwood production fell by more than 10 % after 2008 and this trend continues. Within the EU27 the annual removal of 391 mill. m³ roundwood (20% for fuel) are made by Sweden (17%), Germany and France (each 14%), Finland (11%), Poland (9%).

The world annual average removal for fuelwood for the same year was 1,85 bill. m³ used especially as a major source of energy in many developing countries, who consumed around three quarters of the world's fuelwood. The share of fuelwood in removals was considerably higher in Africa (89%) and Asia (77%), falling to 24% in Europe. By continents, Asia (41%) and Africa (33%) are burning three quarters of world wooden fuel. In contrast, Europe produced 8% and North America only 7% of the world's fuel (2009). A high proportion of global fuelwood is from broad-leaved species (89%). By country India (17%), China (11%), Brazil (8%), and the EU27 (less than 5%) are the main fuel producers. The EU27 is using 82.6 mill. m³ roundwood as fuel. The main wooden fuel producers in Europe are France (31%), Germany (10%) and Sweden, Finland and Italy (each 6%) [FAO, Eurostat 2011].

3. WOOD PROCESSING INDUSTRY

In 2008 the EU27 wood-based manufacturing industry had a turn-over of more than 413 bill. €, employing 2.77 mill. people in 328,300 companies. The wood and wood-products industries employ 1.16 mill. people, the same figure as the furniture industry (1.2 mill.) vs. 0.7 mill. in the paper and paper products industry. In terms of turnover, the paper and products industry makes 180 bill. € (high productivity due to high automatisation), wood and wood products 131.5 bill. € and the furniture industry 115 bill. € (due to more hand labour). Between countries China ranks on top with 1.25 mill. persons (more than EU 27), followed by USA 536,000, Russia 340,000, Indonesia 300,000, Brazil 225,000, Italy 155,000, Poland and Germany (each over 135,000) [FAO, Eurostat 2011].

3.1 Sawn wood

The world production of sawnwood was 362 mill. m³ in 2009 (10% less than in 1999). More than one quarter is processed in the EU27, equal to that of North America (1/3 Canda and 2/3 USA, where actually only 2/3 of the 1999 level was processed), followed by China (9%),

Brazil (7%) and Russia (3%). The continent with the lowest sawn production is Africa and Oceania (each above 2%). In 2007 the EU production of sawnwood peaked with over 115 mill. m³. By 2009 this figure dropped by over 22%. The main share of sawnwood within EU27 (91 mill. m³) in 2009 was held by Germany (23%), Sweden (18%), Austria, Finland and France (each 9%) [FAO, Eurostat 2011].

3.2. Wood based panels

The production lines manufacturing wood based panels have developed more and more, reaching high production capacities (>1.500 m³/day per line). The trend of building new production capacities stopped completely at least within North America and Central Europe after the start of the crises in 2008. Big panel producers of the world are tailoring their own available capacities. Many closures of old or small plants were recorded especially in the USA and the EU27. The prediction, one decade ago, that only a few large industrial groups would operate in the world, concentrating an overwhelming proportion of the wooden based panels capacity, has been further "supported" by the financial crises. Small- and medium-sized producers not involved in this process will only be able to survive by specializing in the manufacture of types and sizes of boards that are "unprofitable" for mega-groups [Barbu, 2009].

The total installed capacity worldwide for wood based composite panels has risen from 2000 to 2010 by more than 25%, reaching 235 mill. m³/year. The increase in capacity of the most recent years was only in South-East Asia and South America. In Europe new production capacities are only being developed in the East, particularly in Russia and Turkey.

Europe and China each hold more than 30% of the world capacity for wood based panels. The production of wood-based panels (comprising particleboard, fibreboard, plywood and veneers) reached 70 mill. m³ in 2007. By 2009 European production retracted by 20%.The main panel producer in Europe is Germany (26%). Turkey increased its capacities at a high rate reaching 2nd place after Germany. Russia will become an important player in this industry with operating capacities of close to 8 mill. m³ at the moment. The main market share in Europe belongs to Austrian group owners Kaindl (Krono Group) and Egger (28%, respectively 12%) and the top 4 of them (including Sonae and Pfleiderer) controll more than half of the European capacity. The top 10 of Europe is producing up to 75% [WbPI, EUWID 2011].

The availability and quality of raw materials determines the type and concentration of the panel industry in Europe. The South is specialized in particleboard, the Alps and central region in softwood mills, pulp & paper and also MDF industry, and in Scandinavia only sawnwood, pulp (58% of total), paper and veneer based products are produced. The huge urban areas provide recycled wood which in the past was only used only for particleboard now also has to be shared with biomass energy producers.

Among the various types of wood-based panels manufactured within the EU, over 60% of production was for particleboard (37.6 mill. m³ in 2009). The EU production of particleboard (PB) was more than twice the level of the output recorded for fibreboard (15 mill.m³), such as hardboard (HB), medium-density fibreboard (MDF) and softboard (SB, also known as insulating board). The level of production in the EU27 of plywood (PY) and of veneer sheets was at 3 mill. m³ and 1.4 million m³ respectively. The largest overall contraction between

2006 and 2009 was recorded for HB (-53%), while the production of PY fell by 35%. The smallest reduction in output was recorded for oriented strand boards (OSB), with an overall decline of less than 6% [Eurostat 2011].

3.2.1. Particleboard (PB)

Particleboard kept its significant market share for decades with its popularity worldwide (above 40%) and in Europe (60%, incl. Russia and Turkey), loses constantly the ground in North America and Central Europe as well. The world production capacity for 2010 was above 96 mill. m³. An unexpected invigoration of production capacities can be seen lately in Eastern Europe by 3 mill. m³ (incl. Russia and Turkey), Latin America by 1 mill. m³. Europe incl. Russia and Turkey still holds the first position worldwide concerning production capacity (54 mill. m³). The main producers of the world by their installed capacities are Germany (8.4 mill. m³), USA and China (est. by less than 8 mill.m³ each), Russia (est. by less than 6.5 mill.m³), Turkey (over 5 mill. m³), Brazil, France and Italy (over 4.3 mill. m³ each), and Spain and Thailand (over 3.2 mill. m³) [WbPI, 2011]. The demand for PB is maintained constant due to the cheap raw materials originated in the recycled wood (harsh competition to biomass based energy generation) and low price compared to MDF (50%). The increased use of recycled material became state of the art and factories fit their equipment for the preparation of this type of raw material. One aspect that could be improved is still the on-line detection of contaminants in recycled material. The main use of PB in Europe is for the furniture industry (54%) because of the existing processing technology, and its light weight and low price compared to other panels. A slight loss in flooring and building share is noticed because of MDF, specifically OSB. A new generation of light particleboards with a density of less than 500 kg/m³ is established. New regulations for free formaldehyde emission of PB (Perforator 4 mg/100g) were implemented since 2009 [Barbu, 2009; EPF, 2011].

3.2.2. Plywood (PY)

Plywood holds the second position (74 mill. m³) worldwide after PB. However, it is less and less mentioned by statistics, due to the severe lack of appropriate raw material, and high labour costs especially in developed countries. Because of this situation there are no significant European capacities for the plywood production (3.5 mill. m³ in 70 small companies). The newly developed MDF and OSB boards tend to substitute it, offering economic benefits in furniture manufacture and construction. Over the last two decades, there has been an increase in plywood production worldwide (+50%). China is now the biggest plywood manufacturer of the world (over 35 mill. m³). Asia without China already surpassed North America (17 mill. m³), with a positive tendency with regards to the evolution of capacities. In South America (over 4 mill. m³), Brazil, is one of the worldwide main plywood exporter. In North America, Central Europe and Oceania, a constant decrease in the production capacities can be noted. Eastern Europe and Russia are other regions with a positive evolution in this respect. In Europe, the processed plywood represents 15% of the world production capacity and is covered by two thirds from imports (China, Brazil, Russia, all above 75%) [Barbu 2011; EPF 2011].

3.2.3. Oriented strand board (OSB)

Oriented strand board seems to be like MDF in its evolution and had a growth of more than 40% in the same decade. In North America, where OSB launched as a building material to the detriment of plywood and PB, 85% of the global production capacity (30 mill. m³) was

concentrated. In the last decade in Europe the annual production capacity has doubled, reaching 5 mill. m³. Related to world capacity (=North America) it represents less than 15%. More than 30% of the EU27 production (3 mill. m³) is exported to Eastern regions. New lines are realised for the very first time in Russia and China. The world forecast for the next years depends strongly on the development of the collapsed building industry in North America. The unprecedented evolution of the installed capacities for OSB production in North America began to decline since the recent crises. The total production capacity of North America in 2010 was 24 mill. m³ but the producers reduced their out-put due to the low request from market. Only 60 to 70% of this capacity was operating in the last years. Some of the temporarily closed mills got bankrupt and merged into other groups. Most of the planed new projects in USA and Canada (over 2 mill. m³) are cancelled or delayed [Barbu, 2009]. Further investments are forecasted for the 1st time in Turkey, Ukraine, and Venezuela. The main use of OSB is for construction (75%) and packaging. VOC of pine strands and increasing requirements for indoor air quality are new optimization fields. The new emission values for formaldehyde were issued by middle of 2009 [EPF, WbPI 2011].

3.2.4 .Medium density fibreboard (MDF)

Over the last 5 years, the medium density production capacity has seen the quickest increasing rate, surprisingly in China (over 10 mill. m³) and its neighbouring regions (1.5 mill. m³), as well as in South America (5 mill. m³), Russia (over 1 mill. m³), Turkey (about 1 mill. m³), not in Central Europe or North America where the initial boom took place. MDF – after 45 years of manufacture, is produced on more than 500 production lines, with a production capacity (over 80 mill. m³) distribution as follows: 46% in China, less than 25% in Europe (incl. Russia and Turkey), and the rest shared between Asian countries (11%, without China), Latin America (9%) and North America (7%). In the same period in North America (-20% in USA), Oceania, and parts of Asia the production activity was stopped and lines have been closed down, dismounted and relocated. For the last five years only one MDF new project was completed in Central Europe while China doubled its installed capacity. New lines are planed only in South America (1.5 mill. m³), China (1 mill. m³), South-Eastern Asia (1 mill. m³), Russia and Turkey (about 1 mill. m³ each) [WbPI, 2011]. The main use of MDF is for furniture (55%) as substrate panels. One third of MDF is produced as thin HDF and coated for flooring. A light overcapacity and price instability have driven manufacturers to keep their production constant or to reduce it. Because the furniture sales suddenly decreased due to the instable financial situation and low number of new buildings in USA and Eastern Europe production figures decreased too. From 2008 on new regulations require a limit of 5 mg/100 g (Perforator) for free formaldehyde emission. A reduction of weight for thicker boards is still greatly demanded by customers [EPF, EUWID 2011].

3.2.5. Fibre based insulation boards in dry process

The fibre based insulation boards market in Europe, particularly in Germany, is presently in a renaissance. In recent years, the European market of insulating materials represented 30 mil. m²/year. Different European manufacturers of conventional wood based panels have also been producing wood-fibre-insulating-boards since the middle of the nineties in different new dry-processes beside the revised wet-process. Wood fibre insulating materials with thicknesses over 200 mm and densities below 50 kg/m³ can be produced for the first time on an industrial scale without gluing multiple thin fibreboards. The manufacture of very low density fibreboards in the dry process requires an activation of the resin over convective media such as hot-air, superheated steam or a mixture of both, and an adaptation of the

pressing technique. These new light fibreboards clearly have better physical characteristics (thermal conductivity) compared to classical products like fibreboards made using the wet process (>150 kg/m³). The physical properties of light wood fibreboard for insulation are not inferior for example to mineral wool. Insulation products made of regenerative raw materials are about twice as expensive as classical insulation products and have only been able to be partly established on a large market [Barbu, 2011].

3.2.6. Hardboard (HB) and softboards (SB) in wet process

Hardboard (HB), manufactured by the wet process, is the board with the longest tradition, after plywood and blockboard. At least in Europe (both type less than 5%), hardboard production is obviously in decline, not due to the board properties (NB: board with very low emissions), but due to environmental problems, especially water treatment owing to the ecological nature of the material and particularly to the performances similar to those insulating materials. On the other hand the softboards (SB < 400 kg/m³) production rose in the same period.

3.2.7. Other wood based composites

The production of wood pellets in North America and the EU grew at a phenomenal rate. Between 2008 and 2009 (7.8 mill. t) it raised about 40 %. More than half of the EU's production was concentrated within Germany (1.5 mill.t) and Sweden (2.0 mill.t) and Latvia (670,000 t), Poland and France (each over 550,000 t), Estonia (close to 500,000 t). An unprecedented development is also evident in Russia which owns the 1st pellets mill with 1 mill. t production capacity in one site [Eurostat, Euwid 2011].

Parquet (not HDF based flooring) had a positive and constant evolution for more than two decades. Nowadays, 100 mill. m² of parquet were produced in Europe. The main manufacturers are Sweden (22%), Poland (12%), Germany (12%) and Spain (10%). The main producer groups are located in Scandinavia but production also takes place in other European and Asian countries. The parquet consumption is 0.23 m² per inhabitant, on average. However, the greatest parquet-consumer countries are Germany (22%), Spain (18%), Italy (15%) and France (11%). The most widespread type of parquet is laminated (80%) due to its reasonable price, high performance, and easy assembly. Although the price of massive parquet and the labour costs are high, the consumed volume remains steady (15%) [HZB, EUWID 2011].

3.3. Furniture

The furniture industry witnesses worldwide profound changes in terms of both the manufacturers and the diversity of products, which need to meet the new requirements of the customers. The traditional furniture manufacturers in the Central Europe and North America are hardly facing up to the competition of the new manufacturers from countries under development in Eastern Europe and South-East Asia which, little by little, are beating them on quantity and the price level. Additionally IKEA and other similar low budget furniture trading chains have greatly influenced the developments of last decades.

The competition of sale prices has become all around the world one of the crucial factor in the marketing of furniture. The need for personalized furniture and satisfying the personal tastes is ever more important in the designing of furniture. The modernization of the furniture

manufacturing processes by the aid of completely controlled production flows and centres, automatically and instantaneously adjustable according to the series to be processed, creates competition in this market. The forecast predicting the migration of the production centres from Western and Central Europe to the East of the continent has not been accepted for a long time. Today, the ultra-conservative investors have to face it as an obvious and painful reality.

5 years ago furniture production reached the value of 200 bill. €. The forecasts for the year 2000 considered that the furniture production in Europe and North America would continue growing – but, unfortunately, this scenario did not come true. Since 2000 until the present, China has managed to double its furniture production and to increase exports threefold; so that Chinese-made furniture represents 25% of the total quantity produced by the USA and EC together. This discrepancy results from production costs, which are 70-80% lower in China than in North America or Central Europe. The huge amount of furniture imports in USA determined a clear downward trend for their domestic production and the relocation of the manufacturing centres outside.

The same tendency is seen in the European market, too. China has become one of the biggest furniture suppliers, after Germany, Italy and Poland. In Germany for instance, an obvious decline in the number of small plants manufacturing custom-made furniture has been recorded over the last decade, in contrast to an unexpected increase in the number of assembling facilities for imported pre-manufactured furniture (threefold). In general the Chinese furniture market, demanding over two thirds of the domestic production, cannot be overlooked.

The furniture consumption in the Europe and North America is not stabilized. This undesirable evolution can be accounted for by the negative demographic development in the industrialized countries, the rise in the cost of living, the increase of the unemployment rate in some regions, and especially the development of a new category of furniture, the so called “do it yourself” (Ikea), with low prices and an acceptable service life and the current fast moving world financial crises [Barbu, 2009]. Pöyry forecasts an increase of the world demand from 12 to 14.7 mill. m² for coating materials by 2015. Especially the melamine based paper coatings will reach 45% market share. This expected development has to follow the booming development in the emerging countries, the apparition of conurbations and new environmental aspects.

3.4. Construction

For the first time for many decades, and because of the unexpected rise in the price of steel, modern wooden construction can compete with the classical systems made of concrete and steel especially. The new wooden structures are favoured by the elements in their structure based on Glue Laminated Timber (GLT), I-beams, OSB faced frames and Cross Laminated Timber (CLT), developed with pre-designed high properties and meeting the same requirements as the rest of the building materials: fireproofness, large spans, multi-floors, low weights at high dimensional stability in various environments and, last but not least, easy and fast assembly are the characteristics of the new generation of wooden constructions.

The tradition and impact of prefabricated houses in Europe is still low. Aspects like energy saving, low costs and fast manufacturing time need to be better explained and spread for a large acceptance and successfully marketing. New European regulations like the Energy

Saving Certificate for houses and new regulation for building with more than seven floors in urban areas could sustain positive developments. The renovation of existing buildings especially the thermal insulation is an activity over a large time span.

3.5 Recovered wood, recycled pulp and paper and fuel wood for biomass energy

3.5.1 Recovered wood [Eurostat, 2011]

Waste treatment operations distinguish between five different treatment types: recovery, energy recovery, incineration, disposal on land, and land treatment/release into water. Almost 25 mill. t of wood waste were treated in the EU (2008), while the figure for paper and cardboard was 13.3 mill. t higher. The highest share of wood waste in the EU (2008) was generated by wood manufacturers (39%). Households accounted for the highest share of waste paper and cardboard (30%). Both wood manufacturing and paper manufacturing accounted for only a small share of the total waste generated by all activities. Looking in more detail at the recycling of wooden packaging some 5.1 mill. t and 25.2 mill. t of paper and cardboard packaging were recycled in the EU (2008). The production of recovered pulp fibre and recovered paper in the EU was 23 mill. t and 50 mill. t respectively (2009). Germany alone accounted for more than half (56%) of the recovered fibre pulp and the addition of Spain and the UK led to a cumulative share of 88%. The main production of recovered paper was in Germany (30%). Together with the UK, France, Italy and Spain accounted for 75% of the EU total. The two largest producers of recovered fibre pulp in the world are China and the EU.

3.5.2 Biomass energy generation from wood (waste) [Eurostat, 2011]

Within the EU, energy from biomass has become increasingly important in recent years, as policymakers seek to ensure diverse and secure energy supplies while at the same time considering the impact of energy policy on climate change. The introduction within the EU of national targets for 2020 concerning the share of renewable energy in gross inland energy consumption, will likely have a significant impact (not only positively) on the forest sector (negatively for panels, pulp and paper production), given that wood and wood waste is currently the largest source of renewable energy. Indeed, the use of biomass from both forests and agriculture is forecast to increase sharply in the coming decades.

Wood for use as an energy source (a fuel) comes not only from tree felling, but also from selective thinning of managed forests and other forestry practices (direct sources). Wood for energy use may also be derived as a by-product from downstream processing in wood-based manufacturing (indirect sources). End-of-life wood and paper products may also be used as a source of energy (recovered wood). Information collected shows that direct sources of total wood used as an energy source in France was 84% which contrasts to the high share of indirect sources in Sweden (81%) and Finland (78%). The share of recovered wood rose in Germany (23%) and UK (29%), which reflects the new landfill legislation that encourages wood waste to be used or traded, as well as the promotion of biomass energy production. Private households were the main users of wood as a source of energy (48%) of the wood used for energy purposes (2007).

Renewable energy sources accounted for only 8% of the EU's gross inland consumption of energy (2008). This share was only 4% in 1990. EU gross inland energy consumption of wood and wood waste was 71 mill. t oil equivalents (2008). Wood and wood waste was the

leading renewable energy resource in the EU, accounting for 47% of all gross inland energy consumption from renewable energy sources and for 68% of the total for biomass and waste (remainder 14% municipal solid waste, 11% biofuels and 7% biogas).

Aside from its conversion into heat through combustion, biomass energy sources may also be transferred into electricity, gas, or liquid fuel. Biomass is increasingly used in complex installations (i.e. the production of combined heat and power or co-combustion technologies for power generation). Net electricity generation from biomass-fired power stations in EU accounted only 3% (2008).

4. SUMMARY

The world roundwood production was the same in the last decade. 8% reduction in the world's industrial roundwood production was recorded for the same time period in the favor of fuelwood. Asia accounted for the highest share (30%) of the world's roundwood production (2009), which still didn't cover its own need.

The world's sawnwood production was 7% lower than a decade before. Europe accounted for more than 35%) of global output in 2009, while production in China and India doubled in the last decade (from relatively low levels). The producers will be constrained to reduce the transportation expenses especially for raw materials, to sell wood and processing wastes directly to biomass energy producers and to take organizational actions destined for making the manufacturing process more flexible. An interesting example is that of briquetting of chips resulted from the wood primary processing (pellets), as well as that of the bark and other process residues conversion in order to efficiently produce heat energy and electric power on site. The overcapacity of sawmills installed in the last years, especially in German speaking region and neighboured countries will be severely reduced by bankrupts and merging.

Northern and Central America produced 40% of the world's wood pulp (1,5 times more than in 1999). The relative contributions of Brazil and China doubled to 8 % and 4% of the world's wood pulp by 2009. Global paper and paperboard production in 2009 was 20% higher than in 1999. Over the last decade, Asia has the position of global leader (42%) as result of China overtaking the USA [Eurostat, 2011].

In the last decade China has become the top producer for wood based-panels producing 36% of the world volume in 2009 (6 times increase) and the forecast will continue to be a positive one. The installed overcapacity for wood based panels and the ongoing financial crises with its dramatic impact on building and furniture sales forced manufactures to reduce their production rate and sales prices to the level of production costs and close systematically the old lines. The reduction of board weight and emissions on the one hand and the increase in use of recycled wood on the other hand is an important goal but not the solution to protect some of the companies against shutting down their activities. A further harsh concentration of the existing capacities in some international acting megagroups could be the short term forecast.

Furniture made from low weight elements (sandwich type or foamcore) and low emission panels especially for the "do it yourself" segment is a probable direction of developments in the near future. Other processing and finishing technologies adapted to the new quality of board (light weight and low emissions) should be extended in the market and accepted by

processing companies.

The different regulations in the EU states subventions of green energy generated from biomass (= approx. same raw materials like for PB) and in environmental protection (waste air, waste water and noise) create precedents for unequal competition inside Europe and between the industries. Some regions also offered important subventions or taxes reductions in order to settle down industrial production sites which also creates different advantages compared to other producers

The forecast for the coming years will continue to be a negative one for North America and Central Europe, stating a consolidation of the available new production capacities and closing of the lines with different accents depending on the effect of the financial crisis on the furniture and building industry from one continent and region to the other.

LITERATURE

Barbu, M.C. 2009. Actual developments of the wood industry. Proceeding of 7th ICWSE, 4-6 June, Brasov, ISSN: 1843-2689, pp. 255-262

Barbu, M.C. 2011. Current developments in the forestry and wood industry. ProLigno, Vol. 7, Nr. 4, pag. 111-124

Eurostat 2011. Forestry in the EU and the world - a statistical portrait. Stastical book. Publications Office of the European Union

Irle, M., Barbu, M.C. 2010. Wood-based Panel Technology, Chapter 1 in Thömen, H. et.al. "Wood based Panels – An Introduction for Specialists". Brunel University Press, London. ISBN 978-1-902316-82-6.

*** EPF (2011): www.epf.org

*** EUWID (2011): www.euwid.org/holzwerkstoffe/

*** FAO (2011): www.fao.org/faostat/

*** WbPI (2011): www.wbpionline.com

Proceedings of the 55th International Convention of Society of Wood Science and Technology
August 27-31, 2012 - Beijing, CHINA

Turkish Wood Based Panels Industry: Future Challenges and Suggestions

Hasan Tezcan Yildirim. [1*]

[1] Doctor Research Assistants, Istanbul University Faculty of Forestry,Istanbul-Turkey.
* *Corresponding author*
htezcan@istanbul.edu.tr

Abstract

World production of wood based panel has been 63.1 million cubic meters in 2005. In 2009 wood based panel production was 75.5 million cubic meters in the world. The amount of production has risen to 12 million cubic meters. China is the world's largest wood based panel's manufacturer. 45% of the world wood based panels production is carried out by China. China plate, respectively, producing 34.5 million cubic meters in 2009, the U.S., Germany and Turkey has been following. Turkish wood based panels industry has shown a tendency of rolling between these periods. Turkey, the world's 4th largest important for the industry as a manufacturer of wood based panels make it clear that a country. Turkey has made great strides in the last 20 years in the forest products industry. There are wood based panels at the beginning of these developments, the share of industry pioneer. Both the development of new materials and techniques of domestic and international market demand have played a decisive role. Turkey's wood panels production, while the 100,000 m^3 in the early 2000s, by 2010 the amount of production is about 5.5 million m^3. Total of 95 facilities are available in the industry, 24 of them particleboard, fiberboard, 16, and 55 producing plywood panels. The sector's total production capacity is approximately 9 million m^3. Given the industry's production of 2,500,000 m^3 of wood for the production of particleboard should, 2,950,000 m^3 of wood required for the production of fiberboard. Approximately 500,000 m^3 of plywood in the wood for the production of wood production for the sector is required, but Turkey give to wood for sector is 4,030,000 million m^3. Therefore, approximately 2,000,000 m^3 of wood vulnerability exists in the industry. The results obtained so far indicate that the demand for Turkish wood based panels industry has made in meeting the GDF's chip wood fiber production is not sufficient. Where the raw material supply problem in the industry, as well as the problems encountered in the forest and on the basis of the villagers living adjacent to, not to the time of product problems related to storage and transportation of raw materials and other related problems are bottlenecks. Problems related to the provision of raw materials and raw materials research, first, the need for future estimates of the level at which the world and close to the periphery countries will be examined, wood composite panel production and trade policy recommendations will be developed.

***Keywords*:** *Wood based panels industry, forest industry, forest products, forest products policy, forest villagers*

Introduction

The forest industry has been an inevitable propelling power of the industry since olden times (Mahapatra and Mitchell, 1997; Ok, 2005; İlter and Ok, 2007; Paul and Chakrabarti, 2011). And thus, the industrial use of wood has continued from the past until today. Use of wood as an industrial material is perceived as a source of income for wood producers (Cubbage et. al, 2007; Toppinen and Kuuluvainan, 2010; Damette and Delacote, 2011). Meeting wood demand is of great importance for the forestry sector. The fact that the wood demand is still being met via illegal methods today highlights the relevance of sustainable forest management and –as it naturally entails- that of certification in terms of industrial wood production (Schanz, 2002; Hetemäki and Nilsson, 2005; Krott, 2005; Ingold and Zimmermann, 2011). The board sector of the wood industry has achieved a giant leap forward, especially in the last ten years. The most important reason for such a big leap forward is the fact that wood is of very little economic value when used in en masse (Yıldırım, 2010). Worldwide board production had a fluctuating course between 2005-2009. Wood production, which was 63.1 million m^3 in 2005, increased to 75.5 million m^3 as of 2009. The world's largest board producer is China, which fulfills 45% of worldwide board production alone. The USA, Germany and Turkey follow China, which produced 34.5 million m^3 of boards in 2009. As the 4th largest board producer worldwide, Turkey is an important country for the sector. From this perspective, it is essential to discuss the current status of the sector and that of the resources owned by Turkey.

As per the latest forest inventory research and management plans made by forestry organization, Turkey has total of 21.2 million ha (which corresponds to 25% of country's surface area). It is estimated that 10.1 million ha of the current forests has an economic function and 10.4 million ha has an ecologic function while 0.7 million ha has a social function OGM (General Directorate of Forestry (2006). 15 million ha of forests are groves while 6 million ha are coppice woodlands. On the other hand, half of the forests are normal while the other half are degraded forests. A portion greater than 99% of the Country's forests is owned by the state while the surface area of forests owned by public legal persons is approximately 7,986 ha. The surface area of forests owned by the private sector is 10,182 ha (which is exclusive of special afforestation practices using poplar and other species). According to OGM's data (2008), total growing stock of Turkey's forests is 1.2 billion m^3 in normal forests and 0.8 billion m^3 in degraded forests. Average growing stock per unit area is 112.5 m^3/ha for normal forests and 8.28 m^3/ha for degraded forests. On the other hand, while the growth of our forests was 36.3 million m^3, the yearly allowable cut given in management plans was 16.3 million m^3. Increase is 3.34 m^3/ha total in normal forests in unit surface area and 023. m^3/ha total in degraded forests. The major part of industrial wood production consists of products with a small diameter and of low value (fiber-chip, wood for paper production and industrial wood). First and second class rate in lumber, which is also classified as industrial wood, is calculated to be 3% (OGM, 2008). It is estimated that in Turkey, 150,000 to 200,000 ha is used for purposes of growing poplar, and approximately 3.0 – 3.5 million m^3 production is used

for meeting the industrial wood requirement annually, while 2 million stere is used as firing wood (Kaplan, 2008).

For the purpose of meeting the total wood requirement, OGM supplies 12-13 million m^3 wood out of their sales to the market. On the other hand, the private sector's production is 2-3 million m^3 while 2.3 million m^3 woods are supplied to the market by means of imports (OGM, 2011). The balance of 4-5 million m^3 consumption is known to be supplied illegally. Although some substitute materials, such as metallic and synthetic materials, are being used widely today, this didn't mitigate the need for wooden products. To the contrary, consumption of wood products is on the rapid increase in parallel to worldwide economic developments and an increase in population (Birler, 1998; Ekizoğlu, 2008; Toppinen and Kuuluvainan, 2010; Yıldırım, 2010). The board sector of the forest industry is of great importance for Turkey. While wood can be an export item once processed, new factories are opened and new employment opportunities arise as the sector grows.

Turkey has achieved major progress in the forest industry, especially in the last 20 years. The board sector is the frontier in such progress. Both the development of new material techniques and the demand in domestic and international markets have had decisive roles in such progress (Ekizoğlu and Yıldırım, 2011). While Turkey's board production was 100,000 m^3 in early 2000s, production increased to 5.5 million m^3 level as of 2010. There are 40 facilities in the sector, 24 of which produce chip board while 16 facilities produce fiber board. Total production capacity of the sector is approximately 9 million m^3. Rapid development of the sector has certain complications. In a general sense, these complications are as follows (Ekizoğlu, 1985; Zengin, 2009; Yıldırım, 2010):
Raw Material Issue: Single biggest cost factor of the chip board and fiber board industry is wood material. Accordingly, raw material issues are among the most important problems for the industry. Considering the actual capacity of chip board industry, the requirement is approximately 7,824,000 stere raw materials. Considering 10,676,000 stere of raw material requirement of fiber board industry, calculated on basis of industry's actual capacity, overall raw material requirement of board sector is around 18,500,000 stere. This will pave the way for imports, which in turn cause losses to the country's economy. Import raw material requirement of the board sector, which suffers a raw material shortage in the current situation, will increase after these investments.
Purpose of Use Issues: The chip board and fiber board industry is able to use raw materials of both high and low quality. Raw material used in these sectors is close to raw material used in paper industry and firing wood and waste raw materials of other forest products can be used in board industry at certain proportions. However, the fact that the raw material that can be used in chip board and fiber board sectors is being distributed to forest villagers for use as firing wood gives rise to an important raw material problem for the board industry.
Transportation Issue: Transportation, namely freight transportation, causes two problems for board sector. First is the inability of transporting board raw materials and second is the fact that transportation is a cost factor that increases the overall cost of raw materials. Transportation's contribution to overall cost increases as does the transportation distance.

Although exact percentages are unknown, increase in raw material costs in turn result in an increase in final product prices and makes it difficult to have stability in market prices. Technical Personnel Issue: The fact that forest industry engineers especially do not have a sufficient level of material knowledge by the time they graduate from their faculties' causes major problems in work environments in factories. It is not possible for employers to cover up such insufficiencies of engineers, and therefore providing employment opportunities in production lines of work to forest industry engineers becomes more difficult.

The basic purpose of this study is to project the future demand based on the board sector data from the past and thereby bringing solution recommendations to known issues. Two distinct scenarios were developed for the purpose of demand projection. While only the yearly change was considered in the first scenario, what the demand would be was calculated on the basis of socio-economic variables in the second scenario.

Materials and Methods

Cases where a dependent variable can be calculated using a single independent variable is very rare In particular, the planning and management of forest resources have a very multi-dimensional structure. Accordingly multidimensional decision taking methods are suitable for the structure of forest resources and more substantial decisions and solution propositions are possible when these methods are used (Daşdemir and Güngör, 2002). The most widely used and most suitable technique for multidimensional decision taking methods and in forestry studies is regression (Altunışık et al., 2002; Yazıcıoğlu and Erdoğan, 2004; Kalaycı, 2006). From this perspective, a multidimensional linear regression model was used in this study. An attempt was made to determine the future demand for wood raw materials to be used in board production using multiple regression. Moreover, wood requirement was determined considering Turkey's current board production and predictions on the amount of raw materials to be needed in the future are listed.

Amount of industrial wood production used in board production between 1980-2010 (WP), population (PPL), Gross Domestic Product per capita in US dollars on basis of current producer prices (GDP$) and number of completed buildings (COMPBLDG) factors were taken as socioeconomic variables and considered as the material in this study. Data pertaining to these factors were taken from General Directorate of Forestry (OGM), Turkish Statistical Institute (TÜİK), Istanbul Chamber of Commerce (ITO) and State Planning Agency and are given in Table 1 below.

Table 1. Values of independent variables between 1980-2010

Years	URM	NFS	GSMH	TAMINS
1980	6,796,950	44,736,957	1,539	63,301
1981	7,312,423	45,922,457	157	57,232
1982	5,839,416	47,107,957	1,375	54,156
1983	6,683,409	48,293,457	1,264	54,532
1984	7,614,403	49,478,957	1,204	57,201
1985	7,425,396	50,664,458	133	52,183
1986	7,570,000	51,826,173	1,462	71,461
1987	7,251,000	52,987,888	1,636	80,520
1988	7,447,000	54,149,603	1,684	83,714
1989	7,460,000	55,311,318	1,959	94,799
1990	6,581,000	56,473,035	2,682	94,489
1991	6,513,000	57,606,124	2,621	92,388
1992	6,897,000	58,739,213	2,708	105,293
1993	7,010,000	59,872,302	3,004	101,712
1994	6,712,000	61,005,391	2,184	99,993
1995	8,046,000	62,138,480	2,759	96,661
1996	7,528,000	63,271,569	2,928	104,776
1997	6,974,000	64,404,658	3,079	106,406
1998	7,051,000	65,537,747	4,168	91,816
1999	7,066,000	66,670,836	3,739	86,777
2000	7,329,000	67,803,927	3,914	90,849
2001	6,777,671	68,201,403	2,878	86,155
2002	8,005,138	68,598,879	3,326	47,094
2003	7,320,498	68,996,355	4,341	50,140
2004	8,253,000	69,393,831	5,487	75,495
2005	8,100,284	69,791,307	6,681	114,254
2006	9,298,696	70,188,783	7,214	114,204
2007	10,053,000	70,586,256	9,212	105,865
2008	11,542,000	71,517,100	8,507	93,013
2009	11,464,000	72,561,312	9,318	93,493
2010	12,570,000	73,722,988	10,190	93,961

“Significant (Sig.)” variables with values that exceed 0.001 or 0.05 must be removed from the model. However, because we believe removal of these variables would affect the basis of the study, we included all the independent variables in the model. Analysis of all models were made using SPSS software suit.

Finding

Multiple regression method was used in order to determine the board production volume and future demand. Independent variables' ability in percentage in explaining dependent variable is given in Table 2.

Table 2. Model Summary

Model	R	R Square	Adjusted R Square	Std. Error of the Estimate	Change Statistics					Durbin-Watson
					R Square Change	F Change	df1	df2	Sig. F Change	
1	,892[a]	,796	,774	747539,142	,796	35,205	3	27	,000	1,471

a.Predictors: (Constant), TAMINS, GSMH, NFS
b.Dependent Variable: URM

We see that independent variables explain dependent variable by 79.6% in the model summary, which consists of the first results of regression analysis carried out for the purpose of determining the amount of industrial wood needed for board production. On the other hand, the model's significance level turned out to be 0.000, and it was ascertained that there is a significant correlation (at 0.001 level) between independent variables included in the model and dependent variable. The model for purpose of determining the industrial wood production volume was formulated in the light of the data given in Table 3.

Table 3. Model data used in projection of industrial wood production volume

Model		Unstandardized Coefficients		Standardized Coefficients	t	Sig.
		B	Std. Error	Beta		
1	(Constant)	9560592,005	1453407,338		6,578	,000
	NFS	-,053	,029	-,300	-1,853	,075
	GSMH	681,002	91,022	1,186	7,482	,000
	TAMINS	-11,885	7,875	-,154	-1,509	,143

a.Dependent Variable: URM

In accordance with the data given in Table 3, industrial wood production model is formulated as follows.

$$Y=-0,053*NFS+681,002*GSMH-11,885*TAMINS$$

With the help of this formula, it is understood that industrial wood production will change directly correlated to changes in population and Gross Domestic Product and inversely correlated to number of completed buildings. Independent variables' values for years between 2011-2010 have been calculated using simple regression and used in corresponding years in multiple regression analysis model. Industrial wood production volume was found on basis of these calculations and given in Table 4.

Table 4. Projection of industrial wood production

Years	Projection of industrial wood production
2011	11,153,206
2012	11,463,410
2013	11,773,614
2014	12,083,818
2015	12,394,022
2016	12,7042,27
2017	13,014,431
2018	13,324,635
2019	13,634,839
2020	13,945,043

On the other hand, according to data of the Chip Board Industrialists Association (2012), Chip Board Factories in Turkey has 17,427 m^3/day established capacity. These factories have an actual daily production of 14,437 m^3 (5,269,505 m^3 per year). On the other hand, capacity of established and active fiber board factories is 13,645 m^3/day (4,980,425 m^3 per year). The yearly wood requirement of active capacities (as opposed to that of the established capacities) are [1] 15.6 million steres of wood for chip board. Likewise, wood needed for fiber board is 21 million steres. Therefore, Turkey's wood requirement only for the board sector is approximately 37 million steres. Current production volume is 20-25 million steres in our calculations. It is understood that this volume is insufficient today and a production of such limited volume will not meet future requirements.

Conclusions and Recommendations

Recommendations about the problems encountered in board production and predictions on the future are given below in the light of the findings of the study:

- In order to meet the industrial wood demand, it is essential to carry out initial demand forecasts and to revisit forecasts each year.
- Industrial plantation operations for the purpose of meeting the needs of forest industry must be accelerated as the demand will increase in the future.
- Generalization of sustainable forest management and certification practices, and prediction of future certified wood demand are essential.
- New practices to increase the productivity of Turkey's forests must be accelerated. Silvicultural practices, which are of great relevance in meeting the quantitative wood demands of the forest industry in particular, must be prioritized. In this context, shortening the management periods, especially in relation to red pine, can be considered as an option.
- It is essential to identify areas to be used for wood production in the scope of functional planning, to carry out practices in accordance with such planning, and to review management plans.

[1] Amount of wood needed to produce 1 m^3 chip board is approximately 2-3 steres. Amount of wood needed to produce 1 m^3 fiber board is 4-4.5 steres. Calculations were based on the aforementioned figures.

- We shouldn't delay in fulfilling the requirements of sustainable forest management and BREED characteristics and international processes must be considered while deciding on wood production policies.
- Material knowledge, management and organization issues must have greater focus in education of Forest Industry Engineers.
- Allocations made for forest villagers must be reviewed with due consideration to the future of the forest industry.
- Because the raw material requirements of the sector will increase due to new initiatives in the future, both the private sector and state must launch afforestation practices, in particular using quick developing species, nearby factories of large capacities. Red Pine and Poplar, which are able to adapt in Turkey's conditions, may be preferred as quick developing species.

References

ALTUNIŞIK, R., COŞKUN, R., YILDIRIM, E., BAYRAKTAROĞLU, S., 2002. *Sosyal Bilimlerde Araştırma Yöntemleri SPSS Uygulamalı*, Sakarya Kitabevi, ISBN 975-8644-07-6.İkinci Baskı, Sakarya.

BİRLER, A.S., 1998. Endüstriyel Plantasyonlar (Orman Ağaçları Tarımı). Çevre ve İnsan. Anadolu Üniversitesi Açıköğretim Fakültesi Yayınları. Anadolu Üniversitesi Yayın No: 1017, Açıköğretim Fakültesi Yayın No: 560, Bölüm 9, 175-188.

CUBBAGE, F., MAC DONAGH, P., SAWINSKI JÚNIOR, J., RUBILAR, R.,DONOSO, P., FERREIRA, A., HOEFLICH, V., MORALES OLMOS, V., FERREIRA, G., BALMELLI, G., SIRY, J., NOEMI BÁEZ, M., ALVAREZ, J., 2007. "Timber investment returns for selected plantation and native forests in South America and the Southern United States," *New Forests*. 33(3):237-255.

DAMETTE, O., DELACOTE, P., 2011. Unsustainable timber harvesting, deforestation and the role of certification. *Ecological Economics*, 70(6). 1, 2.1.

DAŞDEMİR, İ., GÜNGÖR, E., 2002. Çok Boyutlu Karar Verme Metotları ve Ormancılıkta Uygulama Alanları. ZKÜ Bartın Orman Fakültesi Dergisi (4), 1-19.

EKİZOĞLU A., 1985: Türkiye'de Yonga Levha Endüstrisi Sorunları ve Çözüm Yolları. Doktora Tezi, İstanbul

EKİZOĞLU, A., 2008. Orman Endüstri Politikası Ders Notları (Basılmamış).

EKIZOĞLU A., YILDIRIM H.T., 2011. Lecture Notes of Forest Industry Policy (Unpublished). Istanbul, Turkey.

HETEMÄKI, L., NILSSON, S., (Eds.). 2005. Information Technology and the Forest Sector. IUFRO World Series, Vol. 18

INGOLD, K., ZIMMERMANN, W., 2011. How and why forest managers adapt to socio-economic changes: a case study analysis in Swiss forest enterprises, Forest Policy and Economics 13 (2011): 97–103.

İLTER E, OK, K., 2007. Ormancılık ve Orman Endüstrisinde Pazarlama İlkeleri ve Yönetimi. Geliştirilmiş 2. Baskı. Form Ofset Matbaacılık. Ankara, Turkey.

KALAYCI, S., 2006. *SPSS Uygulamalı Çok Değişkenli İstatistik Teknikleri* 2. Baskı, Asil Yayın Dağıtım, Ankara, 975-9091-14-3.

KAPLAN, E., 2008. Türkiye'de Orman Ürünleri Talebi ile Arz Kaynaklarının Değerlendirilmesi Ve Endüstriyel Plantasyonların Yeri. 150th Anniversary of Forestry Education in Turkey. Bottlenecks, Solutions, and Priorities in the Context of Functions of Forest Resources / 17-19 October 2007, İstanbul.

KROTT, M., 2005: Forest Policy Analysis. ISBN 978-1-4020-3485-5 (e-book), Springer [online] www.springeronline.com [Referans Tarihi: 01.02.2007]

MAHAPATRA, A., MITCHELL, C.P., 1997. Sustainable development of non-timber forest products: implication for forest Management in India. Forest Ecology and Management, 94, 15–29.

OGM, 2006. Ministry of Forestry Annual Statistic Database. [online] www.ogm.gov.tr. Accessed 03 August 2007.

OGM, 2008. Evaluation of Production and Marketing Activities 2008. [online] www.ogm.gov.tr. Accessed 15 March 2009

OGM, 2011. General Directorate of Forestry Annual Report 2010, Ankara, Turkey.

OK, K., 2005."Idea Marketing in Forestry: Some Implications from the Turkish Forestry Experience", *Forest Policy and Economics*, vol. 7, s. 493-500.

PAUL, S., CHAKRABARTI, S., 2011. Socio-economic issues in forest management in India. *Forest Policy and Economics*, vol. 13, issue 1, pages 55-60.

SCHANZ, H., 2002. National forest programmes as discursive institutions. Forest Policy and Economics 4, 269–279

TOPPINEN, A., KUULUVAINAN, J., 2010. Forest sector modeling in Europe. State of art and future, Helsinki University.

YAZICIOĞLU, Y., ERDOĞAN, S., 2004. SPSS Uygulamalı Bilimsel Araştırma Yöntemleri, Detay Yayıncılık, Ankara, 975-8326-98-8.

YILDIRIM, H.T., 2010. Türkiye'de odun üretim tüketim ilişkilerinin ormancılık politikası açısından irdelenmesi **(**Examination Of Wood Production-Consumption Relations In

Terms Of Forest Policy In Turkey**)**. İ.Ü. Fen Bilimleri Enstitüsü Doktora Tezi (PhD Thesis)(Yayımlanmamış), İstanbul.

ZENGİN, H., 2009. Yonga Levha ve Lif Levha Endüstrisinde Odun Hammaddesi Sağlanması Sorunları ve Çözüm Yolları. (Problems and Solutions on Providing Wood Raw Material in Sheet and Plate Chip Industries) İ.Ü. Fen Bilimleri Enstitüsü Doktora Tezi (Master Thesis)(Yayımlanmamış), İstanbul.

A Life Cycle Assessment of Forest Carbon Balance and Carbon Emissions of Timber Harvesting in West Virginia, USA

Wenshu Lin [1] *– Jingxin Wang*[2*] *– Pradip Saud*[3]

[1] Lecturer, College of Engineering and Technology, Northeast Forestry University, Harbin, China.
wenshu2009@gmail.com
[2] Professor, Division of Forestry and Natural Resources, West Virginia University, Morgantown WV, USA.
* *Corresponding author*
jxwang@wvu.edu
[3] Graduate Research Assistant, Division of Forestry and Natural Resources, West Virginia University, Morgantown WV, USA.
pradipsaud@yahoo.com

Abstract

Forest management activities such as harvesting and transportation emit carbon dioxide (CO_2) and these emissions are often overlooked when estimating the carbon benefits from forests and forest products. This study assessed the net aboveground biological carbon balance of mixed hardwood forests in West Virginia and carbon emissions from the use of fossil fuels in timber harvesting. A life cycle inventory framework of 'cradle to gate' combined with Monte Carlo stochastic simulation was used to analyze the forest carbon balance and emissions from year 2000 to 2009. The results showed that the annual carbon balance of the forests per hectare was not significantly affected by carbon loss from the volume of removal, fire and limited dead trees, unless the number of dead trees or harvesting intensity are increased. Additionally, it was found that average carbon emissions from fossil fuel consumption were 5.06 ± 0.90 metric tons per thousand cubic meters (Mg/TCM) of timber produced using a manual harvesting systems and 6.84 ± 1.22 Mg/TCM when using a mechanized harvesting system. The forest carbon displacement rate during timber harvesting was affected largely by the hauling process compared to felling, processing, skidding and loading processes. Species group, forest type, and harvest intensity influenced forest carbon displacement rates and carbon in harvested timber. Uncertainty of carbon emissions from fuel consumption and forest carbon displacement rate was also related to hauling distance, payload size, forest type, and machine productivity.

***Keywords*:** A. Carbon balance, B. Life cycle inventory, C. Sensitivity analysis, D. Energy consumption.

Introduction

Increasing concentration of carbon dioxide (CO_2) and other greenhouse gases (GHGs) in the atmosphere inspires development of strategies to mitigate climate change impact (Petit et al. 1999; Vannien and Makela 2004; IPCC 2006). One climate mitigation strategies is to focus on increasing the amount of carbon stored in forests or forest products and quantifying the carbon (C) budgets of forest stands (Raupach et al. 2007; Hennigar et al. 2008). Forests, being the largest terrestrial carbon reservoir (Dixon et al. 1994), may increase or decrease carbon stock using different management strategies and practices (Richard et al. 1997).

An assessment of forest carbon that includes timber harvesting intensity level, forest growth rates, dead trees and forest fire loss is necessary to characterize the net forest carbon balance of the existing forest stock. Similarly, consideration of different forest types, harvesting systems, harvesting residue extraction systems, and truck types, would be useful to illustrate the variation of carbon emission rates that could potentially occur during the timber harvesting process. Thus, it is imperative to analyze and quantify forest carbon balances and variation in carbon emissions traceable to fossil fuel consumption in the process of evaluating forest harvesting and management practices. Therefore, the objective of this study was to evaluate the net carbon offset of central Appalachian hardwood forests under current management and harvesting strategies using life cycle inventory (LCI) approach to address current and future sustainability in terms of carbon balance and carbon accumulation potential of forests. The specific objectives were to (1) assess the forest carbon balance of mixed hardwood forests in West Virginia, and (2) analyze the carbon emissions from fossil fuel combustions of harvesting systems in West Virginia.

Materials and Methods

Data. Natural regenerating forests in West Virginia representing typical central Appalachian forests sequester a vast quantity of atmospheric carbon. This carbon capture serves to offset carbon emissions from fossil fuel consumption in transportation and industrial process. Forestland covers almost 76% of the state and 71% of the forests are privately owned (Milauskas and Wang 2006; USDA FS 2010). Data on forest growth and removals, and harvesting production and costs obtained from published literature and public archives were used, within a cradle to gate (sawmill gate) life cycle inventory framework, following inventory data collection rules (ISO 2006) and good practice guidance for forestry practices (IPCC 2006). The system boundary encompassed harvesting systems that include fuel consumption in terms of felling, processing (topping and delimbing), skidding, loading, and hauling to a sawmill. Site regeneration factor was not included in the boundary. We selected a thousand cubic meter (TCM) volume of harvested hardwood timber as the base functional unit in harvesting system analysis.

Timberland data were obtained from an online Forest Inventory and Analysis database (FIA) maintained by USDA Forest Service (USDA FS 2010). Annual growing stock, annual removal, annual mortality (dead and fire), and annual growth of the forest tree

species group were categorized by species groups. Net volume of live trees above 12.7cm (>5 inches) diameter at breast height (dbh) was included in carbon analysis in regard to commercial uses of these trees for either pulp or structural purposes. Mixed hardwood (MHRD) species were considered for analysis and it comprise almost 95% of the forest area. Inventory data on net volume of live trees and net volume of dead trees were available for 2000, 2004, 2005, 2006, 2007, 2008 and 2009. However, data on net growth volume and harvested volume were only available for the years of 2000, 2006, 2008 and 2009.

The green weight of harvested residue biomass ($BHres_i$) by species group ($i=1, 2, \ldots, 19$) was estimated in metric tons (Mg) using Eq.1. The product of harvested volume (Hv_i) is in m^3 and density is in green weight ($Dengwt_i$) in metric tons/m^3. It was assumed that branches and tops of a tree contains biomass equivalent to 29% extra of the total stem biomass in the Northeastern region (INRS 2007). It was also assumed that only 65% of wood residue can be economically extracted and are available due to technical and topographic feasibility (Perlack et al. 2005). However, these two parameters can be adjusted according to different biomass and operational conditions.

$$BHres_i = 65\% * (Hv_i * Dengwt_i * 29)/71 \qquad \forall\ i. \qquad (1)$$

Where, $BHres_i$ means the harvested residue biomass by species group i;
Hv_i means harvested volume by species group i;
$Dengwt_i$ means the density in green weight by species group i.

Forest Carbon Estimation. Carbon (CHv_i) of tree species (i) in harvested volume (Hv_i) was estimated using Eq. (2) by multiplying the harvested volume (Hv_i) by specific gravity (Sg_i) of the tree species at oven dry weight (Alden 1995) for each tree species and assuming a 50% of the total dry biomass weight is carbon (Smith et al. 2006). Similarly, carbon in wood residue ($CBHres_i$) was estimated at oven dry weight in Mg (Eq. 3). Carbon sequestered by dead trees (CB_D) was also estimated in metric tons. Since forest fire is another important factor for forest carbon loss, we estimated carbon emissions due to fires from 2002 to 2009 based on the data obtained from the West Virginia Division of Forestry (WVDOF 2010). Carbon loss from tree by forest fires (CB_F) was estimated in Mg ha^{-1} using an average estimated carbon content of current forest productivity per unit area times burnt forest area (ha).

Net carbon balance (C_{BL}), in metric tons per hectare ($Mg\ ha^{-1}$), of aboveground stem biomass was estimated (Eq. 4) by subtracting mean carbon removals CH_V, CB_D, and CB_F from existing carbon stock (CS) and adding by the mean carbon growth (CB_G). It was also examined for 200 years using Monte Carlo simulation to evaluate the uncertainty of forest carbon balance using mean (μ) and standard deviation (σ) and assuming a normal distribution of 1000 randomly generated numbers. Forest carbon displacement rate (DC_r) that determines reduction in carbon balance of harvested timber at the expense of carbon emission from fossil fuel consumption was calculated using Eq. (5). TCF_c is total carbon emission from fossil fuel consumption. However, the carbon sequestered by roots, branches, foliage and leaf litter on the forest floor was not considered in this study.

$$CHv_i = 0.5 * Hv_i * Sg_i \qquad \forall i. \tag{2}$$

$$CBHres_i = \frac{BHres_i}{Dengwt_i} * Sg_i * 0.5 \tag{3}$$

$$C_{BL} = CB_G + (CS - CH_V - CB_D - \mathrm{CB_F}) \tag{4}$$

$$DC_r = \frac{CHv_i - TCF_c}{CHv_i} * 100\% \tag{5}$$

Where, CHv_i is the harvested timber carbon of species group *i* (Mg TCM^{-1}); Hv_i is the harvested volume of species group *i* (TCM); Sg_i represents the specific gravity of timber of species group *i*; $CBHres_i$ is the wood residue carbon in species group *i* (Mg TCM^{-1}); $BHres_i$ is the oven-dry weight of harvested residue biomass of species group *i* (Mg TCM^{-1}); $Dengwt_i$ is the density of biomass residue in green weight of species group i (Mg TCM^{-1}); C_{BL} is the net carbon balance (Mg Ha^{-1} for forest; Mg TCM^{-1} for harvested timber); CB_G is the mean carbon growth of forests (Mg Ha^{-1}); *CS* is the existing carbon stock (Mg Ha^{-1}); CH_V is the harvested timber carbon (Mg TCM^{-1}); CB_D is the carbon sequestered by dead trees (Mg TCM^{-1}); CB_F is the carbon loss from forest fires (Mg Ha^{-1}); DC_r is the carbon displacement rate (Mg TCM^{-1}); TCF_c is total carbon emission from fossil fuel consumption (Mg TCM^{-1}).

Carbon Emissions from Fuel Consumptions. C emissions were calculated for both manual and mechanized harvesting systems. Carbon emissions from diesel combustion (CD_c) and gasoline combustion (CG_c) were based on the carbon dioxide emission estimates by USEPA (2005). C emission from lubricant consumption (CL_c) was calculated using the method for industrial product and process by the IPCC (2006). The default carbon content of lubricant, 20.0 kg GJ^{-1} was used on a lower heating value basis. Using the principles outlined in the Good Practice Guidance of IPCC (2006) and by USEPA (2010), the total carbon emission (TCF_c) was estimated (Eq. 6) including C emissions from diesel (Eq. 7), lubricants (Eq. 8) and gasoline (Eq. 9) in timber harvesting, residue extraction, and timber and residue hauling process.

$$TCF_c = CD_c + CL_c + CG_c \tag{6}$$

$$CD_c = \left\{ \sum_{k=1}^{n} Hv \left(\frac{\sigma_{mk}}{Pm_m} + \frac{\sigma_{ok}}{Pm_o} + \frac{\sigma_{pk}}{Pm_p} \right) + \frac{Hv}{pd} \left(d_g * 2\gamma_q + d_p * \gamma_q \right) \right\} \alpha * \delta \quad \forall k. \tag{7}$$

$$CL_c = \left\{ \sum_{k=1}^{n} Hv \left(\frac{\varphi_{mk}}{Pm_m} + \frac{\varphi_{nk}}{Pm_n} + \frac{\varphi_{ok}}{Pm_o} + \frac{\varphi_{pk}}{Pm_p} \right) + \frac{Hv}{pd} \left(d_g * 2\,\partial_l + d_p * \partial_l \right) \right\} \beta * \delta \quad \forall k. \tag{8}$$

$$CG_c = \frac{\tau_{nk}}{Pm_n} * \mathrm{ŋ} * \delta \qquad \forall k. \tag{9}$$

Where, TCF_c is the total carbon emissions, CD_c is the carbon emissions from diesel combustion, CL_c represents carbon emissions from lubricant consumption, CG_c is the carbon emissions from gasoline combustion, *Hv* is the harvested volume (m^3) of timber, *k*

is the k^{th} harvesting system (1 = manual, 2 mechanized); σ, φ, and τ are diesel, lubricant, gasoline consumption rates (liters per hour) of machine *m, n, o,* or *p* in harvesting system *k*; *Pm* is the productive machine hour of the involved machine *m, n, o,* or *p*; *pd* is the net payload (tons) of hauling truck; γ_q and ∂_q are diesel and lubricant consumption rates per km (liters/km) of hauling truck, *dg* is the gravel distance (km), *dp* is the paved distance in km, α is CO_2 emission (Mg) from diesel, β is CO_2 emission (tons) from lubricant, ŋ carbon emission (tons) from gasoline and δ is molecular weight of carbon (tons).

Sensitivity Analysis. In the base case scenario, carbon emissions were estimated for mixed hardwood species skidded for 500 meters distance and hauled 80 km (50 miles) using a 4-axle log truck with a 23 m^3 timber payload size for both mechanized and manual timber harvesting systems. Carbon displacement was analyzed for both harvesting systems and forest group type and residue extraction system. The carbon displacement rate was defined as the carbon emissions resulting from fossil fuel consumption in the harvesting system to the amount of carbon stored in the hauled timber. We categorized mixed hardwood tree species into three major forest type groups based on the national core field guide for North Central and Northeastern regions (USDA FS 2006). The selected major forest groups are (1) Oak-hickory including all oak species, hickory, black walnut and yellow-poplar, (2) Ash-cottonwood, and (3) Maple, beech, basswood and birch. Carbon emissions for mechanized and manual harvesting of mixed hardwood species were simulated to examine the uncertainty of carbon emissions using Markov-chain Monte Carlo (MCMC pack) simulation in R (statistical package). Annual carbon emissions from harvesting systems were proportioned to the system per unit production and simulated for 1000 runs under normal likelihood assumptions.

Results and Discussion

Forest Carbon Balance. During the period 2000 to 2009 in West Virginia, the average annual net volume of standing mixed hardwood forests is 689 ± 30.16 million cubic meters (MCM) with mean carbon stock of 46.76 ± 2.06 Mg ha^{-1}. Annual average additions to forest carbon stocks have been significantly different over the years (p = 1.430e-09) probably due to different growth in volume and removal through harvest and fire. Annual growth in volume of live trees has increased annual carbon accumulation (increase in forest carbon stock) with carbon stock additions also significantly different over the years (p = 0.001386). The annual tree growth added 1.09 ± 0.19 Mg ha^{-1} of C to the existing carbon stock as a statewide average. Annually, 2.6 ± 0.44 million tons (Mt) of C stored in trees were removed through harvesting from timberland with an average removal of 0.16 ± 0.03 Mg ha^{-1} during the period 2000 to 2009. This is equivalent to a removal rate of 44.89 ± 1.69 Mg ha^{-1} for those areas harvested. The mean carbon stock and carbon removed were significantly different among tree species groups. For example, yellow-poplar accounted for an average of 11% of the timberland stock but it constituted an average of 20% of the annually harvested timber volume in West Virginia. Annually, forest fires cause 0.21 ± 0.03 Mg of C loss stored in timberland and it resulted in an average of 0.05 ± 0.02 Mg ha^{-1} carbon loss during the period 2000 to 2009. Since only a small amount of forest carbon loss occurred due to forest fire, it would not significantly reduce net forest carbon balance. An annual carbon loss from net dead trees

is 28.63 ± 15.06 Mg with an average of 6.35 ± 3.09 Mg ha^{-1}. Though a large amount of carbon loss occurred from dead trees, carbon release time in atmosphere would be lagged by the time period required for wood decay. Normally a period of 20 years is required to release carbon from dead trees (Janisch and Harmon 2002).

Simulation of forest growth for the next 100 years showed annual additions to carbon stocks ranging from 0.63 to 1.69 Mg ha-1 (Fig. 1a). The existing carbon balance from 2000 to 2009 would be 41.32 ± 4.11 Mg ha^{-1}. However, the forest carbon balance per hectare would not significantly different from the carbon loss per hectare in coming years because annual forest growth per hectare was attributed to the harvested timber volume and volume loss due to forest fire (Fig. 1b). If we limit the harvesting volume at current rate rather than hectare basis, then the carbon loss trends from forest area would be minimum. Therefore, the continuation of timber harvesting at the current mean annual harvest rate based on hectare would create large gap between carbon balance and carbon loss at constant removal and would be helpful to increase carbon balance through a slight variation in annual carbon accumulation might influenced by dead trees (Fig. 1b). However, this would not be possible in practice because of the increasing demand of wood and wood products. Thus, if we increased current harvesting intensity (volume) by 5% and kept constant for consecutive five years and repeated this process for 100-years period to meet the increasing wood demand, we found that a significant amount of carbon stock would be created and more atmospheric carbon would be sequestered in the forests.

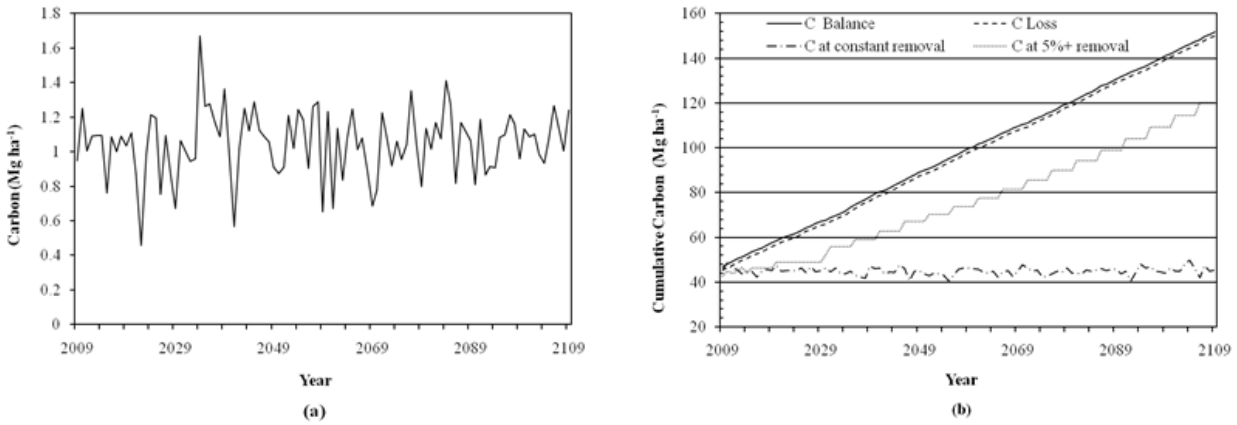

Figure 1. Predicted trends of carbon growth and carbon balance for 100 years:
(a) Carbon accumulation rate per hectare. (b) Cumulative carbon balance from stock and current carbon timber removal rate with the growth rate, constant timber volume removal rate and 5% increment in removal rate at consecutive five years period.

Carbon Emissions from Timber Harvesting and Transportation. Carbon emission rates from consumption of fossil fuel was 5.06 ± 0.90 Mg TCM^{-1} using manual harvesting systems and 6.84 ± 1.22 Mg TCM^{-1} using mechanized harvesting systems with a hauling distance of 80 km or less. Mean carbon emission level from mechanized and manual harvesting systems was not significantly different (p = 0.058) at 95% confidence level. It could be attributed to the similar fuel consumption and productivity rates for loading and hauling in both harvesting systems. Annual carbon emission was directly proportional to

timber volume harvested. Carbon emission in both harvesting systems was lower compared to the average carbon content level (296 kg m^{-3}) of timber harvested that is consistent with the carbon content of (307 kg m^{-3}) for hardwood round logs in the Northeast region (Skog and Nicholson 1998).

Mean carbon emission of combined diesel and gasoline consumption did not differ significantly ($p = 0.106$) while it was significantly different from lubricant consumption ($p = 0.031$) between mechanized and manual harvesting systems. It was 6.06 and 4.61 Mg TCM^{-1} from combined diesel and gasoline consumption, 0.65 and 0.45 Mg TCM^{-1} from lubricant consumption for the mechanized and manual harvesting systems, respectively. In carbon emission level from both harvesting systems, hauling process contributed greater percentage of carbon emission from diesel and gasoline consumption (Table 1). It was followed by felling and skidding in mechanized harvesting system, whereas it was followed by skidding and loading process in manual harvesting system. It was also found that skidding process contributed greater percentage of carbon emissions from lubricant consumption in both harvesting systems.

Table 1. C emissions from fossil fuel due to harvesting hardwood species by harvesting function.

Harvesting	Manual harvesting system		Mechanized harvesting system	
function	Diesel (C %)	Lubricant (C %)	Diesel (C %)	Lubricant (C %)
*Felling	2.61	0.68	24.47	26.23
Processing	-	-	1.64	0.36
Skidding	27.19	83.08	21.65	61.99
Loading	22.71	4.41	16.90	3.10
Hauling	47.48	11.84	35.34	8.32

*Felling in manual harvesting consumes gasoline and topping and delimbing are also associated with felling process.

Carbon Displacement from Forest to Sawmill. Carbon stored in standing trees can be displaced from timberland to sawmill or processing facilities at the expense of carbon emissions from fossil fuel consumption of timber harvesting system. In the base case scenario of mechanized harvesting, the forest carbon displacement rate was 2.31% of the C stored in harvested timber, while it was 1.71% of the C stored in the harvested timber using manual harvesting system. This variation in forest carbon displacement was due to higher carbon emission of using mechanized harvesting system. As hauling distance increased, the carbon displacement rate also increased (Fig. 2a and 2b). It was 4.37% or 3.77%, respectively, for hauling up to 320 km using mechanized harvesting or manual harvesting system. Therefore, longer hauling distance could indirectly decrease the accountability of carbon balance of the harvested timber to some extent.

Approximately 188.5 m^3 (24.8 green Mg ha^{-1}) of logging residue was estimated from harvesting 1000 m^3 of mixed hardwood forests and it contains an average of 56 Mg of carbon. In the base case, payload number was 8, and forest carbon displacement rate was 0.83% and 1.1% of the carbon stored in logging residue using either a cable skidding system or a grappler skidding system, respectively. This difference was due to higher fuel

consumption rate of using grapple skidder in residue extraction. The difference would be greater when hauling for a longer distance, i.e., 1.9% using cable skidder and 2.2% using grappler skidder for hauling up to 320 km (Fig. 2c and 2d). The forest carbon displacement rate varied among forest types (Fig. 2c and 2d) at for different hauling distances. This variation was due to green weight of unchipped residue that limits truck payload size. For example, available residue was 175.02, 147.97, and 153 green metric tons and carbon in wood residue was 55, 52, and 60 Mg for Oak-hickory, Ash-cottonwood and Maple-birch forest group respectively. If the truck payload size is 20 metric ton, then the payload numbers would vary for each forest group, and resulting the hauling cycle number changes for each forest type and fossil fuel consumption rate.

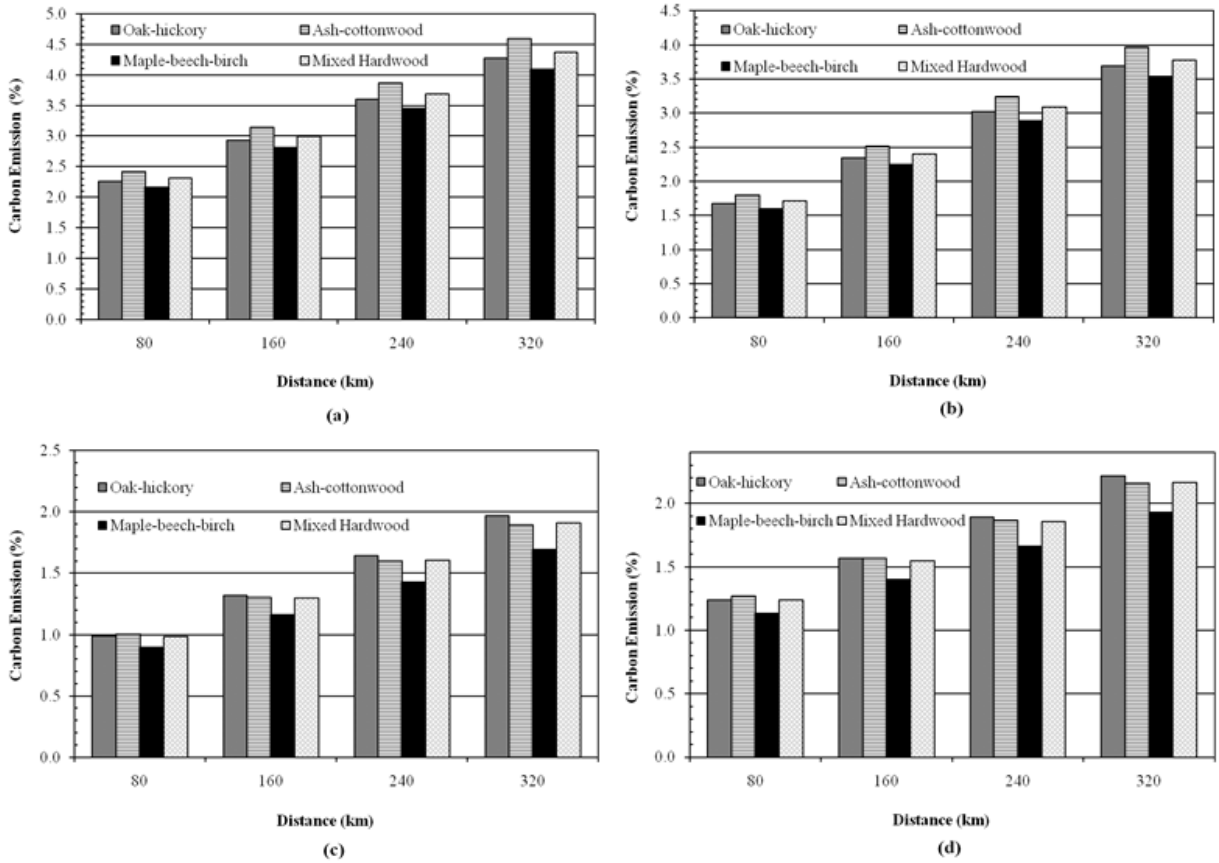

Figure 2. Carbon displacements of four different forest type from the timber harvesting systems and the generated residue extraction system. (a) and (b) timber harvesting under mechanized and manual harvesting systems. (c) and (d) residue extracting under cable and grappler skidding systems.

Sensitivity Analysis and Uncertainty of Carbon Emission. Carbon emission increased with skidding distance (Fig. 3a). It was increased from 0.19-0.47 Mg TCM^{-1} for grappler skidder and from 0.18-0.27 Mg TCM^{-1} for cable skidder when skidding distance changed from 300 to 1,000 m. The amount of carbon emission varied with hauling truck types. In the base case of 80 km hauling distance, the carbon emission amount was approximately the same for all five types of trucks. However, when hauling distance increased up to 320

km, it was found that carbon emission per unit volume of timber transported using a single axle truck was greater than using other truck types (Fig. 3b). A single axle truck has a relatively smaller payload and the similar cycle time though it consumes less fuel compared to other trucks. The use of a single tandem truck (4 axles) or a semi-tractor-trailer (5 axles) would be beneficial in minimizing carbon emissions for hauling a longer distance.

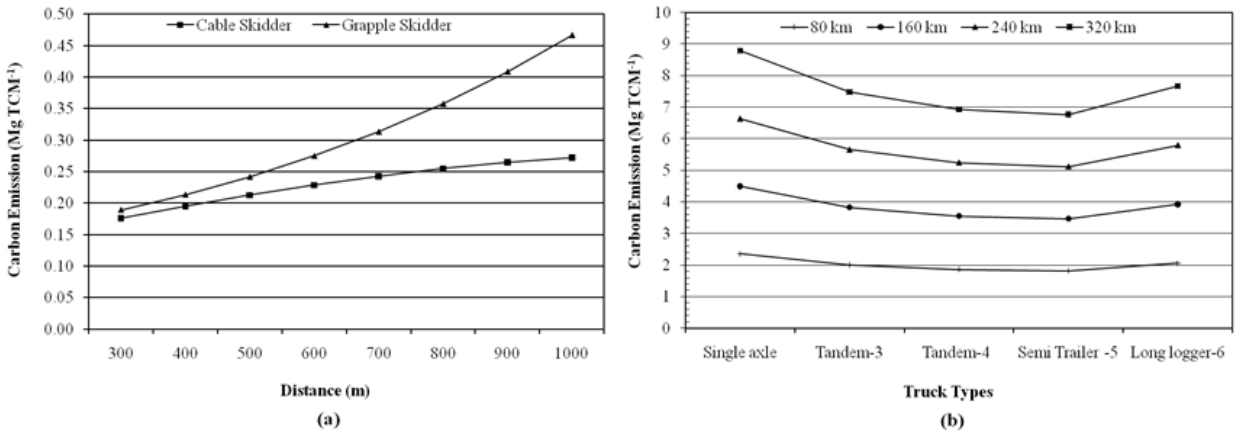

Figure 3. Carbon emission variations during skidding and hauling of mixed hardwood species: (a) by skidder types and skidding distance (meters) and (b) by truck type and hauling distance (km).

Conclusions

Forest carbon removal due to harvesting, fire and limited dead trees does not significantly impair the existing forest carbon stock in West Virginia. However, an increase in the number of dead trees or harvesting intensity could reduce the net carbon balance of timberland. Considering rotation age of natural mixed hardwood forests with slight increase in harvesting intensity would increase forest carbon stock and undermine carbon emissions from fossil fuel consumption of timber harvesting. Such practices would have healthy impacts on carbon stock for timberland and neutralize minor natural depreciation of carbon from fire loss and dead trees.

Natural regeneration in forests, as applicable in the central Appalachian region, entails no fossil fuel consumption in seedling production and plantation and thus results in zero carbon emission level from mechanized instruments. Although mechanized harvesting system emits more carbon into the atmosphere than manual harvesting system, the mean carbon emission does not differ significantly between these two systems. The amount of carbon emissions from fossil fuel consumption due to harvesting is considerably lower than the carbon stored in harvested timber and logging residue. Among harvesting functions, hauling presents a greater effect on carbon emission compared to felling, skidding, topping, delimbing and loading. Hauling distance and truck payload size are the two primary factors that influence carbon emissions, forest carbon displacement rate, and carbon balance in harvested timber. The uncertainty of carbon emissions and carbon

balance of harvested timber depends on harvested timber volume of different forest types and hourly production and fuel consumption of machines in harvesting systems.

References

Alden H.A. 1995. Hardwoods of North America. Gen. Tech. Rep. FPL-GTR-83. Madison, WI: U.S. Department of Agriculture, Forest Service, Forest Products Laboratory. 136 p.

Dixon R.K., Brown S., Houghton R.A., Solomon A.M., Trexler M.C. and Wisniewski J. 1994. Carbon pools and flux of global forest ecosystems. Science. 263:185-190.

EPA (2010) Inventory of US greenhouse gas emissions and sinks: 1990-2008. Available online at: http://www.epa.gov/climatechange/emissions/downloads10/US-GHG-Inventory-2010_ExecutiveSummary.pdf. Accessed on January 20, 2011.

EPA (2005) Average carbon dioxide emissions resulting from gasoline and diesel fuel. Available online at: http://www.etieco.com/content-files/EPA%20emissions%20calc%20420f05001.pdf. Accessed on January 20, 2011.

Hennigar C.R., MacLean D.A. and Amos-Binks L.J. 2008. A novel approach to optimize management strategies for carbon stored in both forests and wood products. Forest Ecology and Management. 256:786-797.

INRS. 2007. Innovative Natural Resource Solutions LLC, Biomass availability analysis-Five counties of Western Massachusetts. Prepared for Massachusetts Division of Energy Resources & Massachusetts Department of Conservation and Recreation. 55p.

IPCC. 2006. 2006 IPCC Guidelines for National Greenhouse Gas Inventories, Prepared by the National Greenhouse Gas Inventories Programme, Eggleston H.S., Buendia L., Miwa K., Ngara T. and Tanabe K. (eds). Published: IGES, Japan. Vol. 4 AFOLU, Chapter 4, 83p.

ISO. 2006. Environment management – Life cycle assessment- Requirements and guidelines. International Organization for Standardization (ISO 14044:2005[E]) 54p.

Janisch J.E. and Harmon M.E. 2002. Successional changes in live and dead wood carbon stores: implication for net ecosystem productivity. Tree Physiology. 22(2-3):77-89.

Milauskas S.J. and Wang J. 2006. West Virginia logger characteristics. Forest Product Journal. 56(2):19-24.

Petit J.R., Jouzel J., Raynaud D., Barkov N.I., Barbola J.M., Basile I., Bender M., Chappellaz J., Davis M., Delaygue G., Delmotte M., Kotlyakov V.M., Legrand M., Lipenkov V.Y., Lorius C., Pépin L. Ritz C., Saltzman E. and Stievenard M. 1999.

Climate and atmospheric history of the past 420,000 years from the Vostok ice core, Antarctica. Nature. 399(6735):429-436.

Perlack R.D., Wright L.L., Turnhollow A.F., Graham R.L., Stokes B.J. and Erbach D.C. 2005. Biomass as feedstock for a bioenergy and bioproducts industry: the technical feasibility of a billion-ton annual supply. Oak Ridge, TN: Oak Ridge National Laboratory. 59 p.

Raupach M.R., Marland G., Ciais P., Quéré C.L., Canadell J.G., Klepper G. and Field C.B. 2007. Global and regional drivers of accelerating CO_2 emissions. Proceedings of the National Academy of Sciences of the United States of America 104:10282-10287.

Richards K.R., Alig R., Kinsman J.D., Palo M. and Sohngen B. 1997. Consideration of country and forestry/landuse characteristics in choosing forestry instruments to achieve climate mitigation goals. Critical reviews in Environmental Science and Technology. 27 (Special): S47-S64.

Skog K.E. and Nicholson G.A. 1998. Carbon cycling through wood products: The role of wood and paper products in carbon sequestration. Forest Product Journal. 48(7/8):75-83.

Smith J.E., Heath L.S., Skog K.E. and Birdsey R.A. 2006. Methods for calculating forest ecosystem and harvested carbon with standard estimates for forest types of the United States. Gen. Tech. Rep. NE-343. Newtown Square, PA: U.S. Department of Agriculture, Forest Service, Northeastern Research Station. 216 p.

USDA FS. 2006. Forest inventory and analysis National core field guide Volume I: field data collection procedures for phase 2 plots. Version 3.1 Northern Edition, 294p.

USDA FS. 2010. Forest Inventory Data Online Version. 2.0. US Department of Agriculture. Forest Service. Available online at http://fiatools.fs.fed.us/fido/index.html. Accessed on Jan 20, 2011.

Vannien P. and Makela A. 2004. Carbon budget for Scots pine trees: effects of size, competition and site fertility on growth allocation and production. Tree Physiology. 25(1):17-30.

West Virginia Division of Forestry. 2010. Fire statistics from recent years. Available online at: http://www.wvforestry.com/dailyfire.cfm. Accessed on June 25, 2010.

An Innovative Approach to Identify Regional Bioenergy Infrastructure Sites

Natalie Martinkus[1] – Aditi Kulkarni[2] - Nicholas Lovrich[3] - Paul Smith[4] - Wenping Shi[5] - John Pierce[6] - Michael Wolcott[7]- Shane Brown[8]*

[1] Graduate Research Assistant, Civil Engineering Department, Washington State University, Pullman WA
[2,5] Graduate Research Assistant, Department of Agricultural and Biological Engineering , The Pennsylvania State University, University Park PA
[3]Regents Professor Emeritus, The Thomas S. Foley Institute for Public Policy and Public Service, Washington State University, Pullman, WA
[4] Professor of Bioproducts Marketing, Department of Agricultural and Biological Engineering, Pennsylvania State University, State College, PA
[6]Affiliate Faculty and Faculty Research Associate, School of Public Affairs and Public Administration, University of Kansas, Lawrence, KS
[7,8]Associate Professor and Professor, Department of Civil and Environmental Engineering, Washington State University, Pullman WA
** Presenter and Corresponding author (Paul Smith)*

Abstract

The Northwest Advanced Renewables Alliance (NARA) has been formed with initial funding from the USDA-NIFA (U.S. Department of Agriculture – National Institute of Food and Agriculture) program to produce aviation biofuels and co-products from woody biomass. Innovative products such as bio-jet fuel (biojet) combine numerous scientific and technical developments to address a significant social need. In order for these innovations to become truly transformational, however, a supply chain of sufficient size must be employed for building and sustaining regional, national, and eventual international impact. Developing major new supply chains for natural resource-based industries must engage communities that represent a convergence of natural resource availability, physical supply chain assets, and a social will and capacity for collective action directed toward sustainable economic development.

This paper describes the development of multiple empirical quantitative measures for core dimensions of community assets. These measures are used to assess community-level resilience and adaptability to change arising from social capital, civic engagement and creative vitality. Community-level social capital and creative capacity, combined with an analysis of physical asset constraints, are merged through GIS application to better understand key community supply chain issues with regard to regional bioenergy infrastructure projects. This knowledge can then be used to develop a more complete understanding of how community social capital and creative capacity might play an

important role in building community support for or addressing community opposition to regional bioenergy infrastructure projects.

Keywords: Biofuels supply chain, bioenergy, creative capacity, social capital, GIS

Introduction

The Northwest Advanced Renewables Alliance (NARA) initiative is focused on developing socially acceptable and economically viable biofuel solutions for the United States Pacific Northwest (PNW) region. Under this project, we are exploring various metrics, methods and analyses to identify potential communities in the PNW states of Idaho, Montana, Oregon and Washington that are "physically" and "socially" able to accommodate and accept potential NARA infrastructure/supply chain nodes and biofuel markets. This paper specifically provides an introduction to some of the physical and social asset tools being developed and deployed to better understand, identify and delineate these NARA communities.

Determination of these pilot communities will be greatly facilitated through an in-depth study using Geographic Information Systems (GIS) to visually display and screen the physical assets and county-level social data, which will enable us to evaluate the creative health and social structure for each state. The advantage of using a GIS-based approach is that both spatial and non-spatial data can be assembled and compared simultaneously using a single quantitative analytical platform. Communities that rank high in both biogeophysical and social characteristics will be considered for final selection as a pilot program. Once the pilot communities are selected, a field study of local stakeholder perceptions will begin to assess the level of receptiveness of various stakeholder groups to the placement of biofuel supply chain nodes in their immediate environment and/or to the adoption of aviation biofuel. This assessment will allow us to "ground truth" our model.

Some of the key physical factors used to determine a site's suitability are proximity to major road and rail, pipeline and petroleum terminals, location relative to major feedstock sources, and a sufficient workforce. Next, Index of Relative Rurality (IRR) scores were considered to determine if population centers of sufficient size and diversity of workforce elements (nearer to 0 on the IRR scale) are located in areas proximate to biomass and related biogeophysical assets. IRR scores indicate potential sites with a population base of sufficient size and scope (typically a "micropolitan" census designation) to permit an effective stakeholder engagement process to explore the potential for collective action around key biomass and biofuel infrastructure as a form of sustainable economic development for their community.

The social characteristics this paper uses to define a promising community include a strong creative arts economy (surrogate for creative thinking capacity), apparent potential for collective action (evidence of social capital attributes), the types and structure of social networks (organizations in which social trust and collective action skills are developed), and support for civic activity (e.g., volunteering). Creative Capacity was examined through the use of the Creative Vitality Index (CVI). CVI serves as a surrogate indicator for the health of the creative arts economy (performing, creative and literary) of a county based on the presence of arts-related businesses, members of the workforce, and non-profit organizations. The work of Richard Florida reported in *The Rise of the*

Creative Class (2002) highlights the strong connection between the presence of these arts-related aspects of local communities and their potential for economic development. The data for US counties were provided by WESTAF (Western States Arts Federation).

Social Capacity was examined with measures of social capital derived from the work of Rupasingha and his colleagues (2000; 2006). The particular two measures used in this project entailed per capita scores for the presence of non-rent seeking organizations[1] and overall social capital scores reflecting: a principal component factor analysis combining non-profit density, census survey participation rate, voter participation level and associated network density. Social Capital, a crucial component of the social assets of a geographical area, is based on an identifiable set of the behaviors, attitudes and values of citizens (Coleman 1990; Putnam 2000; Halpern, 2005) and is the resource that emerges from "the norms and social relations embedded in the social structure of societies that enable people to coordinate action to achieve desired goals" (Borgada et al., 2002). This coordinated collective action is based heavily on "trust", which facilitates the formation of networks and is produced within networks. In turn, these networks are capable of producing purposeful civic activity to achieve shared goals (Coleman, 1988, 1990; Halpern, 2005; Putnam, 2000).

Combined, the paper's biogeophysical and social assets describe both the structural and socio-political components of each community and, in combination with their spatial coincidence, will contribute importantly to the final selection of pilot NARA communities in the four U.S. Pacific Northwest states. This paper's analysis is limited to the evaluation of Montana counties as an illustration of the process.

Methodology

Physical Assets: In order to identify the candidate communities, a GIS analysis was performed on both the physical and social assets in Montana. The physical attributes considered for the analysis include: cities (location and population), major road network, railroad network, 2004 forest residue data (county-level), refined products pipelines, pipeline terminals, and refineries (Figure 1). Assumptions made in this project are based upon the work of Zhang et al. (2011): only cities with a population greater than 1,000 will be considered for potential biofuel facility locations to ensure the availability of a work force; and, potential cities should be located within one mile of state/federal road and railroad networks to ensure that feedstock and co-products can easily be transported. In order to minimize transportation costs, it is important that the conversion facility be located near a pipeline terminal. The terminal will serve as an input point for the finished product, isobutanol. From the terminal, the fuel can then flow to a refinery to be converted into the final product, bio-jet fuel. Using a pipeline will greatly reduce transportation costs, which translates into cheaper overall prices for the aviation biofuel.

A spreadsheet of forest residue volume by county (2004 data) was added into GIS and joined to the county shapefile. The symbology of the County shapefile was changed to graduated colors, and the forest volumes were divided into 6 manually-determined ranges. No data was given on the volume of forest products removed in certain counties

[1]Non rent-seeking organizations: Government restrictions on economic activity produce economic and social benefits called "rents", through licenses, lobbying, restrictions etc. for certain sections of the economic society, at the expense of other sections. Organizations that seek to increase the overall economic wealth instead of capturing "rents" are known as "non rent-seeking organizations" (Krueger, 1974).

in north-eastern Montana and those counties with under 500,000 cu. ft. of forest residues were not color-shaded on the map, resulting in 18 Montana counties with suitable forest residue volume for subsequent consideration and analysis (Figure 1).

ESRI's ArcGIS v.10 ModelBuilder program was used to assess the region's physical assets because of the relative ease with which models can be created to run a series of commands simultaneously in order to solve complex problems. Within the ModelBuilder tool, a weighted analysis can be performed to assign weights to the layers and scaled values to data within a layer, thus enabling the user with a way to compare and prioritize vastly different datasets using the same numerical scale. The ModelBuilder tool was used in this project to identify well-suited communities based on their physical attributes.

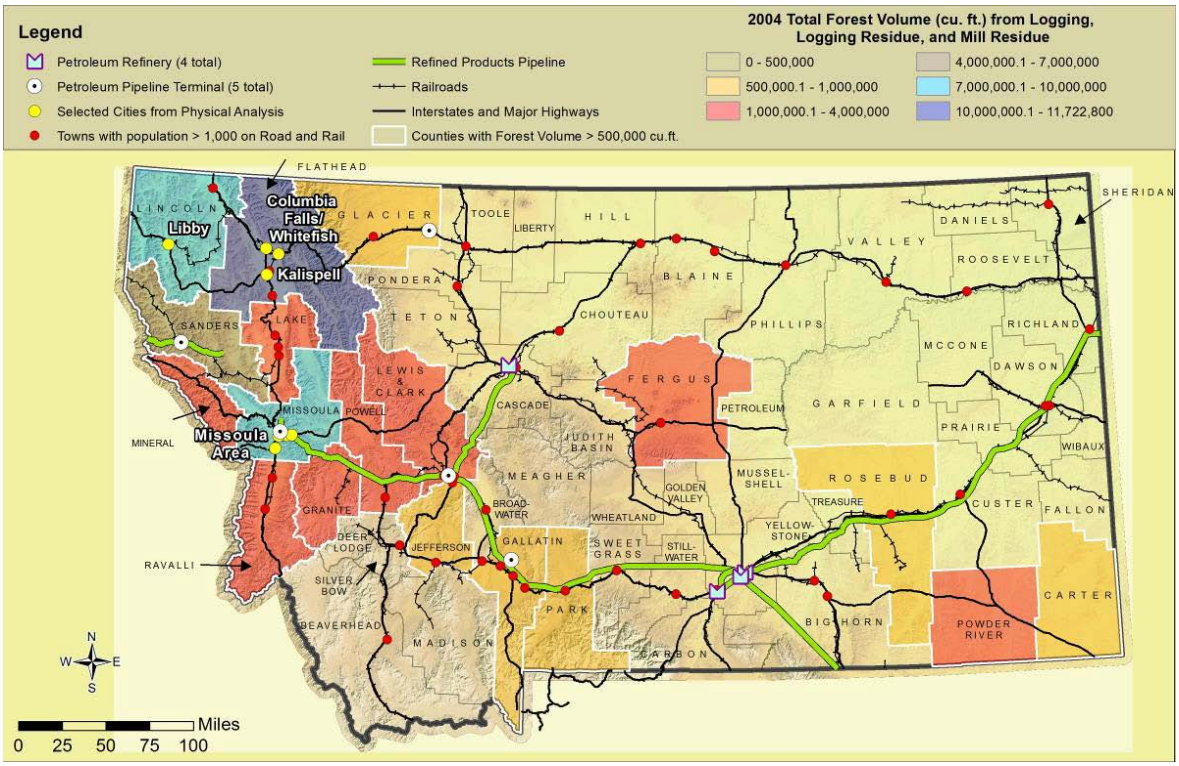

Figure 1. Base Map of Montana with Physical Assets and the 18 Counties with more than 500,000 cu. ft. of Forest Residue

Index of Relative Rurality: We also assessed the degree of "rurality" of a geographical area. To this end we have made use of the IRR, which estimates the degree of rurality of each county, with scores closer to 0 indicating a high level of urbanization and scores closer to 1 representative of high rurality. The IRR is based on four dimensions: population size, density, percentage of urban residents, and distance to the closest metropolitan area (Waldorf, 2006). The counties with scores nearer to 0 on this index that also feature high social asset scores AND spatial proximity to biomass sources and related structural assets will clearly be good candidates for consideration as potential NARA biofuel pilot communities.

Social Assets:

i) Creativity Vitality Index: Creative Capacity assessment was conducted by comparing the creative vitality of the counties within Montana to that of all US counties through the use of the Creativity Vitality Index (CVI). The CVI is an evaluative measure of the health of the creative economy of a given geographical area compared to the national index, and creates a benchmark for future measurement (Western States Arts Federation, 2010). The CVI is a composite score based on two components in a 3:2 ratio that weighs community participation in the arts and concentrations of arts-related employment. Each geographical area is evaluated on these components for the measurement of its CVI score. The national CVI is set at 1.00. This analysis is based on CVI scores of counties and states relative to the national CVI score in 2008.

ii) Social Capital: The level of supportive collective action expected from a particular county is measured through the following two measures:

a. **Putnam Groups (PG) Score:** The sum of per capita presence of non-rent-seeking groups multiplied by a constant for all US counties and has been estimated from various public sources (principally US Census-based statistics and derivative governmental and research centers) by Rupasingha, Goetz and Freshwater (2000). This data has been used in prior studies to predict community-level adaptation to economic change (Rupasingha et al., 2006).
b. **Overall Social Capital (OSC) Score**: This score represents the results of a factor analysis combining, in a single measure, per capita information on all organizations, turnout levels in presidential elections, rate of participation in the US census survey, and the number of tax exempt (non-profit) organizations in each US county.

High Social Capital and CVI scores reflect communities rich in social and creative capital and aids in predicting communities that may act collectively upon the opportunities that engagement with advanced renewable biofuel production presents for the NARA region. Less rural counties with high biomass availability and rich in social attributes may be considered as most suitable locations for pilot programs. Also, more rural areas that are proximate to relatively larger towns with greater biomass availability may also be considered for the pilot program as potential supply chain "procurement" nodes. The literature on "assets-based community development" is replete with examples of communities that have been able to mobilize their social capital and creative problem solving assets for the promotion of community-based economic development and local institutional sustainability.

The social asset analysis using GIS initially involved comparing the IRR values for each county against the highest forest residue-producing counties in the state. Since potential NARA pilot communities must be located in a region with high volumes of biomass, ***the goal is to identify those counties that have high forest residue yields yet also possess suitable human resources to capitalize on the economic development opportunities that may emerge.*** From these communities, we examined the social and creative capital potential. This process leads to geographically-based communities of sufficient size to

permit NARA to engage a sufficient number of stakeholder representatives to facilitate a collaborative process directed toward collective action related to sustainable biofuel production.

Analysis

Physical Assets: In ArcGIS v10, the assumptions were implemented by selecting only those towns in Montana with a population of greater than 1,000 and by creating a 1-mile buffer around all major roadways and railroads. A Euclidean Distance raster of the pipeline terminals within Montana was created to determine the distance from any point in the state to the closest terminal. The resulting raster was then reclassified using the Reclass tool in Model Builder. The distances were divided into 10 equivalent ranges of 40 miles and were assigned a corresponding numerical score from 1-10, with a 10 being the closest to a terminal (0 – 40 miles from a terminal), a 9 being 40 – 80 miles from a terminal, etc. (Figure 1).

The Weighted Overlay tool was then used in Model Builder to combine the buffered road and rail, forest residue volume, and petroleum terminal distance rasters into one weighted raster. All four inputs were given equal weight (25%). Scaled values were assigned to the data within each layer as follows: for the buffered road and rail, any area inside the buffer was given a score of 10 and any area outside the buffer was given a score of 1; the terminal distances were ranked as indicated above; and the forest volumes were ranked with the highest volume range given a score of 10, the lowest volume range a score of 5, and any county with no forest volume data a score of 1. The weighted output raster consists of values ranging from 1 to 10, with a score of 10 indicating those stretches of buffered road and rail that are close to a terminal and in a high-producing forest residue county, and a score of 1 indicating those areas that are outside of the road and rail buffer, have no forest residue volume data, and are located far from a terminal. Nine towns were located in a region with a rank of 10, and include the Missoula area in Missoula County, the Kalispell/Columbia Falls/Whitefish area in Flathead County, and Libby in Lincoln County (all in the northwest region of Montana). These towns may be suited to host a conversion facility based on their county's forest residue volume and their proximity to road, rail, and a pipeline terminal (Figure 1)

Index of Relative Rurality (IRR): Table 1 shows the 18 Montana counties with a forest residue volume of over 500,000 cu. ft. and their corresponding IRR. Those counties with IRR values closer to 0 exhibit relatively lower rurality (higher urbanization) and hence are hypothesized to be better equipped to support NARA infrastructure/supply chain nodes. Accordingly, Table 1 provides IRR detail along with forest residue volume, and social asset scores. Flathead, Missoula, Powell, and Lewis & Clark exhibit both high forest residues and low IRR scores. These counties may be likely candidates for NARA community consideration (Table 1).

Social Assets: Table 1 provides social asset scores for the 18 counties exhibiting forest residue volumes greater than 500,000 cu. ft. Of the three western Montana counties with the greatest forest residue volume, Flathead and Missoula have CVI scores higher than

the national average score of 1.00, indicating higher per capita presence of arts and culture related industries, organizations and occupations as compared to the nation. Missoula is in the top group in regard to overall social capital and Lincoln and Flathead are in the top group for the non-rent-seeking networks (Putnam Group scores) (Table 1). Lincoln's relatively high IRR and Putnam Group score and low CVI score, combined with a large biomass volume and close proximity to Flathead, suggest its value as an important source of biomass material.

Table 1. Top 18 Counties Based on Forest Residues (cu. ft.) (2004) and Corresponding IRR Scores (2000), CVI Scores (2008), PG (2000) and OSC (2009)

County	Forest Residue (cu.ft.) 2004	IRR 2000	CVI 2008	Putnam Groups 2000	Overall Social Capital 2009
Flathead	***11,722,800***	***0.531***	***1.203***	***13.388***	***0.693***
Lincoln	***8,310,650***	***0.654***	***0.539***	***13.850***	***0.713***
Missoula	***8,280,130***	***0.316***	***1.620***	***9.345***	***1.533***
Sanders	5,547,260	0.72	0.313	10.728	1.018
Powell	3,629,180	0.500	0.644	5.656	-0.084
Mineral	2,767,250	0.73	0.362	13.423	1.463
Lake	2,465,490	0.589	0.492	10.260	0.356
Granite	1,713,000	0.75	0.669	3.799	1.599
Powder River	1,681,880	0.88	0.571	20.953	4.511
Lewis and Clark	1,475,520	0.418	0.925	11.643	2.144
Fergus	1,428,070	0.598	0.496	17.603	1.665
Ravalli	1,158,790	0.614	0.743	9.261	0.654
Jefferson	964,112	0.74	0.622	2.025	0.565
Glacier	714,777	0.611	0.378	10.247	-0.472
Carter	693,280	0.91	0.251	13.307	2.541
Park	651,528	0.594	1.035	13.828	1.844
Gallatin	613,440	0.540	1.698	11.127	0.663
Rosebud	604,019	0.75	0.333	9.795	1.038
National Ave.	**--**	**--**	**1.00**	**11.78**	**0.00**

This preliminary analysis focused on Montana and its counties. Going forward, we will analyze all four states in the PNW region to shortlist counties hypothesized to be suitable for NARA activities. Table 2 compares the social attributes of the four NARA-region states to corresponding national scores. The CVI scores for Washington and Oregon are higher than the national mean score of 1.00, indicating a higher per capita presence of arts and culture related industries, organizations and occupations in these areas as compared to the nation. Montana scores are close to the national CVI mean score whereas Idaho lags the region and nation. In terms of PG and OSC state scores, Table 2 shows that, compared to the other states, Montana has a high non-rent-seeking score as well as a high overall social capital score. In the cases of Idaho, Washington and Oregon, the same benefit of simultaneous consideration of biogeophysical and social assets should be apparent. Each of these states features substantial socio-economic diversity, and the

best fit to the needs of the potential sustainable biojet supply chain for the Pacific Northwest will require careful and considerate site selection and stakeholder engagement in the most propitious communities.

Table 2. CVI, PGS and OSC Scores for the PNW Region

Region	Country	CVI (2008)	Putnam Groups (2000)	Overall Social Capital (2009)
Idaho	United States	0.662	6.89	-0.358
Montana	United States	0.921	12.03	1.622
Oregon	United States	1.018	9.61	0.366
Washington	United States	1.014	10.85	-0.518
National	United States	1	11.78	0

Conclusions

The results from the physical attribute analysis suggest the communities of Libby (in Lincoln County), Kallispell/Whitefish/Columbia Falls (in Flathead County) and Missoula (in Missoula County) may be likely candidates for a NARA community based on their proximity to major road and rail, pipeline terminals and high biomass volumes. The results from the social asset analysis indicate that Missoula, Lewis and Clark, and Yellowstone Counties all are less rural, highly urbanized, and have a high potential for creativity and forming networks. Thus, the final selection for our initial target NARA community will be the Missoula greater area in Missoula County, since it contains the desired traits of having both high physical and social assets.

Limitations

First, this paper is limited to Montana and its counties. An in-depth study of all four PNW states and counties is the next step in the ranking and identification of potential NARA communities. Second, this paper provides an initial analysis of biogeophysical and social asset measures and is intended as a primer on the potential metrics, methods and analysis that may be deployed to efficiently determine potentially favorable sites for sustainable economic development activities. Use of CVI scores may be seen as an indicator of a community's willingness and capacity to take on and/or identify innovative solutions to addressing NARA community challenges. The Putnam Groups and Overall Social Capital scores address two dimensions of social capital as networks and may be viewed as the presence of collective capacity to mobilize the political and policy resources necessary to make those solutions happen.

Future work will refine scales and develop additional metrics and indices to further delineate potential sites in Montana and the other three NARA states of Idaho, Oregon and Washington. Finally, these protocols provide an efficient way to quantify conditions conducive to biofuels siting acceptance and, as such, represent powerful tools for developing hypothesis for further testing with the development of on-the-ground validation work protocols.

Literature Cited

Borgada, E.J., Sullivan, J., Oxendine, a. Jackson, M. and Riedel, E. (2002). Civic Culture Meets the Digital Divide: The Role of Community Electronic Networks. *Journal of Social Issues*, 58 (1), 125-140.

Coleman, James S. 1990. *Foundations of Social Theory*. Cambridge, Mass.; Belknap Press.

Florida, Richard (2002). *The Rise of the Creative Class*. New York: Basic Books.

Greenwood, Daphne T. and Richard P.F. Holt. 2010. *Local Economic Development in the 21st Century: Quality of Life and Sustainability*. Armonk, New York: M.E. Sharpe.

Halpern, David. 2005. *Social Capital*. Malden, MA: Polity Press.

Krueger, Anne. 1974. *The Political Economy of the Rent-Seeking Society*. The American Economic Review, Vol. 64, No. 3.

NARA. Web. <*http://nararenewables.org/about*>.

Pierce, J.C., N.P. Lovrich, and H.S. Elway. 2011. "Chapter 1: The Political Culture of Washington State." Governing Washington: Politics and Government in the Evergreen State . Eds. Cornell Clayton and Nicholas Lovrich. Pullman, WA: Washington State University Press.

Putnam, Robert. 2000. *Bowling Alone: The Collapse and Revival of American Community*. New York: Simon and Schuster.

Rupasingha, Anil, Stephen J. Goetz and David Freshwater. 2000. "Social Capital and Economic Growth: A County-Level Analysis." *Journal of Agricultural and Applied Economics* 32: 565-572.

Rupasingha, Anil, Stephen J. Goetz and David Freshwater. 2006. "The Production of Social Capital in U.S. Counties." *Journal of Socio-Economics* 35(1):83-101.

Waldorf, Brigitte S., 2006, "Continuous Multi-dimensional Measure of Rurality: Moving Beyond Threshold Measures." Department of Agricultural Economics, Purdue University, West Lafayette, IN 47907, USA

WESTAF, 2010, "The Creative Vitality™ Index: An Overview." Western States Arts Federation. Web. <*http://www.westaf.org/publications_and_research/cvi*>

Zhang, F, D.M Johnson, and J.W Sutherland. "A GIS-Based Method for Identifying the Optimal Location for a Facility to Convert Forest Biomass to Biofuel." *Biomass and Bioenergy*. 35.9 (2011): 3951-3961. Print.

Quantitative Structural Characters of Lignins Obtained from Residue after Hydrothermal Pretreatment

Jia-Long Wen[1] – Bai-Liang Xue[2] – Feng Xu[3]–Run-Cang Sun[4]*

[1] PHD student, Institute of Biomass Chemistry and Technology- Beijing Forest University, Beijing, China
wenjialonghello@126.com
[2] Master student, Institute of Biomass Chemistry and Technology- Beijing Forest University, Beijing, China
xuebailiang67@163.com
[3] Professor, Institute of Biomass Chemistry and Technology- Beijing Forest University, Beijing, China
xfx315@163.com
[4] Professor and director, Institute of Biomass Chemistry and Technology- Beijing Forest University, Beijing, China
rcsun3@bjfu.edu.cn
* *Corresponding author*

Abstract

Hydrothermally treated (HTT) process was demonstrated to increase enzymatic hydrolysis efficiency of lignocelluloses in the current bio-ethanol production. In this study, to maximize the utilization of enzymatic hydrolysis lignin (EHL), the quantitative information of its structural features were investigated. The structural features of the lignins obtained from different HTT species (softwood, hardwood and grass species) were characterized by FT-IR spectroscopy, gel permeation chromatography (GPC), quantitative ^{13}C and 2D HSQC nuclear magnetic resonance (NMR) spectroscopy. The results reveal that the typical structural features of lignin, such as β-O-4, β-β, and β-5 substructures, are preserved during HTT process. However, some condensed lignin structures from different materials were also detected, especially for pine wood. The degrees of lignin condensation (DC) was decreased in the order of pine (0.63) > birch (0.45) > bamboo (0.15). Interestingly, the lignin from HTT bamboo, *p*-coumaric acid was observed to acylated at γ-position of the lignin, suggested that the HTT process has slight effect on the native ester in the grass lignin. The molecular weights (M_w) of lignin preparations from various HTT biomasses (pine, birch, and bamboo) were 8860, 10840, and 9430 g/mol, respectively. In addition, the lignins isolated from HTT biomass have more uniform molecules, as revealed by low polydispersity values (M_w/M_n, 1.68–1.97).

***Keywords*:** Lignin, Quantitative Structure, S/G ratio, β-O-4, HTT

Introduction

Biorefineries can provide the production of energy, fuels, chemicals and materials as well as food and feed components to enable a lastingly successfully production on the basis of renewable resources [1]. Motivating by the tendency of "biomass refining", lignocellulosic material (LCM) can be "fractionated" into their main components by sequential treatments to give separate streams that may be used for value-added products exploitation. However, the utilization of LCM as chemical feedstock for fuels and chemicals is hindered by the inefficiency. The toughest obstacle of biomass utilization is tight and complex structure of biomass. Therefore, a number of pretreatments, such as including dilute acid, sulfur dioxide, ammonia expansion, and hydrothermal pretreatments, were develop to alleviate the natural obstacle and increase enzymatic hydrolysis [2].

Among these pretreatments, hydrothermal pretreatments are considered to be economically and environmentally attractive technologies aiming at fractionation and utilization of individual components of LCM. These processes have been used for a variety of biomass types and have been shown to work effectively at a commercial scale. The hemicelluloses-based oligosaccharides were firstly removed and collected in the first step [3]. The hydrothermally-treated wood residues were undergone enzymatic hydrolysis to obtain glucose for ethanol production. Furthermore, the enzymatic hydrolysis residues (EHR) are still rich in lignin and small amount of obstinate cellulose. The EHR should be explored as value-added materials to realize the dream of "waste valorization". The objective of this work was firstly to compare qualitative and quantitative structural features of the isolated lignins from hydrothermally pretreated biomass.

Materials and Methods

Materials. *Pinus yunnanensis* (Softwood) and *Betula alnoides* (hardwood) was harvested in October 2010 from Yunnan Province (China). *Bambusa rigida sp.* (grasses) was obtained from Sichuan, China. The content of Klason lignin in *Pinus*, *Betula*, and *Bambusa* is 23%, 24% and 23%, respectively. All chemical reagents used were analytical grade or best available.

Hydrothermal treatment (HTT). The ball-milled wood meals were initially presoaked in deionized water at a solid loading of 5%. Subsequently, the slurry containing water and wood meal was sealed in a 1.0 L high pressure and temperature stainless steel reactor (PARR, America). Then the reactor was purged three times with nitrogen to remove the air/oxygen in the reactor airspace. The ball-milled materials were firstly hydrothermally pretreated at 150 ^{o}C for 2 h. After the reaction completed, the reactor was cooled down to room temperature by cool water, which was installed inside of the reactor.

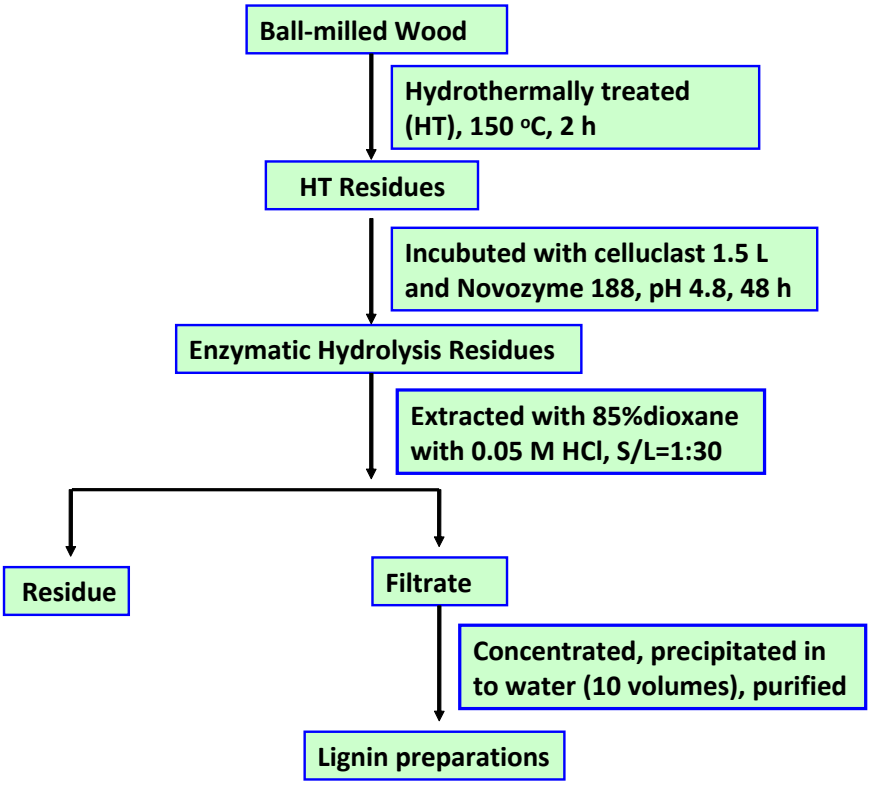

Figure 1. Scheme of lignin isolation from hydrothermally treated residues

Preparation of enzymatic mild acidolysis lignins (EMALs). The EMALs were isolated according to a previous report [4]. The hydrothermally treated wood species (pine, birch and bamboo) (5 g) was suspended in acetate buffer (0.05 mol/L, 100 mL, pH 4.8), with the loading of 200 FPU cellulase (Celluclast 1.5 L) and 200 FPU *β*-glucosidase (Novozyme 188), respectively. The reaction mixture was incubated at 50 ºC in a rotary shaker (150 rpm) for 48 h. After enzymatic hydrolysis, the resulting enzymatic hydrolysis residues (EHRs), which contained carbohydrate impurities, was collected by centrifugation and washed with acidified water (pH=2) followed by freeze-drying. The HERs was then treated with 0.05 M HCl in acidic dioxane-water (85:15, v/v) at 86 °C under nitrogen for 2 hours, respectively. The resulting mixture was filtered and the lignin solution was collected. The solid residue was washed with fresh dioxane until filtrate was clear. The lignin solution and the combined washings were then neutralized with solid sodium bicarbonate. The neutralized solution was finally precipitated in a large quality of acidified water (10 volumes, pH=2) and then the precipitated lignin was collected by centrifugation followed by freeze-drying. To remove the carbohydrate remained in the lignin preparations, the lignins were firstly dissolved in 90% acetic acid, and then the lignin solutions were dropping into 10 volumes of water to induce precipitate. The precipitated lignins were washed with acidified water for several times and then freeze-dried.

Associated Polysaccharides Analysis. The composition of structural carbohydrates was determined using National Renewable Energy Laboratory (NREL) protocol, and analyzed by high-performance anion exchange chromatography (HPAEC) (Dionex, ISC 3000,

Sunnyvale, CA, USA) on a CarboPac PA 20 analytical column (4×250 mm) with pulsed-amperometric detection.

FT-IR Analyses. FT-IR spectra of lignin fractions were conducted using a Thermo Scientific Nicolet iN10 FT-IR Microscope (Thermo Nicolet Corporation, Madison, WI) equipped with a liquid nitrogen cooled MCT detector.

NMR Spectra of EMALs. NMR spectra were recorded on a Bruker AVIII 400 MHz spectrometer at 25 ^{o}C in DMSO-d_6. For the quantitative ^{13}C NMR experiments, 140 mg of lignin was dissolved in 0.5 mL DMSO-d_6. The quantitative ^{13}C NMR spectra were recorded in the FT mode at 100.6 MHz. The inverse gated decoupling sequence (C13IG sequence from Bruker Standard Library), which allows quantitative analysis and comparison of signal intensities, was used with the following parameters: 30^{o} pulse angle; 1.4 s acquisition time; 2 s relaxation delay; 64 K data points, and 30,000 scans. To achieve sufficient relaxation in a feasible time, 20 µl of chromium (III) acetylacetonate (0.01 M) was added as a relaxation agent for the quantitative ^{13}C spectrum to reduce the relaxation delay according to a previous report [5].

Results and Discussion

To understand the quantitative structure and thermal properties of lignins obtained from residue after hydrothermal pretreatment, the purified lignin should be obtained. Herein, the EMAL was isolated according to the existing literature [4]. The carbohydrate contents of EMALs isolated from hydrothermally treated lignocellulosic materials (pine, birch, and bamboo) are given in **Table 1**. It was found that the carbohydrate contents of the lignin preparations varied with different raw-materials. However, the carbohydrate contents in the lignins are low, which will not hinder the structural analysis of lignin in the subsequent sections.

Table 1. Yield and carbohydrate contents of lignin preparations

Samples	Sugar (%)	Ara	Gal	Glu	Xyl	Man	GlcA
Pine	1.63	Tr	0.31	0.40	0.27	0.40	0.20
Birch	1.29	Tr	0.08	0.25	0.86	0.04	0.06
Bamboo	3.46	Tr	0.09	0.61	2.11	Tr	0.29

FT-IR Characterization. The fingerprint region of FT-IR spectra of the EMALs (**Figure 2**) after HTT exhibits typical lignin patterns. The bands at 1593, 1507, and 1421 cm^{-1}, corresponding to aromatic skeletal vibrations and the C–H deformation combined with aromatic ring vibration at 1462 cm^{-1}, are present in these three spectra [6]. For HTT softwood (pine), the composed band system between 1175 and 1065 cm^{-1} showed a maximum at 1138 cm^{-1}. This feature is typical only for G lignins. Another, for hardwood (birch), the same band system showed a maximum at about 1125 cm^{-1}. This is sensitive criterion for GS lignins, indicating the HTT birch lignin belongs to typical GS lignin. However, a band around at 1167 cm^{-1} (C=O vibration of esters) is additionally present in the spectrum of bamboo. Moreover, the whole C=O range between 1800-1633 cm^{-1} is

intense in the spectrum of bamboo. Another intense band at 834 cm^{-1} further indicated that typical HGS lignins of the bamboo.

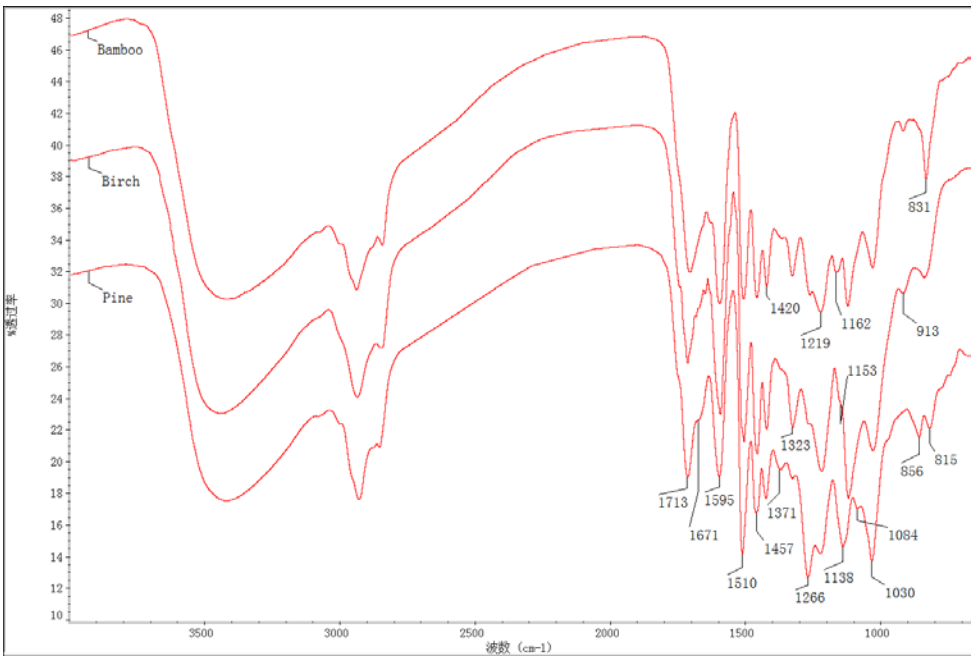

Figure 2. FT-IR spectra of HTT lignins from pine, birch, and bamboo

Estimation of Different Lignin Moieties from Quantitative ^{13}C NMR Spectra. The integral of the 162-102 ppm region was set as the reference, assuming that it includes six aromatic carbons and 0.12 vinylic carbons [7]. It follows that the integral value divided by 6.12 is equivalent to one aromatic ring.

Figure 3 displays the quantitative ^{13}C NMR spectra of the HTT lignins, and Table 2 gives the quantification of the most important lignin moieties. The methoxy groups of the lignins determined by quantitative ^{13}C NMR spectra showed 0.91 (pine EMAL), 1.37 (birch EMAL), and 1.18 (bamboo EMAL) methoxy groups per aromatic ring. Compared with the existing results for methoxy groups of hardwood, softwood and grass, the data presented here is slightly lower, the decrease of aromatic methoxy content is attributed to the demethoxylation during HTT process. In addition, lignin structural moieties, such as aromatic C-O, aromatic C-C, and aromatic C-H, were determined based on quantitative ^{13}C NMR spectra. Furthermore, the content (expressed by per Ar) of lignin inter-linkage β-O-4′, β-β′, and β-5′ were calculated. It was observed that the content of β-β′ and β-5′ is higher in pine than that of in birch and bamboo, suggested that more condensed lignin units presented in the HTT pine EMAL. The degrees of lignin condensation (DC) were also calculated according to Capanema et al. [8, 9]. The DC values were 0.63, 0.45, and 0.15 for the lignins of pine, birch and bamboo, respectively. This also suggested that pine lignin is more condensed.

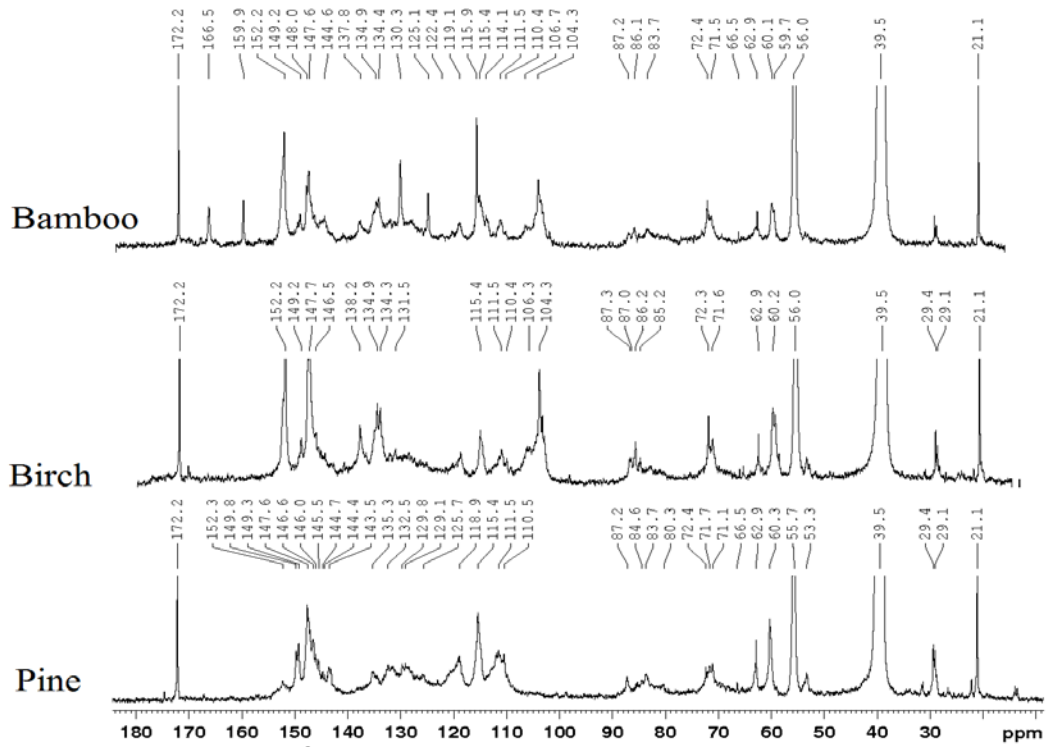

Figure 3. Quantitative ^{13}C-NMR spectra of HTT lignins from pine, birch, and bamboo

Table 2. Main chemical shift assignments in the quantitative ^{13}C-NMR spectra of nonacetylated HTT lignins

		Quantification		
δ (ppm)	Assignments	Pine	Birch	Bamboo
160-140	Aromatic C-O	1.96	2.22	1.87
140-125	Aromatic C-C	1.65	1.79	1.82
125-103	Aromatic C-H	2.37	1.98	2.20
58-54	OCH_3	0.91	1.37	1.18
61.2-58	β-O-4′	0.38	0.39	0.32
54-53	C_β in β-β′, β-5′	0.15	0.08	0.07
	[a] DC	0.63	0.45	0.15

[a] DC, Degree of condensation. For pine wood, DC was calculated by (3.00 - h-units) - [($I_{125\text{-}103}$) + M + 2 × I]; For birch and bamboo, s + g + h=1 (S, G, and H units were calculate from 2D), $I_{theor\ CAr\text{-}H}$= (2s + 3g + 2h), DC=$I_{theor\ CAr\text{-}ii}$—$I_{125\text{-}102\ ppm}$.

2D-HSQC NMR analysis. The inter-linkage and aromatic regions of the HSQC NMR spectra of the three EMALs are shown in **Figures 4 and 5**. The side-chain region (δ_C/δ_H 50-90/2.5-6.0) of the 2D HSQC NMR spectra provided useful information about the inter-coupling bonds present in lignin (β-O-4, β-β, β-5, etc.). As shown in Figure 4, the side-chain regions of the three EMALs in the HSQC spectra were similar except for the associated carbohydrates. The important correlations, such as those from substructures of β-ether (β-O-4) **A**, resinol (β-β) **B**, and phenylcoumaran (β-5) **C** can be readily assigned according to the recent literatures [10].

Table 3. Assignments of ^{13}C-^{1}H cross signals in the HSQC spectra of HTT lignins

Lable	δ_C/δ_H (ppm)	Assignments
C_β	53.1/3.46	C_β–H_β in phenylcoumaran substructures (C)
B_β	53.5/3.07	C_β–H_β in β-β (resinol) substructures (B)
OCH_3	56.4/3.70	C–H in methoxyls
A_γ	59.9/3.35	C_γ–H_γ in β-O-4 substructures (A)
A_γ	59.9/3.80	C_γ–H_γ in β-O-4 substructures (A)
$A_{\gamma'}$	63.1/4.28	C_γ–H_γ in γ-acylated β-O-4 substructures (A′)
B_γ	71.8/3.81	C_γ–H_γ in β-β resinol substructures (B)
B_γ	71.8/4.17	C_γ–H_γ in β-β resinol substructures (B)
A_α	72.0/4.85	C_α–H_α in β-O-4 substructures linked to a S unit (A)
A_β(G/H)	83.5/4.32	C_β–H_β in β-O-4 substructures linked to a G unit (A)
B_α	84.7/4.64	C_α–H_α in β-β (resinol) substructures (B)
A_β(S)	86.0/4.11	C_β–H_β in β-O-4 substructures linked to S (A, *erythro*)
A_β(S)	86.8/3.96	C_β–H_β in β-O-4 substructures linked to S (A, *threo*)
C_α	87.6/5.50	C_α–H_α in phenylcoumaran substructures (C)
$S_{2,6}$	104.2/6.72	$C_{2,6}$–$H_{2,6}$ in syringyl units (S)
$S'_{2,6}$	106.6/7.27	$C_{2,6}$–$H_{2,6}$ in oxidized (C_αOOH) syringyl units (S′)
G_2	111.4/6.96	C_2–H_2 in guaiacyl units (G)
G_5	114.8/6.71	C_5–H_5 in guaiacyl units (G)
G_6	119.8/6.72	C_6–H_6 in guaiacyl units (G)
$H_{2,6}$	128.2/7.17	$C_{2,6}$–$H_{2,6}$ in H units (H)
$PCE_{3,5}$	115.8/6.83	$C_{3,5}$–$H_{3,5}$ in *p*-coumarate
$PCE_{2,6}$	130.2/7.48	$C_{2,6}$–$H_{2,6}$ in *p*-coumarate
PCE_7	144.8/7.51	C_7–H_7 in *p*-coumarate
PCE_8	113.9/6.29	C_8–H_8 in *p*-coumarate

The composition of the lignins is clearly evidenced in the aromatic region of these 2D-HSQC NMR spectra (Figure 5). For birch and bamboo, a significant correlation for the syringyl units (S) was observed at δ_C/δ_H 103.8/6.69 ppm, while their oxidized (α-ketone) structures S' appeared at δ_C/δ_H 106.2/7.28 ppm. With the exception of **S** units, all of the guaiacyl components which are in the lignins can be expressly distinguished. The correlation for the G_2-position is at δ_C/δ_H 110.7/6.96 ppm. In addition, some condensed G_2 was also found at lower field (labeled as condensed structural in Figure 5) [11]. For pine EMAL, G_2 and G_6 was observed to be more condensed. The observations were in agreement with the results obtained from ^{13}C-NMR spectra, in which the degrees of

lignin condensation was decreased in the order of pine (0.63) > birch (0.45) > bamboo (0.15). Specially, the assignments were listed in Table 4 and the major structural features are depicted in **Figure 6**.

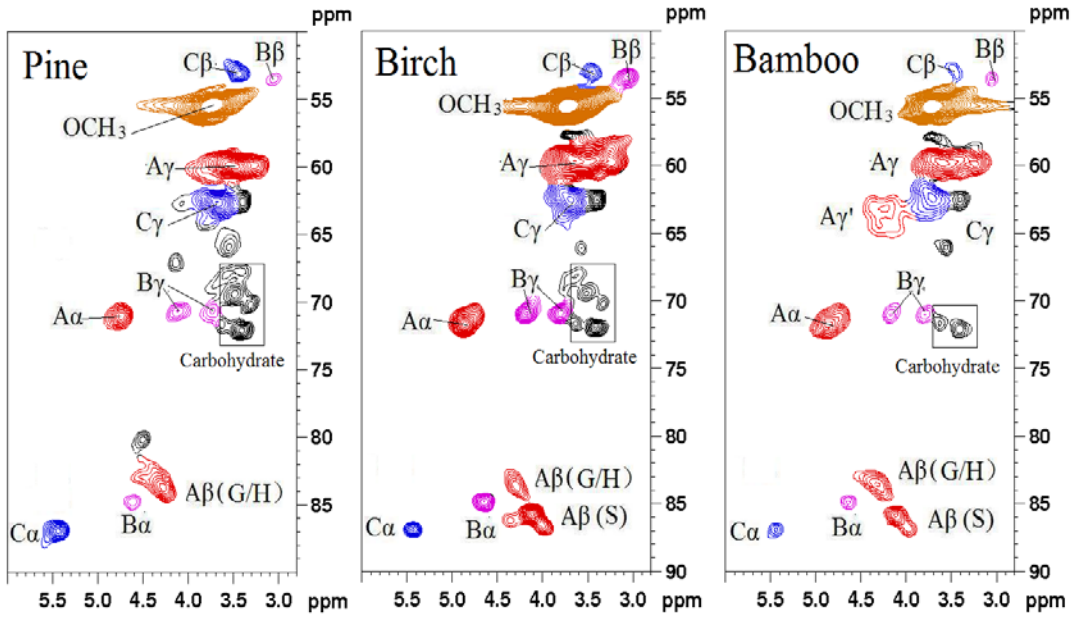

Figure 4. The side-chain regions in 2D HSQC NMR spectra of the lignins

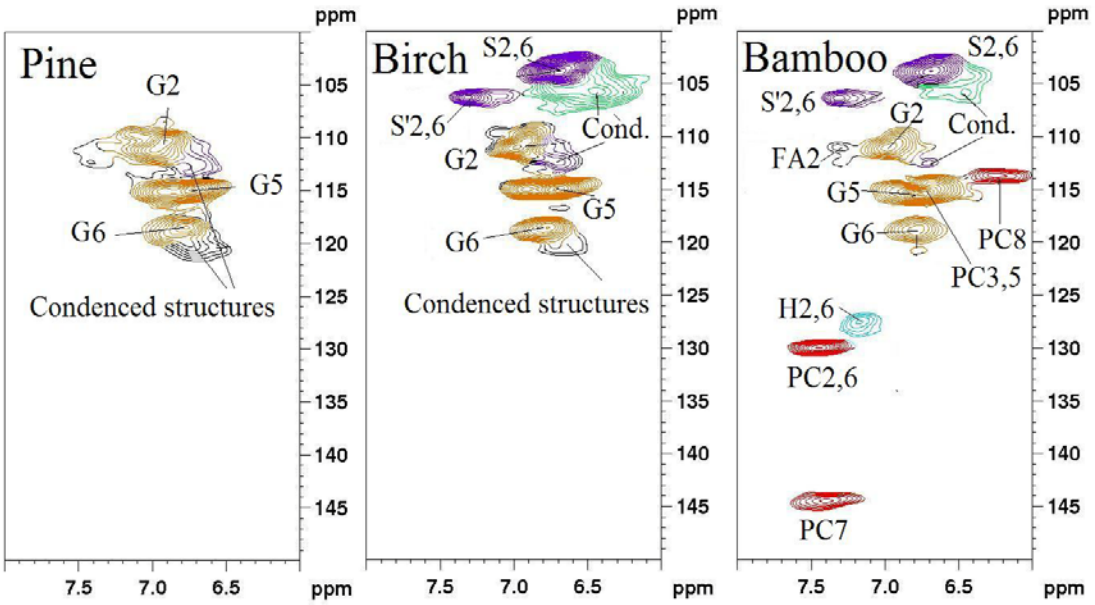

Figure 5. The aromatic regions of 2D HSQC NMR spectra of the lignins

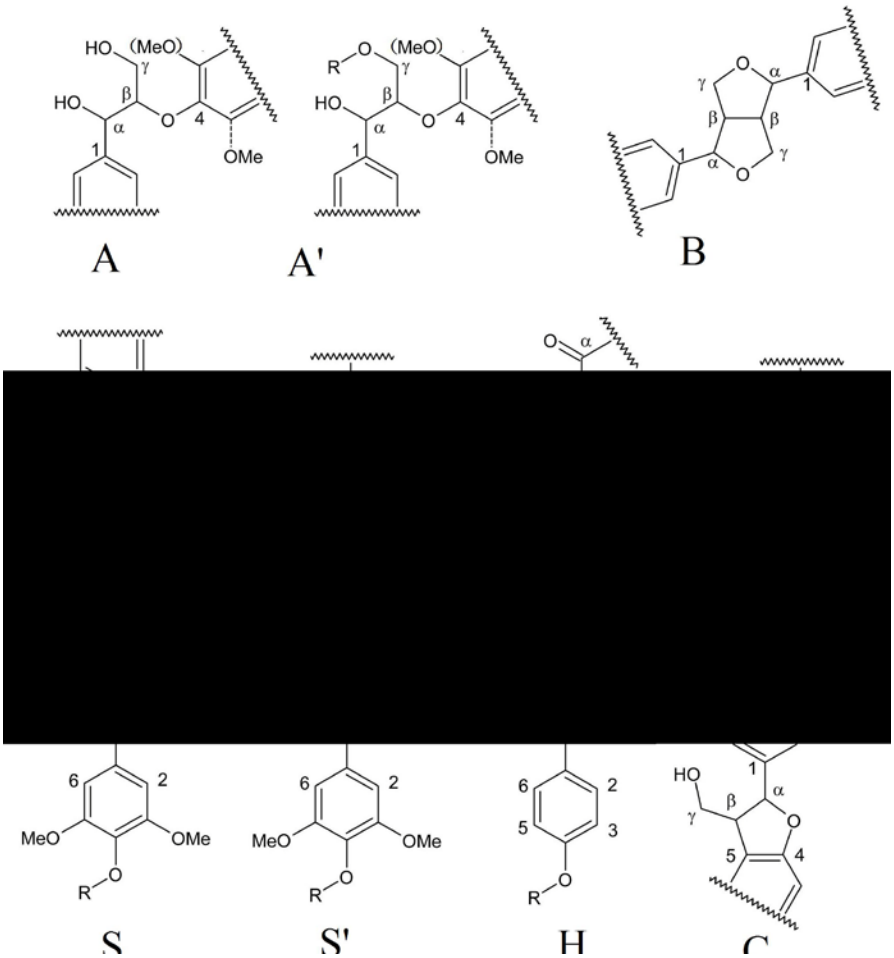

Figure 6. Main lignin substructures in the treated bamboo samples (A) β-O-4 linkages; (A') acylated β-O-4 substructures; (B) resinol structures formed by β-β/α-O-γ/γ-O-α linkages; (C) phenylcoumarane structures formed by β-5/α-O-4 linkages; (S) syringyl unit; (S') oxidized syringyl unit linked a carbonyl or carboxyl group at Cα (phenolic); (H) p-hydroxyphenyl units; (F) *p*-hydroxycinnamyl alcohol end groups; (G) guaiacyl unit; (G') oxidized guaiacyl units with a Cα ketone; (FA) ferulate; (*p*-CA) *p*-coumarate.

Molecular Weights Analysis

Table 4. Weight-average (M_w) and number-average (M_n) molecular weights (g/mol) and polydispersity (M_w/M_n) of the lignin preparations

	M_w	M_n	M_w/M_n
Pine	8860	5260	1.68
Birch	10840	5500	1.97
Bamboo	9430	4950	1.90

Table 4 shows the weight-average (M_w) and number-average (M_n) molecular weights and polydispersity index (M_w/M_n) of lignin preparations isolated from HTT biomass. The molecular weights (M_w) of lignin preparations from various HTT biomasses (pine, birch, and bamboo) were 8860, 10840, and 9430 g/mol, respectively. In addition, the lignin preparations isolated from HTT biomass have more uniform molecules, as indicated by low polydispersity values (M_w/M_n, 1.68–1.97).

Conclusion

Results obtained reveal that the typical structural features of lignin, such as β-O-4, β-β, and β-5 substructures, are preserved during HTT process. However, some condensed lignins from different materials were detected, especially for pine wood. The degrees of lignin condensation (DC) was decreased in the order of pine (0.63) > birch (0.45) > bamboo (0.15). Interestingly, the lignin from HTT bamboo, *p*-coumaric acid was observed to acylated at γ-position of the lignin, suggested that the HTT process has slight effect on the native ester in the grass lignin. The molecular weights (M_w) of lignin preparations from various HTT biomasses (pine, birch, and bamboo) were 8860, 10840, and 9430 g/mol, respectively. In addition, the lignins isolated from HTT biomass have more uniform molecules, as revealed by low polydispersity values (M_w/M_n, 1.68–1.97). The well-characterized lignins will prompt us to utilize the residue after enzymatic hydrolysis.

References

1. Lyko, H., Deerberg, G., Weidner, E. 2009. Coupled production in biorefineries-combined use of biomass as a source of energy, fuels and materials. Journal of Biotechnology.142:78–86
2. Yang, B., Wyman, C.E. 2008. Pretreatment: the key to unlocking low-cost cellulosic ethanol. Biofuels Bioproducts & Biorefining-Biofpr. 2:26–40
3. Tunc M, Sefik., van Heiningen Adriaan, R. P. 2008. Hemicellulose Extraction of Mixed Southern Hardwood with Water at 150 °C: Effect of Time. Industrial & Engineering Chemistry Research. 47 (18): 7031-7037
4. Jaaskelainen, A.S., Sun, Y., Argyropoulos, D.S., Tamminen, T., Hortling, B. 2003. The effect of isolation method on the chemical structure of residual lignin. Wood Science and Technology. 37 (2): 91-102
5. Yuan, T.Q., Sun, S.N., Xu, F., Sun, R.C. 2011. Characterization of lignin structures and lignin-carbohydrate complex (LCC) linkages by quantitative ^{13}C and 2D HSQC NMR. Journal of Agricultural and Food Chemistry. 59:10604–10614
6. Faix, O. (1991) Classification of lignins from different botanical origins by FT-IR spectroscopy. Holzforschung 45:21–27
7. Chen, C.L. Characterization of milled wood lignins and dehydrogenative polymerisates from monolignols by carbon-13 NMR spectroscopy. In *Lignin and Lignan Biosynthesis*; ACS Symposium Series 697; Lewis, N., Sarkanen, S., Eds.; American Chemical Society: Washington, DC, 1998; pp 255-275.
8. Capanema, E.A., Balakshin, M.Y., Kadla, J.F. 2004. A comprehensive approach for quantitative lignin characterization by NMR spectroscopy. Journal of Agricultural and Food Chemistry. 52, 1850–1860.

9. Capanema, E.A., Balakshin, M.Y., Kadla, J.F. 2005. Quantitative characterization of a hardwood milled wood lignin by nuclear magnetic resonance spectroscopy. Journal of Agricultural and Food Chemistry. 53, 9639–9649.
10. Kim, H., Ralph, J. 2010. Solution-state 2D NMR of ball-milled plant cell wall gels in DMSO-d_6/pyridine-d_5. Organic & Biomolecular Chemistry. 8:576–591
11. Shuai, L., Yang, Q., Zhu, J.Y., Lu, F.C., Weimer, P.J., Ralph, J., Pan, X.J. 2010. Comparative study of SPORL and dilute-acid pretreatments of spruce for cellulosic ethanol production. Bioresource Technology. 101:3106–3114

Effect of Species, Particle Size and Compacting Pressure on Relaxed Density and Compressive Strength of Fuel Briquettes

Stephen J. Mitchual [1], Kwasi Frimpong-Mensah [2] and Nicholas A. Darkwa [3]*

[1] Department of Design and Technology Education, University of Education, Winneba, Kumasi Campus, P. O. Box 1277, Kumasi, Ghana.
**Corresponding author:Stephen.mitchual@yahoo.com*
[2] Department of Wood Science and Technology, Faculty of Renewable Natural Resources, Kwame Nkrumah University of Science and Technology, Kumasi, Ghana.
Frimpongmensahk@yahoo.com
[3] Department of Wood Science and Technology, Faculty of Renewable Natural Resources, Kwame Nkrumah University of Science and Technology, Kumasi, Ghana.
Nicdarkwa@yahoo.com

Abstract

Densification of biomass waste materials has provided a great boost to the utilization of wood and agricultural waste for domestic and industrial fuels. However, the processes involved in the production of this fuel makes it more expensive compared to fossil fuels. This is because densification of wood waste into fuel briquettes is not simple and straightforward. This paper reports the results of research conducted to determine the effect of species, particle size and compacting pressure on relaxed density and compressive strength in cleft of briquettes produced from sawdust of tropical hardwoods. Briquettes were made using a laboratory hydraulic press. compacting pressure was varied from 10MPa to 50MPa at an interval of 10MPa. Species used were *Triplochiton scleroxylon*, *Ceiba pentandra*, *Aningeria robusta*, *Terminalia superba*, *Celtis mildbreadii* and *Piptadenia africana*. The results indicate that species, compacting pressure and particle size of sawdust at 5% level of significance have significant effect on the relaxed density and compressive strength of briquettes produced. The multiple correlation coefficient (R) and *adjusted* R^2 for the regression model between relaxed density of briquettes, and species density, particle size and compacting pressure were .93 and .87 respectively. Additionally, the multiple correlation coefficient (R) and *adjusted* R^2 for the regression model between compressive strength of briquettes, and species density, particle size and compacting pressure were .83 and .69 respectively. The regression models suggest that species density, particle size and compacting pressure are good predictors of relaxed density and compressive strength of briquettes produced from sawdust of tropical hardwoods.

Keywords: Briquettes, species, compacting pressure, particle size, relaxed density, compressive strength

Nomenclature

d_1	[mm]	Diameter of briquette at point one
d_2	[mm]	Diameter of briquette at point two
d_3	[mm]	Diameter of briquette at point three
l_1	[mm]	Length of briquette at point one
l_2	[mm]	Length of briquette at point two
l_3	[mm]	Length of briquette at point three
M	[g]	Mass of briquette
M_1	[g]	Mass of the test sample before drying
M_o	[g]	Oven-dry mass of the test sample

Introduction

Sustainable development and the role of energy in the development process worldwide are vital issues that have been gaining more attention and concern over the last few decades. Fossil fuels supplied about 80% of world primary energy demand in 2004 (IEA, 2006) and their use is expected to grow in absolute terms over the next 20–30 years in the absence of policies to promote low-carbon emission sources. The nearly total dependence on energy from fossil sources is clearly not ideal in that crude oil reserves are limited and unevenly distributed in the world, with the most important reserves in politically unstable regions. In the past and present distortions in the supply of crude oil result in sharp increases in crude oil prices and therefore leading to world wide economic uncertainty. Fossil energy use is also responsible for about 85% of the CO_2 emissions produced annually (IEA, 2003). This significantly adds to the greenhouse gas emissions. The above and others are the important reasons to find other means of getting energy for the ever-growing demand for energy world wide. Renewable source of energy are the fastest-growing source of world energy, with consumption increasing by 3.0 percent per year (EIA, 2009). This is due to its environmental friendliness as against the rising concern about the environmental impacts of fossil fuel use and also strong government incentives for increasing renewable penetration in most countries around the world (EIA, 2009). Globally, biomass currently provides around 46 EJ of bioenergy in the form of combustible biomass and wastes, liquid biofuels, solid biomass/charcoal, and gaseous fuels. This share is estimated to be over 10% of global primary energy, but with over two-thirds consumed in developing countries as traditional biomass for household use (IEA, 2006). Previous studies conducted to examine the economic impacts of using biomass energy clearly show that the benefits of production of briquettes for many economies clearly exist. However, there are several important factors that limit its utilization. The main reason is the production cost of various bio energy fuels. The production cost does not match the production price of fossil fuels such as coal. This means the commercial production of biomass is quite far-fetched at present. Hence there is an urgent need to cut down the production cost to make bio-energy affordable. This can be done through research work to improve upon the technologies available for their production as well as providing wider market. This among others will help to lower the production cost of biomass fuel and therefore make it more competitive. In this paper the researchers investigated into the effect of species, particle size (PS) and compacting pressure (CP) on relaxed density (RD) and compressive strength in cleft (CS) of fuel briquettes made at room temperature and low CP.

Materials and Methods

Materials and material preparation. Sawdust from the following selected tropical hardwoods species: *Triplochiton scleroxylon, Ceiba pentandra, Aningeria robusta, Terminalia superba, Celtis mildbreadii* and *Piptadenia africana* were used for the study. These species could be classified into lower density (*T. scleroxylon and C. pentandra*), medium density (*A. robusta and T. superba*) and high density (*P. africana and C. mildbreadii*). The sawdust was sun dried at an average relative humidity and temperature of 75% and 28^{o}C respectively for between five and seven days. Thereafter, the sawdust of each species was classified into PS: PS ≤ 1mm, 1mm < PS ≤ 2mm and 2mm < PS ≤ 3.35mm using an automatic sieve shaker with serial number A060-01/ZG/0038 and model A060-01.

Moisture content. The moisture content of the sawdust was determined in accordance with the European Standard EN 13183-1: (2002). A sample of 2g of sawdust of each species was weighed and placed in a laboratory oven at a temperature of (103 ± 2) ^{0}C and dried until the difference in mass between two successive weighing separated by an interval of two hours was less than 0.01 grammes. The moisture content of the specimen was then computed as follows:

$$Moisture\ content = \frac{M_1 - M_o}{M_o} \times 100$$

Density of species. Density of the six timber species from which sawdust was collected was determined in accordance with ASTM D 2395 – 07a. Five clear specimens of dimension 20mm x 20mm x 30mm were prepared for each species. The oven-dried masses of the specimens were determined. Thereafter they were dipped one-by-one in a paraffin wax and then kept in a desiccator. The volume displacement method which employs the use of Eureka can and a measuring cylinder was used to determine the volumes of the specimen. Density of each specimen was then computed as;

$$Density = \frac{Mass\ of\ specimen}{Volume\ of\ specimen}$$

Briquetting process. A 55.3-mm ID × 52.5-cm height cylindrical mould was utilized to produce the briquettes. Ninety grammes of sawdust of each species and PS was weighed and filled into the mould. The average moisture content of the sawdust was 11.46%. A manual hydraulic press and a piston were used to compress the raw material without a binder against the other end of the mould to form the briquettes. A clearance of about 0.1 mm was provided between the piston and the inner wall of the mould to allow for air escape. The samples were pressed using the following predetermined CP levels: 10MPa, 20MPa, 30MPa, 40MPa and 50MPa. The dwelling time for each press was maintained at 10sec for all the pressing made. This process was repeated for all the six species and PS.

Physical and mechanical properties of briquettes. The RD and CS of the briquettes were investigated using standard testing methods.

Relaxed density of the briquettes was determined 30 days after removal from the press in accordance with ISO3131-1975. The mass of the briquettes was determined using a laboratory electronic balance with an accuracy of 0.01g. The diameter and length of the briquette were measured at three points with a Digital Vernier Calliper. RD was then computed as:

$$RD\ \left(\frac{g}{cm^3}\right) = \frac{108000 * M(g)}{\pi[d_1(mm) + d_2(mm) + d_3(mm)]^2 * [l_1(mm) + l_2(mm) + l_3(mm)]}$$

Compressive strength in cleft of briquettes was determined in accordance with ASTM D 2166-85 using an Instron Universal Strength testing machine with load cell capacity 100KN. The cross-head speed was 0.305mm/min. A sample of briquette to be tested was placed horizontally in the compression test fixture and a load was applied at a constant rate of 0.305 mm/min until the briquette failed by cracking. The CS was then computed as follows:

$$\text{Compressive strength in cleft}\ \left(\frac{N}{mm}\right) = \frac{3 * The\ load\ at\ fracture\ point\ (N)}{[l_1(mm) + l_2(mm) + l_3(mm)]}$$

Results and Discussion

Relaxed density. The result in TABLE 1a (PS < 1mm) indicates that the RD of briquettes made from *C. pentandra,* the species with the lowest density (409Kg/m^3) ranged from 398Kg/m^3 to 716Kg/m^3. That of *C. mildbreadii*, species with highest density (764Kg/m^3) ranged from 453Kg/m^3 to 706Kg/m^3. The lowest RD for all the briquettes produced from PS < 1mm was 366Kg/m^3 (*T. scleroxylon* at CP = 10MPa) and the highest was 741Kg/m^3 (*P. africana* at CP = 50MPa). The result in TABLE 1b for 1mm ≤ PS < 2mm also shows that the RD of briquettes made from *C. pentandra* ranged from 386Kg/m^3 to 692Kg/m^3 whilst that of *C. mildbreadii* ranged from 435Kg/m^3 to 658Kg/m^3. The result also indicates that the lowest RD for 1mm ≤ PS < 2mm was 354Kg/m^3 (*T. scleroxylon* at CP = 10MPa) and the highest was 723Kg/m^3 (*P. africana* at CP = 50MPa). Considering TABLE 1c which indicates the RD for 2mm ≤ PS < 3.35mm, it shows that briquettes made from *C. pentandra* had RD ranging from 373Kg/m^3 to 651Kg/m^3 whilst that of *C. mildbreadii* ranged from 430Kg/m^3 to 655Kg/m^3. Additionally, the lowest RD for this PS was 324Kg/m^3 (*T. scleroxylon* at CP = 10MPa) and the highest was 720Kg/m^3 (*P. africana* at CP = 50MPa). Briquettes densities obtained from this study was consistent with suggestion by some researchers that briquettes made from hydraulic piston press are usually less than 1000Kg/m^3 (Tumuluru, Wright, Kenny and Hess, 2010) and are usually between 300Kg/m^3 - 600Kg/m^3 (Saeidy, 2004). Correlation analysis between RD on one hand, and CP and PS on the other hand indicates that there was a weak significant negative correlation between RD and PS of the briquettes produced (Pearson's r = -.188, p-value = .000; N = 450; 1-tailed, $\alpha = 0.05$). CP was also found to have a very strong positive significant correlation with the RD of the briquettes produced (Pearson's r = .901, p-value = .000; N = 450; 1-tailed, $\alpha = 0.05$). This result generally suggest that the RD of the briquettes produced increases with increasing CP level and that briquettes produced from sawdust of tropical hardwoods with smaller PS are likely to have higher RD than those with larger PS. This result confirms that of other researchers.

Table 1a: *Relaxed density of briquettes for particle size (P) P < 1mm (Kg/m^3)*

	Compacting pressure

Species	10MPa	20MPa	30MPa	40MPa	50MPa
C. pentandra	398	523	622	666	716
T. scleroxylon	366	458	545	594	632
A. robusta	440	543	607	636	695
T. superba	447	557	631	675	727
P. africana	465	567	637	679	741
C. mildbreadii	453	533	611	662	706

Table 1b: *Relaxed density of briquettes for particle size (P) 1mm ≤ P < 2mm (Kg/m^3)*

	Compacting pressure				
Species	10MPa	20MPa	30MPa	40MPa	50MPa
C. pentandra	386	503	606	646	692
T. scleroxylon	354	452	535	591	627
A. robusta	362	466	538	586	658
T. superba	437	548	615	651	680
P. africana	441	534	610	664	723
C. mildbreadii	435	491	562	621	658

Table 1c*: Relaxed density of briquettes for particle size (P) 2mm ≤ P < 3.35mm (Kg/m^3)*

	Compacting pressure				
Species	10MPa	20MPa	30MPa	40MPa	50MPa
C. pentandra	373	489	598	618	651
T. scleroxylon	324	435	508	552	597
A. robusta	345	463	519	571	573
T. superba	396	514	591	649	673
P. africana	417	530	604	658	720
C. mildbreadii	430	487	543	612	655

Križan (2007) and FAO (1990) reported that in reality in briquetting when the fraction of the raw material is smaller, the briquette produced will have a higher density. The reason for this trend is that increasing the CP will lead to the particles of biomass material being closely packed due to reduction of the void ratio and the plastic deformation of the particles (Lindley and Vossoughi, 1989). Additionally, when the raw material is finer it gives a larger surface area for bonding which result in the production of briquette with higher density. Table 2 which shows the Analysis of Variance (ANOVA) of RD of briquettes produced indicates that at 5% level of significance, species, PS, CP and their interactions have significant effects on the RD of briquettes produced. The multiple coefficient of determination value (R^2) and the root mean square error (RMSE) for the ANOVA Model were 0.9907 and 11.24 respectively. Thus, it could be deduced that species, PS and CP and their interactions explain about 99.07% of the variability in the RD of the briquettes produced.

Table 2: *ANOVA of relaxed density of briquettes*

Source	DF	ANOVA SS	Mean Square	F-Ratio	p-value
Species	5	452443.680	90488.736	715.19	< 0.0001*
Particle size	2	174914.253	87457.127	691.23	< 0.0001*
CP	4	4106254.742	1026563.686	8113.63	< 0.0001*
Species*CP	20	45562.164	2278.108	18.01	< 0.0001*
Species*Particle size	10	38280.947	3828.095	30.26	< 0.0001*
Particle size *CP	8	3449.324	431.166	3.41	0.0009*
Species* Particle size* CP	40	22406.809	560.170	4.43	< 0.0001*
Error	360	45548.400	126.523		

*Statistically significant at 0.05 level of significance; DF = Degree of freedom

Multiple regression analysis to establish the relative contribution of species density, PS and CP in the prediction of the RD of briquette and the mathematical relationship between the dependent variable RD and the independent variables; species density, PS and CP is as indicated in TABLE 3. The result (TABLE 3) shows the unstandardized (β) and standardized (Beta) regression coefficients, the multiple correlation coefficient (R), *adjusted* R^2, the value of t and its associated p-value for each of the variables. As shown in table 3 species density, PS and CP collectively explained 87.1% (*adjusted* R^2 = .871) of the variance in the RD of briquette produced. This suggests that the regression model is a good predictor of briquettes' RD (R^2 = 0.872, p-value = .000).

Table 3: *Regression of relaxed density of briquettes on species density, particle size and compacting pressure*

Variables	β	Beta	R	*adjusted* R^2	t	p-value
Constant	334.651				34.238	.000
Species density	.125	.160			9.446	.000
Particle size	-23.997	-.188			-11.109	.000
Compacting pressure	6.639	.901			53.234	.000
			.934	.871		

Additionally, based upon the standardized regression coefficients values (Beta), it could be deduced that CP explained the bulk of the variance in the RD of the briquette produced (Beta = .901, t = 53.234, p-value = .000) and was the best predictor of RD of the briquette. However, species density and PS of sawdust used significantly contributed to the model (Species density: Beta = .160, t = 9.446, p = .000; PS: Beta = -.188, t = -11.109, p = .000). Furthermore, it could be deduced from the unstandardized (β) regression coefficients values that the relationship between the dependent variable RD and the independent variables; species density (S), PS and CP is:

$$\text{Relaxed density} = 334.651 + .125S - 23.997PS + 6.639CP$$

Compressive strength in cleft. Briquette's CS is one of the indices used to assess its ability to be handled, packed and transported without breaking. Table 4a, b and c indicates the CS of briquette produced. The result for PS < 1mm (Table 4a) indicates that at all CP levels the CS of

C. pentandra was exceptionally high compared to that of the other species. CS of *C. pentandra* ranged from 15.81N/mm to 44.58N/mm for CP levels 10MPa to 50MPa. *C. mildbreadii* comparatively had the lowest CS ranging from 1.30N/mm to 12.45MPa for the same CP levels. The result for 1mm≤ P S < 2mm (Table 4b) and 2mm≤ P S < 3.35mm (Table 4c) reflected the trend for PS < 1mm. In both cases the CS of *C. pentandra* was exceptionally higher than that of the other species. Correlation analysis indicated a weak significant positive correlation between PS and CS (Pearson's r = .179, p-value = .000; N = 450; 1-tailed, $\alpha = 0.05$). Additionally, a

Table 4a: *Compressive strength of briquettes for particle size (P) P < 1mm (N/mm)*

	Compacting pressure				
Species	10MPa	20MPa	30MPa	40MPa	50MPa
C. pentandra	15.81	29.23	39.26	40.40	44.58
T. scleroxylon	3.33	9.35	14.27	20.66	30.56
A. robusta	3.97	8.23	16.28	19.48	26.63
T. superba	2.13	6.16	10.44	13.64	18.92
P. africana	1.76	5.95	10.13	17.06	21.14
C. mildbreadii	1.30	3.55	6.69	10.51	12.45

Table 4b: *Compressive strength of briquettes for particle size (P) 1mm ≤ P < 2mm (N/mm)*

	Compacting pressure				
Species	10MPa	20MPa	30MPa	40MPa	50MPa
C. pentandra	7.28	24.34	34.74	42.62	52.60
T. scleroxylon	6.97	14.66	27.53	36.57	38.31
A. robusta	3.47	9.51	14.42	21.62	27.50
T. superba	3.26	6.61	12.50	14.89	18.03
P. africana	2.60	6.99	12.65	17.80	24.05
C. mildbreadii	2.59	5.64	9.63	12.49	16.40

Table 4c*: Compressive strength of briquettes for particle size (P) 2mm ≤ P < 3.35mm (N/mm)*

	Compacting pressure				
Species	10MPa	20MPa	30MPa	40MPa	50MPa
C. pentandra	13.80	26.71	36.73	45.40	51.45
T. scleroxylon	6.98	15.24	27.64	36.86	40.89
A. robusta	2.69	11.90	17.29	21.35	26.88
T. superba	4.22	9.58	13.05	15.80	24.67
P. africana	3.97	15.28	24.24	41.83	55.45
C. mildbreadii	3.62	5.78	10.18	12.66	19.18

strong significant positive correlation between CS and CP of briquettes produced was established (Pearson's r = 0.670, p-value = .000; N = 450; 1-tailed, $\alpha = 0.05$). This result means that the CS

in cleft of the briquettes produced increased with increasing PS and CP. The ANOVA of CS of briquettes produced (Table 5) indicates that at 5% level of significance, CP, species, PS and their

interactions had significant effects on the CS of the briquettes produced (p-value < 0.05). The R^2 and RMSE for the ANOVA Model were 0.9802 and 2.1162 respectively. It could therefore be deduced that the species type of the biomass raw material, its PS and CP could explain about 98.02% of the variability in the CS of the briquettes produced.

The summary of the result of multiple regression to establish the relative contribution of species density, PS and CP towards the prediction of CS of the briquette and the mathematical relationship between the dependent variable CS and independent variables; species density, PS and CP is as indicated in TABLE 6. The result indicates that the unstandardized (β) and standardized (Beta) regression coefficients, the multiple correlation coefficient (R), *adjusted* R^2,

Table 5: *ANOVA of compressive strength in cleft of briquettes*

Source	**DF**	**ANOVA SS**	**Mean Square**	**F-Ratio**	**p-value**
Species	5	29475.439	5895.088	1316.33	< 0.0001*
Particle size	2	2688.496	1344.248	300.16	< 0.0001*
CP	4	36597.173	9149.293	2042.97	< 0.0001*
Species*CP	20	4451.833	222.592	49.70	< 0.0001*
Species*Particle size	10	3592.241	359.224	80.21	< 0.0001*
Particle size *CP	8	902.633	112.829	25.19	< 0.0001*
Species* Particle size* CP	40	2186.188	54.655	12.20	< 0.0001*
Error	360	1612.234	4.47843		

*Statistically significant at 0.05 level of significance; DF = Degree of freedom

the value of t and its associated p-values for each of the variables. The result indicates that species density, PS and CP collectively explained 68.5% (*adjusted* R^2 = .685) of the variance in the CS of briquette produced. This suggests that the regression model is a good predictor of CS of briquettes produced (R^2 = 0.685, p-value = .000).

Table 6: *Regression of compressive strength of briquettes on species, particle size and compacting pressure*

Variables	β	Beta	R	*adjusted* R^2	t	p-value
Constant	19.923				10.081	.000
Species density	-.046	-.454			-17.147	.000
Particle size	2.957	.179			6.770	.000
Compacting pressure	.637	.670			25.267	.000
			.829	.685		

The standardized regression coefficients values (Beta) for the three predictive variables suggest that CP explained the bulk of the variance in the CS of the briquette produced (Beta = .670, t = 25.267, p = .000) and was the best predictor of CS of the briquette produced. That not withstanding species density and PS of sawdust used significantly contributed to the regression model (Species density: Beta = -.454, t = -17.147, p = .000; PS: Beta = .179, t = 6.770, p = .000).

The values of unstandardized regression coefficients (β) also suggest that the mathematical relationship between CS of briquettes produced and, species density (S), PS and CP is:

Compressive strength = 19.923 - .046S + 2.957PS + 0.637CP

Conclusions

From the results of the study it could be concluded that: (1) the type of species, compacting pressure and particle size, as well as their interactions have significant effect on the relaxed density and compressive strength in cleft of briquettes produced, (2) The mathematical relationship between RD and, species density (S), PS and CP is: Relaxed density = 334.651 + .125S – 23.997PS + 6.639CP, (3) The mathematical relationship between CS and, species density (S), PS and CP is: Compressive strength = 19.923 - .046S + 2.957PS + 0.637CP

References

ASTM D2395–2008. Standard test methods for specific gravity of wood and wood-based materials, 299 – 300.

ASTM D2166-85. Standard Test Method of compressive strength of wood.
EN 13183-1: 2002. Moisture content of a piece of sawn timber. Determination by oven-dry method.

FAO, 1990. The briquetting of agricultural wastes for fuel. FAO, Environment and Energy Paper.

International Energy Outlook 2009. US Dept. of Energy. Energy information administration. Report DOE/EIA – 0484.

ISO 3131-1975. Standard test method for density of regular solids.

IEA, 2003. Building the cost curves for the industrial sources of nonCO2 greenhouse gases. Greenhouse Gas R&D Programme, Report No. PH4/25, OECD, Paris.

IEA, 2006b. World energy outlook 2006. International Energy Agency, OECD Publication Service, OECD, Paris.

Križan, P. 2007. Research of factors influencing the quality of wood briquettes.Acta Montanistica Slovaca Ročník 12 (3): 223-230.

Lindley, J. and Vossoughi, M. 1989. Physical properties of biomass briquettes. Transaction of the ASAE. 32(2): 361-366

Saeidy, E. E. 2004. Technological fundamentals of briquetting cotton stalks as a biofuel. A dissertation submitted to Humboldt-Universität, zu Berlin.

Tumuluru, J. S., Wright, C. T., Kenny, K. L., and Hess, R. 2010. A review on biomass densification technologies for energy application. U.S. Department of Energy.

Physico-Chemical Characteristics and Market Potential of Sawdust Charcoal Briquette

[1]*Akowuah J. O.*, [1]*Kemausuor F. and* [2]*Mitchual S. J.*
[1]Department of Agricultural Engineering, Kwame Nkrumah University of Science and Technology, Kumasi

[2]Department of Design and Technology Education, University of Education, Winneba, Kumasi Campus
Corresponding author: *akowuahjoe@yahoo.co.uk*

ABSTRACT

In view of soaring prices of petroleum products on the world market and concerns over the negative impact of deforestation on the environment, briquettes are a better replacement to LPG, kerosene, firewood and charcoal as energy source for heating, cooking and other industrial applications in both urban and rural centres. This study therefore sought to assess the physico-chemical properties of charcoal briquettes produced in Ghana. It also sought to establish demand for and willingness of potential users to substitute charcoal and firewood with a 'Grade B' charcoal briquette. The study employed a two tie approach (laboratory test and interviews using questionnaires). The laboratory experiment sought to determine the physico-chemical characteristics of the briquettes. Data on potential users' acceptability and willingness to use the briquettes were collected from 60 respondent using self-completion questionnaires. Results of physico-chemical assessment of the briquettes were as follows: length (75mm - 120mm), moisture content (5.7% dry basis), density (1.1g/cm^3), ash content (2.6%), fixed carbon (20.7%), volatile matter (71%) and calorific value (4820Kcal/kg). Response to the questionnaire gave the following observations: ease to ignite (97% responded yes), long burning time (78% responded yes), heat output (76% responded high). Moreover, all the respondents indicated that, the briquettes were sparkless, smokeless and have low ash content. Finally, 93% of the respondents indicated their willingness to use the briquettes. Based on the findings, the study concluded that there is indeed future and market potential for the use of biomass briquettes in the study area.

Keywords: Sawdust charcoal briquettes, physico-chemical characteristics, demand and potential user's acceptability

Introduction

As a result of growing worldwide concern regarding environmental impacts – particularly climate change – from the use of fossil fuels coupled with the volatile fossil fuel market and, the need for an independent energy supply to sustain economic development, there is currently a great deal of interest in renewable energy in general and biomass energy in particular. Biomass is one of the most common and easily accessible renewable energy resources and represents a great opportunity as a feedstock for bioenergy (McKendry, 2002). A wide range of biomass resources- crop residues (corn stover, rice husk etc), wood wastes from forestry and industry, residues from food and paper industries, municipal solid wastes (MSW) and dedicated energy crops such as short-rotation perennials- can be utilised to generate electricity, heat, combined heat and power, and other forms of bioenergy.

Traditionally, energy in the form of firewood, twigs and charcoal has been the major source of renewable energy for many developing countries (Emerhi, 2011). In Ghana, it is estimated that, about 90% of bulk woodfuels is obtained directly from the natural forest while the remaining 10% is from wood waste (logging and sawmill residues) and planted forests (EC, 2008). Woodfuels – firewood and charcoal – forms the most dominant source of energy in Ghana and is used significantly in both rural and urban communities for cooking and many other heating applications. According to KITE (1999), about 70% of the total national energy consumption is accounted for by biomass in either direct or processed form, a trend that has continued for the last decade (Fig. 1). The over reliance on forest wood in Ghana mainly for charcoal production, firewood and furniture making has resulted in the depletion of forest reserves at a faster rate – estimated at 3% per year (Trossero, 2002). A similar scenario according to Emerhi (2011), in other sub-Saharan countries has resulted in shortage of fuel wood which has led to the depletion of over 75% of the total forest cover and thus leading to environmental crises. As rightly noted by Stout and Best (2001), a transition to a sustainable energy system is urgently needed for developing countries.

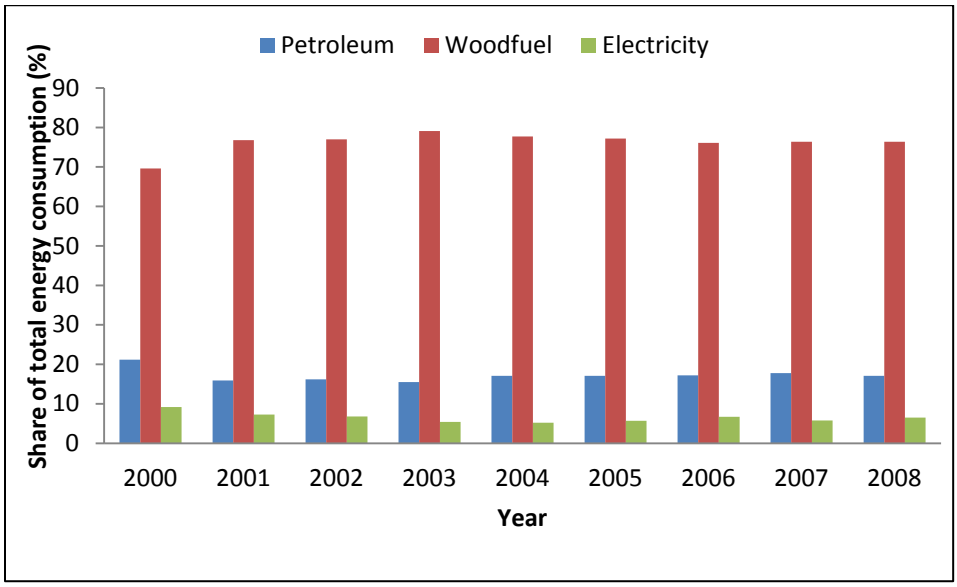

Figure 1: Trend of energy consumption by type of fuel

Among the several kinds of biomass resources, agricultural residues - sawdust, rice husk, corn stover, cotton stalk, groundnut husk etc - have become one of the most promising choices as cooking fuels due to its availability in substantial quantities as waste annually. However, the utilisation of these biomass residues in their natural form as fuel is difficult because of their very low bulk density, low heat release and the excessive amounts of smoke they generate. All of these characteristics make them difficult to handle, store, transport, and utilize in their raw form. One of the ways of improving the thermal value of such biomass is the application of briquetting technology (Wilaipon, 2007). This involves the densification of loose biomass to produce fuel briquette which has better handling characteristics and enhanced volumetric calorific value (Oladeji, 2010). According to Styles *et al*. (2008), briquettes are a key technology for increasing biomass use in both electricity and heat production.

The production of briquettes from sawdust exemplifies the potential of appropriate technology for wood waist utilization. If produced at low cost and made conveniently accessible to consumers, briquettes could serve as complement to firewood and charcoal for domestic cooking and agro-industrial operations. Besides, briquettes have advantages over fuel wood in terms of greater heat intensity, cleanliness, convenience in use, and relatively smaller space requirement for storage (Singh and Singh, 1982; Wamukonya and Jenkins, 1995; Yaman *et al*., 2000; Olorunnisola, 2004). Successful briquette operations are found mostly in developed countries. An example is the industry based on carbonization of sawdust and bark in the southern USA. However, briquetting operations are not successful in developing countries like Ghana and other African countries. This is mostly due to the high cost of production, lack of awareness on its sustainability, availability of market and poor packaging and distribution systems for the product (Emerhi 2011).

Commercial production of sawdust briquette was introduced in Ghana in 1984. Though the briquettes had high prospect as an alternative to firewood and charcoal, it could not be promoted widely especially with the household sector due to operational and marketing challenges. Notably, Oladeji (2010), also reported that, if biomass or agro-waste briquettes are to be used efficiently and rationally as fuel, they must be characterized by determining it parameters such as the moisture content, ash content, density, volatile matter, and heating value among others. Therefore, this study assessed the physico-chemical properties of charcoal briquettes produced in Ghana. It also sought to assess the market potential of charcoal briquettes in the study area to establish demand for and also the willingness of potential users to substitute charcoal and firewood with the sawdust charcoal briquette.

Materials and Methods

Raw material

The samples of sawdust charcoal briquette used for the study were obtained from a briquette producing company in the Kumasi Metropolis. In all, 600kg of briquettes were acquired for the study. The production of briquette at the company is by the extrusion process through the use of screw press briquetting machine at die pressure range of 100-200MPa with no additives such as starch binder. The briquette in (Fig. 2) is carbonised and square sized (0.035m × 0.035m) with a concentric hole diameter of 0.01m.

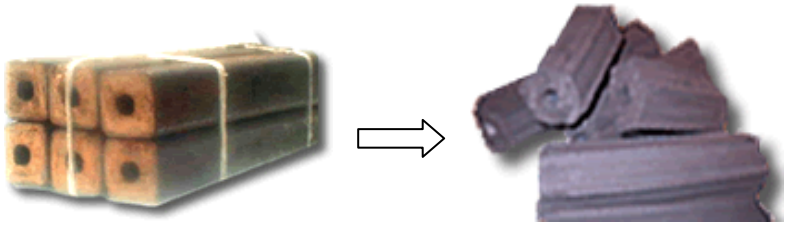

Figure 2: Sample of carbonised sawdust charcoal briquette

Determination of physico-chemical properties of sawdust charcoal briquette

The calorific value, density, proximate and ultimate analysis of the sawdust charcoal briquette was determined prior to distribution to sampled potential users. According to Chaney (2010), proximate analysis is a standardised procedure which gives an idea of the bulk components that make up a fuel, which relate closely to its combustion behavior. Proximate analysis was done to determine the percentage volatile matter content, percentage ash content, moisture content and percentage content of fixed carbon of the briquettes.

Percentage volatile matter (PVM)

The PVM was determined by pulverising 2g of briquettes sample in a crucible and placing it in an oven until a constant weight (A) was obtained. The briquettes were then kept in a furnace at a temperature of 550 ^{o}C for 10 minutes and weighed after cooling in a dessicator to obtain (B). The PVM was then calculated using equation 1:

$$PVM = \frac{A-B}{A} \times 100 \quad \text{(Eq. 1)}$$

Percentage Ash content (PAC)

The PAC was also determined by heating 2g of the briquette sample in the furnace at a temperature of 550 ^{o}C for 4hrs and weighed after cooling in a dessicator to obtain the weight of ash (C). The PAC was determined using equation 2:

$$PAC = \frac{C}{A} \times 100 \quad \text{(Eq. 2)}$$

Percentage moisture content (PMC) on dry basis

The moisture content was found by weighing 2g of the briquette sample (E) and oven drying it at 105 ^{o}C until mass of the sample was constant. The change in weight (D) after 60 mins was then used to determine the sample's percentage moisture content using equation 3:

$$PMC_{(db)} = \frac{D}{E} \times 100 \quad \text{(Eq. 3)}$$

Percentage fixed carbon (PFC)

The PFC was calculated by subtracting the sum of percentage volatile matter (PVM) and percentage ash content (PAC) and percentage moisture content from 100 as shown in equation 4:

$$\text{Fixed Carbon} = 100\% - (\text{PAC} + \text{PMC} + \text{PVM}) \quad \text{(Eq. 4)}$$

Estimation of important chemical elements that make up biomass, namely carbon, hydrogen, oxygen, nitrogen and sulphur were determined through 'ultimate' analysis.These properties were determined in accordance with ASTM analytical methods as prescribed by Jenkins *et al.* (1998). The calorific value of the samples was determined using a bomb calorimeter in accordance with ASTM E711 - 87 (2004). Density of the briquettes was calculated from the ratio of the mass to the volume of briquette in accordance with the method used by Rabier *et al.* (2006).

Of critical importance in the survey which the consumers responded to, include effect of the burning rate of the briquettes, heat output, ease of ignition of the briquettes, rate of devolatisation (how fast the briquettes burned), burning time or combustibility rating (how long the briquette burned before restocking when they are used in cooking and heating), sparking ability, smoke generation and any other effects regarding the burning of the briquettes.

Market survey

10kg of the sawdust charcoal briquettes was given to each of the 60 potential users sampled. The potential users sampled involved households and local hospitality industries operators (e.g. restaurants, hotels, wayside food vendors and bakeries). A survey was then conducted among the recipients of the briquette in order to establish their acceptability and willingness to use the briquettes. The survey was conducted through the administration of structured questionnaires a week after the distribution of the briquettes.

Results and Discussions

Physical characteristics of the briquettes

The quality of the sampled briquettes assessed on the basis of its physical condition was very good. The external surface was smooth and the structure of the cross-section was compact and homogenous. The density of the sawdust charcoal briquette was found to be 1100kg/m^3 which is reasonable and falls within the range recommended by Grover *et al*. (1994) for sawdust briquette produced by screw extrusion process. The hole in the center helps in combustion because of sufficient circulation of air. It also provides sufficient toughness to withstand exposure and shocks of transportation and storage.

Physico-chemical characteristics

The result of the physico-chemical characteristics of the sawdust charcoal briquette is presented in (Table 1).

Proximate analysis		Ultimate analysis		Heating value
Parameter	Value (%)	Parameter	Value (%)	
Volatile matter	71	Carbon	53.07	
Ash content	2.6	Hydrogen	4.1	4820 KCal/kg
Moisture content	5.7	Oxygen	39.6	
Fixed carbon	20.7	Sulphur	0.302	

Nitrogen	0.28

Table 1: Physico-chemical characteristics of sawdust charcoal briquette

Proximate analysis

The proximate analysis of the briquettes examined in this study were limited to percentage volatile matter, percentage ash, percentage fixed carbon and moisture content. The results presented in (Table 1) are discussed here after.

Moisture content

According to Yang *et al.* (2005), moisture content is a very important property which can greatly affect the burning characteristics of biomass. Aina *et al.* (2009) also reported that, moisture content is one of the main parameters determining briquette quality as lower moisture content of briquettes implies higher calorific value. Moisture content affects both the internal temperature history within the solid, due to endothermic evaporation, and the total energy that is needed to bring the solid up to the pyrolytic temperature (Zaror and Pyle, 1982). From Table 1, moisture content of the sawdust charcoal briquette was 5.7% db. This is within the limits of 15% recommended by Wilaipon (2008) and Grover and Mishra (1996), for briquetting of agro-residues. Most durable briquettes of sawdust are of the moisture content of 5% (Aina *et al.*, 2009). Wamukonya and Jenkins (1995), also recommended that, the range of values (7.7-15.1%) and (12-20%) for sawdust and wheat straw briquettes respectively are good for storability and combustibility of briquettes.

Volatile matter, ash content and fixed Carbon

Volatile matter represents the components of carbon, hydrogen and oxygen present in the biomass that when heated turn to vapour, usually a mixture of short and long chain hydrocarbons (Chaney, 2010). Volatile content has been shown to influence the thermal behaviour of solid fuels (Loo and Koppejan, 2008), but this is also influenced by the structure and bonding within the fuel. Chaney (2010) reported that, low-grade fuels, such as dung, tend to have a low volatile content resulting in smouldering combustion which De Souza and Sandberg (2004) described as a heterogeneous flameless combustion process which occurs on the surface or within the porous fuel. They further stated that, it results in incomplete combustion which leads to significant amount of smoke and toxic gases being released.

From the proximate analysis, the percentage content of volatile matter for the sawdust charcoal briquette was 71%. Ash which is the non-combustible component of biomass was determined to be 2.6%. According to Kim *et al.* (2001), ash has a significant influence on the heat transfer to the surface of the fuel, as well as the diffusion of oxygen to the fuel surface during char combustion. The values of volatile matter and ash content observed in this study are good and acceptable. Loo and Koppejan (2008), reported that, the higher the fuel's ash content, the lower its calorific value. *Ibid,* again reported that, biomass generally has a volatile content of around 70-86% of the weight of the dry biomass which makes biomass a more reactive fuel giving a much faster combustion rate during the devolatisation phase than other fuels such coal.

The fixed carbon of a fuel which is the percentage of carbon available for char combustion was determined to be 20.7%. This is not equal to the total amount of carbon in the fuel (the ultimate carbon) since a significant amount is released as hydrocarbons in the volatiles.

Ultimate analysis

From the result of ultimate analysis, the composition of the sawdust charcoal briquette, analysed on an "as received basis", showed 53.07% carbon, 4.1% hydrogen, 39.6% oxygen, 0.28% nitrogen, and 0.302% sulphur. The results agrees with the observations made by Chaney (2010) who reported, that, analysis of biomass using the gas-analysis procedures revealed the principal constituent as carbon, which comprises between 30 to 60% of the dry matter and typically 30 to 40% oxygen. Hydrogen being the third main constituent makes up between about 5-6% and nitrogen and sulphur (and chlorine) normally makes up less than 1% of dry biomass.

The amount of carbon and hydrogen content in the sample examined is very satisfactory as they contribute immensely to the combustibility of any substance in which they are found, (Musa, 2007). Jenkins *et al*, (1998) reported that, the resulting composition of biomass affects its combustion characteristics as the total overall mass decrease in the fuel during the volatile combustion phase of the combustion process as the hydrogen to carbon ratio of the fuel increases, and to a lesser extent, as the oxygen to carbon ratio increases. The low sulphur and nitrogen contents reported is a welcome development as there will be minimal release of sulphur and nitrogen oxides into the atmosphere which is an indication that the burning of the briquettes as fuel will not pollute the environment, (Enweremadu, *et al.,* 2004). Chaney (2010), also reports that, nitrogen, sulphur and chlorine are significant in the formation of harmful emissions and have an effect on reactions forming ash.

Calorific value

Heat value or calorific value determines the energy content of a fuel. It is the property of biomass fuel that depends on its chemical composition and moisture content. The most important fuel property is its calorific or heat value (Aina *et al.,* 2009). The calorific value calculated for sawdust charcoal briquette was 20,175.81kJ/kg (4820 Kcal/kg). This energy value is sufficient enough to produce heat required for household cooking and small scale industrial cottage applications. The results compares well with the results of heating value of sawdust briquette obtained by Chaiklangmuang *et al.* (2008) and most biomass energy for examples, almond shell briquette - 19,490KJ/kg (Jenkins *et al.,*1998), corncob briquette - 20,890 KJ/kg (Oladeji, 2010), cowpea- 14,372.93 kJ/kg, and soybeans-12,953 kJ/kg (Enweremadu, *et al*., 2004).

Respondents' perception on usage of the sawdust charcoal briquette

As shown in (Table 2), the following observations were made in response to the use of the briquettes by the potential users. With ease to ignite, 97% of the respondents indicated it was easy to ignite the briquette. 78% of the respondents also indicated that combustibility rating/burning time was quite long if they compare to the same amount of charcoal they use for their cooking and heating activities. 76% were of the perception that the heat output from the briquette was quite high compared to other fuels such as charcoal which they have been using. On the rate of devolatisation, 75% responded that, though the briquette has high heat output it

burned slowly. The responds implies that the sawdust charcoal briquette used in this study ignites more easily and burn with high intensity for a long time.

More importantly, all the respondents indicated that, the briquettes burned without sparks and smoke. Low ash content was also observed. This shows that the sawdust charcoal briquette will be a better alternative to charcoal and firewood. This agrees Emerhi (2011), who reported that, briquettes improves health by providing a cleaner burning fuel and also provides a better alternative to firewood (40% more efficient, better and longer burning time) as well as helps to protect the environment by reducing the number of trees cut for firewood. Finally, 93% of the respondents indicated their willingness to use the briquettes if available and not very expensive.

Parameter		**Response (%)**	
Usage of product	Cooking	Grilling	Barbequing
	72	18	10
Ease of ignition	Easy	Difficult	
	97	3	
Convenience	Very good	Good	Poor
	27	68	5
Rate of devolatisation	Fast	Slow	Moderate
	6	85	9
Heat output intensity	High	Moderate	Low
	76	20	4
Combustibility rate /burning time	Long time	Short time	
	78	22	
Ash generated	Low	High	
	100	0	
Smoke/sparks	Yes	No	
	100	0	
Eagerness to use	Willing	Not sure	
	93	7	

Table 2: A matrix of user's perception on usage of sawdust charcoal briquette

Conclusion

The findings of this study have shown that, charcoal briquettes produced from sawdust would make good biomass fuel. The physico-chemical characteristics of the briquette assessed in this study showed that the briquettes manufactured from the sawdust has low moisture content, high calorific value and low ash content. There is also an indication that, the briquette is environmental friendly and will help reduce the health hazard associated with the use of fuel wood and reduce deforestation. The survey has revealed that sawdust usually generated in large quantities and usually burned to pollute the environment can be converted into good quality, highly storable and durable high-grade solid fuel briquettes that will be suitable for both domestic and industrial energy production for heat generation.

It can therefore be concluded that, indeed, there is future and market potential for biomass briquettes in the country since the survey revealed a positive attitude for the use of biomass briquettes by the respondents.

References

Aina, O. M., Adetogun, A. C. And Iyiola, K. A. (2009). Heat Energy From Value-Added Sawdust Briquettes of Albizia Zygia. Ethiopian Journal of Environmental Studies and Management Vol.2 No.1. pp 42-49.

ASTM standard E711-87 (2004), Standard test method for gross calorific value of refuse – derived fuel by the bomb calorimeter. Annual book of ASTM standard, 11.04. ASTM International, Available at: http//www.astm.info/standard/E711.htm

Chaiklangmuang, S., Supa S. and Kaewpet, P. (2008). Development of Fuel briquettes from Biomass-Lignite Blends. Chiang Mai J. Sci. 2008; 35(1):43-50.

Chaney, J. (2010). Combustion characteristics of biomass briquettes. Unpublished PhD studies. Available at: http://etheses.nottingham.ac.uk/1732/1/Combustion_Characteristics_of_Biomass_Briquettes.pdf

De Souza, F. and Sandberg, D. (2004). Mathematical model of a smoldering log. Combustion and Flame, vol. 139, pp. 227–238.

Emerhi, E. A. (2011). Physical and combustion properties of briquettes produced from sawdust of three hardwood species and different organic binders. Adv. Appl. Sci. Res., 2(6):236-246.

Energy Commission, Ghana (2008). Report on woodfuel use in Ghana: an outlook for the future. Energy Commission of Ghana.

Enweremadu, C. C, Ojediran, J. O., Oladeji, J. T., and Afolabi, I. O. (2004). Evaluation of Energy Potential of Husks from Soy-beans and Cowpea. Science Focus. 8:18-23.

Grover, P. D. and Mishra, S. K. (1996). Biomass briquetting: Technology and Practices. Regional wood energy development programme in Asia gcp/ras/154/net, FAO Field Document No.46, p48.

Grover, P. D., Mishra, S. K. and Clancy, J. S. (1994). Development of an appropriate biomass briquetting technology suitable for production and use in developing countries. Energy for Sustainable Development Volume 1 No. 1. pp 45-48.

Jenkins, B. M., Baxter, L. L., Jr., T. R. M. and Miles, T. R. (1998). Combustion properties of biomass. Fuel Processing Technology, vol. 54, pp. 17–46.

Kim, H. J., Lu, G. Q., Naruse, I., Yuan, J. and Ohtake, K. (2001). Modeling combustion characteristics of biocoalbriquettes. Journal of Energy Resources Technology, vol. 123, pp. 27–31.

Kumasi Institute of Technology and Environment (KITE), (1999). Energy Use in some peri-urban areas in Kumasi. 4th Floor SSNIT Building Annex, Harper Road, Adum, Kumasi-Ghana. – Unpublished study

Loo, S. V. and Koppejan, J. (2008). The Handbook of Biomass Combustion and Co-firing. Earthscan.

McKendry, P. (2002). Energy production from biomass (part 1): overview of biomass. Resource Technol., (83), 37-46.

Musa, N. A. (2007). Comparative Fuel Characterization of Rice Husk and Groundnut Shell Briquettes. NJREDl. 6(4):23-27.

Oladeji, J. T. (2010). Fuel Characterization of Briquettes Produced from Corncob and Rice Husk Resides. Pacific Journal of Science and Technology. 11(1):101-106.

Olorunnisola A. O. (2004). Briquetting of rattan furniture waste. Journal of Bamboo and Rattans3(2):139-149.

Rabier, F., Temmerman, M., Bohm, T., H. Hartmann, Jensen, P. D., Rathbauer, J., Carrasco, J. and Fernandez, M. (2006). Particale density determination of pellets and briquettes. Biomass and Bioenergy, vol. 30, pp. 954–963.

Singh, A. and Singh, Y. (1982). Briquetting of paddy straw. Agricultural Mechanization in Asia,Africa and Latin America 42-44.

Stout, B. A. and Best, G. (2001). Effective energy use and climate change: needs of rural areas in developing countries. Agricultural Engineering International: the CIGR E-Journal of Scientific Research and Development. Vol. III, 19pp.

Styles, D., Thorne, F. and Jones, M. B. (2008). Energy crops in Ireland: an economic comparison of willow and miscanthus production with conventional farming systems. Biomass Bioenergy, 32, 407- 421.

Trossero, M. A. (2002). Unasylva Newsletter 211, Vol. 53, published by FAO.

Wamukonya, L. and Jenkins, B. (1995). Durability and relaxation of sawdust and wheat-straw briquettes as possible fuels for Kenya. Biomass and Bioenergy 8(3): 175–179.

Wilaipon, P. (2007). “Physical Characteristics of Maize Cob Briquettes under Moderate Die Pressure”. American Journal of Applied Science. 4:995-998.

Wilaipon, P. (2008). Density Equation of Bio-Coal Briquette and Quantity of Maize Cob in Phitsanulok, Thailand. American Journal of Applied Sciences, 5(2):1808-1811.

Yaman, S., Sahan M., Haykiri-acma, H., Sesen, K. and Kucukbayrak, S. (2000). Production of fuel briquettes from olive refuse and paper mill waste. Fuel Processing Technology 68:23-31.

Yang, Y. B., Ryu, C., Khor, A., Yates,N. E., Sharifi, V. N. and Swithenbank, J. (2005). Effect of fuel properties on biomass combustion. part ii. Modeling approach-identification of controlling factors, Fuel, vol. 84, pp. 2116–2130.

Zaror, C. A. and Pyle. P. D. (1982). The pyrolysis of biomass: A general review, Sadhana Academy Proceedings in Engineering Sciences, vol. 5, no. 4, pp. 269–285.

Ethanosolv Pretreatment of Bamboo with Dilute Acid for Efficient Enzymatic Saccharification

Zhiqiang Li, Zehui Jiang, Benhua Fei*
International Centre for Bamboo and Rattan, Beijing 100102, China.
** Corresponding author: jiangzehui@icbr.ac.cn*
Zhiyong Cai

USDA Forest Service, Forest Products Laboratory, 1 Gifford Pinchot Dr., Madison, WI 53726, United States
Xuejun Pan
Biological Systems Engineering, University of Wisconsin, 460 Henry Mall, Madison, WI 53706, United States

Abstract

Bamboo is a potential lignocellulosic biomass for the production of bioethanol because of its high cellulose and hemicelluloses content. In this research, ethanosolv pretreatment catalyzed by sulfuric acid was studied in order to enhance enzymatic saccharification of moso bamboo. The addition of 2% (w/w on bamboo) sulfuric acid in water or 75% (v/v) ethanol was demonstrated effective in pretreatment and fractionation of bamboo. The ethanosolv pretreatment yielded a solid fraction with 84.5% cellulose. The cellulose-to-glucose conversion yields were 77.1% (ethanosolv) and 57.3%(water) after enzymatic hydrolysis of the solid fraction at 50 °C for 48 h using a enzyme loading (15 filter paper units of cellulase/g cellulose and 30 IU β-glucosidase/g cellulose). The concentrations of fermentation inhibitors such as 5-hydroxy-2- methyl furfural (HMF) and furfural were 0.96 g/L and 4.38 g/L, respectively, in the spent liquor after the ethanosolv pretreatment, which were slightly lower than those in the spent liquor from H_2SO_4-water treatment. When the pretreatment spent liquor was diluted with water, dissolved lignin was precipitated and then recovered through filtration. More than 87.2% of the original lignin in untreated bamboo was recovered as ethanol organosolv lignin.

***Keywords*:** Bamboo, Bioethanol, Ethanosolv, Organosolv pretreatment, Dilute acid

Introduction

The first-generation bioethanol which based on corn reached the limit due to limitation in feedstock supply and competition with food and livestock feed market (Gray et al., 2006; Leibtag 2008; Elobeid et al., 2006). The exploitation and utilization of second-generation bioethanol from lignocellulose have attracted much interest of researchers and the governments around the world. However, conversion of lignocellulosic biomass to ethanol is much more difficult than sugar and corn-to-ethanol production due to the recalcitrant nature of the lignocellulosic biomass (Sun et al., 2002). Thus, a pretreatment process is required to enhance its enzymatic digestibility. Many pretreatment methods have been proposed to increase cellulose-to-glucose conversion yield in the bioethanol production process.

Organosolv pretreatment has been evaluated as an effective pretreatment method for high-lignin lignocellulosic biomass (Chum et al., 1990; Pan et al., 2006). It can breaks down internal lignin and hemicellulose bonds and thus, removes the portion of lignin from biomass. Through the removal of the lignin, pore-volume and surface area increase so as to increase substrate enzymatic digestibility. A strong inorganic acid is usually carried out in the organosolv pretreatment as a catalyst which to hydrolyze the lignin-lignin and lignin-carbohydrate bond in biomass (Holtzapple et al., 1984).

Bamboo is the vernacular or common term for members of a particular taxonomic group of large woody grasses (subfamily *Bambusoideae*) (Scurlock et al., 2000). Bamboo has some advantages such as fast growth, high cellulose content and bamboo resource is very abundant in China. So it may be one of most potential bio-energy resources with Chinese characteristics in the future. Some pretreatments have been investigated on bamboo for bioethanol production. Enzymatic saccharification (48 h) using a 35 atm and 5 min steam exploded bamboo produced 426 and 488 mg/(g initial dry sample) of glucose and reducing sugar, respectively(Yamashita et al., 2010). Otherwise, the sugar yield was only 43-85mg/(g initial dry sample) of dilute sulfuric acid pretreatment which carried out at 120-140°C for 30-90min with a sulfuric acid loading of 0.6-1.2% (w/w) (Leenakul et al., 2010). Literature on organosolv pretreatment of bamboo is scarce. In this investigation, the feasibility of an ethanosolv pretreatment using inorganic catalyst was evaluated. Dilute sulfuric acid was applied as the catalyst for ethanosolv pretreatment of moso bamboo and the enzymatic hydrolysis were carried out after the pretreatment.

Materials and Methods

Materials. Moso bamboo (*Phyllostachys heterocycla*) was acquired from the central area of Louisiana, USA. After being air-dried, the culms of mature (4 years old) bamboo were milled using a hammer mill with a screen opening size of 2.0 mm before pretreatment. The average moisture content of ground bamboo was 6.93% (wt). The moisture content of the ground samples was measured under oven-dried (OD) for 24 h at 105±2°C. Commercial enzymes, cellulase and β-glucosidase produced by Novozymes, were

purchased from Sigma-Aldrich (St. Louis, MO). All the chemical reagents used in this study were purchased from Fisher Scientific (Pittsburgh, PA).

Pretreatments. Bamboo samples were pretreated in a microwave accelerated reaction system made by CEM Corporation (Model MARS, CEM Corporation, Matthews, North Carolina, and USA). Each pretreatment was carried out in duplicate; the average results of the two runs were reported. In general, 8 g of raw oven-dry bamboo was loaded into a 100 mL vessel. Prepared pretreatment solution of 50 mL 0.32% (2% on OD bamboo) H_2SO_4 in water or 75% (w/w) ethanol was then poured into the vessel. The vessel positioned at the centre of rotating circular ceramic plate in the microwave oven for treatment at the power level of 400W. The temperature was raised to the 180°C in 10 min and maintained for an additional 30 min. After the pretreatment, the pretreatment spent liquor was separated from the pretreated substrate (solid) by vacuum filtration. The ethanosolv pretreated substrate was washed three times with 50 mL aqueous ethanol with the same concentration (75%) of pretreatment liquor at 60 °C and the washes combined with the spent liquor. The substrate was then washed three more times with water at 60 °C and the washes discarded. The solid substrate then stored at 4°C for enzymatic hydrolysis.

The spent liquor and ethanol washes were combined and mixed with three volumes of water to precipitate the dissolved lignin. The precipitated lignin, described as ethanol organosolv lignin (EOL), was collected on filter paper through vacuum filtration and then washed thoroughly with water and air-dried. The filtrate and water washes were combined to obtain a water-soluble fraction containing monomeric and oligomeric hemicellulosic sugars, depolymerized lignin, and other unidentified components. It was stored in 4°C for fermentation inhibitors and chemicals analysis by high performance liquid chromatography (HPLC).

Enzymatic hydrolysis. Enzymatic hydrolysis of the pretreated bamboo substrates and original raw bamboo was conducted as described previously (Pan et al., 2008). Commercialized microcrystalline cellulose (MCC) was used as a comparison for the enzymatic digestibility. Enzymatic hydrolysis was carried out in 150 mL plastic jars at 50°C on a shaking incubator (Thermo Fisher Scientific, Model 4450, Waltham, MA) at 220 rev/min. Bamboo substrate equivalent to 0.8 g glucan was loaded with 40 mL of 0.05M sodium acetate buffer (pH 4.8). Approximately 1.5 mg of tetracycline chloride was added to control the growth of microorganisms and prevent consumption of liberated sugars. Two enzymes cellulase (15 FPU, Filter Paper Units, per gram glucan) and β-glucosidase (30 IU, international Units, per gram glucan) were loaded into the plastic jars. Hydrolysates were sampled periodically at 1, 3, 6, 12, 24 and 48 hour to analyze glucose concentration. The hydrolysis was conducted in duplicate for each substrate; the average is reported here.

Analytical methods. In-soluble lignin of bamboo and pretreated bamboo substrates was determined according to National Energy Laboratory (NREL) Analytical Procedure: Determination of Structural Carbohydrates and Lignin in Biomass (with modifications). Acid-soluble lignin was measured at 205 nm on a UV-Visible spectrophotometer.

Carbohydrate compositions of the original bamboo, pretreated bamboo substrates and spent liquors were conducted using an improved high-performance anion exchange chromatography (Dionex HPLC system ICS-3000) equipped with integrated amperometric detector and Carbopac™ PA1 guard and analytical columns at 20°C. Fermentation inhibitors including acetic acid, formic acid, furfural, levulinic acid and 5-hydroxylmethylfurural (HMF) were analyzed using the Dionex ICS-3000 equipped with a Supelcogel C-610H column at temperature 30°Cand UV detector at 210 nm.

According to the filter paper assay recommended by the International Union of Pure and Applied Chemists, the cellulase activity was determined and its expression is filter paper units (FPUs). β-glucosidase activity was determined through p-nitrophenyl-b-D-glucoside as the substrate and its expression is International Units (IUs).

Results and Discussions

Comparison of cell wall components of pretreated substates. The cell wall chemical composition can provide some indications of the effect of chemical pretreatment on bamboo chemical structure. Chemical components of untreated bamboo and pretreated bamboo substrates are listed in table1. The untreated bamboo has glucose, xylose and lignin contents of about 41.3%, 22.0% and 24.3%, respectively. There are low content of arabinose (1.1%), galactose (0.3%) and mannose（0.6%) in untreated bamboo. The ethanosolv pretreatment without acid catalyst slightly changed the chemical components composition of bamboo. The ethanosolv pretreatment with acid catalyst were very effective in removing hemicellulose and lignin. As a result, cellulose was enriched in the pretreated substrates as high as 84.5%. This suggested that the ethanosolv pretreatment with sulfuric acid could minimize the loss of cellulose, which served the main resource in bioethanol production. The addition of acid to the liquid mixture played a very important role in catalyzing the removal of hemicellulose and lignin.

Table 1. *Chemical analyses of untreated and pretreated bamboo substrates after 30 min at 180 °C*

Acid charge on OD bamboo (%)	Pretreated solutions	Component weight (%)						
		Arabinose	Galactose	Glucose	Xylose	Mannose	Acid-insoluble lignin	Acid-soluble lignin
Untreated bamboo		1.1±0.1	0.3±0.0	41.3±0.4	22.0±1.0	0.6±0.0	22.8±0.2	1.5±0.0
0	Ethanosolv	1.0±0.1	0.3±0.0	43.7±1.5	21.8±0.9	ND	24.9±0.5	2.2±0.0
2	Ethanosolv	0.1±0.0	ND	84.5±3.1	8.2±0.3	0.8±0.1	5.5±0.1	2.3±0.1
2	Water	0.1±0.0	ND	52.0±2.9	1.8±0.2	ND	35.0±0.4	1.8±0.4

The spent liquor and ethanol washes were combined and mixed with three volumes of water to precipitate the dissolved lignin. The precipitated lignin was collected on filter paper through vacuum filtration and then washed thoroughly with water and air-dried. In contrast to lignin produced by other technical processes, such as kraft pulping, ethanol

organosolv lignin is a sulfur-free low-molecular-weight product of high purity. Generating high-quality lignin is one of the unique advantages of the ethanosolv pretreatment over alternative methods, such as steam explosion, dilute-acid pretreatment, and hot-water treatment, where the only proposed use for the lignin is as a boiler fuel (Pan et al., 2008). High-quality lignin can be used as a substitute for polymeric materials, such as phenolic powder resins, polyurethane foams, and epoxy resins.

The sugars and soluble lignin in the combined liquor of filtrate and water washes were listed in table 2. The concentration was calculated on original spent liquors. More glucose and xylose were detected in ethanosolv pretreatment spent liquors than that in water pretreated spent liquors.

Table 2. *Chemical analyses of pretreated spent liquors*

Acid charge on OD bamboo (%)	Pretreated solutions	Component in spent liquors (g/L)					
		Arabinose	Galactose	Glucose	Xylose	Mannose	Acid-soluble lignin
0	Ethanosolv	0.0±0.0	0.0±0.0	0.8±0.1	0.0±0.0	0.8±0.2	5.5±0.9
2	Ethanosolv	1.6±0.2	0.5±0.0	6.9±0.9	20.5±2.3	0.7±0.1	5.0±0.3
2	Water	0.04±0.0	0.7±0.0	3.3±0.1	8.4±0.6	ND	5.7±0.3

Mass balance of sugars during pretreatments. For an ideal pretreatment, it should provide readily enzymatic digestible substrates. But it is not enough; it should also to maximally recover all the components of original biomass. As shown in table 3, sugars and lignin in two fractions, solid substrates and spent liquors, were calculated based on 100 g untreated raw bamboo. As discussed above in table1, it contained 41.3 g glucose, 22.0 g xylose, 1.1 g arabinos, 0.3 g galactose and 0.6 g mannose from 100 g oven-dry bamboo. The total sugars and lignin recovery was 86.7 g without acid pretreatment. Ethanosolv pretreatment with acid addition obtained lower recovery 81.2 g. Although total components recovery was high, only 41.5 g substrates were obtained. Low substrate yield from ethanosolv pretreatment was due in part to the dissolution of more hemicellulose and lignin. The detected sugars in the spent liquors were 18.8 g (ethanosolv). The spent liquors with so high concentration sugars can be detoxified and then used for ethanol fermentation.

The calculations from these data indicated that total sugar recovery was 87.4 % (ethanosolv) and 63.7 % (water). The glucose recovery was 94.2 % (ethanosolv) and 84.0% (water). While the xylose recovery was quite low, it was 73.6% (ethanosolv) and 28.6 % (water). The result indicated xylose was subject to greater degradation than glucose in acid pretreatment, especially in water pretreated solution. This is one of the reasons why water pretreated spent liquor had high concentration of furfural than ethanosolv pretreated spent liquor, which was listed in table 4.

Table 3. *Mass balance of 100 g oven-dry bamboo powder during pretreatments*

Acid charge on OD bamboo (%)	Pretreated solutions	Component recovery, g								
			Arabinose	Galactose	Glucose	Xylose	Mannose	Lignin	Sum	Recovery
0	Ethanosolv	Substrate	0.9±0.1	0.3±0.0	38.7±1.5	19.3±0.9	ND	23.1±0.5	82.3	86.7
		Liquor	0.0±0.0	0.0±0.0	0.5±0.1	0.0±0.0	0.5±0.2	3.4±0.9	4.4	
2	Ethanosolv	Substrate	0.0±0.0	0.0±0.0	34.6±3.1	3.4±0.1	0.3±0.1	3.2±0.1	41.5	81.2
		Liquor	1.0±0.2	0.3±0.0	4.3±0.9	12.8±2.3	0.4±0.1	20.8±0.3	39.6	
2	Water	Substrate	0.1±0.0	0.0±0.0	32.6±2.9	1.1±0.2	0.0±0.0	23.0±0.8	56.6	68.0
		Liquor	0.0±0.0	0.5±0.0	2.1±0.2	5.2±0.8	0.0±0.0	3.6±0.4	11.4	

Comparisons of fermentation inhibitors formation during pretreatments. The cellulose and hemicellulose removed by ethanosolv pretreatments were partially hydrolyzed to fermentable sugars and even further degraded to potential fermentation inhibitors, such as formic acid, levulinic acid, furfural and Hydroxymethylfurfural (HMF). Furfural derived from pentoses, HMF from degradation of hexoses, and levulinic and formic acids from successive decomposition of HMF. The acid-soluble lignin was also a kind of fermentation inhibitors. Acetic acid released from acetyl groups on hemicelluloses, which could be detected in both acidic and basic pretreatment liquors.

All the potential fermentation inhibitors mentioned above were listed in table 4. The data clearly indicated that the acid-soluble lignin in the spent liquors were slightly different. The total of inhibitors (formic, acetic and levulinic acid, furfural and HMF) were significantly different. There was no inhibitor detected in ethanosolv pretreatment liquors without acid addition. The total inhibitors in organsolv pretreated spent liquor was less than that in water pretreated spent liquors.

Table 4. *Fermentation inhibitors in pretreated spent liquors after 30 min at 180 °C*

Acid charge on OD bamboo (%)	Pretreated solutions	Inhibitors (g/L)						
		Acid-soluble lignin	Formic acid	Acetic acid	Furfural	HMF	Levulinic acid	Total
0	Ethanosolv	5.5±0.9	0.0±0.0	0.0±0.0	0.0±0.0	0.0±0.0	0.0±0.0	0.0
2	Ethanosolv	5.0±0.3	2.4±0.2	1.6±0.4	4.4±0.1	1.0±0.1	2.0±0.3	11.4
2	Water	5.7±0.3	4.0±0.3	5.7±0.4	4.6±0.1	1.2±0.1	0.4±0.0	15.9

Enzymatic hydrolyzability of pretreated bamboo substrates. There are many factors that affect enzymatic hydrolyzability of substrates, such as hemicellulose content, lignin structure, distribution and content, cellulose crystallinity and degree of polymerization, and so on(Mansfield et at., 1999; Alvira et al., 2010). All these known and unknown factors caused bamboo to be a unique biomass for efficient pretreatment not likes agricultural wastes and wood. One of the structural differences is that bamboo has high density and hardness, even for the outer part of bamboo (bamboo green).

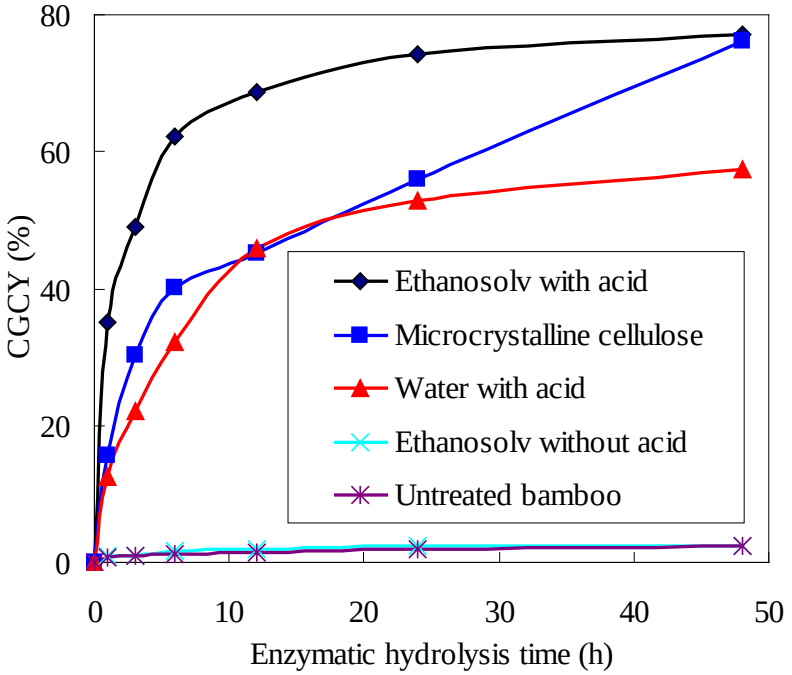

Figure 1. *Comparison of time-dependent enzymatic hydrolysability of different pretreated bamboo substrates with a enzyme loading of 15 FPU cellulase and 30 IU β-glucosidase per gram of cellulose, 50°C, pH 4.8 and on a 220 rpm shaker. CGCY: cellulose-to-glucose yield.*

The enzymatic hydrolyzability of ethanosolv pretreated bamboo substrates were shown in figure 1. Commercialized microcrystalline cellulose (MCC) was used as a comparison for the enzymatic digestibility. The enzymes loading were 15 FPU (Filter Paper Units) cellulase and 30 IU (International Units) β-glucosidase per gram cellulose for all enzymatic hydrolysis. The cellulose-to-glucose conversion yield of untreated raw bamboo after a 48 h hydrolysis was only 2.4%. The cellulose-to-glucose conversion yield of ethanosolv pretreatment without acid addition was just 2.6%, no significantly increasing. Otherwise, the water and ethanosolv with acid pretreatment had significantly improved the enzymatic digestibility of bamboo. Meanwhile, the cellulose-to-glucose conversion yield of ethanosolv pretreatment (77.1%) was higher than that of water pretreatment (57.3%). Which were even higher than microcrystalline cellulose to glucose conversion yield (76.2%)? Including glucose in the spent liquor, the total glucose yield from raw bamboo were 31.0% (ethanosolv) and 20.8% (water), respectively. It was calculated based on 41.3% cellulose content in raw bamboo.

Comparison among the pretreatments, the cellulose-to-glucose conversion yields were increasing with the content of lignin decreasing. The removal of hemicellulose and lignin increased cellulose susceptibility to enzymes. Meanwhile, the cellulose-to-glucose conversion yield of MCC was 76.2%, not reach 100%. The results indicated that besides the content of hemicellulose and lignin, other factors like cellulose crystallinity and degree of polymerization affected the enzymatic digestibility of the substrates together.

Conclusion

Ethanosolv pretreatment without acid addition has no observably influence on cell-wall change or enzymatic digestibility of bamboo. Ethanosolv pretreatment with sulfuric acid as catalyst has significantly hemicellulose and lignin removal and enzymatic digestibility increasing of bamboo substrates. Based on the same acid loading (2% on OD bamboo), the ethanosolv pretreatment has much more hemicellose and lignin removal and the cellulose-to-glucose conversion yield was higher than water-pretreatment. The total glucose yield (including pretreatment and hydrolysis) from raw bamboo were 31.0% (ethanosolv) and 20.8% (water), respectively.

Acknowledgments

The authors are grateful for the support of ‘the Fundamental Research Funds for the International Centre for Bamboo and Rattan’, Grant. No. 1632012001.

References

Alvira P., Tomás-Pejó E., Ballesteros M., Negro M.J., 2010. Pretreatment technologies for an efficient bioethanol production process based on enzymatic hydrolysis: A review. Bioresource Technology, 101, 4851–4861.

Chum H. L., Johnson D. K., Black S. K., 1990. Organosolv pretreatment for enzymic hydrolysis of poplars. 2. Catalyst effects and the combined severity parameter. Ind Eng Chem Res, 29, 156-162.

Elobeid A, Tokgoz S, Hayes D, Babcock B, Hart C., 2006. Long-run impact of corn-based ethanol on the Grain, Oilseed, and livestock sectors: a preliminary assessment. The Food and Agricultural Policy Research Institute (FAPRI) Publications.

Gray K. A., Zhao L., Emptage M., 2006. Bioethanol. Current Opinion in Chemical Biology, 10, 141-146.

Holtzapple M. T., Humphrey A. E., 1984. The effect of organosolv pretreatment on the enzymatic hydrolysis of poplar. Biotechnology and Bioengineering, 26, 670-676.

Leenakul W, Tippayawong N. Dilute Acid Pretreatment of Bamboo for Fermentable Sugar Production. *Journal of Sustainable Energy & Environment,* 2010 (1), 117-120.

Leibtag E., 2008. Corn prices near record high, but what about food costs? Amber Waves, 6, 10-15.

Mansfield, S. D., Mooney, C., Saddler, J. N., 1999. Substrate and enzyme characteristics that limit cellulose hydrolysis. Biotechnology progress, 15, 804-816.

Pan X. J., Gilkes N., Kadla J., Pye K., Saka S., Gregg D., Ehara K., Xie D., Lam D., Saddler J., 2006. Bioconversion of Hybrid Poplar to Ethanol and Co-Products Using an

Organosolv Fractionation Process: Optimization of Process Yields. Biotechnology and Bioengineering, 94, 5, 851-861.

Pan X. J., Xie D., Yu R. W., Saddler J. N., 2008. The bioconversion of mountain pine beetle-killed lodgepole pine to fuel ethanol using the organosolv process. Biotechnology and Bioengineering, 101, 39-48.

Scurlocka J.M.O., Daytonb D.C., Hamesb B., 2000. Bamboo: an overlooked biomass resource? Biomass and Bioenergy 19, 229-244.

Sun Y., Cheng J., 2002. Hydrolysis of lignocellulosic materials for ethanol production: a review. Bioresource Technology, 83, 1-11.

Yamashita Y, Shono M, Sasaki C, et al., 2010. Alkaline peroxide pretreatment for efficient enzymatic saccharification of bamboo. *Carbohydrate Polymers*, 79, 914-920.

Proceedings of the 55th International Convention of Society of Wood Science and Technology
August 27-31, 2012 - Beijing, CHINA

How Improved Pretreatment And Enzyme Complexes Can Help Us Evolve From A Hydrocarbon Based Economy To A Carbohydrate/Biomass Based Society

*Jinguang HU –Valdeir ARANTES –Amadeus PRIBOWO –Keith GOURLAY –Jack SADDLER**

Forestry Products Biotechnology/Bioenergy Group, Wood Science Department, University of British Columbia, 2424 Main Mall, Vancouver BC, V6T 1Z4, Canada

*Corresponding author

Phone: 604-822-9741
Fax: 604-822-8157
Email addresses: jack.saddler@ubc.ca

Abstract

A crucial step in the bioconversion of lignocellulosic feedstocks to biofuels is to cost-effectively maximize the saccharification of the cellulose and hemicellulose components to fermentable sugars. Despite intensive research over the last 30 years, achieving fast, complete and efficient bioconversion of lignocellulosic substrates remains a challenging goal. It is widely acknowledged that the rate and extent of the cellulolytic hydrolysis is influenced, not only by the effectiveness of the enzyme cocktail, but also by the physical and chemical nature of lignocellulosic substrates and the mechanism and effectiveness of the various pretreatment technologies that are used. In this short review, variouspretreatment processes are compared and the different strategies that have been assessed to try to improve the hydrolytic performance of the various enzyme complexes are discussed. We have also tried to summarize the work ofour FPB/Bioenergy group over the past 30 years, in collaboration with multinational companies such as Novozymes (the world's biggest enzyme company, based in Denmark). We describe how considerable progress has been made in the "bioconversion" areaand how forest based residues can be readily converted into useful sugars for the production of "green" fuels and chemicals.

Keywords:lignocellulosic biomass, pretreatment, enzyme, enzymatic hydrolysis.

Introduction

Concerns about increasing levels of carbon emissions, global warming and energy security have encouraged governments around the world to pursue alternative, clean energy strategies(Sims et al., 2010). In the same way that oil, coal and gas are composed of finite hydrocarbons, the carbohydrates in sustainably produced biomass found in forests and agricultural crops can be used as the feedstock for "bioconversion technologies" that can be the basis of sustainably derived products such as bioenergy, biomaterials and biochemicals(Stephen, Mabee and Saddler, 2012). However, the utilization of biomass for biofuels or biochemicals first requires the breakdown of the carbohydrates within the biomass down to their component sugars. In nature, fungi, bacteria, and other microorganisms produce enzymes to break down these sugar polymers(Lynd et al., 2002; Zhang and Lynd, 2004). However, because these polymers serve as structural materials in plants, they have evolved to withstand fast and effective microbial/enzymatic degradation(Himmel et al., 2007). Consequently, in order to efficiently utilize this biomass, the natural degradation process that normally occurs over a long period of time (typically several years) needs to be shortened into a matter of days or even hours/minutes(Sims et al., 2010; Stephen, Mabee and Saddler, 2012)!

Over the past 50 to 60 years, many excellent research groups have been studying ways to acceleratethis biodegradation process to enable technical, and hopefully economic, biomass conversion to these higher value products. It is widely acknowledged that an efficient biomass pretreatment process is required to not only recover as many of the original biomass components (lignin, hemicellulose, cellulose, extractives, etc.) in a useable form, but to also "open up" the biomass matrix and increase enzymes access to the cellulosic component. In parallel, a robust enzyme cocktail that can quickly and efficiently break down the cellulose component at high substrate and low protein concentrations is also an essential requirement if we are to establish an economically viable biomass-to-fuels/chemicals industry(Sims et al., 2010; Himmel et al., 2007; Yang and Wyman, 2008; Gao et al., 2010). In this paper,we have briefly reviewed leading pretreatment technologies and various strategies that groups have used to try to enhance the enzymatichydrolysis step of a biomass-to-fuels/chemicals biorefinery process.In particular,the collective research of our Forest Products Biotechnoloy/Bioenergy (FPB) Research Group is described, summarizing how we have tried to better understand howforest based residues might be broken down into useful sugars for the production of "green" fuels and chemicals.

Pretreatment

Pretreatment is a prerequisite step in any proposedbiochemically based biomass-to-fuels/chemical biorefinery process, both so that the various biomass components can be fractioned and recovered in an effective manner and so that the cellulosic fraction can be "opened up" to enhancethe rate and extent ofenzymatic hydrolysis. It is recognised that the rate and extent of cellulose hydrolysis is influenced not only by the efficiency of the enzyme cocktail but also by the chemical, physical and morphological characteristics of the heterogeneous lignocellulosic substrates(Yang and Wyman, 2008; Chandra et al., 2007; Mosier et al., 2005). Pretreatment strategies have generally been categorized into biological, physical and chemical processes, or a combination of these approaches (Table 1).

Biological pretreatment has been traditionallyapplied as a biopulping option in the pulp and paper industry(Chandra et al., 2007; Tian, Fang and Guo, 2012). In general, bio-based pretreatments haveutilized wood degrading fungi such as soft rot, brown rot, and white rot to modify the chemical composition of the lignocellulosic biomass. Soft and brown rot fungi have been shown to primarily degrade the hemicellulose while white rot fungi mainly attack the lignin(Hammel et al., 2002; Martinez et al., 2005). Even though this pretreatment approach consumes less energy, is environmentally friendly and generates fewer inhibiting compoundsthan thermo/chemical pretreatment technologies, it requires careful growth condition, large spacefor operating and a long pretreatment (incubation) period (at least 10-14 days)(Tian, Fang and Guo, 2012; Wyman et al., 2005). These limitations have made biological pretreatments less commercially attractive.

In contrast, physical pretreatments, such as milling and ultra-sonication, can breakdown feedstock into smaller size without changing their chemical composition(Mosier et al., 2005; Yunus et al., 2010). Physical pretreatments generally enhance enzymatic hydrolysis by disrupting the cellulose crystallinity and/or by increasing the surface areaof the biomass(Yunus et al., 2010; Mais et al., 2002). Although physical pretreatment have been successfully applied to variety of feedstocks, they are typically energetically demanding and do not remove or solubilize the hemicellulose and lignin, both of which generally restrict the accessibility of cellulose to cellulase enzymes(Chandra et al., 2007; Wyman et al., 2005). Physical pretreatments have yet to be shown to be economically viable at a commercial scale.

Chemical pretreatment (typically acid and alkali based) are usually initiated by chemical reactions with the main goal of enhancing enzyme accessibility to the cellulose by disrupting of the biomass structure and solubilizing the hemicellulose and lignin, and to a lesser degree of decreasing the DP and crystallinity of the cellulosic component(Yang and Wyman, 2008; Chandra et al., 2007). For example, organosolv pretreatment has been applied using a variety of solvents and this type of pretreatment has been shown to significantly reduce the lignin content of the substrate(Pan et al., 2006). By combining it with swelling agents such as NaOH and sulfuric acid organosolvpretreatmentcan also partially decrease cellulose crystallinity(Silverstein et al., 2007).Pretreatments that combine both chemical and physical processes are generally referred to as physiochemical processes, and this type of pretreatmenthas received most attention in recent years.For example, steam explosion with the addition of chemical catalyst has shown significant advantages for generating easily hydrolysable substrates from most potentiallignocellulosic biomasssubstrates (Chandra et al., 2007; Arantes and Saddler, 2011).

Unfortunately, manypretreatment conditions that are optimized to result in easily-digestible cellulose (usually at very high severity) typically result in significant loss of the hemicellulose component, which can account for 20-40% of the plant cell-wall polysaccharides(Chandra et al., 2007; Bura, Chandra and Saddler, 2009).The degradation of the hemicelluloses not only reduces the sugar yield of the process, but also results in the formation of degradation products that can be inhibitory to the hydrolysis step but particularly to the yeast used in the subsequent fermentation of the sugars to biofuels such as ethanol (Ohgren et al., 2007; Palmqvist et al., 1996). Lower severity pretreatments allow for the preservation of hemicelluloses in a useable, insoluble form, resulting in an increase in overall sugar recovery. However, the following enzymatic hydrolysis of the cellulosic component becomes more difficult due to the recalcitrant nature of the remaining, lightly-pretreated substrate(Chandra et al., 2007).

Over the past 20 years, our Forest Products Biotechnology/Bioenergy Group at UBC has focused on both steam and organosolv pretreatments, assessing their suitability for application over a range of lignocellulosic substrates.A main goal has been to try and determine which substrate characteristics are primarily responsible for limiting the effective enzymatic hydrolysis of the cellulosic component while developing pretreatment methods that both maximize recovery of the lignin and hemicellulose components in a useable form while enhancing cellulose accessibility to the cellulase complex. We have tried to differentiate between the various lignocellulosic substrate characteristics at the macroscopic (fiber), microscopic (fibril) and nanoscopic (microfibril) level that have been modified during pretreatment and subsequent hydrolysis.

Enzymatic hydrolysis

A significant amount of research has been carried out to both improve the efficiency of the pretreatment step and to improve substrate accessibility to enzymes.However, high enzyme loadings are still typically required(Arantes and Saddler, 2011; McMillan et al., 2011), which contribute to the high costs incurred in the production of biomass-derived biofuels(Arantes and Saddler, 2011; Merino and Cherry, 2007; Somerville, 2006; Wilson, 2009). Past work has generally pursued three main strategies to try to reduce the cost of the enzymatic hydrolysis step. Eitherby minimizing the costs of enzyme production(Wilson, 2009),and increasing the hydrolytic performance of the enzymes(Gao et al., 2011; Hu, Arantes and Saddler, 2011), or by trying to recycle the enzymes for multiple roundsfor hydrolysis (Gregg and Saddler, 1996; Tu et al., 2006).

Enzyme Production: Over the last decade, even though biotechnology companies, such as Novozymes, Genencor International, etc., have reported a significant decrease in the cost of enzyme production, it is generally recognised that a further 3-5 fold reduction is still needed in order for cellulosic ethanol to be economically feasible (Aden and Foust, 2009; Humbird et al., 2010). However,the further cost reductions for enzyme production has been predicted to be challenging(Stephen, Mabee and Saddler, 2012; Wilson, 2009). Therefore, the other two strategies have been attracted considerable attention over the last few years.

Enzyme Specific Activity: Past work has shown that the “specific activity” of the cellulase complexcan be improved by increasing the activity of individual enzymes and/or by producing more efficient enzyme mixtures that act synergistically on the heterogeneous lignocellulosic substrates.Although strategies such as site-directed mutagenesis or directed evolution have been successfully employed to improve individual cellulase properties such as binding affinity, catalytic activity and thermostability(Wilson, 2009; Okada et al., 2000; He Jun et al., 2009),in most cases the extent of improvement achieved on simple, model cellulosic substrates does not directly translate into improved activity on the more complex, heterogeneous lignocellulosic substrates(Zhang, Himmel and Mielenz, 2006). This suggests that the actual catalytic cleavage of the glycosidic bond may not be the key limiting step in the enzymatic hydrolysis of cellulosic biomass. In parallel, alternative strategies have tried toenhance the hydrolytic efficiency of the enzyme cocktail by optimizing the composition of the major cellulase components using statistical design of experiments as well as by supplying these cellulase enzymes with accessory enzymes such as hemicellulases, GH61, and/or non-hydrolytic, chain separating proteins. This approach have been shown to improve enzyme accessibility to the cellulose chains, and therefore,

the overall "specific activity" of the enzyme mixture (Gao et al., 2011; Hu, Arantes and Saddler, 2011; Harris et al., 2010; Quiroz-Castaneda et al., 2011; Arantes and Saddler, 2010).
One of the main projects we have pursued over the years has been to develop/identify an effective enzyme mixture that,at low protein concentrations, allows fast and complete hydrolysis over a range of pretreated lignocellulosic substrates.It is apparent that there are several important cellulase components and accessory enzymes/proteins that are required to achieve a fast and efficient hydrolysis on various lignocellulosic substrates. It is also clear that there is an optimized ratio and/or combination of enzymes that can be developed to achieve maximum substrate hydrolysis yield with minimum enzyme loading depending on the particular lignocellulosic substrate or pretreatment that has been used. In addition, the type and extent of interaction among these enzymes and between enzymes and substrates have been evaluated over the duration of the hydrolysis reaction. For example, we have shown thatthe interaction between the cellulases andxylanases during hydrolysis of steam pretreated corn stover shows considerable synergistic cooperation, resulting in significantly improved cellulose accessibility resulting from increased fiber swelling and fiber porosity(Hu, Arantes and Saddler, 2011). We have shown that byoptimizing the composition of the cellulases/xylanases cocktail,a 7-fold decrease in cellulase loading and a significant increase in the hydrolysis performance could be achieved (5mgC+30mgX vs. 35mgC) (Figure 1).

In parallel with this more applied, enzyme characterization and application work we have also developed and refined techniques such as Simon's Stain to try to quantifychanges in the accessibility of lignocellulosic substrate (Chandra et al., 2008), and substructure-specific Cellulose Binding Modules (CBM's) to try to assess the cellulose amorphogenesis step at the macroscopic (fiber), microscopic (fibril) and nanoscopic (microfibril) level (Gourlay, Arantes and Saddler, 2012). It is hoped that by a better understanding of what constitutes the essential enzyme components andtheir respective roles during biomass hydrolysis, we can both increase our fundamental knowledge of the mechanisms of biomass degradation and also help better design efficient and robust enzyme cocktails that can effectively hydrolyse various lignocellulosic substrates using low protein (enzyme) loadings.

Enzyme Recycling: Due to the high stability of the cellulase enzymes, enzyme recycling is another promising strategy that could be used to further decrease the cost of enzymatic hydrolysis. During a typical hydrolysis process, the enzymes might remain in the liquid phase, or be adsorbed to the solid substrates(Yang et al., 2010; Tu, Chandra and Saddler, 2007). Several approaches have been pursued to try to reuse the enzymes from both phases, such as ultrafiltration membranes(Lu et al., 2002; Tan et al., 1986), enzyme flocculation(Xu and Chen, 2009), enzyme immobilization (Tu et al., 2006)and reutilization of bound enzymes by adding fresh substrates (Yang et al., 2010; Qi et al., 2011). In order to efficiently apply these strategies, a better understanding of how the enzymes interact with the substrate is required. Unfortunately, there is a significant gap in our knowledge on how the various enzymes present in the enzyme mixture adsorb/desorb, to/from the substrate. This is primarily due to the inability of the availableassays to fully resolve the complexity of the enzyme mixture.We have been investigating the individual enzyme adsorption/desorption profiles during hydrolysis of a range of cellulolytic/lignocellulosic substrates using anenzyme-linked immunosorbent assay (ELISA).

Conclusions

In summary, an ideal pretreatment method should be cheap (both capital and operating costs), effective on a wide range of lignocellulosic substrates, require minimum preparation/handling steps prior to pretreatment, ensure recovery of all of the lignocellulosic components in a useable form and provide a cellulosic stream that can be efficiently hydrolyzed with low concentrations of enzymes. So far it is unlikely that one pretreatment process will be declared a "winner" as each method has its inherent advantages/disadvantages.

It is apparent that by optimizing the "cellulase" enzyme cocktail by the addition ofspecific accessory enzymes to the cellulases mixture/complex we can further decrease the required enzyme loading needed to achieve fast and efficient cellulose hydrolysis. However, it is also clear that the "ideal" enzyme cocktail will be influenced by the nature and source of the biomass substrate, its gross and detailed characteristics and by the pretreatment method that is used to both fractionate and open up the cellulosic component. Therefore it is important to define the ideal, "synergistic conditions" between the compromised pretreatment parameters (i.e. between maximising overall sugar recovery while enhancing cellulose accessibility) and the "optimized" enzyme cocktail. This combination will be essential to further improving the economics of a biochemically based biomass-to-fuels and chemicals process.

Table 1. Summary of various pretreatment technology used for lignocellulosic biomass

pretreatment technology	**examples**	**major effects**	**advantages**	**disadvantages**
biological	white/brown -rot fungi	degradation of lignin and hemicellulose	low energy input; environmentally friendly	very slow
physical	ball milling	reduce particle size;decrease cellulose crystallinity	suitable for various substrates; no chemical input	large energy consumption
chemical	dilute acid; alkaline; organosolv; ionic liquid	hemicellulose solubilisation; lignin transformation/ delignification; saponification of intermolecular ester bonds	improve cellulose accessibility/digestibility	equipment corrosion; sugar degradation; toxic substrates; difficult to recover chemicals
physiochemical	steam explosion; AFEX	disrupt LCC; hemicellulose degradation; decrystalline cellulose	short time; cost effective; improve cellulose accessibility/digestibility;	sugar degradation; produce inhibitors for the following biological process

LCC: lignin-carbohydrate complex; AFEX: ammonia fibre expansion

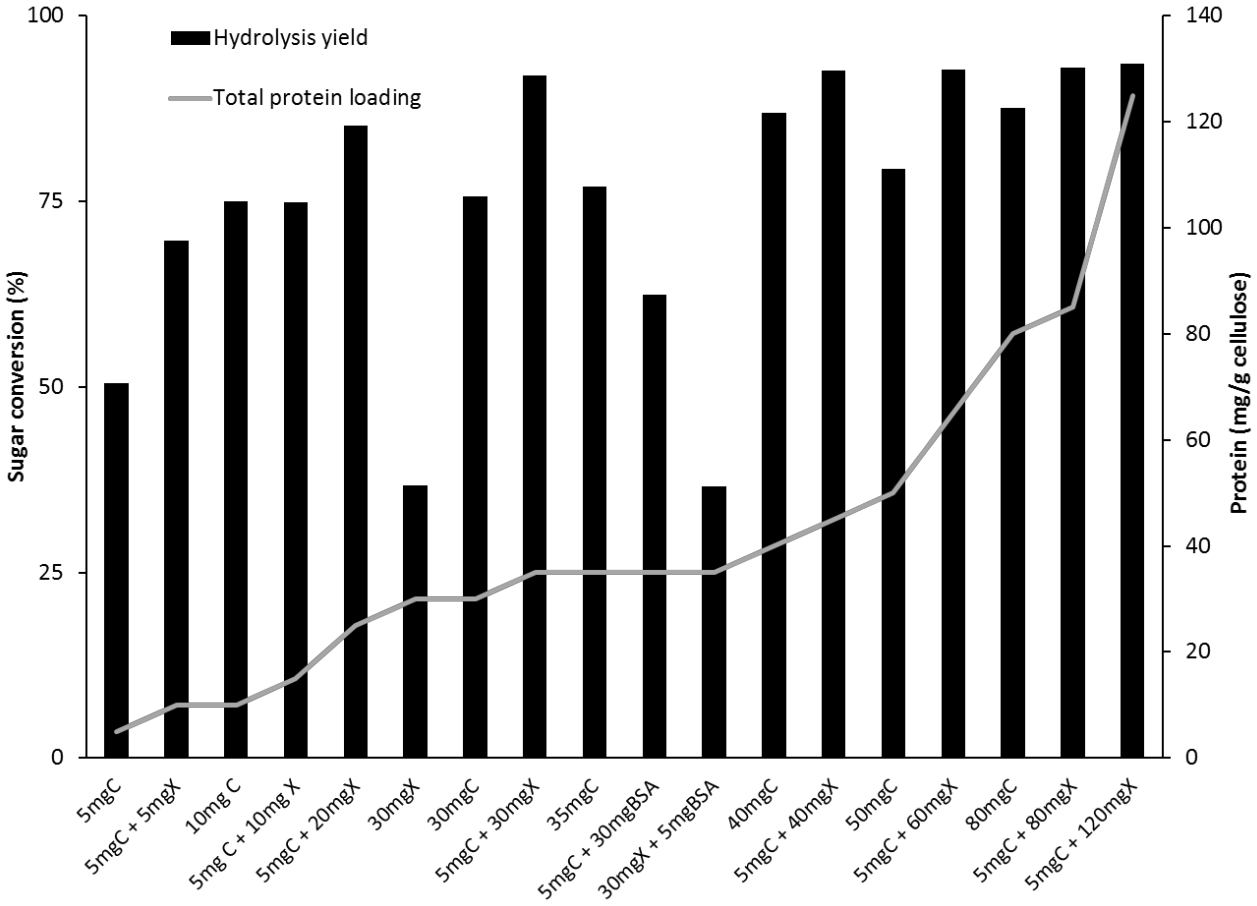

Figure 1. Hydrolysis of steam pretreated corn stover (SPCS) with various combinations of cellulases and xylanases preparations. Total sugar conversion was calculated based on the hydrolysis of the SPCS in 50mM acetate buffer (pH 5.0) at 2% (w/w) solid loading for 72 hours at 50 ºC. Total protein loading was the total enzyme (protein) loading used for hydrolysis. C: cellulases, X: xylanase, BSA (protein control): bovine serum albumin.

References

Aden, A., Foust, T., 2009.Technoeconomic analysis of the dilute sulfuric acid and enzymatic hydrolysis process for the conversion of corn stover to ethanol, Cellulose. 16, 535-545.

Arantes, V., Saddler, J.N., 2010. Access to cellulose limits the efficiency of enzymatic hydrolysis: the role of amorphogenesis, Biotechnology for Biofuels. 3, 4.

Arantes, V., Saddler, J.N., 2011. Cellulose accessibility limits the effectiveness of minimum cellulase loading on the efficient hydrolysis of pretreated lignocellulosic substrates, Biotechnology for Biofuels. 4, 3.

Bura, R., Chandra, R., Saddler, J., 2009. Influence of Xylan on the Enzymatic Hydrolysis of Steam-Pretreated Corn Stover and Hybrid Poplar, Biotechnol.Prog. 25, 315-322.

Chandra, R., Ewanick, S., Hsieh, C., Saddler, J.N., 2008. The Characterization of Pretreated Lignocellulosic Substrates Prior to Enzymatic Hydrolysis, Part 1: A Modified Simons' Staining Technique, Biotechnol. Prog. 24, 1178-1185.

Chandra, R.P., Bura, R., Mabee, W.E., Berlin, A., Pan, X., Saddler, J.N., 2007. Substrate pretreatment: The key to effective enzymatic hydrolysis of lignocellulosics? Biofuels. 108, 67-93.

Gao, D., Chundawat, S.P.S., Krishnan, C., Balan, V., Dale, B.E., 2010. Mixture optimization of six core glycosyl hydrolases for maximizing saccharification of ammonia fiber expansion (AFEX) pretreated corn stover, Bioresour. Technol. 101, 2770-2781.

Gao, D., Uppugundla, N., Chundawat, S.P.S., Yu, X., Hermanson, S., Gowda, K., Brumm, P., Mead, D., Balan, V., Dale, B.E., 2011. Hemicellulases and auxiliary enzymes for improved conversion of lignocellulosic biomass to monosaccharides, Biotechnology for Biofuels.4, 5.

Gregg, D.J., Saddler, J.N., 1996. Factors affecting cellulose hydrolysis and the potential of enzyme recycle to enhance the efficiency of an integrated wood to ethanol process, Biotechnol. Bioeng. 51, 375-383.

Hammel, K., Kapich, A., Jensen, K., Ryan, Z., 2002. Reactive oxygen species as agents of wood decay by fungi, Enzyme Microb. Technol. 30, 445-453.

Harris, P.V., Welner, D., McFarland, K.C., Re, E., Poulsen, J.N., Brown, K., Salbo, R., Ding, H., Vlasenko, E., Merino, S., Xu, F., Cherry, J., Larsen, S., Lo Leggio, L., 2010. Stimulation of Lignocellulosic Biomass Hydrolysis by Proteins of Glycoside Hydrolase Family 61: Structure and Function of a Large, Enigmatic Family, Biochemistry (N. Y.). 49, 3305-3316.

He Jun, Yu Bing, Zhang Keying, Ding Xuemei, Chen Daiwen, 2009.Thermostable carbohydrate binding module increases the thermostability and substrate-binding capacity of Trichodermareeseixylanase 2, New Biotechnology. 26, 53-59.

Himmel, M.E., Ding, S., Johnson, D.K., Adney, W.S., Nimlos, M.R., Brady, J.W., Foust, T.D., 2007. Biomass recalcitrance: Engineering plants and enzymes for biofuels production, Science. 315, 804-807.

Hu, J., Arantes, V., Saddler, J.N., 2011. The enhancement of enzymatic hydrolysis of lignocellulosic substrates by the addition of accessory enzymes such as xylanase: is it an additive or synergistic effect? Biotechnology for Biofuels.4, 36.

Humbird, D., Mohagheghi, A., Dowe, N., Schell, D.J., 2010. Economic Impact of Total Solids Loading on Enzymatic Hydrolysis of Dilute Acid Pretreated Corn Stover, Biotechnol.Prog. 26, 1245-1251.

Lu, Y.P., Yang, B., Gregg, D., Saddler, J.N., Mansfield, S.D., 2002.Cellulase adsorption and an evaluation of enzyme recycle during hydrolysis of steam-exploded softwood residues, Appl. Biochem. Biotechnol. 98, 641-654.

Lynd, L.R., Weimer, P.J., van Zyl, W.H., Pretorius, I.S., 2002. Microbial cellulose utilization: Fundamentals and biotechnology, Microbiology and Molecular Biology Reviews. 66, 506-+.

Mais, U., Esteghlalian, A.R., Saddler, J.N., Mansfield, S.D., 2002.Enhancing the enzymatic hydrolysis of cellulosic materials using simultaneous ball milling, Appl. Biochem.Biotechnol. 98, 815-832.

Martinez, A., Speranza, M., Ruiz-Duenas, F., Ferreira, P., Camarero, S., Guillen, F., Martinez, M., Gutierrez, A., del Rio, J., 2005. Biodegradation of lignocellulosics: microbial chemical, and enzymatic aspects of the fungal attack of lignin, International Microbiology. 8, 195-204.

McMillan, J.D., Jennings, E.W., Mohagheghi, A., Zuccarello, M., 2011. Comparative performance of precommercial cellulases hydrolyzing pretreated corn stover, Biotechnology for Biofuels. 4, 29.

Merino, S.T., Cherry, J., 2007. Progress and challenges in enzyme development for Biomass utilization, Biofuels. 108, 95-120.

Mosier, N., Wyman, C., Dale, B., Elander, R., Lee, Y.Y., Holtzapple, M., Ladisch, M., 2005.Features of promising technologies for pretreatment of lignocellulosic biomass, Bioresour. Technol. 96, 673-686.

Ohgren, K., Bura, R., Lesnicki, G., Saddler, J., Zacchi, G., 2007. A comparison between simultaneous saccharification and fermentation and separate hydrolysis and fermentation using steam-pretreated corn stover, Process Biochemistry. 42, 834-839.

Okada, H., Mori, K., Tada, K., Nogawa, M., Morikawa, Y., 2000.Identification of active site carboxylic residues in Trichodermareeseiendoglucanase Cel12A by site-directed mutagenesis, Journal of Molecular Catalysis B-Enzymatic. 10, 249-255.

Palmqvist, E., HahnHagerdal, B., Galbe, M., Zacchi, G., 1996.The effect of water-soluble inhibitors from steam-pretreated willow on enzymatic hydrolysis and ethanol fermentation, Enzyme Microb. Technol. 19, 470-476.

Pan, X., Gilkes, N., Kadla, J., Pye, K., Saka, S., Gregg, D., Ehara, K., Xie, D., Lam, D., Saddler, J., 2006. Bioconversion of hybrid poplar to ethanol and co-products using an organosolv fractionation process: Optimization of process yields, Biotechnol. Bioeng. 94, 851-861.

Qi, B., Chen, X., Su, Y., Wan, Y., 2011. Enzyme adsorption and recycling during hydrolysis of wheat straw lignocellulose, Bioresour.Technol. 102, 2881-2889.

Quiroz-Castaneda, R.E., Martinez-Anaya, C., Cuervo-Soto, L.I., Segovia, L., Folch-Mallol, J.L., 2011.Loosenin, a novel protein with cellulose-disrupting activity from Bjerkanderaadusta RID A-5206-2008, Microbial Cell Factories.10, 8.

Silverstein, R.A., Chen, Y., Sharma-Shivappa, R.R., Boyette, M.D., Osborne, J., 2007. A comparison of chemical pretreatment methods for improving saccharification of cotton stalks, Bioresour. Technol. 98, 3000-3011.

Sims, R.E.H., Mabee, W., Saddler, J.N., Taylor, M., 2010.An overview of second generation biofuel technologies, Bioresour. Technol. 101, 1570-1580.

Somerville, C., 2006. The billion-ton biofuels vision, Science. 312, 1277-1277.

Stephen, J.D., Mabee, W.E., Saddler, J.N., 2012. Will second-generation ethanol be able to compete with first-generation ethanol? Opportunities for cost reduction, Biofuels Bioproducts&Biorefining-Biofpr. 6, 159-176.

Tan, L.U.L., Yu, E.K.C., Campbell, N., Saddler, J.N., 1986. Column Cellulose Hydrolysis Reactor - an Efficient Cellulose Hydrolysis Reactor with Continuous Cellulase Recycling, Appl. Microbiol.Biotechnol. 25, 250-255.

Tian, X., Fang, Z., Guo, F., 2012.Impact and prospective of fungal pre-treatment of lignocellulosic biomass for enzymatic hydrolysis, Biofuels Bioprod.Biorefining. 6, 335-350.

Tu, M.B., Zhang, X., Kurabi, A., Gilkes, N., Mabee, W., Saddler, J., 2006.Immobilization of beta-glucosidase on Eupergit C for lignocellulose hydrolysis, Biotechnol.Lett. 28, 151-156.

Tu, M., Chandra, R.P., Saddler, J.N., 2007.Evaluating the distribution of cellulases and the recycling of free cellulases during the hydrolysis of lignocellulosic substrates, Biotechnol.Prog. 23, 398-406.

Wilson, D.B., 2009. Cellulases and biofuels, Curr.Opin.Biotechnol. 20, 295-299.

Wyman, C., Dale, B., Elander, R., Holtzapple, M., Ladisch, M., Lee, Y., 2005.Coordinated development of leading biomass pretreatment technologies, Bioresour. Technol. 96, 1959-1966.

Xu, J., Chen, H., 2009. Coupling recovery strategy of cellulase in hydrolyzate after hydrolysis with Tannin flocculation and PEG desorption, Appl. Biochem. Microbiol. 45, 309-312.

Yang, B., Wyman, C.E., 2008.Pretreatment: the key to unlocking low-cost cellulosic ethanol, Biofuels Bioproducts&Biorefining-Biofpr. 2, 26-40.

Yang, J., Zhang, X., Yong, Q., Yu, S., 2010.Three-stage hydrolysis to enhance enzymatic saccharification of steam-exploded corn stover, Bioresour.Technol. 101, 4930-4935.

Yunus, R., Salleh, S.F., Abdullah, N., Biak, D.R.A., 2010. Effect of ultrasonic pre-treatment on low temperature acid hydrolysis of oil palm empty fruit bunch, Bioresour.Technol. 101, 9792-9796.

Zhang, Y.H.P., Lynd, L.R., 2004. Toward an aggregated understanding of enzymatic hydrolysis of cellulose: Noncomplexedcellulase systems, Biotechnol. Bioeng. 88, 797-824.

Zhang, Y.-.P., Himmel, M.E., Mielenz, J.R., 2006. Outlook for cellulase improvement: Screening and selection strategies, Biotechnol. Adv. 24, 452-481.

The Biorefining Story: Progress in the Evolution of the Forest Products Industry to a Forest-Based Biorefining Sector

John N Saddler, Sergios Karatzos and Jinguang Hu

Forest Products Biotechnology/Bioenergy Group
IEA Bioenergy Task 39
Department of Wood Science
Faculty of Forestry
University of British Columbia
2424 Main Mall, Vancouver BC V6T 1Z4
Email: jack.saddler@ubc.ca

Keywords: Biofuels, bioenergy, biorefinery, conventional and advanced biofuels.
(A variation of this manuscript/presentation was given at IUFRO All Div. 5 Conference, Estoril, Portugal, July, 2012)

Abstract
Continued global insecurity around oil supplies has helped keep oil prices volatile and relatively high, influencing the ongoing and significant investment in both conventional (sugar, starch, plant, and animal-oil-derived ethanol and diesel) and advanced (biomass-derived or 'drop-in' like) biofuels and chemicals. It is likely that 'pioneer' advanced biofuel plants will first use biomass residues as their initial feedstock as it is currently difficult to justify the investment in energy crops when there is no clear market for their use. It is also likely that agriculture-based advanced biofuel plants will be predisposed towards using a biochemically based process as sugar- and starch-based processes already use much of the equipment and processes that are conducive to the use of enzymes and microorganisms. In contrast, wood-based processing such as in pulp and paper manufacturing will be predisposed to using thermochemically based processes which build on already existing expertise in areas such as combustion, gasification and pyrolysis. The biorefinery concept has been proposed as a means to extract maximum value from lignocellulosic materials, with the higher value physical/chemical components used for biomaterials and chemicals and whatever is left used for bioenergy/biofuel production. The continued development of new conversion technologies has encouraged these nascent, newer biorefineries to assess a range of lignocellulosic feedstocks with the hope of producing additional value-added bioproducts and more efficient recovery of bioenergy. There are a number of complementary platforms for processing lignocellulosic feedstocks, including traditional platforms (i.e., existing pulping and starch-to-ethanol processes) as well as emerging technologies that are either biological, thermochemical or hybrid-based. However, there is as yet no clear candidate for 'best technology pathway' between the competing routes. Monitoring of larger-scale demonstration projects is one of the activities undertaken by IEA Bioenergy Task 39

to try to derive an accurate, comparative data base. Even at oil prices in excess of $100 a barrel, advanced biofuels will likely not become fully commercial for fivetoten more years without significant government support. The expertise, progress, and goals of the member countries and companies involved with IEA Bioenergy Task 39 will be used to describe progress in the biorefining area and our attempts to commercialise advanced biofuels.

Background

As oil becomes scarcer and more difficult and expensive to source and process, forestry-derived biomass is gradually shifting from being more of a sectoral resource (e.g., for products such as housing, furniture, pulp, and paper) to potentially becoming a major feedstock for the rapidly evolving 'biorefinerysector'. Trends such as the unstable but generally increasing oil prices, global sustainability concerns including climate change and the ongoing economic malaise have all contributed to the growth in both interest and investment in what is generally termed the 'bioeconomy'.

Oil and its derivatives have been the lifeblood of most of the world's industrial economies since the middle of the last century.However, increasing demand for a finite resource is driving up its cost andthe environmental risk of its extraction, while all fossil fuels are known to be the primary cause of increasinggreenhouse gas (GHG) emissions. At the same time the establishedforest-based industrial sector has been going through some major upheavals with the US housing crisis greatly reducing traditional uses such as lumber for housing, while longer term trends, such as the rapid increase in digital media use,significantly reducing the market for products such as newsprint and writing paper. There is a growing realisation that the convergence of the five 'F's' (fuel, food, feed, fiber,and fertiliser), will result in increasing competition for resources from nontraditional competitors. In countries such as Brazil, oil companies such as Petrobras have invested heavily in sugar-cane-to-ethanol production while at the same time becoming world leaders in deep-water oil drilling and extraction. Energy companies such as BP and Shell have invested heavily in a variety of technologies and companies, from wood pellets, through biomass-to-ethanol to algal biofuels. Chemical companies such as DuPont have acquired companies such as Danisco/Genencor, to diversify into areas traditionally associated with a food company (Danisco) whichitself had recently acquired the world's second biggest enzyme company (Genencor). Thus, as various companies and sectors look to expand, the traditional industrial users of the world's forests can anticipate other groups to increasingly look at whether a sustainably produced feedstock (such as a tree), which sequesters carbon from the atmosphere, might provide an alternative approach to making their traditional products of chemicals, fuels, and energy. The OPEC-generated oil crisis of the 1970s and the more recent concerns about GHG emissions have motivated significant R,D,D&D (research, development, demonstration, and deployment) investments in the bioenergy sector over the last few decades. However, there is an increasing realisation that, in the same way that the lower volume but higher value co-products such as plastics, chemicals, dyes, etc., make an oil refinery economically viable (with the bulk products of diesel/gasoline/petrol being of generally lower value), any future bioenergy sector will also require these higher value co-products (biomaterials, biochemicals, etc.) as the basis of a future biorefinery sector.

The agriculture sector is very much at the forefront of this evolution. In the 'swinging sixties' (1960–1969) the issue of the day was not energy but overpopulation and the world's ability to feed all of its people. Oil was thought to be so plentiful and infinite that oil and chemical companies such as BP, ICI and Shell invested in "single-cell-protein" that was derived from the growth of microorganisms on oil derivatives such as methanol. However, primarily through what has been termed the 'green revolution', agriculturalproductivity per hectare has increased steadily over the last 50 years to the extent that agriculture is now the primary source of the most used renewable biofuels such as biodiesel and bioethanol! In the same way thatagriculture provides food, fuel, feed, chemicals, nutraceuticals, etc., it is increasingly likely that, as well as continuing to produce 'traditional' products such as lumber and pulp and paper, the forest sector will also evolve into a biorefinery mode of operation with bioenergy being one of the major complementary markets that will be developed.

Over the last couple of decades a range of biomass conversion technologies have been investigated that have used both forestry and agricultural feedstocks to try to produce fuels and chemicals. These biofuels/bioproducts can compete economically with current oil-derived products while proving to be much more desirable from an environmental and social perspective (i.e., lower carbon emissions, gains in rural employment, etc.)
In the next section we discuss the rapidly evolving bioenergy sector (and biofuels in particular), the potential for the forest sector to become a leading player, and some of the work that organisations such as IEA Bioenergy have played in trying to catalyse the development of a forest-based biorefinery.

The Current Forest Sector

As mentioned earlier, the forest sector is facing major challenges while new conversion technologies, emerging markets and increasing requirements for the sustainable production and use of materials/products are creating a strong drive for transformation in the sector. Traditional forest products such as construction and pulp andpaper represent a 'business as usual'*modus operandi* for the forest-based sector,but they are not sufficient to ensure substantial future growth and revenues for the sector. A change is required to address these challenges and to harness the opportunities of diversifying the product range of the forest industry. This diversification can be achieved by selectively extracting further value from lignocellulosic biomass such as thermal value (bioenergy), chemical functionality (chemicals and fuels)and novel structural applicationssuch as biomaterials like nanocrystalline cellulose. Ideally, the future forestry facilities will be able to exploit a range of value categories from their biomass feedstock and, depending on market conditions, the future forest-based biorefinery sector will be able to move to the product streams that offer the highest economic as well as environmental/social values.
Of the various businesses that constitute the current forest products sector, thepulp and paper industry is best positioned to evolve into abiorefinery approach that would allow easier diversification of itsproduct streams. Most pulp mills already have in-house expertise and assets needed to enhance the fractionation of the cellulose, lignin, hemicellulose, extractives, and other components of forest biomass using a variety of approaches (e.g., Kraft lignin, dissolving pulp). The sector also has well-establishedexpertise in handling and recycling chemicals as well as dealing with waste streams and water recycling. These assets can be readily leveraged to

manufacture lignin and cellulose-derived products beyond traditional pulp and paper products into the wider biorefinery approach.

It should be noted that paper and packaging companies accounted for most forest-based revenue generated globally; the top 10 P&P companies are listed in table 1. Despite the considerable size and global reach of many of these companies, their investment in innovation and the limits to their product diversification tend to be in their traditional market areas, aiming at the production of **whiter** paper or **stronger** tissue paper, rather than making use of their expertise in sustainably producing, accessing and processing the biomass feedstock into different products and markets. Those companies thathave diversified to some extent, such asKimberly-Clark, have developedhigh-value speciality products (e.g.,laboratory and medical consumables). It should be noted that this iscurrently the company with the highest net income on a global basis (table 1).

Table 1: PricewaterhouseCoopers Top Global Forest, Paper & Packaging Industry Companies

Rank 2010	Company name	Country	Sales US $ millions	Net income (loss) US $ millions
1	International Paper	US	25,179	644
2	Kimberly-Clark	US	19,746	**1,843**
3	Svenska Cellulosa (SCA)	Sweden	15,202	773
4	Stora Enso	Finland	13,671	1,021
5	Oji Paper	Japan	13,097	284
6	Nippon Paper Group	Japan	12,502	343
7	UPM—Kymmene	Finland	11,848	745
8	Smurfit Kappa	Ireland	8,865	66
9	Mondi Group	UK	8,269	297
10	Metsalito	Finland	7,139	226

Source: PricewaterhouseCoopers, 2011

Over the last 100 years, at the same time as the forest products sector has been developing the various products that we now take for granted (kraft/mechanical/dissolving pulps, engineered wood products, etc.),the energy sector was evolving from a coal-based sector to one increasinglydependent on oil. There was also an increasing realisation that, although energy applications would continue to grow, lower volume but higher value co-products such as chemicals and plastics would increasingly become the profit centreof the‘oil refining sector’. More recently both cost (oil is getting more expensive and environmentally ‘risky’ to access and process) and environmental/social concerns have encouraged traditional coal- and oil-based sectors to consider if their currenthydrocarbon-based operations could evolve into one based more on sustainably produced carbohydrates.

The Potential, Evolving Forest Biomass Processing Sector

Over the last 50 years or so, the world’s economy has become less dependent on the resource and manufacturing industries with ‘white collar’industries such as banking, insurance, and education

becoming bigger players in the 1980s through 2000. Since 2000, the growth of companies such as Apple, Google, and Facebook have also been contributing to the manufacturing sector's diminished influence. When the world's top companies are reviewed (table 2), although companies such as Toyota are still in the top 10, the fact that a retailer, Wal-Mart, is number one is quite telling. What is also apparent is that the world's increasing need for energy results in oil companies still predominating as the biggest and often most profitable companies. In contrast, the world's forest products companies might be considered to be 'middle-sized' players, with the company with the greatestrevenue in 2009, International Paper, listed as number 362 in the world in terms of revenue (table 2).

Table 2: Top global companies by revenue

Rank 2009	Company name	Country	Sales US $ millions	Net income (loss)US $ millions
1	Wal-Mart Stores	US	408,214	14,335
2	**Royal Dutch Shell**	The Netherlands	285,129	12,518
3	**Exxon Mobil**	US	284,650	19,280
4	**BP**	UK	246,138	16,578
5	Toyota Motor	Japan	204,106	2,256
7	**Sinopec**	China	187,518	5,756
10	**China National Petroleum**	China	165,496	10,272
11	**Chevron**	US	163,527	10,483
14	**Total**	France	155,887	11,741
17	**ConocoPhilips**	The Netherlands	139,515	4,858
362	International Paper	US	23,366	663

Source: CNN Money, 2011

Over the last decade or so, there is growing recognition that we need to think in human generational terms, rather than just short-term 'profitability'over thenextfinancialquarter, with nontraditionalforest-based players such as oil and chemical companies increasinglyassessing the viability of producing their traditional fossil-fuel-derived products from biomass. There have also been parallels in the way the oil- and forest-based sectors have evolved. Historically, the structural characteristics of wood result in its primary application in markets such as housing, furniture, and bridgeswith applications such as pulp and paper being developed relatively more recently (in the last 50 years or so). Similarly, oil was predominantly used for its energy/fuel applications with its potential asa chemical/polymer/plastics feedstock becoming fully realised at the same time as the processes such as kraft andthermochemical pulping were being commercialised in the 1950s and 1960s. There are also parallels when the volume and value of the products that can be derived from a forest- or oil-based feedstock are compared (figure 1). In the oil-based sector, transportation fuels (diesel/petrol/gasoline) represent the main product in terms of volume (70 percent) whileco-products and value-added materials such as plastics represent only 4 percentof the product volume.These nonfuel product categories contribute almost as much to the annual revenues of the industry as do the total fuels component(figure 3). The importance and use of wood as a structural material is reflected in both the high volume and

value ofsolid-wood products (plywood, OSB, engineered wood, lumber, etc.) as well as pulp, paper and packaging products. In contrast, the current chemical and energy products/uses represent a lower volume and an even lowervalue forest product.However, the recent high value of dissolving pulp (although somewhat stabilised in recent months) has indicated how valuable a true forest-based biorefinery might be when pulp is valued more as a 'biomaterial' or 'chemical/polymer' feedstock rather than just a source of paper products. Although forest products companies such as Borregaard, Neucel, Tembec and Lenzinghave shown how a biorefinery can operate and evolve into marketing a range of speciality pulps, chemicals and fuels, a strategy that is being increasing pursued by forest companies is to form partnerships with companies that better understand the markets into which the bioenergy/biomaterials can be sold.Examples of such bioenergy collaborationsinclude Catchlight, which is the Chevron-Weyerhaeuser joint venture in the US and the Stora Enso-Neste oil collaboration in Scandinavia.Both collaborations are focussed on developing the biofuels/bioenergy area with the forest-based company better understanding the logistics, costsand complexity of sourcing, collecting and processing the biomass, and the energy company better understanding the markets and likely value that can be extracted from the renewably sourced carbon (table 3).

Table 3: Examples of collaborations between the petroleum and forest products industries

Oil refiner company ($m revenue in 2010)	Fibre expert company ($m revenue in 2010)	Country	Type of collabouration	Year initiated
Neste Oil (11,890)	Stora Enso (13,671)	Finland	50/50 investment on a demonstration facility in Varkaus	2009
Chevron (198,198)	Weyerhaeuser (6,552)	USA	50/50 Joint Venture named "Catchlight Energy"	2008

Source: Company Websites and annual reports.

As well as forming partnerships with traditional forest products companies, oil and chemical companies are also strategic investors in technology providers such as Amyris (Total), Codexis and Iogen (Shell) as well as purchasing companies (BP's purchase of Verenium) and investing in longer term R&D centre's (BP's investment in the Energy Biosciences Institute). These types of substantial short-andlong-term investments indicate that, while it will likely take a while, 'Big Oil'is assessing the potential of moving from depletingstocks of hydrocarbons to a renewable and hopefully sustainable carbohydrate feedstock!

From a sustainability point of view, the oil refiners find themselves under continuous pressure to develop "greener" fuel blends (e.g., compulsory ethanol blending in the US) and "greener" (biodegradable and/or renewable) materials. In this context, the scope for the petroleum and forestry industries to collabourate is projected to increase.

Figure 1: Comparison of value and volume distribution in the forest and petroleum industries Source: adapted from Browne et al., 2012.

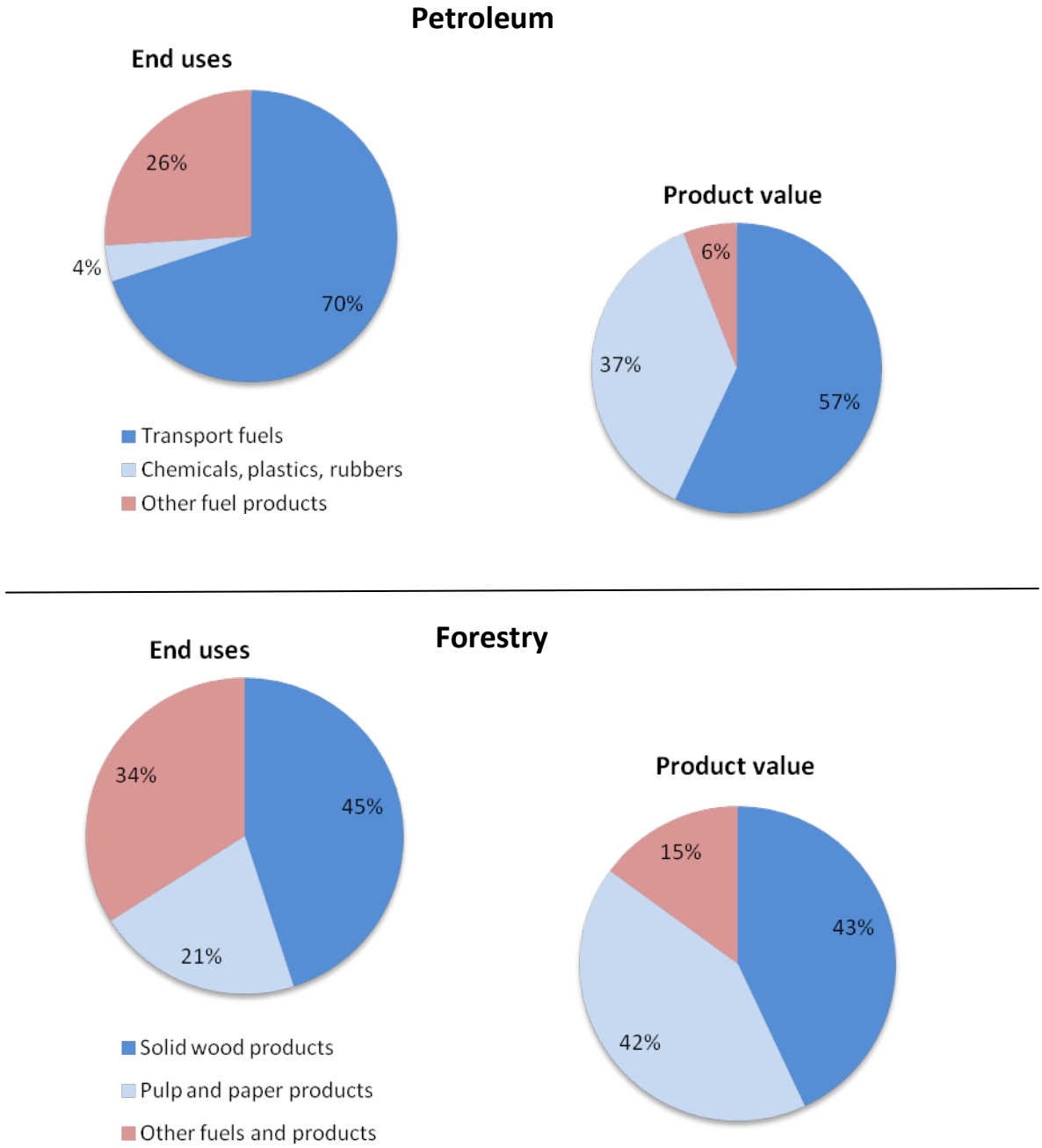

Case Study:Development of Conventional (First Generation) and Advanced (Second Generation) Biofuels

As mentioned earlier, biofuels are the most widely used renewable alternative to oil-based transportation fuels such as diesel and petrol/gasoline. Biofuels can generally be defined as liquid

transportation fuels that are derived from crops (such as sugarcane, corn, rapeseed, or sunflowers) or biomass (such as forestry and agricultural residues or energy crops such as switchgrass, fast-rotation trees, or algae). In direct response to the OPEC oil crisis, pioneering countries such as Brazil and the US greatly expanded their production of 'traditional'or 'conventional'biofuels such as sugarcane or ethanol derived from corn. Other countries such as Germany quickly followed suit by greatly expanding itsproduction of oil seed-bearing crops such as rape/canola. These so-called 'first generation'biofuels technologies (now better defined as 'conventional'or traditional biofuels production) have helped establish much of the infrastructure and policies that are in place to make bioethanol,and to a lesser extent biodiesel, significant commercial realities in many parts of the world. Countries such as Brazil continue to improve on many aspects of sustainability as well as the economics of making ethanol from sugarcane. However, in other parts of the world, various economic and social (e.g., food versus fuel) considerations have encouraged the development of 'advanced'biomass-based biofuels technologies based on biochemical, thermochemical and hybrid process routes (sometimes referred to as second- or third-generation biofuels). The technology pathways to biofuels and bioenergy from biomass are depicted in figure 2.

Figure 2: Pathways to energy products from biomass

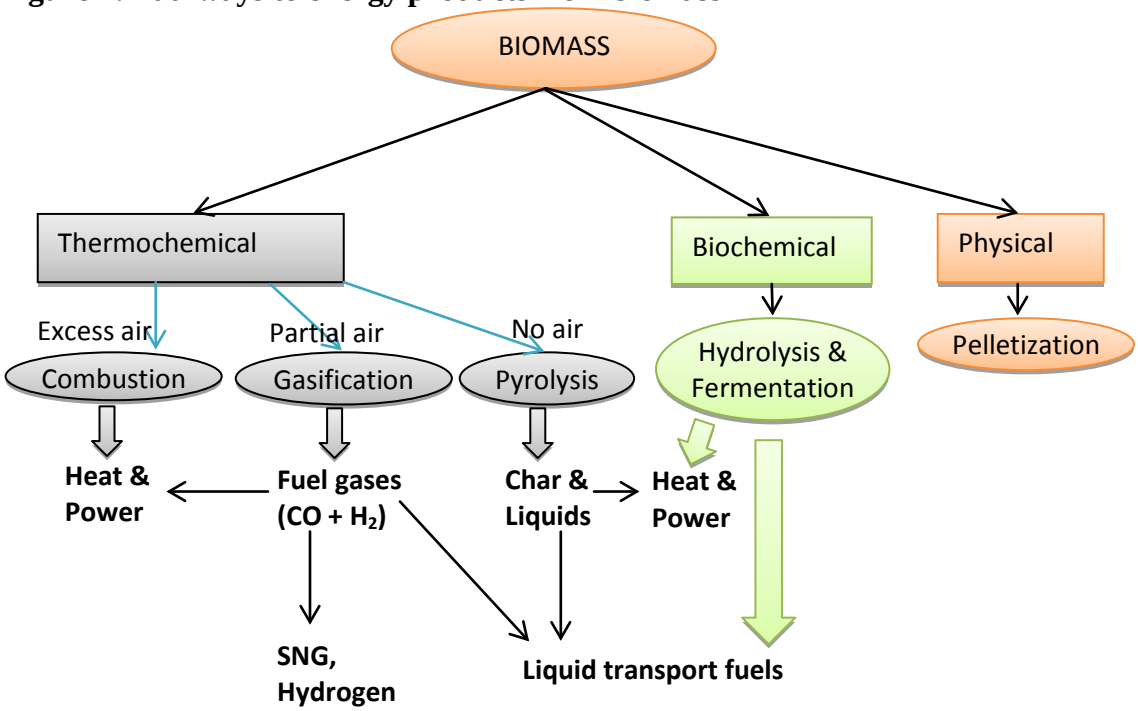

Source: Adapted from BPN, 2011

International Biofuel Targets and the Quest for Economic Viability and Sustainability

As mentioned earlier, there has been significant investment in the development of renewable liquid transportation fuels with various countries developing mandates, directives, targets and roadmaps to facilitate the commercialization of biofuels (BD, 2011). The recently developed IEA (International Energy Agency) biofuels roadmap (IEA, 2011) is one example of a globally

concentrated effort to prepare an action plan and determine global biofuel volume and specification targets. As detailed in the report, if the world aspires to reach the GHG reductions that are described in the "Blue Map" Scenario (energy-related CO_2 emissions are reduced by 50 percentin 2050 relative to their 2005 level), biofuels use will have to grow from its current 2 percentshare of global transportation energy to over 25 percentby 2050. In this way it is estimated that about 2.1 Gt CO_2 emissions per year could be reduced. Although production of some conventional biofuels such as sugarcane-derived ethanol are expected to continue to grow, as they can be produced both sustainably (good GHG savings) and economically (Brazil's experience and increasingly efficient production techniques), future advanced biofuels such as energy-dense hydrocarbon-type diesel and jet fuels will likely be produced by thermochemical means such as by Fischer-Tropsch conversion of gasified biomass and pyrolysis oils.

IEA Bioenergy Task 39: An Example of an International Forum that Can Promote Biorefinery Collabourations

An international example of an organization thatfacilitates collaboration and information exchange in the biofuel-biorefinery sector is IEA's Task 39. The Task is focused on biofuel commercialisation in a biorefinery approach and operates for the interests of its member countries and the overall mission of the IEA. The origins of the International Energy Agency (IEA) coincided with the first of several 'oil price disruptions' initially caused by the OPEC oil crisis of the 1970s. Since then, the IEA has evolved from an agency that tried to better anticipate oil price disruptions to now having a mandate to 'improve the world's energy supply and demandstructure by developing alternative energy sources and increasing efficiency of energy use'. The work of IEA Bioenergy Task 39, 'Liquid biofuels' (http://www.task39.org) is very much at the forefront of the renewable fuels strategy of many countries.With dwindling petroleum reserves and soaring transportation fuel demand from China, India, and other emerging economies, the world needs alternatives such as biofuels and biomaterials. This organization and other global collabouration efforts are indispensable tools in ensuring the success of the evolving bioeconomy.

What is the Likely Structure/Operation of Forest-Based Biorefineries?

Just like oil refineries, biorefineries can provide a wide range of molecules and materials that act as the precursors or products for transportation fuels and commodity/specialty chemicals. Bioenergy, biofuels and biomaterials are the main categories of products that can be produced from forest-derived biomass depending on the feedstock and the process involved (figure 3). It is likely that traditional high-value products such as engineered wood or specialty pulps will continue to be the mainstay of many forest-based biorefineries.Nature designed trees to be primarily composed of 'structurally robust polymeric components' such as cellulose, hemicellulose and lignin and it thus makes sense to first take advantage of wood's'structural' characteristics before conspiring its chemical/energy potential!

There are several conversion technology platforms that are current and potential candidates for a forest-based biorefinery employing either thermochemical processes such as

pyrolysis/gasification or biological processes such as microorganisms/enzymes (biochemical platforms). Although both the thermochemical and biochemical platforms have the capacity to produce fuels, chemicals and to generate power (figure 3),the biochemical approach tends to fractionate the cellulose, hemicellulose, lignin, extractives, etc. through processes such as pretreatment while the thermochemical process carries out this fractionation after all of the biomass has been pyrolysed or gasified first. In either type of biorefinery, the 'energy products' such as biopower and biofuels are likely to result in the greatest product volume while biomaterials/biochemicals such as xylitol or nutraceuticals will havesignificantly smaller markets but with much higher value. In this way it has been suggested that the forest-based biorefinery can develop a diverse range of products, analogous to an oil refinery, and therefore be in a much better position to deal with both market fluctuations and market opportunities. Future forest-based biorefineries should also be 'flexible' or 'modular' in theirdesign so that theycan readily shift from one product stream to another, depending on market prices. Some excellent examples of the development of the biorefinery conceptcan be seen over the last 20 years in the US corn and the Brazilian sugar-based industries. In the early 1980s, Brazil wasthe first country to try to become less dependent on imported oil by aggressively developing an ethanol industry based on itsconsiderable sugarcane industry. However, the Brazilianssoon found out the advantages of being able to diversify their product mix by shiftingto more sugar production when the value of sugar is high (as it currently is) or to ethanol production whenever the international price of oil is high. Similarly, the US corn sector is still a substantial animal feed supplier with corn's use as an ethanol feedstock only recently superseding this traditional market for corn. Thus when oil prices are high (as they are currently) ethanol will continue to look attractive, with the concomitant high price for animal feed resulting in famers planting more corn than other less-profitable crops such as soya. It should be noted that the different biorefinery platforms have advantages and disadvantages. For example, the traditional and biological platforms tend to have lower throughput rates but achieve cleaner product streams (e.g., purer ethanol and chemicals), while the thermochemical platforms tend to provide faster throughput but poorer separation and quite heterogeneous product streams (e.g., pyrolysis oils). In general, each biorefinery platform will involve some form of compromise or tradeoff at more than one level. As a result it is difficult to identify a'best technology pathway'.

Although several pulp mills could be evolved into more of a biorefinerymode of operating,viaeither a thermochemical or biochemical approach, it is likely that 'pioneer' plants will first use any energy produced in-house viadirect combustion, combined heat and power, or black liquor gasification types of approaches.Pulp mills have existing equipment that can be easily retrofitted to perform either pretreatment or biochemical conversion (e.g., pulping digestors) or pyrolysis/gasification (e.g., black liquor gasification) for thermochemical conversion. Althoughthese technologies can fractionate biomass and produce value-added biorefinery-type products, they are likely to be more mid-tolong-term solutions for the forest sector. Biopower is already being used within several pulp mills inexisting operation units such as lime kilns and black liquor gasifiers, although most older pulp mills are rarely self-sufficient in power generation and they often have to buy natural gas or electricity to complement their in-house power.

Figure 3: Potential forest based biorefinery platforms

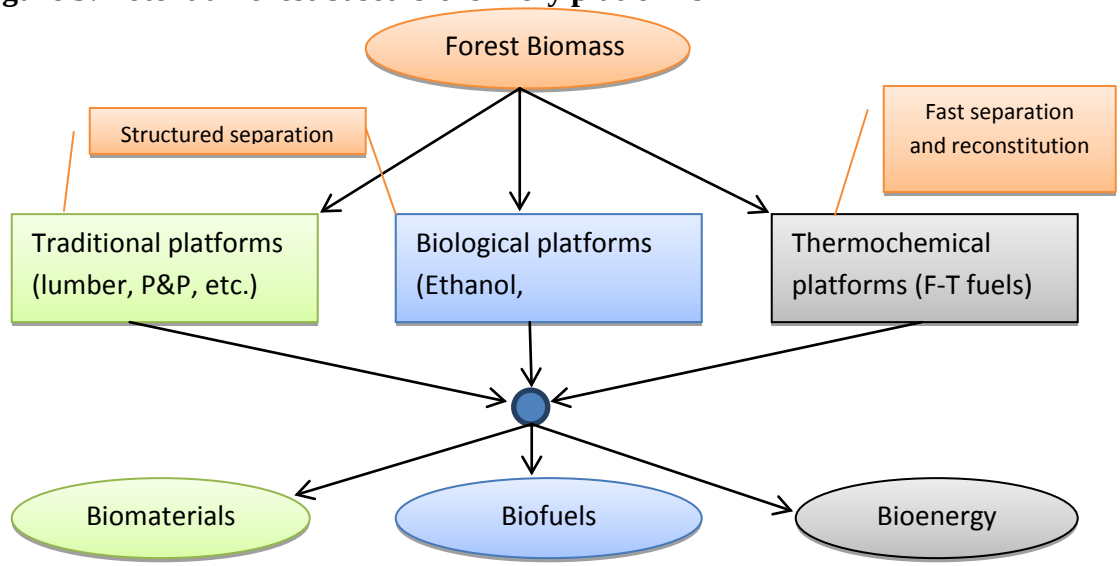

Feedstock-Process Compatibility and Logistics Aspects

In comparison to oil, biomass is a feedstock that is less energy dense, higher in moisture, much more heterogeneous, dispersed in its distribution and, somewhat surprisingly, often requiring more of a 'social license' for itscollection does drillingforoil! Accordingly, biorefinery facilities will have some logistic challenges, which will undoubtedly influence the choice of technology platform, feedstock and markets that might be pursued. For example, thermochemical facilities are likely to be more amenable to scale-up because, in contrast to biochemical processes, they can process highly densified and more hydrophobic forms of biomass such as torrified pellets or bio-oils, which in turn can be transported longer distances than raw biomass(Stephen et al., 2010).Similarly the seasonality of fibre harvest, moisture and ash content, accessibility of fibre, bulk density, and amenability to densification are other characteristics that can vary between different feedstocksand should be taken into account when choosing abiorefinery technology. Matching the right technology to the appropriate feedstock and securing the availability of the raw material will be paramount to the sustainable and profitable operation of asuccessfulforest-based biorefinery.

TheForest Products Association of Canada's (FPAC) 'Biopathways'Strategy

In North America, the current, ongoing financial crisis was partially precipitated by the subprime mortgage crisis that resulted in housing starts (predominantly made out of wood) going from record highs around 2007/2008 to almost record lows in recent history. The evaporation of this core market and the increasing value of the Canadian dollar versus the US dollar resulted in dire financial/employment conditions for the Canadian forest products sector. As one part of an evaluation of how the sector might survive and evolve, the Forest Products Association of

Canada (FPAC), with financial support from the Canadian Forest Service's (CFS) of the federal Natural Resources Canada (NRCan) and input from the recently merged R&D organisation, now termed FP Innovations (formerly Forintek, Paprican, FERIC and part of CFS), created the Canadian Forest Innovation Council (CFIC),whichhelped identify the need to develop a 'biopathways' strategy. The work carried out within the Biopathways project involved a detailed and thorough evaluation of potential strategies for renewal and diversification of the Canadian forest products sector. In its initial work the group assessed both traditional and emerging manufacturing pathways in three selected regions within Canada (northern Ontario, interior British Columbia and the Lac St. Jean region of Quebec) (BPN, 2011). This initial study indicated that, generally,the pathways thatmaximise greatest return on capital expended (ROCE) are the ones that combine current sawmill operations with bioenergy and engineered wood products (EWP)applications and markets, while current pulp and paper operations are best blended with bioenergy and biorefinery technologies and applications. However, it was also apparent that the strategies thatmaximise ROCE are not necessarily the ones that maximise employment indicators and vice versa. It was also evident that different pathways perform differently in each ofthe three regions studied. These recommendations again indicated that there is no 'best technology pathway' and that the desired 'win-win' situations have to be carefully assessed and customised to the industrial and social background of each region. However, the study strongly emphasised the urgent need for renewal in theforest products sector as the opportunities are too great to miss out on and 'business-as-usual' would be unlikely to be successful in the future. The report indicated that, on average, a new technology added to an existing pulp mill will improve ROCE by 3.7 percent, GDP contribution by 10 to 25 percent,and employment by 1 to 4 percent(BPN, 2011).Overall, the report recommendedthat (a) better integration of traditional and novel technologies/products/markets, (b) increased cross-sectoral synergies and (c) better leveraging of existing infrastructure will be key components for the future success of the evolving forest sector. It was also noted that policy support,improved communication between sectors (such as the Catchlight joint venture between Weyerhaeuser and Chevron), increased investment in R&D and hiring new people with the skills and training needed for the future biorefining sector, are all essential components to ensuring the success of the proposed biopathways strategy. More recently, a network of university-based networks working in the forest products sector has been formed (the FIBRE network,http://www.reseauxfibrenetworks.ca) with the goal of helping commercialise university-derived research while training the highly qualified personnel (HQP) that will be needed by the future forest products/biorefining sector. The better integration and close collaboration between FPAC, NRCan, FP innovations and the universities is seen as key to ensuring the effective development of Canada's future forest-based biorefining sector.

Conclusions

The forest-based biorefinerywill continue to have traditional products and markets (lumber, engineered wood, pulp and paper) at its core, making use of wood's inherent structural characteristics. However, the increasing costs (economic, environmental and social) of using fossil-fuel-derived feedstocks to make many of the products from an oil refinery will encourage oil/chemical companies to continue to evaluate carbohydrates as a possible replacement for hydrocarbon-based feedstocks. The commercialisation of the forest-based biorefinerycomes with

a number of challenges, several of which could be addressed through selected partnerships and collaborations, leveraging the relative expertise of sectors such as the forest products and the chemical/oil refining industries. There is considerable potential for the forest products sector to 'learn'from the strategies of the oil refinery, and more recently the agriculture-based biorefinery sectors. It can do this byextracting the maximum value from biomass by supplementing fossil-fuel energy sources with biomass-derived energy and developinghigh-value co-product streams such as nanocrystalline cellulose andnutraceuticals.Although various thermochemical and biochemical-based processes are currently being evaluated as the basis of a 'biorefinery platform', there is as yet no 'best technology platform' and the choice of process is more likely to be influenced by feedstock specificity and the peculiarities and logistics of each region. Althoughthe biorefinery approach to processing forest-derived biomass is poised to play a central role in the future of the forest products sector, part of its success will depend onthe careful selection of technology and markets that will capture the synergistic opportunities between complementary industries and other stakeholders. These collabourations and synergisms can be facilitated via national networks such as the Canadian Biopathways Network and international networkssuch as the Bioenergy Implementation Agreement (IA) of the International Energy Agency (IEA).

References

Biofuels Digest [BD], '*Biofuels mandates around the world'*, (2011),<http://www.biofuelsdigest.com/bdigest/2011/07/21/biofuels-mandates-around-the-world/>,accessed 17 May 2012.

Biopathways Partnership Network [BPN], '*Bio-pathways'*, Forest Products Association of Canada (2011), <http://www.fpac.ca/index.php/en/bio-pathways/>, accessed 17 May 2012.

Browne, T., R. Gilsenan, D. Singbeil and M. Paleologou, '*Bio-energy and bio-chemicals synthesis report'*, Forestry Products Association of Canada (2012), <http://www.fpac.ca/publications/Bio%20Energy%20Final_En.pdf>,accessed 17 May 2012.

CNN Money, '*Global 500 top companies by revenue'*, Cable News Network (2011), <http://money.cnn.com/magazines/fortune/global500/2010/full_list/>, accessed 17 May 2012.

International Energy Agency [IEA], '*From 1st to 2nd generation biofuel technologies; an overview of current industry and RD&D activities'*, (2008), <http://www.iea.org/publications/free_new_Desc.asp?PUBS_ID=2079>,accessed 17 May 2012.

International Energy Agency [IEA], '*Technology roadmap: biofuels for transport'*, OECD/IEA Paris (2011), <http://www.iea.org/papers/2011/biofuels_roadmap.pdf>,accessed 17 May 2012.

PricewaterhouseCoopers, '*Global forest, paper & packaging industry survey: 2011 edition—survey of 2010 results'*, PricewaterhouseCoopers LLP (2011), <http://www.pwc.com/gx/en/forest-paper-packaging/assets/global-forest-survey-2011.pdf>,accessed 17 May 2012.

Stephen, J.D., W.E. Mabee and J.N. Saddler, 'Biomass logistics as a determinant of second generation biofuel facility scale, location and technology selection', *Biofuels Bioproducts and Biorefining*, 4/5 (2010): 503–518, <http://onlinelibrary.wiley.com/doi/10.1002/bbb.239/abstract>,accessed 17 May 2012.

The Antibacterial Performance of Natural Bamboo Fiber and Its Influencing Factors

Li Xia XI [1] *– Dao Chun QIN* [2*]

[1] Ph.D. student, Research Institute of Wood Industry, Chinese Academy of Forestry, Beijing 100091, China.
xilixia123@163.com
[2] Researcher, International Centre for Bamboo and Rattan, Key Laboratory of Bamboo and Rattan Science and Technology of the State Forestry Administration, Beijing 100102, China.
* *Corresponding author*
qindaochun@gmail.com

Abstract

Natural bamboo fiber is a new type of plant fiber using for textile. Its natural antibacterial property has not been investigated fully. In this paper, the nature antibacterial property of natural bamboo fiber was determined with the method of dynamic test referring to GB/T 20944. 3-2008 and compared with other fibers for textile, such as jute fiber, flax fiber, ramie fiber and regenerated bamboo fiber. The bacteria used in the test were *Escherichia coli*． (8099), *Staphylococeus auresu*(ATCC 6538) and *Candida albican*(ATCC 10231).The relationships between the antibacterial property of natural bamboo fiber and its shape, hygroscopicity and extractives were tested to analyze the influencing factors. In the results, compared with natural cotton the bacteriostatic rates of natural bamboo fiber against the bacteria were all zero; that of jute fiber and flax fiber against ATCC10231 were 48% and 8.7%; that of ramie fiber against ATCC 6538 was as high as 90.2%; that of regenerated bamboo fiber against ATCC6538 was higher than 70%. The bacteriostatic rates of the bamboo with different shape were all zero, that of plant fibers was inversely proportional to their moisture regain and the bacteriostatic action against ATCC 10231 of natural bamboo fiber extracted was lower, however, that against 8099, and ATCC 6538 was stronger except extracted with benzene. The results show that natural bamboo fiber has no natural antibacterial property. The shape could not impact the natural antibacterial property of natural bamboo fiber but the hygroscopicity and extractives have influence on that.

***Keywords*:** Natural bamboo fiber, antibacterial property, Influencing factors.

Introduction

As an abundant resource in China and an eco-friendly and multifunctional plant, bamboo has been used in architecture, agriculture, furniture and paper-making for thousands of years. Recently, research on producing textile fiber from bamboo has been conducted. According to different preparation techniques, the bamboo fiber for textile has been divided into two kinds, natural bamboo fiber and regenerated bamboo fiber (Li Qingchun. 2003). The natural bamboo is usually in the form of fiber bundle which is produced by unique chemical and physical technique (Wang Chunhong et al. 2005, Zhang Wei et al. 2007). The regenerated bamboo fiber is made from bamboo pulp, which has a similar processing method to the ordinary viscose fiber (Zhou Hengshu and Zhong Wenyan. 2003).

Clothing manufactured by regenerated bamboo fiber has entered the textile market with a claim for its antimicrobial property, but without scientific evidence (Afrin, T. et al. 2009). With the success of the separation techniques of natural bamboo fiber, people start to pay attention to the antibacterial property of natural bamboo fiber. However, there are different opinions on this issue. High bactericidal rate of natural bamboo fiber against some kinds of bacteria has been reported (Xing Shengyuan and Liu Zheng.2004) and the antibacterial agent in bamboo fiber has been identified as anthraquinone compounds that contain four α-hydroxylation functional groups (Sun Jujuan. 2007). However, results released from other studies have indicated that natural bamboo fiber has no significant antibacterial effect (Zhou Hengshu and Deng Libin. 2005) and even if it does, it is just because of certain natural micro-structure, not the antibacterial constituents (Zhu Liwei et al. 2008).

The aim of this paper was to investigate the natural antibacterial property of natural bamboo fiber and its influencing factors. As cotton, jute, flax and ramie are also plant fiber being used in textiles, they were selected to be compared with natural bamboo fiber. Meanwhile, the antibacterial property of regenerated bamboo fiber was also evaluated and compared with natural bamboo fiber.

Materials and Methods

Materials. Natural bamboo fiber used in this study was produced from the bamboo of Neosinocalamus affinis following the process: bamboo spliting → alkali degumming → acid rinsing → water rinsing → dewatering → shaking → drying → combing. Cotton, jute, flax, ramie and regenerated bamboo fiber used to be compared with natural bamboo fiber were purchased from market. A part of cotton fiber was treated with antibacterial agent SCJ-2000 (produced by Beijing Jlsun High-tech Co. Ltd), while another part of cotton and all of other fibers were untreated. Bamboo bundle used in this study came from the first step of the process and bamboo powder was obtained by grinding the natural bamboo fiber into 40~60 mesh-powder. In this study three repeated sepecimen for each series of test were prepared.

Microorganisms and media. Gram-negative bacteria, *Escherichia coli* (*E. coli*, 8099), gram-positive bacteria, *staphylococcus aureus* (*S. aureus*, ATCC 6538) and fungi *Candida albicans* (C. albicans, ATCC10231) were used as test organism. Nutrient Broth and Nutrition Agar culture medium were prepared for the bacteria growing and Sabouraud's Agar culture medium was used for the fungi culture. Buffer solution used for diluting was phosphate buffer solution (PBS, 0.03mol/L, pH=7.2~7.4).

Evaluation of fiber hygroscopicity. The humidity of the fiber samples was conditioned to balance state on the condition of 20℃ and 65% RH firstly referring to GB 6529-86 Textiles-Standard atmospheres for conditioning and testing. Then the samples were dried to constant weight at 105±2℃ referring to GB/T 9995-1997 Determination of moisture content and moisture regain of textile-Oven-drying method. The moisture regain was evaluated by the following equation:

$$W = \frac{G - G_0}{G_0} \times 100\% \quad (1)$$

Where W is the moisture regain, %, G is the wet weight of the textile fiber, g, and G_0 is the dry weight, g.

Extracting of natural bamboo fiber. Natural bamboo fiber was extracted to remove some kinds of extractives contained in the fiber referring to the determination method of extractives in fibrous raw material stipulated in GB/T2677. The extraction dissolvent used in the test were cold water (room temperature), hot-water (95~100℃), ethanol (density 95%), benzene, benzene/ethanol mixture (2:1, v/v) and 1% NaOH.

Antibacterial test. The antibacterial activity was tested with the shake flask test referring to GB/T 20944. 3-2008 Textiles-Evaluation for antibacterial activity-Part 3: Shake flask method. In the test for investigating the natural antibacterial property of natural bamboo fiber and the effect of bamboo shape on it, the untreated cotton was used as the negative control sample and the antibacterial cotton was used as the positive control sample. The antibacterial properties of test samples were evaluated by calculating the bacteriostatic rate as Equation (2). In the test for investigating the effect of extractive on the antibacterial activity of natural bamboo fiber, the bacterial growth in the flasks containing the natural bamboo fiber extracted and untreated was compared. The effect was evaluated by calculating the efficiency of anti bacteria as Equation (3). Negative number in the result was represented by 0.

$$Y = \frac{W_t - Q_t}{W_t} \times 100 \quad (2)$$

Where Y is the bacteriostatic rate, %, W_t is the average CFU per milliliter for the flask containing the negative control sample after 18h contact, and Q_t is the average CFU per milliliter for the flask containing the test sample after 18h contact.

$$E = \left(1 - \frac{D_t}{D_0}\right) \times 100 \quad (3)$$

Where E is the efficiency of anti bacteria, %, D_t is the average CFU per milliliter for the flask containing the natural bamboo fiber extracted after 18h contact, and D_0 is the average CFU per milliliter for the flask containing the natural bamboo fiber untreated after 18h contact.

Results and Discussion

Antibacterial property. The results of the antibacterial test are shown in Table 1. The untreated cotton as the negative control sample was not effective against bacteria, while the antibacterial cotton was very effective against all test bacteria with a bacteriostatic rate of over 99 % against *E. coli* and 100 % against *S. aureus* and *C. albicans*, indicating dependability of this test. The results showed that natural bamboo fiber was not effective against *E. coli*, *S. aureus* and *C.albicans* since the bacteriostatic rate against all of them was 0. By comparison, the bacteriostatic rate of ramie against *S. aureus* was over 90%, and that of regenerated bamboo fiber was 75.8%. Jute and flax had bacteriostatic activity against *C. albicans* because of bacteriostatic rate of 48% and 8.7%.

Tab.1 Results of the antibacterial test

fiber type	Bacteriostatic rate(%)		
	Escherichia coli	*Staphylococcus aureus*	*Candida albicans*
Untreated cotton	0	0	0
NBF	0（-68.9）	0（-13.2）	0（-41.3）
Jute	0（-15.9）	0（-48.4）	48
Flax	0（-45.0）	0（-88.8）	8.7
Ramie	24.3	90.2	54
RBF	41.4	75.8	0（-12.8）
Antibacterial cotton	>99%	100%	100%

Note: NBF=Natural bamboo fiber, RBF=Regenerated bamboo fiber (the same below)

The bacterial population density on each sample after shaking 18h is shown in Figure 1 in order to compare the inhibiting ability to bacterial growth of each kind of textile fiber. The Histogram shows that compared with natural cotton the population density of *E. coli* and *C. albicans* in natural bamboo fiber increased greatest after 18h. Instead of increasing, *E. coli* density in regenerated bamboo fiber and *S. aureus* density and *C. albicans* density in ramie decreased greatest.The antibacterial performance of regenerated bamboo fiber may largely come from the use of a large amount of chemicals in manufacturing process (Zhang Shiyuan. 2008) and that of ramie has been attributed to the components of pyrimidine, purine or other antibacterial component (Shao Songsheng. 2000).

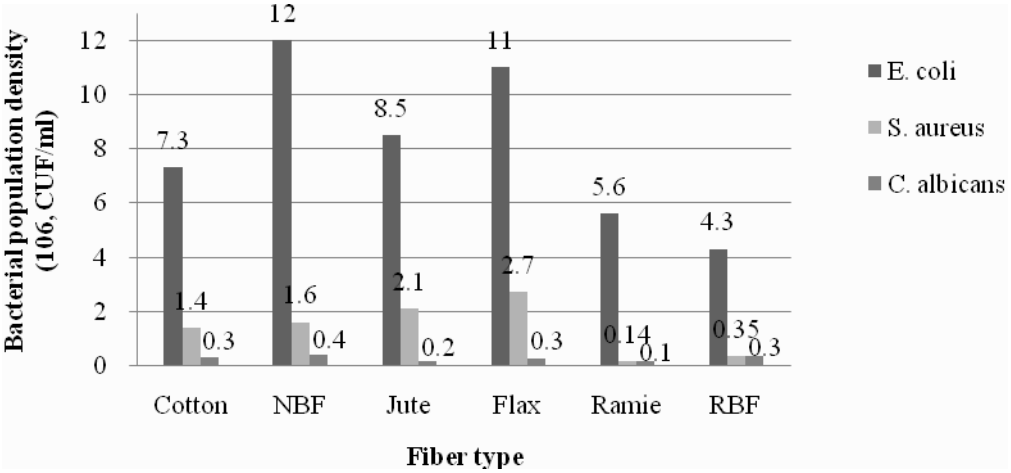

Fig.1 The bacterial population density on each sample after shaking 18h

The effect of bamboo shape. The bacteriostatic rates on the different shapes of bamboo against all the challenge bacteria were all 0 as showed in Table 2 and the bacterial population density of the same bacteria on different shapes of bamboo were nearly equal (Fig.2).

Tab.2 The bacteriostatic rate on different shapes of bamboo

Bamboo shape	Bacteriostatic rate(%)		
	Escherichia coli	*Staphylococcus aureus*	*Candida albicans*
Bundle	0(-69.0)	0(-75.0)	0(-45.5)
Fiber	0(-68.9)	0(-13.2)	0(-41.3)
Powder	0(-54.9)	0(-50.0)	0(-33.4)

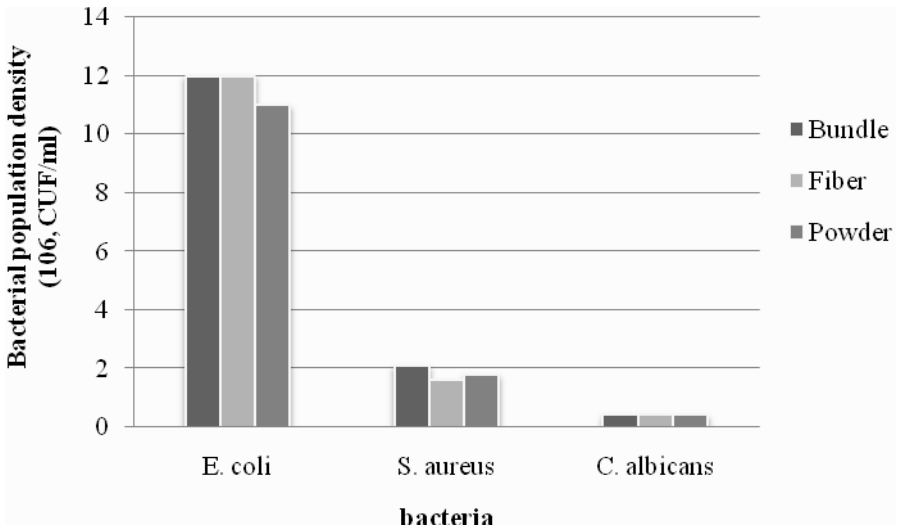

Fig.2 The bacterial population density on different shapes of bamboo

The effect of fiber hygroscopicity. The moisture regains of textile fiber are presented in Table 3, which shows that except the regenerated bamboo fiber the moisture regain of natural bamboo fiber was highest among the plant fibers, while that of ramie was lowest. The moisture regain of fiber is inversely proportional to their degree of crystallization (Wang Yueping et al. 2009). Figure 3 indicates the relationship between the moisture regain of the plant fibers and their bacteriostatic rates. According to the figure presented, it was determined that fiber possessing higher hygroscopicity presented lower bacteriostatic rate. Especially, the fitting correlation coefficient of the bacteriostatic rate against *E. coli* along with the moisture regain was 0.993. However, the regenerated bamboo fiber did not follow this trend (there is no definite relationship between hygroscopicity and its bacteriostatic rate), which may result from its preparation process.

Tab.3 The moisture regain of textile fiber

Fiber name	Moisture regain(%)
NBF	9.80
Cotton	7.75
Flax	9.24
Ramie	6.81
RBF	12.09

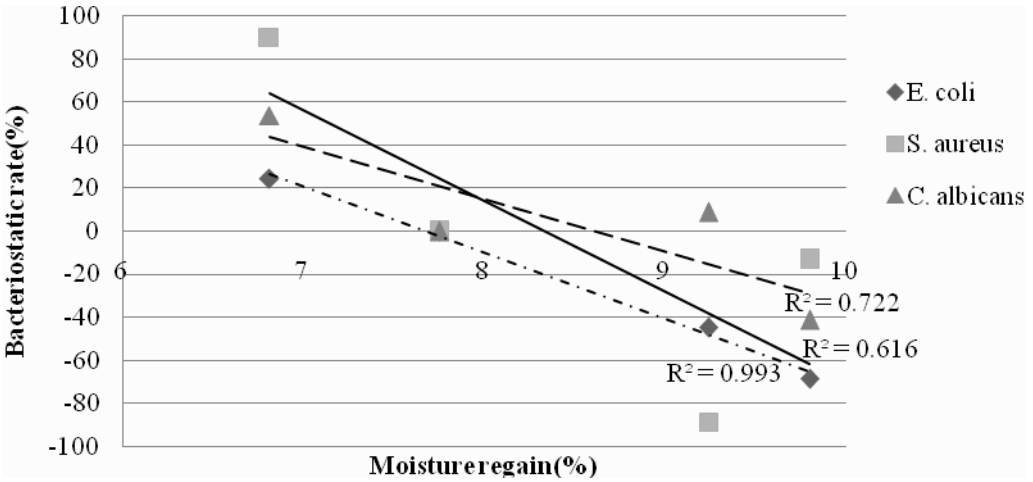

Fig.3 The relationship between moisture regain and bacteriostatic rate

The effect of extractive. It can be seen from Table 4 that extraction was effective in improving the antibacterial performances of natural bamboo fiber against *E. coli* and *S.aureus* except using benzene as the extraction dissolvent. Extraction using hot-water was the most effective method in improving the antibacterial property against *E. coli* with an anti bacteria efficiency of nearly 70% and using 1% NaOH was the best method against *S.aureus* with an anti bacteria efficiency of over 67%. However, there was not

any contribution toward improving the antibacterial activity against *C. albicans* by removing some kinds of extractives from natural bamboo fiber.

Tab.4 Antibacterial Efficiency of different extraction method

Extraction dissolvent name	anti bacteria Efficiency（%）		
	Escherichia coli	*Staphylococcus aureus*	*Candida albicans*
Cold-water	64.35	10.91	0
Hot-water	69.57	30.91	0
Ethanol	18.26	7.88	0
Benzene	0	0	0
Benzene/ethanol	4.35	36.36	0
1% NaOH	58.26	67.88	0

The origins of the extraction influence on the antibacterial property of the natural bamboo fiber may be attributed to three reasons. Firstly the removing of some extractives of natural bamboo fiber such as carbohydrate and inorganic salt (Higuchi, T.1987) which are microbial growth nutrients could improve the antibacterial performance. Secondly the extractives may contain some antibacterial component and the reduction of which may decrease the antibacterial property of the natural bamboo fiber at the same time. And finally, changes in chemical composition changed the pH value of the fiber which could affect the bacteria growth (Sun Fangli et al. 2006). Therefore, we inferred that the combine of the three aspects led to the influence of extraction on the antibacterial property of the natural bamboo fiber.

Conclusion

In this study, the antibacterial property of natural bamboo fiber and its influencing factors were investigated. The antibacterial test results show that natural bamboo fiber has no natural antibacterial property compared with other textile fiber. The fact that the growth of bacteria on different shapes of bamboo was nearly equal may indicate that the shape could not impact the antibacterial activity of natural bamboo fiber. The linear relationship between the moisture regain and the bacteriostatic rate suggests that the hygroscopicity may be a influencing factor in antibacterial performance of fiber. Some extraction method could improve the antibacterial property of natural bamboo fiber against bacteria, therefore, extractives have influence on that.

References

Li Qingchun. 2003. The Properties of Bamboo Fiber and Key Technology in Development. Sichuan Textile Sci. Technol. (5): 56-58.

Wang Chunhong, Wang Rui, Zhu Ruoying, et al. 2005. Producing Process of Bamboo Fiber. J. Tianjin Polytechnic Univ.. 24(4): 16–17.

Zhang Wei, Li Wenbin and Yao Wenbin. 2007. Separating Mechanism of Long Bamboo Fiber and Production Method. J. Beijing Forestry Univ.. 29(4): 63–66.

Zhou Hengshu and Zhong Wenyan. 2003. Development and Application of Bamboo Fiber. Wool Textile J.. (4): 30–36.

Afrin, T., Tsuzuki, T. and Wang, X. 2009. Bamboo fibres and their unique properties. In C.M. Wilson & R.M. Laing (Eds.), Combined (NZ and Aus) Conference of the Textile Institute,2009, Dunedin, NZ.

Xing Shengyuan and Liu Zheng.2004. The performance and product development of bamboo fiber. China Textile Leader. (4): 43-48.

Sun Jujuan. 2007.

Zhou Hengshu and Deng Libin. 2005. Study on the function and the anti-virus finishing of the original bamboo fabric. Progress in Textile Science & Technology. (5): 12-15.

Zhu Liwei, Shi Limin, Jiang Jianxin, et al. 2008. Studies on antibacterial properties of the natural bamboo fabric based on FZ/T 73023-2006. Journal of Donghua University. 34(4): 401-404.

Zhang Shiyuan. 2008. Bamboo fiber and its products processing technologies. Beijing: China Textile & Apparel Press.

Shao Songsheng. 2000. Prospects of bast fiber textiles. China Textile Leader. (1): 66-68.

Wang Yueping, Wang Ge, Cheng Haitao, et al. 2009. Structures of bamboo fiber for textiles. Textile Research Journal. 80(4): 334-343.

Higuchi, T.1987. Chemistry and biochemistry of bamboo. Bamboo J. 4: 132-145

Sun Fangli, Mao Shengfeng, Wen Guifeng, et al. 2006. Anti-mold effects of bamboo timber treated with different solutions. Journal of Zhejiang Forestry College. 23(2): 135-139

Acknowledgements

This research was supported by grant No. 2006BAD19B07 from the National Scientific and Technical Supporting 11th Five-year Plan Project.

The Manufacturing Process Of Bamboo Pellets

Zhijia Liu[a,b], Zehui Jiang[a], Zhiyong Cai[b*], Benhua Fei[a] , YanYu[a], Xing'e Liu[a]*

[a]International Centre for Bamboo and Rattan, Beijing, China, 100102

[b]Forest Products Laboratory, USDA Forest Service, Madison, WI 53705-2398, USA

Corresponding author: [a]Professor Jiang Zehui

[b]Professor Cai Zhiyong, tel: +1 (608) 231 9446 fax: +1 (608) 231 9582

Abstract

Bamboo was a kind of biomass materials and had great potential as a bio-energy resource of the future in China. The physical and combustion properties of bamboo pellets were determined and the effects of moisture content (MC) and sizes of particle on these properties were investigated in this research. The results showed that MC and sizes of particle affected these properties of bamboo pellets. The effects of MC on physical properties including length, diameter, pellet MC, unit density, bulk density were significant at p=0.05. But there were not significantly difference between particle size (PS) and all properties of bamboo pellets. The optimum manufacturing process was 16% MC and PS mixture. All properties of bamboo pellets could meet the requirement of *Pellets Fuel Institute Standard Specification for Residential/Commercial Densified* and the gross calorific value could also meet the minimum requirement for making commercial pellets of DIN 51731 (>17500J/g), respectively. Bamboo pellets would be the proposed new biomass solid fuel and had the potential to be development as commercial pellets.

Key words: Biomass, Bio-energy, Bamboo, Bamboo pellet, Physical property

1. Introduction

There were several alternative energy which could substitute fossil fuel in the future, such as hydro, solar, wind, biomass and ocean thermal energy. Among these energy sources, biomass was the only carbon-based sustainable energy and the wide variety of biomass enabled it to be utilized by most people around the world (Faizal et al., 2010). Bamboo was a kind of biomass materials and had been widely cultivated in the west and south of China. Currently, bamboo resource was very abundant and the total area of bamboo was about five million hectares and that of moso bamboo *(Phyllostachys heterocycla)* was about 3 million hectares in China (Jiang, 2002). Annual yield of moso bamboo was about eighteen million tons, which was widely used to produce furniture, flooring and interior decoration materials. Bamboo, like wood, was mainly composited of hemicelluloses, cellulose and lignin. It had great potential as a bio-energy resource of the future in China.

The biomass pellets and briquettes were a main kind of bio-energy and they had better flow properties. Densification into pellets could reduce material wastage and improve ease of transporting and storage (Adapa et al., 2006). In the recent years, various pellets had been studied such as biomass waste materials (Ayhan and Ayse, 2004), spring-harvested reed canary-grass (Susanne and Nilsson, 2001), switchgrass (Colley et al., 2006), cotton stalk (Abasaeed, 1992), peanut hulls (Fasina and Sokhansanj, 1993), poultry litter (Mcmullen et al., 2004), corn-soybean (Parsons et al., 2006). During the densification process of biomass pellets, the MC and PS of materials were considered as two main factors affected to properties of pellets. Faizal et al. (2009) studied the physical characteristics of briquette contains different mixing ratio of empty fruit bunch fiber and mesocarp fiber. Holt et al. (2006) manufactured fuel pellets using by-products from two cotton gins. The treatments resulted from using different material streams from the ginning process as well as varying quantities of starch and/or crude cottonseed oil during the fuel pellet manufacturing process. The fuel pellet density from the various treatments ranged from 488 to 678 kg/m3. Zimonja and Svihus (2009) conducted to investigate the influence of cereal starch exposed to various processing techniques on physical pellet quality and nutritional value of the diets fed to broiler chickens. The combustion properties of pellets were one of main characteristics for solid fuel. Susanne and Calle (2001) investigated ash problems of spring-harvested reed canary-grass briquettes during the combustion. Ann and Petersen (2006) studied how much greenhouse gas (GHG) was emitted for various kinds of fuel wood, sawdust, pellets, briquettes, demolition wood, and bark (not only CO_2, but also CH_4 and N_2O). Maria (2010) determined the emissions of organic compounds from incomplete burning of oats using gas chromatography and compared to those of softwood pellets. The use of coal-biomass briquettes will effectively reduce the indoor concentration of sulfur dioxide (SO2) emitted during raw coal combustion. Indoor concentrations of SO2 emitted from combustion of either coal-biomass briquettes or low-grade coal in households were measured and were found to be less with coal-biomass briquettes (Yugo et al., 2005). Telmo and Lousada (2011) tested the calorific values of wood pellets from different wood species using a Parr 6300 bomb calorimeter, and softwoods had a high calorific value between 19660.02 and 20360.45kJ/kg, but the hardwoods had a ranging interval between 17631.66 and 20809.47 kJ/kg.

All briquettes prepared from mango leaves, eucalyptus leaves, wheat straw, and saw dust had more heating value than the half of the Indian coal and these could be used as an alternative for the coal and also for fire wood (Varun et al., 2010).

To date, no information was available about bamboo pellets. This study was therefore carried out to determine properties of bamboo pellets, which was manufactured using different MC and PS of bamboo. The purpose of this research analyzed the effect of MC and PS on physical properties of bamboo pellets and provided guidelines for later research.

2. Materials and methods

2.1 Materials

Maso Bamboo was used in the study. The initial MC of samples was about 6.13%, their density was about 0.65g/cm^3. Bamboo materials were cut off to sample size 40mm (longitudinal) by 3-8mm (radial) by 20-30mm (tangential). Then, they were broken down to particles using wood particle

mill at Forestry Products Laboratory of USDA Forest Service. Finally, they were screened to get three different kinds of bamboo PS.

2.2 Pellet Formation

The bamboo pellets were manufactured using laboratory pellet mill (L-175), made by AMANDUS KAHL NACHE HAMBURG COMPANY. The effects of MC and PS of bamboo were carried out at by a 3^2 full-factorials design shown in Table 1. The manufacturing processes were shown:

1. The bamboo particles were separated according their PS. Three kinds of PS, used in the study, were respectively PS1 (the particle diameter was more than 1.18mm), PS2 (the particle diameter was 1.18-0.84mm) and PS3 (the particle diameter was less than 0.84mm).
2. One kilogram (1kg) of bamboo particles with PS1, PS2 and PS3 were respectively put into the conditioning room with temperature 27℃, humidity 65% and temperature 27℃, humidity 90% to adjust their MC to about 8%, 12% and 16%. For the highest MC (16%), bamboo particles were conditioned by adding predetermined amounts of distilled water onto the samples.
3. The bamboo particles were transferred to separate Ziploc bags and sealed tightly. Then they were kept in a conditioning room (temperature 27℃, humidity 65%) for 48h to enable moisture to be distributed uniformly.
4. MC of bamboo particles was tested using drying oven at 105℃ for 8h. The initial and final mass was measured by a digital balance. MC of bamboo particles was calculated basis on the mass loss.
5. The parameters of pellet mill were set to rotary speed 235r/min and pellets diameter 5.9mm.

6. The bamboo particles were continuously feed into pellet mill, and bamboo pellets were formatted.
7. The bamboo pellets were collected and were kept in the laboratory more than a week, and then their properties were tested.

Table 1 Experimental design

Experiment No.	MC (%)	PS (mm)
1	8	PS1
2	8	PS2
3	8	PS3
4	12	PS1
5	12	PS2
6	12	PS3
7	16	PS1
8	16	PS2
9	16	PS3

2.3 Properties Test

(1) Pellet dimension

The pellets were cylindrical in the shape. In order to determine dimensions and unit mass, ten bamboo pellets were randomly selected in each experiment. The length (L) and diameter (d) of every sample were measured using a digital vernier caliper. The mass of bamboo pellets (m) was weighted using a precision digital balance (0.0001 Resolution).

(2) Unit density (ρ_u)

Unit density of bamboo pellets were determined by weighting the individual pellet and calculating its volume basis on its length and diameter as per the following equations.

$$V_u = \pi/4d^2L \quad (1)$$

$$\rho_u = m_u/V_u \quad (2)$$

Where, V_u was the volume of individual pellet, cm^3; d was the diameter of pellet, mm; L was the length of pellet, mm; ρ_u was the unit density, g/cm^3; m_u was the mass of individual pellet, g.

(3) Bulk density (ρ_b)

Bulk densities were calculated as the ratio of the mass of materials to the volume of the container. The bamboo pellets were leveled with the top surface of the container and they were weighed using a precision digital balance (0.0001 Resolution). The volume of container was calculated by measuring its length and diameter.

$$P_b = m_b/V_b \quad (3)$$

Where, ρ_b was the bulk density, g/cm^3; V_b was the volume of cintainer, cm^3; m_b was the total mass of pellets, g.

(4) Pellet MC

Pellet MC was determined by mass loss of samples. Ten bamboo pellets in every process were heated using drying oven under rigidly controlled conditions of temperature (105℃), time (8h). Then they were removed from drying oven and put into a desiccator to cool to room temperature. The next, they were weighted using a precision digital balance (0.0001 Resolution). Samples were returned to drying oven at 105℃ for 2h and they were cooled and weighted. When mass varies of samples was less than 0.2%, their final mass was recorded. MC was calculated using the following equation:

$$MC = (m_i-m_f)/m_f\times100\% \quad (4)$$

Where, MC was pellet moisture content (%), m_i was initial mass of samples (g), and m_f was final mass of samples (g).

(5) Pellet fine (P_f)

Pellet fine was determined using 3.17mm (1/8in) wire screen sieve according to *Pellets Fuel*

Institute Standard Specification for Residential/Commercial Densified. Fifty bamboo pellets were randomly selected and were divided into ten groups. The initial mass of every group sample was weighted using a precision digital balance (0.0001 Resolution). They were placed on wire screen sieve and tilted it from side to side ten times. Then the final mass was weighted and recorded. The pellet fine was calculated using the following equation:

$$P_f = (m_i-m_f)/m_i\times100\% \quad (6)$$

Where, P_f was fine of samples (%), m_i was initial mass of samples (g), and m_f was final mass of samples (g).

(6) Pellet durability (P_d)

Pellet durability was determined by mass loss of samples. Fifty bamboo pellets in every process were randomly selected and weighted using a precision digital balance (0.0001 Resolution). The initial mass was recorded. Then they were put into a vibrating sieve with screen size 3.17mm (1/8in). After ten minutes, they were weighted again and the final mass was recorded. The pellet durability was calculated using the following equation:

$$P_d = 100-(m_i-m_f)/m_i\times100\% \quad (5)$$

Where, P_d was pellet durability index (%), m_i was initial mass of samples (g), and m_f was final mass of samples (g).

(7) Pellet absorption (P_a)

Pellet absorption was determined through mass change of samples. Five bamboo pellets in every process were randomly selected. They were dried at temperature 105℃ until their mass did not change and then the initial mass of samples was weighted using a precision digital balance (0.0001 Resolution). They were kept in the conditioning room (temperature 27℃, humidity 90%) for 24h. Then the final mass of samples was weighted and recorded. The pellet absorption was calculated using the following equation:

$$P_a = (m_i - m_f)/m_i \times 100\% \quad (7)$$

Where, P_a was absorption of samples (%), m_i was initial mass of samples (g), and m_f was final mass of samples (g).

(8) Inorganic ash (Ia)

Inorganic ash of bamboo pellets were determined basis on the percent inorganic material in the bamboo pellets.

1. Five empty crucibles were ignited in the muffle furnace at 600℃, were cooled in the desiccator and were weighted using a precision digital balance (0.0001 Resolution).
2. About 2g bamboo pellets were placed in every crucibles, were determined the weight of crucibles plus bamboo pellets and were placed in the drying oven at 105℃. After 2 h, they were replaced, were cooled in the desiccator to room temperature and were weighted.
3. The crucibles were returned to drying oven at 105℃ for 2h and were cooled and weighted. When weight variance of the crucible was less than 0.2%, the final weight was recorded.
4. The crucibles were placed in the muffle furnace at 600℃ and were ignited until all the carbon was eliminated.
5. The crucibles were removed from muffle furnace and were cooled in the desiccator and weighted using a precision digital balance (0.0001 Resolution).
6. Inorganic ash content was calculated basis on the following equation.

$$Ia = (W_1/W_2) \times 100\% \quad (8)$$

Where, Ia was inorganic ash content, %; W_1 was weight of inorganic ash, g; and W_2 was weight of oven-dry bamboo pellets, g.

(9) Gross calorific value (Gc)

The gross calorific value was the amount of energy per unit mass released upon complete combustion. The calorific value of bamboo pellets was tested using *PARR 1266 Bomb Calorimeter*.

Before testing gross calorific value of bamboo pellets, the calorimeter was calibrated with tablets of benzoid acid whose calorific value was 26465 J/g. In this test, about 1g bamboo pellets was introduced in the bomb, which was charged slowly with pure oxygen (>99.95 vol. %, quality 3.5) to a pressure of 3.0±0.2 MPa without displacing the original air. Any combustion aid was not used and five samples were tested in every condition. The final experimental result was the average value of five samples.

(10) Combustion rate (Cr) and Heat release rate (Hr)

The fire time was recorded according to *PARR 1266 Bomb Calorimeter.* It was time for bamboo pellets combustion was completed. Basis on the amount of total bamboo pellets and fire time, the average combustion rate could be calculated by using following equation.

$$Cr = M/t \quad (9)$$

Where, Cr was the average combustion rate, g/s; M was the mass of bamboo pellets, g; t was fire time in every test, s.

By knowing the gross calorific value and average combustion rate, the heat release rate could be calculated by using following equation (Faizal et al, 2010).

$$Hr = Gc \times Cr \quad (10)$$

Where, Hr was the heat release rate, J/s; and Cr was the average combustion rate, g/s.

2. Results and discussions

2.1 Effects of MC on properties of bamboo pellets

Table 2 showed the effects of MC on some physical properties of bamboo pellets. For every physical property, the data presented were the mean of measurements made on 30 pellets at each MC level. As shown in Table 2, the mean length of bamboo pellets ranged between 12.71mm and 11.69mm. The length values were 12.50mm, 12.71mm and 11.69mm at 8%, 12% and 16% MC levels, respectively. The length of the pellets affected the fuel feeding properties. The shorter the pellets, the easier the continuous flow could be arranged (Paivi, 2001). The mean diameter of bamboo pellets slightly ranged and the values were respectively 6.086mm, 6.036mm and 6.044mm at 8%, 12% and 16% MC level. The dimensions of pellets, both diameter and length, were important factors with respect to combustion. Experience had shown that thinner pellets allowed a more uniform combustion rate than thicker ones, especially in small furnaces (Paivi, 2001). The mean mass value was biggest at 12% MC level, the next was 16% and the last was 8%. The absorption of bamboo pellets also slightly ranged at each MC level. The difference could result from different pore structure of bamboo pellets when they were manufactured using bamboo

particles with different MC levels. The pellet MC slightly increased with increase in particle MC. According to Table 2, the unit density and bulk density values were 1.05g/cm^3, 1.14g/cm^3, 1.20 g/cm^3 and 0.522 g/cm^3, 0.625 g/cm^3, 0.652 g/cm^3 at 8%, 12% and 16% particle MC, respectively. The unit density and bulk density of bamboo pellets were increased with increase in particle MC. Transport efficiency depended on the bulk density of pellets. The strength of pellets was also an important factor connected with handling and transporting. In the research, the strength of pellets included two parameters, durability and fine. Table 2 showed the change of durability and fine of bamboo pellets. The pellet durability increased with increase in particle MC and the values were respectively 95.07%, 97.95% and 98.38%. For pellet fine, however, the smallest value was 16% MC level, the next was 8% and the last was 12%. The unit density was a very important parameter affected the durability and fine of pellets. The unit density of bamboo pellets were increased with increase in particle MC. The bigger the unit density, the higher was durability of pellets and the less was fines of pellets.

Table 3 showed the effects of MC on combustion properties of bamboo pellets. As shown in Table 3, the inorganic ash of bamboo pellets slightly ranged between 1.46% and 1.34%, and the values were 1.46%, 1.38% and 1.34% at 8%, 12% and 16% MC levels, respectively. The proportion of organic material decreased during the formation process of bamboo pellets (Paivi, 2001), which led to the difference of inorganic ash of bamboo pellets. For 16% MC, bamboo pellets were easier formatted in the manufacturing process and the reduction of organic materials was less, which resulted in a minimum inorganic ash content of bamboo pellets. There were no significant difference of gross calorific value of bamboo pellets manufactured using different MC. The slight variance of gross calorific value was due to the heat energy required to vaporize water because of hydrogen released during combustion process of bamboo pellets. The bamboo pellets made of different MC had different combustion rate. The combustion rate for bamboo pellets increased as MC increased from 8% to 16% MC. This was because when MC increased, the dwell time of bamboo particles in the die set was shorter and the air gap between particles of bamboo pellets was also more. Due to better air circulation through the air gap of pellets, the combustion rate of pellets increased (Faizal et al, 2010). In this research, the combustion rate of bamboo pellets manufactured by 16% MC was highest, the next was 12% and the last was 8%. It was also found that the heat release rate of bamboo pellets was also increased with MC increase. The main reason was that combustion rate increased with MC increase even though the gross calorific value seemed to be constant. The value of heat release rate were respectively 3164J/s, 3307J/s and 3377J/s for the 8%, 12% and 16% MC.

In sum, the properties of bamboo pellets, including physical properties (length, diameter, mass, pellet MC, absorption, unit density, bulk density, porosity, durability and fine) and combustion properties (inorganic ash, gross calorific value, combustion rate and heat release rate) were tested. The particle MC affected these properties and analysis of variance results (Table 4) showed that the effects of particle MC on length, diameter, pellet MC, unit density, bulk density were significantly different at p=0.05.

Table 2 Physical properties of bamboo pellets manufactured by different MC particles

MC (%)	L (mm)	d (mm)	Mass (g)	Pellet MC (%)	Pa (%)	ρ_u (g/cm^3)	ρ_b (g/cm^3)	Pf (%)	Pd (%)
8	12.50	6.086	0.3827	4.91	11.12	1.05	0.522	0.41	95.07
12	12.71	6.036	0.4140	4.96	11.35	1.14	0.625	0.54	97.95
16	11.69	6.044	0.3975	5.35	10.95	1.20	0.652	0.27	98.38

Table 3 Combustion properties of bamboo pellets manufactured by different MC particles

MC (%)	Ia (%)	Gc (J/g)	Cr (g/s)	Hr (J/s)
8	1.46	18465.90	0.171	3164.62
12	1.37	18438.78	0.179	3307.79
16	1.34	18457.46	0.183	3377.81

Table 4 Analysis of variance

Properties	Variance	SS	df	MS	F value	P-value	F crit
	Interior-group	21.40	2	10.70	3.69	0.0287103	3.10
Length	Inter-group	251.65	87	2.89			
	Total	273.06	89				
	Interior-group	0.043	2	0.02	16.66	7.471E-07	3.10
Diameter	Inter-group	0.11	87	0.0012			
	Total	0.15	89				
	Interior-group	3.50	2	1.75	5.22	0.0072033	3.10
Pellet MC	Inter-group	29.22	87	0.33			
	Total	32.72	89				
	Interior-group	0.32	2	0.16	11.35	4.16E-05	3.10
Unit density	Inter-group	1.25	87	0.014			
	Total	1.57	89				
	Interior-group	0.28	2	0.14	175.08	3.167E-31	3.10
Bulk density	Inter-group	0.07	87	0.0008			
	Total	0.35	89				

2.2 *Effects of PS on the properties*

Table 5 showed the effects of PS on physical properties of bamboo pellets. As shown in Table 5, the mean length of bamboo pellets decreased with increase in PS and the values were 12.62mm, 12.24mm and 11.94mm at PS1, PS2 and PS3 levels, respectively. The mean diameter and mass of bamboo pellets slightly ranged and the values were respectively 6.052mm, 6.062mm 6.053mm and 0.4006g, 0.3975g, 0.3961g. The pellet absorption also slightly ranged at three PS levels. The variance could result from different pore structure of bamboo pellets and surface/volume ratio of bamboo particles. When water dripped to pellet surface, absorption, spreading and permeability happened at the same time. The pore structure of bamboo pellets affected removing process of water.

The inter-porosity of bamboo pellets, made of PS1, was bigger and more than that of other bamboo pellet, made of PS2 or PS3. The variance of inter-porosity resulted in the difference of surface/volume ratio in the inner of bamboo pellets. High surface/volume ratio in each particle allowed better penetration of moisture. Link et al. (1999) found linear relationship between the absorption maximum of the longitudinal plasmon resonance and the mean surface/volume ratio as determined from TEM. The absorption of bamboo particle was also different for PS1, PS2 and PS3. Barltrop and Meek (1979) found an inverse relationship between particle size and absorption of lead. So particle absorption should be biggest for PS3, the next was PS2 and the last was PS1 in this research. Li et al. (2010) found that water absorption of rice straw particleboard increased with decrease in PS. According to Table 5, the unit density and bulk density values were 1.11g/cm^3, 1.13g/cm^3, 1.16 g/cm^3 and 0.599 g/cm^3, 0.600 g/cm^3, 0.600 g/cm^3 at PS1, PS2, PS3 levels, respectively. The unit density and bulk density of bamboo pellets were increased with increase in PS. The pellet durability increased with increase in PS and the values were respectively 97.96%, 97.21% and 96.23%. For pellet fine, however, the smallest value was bamboo pellets, made of PS1, the next was PS2 and the last was PS3. The smaller particle size made the feedstock slippery and it slid through the holes too easily, thereby reducing pellet strength.

Table 6 showed the combustion properties of bamboo pellets. As shown in Table 6, the inorganic ash of bamboo pellets decreased with the PS increase and the value was 1.45%, 1.38% and 1.32% for PS1, PS2 and PS3, respectively. There were no significant difference of gross calorific value of bamboo pellets manufactured using different PS. The gross calorific value of bamboo pellets was respectively 18463J/g, 18464J/g and 18434J/g. The gross calorific value of all bamboo pellets could meet the minimum requirement for making commercial pellets (>17500J/g), as stated by DIN 51731 (Faizal et al, 2010). The bamboo pellets made of different PS had different combustion rate. The combustion rate for bamboo pellets increased as PS increased. Air circulation affected the combustion rate of pellets when they were burned (Faizal et al, 2010). The bigger PS of bamboo material, the more inner porosity of bamboo pellets, which could led to a better air circulation in the combustion process of bamboo pellets. It was also found that the heat release rate of bamboo pellets was also increased with PS increase even though the variance was no significant. The value of heat release rate were respectively 3271J/s, 3277J/s and 3301J/s for PS1, PS2 and PS3. It came to an experimental conclusion that the combustion process of bamboo pellets manufactured by PS3 was the best, which also proved why its inorganic ash was the lowest in this research.

In sum, the effects of PS on some properties of bamboo pellets were investigated in this research. The PS affected the properties of bamboo pellets, but the variance of these properties was not significant at p=0.05 basis on analysis of variance method.

Table 5 Physical properties of bamboo pellets manufactured by particles with different sizes

PS	L (mm)	d (mm)	Mass (g)	Pellet MC (%)	Pa (%)	ρ_u (g/cm^3)	ρ_b (g/cm^3)	Pf (%)	Pd (%)
PS1	12.62	6.052	0.4006	5.06	11.31	1.11	0.599	0.27	97.96
PS2	12.24	6.062	0.3975	5.20	11.32	1.13	0.600	0.46	97.21

PS3	11.94	6.053	0.3961	4.96	10.79	1.16	0.600	0.49	96.23

Table 6 Combustion properties of bamboo pellets manufactured by particles with different sizes

PS	Ia (%)	Gc (J/g)	Cr (g/s)	Hr (J/s)
PS1	1.45	18463.07	0.177	3271.62
PS2	1.39	18464.22	0.177	3277.22
PS3	1.33	18434.85	0.179	3301.39

2.3 The optimum manufacturing process

The density of pellets was very important to evaluate product properties. Several national standards described the particle density of pellets and briquettes as a quality indicator of densified fuels. The maximum throughout for such a large-scale biomass bulk terminal was set at 40 tons per annum, both solid and liquid biomass, which implied that substantial storage facilities and spaces and handing systems were required. Transport and handing efficiency and amount of storage space depended on the bulk density of pellets. The increase of bulk density reduced the amount of storage space. So in this research, the bulk density was selected to optimize the manufacturing process of bamboo pellets. Table 7 showed the bulk density of bamboo pellets with different MC and PS. According to Table 7, the bulk density values were 0.522 g/cm^3, 0.625 g/cm^3, 0.652 g/cm^3 at 8%, 12% and 16% particle MC, respectively. But for different PS, the bulk density value was very slightly various. Analysis of variance results (Table 8) showed that the effects of MC on bulk density were significantly different and the variance between bulk density and PS was not significant at p=0.05. So the optimum MC was 16%, and Mixture or any kind of PS, used in this research, was selected to manufacture bamboo pellets. The bamboo pellets photo, made in the optimum process, was shown in Figure 1.

Table 7 The bulk density of bamboo pellets with different MC and PS

Process parameters	MC (%)			PS		
	8	12	16	PS1	PS2	PS3
ρ_b	0.522	0.625	0.652	0.599	0.600	0.600

Table 8 Analysis of variance

Process parameters	Variance	SS	df	MS	F value	P-value	F crit
MC	Interior-group	0.28	2	0.14	175.08	3.167E-31	3.10
	Inter-group	0.07	87	0.0008			
	Total	0.35	89				
PS	Interior-group	4.894E-05	2	2.447E-05	0.0060462	0.99	3.10
	Inter-group	0.3521291	87	0.0040475			
	Total	0.3521781	89				

Figure 1 The bamboo pellets with 16% MC and PS mixture

3 Conclusions

It could be concluded from this research that MC and PS affected the properties of bamboo pellets. The effects of MC on some properties such as length, diameter, pellet MC, unit density, bulk density were significant at p=0.05. But there were not significantly difference between PS and all properties of bamboo pellets. The optimum manufacturing process was 16% MC and PS mixture in this research. All properties of bamboo pellets could meet the requirement of *Pellets Fuel Institute Standard Specification for Residential/Commercial Densified*. The gross calorific value of bamboo pellets could also meet the minimum requirement for making commercial pellets of DIN 51731 (>17500J/g), respectively. The experimental result showed that bamboo pellets would be the proposed new biomass solid fuel and had the potential to be development as commercial pellets.

Acknowledgements

This research was financially supported by the ‘Basic Scientific Research Funds of International Centre for Bamboo and Rattan’ (Grant No. 1632012002) and ‘Development and demonstration of bamboo/wood composite LVL and wallboard’ (Grant No. [2008] 16).

References

Adapa, P.K., Singh A.K., Schoenau G.J., Tabil, L.G., 2006. Pelleting characteristics of fractionated alfalfa grinds: hardness models. Power Handling and Processing 18, 1-6.

Ayhan, D., Ayse, S.D., 2004. Briquetting Properties of Biomass Waste Materials. Energy Sources 26, 83-91.

Abasaeed, A.E., 1992. Briquetting of carbonized cotton stalk. Energy 17, 877-882.

Barltrop, D., Meek, F., 1979. Effect of particle size on lead absorption from the gut.

Cattaneo, D., 2003. Briquetting-A Forgotten Opportunity. Wood Energy. University of Brescia.

Colley, Z., Fasina, O.O., Bransby, D., Lee, Y.Y., 2006. Moisture effect on the physical characteristics of switchgrass pellets. Transactions of the ASABE 49, 1845-1851.

Fasina, O.O., Sokhansanj, S., 1993. Effect of moisture content on bulk handling properties of alfalfa pellets. Canadian Agricultural Engineering 35, 269-273.

Fasina, O.O., 2007. Physical properties of peanut hull pellets. ASABE paper No. 076161. St. Joseph, MI: ASABE.

Faizal, H.M., Latiff, Z.A., Wahid, M.A., Darus, A.N., 2010. Physical and combustion characteristics of biomass residues from palm oil mills. New Aspects of Fluid Mechanics, Heat Transfer and Environment, 34-38.

Holt, G.A., Blodgett, T.L., Nakayama, F.S., 2006. Physical and combustion characteristics of pellet fuel from cotton gin by-products produced by select processing treatments. Industrial Crops and Products 24, 204-213.

Jiang Z.H., 2002. World bamboo and rattan. Liaoning Science & Technology Press , China. 43 pp.

Kaliyan, N., Morey, R.V., 2008. Factors Affecting Strength and Durability of Densified Biomass Products. Biomass and Bioenergy, 1-23.

Li, X.J., Cai, Z.Y., Winandy, J.E., Basta, A.H., 2010. Selected properties of particleboard panels manufactured from rice straws of different geometries. Bioresource Technology 101, 4662-4666.

Link, S., Mohamed, M. B., Elsayed, M. A., 1999. Simulation of the Optical Absorption Spectra of Gold Nanorods as a Function of Their Aspect Ratio and the Effect of the Medium Dielectric Constant. J. Phys. Chem. B 103, 3073-3077.

Mahapatra, A.K., Harris, D.L., Durham. D.L., Lucas, S., Terrill, T.H., Kouakou, B., Kannan, G., 2010. Effects of moisture change on the physical and thermal properties of sericea lespedeza pellets. International Agricultural engineering Journal 1, 23-29.

Maria P. (2010) Emissions of organic compounds from the combustion of oats-a comparison with softwood pellets. Biomass and bioenergy, 34, 828-837.

Nalladurai, K.R., 2010. Vance Morey. Natural binders and solid bridge type binding mechanisms in briquettes and pellets made from corn stover and switchgrass. Bioresource Technology 101, 1082-1090.

Paivi, L., 2001. Quality properties of pelletised sawdust, logging residues and bark. Biomass and bioenergy 20, 351-360.

Susanne, P., Calle, N. (2001). Briquetting and combustion of spring-harvested reed canary-grass: effect of fuel composition. Biomass and Bioenergy, 20, 25-35.

Susanne, P., Nilsson, C., 2001. Briquetting and combustion of spring-harvested reed canary-grass: effect of fuel composition. Biomass and Bioenergy 20, 25-35.

Telmo, C., Lousada, J. (2011). Heating values of wood pellets from different species. Biomass and bioenergy, 35, 2634-2539.

Yugo, I., Yamada, K., Wang, Q.Y., Sakamoto, K., Uchiyama, I., Mizoguchi, T., Zhou, Y.R. (2005). Measurement of Indoor Sulfur Dioxide Emission from Coal-Biomass Briquettes. Water, Air & Soil Pollution, 163, 341-353.

Investigation on Production of Bleachable Chemi-Mechanical Pulp from Wheat Straw

Ahmad Jahan Latibari ,
Mohammad Ali Hossein,
Reza Hosseinpour
Department of Wood and Paper Science and Technology
Karaj Branch, Islamic Azad University
Karaj, Iran

Abstract

In an attempt to develop pulping process suitable for small scale implementation, production of bleachable chemi-mechanical pulp from wheat straw was investigated. Four levels (10, 12, 14 and 16% based on oven dry weight of straw) NaOH and one pulping time of 40 minutes at 95°C pulping temperature were used. After digester yield varied between 64.4 and 72.2% and the total yield after defibration was measured as 55.5% and 58.2%. Unrefined pulp freeness varied between 708 and 790 ml CSF. Pulps produced applying 10-16% NaOH, 40 minutes pulping time and 95°C pulping temperature was selected from further evaluation. These pulps were refined to about 365 ml CSF in a PFI mill and then hand sheets were made for strength evaluation. The apparent density of the hand sheets varied between 430-489 kg/m^3, tear index between 6.51-7.11 $mN.m^2/g$, and tensile index between 29.2 -30.8 N.m/g. Significant difference at 99% was not observed between the strength of the pulps. Then pulp produced applying 10% NaOH, 40 minutes pulping time and 95°C pulping temperature were selected for bleaching trials. Totally Chlorine Free (TCF) bleaching sequences was used for bleaching. Pulps bleached applying 4% H_2O_2 and 3.5% NaOH , 3% sodium Silicate, 0.5% MgSO4 and 0.3% DTPA for 2 hours showed the highest brightness of 50.69% compared to 29.2% for unbleached pulp.

Keywords: Wheat Straw, Chemi-Mechanical Pulp, Yield, Strength, Totally Chlorine Free Bleaching

Introduction

Paper was invented using non wood fibers and during the course of its development thru Asia and then Europe, non woods such as wheat straw were utilized. However, the abundant sources of wood in Europe and easy processing of this fiber supply replaced non woods. During late 20th century, global shortage of wood has emerged and paper industry was forced to look for alternatives sources of fibrous raw material. Countries and regions with limited paper production are also trying to develop domestic production capacities, relying on local but unconventional raw material. Two production trends; utilization of non-wood fiber supply and re-utilization of recycled paper have been followed.

Regions like Asia and also some countries in the Middle East concentrated on utilization of non woods as raw material. Therefore, it is believed that the non wood pulp production will take the momentum at the annual rate between 12-15%, even though it seems unrealistic (Pande 2009). In this expansion path, the share of undeveloped countries which are faced with wood fiber supply limitation will be more than fiber rich countries. Annual plant pulping found more and more importance especially in fiber deficient regions and since 1970, the non wood plant fiber pulping capacities increased two to three times as fast as wood pulping capacity on global basis (Hedjazi et al. 2009). It has been estimated that the pulp production from wheat straw in China will reach almost 13 million tons in 2020 (Zhao et al. 2010).

The general desire on non wood pulping initiated interest worldwide and various research groups started research, development, improvement and implementation of non wood pulping (Mackean and Jacobs 1997). Such research activities cover a wide range of pulping processes from conventional soda pulping of bagasse and cereal straw to non conventional fibers such as date palm residues (Kristova et al. 2005). Wheat straw has been the prime non wood fiber supply and different pulping processes have been studied (Ates et al. 2008, Hedjazi et al 2008). Wheat straw Alkaline Peroxide Mechanical Pulping was investigated to develop raw material efficient pulping method (Pan and Leary 2002) and enzyme and hot water treatment of wheat straw was studied to improve the brightness of the wheat straw pulp (Zhao et al 2004 and Mustajoki et at 2010).

For annual plant and wheat straw, mostly soda pulping has been applied. Soda pulping is well-established process with the potential to process vast variety of annual plant raw material, but this process has particular disadvantages such as low yield. Chemi-mechnical pulping has been developed to reach higher yield and more efficient use of raw material. However, the strength properties of this pulp are inferior to normal soda pulp. Therefore, we concentrated on the modification of the chemi-mechanical pulping process to preserve the yield and carbohydrate, providing suitable properties.

In this investigation, our attempts are focused on the development of simple pulping process for wheat straw suitable for small scale production and characterize the pulp properties to be utilized as supplementary pulp for corrugating fine grade paper.

Experimental

Material

Wheat straw in bales was collected from Agriculture and Natural Resources College Experimental Station, Islamic Azad University, Karadj Branch. Samples were cleaned and leaves and debris were separated and then the cleaned straw was chopped into 2-4 centimeter length pieces. The chopped straw was dried at ambient temperature and after reaching

equilibrium moisture, it was stored in plastic bags until used.

Pulping

Experimental conditions for Chemi-Mechanical Pulping (CMP) of wheat straw were set as follow:

Four levels of active alkali (10, 12, 14, and 16%, based on NaOH), one pulping times (40 minutes after reaching the pulping temperature) were studied. Pulping temperature and liquor to straw ratio were constant at 95°C and 8/1 respectively. For each combination of variables, three replica pulps were prepared.

All cooks were performed in a 4 liter rotating digester "Ghomes Wood and Paper Equipment Manufacturing Co." using 100 g of wheat straw chips (dry basis). At the end of each cook, the content of cylinder was discharged on 200 mesh screen and the cooked material was washed using hot water and the remaining liquor was separated by hand pressing the cooked material. Cooked material was defibrated using 25 cm laboratory single disc refiner, and then the pulp was screened using a set of two screens, 14-mesh screen on top of 200 mesh screens. Material remained on 14 mesh screen was considered as rejected (shives) and the fibers passed 14 mesh screen and remained on 200 mesh screen was considered as accepted pulp (screened yield).

Bleaching

The selected CMP pulp from pulping trails were used for bleaching experiments applying Totally Chlorine Free (TCF) bleaching sequence. First the pulp consistency and pH were adjusted at 3% and 5 respectively and then these samples were chelated by 0.3% DTPA for 30 minutes at 70°C in polyethylene bags. At the end of chelating period, the pulp was thoroughly washed with de-ionized water and dewatered manually. TCF bleaching of chelated pulps was performed using a combination of one of the three levels (2, 3 an 4.5% based on the dry weight of the pulp) NaOH and one of the three levels (3, 3.5 and 4%, based on the dry weight of the pulp) H_2O_2. Other chemicals including sodium silicate and $MgSo_4$ were constant at 3% and 0.5% respectively. The pulp consistency, bleaching time and temperature was constant at 3%, 120 minutes and 70°C respectively. Bleaching experiments were conducted in polyethylene bags and hot water bath and during the bleaching periods, the sample was hand kneaded. At the end of each bleaching trail, pulp was thoroughly washed with tap water and the pH of the bleached pulp was adjusted at 3 using diluted sulfuric acid. Finally the pulp was dewatered and hand sheets were prepared for further testing.

Following Tappi test methods were used for pulp analysis: Beating; T248 om-88: Freeness; T227 om-04: Hand sheet preparation; T205 sp-06: Brightness; T452 om-08: Opacity; T425 om-06: Tear strength; T414 om-04: Tensile strength and breaking length; T494 om-92: Burst strength; T403 om-02.

Results

Pulping

Soda pulping has been applied on wheat straw to produce pulps suitable for further chlorine (CEH) bleaching of the pulp for writing and printing paper production. This pulping process requires the application of high temperature in the range of 175°C and consequently, the equipments are under pressure. The pulping yield will be very low and therefore the raw

material efficiency is limited and only high capacity, capital intensive plants can be erected. Therefore, recently, alternative pulping of wheat straw has been investigated. The most recent available reports are on APMP of wheat straw (Pan and Leary 2002, Zhao et al 2004, Mustajoki et at 2010). In this study, we concentrated on the development of simple pulping to produce pulp on small scale suitable as supplementary pulp for fine paper production applying low temperature, but varying active alkali and pulping. To optimize the puling conditions for CMP pulping of wheat straw, in preliminary tests, we had to select different chemical charge and pulping times to reach appropriate pulping condition for suitable pulping yield. It was found that pulping time is not influential on the pulping yield, but the effect of active alkali charge was statistically significant $p<0.05$). Therefore, we measured the strength properties of pulps produced using different active alkali charge. The results of the measurements are summarized in Table 1.

Active Alkali (%)	Digester Yield (%)	Defibration Yield (%)	Initial Freeness (mL CSF)	Refined Freeness (mL CSF)	Apparent Density (kg/m^3)	Tensile Index (N.m/g)	Tear Index ($mN.m^2$ /g)	Brightness (% ISO)
10	72.2	58	790	365	440	56.6	6.51	29.2
12	67.2	56.2	755	367	430	58	6.86	28.4
14	67.2	55.5	772	384	437	60.1	7.11	29.3
16	64.6	58.3	708	343	489	56.2	6.97	30.8

Table 1- Chemi-Mechanical Pulping of Wheat straw (pulping time; 40 minutes, pulping temperature: 95°C and liquor to straw ration:8/1)

The results indicated that the impact of active alkali at 40 minutes pulping time on the strength of the pulps was not significant, but its effect on pulping yield was statistically significant. Therefore, based on the analysis of pulping results and considering the pulping yield and pulp strength (Table 1), pulp produced applying pulping temperature of 95°C, pulping time of 40 minutes and active alkali of 10% was selected for TCF bleaching. The total yield after chemical treatment and defibration of this pulp was measured as 72.2% and 58% respectively. However, the actual defibration yield at continuous pulping operation is usually a few percent higher due to process water circulation and consequent fine saving.

Pulp Bleaching

The results of TCF bleaching trails on wheat straw CMP pulp are summarized in Table 2. Applying 4% hydrogen peroxide and 3.5% sodium hydroxide increased the pulp brightness from the initial value of 29.2% ISO to the final value of 50.69% ISO. Even though TCF bleaching of the wheat straw CMP pulp reduced the yellowness of the pulp, but the existence of the yellow pigments in this pulp do not permit the production of very bright pulps. TCF bleaching of this pulp did not exert any detrimental impact on the strength of the paper.

H_2O_2 (%)	NaOH (%)	Brightness (%ISO)	Opacity (%ISO)	Yellowness (%ISO)	Tensile Index (Nm.g)	Tear Index ($mN.m^2/g$)	Burst Index ($kPa.m^2/g$)
3	2	45.24	46.37	76.13	43.6	9.5	2.23
3	2.5	43.17	49.43	77.04	40.2	8.93	2.69
3	3	47.79	45.68	75.92	39.1	9.04	2.73
4	2	41.78	50.69	77.48	37.5	9.54	2.84
4	2.5	45.58	47.16	76.47	44.7	10.24	2.64
4	3	47.02	46.24	76	43.3	9.55	2.72

4	3.5	50.69	42.85	76.76	33.3	9.97	2.72
5	3	48.69	42.65	76.66	31.1	9.74	3.01
5	3.5	46.19	46.67	77.27	37.4	10.5	2.57
5	4	46.44	46.22	76.5	41.5	9.97	2.49
5	4.5	46.37	46.36	77.13	30.8	9.47	3.23

Table 2- The results of TCF bleaching of wheat straw CMP pulp (Temperature; 70 °C: Time 120 minutes: consistency;3%: sodium silicate;3% and MgSo4:0.5%)

Discussion

The objective of this study was to develop pulping process suitable for small scale production of semi-bleached pulp suitable for low cost fine paper production. The pulps produced applying different dosages of sodium hydroxide ratios and 40 minutes pulping time at 95°C showed promising properties. These pulps were selected for strength evaluation. Pulps were refined to about 360 ml CSF and hand sheets were made. Changing the sodium hydroxide dosage did not significantly influence both tear and tensile indices of the pulps.

Our results are compared with similar research results reported in the literature (Pan and Leary 2002, Zhao et al 2004, Mustajoki et at 2010).The information demonstrated the suitability of wheat straw CMP pulp for fine grade papers as writing and printing papers for mass production.

Even though the pulping yield as CMP pulp is lower than usual CMP, but for material such as wheat straw and the strength of the pulps, it deserves to scarify the yield for better strength of final product.

Conclusion

World paper industry under pressure from environmentalist is searching for alternative raw material for future fiber supply and the situation in fiber deficient countries especially Middle East is so severe that these countries can not develop national paper industry. Therefore, different research groups have been looking at alternative fiber resources including wheat straw, sunflower stalks, as well as corn stalks as investigated.

CMP pulps from wheat straw applying 10% NaOH, 95°C pulping temperature and 40 minutes time provides a good compromise between the yield and strength. This pulp was TCF bleached using 4% H_2O_2 and 3.5% NaOH to the final brightness of 50.69% ISO.

Tensile index, burst index and tear index of this pulp (72.2% total digester yield) were measured as 33.3 N.m/g, 2.72kPa.m^2/g and 9.97mN.m^2/g. Based on the finding of this study, CMP pulping of wheat straw with application of only 10% NaOH as the pulping chemical will open new way for utilization of this unused material, to fulfill the pulp fiber shortage in fiber deficient countries.

Acknowledgements

Islamic Azad University, Karaj Branch provided financial support which we ought to appreciate. Iran Standard and Industrial Research Organization, Packaging Dept. is gratefully acknowledged for testing facilities.

References

Ali, S.H., Asghar, S.M., and Shabbir, A.U. 1991. Neutral sulfite pulping of wheat straw, In proceeding of the Tappi pulping conference. Tappi Press Atlanta,Ga. pp.51-56.

Ates, S., Atik, C., Ni, Y., Gumuskaya, S. 2008. Comparison of different chemical pulps from wheat straw and bleaching with xylanase pre-treated TCF method, Turkish J Agric For 32:561-570.

Hedjazi, S., Kordsachia, O., Patt, R., Jahan Latibari, A., Tschirner, U. 2008. Alkaline sulfite-anthraquinone (AS/AQ) pulping of wheat straw and totally chlorine free (TCF) bleaching of pulps, Ind. Crops Prod. 29:27-29.

Hedjazi, S., Kordsachia, O., Jahan Latibari, A., Tschirner, U. 2009. Alkaline sulfite/anthraquinone (AS/AQ) pulping of rice straw and TCF bleaching of pulps, Appita J. 62(3):137-145.

Khristova, P., Kordsachia, O., Khider, T. 2005. Alkaline pulping with additives of date palm rachis and leaves from Sudan, Bioresources Technol. 96:79-85.

Mckean, W.T., Jacobs, R.S. 1997. Wheat straw as a paper fiber source, Unpublished report. The Washington Clean Center. Seattle. WA. USA. 47p.

Mustajoki, S., Leponiemi, A., Dahl, O. 2010. Alkaline peroxide bleaching of hot water treated wheat straw. Bioresources 5(2):808-826.

Pan, G.X., Leary, G.L. 2002. Alkaline peroxide mechanical pulping of wheat straw, Part 1: Factors influencing the high brightness response in impregnation. Tappi J. Peer Reviewed 9 p.

Pande, H. 2009. Non-wood fiber and global fiber supply, Unisyva,No. 193, 9p.

Tappi standards and suggested methods, 2008. Tappi press. Atlanta,GA. USA.

Xu, E.C., Rao, N.N. 2001. APMP (Alkaline peroxide mechanical) pulps from nonwood fibers. Part 3: Bagasse. In proceeding of the Tappi 2001 pulping conference. 6p.

Wang, D.L.-K., Patt, R. 1989. Alkaline sulfite-anthraquinone pulping of bagasse, Holzforschung 43 (4):261-264.

Zhao, J., Li, X., Qu,Y., Gao, P. 2004. Alkaline peroxide mechanical pulping of wheat straw with enzyme treatment. Applied Biochemistry and Biotechnology 112:13-23.

Zhao, G., Lai, R., He, B., Greschik,T., Li,X. 2010. Replacement of softwood kraft pulp with ECF bleached bamboo kraft pulp in fine paper. Bioresources 5(3):1733-1744.

Shear strain distribution of bonding interface in ductile PF bonded 2-ply bamboo sheet by the method of electronic laser speckle interferometry

Cheng Yong[1] *Mingjie Guan*[2*]

[1]Wood Science and Technology College, Nanjing Forestry University, Nanjing, Jiangsu, China
yongcheng0520@hotmail.com
[2] Bamboo Engineering and Research Center, Nanjing Forestry University, Nanjing, Jiangsu, China
* *Corresponding author*
mingjieguan@hotmail.com

Abstract

The shear strain distribution across a 2–ply bamboo sheet bonded with ductile PF is measured by means of electronic laser speckle interferometry, along with tensile strength experiment to prove shear stain distribution on macroscopic scale. This research will effectively combine macroscopic mechanical property with microcosmic interfacial mechanical property. Study on shear strain distribution of bonding interface will contribute to understand bamboo bonding interface response mechanism under deformation conditions and solve problems of plybamboo deformation or bonding failure. Moreover, it is supposed that this study will be conducive to choosing bamboo-specific adhesives under different conditions.

Key words bamboo, electronic laser speckle interferometry, ductile PF, bonding interface

Introduction

Phenol-formaldehyde resin is commonly used in bamboo-based panels (Yiping Ren. 2008, Mingjie Guan et al. 2005, 2006, Fengwen Sun et al. 1999), for which it is one of the mainly used adhesives in wood-based panels industry. But, due to differences of structure and chemical composition between bamboo and wood, there may be diversities upon characters of bonding interface and the stress transfer mechanism between these two materials (Hongxia Ma. 2009). As previous studies shown, there are many researches on strain and stress of wood bonding interface (Ulrich Müller et al. 2006, Wolfgang Gind et al. 2004, Andreas Valla. 2011). The high spatial resolution of ESPI was sufficient to reveal differences in strain concentration occurring in lap-shear wood specimens bonded with PUR and PRF (Ulrich Müller et al 2005). Stiff latewood bonded with PUR was strained little compared to less stiff earlywood, and stress concentration is evenly compared to PRF with ESPI (Wolfgang Gindl et al 2009). The strain concentration caused by penetration of PUR and PRF into poplar cell cavities was also measured (Wolfgang Gindl 2005). However, studies on strain and stress of bamboo bonding interface are scarce.

In the present study, we tested the micro-scale strain distribution and strain concentration in the vicinity of bonding interface of 2-ply bamboo panels by means of ESPI (electronic speckle pattern interferometry), along with the bonding line shear strength of bamboo-based panels with phenol-formaldehyde resin modified by different content of PVA (polyving akohol). We compared the values glued with phenol-formaldehyde resin to modified phenol-formaldehyde resin on macro- and micro-scale. In addition, we analyzed the failure model of bonding interface of 2-ply bamboo.

Materials and methods

Shear testing

Shear specimens in accordance with DIN EN 302-1-2004 with a total length of 150mm, a width of 20mm and a thickness of 2×5mm, were manufactured from a 5mm thick planed, bleaching moso bamboo. Phenol-formaldehyde resin was manufactured experimentally and modified by different content of polyving akohol (5%, 10%, 20%). These adhesives were used to glue the specimens and then the specimens were all cured in a press 2MPa and at ambient temperature 140℃for 15minutes. After curing, specimens were maintained in a condition room at 65% RH and 20℃ for 1 week until constant weight was attained. Incisions were made by using a circular saw to detect the notches towards the glue line, allowing for a tested bond length of 10mm as suggestion by DIN EN 302-1-2004. Shear testing was done on universal testing machine applying the load at a speed of 2.5mm/min. We tested a sufficient number of specimens to get 10 valid numbers, permitting the bamboo failure to nearest 30%.

ESPI measurement

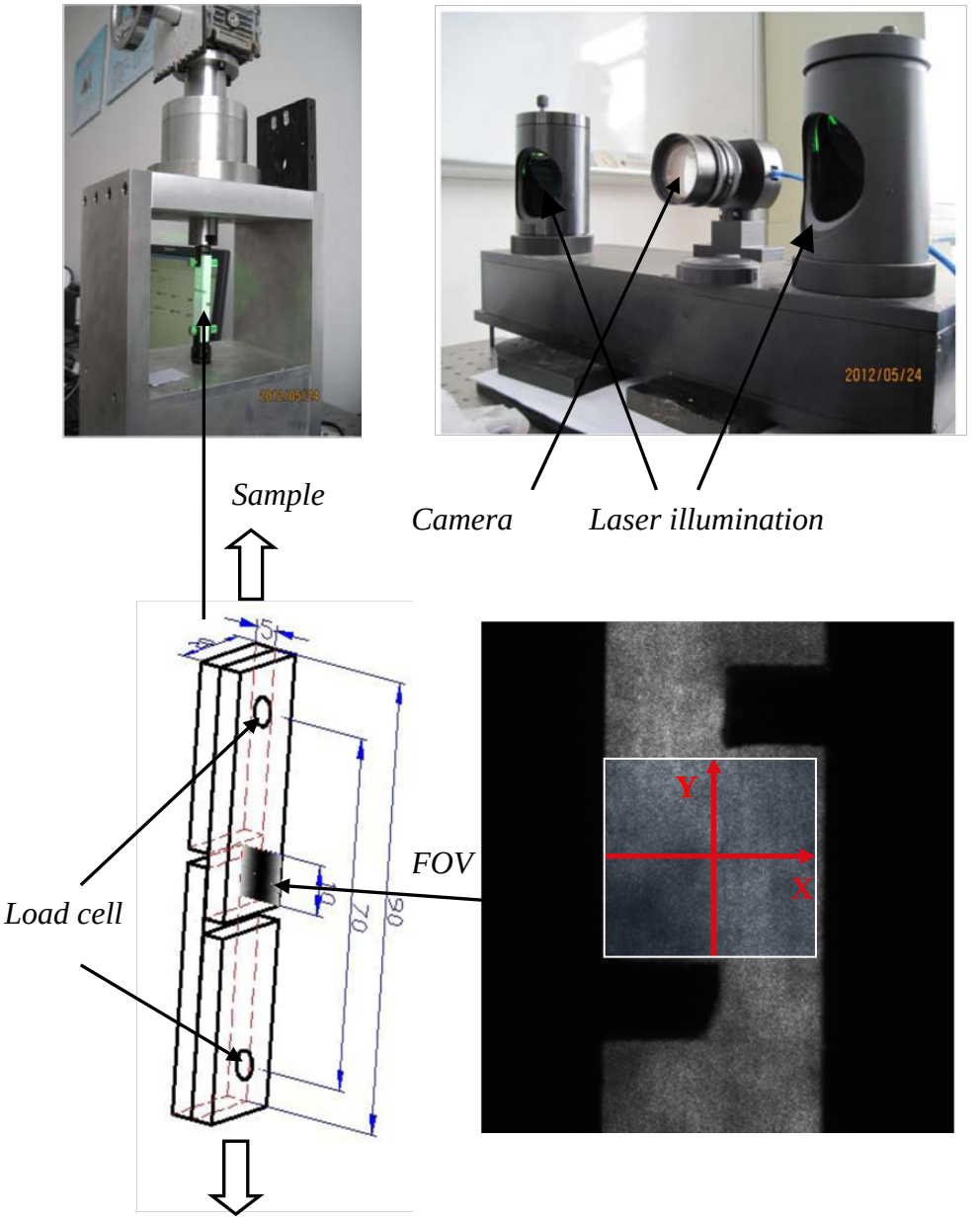

Fig.1 Tensile shear experiment on a lap-shear specimen. One-dimensional deformation of the sample surface was observed by means of electronic speckle pattern interferometry.

In order to monitor shear displacement on the surface of the two lap joint specimens, as depicted in Figure 1, shear testing corresponding to DIN EN 302-1-2004 was performed on a universal testing machine equipped with TS-S1-1XP ESPI system. The basic principle of ESPI technique was explained in detail in a previous paper (Ulrich Müller et al. 2006). With the optical set-up used here, the size of the field of view (FOV) observed with ESPI was 44×35mm^2, working distance between camera and specimen was about 300mm. Specimens were pre-loaded to 50N and then strained in 14 steps of 5N. We conducted the shear testing twice in two directions X and Y, for this kind of ESPI caught the deformation only from the X direction, so each deformation of 2-ply bamboo should be controlled in its elastic stage. At each displacement step, a interference fringe image of the observed field of view was taken. The displacement maps were computed by summing up information from all 14 displacement steps. Each adhesive with 5 specimens

were tested at least five times until all the specimens showed similar results and then we chose only one specimen for calculation.

Results and discussion

Shear strength

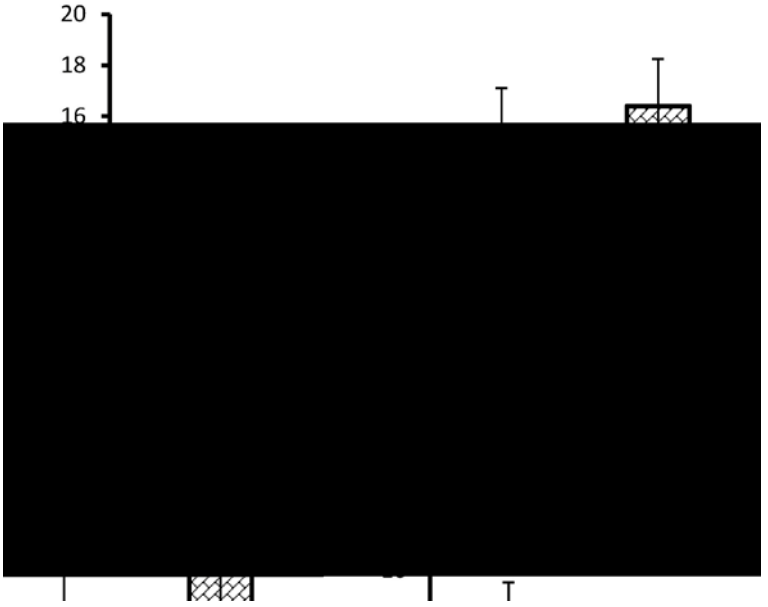

Fig. 2 Shear testing of phenol-formaldehyde resin with different content of PVA (polyving akohol). Sample A to sample D with content of PVA: 0%, 5%, 10%, 20% respectively. The red line equals to the minimum allowed shear strength according to DIN EN302-1-2004.

The shear strength glued with different content of PVA results in clear difference. As depicted in Figure 2, we can see that, with the percentage of PVA increasing, the shear strength start to descend at first, but rebound higher than before later. The maximum strength is 16.39MPa with the percentage of PVA 20%, while the minimum one is 11.95MPa with the percentage of PVA 5%.

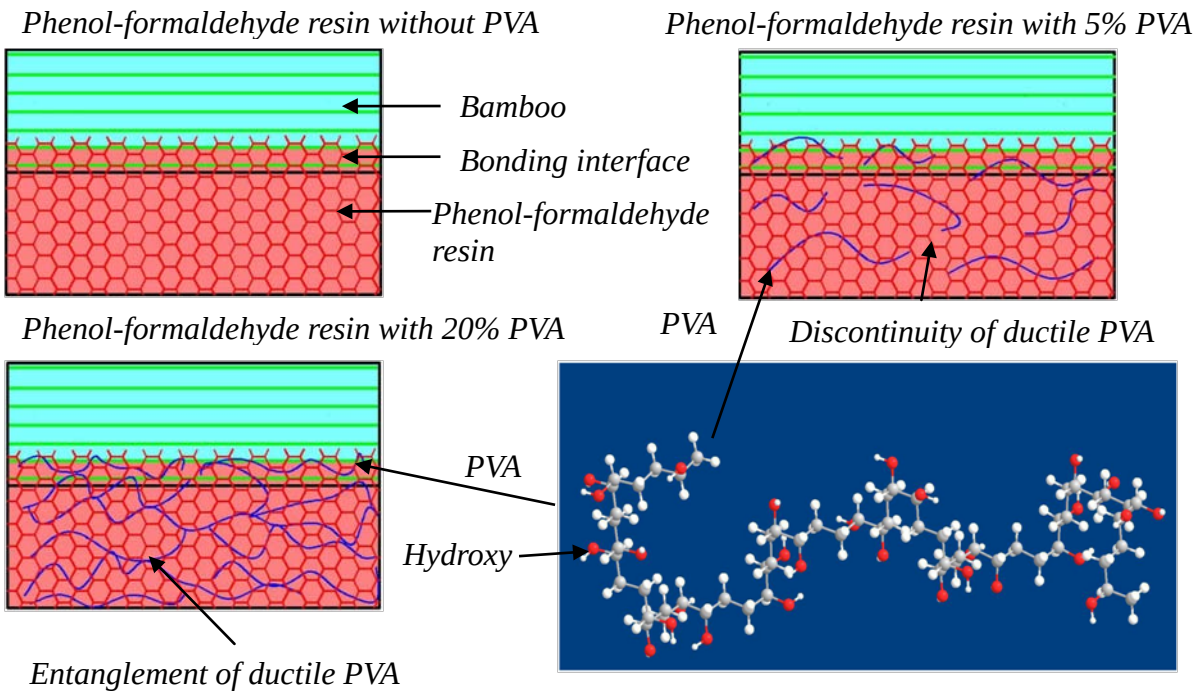

Fig.3 Models to illustrate phenol formaldehyde resin modified by different proportion of ductile PVA

For better understanding the diversity of shear strength, referring to Frihart's bonding model (Charles R. Frihart et al. 2005, Christopher G. Hunt et al. 2007, Robert G. Schimidt et al. 1997), we set up a model to illustrate the difference between bonding interface and substrate considering the influence of PVA and bamboo. As it is shown in Figure 3, phenol-formaldehyde resin, composed of oligomers and monomers, easily forms polymer chain and cross-links by hot-pressing which have a high content of aromatic or resonance-stabilized structure with limited flexibility (Robert G. Schimidt et al. 1997), and easily lead to stress concentration with rigid backbone which are incompatible with ductile bamboo. In the contrast, PVA whose branched hydroxy makes it prone to combine hydroxymethyl of phenol-formaldehyde resin, belongs to the pre-polymerized adhesive with a flexible backbone (Charles R. Frihart et al. 2005). Thereby, more energy resulting from strain concentration in the vicinity of gluing line will be absorbed by interfacial slipping, and then, inducing higher shear strength. As shown in Figure 2, Shear strength decreases with a small number of PVA for entanglement networks created by PVA are not abundant, which leads to strain concentration between two glues while interface slips without obvious overall effect. However, as the percentage of PVA increasing, enough entanglement of PVA will ensure strain transmission (R. Garcia and A. Pizzi. 1998). Interface slipping will remove strain concentration and eliminate interface energy leading to shear strength increase.

In addition, considering the shear deformation of one-direction bamboo, ductile PF may be more suitable for bamboo-based materials than the commonly used stiff PF, for ductile bamboo fibers usually bear more deformation, which is more incompatible with stiff PF.

Shear strain distribution

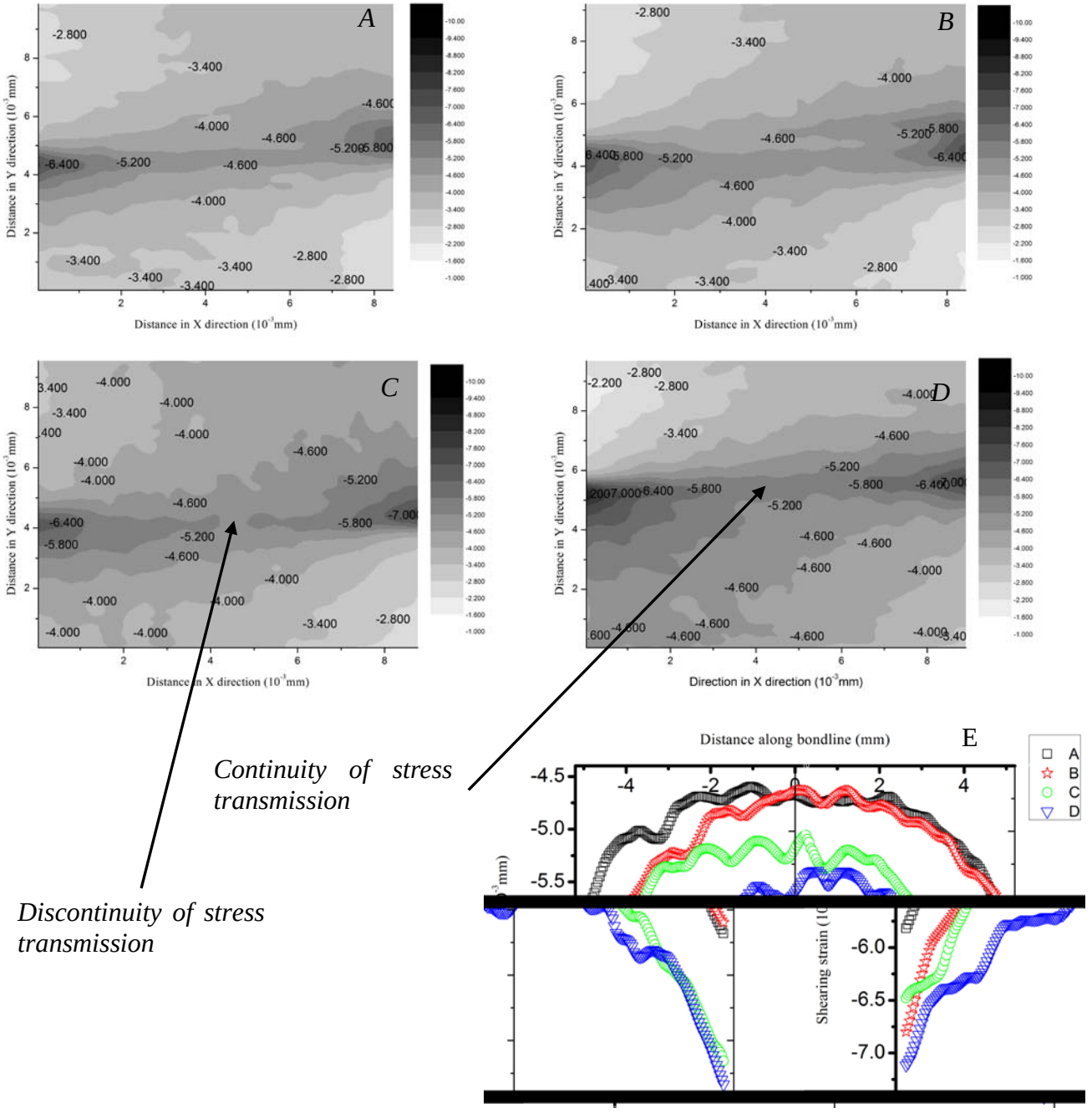

Fig. 4 (A-D) Strain distribution of specimens glued with phenol-formaldehyde resin in different content of PVA with observed fields of view. Sample A, B, C, D represent phenol-formaldehyde resin with PVA, 0%, 5%, 10%, 20% respectively. Scale bars indicate strains multiplied by 10^{-3}mm. (E) Values of strain with different samples (A, B, C, D) along the bond line.

Two-dimensional patterns of in-plane strain distribution across the FOV on tensile specimens glued with different adhesives are shown in Figure 4. In micro-scale strain distribution, ductile PF reflects more obvious than the normal stiff PF with higher strain concentration at both ends of the overlapping area and high gradient of strain along the bondline. Line plots of shear strains along the glue line are shown in Figure 4E, indicating

that the values and the range values of strain are higher with ductile PF. With the percentage of PVA increasing, continuity of stress transmission and isostrain area become larger, resulting in increasing values of shear strain.

In the region of bonding interface, strains from 4.6×10^{-3} to 6.4×10^{-3}mm are observed for PF samples compared with strains from 5.2×10^{-3}-7.2×10^{-3}mm for PF with 20% PVA samples. According to Frihart's models (Charles R. Frihart et al. 2005, Christopher G. Hunt et al. 2007, Robert G. Schimidt et al. 1997), pre-polymerized adhesives could offset the energy created from stress concentration by itself slipping, while being applied lateral load. So it is reasonable for PVA to drive all stiff PF slipping when being applied lateral load, for which its branched hydroxyl combines hydroxyl of hydroxymethyl from PF on hot-pressing. As shown in Figure 4C at the arrow, there are discontinuous breaks in strain distribution with little PVA. In accordance with models we have set before, inadequate entanglement network of each PVA leads to strain transmission failure, which results in bonding interface slipping. However, as the arrow depicted in Figure 4D, the breaks of strain transmission disappear with enough PVA entangling which leads to overall effect. As shown in Figure4E, the values of shear strain increase as a whole with the percentage of PVA increasing, which is another way to demonstrate that flexible bonding interface could improve strain transmission effects.

Conclusion

In terms of shear testing and strain distribution by ESPI along the bond line, it displays marked difference among shear strength and strain distribution glued with PF modified by different content of PVA. The results obtained here have shown that ductile PF could diminish stress distribution in adhesive assemblies and lead to bonding interface slipping, which could effectively reduce destructive energy in their overall strength. The amount of pre-polymerized adhesive-PVA could have a positive influence on the stress transmission and strain distribution in the vicinity of bonding interface, which may contribute to compatibility with ductile bamboo.

Acknowledgements

This research was sponsored by a project funded by the priority academic program development of Jiangsu higher education institutions (PAPD) and Natural Science Foundation of Jiangsu province, China (BK2011822).

References

Yiping Ren.2008. Study on properties and evaluation of adhesive used in bamboo-based structural materials. Doctor degree. Chinese Academy of Forestry. (In Chinese)

Mingjie Guan, Yixin Zhu, Xiaodong Zhang, Qisheng Zhang. 2005. Bending properties of wood-bamboo composite plywood in differently hygrothermal conditions. Journal of Nanjing Forestry University (Natural Science Edition), 29, 106-108. (In Chinese)

Mingjie Guan, Yixin Zhu, Xinan Zhang. 2006. Comparison of bending properties of scrimber and bamboo scrimber. Journal of Northeast Forestry University, 34, 7 and 21. (In Chinese)

Fengwen Sun, Hong Gao, Mingjie Guan, Yanwen Li, Qisheng Zhang. 1999. Several low-cost modified PF adhesives and their bonding properties. Forestry Products Industry, 26, 14-16. (In Chinese)

Hongxia Ma. 2009. Influence gluability and its affecting factors of bamboo/poplar composite. Doctor Degree. Chinese Academy of Forestry. (In Chinese)

Ulrich Müller, Aleksandra Sretenovic, Angela Vincenti and Wolfgang Gindl. 2005. Direct measurement of strain distribution along a wood bond line. Part 1: Shear strain concentration in a lap joint specimen by means of electronic speckle pattern interferometry. Holzforschung, 59, 300-306.

Wolfgang Gindl and Ulrich Müller.2006. Shear strain distribution in PRF and PUR bonded 3–ply wood sheets by means of electronic laser speckle interferometry. Wood Sci Technol, 40, 351-357.

Wolfgang Gindl, Aleksandra Sretenovic, Angela Vincenti and Ulrich Müller. 2005. Direct measurement of strain distribution along a wood bond line. Part 2: Effects of adhesive penetration on strain distribution. Holzforschung, 59,307-310.

Ulrich Müller, Aleksandra Sretenovic and Wolfgang Gindl. 2006. Mechanism of stress transfer in a single wood fibre-LDPE composite by means of electronic laser speckle interferometry. Composites Part A: applied science and manufacturing, 37, 1406-1412.

Wolfgang Gindla,c, Thomas Schōberlb, George Jeronimidisc. 2004. The interphase in phenol–formaldehyde and polymeric methylene diphenyl-di-isocyanate glue lines in wood International Journal of Adhesion & Adhesives, 24,279-286.

Andreas Valla, Johannes Konnerth, Daniel Keunecke, Peter Niemz, Ulrich Müller and Wolfgang Gindl. 2011. Comparison of two optical methods for contactless, full field and highly sensitive in-plane deformation measurements using the example of plywood. Wood Sci Technol, 45,755-765.

Charles R. Frihart. 2005. Adhesive Bonding and Performance Testing of Bonded Wood Products. ASTM Special Technical Publication, 2, 1-12.

Christopher G. Hunt, Rishawn Brandon, Rebecca E. Ibach, Charles R. Frihart. 2007. What does bonding to modified wood tell us about adhesion. IN: Bonding of modified wood: proceedings of the 5th COST E34 International Workshop, Bled, Slovenia, Sept. 6th, 2007. Ljubljana: Biotechnical Faculty, Dept. of Wood Science and Technology, 2007.

Robert G. Schimidt, Charles E. Frazier. 1997. Network characterization of phenol-formaldehyde thermosetting wood adhesive. International Journal of Adhesion & Adhesive, 18, 139-146.

Priya Viswanath and Eby T. Thachil. 2008. Properties of polyvinyl alcohol cement pastes. Materials and Structures, 41,123-130.

R. Garcia and A. Pizzi. 1998. Crosslinked and Entanglement Networks in Thermomechanical Analysis of Polycondensation Resins. Journal of Applied Polymer Science, 70, 1111-1119.

Agricultural Straw Reinforcing Polypropylene by Hot Pressing

Weihong Wang [1*] – *Senlin Yuan*[2] – *Hainggang Wang*[3]
[1] Professor, Key Lab of Bio-based Material Science & Technology of Ministry of Education, Northeast Forestry University, Harbin, CHINA
* *Corresponding author*
weihongwang2001@yahoo.com.,cn

[2] Science Assistant, Key Lab of Bio-based Material Science & Technology of Ministry of Education, Northeast Forestry University, Harbin, CHINA

[3] Engnieer, Key Lab of Bio-based Material Science & Technology of Ministry of Education, Northeast Forestry University, Harbin, CHINA

Abstract

The annual output of straw from agriculture is around 0.79 billion in China. There is 0.15 billion straw need to utilize except those being returned and fertilized. This is an abundant resource even in a global scale. In present research. Straw was used to reinforce thermoplastic.

Straw and thermoplasitc was converted into fiber form and preheating step was introduced before hot pressing. The size of the fibrous plastic and rice straw was discussed as variables. The optimal performance was obtained when high density polyethylene (HDPE) was in fiber form, the weight ratio of HDPE to rice straw fiber was 40:60, and the straw fiber was 16-40 mesh. When the straw/HDPE fiber mixture underwent preheating at 130℃~140℃, the composite significantly improved in physical and mechanical properties.

For PP fiber, Straw/PP fiber composite presented 1.77% of 2h thickness swelling, 0.77 MPa of internal bonding strength, 36.76MPa of flexural strength, and 2.92GPa of elastic modulus. In order to finish the composite, poplar veneer was overlaid on the surface by the aid of polypropylene accumulated on the surface. No other adhesive was used. The tested surface bonding strength of the composite was 1.22MPa and there was no peeling phenomenon presented after impregnating in water. The contact angle detecting proofed that hot pressing process almost did not influence the wettability of veneer compared to common plywood. The research provided a good way to use agriculture straw in composite production.

***Keywords*:** straw; fibrous polypropylene; veneer; composites; hot-pressing

Introduction

The annual output of straw from agriculture is around 0.79 billion in China. There is 0.15 billion straw need to utilize except those being returned and fertilized. This is an abundant resource even in a global scale. Wheat straw has long being tried to use in composite. One of these methods is to reinforce plastic.

Many bio-resources other than wood have been used in wood–plastic composites (WPC) such as rice hull (Madhoushi et. al. 2009, Wang et. al. 2009). However, when straw resources from agriculture are used in extrusion, thermo-degradation often occurred under the combination of high temperature and pressure. The hot-pressing method that is commonly used in the wood industry has rarely been used to produce wood–plastic composites (Chen et. al. 2006, Chaharmahali et. al.2008, Ashori and Nourbakhsh, 2009). In fact, in the hot-pressing process, much larger particles can be used than in extrusion and they can be oriented by spreading. Hot pressing also provides the possibility of producing large panels of composite like pure wood-based composites.

The object of this study is to use straw in WPC industry by hot pressing.

Materials and Methods

Simply mixing cellulosic particles with plastic pellets does not produce satisfactory properties. This is mainly due to insufficient melting of the plastic pellets in the duration of economic hot pressing and the non-uniform distribution of plastic pellets in the bio-fibers. In order to melt the plastic matrix sufficiently, the press platens must maintain at a high temperature and close for a long time. This will result in thermo-deterioration of the wood or other plant-fiber component.

Two additional steps have been inserted in the hot-pressing process. The first key step is to process the plastic pellets into fibers. This will ensure that the plastic matrix has a similar bulk density to the plant fibers and mixes more uniformly. The second additional step is to preheat the mat before hot pressing in order to shorten the hot-pressing duration and evaporate moisture in the plant fibers.

Materials. Wheat straw was collected from a farm in Northeast China. When used, the straw was cut and classified into two groups by screening: one was between 8 and 16 mesh, and the other between 16 and 40 mesh. Commercial high density polyethylene (HDPE) in pellet form was produced by China Petroleum Daqing Petrochemical Company. Some of HDPE pellets were milled into powder, and passed through a 40-mesh screen. Others were processed into fibers. Polypropylene (PP) film was combed into fibers before mix with straw particles.

Preparation of composites. Straw particles and HDPE or PP were uniformly blended in the ratio 60:40 w/w. The mixture was spread in a 16×16 cm square wooden mold. The mat formed after removing the mold was placed between two steel plates and pre-pressed under 0.5 MPa pressure at 140℃ in an oven. After 40-60 min, the mat was put into the

hot press and pressed for 10-12 min under 4 MPa pressure. The straw particles and molten HDPE or PP were removed from the hot press and put into a cold press. The composite was hardened under pressure. Based on the data obtained from a 16×16 cm composite board, a larger board 35×35×1cm in size was hot pressed to verify the results.

In order to finish the composite, poplar veneer was overlaid onto the surface by the aid of polypropylene accumulated on the surface. No other adhesive was used.

Property measurement. The composite board was sawn into 5 cm wide strips to determine its bending strength (BS) and modulus of elasticity (MOE). 5 × 5 cm samples were cut from an unbroken area of the bending samples. Some of these samples were soaked in water to measure the thickness swelling (TS). The remaining samples were used for testing the internal bonding strength (IB). To observe the melting state, the broken interfaces resulting from the IB test were monitored with a stereo microscope. For veneer overlaid straw/PP composite, the contact angle was measured.

Results And Discussions

Effects of preheating on the properties of straw/HDPE powder composite. Preheating the mat before hot pressing could significantly improve the properties of the composite as shown in **Table 1**. All items were improved by more than 30%. This was because, for the same hot-pressing duration, the mat without preheating treatment took longer time to heat up to the set temperature, so the HDPE matrix did not have sufficient time to melt and could not glue the straw particles well. On the other hand, if HDPE matrix got enough time to melt, bio-fibers on surface would take a risk to thermo-degradation. This reduces the reinforcement to plastic matrix. In present research, when the wheat straw/PE mat was preheated at a relative lower temperature, moisture contained in straw could be removed, which avoided forming cavities inside composite boards during hot pressing due to moisture evaporation. Thus, straw particles contacted with HDPE matrix tightly and improved the properties of composites.

Table 1 Effects of straw particle size and preheating treatment on the properties of straw/HDPE powder composite (16cm×16cm×0.9cm)

Treatment	Straw size (mesh)	Density (g/cm^3)	BS (MPa)	MOE (GPa)	2 h TS (%)	24 h TS (%)
Without preheating	16 – 8	0.68 (0.021)	5.66 (0.411)	0.82 (0.069)	30 (2.471)	35 (3.999)
Preheating	16 – 8	0.69 (0.022)	7.44 (0.569)	1.11 (0.073)	20 (1.756)	22 (3.008)
	40–16	0.62 (0.025)	9.05 (0.845)	1.26 (0.096)	14 (1.850)	16 (1.213)

Effects of straw particle size on the properties of straw/HDPE powder composite. A uniform distribution of HDPE powder in the straw particles is important in order to ensure that each particle has bonding points. Otherwise, the lapped particles cannot be

linked tightly together. Water will impregnate the board through these gaps and the straw will swell, which will eventually decrease the properties of the board. As Table 1 showed, the composites with 40–16 mesh particles presented better properties than those with 16–8 mesh particles. In particular the swelling of the former composite was significantly less than that of the latter. Presumably the larger straw particles cannot be easily enclosed by the molten PE matrix. The larger straw particles had a smaller bulk density; this made it more difficult to mix them uniformly with heavier PE powder. All these factors decrease the properties of composites made with large straw particles.

Effects of the form of PE on the properties of composites. The composite with HDPE fibers had better properties (**Table 2**) than the composite with HDPE powder (Table 1). When MAPE was used, the properties improved even more. Usually it is difficult to mix straw particles uniformly with HDPE due to their different bulk densities. The straw particles are much lighter than the same volume of HDPE pellets or powders. In the mixing process, the heavier HDPE powder tends to accumulate in the lower part of the mat, which results in no bonding medium existing between some straw particles.

Table 2 Properties of wheat straw/HDPE fiber composite (16cm×16cm×0.9cm)

HDPE type	Density (g/cm^3)	BS (MPa)	MOE (GPa)	2 h TS (%)	24 h TS (%)	IB (MPa)
HEPE fiber without coupling agent	0.55 (0.029)	11.36 (1.058)	1.12 (0.097)	10 (0.102)	15 (1.397)	0.24 (0.020)
HEPE fiber containing MAPE	0.59 (0.022)	17.61 (1.627)	1.23 (0.198)	9 (0.906)	10 (1.)	0.32 (0.017)

Table 3 Properties of wheat straw/HDPE fiber and straw/PP fiber composites (35 cm×35 cm×1 cm)

	MAPE (%)	Density (g/cm^3)	BS (MPa)	MOE (GPa)	IB (MPa)	2 h TS (%)	24 h TS (%)
Straw:HDPE 60:40	4	0.70 (0.017)	17.00 (1.197)	1.57 (0.152)	0.55 (0.028)		9.00 (0.899)
Straw:PP 60:40			36.76	2.92	0.77	1.77	

In this research, when HDPE pellets were processed into fibers, they had similar bulk density to the straw particles, so an even mixture was easy to produce. The long HDPE fibers could pass through several straw particles and provide more bonding points. Based on the data obtained from the composites of 16×16 cm size, larger composites 35×35 cm in size were pressed. Their properties are listed in Table 3, which indicated that preheating and HDPE in the form of fiber were feasible. Based on the data tested in

previous experiments (Table 1 and 2), samples absorbed more water in the first 2 hours than in later much longer duration.

Properties of veneer overlaid straw/PP fiber composite. The same process was used to press straw/PP fiber composite, which presented much higher mechanical properties and better water resistant (Table 3). In order to decorate the composite, wood veneers were overlaid on its surfaces. Before straw/PP fiber mat was preheated, veneer was laid under and on the surface. The mat and veneers were preheated and hot pressed together. Shear strength between veneer surface and straw/PP composite was 1.22MPa.

To investigate the water resistance of overlaid, the composite with veneers was impregnated in boiling water for 20h and then dried in oven at (63±3) ℃ for 3h. Then the separation at each corner of the composite was observed. The result showed that no separation occurred between veneer and straw/PP fiber composite.

Veneer under high temperature risks thermo-degradation and adversely affects the wet ability of the surface. Contact angle is considered a good way to evaluate surface wet ability. As shown in Fig. 1, veneer underwent hot pressing showed largest contact angle. This indicated that hot pressed surface veneers decreased in wet ability, which is bad for gluing. However, when the veneer was sanded, its contact angle significantly decreased within 30 secs due to the removing of surface oxidation. It is presumed that veneered straw/PP fiber composite could be glued or painted well after sanding treatment. It could be decorated as other traditional wood composites such as plywood or particleboard.

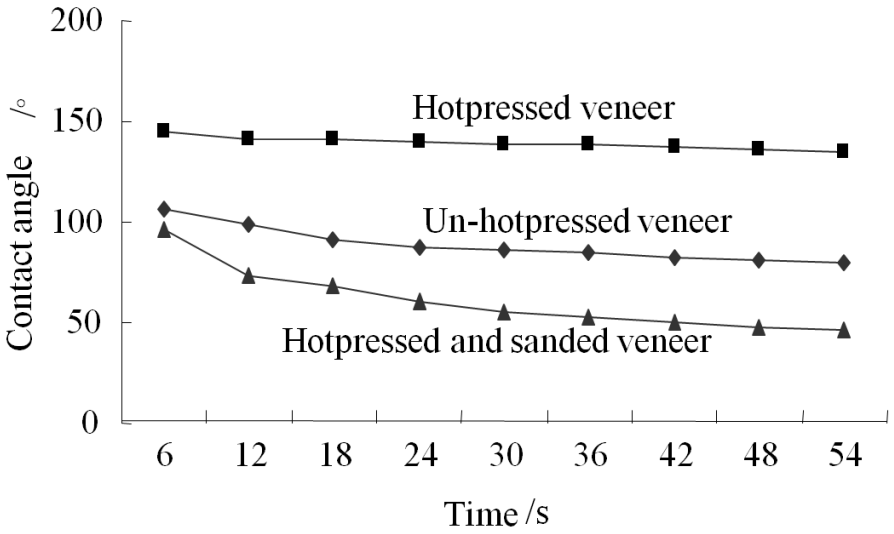

Figure 1 Contact angle of veneer surface

Conclusion

Preheating the mat before hot pressing can provide better properties in the same hot pressing duration. Polymer in fiber form mixes uniformly with straw particles and improves the properties of the composite more significantly than polyer in powder form. When MAPE is used, and the mat is preheated at 140℃ for 40 min and hot pressed at 175℃ for 12 min, the straw–PE fiber composite produced has 17 MPa MOR, 1.57 GPa MOE, 0.55 MPa internal bonding strength, and 9% 24 h thickness swelling.

For PP fiber, Straw/PP fiber composite presented 1.77% of 2h thickness swelling, 0.77 MPa of internal bonding strength, 36.76MPa of flexural strength, and 2.92GPa of elastic modulus.

Veneer could be overlaid directly on the surface of straw/PP fiber composite by the aid of PP accumulated on the surface. No other adhesive was used. Though underwent high temperature, wet ability of surface veneer was not affected after veneer was sanding.

Reference

Ashori A, Nourbakhsh A. 2009. Characteristics of wood–fiber plastic composites made of recycled materials. Waste Management. 29(4): 1291-1295

Chaharmahali M, Tajvidi M, Najafi SK. 2008.Mechanical properties of wood plastic composite panels made from waste fiberboard and particleboard. Polymer Composites. 29(6): 606 – 610

Chen H.C., Chen T.Y., Hsu C.H. 2006. Effects of wood particle size and mixing ratios of HDPE on the properties of the composites. Holz als Roh-und Werkstoff. 64: 172-177

Madhoushi M, Nadalizadeh H, Ansell MP. 2009. Withdrawal strength of fasteners in rice straw fibre-thermoplastic composites under dry and wet conditions. Polymer Testing. 28(3): 301–306.

Wang WH, Wang Qingwen, Dang WJ. 2009. Durability of a rice-hull-PE composite property change after exposed to UV weathering. Journal of Reinforced Plastics and Composites. 28(15):1813-1822

Proceedings of the 55th International Convention of Society of Wood Science and Technology
August 27-31, 2012 - Beijing, CHINA

Characterization of Juvenile Wood in Lodgepole Pine in the Intermountain West

Thomas M. Gorman [1*] *– David E. Kretschmann*[2]

[1] Professor, Department of Forest, Rangeland and Fire Sciences, University of Idaho, Moscow, ID, USA.
* *Corresponding author*
tgorman@uidaho.edu
[2] Research General Engineer, USDA Forest Service, Forest Products Laboratory, Madison, WI, USA.
dkretschmann@fs.fed.us

Abstract

Juvenile wood (core wood) is typically characterized as being less dimensionally stable and having lower mechanical properties than mature wood. Determination of the age of transition from juvenile wood to mature wood can provide basic information needed to assess dimensional stability and better utilize small-diameter trees growing in the intermountain west as solid-sawn products and as structural composites. While there is considerable information available on the variation of specific gravity with the age of the tree for western conifers, specific gravity is not useful for predicting dimensional stability, and as a single predictor of mechanical properties only explains about 50% of the observed variation. Determination of the age of transition between juvenile wood and mature wood, and some of the factors that could effect this transition, is important when making judgments about utilization options for naturally occurring stands of trees in the intermountain west region of the United States.

Lodgepole pine (*pinus contorta*) trees were harvested from four different sites in the US intermountain west to include site variations affecting growth, such as elevation, precipitation, and growing seasons. Bolts were extracted from each tree and processed to extract a single, radial-sawn board from each bolt. From each board, longitudinally-oriented samples were taken for every 5th growth ring, measuring approximately 5 x 5 mm in cross section with lengths ranging from 125 to 350 mm. Longitudinal shrinkage was measured in each sample as it dried from green to oven dry conditions. Later, the average microfibril angle was determined for the same samples.

A good correlation was found between longitudinal shrinkage and microfibril angle, suggesting that either method could be used to determine the juvenile wood transition in lodgepole pine. In addition, a significant difference in the juvenile wood transition period was found between sites. These results are useful for establishing parameters meaningful to the characterization of juvenile wood in the western conifers when utilized as solid-sawn products and structural composites.

***Keywords*:** A. Lodgepole pine, B. Juvenile wood, C. Mature wood, D. Longitudinal shrinkage, E. Microfibril angle.

Introduction

There are approximately 10.19 $\times 10^{12}$ m^3 (net) of softwood growing stock in the western United States, excluding Alaska and the Great Plains (Smith *et al*. 2009). Of the 52.6×10^6 ha of western timberland not reserved for timber harvest and meeting minimum productivity standards, it has been suggested that 11.7 $\times 10^6$ ha are high priority areas for fuel reduction treatments (Figure 1).

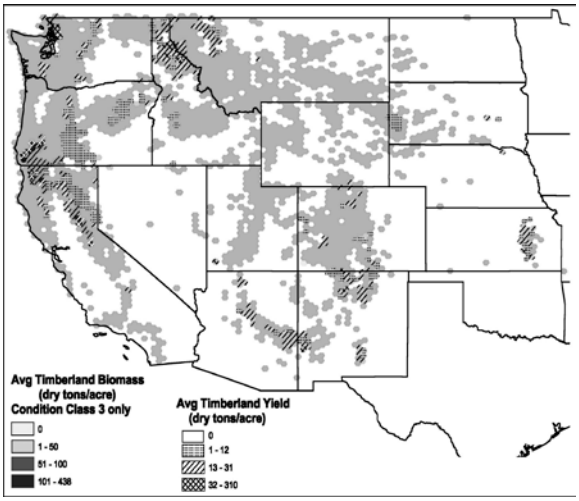

Figure 1. Potential high-priority fuel reduction thinning opportunities on timberland in western United States (Vissage and Miles, 2003)

Most trees in these high priority treatment areas are in diameter classes below 25 cm diameter at breast height (dbh), though the majority of the biomass falls in diameter classes above 25 cm dbh (Woodall 2003). Thinning at risk stands is often imperative to reduce fire risk, even for stands that are eventually to be subjected to controlled burns. Because the costs of fuel reduction treatments often exceeds the value of the material removed, finding higher value uses for the thinnings is a major focus of Forest Service Research (Forest Service 2003).

Historical and contemporary studies have identified the occurrence of juvenile wood to be a major impediment to more efficient utilization. Juvenile core material in a tree shrinks longitudinally much more than does mature material, which can affect the dimensional stability of wood-based products (Gorman 1985). While extensive literature is available on the occurrence of juvenile wood in many western species, especially Douglas-fir, much of the available information is based on variation in specific gravity with tree age (Figure 2). Koch (1994) notes that juvenile wood appears to be less pronounced in lodgepole pine than in most other western species. Determination of the age of transition between juvenile wood and mature wood, and some of the factors that

could effect this transition is important when making judgments about utilization options for naturally occurring stands of trees in the intermountain west.

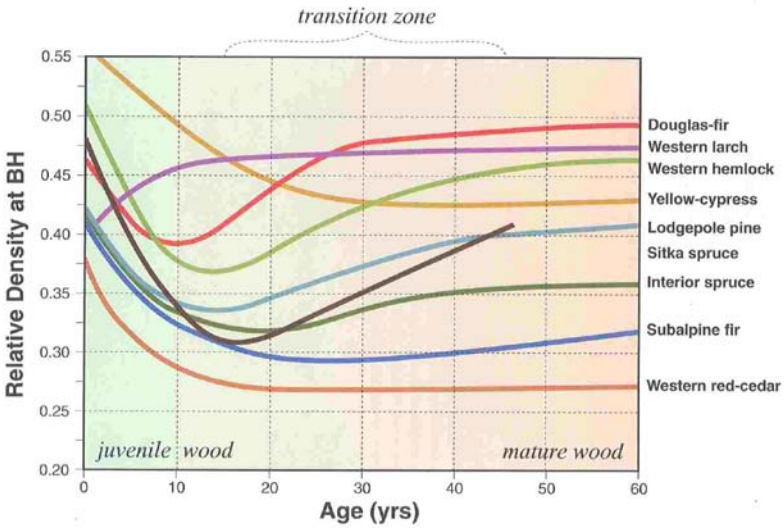

Figure 2. Juvenile wood in western species (Jozsa and Middleton 1994).

Clarke and Saucier (1989) concluded that the period of juvenility in slash and loblolly pine was influenced by environmental factors associated with geographic location. The variation with geographic location appeared to be related to climatic factors such as temperature (length of the growing season) and seasonal rainfall patterns. The study also showed that while planting density did not alter the length of the juvenile wood period, planting density did influence the size of the juvenile wood core, by controlling radial growth. Shuler *et al.* (1989) also note that microfibril angle in young-growth ponderosa pine did not vary significantly with either site index (from 55 to 100) or dbh (from 23 to 36 cm). It has generally been found that the largest variation in microfibril angle in softwoods occurs in the buttlog (Jozsa and Middleton 1994; Schuler, et al. 1989, Voorhies and Groman 1982).

Longitudinal shrinkage and microfibril angle are correlated, and can be used as indicators for demarcation of the juvenile wood-mature wood transition (Clark *et al.* 2006, Harris and Meylan 1965, Yin *et al.* 1994). The objective of this study was to measure longitudinal shrinkage and microfibril angle to estimate the juvenile wood-mature wood transition in lodgepole pine across a wide range of geographic locations in the western U.S. This was intended to provide a better understanding of the fundamental properties that influence utilization options for small-diameter trees harvested from western forests to improve forest health and reduce fire hazards.

Materials and Methods

Sampling was limited to lodgepole pine trees 13 to 33 cm in diameter growing in Idaho and Montana. We sampled and assessed lodgepole pine trees from 1) a relatively dry site with an intermediate growing season (Helena National Forest in Montana), 2) a relatively wet site with a short growing season (Panhandle National Forests in Idaho), and 3) a mid-range precipitation site with an intermediate growing season site (Payette National Forest

in Idaho), and 4) a site with mid-range precipitation and a long growing season (Kootenai National Forest in Montana) (Figure 3).

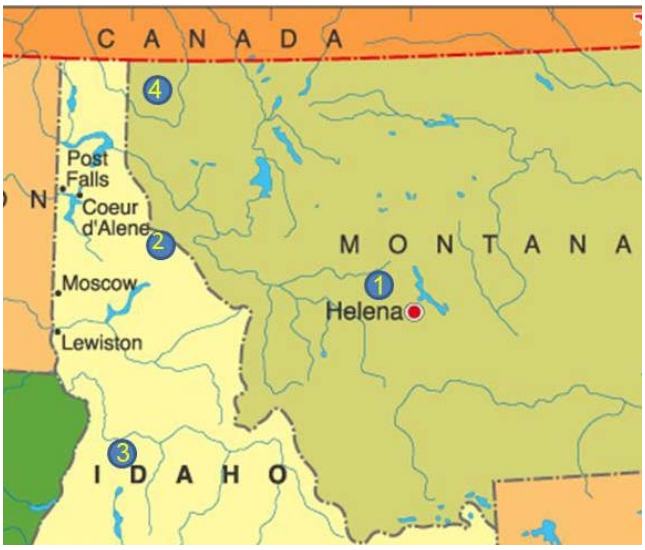

Figure 3. Four sites selected for sampling included 1) dry site, intermediate growing season, 2) wet site, short growing season, 3) mid-range precipitation, intermediate growing season, and 4) mid-range precipitation, long growing season.

Five to six trees were selected from each site. Information on site quality, trees age, and stocking density was recorded for each sampling location. The trees were selected based on straightness of bole and absence of defect. A 1.5 m bolt was cut from the butt-log of each tree and processed to extract a single, radial-sawn board from each bolt.

From each board, longitudinally-oriented samples were taken at the 3rd, 6th, 9th, 12th, 15th, 20th, 40th, and 60th annual growth rings from both sides of the pith, each measuring approximately 5 x 5 mm in cross section, with lengths ranging from 125 to 350 mm (Figure 4). Longitudinal shrinkage was measured in each sample as it dried from green to oven dry conditions. The average microfibril angle was then determined for the same samples using x-ray diffraction techniques (Verrill *et al.* 2001).

a

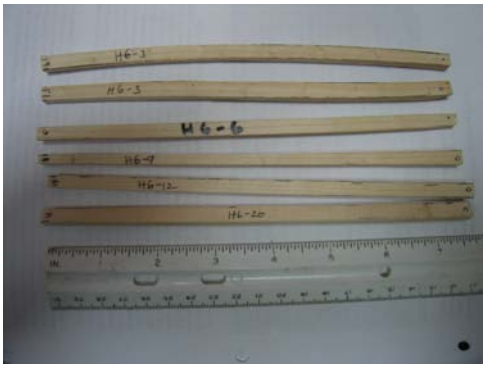

b

Figure 4. Sample preparation consisted of a) sawing a single, radially-oriented board from each bolt, then b) extracting samples to measure green to oven-dry shrinkage.

Results

The longitudinal shrinkage information clearly showed a distinction between the four geographic locations sampled (Figure 5). Both the duration and magnitude of longitudinal shrinkage varied by location, with the greatest shrinkage occurring in the samples collected from the Panhandle National Forests of Idaho. The least shrinkage occurred in the samples collected from the Helena and Kootenai National Forests in Montana, and these samples also exhibited the least overall longitudinal shrinkage.

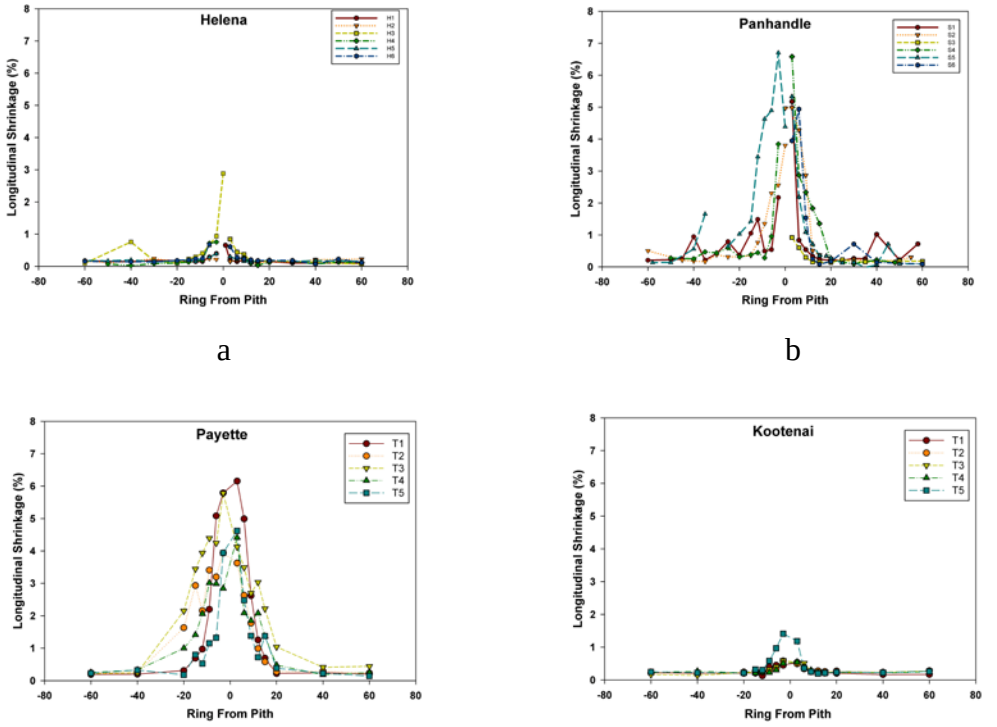

Figure 5—Longitudinal shrinkage values at various ring positions for the trees sampled from the a) Helena National Forest, b) Panhandle National Forests, c) Payette National Forest, and d) Kootenai National Forest sampling locations.

The microfibril angle measurements also showed a distinction between the four geographic locations sampled (Figure 6). Again, the duration and magnitude varied by location, with the greatest duration occurring in the samples collected from the Panhandle and Payette National Forests of Idaho. The least duration occurred in the samples collected from the Helena and Kootenai National Forests in Montana, suggesting that the juvenile wood period was shorter for these two locations than the two locations in Idaho.

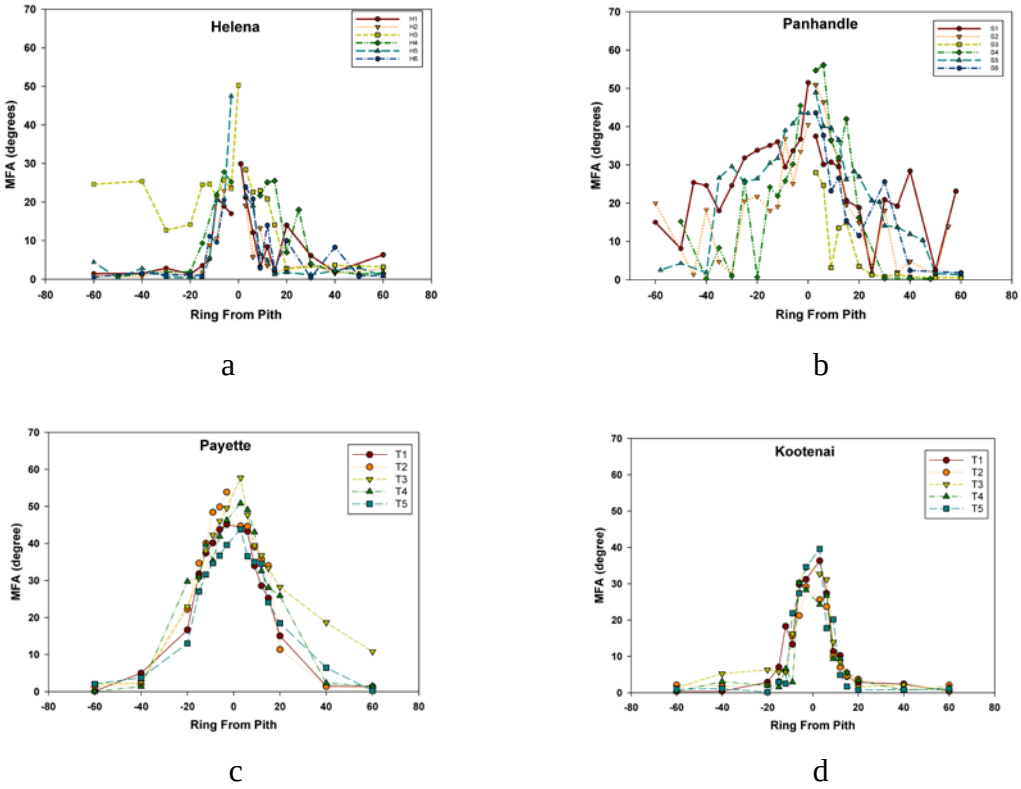

Figure 6—Microfibril angle values at various ring positions for the trees sampled from the a) Helena National Forest, b) Panhandle National Forests, c) Payette National Forest, and d) Kootenai National Forest sampling locations.

A good correlation was found between the lower values of longitudinal shrinkage and microfibril angle, as shown in Figure 7. The values for longitudinal shrinkage varied considerably for each site, especially when the microfibril angle increased beyond 20 degrees. Overall, it appears that either longitudinal shrinkage or microfibril angle could be used to estimate the juvenile wood period for trees located at each of the sites.

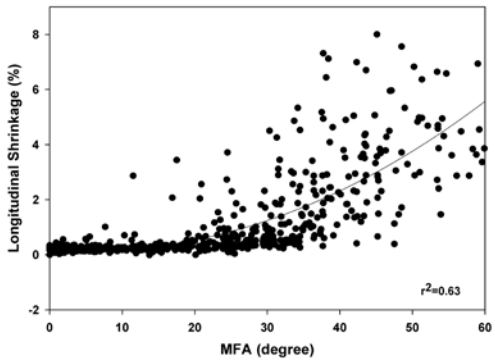

Figure 7. Quadratic regression fit between longitudinal shrinkage and microfibril angle for all measurements.

A segmented regression analysis was applied to each MFA and LS data set to obtain an indication of when the trees transitioned to mature wood. An example of such a regression fit is given in Figure 7. The results are given in Table 1.

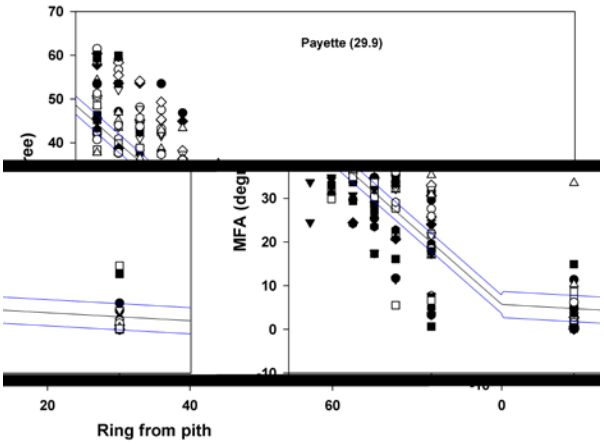

Figure 8. Segmented regression example.

Table 1: Summary of segmented regression prediction of juvenile wood transition

National Forest	Longitudinal shrinkage (years)	Microfibril angle (years)
Helena	8.7	14.0
Panhandle	13.9	30.1
Payette	20.8	29.9
Kootenai	10.0	13.3

Conclusions

A good correlation was found between longitudinal shrinkage and microfibril angle, confirming that either method could be used to determine the juvenile wood transition in lodgepole pine. In addition, significant differences in the juvenile wood transition period were found between the four sites. These results are useful for establishing parameters meaningful to the characterization of juvenile wood in the western conifers when utilized as solid-sawn products and structural composites.

References

Clark, A., III, and J.R. Saucier. 1989. Influence of initial planting density, geographic location, and species on juvenile wood formation in southern pine. Forest Products Journal. 39(7/8):42-48.

Clark, A., R.F. Daniels & L. Jordan. 2006. Juvenile/mature wood transition in loblolly pine as defined by annual ring specific gravity, proportion of latewood and microfibril angle. Wood Fibre Sci. 38: 292–299.

Forest Service. 2003. A strategic assessment of forest biomass and fuel reduction treatments in western states. USDA Forest Service, Washington, DC. 21 p. www.fs.fed.us/research

Gorman. T.M. 1985. Juvenile wood as a cause of seasonal arching in trusses. Forest Products Journal. 35(11/12):35-40.

Harris, J.M. and B.A. Meylan. 1965. The influence of microfibril angle on longitudinal and tangential shrinkage in Pinus radiata. Holzforschung. 19(5):144-153.

Jozsa, L.A. and G.R. Middleton, 1994. A discussion of wood quality attributes and their practical implications. Special Publication No. SP-34. Forintek Canada Corp., Vancouver, BC.

Koch, P. 1996. Lodgepole pine in North America, Forest Products Society, Madison, WI. 1096p.

Larson, P.R., D.E. Kretschmann, A. Clark III, and J.G. Isebrands. 2001. Formation and properties of juvenile wood in southern pines. General Technical Report FPL-GTR-129. USDA Forest Service, Forest Products Laboratory, Madison, WI. 42p.

Smith, W. B., Miles, P.D., Perry, C.H., Pugh, S.A., 2009. Forest Resources of the United States, 2007. Gen. Tech. Rep. WO-78. Washington, DC: U.S. Department of Agriculture, Forest Service, Washington Office. 336p.

Shuler, C.E., D.D. Markstrom and M.G. Ryan. 1989. Fibril angle in young-growth ponderosa pine as related to site index, D.B.H., and location in the tree. Research Note RM-492. USDA Forest Service, Rocky Mountain Forest and Range Experiment Station, Fort Collins, CO. 4p.

Verrill, S. P.; Kretschmann, D. E.; Herian, V. L. 2001. JMFA—A graphically interactive Java program that fits microfibril angle X-ray diffraction data. Res. Note FPL-RN-0283. Madison, WI: U. S. Department of Agriculture, Forest Service, Forest products Laboratory. 44p.

Vissage, J.S.; Miles, P.D. 2003. Fuel reduction treatment: A west-wide assessment of opportunities. Journal of Forestry. 101(2):5-6.

Voorhies, G. and W.A. Groman. 1982. Longitudinal shinkage and occurrence of various fibril angles in juvenile wood of young-growth ponderosa pine. Arizona Forestry Notes No. 16. University of Northern Arizona, Flagstaff, AZ. 18p.

Woodall, C.W., 2003. Coming soon: a national assessment of fuel loadings. J. Forest. 101 (2), 4–5.

Ying, L., D.E. Kretschmann, and B.A. Bendtsen. 1994. Longitudinal shrinkage in fast-grown loblolly pine plantation wood. Forest Prod. J. 44(1):58-62.

Proceedings of the 55th International Convention of Society of Wood Science and Technology
August 27-31, 2012 - Beijing, CHINA

RADIAL VARIATION OF MECHANICAL AND PHYSICAL PROPERTIES OF BLACK SPRUCE CELL WALL DETERMINED BY NANOINDENTATION AND SILVISCAN

Alain Cloutier[1*] *– Cecilia Bustos*[2] *– William Gacitúa*[2] *– Paulina Valenzuela*[3] *– Alexis Achim*[4]

[1] Professor and Director, Wood Research Centre, Université Laval – 2425 rue de la Terrasse, Québec, QC, Canada G1A 0A6
* *Corresponding author*
alain.cloutier@sbf.ulaval.ca
[2]Associate Professor, Centro de Biomateriales y Nanotecnología, Universidad del Bío-Bío, Departamento de Ingeniería en Maderas – Avenida Collao 1202, Concepción, Chile
[3]Research Associate, Centro de Biomateriales y Nanotecnología, Universidad del Bío-Bío, Departamento de Ingeniería en Maderas – Avenida Collao 1202, Concepción, Chile.
[4] Associate Professor, Wood Research Centre, Université Laval – 2425 rue de la Terrasse, Québec, QC, Canada G1A 0A6

Abstract

The mechanical and physical properties of the cell wall can be related to wood properties at the macro scale level. Several techniques became available over the last few years to determine cell wall properties including nanoindentation and the Silviscan technology. The objectives of this study were to determine the modulus of elasticity and hardness of black spruce cell wall secondary layer from pith to bark and determine their relationship with wood density and microfibril angle. Seven black spruce trees were harvested in the Quebec North Shore area, about 500 km northeast of Quebec City. A 50 mm-thick disk was cut from each tree at 2.5 m from the stump. A 50 mm-wide stick with pith included was cut from each disk. Matched samples were cut from this stick for the measurement of density and microfibril angle from pith to bark by the Silviscan technology and modulus of elasticity and hardness of the cell wall secondary layer by nanoindentation. The results showed that latewood cell wall modulus of elasticity had the tendency to increase from the pith to a cambial age of about 20 years in the juvenile wood zone. It stabilized or varied slightly from 20 years and over. Latewood cell wall hardness did not vary significantly from pith to bark. Microfibril angle decreased from the pith to a cambial age of about 20 years and remained fairly constant at higher cambial age. Finally, microfibril angle and cell wall modulus of elasticity vary inversely from pith to bark and appeared to be correlated.

***Keywords*:** Black spruce, cell wall, modulus of elasticity, hardness, microfibril angle.

Introduction

The mechanical and physical properties of the cell wall can be related to wood properties at the macro scale. Several techniques became available over the last few years to determine cell wall properties including nanoindentation and the Silviscan technology. The nanoindentation technique determines the mechanical properties of a material at the submicron and nanoscale level. This method involves the penetration of a tip (indenter), while the penetration depth and load are recorded. The stiffness and hardness of the indented zone can then be calculated (Gindl and Schöberl 2004; Gacitúa et al. 2007; Xing et al. 2009; Bustos Avila et al. 2011; Valenzuela Carrasco 2011; Yin et al. 2011). The Silviscan technology is based on X-ray absorption and diffraction to determine wood density and microfibril angle. It has become a reference in wood characterization but it does not provide a direct measurement of the cell wall mechanical properties.

The objectives of this study were to determine the modulus of elasticity and hardness of black spruce (*Picea mariana*) latewood cell wall secondary layer by nanoindentation from pith to bark and determine their relationship with wood density and microfibril angle determined by the Silviscan technology.

Materials and Methods

Materials. Seven black spruce trees from naturally regenerated stands were felled in the Province of Quebec North Shore area, 500 km northeast of Quebec City, Québec, Canada. A 50 mm thick (L) disk was cut from each tree at 2.5 m height. A 35 mm wide stick with pith included was cut from each disk. This stick was ripped into two samples: a 15 mm (L) thick sample was used for Silviscan analysis and a matched 35 mm thick (L) sample was used for nanoindentation measurements (Fig. 1a).

Nanoindentation on solid wood. A Hysitron Triboindenter® equipped with a three sided pyramid Cube corner diamond indenter tip located at the Nanotechnology Laboratory of the Universidad del Bío-Bío, Concepción, Chile was used to determine the mechanical properties of the tracheid cell walls. From each stick, one specimen of size 3 mm x 3 mm (R x T) was sampled at the latewood-earlywood interface of growth rings 5, 10, 20, 35 and 50 years (Fig. 1b). The five specimens obtained were embedded with Spurr epoxy resin and used for nanoindentation. Axial indentations were performed in earlywood and latewood tracheids across the transverse surface of the secondary (S2) cell wall. A loading function was applied to load a peak force of 100 μN for 60 s with loading and unloading performed at 20 μN/s. In a given indentation experiment, the peak load (P_{max}), the penetration depth at peak load (h) and the initial slope of the unloading curve (S=dP/dh) were obtained. From the indenter geometry and h, the contact area (A) was calculated. The load-displacement data from the nanoindentation test were used to calculate hardness (H) and elastic modulus (E_s) of the cell wall at the indentation location.

a)

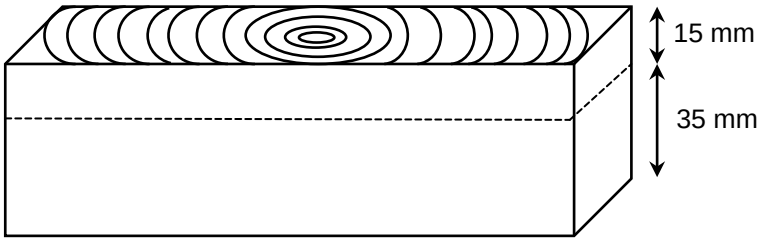

b)

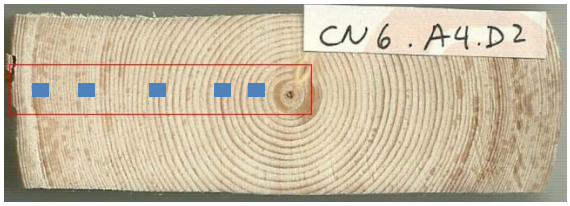

Figure 1. a) Matched samples used for Silviscan analysis (top) and for nanoindentation (bottom); b) typical sample and location of nanoindentation specimens.

The hardness (H) of the samples for an indentation depth (h) can be calculated from the following equation:

$$H = \frac{P_{max}}{A} \quad (1)$$

The combined modulus of the system, or reduced indentation modulus (E_r) was determined from the following expression:

$$E_r = \frac{1}{2}\frac{dP}{dh}\frac{\sqrt{\pi}}{A} \quad (2)$$

where dP/dh is the slope of the tangent to the initial unloading curve in the load–displacement plot. The sample modulus (E_s) can then be calculated as follows

$$E_s = (1 - \upsilon_s^2)\left(\frac{1}{E_r} - \frac{1-\upsilon_i^2}{E_i}\right)^{-1} \quad (3)$$

where the sub-indexes “s” and “i” represent the sample (cell wall, S2 layer) and indenter respectively and ν is the Poisson’s ratio. The indenter modulus E_i is constant and equal to 1240 GPa, with a Poisson’s ratio of 0.07. A Poisson’s ratio of 0.30 was assumed for black spruce cell wall.

Silviscan measurements on solid wood. A matched stick for each of the seven disks sampled (Fig. 1a) was sent to FPInnovations, Vancouver, Canada for Silviscan analysis. The samples were scanned with X-ray from pith to bark. X-ray absorption was used to determine wood density and X-ray diffraction was used to determine microfibril angle (MFA) from pith to bark.

Results and Discussion

Typical nanoindentations performed in the S2 layer of latewood tracheids are shown in Figure 2.

Cell wall modulus of elasticity and hardness. The latewood cell wall modulus of elasticity and hardness from pith to bark of the seven disks studied are shown in Figure 3. Overall, E_s had the tendency to increase from the pith to about 20 years of cambial age. It stabilized or varied slightly from 20 years and over. Hardness did not vary significantly from pith to bark. It remained fairly constant.

Microfibril angle and density. The MFA and average growth ring density from pith to bark determined by Silviscan are shown in Figure 4. Microfibril angle decreased from the pith to about 20 years of cambial age. It remained stable at higher cambial age. Growth rings average density was high close to the pith and decreased quickly until 20 years of cambial age was reached. It increased slightly or remained constant at higher cambial ages. Sudden increases and decreases can be noticed in some MFA plots. These variations of MFA often correspond to variations in growth ring density. This is most likely due to the occurrence of compression wood which is frequent in black spruce.

Correlation between microfibril angle and cell wall modulus of elasticity. The MFA determined by Silviscan and latewood cell wall E_s determined by nanoindentation are plotted against cambial age in Figure 5. Latewood cell wall E_s has the tendency to increase from the pith to about 20 years of cambial age. It seems to remain stable or increase slightly at higher cambial ages. Therefore, even if the average growth ring density is higher close to the pith (Fig. 4), the corresponding tracheid cell walls have a lower E_s. Microfibril angle and E_s vary inversely and a fairly high correlation appears to be present. Statistical analysis is currently performed on the results to quantify the tendencies described in this paper.

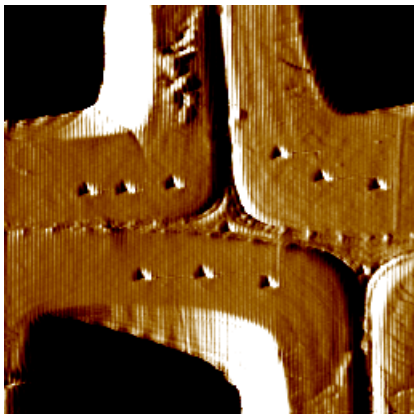

Figure 2. Typical nanoindentations performed in the S2 layer.

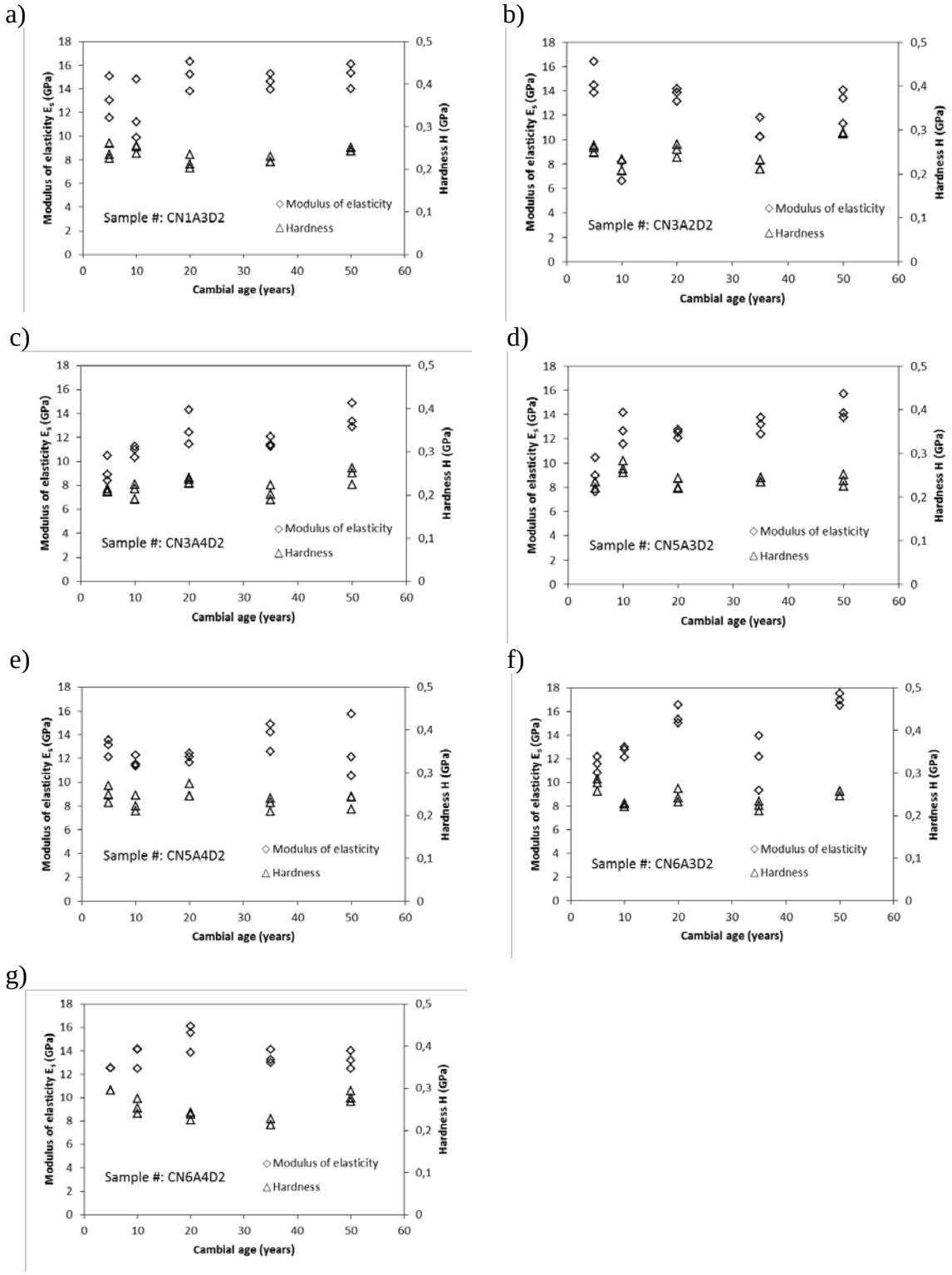

Figure 3. Latewood cell wall modulus of elasticity (E_s) and hardness (H) against cambial age obtained by nanoindentation for the seven samples studied. Each data point is the average of three indentations in a given tracheid S2 layer.

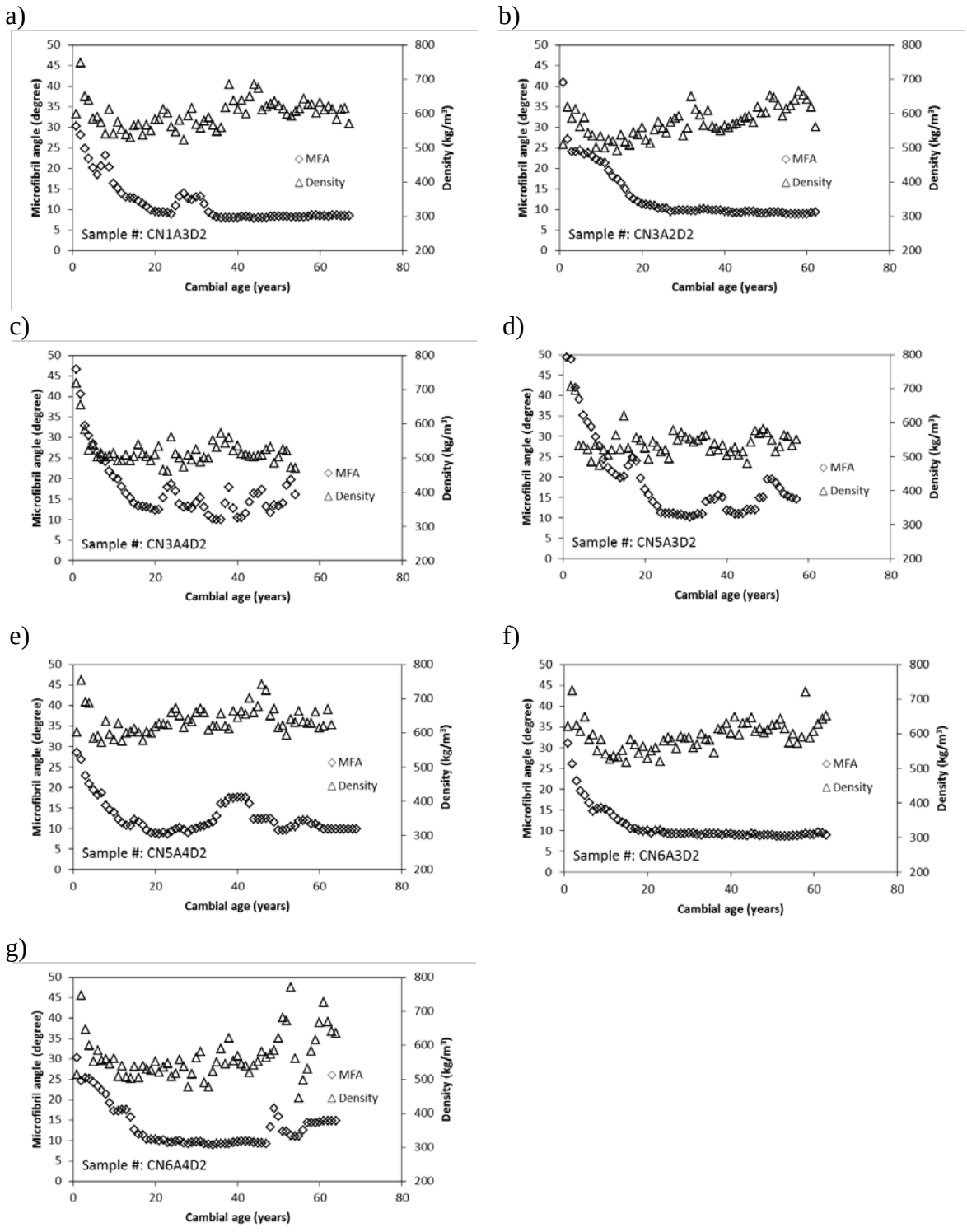

Figure 4. Microfibril angle (MFA) and average growth ring density determined by Silviscan against cambial age for the seven samples studied.

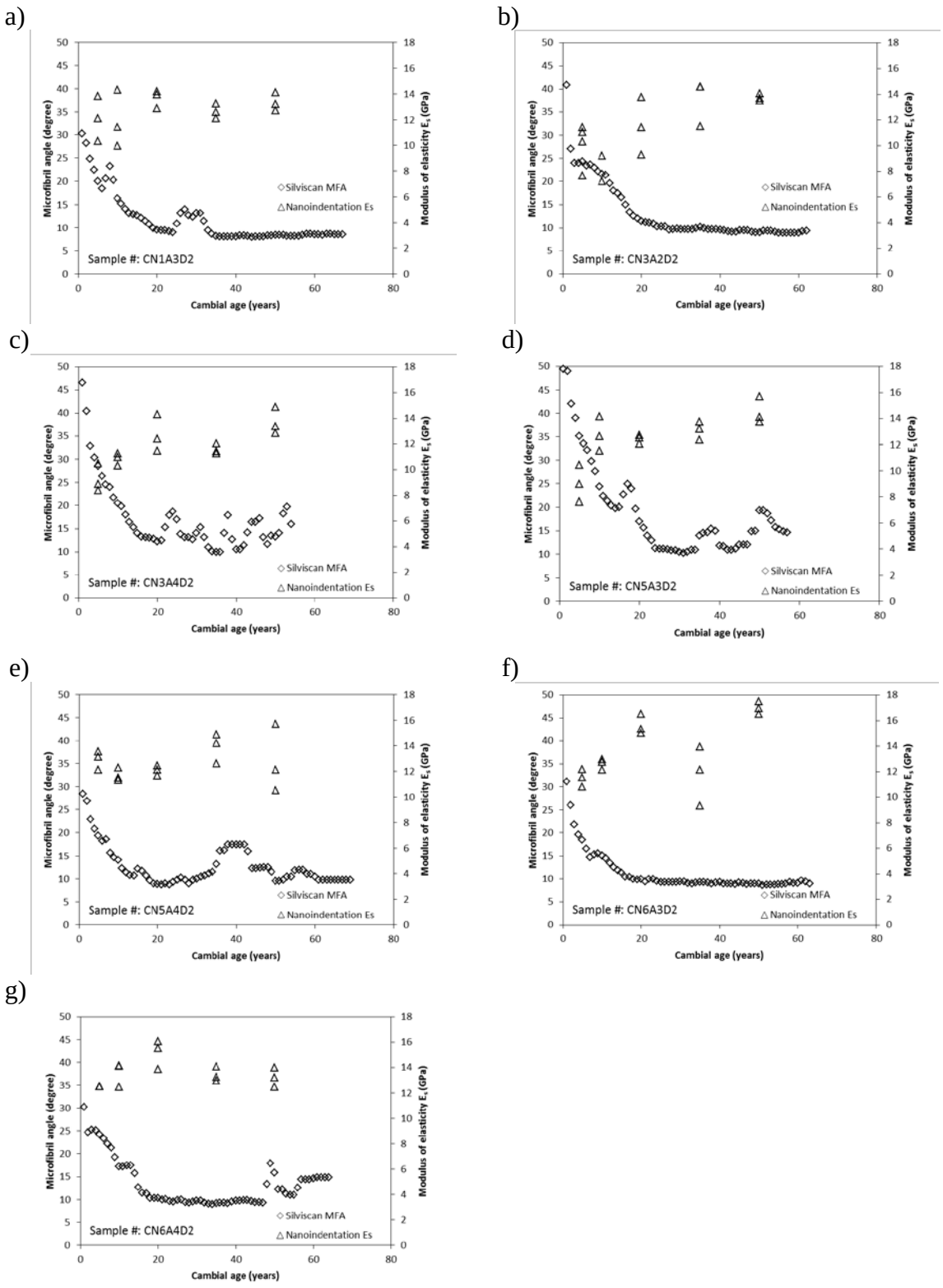

Figure 5. Microfibril angle (MFA) determined by Silviscan and latewood cell wall modulus of elasticity (E_s) determined by nanoindentation against cambial age for the seven samples studied.

Conclusions

The following conclusions can be made from this study:

1. Latewood cell wall modulus of elasticity had the tendency to increase from the pith to a cambial age of about 20 years in the juvenile wood zone. It stabilized or varied slightly from 20 years and over in the mature wood zone;
2. Latewood cell wall hardness did not vary significantly from pith to bark;
3. Microfibril angle decreased from the pith to a cambial age of about 20 years. It remained fairly constant at higher cambial age;
4. Microfibril angle and cell wall modulus of elasticity varied inversely from pith to bark and appeared to be correlated.

Statistical analysis of the data presented in this paper is needed to quantify the tendencies described in this paper. It is currently in process.

Acknowledgements

This work was funded by the Natural Sciences and Engineering Research Council of Canada – Strategic Networks Program, ForValueNet NSERC Strategic Network. The authors would like to thank Dr Maurice Defo from FPInnovations, Vancouver for assistance in the Silviscan analysis of the samples.

References

Bustos Avila, C.; Gacitúa Escobar, W.; Cloutier, A.; Fang, C.H.; Valenzuela Carrasco, P. 2011. Densification of wood veneers combined with oil-heat treatment. Part III: Cell wall mechanical properties determined by nanoindentation. BioResources 7(2): 1525-1532.

Gacitúa, W., Ballerini A., Lasserre, J.P., and Bahr, D. 2007. Nanoindentations and ultrastructure in Eucalyptus nitens with micro and mesocracks. Maderas Cienc. Tecnol. 9(3): 259-270.

Gindl, W.; Schöberl, T. 2004. The significance of the elastic modulus of wood cell walls obtained from nanoindentation measurements. Composites Part A 35: 1345- 1349.

Valenzuela Carrasco, P. N. 2011. Fracturas, propiedades nanomecánicas y anatomía de familias de *Eucalyptus nitens*. Master thesis. Departamento de Ingeniería en Maderas, Universidad del Bío-Bío. Concepción, Chile. 85 p. In Spanish.

Xing, C.; Wang, S.; Pharr, G.M. 2009. Nanoindentation of juvenile and mature loblolly pine (*Pinus taeda* L.) wood fibers as affected by thermomechanical refining pressure. Wood Sci. Technol. 43: 615-625.

Yin, Y.; Berglund, L.; Salmén, L. 2011. Effect of steam treatment on the properties of wood cell walls. Biomacromolecules 12: 194-202.

Fundamental Properties of Masson Pine (*Pinus massoniana* Lamb.) Wood from Plantation

Shuqin Zhang[1] *- Benhua Fei*[2*] *- Yan Yu*[3] *- Hankun Wang*[4]

[1] PhD Student, Chinese Academy of Forestry, Beijing, China.

13810133123@163.com

[2] Researcher, ICBR, Beijing, China

[*] *Corresponding author*

feibenhua@icbr.ac.cn

[3] Associate Researcher, ICBR, Beijing, China

[4] PhD Student, ICBR, Beijing, China

Abstract

Pine is one of the world's three largest fast-growing wood species, among which Masson pine (*Pinus massoniana* Lamb.) is native to a wide area of central and southern China and is a common trees in plantation forestry for replacing or compensating of the loss of the natural forest in southern China. To efficiently utilize the Masson pine plantation wood, it is important to understand its wood properties. In this report, experiments were carried out on the same thin clear wood specimen to determine its basic density, microfibril angle (MFA) and tensile modulus of elasticity parallel to grain (E_L). 1020 Specimens, 1.5 (R)×10 (T)×80 (L) mm, were cut from 19 disks at breast height of Mssson pine plantation trees grown in Huangshan public welfare forest field, Anhui province. MFA was measured by X-ray diffraction. Results indicate that MFA ranges from 9.8° to 45.6° and is large in the juvenile wood and small in the mature wood. There is much less variation and smaller MFA in the mature wood than in the juvenile wood. The average basic density and E_L at about 14% moisture content are 0.428 g/cm^3 and 11.2 GPa， respectively. Coefficient of variation (COV) for basic density and E_L averaged 21% and 48%. It is concluded that MFA, combined with basic density, has a strong relationship to E_L. Nevertheless variations of both MFA and basic density are generally insufficient to explain variations in E_L of wood because variations in the composition of wood can contribute strongly to variations in E_L.

Keywords: Masson pine, Basic density, Microfibril angle, Tensile modulus of elasticity parallel to grain

Introduction

Masson pine (*Pinus massoniana* Lamb.) is a species of pine, native to a wide area of central and southern China, and is considered the most important commercial species for fiber and solid wood products. The species is also a common tree in fast-growing plantation forestry in southern China. According to 7th national forest resources inventory results, the area of Masson pine plantation was 3.36 million hm^2 and its accumulation was 157.93 million m^3 in China. To better and efficiently utilize the Masson pine wood from plantation, it is essential to study the basic wood properties important to manufacturing processes and uses, including density ρ, microfibril angle (MFA), modulus of elasticity (MOE), and so on.

The density of a substance is defined as the ratio of its mass to its volume. For wood, both mass and volume depend on moisture content (MC), so its density is related to MC and is not constant. To make comparisons between species, a standard reference is the combination of oven-dry mass and green volume, referred to as basic density. Bunn (1981) stated "Basic density is probably the single most important intrinsic wood property for most wood products, particularly if we are contemplating adopting short rotations." After Bunn, Bamber & Burley (1983) pointed out "Of all the wood properties density is the most significant in determining end use. It has considerable influence on strength, machinability, conversion, acoustic properties, wearability, paper yield and properties and probably many others." Therefore density can be used as a general measure of wood quality.

MFA refers to the mean helical angle between the cellulose fibrils and the longitudinal cell axis. MFA is perhaps the easiest ultrastructural variable to be measured by X-ray diffraction (XRD) for wood cell walls. MFA is known to have significant influences on longitudinal shrinkage (Harris & Meylan 1965, Meylan 1972) and stiffness (Cave & Walker 1994). Donaldson (2008) comprehensively reviewed MFA's measurement methods, variability and relations to wood properties. So MFA has become an important indicator of wood quality to the forest products industry.

The mechanical properties of wood are usually the most essential characteristics for its application. MOE, especially along the longitudinal axis of wood E_L, is the most representative parameter to describe the wood mechanical property. E_L is usually determined from bending rather than from longitudinal tensile test. E_L values obtained from bending test include an effect of shear deflection, which results in lower E_L values (FPL 2010). This study addressed E_L determined by tensile test parallel to grain of wood.

Materials and Methods

19 Masson pine (*Pinus massoniana* Lamb.) trees were selected and felled from the Huangshan plantation stand aged 40 years in Anhui province. The 19 trees were all straight in form and had an average diameter at breast height (DBH) of 31.2 cm. The details of these sample trees were presented in table 1. A disk approximately 20 cm thick was removed at breast height from each tree. After air-seasoning, these discs were processed to be central

strips (1 cm×8 cm in T×L directions) from north through the pith to south. Then 1.5-mm-thick tangential slices were cut along the growth rings. The nominal dimensions of the thin clear specimen is 1.5 mm (R)×10 mm (T)×80 mm (L).

The experimental procedure was first to measure MFA, then to determine E_L and last to determine basic density of the specimen. The average MFA of specimen was measured by an X-ray powder diffractometer（PHILIPS X'Pert PRO PW3050/60）. A line-focused X-ray beam （Cu-Kα X-ray）was applied to the wood specimen which was mounted in a holder that can

Table 1. Specification of Masson pine plantation sample trees

Tree No.	DBH (cm)	Tree height (m)	Clear length (m)	Growth ring (a)
1	23.8	14.0	7.3	40
2	31.9	19.0	11.0	44
3	25.1	14.0	5.3	33
5	28.9	19.0	13.8	43
7	22.0	17.0	11.8	41
8	23.3	16.3	11.3	43
9	39.8	19.7	9.7	43
10	31.8	18.3	10.0	42
11	30.0	20.0	11.5	44
12	40.3	22.0	11.3	44
13	44.3	20.0	12.0	43
14	43.7	20.0	10.0	43
15	33.5	18.0	8.0	37
16	27.0	16.3	10.8	41
17	28.0	15.6	9.6	34
18	20.6	16.3	12.3	38
19	32.1	18.5	9.5	37
20	34.7	20.0	12.6	44
21	31.6	18.3	10.3	41
Mean	31.2	18.0	10.4	40

be rotated about a horizontal axis (X axis of a right handed cartesian set X, Y, Z). The specimen is mounted at the centre of rotation, with its longitudinal (L) axis set initially in the vertical direction, Z, and usually with its L-T face normal to the X axis. The measurements were made a circle rotation at 0.5 sec/step and scan step size 1°, at a Bragg's angle 2θ=22.4°, using the 2 mm diverging slit and 1 mm receiving slit. A diffractogram (Fig. 1) is produced

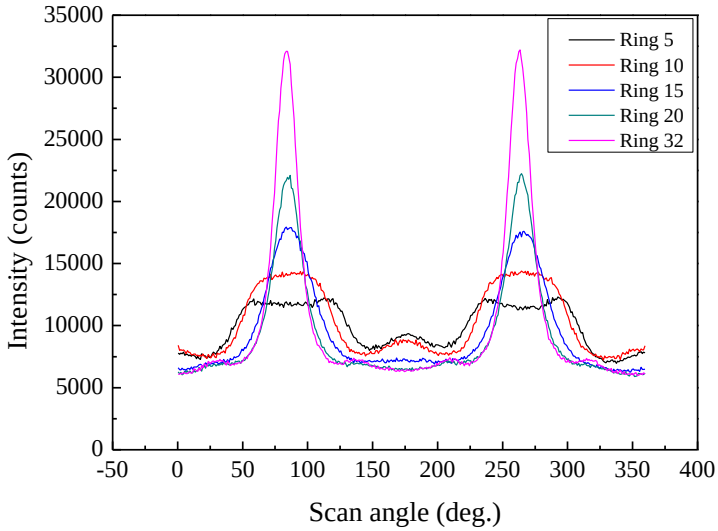

Figure 1. X-ray diffraction profile for specimens from different rings of the wood strip

by the crystalline structure and recorded by a X'Celerator detector. According to the calculation of MFA presented by Cave (1966, 1997), the value of MFA was equal to 0.6 by parameter T obtained from the diffraction intensity around (002) arc. After the MFA of each specimen had been measured, an INSTRON 5848 Micro-Tester was used to perform the axial tensile test on the same specimen to obtain its tensile E_L when the specimen reached the equilibrium moisture content (EMC) in a temperature & humidity chamber with (20±2)℃ and (65±3)% RH. The grip air of 250 N and the static load cell of 2 kN were chosen. The strain of longitudinal deformation was detected by a 25 mm dynamic extensometer. The loading rate was 1.5 mm/min and the max. load was 350 N. The calculation of E_L was as follows

$$E_L = \frac{\sigma_{150} - \sigma_{300}}{\varepsilon_{150} - \varepsilon_{300}} \quad (1)$$

where σ_x and ε_x respectively indicated the stress and strain corresponding to the load of x N. The wood basic density was determined using the conventional gravimetric method with water-saturated volume and oven-dry mass.

Results and Discussion

Wood density and within-tree variation

Figure 2 showed the basic density of 713 Masson pine wood specimens in this study. The average basic density and corresponding coefficient of variation (COV) were 0.428 g/cm^3 and 21%., respectively. Because of the specimen from the same growth ring, in fact, the density was the growth ring density, which was affected by the cell wall thickness, cell diameter, the ratio of earlywood to latewood, chemical content and the age.

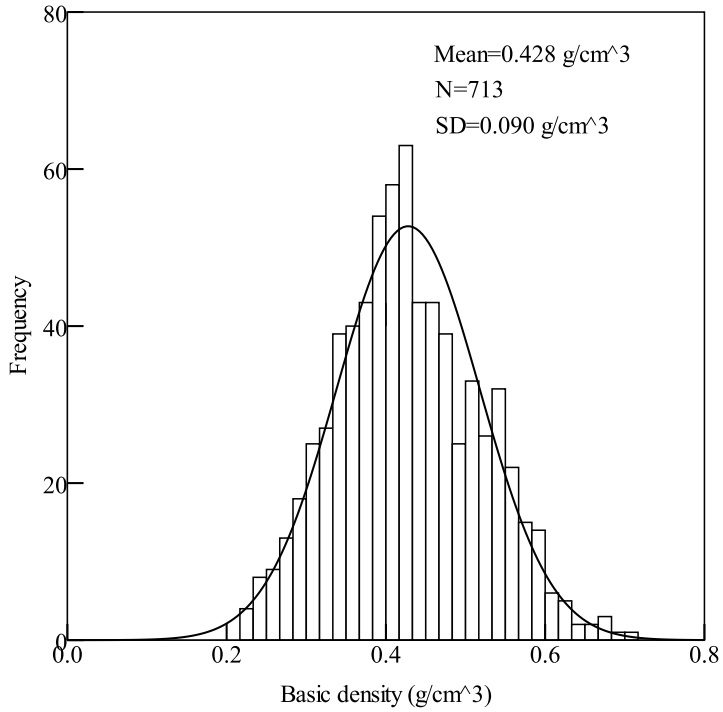

Figure 2. The basic density of Masson pine wood from plantation

The predictable pattern for basic density is that it is lowest near the pith, increasing outwards to about 25th growth ring, thereafter remaining relatively constant (Bunn 1981). For Masson pine, wood density adjacent to the pith averages about 0.378 g/cm^3 whereas the outer wood after 25th ring averages about 0.460 g/cm^3. The figure 3 shows that the basic densities of two sample trees vary with the growth rings. Different trees can have markedly different density gradients across those 25 rings.

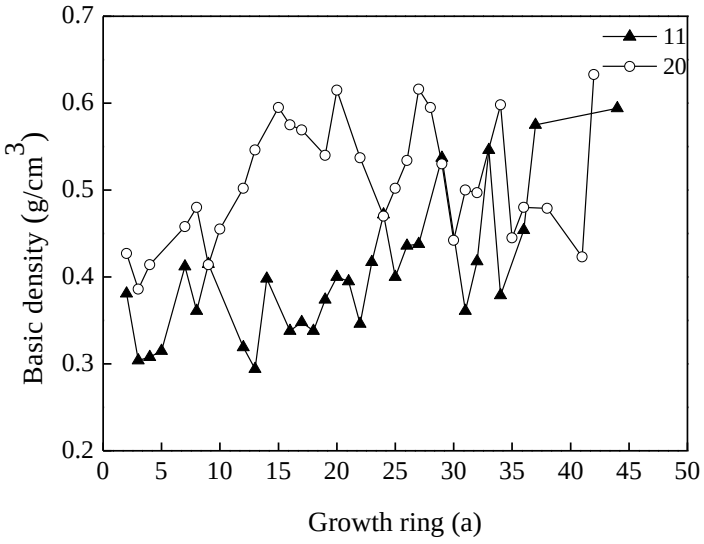

Figure 3. Variation of wood density of Masson pine plantation with growth rings

MFA and within-tree variation

The MFA was systematically studied over a wide range of growth rings in each tree. The distribution of measured MFA summarized in figure 4 angles shows most of the MFA range from 10° to 15°. The average MFA for all 1020 specimens was 17.5°. The MFA were correlated with the distance from the pith and the results were compared (figure 5). The MFA was found to decrease from pith to about 20th ring and then to remain stable in all trees.

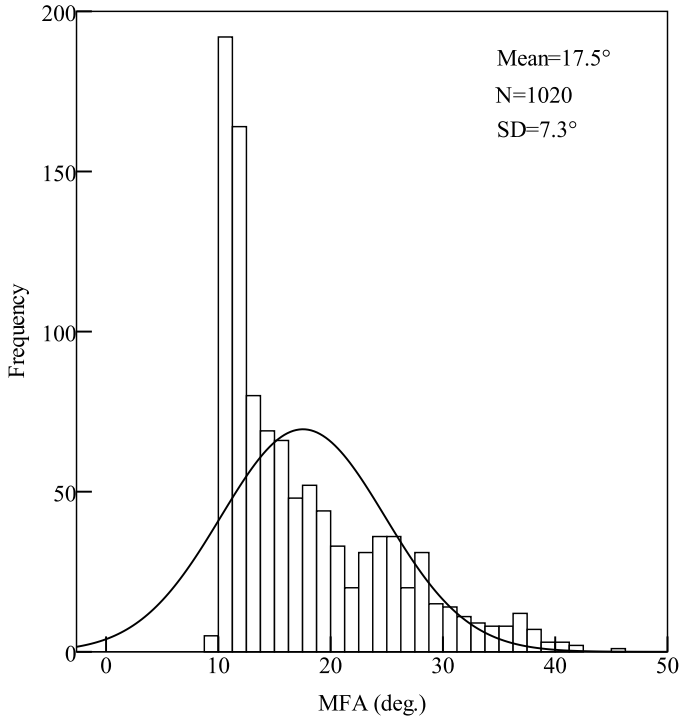

Figure 4. MFA of Masson pine wood from plantation

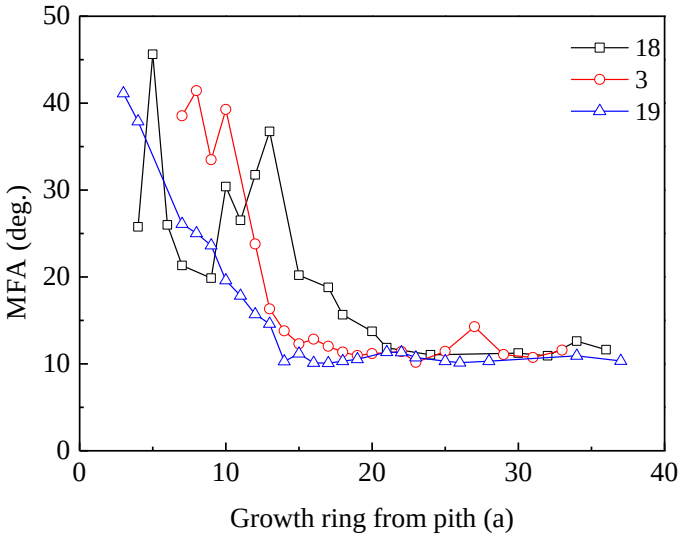

Figure 5. Variation of MFA of Masson pine along the radial direction

The tensile modulus of elasticity parallel to grain E_L

The average tensile E_L for 182 clear specimens at 14% MC was 11.2 GPa. The corresponding COV was approximately 48%. Stress-strain curves for specimens with different MFA are shown in figure 6. It is obvious that specimens with larger MFA show increased extensibility. Longitudinal strain increases from 0.08% to 0.4% as MFA increases from 10.3° to 41.1° when the stress is 17 MPa.

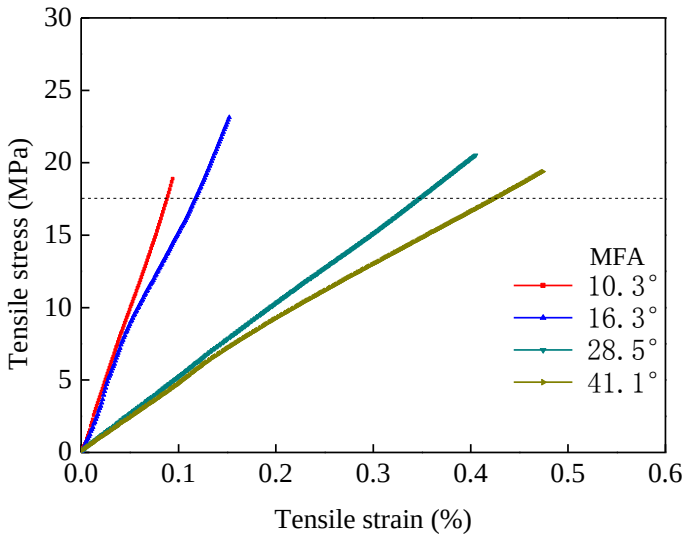

Figure 6. Longitudinal tensile stress-strain curve of Masson pine wood with different MFA (within elastic limit)

Conclusion

It is the first time to experimentally determine the longitudinal tensile modulus of elasticity E_L of Masson pine wood from plantation in China. The average wood basic density, MFA and tensile E_L at 14% MC are 0.428 g/cm^3, 17.5° and 11.2 GPa, respectively. These data may serve as a basis for the efficient utilization of Masson pine. This study has important basic and practical meanings.

References

Bamber R. K. & Burley J. 1983. The wood properties of radiata pine. Slough, UK: Commonwealth Agricultural Bureaux.

Bunn E. H. 1981. The nature of the resource. New Zealand Journal of Forestry. 26(2): 162-199.

Cave I. D. 1966. X-ray Measurement of Microfibril Angle. Forest Products Journal, 16(10): 37-42.

Cave I. D. & Walker J. C. F. 1994. Stiffness of wood in fast-grown plantation softwoods: the influence of microfibril angle. Forest Products Journal. 44(5): 43-48.

Cave I. D. 1997. Theory of x-ray measurement of microfibril angle in wood part 1. the condition for reflection x-ray diffraction by materials with fiber type symmetry. Wood Science and Technology, 31(3): 143-152.
Cave I. D. 1997. Theory of x-ray measurement of microfibril angle in wood part 2. the diffraction diagram x-ray diffraction by materials with fiber type symmetry. Wood Science and Technology, 31(4): 225-234.
Donaldson L. 2008. Microfibril angle: measurement, variation and relationships – a review. IAWA Journal. 29(4): 345-386.
Harris J. M. & Meylan B. A. 1965. The influence of microfibril angle on longitudinal and tangential shrinkage in Pinus radiata. Holzforschung. 19(5): 144-153.
Meylan B. A. 1972.The influence of microfibril angle on the longitudinal shrinkage-moisture content relationship. Wood Science andTechnology. 6(4): 293-301.

Acknowledgements

This work was funded by the National Natural Science Foundation of China (NSFC) Key Program (30730076). Their financial contribution to the project is gratefully acknowledged. I am indebted to staff at ICBR, especially members of the Material Science and Technology of Bamboo and Rattan.

Proceedings of the 55th International Convention of Society of Wood Science and Technology
August 27-31, 2012 - Beijing, CHINA

The Research on Bamboo-wood Corrugated Sandwich Panel

Feng YANG. Benhua FEI

International Centre for Bamboo and Rattan, Beijing, 100102, China

Abstract

The physical and mechanical properties of Bamboo-wood corrugated Sandwich Panels (BCSP) relevant for nonstructural Panels were studied. The Bamboo-wood corrugated Sandwich Panels consisted of 2 face layers and the core particleboard that was made of low-value biomass material (bamboo and wood particles) through hot-mold pressing. The modulus of rupture (MOR), the modulus of elasticity (MOE) and the compressive strength (CS) were determined. The 3-layer composites were also prepared from the corrugated core layer and 2 face layers, and tested in three-point bending and compressive strength. A maximum value of the properties was obtained for bamboo core particleboard and 2 MDF face panels. It was observed that the bending and compressive properties of BCSP (MOR, MOE and CS) were significantly improved due to the pressure, temperature and time of the manufactured sandwich panels. Effect of pressure on physical and mechanical properties of urea-impregnated biomass corrugated composites was the most crucial. It was found that the compressive strength (CS) of composites decreased when pressing time was extended from 7 to 9min, whereas the modulus of rupture (MOR) and the modulus of elasticity (MOE) did not decrease. The bonding and compressive performance of the biomass corrugated composites with UF adhesive was comparable with or better than in the case of the biomass cellular board.

Keywords: Bamboo-wood corrugated Sandwich Panels; physical and mechanical properties; bamboo particles; MDF.

Introduction

The optimized structure with the corrugated structure is rational bearing structure, a favorable compressive strength and shear strength can obtained through applicable Structural Design (Er 2008). Compared with cellular structure, the shear strength of corrugated structure is three to seven times in YZ-direction (Xiong 2001). The current commercial products for Packaging, such as carton, enclosure Material of refrigerator wagon camping house and the conventional corrugated forming method, included roll forming, bending forming and Pull forming (He 2004).

In the present work, some wood-bamboo-based sandwich panels with low-value fiberboard were manufactured with different thickness, core density, and face materials. A three-point bending test was conducted, and the compressive strength (CS) was determined, which was also important for structural calculations.

Pressing factors are critical for core particleboard manufacture, because the temperature, the pressure and the time play a dominant role in mechanical performance. The optimization of laminated plate structures have been considered by a number of authors (Jiang 2002, Gao 1997), but the optimization of wood-bamboo- based sandwich panels, and particularly with corrugated core, appears to be much less well studied. Therefore, the optimum designs of some virtual wood-bamboo-based sandwich structures were analyzed by considering the designs of the manufactured panels.

Materials and Methods

Face and core materials. For core materials, bamboo particle, wood flake and wood fiber from factory milling waste were prepared, which would be produced corrugated core through hot-mold pressing. For face materials, plywood (PW), medium-density fiberboard (MDF) and bamboo parallel strand lumber (BPSL) were prepared. The PW was commercially produced from hardwood veneer with a thickness of 5 mm and MOR of 18 MPa. The MDF was commercially produced from hardwood fiber with a thickness of 5 mm and MOR of 34 MPa. The BPSL was commercially produced from bamboo pieces with a thickness of 5 mm and MOR of 67 MPa.

Manufacture of sandwich panels. Nine types of Bamboo-wood Sandwich Panel with corrugated core were manufactured as listed in Table 1. Sandwich panels with a target thickness of 18 mm at three Layers (2 face Layers and a corrugated core layer) as shown in Figure 1.

Table 1 Experimental geometric data of the manufactured sandwich panels

No.	Face	Core	$MOR_{\parallel}$ (MPa)	$MOR_{\perp}$ (MPa)	$MOE_{\parallel}$ (MPa)	$MOE_{\perp}$ (MPa)	CS(MPa)

1	①	Ⅰ	9．03	7．77	983	660	1．88
2	①	Ⅱ	12．12	10．67	1304	919	3．32
3	①	Ⅲ	16．52	14．11	2904	2244	2．54
4	②	Ⅰ	22．21	20．53	2042	1402	1．64
5	②	Ⅱ	17．81	15．61	2111	1753	3．40
6	②	Ⅲ	24．37	19．81	2736	2571	5．06
7	③	Ⅰ	29．08	23．85	1958	1200	1．24
8	③	Ⅱ	20．39	11．08	4052	600	1．22
9	③	Ⅲ	38．53	14．86	5207	707	3．60

The data are average values of the specimens for the mechanical property test. ①, 5 mm PW; ②, 5 mm MDF; ③, BPSL; Ⅰ, 5 mm corrugated core of wood fiber ; Ⅱ, 5 mm corrugated core of wood flake; Ⅲ, 5 mm corrugated core of bamboo particle; MOR, longitudinal Modulus of Rupture of panel; MOR, transverse Modulus of Rupture of panel; MOE, longitudinal modulus of elasticity of panel; $MOE_{\perp}$ transverse modulus of elasticity of panel; CS, compressive strength.

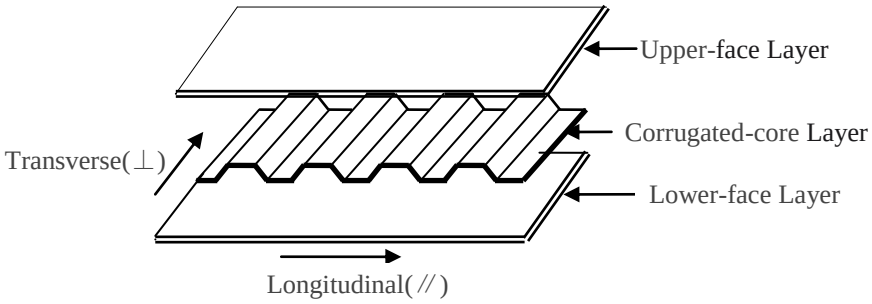

Figure 1 Structure schematic of sandwich panel

The manufacturing procedure of sandwich panels was as follows. The core material was put into a blender and the commercial adhesive of urea-formaldehyde (UF) was sprayed into the particle using a spray gun during material the cycle. The resin content was 9% solid resin of UF based on the oven-dried particle weight. The particle was formed into corrugated core in a size of 400 (width) × 400mm (length) through hot-mold pressing by using a corrugated shape forming steel mold. All face materials were prepared in a size of 400 (width) × 400 mm (length). Before pressing, UF adhesive was spread on the back side of each face material at approximately 130 g/m2 on solid basis using a hard plastic hand roller. The face materials were then symmetrically placed on the top and bottom surfaces of corrugated core so that the grain of the face layer was parallel to the panel length direction (longitudinal direction of corrugated core).

The assembled slabs were pressed through a “hot into and hot out” hot-press molding and the process curve was shown in figure 2. In this study, three main pressing process factors (temperature, pressure and time) of hot-mold pressing were emphatic studied, three different levels were selected in each factor, and the L9 (34) orthogonal experiment design as shown in

Table 2 (the test specimens consisted of 2 MDF face-layers and the core-layer was made of bamboo particle) (LI, 2005).

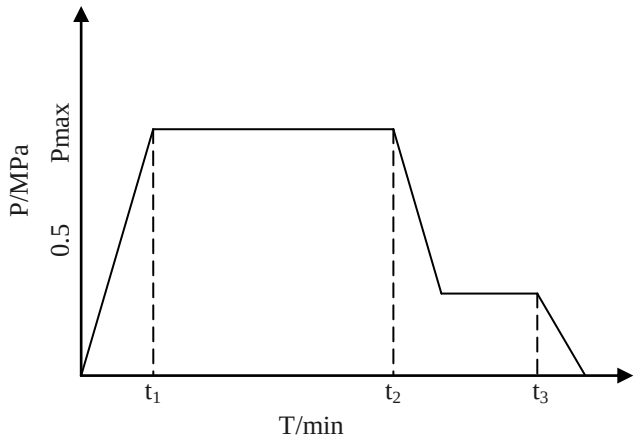

Figure 2 Process curve of hot-press molding

Table 2 The orthogonal experiment factors and levels

level	factor temperature（T）/℃	pressure（P）/MPa	time (t)/min
1	150	2.5	5
2	160	3.0	7
3	170	3.5	9

Testing methods

Prior to conventional evaluation of the mechanical and physical properties, the specimens were conditioned at 20℃ and 65% relative humidity (RH) for at least 2 weeks. The panels were tested based on Test methods of evaluating the properties of wood-based panels and surface decorated wood-based panels (GB/T17657-1999).

All the panels were trimmed and cut into various test specimens as follows: 50 (width)×200 mm (length) for static bending; 100 (width)×100 mm (length) for compressive strength (CS). The static bending tests were conducted on four specimens from each treatment (total 36 samples), using a three-point bending test over an effective span of 150mm at a loading speed of 10 mm/min; four test specimens were prepared from each treatment (total 36 samples) for the CS. Comparison of property values of the Bamboo-wood Corrugated Sandwich Panel (BCSP) with Wooden Cellular Panel can describe the position of BCSP among the well-known nonstructural panels.

Results and discussion

The experimental geometric data of BCSP are listed in Table 1. Results indicate that both bending and CS properties of BCSP, which consisted of 2 MDF face-layers and the core-layer made of bamboo particle, achieved optimal among experimental geometric data. The BCSP exhibited a better mechanical properties and was chosen as materials in orthogonal experiment.

Table 3 shows the test results of orthogonal experiment of the test specimens and these range analysis results are shown in Table 4. From the above results, the pressure of the manufactured sandwich panels was the most effective factor to improve the mechanical properties among the three factors. The temperature and the time of the manufactured sandwich panels had less significant effects on mechanical properties of the test specimens

Table 3 The test results of orthogonal experiment

No.	T(℃)	P(MPa)	t(MPa)	$MOR_{//}$ (MPa)	$MOR_{\perp}$ (MPa)	$MOE_{//}$ (MPa)	$MOE_{\perp}$ (MPa)	CS (MPa)
1	155	2.5	5	16.743	13.029	2270	2034	5.090
2	155	3.0	7	20.414	20.952	4723	2594	5.570
3	155	3.5	9	29.719	22.258	5746	3445	5.765
4	160	3.0	5	22.442	19.936	4769	2277	6.177
5	160	3.5	7	30.668	25.136	5947	3677	6.774
6	160	2.5	9	18.458	15.499	3077	2683	4.013
7	165	3.5	5	21.234	20.761	4380	2616	5.638
8	165	2.5	7	21.308	11.749	3845	2305	5.177
9	165	3.0	9	21.860	13.936	3266	2646	5.544

Table 4 The range analysis of the process variables affecting to panel

Level	$MOR_{//}$(MPa)			$MOR_{\perp}$(MPa)			$MOE_{//}$(MPa)			$MOE_{\perp}$(MPa)			CS(MPa)		
	T	P	t	T	P	t	T	P	t	T	P	t	T	P	t
1	22.292	20.503	20.140	18.746	13.426	17.909	4246	3064	3806	2691	2341	2309	5.475	4.760	5.638
2	23.856	23.239	25.797	20.190	19.608	20.612	4598	4253	4838	2879	2506	2859	5.655	5.764	5.840
3	21.467	29.207	27.012	15.482	25.385	19.898	3830	5358	4030	2522	3246	2925	5.453	6.059	5.107
range	2.389	8.704	6.872	4.708	11.959	2.703	768	2294	1032	357	905	616	0.202	1.299	0.733

Figure 3 indicates that the temperature had a significant effect on panel plasticizing and adhesive curing. The bending and CS values of BCSP increased with the increase in temperature (150 ℃ to 160 ℃), which indicated that mechanical properties had a tendency to increase with increasing temperature. When the temperature of the slab increased, the

adhesive viscosity decreased, bamboo material were heated to bate, and liquidity increased, all of which had more advantage to enhance the contact between the material and adhesive and improve the internal bonding strength.

Moreover, the increase of temperature was beneficial to the form of temperature gradient in the thickness direction of the panel, which caused the High-hard surface, and resulted in the increase of mechanics performance. However, a reverse trend was found in a higher temperature (160 ℃ to 170 ℃). The reduction in mechanical properties might be due to the following reasons: material degradation under high temperature, and even coking phenomenon lead to the increase of brittle surface. As a result, less value was being obtained.

Results of statistical analysis (Fig. 3) show that the pressure has a significant effect on the bending and CS properties. The effect on bending and CS values of BCSP was clearly observed. This was because the much closer contact between internal material and adhesive, the more improvement of the bonding strength. The trend of CS increase slowed when the pressure values reach over 3.0 MPa. The reason may be that the it can satisfy the needs of gluing between the strands. No significant effects were observed when the pressure increased. Additionally, the curing degree becomes a major factor influencing mechanical properties.

Figure 3 shows time factor has a significant effect on bending and CS values. The bending and CS strength of BCSP increase with increasing time (5min to 7min). The results indicate that the extension of time can promote curing of the glue to achieve a better mechanical properties within a certain range. The time values of the sandwich panels were in the range of 7 min to 9 min, MOR⊥、MOE⊥ and CS values of BCSP had a tendency to decrease with increasing pressing time because of degradation and embrittlement of bond line. Whereas the MOR∥ and MOE∥ values generally were not significantly affected. At different direction, the higher pressing time may play a subdominant role where mechanical properties are concerned during resin cured in the panels.

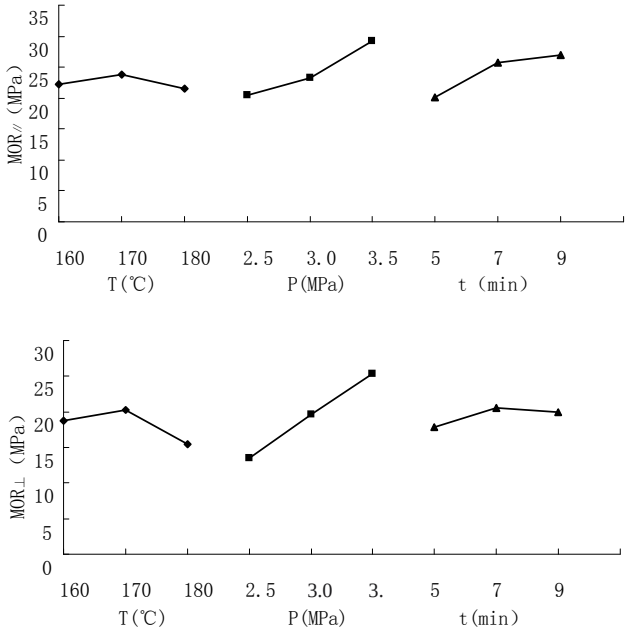

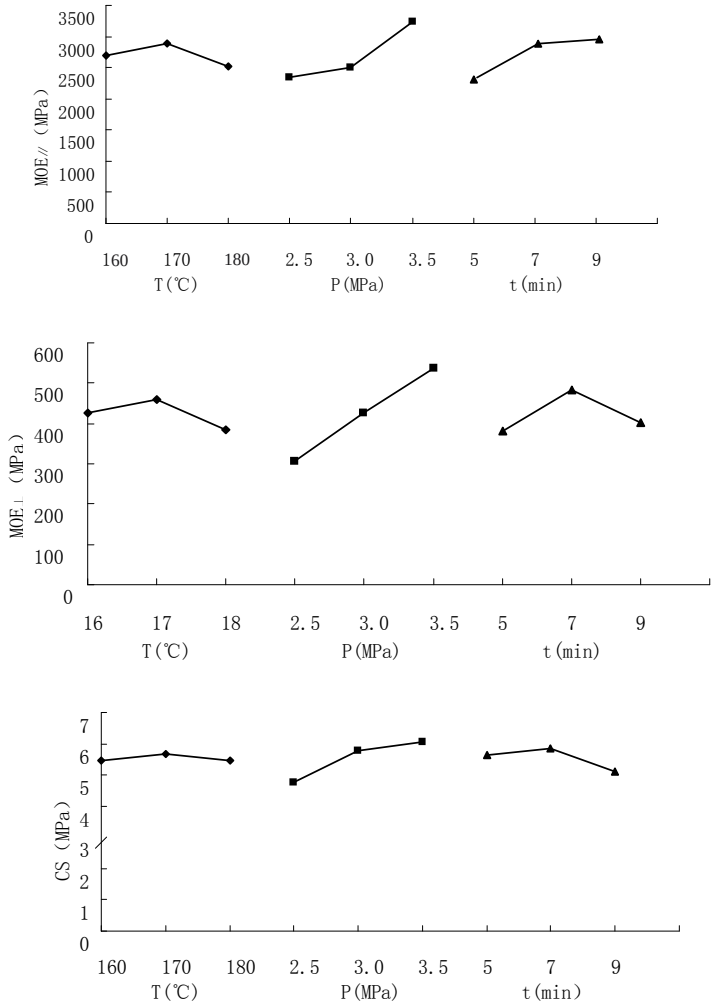

Figure 3 Technology factors affecting to mechanical properties of BCSP

Conclusions

The manufacture of BCSP from corrugated strands of moso bamboo (Pyllostachys pubescens Mazel) appeared to be technically feasible. Strength properties were improved with increasing pressure mainly; Temperature and time had less significant effect on strength properties. The Optimum technologic parameters of BCSP manufacturing are as follows: 160 ℃of temperature in core pressing, 3.0 MPa pressure in core pressing, 7 min time in core pressing. Compared to the commercial nonstructural products, BCSP showed superior strength properties. It is recommended that further research should be done to investigate other properties of BCSP, such as biological resistance, weather-ability, finishing properties, and fastener-holding capacity.

References

Er, Y.P. 2008. Study on Load Carrying Performance of Corrugated Board Structure. Packaging Engineering. 29 (1):66-68.

Xiong, H.Z. 2001. Contrast of Rigidity Between Honeycomb Cardboard and Corrugated Cardboard. Journal of Beijing Technology and Business University (Natural Science Edition). 9(3):42-46.

He, C.P.2004. The Design of Bending Forming Mould of Corrugated Plate. Special Purpose Vehicle. 4(3)：31- 34.

Jiang, Z.H. 2002. The Research and Development on Bamboo/Wood Composite Materials. Forest Research. 15(6):712-718.

Gao, J.Z.1997. The Influence of Mul-corrugated Board Pressure Structure and the Component Forming. New agricultural mechanization. 2：39- 40.

LI, Y.Y.2005. Experimental Design and Data Processing. Beijing.: Chemical Industrial Press.

Suitabilityof Changbai Larch Plantation for LVL Products

Suyong Huang[1] - Brad Jianhe Wang[2] - Jianxiong Lu[3] - Chunping Dai[2] - Yuancai Lei[3]*

[1]Post Doctor Fellow, Chinese Academy of Forestry, Beijing, P. R. China 100091
[2]Research Scientist, FPInnovations - Wood Products, Vancouver, B.C., Canada V6T 1W5
[3]Research Scientist, Chinese Academy of Forestry, Beijing, P. R. China 100091

**Corresponding author*
brad.wang@fpinnovations.ca

Abstract

The objective of this work was to examine the feasibility of Changbai larch (*Larixolgensis* Henry) plantation for manufacturing LVL products. Nine representative larchlogs were sampled from each of four typical standsin the northern part of China. They were bucked and conditioned for veneer peeling. Veneer was then clipped, dried and stress graded with a production-line Metriguard veneer grader. Veneer properties were subsequently analyzed and benchmarked against common second-growth softwood species in Canada. All larch dry veneer sheets werefurther segregated into four E grades based on dynamic modulus of elasticity (MOE),and fourLVL billets weremanufactured from eachE grade. The performance of those 16 LVL billets were evaluated in terms of flatwise and edgewise bending stiffness and strength. The results demonstrated that comparing with Canadian western hemlock (Tsugaheterophylla (Raf.) Sarg) and amabilis fir (Abiesamabilis (Dougl.) Forbes) with an average rotation of 68 years, Changbai larch has significantly higher veneer density and ultrasonic propagation time (UPT), and also higher veneer MOE. About 85% of larch veneer could be suitable for manufacturing 1.8E or higher grade commercial LVL. A high correlation existed in bending MOE and modulus of rupture (MOR) between the larch LVL andveneerfor both edgewise and flatwise modes. Thus, the bending performance of larchLVL products can be accurately predicted with regard to veneer E grade.

Keywords:Changbai larch,Amabilis fir, Laminated veneer lumber (LVL), Modulus of elasticity (MOE), Stress grade, Veneer, Western hemlock

Introduction

Changbai larch (*Larix olgensis* Henry) is one of the most important commercial plantation species in the northern part of China. This species has a high growth rate and high survival rate due to its strong resistance to pests, diseases, and inclement weather (Liu 2004). With an increasing volume of plantations reaching a target rotation age, this species has become one of the major fiber stocks in China. Its logs are generally very knotty, which could affect the appearance grades and some mechanical properties of end products, so pulp has been the predominant industrial application for this species (Li 2001; Liu 2004; Sun and Pang 2005; Zhang et al. 2005), followed by lumber (He *et al.* 2009).

Opportunities exist to utilize plantation species, such as hybrid poplar(*Populus hybrids)*, black spruce (*Picea mariana)*, and aspen (*Populus tremuloides),*for manufacturing high-value wood composite products or engineered wood products (Wang 2001; Wang and Dai 2001; Knudson and Wang 2002, Knudson et al. 2002; Knudson et al. 2006; Wang and Dai 2005; Wang et al. 2010). Such potential products include glulam, structural composite lumber like laminated veneer lumber (LVL), parallel strand lumber (PSL or Parallam), veneer strand lumber (VSL) and oriented strand lumber (OSL) etc. and newer products such as cross laminated timber (CLT) for niche markets. The advantage of those products is that their performance is not necessarily limited by wood properties. They offer opportunities to convert low-value plantation logsto higher value next generation building products.

Traditionally, forest resourcesare mainly characterized through tests on clear wood and full size lumber (Zhang et al. 2005; Wang and Dai 2012). Veneer is a basic element for manufacturing plywood, LVL and PSL. Compared to dimension lumber, those veneer products have higher and more uniform stiffness and strength, greater dimension/dimensional stability and minimum defects. While growth characteristics of this larch species in China have been well documented, little is known about its veneer properties in relation to its site, stand management and tree growth. Virtually no effort has been undertaken to use this species for manufacturing veneer-based products, particularly LVL.

To maximize the value return from the larch plantations in China, a national research program was recently initiated to characterize this resource through veneering with regard to stand density, growth rate, and stem position and to determine its suitability for veneer products particularly LVL (Huang et al. 2012). As part of the initiative, the key objective of this work was to investigate the suitability of the larch plantation for LVL products. By analyzing the distribution of main larch veneer properties, a benchmark study can be done against other common softwood species to determine its suitability for LVL manufacturing and respective grade outturns. By manufacturing LVL billets from segregated larch veneer and conducting tests on their bending performance, the correlation between larch LVL and veneer properties can be established to identify the best product potential from this resource.

Materials and Methods

Tree sampling and cutting. In this study, the sample trees were obtained from Mengjiagang Forestry Center, Jiamusi, Heilongjiang province, China. This site is located in the

Xiaoxinganling Mountain zone. The site belongs to the East Asian continental monsoon climate zone. Four typical stands were selected with varying initial spacing (or density), final density, and stand management practices. Nine representative trees were systematically selected from each stand, three each from large (30 cm), medium (25 cm), and small (20 cm)DBH classes, respectively. They were harvested, trimmed, and bucked. Six 1.25 m long bolts were systematically cut along the entire stem to peel 2.6 mm thick veneer. The live crown width, length, and DBH were measured from each tree before felling. After felling, the total height and diameter of the five biggest branches were measured as well as the diameter at different tree heights for calculating the tree taper. Clear wood specimens were also sawn from matched bolts for mechanical testing to permit comparison and validation and subsequent evaluation of product options (Huang et al. 2012). Table 1 shows the characteristics of the 9 sample trees from each stand with the mean DBH and tree height.

Table 1. Sampling schemes and stand characteristics of larch trees

Stand no.	Initial density (trees/ha.)	Final density (trees/ha.)	Site index		Mean DBH (cm)	Number of trees
			Age (year)	Mean tree height (m)		
1	3000	580	46	21.8(1.59)*	24.5(5.58)	1-9
2	4000	487	53	21.5(1.06)	23.2(4.54)	10-18
3	5000	305	53	22.3(1.05)	25.0(3.64)	19-27
4	6000	200	49	22.0(1.03)	26.8(4.80)	28-36

*Standard deviation

As shown in Figure 1, each tree was bucked into 6 segments with a mark from butt to top (crown) along the entire stem to indicate its stem position. Among which, the first segment (1300 mm from the butt) was right on the breast height for basic density measurement and veneer processing. Then, the 5 consecutive segments 2 to 6 were cross cut with a length of 2500 mm. After that, all segments were transported to the Chinese Academy of Forestry (CAF) in Beijing. In the pilot plant, each segment (from 2 to 6) was further cross cut to obtain 5 disks, starting from the bottom and labeled A to E for determining various wood characteristics. Disk A (30 mm thick) was used to determine chemical properties such as pH, acid, and alkali buffer values; disk B (30 mm thick) provided the sapwood and heartwood area ratio; disk C (50 mm thick) was used to observe anatomical symptoms such as annual ring width; section D (1250 mm long) was used to determine clear wood macro- and micro- mechanical properties, and section E (1250 mm long) was used for veneering.

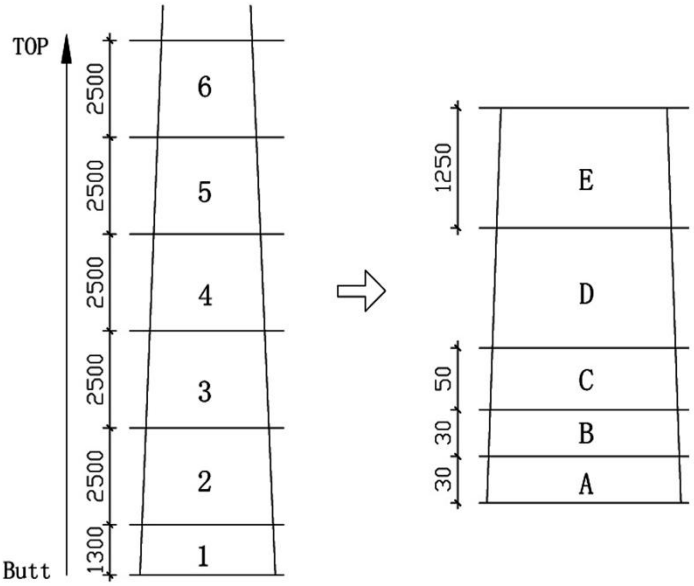

Figure 1. Bucking and cross cutting of one sample tree

Veneer peeling,clipping, drying and grading. Each 1250 mm long section E (bolt) from segments 1-6 was transported to a plywood mill for veneer processing. The bolts were conditioned in a pond at 60 ºC for 48 hours before peeling with an industrial lathe equipped with a nose bar. The lathe settings were: horizontal gap = 2 mm, pitch angle = 89.5º, and vertical gap = 1.2 mm. The core drop size was 38 mm. The target veneer thickness was 2.6 mm (about 1/10 inch). Each veneer ribbon was clipped into 600 mm sheets in width sequentially from sap (bark) to core (pith). Then each sheet was coded with a number in combination with tree number, segment number, and veneer sheet number for easy identification. After that, each sheet was dried using a press dryer with a temperature of 120 to 130 ºC. A total drying time of about 15 min was used to achieve a target veneer moisture content (MC) of 3 to 6%, which is ideal for gluing. The dryer was opened once to evaporate steam after pressing about 7 min.

All dry sheets were shipped back to CAF in Beijing for nondestructive tests. Each sheet was fed through a full scale Metriguard 2800 veneer tester (Metriguard Inc. 2012). This tester uses a variety of property measurements for sorting veneer. These may include ultrasonic propagation time (UPT), density, or dynamic MOE. The density is measured by microwave cavity resonators. The data for each sheet were then downloaded from the tester for further analysis.The total number of veneer sheets was 2291 for density, UPT and dynamic MOE measurements. Note that the veneer dynamic MOE is computed as follows,

$$\mathrm{MOE} = \rho \times \left(\frac{L}{\mathrm{UPT}}\right)^2 \qquad (1)$$

where ρ is veneer density and L is the span for the UPT measurement.

Data were first plotted for population cumulative distribution of each veneer property for the four combined stands. The comparison was made to benchmark this larch species against common

second growth western hemlock (Tsuga heterophylla (Raf.) Sarg) and amabilis fir (Abies amabilis (Dougl.) Forbes) with an average rotation of 68 years in Canada.

All 2291 veneer sheets were subsequently sorted into four E grades based on dynamic modulus of elasticity (MOE) with three E breakpoints, 10, 12 and 14 GPa for LVL manufacturing. The selection of those breakpoints was just for the convenience of veneer segregation since no stress grading rules are currently available.

Pilot plant LVL manufacturing and testing. An industrial single opening press (2440 mm x 1200 mm) was used to manufacture 15-ply larch LVL billets (1200 mm x 600 mm). A plywood phenol formaldehyde (PF) adhesive with a solids content of 55% was used to bond the veneer sheets. Four billets from each E grade were loaded into the press side by side for hot pressing. A total of sixteen LVL billets were made with the following manufacturing parameters: glue spread level, 150 g/m^2 per single glueline; pressing temperature, 145°C; target thickness, 37mm (thickness control); and pressing time, 40min. After unloading, all billets were stacked and stored for one week before cutting bending specimens. The bending MOE and modulus of rupture (MOR) were measured in both flatwise and edgewise modes in accordance with GB/T20241-2006(China Standard Press 2006), which is equivalent to Japanese LVL Standard (JAS SIS-24 1993).

Results and Discussion

Benchmarking larch veneer properties. Table 2 summarizes the veneer properties in terms of four individual stands. For each stand, the total number of veneer sheets was also calculated, reflecting a measure of veneer yield. The same number of trees harvested from each stand resulted in different veneer yields, mainly due to the difference in the tree mean DBH (Table 1). The coefficient of variation (COV) ranged from 8.6 to 12.1% for veneer density, 7.0 to 7.9% for veneer UPT, 12.9 to 13.4% for dynamic veneer MOE. Comparatively, the stand 1 yielded the highest veneer density and MOE than the other three stands ($p = 0.05$).Based on Table 2, the within-stand variation seemed to be higher than the between-stand variation.

Table 2. Properties of larch veneer in relation to stands

Stand no.	No. of sheets	Density (g/cm^3)		UPT (μs)		MOE (GPa)	
		Mean	Std. Dev.	Mean	Std. Dev.	Mean	Std. Dev.
1	517	0.539	0.046	200.9	15.9	13.1	1.7
2	490	0.535	0.061	203.6	14.3	12.8	1.7
3	619	0.523	0.543	202.9	15.3	12.7	1.7
4	665	0.520	0.631	204.1	15.1	12.4	1.6

Figure 2 shows the density cumulative distribution function (CDF) of Changbai larch veneer in comparison with western hemlock and amabilis fir veneer. The data of hemlock and amabilis fir were cited from a recent hem-fir study with an average rotation age of 68 years (Wang et al. 2010). There existed a large variation in the veneer density for each specis. The larch veneer

density generally ranged from 0.40 to 0.70 g/cm^3, which is significantly higher than hemlock and amabilis fir ($p = 0.05$).

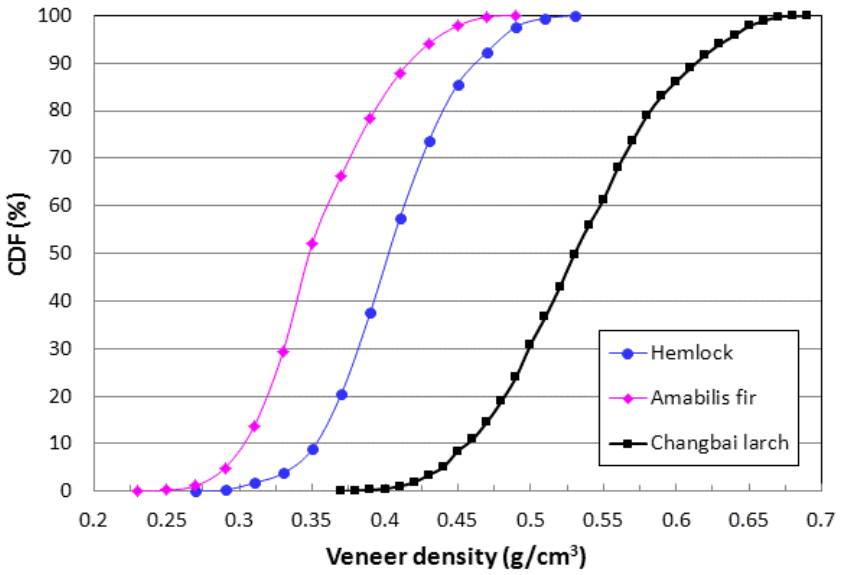

Figure2. CDF of veneer density compared by species

Figure 3 shows the UPT cumulative distribution function (CDF) of Changbai larch veneer in comparison with western hemlock and amabilis fir veneer. The UPT is generally affected by grain angle, knots and other wood defects. There existed a large variation in the veneer UPT for each specis. By comparison, the larch veneer had the highest UPT, followed by hemlock and amabilis fir veneer. This may indicate that the larch has a larger microfibril angle than the other two species.

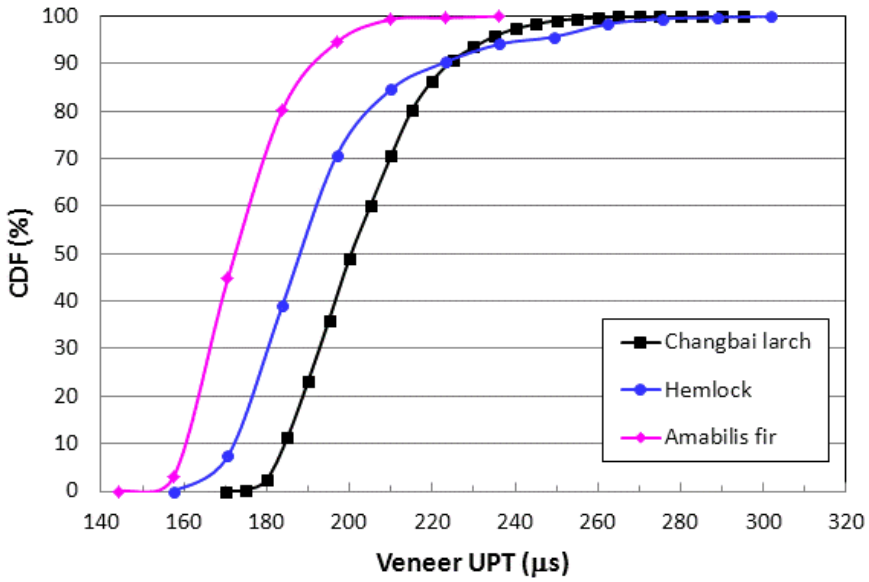

Figure3. CDF of veneer UPT compared by species

Figure 4 shows the dynamic MOE cumulative distribution function (CDF) of Changbai larch veneer in comparison with western hemlock and amabilis fir veneer. There existed a large variation in the veneer MOE for each specis. By comparison, the larch veneer had the highest MOE, followed by amabilis firand hemlock. On average, a conversion factor of approximately 1.10 can be used to link product MOE with veneer MOE using conventional pressing schedules with a panel compression ratio (CR) ranging from 7-13% (Wang and Dai 2001). Based on Figure 4, about 85% of the larch veneer from the four standscombinedcan be used to manufacture higher grade LVL, meeting 1.8E (12,411 MPa) or higher grade LVL requirements.

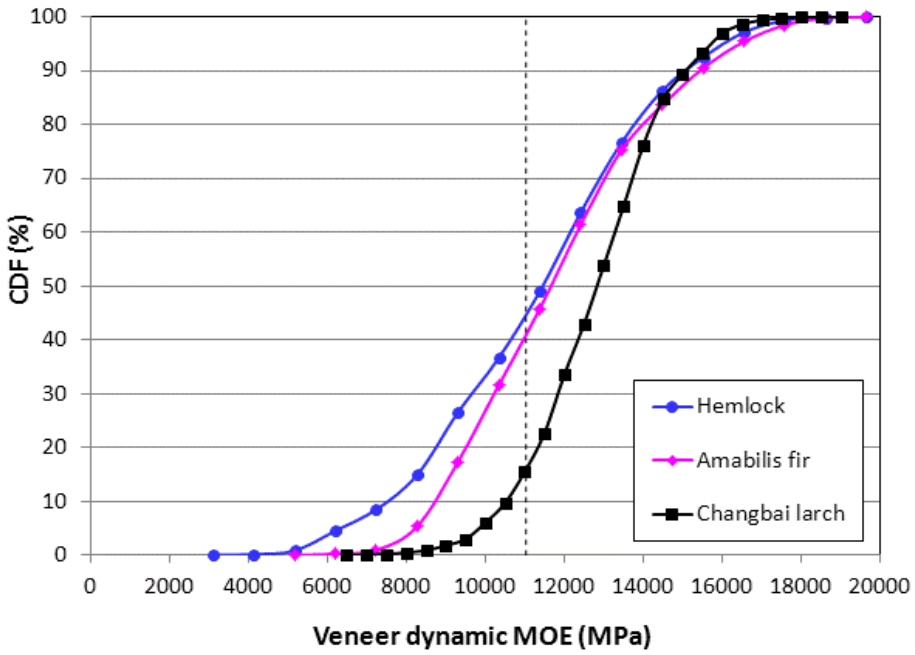

Figure 4.CDF of veneer dynamic MOE compared by species

In summary, comparing with Canadian hemlock and amabilis fir (68-year old on average), Changbai larch has significantly higher veneer density and UPT, and also higher veneer MOE. Under the circumstance of such a large variation of veneer properties, veneer stress grading is deemed necessary for structural applications of the larch veneer.

Stress grading of larch veneer. Table 3 summarizes the properties of each E grade after sorting with the following three E breakpoints: 10, 12 and 14 GPa. There was a clear descending trend from E1 to E4 for both veneer MOE and density. Compared with the unsorted population, the within-grade variation of veneer MOE and density was significantly reduced, which is beneficial to manufacturing of consistent LVL products.

Table 3. Properties of larch veneerE grades

Veneer E grade	MOE threshold (GPa)	Number of sheets	Dynamic MOE(GPa）		UPT (μs)		Density (g/cm^3)	
			Mean	Std. Dev.	Mean	Std. Dev.	Mean	Std. Dev.
E1	>14	545	15.86	0.65	191.0	9.3	0.59	0.04
E2	12-14	1023	13.37	0.79	199.0	11.7	0.54	0.05
E3	10-12	628	11.21	0.54	210.5	15.1	0.50	0.06
E4	<10	95	9.22	0.74	226.8	17.3	0.47	0.05
Population	Unsorted	2291	12.79	1.75	203.4	16.0	0.53	0.06

Correlation between larch LVL and veneer. Based on the measurement of final LVL thickness, it was found that the compression ratio (CR) of larch LVL was about 11-13%, which helps enhance the bending properties of LVL. Table 4 summarizes the bending MOE and MOR of larch LVL and veneer MOE. By comparison, LVL had a higher MOE than veneer for both edgewise and flatwise bending modes. The higher veneer E grades yielded higher LVL bending MOE and MOR.

Table 4. Properties of larch veneer and LVL

Veneer E grade	Veneer MOE (GPa)		LVL MOE (GPa)				LVL MOR (MPa)			
			Edgewise		Flatwise		Edgewise		Flatwise	
	Mean	Std. Dev.	Mean	Std. Dev.	Mean	Std. Dev.	Mean	Std. Dev.	Mean	Std. Dev.
E1	15.79	0.53	19.53	0.75	18.35	0.98	98.27	9.51	90.88	8.25
E2	13.41	0.30	16.79	0.81	16.36	1.04	86.00	6.76	75.81	11.70
E3	11.01	0.35	12.86	0.64	12.29	0.72	61.28	5.23	61.53	7.52
E4	9.15	0.64	10.96	0.34	11.02	0.52	53.06	4.32	48.57	4.99
Total	12.34	2.55	15.73	3.20	15.10	2.91	79.68	18.99	70.97	17.04

Figure 5 shows the correlation between LVL edgewise bending MOE and MOR and mean MOE of veneersheets built into each billet. The correlation was excellent giving an equal R^2 of 0.91. Similarly, Figure 6 shows the correlation between LVL flatwise bending MOE and MOR and mean MOE of veneersheetsassembled into each billet. The correlation was also good giving an R^2 of 0.90 and 0.82, respectively. The results indicate that the performance of larch LVL can be accurately predicted with regard to the veneer E grade.

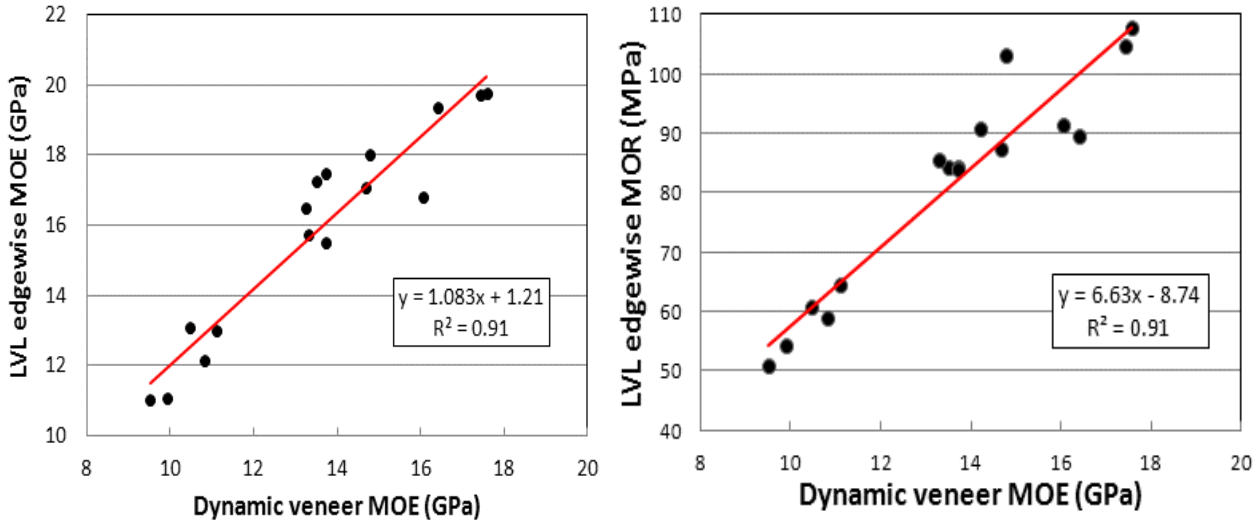

Figure 5.Correlation between larch LVL edgewise bending performance and veneer MOE

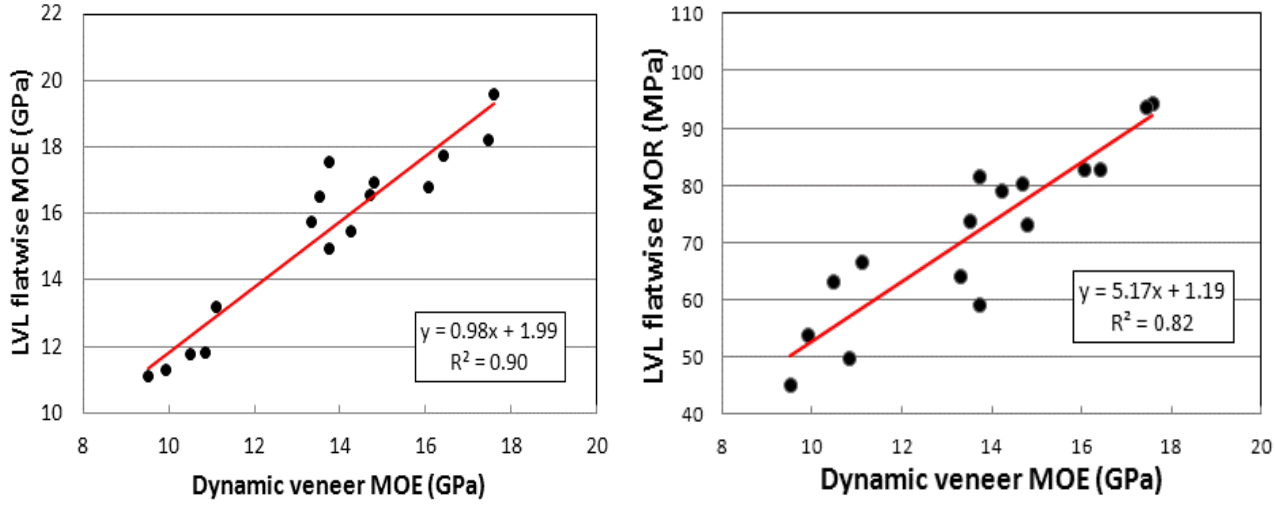

Figure 6.Correlation between larch LVL flatwise bending performance and veneer MOE

Conclusions

A significant variation existed in properties of Changbai larch veneer within each stand and population. The within-stand variation seemed to be higher than the between-stand variation. Comparing with Canadian second growth hemlock and amabilis fir, Changbai larch had significantly higher veneer density and UPT, and also higher veneer MOE. About 85% of the larch veneer from the four stands combined could be suitable for manufacturing 1.8E or higher grade commercial LVL. A high correlation was found between the larch LVL and veneerin terms of both edgewise and flatwise bending modes. The results demonstrate that Changbai larch is suitable for manufacturing LVL products with higher grade outturns, and the performance of larch LVL is predictable in relation to veneer E grade.

Acknowledgements

This work was part of a research program sponsored by the Special Overseas Cooperation Fund for Chinese Academy of Forestry (CAFYBB2008008) and the National Natural Science Foundation of China (No. 30825034). The authors would like to thank FPInnovations for their cooperation. We sincerely thank Dr. Rongjun Zhao, Dr. Xinting Xing, and research assistants Weiwei Shangguan and Yali Shao for their participation in sampling trees and conducting clear wood tests. We also thank Dr. Dongsheng Chen for providing stand information. We further thank the staff from Sanli Company for their help in veneer peeling and the management team at the Mengjiagang Forest Centre for their assistance in field work and log conversion.

References

China Standard Press. 2006. Laminated veneer lumber. GB/T 20241-2006. Beijing.

He, L., X. Wang, D. Zhao, C. Yan and L.C. Shi.2009. Research on classification by appearance of larch timber and vibration inspection tests. Forestry Machinery & Woodworking Equipment, 37(10), 24-26.

Huang, S.Y., B. J. Wang, J. Xiong, C. Dai and Y. Lei. 2012. Characterizing Changbai larch for veneer products. Part 1. Effect of stand density. BioResources. 7(2):2444-2460.

JAS SIS-24. 1993. Japanese agricultural standard for structural laminated veneer lumber.

Knudson, R. and B. J. Wang. 2002. Manufacture of LVL and plywood from short rotation hybrid poplar. Forintek Canada Corp. General Report- 2019. 90pp.

Knudson, R., B. J. Wang and L. Chen. 2002. Evaluation of Saskatchewan-grown hybrid poplar for veneer products and oriented strand board (OSB). Forintek Canada Corp. General Report-3533. 25pp.

Knudson, R. M., B. J. Wang and S. Y. Zhang. 2006. Properties of veneer and veneer-based products from genetically improved white spruce plantations. Wood and Fiber Sci. Vol. 38 (1): 17-27.

Li, F. S. 2001. Effect of cultivation measures on economic benefit of Larix olgensis pulp forest. J. For. Res. 12(3), 179-182.

Liu, Y. X. 2004. Compilation of properties and utilization of wood produced from Northerneast

part of China. Chemical Industry Press, Beijing.
Metriguard Inc. 2012. Veneer testers.http://www.metriguard.com/catalog/5%20-%2016%20Veneer%20Testers.pdf.
Sun, S. F. and Y. M. Pang. 2005. Study on management of pulpwood plantation of Larix Olgensis. Forest Resources Management (3), 51-54.
Wang, B. J. 2001. Characterizing aspen veneer for LVL/plywood products. Forintek Canada Corp. Report-2019. 16pp.
Wang, B. and C. Dai. 2001. Characterizing veneer stress grades for LVL/plywood products. In: Proceedings of Symposium on Utilization of Agricultural and Forestry Residues. Oct. 2001. Nanjing, P. R. China.270-276.
Wang, B. J. and C. Dai. 2005. Hot-pressing stress graded aspen veneer for laminated veneer lumber (LVL). Holzforschung 59(1), 10-17.
Wang, B. J. and C. Dai. 2006. Veneer grading strategies for LVL production. In: Proceedings of the 2nd International Symposium on Veneer Processing and Products. Vancouver. B. C. pp 263-275.
Wang, B. J., C. Dai, G. Middleton and D. Munro. 2010. Characterizing short-rotation coastal hemlock and amabilis fir veneer properties: preliminary results. Report to Coastal Forest Sector Hem-fir Initiative. FPInnovations-Wood Products. 23pp.
Wang, B. J. and C. Dai. 2012. Systematic resource characterization through veneering and non-destructive testing. Submitted to Wood and Fiber Science, 20 pp.
Zhang, J. H., S. G.Zhang, S. L.Shi, H. R.Hu, and S. Z. Zhang. 2004. Paper-making properties of Larix kaempferi pulpwood. Journal of Beijing Forestry University 26(5), 71-74.
Zhang, S.Y., Y. C. Lei and C. Bowling. 2005. Quantifying stem quality characteristics in relation to initial spacing and modeling their relationship with tree characteristics in black spruce (Picea mariana). Northern Journal of Applied Forestry, 22(2), 85-93.

Influence of Compression Treatment on the Surface Free Energy of Poplar Wood Calculated by Different Methods

Wending Li. [1] *– Yang Zhang*[2*] *– Yufei Wu*[3] *– Cong Liu*[4] *– Kien Nguyentrong*[5]

[1] Ph. D. student, College of Wood Science and Technology, Nanjing Forestry University, Nanjing, China.
wending15@163.com
[2] Professor, College of Wood Science and Technology, Nanjing Forestry University, Nanjing, China.
* *Corresponding author*
yangzhang31@126.com
[3] Associate Professor, College of Wood Science and Technology, Nanjing Forestry University, Nanjing, China.
[4] Ph. D. student, College of Wood Science and Technology, Nanjing Forestry University, Nanjing, China.
spriteno1@126.com
[5] Associate Professor, Wood Technology Faculty, Vietnam Forestry University, Hanoi, Vietnam
trkiennghia@yahoo.com

Abstract

The advancing contact angles of three test liquids on wood surface were used to determine the surface free energy (SFE) of compressed poplar wood with different compression ratios (CR), namely 12%, 25%, 34%, 48% and 58% and normal wood without compression. Four widely applied approaches for surface free energy and components of wood with compression treatment: critical surface tension approach (CST), geometric mean approach (GM), harmonic mean approach (HM) and acid-base approach (AB) was discussed. The surface free energy and components of poplar wood calculated by the four approaches were compared in this paper. The results show that the critical surface tension value (γ_c) increases slightly by increasing compression ratios of poplar wood and the maximum value is 70.4mJ.m^{-2} at CR of 48%. According to HM approach, compression treatment just changes the polar component of poplar wood. The Lifshitz – van der Waals component values (γ_s^{LW}) of wood compressed or not keep unchanged at 18.4 mJ.m^{-2}. The values of SFE of poplar wood calculated by the four methods vary greatly. The highest SFE value (γ_s)is

obtained by GM approach (96.1 $mJ.m^{-2}$), followed by CST approach (63.2 $mJ.m^{-2}$), HM approach (53.3$mJ.m^{-2}$) and AB approach (30.7$mJ.m^{-2}$).

***Keywords*:** Surface Free Energy, Compression Ratios, Mechanical properties, Component, Approach

Introduction

Wood is a complex material which is constituted by cellulose, hemicelluloses, lignin and extractives and has a heterogeneous, rough and even porous surfaces. Compression treatment will not only enhance physical and mechanical properties of wood materials, such as modulus of elasticity, shear strength, tensile /compressive strengths, surface hardness, abrasion resistance and thermal conductivities, but also improve its surface characteristics(Asako et al. 2002, Büyüksar 2012, Bekhta et al.2009). Surface properties plays an important role on depth of penetration of adhesive into the wood, uniform distribution of adhesive and bonding quality between veneer sheets. Büyüksar determinated the wettability of panels produced from thermally compressed wood veneer at 200℃ and found the contact angle increased due to chemical changes such as degradation of the most hygroscopic compounds(Büyüksar 2012).

Surface free energy is an important parameter in evaluating chemical properties of solid materials surfaces and represents a measure of the material wettability(Cerne et al.2008). It reflects the state of imbalance in intermolecular interactions present at the phase boundary of two mediums and is increasingly used as a measure of adhesive properties in gluing, painting, lacquering, especially in area of wood-based composites(Rudawska et al. 2009). A number of theories for the calculation of surface free energy have been applied to wood(Gindl et al. 2001), i.e. critical surface tension approach (CST), geometric mean approach (GM), harmonic mean approach(HM), and acid–base approach (AB).

Currently, there is no information on surface free energy of wood with compression treatment in the literature. In this paper, five compression ratios of poplar wood, namely 12%, 25%, 34%, 48% and 58% and normal wood without compression were considered. The objective is to calculate the surface free energy of poplar wood using the four approaches and to analyze their differences of compression treatment statistically.

Materials and Methods

Materials. Poplar wood (*populus euramevicana cv. 'I-214'*) is taken from a piece of veneer stored under controlled conditions of temperature and humidity (20℃/65% RH). Six samples are cut from this veneer with dimensions of 10cm ×10cm× 2mm. Each sample is sanded (grit 500), firstly 20 times perpendicular to the grain and then 20 times parallel to it. Then, five kinds of samples are prepared, compressed with compression ratios (CR) of 12%, 25%, 34%, 48% and 58% respectively and normal wood without

compression. At last, nine specimens are tailored from each sample with dimensions of 3cm ×1cm.

Contact angle measurements. To calculate the surface free energy of wood reliable, measurement of contact angle are performed using three or more testing liquids with known properties: distillated water, n-hexane (99.6%, Nanjing Chemical Reagent Co. Ltd. Nanjing), glycerol (99.0%, Tianjin Damao Chemical Reagent Co. Ltd.).The testing liquid surface tensions and their components are presented in Table 1.The contact angle is defined as the angle between solid surface and a tangent, drawn on the drop-surface, passing through the triple-point atmosphere–liquid–solid. The contact angles are determined using a tensionmeter (Sigma 701, KSV, Finland). We use Wilhelmy plate method to measure the contact angle of specimens.

Table 1 Data of surface tension and components of test liquids at 20 ℃ (mJ.m^{-2})

Test liquids	γ_L	γ_L^d	γ_L^p	γ_L^+	γ_L^-
Water	72.8	21.8	51	25.5	25.5
n-Hexane	18.4	18.4	0	0	0
Glycerol	64.0	34.0	30.0	3.9	57.4

Subscript letter L indicates liquid. γ_L, surface tension, γ_L^d, dispersed component, γ_L^p, polar component, γ_L^+, electron-acceptor (polar), γ_L^-, electron-donor component (polar).

The specimens are suspended from the electronic microbalance (precision 1 μN) and move in and out of the test liquids at a speed of 1mm.min^{-1}. The force acting on the balance is continuously measured. Advancing and receding contact angles are obtained from immersion and emersion, respectively. The contact angle (θ) is calculated according to Equation (1),

$$F - F_b = 2(l + d)\gamma_L \cos\theta \quad (1)$$

where F is the measured vertical force, F_b is the buoyancy force, l and d is the length and thickness of a specimen, and γ_L is the surface tension of test liquid.
The contact angles determined with each test liquid on three specimens with same compression treatment are measured.

Calculation of surface free energy. The fundamental formulation of determining the surface free energy a solid is the Young equation (2),

$$\gamma_L \cos\theta = \gamma_S - \gamma_{SL} \quad (2)$$

where γ_L is the surface tension of test liquid, θ is the contact angle, γ_S is the surface free energy of the solid and γ_{SL} is the solid/liquid interfacial energy(Luan et al. 2011).

Among the various possible thermodynamic approaches to determine γ_S and γ_{SL}, the most important methods represented by critical surface tension approach (CST), geometric

mean approach (GM), harmonic mean approach (HM) and acid–base approach (AB) has been selected for this study.

Critical surface tension approach. The major historical step in contact angle research is Zisman(Zisman 1963). Contact angles of a homologous series of liquids that consists of dispersive polar and nonpolar test liquids on many different low-energy solids are measured. A plot of $\cos\theta$ versus γ_L is generated and a linear fit for the same is obtained. By extrapolating the linear curve to $\cos\theta$=1, the values of critical surface tension (γ_C) of wetting can be obtained according to Equation (3),

$$\gamma_C = \gamma_L + \frac{\cos\theta - 1}{b} \quad (3)$$

where b is slope of the regression line.

Geometric mean approach. The geometric mean approach was developed by Owens-Wendt(Rossi et al. 2012). The total surface free energy γ_S is divided into a dispersed (γ_S^d) and polar (γ_S^p) component according to the formula $\gamma_S = \gamma_S^d + \gamma_S^p$. The interfacial tension between a solid and a liquid is evaluated by the geometric mean equation according to Equation (4),

$$\gamma_{SL} = \gamma_S + \gamma_L - 2(\sqrt{\gamma_S^d \gamma_L^d} + \sqrt{\gamma_S^p \gamma_L^p}) \quad (4)$$

where γ_{SL} is the solid/liquid interfacial energy. γ_L is the surface tension of test liquid, γ_S^d and γ_S^p is the dispersed and polar component of surface free energy of the solid, respectively, γ_L^d and γ_L^p is the dispersed and polar component of surface tension of test liquids, respectively.

Owens-Wendt combined Equation (4) with Equation (2), which gives the following Equation (5),

$$\gamma_L(1+\cos\theta) = 2(\sqrt{\gamma_S^d \gamma_L^d} + \sqrt{\gamma_S^p \gamma_L^p}) \quad (5)$$

where θ is the contact angle.

To obtain the values of γ_S^d and γ_S^p of a solid, the contact angle θ of at least two test liquids with known surface tension components on the solid must be measured.

Harmonic mean approach. It was proposed by Wu that the interfacial energy (γ_{SL}) between a liquid and a solid can be evaluated by the harmonic mean equation as follows(Wu 1971):

$$\gamma_{SL} = \gamma_S + \gamma_L - \frac{4\gamma_S^d \gamma_L^d}{\gamma_S^d + \gamma_L^d} - \frac{4\gamma_S^p \gamma_L^p}{\gamma_S^p + \gamma_L^p} \quad (6)$$

Similar to geometric mean approach , the dispersed (γ_S^d) and polar (γ_S^p) components of surface free energy of the solid can be calculated by Equation (7) which is from combining Equation (6) with Equation (2).

$$\gamma_L(1+\cos\theta) = \frac{4\gamma_S^d \gamma_L^d}{\gamma_S^d + \gamma_L^d} + \frac{4\gamma_S^p \gamma_L^p}{\gamma_S^p + \gamma_L^p} \quad (7)$$

***Acid–base approach*.** In this approach, the surface free energy is regarded as the sum of a Lifshitz–van der Waals component γ^{LW} and acid–base component γ^{AB}. The acid–base component γ^{AB} can be further subdivided according to Equation (8),

$$\gamma^{AB} = 2\sqrt{\gamma^+ \gamma^-} \quad (8)$$

where γ^+ is the electron–acceptor parameter of the acid–base surface free energy component or Lewis acid parameter of surface free energy and γ^- is the electron–donor parameter of the acid–base surface free energy component or Lewis base parameter of surface free energy (Gindl et al. 2001) .The approach for surface free energy component of solid is given by Equation (8),

$$\gamma_L(1+\cos\theta) = 2\sqrt{\gamma_S^{LW}\gamma_L^{LW}} + 2\sqrt{\gamma_S^+\gamma_L^-} + 2\sqrt{\gamma_S^-\gamma_L^+} \quad (9)$$

In order to get the surface free energy components (γ_S^{LW}) and parameters (γ_S^+ and γ_S^-) of a solid, the contact angles of at least three liquids with known surface tension components of γ_L^{LW} , γ_L^+ and γ_L^- have to be determined.

Results and Discussion

Influence of compression treatment on contact angle. From the Wilhelmy plate method, both advancing and receding contact angles can be obtained by immersion and emersion of the specimens. The advancing contact angles determined with three test liquids on the poplar wood treated with different compression ratios are given in Table 2.

Table 2 Contact angles for test liquids measured on specimens treated with different CR

CR(%)	Advancing contact angle(degree)					
	Distillated water		n-Hexane		Glycerol	
	x[a]	S[b]	x	S	x	S
0	60.7	0.26	_	-[c]	112.7	1.13

12	75.0	1.80	_-	118.9	4.45
25	61.0	4.84	_-	114.8	1.12
34	78.3	5.14	_-	111.3	2.09
48	60.6	0.98	_-	117.7	3.00
58	91.1	2.73	_-	138.5	1.14

[a] Mean value. [b] Standard deviation. [c] Advancing contact angle is not obtained.

Hexane is a low energy liquid and can penetrate into the porous structure of the wood, which prevented us from obtaining the contact angle measurements(Asako et al. 2002). The receding contact angles determined on the specimens are zero degree for all liquids, due to the phenomena of contact angle hysteresis(Gindl et al. 2001). We attribute this pronounced contact angle hysteresis to swelling behavior and surface roughness(Shang et al.2008). A one-way analysis of variance (ANOVA) identifies that the influence of compression ratios on contact angles for distillated water and glycerol are both highly significant (probabilities (P) < 0.01). The contact angles obtained with glycerol are significantly bigger than obtained with distillated water correspondingly (Table 2).

Influence of compression treatment on surface free energy. Figures1, 2, 3, and 4 show the surface free energy and components values of poplar wood, which are treated with different compression ratios and calculated by four approaches, respectively. From one-way ANOVA, the probabilities (P) are all appreciably lower than 0.01, thus implying that the observed differences are highly significant.

Critical surface tension approach (CST) is based on a single-probe liquid approach in which only the total surface tension of liquid is considered as the required parameter to obtain the surface free energy of a solid. Critical surface tension value (γ_C) of the solid is not the surface free energy, but only an empirical parameter related closely to this quantity(Gindl et al. 2001, Ahadian et al. 2009). Zisman found that the bigger γ_C of a solid is, the more liquids can spread on its surface, the better wettability of the solid(Zisman 1963, Wu 1979). In this research, the value of γ_C increases slightly by increasing compression ratio and the maximum value is 70.4mJ.m^{-2} at CR of 48%, due to densification occurring in the surface of wood. The average improvement on critical surface tension with increasing CR were 0.5%, 3.7%, 3.9%, 11.4% and 5.0% corresponding to CR of 12%, 25%, 34%, 48% and 58%, respectively, in comparison to the normal wood specimen (Fig. 1). Dispersed and polar component can't be calculated by critical surface tension approach.

The geometric (GM) and harmonic mean (HM) approaches are very similar. The dispersed and polar components of liquid surface tension are considered in the calculations. Figure 2 shows the total surface free energy γ_S, dispersed components γ_S^d and polar components γ_S^p of poplar wood corresponding to the compression ratio using geometric mean approach (GM). The γ_S, γ_S^d and γ_S^p of normal wood specimens are 96.1mJ.m^{-2}, 93.9mJ.m^{-2} and 2.16 mJ.m^{-2}, respectively. It shows predomination of dispersed component of poplar wood. With increasing of the compression ratio, γ_S decreases slightly until CR of 25% and follows by a mild increase until the end of the testing. The standard deviations of these values are very big. The dispersed component

γ_S^d decreases linearly and sharply to 22.1 mJ.m^{-2}, corresponding to the CR of 58% (correlation coefficients R^2=0.903). On the contrary, polar component γ_S^p increases linearly with the increase of CR (R^2=0.950) (Fig. 2).

The values of total surface free energy γ_S and of their components γ_S^d and γ_S^p calculated by harmonic mean approach (HM), are showed in Figure 3. It is clear from Figure 3 that the better second polynomial fit are obtained for γ_S and γ_S^p (R^2=0.958 and R^2=0.939, respectively). Both the γ_S and γ_S^p show raised trend in the beginning and gentle trend afterwards increasing with the CR. This may be due to the fact that as the roughness of wood decrease with the increasing CR of poplar wood, the wood-liquid interfacial contact area increases which leads to a improvement of the wettability (Selvakumar et al. 2010). Nevertheless, the γ_S^d basically maintains constant from 10.1 mJ.m^{-2} to 7.1 mJ.m^{-2}. So we can infer that compression treatment of poplar wood just changes the polar component based on harmonic mean approach.

To the three-probe liquids method, as a product of γ_S^+ and γ_S^- of surface free energy,the polar component of γ_S^{AB} can be used in treating the contribution of acidic and basic character to the adhesion across an interface(Gindl et al. 2001). Figure 4 displays the changes in the total surface free energy (γ_S), the Lifshitz-van der Waals component γ_S^{LW}, the acid-base component γ_S^{AB} (concludes electron-acceptor parameter γ_S^+ and electron-donor parameter γ_S^-) that were obtained using acid–base approach (AB). Like GM approach, the values of γ_S and γ_S^{AB} calculated by AB approach both decrease slightly until at CR of 25% (19.5mJ.m^{-2} and 1.1 mJ.m^{-2}, respectively) and follow by a mild increase until the end of the testing with the increasing of CR (Fig. 4). However, all the values of γ_S calculated by AB approach are 60% lower than by GM approach correspondingly. The values of γ_S^{LW} keep unchanged at 18.4 mJ.m^{-2} with increasing of CR. The values of γ_S^+ are very low (less than 1.0 mJ.m^{-2}) and alter slightly. On the contrary, it shows predomination of electron-donor component γ_S^- (even higher than γ_S) and presents raised trend of γ_S^- from 64.1 mJ.m^{-2} to 126.1mJ.m^{-2} with increasing of CR (Fig. 4).

Comparision of different approaches. The values of γ_S, γ_S^d (or γ_S^{LW}), γ_S^p (or γ_S^{AB}), γ_S^+ and γ_S^- of normal poplar wood without compressed using above four approaches, are compared in Figure 5.The highest value of γ_S is calculated by GM approach (96.1 mJ.m^{-2}), followed by CST approach (63.2 mJ.m^{-2}), HMapproach (53.3mJ.m^{-2}) and AB approach (30.7mJ.m^{-2}).

The value of γ_S calculated by the GM approach is 80% higher than by the HM approach and its standard deviation is much bigger than other approaches. The γ_S^d is predomination component (accounted for 98% of γ_S) by GM approach , while γ_S^p is the predomination componen(accounted for 80% of γ_S) by HM approach(Fig. 5). The difference between GM and HM approach is that the former utilizes a linear relationshipfor determining γ_S,

γ_S^d and γ_S^p respectively, whereas HM approach basically uses a non-linear relationship(Ahadian et al. 2009).

Using the acid-base approach for the calculation of the surface free energy, the value of γ_S is lower than other approaches. The dispersed component (γ_S^d or γ_S^{LW} =18.4mJ.m^{-2}) is larger than the acid-base component (γ_S^p or γ_S^{AB} =12.3mJ.m^{-2}). According to acid-base approach, poplar wood represents a monopolar surface with fact that electron-donor component (64.1 mJ.m^{-2}) is much stronger than the electron–acceptor component (0.6 mJ.m^{-2}).

Conclusions

In this study, the SFE values and its components of poplar wood were obtained using four methods, namely critical surface tension approach (CST), geometric mean approach(GM), harmonic mean approach (HM) and acid-base approach(AB). The influence of compression treatment on the SFE of poplar wood was also discussed. The γ_C value of poplar wood increases slightly by increasing CR and the maximum value is 70.4mJ.m^{-2} at CRs of 48%.GM approach gives higher values for SFE compared to other approaches. With increasing of the CR, γ_S decreases slightly until at CR of 25% and follows by a mild increase while the γ_S^d decreases linearly to 22.1 mJ.m^{-2} at CR of 58%. According to HM approach, both the γ_S and γ_S^p show raised trend in the beginning and gentle trend afterwards increasing with the CR. Also, we can infer that compression treatment just changes the polar component of poplar wood. All the γ_S values calculated by AB approach are much lower than by GM approach correspondingly. The γ_S^{LW} values keep unchanged at 18.4 mJ.m^{-2} with poplar wood compressed or not.

To normal poplar wood, the values of SFE calculated by the four methods vary greatly. The highest value of γ_S is calculated by the GM approach (96.1 mJ.m^{-2}), followed by CST approach (63.2 mJ.m^{-2}), HMapproach (53.3mJ.m^{-2}) and AB approach (30.7mJ.m^{-2}). γ_S^d is the predomination component (accounted for 98% of γ_S) by GM approach , while γ_S^p is the predomination componen (accounted for 80% of γ_S) by HM approach.

Acknowledgments

This work was supported by the funding of forest science and technology transfer for State Forestry Administration (2010 No.33) and the funding of industrialization transfer from scientific achievements of the university in Jiangsu province (JH10-15).

References

Y. Asako, H. Kamikoga, H. Nishimura, and Y. Yamaguchi. 2002. Effective thermal conductivity of compressed woods. International Journal of Heat and Mass Transfer 45: 2243-2253.
Ü. Büyüksar. 2012. Surface characteristics and hardness of MDF panels laminated

with thermally compressed veneer. Composites Part B.
P. Bekhta, S. Hiziroglu, and O. Shepelyuk. 2009. Properties of plywood manufactured from compressed veneer as building material. Materials and Design. 30:947-953.
L. Cerne, B. Simoncic, and M. Zeljko. 2008. The influence of repellent coatings on surface free energy of glass plate and cotton fabric. Applied Surface Science. 254: 6467-6477.
A. Rudawska, E. Jacniaka. 2009. Analysis for determining surface free energy uncertainty by the Owen–Wendt method. International Journal of Adhesion & Adhesives. 29: 451-457.
M. Gindl, G. Sinn, W. Gindl, A. Reiterer, and S.Tschegg. 2001. A comparison of different methods to calculate the surface free energy of wood using contact angle measurements. Colloids and Surfaces, A: Physicochemical and Engineering Aspects. 181:279-287.
Z. J. Luan, Y. Wang, F. Wang, L. Y. Huang, and L. Meng. 2011. The surface free energy of pyrite films prepared by sulfurizing the precursive electrodeposited films. Thin Solid Films. 519:7830-7835.
W. A. Zisman, Ind. Eng. Chem. 55,19(1963).
D. Rossi, S. Rossi, H. Morin, and A. Bettero. 2012. Within-tree variations in the surface free energy of wood assessed by contact angle analysis. Wood Science Technology. 46: 287-298.
S. Wu, J. Polym. Sci. Part C. 34, 19(1971).
J. Y. Shang, M. Flury, J. B. Harsh, and R. L. Zollars, J.Colloid Interface Sci. 328, 2(2008).
S. Ahadian, M. Mohseni, and S. Moradian. 2009. Ranking proposed models for attaining surface free energy of powders using contact angle measurements. International Journal of Adhesion & Adhesives. 29: 458-469.
S. Wu, J. Collid Surf. Sci. 605, 71(1979).
N. Selvakumar, H. C. Barshilia, and K. S. Rajam. 2010. Effect of substrate roughness on the apparent surface free energy of sputter deposited superhydrophobic polytetrafluorethylene coatings: A comparison of experimental data with different theoretical models. Journal of Applied Physics. 108, 013505.

Sustainable Chemistry in Wood Transformation

Tatjana Stevanovic

Wood Sciences and Forestry Department, Laval University, Quebec, Canada

Phone: 1-418-656-2131 ext 7337

Fax: 1-418-656-2091

e-mail: Tatjana.Stevanovic@sbf.ulaval.ca

Abstract

Wood Chemistry is fundamental to the future developments related to forest biorefinery. The idea is to transform forest biomass as completely as possible into innovative chemical products, fuels and/or energy. Wood Chemistry is sustainable as it harbors the principles of green chemistry. Future forest biorefineries will function at first as integrated, which means that the valorization of the by- products will be integrated in the existing pulp or sawmills. The huge quantities of bark produced by forest industry are no longer regarded as wastes, but rather as important by-products, the extraction of which can produce valuable bioactive molecules which could serve to design innovative foodstuffs, pharmaceuticals and cosmeceuticals. The example of extraction of black spruce (*Picea mariana)* bark developed in our laboratory is used to demonstrate integration of several sustainable chemistry and engineering principles in that context. Wood welding is an innovative new technology for bonding solid wood without adhesives. Our results on rotational dowel welding of two Canadian hardwood species (sugar maple and yellow birch) indicate the possibility to produce laminated timber assembled only with wood dowels. This technology relies on wood chemistry, as the friction between wood slat and wood dowel rotating at high speed causes the thermal transformation of wood components, the products of which solidify and bond two pieces, once the pressure is released. The dowel welded wood panels produced by this technology without adhesives or metal parts are suitable for furniture application and are easily and completely recyclable. The gases released in minimal quantities by wood welding are not harmful to human health. This technology includes several principles of sustainable (green) chemistry and sustainable engineering. The public awareness of environmental and health implications related to wood transformation will definitely cause a shift towards sustainable wood transformation based on principles of green chemistry and sustainable engineering.

Keywords: sustainable, wood chemistry, bioactive forest extractives, biorefinery, wood welding, dowel-welded panels, sustainable engineering

Introduction

The principles of sustainable or green chemistry represent guidelines for the sustainable development of wood transformation which has entered a new era in which every atom counts. Let us start by citing the definition of sustainable chemistry such as presented at the official site of EPA (Environmental Protection Agency) [1]:

"Green chemistry also known as sustainable chemistry, is the design of chemical products and processes that reduce or eliminate the use or generation of hazardous substances. Green chemistry applies across the life cycle of a chemical product, including its design, manufacture, and use.**",** Inspired by these principles, the same author (Anastas) has presented the 12 principles of green engineering into which wood engineering is perfectly integrated.

One of the 12 sustainable chemistry principles [2], as published by American Chemical Society (ACS): **Prevention Instead of Treatment** : It is better to prevent waste than to treat or clean up waste after it is formed, has been making part of wood transformation practices for a long time, to the point that the word waste has silently disappeared and replaced by "residue". Sawdust, shavings, small diameter wood etc.- represent the examples of use as feedstock for panel and pulp and paper industries for a long time. The wood engineering practices have moved yet another step further by adopting the biorefinery concept of wood transformation as a holistic approach to forest biomass transformation. In that sense the sustainable engineering principle: **Integrate Material and Energy Flows**: Design of products, processes, and systems must include integration and interconnectivity with available energy and materials flows, has been adopted in many examples of biorefinery concept applied to forest resources. The co-generation of energy by combustion of the residues within the same mill is a common practice now; the multiple projects on cellulosic ethanol or production of nano-cellulose from highly purified chemical pulp are under development or pyrolysis of forest biomass for production of biofuels, to name just some of them. The good knowledge of wood chemistry is essential for all further developments and design of innovative products by wood industry within the biorefinery concept. One of such examples where the fundamental knowledge of wood chemistry was essential for developments is certainly the nano-cellulose and the large number of its possible applications, all of which fundamentally repose on the supramolecular structure of cellulose I, the information gained through wood chemistry (and physics) studies of cellulose in its native state. The studies in the field of lignin chemistry have allowed progress in chemical pulping technologies which are yielding various types of industrial lignins some of which are being studied and developed for applications in materials. The wood chemistry studies have also provided indispensable information about hemicelluloses of cell walls which is inspiring new developments related to their application in materials or as sources of chemicals and fuels. Finally, the huge body of knowledge is now available about the substances extraneous to cell walls which are loosely distributed in the porous structure of wood and therefore available to different solvent systems, for which they are named wood extractives. Wood extractives represent certainly the most complex category of wood constituents and despite the small quantities in which they are typically present (rarely exceeding 5% of o.d. temperate zone woods) they are determining several physico-chemical and technological properties of wood. Their amazing structures and properties related to their bioactivities have inspired numerous studies and are stimulating the ongoing research in my laboratory.

Wood transformation is inherently applying several principles of green chemistry and green engineering, of which the following: **Renewable RatherThan Depleting**: Material and energy inputs should be renewable rather than depleting, is so obviously applied at all times. Dealing with a renewable material such as wood, our industry is applying this principle to a large extent and it should secure its position in all future developments. I shall describe here two processes of innovative wood transformation and how the sustainable (green) chemistry and engineering principles apply to them. One is about the phenolic extractives from residues of wood transformation and the other is about the innovative technology of welding solid wood without adhesives.

Extraction Of Bioactive Molecules And Forest Biorefinery

In the first part of this presentation I should like to make a case that the sustainable engineering principle: **Design for Separation and Purification Operations**: should be designed to minimize energy consumption and materials use, is applied along with the green (sustainable) chemistry principle: **Atom Economy:** Design (synthetic) methods to maximize the incorporation of all materials used in the process into the final product, are applied in the processes of the forest biomass extraction. We shall explore here a specific way to contribute to the atom economy by saving the bioactive molecules available from wood transformation residues (such as bark, the residue of wood transformation most readily available and in most important quantities) through extraction, followed by the design of innovative bio=products based on the extracts and their fractions and /or constituents.

We have been studying the bark extractives available from commercial wood species of Canada for more than a decade now and we consider that there is a real potential to integrate the extraction as part of the biorefinery concept into some of the existing wood transformation mills, the sawmills representing the good candidates as they make part of primary transformation of wood. Such integration would consist of implementing the extraction with green solvents (primarily water and ethanol) of residual bark remaining after wood transformation, the most abundant industrial residue available, in order to produce an extract containing bioactive molecules which would be applicable for design of high value products. The extracted bark would still be available as source of fibers or for the energy production, the latter being its most important current use in Quebec and Canada. This would make a perfect example of application of sustainable chemistry principles by saving the atoms in the molecules so ingeniously synthesized by nature and by applying the simple extraction and separation procedures and green solvents such as water or ethanol, thus respecting the previously discussed sustainable engineering principle. To illustrate such a concept we shall present the results available so far for black spruce (*Picea mariana*) bark and its aqueous extract rich in polyphenols.

Black spruce (*Picea mariana* (Miller) B.S.P) is one of the most important industrial species from Canadian forests and its bark is available in huge quantities as a result of wood transformation. We have demonstrated recently that the hot water extract from black spruce bark has important antioxidant and anti-inflammatory properties which could qualify this extract as natural product available for design of applications such as antioxidants of natural (plant) origin (versus synthetic antioxidants, the toxicity of which has been questioned), as the first example (Diouf *et al.*, 2009) [4]. In another investigation, this extract was further characterized and it was determined that it had a high content of total phenols and flavonoids as well as a low toxicity on normal human keratinocytes and an adequate chemical reactivity towards different free radicals involved in

psoriasis, a skin disorder affecting up to 2 % of the world's population (Garcia-Perez *et al.*, 2010) [5], which could be a basis for a potential very high value pharmaceutical application of the water extract of black spruce bark and its fractions. All these results taken together indicate the water extract of black spruce bark as a valuable source of bioactive molecules.

Given the fact that the crude water extract is composed of several families of water soluble molecules, we have decided to fractionate it further in order to enhance its biological activity and to identify and characterize the major constituents of ethyl-acetate fraction, since it is particularly rich in polyphenols. The results on the identification of the molecules present in this fraction demonstrate that it is composed mainly of lignans, neolignans, cinnamic acids, flavonoids and stilbenes, along with minor quantities of other phenols and terpene derivatives (Garcia-Perez et al., 2012) [6]. The most important constituents of the ethyl-acetate fraction determined by combination of physico-chemical methods (chromatographic separation, UV, optical activity determination) and ^{1}H and ^{13}C NMR spectroscopy analyses are presented in Figure 1.

l

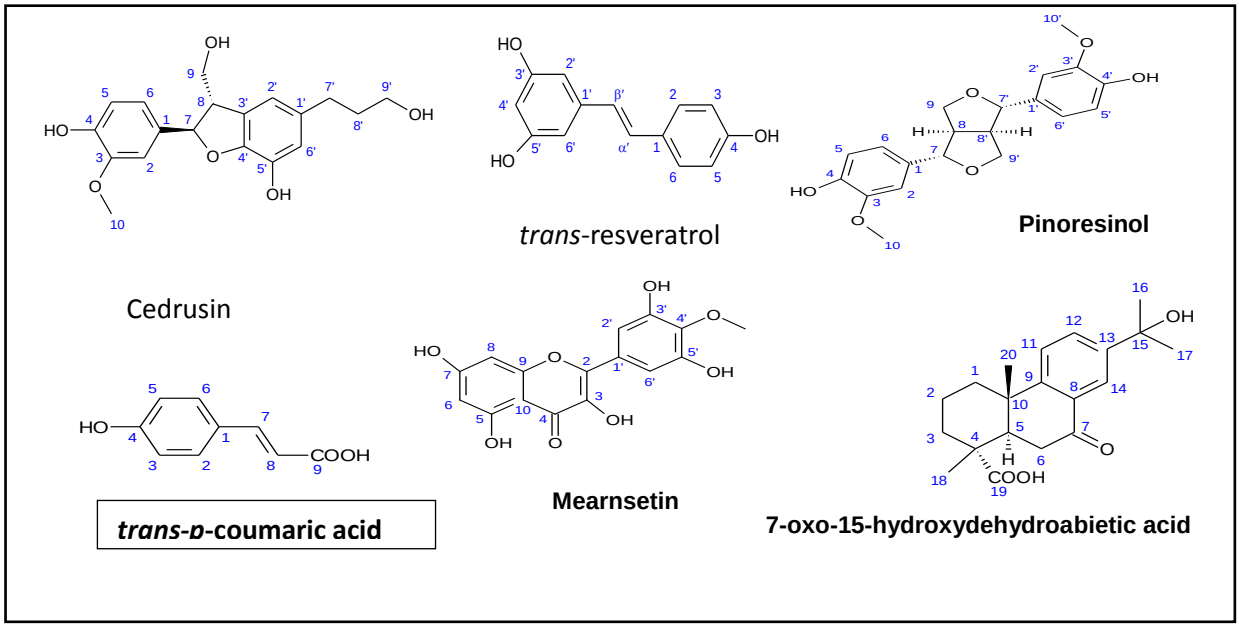

Figure 1: The major constituents of the ethyl acetate fraction of water extract of black spruce (*Picea mariana*) bark (from [6])

Interestingly, one of the major constituents determined in this fraction of the black spruce bark water extract is the stilbene resveratrol, the common constituent of grapes and wines, chocolate and peanuts, which confirms therefore our point that the forest and agricultural resources belong to the same world (Stevanovic *et al.*, 2009) [7]and that there is an evident need that these two sectors exploit better their synergy. The concentration of *trans*-resveratrol calculated on oven dry mass of black spruce bark is 109 □g/g, while its concentration in grapes is only 40□ □g/g, which makes black spruce bark an interesting alternative source of this valuable bioactive molecule (Garcia-Perez *et al.*, 2012) [6].

These results have inspired our recent study in which we explored the water extract of black spruce bark obtained on a larger scale in order to compare its properties with those of the extract obtained in laboratory. The hypothesis of our study was that the extract obtained on the larger

scale would essentially preserve the qualities of the laboratory studied one and that it would be non-toxic when tested by acute oral toxicity test performed on Sprague- Dawley rats. Indeed, the results obtained in that study (results not yet published) have confirmed the same chromatographic profile and the comparable contents of the total phenols constituents in the extract obtained on laboratory and larger scale. The acute oral toxicity test performed with the crude water extract of black spruce (*Picea mariana*) bark on rats has shown that the crude extract in form of powder does not have any adverse effects. All these results taken together indicate the real potential of innovative bio-products based on application of the water extract of black spruce bark and of its fractions as natural health products, antioxidants, as food supplements, pharmaceuticals or as ingredients of novel cosmetic products.

Sustainable Production Of Laminated Wood Panels By Rotational Dowel Welding

Rotational wood-dowel welding has been shown to rapidly produce wood joints of considerable strength without any adhesive. This technique represents an opportunity to increase productivity, reduce costs of the furniture production, eliminate the need for synthetic adhesives of petrochemical origin and significantly reduce (eliminate) the time required for the gluing process. The following principles of sustainable chemistry and engineering are evidently applied here: **Use of Renewable Feedstocks**: Use renewable raw material or feedstock rather whenever practicable, and **Maximize Efficiency**: Products, processes, and systems should be designed to maximize mass, energy, space, and time efficiency, and finally the sustainable engineering principle-**Minimize Material Diversity**: Material diversity in multicomponent products should be minimized to promote disassembly and value retention, are evidently applied.

The objective of the study was to define optimal wood-dowel welding parameters for two North American hardwood species frequently used for indoor appearance products: sugar maple (*Acer saccharum*) and yellow birch (*Betula alleghaniensis*). Optimized parameters for individually studied species were determined using a rotational wood-dowel welding machine specially designed for the needs of the project. A comparative analysis of wood-dowel welding parameters was performed. The investigated parameters for two studied wood species were grain orientation, rotational speed and insertion speed. Temperature profile measurements at the interface during rotational wood-dowel welding were also carried out and the maximum temperature in the welding zone was measured. That temperature was used in the study of the gases released in form of fume observed in the process of welding. Optimal welding mechanical properties were determined from the dowel withdrawal strength test, using a standard tensile strength test. Results revealed a significant interaction between species, rotational speed, and insertion speed (Belleville et al., 2012) [8]. Sugar maple produced wood joints with higher withdrawal strength than yellow birch. The best results for sugar maple and yellow birch were obtained with a rotational speed of 1000 RPM. A 25 mm s^{-1} insertion speed produced significantly stronger welded joints in sugar maple than at 12.5 mm s^{-1}. For yellow birch, a 16.7 mm s^{-1} insertion speed provided the best results. Both wood species and rotational speed had a significant effect on maximum temperature at the interface during welding. Peak welding temperatures measured with optimal parameters were determined to be 244˚C and 282˚C for sugar maple and yellow birch, respectively. To prepare panel specimens, 25x30x225 mm slats of sugar maple and yellow birch wood were cut from clear wood material. For each panel, 12 slats were attached by 96 wood-welded dowels (always matching the wood species of the slats) to assemble a 30x 225x300 mm panel, as illustrated in Figure 2.

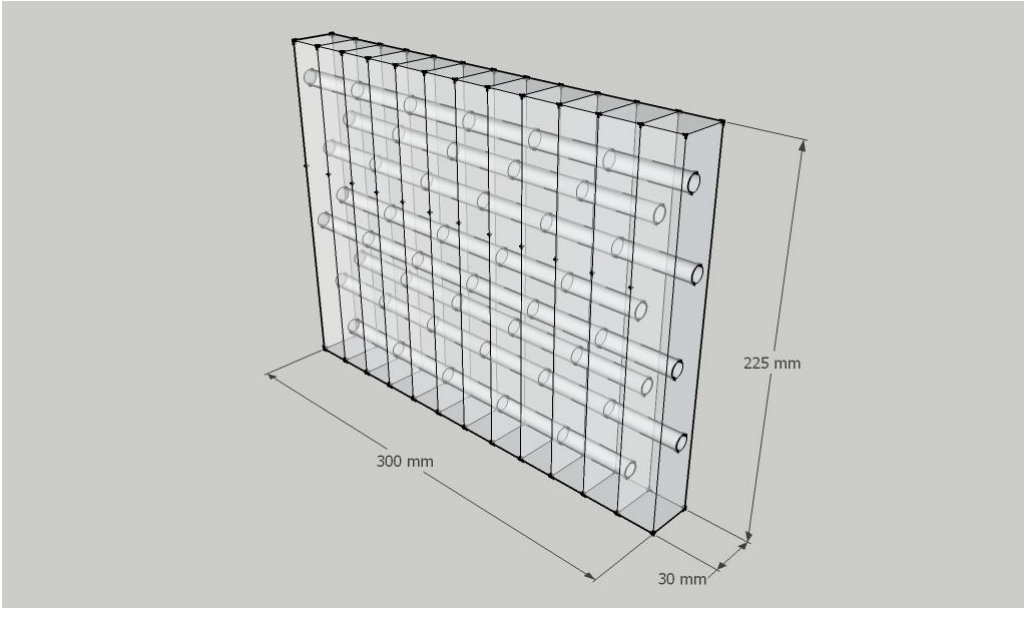

Figure 2 Scheme of a dowel-welded panel (Belleville et al., 2012 [9])

The optimal welding parameter sets were applied for the fabrication of the panels from each wood species, based on the results of our previous study (Belleville et al. 2012) [8]: 1000 rpm rotational speed and 25 mm s^{-1} insertion rate for sugar maple, and 1000 rpm and 16.7 mm s^{-1} for yellow birch.

Plain-shank dowels of sugar maple and yellow birch wood, 9.68 mm in diameter and 96 mm in length, were commercially manufactured by a local supplier. Dowels were welded by inserting them into pre-drilled holes 7.67 mm in diameter and 50 mm deep into two adjacent slats. The same species was used for each dowel and slat combination as mentioned previously and illustrated in Figure 3.

Figure 3. Cross section of wood dowel welded through two wood slats (Belleville et al., 2012) [9].

Rotational wood-dowel welding offers a promising alternative for panelling applications in the furniture industry. Friction between the dowel and substrate during insertion (less than 3 s) combined with high-speed dowel rotation causes the temperature to rise, which induces the thermochemical transformations of lignin and carbohydrates (hemicelluloses in particular) which provide "molten" material which upon the release of pressure solidifies and ultimately induce the wood to weld. The usual adhesive used in hardwood panelling is polyvinyl acetate (PVA), which requires long curing time (up to 24 hours) and multiple handling. These constraints limit the production flow and flexibility required for customized production. Dowel wood welding in addition to improving the efficiency of production, reduces the use of petrochemicals and is therefore contributes to lowering of production costs. Our study of gases released in fume occurring during welding has proven that no toxic or otherwise health harmful gases are released (unpublished results). Rotational wood-dowel welding of North American wood species provides a promising alternative to gluing. The results confirm that wood-dowel welding could be suitable for producing panels from certain North American species. The technique could help improve production flow and flexibility by eliminating long curing times for adhesive polymerization as well as multiple handling. Moreover, manufacturers would no longer need to buy or store petrochemically derived adhesives. Furthermore, because welded panels are made entirely of wood, they are also fully and easily recyclable. We also studied the adhesion mechanisms in wood-to-wood welding by analysing the material collected from the welding zone by Py-GC-MS, XPS and FT-IR. It appears that the welding mechanism could be related to the mechanisms involved in fast pyrolysis, characterized by high pressures applied which are limiting the availability of the oxygen at the interface. Rapid quenching, at the moment of the pressure release and interruption of rotation, may "freeze" the intermediate degradation products of fast pyrolysis. During welding, the wood cells adjacent to the connected surfaces collapse due to frictional forces and the generated heat enhances the decomposition of wood components. The results of our investigation indicate that thermal treatment of birch and maple wood degrades hemicelluloses through acid hydrolysis and dehydration mechanism and affects lignin polymer through depolymerisation reactions. Although lignin appears to be a major contributor to wood welding, we have also determined the increased amounts of polysaccharide-derived products in the welding zone. We have clearly demonstrated the importance of wood species, and therefore of its wood chemistry, for chemical changes occurring at the welding interface during wood-dowel welding, which could explain, at least in part, the better mechanical performance of welded maple compared to birch.

The results on identification of gases emitted during the process of wood welding show similar proportions of non-condensable gases for the two studied species. Most of the volatile compounds identified during pyrolysis were non-toxic products derived from degradation of wood polymers. The proportion of detected VOCs was relatively low and below the exposure limits. The composition of the non-condensable gases (NCG) was close to that found in pure air. No carbon monoxide was produced during welding, and only traces of hydrogen and carbon dioxide were present. The knowledge gained on VOCs provides valuable information for air safety inspections important for future implementation of wood-welding technology. Hence, wood welding appears to be an ecological technique for assembling furniture components and other applications, and is not harmful for human health.

The wood-welding technology developed by our team with a specially designed machine can be applied to the eco-conception of wood-welded panels for furniture and other indoor appearance applications. Our preliminary results with dowel-welding of black spruce indicate a potential of applying this technology in green (sustainable) construction, in the same line with the results published on manual dowel welding of Norway spruce (Bocquet *et al.*, 2007 a,b) [10], [11]

Conclusions

The transformation of wood yields various forms of residues among which barks are the most abundant. Transforming bark extracts into value added products implies the use of a renewable residue and contributes to saving atoms in molecules recovered by extraction, all by utilisation of water and other green solvents, thus encountering several principles of sustainable chemistry and sustainable engineering.

Wood welding with rotating dowels is the new and innovative technology of assembling wood slats into laminated panels without any synthetic adhesives, in couple of seconds, thus saving energy and protecting environment. This technology relies on wood chemistry and implicates several sustainable chemistry and engineering principles, producing ecological panel fully recyclable at the end of service life.

The public awareness of environmental and health implications of wood transformation will definitely cause a shift towards sustainable wood transformation based on principles of green chemistry and sustainable engineering.

Acknowledgments: My present and former graduate students and postdoctoral fellows: Martha-Estrella Garcia-Perez, Benoit Belleville, Gina Rodriguez-Baca, Ying Sun, Sanja Erakovic, Maria Prado, Papa Diouf and Mariana Royer are gratefully acknowledged for their contributions to the presented results and for providing continuous inspiration for my research.

References

[1] EPA (Environmental Protection Agency) definition of green chemistry and its 12 principles:

http://www.epa.gov/greenchemistry/

[2] ACS Green Chemistry Institute: 12 principles of green chemistry:

http://portal.acs.org/portal/acs/corg/content?_nfpb=true&_pageLabel=PP_ARTICLEMAIN&node_id=1415&content_id=WPCP_007504&use_sec=true&sec_url_var=region1&__uuid=d256ee0d-7e3d-4ed1-80f7-f598bf701bd0

[3] Anastas, P. and Zimmerman, J.B., "Design through the Twelve Principles of Green Engineering", Environmental Science and Technology, 2003, 37(5), pages 94A-101A

[4] Diouf, P. N., Stevanovic, T., and Cloutier, A. (2009). Study on chemical composition, antioxidant and anti-inflammatory activities of hot water extract from Picea mariana bark and its proanthocyanidin-rich fractions. *Food Chemistry*, **113**(4), 897-902.

[5] Garcia-Pérez, M. E., Royer, M., Duque-Fernandez, A., Diouf, P. N., Stevanovic, T., Pouliot, R. (2010). Antioxidant, toxicological and antiproliferative properties of Canadian polyphenolic extracts on normal and psoriatic keratinocytes. *J Ethnopharmacol*, **132**(1), 251-258.

[6] García-Pérez M-E, Royer M, Desjardins, Y., Pouliot R., Stevanovic, T (2012) : Picea mariana bark: A new source of trans-resveratrol and other bioactive polyphenols. Food Chemistry . in press http://dx.doi.org/10.1016/j.foodchem.2012.05.050

[7] Stevanovic, T., Diouf, P.N., Garcia-Perez, M-E. (2009) : «Bioactive polyphenols from healthy foods and forest biomass». *Current Nutrition and Food Science*, Vol. 5, 264-295

[8] Belleville B, Stevanovic T, Pizzi A, Cloutier A, Blanchet P (2012) *Determination of optimal wood-dowel welding parameters for two North American hardwood species*. Journal of Adhesion Science and Technology *in press*, DOI:10.1080/01694243.2012.687596)

[9] Belleville, B., Stevanovic, T., Salenikovich, A., Cloutier A., Pizzi, A., Blanchet, P. (2012) : ‘’Production and properties of wood-welded panels made from two Canadian hardwoods’’ submitted to *Wood Sci. Technol.*

[10] Bocquet, J.-F., A. Pizzi, and L. Resch. 2007a. Full-scale industrial wood floor assembly and structures by welded-through dowels. *Holz Roh Werkst.* 65(2): 149-155.

[11] Bocquet, J.-F., A. Pizzi, A. Despres, H. R. Mansouri, L. Resch, D. Michel, and F. Letort. 2007b. Wood joints and laminated wood beams assembled by mechanically-welded wood dowels. *J. Adhes. Sci. Technol.* 21(3-4): 301-317

Preparation and Characterization of Rosin-Based Polymeric Monomer

Jifu Wang[1,2], Chunpeng Wang[1,2], Chuanbing Tang[3], Fuxiang Chu[1,2]*

1.Institute of Chemical Industry of Forest Products, Chinese Academy of Forestry ; Key Lab. of Biomass Energy and Material, Jiangsu Province; National Engineering Lab. for Biomass Chemical Utilization; Key and Lab. on Forest Chemical Engineering,SFA, Nanjing 210042，China;

2.Institute of Forest New Technology, Chinese Academy of Forestry, Beijing 100091，China

3. Department of Chemistry and Biochemistry and Nanocenter, University of South Carolina, Columbia, South Carolina 29208, USA

* *Corresponding author*
chufuxiang@caf.ac.cn

Abstract

Rosin, a robust inexhaustible raw material from pine tree has attracted much attention due to its utilization as a feedstock for the preparation of polymer in the age of the depletion of crude oil. Maleopimaric acid (MPA), one of most important rosin derivative obtained from the Diels-Alder reaction between the gum rosin and maleic anhydride was reported and characterized. MPA can be obtained with low cost and high purity while compared with other rosin derivative, which enable it to be used as intermediate compound for the preparation of functional material. In this paper, we report a convenient and efficient method to prepare and purify MPA. In addition, a novel vinyl ester of maleopimaric acid (AMPA) was also synthesized by subsequent reaction with oxalyl chloride and allyl alcohol. The structure and properties of these rosin derivatives were characterized by FT-IR, GC-MS, ^{1}H NMR, ^{13}C NMR and DSC. The results showed that MPA and AMPA was high purity. Particularly, AMPA can be performed through thermal initiation without free radical initiator, which indicated that these rosin derivatives have a great potential to prepare the rosin-based unsaturated and epoxy resin.

***Keywords*:** Rosin, Monomer, Free Radical Polymerization.

Introduction

Synthetic polymer consumed ~ 7% of fossil fuels world each year. As the depletion of fossil oil and environmental awareness, the utilization of renewable source to prepare the polymer has been receiving much attention.[1] Rosin, an important renewable resource generated by pine, is produced about 10 million tons in the world, which has been regarded as one of promising alternative feedstock.[2,3] Up to now, a large number of rosin derivatives that acted as additives or monomer have been widely employed in the modification the existing polymer or develop the novel one.[2,4] Generally, these rosin based polymers are divided into main chain and side chain polymers according to the position of the moiety of rosin in the structure of the polymer.[4,5] Main chain polymers such as polyesters, polyamides, polyimides, polyamideimides, polyester polyols, epoxy resin and polymer with diabietyl ketone structure have been widely reported.[6-13] And the side polymer that generally synthesized by free radical polymerization, require the high purity of the monomer.[14] However, rosin is a mixture that mainly composed of diterpene resin acids (about 90 %), and other non-abietane compounds (about 10%) , which result in less progress in the development of the rosin based polymeric monomers with free radical polymerization capability. [14-16]Although there has been a growing interest in the synthesis of rosin based monomers with vinyl, allyl and acrylic group, the purity of monomer is still the main issue that impeded its application. In our previous work, we have synthesized a range of high purity rosin-base monomers by using dehydroabietic acid as starting material, and the nature of properties of rosin such as hydrophobic, bulky, thermal stability, et al, have imparted into a novel synthetic polymer though the controlled/living free radical polymerization and click reaction.[14-20] Herein we reported a strategy to synthesize a novel rosin based monomer with allyl and anhydride group, which has a great potential to be used as epoxy or unsaturated resin precursor that are capable of free radical polymerization. Maleopimaric acid, one of most important rosin derivative from the Diels-Alder reaction between the levepimaric acid and maleic anhydride, was synthesized in the first step and then used as starting material to synthesize the rosin based polymeric monomer. Additionally, FT-IR, GC-MS, ^{1}H NMR, ^{13}C NMR and DSC were employed to characterize the structure and properties of the rosin based polymeric monomer. We believe that our report could be an exemplary synthetic strategy for development of rosin based polymeric monomers with anhydride group.

Materials and Methods

Materials. Gum rosin was obtained from Wuzhou Chemical, China and used as received. Tetrahydrofuran (THF), maleic anhydride, acetate acid, petroleum ether, ethyl acetate, triethylamine (TEA) and Oxalyl chloride ($C_2Cl_2O_2$) were purchased from Shanghai No.4 Reagent & H.V. Chemical Co Ltd, China and used as received. Allyl alcohol was obtained from Shanghai Orgpharma Chemical Co., Ltd and used as received.

Synthesis of Maleopimaric acid (MPA). 100 g gum rosin was added into a three necks round bottom flash equipped with mechanical stirrer, thermometer, condenser and nitrogen inlet. The gum rosin was heat to 180 ^{o}C and maintained at this temperature for 1 h under the nitrogen atmosphere. 30 g maleic anhydride was then added and stirred at 180 ^{o}C for 3 h followed by raising the temperature to 220 ^{o}C and maintaining for 1 h. The reaction was cooled to 100 ^{o}C and 200 ml acetic acid was added. After the temperature was cooled to room temperature, the yellow solid (crude MPA) was obtained. The crude product was recrystallized twice from acetic acid and obtained 55 g white crystal.

Synthesis of rosin based polymeric monomer. MPA(10 g, 0.025 mol) was dissolved in 50 ml THF and added to a round bottom flask. oxalyl chloride (2.95 ml , 0.03 mol) was injected and stirred at 50 ^{o}C for 4 h. The gas generated in the reaction was absorbed by base solution. After removed of the unreacted oxalyl chloride by vacuum distillation, the MPA chloride was obtained. 50 ml THF, allyl alcohol (1.46 g,0.025 mol) and triethylamine (3.5 ml , 0.025 mol) were then added into the flask. The mixture was stirred at room temperature for 12 h and the crude rosin based polymer (AMPA) was obtained. AMPA was further purified by the silica gel chromatography (petroleum ether/ ethyl acetate= 8/2 as eluent).[21]

Characterization. Fourier transform infrared (FTIR) analysis was performed using a Nicolet iS10 FTIR spectrometer by an Attenuated Total Reflectance (ATR) method. Gas Chromatography-Mass Spectrometry (GC/MS) analysis was carried out on Agilent 6890N Network GC system and Agilent 5973 mass selective detector. GC was performed on Agilent HP-5 capillary column (30m×0.25mm×0.25μm) with an oven temperature of 60 ^{o}C →100 ^{o}C (5 ℃/min, 10min))→280 ^{o}C (20 ^{o}C /min, 9min)→280 ^{o}C (20 min). Carrier gas was He at a flow-rate of 1.0 mL/min. The temperature of injection port was 250 ^{o}C. 0.2 μL of sample was injected into the GC system. The mass spectrometer was operated in electron ionization mode. The temperature of ion source was 230 ^{o}C. The ion of the investigated compounds was detected in the range from 10 to 800 amu. The compound was dissolved in tetrahydrofuran and the amount of the components respectively was determinated by peak area normalization method. The ^{1}H NMR and ^{13}C-NMR spectra of MPA and AMPA were scanned on Brucker DRX500 with $CDCl_3$ as solvent. Differential scanning calorimetry (DSC) was run on Perkin Elmer Diamond DSC. 3~4 mg sample was enclosed in aluminum pans. A dry nitrogen flow was used as protective gas. The temperature was increased at rate of 20 K/min from 30 ^{o}C to 250 ^{o}C. The change of enthalpy caused by the polymerization was investigated. And the second scan of the sample was carried out for measurement of the glass transition temperature (Tg).

Scheme 1. Synthesis of MPA and AMPA

Results and Discussion

Synthesis of Maleopimaric Acid (MPA).

Iomerization of resin acid to levopimaric acid under the heat or acid condition, allow us to develop more rosin derivatives by the Diels-Alder reaction. In this work, gum rosin was used as starting material to synthesize the MPA, which can decrease the cost, while compared to the employment of abietic acid.[9] Gum rosin was heat to 180 ^{o}C and carried out the isomerization so that other resin acid would convert to levopimaric acid prior to Diels-Alder reaction with maleic anhydride. The successful synthesis of MPA was rectified by the FTIR spectrum of MPA and showed that the formation of anhydride group is evidenced by the absorption bands at 1842cm^{-1} and 1778 cm^{-1}. The presence of preexisting carboxyl group from the resin acid is reflected by the absorption at 1693 cm^{-1}. The structure and purity of MPA were also confirmed by ^{1}H NMR and ^{13}C NMR. ^{1}H NMR (500 MHz, $CDCl_3$) δ: 5.54 (s, 1H, C*H*=C); 3.10 (d, 1H, C*H*C=O); 2.73 (d, 1H, C*H*C=O); 2.5 (d, 1H, C*H*C=CH); 2.27 (m, 1H, CC*H*$(CH_3)_2$). ^{13}C NMR (125 MHz, $CDCl_3$) δ: 185.4 (*C*OOH); 172.7-170.9 (O=*C*O*C*=O); 148.1 (*C*=CH); 125.1 (C=*C*H); 49.1 (C=O*C*H*C*HC=O); 46.8 (*C*C=O).[17]

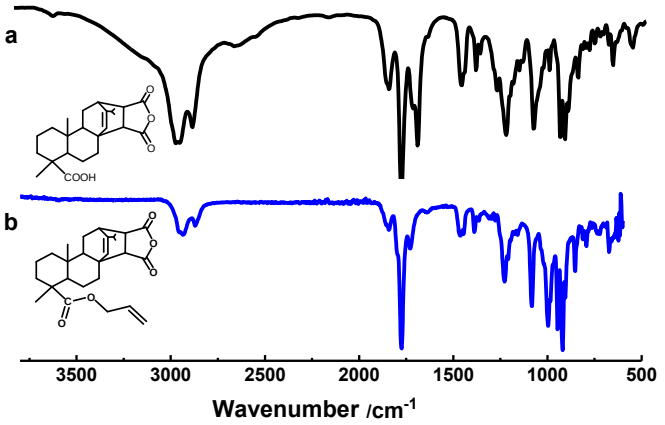

Figure1.FTIR spectra of (a) MPA and (b) AMPA

Synthesis of rosin based polymeric monomer

The synthesis route and chemical structure of rosin based polymeric monomer were showed in Scheme 1. Due to the steric effect of moiety of MPA, the synthesis of rosin based polymeric monomer (AMPA) was carried out with two steps. The carboxyl group of MPA was converted to acyl chloride and then reacted with allyl alcohol in present of catalyst triethylamine. As shown in fig.1, the appearance of new absorption peak at 1729 cm-1 and 1636 cm-1, which arise from the ester (carbonyl group) and double bond (from allyl alcohol) respectively, indicating that allyl alcohol has successfully grafted into MPA by esterification. The structure and purity of AMPA were further confirmed by GC-MS, ^{1}H NMR and ^{13}C NMR. In fig.2a, there is a sharp peak at 32 min, suggesting that AMPA was high purify compound (>99 wt %) after chromatograph separation. The molecule weight of MPA can be observed in fig.2b by the molecular ion peak (m/z=440). ^{1}H NMR (500 MHz, $CDCl_3$) δ: 6.02 (m, 1H, C*H*=CH_2); 5.54 (s, 1H, C*H*=C); 5.30 (d, 2H,

CH=CH_2); 4.61 (m, 2H, OCH_2CH=CH_2); 3.10 (d, 1H, C*H*C=O); 2.73 (d, 1H, C*H*C=O); 2.5 (d, 1H, C*H*C=CH); 2.27 (m, 1H, CC*H*(CH_3)$_2$). ^{13}C NMR (125 MHz, $CDCl_3$) δ: 175.4 (*C*OOCH_2); 172.7-170.9 (O=*C*O*C*=O); 148.1 (*C*=CH); 132.0 (*C*H=CH_2); 125.1 (C=*C*H); 118.0 (CH=*C*H_2); 49.1 (C=O*C*H*C*HC=O); 46.8 (*C*C=O).[21]

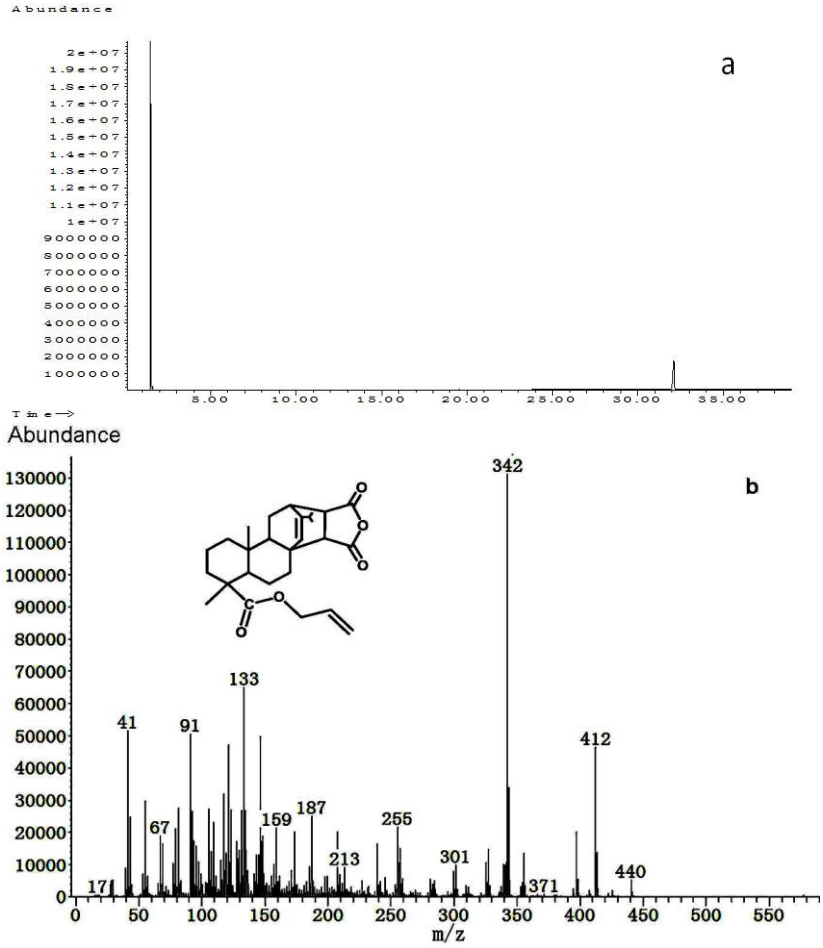

a:GC; b:MS
Figure 2.GC-MS spectra AMPA

Thermal properties of rosin based polymeric monomer

DSC was used to investigate the change of heat flow of AMPA during the heating. About 3 mg of AMPA was enclosed in aluminum pans and heated from 30 ^{o}C to 250 ^{o}C at rate of 20 ^{o}C/min under nitrogen atmosphere. As showed in fig.3a, there was an endothermic peak appearing when the temperature reached to 70 ^{o}C, indicating the melting of the crystal (AMPA). After the completion of melting at 128 ^{o}C, it was surprising to observe that an exothermic peak appeared probably due to the polymerization of AMPA. This assumption was verified by the second scan of sample from fig.3a, which exhibited a conspicuous Tg slope (98 ^{o}C) in fig 2b. The ability of AMPA for the thermal initiation polymerization may be explained by the existence of anhydride group that may activate vinyl group. Thus, AMPA is a novel rosin based

polymeric monomer with anhydride group, which can be initiated by the heat, and have a great potential to be utilized as a component for unsaturated and epoxy resin.[21]

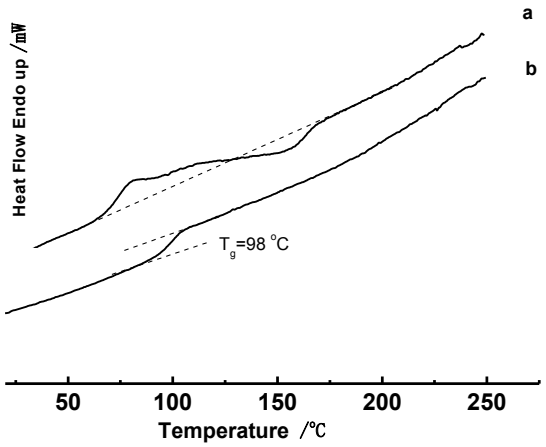

a, first scan; b, second scan
Figure 3.DSC curves of AMPA

Conclusion

In conclusion, we have synthesized a novel rosin based monomer (AMPA) with anhydride group. The synthetic strategy involved two steps. In the first step, maleopimaric acid (MPA) was prepared by using the low-cost gum rosin as a staring material and recrystallized in acetic acid to purify. Subsequently, MPA was employed as a feedstock to synthesize the expected monomer (AMPA) through the esterification with allyl alcohol. The structure and purity of AMPA were confirmed by FT-IR, GC-MS, ^{1}H NMR, ^{13}C NMR. The purity of AMPA can reach 99 wt % and Tg is 98 ^{o}C for its homopolymer. Due to the nature of AMPA's molecular structure, polymerization of AMPA can be performed through thermal initiation without free radical initiator. In addition, the nature of AMPA's molecular structure also allow itself to be used as a component for unsaturated and epoxy resin. Synthesis of AMPA provides a new avenue to prepare other rosin based polymeric monomer, which could extend the application of rosin to polymer area.

Acknowledgement

We would like to acknowledge support from China international science and technology cooperation (2011DFA32440) and Special Fund for Fundamental Research from Research Institute of New technology of Chinese Academy of Forestry (CAFINT2010C05), (CAFYBB2010003).

Reference

(1) Williams, C. K.; Hillmyer, M. A. *Polymer Reviews* **2008**, *48*, 1.
(2) Maiti, S.; Ray, S. S.; Kundu, A. K. *Progress in Polymer Science* **1989**, *14*, 297.

(3) Song, Z. *Journal of Chemical Industry of Forest Products* **2002**, *36*, 29.
(4) Wang, J.; Lin, M.; Wang, C.; Chu, F. *Polymer Materials Science & Engineering*, **2009**, *25*, 170.
(5) Wang, J. *Materials Review* **2011**, 71.
(6) Bicu, I.; Mustata, F. *Journal of Applied Polymer Science* **2004**, *92*, 2240.
(7) Kim, S. J.; Kim, B. J.; Jang, D. W.; Kim, S. H.; Park, S. Y.; Lee, J.-H.; Lee, S.-D.; Choi, D. H. *Journal of Applied Polymer Science* **2001**, *79*, 687.
(8) Le Thi Nhut, H.; Pascault, J. P.; Lam Thanh, M.; Chu Pham Ngoc, S. *European Polymer Journal* **1993**, *29*, 491.
(9) Liu, X.; Xin, W.; Zhang, J. *Green Chemistry* **2009**, *11*, 1018.
(10) Liu, X. Q.; Xin, W. B.; Zhang, J. W. *Bioresource Technology* **2010**, *101*, 2520.
(11) Mustata, F. R.; Tudorachi, N. *Industrial & Engineering Chemistry Research* **2010**, *49*, 12414.
(12) Liu, Y. *Journal of Guangxi University : Natural Science Edition* **2005**, *30*, 348.
(13) Zhang, Y.; Heath, R. J.; Hourston, D. J. *Journal of Applied Polymer Science* **2000**, *75*, 406.
(14) Wang, J.; Lin, M.; Wang, C.; Chu, F. *Journal of Applied Polymer Science* **2009**, *113*, 3757.
(15) Wang, J.; Yao, K.; Korich, A. L.; Li, S.; Ma, S.; Ploehn, H. J.; Iovine, P. M.; Wang, C.; Chu, F.; Tang, C. *Journal of Polymer Science Part A: Polymer Chemistry* **2011**, n/a.
(16) Zheng, Y.; Yao, K.; Lee, J.; Chandler, D.; Wang, J.; Wang, C.; Chu, F.; Tang, C. *Macromolecules* **2010**, *43*, 5922.
(17) Wang, J.; Chen, Y. P.; Yao, K.; Wilbon, P. A.; Zhang, W.; Ren, L.; Zhou, J.; Nagarkatti, M.; Wang, C.; Chu, F.; He, X.; Decho, A. W.; Tang, C. *Chemical Communications* **2012**, *48*, 916.
(18) Wang, J.; Wu, H.; Lin, M.; Wang, C.; Chu, F. *Paint & coatings industry* **2009**, *39*, 13.
(19) Wilbon, P. A.; Zheng, Y.; Yao, K.; Tang, C. *Macromolecules* **2010**, *43*, 8747.
(20) Yao, K.; Wang, J.; Zhang, W.; Lee, J. S.; Wang, C.; Chu, F.; He, X.; Tang, C. *Biomacromolecules* **2011**, *12*, 2171.
(21) Wang, J.; Chang, L.; Yu, J.; Nan, J.; Liu, Y.; Lin, M.; Wang, C.; Liu, M.; Cai, Z.; Chu, F. *Biomass Chemical Engineering* **2012**, *46*, 1.

Proceedings of the 55th International Convention of Society of Wood Science and Technology
August 27–31, 2012 - Beijing, CHINA

Life-Cycle Inventory Analysis of Manufacturing Redwood Decking

Richard D. Bergman[1] – Han-Sup Han[2] – Elaine Oneil[3]—Ivan L. Eastin[3]*

[1] Research Forest Product Technologist, U.S. Forest Service Forest Products Laboratory, Madison, Wisconsin, USA
* *Corresponding author*
rbergman@fs.fed.us
[2] Professor, Forest Operations and Engineering, Department of Forestry and Wildland Resources, Humboldt State University, Arcata, California, USA
[3] Research Scientist and Executive Director (CORRIM), School of Forest Resources, University of Washington, Seattle, Washington, USA
[4] Professor and Director, Center for International Trade in Forest Products, University of Washington, Seattle, Washington, USA

Abstract

Green building has become increasingly important. Therefore, consumers and builders often take into account the environmental attributes of a building material. This study determined the environmental attributes associated with manufacturing 38-mm × 138-mm (nominal 2 × 6) redwood decking in northern California using the life-cycle inventory method. Primary data collected from four redwood mills represented over 83% of redwood lumber production. The primary data were then weight-averaged on a per-unit basis of one m^3 of planed redwood decking (380 oven dry (OD) kg/m^3) to calculate material flows and energy use. The cumulative unallocated energy consumption associated with manufacturing 1.0-m^3 planed redwood decking from 1.8 m^3 of incoming logs was found to be 1,500 MJ/m^3 with 14% of the energy provided by burning wood residues. Emission data produced through modeling the production process found that the estimated total biomass and fossil carbon dioxide emissions were 20.6 and 69.7 kg/m^3, respectively. Our analysis estimated that 38-mm × 138-mm redwood decking stores 697 kg CO_2-equivalents per m^3 of planed redwood decking assuming carbon content of wood of 50%. The amount of carbon stored in redwood decking exceeds the total carbon emissions during manufacturing by a factor of eight. Therefore, low carbon manufacturing emissions and redwood decking's ability to store carbon when in-use are positive environmental attributes when selecting a decking product.

***Keywords*:** Life-cycle inventory, LCI, redwood decking, manufacturing, environmental attributes.

Introduction

Categorizing building materials with positive environmental attributes is the result of the drive for green building. Green building is the practice of improving energy efficiency, construction, and operation of buildings while decreasing overall environmental burdens. By 2013, the green building market for new non-residential construction could triple to $96–140 billion from $42 billion in 2008 (MHC 2010). Creating a science-based green building policy for the building industry would aid in producing sustainable building practices. However, to create such a policy and to address environmental claims, scientific approaches such as life-cycle analysis will be required to assess building materials and practices for their environmental attributes.

The goal of this study was to document the life-cycle inventory (LCI) of redwood (*Sequoia sempervirens*) decking production from incoming logs to redwood decking in northern California. The present study listed material flow, energy consumption, and emissions for the redwood decking manufacturing process on a per-unit basis. Primary data collected by surveying redwood sawmills primarily used a questionnaire. Peer-reviewed literature provided secondary data per CORRIM guidelines (CORRIM 2010). Material balances constructed with a spreadsheet algorithm used data from primary and secondary sources. From material and energy inputs and reported emissions, SimaPro 7 software (PRé Consultants, Amersfoort, Netherlands) modeled the estimates for environmental outputs (PRé Consultants 2012).

Methodology

Scope. This study covered the manufacturing redwood logs leaving the forest landing to redwood decking leaving the sawmill according to ISO 14040 and 14044 standards (ISO 2006a,b). LCI data from this study will help conduct a comparative life-cycle assessment (LCA) for redwood decking to other non-wood decking materials. To construct a full LCA, this manufacturing LCI will be linked to forest resources (upstream) and product transportation (downstream). The LCI provided a gate-to-gate analysis of cumulative energy of manufacturing as well as transportation of raw materials. Analyses included redwood's contribution to cumulative energy consumption and emission data.

Four redwood mills representing over 83% of redwood lumber production provided 2010 primary data. In 2011, site visits were conducted at the four mills. The surveyed mills provided detail annual production data on their facilities including on-site energy consumption, electrical usage, log volumes, and decking production for 2010.

Functional unit. Delineating system boundaries determined the unit processes to include and standardized material flows, energy use, and emission data. The present study selected a functional unit of one m^3 of decking material with 38-mm thickness and assumed no spacing between deck boards. Based on U.S. industry measures, converted green and dry wood decking using the following conversions: 2.36 m^3 and 1.62 m^3 per thousand board feet (bf), respectively, since wood shrinks as it dries from its green state to its final dry state and is planed (Bergman 2010). For dry redwood decking, 10 m^2 at 38-mm thickness equals 0.38 m^3 (231 bf). Results were reported per m^3 of planed redwood decking.

Unit processes. Five main unit processes were identified in manufacturing redwood decking. These included resource transport, log yard, sawing, drying, and planing with energy generation considered an auxiliary process. All emissions (i.e., environmental outputs) and energy consumed were assigned to the redwood decking and none to the co-products (i.e., redwood decking residue). The present study was consistent with the Mahalle and O'Connor (2009) LCA study on western redcedar (*Thuja plicata*) where the price for decking is much higher than the co-products is (10 to 1. Therefore, no primary energy and environmental outputs were allocated to the mill residues. Green wood residues included sawdust, chips, hog fuel, and bark. Some mills ground all wood residues into hog fuel. Diesel logging trucks transported the redwood logs from the forest landing to the log yard. Logs in the log yard were wetted to maintain log quality and prevent checking or splitting depending on the season and the mill. Log stackers or front-end loaders transported logs from the yard to the sawmill. Sawing the logs produced rough green redwood decking. The sawing process (less the bark) produces rough green decking (59.9%), wood chips (22.7%), sawdust (9.5%), hog fuel (5.0%), and shavings (1.9%). The three processing options for rough green decking include 1) planing on all four sides and selling as green decking (7.6%), 2) selling as-is (28.4%), or 3) drying, planing and selling as dry decking (64%). Drying rough green decking occurs mostly by air-drying with minimal kiln-drying to reach the desired moisture content (MC). After drying, the rough dry decking was planed on all four sides producing shavings.

System boundary. Boundary selection helps track the material and energy flows crossing the boundary precisely. To track flows tied to redwood decking production, two system boundaries were considered. One—the cumulative system boundary—is shown by the solid line in Figure 1 and includes both on- and off-site emissions for all material and energy consumed. Fuel resources used for the cradle-to-gate production of energy and electricity were included within the cumulative system boundary. The on-site system boundary (dotted line in Figure 1) covered emissions occurring only at the mill from the four unit processes involved: log yard, sawing, drying, and planing. Off-site emissions include grid electricity production, transportation of logs to the mill, and fuels produced off-site but consumed onsite. Ancillary material data such as motor oil, paint, and hydraulic fluid were collected and were part of the analysis.

Results and Discussion

By surveying four redwood mills in northern California in 2010, detailed primary data on mass flow, energy consumption, and fuel types provided life-cycle information including air emission data. SimaPro 7 modeled weight-averaged survey data to estimate non-wood raw material use and emission data on a 1-m^3 unit basis.

To confirm the data quality, a mass balance was performed and the results are summarized in Table 1. In performing the mass balance for redwood decking, all of unit processes located within the site system boundary were considered. Using a weight-averaged approach, 648 OD kg (1.8 m^3) of incoming redwood logs with a green density (127% MC) of 803 kg/m^3 produced 1.0 m^3 (380 OD kg) of planed redwood decking. The sawing process yielded 388 kg of rough green decking with no loss of wood substance occurring during the drying process. Planing the rough lumber into a surfaced decking product reduced the 388 OD kg of rough dry decking to 380 OD kg of planed dry redwood decking, for a 2% reduction in mass. Some wood waste was converted

on-site to thermal energy in a boiler; boilers burned all 8 OD kg of dry shavings produced onsite for thermal process energy. Overall, an average redwood log was reduced to 58.6% (380/648) of its original mass during its conversion to planed dry redwood decking.

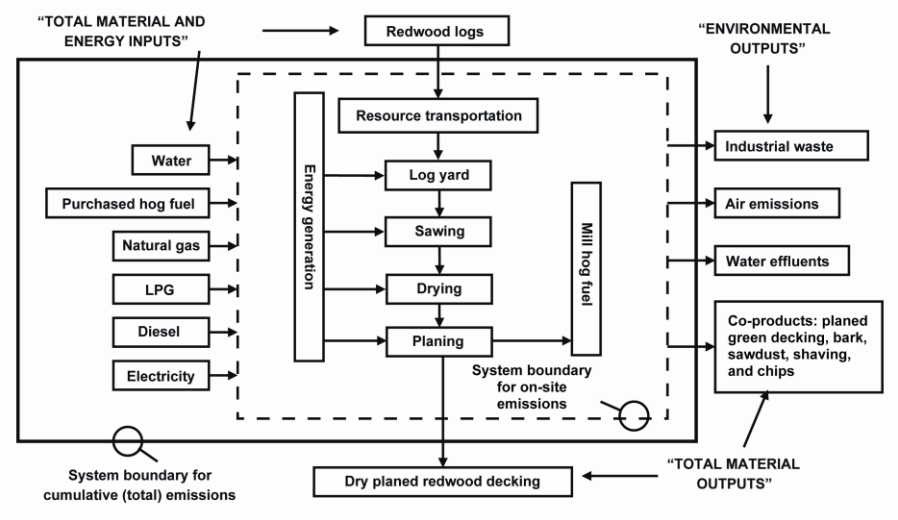

Figure1: System boundaries for redwood decking manufacturing

Table 1: Mass balance of redwood decking

	Sawing process		Boiler process	Dryer process		Planer process		All process combined		
Material (OD kg)	In	Out	In	In	Out	In	Out	In	Out	Diff
Green logs (wood)	648	-	-	-	-	-	-	648	0	–648
Green logs (bark)	71	-	-	-	-	-	-	71	0	–71
Green chips	-	147	-	-	-	-	-	0	147	147
Green sawdust	-	68	-	-	-	-	-	0	68	68
Green bark	-	71	-	-	-	-	-	0	71	71
Green shaving	-	12	-	-	-	-	-	0	12	12
Green hog fuel	-	32	-	-	-	-	-	0	32	32
Rough green decking	-	388	-	388	-	-	-	388	388	0
Rough dry decking	-	-	-	-	388	388	-	388	388	0
Planed dry decking	-	-	-	-	-	-	380	0	380	380
Dry shavings	-	-	8	-	-	-	8	8	8	0
Sum	719	719	8	388	388	388	388	1503	1495	-8

Redwood decking in service stores carbon. Carbon content for wood products is assumed to be 50% by mass of oven-dried (OD) wood. Therefore, the carbon stored in one m^3 (380 OD kg) of redwood decking is equivalent to 697 kg CO_2.

Table 2 shows the cumulative unallocated energy consumption for a cubic meter of planed dry redwood decking. Cumulative energy consumption for manufacturing redwood decking was 1,500 MJ/m^3 with wood fuel comprising about 14%. Coal (33.2%), natural gas (20.0%), and crude oil (17.4%) were the three highest energy resources consumed during product production. Coal makes up about 35% of the grid in the western United States. Therefore, coal has the highest energy consumption because the mills use grid electricity. Because of the minimal kiln-drying that occurs during the production of redwood decking, less than 10 kg of wood fuel was burned in boilers on-site for energy per cubic meter of redwood decking made. Usually, most energy for processing wood products comes from wood fuel generated on-site and burned on-site (Puettmann et al. 2010). However, redwood decking is not the only wood product to have a low energy consumption profile. Douglas-fir (*Pseudotsuga menziesii*) used for structural lumber is usually not kiln-dried, and therefore, is installed green and dries in place. Thus, the energy profile for green Douglas fir looks similar to redwood decking (Milota et al. 2005; Puettmann and Wilson 2005).

Table 2: Cumulative energy (higher heating values (HHV)) consumed during production of planed (surfaced) redwood decking—cumulative, unallocated gate-to-gate LCI values[a]

Fuel[b,c]	(kg/m^3)	(MJ/m^3)	(%)
Wood fuel/wood waste	9.95	208	13.8%
Coal[d]	19.1	499	33.2%
Natural gas[d]	5.52	301	20.0%
Crude oil[d]	5.77	263	17.4%
Hydro	0	95.8	6.4%
Uranium[d]	0.000357	136	9.0%
Energy, unspecified	0	2.27	0.2%
Total	—	1,500	100%

[a] Includes fuel used for electricity production and for log transportation (unallocated).
[b] Values are unallocated and cumulative and based on HHV.
[c] Energy values were found using their HHV in MJ/kg: 20.9 for wood oven-dry, 26.2 for coal, 54.4 for natural gas, 45.5 for crude oil, and 381,000 for uranium.
[d] Materials as they exist in nature and have neither emissions nor energy consumption associated with them.

Most wood products consume more energy per cubic meter of final product during the manufacturing stage than redwood decking. For making hardwood lumber in the southeastern United States, cumulative allocated energy consumption for one m^3 of planed dry hardwood lumber is 5,860 MJ/m^3 with 66% from wood fuel (Bergman and Bowe 2012). The values listed in Puettmann et al. (2010) and Bergman and Bowe (2012) studies use mass allocation. The present study allocates all primary energy to redwood decking and none to its residues. Primary energy is energy embodied in the original resources such as crude oil and coal before conversion. However, cumulative unallocated energy for manufacturing redwood decking is still only 26% of southeastern hardwood lumber (Bergman and Bowe 2012). The low cumulative energy for redwood decking occurred because of minimal use of kiln drying, which is the most energy-intensive part of producing dry lumber products.

Table 3 lists the unallocated environmental outputs for manufacturing one m^3 of redwood decking for the cumulative and on-site system boundaries. The cumulative values included all emissions and were higher than the on-site emissions. For the cumulative system boundary, biogenic CO_2 and fossil CO_2 were 20.6 and 69.7 kg/m^3. Fossil CO_2 for the cumulative case was about eight (69.8/8.94) times the fossil CO_2 emitted for the on-site case. For on-site, the only sources of fossil CO_2 came from rolling stock such as front-end loaders moving logs and forklifts moving lumber around the mill. Additionally, mercury emissions to air dropped by a factor of 11 (0.176/0.0152) because emissions from grid electricity consumed at the mill were not included in the on-site case.

Table 3: Environmental outputs for manufacturing one m^3 of planed redwood decking

Substance	Cumulative (kg/m^3)	On-site (kg/m^3)
Water effluents		
BOD5 (Biological oxygen demand)	2.09E-01	1.69E-01
Chloride	1.71	0.389
COD (Chemical oxygen demand)	2.21E-02	1.02E-02
DOC (Dissolved organic carbon)	2.17E-03	1.87E-03
Oils, unspecified	3.14E-03	2.11E-03
Suspended solids, unspecified	7.07E-02	2.58E-02
Industrial waste[a]		
Waste in inert landfill	0.267	0.267
Waste to recycling	0.222	0.222
Solid waste[b]	0.111	0.092
Air emissions		
Acetaldehyde	1.19E-04	1.04E-04
Acrolein	4.06E-04	3.35E-04
Benzene	4.98E-04	3.92E-04
CO	0.239	4.97E-02
CO_2 (biomass (biogenic))	20.6	16.2
CO_2 (fossil)	69.8	8.94
CH_4	5.06E-04	4.16E-04
Formaldehyde	1.09E-06	3.08E-07
Mercury	0.176	1.52E-02
NO_x	6.15E-04	3.95E-05
Non-methane VOC	1.61E-02	8.41E-03
Particulate (PM10)	5.77E-02	4.55E-02
Particulate (unspecified)	2.67E-02	1.70E-03
Phenol	3.79E-07	3.68E-07
SO_x	0.399	0.0127
VOC	5.21E-02	5.14E-03

[a] Includes solid materials not incorporated into the product or co-products but left the system boundary.
[b] Solid waste was boiler ash from burning wood. Wood ash is typically

used a soil amendment or landfilled.

Coal power plants are major emitters of mercury in the United States (Pirrone et al. 2010). Sulfur dioxide is similar to mercury as its emissions follow coal power production. Biogenic (biomass) CO_2 decreased by about 21% because some wood fuel burned to provide thermal energy for the mills was burned off-site (outside the system boundary), and then the boiler steam was pumped to mills. Solid waste (wood boiler ash) follows wood fuel consumption.

Conclusions

The amount of carbon stored in redwood decking is about eight times the total carbon dioxide emissions released during manufacturing. Therefore, low carbon manufacturing emissions and redwood decking's ability to store carbon when in use similar to other wood products are positive environmental attributes when selecting a decking product.

Air-drying redwood decking dramatically lowers energy consumption during product production. Wood product production usually consumes more fossil and wood fuel than found for redwood decking manufacturing. The main reason is that most wood product manufacturing facilities especially when processing hardwoods kiln-dry their final product when it is freshly cut or green. An additional benefit, redwood decking can typically equilibrate to exterior conditions without any issues after installation.

References

Bergman, R.D. 2010. Drying and control of moisture content and dimensional changes. In: Wood handbook—wood as an engineering material. General Technical Report FPL–GTR–113. Madison, WI: U.S. Department of Agriculture, Forest Service, Forest Products Laboratory. pp. 13-1–13-20.

Bergman, R.D. and Bowe, S.A. 2012. Life-cycle inventory of hardwood lumber manufacturing in the Southeastern United States. Wood and Fiber Science 44(1):71–84.

CORRIM. 2010. Research guidelines for life-cycle inventories. Consortium for Research on Renewable Industrial Materials (CORRIM), Inc., University of Washington, Seattle, WA. 40 pp.

ISO. 2006a. Environmental management—life-cycle assessment—principles and framework. ISO 14040. International Organization for Standardization, Geneva, Switzerland. 20 pp.

ISO. 2006b. Environmental management—life-cycle assessment—requirements and guidelines. ISO 14044. International Organization for Standardization, Geneva, Switzerland. 46 pp.

Mahalle, L., O'Connor, J. 2009. Life Cycle Assessment of Western Red Cedar Siding, Decking, and Alternative Products. FPInnovations – Forintek Division, Western Region. 126 pp.

MHC. 2010. Green outlook 2011: Trends driving change. McGraw-Hill Construction (MHC), New York. 32 pp.

Milota, M.R., West, C.D., Hartley, I.D. 2005. Gate-to-gate life inventory of softwood lumber production. Wood and Fiber Science 37 (Special Issue): 47–57.

Pirrone, N., Cinnirella, S., Feng, X., Finkelman, R.B., Friedli, H.R., Leaner, J., Mason, R., Mukherjee, A.B., Stracher, G.B., Streets, D.G., Telmer, K. 2010. Global mercury emissions to the atmosphere from anthropogenic and natural sources. Atmospheric Chemistry and Physics, (10): 5951–5964.

PRé Consultants. 2012. SimaPro 7 Life-Cycle assessment software package, Version 7. Plotter 12, 3821 BB Amersfoort, The Netherlands. http://www.pre.nl/. (accessed May 8, 2012).

Puettmann, M.E., Bergman, R.D., Hubbard, S., Johnson, L., Lippke, B., and Wagner, F. 2010. Cradle-to-gate life-cycle inventories of US wood products production – CORRIM Phase I and Phase II Products. Wood and Fiber Science 42 (CORRIM Special Issue):15–28.

Puettmann, M.E. and Wilson, J.B. 2005. Life-cycle analysis of wood products: Cradle-to-gate LCI of residential wood building materials. Wood and Fiber Science 37 (Special Issue):18–29.

Mid-rise Wood Frame Construction: Structural, Fire Safety, Environmental and Architectural Considerations

Kevin Cheung[1] *– Fang Xu*[2]

[1] Chief Engineer, Western Wood Products Association, 522 SW Fifth Avenue, Suite 500, Portland, Oregon 97204-2122, USA.
kcheung@wwpa.org
[2] Director, American Softwoods China Office, Rm. 805, Tower 3, Wellington Park, 183 Huai Hai Road, Shanghai 200030, CHINA.
xu_fang@amso-china.org

Abstract

In the United States, low-rise wood construction is the predominant in residential construction. Mid-rise wood frame construction of 4 and more stories is increasingly popular in the last 30 years spreading across the country. Mid-rise wood frame buildings are being built atop of 1- to 2-story concrete construction to achieve even higher height. This type of construction project is common for apartments and condominiums, hotel and motels, and senior living facilities.

The International Building Code is used throughout the United States providing provisions for structural and fire safety considerations. Most recent projects of mid-rise wood frame construction are targeted to achieve levels in the Leadership in Energy & Environmental Design standards.

***Keywords*:** A. Mid-rise Wood Frame Construction, B. Structural, C. Fire Safety, D. Environmental, E. Architectural.

Introduction

In the United States, wood construction is predominant used in residential construction mostly 1 to 3 stories single family detached homes. Mid-rise wood frame construction of 4 and more stories is becoming popular in the United States and Canada. Started in the U.S. West Coast cities in the 80's, mid-rise wood frame construction has been spreading across the United States. Mid-rise wood frame buildings can be built atop of 1- to 2-story concrete construction to achieve even higher height. This type of construction is common for apartments and condominiums with amenities from affordable to luxury, hotel and motels in city centers as well as suburban areas, university student housing, and senior living facilities.

Designers have developed solutions to the design challenges. Code-compliant wood frame construction provides for good performance in safety for fire events, structural capacity during earthquakes and hurricanes, and serviceability.

In British Columbia of CANADA since 2009, the building code allows for mid-rise wood frame buildings of six stories. The Chinese code is being revised to make possible mid-rise construction of 3 stories of wood frame construction atop 4 stories of concrete construction.

United States Experience of Mid-rise Wood Frame Construction

Mid-rise wood frame buildings of 4 stories and higher in the United States can be built over 1- to 2-story concrete construction with or without 1- to 2-level underground parking. A typical development provides 40 to 250 living units and is required by building code to be of one-hour fire resistance rating. The parking garage is three-hour-rated minimum fire resistance. Figure 1 is the photos of a mid-rise wood frame building completed in 2010.

Figure 1: The MATISSE Apartment project in Portland, Oregon,United States completed in 2010 – Left: construction of 2-story underground reinforced concrete construction, Middle: 5-story wood frame over 1-story reinforced concrete with post-tension slab, Right: completed project. Photos: R&H Construction, General Contractor of the project.

Activation of the sprinklers as construction proceeds enhances fire protection during construction. The stairwells and elevator shafts require two-hour fire-resistance-rated wood frame or masonry construction. By using post-tensioning concrete slab to support the wood frame, the slab thickness is reduced to keep overall building height to the

minimum to be under the building code permitted allowable height. The typical size of apartment and condominium units is between 600 and 1,900 ft^2.

The use of 2x6 exterior wood frame wall is common to allow for the installation of thick insulation material to reduce heat loss in cold weather periods. The floor topping of lightweight concrete or gypcrete provides for enhanced sound control. Both solid-sawn lumber and/or wood I-joists are used to provide the floor framing. During construction of the wood frame, heaters and dehumidifiers may be used to reduce the moisture from the concrete and the wood framing materials.

High density housing. Many of the mid-rise wood frame construction projects are developed as high density housing achieving 100 to 140 units per acre. Figures 2, 3, 4, 5 and 6 showcase a number of high density housing projects.

Figure 2 Fashion Walk: 5 stories of wood frame over two levels of exposed concrete parking. A seven-story building utilizied a sloping site to pick up an additional story. Photos courtesy of Tim Smith, President, Togawa Smith Martin, Inc.

Figure 3 Esprit: A high density residential development of 5 stories wood frame over one level of concrete parking garage out. Photos courtesy of Tim Smith.

Figure 4 Americana: 5 story wood frame over one story retail podium of concrete construction. A typical European infill project creating high density housing with active retail base designed for 100 units per acre. Photos courtesy of Tim Smith.

Figure 5 Casa Heiwa: A 5-story wood framed building in California, built in 1995, achieved high density of 100 units per acre. Photos courtesy of Tim Smith, President, Togawa Smith Martin, Inc.

Figure 6 Union Square & Elan: 7 levels residential building - one level of concrete and 6 levels of wood framing. Density of 130-140 units per acre. Photos courtesy of Tim Smith, President, Togawa Smith Martin, Inc.

Environmental Benefits

Mid-rise wood frame projects are often targeted for certification to the Leadership in Energy & Environmental Design (LEED) standard. The use of wood in construction is environmentally friendly as carbon is stored in the wood used. The manufacturing of wood products produces greenhouse gas emissions significantly less than that from other building materials.

A carbon calculator from WoodWorks is available at www.woodworks.org for estimation of stored carbon dioxide equivalent in wood products used in construction projects.

Rick Bergman of the U.S. Forest Products Laboratory studied carbon impact factors for a range of wood products and its alternatives. With the use of life cycle assessment, he quantified the net CO_2 balance as total carbon footprint, see Table 1. He concluded that all wood products have a negative carbon dioxide balance from cradle-to-gate.

Product	Unit	Category	A	B	C	D	Alternative	E
Hardwood Lumber	One board foot	NE/NC	0.89	0.59	1.84	2.63	PVC	**-4.16**
	One board foot	SE	1.08	0.79	1.77	2.64	PVC	**-4.12**
Softwood Lumber	One 2x4 'stud'	NE/NC	1.85	1.23	6.63	6.97	Steel stud	**-13.0**
	One 2x4 'stud'	SE	3.90	3.32	8.42	7.01	Steel stud	**-14.9**
Wood Flooring	1 square foot	Solid wood	1.06	0.69	2.12	-0.13	Linoleum	**-1.61**
	1 square foot	Engineered	0.98	0.52	1.10	-0.22	Linoleum	**-0.42**
Doors	One door	Solid wood	46.5	29.4	100	228	Steel door	**-311**
Decking	One deck board	Treated pine	5.18	1.70	16.1	11.9	WPC	**-24.5**
Siding	100 square feet	WRC	37.7	5.96	77.7	20.4	Vinyl	**-66.3**
Poles	One 45' pole	Treated wood	454	431	1160	1380	Concrete	**-2520**
OSB	One 4'x 8' sheet	SE	19.0	10.7	34.7	-	n/a	**-26.3**
Plywood	One 4'x 8' sheet	PNW	5.72	4.13	25.5	-	n/a	**-23.9**
	One 4'x 8' sheet	SE	10.1	6.48	30.9	-	n/a	**-27.3**

Table 1 Carbon Impacts of Wood Products

The wood product carbon impact equation A-B-C-D = E

in which

A is Manufacturing Carbon
B is Bio-fuel
C is Carbon Storage
D is Substitution
E is Total Carbon Footprint or Carbon Credit

These data in Table 1 are compiled from life cycle assessment (LCA) of the various products. All "carbon" values are kilograms of CO_2. To convert from CO_2 to elemental carbon, multiply by 0.27. For comparison, a car produces 8.8 kg of CO_2 when it burns one gallon of gasoline.

U.S. Building Code

The International Building Code (IBC) is a model code used throughout the United States. Each local government adopts IBC with amendments to address local preferences and conditions. IBC provides provisions for safety considerations in design and construction of building structures including the allowable building height, number of stories and floor area for wood frame construction. These allowable can be increased when additional measures to provide for fire protection are used such as sprinkler system for fire suppression.

Designers has successfully addressed the design challenges from the increasing height of wood framed buildings that includes wood shrinkage, lateral shear force resistance, overturning moment resistance (including compression perpendicular to the grain on wood members and hold-down anchor design) and fire regulations (risk of fuel load and egress of occupants) that are requirements of IBC.

The IBC allows the ground floor, when non-combustible construction is used such as reinforced concrete, to be treated as a separate building when considering the limitation of number of stories. This is called podium construction as shown in Figure 7.

Figure 7: Podium Construction in San Francisco, California in 2010

Some local building regulations allow wood frame construction for up to five stories over a podium construction. The podium structure is limited to one story in Portland, Oregon, and to 2 stories in Seattle, Washington as shown in Figure 8.

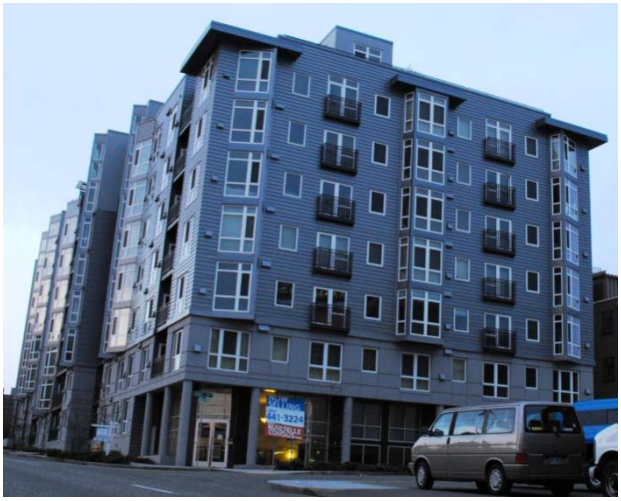

Figure 8: Marselle Condos in Seattle, Washington – a 160,000 square feet condo project of IBC Type III construction has five floors of wood construction over a two-story concrete podium construction.

Chinese Codes and Standards

Wood frame construction was introduced into China in the early 1990s. To provide design professionals, builders, and architects with guidelines on design and construction of wood frame construction, the Chinese code development body, in cooperation with industry associations from the U.S., Canada, and Europe, adopted the North American wood frame construction in 2003 in to the China Timber Structure Design Code GB50005. A three-story wood frame building in Shanghai is shown in Figure 9.

Figure 9: Three-story wood frame building in Shanghai, CHINA completed in 2004

Following the release of GB50005, the Chinese wood industry developed product standards in response to the need for conformity assessment and development of the wood frame construction market. These standards provide performance criteria for the use of engineered wood products in structural applications as alternatives to the solid sawn lumber products.

China timber structure design code (GB50005-2003). The most recent revision of the standard was completed in 2003. One major revision was the inclusion of design requirements on wood frame construction. Both prescriptive design method, which is primarily used in the design of floor and wall system, and engineered design method are provided in this version. Besides, design strength of shearwall and diaphragm are also included. Despite the fact that use of wood frame construction is limited in buildings up to three stories, the release of GB50005 paved the road for use of hybrid wood frame construction over three stories of concrete construction in the future. The committee of China Timber Structure Design Code is currently in the process of revising China Timber Structure Design Code (GB50005-2003) in the hope that more information about the use of engineered wood products and connection design will be included in the future.

Technical Specification for Wood Frame Construction (J11461-2009). Following the release of the China Timber Structure Design Code (GB50005-2003) in 2003, Shanghai local government developed this technical specification in 2009 in an effort to expand application of wood frame construction (WFC) method from three story WFC buildings to four story (one story concrete/masonry/steel buildings topped with three story WFC buildings) and five story (four story concrete/masonry/steel buildings topped with one story WFC buildings) hybrid construction buildings. Given the fact that design requirements on seismic resistance and durability issues covered in GB50005-2003 are not sufficient enough for designers to adequately perform their design services in some cases, this technical specification provides users with two separate chapters specifically dealing with these issues.

Chinese Building Fire Code (GB50016). Chinese Building Fire Code is a nationally enforced mandatory code, providing designers with design requirements on all the issues associated with fire safety design. In the most recently revised version, wood frame hybrid construction is allowed to be built up to seven stories (four story concrete/masonry/steel sub-structure + three story wood frame construction) as long as at least two hour fire resistance is provided between the substructure built with non-combustible material and superstructure constructed with wood frame construction. At the moment, this revised version is pending the official approval from Chinese government agencies. It is believed that the release of this standard will be helpful to significantly expand use of wood frame construction in multi-story residential as well as commercial buildings.

Technical Specification for Light-gauge Metal Plate Connected Wood Trusses. The design requirements on wood trusses provided in GB50005-2003 is insufficient and generic, which is hard to be used by designers when they run into projects associated with use of wood trusses. As such, the GB50005 committee, in cooperation with Canadawood, Europeanwood, MiTek and several other major truss manufacturers in China, developed the standard in 2010 in the hope to provide designers with viable method in design of wood trusses. The standard was developed based upon ANSI/TPI 1 – National Design Standard for Metal Plate Connected Wood Truss Construction and TPIC- Truss Design Procedures and Specifications for Light Metal Plate Connected Wood Trusses.

The Hygrothermal Performance of Wood Frame Wall System in Suzhou Lake Tai Climate Zone

Xiaohuan WANG

Assistant Research Fellow, Beijing Forestry Machinery Research Institute of State Forestry Administration, China

Benhua FEI

Research Fellow, International Bamboo and Rattan Network Center, China

Jun NI

President, Suzhou Crownhomes co., Ltd., China

Abstract

Long-term on-site assessment of hygrothermal performance is necessary for developing energy-efficient and durable wood frame wall system. In this paper the hygrothermal performance of cavity insulation wall was examined from temperature, relative humidity, air pressure in cladding ventilation and wood material surface temperature throughout the year in Suzhou Lake Tai of hot summer & cold winter climate zone. The results clearly demonstrated the effect of the cavity insulation, cladding cavity ventilation, air and vapor barrier. Thermal performance was proved very well because of the wall cavity insulation. Cladding ventilation including openings was effective at lowering relative humidity of insulated wall cavities. Condensation and mold growth were not found inside the wall during the whole testing period. Wood frame wall system exhibited very good hygrothermal performance to be widely used in hot summer & cold winter climate zone in central China.

Key words: hygrothermal performance, wood frame wall, insulation, vapor retarder

Introduction

Long-term on-site assessment of hygrothermal performance is necessary for developing energy-efficient and durable wood frame wall system. Dynamic changes of temperature, relative humidity and moisture content can reveal the function of each material in multilayer wall. Heat and moisture transfer through wall was measured under the different materials and climatic conditions[1-4]. These studies revealed the factors that affect the wall hygrothermal performance, such as ventilation, airtightness, insulation, infiltration and vapor diffusion. Experiments and simulation results have helped to improve hygrothermal performance of the exterior wall system, and professional guidance or recommendations were provided [5-7].

China is divided into five climate zones for having a vast terrain territory. Suzhou is identified as a hot summer & cold winter climate zone, which is a north subtropical monsoon climate of hot summer, cold and dry winter, wet and humidity. Complicated environment conditions increase the difficulty of building wall design to maintain energy saving and durability. The increasingly wood frame houses were built in hot summer & cold winter climate region. However, hygrothermal performance of wood frame wall system is still unknown under this climatic condition.

This study is developing and implementing an on-site systems engineering approach to monitor long-term changes in the hygrothemal responses of wall system. The medial and lateral wall, ventilation cavity and insulated wall cavity conditions were monitored for air temperature, relative humidity, air pressure in cladding ventilation and wood material surface temperature in Suzhou Lake Tai of the hot summer & cold winter zone climate. The results will be used to support the future design standards regarding exterior wall requirements

Tested building and Wall configuration

Suzhou Crownhomes co., Ltd established a low-carbon demonstration wood house at park by the side of Suzhou Lake Tai (see figure 1). The building is a post and beam construction consisted of glulam. The wall thickness was 125mm filled in the main frame structure. Configuration and materials of multilayer wall illustrated in figure 2. Thermal insulation was by inserting the premium loose-fill fiberglass insulation into the cavity between studs in the exterior wall, which was then covered on interior panel with gypsum board and the exterior panel with OSB sheathing. The continuous polyethylene films were used as interior vapor retarders placed on the interior surface of cavity insulation.

Figure 1 Demonstration test house

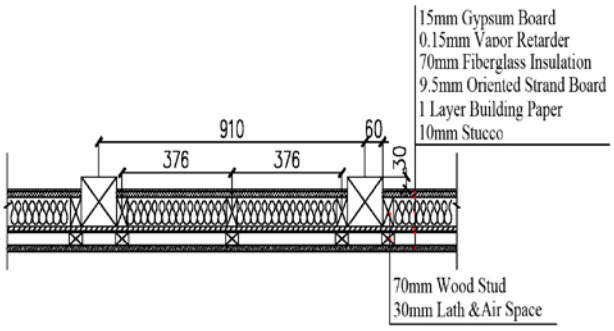

Figure 2 Configuration of multilayer wall

Instrumentation and sensor locations

One frame in the south exterior wall was chosen to be tested according to the field conditions of the house. Air temperature and relative humidity were monitored by JWSK-6ACC05 sensor with accuracy of 0.1. Surface temperature was measured using type T thermocouples, calibrated to 0.1K. Ventilated cavity pressure was measured by JQYB atmospheric pressure transmitter with accuracy of 0.1kPa.

Sensors were connected to the data collection equipment, which continuously monitor the hygrothermal performance of the test wall. Data were recorded and stored in computer every minute, and could be extracted every 30 min or every hour flexibly to analyze by operating software. The monitor process began in June 2010, and the testing has been done continuously 2 years.

The sensor locations are illustrated in figure 3. Sensors of air temperature and relative humidity (RHT1~ RHT10) were distributed in each layer from the medial to lateral wall. These were installed 300mm from the top and bottom of the test wall respectively. Sensors of air pressure (P1 and P2) were placed in cladding ventilation cavity, which locations were same as RHT4 and RHT9.

Sensors of surface temperature (T1~T6) of stud and OSB were located in cavity insulation. T1 and T5 were located in the center of top and bottom wood plate, T2 and T4 were located in exterior sheathing board, 300mm from the top and bottom wood plate respectively. T3 and T6 were located in stud and the exterior sheathing board respectively, centered vertically between the top and bottom plates.

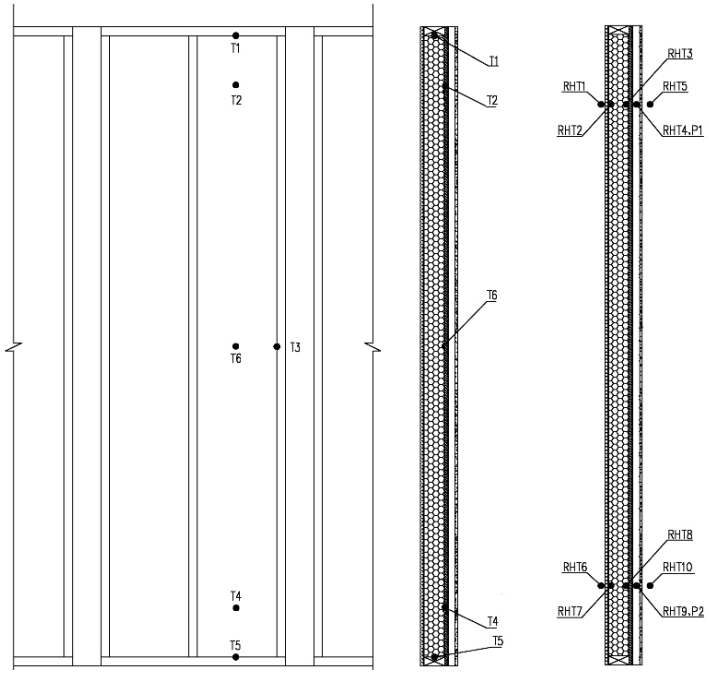

Figure 3 Schematic drawing of sensor locations in the test wall

Results and discussion

The trend was basically identical between RHT1~RHT5 and RHT6~RHT10 described in [7]. Figure 4 and figure 5 only present air temperature and relative humidity changes of RHT1~ RHT5 in the last one year in addition to the August data failed in this paper. Air temperature of the medial wall varies were less during the period of April to October than the period of November to May. Air temperatures of the medial wall were closer to air temperatures of the interface between the gypsum board and insulation layer. Air temperature changes trend of the interface between the insulation layer and OSB sheathing board was closer to air temperature of the lateral wall, which confirmed that effective function of the insulation layer. January was the indoor coldest month from the changes of the whole year. Although air temperature of the lateral wall was near to −3.0℃, air temperature of the medial wall could maintain 11℃. The peak of each interface air temperature clearly showed the hysteresis behavior from the medial to lateral of the test wall.

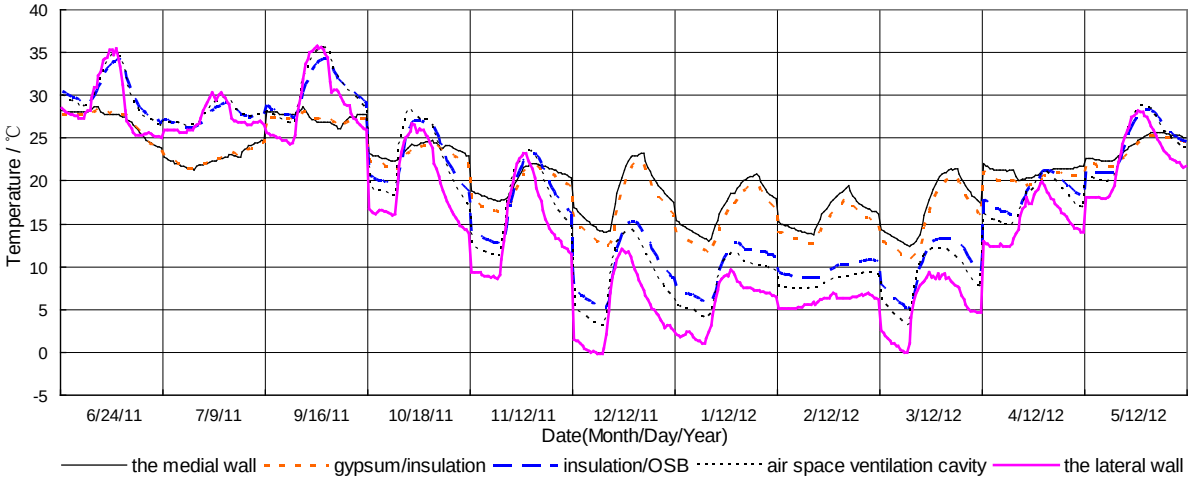

Figure 4 Changes of interface air temperatures for the whole year

Relative humidity changes over time clearly suggested the opposite state compared with temperature. Relative humidity range of the lateral wall was from 30% to 99%, but relative humidity range of the medial wall was lower, more steady and proper to live. Relative humidity of the medial of wall was always little lower and nearer to relative humidity of interface between the gypsum board and insulation layer. Relative humidity changes trend of the interface between the insulation layer and OSB sheathing have been shown the same as those of the lateral wall, which were different with relative humidity of the gypsum board cavity-side obviously. It was shown that the vapor retarder of polyethylene film really prevented the vapor into the indoor through wall cavity.

Relative humidity of the interface between the insulation layer and OSB sheathing was stable comparatively, and lower than relative humidity of inside the cladding cavity. Apparently, the waterproof and moisture permeable building paper was very indeed effective in condition of the high relative humidity of outdoor. But relative humidity of the OSB cavity-side was lowest when relative humidity of each the medial and lateral wall was high in summer, especially in July. The moisture was restrained from indoor into wall cavity by vapor retarder of polyethylene film. The temperature of ventilated cavity up to 36.7℃ in July, when the highest relative humidity was 83.9%. However, the time was not so long under this high temperature and relative humidity state. There was not mold growth according to reference [8].

Both the stucco and air space ventilation cavity resistance to moisture was obviously effective since data showed relative humidity inside the cladding cavity before reached the maximum was always lower than relative humidity of the lateral wall, and the peak of relative humidity inside the cladding cavity clearly showed the hysteresis behavior.

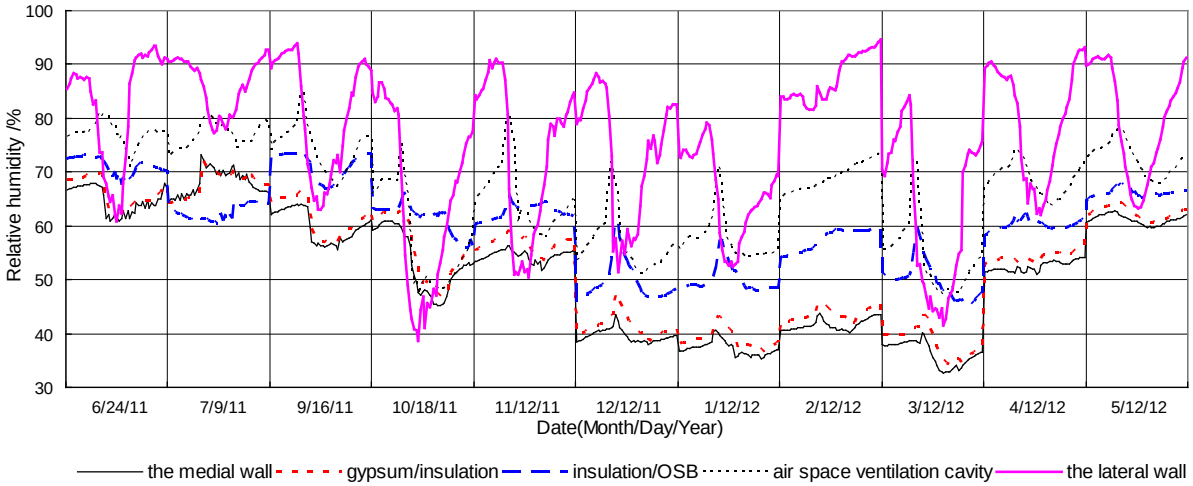

Figure 5 Changes of interface relative humidity for the whole year

Temperature and relative humidity data measured at the coldest day of outdoor monthly from October to March of next year were chosen to analyze for illustrating the state of heat and moisture transfer through the multilayer wall. Temperature and relative humidity gradients through the test wall profile were obvious in Figure 6. Temperatures were reduced from medial to lateral wall, and the trends of relative humidity were opposite. Temperature difference was the largest between gypsum board and OSB sheathing in the process of heat transfer from medial to lateral wall. The largest temperature difference has reached 8.2℃ happened in December. The insulation kept the indoor warm. Temperature difference between ventilated cavity and lateral wall was about 4℃. There was a certain heat barrier because of air space. Figure 7 showed the surface temperature of SPF frame dimension lumber and OSB sheathing. The surface temperatures of OSB sheathing (T2, T4 and T6) developed continuously along with the changes of the lateral wall temperatures. The surface temperatures of wood frame (T1, T3 and T5) developed smaller than those of OSB sheathing. All surface temperatures were above 0℃. So the risk of water condensation in the wall could be eliminated in winter.

Relative humidity gradients were largest between ventilated cavity and lateral wall. The maximum difference was 34% happened in December. In winter relative humidity maximum gradient was 14.6% from the interface between the gypsum board and insulation layer to the interface between the insulation layer and OSB sheathing. So the vapor retarder of polyethylene film was perfect. But at the same time relative humidity of medial wall didn't attain to 40%. Therefore, the indoor environment was felt little dry.

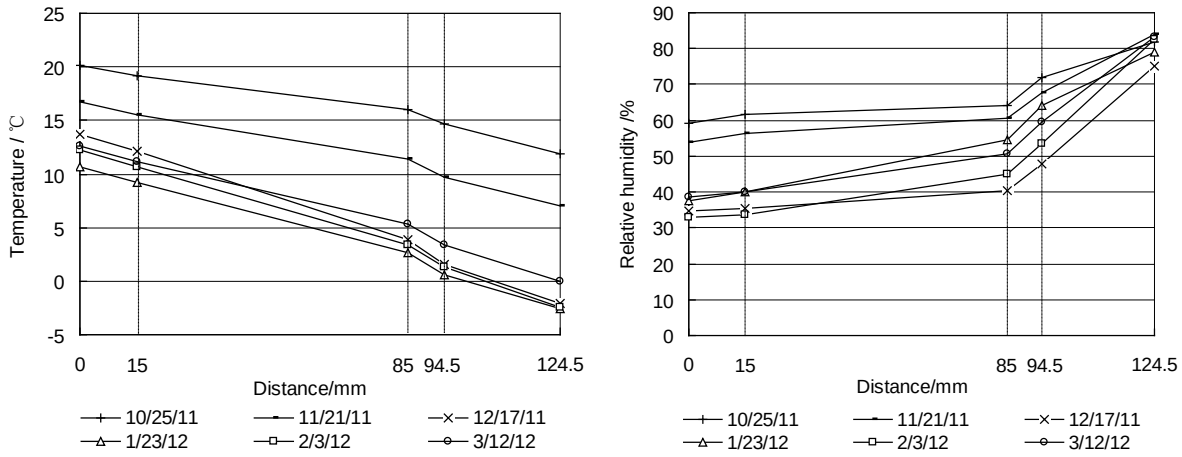

Figure 6 Temperature and relative humidity gradients through the test wall profile

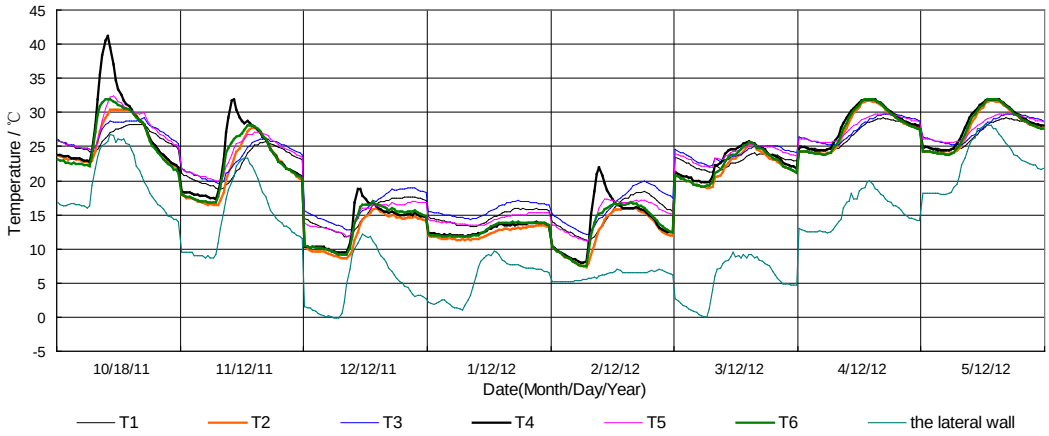

Figure 7 Surface temperature of wood materials of SPF and OSB

Figure 8 showed the air pressure of the top and bottom in cladding ventilation cavity. The top air pressure P1 was always less than the bottom air pressure P2. The average difference of air pressure was 0.12kPa. This indicated airflow entering low on the wall and exiting at the top through ventilation holes in metal strips. Winter air pressure was higher than other seasons' from the whole year data.

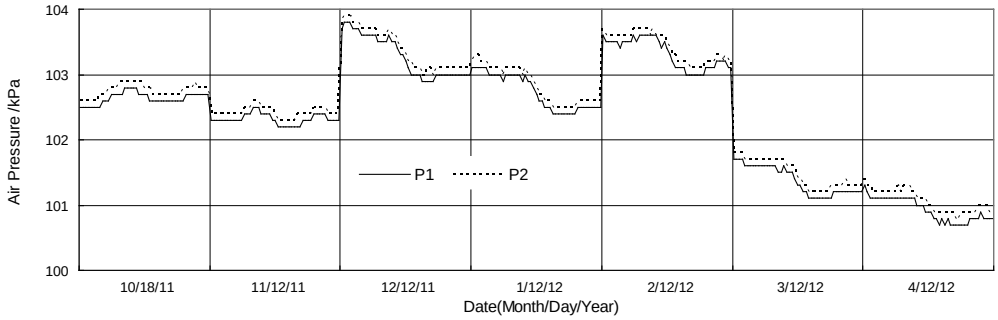

Figure 8 Air pressure in cladding ventilation cavity

The result analysis of two years data seems that the application of wood frame wall

system in demonstration test house is very successful in Suzhou Lake Tai climate zone. Thermal performance of this system was good and no mold growth and water condensation occurred inside the wall during the testing period. Most time of temperature and relative humidity indoor were perfect or acceptable in addition to January night. The increasing humidity should be needed to protect the dry glulam against split in winter.

Conclusions

Long-term on-site assessment of hygrothermal performance was presented in this paper. The results indicated that water vapor control strategy performed well at reducing summertime mold growth and wintertime condensation in testing wall assemblies in Suzhou Lake Tai of hot summer & cold winter climate zone. Vapor retarder, waterproof & moisture permeable building paper and cladding ventilation cavity could increase the moisture tolerance and reduce risks related moisture for multilayer wall. Thermal performance was on perfect level because of cavity wall insulation from the whole testing period. Therefore, the same configuration design as testing exterior wall can be widely used in China hot summer & cold winter climate zone.

Acknowledgements

This research has been supported by the forestry industry research special funds for public welfare projects, State Forestry Administration of China, contract No. 201204701 and leading talent project in Suzhou Wuzhong District, contract No. WC201107.

References

1. Gatland S.，Karagiozis A. (2007). The hygrothermal performance of wood-framed wall systems using a relative humidity-dependent vapor retarder in the Pacific Northwest. Thermal Performance of the Exterior Envelopes of Whole Buildings X International Conference, December 2-7.
2. Jan Toman, Alena Vimmrová, Robert Černý. (2009). Long-term on-site assessment of hygrothermal performance of interior thermal insulation system without water vapour barrier. Energy and Buildings, 41(1): 51-55.
3. Maref, W., Tariku, F. & B. Di Lenardo. (2008). NRC-IRC develops evaluation protocol for innovative vapour barrier, Construction Innovation, 13, (2): 6.
4. Robert Tichy, Chuck Murray. (2007). Developing innovative wall systems that improve hygrothermal performance of residential buildings. Washington State University, March.
5. Glass, Samuel V., TenWolde, Anton. (2007). Review of in-service moisture and temperature conditions in wood-frame buildings. General Technical Report FPL-GTR-174. Madison, WI: U.S. Department of Agriculture, Forest Service, Forest Products Laboratory.
6. Karagiozis A, Desjarlais A. (2007). Developing innovative wall systems that improve hygrothermal performance of residential buildings, Oak Ridge National Laboratory, May.
7. Tariku F.,Maref W., Di Lenardo B., Gatland, S. (2009). Hygrothermal performance of RH-dependent vapour retarder in Canadian coastal climate. 12th Canadian Conference of Building Science and Technology, Montreal, QC, May 6-8.
8. Xiaohuan Wang. (2011). Research on thermal performace of wood frame wall, Beijing: Chinese

Academy of Forestry.
9. Jian Li. (2009). Wood science research, Beijing: Science Press, pp30.

From a Production Orientation to a Stakeholder Orientation: The Evolution of Marketing Sophistication in Private, Multi-site U.S. Sawmills

Xiaoou Han
Ph. D Candidate
Department of Wood Science and Engineering
College of Forestry
Oregon State University
Corvallis, OR 97331
xiaoou.han@oregonstate.edu

Eric Hansen
Professor
Department of Wood Science and Engineering
College of Forestry
Oregon State University
Corvallis, OR 97331
eric.hansen2@oregonstate.edu

Abstract

Marketing can be thought of as a means of satisfying stakeholder needs in a social context. The role of marketing within a firm and the way it is conducted serve as indications of the sophistication of a firm. When marketing is purely a selling function, the company is likely production oriented. Conversely, marketing as an integrator or relationship-builder implies a more sophisticated market-orientation. Based on previous research, it is clear that marketing is changing over time. This study is focused on the "real" marketing sophistication and practice present in the US sawmilling sector. Here, marketing sophistication is used to mean the "degree of market orientation." It also explores the evolution of marketing sophistication in the sawmilling sector during the past years and the direction towards which marketing will develop. Finally, it investigates the interface between marketing and sales departments which can have essential impacts on marketing sophistication.

Key words: marketing sophistication, evolution, recession, customer, stakeholder

Introduction

During the early years when demand was high and customer needs were relatively unified, companies were mainly focused on producing large volumes of commodity products and would rely on a sales force to sell those products to customers. As the marketplace changes over time, especially with respect to customer needs and competitors, companies must become more sophisticated in their marketing approach to remain competitive. Instead of focusing only on production, companies should put more efforts to satisfy customers and other stakeholders.According to Narver and Slater (1990), a market orientation is a focus on customers and competitors and an ability to bring information about each back into the organization and effectively integrate it into operations (Narver and Slater 1990). This perspective is broadened by adding the idea of "stakeholder orientation" (Ferrell et al. 2010).

The forest industry is traditionally production-oriented and competes on low cost. Marketing is implemented as a sales-tool. However, the marketplace has evolved and become much more sophisticated. Marketing has to keep up with the change, especially during recession and times when the companies are facing severe challenges. Therefore, the understanding and approach of marketing must be improved to provide forest product companies with continuous competitive advantages. Hence, the objectives of this study, in the context of private-owned, multi-site, medium-sized U.S. sawmills are the following:

1) To learn the current situation of marketing sophistication

2) To investigate the evolution of a marketing sophistication

3) To assess the role ofmarketing departments in sawmilling companies

Theoretical background

Market orientationconceptualization

Lear's (1963) work is the earliest literature that can be found discussing market orientation and it can be considered quite similar to customer orientation. However, after decades of development, market orientation has turned into a rich concept including multiple dimensions. It is considered as the actual implementation or interpretation of the marketing concept (Kohli and Jaworski 1990).Narver and Slater (1990) and Kohli and Jaworski (1990) are the two well-know "camps" regarding market orientation. Narver and Slater (1990) consider market orientation as an organizational culture consisting of three components, namely, customer orientation, competitor orientation and interfunctional coordination. However, Kohli and Jaworski (1990) understand market orientation as a behavioral process of intelligence generation, intelligence dissemination and responsiveness. They provide two perspectives to approach market orientation with the same focus - the customers. The two perspectives are different but can be integrated as a whole.

From the cultural perspective, market orientation could be understood as attitudes and values that are shared by the people in the organization. It is like "an invisible hand" guiding individuals' behavior (Lichtenthal and Wilson 1992). The behavioral view of market orientation provides a framework of implementation of market orientation (Vazquez et al 2001). Cadogan and Diamantopoulos (1995) synthesize these two perspectives and suggest a reconstruction of market

orientation (Figure 1).

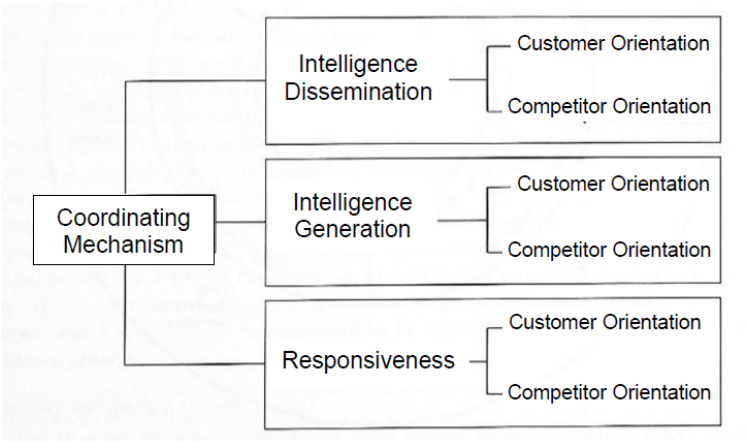

Figure 1: An integrated model of market orientation (adapted from Cadogan and Diamantopoulos, 1995)

In this integrated construct of market orientation, the three behavioral components- intelligence generation, intelligence dissemination and responsiveness-are led by customer orientation and competitor orientations. The coordinating mechanism dictates the manner in which these three behaviors are performed. That is to say, the activities associated with a market orientation take place following the process of intelligence generation, intelligence dissemination and responsiveness. The activities and the process that take place are oriented towards customers and competitors. Also, a coordinating mechanism steers the entire process to make sure things can be done effectively and efficiently. It focuses on the communication within a functional group as well as on the interaction among different functional groups.

The scope of a market orientation has expanded to include other stakeholders.Besides customers and competitors, other factors such as suppliers and communities could each highly influence companies (Lusch and Laczniak 1987). Taking such factors into consideration, the idea of stakeholder orientation is suggested(Maignan and Ferrell 2004, Ferrell et al. 2010). A stakeholder orientation emphasizes the importance of all individuals and organizations that have a "stake" in the company. It is suggested to be an extension of a market orientation, broadening the focus of the concept from just customers and competitors to all stakeholders.

As mentioned earlier, the stakeholder perspective is proposed and it enriches the concept of marketing. From the stakeholder perspective, marketing not only focuses on customers but also takes employees, suppliers, communities, etc. into consideration. Ferrell et al. (2010) proposes the definition of a stakeholder orientation as "the organizational culture and behaviors that induce organizational members to be continuously aware of and proactively act on a variety of stakeholder issues." A stakeholder orientation has concerns for a variety of parties rather than being centered on any specific group. On the contrary, a traditional market orientation identifies customers and competitors as the key focus while paying little attention to other stakeholders.

Although a stakeholder orientation does not put more importance on any specific group than the others, neither does it consider them equal. Different stakeholder groups may be prioritized depending on the issue. Bringing this idea together with the integrated construct of market orientation, the focus of each behavioral component can possibly be expanded from a customer and competitor orientation to a stakeholder orientation (Figure 2).

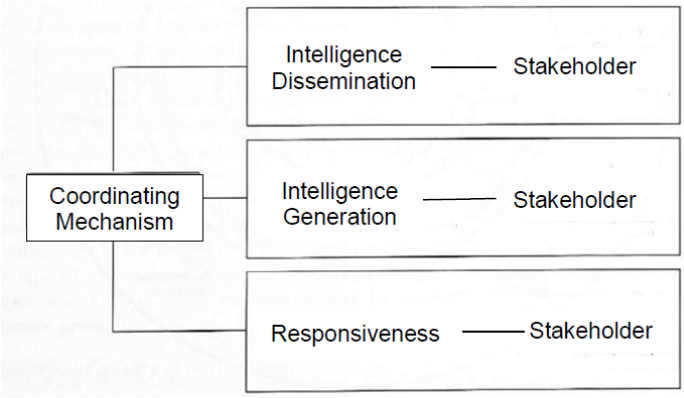

Figure 2: An integrated model of market orientation, from a stakeholder view

Marketing and sales

The distinction between the marketing department and the sales department is receiving increasing attention in the generic marketing literature, although in the past they were not well distinguished. In some research, sales is considered a subunit under the marketing department managed by the marketing executive (Dashpande and Webster 1989; Ruekert et al. 1985), while some authors only talk about the marketing department and don't even mention the sales department (Dastmalchian and Boag 1990). In fact, sales and marketing are two different concepts with different mind-sets or thought worlds behind them.

The role of either a sales department or a marketing department can differ between companies, thus, the distinction of these two departments can vary from one company to another. However, there are some perspectives regarding sales-marketing distinction that can fit the situations of most companies. An example would be that sales is suggested to be short-term oriented and marketing is long-term oriented (Homburg et al.2008; Rouziès 2005). Sales people are normally motivated by month-to-month or quarter-to-quarter goals while marketers often aim for sustainable competitive advantages which may take years to achieve. Also, sales is considered people-oriented (or individual-oriented), for the salespeople often focus on building relationships with the individual customers whom they directly deal with, while marketing has its focus more on analysis of the customer group and market research, in order to get higher level knowledge and better understanding of a larger scope.

It becomes more complicated when scholars try to differentiate sales and marketing using the notion of product-orientation vs. customer-orientation. According to Rouziès et al. (2005), sales is customer-oriented, for the salespeople normally work with a certain group of customers. They

promote various products and services to their customers and make efforts to build good relationships with them. Different from sales, marketing mainly focuses on a certain product or product line. This aligns with Cespedes (1994) and Homburg and Jensen (2007) that sales is customer-oriented while marketing is product-oriented. However, Lear (1963) considers sales as product-oriented and marketing as customer-oriented.According to Lear (1963), a product-oriented firm is likely to have a sales department in which people focus more on products, while in a market-oriented company, there will be a marketing department focusing on the market. Another important aspect regarding marketing and sales department is the marketing and sales interface. As two different but closely connected departments in one company, the marketing department and sales department interact and collaborate in a number of ways. Simply speaking, the marketing department can lead, follow or be independent from the sales department (Day 1999; Kotler et al. 2006). However, the actual situation of marketing and sales configuration is rather complicated. Homburg et al. (2008) creates five categories with each category representing one type of marketing and sales configuration. In each category, the marketing department maintains a different level of knowledge, ranging from low to high, regarding products and marketing and so is the sales department. Also, the marketing department can be either short-term focused or long-term focused and the situation of the sales department is similar. The collaboration and communication between the marketing department and the sales department varies among categories.

Marketing sophistication in the forest sector

The term ‘marketing sophistication’ means the degree of market orientation in an organization.Traditionally, marketing in the forestry sector is largely production-oriented. Take sawmills for example. During the “good old days”, sawmills would just produce as much as they could. Production was their major focus and lumber they produced could be sold very quickly. However, the market is changing. Sawmills in the U.S. are facing increasing competition from other parts of the world. Hansen et al. (2002) suggest that the lumber from European countries is gaining market share in the U.S. market, although it was just a temporal phenomenon. Also, market needs to become more diversified with the growing sophistication of customers with more specific demands. The traditional commodity strategies can no longer satisfy the customers. In addition, the recession that started in 2008 brings more challenge to the industry. Many sawmills shut down during the recession. Some other sawmills are suffering from low profit and high inventories. There are calls for a development of marketing sophistication in the industry and at this point they seem especially urgent. Recent work focusing on marketing in the forest industry companies provides some evidence of increased marketing sophistication (Tibbets 2009, Juslin and Hansen 2003, Hansen et al. 2002). On the other hand, other results show that marketing in forest industry companies is not well implemented (Hansen 2006). Despite the evidence in both directions, there is limited understanding regarding the “real” marketing sophistication and practice in the forest industry.

Methods

Data wascollected throughin-person interviews. A semi-structural interview protocol was created and pre-tested on individuals in both academia and industry. The pre-tests were conducted following the same procedures as the actual interviews. Marketing managers and CEO/president of the private, multi-site, medium-sized, US sawmilling companies were the targets for

interviews. They were sampled from the softwood and hardwood sawmills located in different regions of the U.S. In total, 19 interviews were conducted with 14 sawmills. The interviews were verbally transcribed and analyzed using the qualitative software NVIVO. Themes and important information were identified to address the objectives outlined in the beginning of this paper.

Results

We found that in most of the sawmills studied sales plays a larger role than marketing. The sales/marketing department in these sawmills largely operates focusing on sales. The major function of the department includes making phone calls to current/potential customers, establishing and maintaining relationships and then selling products. Marketing tends to be interpreted as advertising and promotion, which in general are led bythe sales department and are not really important to most of the sawmills. Although the overall marketing sophistication (market orientation) in the sawmills is still relatively low, there are evidences indicating that it has evolved from the traditional production orientation towards a market orientation and a stakeholder orientation. We learned that instead of being production-oriented and concentrating on mass production at low costs, the sawmills now put more effort into understanding the market environment and demands, and then implement strategies and activities accordingly. The analysis is still on-going, but some patterns already emerged from the interview data.

Companies now pay more attention to the stakeholders relevant to their business, including customers, competitors, community, environmental world, etc. as external stakeholders. Customer seems like the most important stakeholder group for the companies. Customer wants and needs become essential to the sawmills. To retain current customers and gain potential customers, the sawmills need to be more customer-oriented-to identify what they want and provide the products and services wanted. This was not considered an important issue years ago when market demand was quite high. During the recession time when market demand was relatively low, sawmills became more proactive in terms of satisfying their customers. Although the major focus of most sawmills interviews is still on the domestic market, the oversea customers are of growing importance nowadays due to the shrinkage of the U.S. market. Developing countries such as China and India still maintain a relatively high demand for lumbers and other forest products. They can be a good potential market for U.S. sawmills.

Also, the environmental world is of a great importance to the sawmills.Sawmills are expected to be environmentally responsible with its operations.One way the companies address it is to provide third-party certified products. They also promote the fact that they manage their forest land in a sustainable manner to build a positive public image. Furthermore, some sawmills actively participate in national programs and industry associations in order to promote the forest sector as a whole.

Overall, the evolution of marketing sophistication gains a firm better understanding of the customers and the market environment. It also helps a firm to better respond to various demands from customer and other stakeholders and thus enhances firm competitiveness within the forest sector. Eventually, it may increase the competitiveness of the forest sector.

References

American Marketing Association.1948. Report of the Definitions Committee. Journal of Marketing 13(2):202-217.

Bartels, R. 1962. The Development of Marketing Thoughts. Richard D. Irwin, Inc, Homewood, IL.

Berg, B. L. 2009 Qualitative Research Methods. Pearson education, Inc. Boston.

Cadogan, J. W. and A. Diamantopoulos. 1995. Narver and Slater, Kohli and Jaworski and the market orientation construct: integration and internationalization. Journal of Strategic Marketing. 3(1):41-60.

Cespedes, F. V. 1994. Industrial marketing: managing new requirements. Sloan Management Review. 35(3):45-60.

Day, G. 1999. Aligning organizational structure to the market. Business Strategy Review. 10(3): 33-46.

Hansen, E., J. Seppälä, and H. Juslin. 2002. Marketing Strategies in the Western Softwood Sawmill Industry. Forest Products Journal. 52(10):19-25.

Dastmalchian, Aand D. A. Boag. 1990. Environmental dependence and departmental structure: case of the marketing function. Human Relations. 43 (12): 1257–1276.

Deshpandé, R and F. E. Webster. 1989. Organizational Culture and Marketing: Defining the Research Agenda. Journal of Marketing. 53 (1): 3–15.

Deshpande, R and G. Zaitman. 1982. Factors affecting the use of market research information: a path analysis. Journal of Marketing Research, 19 (1): 14-31.

Fern, E. F. 1982. The use of focus groups for idea generation: the effects of group size, acquaintanceship, and moderator on a response quality and quantity. Journal of Marketing Research. 19, 1-13.

Ferrell, O. C., T. L. Gonzalez-Padron., G. T. M. Hult and I. Maignan. 2010. From market orientation of stakeholder orientation. Journal of Public Policy and Marketing. 29 (1): 93-96.

Hibbard, B.H and A. Hobson. 1916. Marketing farm product by parcel post and express. American Economic Review. 6 (3): 589-608..

Homburg, C and O. Jensen. 2007. The thought worlds of marketing and sales: which differences make a difference?. Journal of marketing. 71(3):124-142.

Homburg, C., J. P. Workman and H. Krohmer. 1999. Marketing's influence within the firm. Journal of Marketing. 63 (2): 1-17.

Homburg, C., O. Jensen and H. Krohmer. 2008. Configurations of marketing and sales: a taxonomy. Journal of Marketing. 72 (2): 133-154.

Hunt, Shelby D. 2007. A Responsibilities Framework for Marketing as a Professional Discipline," Journal of Public Policy &Marketing, 26 (Fall), 277–83.

Juslin, H. and E. Hansen. 2003. Strategic Marketing in the Global Forest Industries. Author's Academic Press. Corvallis, Oregon. 610 pp.

Kohli, A.K. and B.J. Jaworski. (1990). Market Orientation: The Construct, Research Propositions, and Managerial Implications. Journal of Marketing. 54(2):1-18.

Kotler, P. 2003. A Framework for Marketing Management. Pearson Education, Inc, Upper Saddle River, NJ.

Kotler, P., N. Rackham and S. Krishnaswamy. 2006. Ending the war between sales & Marketing. Harvard Business Review. 84 (7-8): 68-78.

Kotler, Phillip. 1977. From Sales Obsession to Marketing Effectiveness. Harvard Business Review. 55(6): 67-75.

Lichtenthal, J. D and D. T. 1992. Becoming market oriented. Journal of Business Research. 24 (3)3: 191-207.

Lusch, R. F. and G. R. Lazniak. 1987. The Evolving Marketing Concept, Competitive Intensity, and Organizational Performance. Journal of the Academy of Marketing Science. 15 (3): 1-11.

Lear, R.W. 1963. No Easy Road to Market Orientation. Harvard Business Review 41(5):53-60.

Maignan, I. and O.C. Ferrell. 2004, Corporate social responsibility and marketing: an integrative framework, The Journal of the Academy of MarketingScience. 32 (1): 3-19.

Narver, J.C. and S.F. Slater. 1990. The Effect of a Market Orientation on Business Profitability. Journal of Marketing. 54(4):20-35.

Powell, F.W. 1910. Co-operative Marketing of California Fresh Fruit. Quarterly Journal of Economics 24(2):392-418.

Tadajewski, M. 2009. Eventalizing the marketing concept. Journal of Marketing Management 25(1/2):191-217.

Tibbetts, A. 2009. A Qualitative Benchmark Study of the Evolution of Oregon's Forest Products Industry's Emphasis on Marketing. Senior Thesis. Wood Science and Engineering. Oregon State University. Corvallis, Oregon.

Rouziès, D., E. Anderson., A. K. Kohli., R. E. Michaels., B. A. Weitz and A. A. Zoltners. 2005. Sales and marketing integration: a proposed framework. Journal of personal selling and sales management. 25(2): 113-122.

Ruekert, R. W., O C Walker Jr., and K. J. Roering. 1985. The Organization of Marketing Activities: A Contingency Theory of Structure and Performance. Journal ofMarketing. 49(1): 13-25.

Vázquez, R.; M. L. Santos and L. I. Álvarez.2001. Market orientation, innovation and competitive strategies in industrial firms. Journal of Strategic Marketing. 9 (1):69-90.

Weld, L.D.H. 1915. Marketing Distribution: The University of Minnesota. American Economic Review 5:125.

Weld, L.D.H. 1917. Marketing Agencies between Manufacture and Jobber. Quarterly Journal of Economics 31(4):571-599.

Determination of Volatile Organic Compound Emission from Wood-based Panels

Wang Yu[1] *- Shen Jun*[1*] *- Zhu Haiou*[2] *- Pan Yanwei*[1]

[1] College of Material Science and Engineering, Northeast Forestry University, Harbin.
** Corresponding author*
zhiziwangyu@126.com
shenjunr@126.com
panyanweichenggong@163.com
[2] Jiangsu Entry-Exit Inspection and Quarantine Bureau, Nanjing, P. R. China
zho@dicp.ac.cn

Abstract

The potential impact of volatile organic compound (VOC) on the health and wellbeing of people has become an increasingly important issue over the last twenty five years, now people pay more attention to VOC emissions from all material that applied to indoor decoration and refurbish. As a consequence, the emission of VOC as a whole (other than formaldehyde) from wood products has under monitoring.

VOC emissions from wood-based panels were determined by a $1m^3$ small-scale environmental chamber and analyzed by high performance liquid chromatography (HPLC) and gas chromatography (GC). The result showed that the concentration of formaldehyde emissions from particleboard, plywood, high density fiberboard (HDF) and block board was higher than that of the TVOC concentration, especially HDF. Concentrations of formaldehyde and TVOC emission from particleboard, plywood and HDF were higher than that of the block board. The content of VOC monomers in each of the sheet was different; acetaldehyde and acetone were the main aldehydes and ketones compounds.

The equilibrium concentration of formaldehyde, TVOC and aldehydes and ketones (except formaldehyde) emission from material we tested had the same trend, HDF was the highest one, particleboard and plywood were followed and block board had the lowest equilibrium concentration.

***Keywords*:** Small-scale chamber, Wood-based Panels, Formaldehyde, Volatile Organic Compound(VOC).

Introduction

Wood-based panels are commonly used in indoor decorating and refurbishing, which release a great amount of VOC in usage, due to the wood natural characteristics, urea-formaldehyde adhesives commonly used and the influence of process parameters. Rishdmresearch showed that a large number of VOC was emitted from wood itself, especially in new sawn softwood. Longling[1] and others' research found that final moisture content had a great impact on the release amount of aldehydes compounds and polarity VOC and less effect on terpenes when fir was drying, both decreasing drying temperature and increasing final moisture content could significantly reduce the release amount of aldehydes compounds, methanol, acetate and formic acid emission from wood-based panels. Maria[2] measured formaldehyde, acetaldehyde and VOC emission from wood-based panels sold in Swedish market, the results showed that the VOC concentration emission from plywood, particleboard, HDF and oriented standard board (OSB) was relatively high, there was no phenol in detected compounds, even in the boards production with phenol-formaldehyde. This paper used a $1m^3$ small-scale environmental chamber, ultraviolet spectrophotometer, gas chromatography-mass spectrometer (GC-MS) and high performance liquid chromatography (HPLC) to analyze formaldehyde, VOC and aldehydes and ketones emission from Particleboard, plywood, HDF and blockboard, to understand the VOC release level of wood-based panels sold in market.

Materials and Methods

In this study, we detected formaldehyde and VOC emission from the four kinds of wood-based panels. We also qualitative and quantitative the monomer of aldehydes and ketones.

Test material and instrument. Particleboard, plywood, HDF and blockboard were produced in certain wood-based panels factories of Heilongjiang Province. According to HJ571-2010 <Technical requirement for environmental labeling products—Wood based panels and finishing products> [3], the specimens were dealt with in a standard –related method before they were tested. The specimen was 645mm×820mm×16mm, and the summation of exposed area was $1m^2$. To prevent the high release from the boundary of board, each edges were sealed with aluminum belt, and then the sealed specimen was wrapped with polytetrafluoroethylene and was stored at below 23℃ environmental condition. Tables1, 2, 3 and 4 were the process parameters of each test material.

Table1 the process parameters of particleboard

Parameters	Thickness /mm	Density /gm^{-3}	Hot-pressing temperature/℃	Hot-pressing time/s	Hot-pressing pressure /MPa
particleboard	16	0.77	195/192	204-206	250-260(total)

Table2 the process parameters of plywood

parameters	Raw material	Thickness /mm	Hot-pressing temperature /℃	Hot-pressing time /s	Hot-pressing pressure /MPa	Glue content/g	Types of glue

plywood	Mixed wood chip	7	195-200	20-30	120-130	120	UF, melamine resin

Table3 the process parameters of blockboard

parameters	thickness/mm	Moisture content/%	Hot-pressing temperature /℃	Hot-pressing time /s	Hot-pressing time /MPa	substrate	Surface board	Types of glue
blockboard	16.8-17.2	7-10	120/117	90	0.85	poplar	mahogany	UF

Table4 the process parameters of HDF

parameters	thickness/mm	density/gm^{-3}	Hot-pressing temperature /℃	Hot-pressing time/s	Hot-pressing pressure /MPa	Glue content/g	Types of glue
HDF	12	880	190	278	50	240	UF

Other material: Tenax tube, 2, 4- dinitrophenylhydrazine (DNPH) sampling tube, TVOC standard sample, n –hexadecane standard sample, n-hexane standard sample, TO11/IP-6A aldehyde/ketone-DNPH mix, acetonitrile (chromatographically pure), deionized water.

Main instrument: Gas chromatography-mass spectrometer (GC-MS, TRANCE DSQ, American Thermo Company), Chromatographic column: DB-1-MS quartz capillary column (60m×0.25mm×0.25μm); High performance liquid chromatography (HPLC-1100), Chromatographic column: Zordax Ods (4.6mm×250mm×5μm); thermal desorption (ATD 650, American PE company); ultraviolet spectrophotometer (UV 1550, shimadzu seisakusho Ltd); MODEL 9600 adsorption tube aging device (flow was 10 to 250ml/min, the highest temperature was 400℃); 1m^3 small-scale environmental chamber allocates with air cleaning system, temperature and humidity regulating systems and ventilation system.

Sampling system: LFS-113DC dual-mode low flow gas sampling pump (constant flow 5~200min/L, the flow was 1~350ml/min when pressure kept constant), VER IFLOW-500 electronic flow meter (the range of flow was 1 to 500mL/min and with ±5% accuracy), silicone tube, stealing belt and drying tower.

Test principle and condition

Test principle. The condition of 1m^3 small-scale environmental chamber was 23℃ temperature, 50% relative humidity and 1h^{-1} air exchange rate. First, the chamber's background concentration of TVOC were measured, please put the specimen into the chamber when the chamber conditions was stable. The gas was collected by a dual-mode low flow gas sampling pump, the sampling time and sampling rate was respectively 25min and 200ml/min. The gas was collected on 24th hour, 3rd day, 7th day, 14th day, 21st day and 28th day during the experiment period. TVOC was collected by Tenax tube, aldehydes and ketones were collected by 2, 4- dinitrophenylhydrazine (DNPH) sampling tube.

The thermal desorption system analyzing condition. The thermal desorption temperature and time of sampling tube were 280℃ and 10min, the flow of desorbed gas was 50ml/min; the trapping temperature and heating rate of trapping tube were -20℃ and 40℃/sec; the transmission line temperature was 220℃, split ratio was 50.

GC/MS analyzing condition. The polarity index of capillary column was less than 10, the column length was between 50m to 60m, the inner diameter was between 0.20mm to 0.32 mm and the film thickness was in 0.2μm to 1.0μm. The column temperature first was 40℃ retention 1min, and then at the rate of 5℃/min heating to 100℃ no retention, finally at the rate of 10℃/min heating to 250℃ retention 10 min. The GC/MS interface temperature was 250℃, the whole scanning range was in 25u to 350u, using the high purity helium as carrier gas and the column velocity was 1.0ml/min, selecting EI ionization mode, the ion source temperature was 250℃.

HPLC analyzing condition. Chromatographic experiments were performed on C18 column (4.6 mm×250 mm,μ5m), the mobile phase was acetonitrile and water; the detection wavelength was 360nm, column temperature was 35℃, the flow rate was 1.0 ml/min, injection volume was 25μl, the gradient eluation program saw table5.

Table 5 HPLC gradient eluation program

Time %	Acetonitrile %	Water %
0	60	40
20	75	25
30	100	0
35	60	40

VOC analyzing method. First, analysis on the standard sample, the aldehyde standard sample contains 15 kinds 2, 4-DNPH aldehyde derivatives, including formaldehyde, acetaldehyde, acrolein, etc., the concentration of each standard sample was all 15μg/ml. The concentration of acetonitrile was respectively diluted to 10μg/ml, 4μg/ml, 1μg/ml, 0.4μg/ml and 0.1μg/ml when analyzed, we could obtain the standard sample chromatogram by HPLC analyzing (figure1). Formaldehyde was quantitative by Acetyl acetone Spectrophotometers.

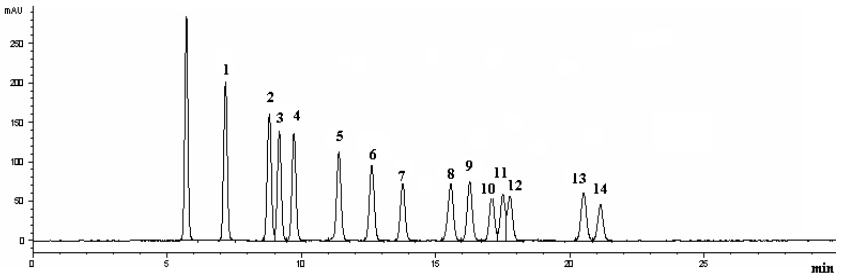

Figure 1 the liquid chromatogram of mixed aldehydes standard sample

1, acetaldehyde	2, acrolein	3, acetone	4, propionaldehyde	5, crotonaldehyde
6, butyraldehyde	7, benzaldehyd	8, isovaleraldehyde	9, valeraldehyde	10, o-tolualdehyde
11, m-tolualdehyde	12, p-tolualdehyde	13, hexanal	14, 2,5-dimethyl benzaldehyde	

Then, analysis on the sample, elution the DNPH sampling tube with acetonitrile, the volume of acetonitrile was 5ml, sample was detected and analyzed by HPLC. Using Tenax tube collected VOC, and using thermal desorption did the high temperature thermal desorption ten minutes at 250℃, then detection by GC/MS.

According to the peak retention time of three kinds of particleboard on the GC/MS and HPLC, comparing with the standard sample map, identified VOC components and calculated concentration of each component.

Some standards about using chamber test VOC regulated that the background concentration of individual target VOC and TVOC should not exceed 2μg/m^3 and 20μg/m^3 respectively [4-6]. Before the test, washing the internal chamber with deionized water and bilwing dry with fan. We could start test when each parameter of chamber was stable. During the sampling period, the gas orderly through activated carbon device, distill water, to remove the volatile compounds. The effect of background concentration had been removed in this experiment.

Result and discussion

Accordingly to JIS A 1901:2009<Determination of the emission of volatile organic compounds and aldehydes for building products-small chamber method> [6], the range of TVOC is between n-hexane and n-hexadecane with gas chromatography, including the two chemical substances. The calculated TVOC is converted to the sum of peak areas using the toluene response factor, the concentration of TVOC was the sum of identified target VOC and unidentified VOC.

Table 6 the result of VOC emission from wood-based panels

specimen	formaldehyde μg/m^3		aldehydes and ketones (except formaldehyde) μg/m^3		TVOC μg/m^3	
Time (day)	1	28	1	28	1	28
Particleboard	140.8	98.3	111.1	22.4	100.8	20.8
Plywood	311	117.5	58.6	30.7	19.8	11.8
HDF	1541.3	1099.0	73.7	49.5	351.7	65.1
Blockboard	41.83	20.33	5.45	2.55	2.69	1.54

Table6 was the result of VOC emission from wood-based panels. From table2 we could see that the initial and steady-state concentration of all substance that emission from HDF which made of various kinds mixed polished wood fiber and urea-formaldehyde were both the highest in the four test boards, except the aldehydes and ketones initial concentration. The TVOC release amount was 351.7μg/m^3 1 day later and that equaled to 3.5 times of particleboard at the same time. One month later, the TVOC concentration was 65.1μg/m^3, and the formaldehyde concentration decreased to 1099μg/m^3 from 1541.3μg/m^3 (0.89ppm).

In the other three kinds of boards, the initial and steady-state concentration of TVOC that emission from particleboard production of softwood chips and urea-formaldehyde were much higher, correspondingly the formaldehyde concentration emission from plywood

production of birch veneer and phenolic aldehyde was higher than the others. The initial aldehydes and ketones compounds (except formaldehyde) concentration emission from particleboard was much higher, but the equilibrium concentration of plywood was higher one month later. What caused the phenomenon was that hexanal and butyraldehyde completely released in aldehydes and ketones compounds emission from particleboard, and that the two substances were both with high initial concentration and very low equilibrium concentration (closed to zero). The aldehyde and ketones compounds emission from plywood were acetone and benzaldehyde, with the time prolong, acetone released completely, we could not detect it on the 7th day, but benzaldehyde was with a low release rate, from the beginning to ending, the concentration total decreased 35.9%. All kinds of substances emission from blockboard production of poplar substrate, peach blossom core surface layer and urea-formaldehyde were very low, TVOC equilibrium concentration was 1.54μg/m^3 one month later, at the moment the formaldehyde concentration was 20.33μg/m^3 (0.016ppm).

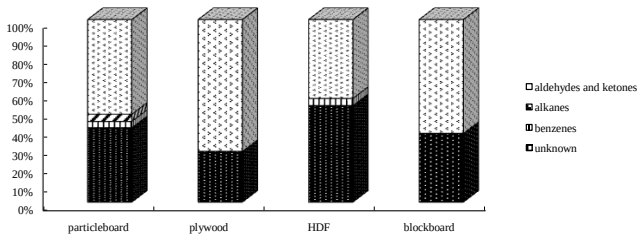

Figure 2 the percentage of individual VOC

Figure2 was the percentage content graph of individual VOC emission from wood-based panels, from figure2, we could see that VOC emission from wood-based panels were main aldehydes and ketones compounds, alkanes, benzenes and some unknown substances, where aldehydes and ketones compounds and unknown substances accounted for a large proportion.The main component of aldehydes and ketones were carcinogenic acetaldehyde and acetone, and aldehydes and ketones might produce in oxidative decomposition of unsaturated fatty acid when wood chipped and dried. Some research showed[7] that the drying temperature and humidity seriously influent the form of aldehydes and ketones, therefore, controlling the release level of aldehydes and ketones compounds based on production origin, reducing the release concentration basically.

Beside aldehydes and ketones compounds and unknown substances, there were alkanes (n-undecane) and benzenes emission from particleboard, and only small amount benzenes in HDF. The detected benzenes were main toluene, ethylbenzene, xylene and styrene, of which the xylene release amount was the biggest. Some researches proved[8] that if people inhaled higher toluene and xylene in short time, it might make central nervous system paralysis, and severe patients might be coma, failure in respiratory cycle and death. Long-term exposure in higher concentration of toluene and xylene would cause chronic benzene poisoning, resulting in obstacle anaemia, fetal congenital defect, therefore, people should pay enough attention to benzenes emission from wood-based panels.

Conclusion

Using $1m^3$ small-scale environmental chamber measures formaldehyde and VOC emission from wood-based panels with higher utilization rate, formaldehyde was collected by distill water and quantitative by acetylacetone spectrophotometry; then using Tenax tube, gas chromatography-mass spectrometer (GC-MS) and high performance liquid chromatography (HLPC) adsorbs the gas and quantity VOC and aldehydes and ketones compounds except formaldehyde, to understand the release level VOC emission from wood-based panels sold in markets.

The formaldehyde concentration was relatively high, especially HDF, the formaldehyde release amount of the other three boards from high to low was plywood, particleboard and blockboard, orderly. Comparing with formaldehyde, the equilibrium concentration of TVOC was very low, and the equilibrium concentration of particleboard was higher than plywood.

Formaldehyde and TVOC emission from blockboard were both lower than the other three boards, acetaldehyde and acetone were the main aldehydes and ketones emission from boards, there were alkanes (n-undecane) and benzenes emission from particleboard, and only small amount benzenes in HDF, we detected no individual VOC in plywood and blockboard.

References

[1] Long Ling, Lu Xixian. VOC Emission from Chinese Fir (Cunninghamia lanceolata) Drying[J]. Scientia Silvae Sinicae, 2008,44(1):107-116.
[2] Maria Risholm-sundman. VOC Emission from Wood-based panels[J]. China Wood-based Panels,2003,6(15-18).
[3] HJ 571-2010, Technical requirement for environmental labeling products—Wood based panels and finishing products[S].
[4] BIFMA M 7.1:2007, Standard test method for determining VOC emissions from office furniture systems, components and seating[S].
[5] ISO 16000-9(2006). Indoor air – Part 6: Determination of the emission of volatile organic compounds from building products and furnishing – Emission test chamber method.
[6] JIS A 1901:2009, Determination of the emission of volatile organic compounds and aldehydes for building products – Small chamber method[S].
[7] M.Z.M. Salem, M. Böhm, J. Beránková, J. Srba, Effect of some manufacturing variables on formaldehyde release from particleboard: Relationship between different test methods, Build. Environ. 46 (2011) 1946-1953.
[8] M.Z.M. Salem, M. Böhm, J. Srba, J. Beránková, Evaluation of formaldehyde emission from different types of wood-based panels and flooring materials using different standard test methods, Build. Environ. 49 (2012) 86-96.

Acknowledge

This research is supported by National Nature Research Fund Project (31070488), and Special Research Fund Project for Science and Technology Innovation Talent From Harbin Technology Division (2010RFXXS023).

New Approach to Remove Metals from Chromated Copper Arsenate (CCA)-Treated Wood

Todd F. Shupe [1] – Chung Y. Hse[2] – Hui Pan[3]*

[1] Professor, School of Renewable Natural Resources, Louisiana State University Agricultural Center, Baton Rouge, LA 70803, USA

* *Corresponding author*

tshupe@agcenter.lsu.edu

[2] Principal Wood Scientist, Southern Research Station, USDA Forest Service, Pineville, LA USA

chse@fs.fed.us

[3] Assistant Professor, Calhoun Research Station, Louisiana State University Agricultural Center, Calhoun, LA 71225, USA

hpan@agacenter.lsu.edu

Abstract

Recovery of metals from chromated copper arsenate (CCA)-treated southern pine wood particles was investigated using binary acid solutions consisting of acetic, oxalic, and phosphoric acids in a microwave reactor. Formation of an insoluble copper oxalate complex in the binary solution containing oxalic acid was the major factor for low copper removal. Furthermore, the possible complexation of acetic/oxalic acid in the organic phase, the decomposition of oxalic acid in acetic acid at high temperatures, and the promotion of the formation and precipitation of the copper oxalate by phosphoric acid may induce an antagonistic effect which adversely influenced the effectiveness of the copper extraction. It was found that the addition of acetic acid into phosphoric acid enhanced the chromium recovery rate of the mixed acid solution. This synergistic effect of mixed acetic acid and phosphoric acids is considered one of the most interesting and significant discoveries in the study.

Keywords: Binary acid solution; CCA-treated wood; microwave extraction,

Introduction

Our recent studies on removal of CCA elements from spent CCA-treated wood have focused on the application of the microwave energy to facilitate acid extraction. A preliminary study (Yu *et al*. 2009) has shown: (1) microwave-assisted acid extractions with oxalic, acetic, and phosphoric acids have reduced the reaction times from hours to minutes compared to the conventional methods, (2) oxalic acid effectively removed arsenic and chromium but not copper, (3) acetic acid extraction was highly effective for the removal of arsenic and copper but not for chromium, and (4) extraction using phosphoric acid was less effective as compared to both oxalic and acetic acids. These results indicated that none of the individual acids were able to effectively remove all three CCA elements simultaneously, but showed a potential complementary effect for extraction. For instance, oxalic acid removed chromium very effectively but not copper, and acetic acid effectively extracted copper but not chromium. The results strongly suggested the opportunity for a two-acid process by either a synergistic extraction effect of the combined acids or a two-step process of consecutive acid extraction. In this study, two acids were mixed, and the extraction potential was evaluated. The acids studied were oxalic, acetic, and phosphoric. The objectives of the study were to develop a cost-effective microwave-based dual acids extraction system to maximize removal of CCA elements from spent-CCA-treated wood. This was addressed by optimizing of the acid combinations and concentration, extraction times, and reaction temperature to minimize any environment impact.

Materials and Methods

CCA-treated southern pine (*Pinus* sp) guard rail posts were obtained from Arnold Forest Products Co. in Shreveport, La. The posts were reduced to sawdust on a table saw. The sawdust was screened to collect sawdust that passed through a 40-mesh sieve and retained on a 60-mesh sieve and then dried to a constant weigh in an oven maintained at 50 ^{o}C. The dried sawdust was stored in heavy duty zip lock polyethylene bag and used without further treatment. All acids used were of reagent grade and obtained from commercial sources. Deionized water was used.

The acid extractions were carried out in a Milestone MEGA 1200 laboratory microwave oven. Unless otherwise stated, 1 g wood meal was weighted into a 100 ml Teflon reaction vessel with a magnetic stirring bar. The acid solutions were prepared in percentage concentration by weight of acid in gram per volume of deionization water (g/v). Twenty ml of a designated concentration and mixed ratio of the binary acid solutions of acetic/oxalic, acetic/phosphoric, or phosphoric/oxalic acids were then added to the reaction vessel and thoroughly mixed. The reaction vessel was then placed on the rotor tray inside the microwave cavity. The temperature was monitored using an ATC-400FO automatic fiber optic temperature control system. Based on monitored temperature, the output power was auto-adjusted during acid extraction. In this study, the temperature was increased from room temperature to 160 °C at a

heating rate of 32.5 °C/min. and then was kept constant for 30 min., unless otherwise noted. After a cooling period of 30 min at the end of acid extraction, the extracted liquids were vacuum-filtered through Whatman No. 4 filter paper and then diluted to 100 ml in a volumetric flask for determination of the CCA elements. The solid wood residue retained on the filter paper was oven-dried and then subjected to acid digestion prior to the determination of chromium, arsenic, and copper. Samples were digested in accordance with American Wood Protection Association Standard A7-93 (AWPA, 2008). The procedure required that the solid residues be accurately weighed into 100 ml test tubes. For each gram of solid residue, 15 ml of nitric acid was added. A digestion blank along with the samples was also prepared. The test tubes were placed into an aluminum heating block and the temperature was increased and maintained at 120 °C until a transparent liquid was obtained. The transparent liquid was cooled to room temperature and 5 ml of hydrogen peroxide was drop-wise added. If the solution was not clear after this treatment, the temperature was increased and another 5 ml of hydrogen peroxide was added. The sample was continually heated until approximately 1 ml of sample solution remained in the test tube. The sample was carefully transferred into a 25 ml volumetric flask and then diluted with distilled water to a 25 ml solution for the determination of the chromium, arsenic, and copper in the residue. The concentration of chromium, arsenic, and copper in both samples (i.e., acid extracted solution and digested solution) was determined by inductive coupled plasma atomic emission spectroscopy (ICP-AES). The recovery rate of the elements in acid extraction was then determined by the following equation:

$$\text{Recovery rate (\%)} = Ws / (Ws + Wr) * 100\%$$

Where Ws is the weight of the CCA elements in acid extracted solution and Wr is the weight of CCA elements in the wood residue

Results and Discussion

Recovery of metals from CCA-treated wood with binary oxalic and acetic acid solutions in a microwave reactor

All mixed acids resulted in more than 98 and 99% recovery for arsenic and chromium, respectively. However, it should be noted that average copper recovery ranging from 30.11 to 34.57% was surprisingly ineffective based on the previous finding that 97.5% copper removal was attained with only acetic acid extraction in a microwave reactor (Yu *et al*. 2009). This result strongly suggests possible physical interactions as well as chemical reactions in the binary acid solution hindered the reactive extraction of acetic acid. The formation of an insoluble complex of oxalic acid and copper during acidification of CCA-treated wood with organic acids is well recognized (Bull 2001; Humer *et al*. 2004; Kakitani *et al*. 2009; Pizzi 1982, 1990). Furthermore, in a liquid-liquid equilibrium involved in the reactive extraction of an organic acid, the formation of mixed acid complexes containing acetic and oxalic acids in the organic phase have been reported (Kirsch and Maurer 1998). In addition, it was reported that in

anhydrous acetic acid at high temperatures oxalic acid can decompose quickly (Pszonicki and Tkacz 1976). Thus, it is possible that the mixed oxalic and acetic acids solution may have induced an antagonistic effect and adversely influenced the effectiveness of the copper extraction, suggesting that the binary mixed solution of oxalic and acetic acid is not suitable for CCA extraction.

Recovery of CCA-treated wood with phosphoric acid and oxalic or acetic acids in a microwave reactor

In the mixed phosphoric and oxalic acids solution, the recovery rate of chromium and arsenic approached 100%. However, the highest copper recovery rate was only 52%, which is substantially less than that of 79% obtained in the simple phosphoric acid extraction in a microwave reactor in a previous study (Yu *et al*. 2009). This result indicates that phosphoric acid in the binary solution appears to promote the formation and precipitation of insoluble copper oxalate in the wood. This suggests that the binary solution of oxalic acid and phosphoric acid is also not suitable for CCA extraction. In a two-step extraction process using oxalic acid as the first step with a 1-h pre-extraction followed by a 3-h extraction with phosphoric acid in the second step, Kakitani *et al*. (2006) also concluded that the use of inorganic acids under the experimental conditions were ineffective for remediation of CCA-treated wood.

In the mixed solution consisting of phosphoric acid and acetic acid, the arsenic and copper were recovered at high efficiency as expected. But the recovery of chromium is the most interesting result in the study. Yu *et al*. (2009) found that extractions with neither acetic acid nor phosphoric acid alone can effectively recover chromium. In this present study, the addition of 1.0% acetic acid into a series of concentrations of phosphoric acid enhanced the chromium recovery rate of the mixed acid solution (i.e., removal of chromium increased as the phosphoric acid increased). It should be noted that all three CCA elements were recovered in high efficiency with the maximum chromium recovery rate of 98.1% when phosphoric acid concentration was 3.5%. This synergistic effect of mixed acetic acid and phosphoric acids is considered one of the most interesting and significant discoveries in the study. The potential for the development of this binary acid solution into a highly efficient CCA recovery system is apparent. The results suggest that the optimization of process variables such as reaction temperature, reaction time, concentrations and mix ratio is needed for a highly efficient CCA recovery system.

Optimization of the synergistic effects of the CCA recovery rate of a phosphoric and acetic acid system

Analysis of variance (ANOVA) indicated phosphoric acid concentration had a significant effect on the CCA recovery rate, but the effect of the acetic acid concentration was not significant. The average recovery rates were 99.3%, 97.5%, and 98.4% for arsenic, chromium, and copper, respectively, when the concentration of phosphoric was 2.75% regardless of the concentration of the acetic acid. The results also show that there was no significant improvement in average chromium recovery rate by raising phosphoric acid concentration above 2.75%, however, the chromium

recovery decreased significantly with a decrease in phosphoric acid concentration below 2.75%. This concentration (i.e., 2.75%) was elected for additional studies in the following process optimization experiment.

It is important to note that even though the effect of acetic acid concentration was statistically not significant, the recovery rate of greater than 99% was attained for all CCA elements as acetic acid concentration increased to 2.0%. The additional capability of further increase in recovery rate is considered important in the development of a scaled up extraction process.

The concentration of phosphoric acid is an important factor in this binary acid extraction. Figure 1 shows the average extraction rate change as the phosphoric acid concentration increased for chromium extraction as compared to that of arsenic and the copper. Chromium has the highest resistance to extraction because of its strong bonding with lignin (Pizzi 1990). However, it is not fully clear how the addition of acetic acid into phosphoric acid resulted in an enhancement regarding the recovery of chromium. Nevertheless, the use of chemical activation of wood with phosphoric acid has been known for many decades and has been applied to different cellulose and lignocellulosic materials for the preparation of activated carbon (Zuo *et al*. 2009; Jogtoyen and Derbyshire 1998) and flame-retardant products (Inagaki *et al*. 1976). Studies have shown that during thermal treatment the phosphoric acid treated lignocellulosics begin to lose carbonyl and methyl groups in hemicelluloses at 50 ^{o}C, composition of lignin starts to change at 100 ^{o}C, and substantial oxidation of cellulose to form ketones occurs at 150 ^{o}C (Jogtoyen and Derbyshire 1998). Also, the bond cleavage reaction of the biopolymer chains occur around 150 ^{o}C (Solum *et al*. 1995). Furthermore, it was shown that the treatment of cellulose with phosphoric acid also resulted in reduced substrate crystallinity and increased accessibility (Nilsson *et al*. 1995; Saito *et al*. 1994). Thus, it is possible that these characteristic reactions of phosphoric acid may each contribute to a different degree toward chromium recovery. For instance, the composition and structural changes in lignin induced by phosphoric acid treatment may weaken the bond binding the metal-lignin complexes to increase the chromium removal. Furthermore, decreased crystallinity and cellulose surface exposure by solubilization of hemicelluloses by the phosphoric acid treatment may result in increasing access for acetic acid to enhance the recovery rate. Additional studies on the influence of particle size on metal recovery rate with a focus on the accessibility factor as well as the effect of phosphoric acid treatment on the distribution of hemicelluloses and lignin compositions between acid solution and extracted wood residues are in progress. These studies should provide additional new data to elucidate the synergistic effect of the binary solution.

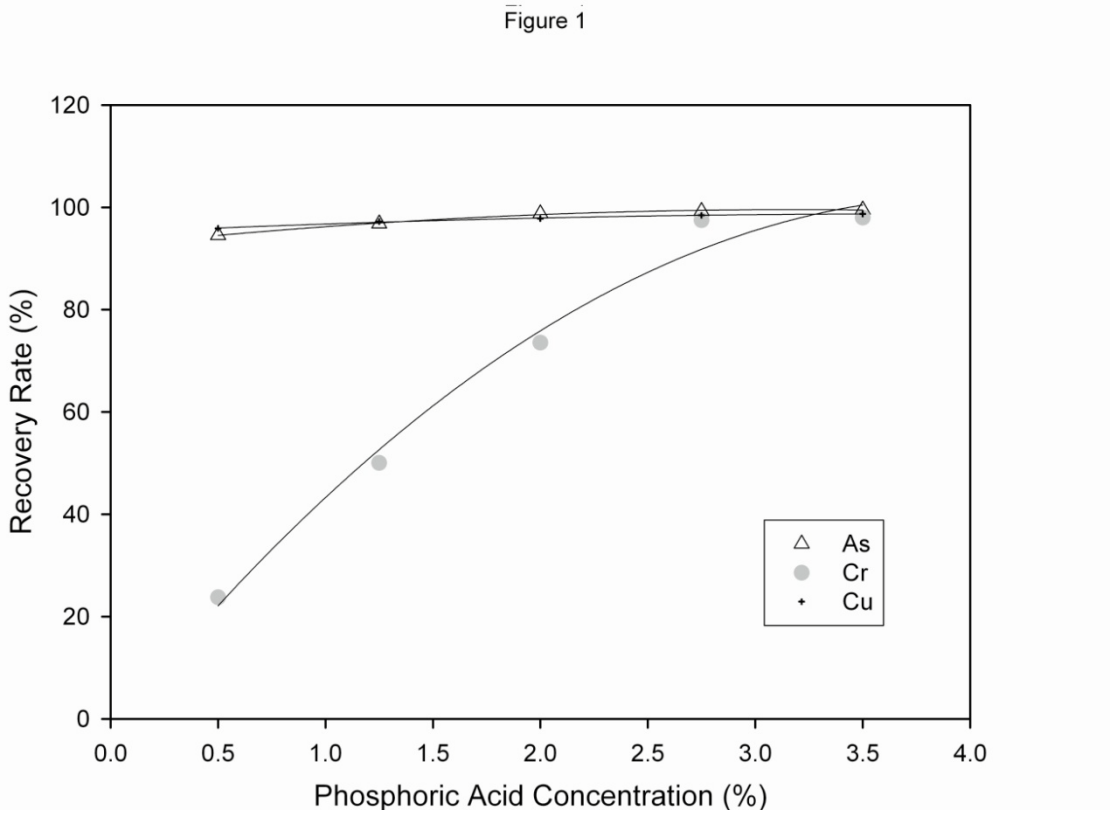

Figure 1. Effect of phosphoric acid concentration on the recovery rate of metal elements from CCA treated wood. Extraction was carried out in microwave reactor at 160 ^{0}C and 30 min.

Conclusions

The effect of microwave-assisted acid extraction of metals from chromated copper arsenate (CCA)-treated southern pine was studied. The results show that diluted phosphoric acid mixed with acetic acid is very effective to recover CCA elements in a microwave reactor in a short period. The advantage of this method is a shorter extraction time and a one step process to achieve the complete recovery of CCA elements. The concentration of phosphoric acid and temperature of the microwave reactor were two important factors. A binary acid solution consisting of 2.75% phosphoric acid and 0.5% acetic acid, reaction time of 10 min., and temperature of 130 ^{0}C is the minimal reaction condition to achieve the maximum recovery rate of all CCA elements. Further research such as the acetic acid concentration, reaction time, and temperature should be studied. Also, research on larger sized wood chips should be done to enhance the practical application of this method.

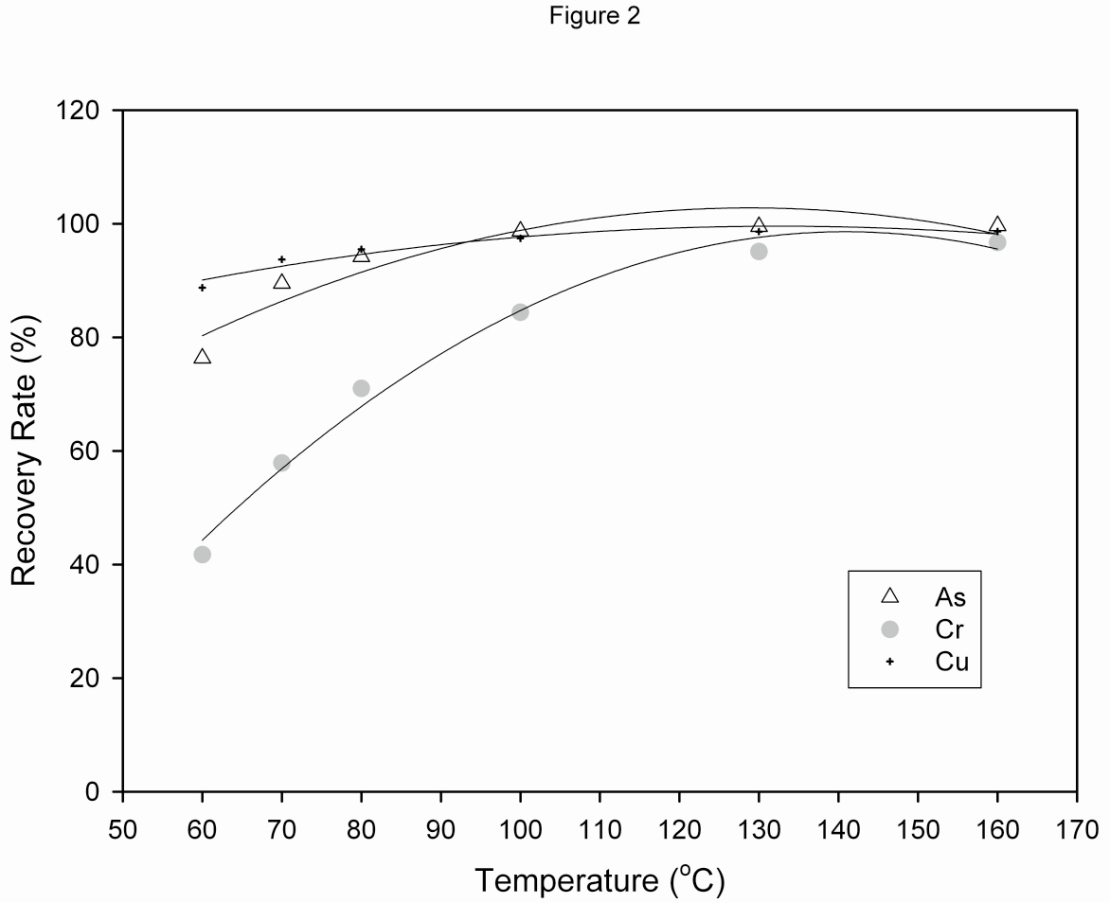

Figure 2. Effect of temperature on recovery rate of metal elements from CCA- treated wood. Extraction was carried out in a microwave reactor at a fixed acid mixture solution of 2.75% phosphoric acid and 0.5% acetic acid.

References

AWPA, (2008) Annual Book of Standards 2008. American Wood Protection Association, Birmingham, AL.

Bull, D.C. (2001) The chemistry of chromate copper arsenate II. Preservative-wood interactions. Wood Sci.Technol. 34, 459-466.

Humer, H., Pohleven, F., Sentjurc, M. (2004) Effect of oxalic acid, acetic acid, and ammonia on leaching of Cr and Cu from preserved wood. Wood Sci. Technol. 37, 463-473.

Inagaki, N., Nakamura, S., Asai, H., Katsuura, K. (1976) Phosphrylation of cellulose with phosphoric acid and thermal degradation of the product. J. Appl. Polym. Sci. 20, 2829-2836.

Jogtoyen, M., Derbyshire, F. (1998) Activated carbons from yellow poplar and white oak by H_3PO_4 activation. Carbon 36, 1085-1097.

Kakitani, T., Hata, T., Kajimoto, T., Imamura, Y. (2006) Designing a purification process for chromium-, copper-, and Arsenic-contaminated wood. Waste Manage. 26, 453-458.

Kakitani, T., Hata, T., Kajimoto, T., Koyanaka, H., Imamura, Y. (2009) Characteristics of a bioxalate chelating extraction process for removal of chromium, copper and arsenic from treated wood. J. Environ. Manage. 90, 1918-1923.

Nilsson, U., Barron, N., McHal, L., McHale, A.P. (1995) The effects of phosphoric acid pretreatment on conversion of cellulose to ethanol at 45 ^{0}C using the thermotolerant yeast *Kluyveromyces Marxianus* IMB3. Biotehnol. Lett. 17, 985-988.

Pizzi, A. (1982) The chemistry and kinetic behavior of Cu-Cr-As/B wood preservatives. IV. Fixation of CCA to wood. J. Polym. Sci.: Polym. Chem. Edit. 20, 739-764.

Pizzi, A. (1990) Chromium interactions in CCA/CCB wood preservatives. 2. Interactions with lignin. Holzforschung 44, 419-424.

Pszonicki, L., Tkacz, W. (1976) Complexes of morin and quercetin with boric acid and oxalic acid in acetic acid medium. Fluorimetric determination of boron. Anal. Chim. Acta 87, 177-184.

Saito, N., Shimizu, Y., Taqkai, M., Hayashi, J. (1994) Super absorbent materials prepared from lignocellulosic materials by phosphorylation IV. Fine structure and water absorbency. Sen-I Gakkaishi 49, 197-201.

Shiau, R.J., Smith, R.L., Avellar, B. (2000) Effects of steam explosion processing and organic acids on CCA removal from treated wood waste. Wood Sci.Technol. 34, 377-388.

Solum, M.S., Pugmire, R.J., Jagtoyen, M., Derbyshire, F. (1995) Evolution of carbon structure in chemically activated wood. Carbon 33, 1247-1254.

Yu, B., Hse, C.Y., Shupe, T.F. (2009) Rapid microwave-assisted acid extraction of metals from chromate copper arsenate (CCA)-treated southern pine wood. IRG/WP 09-50262. International Research Group on Wood Preservation. Stockholm, Sweden.

Zuo, S.L., Yang, J.X., Liu, J.L., Cai, X. (2009) Significance of the carbonization of volatile pyrolytic products on the properties of activated carbons from phosphoric acid activation of lignocellulosic material, Fuel Process. Technol., 90 994-1001.

Quality of Beech Standing Trees Related to Properties of Structural Timber

Rastislav Lagaňa[1*] – *Marian Babiak*[2]

[1] Research Scientist, Department of Wood Science, Technical University in Zvolen, Slovakia.
* *Corresponding author*
lagana@tuzvo.sk
[2] Professor, Department of Wood Science, Technical University in Zvolen, Slovakia.
babiak@tuzvo.sk

Abstract

Beside the traditional spruce structural timber, beech is one of the hardwood species that is recently more utilized for structural purposes in Europe. This study deals with a quality of standing trees that could predict properties of structural timber. Beech trees originated from two different silvicultural stands were evaluated using nondestructive technique. From stands, 14 dominated trees were selected. The sound velocity was measured on 2m length above breast height at four places that were related to slope of a stand and North-South direction. From each tree, 4 plain sawn boards (50x100x2000 – R, T, L) were prepared. Modulus of elasticity, shear modulus and bending strength were measured according to EN 408. Results showed strong relations between nondestructive assessed properties of standing trees and properties of structural timber. An ultrasound method showed to be an alternative predictor of quality of beech stands that could be harvested for construction purposes.

***Keywords*:** forest stands quality, beech, structural timber, nondestructive, characteristic values.

Introduction

For the last decade, there were several studies performed that tried to use standard assessed features of forest stands for prediction of wood properties. Houllier at al. (1995) analyzed the influence of silviculture, site quality the wood production of Norway spruce from both a quantitative and a qualitative point of view. Tree and stand volume, stem taper, wood basic density, proportion of juvenile wood as well as knottiness their considered as the result of growth processes. Lyhykäinen 2009 used stem and crown dimensions variables for estimating yields and grades of lumber of Scots pine stems. Direct method of quality evaluation of standing trees related to clear wood mechanical properties presented Wang at al. (2001). His stress wave approach showed significant relations of the mean values of stress wave speed and dynamic modulus of elasticity for trees with those determined from small, clear wood specimens. Similar approach used Dzbeński and Wiktorski (2010) and compared wave propagation of Pine standing trees with 1.2m long samples properties tested in bending.
Aim of this study was to address a quality of a forest stand and its relation to quality of structural timber. We used Wang's approach and compared quality of beech standing trees assessed by an ultrasound method and compared the results to properties of structural beech timber determined according to EN 408.

Materials and Methods

Dynamic modulus of elasticity calculated from sound velocity and density was determined on standing trees. Material from the measured locations was used for preparation a samples for measuring of bending strength, modulus of elasticity and shear modulus according to EN 408. Results were compared and relationship between destructive and nondestructive properties was analyzed.

Materials. Two sets of materials came from two beech forest stands of different silvicultural treatments. From each stand seven trees were used in this study. Ultrasound velocity was taken at 4 positions of a standing tree using Sylvatest Duo device. These positions were related to cardinal points. The first probe of the device (receiver) was plug into a predrilled hole at the breast height. The second probe (transmitter) was plug into a hole that was placed parallel to the trunk, two meters above the first one. The readings were taken two weeks before harvesting of the trees. After cut down, moisture content (MC) samples were taken from four measured positions at the breast height. Four tangential boards from each trunk were cut and dried to final moisture content of 12 % and further conditioned at T=20°C and RH=65% for 1 month. After that, boards were sized to the final dimensions of 50x100x2000 mm^3 (R, T, L).

Mechanical properties. MOR and MOE of boards were evaluated according to EN 408 standard in 4 point bending. For evaluation of shear modulus, a single span method was used. Density and moisture content were tested using a clear sample from the middle part of a board taken immediately after the bending test. Measured properties were adjusted to 12% of MC using the property-MC relationship given by the standard. Dynamic modulus of a standing tree was calculated from the ultrasound velocity and the density at the green MC according to equation (1).

$$Edyn = \rho_{MC}.c^2 \quad (1)$$

where ρ_{MC} is density of the standing tree at the breast height under the bark and *c* is the velocity measured between two probes at 2 m distance.

Results and discussion

Results published in a previous study (Lagana and Babiak 2011) showed that there is no effects of beech stands or cardinal points position on dynamic modulus of trees. Thus, basic statistics, given in the Table 1, contain all measured data. Average moisture content at the breast height was 87.8%. Density of trees was calculated from the density at 12% of MC, green MC and swelling coefficient.

Table 1. Basic statistic of properties of standing beech trees and boards measured according to EN 408. Velocity is given as measured at green MC, other properties are adjusted to MC = 12%.

	Green MC, %	velocity ms^{-1}	Edyn, MPa	density, kgm^{-3}	MOR, MPa	MOE, MPa	G, MPa
Sample size	54						
Mean	87.8	4 071	17 257	680.0	90.3	13 604	729
Coeff. of var., %	6.9	3.4	7,0	3.9	14.7	8.3	10.1

Practical results are correlations between nondestructive identification property and properties of structural timber. Correlation between ultrasound velocity and bending strength is small (Figure 1). Based on number of samples, the correlation coefficient R = 0.266 was not significant on confidence level a=0.05. Ultrasound velocity readings are not sufficient to predict strength properties of beech timber.

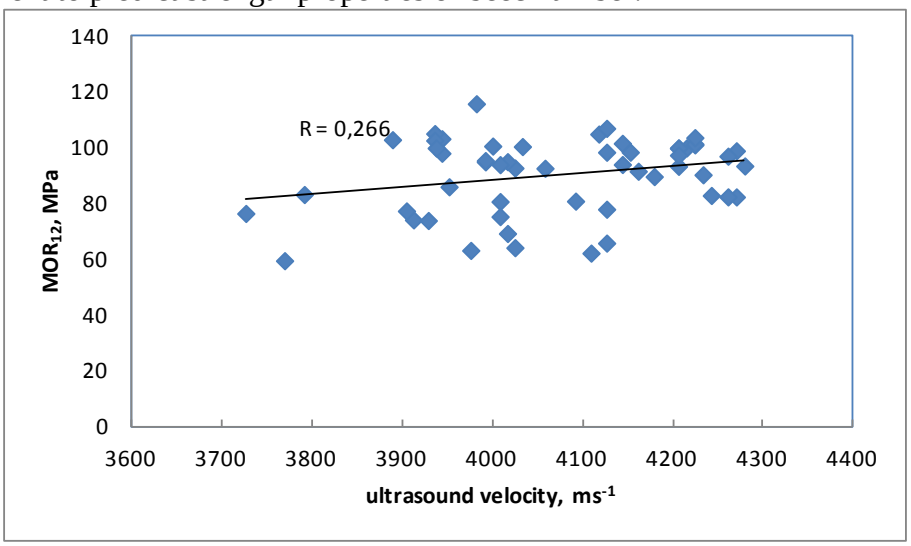

Figure 1 Correlation between ultrasound velocity of a standing beech tree and MOR at 12% of MC determined according to EN 408.

More reliable correlation is given, when density is involved in calculation of dynamic modulus according to equation (1). Figure 2 shows significant correlation of dynamic modulus of standing trees and MOR at 12% of MC.
The next two figures (Figure 3 and 4) show correlation of MOE and shear modulus of dynamic modulus of standing tree. The correlation was the highest between dynamic and static moduli. It could be conclude that the dynamic modulus of elasticity is more reliable feature of a beech standing tree and should be used for quality evaluation rather than ultrasound velocity. Unfortunately, this will involve a challenge in fast and precise determination of tree density.
It should be pointed out that the correlation coefficients are lower than those obtained in Wang's (2001) or Dzbenski's (2010) studies. A reason can be seen in specific properties of beech wood that are related to its structure. Despite of the uniform density of beech wood, this ring-porous species performed much higher variability in MOR than coniferous species. Another possible reason could be high variation of spiral grain angle within beech trunk that was observed in failure modes of bending tests.

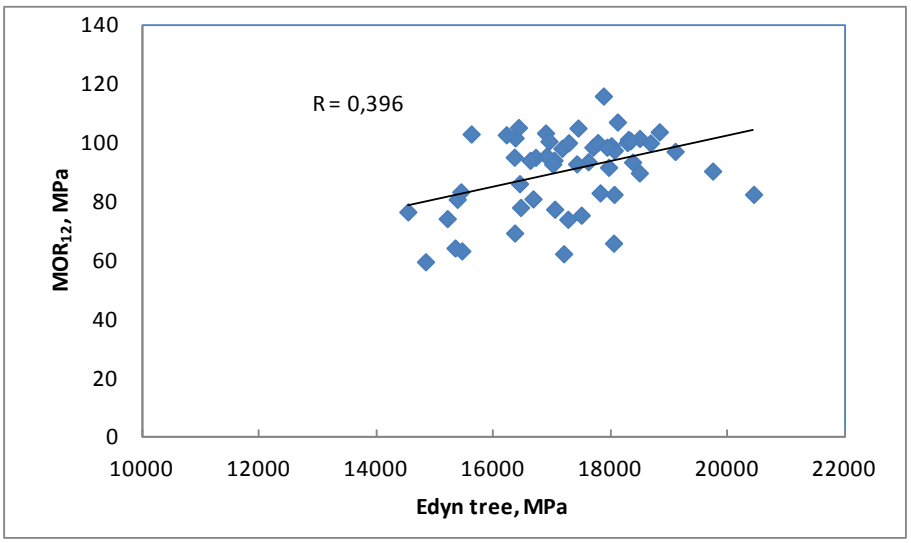

Figure 2 Correlation between dynamic modulus of a standing beech tree and MOR at 12% of MC determined according to EN 408.

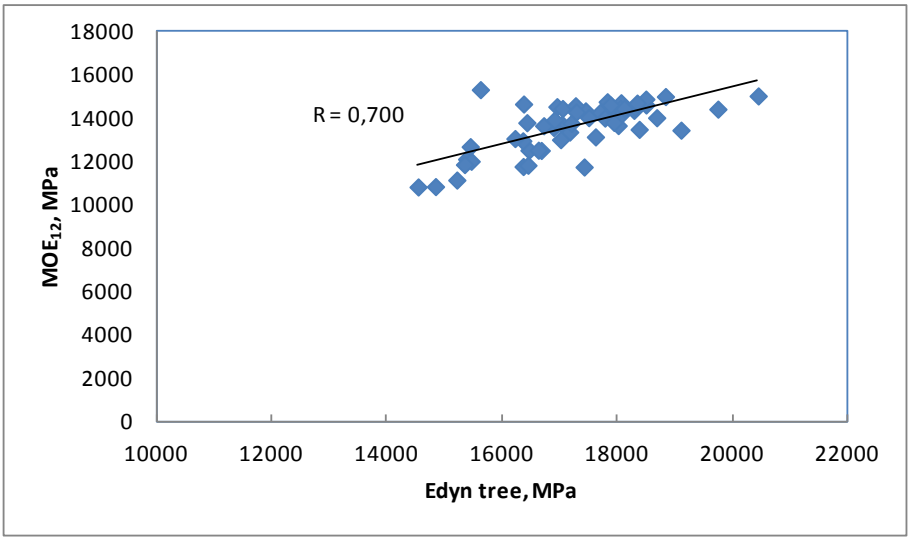

Figure 3 Correlation between dynamic modulus of a standing beech tree and MOE at 12% of MC determined according to EN 408.

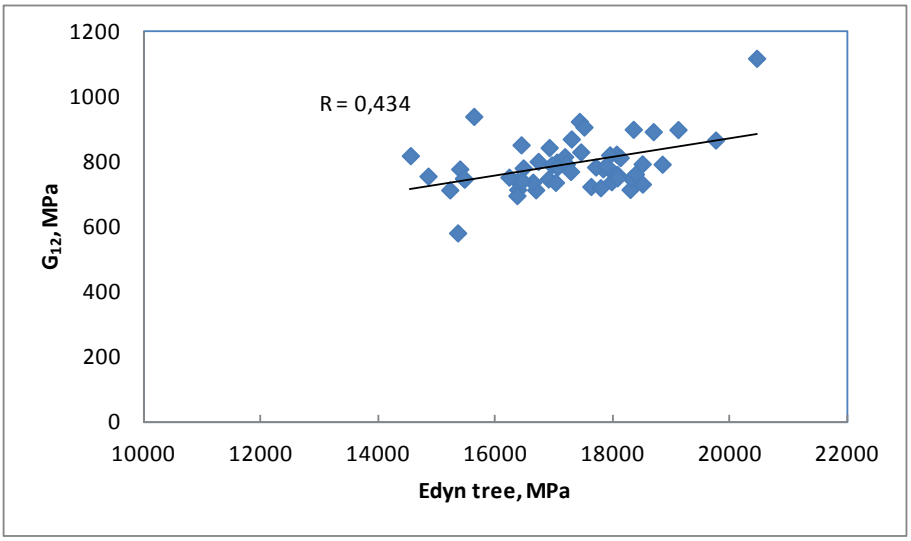

Figure 4 Correlation between dynamic modulus of a standing beech tree and shear modulus at 12% of MC determined according to EN 408.

Conclusion

Quality of structural beech timber could be reliably evaluated on the standing trees using an ultrasound method. Quality assessment should also include determination of green wood density. Results showed significant relations between nondestructive assessed dynamic modulus of standing trees and properties of structural timber such as bending strength, modulus of elasticity and shear modulus. Comparing to other wood species, the studied correlations were smaller than correlations of coniferous species such as pine or spruce. Nevertheless, an ultrasound method was confirmed to be an alternative predictor of quality of beech stands that is harvested for construction purposes.

Acknowledgement

This contribution is a result of the project implementation: Extension of the centre of Excellence „Adaptive Forest Ecosystems“, ITMS: 26220120049, supported by the Research & Development Operational Programme funded by the ERDF

Literature

Dzbeński, W., Wiktorski, T. 2007. Ultrasonic evaluation of mechanical properties of wood in standing trees. In Proceedings of the COST E 53 Conference - Quality Control for Wood and Wood Products. 15th - 17th October 2007, Warsaw. Poland: 21-26.

Houllier, F., Lebanb, J.M., Colinb, F. 1995. Linking growth modelling to timber quality assessment for Norway spruce. Forest Ecology and Management. 74(1): 91–102.

Lagana, R., Babiak, M. 2012. An effect of crown development conditions on beech timber quality. In: Forest Products Society’s 65th International Convention proceedings of abstracts, 19. – 21. 6. 2011, Portland, Oregon, USA.

Lyhykäinen, H., Mäkinen, H., Mäkelä, A., Usenius, A. 2009. Predicting Lumber Grade and By-Product Yields for Standing Scots Pine Trees. In the Proceedings of the International Conference: Forest growth and timber quality: Crown models and simulation methods for sustainable forest management. Gen. Tech. Rep. PNW-GTR-791. Portland, OR: U.S. Department of Agriculture, Forest Service, Pacific Northwest Research Station. pp. 157–166.

Wang, X., Ross, R.J., McClellan, M., Barbour, R.J., Erickson, J.R., Forsman, J.W., McGinnis, G.D. 2001. Nondestructive evaluation of standing trees with a stress wave method. Wood & Fiber Sci. 33(4):522-533.

Liquefied Wood as an Adhesive

Milan Sernek[1*] *– Aleš Ugovšek*[2]

[1] Associate professor, Department of Wood Science and Technology, Biotechnical Faculty, University of Ljubljana, Rozna dolina, C. VIII/34, 1001 Ljubljana, SLOVENIA
* *Corresponding author*
milan.sernek@bf.uni-lj.si
[2] Graduate student, Department of Wood Science and Technology, Biotechnical Faculty, University of Ljubljana, Rozna dolina, C. VIII/34, 1001 Ljubljana, SLOVENIA
ales.ugovsek@bf.uni-lj.si

Abstract

The goal of this study was to develop environmentally friendly adhesives derived from natural, renewable resources. Liquefied wood is a naturally-based product which has the potential to be used as an adhesive. This study considered liquefied wood as an independent material for wood bonding. The liquefaction process was carried out in a laboratory reactor using wood sawdust from black poplar (*Populus nigra* L.), ethylene glycol was used as the solvent, and sulphuric acid as a catalyst. The results of the research revealed that a mass ratio between the wood and the solvent of 1:3, and 120 minutes of heating at 180 °C, was optimal for liquefaction. Using an additional procedure, the mass ratio was reduced to a final value of 1:1. The bonding was carried out in a hot press at different pressing temperatures and times. The test specimens were tested according to the standards EN 12765 and EN 205. A press temperature of 180 °C and a pressing time of 12 minutes were determined to be optimal for the bonding of 5 mm thick wood lamellas with the liquefied wood used in this study. Liquefied wood shows good potential for use in wood bonding, but needs some additional modification in terms of strength and durability in order to be able to satisfy the requirements of the European standards for thermosetting adhesives for non-structural applications.

Keywords: Adhesive, Curing, Liquefied wood, Shear strength

Introduction

Liquefied wood is a product of the thermochemical reaction between wood (wood residues), solvent, and added catalyst. Liquefied wood has the potential to be used for bonding of wood. Over the last 20 years there have been many attempts to use liquefied wood as a part of the adhesive formulation. In the earlier years, the development of liquefied wood adhesives was based on liquefied wood that was prepared with phenol and added formaldehyde (Alma and Bastürk 2001, Alma and Bastürk 2006, Li et al. 2004, Fu et al. 2006, Zhang et al. 2007). Many studies were performed in connection with the application of liquefied wood to epoxy resin systems (Kobayashi et al. 2000, Kobayashi et al. 2001, Asano et al. 2007, Wu and Lee 2010), and there have been some other attempts to blend liquefied wood with synthetic resins such as diisocyanates (Juhaida et al. 2010), urea-formaldehyde (Antonović et al. 2010) melamine-formaldehyde, melamine-urea-formaldehyde (Kunaver et al. 2010) and phenol-formaldehyde resin (Ugovšek et al. 2010).

One of disadvantages of adhesives made from liquefied wood is low shear strength of the adhesive bond. This shortcoming can be resolved in different ways: with addition of synthetic resin such as urea-formaldehyde or melamine-formaldehyde; or by optimizing the pressing parameters. The objective of this study was to examine the influence of the press temperature and the pressing time on the shear strength of bonded specimens.

Materials and Methods

Preparation of the liquefied wood. Sawdust of the black poplar (*Populus nigra* L.) was used for the production of liquefied wood (LW). Prior to the liquefaction process, the sawdust was dried in a laboratory oven (103°C, 24 h). A mass ratio of 1:3 between black poplar wood and ethylene glycol (EG) as the solvent was used for liquefaction. 3% of sulphuric acid (SA), based on the EG mass, was added as a catalyst. Liquefaction was carried out for a period of 120 minutes in a 1000 mL three-neck glass reactor, which was immersed in an oil bath that was preheated to 180°C and was equipped with a mechanical stirrer. After liquefaction, the reactor was immersed in cold water in order to quench the reaction.

The liquefied product was then diluted with a mixture of 1,4-dioxane and water (4/1, v/v), and filtered through filter disks (Sartorius filter disks grade 388). In order to obtain the LW without the mixture of 1,4-dioxane and water, a rotary evaporator (Büchi, Rotavapor R-210) was used for evaporation at 55°C and at reduced pressure, from 100 kPa to 1 kPa, which was achieved by means of a vacuum pump (Vaccubrand, PC 3003 Vario). After evaporation of the 1,4-dioxane, the EG in the LW, too, was evaporated (at 120°C, 1 kPa) to achieve a final wood/EG mass ratio of 1:1.

Bonding of the specimens. Solid beech wood lamellas (*Fagus sylvatica* L.) with a thickness of 5 mm were used as a substrate for the preparation of two-layered specimens, which were bonded according to EN 205 by means of conventional hot-pressing. Prior to the bonding, all of the wood lamellas were planed in order to ensure smooth and flat

surfaces. Two lamellas were bonded together with LW. 200 g/m^2 of LW was applied to one surface by means of a roller, and a specific press pressure of 0.6 MPa was used. The bonding process was divided in two parts:

1. The lamellas were bonded using LW at different press temperatures (120, 150, 180, 200 and 220°C) for 15 minutes.
2. The lamellas were bonded with LW at the optimal press temperature ascertained in the first part, but using different pressing times (6, 9, 12, 15 and 18 minutes).

Testing of the specimens. Shear specimens were cut from the bonded lamellas and tested after 7days of conditioning in a standard climate (20 ± 2°C, relative humidity (RH) 65 ± 5%). All the shear tests were carried out using a ZWICK/Z005 universal testing machine, according to the standard EN 205 and EN 12765.

Results and Discussion

The effect of press temperature on the shear strength and wood failure of specimens bonded with LW is presented in figure 1. Press temperatures of 120 and 150°C are inadequate for satisfactory bonding, since the shear strength and wood failure of bonded specimens is lower compared to that of specimens bonded at higher temperatures. Specimens bonded at 180, 200 and 220°C showed comparable shear strength and nearly 100 % of wood failure. Wood failure is high in spite of relatively low shear strength values, when compared with the standard values. The latter is the consequence of the visibly damaged wood surface where LW was applied. It can be concluded that press temperature influences the shear strength of the specimens bonded with LW and that a minimum temperature of 180°C is considered to be sufficient for the bonding of wood lamellas with LW for further investigations.

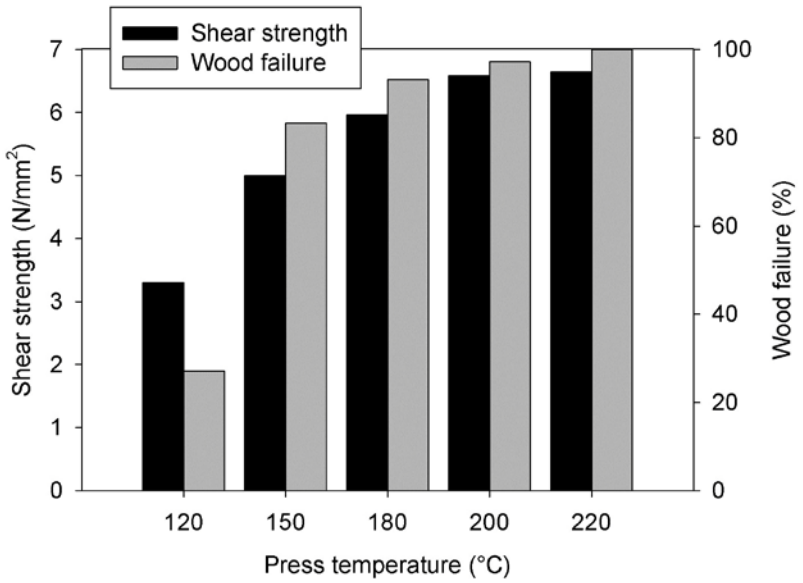

Figure 1. The influence of press temperature on the shear strength and wood failure of specimens bonded with liquefied wood

The influence of pressing time on the shear strength and wood failure of specimens bonded with LW is shown in figure 2. The specimens bonded for 6 minutes remained together after pressing, but some of them fell apart after a 7 days of exposure to a standard climate. Shear strength was low and so was the wood failure. The specimens that were bonded for 9 minutes attained higher shear strength, but still lower than the specimens bonded for a longer time. It is clear that pressing times of 12, 15 and 18 minutes were all long enough to achieve a satisfactory shear strength (over 6 N/mm^2) and wood failure (around 90%). The differences between them are not significant. A pressing time of 12 minutes at 180°C was determined to be optimal for the bonding of the 5 mm thick beech wood lamellas with LW used in this study.

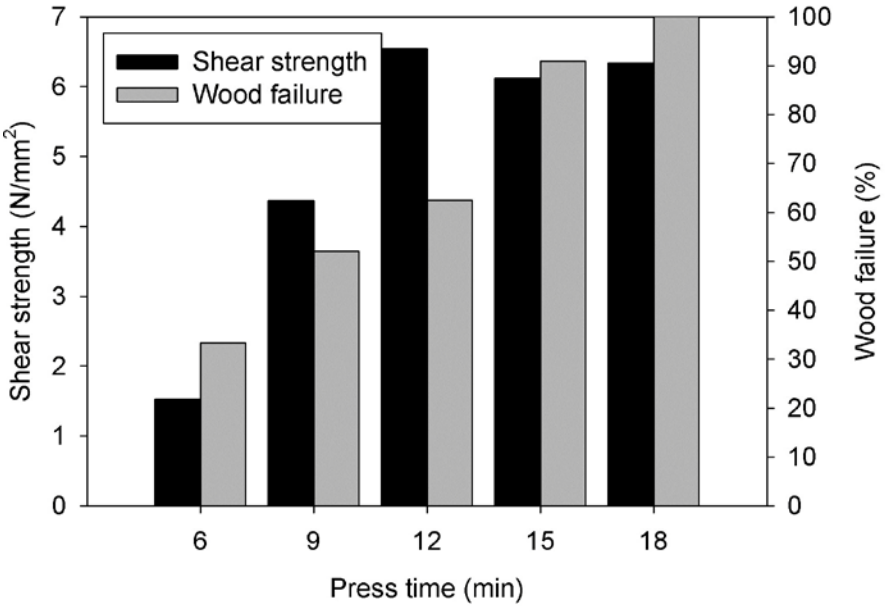

Figure 2. The influence of pressing time on the shear strength and wood failure of specimens bonded with liquefied wood

Conclusions

Liquefied wood showed good potential for use in wood bonding. A press temperature of 180°C and a pressing time of 12 minutes were determined to be optimal for bonding of the 5 mm thick beech wood lamellas with liquefied wood. However, the shear strength was too low (between 6 and 7 N/mm^2) to attain the standard requirements. Despite this, wood failure was high (between 90 and 100%), presumably due to the wood surface damage. Further investigations are necessary to analyze the bondline and to ascertain the cause of this problem.

Acknowledgements

The authors gratefully acknowledge the financial support of the Slovenian Research Agency through Project J4-2177 and Research Program P4-0015.

References

Alma, M. H.; Bastürk, M. A. 2001: Cocondensation of NaOH-catalyzed liquefied wood wastes, phenol, and formaldehyde for the production of resol-type adhesives. Ind. Eng. Chem. Res. 40: 5036-5039.
Antonović, A.; Jambreković, B.; Kljak, J.; Španić, N.; Medved S. 2010: Influence of urea-formaldehyde resin modification with liquefied wood on particleboard properties. Drvna Industrija. 61(1):5-14
Asano, T.; Kobayashi, M.; Tomita, B.; Kajiyama, M. 2007: Syntheses and properties of liquefied products of ozone treated wood/epoxy resins having high wood contents. Holzforschung. 61: 14-18.
EN 12765: 2002: Classification of thermosetting wood adhesives for non-structural applications: 9pp.
EN 205: 2003: Adhesives - Wood adhesives for non-structural applications - Determination of tensile shear strength of lap joints: 13pp.
Fu, S.; Ma, L.; Li, W.; Cheng, S. 2006: Liquefaction of bamboo, preparation of liquefied bamboo adhesives, and properties of the adhesives. Front. For. China. 2: 219-224.
Juhaida, M. F.; Paridah, M. T.; Mohd. Hilmi, M.; Sarani, Z.; Jalaluddin, H.; Mohamad Zaki, A. R. 2010: Liquefaction of kenaf (Hibiscus cannabinus L.) core for wood laminating adhesive. Bioresource technology. 101: 1355-1360.
Kobayashi, M.; Hatano, Y.; Tomita, B. 2001: Viscoelastic Properties of Liquefied Wood/Epoxy Resin and its Bond Strength. Holzforschung. 55: 667–671.
Kobayashi, M.; Tukamoto, K.; Tomita, B. 2000: Application of liquefied wood to a new resin system-synthesis and properties of liquefied wood/epoxy resins. Holzforschung. 54: 93–97.
Kunaver, M.; Medved, S.; Čuk, N.; Jasiukaityte, E.; Poljanšek, I.; Strnad, T. 2010: Application of liquefied wood as a new particle board adhesive system. Bioresource Technology. 101: 1361-1368.
Li, G.; Qin, T.; Tohmura, S.; Ikeda, A. 2004: Preparation of phenol formaldehyde resin from phenolated wood. Journal of forestry research. 15(3): 211-214.
Ugovsek, A.; Kariz, M.; Sernek, M. 2010: Bonding of beech wood with an adhesive mixture made of liquefied wood and phenolic resin, in: Németh R. and Teischinger A. (Eds.). Proceedings of the "Hardwood Science and Technology" - The 4th conference on hardwood research and utilisation in Europe. Sopron, Hungary, 17-18 May 2010, 64-68.
Wu, C.; Lee, W. 2010: Curing behavior and adhesion properties of epoxy resin blended with polyhydric alcohol-liquefied Cryptomeria japonica wood. Wood Science and Technology. http://www.springerlink.com/content/c35529h734w12m78/fulltext.pdf.
Zhang, Q.; Zhao, G.; Yu, L.; Jie, S. 2007: Preparation of liquefied wood-based resins and their application in molding material. For. Stud. China. 9(1): 51-56.

Proceedings of the 55th International Convention of Society of Wood Science and Technology
August 27-31, 2012 - Beijing, CHINA

Water in Wood Studied by Time-domain NMR

Minghui Zhang [1*] – *Ximing Wang* [1] – *Rado Gazo*[2]

[1] Professor, College of Materials Science and Art Design, Inner Mongolia Agricultural University, Hohhot, P.R. China
** Corresponding author*
zhangminghui@imau.edu.cn
[2] Professor, Department of Forestry and Natural Resources, Purdue University, West Lafayette IN, USA.
gazo@purdue.edu

Abstract

Time-domain nuclear magnetic resonance (TD-NMR) technique can easily distinguish water states according to spin-spin relaxation time (T2) and give more quantitative information on water in wood than any other method. In this study, water states in hard wood are investigated with TD-NMR. Also, water migration during drying is also analyzed.

The results of this study show yellow poplar has at least 4 water states according to T2 values at high moisture content. The longest T2 is about 400 ms for free water and the shortest T2 is about 1 ms for bound water. The amount of different water states in hard wood sample decrease at the same time with drying while bound water has slow decreasing rate.

Through TD-NMR technique, water states in wood drying is distinguished easily, but also, different water state migration can be analyzed quantitatively. This technique will benefit wood drying modeling and simulation.

Key words: Water states, Migration, NMR, Relaxation time.

Introduction

Wood is a natural polymer material whose physical properties decided not only by its chemical composition and lignocellulosic structures but also the amount of moisture in it as a hygroscopic natural gel. Water in wood was extensively studied by many researchers in the past decades. Most of them studied bound and free water separately since it was difficult to identify these two water states simultaneously (Skaar 1988). However time-domain nuclear magnetic resonance (TD-NMR) can give more quantitative information on water in wood than any other method (Araujo, Mackay et al. 1992).

Nuclear magnetic resonance **(**NMR) relaxation is a powerful tool for understanding wood structure and dynamics of water in wood since abundant hydrogen nuclei in both wood chemical composition and water can be detected by time domain NMR techniques. Time domain NMR techniques are widely used in wood studies since they are quick, nondestructive and quantitative. Most of these studies are related to moisture content (MC) determination techniques (Nanassy 1976; Sharp, Riggin et al. 1978; Hartley, Kamke et al. 1994; Thygesen 1996; Casieri, Senni et al. 2004; Merela, Oven et al. 2009;) and water characterizing in wood (Menon, Mackay et al. 1987; Araujo, Mackay et al. 1992; Labbe, De Jeso et al. 2006; Cox, McDonald et al. 2010).

Usually bound and free water in wood during drying are studied separately since it is difficult to identify these two water forms simultaneously with traditional methods. Since TD-NMR technique can easily distinguish water states according to spin-spin relaxation time (T2) and give more quantitative information on water in wood, we use this technique to investigate water states and migration during yellow poplar drying.

Materials and Methods

A cylindrical sample of approximately 10mm diameter and 20mm length (longitudinal direction) were cut from fresh yellow poplar disk at heart wood section. The fresh sample was weighed. Free induced decay (FID) and spin-spin relaxation time (T2) data were collected every hour automatically during the sample drying in NMR probe with 40^0C. Also the sample's weight was measured at different time interval during drying. When the sample's weight does not change within 2 days, it was put into oven with 105^0C for 24 hours drying to get oven-dried weight. The FID and proton spin-spin relaxation T2 NMR measurements were conducted with console made from Bruker operating at 22.6 MHz at homebuilt magnetic body. The dead time is 10μs. T2 was carried out using the CPMG sequence with echo time 0.4 ms. Data was acquired setting 3000 echoes.

All experiments were performed at 40^0C. The sample wrapped with plastic in NMR tube was maintained at this temperature in water bath for 24h before measurements were taken. In this study, we determined nanomechanical and localized properties (mainly of the S2 layer and middle lamella) before processing solid wood samples**.** We also established the

potential decrease in mechanical properties for wood and proposed a modified rule for mixture.

Results and Discussion

a) Water states during drying

Figure 1a and b shows yellow poplar's continuous T2 relaxation times distribution during drying at different MC. The continuous T2 relaxation times distribution represents water states distribution.

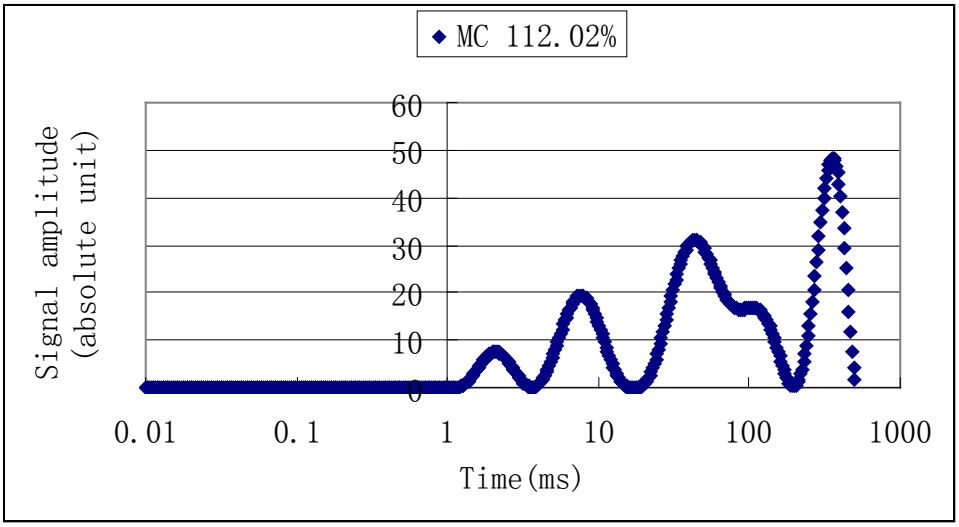

Figure 1a: T2 relaxation profile during drying at MC112.02%

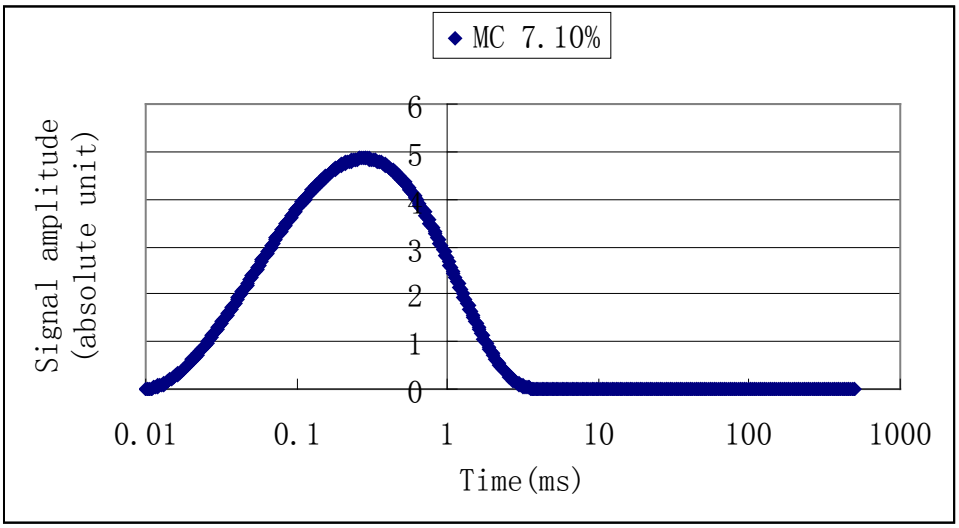

Figure 1b: T2 relaxation profile during drying at MC 7.10%

We can get the sample's initial MC = 112.02% with 5 water states and MC = 7.10% with only one water state. According to Cox, McDonald et al. (2010), T2 relaxation time for

bound water is about 1 ~ 10ms and above 10ms for free water while wood proton relaxation time is about 10 ~ 15μs. Figure 1b shows there is much shorter bound water component than 1 ~ 10ms. This component does not exsist when the sample is in higher MC level. This phonomenon further explains wood drying is a complex process. In the process, water states will change with time. Table 1 tabulates the T2 relaxation times distribution for yellow poplar MC = 112.02% at 40^0C during drying. From the table 1, we can tell it is hard to distinguish bound water and free water when T2 relaxation time distribution is continuous between 3.72ms and 16.62ms.

Table 1 T2 (ms) distribution for yellow poplar MC = 112.02%

bound water		free water		
T2a	T2b	T2c	T2d	T2e
1.15-3.56	3.72-16.62	18.12-72.59	73.46-176.59	180.46-499.99

From figure 2, the water states distribution changes are apparently. The T2 relaxation times get shorter with MC decreasing. The free water components lose quickly, especially for long T2 components. Although the components for T2 less than 10ms are changed, they do not change too much. Their amounts basically keep constant. The number of water states during drying changes with time. From figure 1 and 2, it is shown there are five water states at MC = 112.02%, four at MC = 98.87%, three at MC = 31.94% and one at MC = 7.10%. It is related to the MC.

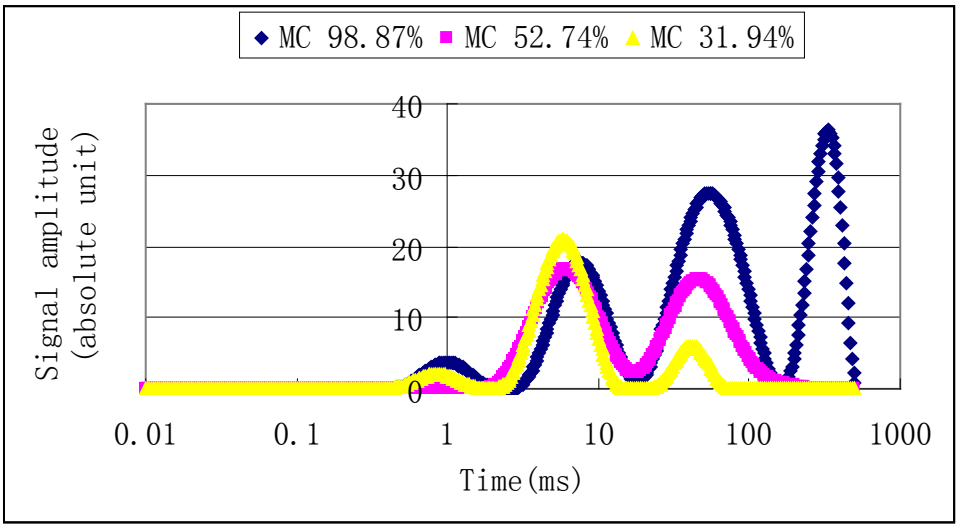

Figure 2: T2 relaxation profile during drying at different MC

b) Water migration during drying

Figure 3 is a typical FID curve for the sample with MC = 4.03%.The component magnetizations with decayed fast part in FID are associated with wood protons while the

slow decayed part is associated with water protons. The water signal starts to decay from 60 to 70μs (Xu, Araujo et al. 1996).

Since signal amplitude is proportional to the number of protons, it is reasonable to calculate MC through NMR signal amplitude. Figure 4 shows the relation between MC determined gravimetrically and NMR signal amplitude. This is highly linear relation with $R^2 = 0.998$. So we can get the MC of the sample during drying any time through this regression line.

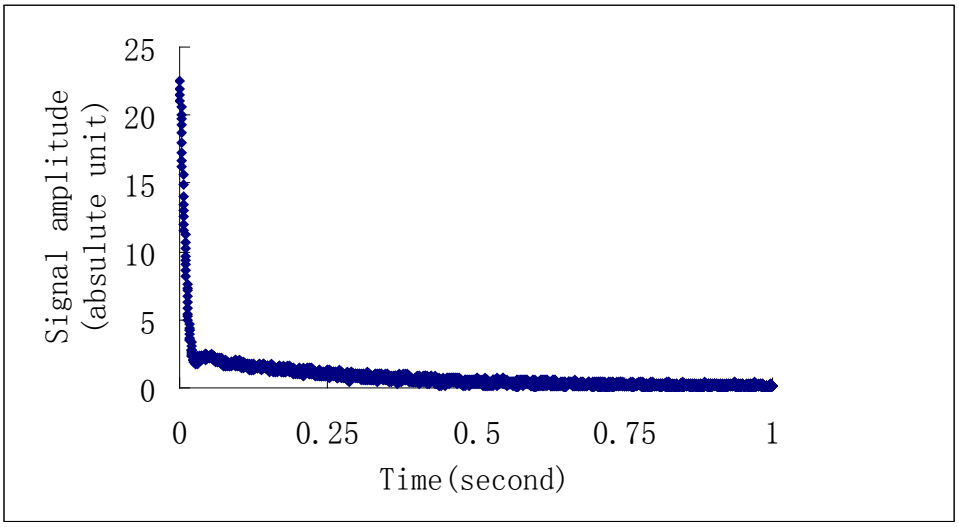

Figure 3: Yellow poplar FID curve for MC = 4.03%

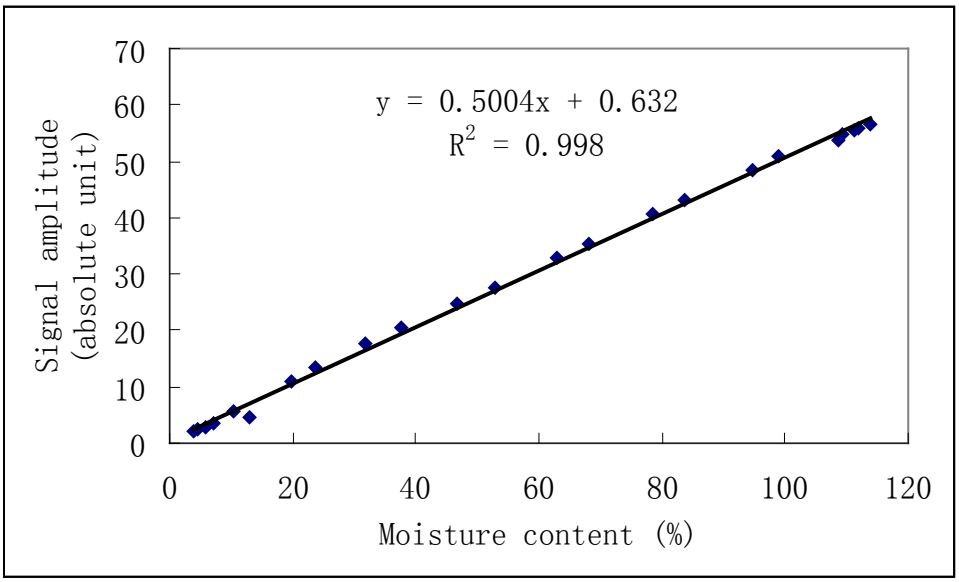

Figure 4: Relation between MC determined gravimetrically and NMR signal amplitude

Figure 5a is the yellow poplar sample MC changes with drying time at 40^0C. Moisture loses very quickly at the beginning of drying and begins to slow down when the MC is about 20%. It seems the curve can be divided two parts: one part seems following linear

function; the other seems following exponential function. The transition point is at MC = 20%. The drying time at that point is 150 hours.

The regressions for these two parts are made separately in order to verify above thoughts. The results from figure 5b and 5c show that it is highly linear between MC and drying time for the first 150 hours with $R^2 = 0.9994$. Also, there follows exponential function between MC and drying time after 150 hours indeed with $R^2 = 0.9665$.

Free water mostly loses in the first part. This is also been seen from figure 2. Since 20% MC is lower than fiber saturation point, some bound water also loses in the first part. The shorter of T2 for bound water, the tighter for the hydrogen bond between water molecule and wood substance. So the drying rate slows down after MC = 20%.

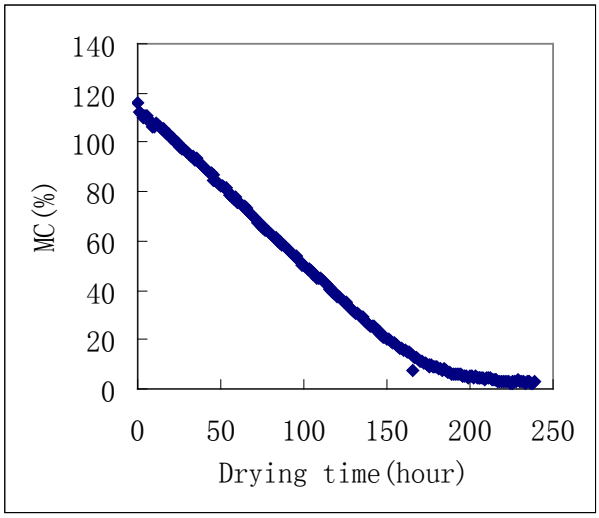

Figure 5a: Yellow poplar sample MC changes with drying time

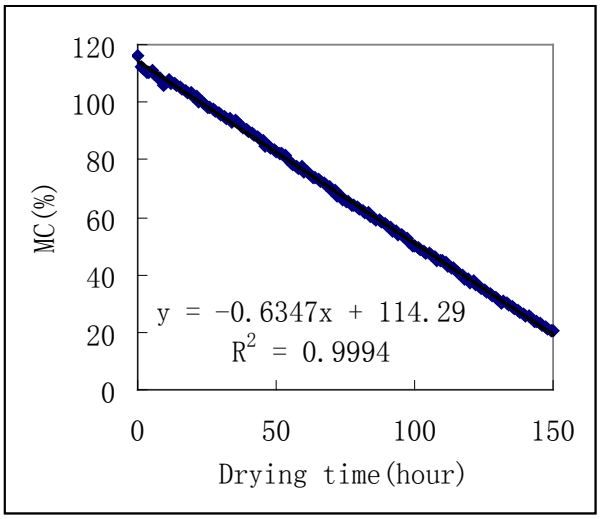

Figure 5b: Yellow poplar sample MC changes with the first 150 hours

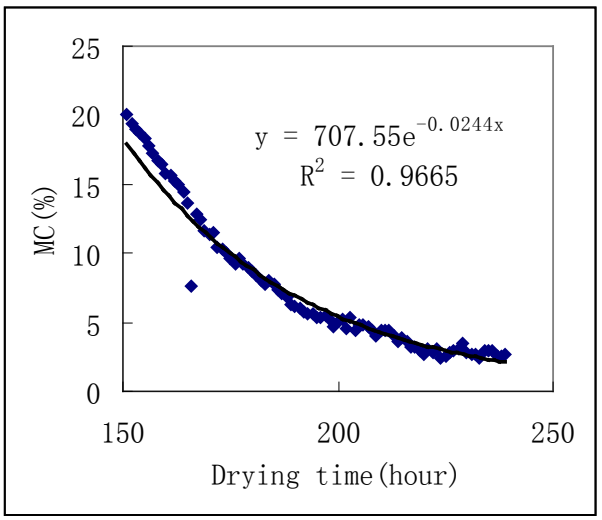

Figure 5c: Yellow poplar sample MC changes after 150 hours

Figure 6 shows free and bound water changes with MC during drying. It is apparent that bound water does not change too much above 50% MC. However we can see the bound water has the little increasing tendency with MC decreasing. The explanation for this result is probably some free water being turned into bound water in drying process. There is a big jump for bound water amount at MC around 46%.The bound water amount starts dropping from MC around 46%. This result shows both free and bound water happen to lose above fiber saturation point.

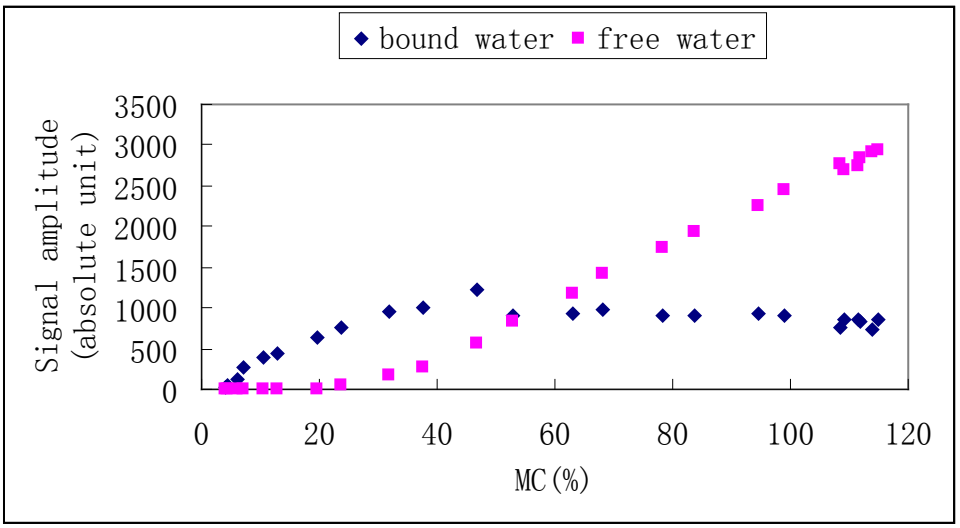

Figure 6: free and bound water changes with MC during drying

Conclusions

It has been shown TD-NMR technique is a powerful tool to distinguish water states through T2 relaxation time during wood drying.

Based on our experiment, the following conclusions can be made about water states and migration in yellow poplar drying with 40^0C: 1.Yellow poplar has at least 4 water states according to T2 values at moisture content above 100%; 2.Water states in wood will change with drying time. The T2 value will get shorter with MC decreasing. 3. Water migration in yellow poplar drying can be divided into two phase – one is following linear function and the other is exponential function. 4. It is apparent that bound water does not change too much above 50% MC. 5. Both free and bound water in yellow poplar drying happen to lose above fiber saturation point.

References

Araujo, C. D., A. L. Mackay, et al. (1992). "Proton Magnetic-Resonance Techniques for Characterization of Water in Wood - Application to White Spruce." Wood Science and Technology **26**(2): 101-113.

Casieri, C., L. Senni, et al. (2004). "Determination of moisture fraction in wood by mobile NMR device." J Magn Reson **171**(2): 364-372.

Cox, J., P. J. McDonald, et al. (2010). "A study of water exchange in wood by means of 2D NMR relaxation correlation and exchange." Holzforschung: International Journal of the Biology, Chemistry, Physics, & Technology of Wood **64**(2): 8p.

Hartley, I. D., F. A. Kamke, et al. (1994). "Absolute Moisture-Content Determination of Aspen Wood Below the Fiber Saturation Point Using Pulsed Nmr." Holzforschung **48**(6): 474-479.

Labbe, N., B. De Jeso, et al. (2006). "Time-domain H-1 NMR characterization of the liquid phase in greenwood." Holzforschung **60**(3): 265-270.

Menon, R. S., A. L. Mackay, et al. (1987). "An Nmr Determination of the Physiological Water Distribution in Wood during Drying." Journal of Applied Polymer Science **33**(4): 1141-1155.

Merela, M., P. Oven, et al. (2009). "A single point NMR method for an instantaneous determination of the moisture content of wood." Holzforschung: International Journal of the Biology, Chemistry, Physics, & Technology of Wood **63**(3): 4p.

Nanassy, A. J. (1976). "True dry-mass and moisture content of wood by NMR." Wood Science **9**(2): 104-109.

Skaar, C. (1988). Wood-water relations. Berlin ; New York, Springer-Verlag.

Sharp, A. R., M. T. Riggin, et al. (1978). "Determination of moisture content of wood by pulsed nuclear magnetic resonance." Wood and Fiber **10**(2): 74-81.

Thygesen, L. G. (1996). "PLS calibration of pulse NMR free induction decay for determining moisture content and basic density of softwood above fiber saturation." Holzforschung **50**(5): 434-436.

Xu, Y., C. D. Araujo, et al. (1996). "Proton spin-lattice relaxation in wood - T-1 related to local specific gravity using a fast-exchange model." Journal of Magnetic Resonance Series B **110**(1): 55-64.

Acknowledgments

This research is supported by the National Natural Science Foundation of China (30800866/ C1603 and 31160141/ C1603)

Analysis of Heat and Moisture Transfer in a Center-Bored Timber whose Outer Surface is Sealed

Jun-Ho Park[1]– Yonggun Park[1]– Yeonjung Han[1]– Joon-Weon Choi[2]–

In-Gyu Choi[2]– Jun-Jae Lee[2]– Hwanmyeong Yeo[3]*

[1] Graduate Student, Dept. of Forest Sciences, CALS, Seoul National University, 599 Gwanak-ro, Gwanak-gu, Seoul – South Korea.
[2] Research Institute for Agriculture and Life Sciences, Professor, Dept. of Forest Sciences, CALS, Seoul National University, 599 Gwanak-ro, Gwanak-gu, Seoul – South Korea.
[3] Research Institute for Agriculture and Life Sciences, Associate Professor, Dept. of Forest Sciences, CALS, Seoul National University, 599 Gwanak-ro, Gwanak-gu, Seoul – South Korea
* *Corresponding author*
hyeo@snu.ac.kr

Abstract

A lot of time and energy are required for drying green timber that has a large cross section. This type of wood also has a high possibility of drying check occurrence due to evolving internal drying stress resulting from long-lasting big internal moisture gradients. Meanwhile, efforts to produce fast water emission by using a low temperature and moisture gradient in wood have been continued for drying wood without drying defects. We figured out a way to rapidly dry green timber that has a large cross section so that it does not make cracks and uses a small amount of thermal energy for drying. We applied a center-boring process, drilled a hole along the central longitudinal axis, and the outer surface of the timber was sealed. The center-boring reduces the heat and the moisture movement distance inside the wood and the outer-surface sealing changes the direction of drying stress. Through this center-bored timber drying process, drying-check free large solid structural timber can be manufactured as well as high grade wood flour, raw material of wood-based panel and woody biomass without extra cost. Because the check-free center-bored timber is light and has a uniform moisture profile, it is good for the beam and column construction. Also, its boring part can be used for hiding electrical wire line which is exposed in ordinary beam and column structures.

***Keywords*:** center-bored timber, MC variation, drying, pitch pine, sealed outer surface, heat transfer, moisture movement

Introduction

It should be applied to an appropriate process to dry wood to recommended low moisture content for efficient use of wood. Usually drying for large cross-sectional timber takes a long time and creates a lot of drying defects. To solve these problems, many drying methods such as high temperature/humidity drying and high-frequency drying, have been proposed. In this study, we developed the outer-surface sealed center-bored timber drying, drying after boring central part of timber along longitudinal axis and sealing the outer surface, which increases the drying rate by reduction of heat and moisture moving distance and prevents occurrence of drying checks. It also has the advantage that byproduct, high grade wood flour, from boring process can be acquired without extra cost. In this study, pitch pine tree needed species regeneration is used. The afforestation area of pitch pine in Korea is approximately 0.4 million ha. Most of these trees have been used for manufacturing wood composite not solid wood.

Materials and Methods

Materials. The species used in the experiments was pitch pine. Center-bored round wood with an outer diameter of 140mm, inner diameter of 80mm was prepared. The length of the specimens was 1.2m. Average initial MC was 30%.

Methods. Pitch pine tree was cut in length of 3m. Pitch pine tree was manufactured as round wood with an outer diameter of 140mm. The round timber was center bored by drilling bit with diameter of 80mm. The center-bored timber was cut in length of 1.4m. Before sealing the outer surface of the center-bored timber, initial MC content specimens with 0.1m (100mm) thickness were cut from both end of the 1.4m center-bored timber. Outer surface of 1.2m center-bored timber was sealed. And center-bored timber was dried at 95℃ for 48 hours according to temperature and humidity conditions of Figure 2. The outside size of dryer is 2,300 mm (length) × 1360mm (width) × 1080mm (height).And inside size is 1,570 mm (length) × 1,200 mm (width) × 640mm (height). Temperature and humidity was controlled by hot-wires located at the bottom of the dryer and steam heater. Wind velocity of longitudinal direction of wood was maintained by air blower on the side of the dryer. The wind velocity measured by anemometer (8386A, TSI Inc.) was at a speed of about 3 m/s.
To measure the internal temperature change during drying, thermocouples were inserted into the wood. Temperature was measured and recorded using data logger (CR1000, Campbell Scientific Inc.) for analyzing heat transfer. And To determining average internal moisture content of wood, the weight of the specimens was measured during drying. In addition, to analyzing moisture transfer, outer, center, and inner part (Figure 1) specimens were cut and weighed at 8 hour intervals during drying

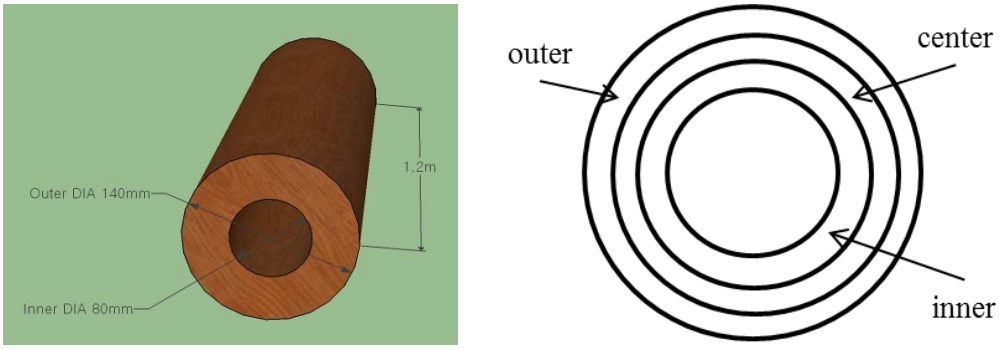

Figure 1. Dimension of center-bored timber and measuring part of MC (outer, center, inner)

Results and Discussion

In this study, heat and moisture transfers in and/or on the outer-surface sealed center-bored timber (sealing wood) and seal-free center bored timber (control wood) were analyzed. The change of MC of sealing wood and control wood during pitch pine center-bored timber drying is shown in Figure 2. MC decrement of sealing wood was a little bit slow compared with control wood, but it is not different significantly. The final MC after 48 hours was about 5%.

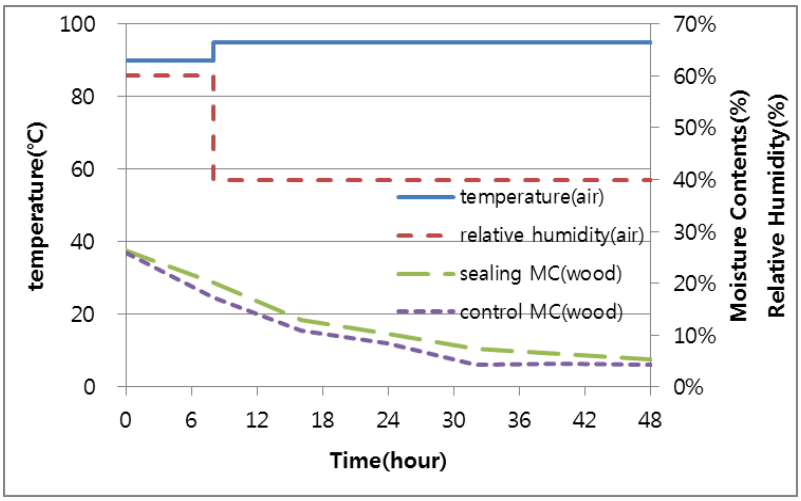

Figure 2. MC variation of sealing wood and control wood by drying schedule

Temperature changes of sealing wood and control wood during drying were shown in Figure 3 and 4. Wood temperature was increased during approximately 3 hours to reach around the setting temperature. In the case of control wood, temperature difference between surface and inner part of control wood was maintained with about 10℃ during 18 hours after beginning of drying. Whereas, temperature difference between surface and inner part of sealing wood was maintained within 5℃ during 18 hours after beginning of drying. It means that heat transfer into outer surface sealing wood very quickly. Because

space between outer surface and sealing material was filled with a high temperature steam, it seems that the heat transfer rate in outer surface sealing wood is higher.

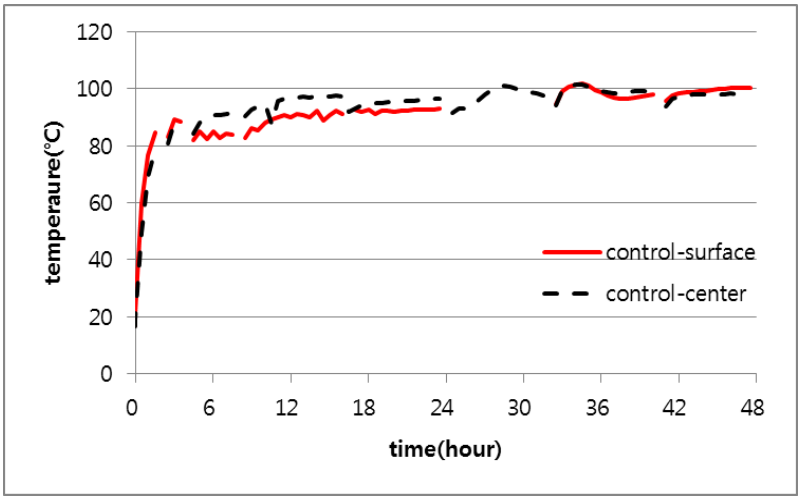

Figure 3. temperature change of control wood during drying

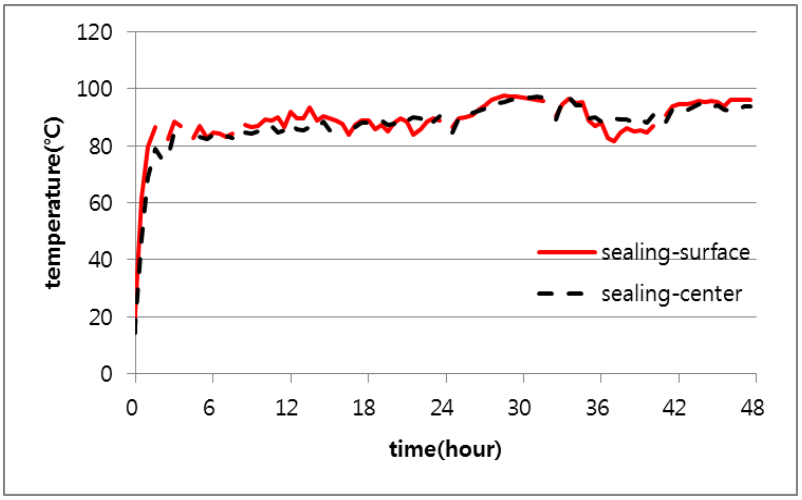

Figure 4. temperature change of sealing wood during drying

Changes of MCs of each part in center-bored timber during drying are shown in Figure 5, 6. Drying time of sealing wood was considerably shorter than expected. Compared to control wood, the moving distances of water molecules in outer-surface sealing wood are much longer. However, the actual drying time of the sealing wood was not increased significantly.

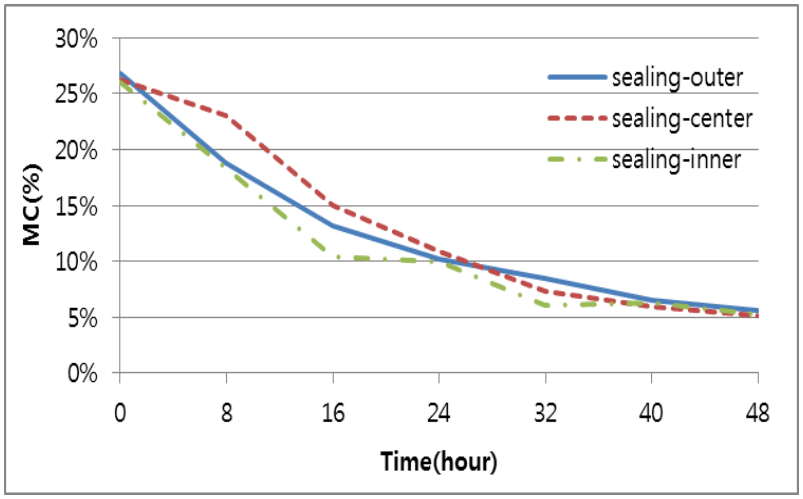

Figure 5. Partial MC variation during drying of sealing wood

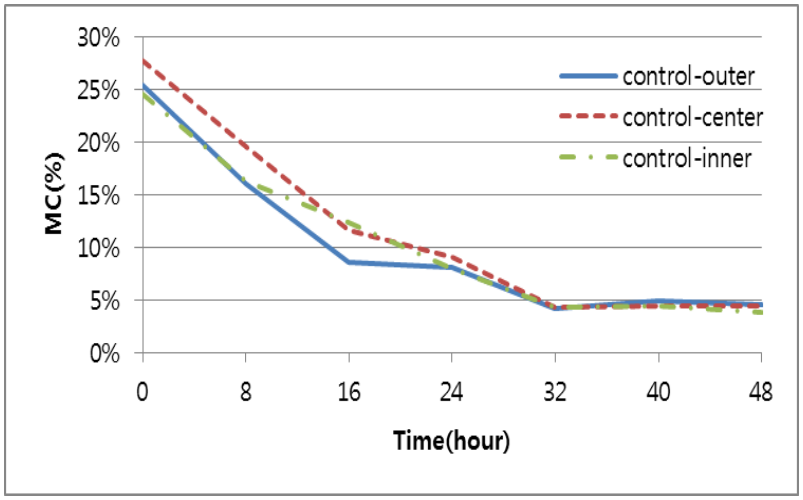

Figure 6. Partial MC variation during drying of control wood

In case of control wood, MCs of outer surface and inner surface are lower than MC of center part of wood prior to drying. And this tendency was maintained during drying and to ending the drying process. However, in case of sealing wood, drying rate of outer surface is lower than center part and inner surface.

This slower drying of outer part prevents the occurrence of tension stress on the outer surface. Also the tension stress occurred on inner surface part could not affect to cause drying check due to geometric characteristics of center-bored timber. Concave and closed curve shape of the hole in the cross section of timber dose not allowed increasing a gap between wood tissues. 6 surface drying checks were found on the outer surface of control wood. The length of surface check was 103.4±55.8mm. Whereas outer-surface sealed center-bored timber (sealing wood) was dried without drying check.

In this study, center-boring, sealing, and drying method and process was developed. Drying after sealing the outer surface of the timber was applied to manufactured defect-free center-bored timber. Also, MC measurement method using NIR during drying

center-bored timber was developed to control the drying process and determine when the drying process should be finished.

References

Hee-Suk Jung, Ho-Yang Kang, Jung-Hwan Park, Nam-Ho Lee Hyoung-Woo Lee, Chun-Won Kang, Hwanmyeong Yeo. 2008. A New Introduction to Wood Drying. Seoul National University Press. Seoul.

Hwanmyeong Yeo, Chang-Deuk Eom, William B. Smith., Kug-Bo Shim, Yeonjung Han, Jung-Hwan Park, Do-Sik Lee, Hyoung-Woo Lee, Moon Jae Park, Joo-Saeng Park, Nam-Ho Lee. 2007. Effects of center boring and kerf treatment on kiln-drying of larch square and round timbers. Forest Product Journal. 57(11): 85-92

Nanotechnology Applications in Forest Products: Current Trends

Douglas J. Gardner and Yousoo Han
University of Maine
Advanced Structures and Composites Center
Orono, Maine 04469

Abstract

Over the past several decades, a significant world-wide research effort has been made in the application of nanotechnology to forest products. Nanotechnology is the understanding and control of matter at dimensions of roughly 1 to 100 nanometers, where unique phenomena enable novel applications. Encompassing nanoscale science, engineering and technology, nanotechnology involves imaging, measuring, modeling, and manipulating matter at this length scale. Nanotechnology research roadmaps have been developed and applied to forest products globally. Many of the applications being developed provide great potential for improved forest products that offer improved material properties for a variety of consumer products. In considering nanotechnology and forest products, we can apply nanomaterials to forest products in the form of coatings, biocides and modified resins or we can derive nanomaterials from wood. Nanomaterials derived from renewable biomaterials like wood, especially cellulose and lignin will undoubtedly play a large role in future nanotechnology research efforts. Research focus areas for nanotechnology applications in forest products include: polymer composites and nanoreinforced materials; self-assembly and biomimetics; cell wall nanostructure; nanotechnology for sensors, processing and process control; and analytical methods for nanostructure characterization. High profile nanotechnology applications in forest products include optically transparent cellulose nanofiber paper and optically transparent cellulose nanocomposites for flexible electronic displays. Future needs of nanotechnology in forest products include the ability to have scalable nano-manufacturing by adapting conventional manufacturing processes or developing novel process equipment. It appears that we may be on the cusp of significant commercial applications of novel nanotechnology applications in forest products.

Keywords: nanotechnology, research, forest products, cellulose nanofibrils, applications

Introduction

Nanotechnology is the understanding and control of matter at dimensions of roughly 1 to 100 nanometers, where unique phenomena enable novel applications. Encompassing nanoscale science, engineering and technology, nanotechnology involves imaging, measuring, modeling, and manipulating matter at this length scale. Nanotechnology research and development (R&D) in the U.S. is high priority research across all segments of science and engineering since the enactment of the National Nanotechnology Initiative (NNI) in 2001. The forest products industry in the U.S. developed a nanotechnology research roadmap in 2005 and more recently in 2010, recognized the study of cellulose-based nanomaterials as a signature research initiative. Nanotechnology research roadmaps have been developed and applied to forest products globally. Research focus areas for nanotechnology applications in forest products include: polymer composites and nanoreinforced materials; self-assembly and biomimetics; cell wall nanostructure; nanotechnology for sensors, processing and process control; and analytical methods for nanostructure characterization.

Nanotechnology Applications in Forest Products

At first glance, applications of nanotechnology in forest products might appear to be a relatively new development, but in actual fact, nanoscale materials have been used in the production of sized and coated paper for over a century. Colloidal materials which are systems consisting of a mechanical mixture of particles between 1 nm and 1000 nm dispersed in a continuous medium, usually water, are commonly used in paper chemicals, as well as in paints and coatings to protect wood. The terminologies used to describe nanomaterials become important because the term nanotechnology was first coined in 1974. Even though the term nanotechnology is relatively new, we have been in fact utilizing nanomaterials in production of man-made materials for many centuries and a number of good examples can be found in the popular scientific media including glazings for pottery, carbon nanofiber reinforced steel, emulsions for food, etc.

In considering nanotechnology and forest products, nanomaterials can be applied to forest products in the form of coatings, biocides and modified resins or nanomaterials can be derived from wood. Nanomaterials derived from renewable biomaterials like wood, especially cellulose and lignin will undoubtedly play a large role in future nanotechnology research efforts. High profile nanotechnology applications in forest products include optically transparent cellulose nanofiber paper and optically transparent cellulose nanocomposites for flexible LED displays. Wood protection applications have been a significant focus of nanotechnology including the utilization of nanobiocides and nanocarrier delivery systems in wood preservatives. Wood coating applications of nanotechnology are now becoming common in the consumer marketplace where coatings with improved scratch and abrasion resistance, hydrophobicity, ultraviolet light blocking and dust free surfaces are touted by commercial manufacturers.

Cellulose Nanomaterials

Cellulose nanomaterials are a large focus of research across the world as evidenced by six comprehensive literature reviews appearing in the peer reviewed literature in 2010 and 2011 [1-6]. Cellulose nanofibers (CNF) are prepared in four different forms: 1) bacterial cellulose nanofibers, 2) cellulose nanofibers by electrospinning, 3) micro- or nano-fibrillated cellulose plant cell fibers, and 4) nanorods or cellulose nanocrystals. Processing techniques have a significant impact on the adhesion properties of the resulting cellulose nanofibers in composite material applications. The behavior of cellulose surfaces in polymers as well as their interaction with different chemicals is of great importance in their current and future applications in nanocomposites. The mechanical performance of nanocomposites, for instance, is dependent on the degree of dispersion of the fibers in the matrix polymer and the nature and intensity of fiber-polymer adhesion interactions. Challenges in the scale-up of producing commercial quantities of cellulose nanofibrils for materials applications include: scalable processing methodologies, adequate methods to dry the fibrils and maintain the nanoscale dimensions, and reduction in energy requirements and production costs.

Cellulose nanomaterial applications that appear to be close to commercial production include: cellulose nanopaper, paper and paperboard coatings, aerogels and foams from nanofibrillated cellulose, bacterial cellulose for clothing, artificial veins and bone scaffolding, as well as spray dried cellulose nanofibrils as a pharmaceutical excipient. Barriers to the commercialization of CNF are based on large scale supply availability. So far, only modest investment has been made in scale up processes from lab to pilot scale. Certain applications will require large quantities of CNF to evaluate in larger scale, real world manufacturing processes. There is a lack of significant, coordinated effort among research organizations (academia, government, industry) and potential customers in transitioning CNF technologies into the marketplace. Also, there are uncertainties in CNF pricing under commercial production conditions, potential safety issues and regulations. One positive step that is currently underway is the development of ISO cellulose nanomaterial standards.

Future Needs of Nanotechnology in Forest Products

Future needs of nanotechnology in forest products include the ability to have scalable nano-manufacturing by adapting conventional manufacturing processes or developing novel process equipment. For example, a goal might be to adopt papermaking processes where we currently self-assemble wood cells on the micron and millimeter length scale at 100 kilometers per hour. Novel composite manufacturing processes will need to be developed for automobiles, adhesives, ballistic applications, coatings, biomedical applications as well as drug delivery. Concerns, challenges and opportunities of nanotechnology in forest products will include addressing consumer perception issues of sustainability as well as health risks. There may be market opportunities to improve existing products with nanotechnology such as the development of intelligent packaging.

It appears that we may be on the cusp of significant commercial applications of novel nanotechnology applications in forest products. The current applications of nanomaterials in wood protection and wood coatings as well as the near to market potential for some cellulose nanofibril material applications is an exciting development in the forest products industry. Perhaps the future is now?

References

1. Eichhorn SJ, Dufresne A, Aranguren M, Marcovich NE, Capadona JR, Rowan SJ, Weder C, Thielemans W, Roman M, Renneckar S, Gindl W, Veigel S, Keckes J, Yano H, Abe K, Nogi M, Nakagaito AN, Mangalam A, Simonsen J, Benight AS, Bismarck A, Berglund LA, Peijs T (2010) Review: current international research into cellulose nanofibres and nanocomposites. J. Mater. Sci. 45: 1-33
2. Habibi Y, Lucia LA, Rojas OJ (2010) Cellulose nanocrystals: chemistry, self-assembly, and applications. Chem. Rev. 110: 3479-3500
3. Siqueira, G, Bras, J, Dufresne, A (2010) Cellulosic bionanocomposites: a review of preparation, properties, and applications. Polymers 2: 728-765
4. Siro I, Plackett D (2010) Microfibrillated cellulose and new nanocomposite materials: a review. Cellulose 17: 459-494
5. Klemm D, Kramer F, Moritz S, Lindstrom T, Ankerfors M, Gray D, Dorris A (2011) Nanocelluloses: a new family of nature-based materials. Angew. Chem. Int. Ed. 50: 5438-5466
6. Moon RJ, Marini A, Nairn J, Simonsen J, Youngblood J (2011) Cellulose nanomaterials review: structure, properties and nanocomposites. Chem. Soc. Rev. 40: 3941-3994

Mechanical Characterization of Wood-Adhesive Interphase with an Improved Nanoindentation Technique

*Yan YU[1,2]----C.R. FRIHART[2] --- J.E. JAKES [2]--- Z.H. JIANG[1]**
[1] International Center for Bamboo and Rattan, Beijing, China, 100102.
* *Corresponding author*
yuyan@icbr.ac.cn
[2] USDA Forest Service, Forest Products Laboratory, Madison, Wisconsin, USA.

Abstract

An improved nanoindentation method was used to assess the hardness and elastic modulus of the bulk adhesive and wood cell walls within wood-adhesive bondlines. Improvements include a specimen preparation technique that does not require any embedment. Also, a structural compliance method was used to remove from the nanoindentation measurements artifacts arising from edges near to the nanoindents and specimen-scale flexing. Interphases between southern pine and the four adhesives phenol formaldehyde (PF), urea formaldehyde (UF), epoxy, and emulsion polymer isocyanate (EPI) were characterized. The hardness of PF was measured to be 0.87 GPa, nearly 2-3 times larger than UF, epoxy and EPI. The elastic modulus of PF was 8.8 GPa, comparable to that of UF but nearly 2-3 times larger than that of epoxy and EPI. Furthermore, we observed that the hardness of wood cell walls increased near the adhesive line for PF and UF bondlines, which strongly supports the idea that some low-molecular components of PF and UF infiltrate into the wood cell wall and improve its mechanical performances after curing. Similar increases were not found for epoxy and EPI bondines. Our results support that the widely known durable and strong bonding of wood with PF is related to the excellent mechanical performances of PF resin itself and its ability of infiltrate into and reinforce wood cell walls.

***Keywords*:** wood bonding, interphase, nanoindentation, adhesive

Introduction

All of the potential applications of wood based composites require the formation of mechanically stable and durable bonds between wood elements and adhesives. A full understanding of the mechanisms of bond formation in the adhesive bonding of wood is necessary for the development of wood composites with improved performance. Adhesive penetration into wood structure is believed to be vital to the durability of wood-adhesive bondlines (Frihart, 2009). Adhesive penetration includes both adhesives flowing into the micron-scale cavities of wood, such as empty lumina, and adhesives infiltrating into the cell walls and modifying them. Understanding how infiltrated adhesives affect wood cell wall properties is critical to understanding how to make durable wood-adhesive bondlines.

Recently, several investigators used nanoindenatation to characterize wood-adhesive bondlines, which is based on the reasonable assumption that the infiltration of adhesives into wood cell walls might change their mechanical properties (Konnerth and Gindl, 2006; Konnerth et al, 2007). However, in this previous work the researchers first embedded wood specimens in an epoxy medium to facilitate sample preparation for nanoindentation. The possibility of undesired chemical modifications caused by the epoxy cannot be totally avoided. Furthermore, the nanoindentation tests adopted the standard Oliver-Pharr method (Oliver and Pharr, 1992) for data analysis. This method assumes the tested samples are homogeneous half spaces and are rigidly supported in the testing machine. However, these assumptions will be violated during testing of cell walls because of the free edge between the cell wall lamina and lumen, which are usually in close proximity to the indents, elastic discontinuities across the cell wall, and the possibility of flexing of the cellular structure during indenting. Jakes et al (2008, 2009) recently proposed a structural compliance method to correct for the above factors. This method has been demonstrated to be effective in the micromechanical measurement of wood cell walls (Jakes et al, 2008). In this paper, a specimen preparation technique that eliminates the need for epoxy embedment (Jakes et al. 2008, 2009) and this structural compliance method were adopted to characterize the mechanical properties of cell walls and adhesive in four wood adhesive bondlines, namely PF, UF, epoxy and EPI.

Materials and Methods

Materials. Southern pine veneers with a thickness about 5 mm were bonded together with PF, UF, epoxy and EPI adhesives with the bonding parameters shown in Table 1.

Sample preparation. The common method of embedding wood or wood composites specimens in an epoxy medium was rejected in this study because it might result in unpredictable chemical modifications in the cell walls. A new sample preparation procedure developed by Jake et al. (2008) was used to eliminate these possible artifacts.

First, small blocks (5×5 mm in cross section) containing the bondline were cut from the two-ply wood laminates. A gently sloping apex was created using a sliding microtome on

the transverse surface of the blocks with the apex positioned in the bondline (Fig. 1). Next, an ultramicrotome (Leica UC6) fit with a diamond knife was used to cut the tip of the apex. This preparation technique produces an exceptionally smooth and flat surface area of approximately 0.2 mm^2.

	Temperature(℃)	Time (Min)	Pressure (MPa)	Application Rate (g/m^2)
PF	158	6	1.2	80
UF	125	5	1.4	150
Epoxy	Room temperature	180	0.86	174
EPI	Room temperature	Overnight	1.4	180

Nanoindentaion. The polished blocks were glued to steel discs and transferred onto the magnetic holder of a Hysiron TriboIndenter equipped with a diamond Berkovich probe with radius less than 100 nm. During the test period, the relative humidity (RH) in the chamber of the instrument was maintained between 42 and 45% using a glycerin-water bath. Specimens were placed inside the enclosure overnight to allow equilibration with the conditions inside the enclosure. Nanoindentation testing was performed both on the pure adhesives and the cell walls with different distance to bondline. To account for potential artifacts arising from edges nearby the nanoindents and specimen-scale flexing, the structural compliance method was employed. More detailed information on this method could be found in Jakes et al (2008, 2009). Residual indents were imaged with a Quesant (Agoura Hills, CA, USA) atomic force microscope (AFM) incorporated in the TriboIndenter.

Results and Discussion

Table 1 Bonding parameters for the four kinds of adhesives

Figure 1 Schematic diagram showing the procedure of unembeddment sample preparation

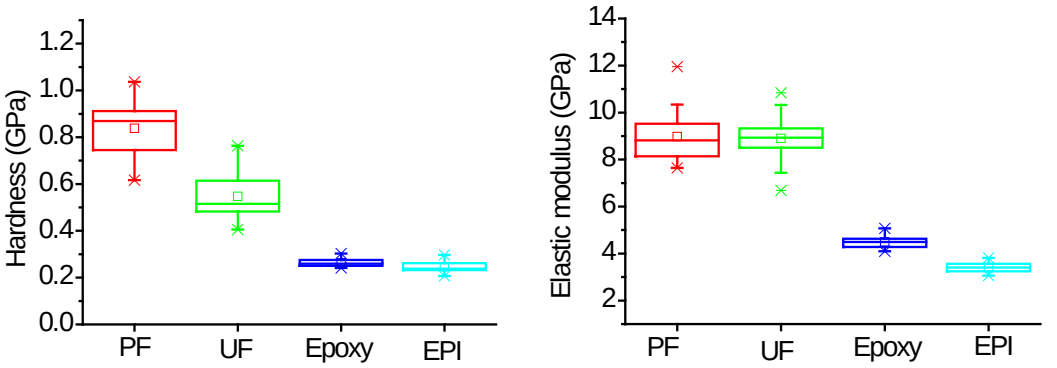

Figure 2 The elastic modulus and hardness of the four wood adhesives

Figure 2 shows the elastic modulus and hardness of the four wood adhesives tested. The elastic modulus of PF was about 8.8 GPa, comparable to that of UF but nearly 2-3 times of epoxy and EPI. EPI has the lowest elastic modulus (3.3 GPa) among the four wood adhesives. The hardness of PF resin was measured to be 0.87 GPa, nearly 2 times the hardness of UF and 3 times the hardness of epoxy and EPI. EPI has the lowest hardness (0.25 GPa) among the four adhesives. Our results indicate PF resin is the most rigid wood adhesive, which is mainly because of its aromatic phenol groups linked by methylene groups along the chain and between chains. EPI is the softest adhesive because of its flexible linear polyester backbone. According to the view point of Frihart (2009), wood adhesives could be classified into two groups. One is *in situ* polymerized adhesives, which is made up of small molecules that cross-link to form relatively rigid polymers after curing. PF, UF and epoxy belong to this group. The other group is called pre polymerized adhesives, consisting of higher MW molecules and is rather flexible after curing. EPI belongs to this group. However, significant difference can also exist among the same group of adhesives, which originates from their different chemical structure.

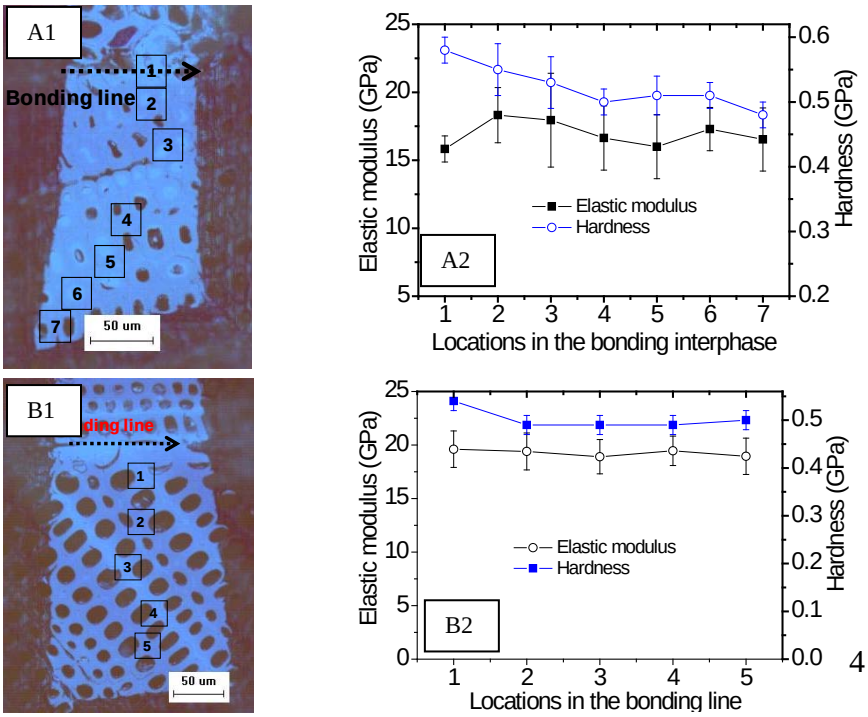

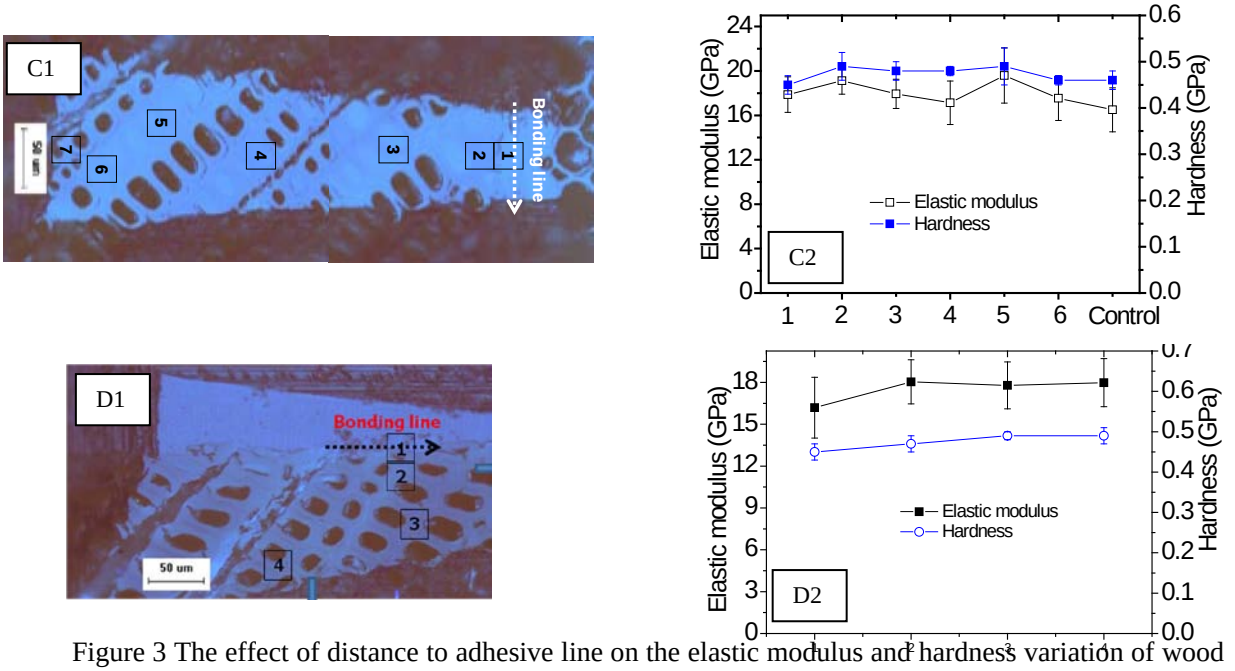

Figure 3 The effect of distance to adhesive line on the elastic modulus and hardness variation of wood cell wall. A: PF; B: UF; C: Epoxy; D: EPI. The higher is the x-axis number, the greater is the distance to adhesive line.

Figure 3 shows the change of elastic modulus and hardness of wood cell walls with the distance to the adhesive line. For PF resin bondlines, cell wall hardness increased significantly for cell walls near the bondlines, while this trend is not so obvious for elastic modulus. The result strongly supports the idea that some low-molecular segments of PF resin penetrate into the wood cell wall and improve it mechanically after curing. However, similar patterns of variation were not observed for the other three adhesive bondlines. For UF resin bondlines, only the cell wall very close to the adhesive line was significantly hardened because the penetration of UF was not as deep into the wood structure as that of PF resin. Although epoxy was found to have a very good capability of flowing into lumina far from the bondlines, changes in wood cell wall mechanical properties were not observed. As for EPI adhesive, no changes in mechanical properties were observed; likely because adhesive infiltration into cell wall will be limited because EPI has too large molecular weight.

Conclusions

1. Of the wood adhesives tested, PF has the highest elastic modulus and hardness, followed by UF, epoxy and EPI in turn.
2. Wood cell walls near UF and PF bondlines had increased hardness, but the elastic modulus was not modified.
3. Mechanical properties of wood cell walls near epoxy and EPI bondlines were not modified. .

4. The durability and strength of wood-PF bondlines is likely because of the high mechanical properties of the PF itself and its ability to infiltrate and strengthen wood cell walls near the bondline.

Acknowledgement
This research is financially supported by National Nature and Science Foundation of China (31070491)

Reference

Frihart, C.R. (2009) Adhesive groups and how they relate to the durability of bonded wood. Journal of Adhesion Science and Technology, 23: 601–617.

Jakes, J.E., Frihart, C.R., Beecher, J.F., Moon, R.J., and Stone, D.S. (2008) Experimental method to account for structural compliance in nanoindentation measurements. Journal of Materials Research, 23(4): 1113-1127.

Jakes, J.E., Frihart, C.R., Beecher, J.F., Moon, R.J., Resto, P.J., Melgarejo Z.H., Su, O.M. rez, Baumgart, H., Elmustafa, A.A., and Stone, D.S. (2009) Nanoindentation near the edge. Journal of Materials Research, 24(3): 1016-1031.

Konnerth, J., Gindl, W. (2006) The interphase in wood-adhesive bond lines by nanoindentation. Holzforschung. 60:429-433

Konnerth, J., Valla, A., Gindl, W. (2007) Nanoindentation mapping of a wood-adhesive bond. Appl. Phys. A. 88:371-375

Oliver, W.C., Pharr, G.M. (1992). An improved technique for determining hardness and elastic modulus using load and displacement sensing indentation experiments. J. Mar. Res. 7: 1564-1583

Proceedings of the 55th International Convention of Society of Wood Science and Technology
August 27-31, 2012 - Beijing, CHINA

Effect of Impregnated Inorganic Nanoparticles on the Surface Chemical Composition of the Kenaf Bast Fibers

Kaiwen Liang[1] *and Sheldon Q. Shi*[2]*

[1] Assistant Research Assistant Professor, Department of Mechanical and Energy Engineering, University of North Texas, Denton, Texas 76207, USA

[2] Associate Professor, Department of Mechanical and Energy Engineering, University of North Texas, Denton, Texas 76207, USA
* *Corresponding author*
Sheldon.Shi@unt.edu

Abstract

The objective of this research was to study the effect of impregnated inorganic nanoparticles on the surface chemical composition of the kenaf bast fiber. High quality kenaf bast fibers were obtained from a chemical retting process. An in situ inorganic nanoparticle impregnation (INI) process was used to introduce the $CaCO_3$ nanoparticles into the retted kenaf bast fibers. X-ray photoelectron spectroscopy (XPS) and scanning electron microscopy (SEM) were used for the surface analysis. It was found that some lignin-based components in the retted fibers were further removed during the INI treatment. The O/C ratio on the fiber surface was increased by over 35% after the INI treatment. The inorganic nanoparticles $CaCO_3$, with different shapes and sizes, appeared at the surface of the impregnated fiber after treatment. Heterogeneous $CaCO_3$ nanoparticle distribution was observed on the INI treated fibers.

***Keywords*:** kenaf, nanoparticle, impregnation, X-ray Photoelectron Spectroscopy (XPS), Scanning Electron Microscopy (SEM)

Introduction

Kenaf is a warm season annual grow fiber crop. It grows in large amounts every year in the United States. In Texas, the growth of kenaf was about 2,300 acres in 1998, 5,600 acres in 1999 and as much as 7,000 acres in 2000 (1). Kenaf is currently a relatively underutilized biomass in Texas. Kenaf bast fiber is attractive also due to its high cellulose content and good mechanical properties. The cellulose content of kenaf bast fiber is about 46 to 57 % (2). The tensile strength and modulus of single kenaf fiber can be as high as 11.9 GPa and 60.0 GPa, respectively (3-4). Thus, the kenaf bast fiber is an excellent cellulose resource for fiber based products, such as newsprint and paper products. It is also a good reinforcement material for natural fiber composites for structural component design for automotive industries (4-10). By introducing the nano or micro particles into the micro pore structure of the cellulosic fibers, the compatibility between natural fibers and thermoplastics can be improved, while the air pocket defect in the natural fiber composites can be reduced (11-12). The objective of this study was to investigate the effect of impregnated inorganic nanoparticles in the kenaf bast fibers on the fiber properties, such as morphology, chemical components, surface roughness and modulus.

Materials and Methods

Materials. In the fiber retting experiments, Kenaf stems (Hibiscus cannabinus, L.) were obtained from Kengro Incorporation, Charleston, MS. After the bast and core were separated using a crushing process, the bast was cut into 5.1 cm in lengths. The bast was then dried until a 8% moisture content was achieved at 22 ºC and 50% relative humidity environment. The retting chemicals such as sodium hydroxide in lab grade, and acetic acid in regent grade and inorganic nanoparticle impregnation chemicals such as sodium carbonate and calcium chloride were purchased from Thermo Fisher Scientific Inc.

Chemical Retting of Kenaf Fiber. The procedure of chemical retting of kenaf fiber followed the details described in previous published paper (13).

Inorganic Nanoparticle Impregnation of Kenaf Fiber. The procedure of inorganic nanoparticle impregnation of kenaf fiber followed the details described in previous published paper (14).

X-ray Photoelectron Spectroscopy (XPS). XPS analysis was performed using a PHI 1600 XPS Electron Scanning Chemical Analysis instrument (Physical Electronics, Inc., Chanhassen, MN) with a PHI 10-360 spherical detector. An achromatic Mg K_alpha X-Ray source was operated at 300 W and 15 kV. XPS data was collected with PHI surface analysis software version 3.0 and analyzed with CasaXPS analysis software version 2.2.88. High resolution scans were energy referenced to C 1s CHx environment at 285 eV. For this technique, the specimens were left inside the vacuum chamber overnight for degasing.

Scanning Electron Microscopy (SEM). A JSM-6500F field emission scanning electron microscope (FESEM) (JEOL USA Inc., Peabody, MA) was used to evaluate the morphology of the retted and impregnated kenaf fibers. The samples were coated with gold before SEM measurements. The electron beam spot size used in X-EDS is about 5 nm in diameter.

Results and Discussion

Surface Chemical Composition of the Fibers. XPS is an analytical technique used to detect the surface composition of cellulosic fiber. XPS can provide quantitative information on different bonded carbon atoms on the fiber surface besides the chemical composition. Thus chemical retted and inorganic nanoparticle impregnated kenaf fibers were first investigated by XPS. The surface composition of the retted and impregnated fibers is shown in Table 1. Carbon (~285 eV) and oxygen (~533 eV) were the main elements detected in the fibers in XPS survey scan. The presence of $CaCO_3$ was evidenced by the calcium characteristic peak (Ca2p) at a binding energy around 350 eV. The content of calcium in fiber increased after fiber inorganic nanoparticle impregnation treatment. Carbon was the dominant element at the surface of these two fibers and the O/C ratio for the components of the surface was different. Kenaf fiber is mainly composed of cellulose, hemicellulose, lignin and pectin (15). Some of the hemicelluloses and lignin were removed from the fibers during alkali retting treatment of the fibers. The O/C ratio of pure cellulose fibers is around 0.80 (16). The O/C ratio of retted fiber was 0.43 and very similar to the reported data for alkali treated kenaf fiber (17). Following the inorganic nanoparticle impregnation treatment, the O/C ratio the fiber was raised to 0.59, increased by over 35%. Thus, oxygen rich cellulose dominated at the fiber surface after the inorganic nanoparticle impregnation treatment of retted fiber.

Table 1. Surface Composition of Inorganic Nanoparticle Impregnated (INI) Kenaf Bast Fibers with Chemical Retted Fibers Used as Control.

	Surface composition (%)				
Sample	O	C	N	Ca	O/C
retted fiber	27.72	64.79	7.47	0.22	0.43
impregnated fiber	33.73	57.37	7.49	1.41	0.59

Figure 1 is the deconvoluted high resolution C 1s XPS spectra which detailed the analysis of the fiber composition. Chemical shifts of carbon (C1s) in cellulose includes C-C-OH, C-OH, C-OR, and O-C-O, and those of lignin are mainly CHx and C-OR (16, 18). The new peak C5 in deconvoluted C 1s XPS high resolution spectra of impregnated kenaf fibers (Figure 1b) appeared from inorganic carbonates (CO_3^{2-}) (19) introduced by the inorganic nanoparticle impregnation treatment of retted fiber. Table 2 summarizes deconvoluted C 1s XPS high resolution spectra peaks assigned to the corresponding functional groups with correlative data. After the inorganic nanoparticle impregnation treatment of retted fiber, the intensity of component peak C1 which corresponding to C-C and C-H chemical groups decreased significantly. In contrast, the content of O-C-O and O-C=O chemical groups increased by 46.96% and 64.54%, respectively. The inorganic carbonates (CO_3^{2-}) component peak appeared and the content of calcium increased (Table

1) after the treatment. Therefore, some of the lignin-like components was further removed from retted fiber during the inorganic nanoparticle impregnation treatment, and $CaCO_3$ inorganic nanoparticles were successfully generated at the surface of the impregnated fiber after treatment.

Scanning Electron Microscopy (SEM) of the Fibers. Figure 2 shows the SEM micrographs of the chemical retted and inorganic nanoparticle impregnated kenaf fibers. There were some residues or impurities left between the fibers which could not be removed by alkali chemical retting treatment (Figure 2a). In contrast, much less residues were observed between the fibers after INI treatment. Some of the kenaf fiber component may be further removed during high temperature treatment like 160 ºC INI treatment. There were large amount of inorganic particles at the surface of the impregnated fiber (Figure 2b) and some particles grow from inside of the fibers to outer surface (Figure 2d). The inorganic particles were in different shapes. Some were square, and the others were sphere. The particle sizes showed a wide distribution ranging from 80 nm to 6 µm. The surface of the impregnated fiber (Figure 2d) was rougher than that of the retted fiber (Figure 2c).

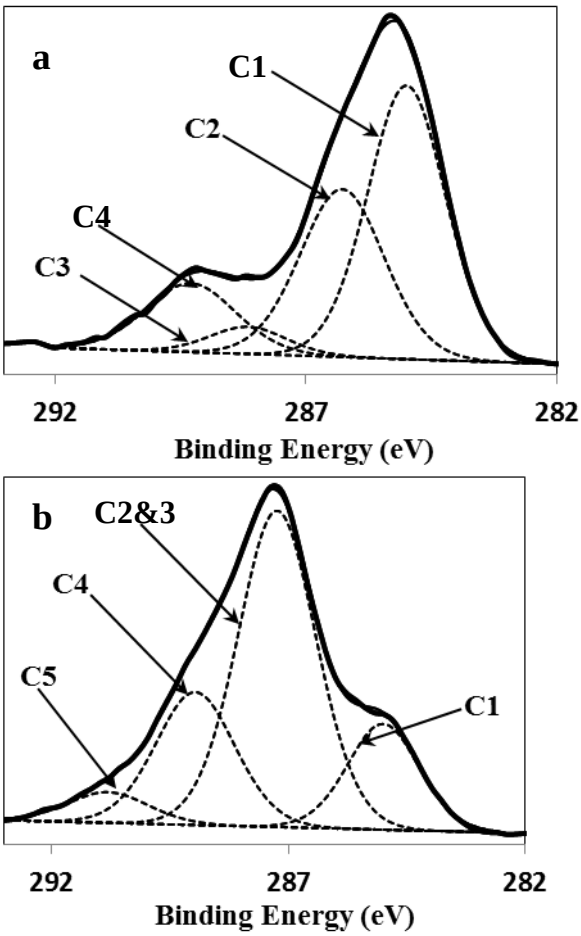

Figure 1. Deconvoluted C 1s XPS high resolution spectra of (a) chemical retted and (b) inorganic nanoparticle impregnated kenaf bast fibers.

Table 2. C 1s Component Intensities of Inorganic Nanoparticle Impregnated (INI) Kenaf Bast Fibers with Chemical Retted Fibers used as control.

	C1 (C-C, C-H)	C2 (C-O)	C3 (O-C-O)	C4 (O-C=O)	C5 CO_3^{2-}
Binding energy (eV)	285	286.5	288.1	289	290.8
retted fiber	48.73 %	32.35 %	4.79 %	14.13 %	0
impregnated fiber	16.69 %	54.58 %		23.25 %	5.47 %

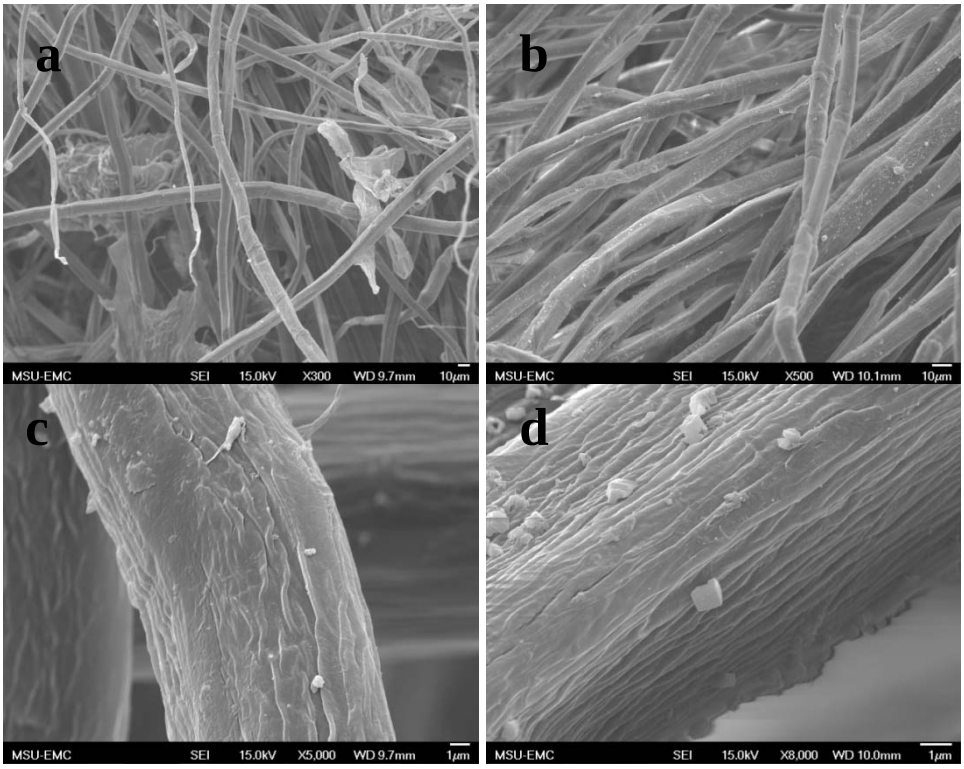

Figure 2. Scanning electron micrographs (SEMs) of the [a (X300) & c (x5000)] chemical retted and [b (X500) & d (x8000)] inorganic nanoparticle impregnated kenaf bast fibers.

Conclusions

XPS was used to study the surface chemical composition of the cellulosic fibers impregnated with the $CaCO_3$ inorganic nanoparticles. It showed that some of the lignin-like components were removed from the retted fiber during the inorganic nanoparticle impregnation treatment. The O/C ratio on the fiber surface was affected by the INI treatment with an increase of over 35%. The $CaCO_3$ appeared at the surface of the impregnated fiber after treatment. Heterogeneous particle size distributed on the fiber surface and various particle shapes observed.

Acknowledgements

The research presented was supported by National Science Foundation (NSF) under grant no. CMMI 0928641.

References

(1) Rymsza, T. Advancements of kenaf in the USA kenaf paper and nonpaper developments http://www.visionpaper.com/PDF_speeches_papers/007anwpp.pdf (accessed May 2012).
(2) Han, J.S. Proceedings of the Korean society of wood science and technology annual meeting 1998, 3–12.
(3) Bolton, A.J. Mat. Tech. 1994, 9, 12.
(4) Karnani, R.; Krishnan M.; Narayan, R. Polym. Eng. Sci. 1997, 2, 476-483.
(5) Rana, A.K.; Mandal, A.; Mitra, B.C.; Jacobson, R.; Rowell, R.; Banerjee, A.N. J. Appl. Polym. Sci. 1998, 69, 329-338.
(6) Eichhorn, S.J.; Baillie, C.A.; Zafeiropoulos, N.; Mwaikambo, L.Y.; Ansell, M.P.; Dufresne, A.; Entwistle, K.M.; Herrera-Franco, P.J.; Escamilla, G.C.; Groom, L.; Hughes, M.; Hill, C.; Rials, T.G.; Wild, P.M. J. Mater. Sci. 2001, 36, 2107-2131.
(7) Sanadi, A.R., Hunt, J.F.; Caulfield, D.F.; Kovacsvolgyi, G.; Destree, B. Proceedings of 6th Intern. Conf. on woodfiber-plastic composites. 2002, 121-124.
(8) Joseph, K.; Thomas, S.; Pavithran, C.; Brahmakumar, M. J. Appl. Polym. Sci. 1993, 47, 1731-1739.
(9) Joseph, P.V.; Joseph, K.; Thomas, S.; Pillai, C.K.S.; Prasad, V.S.; Groeninckx, G.; Sarkissova, M. Composites: Part A 2003, 34, 253-266.
(10) Tajvidi, M.; Falk, R.H.; Hermanson, J.C. J. Appl. Polym. Sci. 2005, 97, 1995-2004.
(11) Shi, S.Q.; Lee, S.; Horstemeyer, M. Proceeding of the American Society for Composites, September 17-19, University of Washington, Seattle, WA, 2007.
(12) Lee, S.; Shi, S.Q.; Barnes, M.H. Proceedings of Advanced Biomass Science and Technology for Bio-Based Products. May 23-25, Beijing, China. Chinese Academy of Forestry. 2007 pp.173-181.
(13) Shi, J.; Shi, S.Q.; Barnes, M.H., Horstemeyer, M.; Wang, J. and Hassan, E-B.M. International Journal of Polymer Science 2011, doi:10.1155/2011/212047.
(14) Shi, J.; Shi, S.Q.; Barnes, M.H., Horstemeyer, M. and Wang, G. International Journal of Polymer Science 2011, doi:10.1155/2011/736474.
(15) John, M.J.; Thomas, S. Carbohydrate Polymers 2008, 71, 343-364.
(16) Pommet, M.; Juntaro, J.; Heng, J.Y.Y.; Mantalaris, A.; Lee, A.F.; Wilson, K.; Kalinka, G.; Shaffer, M.S.P.; Bismarck, A. Biomacromolecules 2008, 9, 1643–1651.
(17) Sgriccia, N.; Hawley, M.C.; Misra, M. Composites: Part A 2008 39, 1632-1637.
(18) Csiszár, E.; Fekete, E. Langmuir 2011, 27, 8444–8450.
(19) Pothan, L.A.; Simon, S.S.; Thomas, S. Biomacromolecules 2006, 7, 892–898.

Proceedings of the 55th International Convention of Society of Wood Science and Technology
August 27-31, 2012 - Beijing, CHINA

Timber Use in the Chinese Gardens and Architecture

Ying JIANG

Abstract

Chinese civilization originated in the middle and lower reaches of the Yellow River – the area that is featured by distinctive four seasons and dense forests. The unique natural and climate conditions nurture the famous Chinese philosophy-Taoism, as well as its unique timber constructions. Traditional Chinese timber constructions have experienced thousands of years' of development. During this process, timber has become a favored material by the Chinese people and used widely. However, with recent economic and population growth, forest resources are decreasing, and the timber constructions can be rarely seen as timber is mainly used for non-structural industrial uses, instead. Thanks to the development of science and technology, wood products now can be manufactured with better physical properties that can last longer and be applied in a broader scope.

Key word：Timber　Traditional Chinese architecture　Five Elements

Chinese civilization originated in the Yellow River basin. The vast plain on the basin once had fertile soil, rivers, and dense forest in the ancient times. Rich wood resource provided people fine building materials. Meanwhile, it created the world famous traditional Chinese timber constructions.

1 Reasons why timber constructions appear and become mainstream in China

Timber, one of the oldest building materials, has been used for thousands of years. Why our ancestors choose timber as the building materials? There are several points in the industry.

First, in the ancient times, the weather and geographical condition is suitable for growing plants in the Yellow River basin. The dense forest and river here make it easy to get raw materials and transport them. Timber becomes the first choice to build houses because it is lighter and more easily to cut and process.

Second, the Chinese philosophy- Taoism believes in the unity of man and nature, and yin-yang and five elements. It believes that the basic substances that compose the world are metal, wood, water, fire and soil, and each of them corresponds to one of the five directions—west, east, north, south and central. Soil represents Central on behalf of the load of all earth things and soil would have a high status. Chinese ancient buildings are often built above tall soil units. Such as Caocao's construction in the Three Kingdoms period, which is famous for poetry and famous Dongjak are built on the high platform. Ming and Qing Imperial Palace in Beijing, the hall is built on the "earth" shaped triple white marble on the platform. Behalf of the state of the Altar also adopt "colored earth" symbol. five elements of wood represent east and symbol of spring and vitality; while Gold acting on behalf of the West and a symbol of force and punishment to kill; water, fire for the intangible thing, therefore, the five elements represent the most advocates of the five substances, only "soil" and "wood" is the most suitable for the construction of housing people live. Therefore, the basic materials of the Chinese ancient architecture are "soil and timber". People live in the space surrounded by the "wood" hosted by the "soil". The yin and yang concept stresses the contrast with the conversion of the things, a tree thanks to the available material become into the pillars of the construction of Buildings, after the use of a number of years decadent gradually come into the soil which the Taoists emphasized the negative yin yang, again and again with endless process.

Third, both Taoism and Confucianism—another Chinese traditional philosophy—emphasize this life. All the buildings for people, places, government offices, houses, temples, are mainly made from wood. Timber structure buildings can be easily build, remove and renovate, just conform to the idea of emphasize this life but not eternal.

2 The development of timber constructions in ancient China

Like birds' perch on the trees and beasts live in the caves, the ancient Chinese first settled in caves with wood roofs. Then the progress of technology and experience brought out pillars and beams, and later formed an integrated structure system.

The main structures of ancient Chinese timber constructions are post-and-lintel construction, column-and-tie construction and well railing construction. The first one is most widely used among the three.

The carrying beam post-and-lintel construction was added to Liang in the column and the beam also lifts the short columns with and beams also known as the stacked beam type. This framework of the roof weight by rafters, purlins, beams, columns, spread to basis. The post-and-lintel construction frame has been existed in the late Spring and Autumn Period and thanks to improvement which gradually formed a complete set of practices. See the first image is unearthed in the Eastern Han Dynasty, Chengdu, Sichuan courtyard brick, it has been developed until the Tang Dynasty and emerge of the hall and hall are two types to create a French hall Buddha Temple, Wutai, in Shanxi province.

Chuan Dou-style timber frame column along the depth direction of the housing, but more dense between column spacing, column directly under the weight of the purlins, without the overhead of carrying beam through each column and several layers of "Chuan Fang" and composed of a bundle of architecture. Chuan Dou-style is characterized by smaller column and "Chuan Fang" columns in series with the purlin direct hold on the stigma along the purlin direction, and then the bucket Fang columns in series to form an overall framework. In contrast, Chuan Dou-style timber frame materials with strong integrity, but the columns arranged in dense, only when the little indoor spatial scales (such as room, miscellaneous house) to use. But post-and-lintel construction frame can be used to span a larger beam in order to reduce the number of columns to obtain a larger indoor space； It is suitable for the construction of palaces, temples, etc. Chuan Dou-style timber frame no later than the Han dynasty is already quite mature and spread to the present. Now is common to use wooden structures in the southern China.

Wells dry wooden structure logs (or square timber) made of stacked pile structure, most of the logs by simple processing with vertical and horizontal stack to form a rectangular space. This structure not only in China can be seen but also in the forest-rich countries. As early as three thousand years ago in China the Shang Dynasty tombs found that the well was dry wooden coffin (that was sets of coffins) using. Yunnan in the Han Dynasty found objects ornamentation also can be seen this structure. According to records, the Han Dynasty in the palace garden has a tall well stem floor.

A major feature of the structure of the Chinese wood is brackets. Bracket is on the columns and beams junction from layers stuck arched bearing members. Brackets appearance made the roof can be with a greater degree of overhang so as to forming a beautiful roof contour. Two thousand years ago preserved artifacts of the Warring States era can already see the image of the early brackets. Brackets in the Tang Dynasty enjoyed development and then with the provisions of the folk may not be used. The evolution of the brackets can be seen as an important symbol of Chinese traditional wood frame construction shape and also to identify an important basis for building era of the ancient wooden architecture. Brackets' evolution in general can be divided into three stages. The first phase is the Western Zhou to the Northern and Southern Dynasties. At this point, the stigma of brackets was not links to each other and even as an independent load-bearing component. The second phase was the Tang Dynasty to the Yuan Dynasty. Then the brackets were no longer isolated components of the supporting frame or cornice, but an inseparable part of level in the framework. The third phase of the Ming Dynasty to the Qing dynasty. The brackets development was no longer play maintaining architecture integrity role. Its use of materials and scale is much narrower than the Song-style.

A number of characteristics of the structural system and architectural forms of ancient Chinese architecture to the Han Dynasty had been basically formed. Chinese ancient wooden structures in addition to widely used in palaces, temples, houses and other low-rise buildings, but also used to build multi-storey or high-level Chong building Court. Which can be seen a lot of carved architectural pattern of the story unearthed relics in the Warring States period, multi-storey pavilion since the Qin and Han Dynasty, an increase in the construction of the Northern Dynasties pavilion-style pagoda very popular and the most notably construction of the North Wei Xiping Yongning Temple in Luoyang. The height of the tower in the ancient records was more than forty Zhang (approximately 133 meters). Showing the level achieved by the wooden structure technology. Existing high-level wooden structure in kind and the released of Jiata Buddha Palace Temple in Shanxi built in 1056 (Ying County Wooden Pagoda) as representative. Since the completion to the moment was over 900 years and had experienced several earthquakes test and remained still stand.

The wooden structure of the skilled construction technology and timber processing experience economic prosperity, they generated a lot of beautiful buildings and gardens. Landscape architecture in the garden usually by the form of wooden structure - Pavilion, platform, floor, pavilion, bridge, House, Villa, Temple and the form of a wealth landscape architecture which add infinite charm to artificial garden natural landscape.

3 The development of timber constructions in modern China

Timber has become a favored material by the Chinese people and used widely after a

long period. Yet the long-term logging has reduced the amount of large diameter class wood that is suitable for construction. To build the Imperial Palace, people in the Ming Dynasty search wood in virgin forest in Sichuan, Guangxi, Yunnan and Guizhou Provinces. Until the Qing Dynasty, the former royal special Phoebe sheareri can be hardly found. In early Kangxi period, when rebuilding the Taihe Palace, the columns in the main hall is made from Manchu yellow pine, covered with spliced pieces of Phoebe sheareri.

The situation is the same in folk areas. Large diameter class wood with high quality become fewer and fewer. Most fine wood is used to make furniture and decorations. Many mansions are made from similar wood but with worth performance. Ordinary houses start to use bricks instead. The division of bricks and timber usage begins from the Qing Dynasty. Kaiyuan Temple in Suzhou is a famous brick building in this period. Meanwhile, the peak of furniture design- furniture in Ming Dynasty appears. Chinese historic gardens show unity and harmony with the delicate wooden furniture.

In 1824, a British named Joseph Aspdin invented cement. Later in 1865, French gardener Joseph Monier invented reinforced concrete. Until early 20th century, some buildings designed by European designers in Shanghai, such as Asia Building, Shanghai Club and East Wind Hotel, totally or partly used reinforced concrete structure.

Because of the urban development, population increase, woodland reduction and invention of new building materials, timber has been used less and less in our daily lives. Things also happen in landscape architecture for more and more reinforced concrete has taken place of timber.

People have been exploring the antiseptic and panel processing technology over the years. In the 1830s, two patents promoted the industrialization of wood antiseptic—one is Moll's creosote antiseptic, the other is Bethel's full-cell process. The antiseptic technology extended the service life of timber and improved its weather resistance, and reduced the damage by corrosion and worms.

Chinese has used timber to make houses, furniture and decorations for thousands of years. As timber becomes a favored material by the Chinese people, the vast forest has shrunk, and many rare woods vanished. Thanks to the natural forest resources protection project, most of the natural forest and secondary forest areas have prohibited logging. Timber import is the only way to make up the shortage of wood.

4 The advantages of timber

Compared to other building materials, timber has following advantages:

(1) Compared to steel and concrete, timber is one of the green materials for trees can improve natural environment during the growth.

(2) Timber has low thermal conductivity and performs well in heat insulation. An experience shows that a 150mm thick timber structure wall has the same heat-retaining capacity with a 610mm thick brick wall, and timber constructions can save energy of 50%—70% compared to concrete structure. Timber can both comfort and feast people with its low thermal conductivity and natural wood grain.

(3) Timber is light in weight and short in building period. Timber structure can use fabricated construction which has a stronger adaptation to weather. Besides, winter construction is unconstrained for timber adapts to low-temperature operation.

(4) Being a renewable resource, timber is much better than masonry concrete and steel structure in energy consumption, emission of greenhouse gases, air and water pollution, and development of ecological response. After removing, the left materials can do a secondary operation expediently.

(5)The progress of high- performance synthetic resin glue, fire retardant, antiseptic, rotary-cut technology has improved the fire resistance and durability of wood, and save the material at the same time. Making all kinds of weather-resistant structural boards becomes available.

5 Conclusions

Timber has carved deeply both in Chinese architectural history and every individual's mind. However, the long-term immoderate logging destroyed forest, vegetation and ecological environment, and almost made timber disappear from the stage of architecture. With the development of new technology, timber has returned with a brand new look. We are looking forward to timber- the beloved building material- will shine again.

Proceedings of the 55th International Convention of Society of Wood Science and Technology
August 27-31, 2012 - Beijing, CHINA

History and Hardwood Species of HMS Charybdis

Marc Milner[1] *– Meng Gong*[2*] *– Xiaomei Jiang*[3] *– Bo Lu*[4]

[1] Professor, Department of History, University of New Brunswick, Fredericton, New Brunswick, Canada
milner@unb.ca

[2*] Research Scientist, Wood Science and Technology Centre, University of New Brunswick, Fredericton, New Brunswick, Canada
* *Corresponding author*
mgong@unb.ca

[3] Professor, Research Institute of Wood Industry, Chinese Academy of Forestry, Beijing, China
xiaomei@caf.ac.cn

and

[4] Assistant Professor, Research Institute of Wood Industry, Chinese Academy of Forestry, Beijing, China
liubo@caf.ac.cn

Abstract

HMS Charybdis was a 21-gun steam-auxiliary screw corvette, which was built for the Royal Navy in 1859. It is generally believed to be the last wood-framed major warship built by the British. HMS Charybdis spent her entire service life operating in the Far East and the Pacific. In 1880, HMS Charybdis was offered to Canada as a training ship, Canada's first warship, to help with the creation of a Canadian navy. In 1884, she was sold and broken-up in Halifax, Canada.

Due to the price and availability of naval timber (mainly English oak) in the early eighteenth century, African timber was purchased by the British navy to substitute oak for building warships. The species of the wood framing from HMS Charybdis was identified in this study to be *Autranella spp.*

***Keywords*:** A. HMS Charybdis, B. History, C. Hardwood, D. *Autranella spp.*

Brief History of HMS Charybdis

HMS Charybdis is generally believed to be the last wood-framed major warship built for the Royal Navy by the British. She was a 21-gun steam-auxiliary screw corvette launching in 1859, Figure 1, 2250 tons, 1400 H. P., 200 by 40 by 20 feet in size with a speed of 11 knots (Tolson 1979). The regulation crew was 180. Guns were mounted on the gun deck for broadside firing.

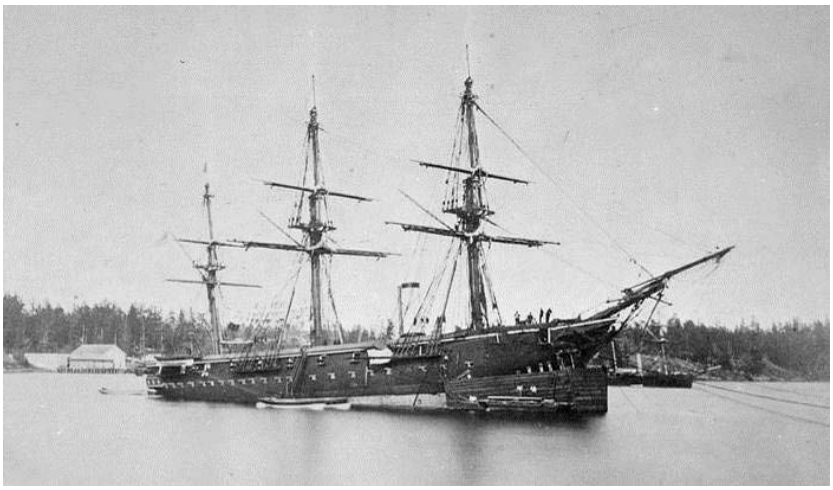

Figure 1. HMS Charybdis.

Upon completion Charybdis was immediately sent to the East Indies Station in 1860, and then soon after (1861) moved to the China Station. The rest of the 1860s were spent in the Pacific, including assignment to the Pacific Station, based in Esquimalt, British Columbia, from 1862 to 1867. In early 1867 Charybdis was transferred to the Australian Station for two years, and then served as part of the Royal Navy's "Flying Squadron" in 1869, visiting ports in South America, Japan and Australia. She returned to Esquimalt and the Pacific Squadron in early 1869. After a refit in England in 1870, Charybdis returned to the Far East, and by 1873 she was serving on the China Station again. In 1873 she was sent south to conduct anti-piracy patrols in the Straits of Malacca, and was involved in the Southern Malayan state disputes in 1874.

By 1880 HMS Charybdis had returned to Britain after two decades of hard foreign service, her machinery – now antiquated – was worn-out and not worth replacing. Charybdis was offered to Canada as a training ship to help with the creation of a Canadian navy. Captain Scott, a retired Royal Navy officer, was sent to England to get Charybdis (Tolson 1979). Stripped of her armament, it took 32 days for Charybdis to arrive in Saint John, New Brunswick, in late 1880 (Tolson 1979). When the war scare finally ended Charybdis was returned to the Imperial government in October 1881. Tolson (1979) wrote "The Charybdis began her antics, refusing to stay at anchor, lunging around the harbour smashing into other vessels." "Two Members of Parliament declared she was nothing but a shire elephant and were all for returning the gift to England."

Finally Charybdis was towed to Halifax in August 1882, and lay idle there until 1884 when she was sold and broken-up.

All that now survives of HMS Charybdis are the gateposts of the Scott Manor house in Bedford, Nova Scotia, Canada, Figure 2. Two decorative posts with fat acorns on top carry handing garden gates. The wood was given to retired Fleet Surgeon J. Ternan, R.N., around 1883 (Tolson 1979).

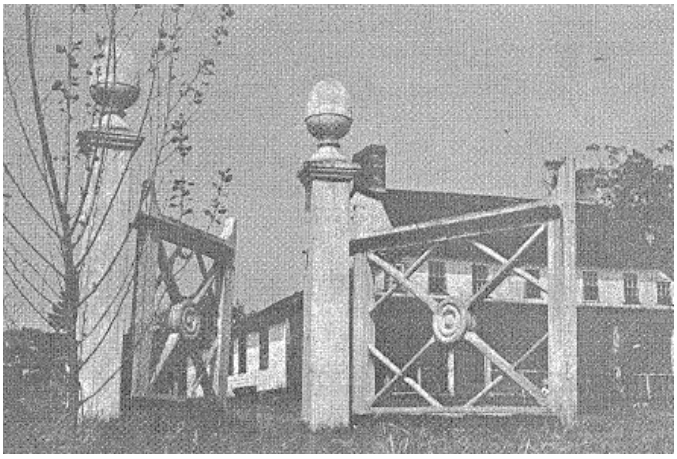

Figure 2. Gates made from HMS Charybdis.

Naval Timber Supply in Early 18th Century in Britain

The English oak (*Quercus robur*) was the favoured native timber tree for ship building due to its numerous qualities such as durability and strength. The sapwood is not suitable for any use as it is prone to decay if exposed to damp, but the heartwood is tough and resilient when dry (Lambert 1991). The presence of tannic acid is largely responsible for the durability of the timber, although it reacts adversely with iron. Oak can be bent using steam or hot sand, and keeps its shape when fully seasoned. Table 1 gives a list of materials estimated in the fabrication of a 74-gun ship of 1,745 tons (Lambert 1991).

Table 1. Materials in the fabrication of a 74-gun ship of 1,745 tons (Lambert 1991).

Material	Item	Load	Weight (tons)
Oak	Timber	739 (at 55 lbs / ft^3)	1,339
	Thickstuff	160 (at 55 lbs / ft^3)	
	Plank	192 (at 55 lbs / ft^3)	
Fir	Timber	74 (at 35 lbs / ft^3)	117
	Deals	76 (at 35 lbs / ft^3)	
Elm	Timber and plank	12 (60 lbs / ft^3)	16
Copper			46
Iron			90
Lead			5
Total			1,613

In addition to ship building and house construction, oak was in increasing demand for barges, machinery and transport facilities of the industrial revolution in the 18th century, when it required more timber than iron. The total quantity of oak timber from the Royal Forests kept decreasing from 1812 to 1824 (Lambert 1991), Figure 3. The supply of naval timber had been a source of concern as early as in 1771 when a Committee of the House of Commons investigated the issue (Lambert 1991). It was then discovered that the problem of timber supply was more closely related to price than availability. Table 2 gives the average price of timber per load in pounds sterling (Lambert 1991). Since a new fleet would use far more timber than one largely reconstructed from existing ships that time, the British Navy was, by 1831, spending more money on African timber than English oak and was prepared to substitute African timber for oak. Since then, tropic African hardwoods were used extensively for framing of the mid-18th century vessels such as the HMS Charybdis, as they were intended for service overseas on tropical or semi-tropical stations.

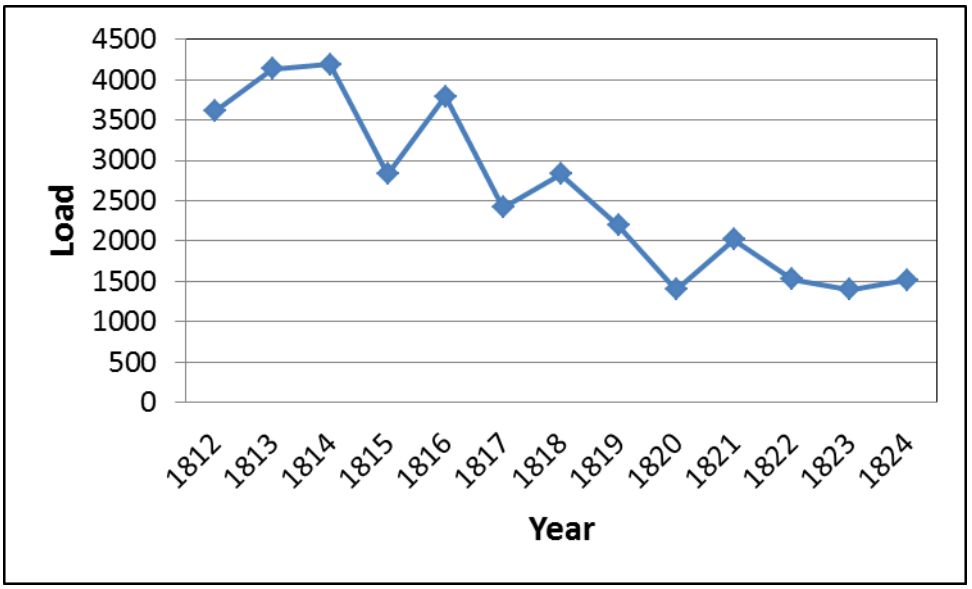

Figure 3 – Supply of oak timber from the Royal Forests

Table 2. Average price (pounds sterling per load) of timber.

Timber		Year	
		1818	1823
English oak	Rough	8.19.6	8.10.6
	Sided	13.8.0	12.14.7
African hardwoods	Sided		8.13.3

Species Identification of the Wood from HMS Charybdis

A wood sample was obtained from the Scott Manor house. The airdry density of the sample was measured at the Wood Science and Technology Centre, the University of New Brunswick, Canada. Micro slides of three standard sections were prepared using a microtome at the Chinese Academy of Forestry, China. Images were accordingly taken under a microscope, Figures 4-6. The major features are described as follows.

Growth ring boundaries distinct to indistinct. Wood (heartwood) brown to red. Texture fine and even grain straight. Airdry density (airdry weight / airdry volume) 0.960 g/cm^3. Vessels diffuse-porous, radial orientation of vessel multiples more or less evident, radial rows of 2-4 vessels or more, perforation plates simple, intervessel pits alternate. Fibres very thick-walled. Longitudinal parenchyma present, apotracheal, diffuse to diffuse-in-aggregates, in narrow bands (up to three cells wide), 6-9 cells per strand. Rays composed of two or more cell types, heterocellular, procumbent ray cells with mostly 2–4 rows of upright and/or square marginal cells, multiseriate, 2–3 cells wide; uniseriate rays composed exclusively of square and/or upright cells. Spiral thickenings absent.

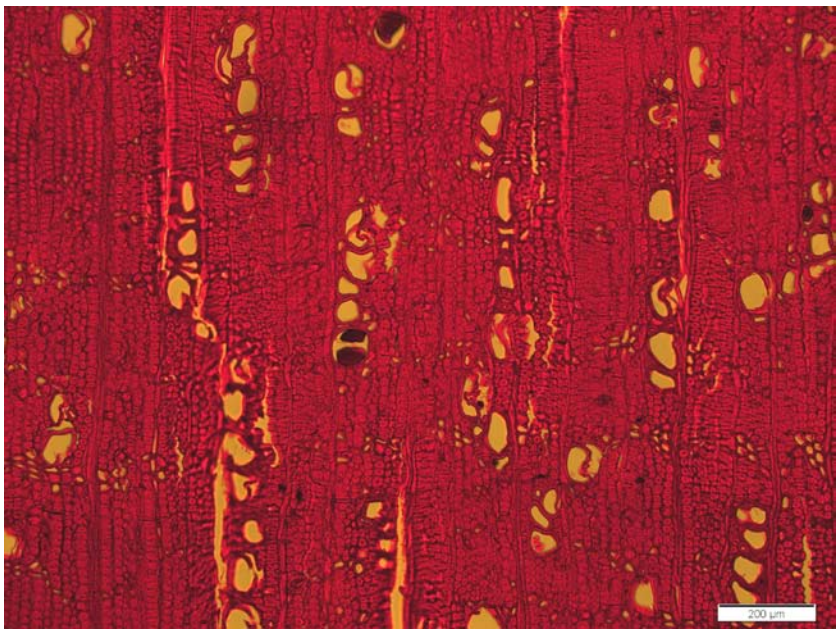

Figure 4. Major features on cross section: diffuse-porous wood with vessels being arranged in radial pattern, very thick-walled fibres, apotracheal longitudinal parenchyma diffuse-in-aggregates forming narrow bands.

Figure 5. Major features on radial section: perforation plates simple, longitudinal parenchyma 6–9 cells per strand, heterocellular rays consisting of procumbent cells with 2–4 rows of upright and/or square marginal cells.

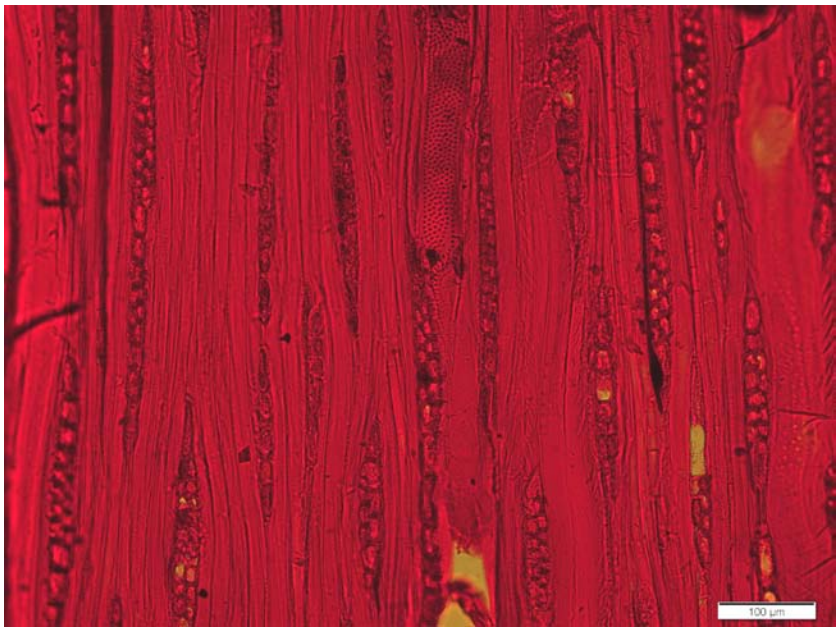

Figure 6. Major features on tangential section: multiseriate rays 1–3 cells wide.

Based on the above features observed, comparison with available micro slides and source of wood sample, it can be concluded that the species of hardwood sample from HMS Charybdis is *Autranella spp*., which belongs to the family Sapotaceae. One of common names could be Mukulungu (Forest Products Laboratory 2012).

This kind of hardwood is distributed in tropic Africa. It is very durable though there may be slight termite attack, resistant to dilute acids and weathering. The wood is widely used for heavy construction, ship and boat building, heavy-duty flooring, bridges, sluice gates and other waterworks, railway sleepers, and poles.

References

Forest Products Laboratory. 2012. Wood Properties (Techsheets) - Tropical Hardwoods. http://www.fpl.fs.fed.us/documnts/TechSheets/Chudnoff/African/htmlDocs_africa/autranella.html. U.S. Department of Agriculture, Forest Products Laboratory, Madison, WI, USA.

Lambert, A. 1991. The Last Sailing Battlefleet: Maintaining Naval Mastery 1815 – 1850. Conway Maritime Press, London, UK.

Richter, H.G. and Dallwitz, M.J. 2012. Commercial Timbers: Descriptions, Illustrations, Identification, and Information retrieval. In English, French, German, Portuguese, and Spanish. Version: 25th June 2009. http://delta-intkey.com'. http://delta-intkey.com/wood/en/www/sapaucon.htm.

Tolson, E. C. 1979. The Captain, the Colonel and Me. Fort Sackville Press, Bedford, NS, Canada.

The Carving Craftsmanship' s Process Principle And Measures Of The Ming And Qing Furniture Artisan

Xiaoting Niu, Doctor Graduate Student
Fenghu Wang, Professor
Materials Science and Engineering College
Northeast Forestry University
No. 26, He Xing Road
Xiang Fang District
Harbin 150040
P.R. CHINA
E-mail: mark_niu2005@126.com
E-mail: fenghuwa@hotmail.com

Abstract: The wood-carving is a Chinese traditional decorative art, which is to carve the three-dimensional configuration designed by artisan on the furniture components. For thousand years, the traditional skill has been inheriting with the way of teacher and pupil generation, and formed a set of systematic operational approach. This paper , based on sorting of the carving technique' s process principle and measures of traditional artisan, would divide carving handcraft into four processes of shencai huagao, yiwen tayang, cupi zaozhi and chanxue suxing. And combined the specific cases, discussed the operative skills of every process , analysed the internal rationality and scientific of process principle and measures of traditional artisan. It will plays a significant role in inheriting the national intangible cultural heritage of Ming style furniture production techniques and Jingzuo style furniture manufacturing technology, and producing the Ming and qing hardwood furniture.

Key words: Ming and qing furniture; Artisan; Carving craftsmanship; Process principle; Procedure measure

INTRODUCTION

Woodcarving is a kind of Chinese characteristics adornment art. And its history is long, It can be traced back to 7000 years ago. As in Hemudu cultural sites had unearthed a woodcarving of fish. The original of the old history already cannot take an examination of this. But from the existing historical and cultural relics know woodcarving art is in the jade, stone, bones, teeth sculpture art such as under the influence of the germination. And its application in the furniture should be at least in the Shang dynasty[1].After thousand years, the intelligent of the artisan search and to Ming and Qing dynasties has formed a fully mature sculpture technology and the necessary tools to use a method. It could be said that, carving techniques is the important component of Ming and Qing dynasty furniture and also is one of the unique technological characteristics. Specific is refers to the use of different type cut, shovel, scraper, line saw tool and to shovel out 3 d form of artwork .This paper is on the basement of the traditional carving process principle and artisan frequently using process measures. And dividing the artwork according to the material extension, coarse grain sample cut billet system, shovel cutting model four working procedure and combined with some examples. This paper discusses the process of every operation skills and analyzes the inner reasonable and scientific way. This to "Ming dynasty furniture manufacture technique", "Jingzuo hardwood furniture manufacture technique" and other countries intangible cultural heritage and to inherit the Ming and Qing dynasties hardwood furniture of significance of reference to the modern production.

SHENCAI HUAGAO

Shencai Huagao refers to the carving timber wood material according to the particular sculpture and space layout. One of the specific conditions of the carving timber wood refers to the wood grain material characteristics and surface characteristics. In particular, the timber wood grain characteristics refers to the wood texture and the surface feature that is refers to the modelling of material characteristics and regularity of distribution on the surface. In practice, the traditional furniture of this two carved artisan constantly understanding and summarized, and gradually formed a set of effective design principles. The three main technical points for muwen shuli, yiwen lixing and yixing suxing.

" Muwen shuli " means to grasp the wood texture and the trend of carving pattern of the position. If the relation between the position is suitable, wood texture will be fluctuation and flow which is changeable. and Such as the round-backed armchair by the dedication of a shallow relief (figure 1) design conception is very clever. first is the whole piece of flower live position clearly by the three groups of wood texture to common curve to the changes in the trends. It made it to be the visual center of the backboard. and the pattern , the size and the direction is not the free one without consideration. For example, the position is back on top of the outermost curve peaks parts of boundaries. and the bottom is back on the outermost curve around the peaks of parts of boundary. Then the head of appearance with internal to the three group is also the curve of the

wood grain, especially leading to the chest and the "S" curve is clearly on the top .The curve of the wood grain curve are linked. there are real meaning of broken is even better. Conversely, if the relationship between the two processes is not good, the flower pattern to live with wood texture of strewn at random to cross will not only affect the appearance of the flow of feeling and their own line of kind of the flower live integral aesthetic feeling. But also affects the flower patterns and the wood itself live connected soundness. It still have this relief. As an example, on the assumption that the position of the dedication of the best in these three groups within the curve of the wood grain to the middle. The size is also not influenced by it. It is obviously will be destroyed by the formation of the stable before the visual centre. And can affect the body's natural indirect dynamic beauty.

Figure 1 The shallow carving of the round-backed armchair

Figure 2 The curving of Southern Official's Hat Armchairs on the top of backboard

" Yiwen lixing " is the further of wood lines presenting ".And the concrete is through the wood natural texture that is kind of the patterns and the carved wood texture to be the perfect fusion. In the growth of wood wheeled way contributed to the log size. This is also a flower patterns and the natural texture of corresponding created prerequisites for. Such as the chair by the dedication of the curving cut decorative pattern design is to "to the texture" type well reflect (figure 2). From its first linear texture feature of its diameter is that by cutting board created. By learning and wood and wood processing theory, It is known that the size of the board wood cutting straight lines, and wood arrange grain growth direction of plank wood fiber connection strength far outweigh the vertical direction of plank wood growth wood fiber connection strength. And the length direction size is curving flowers. The curving flowers pattern width size 2 times much. The internal cloud careless grain branches and leaves out the wood straight grain direction extension and dedication of edge connect. It is not only the obvious straight texture photograph .The more important is the strength consideration of the type of the branches. It is same kind of way as we said.

" Yixing suxing " is the material itself according to the morphological characteristics and material characteristics of the whole to shape carved image. The key technology is mainly to the wood carving and type surface of grasping the characteristics. The experienced carved on the understanding of the basic material form artisan based on the characteristics of it. The main methods used in small root of his works, such as chrysanthemum pear symbolizes root furnishing articles (figure 3). Sculpture artisan cleverly borrow root slipped out of the morphological characteristics. It will cause body below the slender. In the Ming and Qing dynasty, This method is reflected in two aspects. On the one hand, it is the trend of the wood texture to enhance the furniture the structure of the components,And the specific is straight grain out straight materials, song lines out QuCai, such as chrysanthemum pear round-backed armchair (figure 4), such as the leg side wipe linear component is much by texture straight plank made, and five meet chair circle are five sections with chair circle arc corresponding song plate type made; On the other hand, it is reflected in the root of furniture production, such as root square table (figure 5) four legs and tooth board are saving a pick up by roots, it is originality alone rhymes.

Figure 3 chrysanthemum pear symbolizes furnishing articles

Figure 4 chrysanthemum pear round-backed armchair

Figure 5 roots square table

Master the above three methods. Here is curving flowers. According to the samples from it (figure 6).It is known that the light of wood texture, tooth board a three-step distribution, has the obvious bump change, specific for both ends of the texture are up have larger radian is outspread,

and in the middle parts of the texture appears quite gentle, and slightly upward spike. Therefore, in the design volume hook when moire should also be follow the basic rules of the texture, and finally formed the ends for larger volume hook lines radian. And the distribution is more intensive. Also in the middle are smaller and the distribution is more sparse pattern space layout.

YIWEN TAYANG

" Yiwen Tayang " refers to the direction of law of the development of wood engraving materials. It will copy transparent soft materials such as in the pattern of artwork. Expand the engraving posted on the surface of the part process. The three main technical points is like this, miaogao huayang, wenli shenshi and gaoyang tatie.

" Miaogao huayang " refers to the pattern with good design make it into the white paper own the transparency and softness. It has two purpose. One of them is to preserve the sample design. The last one is to further master of kind of the design and the rule. The key techniques have three points. One for the size of the special paper. It need to be the same size to the one you need. But when the component has the type in special. It should be based on the size and some more. Because it's easy to operation of the one mistake and stick dissatisfaction component. But need explanation is due to the Ming and Qing dynasty furniture sculpture designs with symmetry characteristics of more. So the paper determine the size of the artisan. It usually in the form of kind of the painting for shaft centreline folded in half and half to pattern (known as mother lines) size shall prevail[2]. This not only reduce trace complex flower pattern live extension of the error, and also ensure the consistency of kind of the flower around live. In addition, it is very important also. Its permeability and softness not beautiful would affect "extension kind" the work efficiency and accuracy of kind of the live copy flower, can also affect parts of carving wood texture analysis of the direction that it cannot be sure go in the direction of the sword. And may even make joint in sculpture on the surface of the part which can lead to carved flower patterns and the design of living at first flower pattern deviation between it; The second is some of kind of the painting. It embodied in a long components for the flowers of the extension kind live. Because components flower pattern live far outweigh the general specification for the length of the length of the paper. This needs to be clearly label out two pattern of some specific position. Three for grain appearance depth level and the expression of the relationship with. Its main is to point in the topology sample, the patterns and the pattern of the relationship between with express clear. Especially in have multilayer engraving content, use different degree to express the different layer.

"Wenli shenshi" refers to the sample should look carefully from the law before post carved wood panel. And with the flower with good appearance of extension live corresponding to each other. In order to ensure the consistency of the two. "gaoyang tatie" refers to the " wenli shenshi ". And on the basis of extension good sample will be accurately paste desire to graven component surface. The key technology has two, one for the halfway point of the corresponding position.

The main means to ensure the extension of kind of the draft of the centre position and sculpture component to the unity of the centre. The key point also have two. one for paste concentration control. It must not be too loose that will affect the bonding strength. And too thick will not only influence the level of extension draft paste, but also affects the wood texture identification. Secondly paste the master way. To follow by the centre is to both ends of the principle. And the concrete is in alignment flowers line and sculpture live in the centre position after component that with one hand holding flowers live the centre line of the fixed position pattern. And from the centre of the component position began to brush paste. It will take place from the centre line and began to finish with the end of the paste component gradually wood texture flattening the direction, and to ensure that the flowers with live sample component surface no bubble between phenomenon, complete, and then use the same method in the component surface flat spend half live extension pattern. But in a long paste, It is part of sample component. In the following this principle, under the premise of should also ensure that pattern to docking accurate, and it will be joining together of excess pattern. In addition, the curving flowers line kind of the double or the round when need to establish standards, to ensure that the two sides pattern can paste together. For the former two carved the centre line of the component is still in for reference standards and only to determine a carving of the centre line. The latter is adjacent to the one round reference standards. It can be better to identify each pattern on adjacent live docking and accuracy of the same level.

Finally, for example the carving machinery in cloud shape board. We have a key presentation like this (figure 6). You will know it as you see the samples. It is known that the component to the carved of curving flowers. The curving flowers for practice. and belongs to the most simple a layer of grain appearance layout, but in different parts have a different size. Have a basic understanding of it. And it can be carried on in grain extension samples. First, to roll off the centerline of the extension draft grain position and light meat tooth board of the centre position corresponding, determined, with the right hand hold down the volume hook grain the centre line of the extension draft position. Then the draft with the left hand extension left part of this. And from the centre line position began to besmear brushs component to paste, side brush, part of the trend towards from the centre line began. The extension will gradually left along the wood grain direction develop draft show flat. Finally by the same method will be part of the pattern right extension draft paste in component surface.

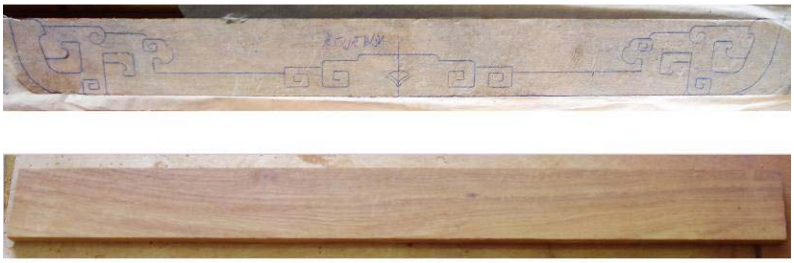

Figure 6 The sketch map of Yiwen Tayang

CUPI ZAOZHI

" Cupi Zaozhi" refers to the flower carving component of the sample paste live pattern characteristics by using chiseled grinding machining method. The file to its grain appearance profile and the hierarchical relationships for
preliminary machining process. The three main technical points, respectively, for pattern analysis, lunkuo dingxing and lidao kaixian.

"Pattern analysis" refers to the carved flowers to live of kind of the structure, characteristics and laws to outline comb. Especially in the area of multi-level carved flower living pattern. This process is very important. " Lunkuo dingxing ", It is mainly refers to the curve of the component type sculpture outside outline or curving flowers. The curving pattern to live before chiselled. Thus, it can not only help to take live of kind of the further chiseled, but also can greatly improve the work efficiency. The key techniques have four point. One for drilling wear bow. First use it in close to take live outline of edge (about 2 ~ 3 mm) of hollow out regional drilled through a round hole. Need explanation is again to complex drilling curving flowers. The curving flowers pattern, It make sure to do precisely clear row holes, lest appear processing error. Secondly, The technical difficulties is mainly to the "search direction" master, shipped to "stable" saw, the strength should be skillful, and should make the movement direction and sculpture hacksaw components of vertical plane. Modern processing is used instead of the electric drill and drill, saw the Sougongzi with alternative, enhanced the production efficiency. Three for "flash volumes even". It is mainly refers to with different types of wood trim amid the "bow type search" residual saw mark flash. In order to make flower live from each of kind of the handover and place such as the corner has fruity effect. The depth of the grinding file must be based on the characteristics and the degree of kind of the round and decide, filing too thin or too thick are not suitable for the further after carving. "Lidao kaixian" refers to the length of the appearance of the matters and spend live to choice and the corresponding flat or round cut cut, press from top to bottom, its principle, along the flower pattern on the movements of the line to live on its outline "zaoxian" processing, should be accomplished with trenchant primary and secondary, different depth. [3]The technical difficulties are mainly embodied in the chisel type of choice and control of the way the cut. Especially when the interface measures carving, accurately grasp the incision size

options radian. In general, the arc of the knife to smooth in the radian measures. For the latter is mainly refers to the strength of the control and cut the shipment of cut cut pressure control. In the specific chiseled, no matter cut or cut all round flat blade surface should make the cut in to chiseled outline of the lateral pattern, and in the cut, we should pay attention to gouge in the overlap .In order to avoid the knife scar fracture and chiseled depth caused by uneven line kind of the outline of inconsistent phenomenon, chiseled strength also want to have a difference, should be based on hierarchical structure pattern decision from inner to outer in order of sequence is abate, and pay special attention to the form and form of taking over parts of the chiseled, to try to minimize carved dynamics, do "let" to the processing of the details as far as possible in the process of carved in the shovel to solve. In addition, but also learn how borrows the hard, do one take.

Finally, we have the example of the carving. The processing technology of the "cupi zaozhi" key points discussed. The former analysis, we can conclude that the tooth board has irregular shape layout, and the volume hook flower carving grain live for practice curving. Therefore, in chiseled coarse grain appearance before the billet, should to roll off the appearance of grain to finalize the design contour machining (figure 7). After completion, it need to comb different size (grain direction and turn off with order. Due to the volume hook pattern levels for curving flowers. The curving flowers of a structure, therefore, in its thick slab of stage just clear cut size different roll off the outline of grain characteristics and relationship with can, and size roll off the hook grain head depth levels vary, compared with both, big volume hook lines of head than small volumes to tick off the hook head deep grain some (figure 8).

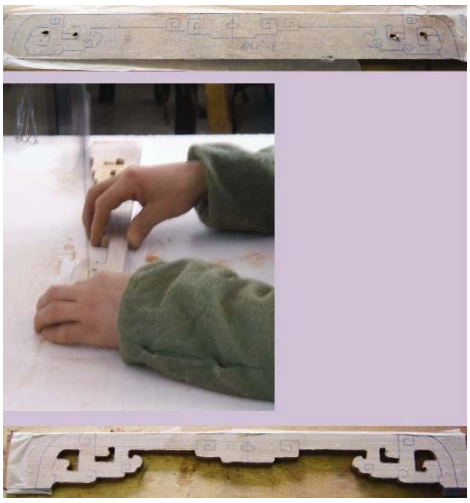

Figure 7 The sketch map of Contour finalize

Figure 8 The sketch map of Cupi Zaozhi

CHANXUE SUXING

" Chanxue Suxing" is refers to the use of different flat shovel types, round shovel, Ames hook etc

sculpture tool sets of live thick billet for advertisers, further clear spend live texture context, accurate shape flower live of kind
of the outline and their levels of structure change. And make flower pattern to live round vivid. The four main
technical points is, wenyang buhua, shunwen chanxue, tezheng bawo and guamo paoguang .

"Wenyang buhua" refers to the flower pattern with live ACTS the role of the depth of the fine process, continue to use the brush in the sculpture members to take live carved perfect modelling of kind of the form. Its main features in the round, curving flowers and high relief shovel cutting model.

"Shunwen chanxue" means carved wood grain growth direction along the component to use the knife. So not only makes the shovel out of the plane cutting flat, smooth and still can minimize the shovel cutting process of the resistance of the wood fiber blade. The principle of the sword is fast, accurate and malicious.In specific shovel cut, it still should focus on the whole, always pay attention to grasp the depth of kind of the flower live level change, carved on step by step, and to pay attention to some of the shovel between mark. It should be a spade a spade spade cut to pressure. In addition, it still should pay attention to grasp the shovel cut flowers live in the process of grain appearance. Different shovel cutting direction caused by the differences of wood texture to. In order to better achieve the purpose of the type to texture. Luck of the shovel skills and the method of the same basic cut, here no longer etc.

"Tezheng bawo" means in specific shovel cut model process to the different characteristics of the flower pattern live precisely control. Because different flowers all have different kind live preferences, this also is all the carved flower pattern can contain live whether the key verve. As in furniture of Ming and Qing dynasty is all kinds of flowers in the living pattern. It is mainly in face and facial features of characterization. Women are more oval face, two eyes and mouth carved out more equilateral triangle.Men are different, the different age has different kinds of carved method. The old people's eyes to wrinkle, eyebrows to highlight, the middle-aged and young people don't. Be like again carved dragon pattern is also very fastidious, one must pay attention to the head carving. Head is mainly forehead parts and eyes, carved verve majesty, central body to stout, dragon Angle to the uniform, neck and a horse, neck feathers to carved elegant feeling, the wind tail, regional different technique is differ carved, and so on. [4]

"Guamo paoguang" refers to the use of scraper, stone, grass and other tools to burnish amid all the carved flower of kind of the live on form "the grinding, till the surface to smooth mellow. But need explanation is for carved by cork, construction, furniture of components, especially character of the facial features generally do not polishing processing. Because burnish is easy to make its lost the feeling of lifelike. One of the "the grinding" is a word from the duty to understand, "fix" refers to the use of different shapes of scraper piece of sculpture of flowers

pattern and live parts to the son overhauled find type, the sword direction should go with wood texture of the direction. "Ground" is refers to the use of different specifications of stone and file to find good grass type of flower pattern and live to son surface grinding polish and grind the direction along the wood texture should also. Otherwise, it will destroy the surface of the wood texture [5]. In addition, the use of traditional grinding tools also different, of which the stone and has a thick stone and stone cent, dry grinding with thick stone, the joint with stone, mainly for furniture plane type component burnish, rub is mainly used for carving grass component and irregular component type of joint, the modern grinding tool is changed to different types of coarse sand paper and fine sand paper burnish. Both of the grinding effects and differences. The latter is much less than the more soft and smooth than the former.

Finally, we have the example of the carving. The processing technology "chanxue suxing" discussed the key points (figure 9). The analysis of former can be straight, tooth board on the hook for single cloud carved party structure, and for a sculpture, the tooth board don't need to draw up the ancient time. In the process of cutting the shovel model, the author only need to clear tooth board wood grain direction, and the wood grain direction shovel cut, under the premise of further clear size party into relationship between moire hook and relationship of scale. Using different types of scraper piece of scraping the light off the root of the remainder of the cloud party carved traces and grain appearance outside of the surface to the son. Finally the grass with amid the wood texture to, under the premise of combining party the morphological characteristics of cloud hook tooth board for joint polishing.

Figure 9 The sketch map of Chanxue Suxing

EPILOGUE

Wood carving is a Chinese decorative art. It consist of primitive simplicity and elegant design,

elegant beautiful forms (such as the line carve, curving flowers. the curving flowers in the round, engraving and fill in the moment, ash, etc), Both at home and abroad win the very high reputation. One thousand years, intelligent of the artisan in practice and summarizes the inquiry, to Ming and Qing dynasties has formed a fully mature sculpture technology and the necessary tools to use a method. And the way to teacher and pupil it circulates. It could be said that the carving techniques Ming and Qing dynasty furniture manufacturing technology is the important component of Ming and Qing dynasty furniture also is one of the special craft characteristics. This paper , based on sorting of the carving technique' s process principle and measures of traditional artisan, would divide carving handcraft into four processes of shencai huagao, yiwen tayang, cupi zaozhi and chanxue suxing. And combined the specific cases, discussed the operative skills of every process , analysed the internal rationality and scientific of process principle and measures of traditional artisan. It will plays a significant role in inheriting the national intangible cultural heritage of Ming style furniture production techniques and Jingzuo style furniture manufacturing technology, and producing the Ming and qing hardwood furniture.

ACKNOWLEDGMENT

This study was supported by Heilongjiang provincial humanities and social science project(12514035).And we especially thank miss Zhaojing for the help of English translation.

REFERENCES

[1] Li ZS, The pictorial handbook of China furniture history. Wuhan: Hubei arts press，2001.(in chinese)
[2] Niu XT，Wang FH, Zhao JX(2009). The modern carving technology in min and qing style furniture. China Forestry Products Industry, 36 (3): 35. (in chinese)
[3] Niu XT，Wang FH, Zhao JX(2009). The modern carving technology in min and qing style furniture. China Forestry Products Industry, 36 (3): 36. (in chinese)
[4] Niu XT(2010). The interviews to Suzuo style furniture craftsmen. Furniture, 177: 66-67. (in chinese)
[5] Niu XT，Wang FH, Zhao JX(2009). The modern carving technology in min and qing style furniture. China Forestry Products Industry, 36 (3): 37. (in chinese)
[6] Hu DS, Zheng MZ. Cultural relics collection grading standards illustrations—Furniture. Beijing：Cultural relic press，2009. (in chinese)
[7] Wang SX. Ming style furniture cuizhen. Shanghai: Shanghai People's Publishing House, 2005. (in chinese)

The Feature and Future Development of Sino-lacquer Furniture

Shasha Song, Benhua Fei

(International Centre for Bamboo and Rattan, Beijing, 100102, China)

Abstract

This thesis aimed to make innovation in the features of modern lacquer furniture based on the preservation of the essence of traditional lacquerware, thus contributing to richer language of lacquer furniture, which made it easier for people with different cultural backgrounds to know more about lacquerware. Therefore, it provided ways for lacquer furniture to penetrate into people's daily life, during which the lacquer furniture would become more artistically appealing. Through the comparative analysis and studying of the features, decoration and patterns of traditional and modern lacquer furniture, with the reference of the design theory, the production techniques and craftsmanship of modern furniture, the thesis made deep exploration into the development of modern lacquer furniture with a special flavour of traditional cultural craftsmanship as well as the infusion of modern artistic style and scientific techniques. Lacquer furniture was basically made of woody material, with the surface painted with Chinese lacquer most of the time, which made it both natural and environmentally-friendly. In patterns, lacquer furniture tried to achieve excellence in form, appeal in taste, and validity in application; in colors, red and black were the most representative and symbolic colors, which were the reflection of national spirit and individuality. Besides, the processes in which the methods and techniques grew integrated and comprehensive, the decorated pattern evolved from simple natural design to diversified artificial permutation both embodied the development of the artistic expression of our nation with the help of the special rhythm and artistic device in modern life. Instead of being traditional or modern, the style and pattern of the lacquer furniture would rather be of more cultural deposits, flavour of the nation as well as the aesthetic sentiment of the time. On basis of this, modern lacquer furniture should encourage more innovation and re-exploration of lacquerware's value, thus promoting the transformation of lacquerware and the recreation of the promising market.

Key words: lacquer furniture; features; decoration; development

Introduction

1. Lacquer art and furniture

1.1 lacquerware art

Lacquer art use the natural lacquer as main coating, and the manufacture foundation is the traditional lacquer decoration techniques and craft (Qiao, 2004). Lacquer art is Chinese traditional arts and crafts, after thousands years of development, it has progressed from the initial functional to later decorative. Until today, it becomes an independent art language, no longer exists alone with the traditional craft in material technology field. Because of the impact of western art and development and utilization of new paint material, modern lacquer art is creating new vitality based on the traditional, and becoming an indispensable form of decoration and means. So lacquer craft appears ever more richly and vividly in the shock between the new and the old, the traditional and the modern.

Lacquerware has good characteristics comparing to other artifacts. One is the compatibility, namely lacquer decoration can be used in different objects, such as wood, bamboo, leather, ceramics, metal, jade, glass, and cloth. The second is the practicability, paint finishing the surface of the artifacts which the features is very hard after dry solid film, not afraid of acid or corrosive erosion, and have moisture-proof, mothproof, moth-proofing, anticorrosion and protect function. The third is decorativeness, it can be personalized adornment for all kinds of objects combined with the needs of modern life.

Therefore, modern lacquer art is not only the concept of lacquerware and lacquer craft in the traditional sense, but also contains the meaning of lacquer art. It includes lacquerware, lacquer painting and painted sculpture in fields of decorative arts and pure art, and has become a very broad, inclusive and comprehensive art form.

1.2 Lacquer furniture

Furniture, as a social part of the material culture of a state or a nation, is a product of economic and cultural development of an era, and it reflects historical features and cultural tradition of the time, the state or nation. Lacquer art have a long history of used in furniture, and lacquer furniture has been represents the highest level of the crafting in the genealogies of Chinese classical furniture that are the pricey specialty items and collections for grandees. The fundamental reason of Chinese ancient lacquer furniture developing so fast is getting official support and arousing the attention of the whole society.

As early as in the Warring States period, productions of lacquer furniture have been managed by special official, and have begun to be taken charge of special management agencies in Han dynasty. And in the Tang dynasty, lacquerware has been listed as one of the taxes objects. From the Tang dynasty to Qing dynasty, the production of folk lacquer furniture develop quickly because of official more emphasis on the design and manufacture of lacquer. They competed in skill, and made the development of the Chinese lacquer furniture reaching the unprecedented level no matter in crafting or the style design. Ming and Qing Dynasties were splendent time and representative of the Chinese classic furniture (Figure 1 and 2). These periods of lacquer furniture focused more on function and formal sense in styling, and take a combination of circle line, arc line and curve line. It abandoned cumbersome and gorgeous in form, also supplemented by lacquer art craft such as lacquer decoration, sculpture, painting and enchase, and formed the Ming and Qing lacquer furniture characteristics finally. From the Ming and Qing dynasty furniture, it can be seen retained lacquer furniture that there was wide variety of products, such as beds and desks, chairs and stools, cabinets, benches and screens, etc. The means of artistic expression are rich and varied, such as jade inlay, gold lacquer painted, carved fill in gold lacquer, carved ash and embellish color, which shown the skills of wonderful artificial excelling nature with lacquer technology, and manifests the intelligence of the working people of ancient China.

Fig.1 Lacquer furniture of Ming Dynasty (http://www.aigunet.com)

Fig.2 Lacquer furniture of Qing Dynasty (http://www.aigunet.com)

Lacquer furniture indicates the development of science and technology and the evolution of the spiritual culture, provides important reference value for design concept and art style of national furniture with modern Chinese characteristics.

2. Features of modern lacquer furniture

Lacquer art is grafted onto modern furniture, combined with decorative drafting, modern modeling, and modern use function. And then constitute effect on the overall aesthetic and form

Chinese modern lacquer furniture, which make it unique feature and colorful sacred in the modern furniture. It embodies the fashional features and prominent humanization at the same time, and adapts to the modern human body need, the room pattern and aesthetic concept. Lacquer furniture is not only an important part of the indoor environment but also has the function of organize and adorn space (Zhang, 2000). It is not only the physical products but also works of art. It makes the space full of spirituality by ingenious display and arrangement, but the absence of ornamental display will be vapid. It will have artistic effect of surprise, full of vitality, and revitalizing brightness by adorning a few of lacquer furniture in the room.

2.1 Environmental protection of materials

Woody material and natural lacquer were becoming the material of first selection for lacquer furniture. In the environmental friendliness, wood has “4R” characteristics (reduce, reuse, recycle, renew), which is considered with material of humanity characteristics. Woody materials have been used for making furniture that has excellent regulating action for interior microclimate environment and improves the quality of human life. Raw lacquer is a natural paint and natural organic compound, has a reputation as king of all paints (Figure 3 and 4). Raw lacquer is human treasure endowed by nature, and has so many excellent properties that general synthetic paint can’t match. The ancients found raw lacquer, and used it to decorate bamboo and wood wares, which were widely used in all aspects of life as the important technologic coating.

Fig.3 Lacquer tree

Fig.4 Raw lacquer

2.2 Artistry

Lacquer furniture with good properties, can be decorated on wood, bamboo, metal, glass and cloth, etc. It decorated all kinds of commodity to meet personalized need, which have not only the beautiful appearance but also many beautiful potential. These beautiful potential integrates natural beauty of materials and technological beauty of artificial art, both also contains spiritual beauty of lacquer art. Through the artisan digging, fashionable element will be injected onto lacquer art constantly, got colorful reflection, and there will be more market space that can be further excavated and utilized. In addition, lacquer art can be used in combination with other

materials, which may make unexpected outcomes (Figure 5).

Fig.5 Lacquerware art

Decorative patterns of lacquer furniture are complete composition, well-proportioned, extensive subjects, content rich and beautiful patterns, and pursue artistic beauty of rhythm and rhyme. It endows combination of rich color and modern life, forming new life constantly to make the decorative patterns get modeling of rhythm harmony, structure of novel and rich, color of bright and beautiful, style of flexible and varied, which makes them richer in artistic of times.

2.3 Decorative

Throughout development history of the lacquer furniture, we can clearly see the lacquerware art form the elegant style and formal beauty after several thousand years of accumulation and exploration. As craftsmanship gradually mature, lacquer furniture not only pursues practical function, but also gradually strengthens exploration of lacquer art decoration.

Modern lacquer furniture have new breakthrough in creating design based on inherit the traditional and innovation combining with times feature of reacted national culture on lacquer furniture decorative design. Modern lacquer furniture decorative has beauty of form with intensive artistic effect to impress appreciator. According to simple or complicated demand, the composition form of lacquer furniture surface is decorative. It embodies decorative characteristics of “vivid” and “charm” by overall modeling and local decorative in relation to each other. The images of the structure achieve the ideal artistic combining with the change of time and space. Color design harmonizes and unified whole furniture, which produces different effects, such as luxuriant effects, simply effects, elegant effects, beautiful effects, bright effects.

2.4 National character

In the traditional design of creation, lacquer furniture is the art symbol of our country and national traditional culture, which has accumulated the culture, aesthetic and value concepts at a certain point in time (Kumanotani, 1995; Cooper, 1985).

Natural raw lacquer was called “magic liquid”, which gives us Oriental nation brilliant lacquer culture. Red and black not only the most representative and symbolic color for lacquerware art but also the typical color of our nation. Actually, it is the embodiment of our national views of color, and also reflects our national spirit and characteristic. In ancient times, ancestors loved red and black because the red symbolizes auspicious, festive and health, and the black symbolizes extensive and profound, steady symbol, all of which were our national character (Shen, 1991). So, we can develop our national unique artistic expression using the decoration patterns of modern lacquer furniture with the unique rhythm and artistic techniques of modern life.

2.5 Practicality

Lacquer furniture is both environmental protective and convenient when used in the life. Designers fully consider the practical function, cognitive function and aesthetic function of the traditional lacquer furniture, which makes the external form be consistent with function, and really reflects the design ideas of both form and spirit, manufacturing for use. And the modern lacquer furniture gradually deviates from practical track to pure visual aesthetic, so that appears pure spiritual modern lacquerware. It should be the perfect unity of art and technology, harmoniously and uniformly for practical and aesthetic for lacquer furniture. So, modern lacquer furniture emphasize on the high fusion of art works and practical functions in daily life (Figure 6 and 7).

Fig.6 Modern lacquer furniture

Fig.7 Modern lacquer furniture

3. Development of modern lacquer furniture

Our contemporary lacquer art has appeared out of touch with people's daily life. Lacquer is scarcely used in daily life and lacquer art is gradually going away from people, which result in downturn and atrophy for industry of lacquerware. Therefore, we should not stay in direct economic value for understanding of lacquer art, but ought to focus on cultural value and industrial value. At the same time, with the rapid development of China's economy and the improvement of consumption capacity, and the increasing need for high-grade furniture, so there is a very significance for the development of modern lacquer furniture in the information age.

Furniture is closely related to human life, and has a never retreating market. Bamboo, wood and metal are the main material for furniture, and lacquer craftwork combines with bamboo technology, woodworking and metal process in historical tradition. So it is a new approach to develop a new form of lacquer technology combining with bamboo, wood and metal. The comprehensive and fringe new form, which can be a few painted or local painted using various techniques, not only can change the inherent pattern of lacquer, but also can reduce the costs. It increases the varieties and culture grade of furniture, and is also the innovation of traditional lacquer art for adapt to the modern mass market.

To explore and utilize greater market potential, lacquer furniture can be infused elements of popularity and fashion. In addition, lacquer furniture combined with other materials to use, also will produce the unexpected results. Most of the modern industrial products are stereotyped. In fact, it will cause the unlimited business opportunities if a little changes are made on some details. Therefore, for developing lacquer furniture, there are many opportunities which are not taken into action or even sill not known.

Seek a road of modern lacquer furniture industrial design by using developed mechanized, semi-mechanized, spraying and batches of lacquer furniture with keep the traditional manual work at the same time. It will be beneficially to develop on manufacture lacquerware (including synthetic coatings), mold-making (including plastic mold and the bottom formwork process), finishing (including spraying) and grinding push light (including grinding and pushing light), etc. There is a good beginning for striding forward gradually to the road of the industrial design, but it should be further practiced to sum up experience, accept modern design concept, and walk. So, it should develop and produce assorted furniture based on traditional lacquer art charm in combination with modern design concept and mechanization production methods. To meet different consumer groups' needs, and let more people understand lacquer furniture, it is necessary to combine lacquer furniture artistry and technology with manufacturability and practicability.

In a word, lacquerware art is an ancient artistic class, which still occupied the position of leading

role in many of the traditional art field. But today it is associated with the antique and collection. To make the traditional lacquer art steady progress and keep up with the times, it must walk on the road of development of variety. Because most of the traditional lacquer furniture were ancient dignified and elegance sedate, both tone or shape of which were shown slightly thick and conservative in the modern family. It is necessary to convert old lacquer art to modern furniture design, which must be combined the tradition with modern to express the international design concept (Song, 2008). Therefore, the design concepts are much more popular than the furniture and the vessel themselves in the home-design at present. So according to the modern development of Chinese furniture, the modern lacquer furniture design and development are connected to the international design concept and classical oriental styles, which makes lacquer furniture become a popular trend by combining with classic, environmental protection and fashion.

Conclusions

Lacquer furniture, reflecting a traditional culture of our Chinese nation, has the strong cohesion and is also the carrier of national thought, and has created aesthetic value with oriental characteristic. So, lacquer furniture was the pure traditional things that has several thousand years of history. To make it has the characteristics of modern lacquer art, it is better try to integrate lacquer art furniture into phases of all ages with the change of times. The media, languages, means and skills of lacquer furniture are developing in the constant changes. It absorbs, discards, inherits and innovate in the interaction among different times, different areas and different art. Furthermore, it not only keeps the fine tradition but also absorbs essence of cultures and arts with the times standards, and occupies its proper market position.

To sum up, it must be found potential from traditional lacquer furniture to seek the opportunity to develop modern lacquer furniture. With exploring and innovation of modern lacquerware art at home and abroad, the design of lacquer furniture will be integrated with the new design concept and the technique. It should be broken through ways of feeling and thinking to create the lacquer furniture as a “wisdom living” which should be collision with hearts. It not only walk more close to fashion taste of the modern residence design, but also still make the traditional culture and technology of lacquer art continue to carry forward. Hopefully, it has certain reference significance to the development of lacquer furniture. As a result, we also can realize that their influence just can’t be understated from seeking development opportunities of modern lacquer furniture. We should study it and love it with an attitude of reverence for precious cultural heritage. And the lacquerware art has beautified our life and inherited our culture all the time which should be hand down from one generation to another.

References

Qiao, S.G. 2004.Chinese traditional craftwork—lacquer art. Zhengzhou: Daxiang Press.

Zhang, Y. 2000. Lacquer art and environmental art. Journal of Chinese Lacquer.1(19):14-17.

Kumanotani,J. 1995. Urushi(oriental lacquer)-a natural aesthetic durable and future-promising coating. Progress in Organic Coatings.26 (2-4):163-195.

Cooper, E. 1985.The culture of craft production in the People’s Republic of China Anthropology of Work Review.6(1):12-15.

Shen, F.W. 1991.The history of the traditional Chinese lacquer art. Beijing: People's Fine Arts Publishing House.

Song, S.S. 2008.Comparative study on lacquerware art of modern and Han Dynasty. Master Dissertation of Northeast forestry university,

Proceedings of the 55th International Convention of Society of Wood Science and Technology
August 27-31, 2012 - Beijing, CHINA

Wood, the Most Interesting, Innovative and the Best Material for Our Society

Eva Haviarova [1*]

[1] Associate Professor, Department of Forestry and Natural Resources, Purdue University, West Lafayette, IN, USA.
ehaviar@purdue.edu

Abstract

Wood is the only material which is renewable, recyclable, biodegradable, and the most suitable material for creation of beautiful, sustainable and earth friendly products. High valued physical, mechanical, environmental and aesthetic properties are unique only to wood. In terms of its use, wood has been serving humans as a superior material for centuries. Examples are easy to find from great inventions of the past to the most interesting and futuristic nano-scale wood products; and from the great architectural wonders of ancient civilizations to the contemporary structures with the most favorable ecological footprints. Despite its vast importance, wood is currently undervalued as an essential ecological material for the future. Therefore, there is a need to rediscover its uniqueness in order to better understand its large potential and importance in our societies. Wood should be more appreciated and promoted for variable uses in almost every aspect of our lives.

***Keywords*:** wood - renewable, recyclable, biodegradable material; nano-scale wood products

Introduction

Wood is the only renewable, recyclable, biodegradable material. It is also highly recommended material suitable for creation of beautiful, sustainable and earth friendly products. Yet, there is an ever growing trend—lack of interest in wood products by the modern generation and that wood and wood products trade are losing its importance. Therefore there is a strong need to remind all potential users and the general public of reasons why wood is the greatest material out there.

Superior Material Properties

Combination of highly valued physical, mechanical, aesthetic and environmental properties are unique only to wood. Numerous technical textbooks have been written about this subject and are used mainly by academic audience (Haygreen and Bowyer 1996). Some properties are going to be highlighted because of their relevance to a broader spectrum of users such as: architects, designers, product developers, artists or craftsmen whom should remain interested in wood material (Fig.1).

Figure 1. Wood is the unique material used by variety of users: architect, designer, product developer, artist or craftsmen.

Physical properties such as - broad spectrum of natural colors, texture, variable density, odor, thermal conductivity, acoustic insulation, electrical, nano-dimensional properties, friction, nuclear and others are reasons why wood is used in so many unique applications (Fig. 2).

Figure 2. Examples of unique application of wood using its physical proprieties.

Properties such as wood - moisture relation and its result in dimensional instability could be perceived negatively, yet it could be also used as an advantage by the clever designer.

Green furniture makers (Shea1971, Alexander 197) used shrink and swell techniques to built furniture which will get stronger over time (Fig. 3).

Figure 3. Shrink and swell joinery examples used in Shaker's furniture, oriental furniture and school furniture.

For many users, wood is perceived as a challenging material and yet there is a great need to understand the behavior of this orthotropic material. Empirical knowledge of proper wood utilization is apparent in many great masterpieces created in the past (Jackson 1989). In contemporary applications it is often detected that a lot was forgotten. However, not even suitable application could be solved with advanced finishes and treatment that could convert the hygroscopic nature of wood into a product with water resistant or even waterproof properties. Just as an example, wood was and still is used for functional bathtubs (Fig. 4).

Figure 4. a) Traditional bathtub, b) & c) contemporary bathtub designs.

Mechanical properties – variable strength based on different wood species, elastic properties such as flexibility, bendability and durability contributed to many products with long lifespan and great performance. Man contributed immensely to engineering properties of wood with the ability to form a variety of wood-based composite materials, which are created from big or small wood particles or residues. These materials are more uniform with specifically designed strength properties. They are more and more utilized to create unique small and large scale structures (Fig. 5).

Figure 5. Examples of composite materials and their use in unique furniture.

Bending wood - with help of some plasticization treatment, craftsmen bent wood for centuries (Gehry 1992). Compression bending is an example of how we could obtain incredible shapes made of wood (Fig. 6).

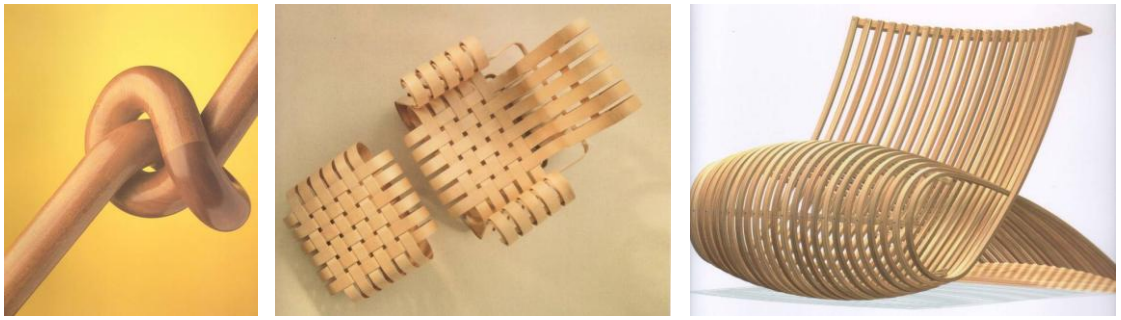

Figure 6. a) Compression bending and b) & c) furniture by Frank Gehry.

Aesthetic properties - among many are variability in appearance based on color and texture, natural soothing feel, warmth and comfort. Wood is a material with status, graceful aging, and with presence of unique character marks. Above all, wood is the material of superior workability, chosen by many craftsman and artists (Lefteri, 2003).

Figure 7. Examples of aesthetic properties are in a) graceful aging of musical instruments, b) workability, and c) use of character marks in art objects.

Environmental nature or wood - is described by renewable, recyclable, biodegradable, sustainable (green) material properties. Wood can be by design slow or fast grown material and has an ability to be preserved for centuries in durable products (carbon sequestering) (Bowyer 2012). Results of Life Cycle Analysis (LCA) are also showing the superiority of wood when compared to other non renewable materials for environmental applications. Nevertheless, heating power and energy from wood residues is an important attribute in today's world.

Wood Utilization

In terms of its use, wood has been serving humans as a superior material for centuries. Examples are easy to find from great inventions of the past to the futuristic nano-scale wood products. Wooden artifacts with superior construction were found in Egyptian tombs (Desroches – Noblecourt 1963). Ancient drawings are documenting how need for wood conquered and transformed the world (Fig. 8).

Figure 8. a) Timber procurement by Uruk civilization, b) & c) & d) Egyptian furniture.

Ship building needed to secure power, expanding empires built cities and towns, metallurgy, glass production, and even a taste for sugar lead to massive deforestation—a movement to a new world with abundant wood resource and consequently to a massive shift of power. This was a repetition of an age-old process that has occurred again and again until today (Perlin 1989). However, we can learn from past mistakes and break out the cycle of deforestation and land degradation that undermined earlier civilizations by responsible use of natural resources and practicing recycling, renewability principles, and applying healthy policies.

Wood for transportation - *w*ood made trade possible from ancient to present times. Ships, chariots, carts, wagons, and other transportation vessels were made for centuries from wood (Fig. 9). It was and still is a priced commodity.

Figure 9. Wood for a) ship building, b) chriots and c) vagons.

Wooden tools, equipment, and musical instruments - *b*efore steel was used, high density wood was used for the most intricate machines. Woodworking tools are still made of wood. Its flexibility and strength is still valued in sports equipment such as baseball bats, skate boards, hokey sticks and others. Acoustic properties of wood for production of musical instruments are perceived more like an art than science but proper selection of wood material is essential for production of high quality musical instruments (Fig. 10). For example, the guitar body is often made of spruce and maple, but components such as the bridge could be made of ivory, ebony or other priced woods while protecting endangered woods is enforced.

Figure 10. a) Ash baseball bat b) Chinese musical instrument, c) bass acoustic guitar

Wood for incense - sandalwood was prized as an incense wood in China. Phoenicians cut down cedars for export to Egypt (Perlin 1989). Cedar was traded by early civilizations and is still used today as an incense material for closets. Wood in general is claimed to have bacteria eliminating properties and is often used for cooking utensils (Fig. 11).

Figure11. a) b),c) Culinary utensils, d) cedar wood shoos incense.

Non wood forest products - such as bamboo is growing one meter a day and is an important material with more than 1,000 uses. Rattan and other similar materials are also of high importance.

Wood for structures – are everywhere from the great architectural wonders of ancient civilizations to the contemporary structures with the most favorable ecological footprints. Examples are endless such as London Olympic Velodrom (Fig. 12a), England; Metropol Parasol in Sevilla, Spain (Fig. 12b); Westminster Hall, in London England; Sakyamuni Temple in Shanxi province, China; China's oldest surviving fully-wooden pagoda Fugong Temple (Fig. 12c); the Hanging Temple of Mount Heng and in Shanxi province, China which was built from local hemlock forests over 50 meters up the side of a sheer cliff in 491**A.D.** How and why it got there? Wood as a material is also suitable for contemporary modular concepts, organic or biodegradable structures and modern homes with favorable eco footprints.

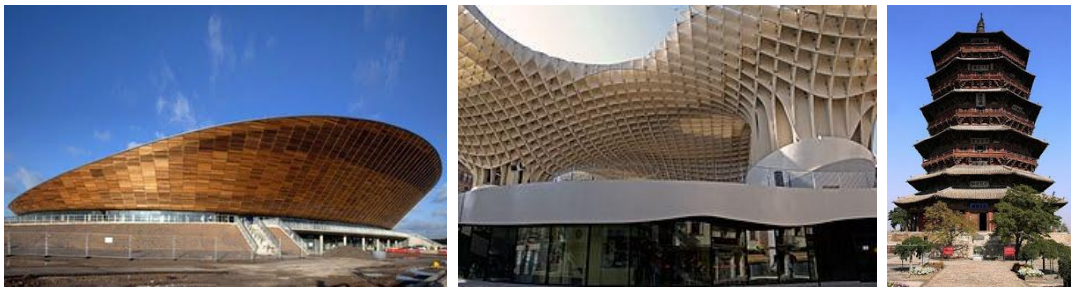

Figure 12. a) London summer Olympic veldrome, b) Metropol Parasol in Sevilla, c) The Fugong Temple Wooden Pagoda.

Wood for prized objects- *w*ood shaping of any kind, especially wood carving into artistic object is the best example how ageless value could be added to a natural material (Fig. 13). For example, furniture from Egyptian tombs is still relevant in terms of structural integrity and could easily compete with any contemporary furniture in terms of its strength and durability. Furniture evolved from prehistoric times and during all architectural periods, wood has remained an essential material for its construction. There is a big lesson to be learned from many of these objects and hopefully preserved for future generations.

Figure 13. a) Chair from tree trunk, b) horse and c) face carvings.

Conclusions

Despite its vast importance, wood is currently undervalued as an essential ecological material. Therefore, there is a need to rediscover its uniqueness in order to better understand its large potential and importance in our societies. Wood should be more

appreciated and promoted for variable uses. There is a large amount of products made of wood and as we say, wood is with us almost every moment of our lives from cradle of wood to wooden casket.

To cultivate love and passion towards wood as a superior material and to teach students and the general public how to use it responsibly and to its full potential is an obligation of every educator in the forest products field. Let me present few examples from the Wood Research Laboratory at Purdue University, USA, where wood products design is approached in combination of aesthetic, strength, manufacturing and environmental design concepts (Fig. 14).

Figure 14. Examples of students design work at Purdue, WRL.

References

Alexander, J. 1978. Making a Chair from a Tree: an Introduction o Working Green Wood. The Taunton Press, Inc. Connecticut.

Bowyer, J. 2012. Carbon 101: Understanding the Carbon Cycle and the Forest carbon Debate. Dovetail Partners Inc.

Desroches-Noblecourt, C. 1963. Tutankhamen. New York Graphic Society, New York.

Genry, F. 1992. New Bentwood Furniture Designs. The Lake St. Louis Historical Society, Montreal.

Haygreen, J. and J. Bowyer. 1996. Forest Products and Wood Science: An Introduction. Iowa State University Press, Ames, Iowa.

Jacson, A., D. Day and S. Jennings. 1989. The Complete Manual of Woodworking. William Collins Sons & Co. Ltd.

Lefteri, Ch. 2003. Materials for Inspirational Design. Roto Vision SA, Switzerland.

Perlin, J. 1989. A Forest Journey: The Role of Wood in the Development of Civilization. Harvard University Press.

Shea, J. 1971. Making Authentic Shaker Furniture. Over Publications, Inc., New York.

Proceedings of the 55th International Convention of Society of Wood Science and Technology
August 27-31, 2012 - Beijing, CHINA

DEVELOPING A WOOD CULTURE FOR NON-RESIDENTIAL CONSTRUCTION

Alain Cloutier[*]

Professor and Director, Wood Research Centre, Université Laval –
2425 rue de la Terrasse, Québec, QC, Canada G1A 0A6

** Corresponding author*
alain.cloutier@sbf.ulaval.ca

Abstract

Light frame wood construction has been used for decades in North America for residential construction. However, wood as a construction material for non-residential buildings almost disappeared in Eastern Canada and was replaced by steel and concrete. Over the last 10 to 15 years, important efforts were made in Eastern Canada and in the Province of Quebec in particular to develop a wood culture and promote the use of wood for non-residential construction. In 2008, the Quebec Government adopted a policy to favor the use of wood in public buildings construction provided that the design meets building code requirements and that the construction cost is no more than 5 % higher than for a standard steel and concrete project. Laval University has been very active in the development of this policy and is committed to the development of wood culture in general. Two major building projects were realized on campus since 2004: the Gene-H.-Kruger Building and the TELUS Stadium. A 44 meter span wooden bridge was also built at Montmorency Forest, Laval University's experimental forest station. These projects were realized as demonstrations that wood can be used for non-residential building economically while valorizing the aesthetic character of wood. They were also aimed at showing the variety of wood-based products available in the market. Wood construction for non-residential buildings is gaining ground in Quebec but work remains to be done. Some of the significant aspects that need to be improved include the development of tools and documentation for engineers and architects involved in these projects, better training programs at the technical and professional levels, and pursue research in the areas of wood based products and construction.

***Keywords*:** wood culture, wood construction, wood bridge, carbon neutral construction.

Introduction

Light frame wood construction has been used for decades in North America for residential construction. However, wood as a construction material for non-residential buildings almost disappeared after the Second World War in Eastern Canada and was replaced by steel and concrete. Over the last 10 to 15 years, important efforts were made in Eastern Canada and in the Province of Quebec in particular to develop a wood culture and promote the use of wood for non-residential construction. In 2008, the Quebec Government adopted a policy to favor the use of wood in public buildings construction provided that the design meets building code requirements and that the construction cost is no more than 5 % higher than for a standard steel and concrete project (MRNF 2008). In 2011, the Quebec Government put together a working group, the Beaulieu Commission, to enquire on the reasons explaining the slow development of non-residential wood construction and recommend measures to correct that situation. In parallel, Laval University has been very active in promoting the use of wood as a construction material for non-residential buildings and is committed to the development of wood culture in general. The Quebec Government policies and Laval University actions to promote the use of wood in non-residential construction will be described in this paper.

Methods used to Promote Wood as a Construction Material

Wood Use Strategy for Construction in Quebec

The Wood Use Strategy for Construction in Quebec (MRNF 2008) was put in place to increase the use of structural and appearance wood in domestic building construction, mainly in non-residential and multi-family construction by about 60% from 2006 to 2014. The aims of this strategy were to support the Quebec wood products industry and reduce greenhouse gas emissions. Two main courses of action were set within this strategy: 1) the Quebec Government should lead by example, using wood in its own buildings. Public order givers must consider the option of using wood when preparing their initial plans and specifications; 2) increase the use of wood in multi-family and non-residential construction by supporting innovation, develop tools to support designers and promote a new appreciation of wood in Quebec. Three specific measures were set to support innovation: 1) technology transfer to construction professionals and promoters; 2) applied research and development to develop new products and systems; and 3) university research involving training of highly qualified people.

Beaulieu Commission on the Utilization of Wood in Building Construction

The Beaulieu Commission was launched in March 2011 to enquire on the reasons explaining the slow development of non-residential wood construction and recommend measures to correct that situation. They published their final report in February 2012 (Beaulieu 2012). The Commission pointed out that progress has been made on the use of wood in non-residential construction but slower than expected. A number of recommendations were made to improve the situation:

1. Improve availability of documentation, design tools, technical support and training for engineers and architects;

2. Improve training programs on the use of wood for non-residential construction at high school, technical school and university levels;
3. Make timber construction course mandatory for civil engineering students;
4. Improve continuing education on wood construction;
5. Develop research chairs.

Showcase Projects at Laval University

Laval University offers undergraduate and graduate training programs in forestry in general and in wood science and engineering in particular. Laval is strongly committed to promote the use of wood in non-residential construction and to contribute to the development of a wood culture in general. Since 2005, three major wood construction projects were completed at Laval: the Gene-H.-Kruger Building, the TELUS Stadium, and the Montmorency Forest Wood Bridge. These projects will be described below.

Results and Discussion

Gene-H.-Kruger Building

The Gene-H.-Kruger Building is shown in Figure 1. Opened in October 2005, it is the home of the Wood Research Centre at Laval University. It is used for teaching and research in wood science and engineering at the undergraduate and graduate levels. The whole structure is made of black spruce and Douglas-fir glulam beams. Exterior siding, windows and interior wall panels are made of wood and wood-based panels. The building usable area is about 8000 m^2. It includes 18 laboratories, three classrooms, one conference room of 100 person capacity, one meeting room of 20 person capacity and Faculty, postdoctoral fellows and graduate student offices.

TELUS Stadium

The TELUS Stadium is shown in Figure 2. Its main function is as a soccer field but it is also used for rugby and football. It was opened in January 2012. It can host 500 spectators. The field has a size of 60 m × 100 m. The main structure is made of 13 black spruce glulam arches of 72 m span installed at 9 m interval. Steel bars are also used in the structure, therefore forming a hybrid structure. Black spruce from northern Quebec with particularly slow growth, small knots and high mechanical properties is used in the main arches.

Montmorency Forest Wood Bridge

The Montmorency Forest Wood Bridge is shown in Figure 3. It was opened in June 2011. The Montmorency Forest is Laval University forest experimental station located 75 km north of Quebec City, Canada. It is a 6664 ha forest managed by the Faculty of Forestry, Geography and Geomatics of Laval University. It is used for teaching, research and recreation. The wood bridge shown in Figure 3 is used to cross the Montmorency River, a tributary of the St-Laurence River. The bridge has a 44 m span and a width of 4.8 m. The structure is made of 12 glulam arches and 10 glulam beams made of black spruce from northern Quebec. The bridge was built and installed on the principle of a carbon neutral project. Therefore, 1941 trees were planted on the Montmorency Forest territory to compensate the balance of 129.4 tons of CO_2 emitted in this project.

a)

b)

c)

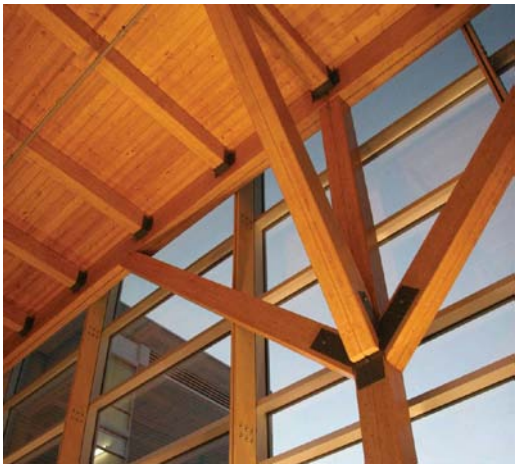

d)

e)

f)

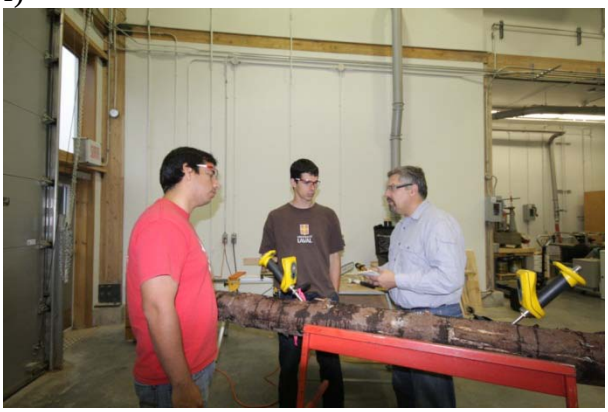

Figure 1. Gene-H.-Kruger Building at Laval University. a) main entrance; b) back entrance; c) wood structure; d) main hallway; e) conference room; f) laboratory.

a)

b)

c)

d)

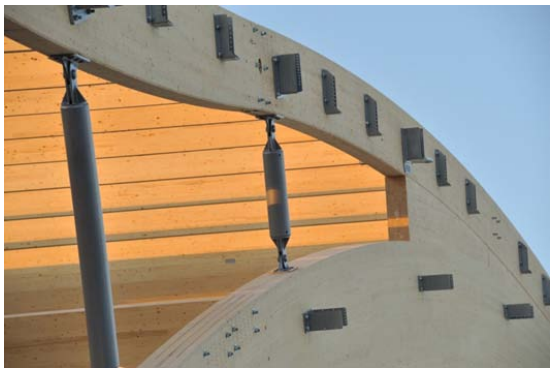

e)

f)

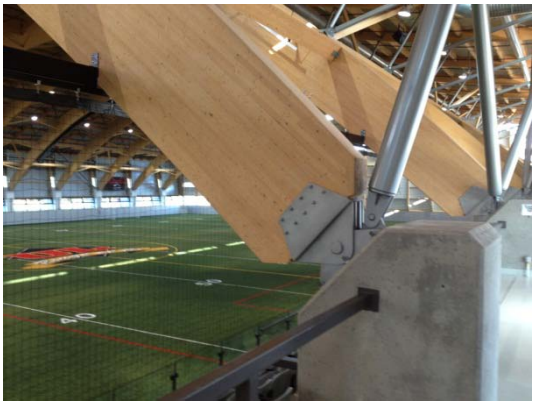

Figure 2. TELUS Stadium, Laval University, Quebec City, Canada. a) location on campus; b) main entrance; c) hybrid structure; d) hybrid structure during construction; e) assembly and installation of main arches; f) glulam connectors to concrete base.

a)

b)

c)

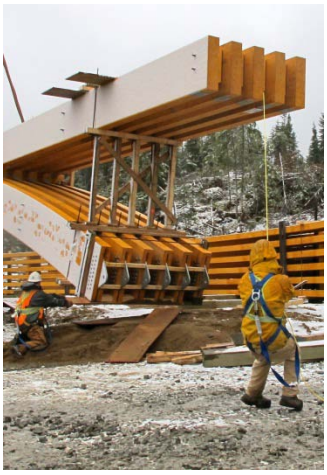

d)

e)

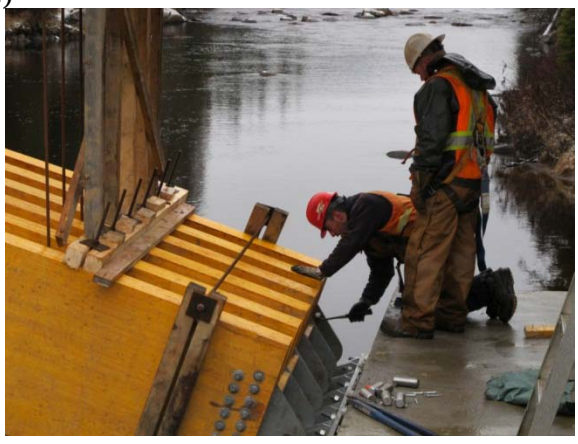

Figure 3. Montmorency Forest Wood Bridge. a) completed project; b) installation of bridge section with a crane; c) installation of bridge section and connectors; d) installation of bridge section and connectors to concrete base; e) installation of connectors to concrete base.

Conclusions

Significant efforts are currently deployed in the Province of Quebec, Canada to develop a wood culture in the area of non-residential construction. Progress were made and interesting showcase projects were realized at Laval University, elsewhere in Quebec and elsewhere in Canada such as FPInnovations laboratories in Quebec City and Vancouver, and the Faculty of Forestry at the University of British Columbia. More work remains to be done to insure a faster development of wood construction in the Province of Quebec. Some of the significant aspects that need to be improved include the development of tools and documentation on wood construction for engineers and architects involved in these projects, better training programs at the technical and professional levels, and pursue research in the areas of wood-based products and wood construction.

References

Beaulieu, L. 2012. Rapport du groupe de travail visant à favoriser une utilisation accrue du bois dans la construction. Ministère des Ressources naturelles et de la faune, Gouvernement du Québec. 67 p. In French. (http://www.mrnf.gouv.qc.ca/publications/forets/entreprises/rapport-beaulieu.pdf)

MRNF 2008. Stratégie d'utilisation du bois dans la construction au Québec. Ministère des Ressources naturelles et de la faune, Gouvernement du Québec. 19 p. In French. (http://www.mrnf.gouv.qc.ca/publications/forets/entreprises/strategie-developpement.pdf)

Other links of interest:

http://www.ffgg.ulaval.ca/fileadmin/images/Faculte/Foret_Momo/Fiche_technique_pont_de_bois.pdf

http://www.crb.ulaval.ca/index.php?id=30

Proceedings of the 55th International Convention of Society of Wood Science and Technology
August 27-31, 2012 - Beijing, CHINA

Rediscovering Wood Culture and Approaching "Wood is Good"

Chia-Hua Lee[1] – Wen-Pin Hou[2]*

[1] Researcher, Internatioanl Wood Culture Society, Kaohsiung, TAIWAN.
* *Corresponding author*
chiahua.lee@iwcs.com
[2] Director, International Wood Culture Society, Newport Beach CA, USA.
mike.hou@iwcs.com

Abstract

International Wood Culture Society (IWCS) is a non-profit and non-governmental international organization, dedicated to the research, education and promotion of wood culture. IWCS promotes the concept "Wood is Good" from the cultural perspective, which provides a different way to a better understanding of the meaning and the importance of wood in human history and in our daily life. To do so, IWCS is currently carrying out the following three projects: the Knowledge Project, the Experience Project, and the Life Project.

IWCS is in a continuing effort to establish an interdisciplinary platform for the exchange of ideas concerning the foundation, application and practices of wood culture, in order to yield systematic and applicable approaches for both research and everyday life. In so doing, IWCS aims to bring to light that studying wood culture improves human relationship with nature and opens new possibilities for a sustainable future.

***Keywords*:** Wood is good, Culture perspective, Interdisciplinary platform, Wood culture, Sustainable future.

TGA and DSC Analysis of Boron Modified Phenol Formaldehyde Polymer

Ertugrul ALTUNTAS [1], Mehmet Hakki ALMA [1], Zeki CANDAN [2]*

Oktay GONULTAS [2], and Murat ERTAS [3]

[1] Department of Forest Products Engineering, Faculty of Forestry
Kahramanmaras Sutcu Imam University, 46060, Kahramanmaras, TURKEY
[2] Department of Forest Products Engineering, Faculty of Forestry
Istanbul University, Sariyer, 34473, Istanbul, TURKEY
[3] Department of Forest Products Engineering, Faculty of Forestry
Bursa Technical University, Bursa, TURKEY
* *Corresponding author*
forestproductsengineer@yahoo.com

Abstract

The objective of this research was to evaluate thermal characteristics of boron modified phenol formaldehyde polymer. Boron – based phenol formaldehyde polymers were synthesized by using boric acid at different reaction conditions such as temperature and time. Thermogravimetric analysis (TGA) and differential scanning calorimetry (DSC) analysis of the boron modified polymer or neat polymer were performed. The results acquired in this study showed that the thermal characteristics of the phenol formaldehyde polymer were affected by the boron modification. The PF polymer modified with boron had higher thermal stability than those of the unmodified or commercial PF polymer. It can be also concluded that the boron modification has not important effect on the T_g or T_m values of the synthesized polymer.

***Keywords*:** A. Boron modified phenol formaldehyde polymer, B. Thermogravimetric analysis, C. Differential scanning calorimetry, D. Thermal analysis

Introduction

Phenolic resins have been synthesized with condensation polymerization of phenol (C_6H_5OH) and formaldehyde (CH_2O). It can be seen in Figure 1 (Altuntas, 2008).

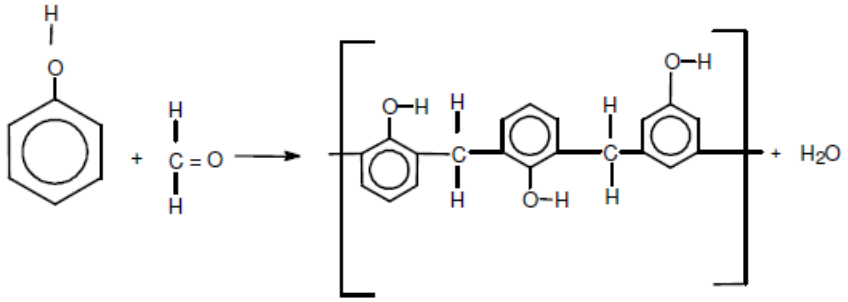

Fig. 1 Phenol-Formaldehyde Reaction

Phenolic resin is widely used as an adhesive in wood composite panel industry. Phenolic resins have been modified with some materials to improve physical and mechanical properties, to increase dimensional and thermal stability, to decrease thermal expansion and water absorption, to change electrical properties (Altuntas, 2008).

Boron compounds are also widely used in industrial applications. Its importance and using area are increasing year by year. Boron compounds have been generally identified and sold according to its B_2O_3 content in industry. They use in glass industry, ceramic industry, cleaning industry, fire retardant materials manufacture, medicine, health, chemistry, agriculture, metallurgy industry, energy industry, automobile industry, waste cleaning process, pigment and dryer, nuclear applications, and protection of wood materials (Ertugrul, 2004).

Materials and Methods

Materials

In this study, phenol (C_6H_5OH), formaldehyde (CH_2O), hexamethylenetetramine (HMTA), acetone, boric acid (H_3BO_3), magnesium oxide (MgO), and zinc stearate were used. Commercial phenol formaldehyde was supplied from ARBAK Chemistry Company, in Istanbul, Turkey.

Synthesis of Boron-Phenol Formaldehyde Polymer

In synthesis of boron- phenol formaldehyde; molar ratios of phenol, formaldehyde, and boric acid were 3:3.6:0.8, respectively. After reactions water was removed using vacuum. Boron phenol formaldehyde polymers were synthesized by using boric acid at different reaction conditions such as temperature and time. Experimental design of this present study is shown in Table 1.

Table 1 Experimental Design of the Boron-PF Synthesis

Polymer Groups	Temperature (°C)	Time (minute)
BPF-1	70	30
BPF-2	70	60
BPF-3	70	90
BPF-4	70	120
BPF-5	90	30
BPF-6	90	60
BPF-7	90	90
BPF-8	90	120
BPF-9	110	30
BPF-10	110	60
BPF-11	110	90
BPF-12	110	120
BPF-13	120	30
BPF-14	120	60
BPF-15	120	90
BPF-16	120	120

TGA Analysis

Thermal stability of boron modified phenol formaldehyde polymer (BPF), neat phenol formaldehyde, and commercial phenol formaldehyde were evaluated by thermogravimetric analysis (TGA). The BPF, neat PF, and commercial PF were exposed to a heating rate of 10°C/min over a temperature range of 25°C to 800°C to carry out TGA. Nitrogen gas was used as the inert purge gas in order to avoid unwanted oxidation of the polymer. Flow rate of nitrogen gas was 20 mL/min.

DSC Analysis

The BPF, neat PF, and commercial PF were evaluated by differential scanning calorimetry (DSC) to determine T_g and T_m characteristics. DSC analysis was performed on 10 mg samples with a heating rate of 10°C/min under nitrogen with a flow rate of 30 mL/min. The BPF, neat PF, and commercial PF were heated from 20°C to 400°C for DSC analysis.

Results and Discussion

The T_d and weight loss values of the BPF, neat PF, and commercial PF are shown in Table 2. The results obtained in this study showed that the boron modification affected the thermal stability properties of phenol formaldehyde polymer.

Table 2 TGA Results of BPF, Neat PF, and Commercial PF

Polymer Groups	T_d (°C)	Weight Loss at T_d (%)	Weight Loss at 800 °C (%)
BPF-1	428,41	37,97	89,87
BPF-2	460,46	15,97	74,85
BPF-3	469,88	25,01	83,93
BPF-4	442,21	36,53	82,07
BPF-5	480,54	22,32	75,42
BPF-6	443,91	30,49	88,24
BPF-7	462,66	27,66	77,93
BPF-8	440,36	19,83	85,10
BPF-9	448,49	30,48	87,27
BPF-10	506, 86	5,79	88,26
BPF-11	442,06	28,25	91,38
BPF-12	449,06	29,56	93,86
BPF-13	443,07	29,35	83,18
BPF-14	443,41	22,08	81,55
BPF-15	434,88	22,49	93,43
BPF-16	451,56	26,32	94,04
Neat PF	460,79	33,16	100,00
Commercial PF	453,45	31,85	100,00

As shown in Table 2, T_d values of the boron-modified PF polymers ranged between 428.41°C and 506.86°C. Some of the BPF groups had higher T_d values than those of neat or commercial resin. The highest T_d value was determined in the BPF-10 group. All BPF groups sowed lower weight loss values at T_d than those of neat PF or commercial PF, except BPF-1 and BPF-4 groups.

TGA curves of commercial PF polymer and boron-modified PF polymer (BPF-10) are shown in Figure 2 and Figure 3, respectively.

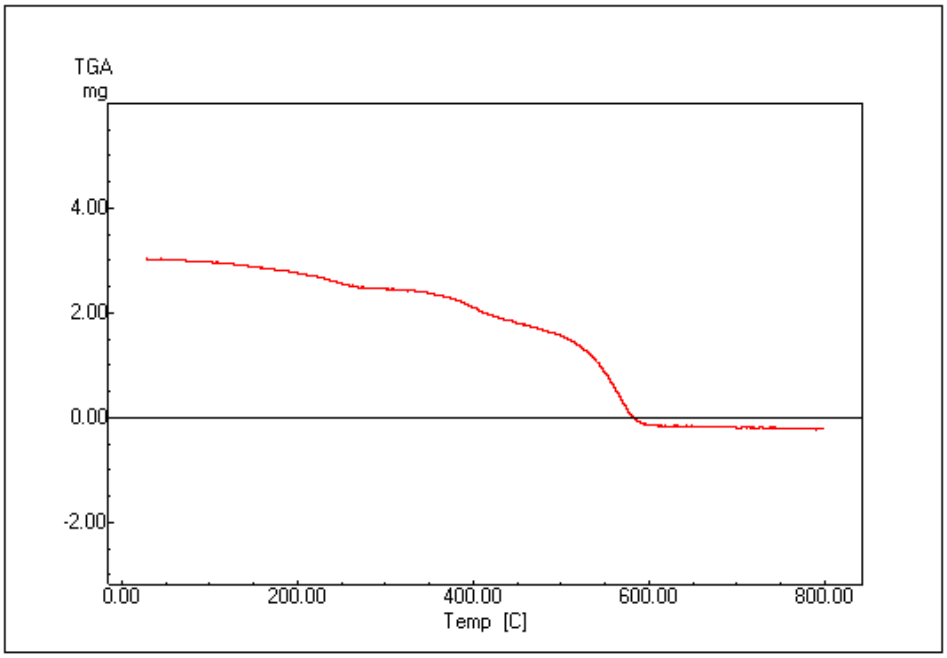

Fig. 2 TGA Curve of Commercial PF

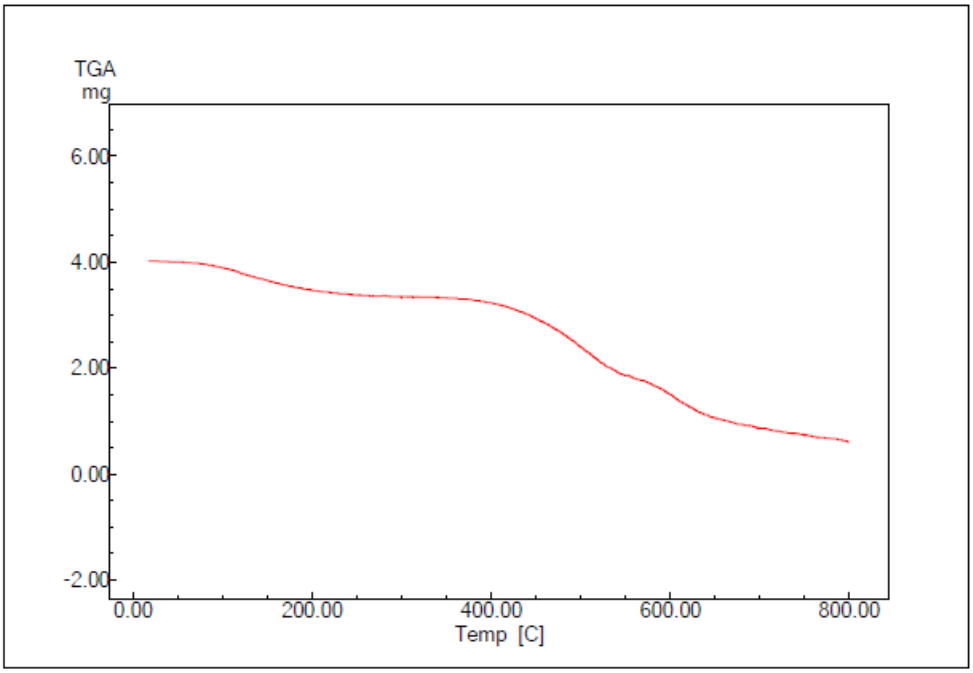

Fig. 3 TGA Curve of BPF-10

The lowest weight loss value at T_d was observed in the BPF-10 group with 5.79%. The results indicate that boron modification increased the thermal stability of the PF polymer. As for the weight loss values at 800°C, the boron-modified PF polymers had lower values than those of neat PF or commercial PF.

The T_g and T_m values of the BPF, neat PF, and commercial PF are shown in Table 3. The results acquired in the DSC analysis showed that the boron modification has some effects on the T_g and T_m values of phenol formaldehyde polymer.

Table 3 DSC Results of BPF, Neat PF, and Commercial PF

Polymer Groups	T_g (°C)	T_m (°C)
BPF-1	121,37	136,11
BPF-2	146,53	149,00
BPF-3	123,20	137,31
BPF-4	136,16	169,95
BPF-5	143,46	154,01
BPF-6	151,23	160,89
BPF-7	149,35	156,31
BPF-8	134,43	135,90
BPF-9	152,88	157,47
BPF-10	149,57	157,57
BPF-11	154,11	160,29
BPF-12	153,84	160,43
BPF-13	147,61	156,38
BPF-14	151,67	159,23
BPF-15	152,76	159,80
BPF-16	151,82	159,01
Neat PF	126,76	141,02
Commercial PF	147,28	151,36

As shown in Table 3, T_g values of the boron-modified PF polymers ranged between 121.37°C and 154.11°C. T_g was 126.76°C for neat PF polymer, while 147.28°C for commercial PF polymer. Except some groups, the T_g values of PF polymers fell within a narrow range. According to T_m values, the boron-modified PF groups had similar values with neat or commercial PF.

DSC curves of commercial PF polymer and boron-modified PF polymer (BPF-10) are shown in Figure 4 and Figure 5, respectively.

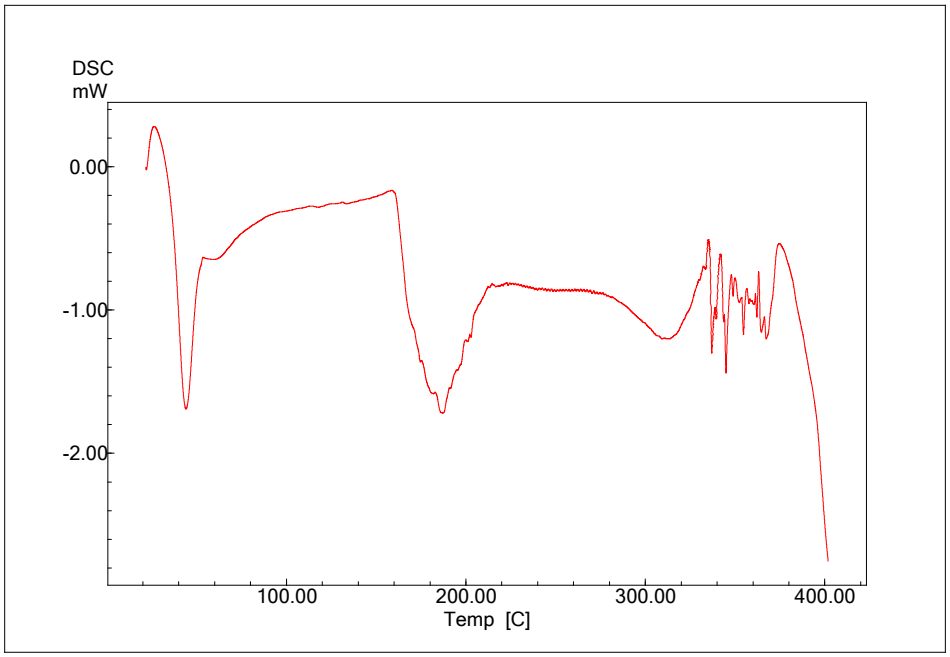

Fig. 4 DSC Curve of Commercial PF

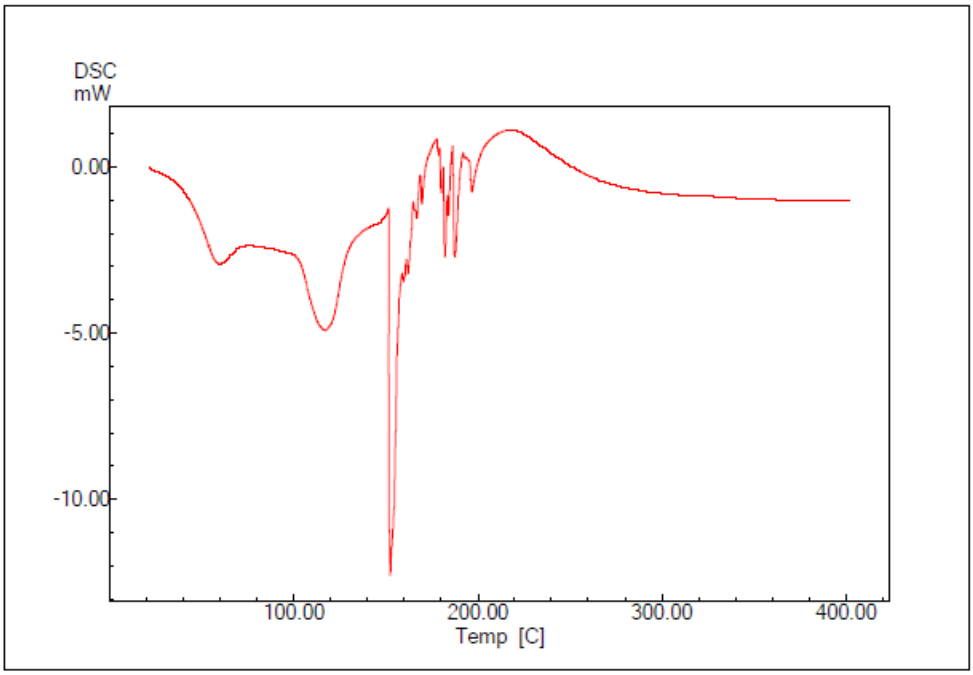

Fig. 5 DSC Curve of BPF-10

The results obtained from the DSC analysis indicated that the boron modification has no negative effect on the T_g or T_m values of the boron-modified PF polymers. Thus, the PF polymers modified with boron compounds could be processed as same as neat or

commercial PF polymer. It also could be stated that both the boron-modified PF and neat PF could be used with together.

Conclusions

The main goal of this study was to enhance thermal performance of PF resin. Thus, PF resins were modified with boron compounds using different time or temperature levels. The results obtained in this study showed that the thermal characteristics of the phenol formaldehyde polymer were affected by the boron modification. The PF polymer modified with boron had higher thermal stability than those of unmodified or commercial PF resin. It could be also concluded that the boron modification has not an important effect on the T_g or T_m values of the PF polymers. PF polymer could be modified with boron compounds to improve its thermal durability without changing its processability. Therefore, the boron-modified PF could be used in wide range of applications.

References

Altuntas, E., 2008, Polymer with boron-wood composites, M.Sc. Thesis, 99 pp., Kahramanmaras Sutcu Imam University, Kahramanmaras, Turkey.

Ertugrul, E, 2004, Bor ve toryum maddeleri sektörü, Türkiye Kalkınma Bankası Araştırma Müdürlüğü Yayınları, Ankara, s: 04–75.

Acknowledgements

The authors thank Kahramanmaras Sutcu Imam University Research Fund for its financial support in this study (Project No: 2007/3 – 19. The author also would like to express their appreciation for the financial support provided by Tubitak, Ankara, Turkey. ARBAK Chemistry Company (Istanbul, Turkey) is greatly appreciated for raw material supply.

Anatomical Investigation of Thermally Compressed Eucalyptus Wood Panels

Kamile TIRAK HIZAL[1*] Dilek DOGU[2] Zeki CANDAN[2] Oner UNSAL[2]

[1] Department of Forest Products Engineering, Faculty of Forestry
Duzce University, Duzce, TURKEY
[2] Department of Forest Products Engineering, Faculty of Forestry
Istanbul University, Istanbul, TURKEY
* *Corresponding author*
ktirak@istanbul.edu.tr

Abstract

Effects of temperature and press pressure on the anatomical structure of solid-wood panels produced by using Turkish River Gum (*Eucalyptus camaldulensis* Dehnh.) wood were evaluated. The logs were obtained from Mersin, South of Turkey. Solid wood panels with dimensions of 150 by 500 by 18 mm were hot-pressed using a laboratory hot press at a temperature of either 150°C or 180°C and pressure of 2 MPa for 45 min. Light Microscopy (LM) and Stereo Microscopy (SM) were employed to reveal deformations in the anatomical structure of the panels subjected to varying thermal compression conditions. Anatomical investigations were also performed for untreated wood samples for comparison purposes. All microscopic studies were realised visually only on cross sections, radial sections, and tangential sections. Possible cracks, collapse, buckling, degradations, fractures and ruptures on vessel walls, ray parenchyma cells, fibers, axial parenchymas, and pits were investigated.

***Keywords*:** A. Thermal modification, B. Thermal compression, C. Anatomical structure, D. Cellular failures, *Eucalyptus* spp.

Introduction

Wood modification methods improve the properties of wood (Hill, 2006). Beside these material improvements the timber quality after modification is also of importance. Thermal compression of wood is a modification method that combines thermal and mechanical processes, resulting in densification of wood.

During the thermal compression process solid wood is exposed to compressive stresses in radial or tangential directions in addition to temperature effects. Changes in the anatomical structure of wood at various temperatures have been studied in detail (Fengel and Wegener 1989; Terziev et al. 2002; Boonstra et al. 2006; Persson et al. 2006; Awoyemi and Jones 2010).

Dogu et al. (2010) reported that there are significant interactions between process conditions and anatomical structure of wood during thermal compression. The wood exhibited different behavior in almost all process condition, and the process conditions showed different effect related to anatomical structure of wood. The authors also indicated that same pressure level has much more effect in the wood deformation at higher temperatures.

In this paper preliminary results of the study about on the effects of varying temperatures and press pressures on anatomical structure of solid-wood panels produced by using Turkish River Gum (*Eucalyptus camuldensis* Dehnh.) wood were explained. This study is a part of study which has different press pressure and temperature. So in our next study all details will be given.

Materials and Methods

Materials

This study was performed by using wood samples obtained from two different thermal processes. Commercial Turkish River Gum solid panels having no defects with dimensions of 150 by 500 by 18 mm were hot pressed using a laboratory hot press at a temperature of either 150 °C and 180 °C and pressure of 2 Mpa for 45 min. (Table 1).

Table 1 Experimental Design of the Thermally Compressed Wood Panels

Groups	**Press Pressure (MPa)**	**Temperature (°C)**	**Pressing Time (min)**
Control	-	-	-
A	2	150	45
B	2	180	45

A total of 5 panels two for each group were used. The panels were pre-dried to a moisture content of 19% before hot pressing. Non-treated control specimens were used for comparison purposes.

Methods

Light microscopy (LM) was employed to reveal deformations in the anatomical structure of the panels subjected to varying thermal compression conditions. Small samples with dimensions of 10 mm (R)x10 mm (T)x20mm (L) were cut for LM evaluations. The samples were kept under vacuum in the presence of alcohol, glycerin, and at room temperature in order to become softened and were then cut into thin sections (about 20 µm) by using a Leica sliding microtome. The sections were then stained with picro aniline blue to supply good contrast between cell walls. The sections were observed under an Olympus BX51 Light Microscope. Images were taken by using analysis FIVE Software and DP71 Digital Camera installed and adopted on the microscope.

Results and Discussion

Microscope investigations performed on the each treatment group were evaluated together for cross-section, radial section and tangential section to better understand the effects of temperature and pres pressure on the anatomical structure of the wood. Images of untreated wood samples are shown in Fig.1 (LM).

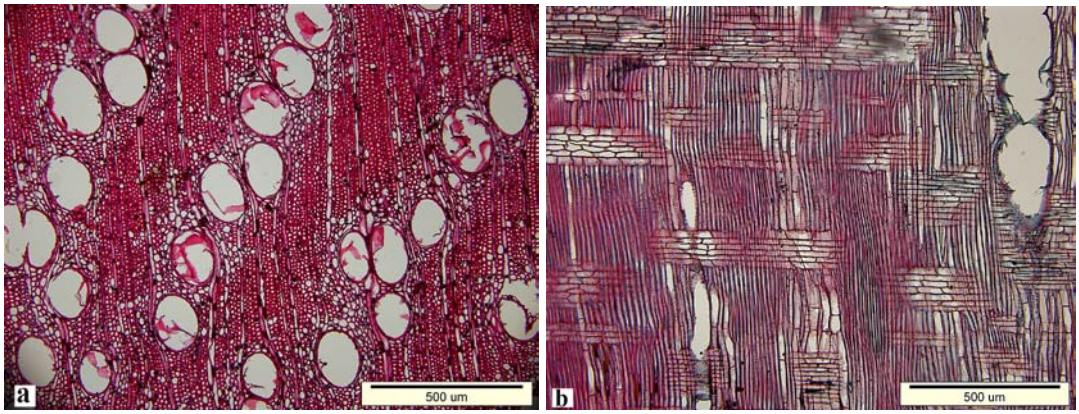

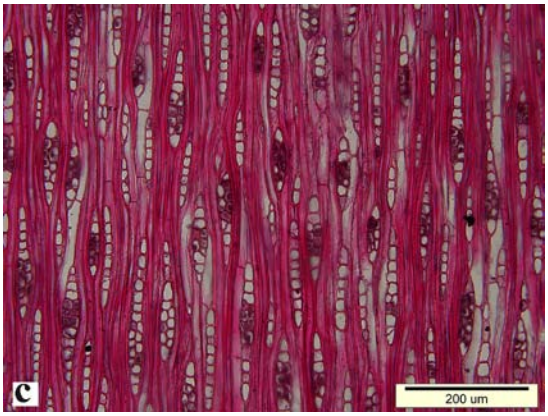

Fig 1. Light micrographs of untreated wood: a) Cross section, b) Radial section, c) Tangential section

Cross Section

Depending on the effects of press pressures and varying temperatures, rays and fibers showed squeeze in the radial directions in Group A (150ºC – 2 MPa) and Group B (180 ºC – 2 MPa).

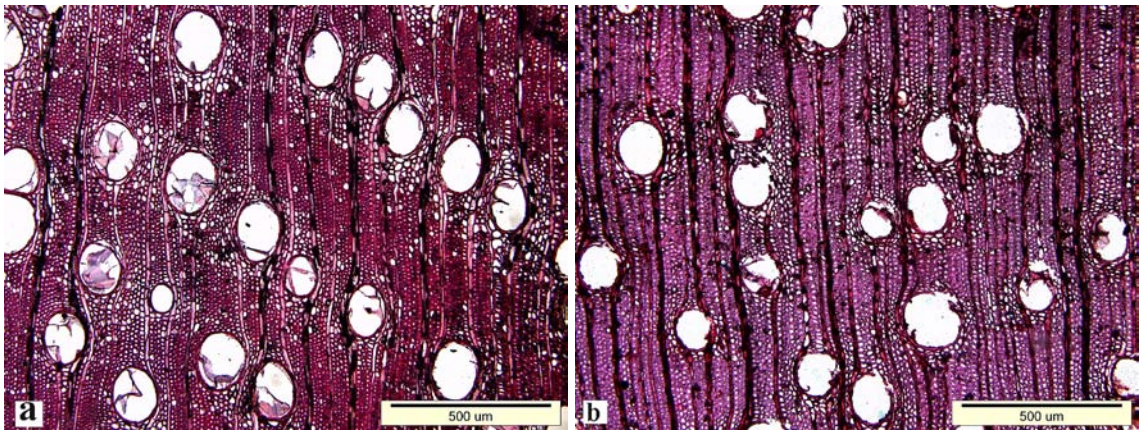

Fig 3. Radial squeeze in Group A(a) and Group B(b)

Turkish River Gum is a diffuse-porous hardwood with similar sized vessels distributed over its structure. The vessel surrounded by paratraheal parenchyma which are thin-walled elements. So cell collapse occurred in almost axial parenchyma in Group A (Fig 4b, arrow 1) and Group B (Fig. 4c, arrow 2). Severe degradation and cracks was observed in the vessel cell wall in Group B (Fig 4c and Fig 4d), whilst severe degradation and cracks was not observed in Group A (Fig. 4a and Fig 4b, arrow 2).

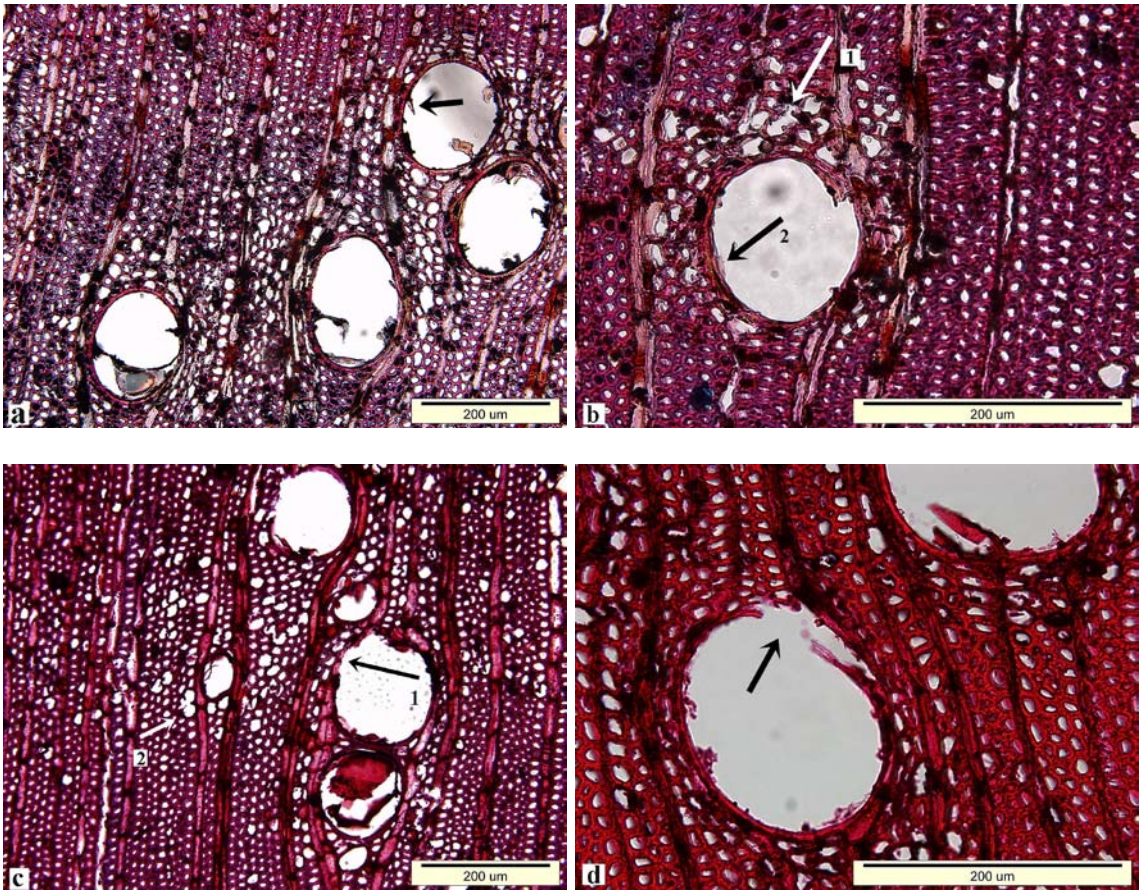

Fig 4. a) Axial parenchyma collapse (arrow) in Group A, b) Vessel cell wall degradation (arrow 2) in Group A c) Vessel cell wall degradation (arrow 1) and axial parenchyma collapse (arrow 2) in Group B, d) vessel cell wall degradation (arrow) in Group B.

Radial Section

No radial and tangential cracks were observed on vessel cell wall while ruptures were seen on vessel cell wall layers. Ruptures in the cell walls of ray parenchyma and cross-field pits were seen in each group, especially severe in Group B (Fig 5).

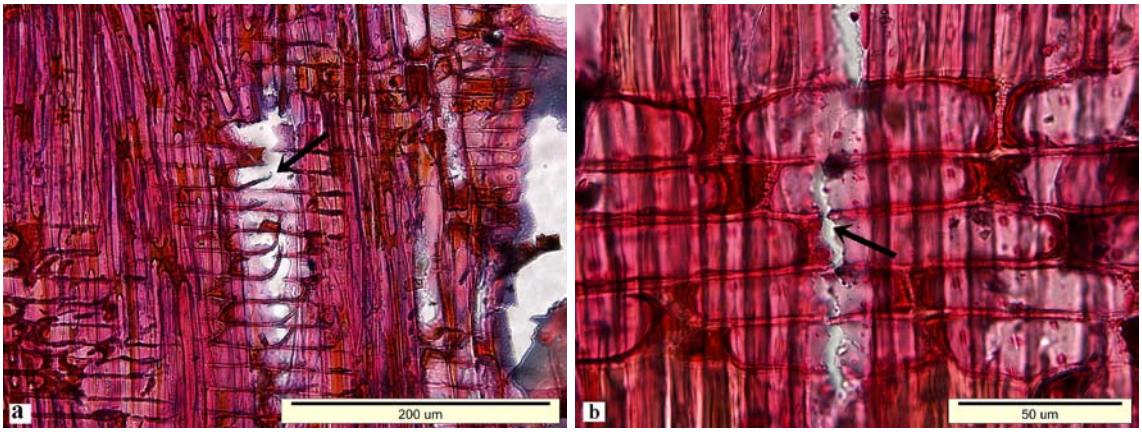

Fig 5. a) Ruptures on cross-field pits and ray parenchyma in Group A, b) Longitudinal ruptures on cross-pitting and ray parenchyma in Group B.

Tangential Section

Cell wall degradation in ray parenchyma in Group A and cracks between ray parenchyma were occurred in Group B were observed (Fig 6). No visible cracks and deformation were in fibre cells.

Fig 5.a) Deformation in ray parenchyma cells in Group A, b) Cracks between ray parenchyma cells in Group B.

Conclusions

The influences of varying temperature (150 ºC and 180 ºC) and press pressure (2 MPa) on the anatomical structure on thermally compressed solid-wood panels were investigated. Microscopic investigations showed that deformations were on axial parenchyma and vessel cell walls. The results show that the same pressure level has much more effect in the wood deformation at higher temperatures.

The wood exhibited much degradation in Group B (180 ºC – 2 MPa), vessel cell walls were all degraded and axial parenchyma were collapsed.

Tabarsa and Chui (2001) stated that when radial compression to aspen, the weakest elements (vessels) exhibited the most deformation in the elastic regime. With increasing compressive load, deformation in the vessels increased until they collapse.

Determination of changes in anatomical structure of wood is important for the development of a new product by means of using wood modification methods. Wood species show specific anatomical properties all modifications affect them differently. Therefore, it is important to know the effects of modification methods on the anatomical properties of wood species.

References

Awoyemi, L., and Jones, I.P. 2010. Anatomical explanations for the changes in properties of western red cedar (*Thuja plicata*) wood during heat treatment, Wood Science and Technology DOI 10.1007/s000226-010-0315-9

Boonstra, M.J., Rijsdijk, J.F., Sander, C., Kegel, E., Tjeerdsma, B., Militz, H., Acker van, J., and Stevens, M. 2006. Microstructural and physical aspects of heat treated wood. Part 1 Softwoods, Maderas. Ciencia y tecnologia 8(3), 193-208.

Dogu, D., Tirak, K., Candan, Z., and Unsal, O. 2010. Anatomical Investigaton of Thermally Compressed Wood Panels, BioResources 5(4), 2640-2663.

Fengel, D., and Wegener, G. 1989. Wood Chemistry Ultra Structure Reactions, Walter De Gruyter

Persson, M.S., Johansson, D., and Morén, T. 2006. Heat Treatment of solid wood: Effects on absorption, strength and color, Doctoral Thesis Paper V, Effect of heat treatment on the microstructure of pine, spruce and birch and the influence on capillary absorption, Luleå University of Technology, LTU Skellefteå, Division of Wood Physics.

Tabarsa, T., Chui, Y., H. 2001. Characterizing Microscopic Behavior of Wood Under Transverse Compression. Part II. Effect of Species and Loading Direction, Wood and Fiber Science, 33(2), pp. 223-232.

Terziev, N., and Daniel, G. 2002. “Industrial kiln drying and its effect on microstructure, impregnation and properties of Scots pine timber impregnated for above ground use. Part 2. Effect of drying on microstructure and some mechanical properties of Scots pine wood, Holzforschung 56(4), 434-439.

Tensile Properties Of Bamboo Units In Different Sizes

Wang Ge[1], *Chen Hong*[1], *Yu Zi-xuan*[1], *Sheldon Q. Shi*[2],

Cheng Hai-tao[1], *Qiu Ya-xin*[1]

[1]International Center for Bamboo and Rattan, Beijing, 100102, China

[2]Mechanical and Energy Engineering, University of North Texas, Denton, TX

76203-1277, USA

Abstract

The objective of this study was to effect of specimen size on the mechanical properties. Both single bamboo fibers and bamboo fiber bundles isolated chemically and mechanically were tested. The tensile strength of chemically macerated single bamboo fiber was 47.58% higher than that of fibers isolated mechanically. Meanwhile, tensile strength and tensile modulus of chemically macerated fiber bundles were over 2.10 times and almost 1.43 times higher than that of the mechanically isolated ones. As both chemically macerated, fiber bundles' tensile strength, decreased by 65.73%, tensile modulus by 12.25%, and elongation by 9.69%, comparing with single fibers. For mechanical isolation, tensile strength, tensile modulus and elongation of fiber bundles were 68.81%, 52.34% and 60.93% lower than that of single fibers, respectively. Compared with single bamboo fibers and bamboo fiber bundles, the tensile strength of bamboo strips reduced by 81.72% and 41.38%, whereas tensile modulus decreased by 57.25% and 10.30%, respectively. And mechanical properties of bamboo strips were lower than that of samples made from outer portion of the bamboo but higher than that of samples made from inner portion of the bamboo. In the tensile properties were different among single bamboo fibers, bamboo fiber bundles and bamboo strips. The smaller the specimen size, the higher the tensile properties. It was shown that the tensile strength, tensile modulus and elongation reduced increasingly, and those decreasing levels were more significant when fibers were isolated mechanically.

Keywords: single bamboo fibers, bamboo fiber bundles, bamboo strips, mechanical property, changing regularity

Introduction

Bamboo resource is abundant in the world, especially in China. With the growing market for bamboo in China, bamboo units in different sizes, such as single bamboo fibers, bamboo fiber bundles and bamboo strips, are becoming the primary feedstock in the paper making, textile, and fiber-based composite. The mechanical performance of products in such fields is highly dependent on the properties of bamboo units. To improve utilization and manufacture of bamboo materials, there is an increasing need for more detailed knowledge regarding mechanical properties and relations between bamboo units in different sizes.

Jayne (1959) tested the mechanical properties of earlywood and latewood fibers from 10 gymnosperm species. It was found that fibers were generally Hookean in nature, displaying a proportional stress-strain relationship. Kersavage (1973) obtained the average tensile stress and modulus of Douglas fir fibers as 0.85 GPa - 0.91 GPa and 23.60 GPa - 24.50 GPa, respectively. Mott et al. (2002) investigated the variations in mechanical properties of individual southern pine fibers and compared engineering properties of earlywood and latewood tracheids with respect to the tree height and juvenility. Groom et al.(2002) reported the definition of juvenile, transition and mature zone as classified by fiber stiffness, strength, microfibril angle, and cross-section area. Subsequently, Burgert et al. (2005) compared the tensile properties of mechanically and chemically isolated spruce fibers by micro-tensile investigation. Recently, Yu et al. (2011) presented an improved technique for single plant fiber characterization, which is easy to conduct, and the results are more accurate.

Zhai et al. (2012) investigated the mechanical properties and structures of windmill palm fiber bundles, and found that the fiber bundles from the inner layer of windmill palm showed higher tensile strength (0.11 GPa) and Young's modulus (1.25 GPa) than that from the other layers.

Recently, many studies have been conducted on the mechanical properties of bamboo strips. Wang (2003) explored that the fracture mechanism of bamboo / Chinese fir composite in bending and shearing tests by observing the images obtained by SEM. For longitudinal 3-point the bending and shearing strength test, the failure form if the composite was crack at tangential direction in Chinese fir or bamboo themselves under the air-dry condition, and the glue line was not breakage. But after water soaked, the failure form of the composite was peeled out at the glue interface between Chinese fir or bamboo and adhesive. Li (2009) studied the tensile properties of bamboo using the digital speckle correlation method (DSCM) and discovered that the mechanical properties of bamboo were lower than that of bamboo fibers because of the slips occurred between fibers when factures happened.

In this paper, the effect of bamboo element sizes (single bamboo fibers, bamboo fiber bundles and bamboo strips) and the isolation method (chemically and mechanically) are investigated. In two previous papers (Wang, 2011; Chen, 2011), four single plant fibers, including single

bamboo fibers, single Chinese fir fibers, single kenaf fibers and single ramie fibers, were tested. The single bamboo fibers shown higher tensile stress, 1.78 GPa, other three tensile stress were 1.26 GPa, 1.02 GPa, 1.00 GPa, respectively. Therefore Cizhu bamboo were chosen as material in our research.

Methods

Samples Preparation

Materials were from the 1-yr-old Cizhu bamboo (*Neosinocalamus affinis*) grown in Chengdu, Sichuan province, China, with an initial moisture content of 8-12%.

Single bamboo fibers were isolated both chemically and mechanically. The bamboo samples were cut into strips (20 mm longitudinally and 2×2 mm in cross-section), and immersed in the chemical solution at a temperature of 60℃ for 42 h to separate. The other bamboo fibers were isolated mechanically using tweezers from 90-um-thick tangential slices after being softened with about 40 h of hot water treatment.

Bamboo fiber bundles: Bamboo fiber bundles were also isolated chemically and mechanically. Bamboo strips (15x 4×2 cm (length x width x thickness) were immersed in alkaline solution for being soften, then were isolated using a comb. The mechanically isolated bamboo fiber bundles were obtained using tweezers from the strips being fibrillated 6 times in the instrument designed at International Center for Bamboo and Rattan. In our previous studies, it was found the tensile strength of bamboo strips fibrillated 4-8 times were stable keeping between 0.09 GPa and 0.10 GPa. Although the tensile strength was 47.6% lower than that of bamboo strips without fibrillation treatment, the bamboo strips fibrillated 4-8 times was well distributed and suited to be used as primary units in the process of bamboo based composites. The strips being fibrillated 6 times were chosen for this study.

The bamboo strips were selected between 4-6 m from the bottom of the trunk. Tensile samples, including bamboo strip, outside of bamboo strip and inside of bamboo strip, were cut into a dog born shape in accordance with requirements described in GB/T 15780-1995 as shown in Figures 1 and 2 using a laser cutting machine (CMA-6040, Guangdong, China).

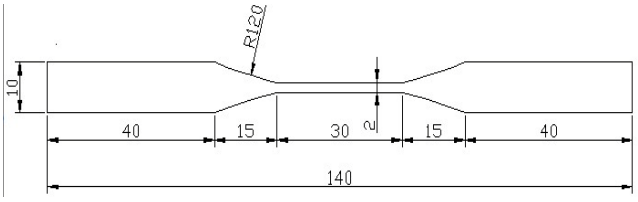

Figure 1. Bamboo strip sample

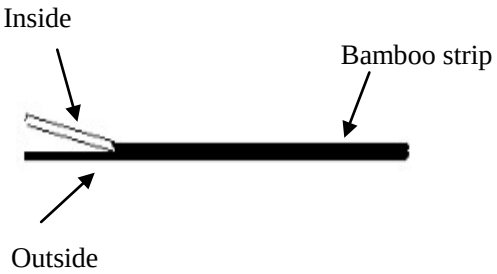

Figure 2. Bamboo samplemaking

Tensile properties testing

Testing of single bamboo fibers: Tensile strength testing of the single bamboo fibers was conducted following the testing procedure described by Cao (2010). In brief, the fibers were first glued on an organic, channeled glass with one droplet of glue in each end, and then placed in an oven at 60℃ for 24 h followed by 22℃for at least 24 h. The tensile testing of the single fibers was conducted with newly designed instrument (SF-Microtester I) located at the International Center of Bamboo and Ratten, Beijing, China. A constant strain rate of 48 um/min was set at 25 ℃ and 20% RH. Fibers were removed from the tensile apparatus immediately upon failure and saved for subsequent cross-sectional area measurement with a confocal laser scanning microscope (CLSM; Zeiss, LSM 510 Meta, Germany) for tensile modulus and strength calculations, Figure 4 (a). Ten samples were tested for chemically and mechanically isolated single bamboo fibers.

Testing of bamboo fiber bundles: Bamboo fiber bundles were glued onto an organic, channeled glass designed to carry the fiber bundles and to be easily fixed with one droplet of glue in each end (Fig. 3). The free length of the fiber bundles were about 10 mm. Before the testing, the samples should be kept at the room temperature for at least 3 h for glue droplet solidifying. The tensile testing of single fibers was conducted at a high-resolution commercial mechanical tester (Microtester 5848, Instron, USA) with a constant strain rate of 48 um/min in the room environment (25 ℃ and 20% RH). To calculate tensile stress and modulus of bamboo fiber bundles, the cell wall cross section-sections were determined. The tested fibers were stained with a dilute concentration of acridine orange, attached to a glass slide and covered with a number 1 cover slip. The images of cell wall cross section were obtained by CLSM and the areas were calculated by the software in the CLSM (Fig. 4 (b). Six samples were tested.

Figure 3. Typical images pf bamboo bundle samples

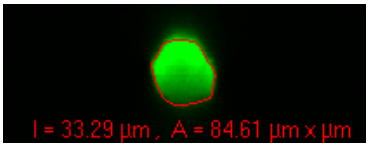

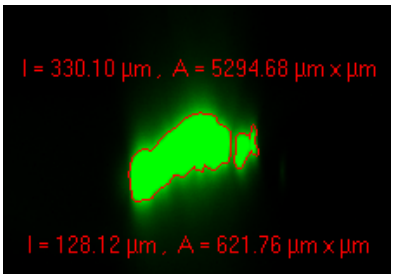

(a) cross section of single bamboo fiber (b) cross section of bamboo fiber bundle
Figure 4. Typical CLSM images of area of cross section

Testing of bamboo strip: The testing of bamboo strip was performed by a high-resolution commercial mechanical tester (Microtester 5848, Instron, USA) with the strain rate at 2 mm/min at a ambient environment of 25℃and 55% RH. Ten samples were tested for each types.

Results and Discussion

Tensile Properties of Single Bamboo Fibers

Table 1
Tensile properties of single bamboo fibers isolated by different methods (TS - Tensile Strength, TM - Tensile Modulus, E - Elongation)

Single Bamboo Fibers	T S/GPa(CV)	TM/GPa(CV)	E/%(CV)
Chemically Isolated	1.77(0.15)	26.85(0.06)	2.89(0.16)
Mechanically Isolated	0.93 (0.19)	34.62(0.17)	4.30(0.17)

Tensile properties of single bamboo fibers isolated chemically and mechanically are shown in Table 1. Isolation methods affected the mechanical properties of single bamboo fibers significantly. Tensile strength of chemically isolated fibers was higher than that of mechanically isolated fibers, whereas the modulus and elongation were lower.

An analysis of the chemical component of the fibers was conducted by FT-Raman spectra to explain why the tensile strength of fibers isolated chemically was higher while the modulus and elongation was lower comparing with the fibers isolated mechanically. In Fig. 5, the most intense band in the fingerprint region at 1600 cm^{-1} for mechanically isolated fibers, attributing to aryl ring stretching and aryl ring symmetric vibration, meant the existence of lignin. Big differences were observed in the fingerprint regions, with the absence of the peak at 1600 cm^{-1} for chemically isolated fibers. Therefore, we can conclude that lignin degradation happened in the chemically isolated fibers. Zhang (2011) found that the tensile strength of single Chinese fir fibers increased, while the modulus and elongation decreased when the lignin content was reduced.

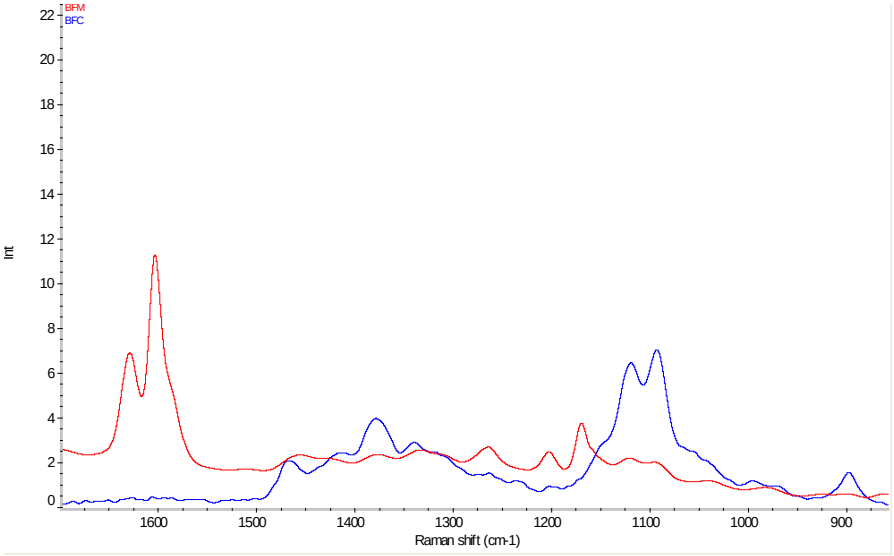

Figure 5. FT-Raman spectra of single bamboo fibers isolated chemically and mechanically in the fingerprint area. (BFC- bamboo fiber isolated chemically, BFM- bamboo fiber isolated mechanically)

Table 2
Assignment of bands in the FT-Raman spectrum of cell wall polymers(Agarwal, 1997)

	Wavenumber(cm-1)	Band assignment
Lignin	1600	Aryl ring stretching,symmetric
	895	HCC and HCO bending at C6
Cellulose	1377	HCC,HCO and HOC bending
	1456	HCH and HOC bending
Carbohydrates	1095	CC and CO stretching

The cell wall structure model established by Boyd (1982)allowed for an essentially lamellar distribution of cellulose, but a non-lamellar distribution of lignin. Neighboring cellulose fibrils linked to each other and formed the disc-shaped openings filled up with matrix made up of hemicellulose and lignin. With the degradation of cellulose in the cell wall, cellulose fibrils aggregated more and connected each other more in longitudinal direction, which increased fracture resistant. Meanwhile, Chen (2011) also found that the cross section area of mechanically isolated fibers was smaller comparing with those isolated chemically. On the other hand, no fracture is observed (Fig. 6(a) on the surface of fiber isolated chemically, while predominant plane fractures were (Fig. 6 (b) produced when the fiber was peeled with fine tweezers, which may be another reason for the lower tensile strength of mechanically isolated fibers.

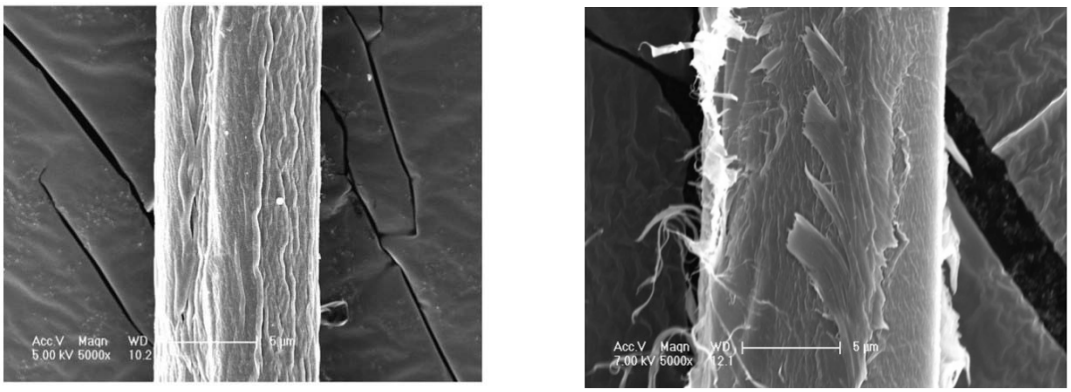

(a) Fibers isolated chemically *(b) Fibers isolated mechanically*

Figure 6. ESEM images of single bamboo fibers isolated differently（Chen, 2011）

Tensile Properties of Bamboo Fiber Bundles

It is seen from Table 3 that tensile strength, modulus and elongation of chemically isolated bamboo fiber bundles were all higher than that of mechanically isolated bamboo fiber bundles.

Table 3
Tensile properties of bamboo bundles made by different methods

Bamboo Fiber Bundles	TS/Gpa（CV）	TM/GPa（CV）	E/%（CV）
Chemically Isolated	0.61（0.37）	23.56（0.35）	2.61（0.32）
Mechanically Isolated	0.29（0.71）	16.50（0.42）	1.68（0.31）

For the chemical isolation process, the first alkali treatment lead to a large removal of lignin (Xu, 2006). This process, removed part of lignin-rich middle lamella, which reduced the damage caused by the comb. In contrast, bamboo fiber bundles isolated mechanically (fiber bundles were peeled with tweezers from fibrillated bamboo strips) was damaged more directly in middle lamella and single bamboo fibers in the fiber bundles. In addition, the failures happened near the glue droplet of the mechanically isolated bamboo fiber bundles were much more comparable to the fiber bundles isolated mechanically. That also revealed that the mechanical isolation caused more damage because of the stress concentration.

Tensile Properties of Bamboo Strip

As shown in Table 4, the tensile strength and modulus along the grain direction of samples made from outer portion of bamboo were nearly double compared to those made from the inner portion of bamboo, while the tensile strength and modulus of bamboo strips were higher than that of samples made from outer portion of the bamboo but lower than that of samples made from inner portion of the bamboo.

Table 4
Tensile properties of bamboo strips (BS — bamboo strips, IBS —inside of bamboo strips , OBS — outside of bamboo strips)

Samples	TS/GPa(CV)	TM/GPa(CV)	E/%(CV)
BS	0.17 (0.34)	14.80 (0.12)	--
OBS	0.20 (0.21)	18.40 (0.17)	--
IBS	0.11 (0.27)	10.60 (0.07)	--

The structure of bamboo is mainly responsible for such results. Bamboo can be considered as a natural composite. The cells in bamboo can be classified into two types: 1)the cell in basic tissues for transmitting load which has high tensile strength, low modulus and low density; 2) vascular bundles structurally consisting of fibers, lignified vessels and etc. The fibers in vascular bundles, with high tensile strength, modulus and density, are the main component responsible to the mechanical properties of bamboo (Zhao, 2002). Vascular bundles were surrounded in the basic tissues and decreased from inner to outer portions of the bamboo, which meant the fibers in outer portion of bamboo was more comparable to those from the inner portion of bamboo as shown in Figure 7 (Jiang, 2002). The amount of vascular bundles determined the mechanical properties of bamboo, more vascular bundles higher tensile strength and modulus (Amada, 1997).

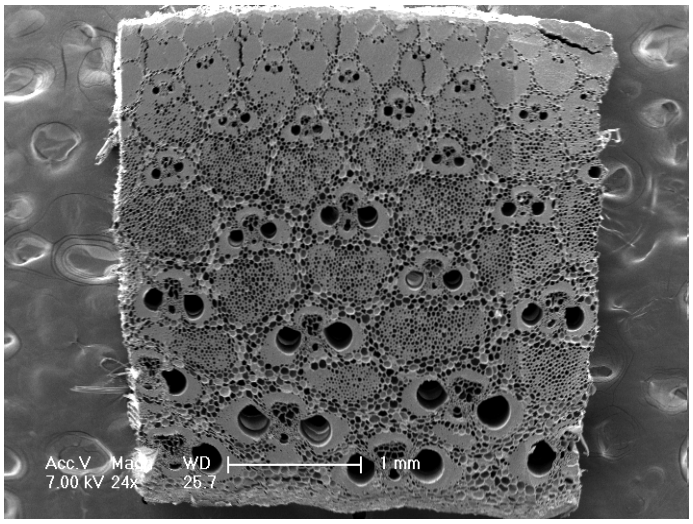

Figure 7. Distribution of vascular bundles in the cross-section of bamboo strip

During the test, shear failure happened first at one end of most samples, followed by the tensile failure. Most of the specimens that in shear failures were those made from the outer portion of the bamboo. Most of the specimens that failed in tension were those made of the inner portion of bamboo. Generally speaking, that strength of the specimen that in shear failure is higher than that failed in tension.

Relationship of Tensile Properties Between Bamboo Units in Different Sizes

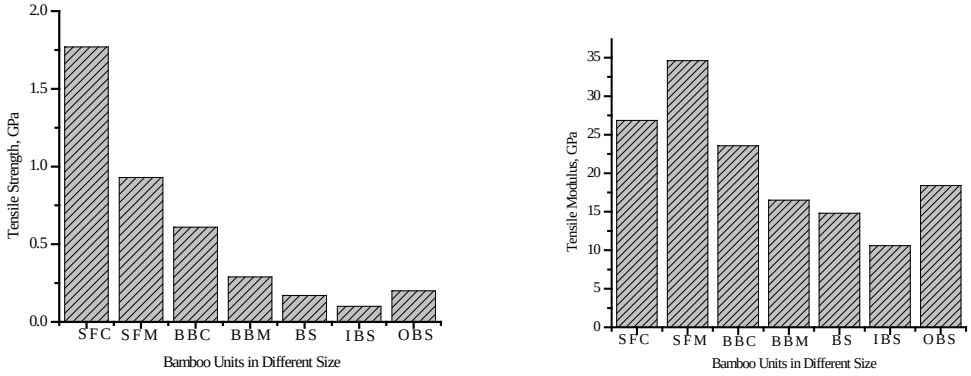

Figure 8. Regularity of tensile properties of bamboo units in different sizes (SFC — single fibers isolated chemically, SFM — single fibers isolated mechanically, BBC — bamboo bundles isolated chemically, BBM — bamboo bundles isolated mechanically, BS — bamboo strips, IBS —inside of bamboo strips, OBS — outside of bamboo strips)

The average tensile strength, modulus and elongation of single bamboo fibers isolated chemically were 1.78 GPa, 23.56 GPa, and 2.89%, respectively. For the fibers isolated chemically, the tensile strength of the bamboo fiber bundle , decreased by 65.73% compared to the bamboo single fibers, the modulus by 12.25% , and the elongation by 9.69%. For the mechanically isolated single bamboo fibers, an average tensile strength of 0.93 GPa, an average modulus of 34.62 GPa and an average elongation of 4.3% were obtained as shown in Figure 8. For both chemically macerated bamboo fiber bundles and single bamboo fibers, tensile strength, modulus and elongation of bamboo fiber bundles were obtained as 68.81%, 52.34% and 60.93%, respectively, which were lower than that of single bamboo fibers. It was attributed to most failures happened in the tissues between the single fibers. This phenomenon was also illustrated by the shapes of failures shown in Figure 9, Shao (2009) studied the behaviors of Mode I (crack opening mode) interlaminar fracture parallel to grain of moso bamboo and observed the crack propagation developed along the longitudinal interface between fibers or ground tissue indicating that the longitudinal interface strength was weak among bamboo cells.

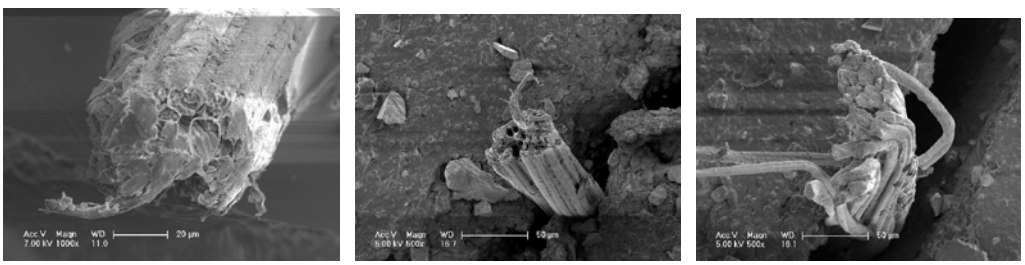

Figure 9. Typical ESEM images of fracture modes of bamboo fiber bundles

As shown in Figure 10, some bamboo fiber bundles contain parenchyma with lower tensile

strength in comparison with the single bamboo fibers (Shao, 2009). As the existence of weak interface among the parenchymas, the crack propagation easily happened resulting in ultimate failure (Tian, 2012).

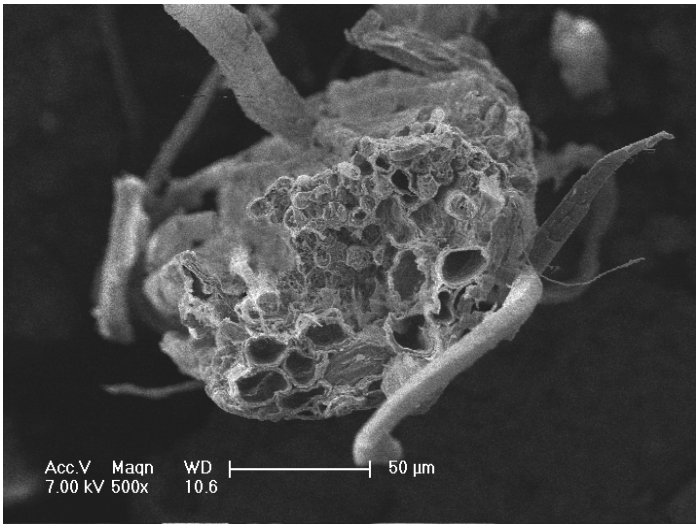

Figure 10. Typical ESEM images of parenchyma cell in the bamboo bundles

The isolation method also affected the mechanical properties of the fiber. For both single bamboo fibers and bamboo fiber bundles, the chemical treatment caused less reduction of the properties compared to the mechanical one.

As shown in Figure 8, the tensile strength of bamboo strips reduced by 81.72% compared to the single fiber, and 41.38% compared to the fiber bundle, whereas the modulus decreased by 57.25% copared to the single fiber, and 10.30% compared to the fiber bundle. And percent loss of tensile strength was more than that of modulus. Bamboo is made up of vascular bundles with basic tissue in between, where the interface is weak (Shao, 2007). Crack propagation first happened in basic tissue area when the stress was just enough to cause a crack. With adding more stress, slips would happen on the interface between bamboo fiber bundles and basic tissue, then cracks would appear on the other weak interface. In the end, the bamboo fiber bundles were pulled out slowly from basic tissue (Tian, 2012). Compared with single bamboo fibers and bamboo fiber bundles, there are many multi-scale weak interfaces in bamboo that lead to a huge decrease of mechanical properties.

Conclusions

The mechanical properties of bamboo units in different sizes (single bamboo fiber, bamboo fiber bundles and bamboo strips) were characterized. The fibers obtained from two isolation methods were compared. For the single bamboo fibers, the tensile strength of chemically isolated samples is higher than that of mechanically isolated ones, whereas the modulus and elongation are lower. For the bamboo fiber bundles, the tensile strength, modulus and elongation of chemically treated samples are higher comparing with the mechanically isolated

ones.

Relationships of the mechanical properties of bamboo units as a function of bamboo sizes were established. For the bamboo strips, the tensile strength and modulus were lower than that of samples made from the outer portion of than bamboo but higher than inner portion of the bamboo. For the chemical isolated fiber, the tensile strength of the bamboo fiber bundle was decreased by 65.73% compared to that of the single fiber, modulus by 12.25%, and elongation by 9.69%. For both isolated mechanically single bamboo fibers and bamboo bundles, the tensile strength, modulus and elongation of bamboo fiber bundles were 68.81%, 52.34% and 60.93% lower than that of single bamboo fibers, respectively. In addition, the mechanical properties of bamboo fiber bundles with chemical treatment decrease more comparing to fiber bundles isolated mechanically. Compared with the single bamboo fibers and bamboo fiber bundles, the tensile strength of bamboo strips reduced by 81.72% and 41.38%, respectively, whereas the modulus was reduced by 57.25% and 10.30%, respectively.

References

Agarwal U P, Ralph S A. FT-Raman Spectroscopy of wood: identifying contributions of lignin and carbohydrate polymers in the spectrum of black spruce (*Picea mariana*). Applied Spectroscopy. 51: 1648-1655.

Amada S, Ichikawa Y, Munekata T, et al. 1997. Fiber texture and mechanical graded structure of bamboo. Composites Part B, 28: 13-20.

Boyd J D. 1982. An anatomical explanation for visco-elastic and mechanosorptive creep in wood, and effects of loading rate on strength. In: New Perspective in Wood Anatomy. Ed. Bass, P. Martinus Nijhoff/Dr W Junk Publishing, La Hague. 172-222.

Burgert I, Keckes J, Fruhmann K et al. 2002. A comparison of two techniques for wood fibre isolated-evaluation by tensile tests on single fibres with different microfibril angle. Plant Biology. 4: 9-12.

Burgert I, Eder M, Fruhmann K etal. 2005. Properties of chemically and mechanically isolated fibres of spruce (Picea abies [L.] Kart.). Part 3: Mechanical characterisation. 59: 354-357.

Cao S P. 2010. The measurement and evaluation of tensile properties of plant individual fibers. MS thesis, Chinese Academy of Forestry, Beijing, China.14-16 pp.

Chen H, Wang G, Cheng H T. 2011. Properties of single bamboo fibers isolated by different chemical methods. Wood Fiber and Science. 43 (2): 111-120.

Groom L, Shaler S, Mott L. 2002. Mechanical properties of individual southern pine fibers. Part III. Global relationship between fiber properties and fiber location within and individual tree. Wood and Fiber Science.34 (2):238-250.

Jayne. B.A. 1959. Mechanical properties of wood fibers. Tappi. 42 (6):461-467.

Jiang Z H. 2002. Bamboo and rattan in the world. Liaoning, Liaoning Science and Technology Press, 27 pp.

Kersavage P C. 1973. A system for automatically recording the load-elongation characteristics

of single bamboo fibers under controlled relative humidity conditions. USDA. U.S. Government Printing Office.

Li X Z. 2009. Research on mechanical and failure properties of moso bamboo. PhD dissertation. Chinese Academy of Forestry, Beijing, China. Pp45-53.

Mott L, Groom L, Shaler S. 2002. Mechanical properties of individual southern pine fibers. Part II. Comparison of earlywood and latewood fibers with respect to tree height and juvenility. Wood and Fiber Science.34 (2):221-237.

Shao Z P. 2007. Wood damage-fracture and wood meso-damage elements. Scienc Silvae Sinicae. 43 (4):107-110.

Shao Z P , Fang C H, Tian G L. 2009. Mode I interlaminar fracture property of moso bamboo (*Phyllostachys pubescens*). Wood Science and Technology.43 (5-6):527-536.

Tian G L, Jiang Z H, Yu Y et al. 2012. Study on the toughness mechanism of bamboo by in-situ tension. Journal of Beijing Forestry University.

Wang G. 2003. Moso bamboo/Chinese fir laminated composite and its properties. PhD dissertation. Chinese Academy of Forestry, Beijing, China. 48-53 pp.

Wang G, Shi S, Wang J W et al. 2011. Tensile of four types of individual cellulosic fibers. Wood and Fiber Science. 43 (4): 1-12.

Xu W, Tang R C. 2006. Extracting natural bamboo fibers from grude bamboo fibers by caustic treatment. Biomass Chemical Engineering. 40 (3): 1-5.

Yu Y, Jiang Z H, Fei B H, et al. 2011. An improved microtensile technique for mechanical characterization of short plant fibers: a case study on bamboo fibers. Journal of Materials Science. 46: 739-746.

Zhao R J， Yu Y S. 2002. Technology of Bamboo Board. Beijing: China Forestry Press, 1-8.

Zhang S Y. 2011. Chemical components effect on mechanical properties of wood cell wall. PhD dissertation. Chinese Academy of Forestry, Beijing, China.48-55 pp.

Zhai S C, Li D G, Pan B, et al. 2012. Tensile strength of windmill palm (Trachycarpus fortunei) fiber bundles and its structural implications. Journal of Material Science. 47: 949-945.

Acknowledgment

This work is funded by the key technology of making large span bamboo engineering structural component (201204701). Also, Dr. Lin kindly assisted with preparing the manuscript. The constructive comments from the anonymous reviewers are greatly appreciated.

Research on Inhibition Effect of MDF Pyrolysis Condensate Liquids against Two Kinds of Fungi

Shihua Chen

Yongshun Feng

Sijin Li

Jun Mu

College of Materials Science and Technology, Beijing Forestry University,

Beijing, China

Abstract

Medium density fiber board pyrolysis condensate liquid with nitric compounds in it can be used as fungal inhibitor. Fungal experiments to test the fungicidal effectiveness against white rot fungus *Coriolus versicolor* and brown rot fungus *Gloeophyllum trabeum* of medium density fiber board pyrolysis condensate liquids obtained under different pyrolysis conditions were carried out. In the experiment, wood vinegar and bamboo vinegar were served as reference for comparison. Liquids components were analyzed by gas chromatography mass spectrometry. The result showed that medium density fiber board pyrolysis condensate liquids had obvious inhibition to both of the fungi. The inhibition rate was up to 52.64% against *Coriolus versicolor* and up to 27.02% against *Gloeophyllum trabeum.* The antifungal activity of medium density fiber board pyrolysis condensate liquid was better than wood vinegar and bamboo vinegar. Gas chromatography mass spectrometry analysis showed that there are more nitric compounds and less acids, phenols and ketones in medium density fiber board pyrolysis condensate liquid than wood vinegar. According to the results of fungal experiments and components analysis, pyrolysis condensate liquids had better antifungal effects with more nitric compounds. Pyrolysis condensate liquid of waste medium density fiber board will be a valuable material to develop with good antifungal effect.

Key words: MDF, pyrolysis liquids, antifungal activity, GC-MS analysis.

Introduction

Wood products play important role in our lives. According to statistics of State Forestry Bureau, the production of wood-based panel of 2011 is 1.6543×10^8 m^3, a 7.7 % increase as compared with that of 2010. In this situation, how to deal with the waste wood-based board becomes an issue that should be focused (Chen et al. 2007). Pyrolysis is believed to be a promising and effective way to reuse waste wood-based board and is friendly to the environment. However, the pyrolysis process of waste wood-based board is not the same as conventional biomass. Adhesive in waste wood-based board influences the pyrolysis process and products (Girods et al. 2007).

According to previous studies, the liquid products of pyrolysis of wood and bamboo have extensive applications. Wood vinegar has been found to have the function of promoting plant growth, antibacterial, anti-corrosion and can be used for wood preservation (Wang et al. 2004). There are some differences between medium density fiber board (MDF) pyrolysis condensate liquid and wood vigenar in composition and propeties. The pyrolysis liquids of MDF are weak alkaline because of the existence of nitrogen-containing compounds (Mu et al. 2011). The liquids can be used as basic solvents and additives in pesticides and in many other ways. A study on characteristic and bio-efficiency of the pyrolysis liquids from wood, particleboard, plywood and fiberboard showed that the inhibition of these liquids on the fungi were different due to different compositions (Nakai et al. 2007).

In this paper, fungal experiments to test the fungicidal effectiveness against white rot fungus *Coriolus versicolor* and brown rot fungus *Gloeophyllum trabeum* of MDF pyrolysis condensate liquids obtained under different pyrolysis conditions were carried out. In the experiment, wood vinegar and bamboo vinegar were served as reference for comparison. Liquids components were analyzed by gas chromatography mass spectrometry (GC-MS). This study could be a basic research for a further study of the possible application of the pyrolysis liquids.

Materials and Methods

Preparation of Samples

Adhesive contained in MDF was mainly urea formaldehyde (UF) resin. MDF pyrolysis liquids samples were obtained from pyrolysis at final temperature fixed at 300℃, 400 ℃, 500 ℃, 600 ℃with the heating rate of 100 ℃/h and 150 ℃/h respectively. MDF(500/150) referred to MDF pyrolysis condensate liquid obtained at final temperature of 500 ℃ with heating rate of 150 ℃/h in the following paragraphs. Wood vinegar and bamboo vinegar were provided by manufactory.

Fungal Experiments

Potato dextrose agar (PDA) medium was autoclaved for 15 min at 121 ℃, 103.4 kPa. Then the pyrolysis liquid was diluted in PDA medium to a concentration of 0.5%. The mixture was poured into Petri dish (80 mm diameter) and left in Horizontal laminar flow table for cooling. The Petri dish was then centrally inoculated with a 5 mm fresh plug of fungi (7 days old). Petri dish with PDA medium only was used as control. Three replicates were set up for all tests and controls. All cultures were incubated in a incubator at 25℃until the growth of the fungi in the controls had reached the edge of the Petri dishes.

The colony diameter was measured and the inhibition was calculated according to the following equation:

$$I=[(C-T)/C]\times 100\%,$$

where I is the inhibition(%), C is the colony diameter of mycelium from control Petri dishes(mm) and T is the colony diameter of mycelium from the Petri dishes containing the liquids(mm) (Kartal et al. 2011).

GC-MS Analysis

Samples prepared from pyrolysis liquids were qualified by GC-MS. A column (RTX-5) with a diameter of 0.25 mm and length of 30 m was maintained at 50 °C for 5 min, then the temperature was raised to 280 ℃at a heating rate of 10 ℃/min and held at 280 ℃for 20 min. Nitrogen was used as carrier gas. The injection (injection volume of 1.0 μl) was performed at 280 ℃in the split mode (20:1). The mass spectrometer was operated in the electron ionization (EI) mode with ionization energy of 70 eV.

Results and Discussion

Bio-efficiency of Pyrolysis Liquids

The inhibition effects of MDF pyrolysis condensate liquids against white rot fungus *Coriolus versicolor* and brown rot fungus *Gloeophyllum trabeum* are shown in Figure 1 and 2 with wood vinegar and bamboo vinegar as contrast. The result showed that MDF pyrolysis condensate liquids had obvious inhibition to both of the fungi. The inhibition effects on *Coriolus versicolor* of all the three kinds of pyrolysis liquids were better than that on *Gloeophyllum trabeum*.

The inhibition rates against white rot fungus *Coriolus versicolor* and brown rot fungus *Gloeophyllum trabeum* of pyrolysis liquids obtained under different pyrolysis conditions are shown in Figure 3 and 4. The antifungal activity of MDF pyrolysis condensate liquid was

better than wood vinegar and bamboo vinegar with the inhibition rate up to 52.64% against *Coriolus versicolor* and up to 27.02% against *Gloeophyllum trabeum.* For MDF, pyrolysis liquids obtained at final temperature of 500℃ and 600℃ had better antifungal effects than those obtained at temperature of 300 ℃and 400 ℃which could be attributed to more anti-fungal functional groups generated at that condition.

Figure 1 The inhibition effects against Coriolus versicolor of different kinds of pyrolysis condensate liquids

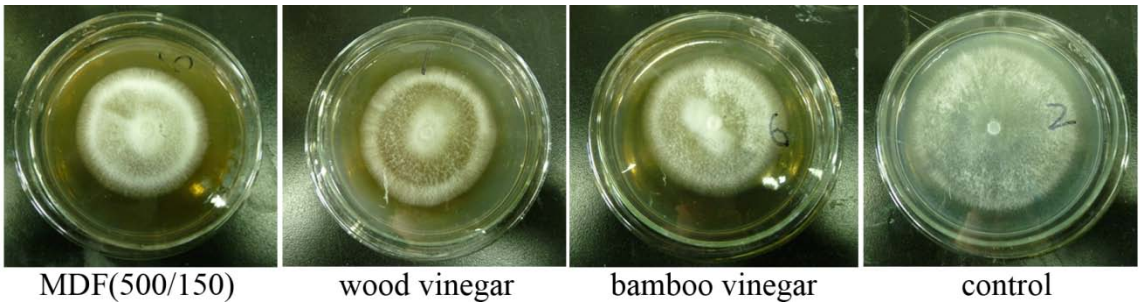

Figure 2 The inhibition effects against Gloeophyllum trabeum of different kinds of pyrolysis condensate liquids

Inhibitory effects in vitro of filtrates from biomass slurry fuel production on the growth of brown-rot and white-rot fungi suggested that higher concentrations of the filtrates are critical for inhibition and the filtrates contain some components such as phenolic compounds from lignin degradation for induction of antifungal activity against brown-rot fungi only (Kartal et al. 2004). In our experiment, the antifungal activity of MDF pyrolysis condensate liquids were better than wood vinegar and bamboo vinegar to both of the fungi. The inhibition effects on white-rot fungus of all the three kinds of pyrolysis liquids were better than that on brown-rot fungus.

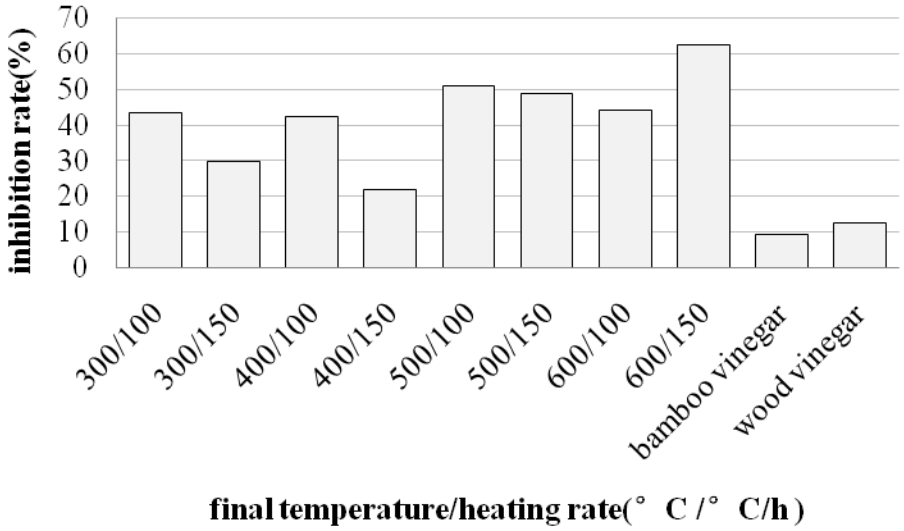

Figure 3 The inhibition rates against Coriolus versicolor of MDF pyrolysis condensate liquids obtained under different pyrolysis conditions

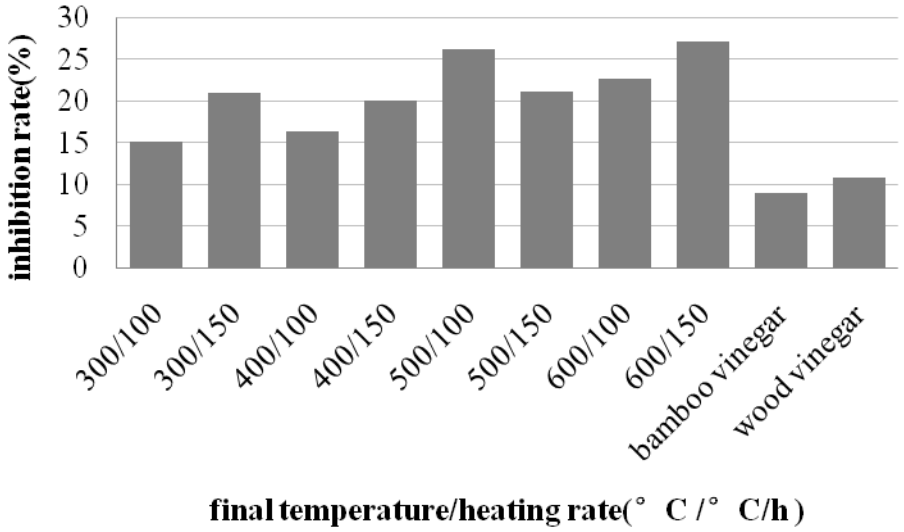

Figure 4 The inhibition rates against Gloeophyllum trabeum of MDF pyrolysis condensate liquids obtained under different pyrolysis conditions

Study of Pyrolysis Liquids Compositions

Main compositions of MDF(500/150) and wood vinegar analyzed by GC-MS are listed in Table 1. MDF pyrolysis condensate liquid contained more nitric compounds, sugars and alcohols than wood vinegar which was rich in acids, phenols and ketones. These linear and cyclic nitric compounds might be generated from decomposition and reaction in the pyrolysis process of UF resin added in the wood-based panel. The distinctive nitric compounds from MDF reveal the chemical interaction between UF resin and wood components. The detailed

chemical reactions now can not be well explained. Such nitric compounds make pyrolysis liquids of waste wood-based composites different from those of general biomass and will influence the utilization of pyrolysis liquids.

Table 1 Main compositions of pyrolysis condensate liquids analyzed by GC-MS

MDF(500/150)	Kinds	Relative content /%	Wood vinegar	Kinds	Relative content /%
Acids	2	34.23	Acids	2	64.46
Phenols	4	4.92	Phenols	5	7.27
Ketones	2	0.63	Ketones	12	9.23
Esters	4	5.14	Esters	4	5.68
Ethers	1	0.57	Aldehydes	2	2.38
Alcohols	1	6.02	Alcohols	1	2.67
Sugars	1	5.24	Sugars	1	0.88
Nitric compounds	11	13.09	Nitric compounds	1	0.72

The pyrolysis process of wood was very complicated, including the thermal degradation of cellulose, hemicellulose and lignin. Wood vinegar contained 16 kinds of ketones, 14 kinds of phenolic and other compounds like esters, aldehydes and alcohols besides the main components acetic acid (Xu et al. 2006). In addition, there are nitric components in wood vinegar like amine, methylamines, dimethylamine and pyridine of trace content (Wang et al. 2004). The result of this paper was in consistent with the mentioned studies and showed that pyrolysis liquids were influenced a lot by the nitric compounds transferred from UF resin.

Pyrolysis condensate liquids with different composition had different fungi inhibition effects. According to the results of fungal experiments and components analysis, we found that pyrolysis condensate liquids had better antifungal effects with more nitric compounds. Acidic environment is suitable for fungal growth. According to previous experiments, the pH of MDF pyrolysis condensate liquid was around 9 with nitric compounds in it while wood vinegar and bamboo vinegar were acidic (Mu et al. 2011). As shown in the antifungal l experimental results, the alkaline pyrolysis liquid had better fungi inhibition effect.

Conclusions

MDF pyrolysis condensate liquids had obvious inhibition to both white rot fungus and brown rot fungus. The inhibition rate was up to 52.64% against *Coriolus versicolor* and up to 27.02% against *Gloeophyllum trabeum.* The antifungal activity of MDF pyrolysis condensate liquid was better than wood vinegar and bamboo vinegar. GC-MS analysis showed that there were more nitric compounds and less acids, phenols and ketones in MDF pyrolysis condensate liquid than that in wood vinegar. According to the result of fungal experiments and components analysis, pyrolysis condensate liquids had better antifungal effects with more nitric compounds. Pyrolysis condensate liquid of waste MDF with good antifungal effect

would be a valuable material to develop.

References

Chen, Z.L., Fu, F., Ye, K.L. 2007. Present condition of wood resources utilization in china and technical measures of wood recycle. China Wood-based Panels. 5: 1-3.

Girods, P., Rogaume, Y., Dufour, A., Rogaume, C., Zoulalian, A. 2007. Low-temperature pyrolysis of wood waste containing urea–formaldehyde resin. Renewable Energy. 33: 648–654.

Wang, H.Y., Yang, G.T., Zhou, D. 2004. Research Situation and Comprehensive Utilization of Wood Vinegar. Journal of Northeast Forestry University. 32(5): 55-57.

Mu, J., Yu, Z.M., Zhang, D.R., Jin, X.J. 2011. Pyrolysis characteristics of disused composite panels and properties of its products. Journal of Beijing Forestry University. 33(1): 125-128.

Nakai, T., Kartal, S.N., Hata, T., Imamura, Y. 2007. Chemical characterization of pyrolysis liquids of wood-based composites and evaluation of their bio-efficiency. Building and Environment. 42: 1236-1241.

Kartal, S.N., Terzi, E., Kose, C., Hofmeyr, J., Imamura, Y. 2011. Efficacy of tar oil recovered during slow pyrolysis of macadamia nut shells. International Biodeterioration & Biodegradation. 65: 369-373.

Kartal, S.N., Imamura, Y., Tsuchiya, F., Ohsato, K. 2004. Preliminary evaluation of fungicidal and termiticidal activities of filtrates from biomass slurry fuel production. Bioresource Technology. 95: 41-47.

Xu, S.Y., Chen, J.J., Cao, D.R. 2006. Analysis of Components in Wood Vinegar. Guangzhou Chemistry. 31(3): 28-31.

Acknowledgements

This study was funded by National Natural Science Foundation of China (31170533).

High-level Expression and Characterization of Thermostable Esterase from *Thermoanaerobacter Tengcongensis* in *Escherichia coli*

Ruobing Deng, Xun Li*, Hong Gao, Fei Wang

China College of Chemical Engineering, Nanjing Forestry University,

Nanjing 210037, China

Jiangsu Key Lab of Biomass-Based Green Fuels and Chemicals,

Nanjing 210037, China

Abstract

A novel thermostable esterase from *Thermoanaerobacter tengcongensis* MB4T was successfully over-expressed in *Escherichia coli* and characterized. Two plasmids pET28a (T7 strong promoter) and pTrc99A (*trc* strong promoter) were used as the expression vectors. The results indicated that plasmid pTrc99A was more suitable for this esterase expression and the efficiency of the *trc* promoter for our analysis is much higher than T7 promoter. The recombinant esterase, having a molecular mass of 43 kDa determined with SDS-PAGE, was purified to homogeneity through heat treatment and DEAE-SepharoseCL-6B. The pTrc99A-est esterase showed maximum activities towards short-chain p-NP esters (C4). The esterase was optimally active at 70^0C (over 15 min) and at pH 7.5. It is highly thermostable, with a residual activity greater than 80% after incubation at 70^0C for more than 2 h.

Key words:
Esterase, over-expression, characterization, *Thermoanaerobacter tengcongensis, E.coli*

Introduction

Lipolytic enzymes (EC 3.1.1.x), represent a hydrolases group, which specifically works over carboxylic ester, and hence has a potentially broad spectrum of biotechnological uses. Lipolytic enzymes can be classified into three main groups: esterase/carboxylesterase (EC 3.1.1.1, carboxyl ester hydrolases), which prefer water-soluble substrates and catalyze the hydrolysis of glycerol esters with short acyl chain (≤10 carbon atoms) to partial gly cerides and fatty acids; true lipases (EC 3.1.1.3, triacylglycerol hydrolases), which display maximal activity towards water- insoluble long-chain triglycerides(≥10 carbon atoms); and various types of phospholipase (Arpigny et al. 1999, Pleiss, J. et al. 1998). The three-dimensional (3D) structures of both enzymes show the characteristic -hydrolase fold (David L. et al. 1992). Recently, esterase has been identified containing a Gly-x-x-Leu motif (Wei Y. et al. 1995) as well as enzymes showing high homology to class α/β-lactamases (Petersen et al. 2001).

Moreover, Esterase plays a major role in degradation of synthetic materials and the synthesis of optically pure compounds, perfumes, and antioxidants (Panda, T. et al. 2005). As applications for esterase are found in various fields, there are growing interest in this enzyme. Furthermore, the esterase in this report is not a true lipase but a novel thermostable esterase (Zhang, J. et al. 2003), which have been isolated from thermophilic organism, *Thermoanaerobacter tengcongensis* (Xue, Y. et al. 2001), and this kind of enzymes have been found a number of commercial applications because of their overall inherent stability (Demirijan, D. et al. 2001), such as the field of the petroleum, chemical and pulp and paper industries, for example, thermostable enzymes have been used for the elimination of sulphur containing pollutants through the biodegradation of compounds like dibenzothiophene (Bahrami, A. et al. 2001). Besides, the gene of this enzyme has been cloned and expressed in E.coli by using the plasmid pET23b as the vector (Zhang, J. et al. 2003), *E. coli* remains the most widely used host for recombinant protein expression. It is easy to transform, grows quickly in simple media, and requires inexpensive equipment for growth and storage. Different strategies like promoter strength (Boer, H. et al. 1983), Combination of plasmids (Khushoo, A. et al. 2005) were used to overcome the limitations.

In this work, we compared the expression of the thermostable esterase from *Thermoanaerobacter tengcongensis* cloned in two different plasmids pET28a (T7 strong promoter) and pTrc99A (*trc* strong promoter) in order to find a suitable plasmid for high-level expression of this esterase. As a result we found that pTrc99A (*trc* strong promoter) was more suitable for this esterase expression. Then we purified and characterized the esterase cloned in plasmid pTrc99A. This knowledge may be applied in the strategy for the selection of suitable plasmid for this esterase expression.

Results

Cloning and Overexpression of *Est* from *T. tengcongensis* in *E. coli*

Genomic DNA obtained from the *T. tengcongensis* was used as a PCR template. A DNA fragment of about 1100 bp length was obtained with PCR amplification with primers described above, and was confirmed by the sequence analysis. The expression plasmid pTrc99A-*est* and pET28a-*est* were successfully constructed and were transformed into *E. coli* TOP10 and *E. coli* BL21DE3 respectively for protein expression. For strain Top10/pTrc-99A-*est*, the expression of the esterase was confirmed by SDS-PAGE analysis (Fig.1, lane 1). And the molecular weight of this protein (43 kDa) on SDS-PAGE (Fig.1, lane 2) was found consistent with the expected molecular weight size. As a negative control, no *T. tengcongensis* esterase protein or activity was detected in the vector-transformed strain (Fig.1, lane 1). However, the result of the enzyme expression in strain BL21DE3/pET-28a-*est* (Fig.2),

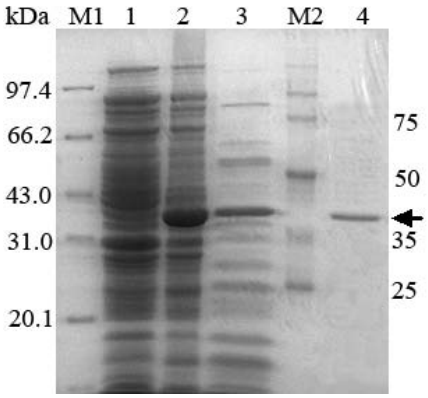

shows that the esterase was not successfully over-expressed with pET-28a in *E. coli.*

Figure 1. Overexpression and purification of T. tengcongensis lipase (est) in E. coli. Lane M1, Lane M2, protein molecular weight markers (in kDa); lane 1, total proteins from strain Top10/pTrc-99A; lane 2 total proteins from strain Top10/pTrc-99A::est; lane 3, supernatant of concentrated proteins fromTop10/ pTrc-99A::est. lane 4, purified lipase.

Figure 2. Overexpression and purification of T. tengcongensis lipase (est) in E. coli. Lane M, protein molecular weight markers; lane 1, total proteins from strain BL21DE3 (condon plus)/pET-28a; lane 2 total proteins from strain BL21DE3 (condon plus)/pET-28a::est

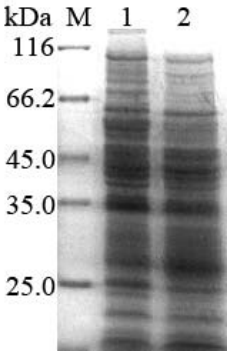

Enzyme purification

Purfication was achieved by heat treatment and DEAE Sepharose Fast Flow. Table 1 depicts specific activity and the purification fold after these steps. The purity of the esterase after the purification increased approximately 12-fold over the crude extract. The purified lipase showed a single band in 12% SDS–PAGE gel (Fig.1, lane 4).

	Total protein (mg)	Total acctivity (U)	Specific activity (U/ mg)	yield (%)	Purification (fold)
Crude extract	329	2782	8	100	1
Heat treatment	44	1984	45	71	5
DEAE-SepharoseCL-6B	6	570	99	20	12

Table 1 Activity and yield of the recombinant esterase in purification procedure

Substrates specificity

The esterase expressed with pTrc99a showed maximum activities towards short-chain *p*-NP esters (C2 and C4), middle activities towards middle-chain *p*-NP esters (C6 to C10) and little activity towards long-chain *p*-NP ester (C16) (Fig. 3). However the esterase expressed with pET-28a showed little activity towards all of

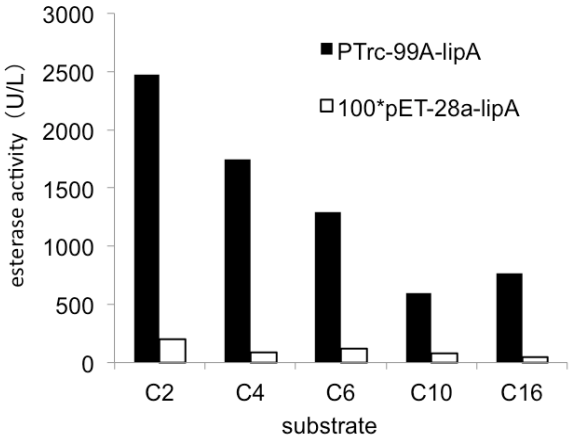

these substrates.

Figure 3. Determination of the substrate specificity of the esterase (Est). The p-NP-acetate (C2), p-NP-butyrate (C4), p-NP-caproate (C6), p-NP-caprate (C10), and p-NP-palmitate (C16) were selected as the substrates. The reactions were conducted using the standard assay conditions (see Materials and methods section), and the highest esterase activity towards p-NP-butyrate (C4) was defined as the 100% level (about 99 U mg−1).

Effects of pH and temperature on the esterase activity

The pH profiles showed that the esterase was active over a broad pH range (pH 7.0–8.0) and the optimum pH was 7.5 (Fig. 4B). The temperature activity curve for the recombinant lipase

was shown in Fig. 4A. The temperature for the optimum of the esterase was 70^0C. The thermal stability of the esterase was studied by measuring the residual activity after incubation for different periods at temperatures ranging between 65 and 80^0C. The half life of the thermostability at 80^0C was more than 60 min. (Fig. 4C).

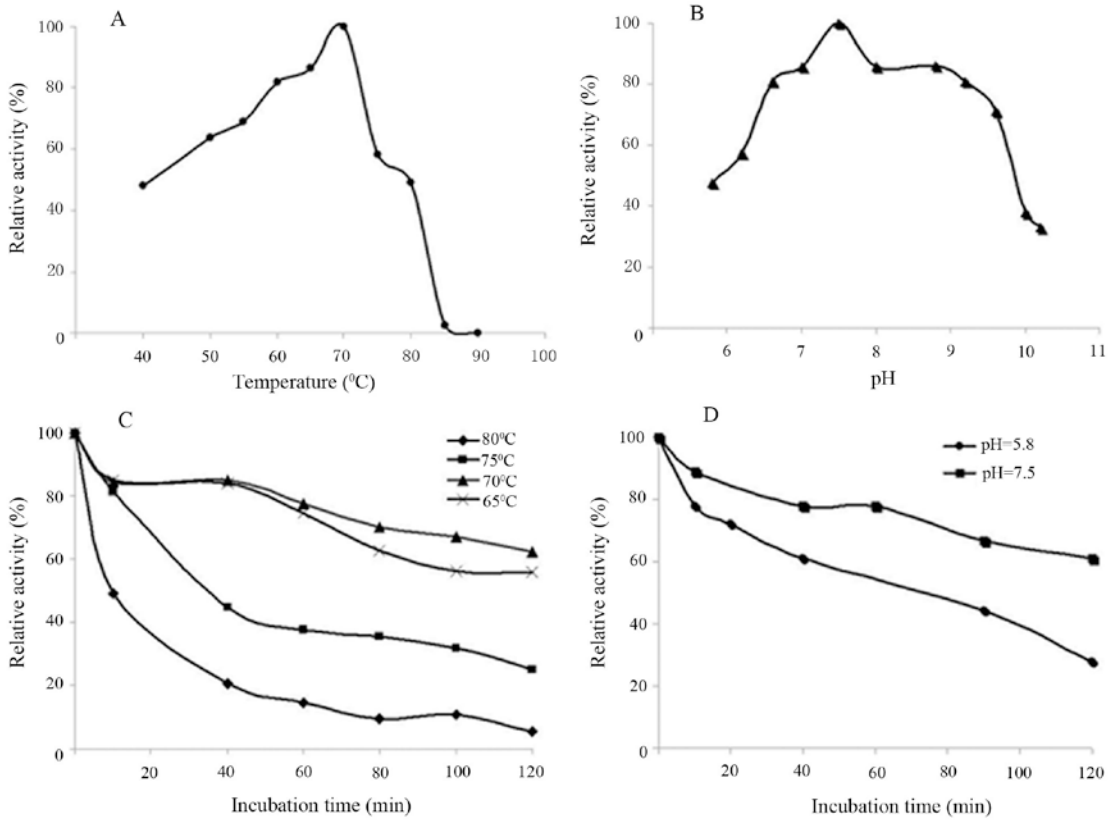

Figure 4. Effects of temperature and pH on esterase activity and stability. (A) Determination of esterase activity at various temperatures at pH 7.5 for 15 min, using p-NP- butyrate as a substrate. The highest activity at 70^0C was defined as 100% level (5.014 U mL^{-1}). (B) Determination of esterase activity at various pHs at 65^0C for 15 min, using p-NP- butyrate as a substrate. The highest activity at pH 7.5 was defined as 100% level (3.51 U mL^{-1}). (C) Determination of the effects of temperature on esterase stability by incubating the purified esterase at various temperatures for up to 2 h and measuring the remaining activity. The original enzyme activity before treatment was defined as 100% (4.01 U mL^{-1}). (D) Determination of the effects of pH on esterase stability by incubating the purified esterase at various pHs for up to 2 h and measuring the remaining activity. The original enzyme activity before treatment was defined as 100% (3.008 U mL^{-1}).

Discussion

Our results showed that the recombinant esterase of *T. tengcongensis* MB4T was successfully over-expressed in *E. coli*. The expression level of the esterase in pTrc99A was about 100 times higher than that in pET-28a. A number of central elements are essential in the design of

recombinant expression systems (Baneyx, F. 1999, Jonasson, P. et al. 2002). Promoter strength affects the amount of transcripts produced and thereby increasing the protein expression. So the plasmids we selected in this study (pTrc99A and pET-28a) were both controlled by strong promoter (*trc* and T7).

However the result shows that the efficiency of the trc promoter for our analysis is much higher than T7 promoter. Briefly many different types of promoters can affect the level of gene expression in *E. coli* and suitability of promoters is important for hith-level expression (Hannig, G. and Makrides, S.C. 1998). Furthermore, the copy number of the expression vector is an important factor for high-level expression (Kobayashi, M. et al. 1991). Plasmid pTrc99A is a high-copy-number of about 100 (Amann, E. et al. 1988), while plasmid pET-28a is a medium-copy-number of 40-50 copies/cell (Kleefeld, A. et al. 2009). It is consistent with the result of our study. In addition, a highly repressible promoter is particularly important for case in which the protein of interest is toxic or detrimental to the growth of the host cell (Hannig, G. and Makrides, S.C. 1998, Amann, E. et al. 1988, Yike, I. et al.). So the reason why pET-28a can not be suitable for this esterase expression maybe the target protein expressed with pET28a is toxic or detrimental to the growth of to the host cell *E. coli* BL21DE3.

The recombinant enzyme was purified by the heat treatment and DEAE Sepharose Fast Flow presented as a single protein band on SDS-PAGE with a molecular weight of 43 kDa. In addition, the result shows that this esterase is indeed highly thermostable. The studies on substrate specificity demonstrated that the recombinant esterase had the strong catalytic ability to the substrates with short carbon chain. These properties would be important for the lipase to be applied in industry. However, modern methods of enzyme engineering, especially directed evolution will certainly provide suitable esterase variants with increased use in organic synthesis and other areas of application in the near future.

Acknowledgments

This work was supported by grants from the programs of State Forestry Administration, China (No. 201004001, 2009-4-63), and a project funded by the priority academic program development of Jiangsu Higher Education Institutions (PAPD).

Reference

Amann, E. Ochs, B. and Abel, K.J. 1988. Tightly regulated tac promoter vectors useful for the expression of unfused and fused proteins in *Escherichia coli*. Gene. 69: 301–315.

Kleefeld, A. Ackermann, B. Bauer, J. et al. 2009. The fumarate/succinate antiporter DcuB of *Escherichia coli* is a bifunctional protein with sites for regulation of DcuSdependent gene expression. Journal of Biological Chemistry. 284: 265-275.

Arpigny, J.L. Jaeger, K.E. 1999. Bacterial lipolytic enzymes: classification and properties. Biochem. J. 343: 177–183.

Bahrami, A. Shojaosadati, S. Mahbeli, G.. 2001. Biodegradation of dibenzothiophene by thermophilic bacteria. Biotechnol. Lett. 23: 899–901.

Baneyx, F. 1999. Recombinant protein expression in *Escherichia coli*. Curr. Opin. Biotechnol. 10: 411–421.

Boer, H. Comstock, L.J. Vasser, M. 1983. The tac Promoter: A Functional Hybrid Derived from the *trp* and *lac* Promoters. Proc. Natl. Acad. Sci. 80: 21-25.

David, L. Ollis, Cheah, E. et al. 1992. The α/β hydrolase fold. Protein Engneering. 5: 197-211.

Demirijan, D. Moris-Varas, F. Cassidy, C. 2001. Enzymes from extremophiles. Curr. Opin. Chem. Boil. 5: 144–151.

Hannig, G. Makrides, S.C. 1998. Strategies for optimizing heterol- ogous protein expression in *Escherichia coli*. Trends Biotechnol. 16: 54–60.

Zhang, J. Liu J.f. Zhou, J. et al. 2003. Thermostable esterase from *Thermoanaerobacter tengcongensis*: high-level expression, purification and characterization. Biotechnology Letters. 25: 1463–1467.

Jonasson, P. Liljeqvist, S. Nygren, P.A. et al. 2002. Genetic design for facilitated production and recovery of recombinant proteins in *Escherichia coli*. Biotechnol Appl Biochem. 35: 91–105.

Khushoo, A. Pal, Y. Mukherjee, K.J. 2005. Optimization of extracellular production of recombinant asparaginase in *Escherichia coli* in shake-flask and bioreactor. Appl Microbiol Biotechnol. 68: 189-197.

Kobayashi, M. Kurusu, Y. Yukawa, H. 1991. High-Expression of a Target Gene and High-Stability of the Plasmid, Applied Biochemistry and Biotechnology. 27: 145-161.

Petersen, E.I. Valinger, G. Solkner, B. et al. 2001. A novel esterase from Burkholderia gladioli shows high deacetylation activity on cephalosporins is related to -lactamases and DD-peptidases. J. Biotechnol. 89: 11-25.

Pleiss, J. Fischer, M. Schmid, R.D. 1998. Anatomy of lipase binding sites: the scissile fatty acid binding site. Chem Phys Lipids. 93:67–80.

T. Panda, B.S. 2005. Gowrishankar, Production and applications of esterases, Appl Microbiol Biotechnol. 67, 160–169.

Wei, Y. Schottel, J.L. Derewenda, U. et al. 1995. A novel variant of the catalytic triad in the Streptomyces scabies esterase. Nat. Struct. Biol. 2: 218-223.

Xue, Y. Xu, Y. Liu, Y. et al. 2001. *Thermoanaerobacter tengcongensis* sp. nov., a novel anaerobic, saccharolytic, thermophilic bacterium isolated from a hot spring in Tengcong, China. Int. J. Syst. Evol. Microbiol. 51: 1335–1341.

Yike, I. Zhang, Y. Ye, J. et al. 1996. Protein Expression, Purif. 7: 45–50.

Proceedings of the 55th International Convention of Society of Wood Science and Technology
August 27-31, 2012 - Beijing, CHINA

FTIR Investigation of Phenol Formaldehyde Resin Modified with Boric Acid

Ertugrul ALTUNTAS [1], Mehmet Hakki ALMA [1], Oktay GONULTAS [2]*

Zeki CANDAN [2], and Murat ERTAS [3]

[1] Department of Forest Products Engineering, Faculty of Forestry
Kahramanmaras Sutcu Imam University, 46060, Kahramanmaras, TURKEY
[2] Department of Forest Products Engineering, Faculty of Forestry
Istanbul University, Sariyer, 34473, Istanbul, TURKEY
[3] Department of Forest Products Engineering, Faculty of Forestry
Bursa Technical University, Bursa, TURKEY
** Corresponding author*
o_gonultas@hotmail.com

Abstract

Phenol formaldehyde resin produced under alkaline conditions has been commonly used in wood-based panel industry. Modification with boron compounds is of importance for enhancing thermal, mechanical, and electrical properties of the resin. In this study, boron modified phenol formaldehyde polymer (BPF) was synthesized using boric acid at different temperatures and times in alkaline condition. Functional group analysis was investigated by FTIR instrument. FTIR spectra obtained in the BPF was compared with commercial phenol formaldehyde (PF). The results acquired in this study showed that B-O bond which is characteristic for polymers including boron compounds was observed in the BMPF. This result also indicates that chemical bonding was existed between phenol formaldehyde and boron compounds.

***Keywords*:** Boric acid, phenol formaldehyde, boron modification, FTIR

Introduction

Phenolic resin is widely used as an adhesive in wood composite manufacturing. Phenolic resins have been modified with some materials to improve physical and mechanical properties, to increase dimensional and thermal stability, to decrease thermal expansion and water absorption, to change electrical properties (Altuntas, 2008).

Boron compounds are of a great importance in many industrial applications and its using area is increasing year by year They use in glass, ceramic, cleaning, fire retardant materials manufacture, medicine, health, chemistry, agriculture, metallurgy, energy, automobile, waste cleaning process, pigment and dryer, nuclear applications, and protection of wood materials (Ertugrul, 2004).

In this study, FTIR analysis was performed to determine the effects of temperature and reaction time on functional groups of the boron modified phenol (BPF) resin.

Materials and Methods

16 BPF polymers were produced as shown in Table 1. Phenol, formaldehyde, boric acid and NaOH were supplied by Merck Co. as analytical reagent grade. Commercial PF was provided from ARBAK Chemical Inc. Istanbul, Turkey.

Table 1. Experimental Design of The BPF Samples

Groups	Phenol:Formaldehyde: Boric Acid Ratio (g)	NaOH (g)	Temperature (°C)	Reaction Time (min)
1	23.500:24.375:4.125	0.1	70	30
2	23.500:24.375:4.125	0.1	70	60
2	23.500:24.375:4.125	0.1	70	90
4	23.500:24.375:4.125	0.1	70	120
5	23.500:24.375:4.125	0.1	90	30
6	23.500:24.375:4.125	0.1	90	60
7	23.500:24.375:4.125	0.1	90	90
8	23.500:24.375:4.125	0.1	90	120
9	23.500:24.375:4.125	0.1	110	30
10	23.500:24.375:4.125	0.1	110	60
11	23.500:24.375:4.125	0.1	110	90
12	23.500:24.375:4.125	0.1	110	120
13	23.500:24.375:4.125	0.1	120	30
14	23.500:24.375:4.125	0.1	120	60
15	23.500:24.375:4.125	0.1	120	90
16	23.500:24.375:4.125	0.1	120	120

Spectroscopic measurements were performed in a SHIMADZU FT-IR 8800 spectrophotometer using the standard KBr method (150 mg KBr plus, 5 mg polymer). FTIR spectra were collected in the wave number range between 4000 and 400 cm^{-1}.

Results and Discussions

The FTIR spectra of the polymers that produced 70, 90, 110 and 120°C and commercial PF samples are shown in Fig. 1, Fig.2, Fig 3, Fig. 4 and Fig. 5, respectively. The main bands and assignments in the FTIR spectra of the BPF and commercial PF are summarized in Table 2.

Table 2. Infrared Bands and Assignment of PF and BPF Polymers

Assignments	Band Position of PF (cm-1)	Band Position of BMPF (cm-1)	References
phenolic OH strech	3220	3228-3211	Liu et al. 2002; Shukla et al. 2010
Aliphatic –CH2 asymmetric stretch	2920	2918-2920	Liu et al. 2002; Costa et al. 1997; Mirski et al. 2008; Pan et al. 2009
Aliphatic –CH2 symmetric stretch		2846	Costa et al. 1997; Pan et al. 2009
Aryl ketone or aldehyde C=O stretch		1705-1676	Perez et al. 2007; Mirski et al. 2008; Pan et al. 2009
C=C stretching vibration of aromatic ring	1602	1647	Shen et al. 1982;Gao et al. 2000; Liu et al. 2002; Costa et al. 1997
Aromatic C–C stretch	1598	1602	Costa et al. 1997; Yangfei et al. 2008;Pan et al. 2009; Shukla et al. 2010
CH_2 deformation	1438	1444	Liu et al. 2002; Costa et al. 1997; Pan et al. 2009;Yangfei et al. 2008
B-O		1382	Colin, 1994; Liu et al. 2002
Phenolic OH in plane deformation	1357		Shen et al. 1982;Gao et al. 2000; Costa et al. 1997; Pan et al. 2009
C–O and OH bending modes in phenol	1250-1240	1224	Shen et al. 1982;Gao et al. 2000; Liu et al. 2002; Costa et al. 1997
symmetric vibration of the ether bond	1101	1101	Shen et al. 1982;Gao et al. 2000; Costa et al. 1997; Poljansek et al. 2006; Shukla et al. 2010
Aliphatic ethers C–O–C stretch	1002	1018-1012	Liu et al. 2002; Pan et al. 2009
Tetra substituted ring		883	Pan et al. 2009
Adjacent 2H, para-substituted		817	Costa et al. 1997; Perez et al. 2007; Pan et al. 2009
C-H out of plane deformation	752	756	Liu et al. 2002; Costa et al. 1997; Perez et al. 2007; Poljansek et al. 2006; Pan et al. 2009; Shukla et al. 2010

Significant changes were noticed in the intensity of bands at 2918, 2617, 2362, 2262, 1890, 1602, 1386, 1228, 1103, 1008, 817, 756 cm-1 diminished with increasing reaction temperature and reaction time. The new peak occurs around 1650cm^{-1} with above at 110°C from produced by oxidized reaction (Yangfei et al. 2008). Peak 3220 cm-1 was noticed to shifts markedly towards from 3228 to 3211 cm-1 because changes take place in the H bonding and the number of OH groups decreases. This is probably due to condensation processes and crosslinking (Costa et al. 2007).

The absorbance peaks of phenol borat (B-O) in this study have been identified at 1382 cm^{-1}.The peak was not observed for commercial PF polymer. This result is agreement with Liu et al. (2002). According to FTIR analysis, we can say to boron reacts with PF polymers under different production process.

Figure 1. The FTIR Spectra of Group 1

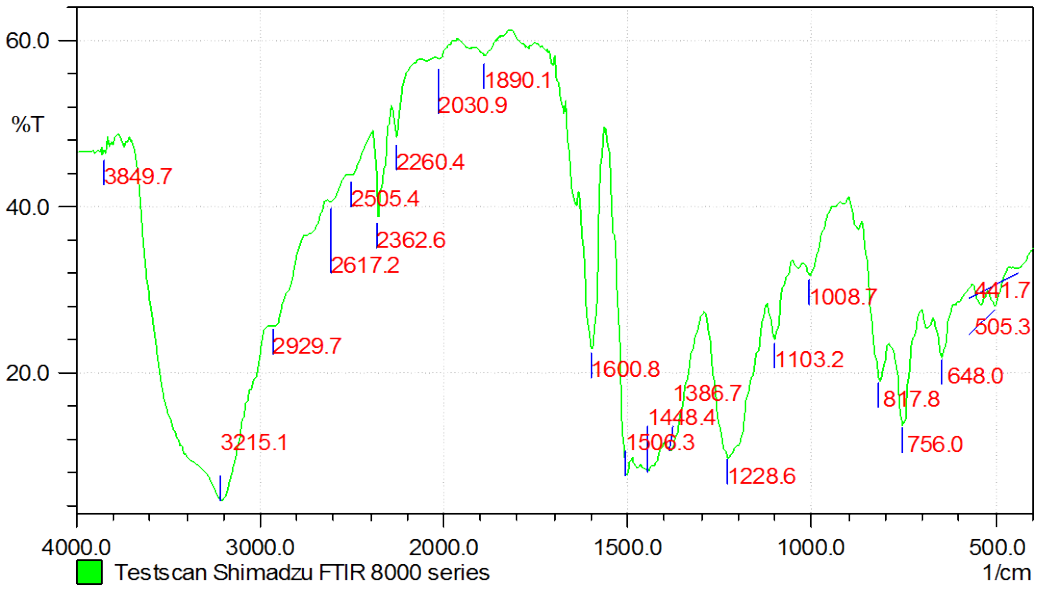

Figure 2. The FTIR Spectra of Group 5

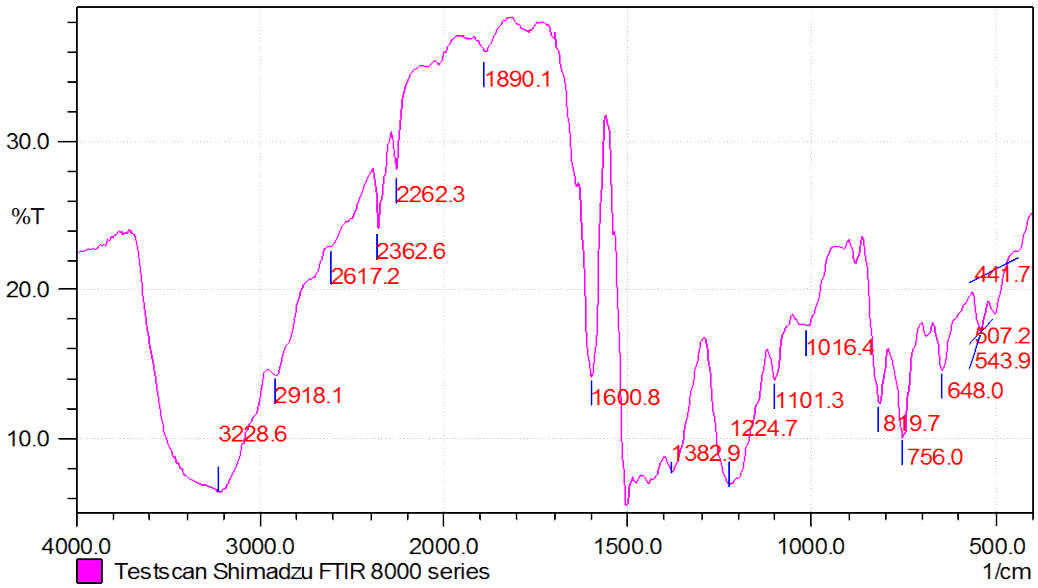

Figure 3. The FTIR Spectra of Group 9

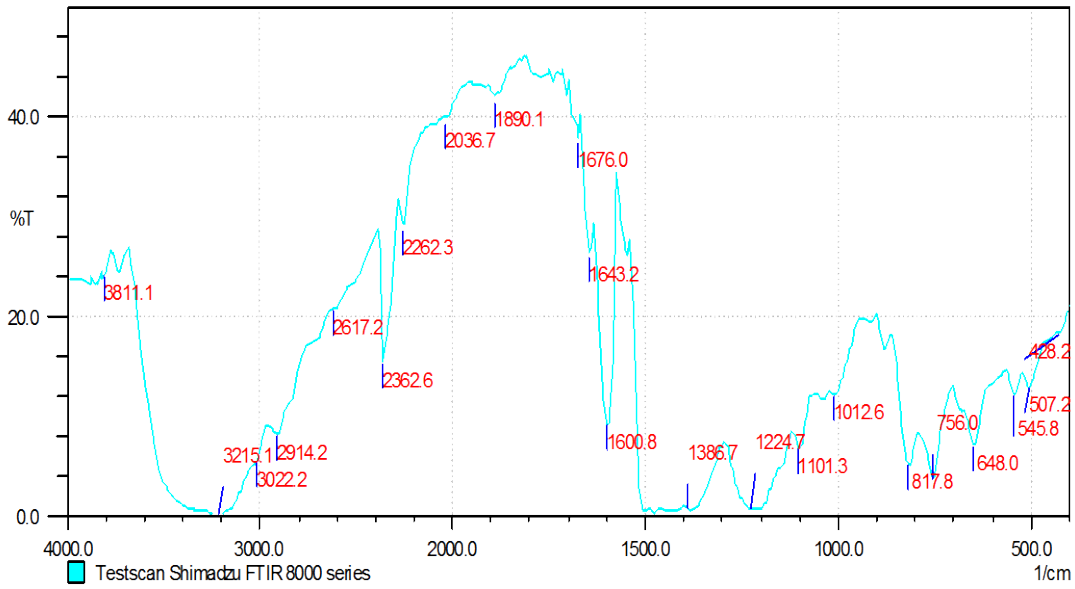

Figure 4. The FTIR Spectra of Group 13

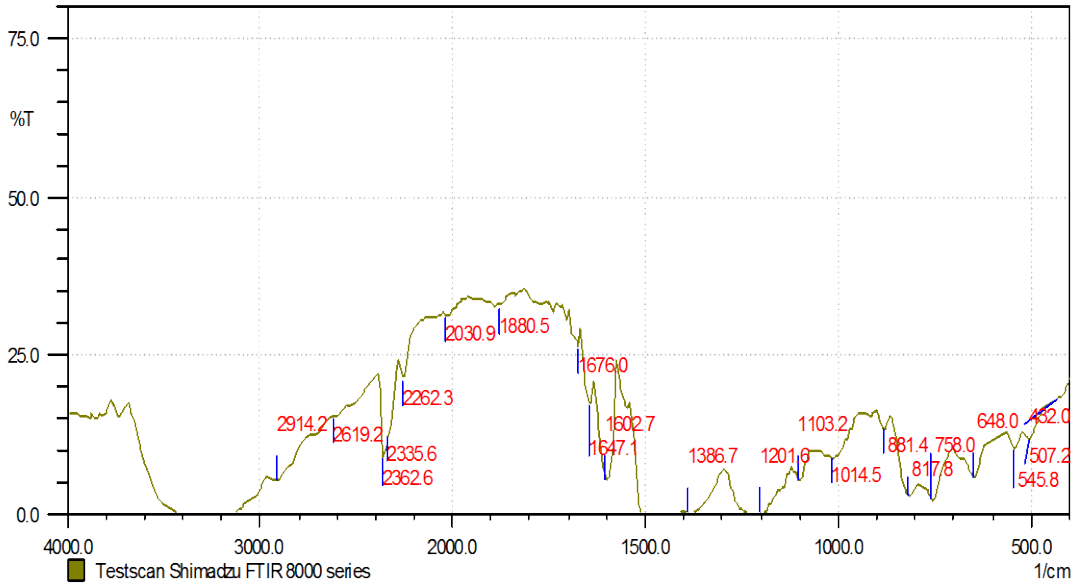

Figure 5. The FTIR Spectra of Commercial PF

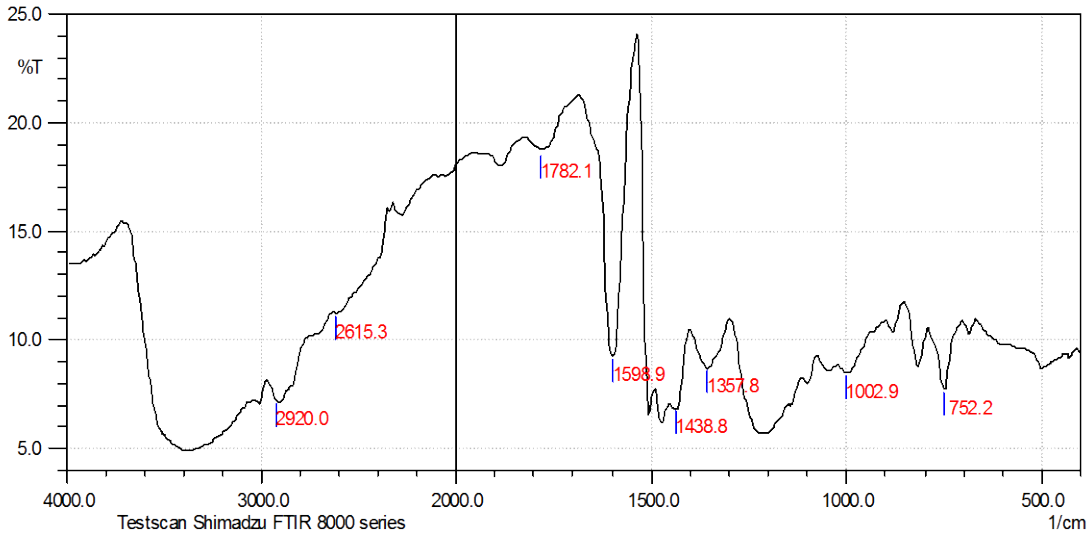

Conclusions

The effects of temperature and reaction time on the functional groups of the boron modified phenol (BPF) resin were investigated in this present study. The absorbance peaks of phenol borat (B-O) have been identified at 1382 cm^{-1}. The peak was not observed for commercial PF polymer. This result is agreement with Liu et al. (2002). The results obtained from FTIR analysis showed that boron reacts with PF polymer under different production parameters.

Acknowledgements

The authors thank Kahramanmaras Sutcu Imam University Research Fund for its financial support in this study (Project No: 2007/3 – 19. The author also would like to express their appreciation for the financial support provided by Tubitak, Ankara, Turkey. ARBAK Chemistry Company (Istanbul, Turkey) is greatly appreciated for raw material supply.

References

Costa, L. Rossi, L. Montelera, D. Camino, G. Weil, E. D. Pearce, E. M. 1997. Structure-charring relationship in phenolformaldehyde type resins. Polymer Degradation and Stability 56: 23-35

Gao, J. Liu, Y. Yang, F. 2000. Boron-containing Bisphenol-A Formaldehyde Resin. J. Applied Polymer Science. 76: 1054–1061

Liu,Y. Gao, J. Zhang, R. 2002. Thermal properties and stability of boron-containing phenol-formaldehyde resin formed from paraformaldehyde. Polymer Degradation and Stability. 77:495–501

Mirski,R. Dziurka,D. Janina, L. 2008. Properties of Phenol–Formaldehyde Resin Modified with Organic Acid Esters. Journal of Applied Polymer Science, Vol. 107, 3358–3366

Pan, H. Shupe, T.F. Hse, C.Y. 2009. Characterization of novolac type liquefied wood/phenol/formaldehyde (LWPF) resin. Eur. J. Wood Prod. 67: 427–437

Perez, J.M. Rodriguez, F. Alonso, M.V. Oliet, M. Echeverria, J.M. 2007. Characterization of a novolac resin substituting phenol by ammonium lignosulfonate as filler or extender. BioResources. 2(2): 270-283

Poljansek, I. Urska, S. Krajnc, M. 2006. Characterization of Phenol–Urea–Formaldehyde Resin by Inline FTIR Spectroscopy. Journal of Applied Polymer Science, Vol. 99:2016–2028

Shukla, P.Yadaw,S. B. Srivastava, D. 2010. A Study on the Kinetics of Condensation Reaction of Phenol-Modified Cardanol–Formaldehyde Resin. International Journal of Chemical Kinetics. 42 6: 380–389

Shen, D.Y. 1982. Application of Infrared Spectroscopy on Studies of Macromolucules. Beijing: Science Pres.

Yangfei, C. Zhiqinb, C. Shaoyi, X. Hongbo, L. 2008. A novel thermal degradation mechanism of phenol–formaldehyde type resins. Thermochimica Acta 476: 39–43

Application of Finite Element Analysis in Properties Test of Finger-jointed Lumber

HE Sheng[1], FU Feng[1], LIN Lan-ying[1], CAO Ping-xiang[2]

(1. Research Institute of Wood Industry, Chinese Academy of Forestry, Wood Functional Materials Lab, Beijing, 100091, China.

2. College of Wood Industry, Nanjing Forestry University, Nanjing 210037, Jiangsu, China)

Abstract

Finger joints have been used to produce engineered wood products for their excellent mechanical performance. The properties of finger-jointed lumber are affected by many different factors. End-pressure is one of the important parameters in the finger-jointed lumber production and it should be identified before the finger joints are jointed.
The mechanical properties are the most concerned properties for structural used finger-jointed lumber. The mainly mechanical properties include the modulus of elasticity and the bending strength. Experimental tests are commonly used in the testing of these properties at present. With the development of nondestructive test technology, many researchers applied such methods in the testing of mechanical properties for wood based products.
Finite element analysis (FEA) has been used as a numerical method for the modeling of properties of different materials. In this paper, ANSYS, a software for FEA, was used to modeling the end-pressure, modulus of elasticity and bending strength of finger-jointed lumber made from *Pinus Sylvistriv* var. under three different fitness lever.
FEA applied in the end pressure tests showed a narrower range compared with the modeling results. Besides, the upper limit obtained from modeling process is close to the optimum end pressure which obtained from experimental test. It indicates that the FEA can be used in the prediction of the end pressure for finger-jointed lumber.
The modeling results for modulus of elasticity (MOE) test were about 20% higher than experimental results. The error may result from the neglection of the natural flaws existing in the lumbers and the manufacturing deficiencies when conducting the modeling process. Moreover, the modeling results showed the same trend as experimental test results under three different fitness levels.

The modeling results for bending strength (MOR) test of finger-jointed lumber also showed some discrepancies compared with the experimental test results. The plastic deformation developed from the loading of end pressure in finger-jointed lumber manufacturing process caused the decrease of the fitness and lengthened the finger joints which is helpful for guarantee the strength of the finger-jointed lumber. But in the modeling process, the effect of the factor was neglected. Also, the damage of the finger joints under end pressure when fitness is 0mm which was not taken into account in the modeling process resulted in the different trend between experimental and modeling results of MOR for finger-jointed lumber under three fitness levers.
The conclusion could be made that FEA is a feasible way in analyzing the properties of finger-jointed lumber if the errors could be eliminated properly. Some modifications should be made on the models in order to realize the modeling of the properties of finger-jointed lumber more accurately.

Keywords: finite element analysis; finger jointed lumber; end-pressure; modulus of elasticity in static bending; bending strength

1. Introduction

Finger joint is a type of end joint developed from scarf joint; it has been used for many years (Roland, 1981). Such joints can not only joint the short pieces of lumber to long ones, but also effectively enhance the utilization of low-grade materials. They are commonly used to produce engineered wood products for their excellent mechanical performance (Cecilia, 2003). Finger-jointed lumber production has now become the most extensively applied method for splicing lumbers together endwise.

The properties of finger-jointed lumber are affected by many different factors such as the wood species, adhesive, length of finger joints, processing parameters, et al. End-pressure refers to the pressure applied on the end of the lumbers to be jointed lengthwise, which bring the mating surfaces so close together that the glue forms a thin and continuous film between them (Cecilia, 2003).Several authors research on end pressure indicated that the pressure must be applied to force fingers together to form an interlocking connection (Raknes,1982), however, the excessive pressure which cause the cell damage or spitting of the finger root could induce the decrease of the strength of finger joints (Marra 1984, Kutscha and Caster,1987). So the end pressure should be identified before the finger joints be jointed. Finger-jointed lumber is classified as two different groups according to it's use, structural and nonstructural use finger-jointed lumber. Nonstructural use finger-jointed lumber is more emphasis on the appearance quality while the structural use finger-jointed lumber focus on the mechanical properties. The mainly mechanical properties to be tested for structural use finger-jointed lumber include the modulus of elasticity in static bending and the bending strength. The mainly method for testing these properties at present is experimental method. With the rapid development of the nondestructive test technology, more and more researchers applied these methods such as the acoustic emission method (Kiyoko Y, et al, 2007), stress wave method (Liang, et al, 2008), ultrasonic method (Lin, et al, 2007), vibration method (Zhang, et al, 2005), the near infrared spectrum technology (Zhao, et al, 2009) in the testing of mechanical properties tests for wood based products.

As an efficient method of numerical analysis, finite element analysis（FEA）is now extensively used in the modeling analysis of materials' properties. Several researchers have successfully applied this method in the properties analysis for wood based materials (Tabiei A. et al, 2000, Moses D.M. 2004, Serrano E. 2004, Davalos J.F. 1995)

In order to save materials which should be used in experimental tests, the present study investigated the end-pressure range, the modulus of elasticity in static bending and the bending strength for *Pinus sylvistriv* var. finger-jointed lumber under three different fitness ratio (0mm, 0.1mm, 0.3mm) using ANSYS, a software for FEA. With the FEA modeling results compared with the experimental test results, it's possible to find the relationship between these two kinds of results and use the FEA to predict the properties of finger-jointed lumber.

2. Materials and Methods

2.1 Materials

The dimensions of the lumbers used in the experiment are 600×88×24mm^3 (Length×Width×Thickness). The moisture content (M.C.) of the lumbers ranges from 8% to 11% while the density ranges from 0.4 to 0.7g/cm^3. The resin used in the production of finger-jointed lumber was a mixture of water-borne carbamate emulsion (the main agent) and macromolecular isocyanate (the firming agent) with a mixture ratio of 100:15 (Dynea, Shanghai). The solid content of the resin is 53%, and the pH is 7.3. The amount of resin sprayed on the finger joints is 250-300g/m^2.

2.2 Methods

2.2.1 Finger joints manufacturing

Finger joints with three different fitness ratio were cut in the cutting machine (FS-520R, Japan) according to the parameters showed in Table 1.

Tab.1 Parameters of finger-jointed lumber

Fitness/mm	Length of Fingers/mm	Tip Thickness/mm	Pitch/mm	Slope
0	25	1.2	8.2	1/8.6
0.1	23.7	1.3	8.2	1/8.6
0.3	21	1.5	8.2	1/8.6

2.2.2 End-pressure testing

A series of 15 finger-jointed lumbers were produced in the end-pressure test experiment. Each fitness lever was represented by 5 finger jointed lumbers. The two finger joints of the same fitness were jointed together by hand after sprayed with resin. They were subsequently loaded lengthwise on the cross section of the lumber in a mechanical experimental machine (INSTRON 5582, America) until they were compressed to crush. At the same time, keep a record of the curve of Load-Displacement when the finger joints were loaded.

2.2.3 Finger-jointed lumber manufacturing

54 finger-jointed lumbers were manufactured in the finger jointing machine (FJ-500OA-2, Japan). Each fitness lever was represented by 18 finger-jointed lumbers. The end pressure applied on the finger joints was determined by the end pressure test experiment. Keep the pressure for 5~10s and then the finger-jointed lumbers were kept in room temperature for at least 48h to let the glue cure completely. All finger-jointed lumbers were tested for modulus of elasticity in static bending (MOE; n=18) and bending strength (n=18). Analysis of variance (ANOVA) was performed to compare the means of each test ($P < 0.05$).

2.2.4 FEA for finger-jointed lumber

The lumber was assumed to be an orthotropic, linear elastic and nonlinear elastoplastic material having the following engineering constants and yield stress as show in Table 2 and Table 3. The data input for the glue and gaskets (Zheng et al, Li et al) were listed in Table 4.

Tab.2 The elastic constants of different directions for *Pinus sylvestris* var.

Elastic Constants											
E_L/MPa	μ_{LR}	μ_{LT}	E_T/MPa	μ_{TR}	μ_{TL}	E_R/MPa	μ_{RT}	μ_{RL}	G_{RT}/MPa	G_{LT}/MPa	G_{LR}/MPa
9171	0.472	0.558	460.4	0.337	0.033	831.6	0.765	0.053	44.48	521.7	666.7

Tab.3 The yield stress of different directions for *Pinus sylvestris* var.

	Longitude	Radial	Tangential
Tensile(MPa)	32.290	4.00	4.00
Compression(MPa)	11.031	4.74	4.36
Shear(MPa)	4.130	4.41	4.13

Tab.4 Parameters of adhesive and gaskets

Materials	Constants for Materials	
	E/MPa	μ
Adhesive	3000	0.37
Gaskets	1000	0.2

Take the software of ANSYS to set up the 3-D models for end-pressure test, modulus of elasticity and bending strength tests. Choose Solid45 as the finite element type and mesh the model with free meshing method.

1) FEA of end-pressure test

Figure 1 and figure 2 shows the model created by ANSYS and its mesh results for the end-pressure test of finger-jointed lumber. The three dimensional displacement constraints were added to one end of the model and the pressure was applied on the other end following the load step which was shown in figure 3. Then the calculation was carried out in the software and the relation between the displacement and load step (the same as load) was output in the post-process part of the software.

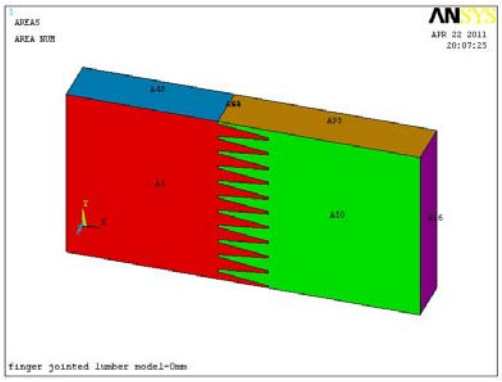

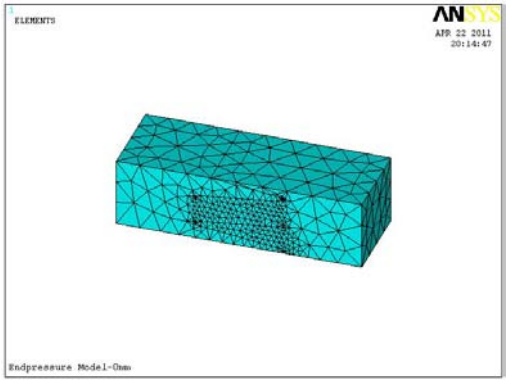

Fig.1 End-pressure FE model(fitness 0mm) Fig.2 Mesh result of end-pressure FE model(fitness 0mm)

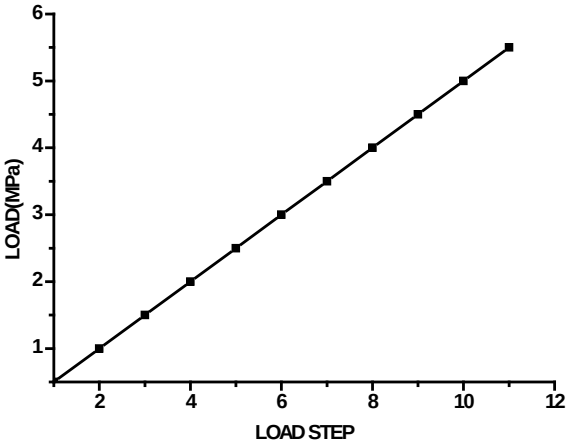

Fig.3 Loading rate of end-pressure test

According to the principles for finger-jointed lumber manufacturing, the end pressure applied on the finger joints should not be too large to result in the fracture of the lumber which may decrease the strength of the finger-jointed lumber. Thus the stress of the elements under pressure should not be larger than the yield stress of the lumber, and the end pressure which caused the damage of the elements is the upper limit whereas the lower limit pressure should be high enough to cause the plastic deformation ensuring the good adhesion of the finger joints.

2) FEA of MOE

Figure 4 and figure 5 shows the model created by ANSYS and its mesh results for the MOE test of finger-jointed lumber. After adding the appropriate displacement constraints to the model and applying the pressure on the loading gaskets follow the load step which was show in figure 6, the calculation was carried out in the software.

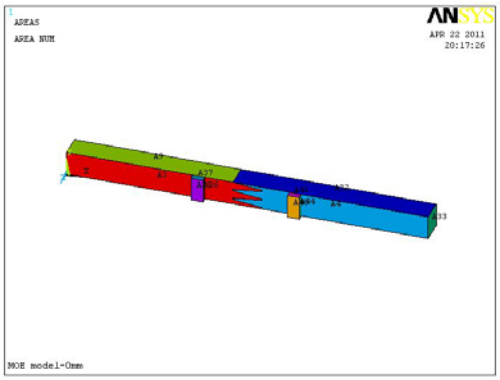

Fig.4 MOE FE model(fitness 0mm)

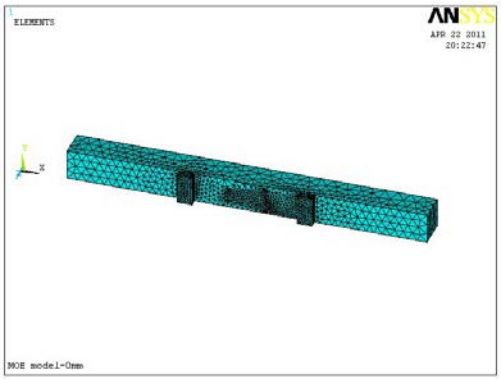

Fig.5 Mesh result of MOE FE model(fitness 0mm)

When the calculation was done, check the modeling results and find out the node which exhibited the largest deformation along the loading direction. Then output the displacement-load curve for the node and keep a record of the displacement when the load increases from the lower limit to upper limit. The MOE of the finger-jointed lumber can be calculated according to the equation (1) below.

$$E = \frac{23Pl^3}{108bh^3 f} \qquad (1)$$

Where E is the MOE of finger jointed lumber (MPa); P is the load difference between the upper limit and lower limit (N); l is the span length (mm); b is the width of the specimen (mm); h is the height of the specimen (mm); f is the deformation of specimen when the load increase from the lower limit to upper limit (mm).

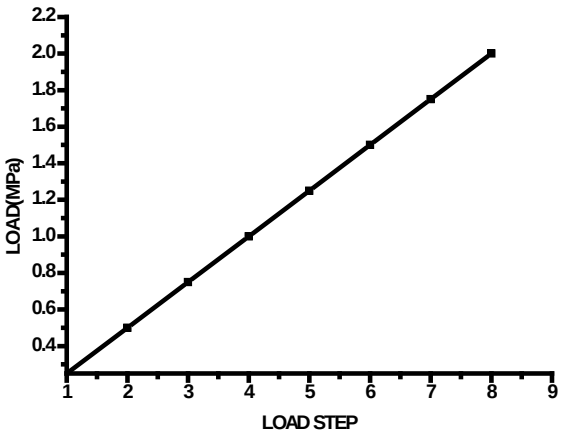

Fig.6 Load rate of MOE test

3) FEA of bending strength

Figure 7 and figure 8 shows the model created by ANSYS and its mesh results for the bending

strength (MOR) test of finger-jointed lumber. Add the appropriate constraints to the model and applying the pressure on the loading gasket follow the load step which was show in figure 9. Then the calculation was carried out in the software and the relation between the displacement and load step (the same as load) was output in the post-process part of the software.

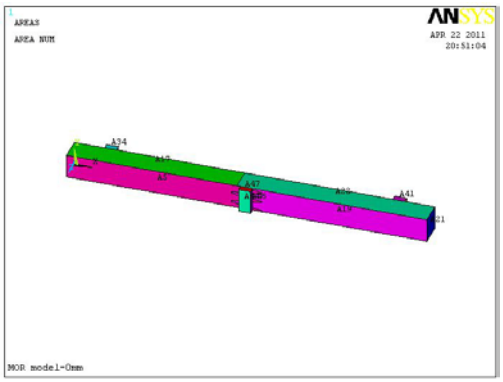

Fig.7 MOR FE model(fitness 0mm)

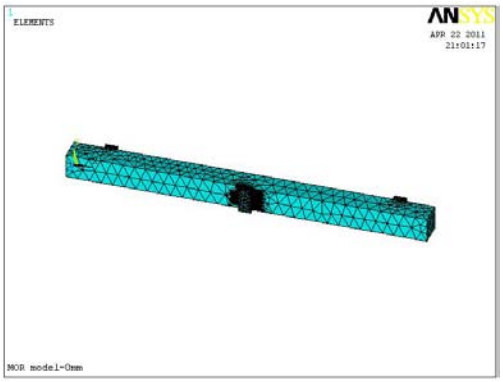

Fig.8 Mesh result of MOR FE model(fitness 0mm)

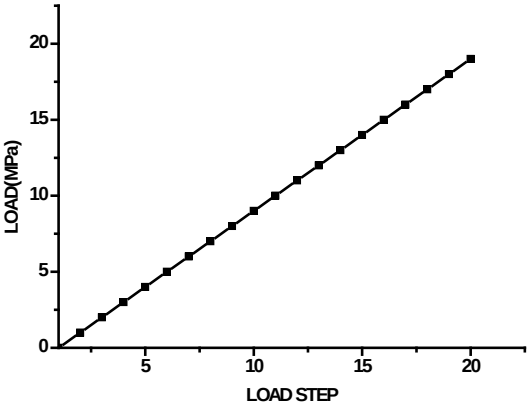

Fig.9 Load rate of MOR test

After the calculation was done, check the modeling result and find the node which exhibited the stress exceed the yield stress of the lumber. Then output the displacement-load curve for the node and keep a record of the pressure when the deformation reached the highest value. The bending strength of the finger-jointed lumber can be calculated according to the equation (2) below.

$$\sigma = \frac{3P_{\max} l}{2bh^2} \qquad (2)$$

Where σ is the bending strength of finger jointed lumber (MPa); P_{max} is the ultimate bending load (N); l is the span length (mm); b is the width of the specimen(mm); h is the height of the specimen(mm).

3. Results and discussion

3.1 end-pressure test

When the load was applied on the end of finger joints, the stress were mainly concentrate on the top of the finger joints according to the modeling results. With the increasing of pressure, elastic deformation was first developed, when the stress exceeded the elastic limited stress, the plastic deformation was then developed. After the stress exceeded the yield stress of the lumber, it indicates that the collapse happened in the finger joints which would affect the ultimate strength of the finger-jointed lumber.

The appropriate end-pressure for finger-jointed lumber manufacturing is between the value causes the plastic deformation and failure of the finger joints. Figure 10 shows the modeling results and experimental results of end pressure test for finger joints at three different fitness levers (0mm; 0.1mm; 0.3mm). From the modeling results, it can be concluded that the end pressure range are 1.5MPa~3.0MPa, 2.0MPa~3.5MPa and 2.5MPa~4.5MPa for fitness 0mm, 0.1mm and 0.3mm respectively.

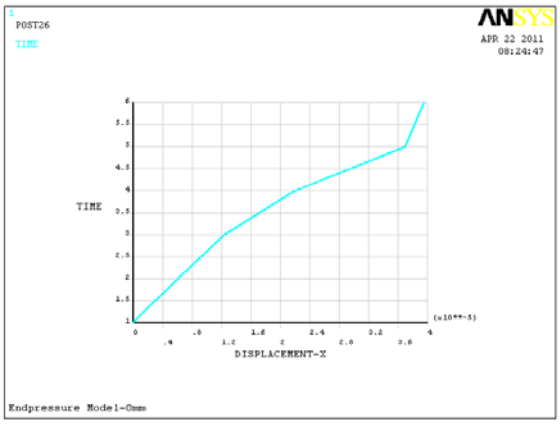

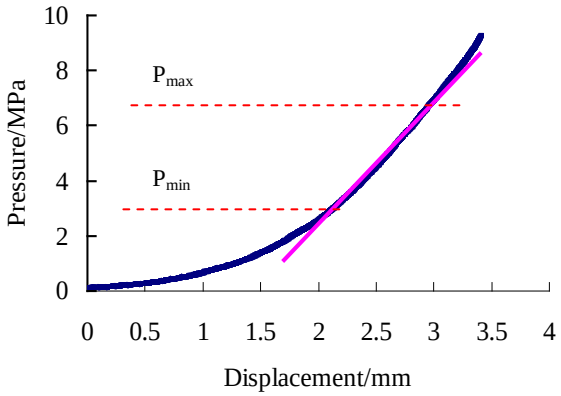

a) Fitness-0mm

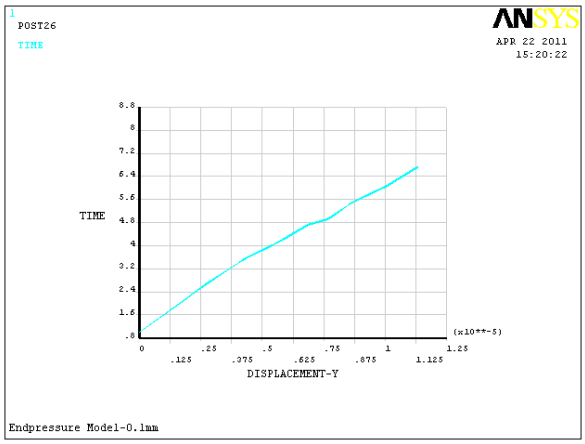

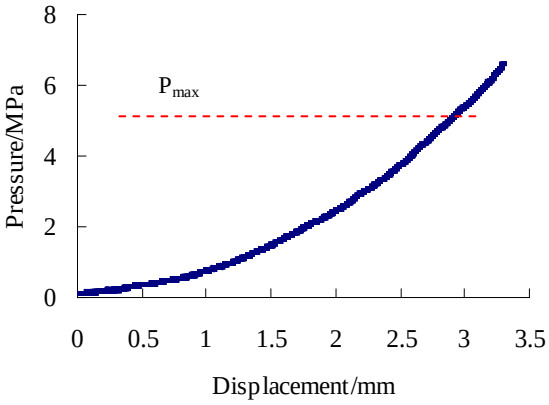

b) Fitness-0.1mm

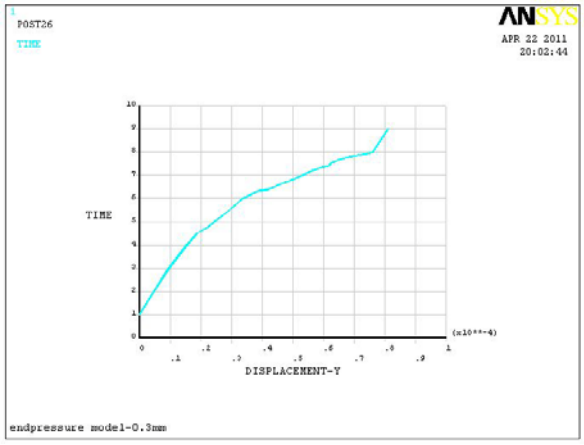

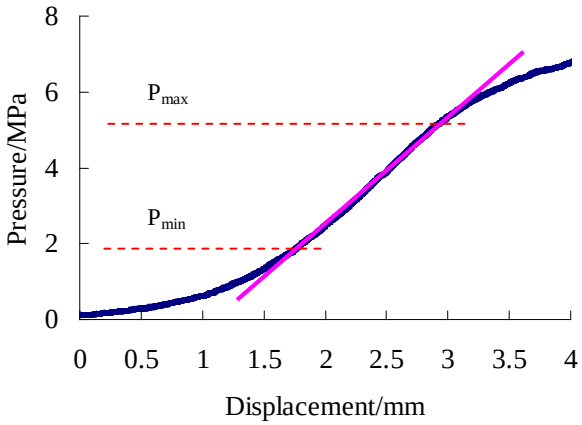

c) Fitness-0.3mm

Fig.10 Modeling and experimental results for end-pressure test

The modeling results showed some discrepancies compared with the experimental results. First, the node developed elastic deformation when the end pressure was low in the modeling process while the displacement increases fast with the increase of pressure in the experimental process because two finger joints can not fit seamlessly which cause a process that two finger joints fit together (the gap between them eliminated gradually under low end pressure). The difference showed in the initial part of the pressure-displacement curves of modeling and experimental results. Secondly, as the table 5 shows, both the lower limit (P_{min}) and upper limit (P_{max}) of end pressure in modeling tests were lower than the experimental test results, extremely for the upper limit. It was mainly caused by the different ways of judging the failure of finger joints under pressure. In the experimental tests, the upper limit of end pressure was set as the macroscopic crack developed in the finger joints, whereas the failure was accounted as the stress on one node of exceeded the yield stress in the modeling process; when one node of the model reached the failure, the others are still in good state. Thus, it is reasonable that the end pressure was smaller in FEA than experimental test results.

Tab.5 Comparison of end-pressure between experimental and modeling results

Fitness/mm	Experimental results/MPa		Modeling results/MPa	
	P_{min}	P_{max}	P_{min}	P_{max}
0	2.6	5.8	1.5	3.0
0.1		5.9	2.0	3.5
0.3	2.6	5.3	2.5	4.5
Average	2.6	5.7	2.0	3.7

As the appropriate end pressure range was determined through experimental and modeling tests, three levels of the end pressure (2.6MPa; 3.5MPa; 4.4MPa) were selected in a experiment conducted to find the optimum end pressure for *Pinus Sylvistriv* var.

finger-jointed lumber. The experiment test results showed that finger-jointed lumber manufactured when end pressure was 3.5MPa exhibited the highest mechanical strength compared with other two levels of end pressure (He, 2011). It is close to the upper limit of the modeling test results. So it can be concluded that the optimum end pressure for finger-jointed lumber manufacturing could be found through FEA process.

3.2 MOE test

Under low pressure, the stresses spread on the finger-jointed lumber were quite uniform. In the direction along the load, elements exhibited the largest deformation. Figure 11 shows the relationship between the displacement and time (the same as load) of the node which developed the largest deformation. According to the national standard for testing the MOE of wood, the deformation taken in the calculation of MOE should be the increment when the load increases from 300N to 700N. It can be drawn from the figure 11 that when fitness is 0mm, the corresponding deformation is 0.45mm, whereas the deformation when fitness is 0.1mm and 0.3mm are 0.4mm and 0.44mm respectively. Thus the MOE for finger-jointed lumber of three different fitness are 16.36GPa, 18.40GPa and 16.73GPa respectively.

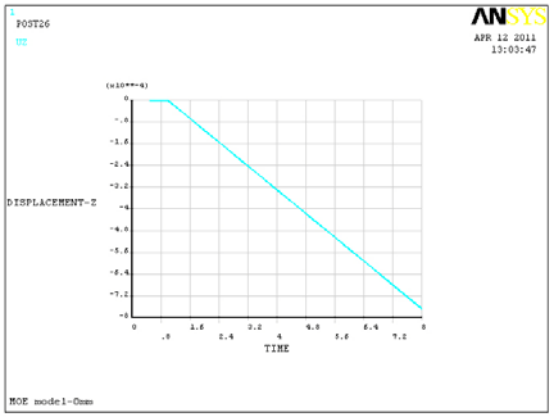

a)Fitness-0mm

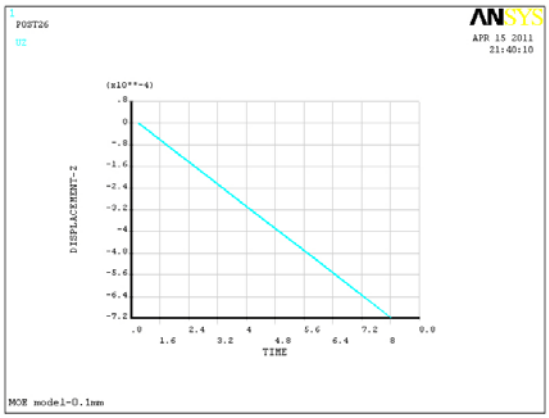

b)Fitness-0.1mm

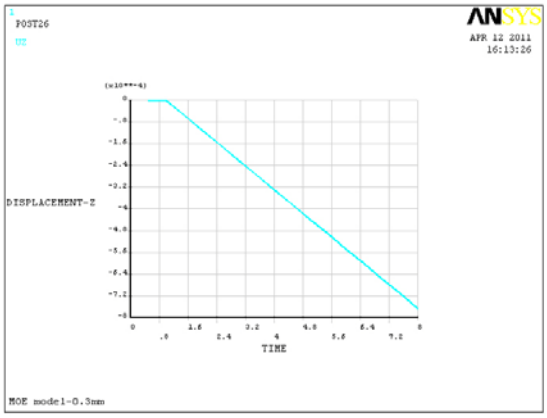

c)Fitness-0.3mm
Fig.11 The modeling results for MOE test

As the table 6 shows, the modeling test results for MOE were more than 20% higher than the experimental test results under three different fitness levers. The error may comprise of two parts. First, knots, rot, oblique grain and other flaws would weaken the strength of the timber which results in the strength decrease of finger-jointed lumber (Xu, 2000). However, in the modeling process, the timber was regarded as a cylinder symmetry and orthotropic material without taken the defects of timber into account. The parameters input in the modeling process were measured using flawless specimens. So it is possiblely cause the difference between these two testing methods. Besides, the other cause of the error could be the manufacturing deficiencies such as the broken of the finger joints, the impurity of the glue mixed with sawdust, ect., these will greatly affect the strength of the finger-jointed lumber (Liu, 1995); but they were neglected in the modeling process.

Tab.6 Comparison of MOE properties between experimental and modeling results

Fitness/mm	Experimental result/GPa	Modeling result/GPa	Error/%
0	13.42	16.36	21.9
0.1	14.40	18.40	27.8
0.3	13.19	16.73	26.8

As both the experimental and modeling results shown, the MOE of finger-jointed lumber when fitness was 0.1mm exhibited the highest value whereas the MOE for fitness 0mm and 0.3mm didn’t show significant difference. The filling of adhesive in the tip top will definitely increase the strength of finger-jointed lumber, thus it is natural that the MOE for fitness 0.1mm is higher than the lumber of fitness 0mm. However, with the increase of fitness, the length of finger joints decrease which result in the decrease of bond area. As the results for scarf joint shows, the increase of bond area would make the joints to withstand higher load (Roland, 1981), namely increase the strength of the joints, including the MOE. So it is reasonable that the MOE for lumbers of fitness 0.3mm were lower than fitness 0.1mm. The

combined effects of filling of adhesive and the length of finger joints resulted in the insignificant difference for lumbers of fitness 0mm and 0.3mm.

3.3 Bending strength test

With the increase of pressure, the deformation of the finger-jointed lumber along the direction of the load increases until the stress in the finger joints reaches the yield stress. The load (corresponding to load step) when the node reaches failure is the ultimate load of bending for finger joints. Figure 12 shows the relationship between displacement and time (load step) for node which reached the yield stress. The ultimate load of bending under three different fitness levers for finger-jointed lumbers were 2600N, 2400N and 1500N respectively from the figure. Thus the corresponding bending strength were 78.0MPa, 72MPa and 45.0MPa.

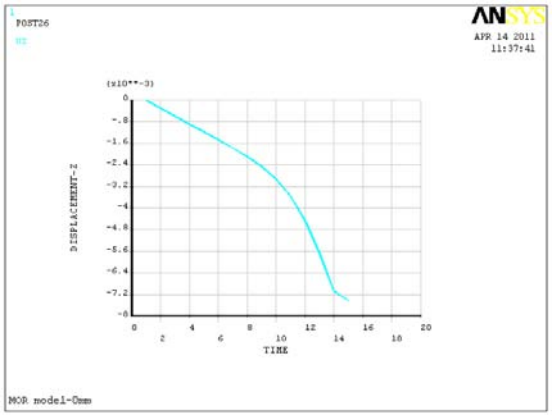

a) Fitness-0mm

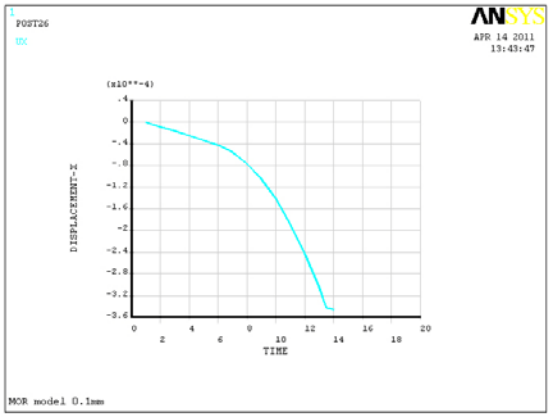

b) Fitness-0.1mm

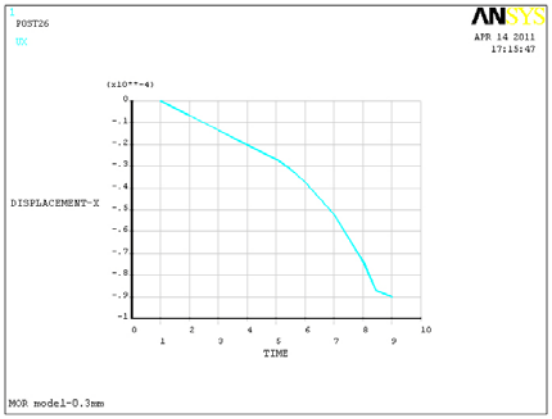

c) Fitness-0.3mm
Fig.12 Modeling results for MOR test

Compared with the experimental results, the modeling results showed some discrepancies in table 7, especially for lumbers manufactured when fitness is 0.3mm (35.3%). The lumbers of fitness 0.1mm exhibited the highest value for MOR while the corresponding value for fitness 0mm and 0.3mm almost at the same lever in the experimental results. However, the MOR for fitness 0mm shows the highest value in modeling result, fitness 0.1mm followed, and the lowest is the lumbers of fitness 0.3mm.

Tab. 7 Comparison of MOR properties between experimental and modeling results

Fitness/mm	Experimental result/MPa	Modeling result/MPa	Error/%
0	68.4	78.0	14.0
0.1	75.9	72.0	-5.1
0.3	69.6	45.0	-35.3

Same as the explanation for results of MOE, the filling of adhesive in tip top will increase the strength which makes the MOR for lumbers of fitness 0.1mm higher than that for fitness 0mm; but when the fitness is too large (0.3mm), the length of finger joints decrease too much, it will affect the strength of finger joints to a large extend. Also, the filling of adhesive in large tip top gap will decrease the strength as bond area for adhesive and the lumber will develop the concentration of stress because adhesive has different prosperities compared with wood, thus the MOR for lumber of fitness 0.3mm is lower than that when fitness is 0.1mm.

The modeling process is different from the actual condition in experimental process to a certain extent. The finger joints would have some plastic deformation when load with end pressure in finger-jointed lumber manufacturing process. This phenomenon will cause the decrease of the fitness and lengthen the finger joints which is helpful for guarantee the strength of the finger-jointed lumber. But in the modeling process, the effect of the factor was neglected, so it can be seen that the modeling results for fitness 0.1mm and 0.3mm are lower

than the experimental results. For lumbers of fitness 0mm, the compression under end pressure would cause some damage to the finger joints as there were no tip top gaps between two finger joints, and then it would decrease the strength of the finger-jointed lumber. This was not taken into account in the modeling process, so the modeling results were higher than experimental results in such condition.

4 Conclusions

FEA applied in the end pressure tests showed a narrower range compared with the modeling results. This was mainly caused by the different ways of judge the failure of finger joints under pressure. In the experimental tests, the upper limit of end pressure was set as the macroscopic cracking developed in the finger joints; whereas the failure was accounted as the stress on one node of exceed the yield stress in the modeling process. Moreover, the upper limit from modeling results is close to the optimum end pressure for finger-jointed lumber manufacturing which obtained from experimental test. It indicates that the FEA can be used in the prediction of the end pressure for finger-jointed lumber.

The modeling results for MOE test of finger-jointed lumber were about 20% higher than experimental results. The error may result from the neglection of the natural flaws existing in the lumbers and the manufacturing deficiencies when conducting the modeling process. Besides, the modeling results showed the same variation tendency for MOE of finger-jointed lumber under three different fitness levels. Thus the conclusion could be made that FEA is a feasible way in analyzing the MOE of finger-jointed lumber if the errors could be eliminated properly.

The modeling results for MOR test of finger-jointed lumber also showed some discrepancies compared with the experimental test results. The modeling process was different from the actual condition in experimental process to a certain extent. The plastic deformation developed from the load of end pressure in finger-jointed lumber manufacturing process caused the decrease of the fitness and lengthen the finger joints which is helpful for guarantee the strength of the finger-jointed lumber. But in the modeling process, the effect of the factor was neglected. Also, the damage of the finger joints under end pressure when fitness is 0mm which was not taken into account in the modeling process resulted in the different trend between experimental and modeling results of MOR for finger-jointed lumber under three fitness levers.

In order to realize the modeling of the properties of finger-jointed lumber, some modification should be made on the models. Further studies are in progress to investigate the ways for diminishing of the errors in the modeling processes.

References

Cecilia B. et al, Effect of curing time and end pressure on the tensile strength of finger-jointed black spruce lumber, forest product journal 2003;53(11):85-89.

Davalos J. F., Kim Y Ch, et al. A layerwise beam element for analysis of frames with laminated sections and flexible joints[J]. Finite Elements in Analysis and Design, 1995, 19: 181-194.

He S. Study of finite element modeling analysis for Pinus *sylvestris* L. var. finger-jointed lumber[D]. Jiangsu: Nanjing Forestry University. 2011.

Kiyoko Y, Takeshi O, Yasuhide M, et al. Evaluation of Sugi finger–jointed laminae with a knot and starved joints by acoustic emission[J]. J. Fac. Agr., Kyushu Univ., 2007,52 (1):111–116.

Kutscha P., R.W. Caster, Factors affecting the bonding quality of hem-fir finger-joints. Forest Prod. J. 1987,37(4):43-48.

Liang S.Q. et al, Developments and applications of nondestructive tests for wood in North America[J]. China wood industry, 2008,22(3):5-8.

Lin L.Y. et al, Comparative study of MOE on three methods of nondestructive test forecasting four kinds of lumber[J]. Wood processing machinery, 2007,18(3):24-29.

Li X.M. Research on Mechanical Property Simulation of Timber with Finite Element Method and Optimization of Timber[D]. Inner Mongolian: Inner Mongolian Agricultural university. 2009.

Liu Z.F. The influence of flaws in finger joints on the strength of finger-jointed lumber[J]. Forestry Abroad,1995,25(1): 99-101.

Marra G. The role of adhesion and adhesives in the wood products industry. In: adhesives for wood. Research applications, and needs. R. H. Gillespie, ed. USDA forest serv., Forest Prod. Lab., Madison, WI. 1984, pp.2-9.

Moses D.M., Prion H.G.L.. Stress and failure analysis of wood composites: a new model [J].Composites: Part B, 2004, 35: 251–261.

Roland W. Finger-jointed wood products. Research paper FPL 382, 1981.

Raknes, E. The influence of production condition on the strength of finger-joints. In:Proc. Procdution, Marketing and Use of Finger-jointed Sawnwood. C.F.I.. Prins, ed. Timber

Committee of the United Nations Economic Commission for Europe. Martinus Nijhof/Dr. W. Junk Publishers. The Hague, The Netherlands. 1982, pp.154-168.

Serrano E. A numerical study of the shear-strength-predicting capabilities of test specimens for wood–adhesive bonds[J]. International Journal of Adhesion & Adhesives, 2004, 24: 23–35.

Tabiei A, Wu J. Three-dimensional nonlinear orthotropic finite element material model for wood [J].Composite Structures, 2000, 50:143-149.

Xu Y.J. The properties of timber[J].Wood in China,2000(5): 21-22.

Zhang H.J. et al, Measuring elastic modulus of wood using vibration method[J]. Journal of Beijing Forestry University, 2005(11):91-94.

Zhao R.J. et al, Estimation of Modulus of Elasticity of Eucalyptus Pellita Wood by Near Infrared Spectroscopy[J]. Spectroscopy and Spectral Analysis, 2009(9):2392-2395.

Zheng X.L. et al, Numerical analysis for effect of adhesive thickness on the stress distribution in butt joint[J]. Adhesion In China, 2004,25(5):30-32.

The Papermaking Potential of Canola Residues; Viable Raw Material

Reza Hosseinpour

Department of Wood and Paper Science, Science and Research Branch, Islamic Azad University, Tehran, Iran. hosseinpourreza@gmail.com

Ahmad Jahan Latibari

Department of Wood and Paper Science, Karaj Branch, Islamic Azad University. Karaj, Iran. latibari_24@yahoo.com

Abstract

Non-wood pulping is gaining momentum not only in fiber deficient regions, but also new interest is shown in North America and Scandinavia. Among non-woods fiber sources, chemical pulping of wheat straw and bagasse has been practiced for a long period and reached its mature stage, but uncommon non-wood fibers are being studied. Among such uncommon fiber sources, canola residue is unique. Its woody stem grows to the height of almost 1.5 meter and its diameter reaches 10 mm. Such woody stem exhibits pulping potential which has not been explored. This is on the contrary to the availability of its vast quantities after harvesting. Wheat straw and even bagasse is used as cattle feed in some countries, but canola residue is not suitable for such application. This also indicates the need for pulping study. The objective of present study was to analyze the potential application of canola residue in pulping. At first, the fiber characteristics and chemical composition were assessed and compare with other non-wood fibers. Then different pulping were conducted applying different chemical treatments, and the corresponding pulp properties were characterized. Generally, the result demonstrated the unique behavior of canola lignin toward chemical treatment. After mild chemical treatment applying a mixture of sodium sulfite and sodium hydroxide, pulp brightness reached almost 44% and strength of pulp were comparable with those from bagasse and wheat straw. Such unique behavior confirms its potential as supplementary pulp for paper production.

Keywords: Canola, CMP, Brightness, Tensile, Tear.

Introduction

Many developing countries have shown interest in establishing domestic paper production capacities and to fulfill their growing demand for paper commodities and to become self-sufficient. In order to satisfy this requirement, paper production facilities have been forced to utilize uncommon raw materials, especially non-wood fibers. In addition, shortage of wood fiber, the cost-effectiveness and abundance of this fiber sources make non-woods reasonable candidates for pulp and paper production (Fatehi et al., 2009). By far, cereal straws have been the major source of non-woods for the paper production (Sun et al., 2001). However, the results on chemical pulping and papermaking properties of several other non-woods are also available in the literature (Ghatak, 2002; Tutus and Eroglu, 2003).

Among agricultural crops, canola has been cultivated to produce seeds for edible oil production, and the interest in its cultivation is increasing around the globe. The canola woody stem has a diameter of one cm and an average height of 1.5 m. After harvesting, the volume of woody stem remaining in the fields is approximately 7 tons/ha. In contrast to cereal straw, the canola stem cannot be used as cattle feed. It is available at a very low cost and apparently suitable for pulping (Sefidgaran et al. 2005).

So far the chemical pulping of non woods has been practice successfully and the unbleached chemical pulps of non-woods has been used in the production of corrugated-medium grades, and the bleached ones can be used in the production of printing and writing papers (Fatehi et al., 2009). However, recent reports and finding have shown that, the chemimechanical pulping (CMP) process provides the advantages of a mild chemical treatment and of high pulping yield compared with the chemical pulping process. Due to the importance of emerging CMP pulping, the CMP pulping of woody materials has also been investigated and promising results have been reported (Janson and Mannstrom, 1981; Law and Daud, 2000; Guerra et al., 2005), but the CMP of non-woods and their corresponding paper properties have received much less attention. Recently, the potential application of canola straw on medium density fiberboard (MDF) has shown promising results (Yousefi, 2009).

The objective of the report is to provide the information on the papermaking potential of canola residues and to provide data on different pulping of this raw material.

Fiber Morphology and Chemical Characteristics

Canola fiber length, fiber width, and lumen width are listed in Table 1. The average fiber length of canola (1.32mm) is longer than that of corn, wheat straw, bangkot, and sunflower, but is shorter than that of bamboo (3.49 mm) and of kenaf (2.32 mm). Canola fiber width (31 μm), lumen width (19.5 μm), and cell wall thickness are higher than that of other non-woods in Table1 (Hosseinpour et al. 2010).

Species	Fiber length (mm)	Fiber width (μm)	Cell wall thickness (μm)	Lumen width (μm)	References
Canola	1.32+-0.5	31+-7.4	3.75	19.5+-6.5	Our data

Corn	0.903	18.45	3.69	11.07	Latibari et al. 2009
Wheat straw	0.74	13.2	4.6	4	Deniz et al 2004
Bamboo	3.49	17.7	5	7.7	Lwin et al 2001
Bongkot	0.82	27	-	-	Loutfi & Hurter 2004
Kenaf (bark)	2.32	21.9	4.2	11.9	Ververis et at 2004
Sunflower	1.28	22.1	3.3	15.6	Eroglu et al 1992

Table 1- Properties of depithed Canola fibers and other non-wood fibers

The chemical composition of canola straw is listed in Table 2 (Hosseinpor et al. 2010).

Species	α-Cellulose (%)	Lignin (%)	Holocellulose (%)	Pentosans (%)	Ash (%)	Alcohol-Acetone extractives (%)	Hot water solubility (%)	Cold water solubility (%)	1% NaOH solubility	Reference
Canola	48.5	20	77.5	17	6.6	6.6	5	13.8	50.3	Our data
Corn	33.6	17.4	64.8	-	7.5	9.5	14.8	-	47.1	Usta et al, 1990
Wheat straw	38.2	15.3	74.5	-	4.7	7.8	14	10.7	40.6	Deniz et al. 2004
Rice straw	48.19	17.3	70.85	24.5	16.6	3.52	16.24	10.65	49.15	Tutus et al. 2004
Bongkot	42.7	17.2	70	27.2	0.7	0.9	2.8	-	17.2	Loutfi &Hurter 2001
Sunflower	37.5	18.2	74.9	-	8.2	7	16.5	15.5	29.8	Eroglu et al. 1992

Table 2- Chemical composition of depithed canola fibers and other non-wood fibers

Evidently, the holocellulose content of canola is somewhat higher than that of wheat straw, but similar to that of hardwood or bagasse, while the α-cellulose content of canola straw is lower than that of others. As is well known, the total hemicelluloses and cellulose contents of lignocellulosic materials is expressed as holocellulose content. Thus, these results indicate that the hemicellulose content in canola straw is higher than in other raw materials listed in Table 2. Also, the lignin content of all samples is comparable.

CMP Pulping

CMP pulping of canola residues were performed applying mild chemical condition in a rotary digester. The liquor-to-fiber ratio was 7:1, while the pH was approximately 13. The CMP process was conducted in three different stages. Firstly, the pretreatment of canola straw was carried out using the chemicals. In this stage, the temperature of the digester was raised to 125 ^{o}C in 23 min, and kept at this temperature for 15 min. Secondly, the pretreated canola straw was refined three times using a single disk refiner under an atmospheric pressure. After refining, the pulp samples were washed thoroughly with water, and the total yield of pulps was determined. Then, the fibers were screened using a 14-mesh screen to determine the

amount of rejects. Thirdly, to further improve the property, a post-refining was performed on the canola straw CMP, using a PFI refiner according to TAPPI T 248. The characteristics of canola canola straw CMP were evaluated in accordance with TAPPI test methods. The tensile, tear and burst strengths were measured according to TAPPI T 494, T 414 and T403, respectively. The thickness of paper-sheets was measured according to Tappi T 411 and then the apparent density was determined considering the actual basis-weight and thickness of the paper-sheets.

Sample/Reference	NaOH (%)	Na_2SO_3 (%)	Total yield (%)	Reject (%)	Cellulose (%)	Holocellulose (%)	Lignin (%)	Ash (%)	Non-wood species
1	4	8	68.9	5.9	23.7	48.8	14.5	2.06	Canola Starw
2	4	10	67.3	5.5	23.2	49.2	13.4	2.01	
3	8	8	63.3	6.8	22.4	44.7	13.6	1.89	
4	8	10	63.1	5.0	22.1	45.0	13.7	1.88	
5	12	8	61.4	4.4	20.9	44.0	14.3	1.84	
6	12	10	60.7	3.9	20.7	43.6	12.7	1.82	
7	12	12	60.0	3.3	20.0	43.8	12.3	1.80	
Peng &Simonson,1992	5.8	-	72	-	-	-	17.6	-	Bagasse
Mirskokraei et al. 2005	4	8	-	-	-	-	17.8	-	Bagasse
Petit-Conil et al. 2001	5.2	-	71	2.1	-	-	-	-	Wheat Straw

Table 3- Pulping condition and chemical composition of Canola straw CMP

The effect of the chemical charges on the CMP pulping and the properties of canola straw CMP are summarized in Table 3. By increasing the charge of the chemicals, the total yield and the amount of rejects were reduced. The relatively low yield of canola straw CMP pulps is attributed to the great loss of lignin, α-cellulose, and holocellulose, which were 20%, 48.5%, 72.5% (Tables 2). Additionally, a lower charge of the chemicals applied in the pretreatment of bagasse CMP and of wheat straw CMP in the literature than that applied in the pretreatment of canola straw CMP in the present work (Table 3). However, a similar yield, but at higher lignin content, was obtained for bagasse CMP and for wheat straw CMP than for canola straw CMP (Table 3).

Sample ID	NaOH (%)	Na_2SO_3 (%)	Total Yield (%)	Apparent Density ($g/cm^{3)}$	Tensile Index (N.m/g)	Burst index ($kPa.m^2/g$)	Tear index ($mN.m^2/g$)
1	4	8	68.9	0.46	15.94	1.6	3.50
2	4	10	67.3	0.48	16.02	1.2	3.52
3	8	8	63.3	0.50	15.31	1.4	3.35
4	8	10	63.1	0.50	15.25	1.5	4.21

5	12	8	61.4	0.59	15.47	2	4.20
6	12	10	60.7	0.50	18.61	1.7	4.64
7	12	12	60.0	0.52	17.79	1.8	3.93

Table 4- Properties of canola straw post refined CMP pulp

The tensile index at a given apparent density for canola straw CMP is similar to that for bagasse CMP reported by Peng and Simonson (1992). The tensile index and apparent density of the paper-sheets increased by 15–24% and 18– 20%, respectively, by the post-refining treatment Table 4). It is shown that a modest post-refining treatment of canola straw CMP can improve the tensile strength significantly. As described earlier, the post-refining improved the fiber straightening, as evidenced by the decreases in curl and kink index. In this case, the increase in the amount of fines as well as in the fiber straightening can account for the pronounced tensile improvement. The increase in the apparent density is attributed to the improvement in the fiber bonding.

By increasing the dosage of the chemicals, the burst and tear indices increased somewhat. Peng and Simonson (1992) reported a much lower tear index (1.5–2 Nm^2/kg) for the bagasse CMP. In another study, similar burst and tear indices were reported for an industrially produced wheat straw CMP (Sig-oillot et al., 1997). These results imply that the wheat straw CMP and the canola straw CMP had similar strength properties. It is also evident, by post-refining of canola straw CMP, the burst index increased by 20–43%, while the tear index increased by 3–6%.

The significant improvement in the burst index from the post-refining treatment is attributed to the straightening of fibers that improves the fiber bonding, as addressed earlier.

Neutral Sulfite Pulping

Ahmadi et al (2010) investigated the performance of canola straw in neutral sulfite semichemical (NSSC) pulping. Different dosages of active alkali and pulping times at sodium sulfite to sodium carbonate ratio of 3:1 and pulping temperature of 170 ^{o}C were applied. Both digester and defibration yields were measured and then the strength of the selected pulps was evaluated. The results of the measurements on the selected pulps are summarized in Table 5.

Active alkali (%)	Pulping time (min)	Total yield (%)	Kappa No.	Tear index ($mN.m^2/g$)	Tensile index (N.m/g)	Breaking length (km)	Burst index ($kPa.m^2/g$)
8	20	72	66	6	35.6	3.63	1.7
10	20	71.5	65	6.2	38.2	3.89	1.75
12	20	69	64.5	6.4	39.2	3.99	1.87
14	20	68.5	63.5	6.6	42	4.28	2.03
16	20	67	56.5	6.9	44	4.48	2.04
12	40	63.5	50	7.4	57.8	5.89	2.46
12	60	58.7	45	7.5	66.5	6.78	2.57

Table 5- The properties of selected NSSC pulps from canola residues

It has been expressed that the performance of canola residues in NSSC pulping varies considerably and the pulping yield is usually low. It is possible to reach defibration yield between 54.5-72% (digester yield between 58.5-87%), but reaching higher yield is difficult using this material. However, with careful refining and back water circulation, defibration yield can be improved. Changing the alkali charge between 8% and 16%, increased the tear strength index from 6 to 6.9 $mN.m^2/g$, breaking length from 3.63 km to 4.48 km, burst strength index from 1.7 to 2.04 $kPa.m^2/g$ and tensile strength index from 35.6 to 44 Nm/g. It can be concluded that canola residues can be considered suitable for unbleached NSSC pulp production to be used as substitute pulp in the production of corrugating medium paper.

Soda Pulping

Enayati et al. (2010) hace examined the application of soda pulping on canola residues applying active alkali (% NaOH) between 15-22% based on the dry weight of the straw, liquor to straw ratio of 8:1 at 170 ^{o}C pulping temperature and different pulping times. The results of pulping yield and kappa number is shown in Table 6.

NaOH (%)	Pulping time (min.)	Screen yield (%)	Reject (%)	Kappa No.	Degree of polymerization
15	60	35.2	14.5	101.2	-
15	80	36.9	12.7	97.3	-
15	100	37.0	11.0	94.6	-
18	60	43.3	4.6	89.8	-
18	80	42.6	3.5	83.5	-
18	100	42.2	3.1	82	-
20	60	40.5	1.5	70.7	1435
20	80	39.1	1.4	54	1511
20	100	38.5	0.9	36.0	1553
22	60	37.3	0.6	40.0	1579
22	80	37.2	0.4	25.9	1448
22	100	36.6	0.3	24.2	1408

Table 6- The results of soda pulping of canola residues (Enayati et al. 2010)

The pulping results indicated that at higher chemical charge, the pulping yield is scarified and the reject is unexpectedly high even after 100 minutes pulping time. However, increasing the alkali charge improved the performance of the soda pulping of this material but the total yield was reduced significantly producing uniform pulp. The kappa number of the pulps varied between 70.1 and 36. Therefore, even 20% active alkali charge did not produce bleachable pulp to be able to produce bleachable pulp. Therefore, the active alkali charge should be increased to 22%.

Pulp produced applying 22% active alkali, and 100 minutes time at 170 ^{o}C was selected for Elemental Chlorine Free (ECF) bleaching under D_0EpD1 with 2.8 kg/ton charge of chlorine dioxide and 1.2% NaOH and 0.3% hydrogen peroxide. The brightness of the bleached pulp was raised from the unbleached value of 36.5% ISO to the final value of 78.4% ISO.

Bleaching partially reduced the strength properties of the canola soda pulp and the tensile index was reduce from 24 Nm/g to 23.1 Nm/g, tear index from 5.07 $mN.m^2$/ to 4.76 $mN.m^2/g$ and burst Index was improved from 1.22 $kPa.m^2/g$ to 1.39 $kPa.m^2/g$. The overall results showed the promising potential of canola soda pulp to be used in combination with wood pulps in paper making.

References

Ahmadi, M., Jahan Latibari, A., Faezipour, M., Hedjazi, S. 2010. Neutarl sulfite pulping of canola residues. Turk. J. Agric. For. 34(2010):11-16.

Enayati, A.A., Hamzeh, Y., Mirshokraei,S.A., Molaei,M. 2010. Paper making potential od Canola stalks. Bioresources 4(1): 245-256.

Eroglu, H., Usta, M., Kirci, H., 1992. A review of oxygen pulping of some non-wood plants growing in Turkey. Tappi Conference, Boston, USA: 215 –222.

Fatehi, P., Tutus, A., Xiao, H., 2009. Cationic PVA as a dry strength additive for rice straw pulp. Bioresour. Technol. 100 (2), 749–758.

Ghatak, H.R., 2002. Papermaking potential of congress grass: pulpability and fiber characteristics. Tappi J. 1 (1), 24–27.

Guerra, A., Mendonça, R., Ferraz, A., 2005. Bio-chemimechanical pulps from *Eucalyptus grandis*: Strength properties, bleaching, and brightness stability. J. Wood Chem. Technol. 25 (4), 203–216.

Hosseinpour, R., Jahan Latibari, A., Farnood, R., Fatehi, P., Sepiddehdam, S.j., 2010. Fiber morphlogy and chemical composition of canola (Brassica napus) stems. IaWA Joiunal 31(4):457-464.

Jahan Latibari, A., Golbabaei, F. Ziadzaheh, A. Farzi, M. Vazzirian, A., 2009. Investigation on size distribution and fiber dimensions of corn stalks. Iranian J. Wood Paper Res. 1: 1–14.

Loutfi, H., Hurter, R.W., 1997. Bongkot-A potential source of nonwood fiber for paper making. Proceedings of Tappi Pulping Conference, San Francisco, California 2: 817– 819.

Lwin, M. K., Han,Y.Y., Maung, K.W., Moe, A.Z., Than, S.M., 2001. An investigation on morphology, Anatomy and chemical properties of some Myanmar Bamboos. Proceedings of the Annual Research Conference, Yangon, Myanmar: 267–288.

Janson, J., Mannstrom, B., 1981. Principles of chemical pretreatment in the manufacture of CMP and CTMP from hardwood. Pulp Paper Can. 82 (4), 51–63.

Law, K.N., Daud, W.R.W., 2000. CMP and CTMP of a fast-growing tropical wood:*Acacia mangium.* Tappi J. 83 (7), 61–68.

Mirshokraie, S.A., Abdulkhani, A., Enayati, A.A., Latibari, A.J., 2005. Evaluation of mechanical and optical properties of modified bagasse chemi-mechanical pulp through acetylation in liquid phase. Iran. Polym. J. 14 (11), 982–988.

Peng, F., Simonson, R., 1992. High-yield chemimechanical pulping of bagasse. Part 4. Baggase CMP with sodium hydroxide/hydrogen peroxide pretreatment. Appita J. 45 (2), 104–108.

Petit-Conil, M., Brochier, B., Labalette, F., Combette, P., 2001. Potential of wheat straw to produce chemimechanical pulps suited to corrugating papers manufacture. In: TAPPI Pulping Conference, Seattle, WA, pp. 929–939.

Sefidgaran, R., Resalati, H., Kazemi, N.S., 2005. A study of potentials for producing soda pulps from canola straw for making fluting paper. Iran. J. Nat. Resour. 2,433–446.

Sigoillot, J.C., Petit-Conil, M., Ruel, K., Moukha, S., Comtat, J., Laugero, C., Joschleau,J.P., de Choudens, C., Asther, M., 1997. Enzymatic treatment with manganese peroxidase from Phanerochaete chrysosporium for enhancing wheat straw pulp characteristics. Holzforschung 51 (6), 549–556.

Sun, R.C., Sun, X.F., Wen, J.L., 2001. Fractional and structural characterization of lignins isolated by alkali and alkaline peroxide from barely straw. J. Agric. Food Chem. 49, 5322–5330.

Technical Association of pulp and paper Industry, 2009. Standard test Methods, Tappi Press, Atlanta, GA. USA.

Tutus, A., Eroglu, H., 2003. A practical solution to the silica problem in straw pulping. Appita J. 56 (2), 111–115.

Yousefi, H., 2009. Canola straw as a bio-waste resource for medium density fiberboard (MDF) manufacture. Waste Manage. 29, 2644–2648.

Tutus, A., Deniz,I., Eroglu, H., 2004. Rice straw pulping with oxide added soda-oxygen-anthraquinone. Pakistan J. Biol. Sci. 7(8): 1350 –1354.

Usta, M., Kirci, H., Eroglu, H., 1990. Soda-oxygen pulping of corn (*Zea mays indurata sturt*). Proceeding of Tappi Pulping Conference, Toronto, Canada: 307–312.

Ververis, C., Georghiou,K., Christodoulakis, N., Santas, P., Santas, R., 2004. Fiber dimension, lignin and cellulose content of various plant materials and their suitability for paper production. Ind. Crops Prod.19: 245–254.

Modulus of Elasticity and Hardness of Compression and Opposite Wood Cell Walls of Masson Pine

Yanhui Huang[1] *- Benhua Fei*[1]* *- YanYu*[1] *- SiqunWang*[2] *- Zengqian Shi*[2] *-*

Rongjun Zhao[3]

[1] International Center for Bamboo and Rattan, Beijing, China.
* *Corresponding author*
feibenhua@icbr.ac.cn
[2] Center for Renewable Carbon, University of Tennessee, Knoxville, USA.
[3] Chinese Academy of Forestry, Beijing, China

Abstract

Compression wood is commonly found in Masson pine. To evaluate the mechanical properties of the cell wall of Masson pine compression and opposite wood, nanoindentation was used. The results showed that the average values of hardness and cell wall modulus of elasticity of opposite wood were slightly higher than those of compression wood. With increasing age of the annual ring, the modulus of elasticity showed a negative correlation with microfibril angle, but a weak correlation was observed for hardness. In opposite and compression wood from the same annual ring, the differences in average values of modulus of elasticity and hardness were small. These slight differences were explained by the change of microfibril angle (MFA), the press-in mode of nanoindentation, and the special structure of compression wood. The mechanical properties were almost the same for early, transition, and late wood in a mature annual ring of opposite wood. It can therefore be inferred that the average modulus of elasticity (MOE) and hardness of the cell walls in a mature annual ring were not being affected by cell wall thickness.

***Keywords*:** Compression wood, Cell wall, Modulus of elasticity, Hardness, Nanoindentation

Introduction

Compression wood develops because of the mechanical compression that occurs on the lower sides of leaning trunks and branches of gymnosperm trees. Wood from the corresponding upper side of these stems and branches is called opposite wood. The characteristics of opposite wood are similar to normal wood; that is, wood that has not grown and developed under the compressive or tensile loads associated with applied bending forces. In contrast to normal or opposite wood, the distinct characteristics of compression wood are higher lignification and density. Compression woods have a unique cell wall structure and tracheid formation characterized by the lack of an S_3 layer and helical cavities in the S_2 layer of the cell wall, rounded cross sections and distorted tracheid tips, and high microfibril angles (Timell 1987). The chemistry of tracheids in compression wood is characterized by lower contents of cellulose and higher contents of lignin compared to a tracheid in normal wood (Timell 1987).
Masson pine (*Pinusmassoniana*) is an important commercial species in the south of China and is used mainly in construction, furniture, indoor decorating, and pulp and papermaking. Compression wood is commonly found in the stems and branches of plantation Masson pine. The compression wood has an important influence on the mechanical properties of wood and wood-based products because for its specific structure and chemical composition. The macro-mechanical properties of compression wood have been subjected to detailed research; however, the mechanical properties at the cellular and subcellular level of compression wood are not well reported. Burgert *et al.* (2004) measured the longitudinal mechanical properties of single fibers of four compression wood types at the cellular level. Gindl *et al.* (2004) and Konnerth *et al.* (2009) investigated the relationship between cell wall mechanical properties of tracheids and microfibril angle (MFA) with normal, early, and late wood, as well as compression and opposite wood at the subcellular level by using a nano-indentation technique. For compression and opposite wood, there has been no detailed and systematic examination of the influence of MFA on the mechanical properties of the cell wall S_2 layer of tracheids, especially looking at the mechanical properties within an annual ring.
To better understand the mechanical properties of the cell wall S_2 layer of compression and opposite wood, this research aims to discuss systematically the influence of microfibril angle (MFA) on the longitudinal modulus of elasticity (MOE) and hardness of compression and opposite wood of Masson pine. The mechanical properties of the cell wall S_2 layer of opposite wood within an annual ring are also examined and discussed.

Materials and Methods

The experimental Masson pine was 32 years old, growing in the Huangshan Gongyi Forest Farm in Anhui province. A 4 cm thick disk containing compression and opposite wood was taken from the Masson pine crooked trunk at a height of 1.5 m. The disk was then dried in air for one month. After drying, one 10 mm wide center strip was sawn from the disk, and six slices containing latewood from the 2nd, 4th, 6th, 9th, 15th, and 24th annual rings (counted from the pith) were removed from the strip on the compression and opposite sides. The nominal size of the slices was about 40×1×10 mm (longitudinal × radial × tangential).

All the slices were conditioned at 20°C and 60% relative humidity for a week before measuring the microfibril angle using X-ray diffraction (X'PERTPRO, Philips Analytical, Almelo, Holland). The radiation source was CuKa (λ=0.154 nm). The tube voltage and current were 40 KV and 40 mA. The X-ray beam size was 4 by 2 mm, and the scattering angle 2θ was 22.4°. The scan time of each sample was 3 minutes. The results were analyzed to extract diffraction strength curves and calculate the mean microfibril angle (MFA). The MFA was determined using the method developed by Cave (1966).
The 12 slices were cut to the final dimensions of 1 mm in the radial direction, 1 mm in the tangential direction, and 10 mm in the longitudinal direction. The specimens were embedded in fresh Spurr low viscosity epoxy resin (Spurr 1969). The embedding was performed in a flat mould with the wood specimen in the middle of the flat surface. The mould containing the wood samples and the epoxy resin was then placed in a vacuum oven. After being kept in a vacuum for a minimum of 12 h, the embedded samples were heated to 70°C for 8 h until the resin cured. The resin-embedded sample was cut out from the mould and then mounted onto an ultra-microtome(American Optical Corp. USA). The transverse surface of the wood was leveled using a glass knife and then cut using a diamond knife for a smoother surface. Finally, the samples were conditioned for at least 24 h at 22°C and 40% relative humidity in the nanoindenter laboratory.

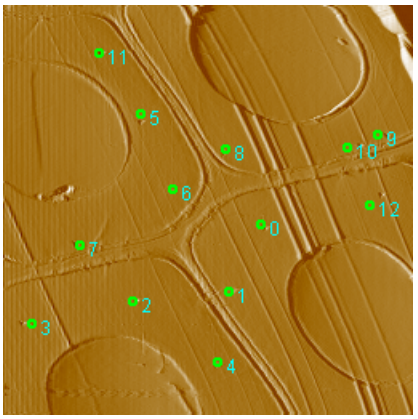

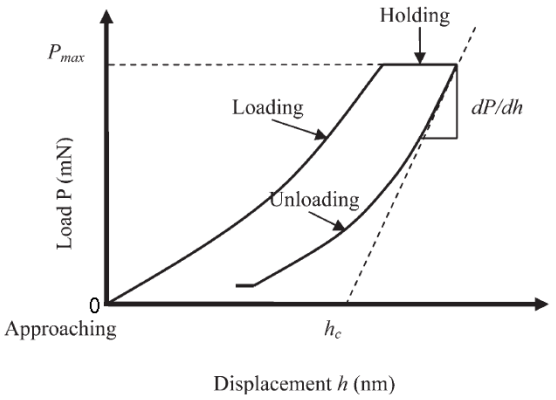

Figure 1.Indentsites on compression wood Figure 2 Nanoindent load-displacement curve

The sample was directly placed into a specially designed holder and then fixed on a motorized sample stage by magnetic force. A nanoindenter (Hysitron Inc. USA) equipped with a three-sided pyramid diamond Berkovich type indenter tip was chosen to conduct the nanoindentation tests. The peak load and loading-unloading rate were 150 μN and 30 μN/s. The load holding time was 5 s between loading and unloading segments to allow for thermal drift corrections. The indent depth was about 120 nm under these conditions. The target region was scanned before and after each experiment using the instrument video system to determine the actual positions and quality of the indentations (Fig. 1). The indents were made near the middle of the cell wallS_2 layer and distributed within the radial and tangential walls so as to reduce the error caused by the angle of tip. At least five tracheids from latewood were examined for each annual ring, and at least 50 measurements were taken for each of the rings investigated in this study.

A typical load-displacement curve of an indentation is shown in Figure 2. It was found that both elastic and plastic deformation occurred during loading and only the elastic part of the displacement was recovered when unloading. Nanoindentation hardness (H) is defined by the following equation,

$$H = P_{max}/A \quad (1)$$

Where P_{max} is the peak load and A is the projected contact area that is calculated from the empirical formula $24.5hc^2$, where hc is the contact depth of the indent.
The sample modulus (E_s) can be calculated as follows,

$$E_s = (1 - \nu_s^2)\left(\frac{1}{E_r} - \frac{1 - \nu_i^2}{E_i}\right) \quad (2)$$

where E_i and ν_i are respectively the elastic modulus and Poisson ratio of the tips. For diamond tips, E_i is 1141 GPa, and ν_i is 0.07. ν_s is the Poisson ratio of samples. It should be pointed out that the E_s and E_r are almost identical for soft materials like bamboo and wood, which eliminates the need to obtain the Poisson ratio of the samples. E_r is called the reduced elastic modulus, and can be obtained from the following equation,

$$Er = S\sqrt{\pi / A} / 2\beta \quad (3)$$

where β is a constant that depends on the geometry of the indenter (β = 1.034 for a Berkovich indenter) and S is the initial slope of the unloading curve(this slope is the elastic contact stiffness). In these tests, a range covering 70 to 90% of the unloading curve was chosen for calculating $S(d_p/d_h)$.

Results and Discussion

Nanoindentation is a very effective method for investigating the mechanical properties of the cell wall S_2 layer (Yu *et al.*2012). Compared to other methods, there is no need for any chemical pretreatment of the sample, and the measured values are very consistent with a variation coefficient of about 10% for MOE and less than 8% for hardness.

Modulus of Elasticity (MOE) The MOE of the cell wall S_2 layer of opposite wood and compression wood are summarized in Tables 1 and 2. The average MOE of opposite wood is slightly higher at 17.71 GPa than that of compression wood (16.65 GPa). A similar increase of the Young's modulus of opposite wood was found by Gindl (2002).The MOE has been shown to have a highly negative correlation to the value of MFA (Cave 1968, 1969; Page *et al.* 1977; Wu *et al.* 2009). As can be seen from Tables 1 and 2, compression wood had an average MFA 10° greater than opposite wood. However, the average MOE of compression wood was a little lower than opposite wood. When making nanoindentation measurements, the MOE is determined from the press-in mode of tip, which does not give the same results as measurements taken in tensile mode. Thus the MFA has a smaller influence on indentation than tension results. Furthermore, other factors must also play a role. Mark and Gillis (1973) showed that the MOE of

cellulosic fibers with a MFA exceeding 25° was insensitive to the properties of the cellulose.
Instead, it depended largely on the other characteristics. The compression wood had thick cell wall S_2 and S_1 layers, which could provide support when the tip was pressed in and pulled out. Schniewind (1962) points out that a high concentration of lignin in the secondary wall could lead to a higher lateral stability of the microfibrils. Hence, the special structure of compression wood, characterized by thick cell wall S_2 and S_1 layers and a high content of lignin, reduces the difference in average MOE resulting from MFA.

Table 1 Cell Wall S2Layer Mechanical Properties and MFA ofOpposite Wood

	O2	O4	O6	O9	O15	O24
MOE(GPa)	17.34	15.75	16.66	17.16	18.90	20.46
Hardness(GPa)	0.5317	0.4766	0.4881	0.4423	0.4605	0.5216
MFA (°)	22.54	26.01	17.02	14.58	11.53	12.57

Table 2 Cell Wall S2Layer Mechanical Properties and MFA ofCompression Wood

	C2	C4	C6	C9	C15	C24
MOE(GPa)	14.72	15.54	15.89	17.16	19.05	17.53
Hardness(GPa)	0.4483	0.4084	0.4256	0.4863	0.4807	0.5073
MFA (°)	32.34	33.28	29.00	19.91	25.18	25.19

Generally, the MOE showed an increasing tendency with increase of annual ring age for both compression wood and opposite wood (Tables 1 and 2), especially from annual ring 6, which was in good agreement with the adaptability growing of structure and function of trees (Meinzer *et al.* 2011). However, the tendency of MFA with annual ring age was to decrease (Fig. 3) (Cave and Walker1994).

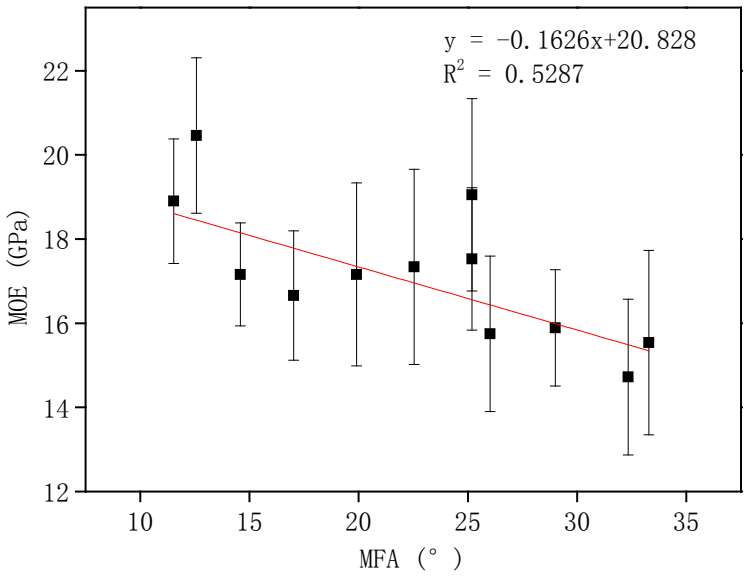

Figure 3 Variation of MOE with MFA for all tested wood samples

MFA is known as a particularly important factor for mechanical properties of wood (Burgert *et al.* 2004; Tze *et al.* 2007; Wu *et al.* 2009), and a decrease in MFA would result in an increase of MOE in both opposite wood and compression wood. Linear regression analysis (Fig.3) shows a weak relationship between MFA and MOE (R^2 = 0.5287) that also indicates that the cell wall MOE is influenced by multiple factors, such as entrained epoxy resin, as well as cell wall structure and components.
For samples taken from the same annual ring, the average value of MOE of opposite wood was higher than that of compression wood, which can be explained by the difference in MFA. However, the difference in the corresponding annual rings of MOE was small (about 1 GPa). The press-in mode of nanoindentation could be an important factor. Considering the special structure of the cell walls of compression wood, for example, the lack of an S_3 layer and the presence of large helical cavities in the S_2 layer, means that the embedding Spurr epoxy resin can easily enter these large helical cavities. The presence of the epoxy resin reinforces the cell walls of the compression wood and reduces the effect of MFA on the mechanical properties of the cell wall. Furthermore, as previously mentioned, the thick cell wall S_2 and S_1 layers and their high content of lignin may also have reduced the difference. Hence, it seems reasonable that there should be a somewhat low correlation coefficient between MFA and MOE in Figure 3. The MOE of the second annual ring was high (17.34GPa), which may have been caused by entrained resin in the samples.

Hardness The average cell wall hardness of opposite wood and compression wood were not significantly different (0.4868GPa and 0.4594GPa). This similarity is supported by the results of Gindl *et al.* (2004) and Yu *et al.* (2007).Yu *et al.* (2007) indicated that the MFA does not greatly influence hardness. So when the MFA reaches a certain critical value, the composition and packing density of the cell walls will act as the determinant of cell-wall hardness (Yu *et al.*2007). Gindl *et al.* (2004) also indicated that the indentation hardness was governed by the matrix at the macro level, for example, lignin content.
As is shown in Tables 1 and 2, there was a increasing trend of variation in cell wall hardness from annual ring 9 of opposite wood and compression wood, which could be also supported by Meinzer *et al.*' theory of adaptability growing (2011).In the same annual ring, it appeared that there was no consistent rule for the average values of hardness of opposite and compression wood. This also indicates that MFA has little influence on the cell wall hardness of opposite wood and compression wood. According to macro-scale mechanical measurements, compression wood has a high lignin content and density, which results in high hardness level in bulk wood samples. However, Wu *et al.*(2009)also did not observe any distinct difference while making observations at the nanometer level. It was proposed that the special structure of the cell wall of compression wood would be the main factors rather than lignin content on cell wall hardness.

Mechanical Property Variation within an Annual Ring Figure 4shows the average MOE and standard deviationof cell wall of early, transition, and late wood within the 24th annual ring of Masson pine opposite wood. The average MOE of the cell wall of early (19.95 GPa), transition (19.95 GPa), and late (21.08 GPa) wood were not significantly different. Variation of MOE is highly dependent on changes in MFA (Cave 1968, 1969;

Page *et al.* 1977).Since there is little variation of MFA in mature wood annual rings (Eder *et al.*2009), it is reasonable to assume that the difference of cell wall MOE should also be insignificant. Eder *et al.* (2009) also reported that the mechanical properties of spruce single fibers were similar throughout an annual ring in transition wood, which also supports the results in this study.
As Figure 4 shows, the distribution range of the standard deviationof cell wall MOE of early wood was larger than that of late wood and transition wood, which was due to the location of the nanoindentations and the thickness of cell wall.

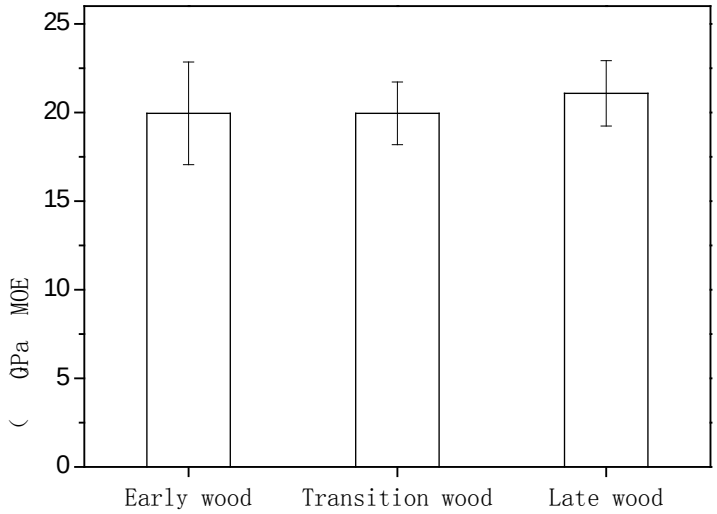

Figure 4 Cell wall MOEs and standard deviations of early, late, and transition wood within the 24th annual ring of Masson Pine opposite wood (error bars represent standard deviation).

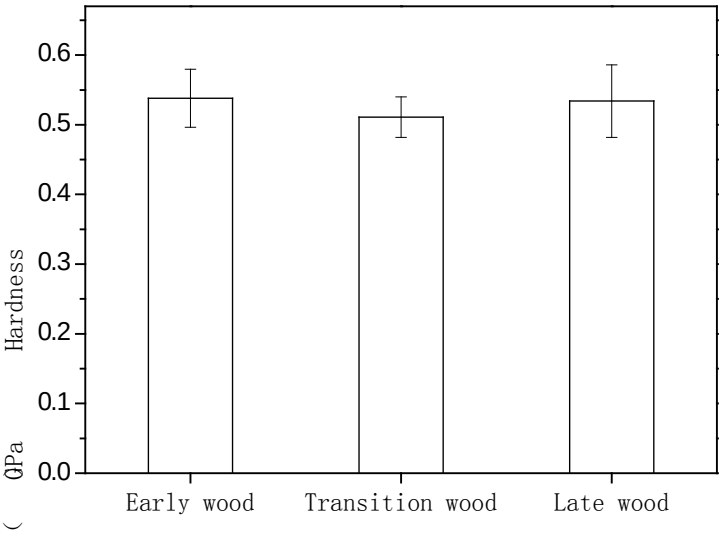

Figure 5 Cell wall hardness and standard deviation of early, late, and transition wood within the 24th annual ring of Masson Pine opposite wood (error bars represent standard deviation).

Generally, the thickness of the cell wall was different among early, transition, and late wood in the same annual ring. The early wood had a thinner cell wall than that of late wood and transition wood. Thus, the thinner the cell walls, the higher possibility of dislocation of the indentation tip. The MOE was slightly higher when the location of tip insertion neared the fringe of the cell wall, but a little lower when it was near the edge of the cell cavity. Therefore, for early wood, the MOE value was less repeatable than for other woods. The distribution range of standard deviations of cell wall MOE was also large.

For hardness, as with measurements of MOE, no difference existed among early, transition, and late wood in the same annual ring (Fig.5). However, the standard deviations of cell wall hardness did not match that of cell wall MOE. According to Yu *et al.* (2007) and Gindl *et al.* (2004), indentation hardness is governed by the characteristics of the matrix. Since the cell wall hardnesses were similar in early, transition, and late wood of the same annual ring, it was reasonable to infer that the matrix properties in a mature annual ring were also similar.

Conclusions

Nanoindentation is a very powerful method for investigating the mechanical properties of the cell wall S_2 layer of compression wood at the nanoscale. The average values of the hardness and MOE of opposite wood were slightly higher than those of compression wood. The MOE increased with increasing annual ring age for both compression and opposite wood, which is mostly due to a decreasing trend in MFA. An increasing trend was also observed for hardness form annual ring 9. In opposite and compression wood taken from the same annual ring, the differences in average values of modulus of elasticity and hardness were all insignificant. The lack of difference was explained by the change in MFA, the press-in mode of nanoindentation, and the special structure of compression wood. For early, transition, and late wood within the same opposite wood annual ring, the MOE and the hardness were both very similar. It is reasonable to infer that the thickness of the cell wall S_2 layer has no effect on the nanoindentation testing values in a mature annual ring.

Acknowledgments

This work was financially supported by projects from the National Natural Science Key Foundation of China (Grant No. 30730076) and the USDA Wood Utilization Research Grant.

References

Burgert, I.,Fruhmann, K.,Keckes,J.,Fratzl, P., and Stanzl-Tschegg, S. 2004. Structure function relationships of four compression wood types: Micromechanical properties at the tissue and fibre level. Trees. 18(4):480-485.

Cave, I. D. 1966. Theory of X-ray measurement of microfibril angle in wood. Forest Prod. J. 16:37-42.

Cave, I. D. 1968. The anisotropic elasticity of the plant cell wall. Wood Sci. Technol. 2(4): 268-278.

Cave, I.D., and Walker, J.C.F. 1994. Stiffness of wood in fast-grown plantation softwoods: Theinfluence of microfibril angle. For. Prod. J. 44:43-48.

Eder, M., Jungnikl, K., and Burgert, I. 2009. A close-up view of wood structure and properties across a growth ring of Norway spruce (*Piceaabies* [L] Karst.). Trees. 23: 79-84.

Gillis, P. P., and Mark, R. E. 1973. Analysis of shrinkage, swelling and twisting of pulp fibers. Cellulose Chem. Technol. 7: 209-234.

Gindl,W. 2002. Comparing mechanical properties of normal andcompression wood in Norway spruce:The Role of lignin incompression parallel to the grain. Holzforschung. 56: 395-401.

Gindl,W., Gupta,H. S.,Schöberl, T.,Lichtenegger, H. C., andFratzl, P. 2004. Mechanical properties of spruce wood cell walls by nanoindentation. Appl. Phys. A. 79:2069-2073.

Konnerth, J., Gierlinger, N., Keckes, J., and Gindl, W. 2009. Actual versus apparent within cell wall variabilityof nanoindentation results from wood cell walls relatedto cellulose microfibril angle. J. Mater. Sci. 44:4399-4406.

Meinzer, F. C., Lachenbruch, B., and Dawson, T. E. 2011. *Size and Age-related Changes in Tree Structure and Function*. Springer, Dordrecht, 510 pp.

Page, D. H., EI-Hosseiny, F., Winkler, K., and Lancaster, A. P. S. 1977. Elastic modulus of single wood pulp fibers. Tappi. 60(4): 114-117.

Schniewind, A. P. 1962. Mechanical behavior of wood in the light of its anatomic structure. In: Schniewind, A. P. (ed.), *The Mechanical Behavior of Wood*, Conf. Univ. CA, Berkeley, 136-146.

Spurr, A. R. 1969. A low-viscosity epoxy resin embedding medium for electron microscope. J. Ultrastruct. Res. 26:31-43.

Timell, T. E. 1987. *Compression Wood in Gymnosperms*, Vol. 1, Springer Verlag, Heidelberg.

Tze, W. T., Wang, S., Rials, T. G., Pharr, G. M., and Kelley, S. S. 2007. Nanoindentation of wood cell wall: Continuous stiffness and hardness measurement. Comp. A–Appl. Sci. Manufact. 38:945-953.

Wu, Y., Wang, S., Zhou, D., Xing, C., Zhang, Y., and Cai, Z. 2010. Evaluation of elastic modulus and hardness of crop stalks cell walls by nano-indentation. Bioresource Technology. 101: 2867-2871.

Yu, Y., Fei, B., Wang, H., and Tian, G. 2012. Longitudinal mechanical properties of cell wall of Masson pine (*Pinusmassoniana* Lamb) as related to moisture content: Ananoindentation study. Holzforschung. 65(1): 121-126.

Yu, Y., Fei, B., Zhang, B., and Yu, X. 2007. Cell wall mechanical properties of Bamboo investigated by in-situ imaging nanoindentation. Wood and Fiber Science. 39(4):527-535.

Livelihood of the Bamboo base: Challenges and Opportunities

Samir Jamatia
Advisor, Twipra Bamboo & Cane Handicrafts, Agartala, Tripura
Member, International Network for Bamboo and Rattan, India
Mobile: +91-9436496101. Email:jamatiasamir@yahoo.com

Abstract

Bamboo is a versatile input and is used as building material, paper pulp resource, scaffolding, agriculture implements, weaving material, plywood and particle board manufacture, basketry, furniture, pickled or stewed bamboo shoots, medicines, etc. Resource management and technical improvements can convert this fast-growing grass into a durable raw material for construction purposes and a wide range of semi-industrialized products. New industrial applications and modern construction design have both demonstrated bamboo's huge potential.
The combined value of internal and commercial uses of bamboo in the world is about Rs 50,000 crores annually. This is supposed to double by 2015. In India archaic legislation and lack of awareness have inhibited the bamboo based industrialization process. The biggest impediment towards a bamboo based sector from developing has been the irregular and scant supply of bamboo for entrepreneurial use. An efficient regulatory institution is essential for markets to grow in a sustainable manner, especially where environment concerns are coupled with business development. Transaction costs must be minimal, information availability maximal with a clear focus on maintaining the forest cover. Unfortunately, the regulatory structure as regards the bamboo industry has remained caught in the quagmire of archaic forest laws. Therefore, what is definitely needed is the linkages that industrialization of the bamboo sector can provide, given the huge linkages with rural livelihood. However, only when there is a viable entrepreneurial activity of any bamboo based product, will the market tend to provide the supply and demand linkages and it is only then that livelihood benefits will accrue.

Introduction

Although recorded history finds mention about the various uses of bamboo as early as 7th century AD during the days of Kingdom. Yet in India, no quantified information is available regarding the actual bamboo base policy for any of these products except for the paper and pulp industry, and the contribution of bamboo in the family income of various categories of consumers. On the resource front also there is no quantification regarding bamboo availability from non-forest land. Being essentially a forest based material, bamboo, although a non wood fibre source is included with wood, in all Indian studies, including those pertaining to raw material for the pulp and paper industry. In the national statistics, therefore it is often difficult to separate the contribution and role of bamboo fibres. On the other hand, non-wood forest products, including bamboo, do not have standard classifications. They are usually classified according to their structure (roots, leaves, bark) or the end use (medicine, food, beverages, utensils, etc.). Bamboo product classification is even more complicated due to the multi-functionality. Most of the economic activities related to bamboo are not recorded officially. Accurate statistical information on trade in Bamboo is also difficult to find, and even internationally. The main reason for this is that international trade statistics suffer from outdated customs codes.

Bamboo – Its Characteristics and Uses

The many characteristics of bamboo make it an enduring, versatile and highly renewable resource. Bamboo has more than 1,500 documented uses, ranging from fuelwood to light bulbs, medicine, poison and toys to aircraft manufacturing. Over 1,000 million people live in houses made of bamboo or with bamboo as the key structural, cladding or roofing element.

• Its biological characteristics make it a perfect tool for reducing carbon dioxide levels in the atmosphere. It generates more oxygen than equivalent strands of trees, lowers light intensity, protects against ultraviolet rays and is an atmospheric and soil purifier.

• Bamboo is an enduring and versatile natural resource. The great diversity of species makes bamboo adaptable to many environments.

• Bamboo grows very fast and has a short growth cycle. Bamboo not only grows much faster than wood, it also needs relatively little water. It is the fastest growing canopy, growing three times faster than most eucalyptus species. Commercially important species usually mature in four to five years (versus 10 to 25 years for most soft woods). Annual harvests are subsequently possible.

• Bamboo prevents soil erosion. Its anti-erosion properties create an effective watershed, stitching the soil together along fragile river banks, deforested areas, and in places prone to earthquakes and mud slides. The sum of stem flow rate and canopy intercept of bamboo is 25% which means that bamboo greatly reduces rain run-off, preventing massive soil erosion. Thus, bamboos help control landslides, keep flooded rivers along their natural course and slow the speed of the water flow.

• Bamboo is foremost in biomass production, with up to 40 tonnes per hectare per year in terms of culms only in managed stands. An estimated one-quarter of the biomass in tropical regions and one-fifth in subtropical regions comes from bamboo.

• Bamboo is one of the world’s best natural engineering materials. Due to its high tensile strength, it is an essential structural material in earthquake architecture and is one of the strongest building materials. Its strength-to-weight ratio is better than that of teak wood and mild steel. Bamboo's tensile strength is 28,000 lb per square inch versus 23,000 for mild steel. This makes bamboo wood a potential alternative, at least in some applications, to steel which requires more energy for manufacturing/production. Its strength and flexibility make it a viable material for building shelters that offer protection against hurricanes and earthquakes. * In Bangladesh, 73% of the population lives in bamboo houses. Bamboo based pre-fabricated houses also can be constructed quickly with new and

emerging techniques and is thus an important post-disaster relief material. It is extensively being used in Tsunami rehabilitation in India. Bamboo reinforcement in concrete piles is used by the Indian Railways.

• As a food source, bamboo shoots have provided nutrition for million of people worldwide. In Japan, the antioxidant properties of pulverized bamboo bark prevents bacterial growth and it is used a natural food preservative. Taiwan alone consumes 80,000 tons of bamboo shoots annually constituting a $50 million industry.

• Bamboo is a viable replacement for wood. Its qualities of strength, light weight and flexibility make it a viable alternative to tropical timber that is used in the furniture and building materials industries.

• It is a critical element of the economy. Bamboo and its related industries provide income, food and housing to over 2.2 billion people worldwide. There is a 3-5 year return on investment for a new bamboo plantation.

• Bamboo is a renewable resource for agro-forestry products. Bamboo is a high-yield renewable natural resource. Ply bamboo is now being used for wall panelling, floor tiles, for paper making, briquettes for fuel, raw material for housing construction, and rebar for reinforced concrete beams. It can be used to produce many items of daily use that are currently made out of plastic or other less eco-friendly materials.

• Bamboo is being used as an input or raw material in certain industries. It has been primarily been used in the paper industry in bulk quantities as a raw material for paper pulp. Bamboo is also used in manufacturing wood substitutes, composites, utility products including Agarbatti (incense sticks).

---

* In Limon, Costa Rica, only the bamboo houses from the National Bamboo Project stood after their violent earthquake in 1992.

• Bamboo is also a source of energy. Gasifiers can produce electricity using bamboo as fuel. These can also be used for thermal applications replacing furnace and diesel oil. Charcoal and its processed form in powder and briquettes can also be manufactured. It is superior to other sources of charcoal in terms of calorific value. Bamboo charcoal can also be used as a raw material for activated carbon manufacturing which is used as adsorbent in different industries like vegetable oil, beverage, pharmaceuticals etc. Goldsmiths prefer bamboo charcoal in making jewels.

In sum, bamboo’s excellent growth, environmental, mechanical and engineering properties make it a fine alternative to tropical timber. Its potential for different value added products and application make it an extremely important material for dispersed employment generation and economic activities. Perhaps these properties and potential usage coupled with increased urgency of environmental issues ought have been sufficient to change the attitude towards bamboo, and solved the problems of tropical deforestation. However it is not so. “Bamboo of the poor man" (India), "friend of the people" (China) and "brother" (Vietnam), bamboo is a wonder plant that grows over wide areas of North Eastern India. Millions of people depend on this plant for their livelihood. It has become so much a part of the culture and memory of societies that the existence of a Bamboo Age has not been ruled out. Its use in food and cooking goes far back in history" representing a social stigma.

Bamboo based Products – An Appraisal

Literature regarding the multiple uses of bamboo highlights the utility of bamboo for house construction, bamboo ply, agricultural implements, handicraft, irrigation, brooms, medicine, food, fuel, fodder, paper & pulp etc, especially bamboo as a perfect substitute for some wood based products. The products that can be made from Bamboo can be broadly be categorized into:

1. Wood Substitutes and Composites,
2. Industrial Use and Products,
3. Food Products,
4. Construction and Structural Applications.

Apart from this broad classification various handicraft and cottage industry products are also made from bamboo. However, this category of products is not discussed as bamboo based industrialization and its prospects limit the scope of the study. Also the input of bamboo as a resource raw material in the paper and pulp industry is also not explicitly dealt with as a bamboo based product but discussed in the next chapter under the resource situation in North Eastern Region.

Wood Substitutes and Composites

This category of products essentially comprises of boards and sticks of varying descriptions and uses, and which can further be used to manufacture finished products like wooden floors or blinds or goes into another industry as an input like incense sticks.

Bamboo Based Panels: China started producing bamboo panels in the early 19th century. At present more than 20 different types of panels are produced in Asia. Bamboo fibre is longer than wood fibre, which gives bamboo some technological advantages. The panels are widely used in modern construction as structural elements or as forms for concrete mouldings. They are also used for flooring, roofing, partitions, doors and window frames. Bamboo panels have some advantages over wooden board due to their rigidity and durability. Various types of bamboo veneers, panels and boards can be broadly classified as follows: veneers, strip boards, mat boards, fibreboards, particle boards, medium density boards, combinations of these, and combinations of these with wood and other ligno-cellulose materials and inorganic substances. Composites of bamboo and jute are also possible to make panels.

Bamboo Flooring: Bamboo flooring is a quality product that can be used widely and has a large, global consumer market. It has certain advantages over wooden floors due to its smoothness, brightness, stability, high resistance, insulation qualities and flexibility. Bamboo flooring has a soft natural lustre and maintains the natural gloss and elegance of bamboo fibre. This flooring is attractive to the demanding markets in Europe, Japan and North America. The estimated annual production of bamboo flooring in China was 17.5 million square metres in 2004, with about 65% being exported (Customs General Administration of China, 2004).

Bamboo Sticks for Blinds and Incense Industry: The art of making screens and blinds from bamboo is not new to India. For centuries, people have woven elegant screens from bamboo that have provided privacy, protection from the sun and added aesthetic appeal to living spaces. Mechanized blind making units can be economically viable enterprises. Again, bamboo sticks making units can substitute the wood that is used in the incense stick, and that industry in North Eastern Region India is estimated to be worth US$400 million. It can also be used in match sticks.

Bamboo Furniture: Traditional bamboo furniture uses natural round or split bamboo. A new type of ‘pack-flat,’ ‘knockdown’ furniture uses glue-laminated bamboo panels. Unlike the traditional design,

this furniture may be shipped in compact flat packs, to be assembled on the spot. The new design overcomes many of the problems of traditional bamboo furniture, such as high labour and transportation costs, low productivity, instability, varying quality and susceptibility to insects and fungi. At the same time, it retains the distinct physical, mechanical, chemical, environmental and aesthetic features of bamboo. Export of laminated bamboo furniture is growing rapidly. However, trade statistics currently do not capture the value, owing to the absence of a special code for bamboo furniture. It is usually classified as wooden furniture.

Industrial Products

Traditionally the industrial use of bamboo has been in the paper and pulp industry. Apart from this, the industrial products from Bamboo, essentially comprises of converting into fuel or electricity through gasification. Through pyrolysis, bamboo can be converted into three valuable products - bamboo charcoal, oil and gas. Changing the pyrolysis parameters can change the product shares depending on the purpose and market conditions. Bamboo based producer gases can be used as a substitute for petroleum. Bamboo charcoal is an excellent fuel for cooking and barbequing. There can also be the use of activated charcoal. This is used as a deodorant, purifier, disinfectant, medicine, agricultural chemical and absorbent of pollution and excessive moisture. The industrial use is using bamboo waste for gasification and thereby producing electricity.

Bamboo for Paper and Pulp: Several bamboo-producing countries, such as China, North Eastern Region and India, use bamboo in paper and pulp. Bamboo paper has practically the same quality as paper made from wood. Its brightness and optical properties remain stable, while those of paper made from wood may deteriorate over time. The morphological characteristics of bamboo fibres yield paper with a high tear index, similar to that of hardwood paper. The tensile stiffness is somewhat lower compared with softwood paper. The strain strength is between that of hardwood and softwood papers. The quality of paper may be improved by refining the pulp.

Bamboo Charcoal for Fuel: Bamboo charcoal is traditionally used as a substitute for wood charcoal or mineral coal. It can serve as a fuel, absorbent and conductor. The calorific value of bamboo charcoal is almost half that of oil of the same weight. Activated bamboo charcoal can be used for cleaning the environment, absorbing excess moisture and producing medicines. The absorption capacity of bamboo charcoal is six times that of wood charcoal of the same weight. China is a leader in its production. At present, Japan, the Republic of Korea and Taiwan Province of China are the main consumers, but its importation is rapidly expanding in Europe and North America. There are three main reasons contributing to the success of bamboo charcoal in international trade:

- Bamboo grows faster and has a shorter rotation compared with tree species;
- The calorific value and absorption properties of bamboo charcoal are similar to or better than those of wood charcoal; and
- It is cheaper and easier to produce.

Bamboo Based Gasifier for Electricity: Gasification of bamboo can produce energy and a range of valuable by-products. It reinforces a commitment to clean and renewable electricity and thermal energy. It can utilise waste generated by processing operations, substitute the use of fossil fuels, and lower operating costs. Bamboo can be cut into small pieces and used in the Gasifier. The requirements for the gasification units are a small proportion of the total availability. A 100 Kw Gasifier would require only about 1000 tonnes per annum, the equivalent of a truckload every three days on the average. An added advantage of gasification of bamboo is that 15% of the biomass would also be available as a by-product in the form of high grade charcoal. In the case of a 100 Kw Gasifier, around

135 tonnes of charcoal would be available each year to meet local needs of fuel. It is clean, cheap & renewable source of energy. Further, it does not depend on quality, species, and maturity of bamboo.

Bamboo based fibre and fabric: The most recent advancement in bamboo is the manufacturing of fibre for making yarn and into various fabrics. There are several spinning mills using 100 per cent bamboo yarn, and Indian companies such as Raymond, BSL Ltd of Bilwara group and Paramount Textile Mills Ltd, Madurai, have already launched fabrics made out of bamboo. Bamboo fabrics are naturally anti-microbial and due to the presence of micro pores in the fabric absorb, they three times more moisture than cotton, making it a superior product. Apart from the ones outlined above, bamboo extracts contain valuable elements that can also used an input in several industrial products. For example, bamboo can be used in pharmaceuticals, creams, and beverages. Traditional medicines like Chawanprash use bamboo extracts.

Food Products

Under this category, it is essentially bamboo shoots that are consumed after being cooked. Bamboo shoots carry the potential of value added economic activity at the entrepreneurial and community level through cultivation, processing and packaging. Its use in food and cooking goes far back in history. China earns US$130 million annually from exports of edible bamboo shoots. About 200 species of bamboo can provide edible and palatable bamboo shoots. **Fresh bamboo shoots are delicious and healthy, with high fibre content. Bamboo vegetables can be found in Chinese grocery stores and restaurants worldwide. After cooking the shoots are still crisp, because cooking does not destroy their texture. Cooked bamboo shoots can be stored in containers and shipped worldwide. In North Eastern Region on Bamboo Shoot units: Luit Vally, Jorhat (Assam), DIMROO Food Industry, Tura (Meghalaya), L Doulo Builders & Suppliers, Dimapur (Nagaland), Nagland Fruits & Vegetables Processing Plant, Dimapur (Nagaland), MAGFRUIT, Imphal (Manipur), AEGIES, Imphal (Manipur).

Construction and Structural Applications

Advances in structural engineering and the development of bamboo composites have opened new vistas for lightweight, durable and aesthetic construction for a variety of applications, enabling informed choices for housing, community and functional structures.

****** Bambusa balcooa, Dendrocalaimus B.brandisii, Dendrocalaimus giganteus, Dendrocalaimus hamiltonii, Dendrocalaimus strictus, Meloccana bambuisodes, Bamboo Shoots available from the following species are also of good quality - D. tulda, D. hamiltonii, M. Bacifera (Muli).

Bamboo housing: There are three main types of bamboo housing, a) traditional houses, which use bamboo culms as a primary building material; b) traditional bahareque bamboo houses, in which a bamboo frame is plastered with cement or clay; and c) modern prefabricated houses made of bamboo laminated boards, veneers and panels. These buildings are usually cheaper than wooden houses, light, strong and earthquake resistant, unlike brick or cement constructions. New types of prefabricated houses made of engineered bamboo have distinct advantages. They can be packed flat and transported at a reasonable cost. They are better designed and environmentally friendly. Bamboo materials are widely available and can be cultivated at a low cost.

The properties and uses of bamboo vary at different stages of growth and its appropriateness at different stages of growth is as follows:

- Up to 30 days - Bamboo shoots to be used as food
- Between 6-9 months - for basketry

- Between 2-3 years - for laminates and boards
- Between 3-6 years - for construction
- Bamboo gradually loses strength after the sixth year and up to 12 years.

Bamboo based Industrialization – Prospects and Problems

This natural resource has played a major role in the livelihood of rural people and in rural industry, especially in tropical regions. Over 2.2 billion people the world over are dependent on bamboo and its related industries for income, food, and housing. Although the rural communities have traditionally been using bamboo, the utilisation has been highly localized as bamboo has often been viewed as an inferior substitute of timber. For example, although over 1 billion people in the world live in bamboo houses, yet there has been little effort to build such houses (using pre-fabricated structures or otherwise) commercially. Traditionally, bamboo has been harvested in the natural forest and its use has been limited to temporal constructions and low-quality utensils prone to rapid decay. Consumption or utilisation has therefore been direct and restricted to poorer people with low income and low purchasing power. Market linkage has as a consequence been weak or non-existent in most countries including India.

Yet, bamboo, as noted, has versatile uses as building material, paper pulp resource, scaffolding, agriculture implements, weaving material, plywood and particle board manufacture, basketry, furniture, pickled or stewed bamboo shoots, medicines, etc. Resource management and technical improvements can convert this fast-growing grass into a durable raw material for construction purposes and a wide range of semi-industrialised products.

New industrial applications and modern construction design have both demonstrated bamboo's huge potential in NER, but the bamboo sector in China is the only one reported to be thriving. The Chinese has been able to successfully industrialize the use of bamboo by integrating the bamboo sector with domestic and international markets. In the last 20 years China has established an integrated chain of bamboo plantations, its semi-processing and industrial product manufacturing such as bamboo flooring, furniture, furnishings, charcoal and fresh bamboo shoots for the domestic and export markets. Its focused intervention to harness bamboo’s potential has led to increase in its productivity by more than 10 times since 1970 when it was 2-3 tonnes/ha/annum. The combined value of internal and commercial uses of bamboo in the world is about rupees 50,000 crores annually. This is supposed to double by 2015. More than half of the world’s consumption of bamboo is in China. China’s export of bamboo products is close to rupees 10,000 crores. As against this, India’s size of the domestic bamboo economy is estimated at rupees 2043 crores. The market potential was, however, estimated at rupees 4463 crores, which could grow to rupees 26,000 crores by 2015 (Planning Commission, 2003).

The bamboo sector in most other countries is still a part of the informal and backward rural economy. There has been an inability to grab the large potential, which has been successfully demonstrated by the Chinese bamboo industry. This raises the question of the bottlenecks facing bamboo development. Many of these inhibiting factors are at the policy level and are additional to a lack of knowledge among the important stakeholders and a widespread stigma of bamboo as a poor man's timber. In India it has been no different. Both the law and lack of awareness about its industrial application has been the primary bottleneck inhibiting a bamboo based industrialization process from taking shape. Presently it is underutilized and found in abundance.

The biggest impediment towards a bamboo based sector from developing has been the irregular and scant supply of bamboo for entrepreneurial use. The paper and pulp industry in India, which has been traditionally using bamboo for over half a century, has constantly innovated to reduce the use of

bamboo in its manufacturing process due to this uneven and scant supply. And after the consumption of the paper mills (who usually have long term contracts with the forest departments), very little is left for any other application. This pattern is true for all Indian states. The present regulatory regime in India is the unambiguous culprit for this irregular and inadequate supply.

An efficient regulatory institution is essential for markets to grow in a sustainable manner, especially where environment concerns are coupled with business development. Transaction costs must be minimal, information availability maximal with a clear focus on maintaining the forest cover. Unfortunately, the regulatory structure as regards the bamboo industry has remained caught in the quagmire of archaic forest laws, whereby bamboo is defined to be a tree, and therefore felled bamboo is classified as timber. This is subject to transit and trade restrictions.

Bamboo is also subject to harvesting permissions in many parts of the country if grown on private lands and which then becomes the basis for imposing the need for transit permits. This has resulted in throttling of the bamboo sector and has discouraged private plantations. The irregular and scant supply of bamboos for processing, despite the world's largest area under bamboos has been a natural corollary. Clearly the expansion of a bamboo based sector has not happened due to the restrictions in place.

If the restrictions are removed, the sector still might not grow, but can impact livelihood benefits percolating down. This should justify an initial policy initiative through subsidies, incentives and other handholding measures. Economic subsidy can be justified when social benefits outweigh private benefits. So in the bamboo sector the understanding of livelihood benefits is crucial understand.

The economic and social benefits for example, from activities related to bamboo based value added products and applications was worked out to be 8.6 million jobs (new) in the Tenth Plan, besides building up large bamboo resource and market opportunities worth rupees 6,500 crore with an investment of rupees 2,600 crore, enabling 5 million families of artisans and farmers crossing the poverty line, according to the ***National Bamboo Mission. The expansion of handicraft, cottage and tiny sector can potentially create 3 million jobs, according to estimates of the Planning Commission (2003). On the other hand, generation of power through gasifiers using bamboo resources exemplifies assiduous application of technology that can alleviate the present power shortage in most states and thus help improve the overall economy.

There has been a growing awareness in recent years about the importance of bamboo being an important means of economic growth and of improving the socio-economic conditions of the rural poor. Bamboo as an industrial material can substitute wood to a great extent and that too at low cost. Bamboo has been traditionally harvested from forest lands in India and the homesteads which may have a few clumps of one of the many species of bamboo for household use but very little intervention in terms of purposive planting has been done in the past. Convincing and informing users and policymakers of bamboo's versatility may fit in with a strategy of poverty alleviation and reducing pressure on tropical forests. Smallholders at the forest fringe can, in particular, improve their livelihood by processing bamboo or growing it in their backyard.

Bamboo as a resource needs to be seen as a form of development, with the primary value addition done closer to the resource in order to reap the livelihood benefits. At the same time, a larg stock of bamboo contributes to broader environmental goals of erosion control, reforestation and watershed management.

***See http://agricoop.nic.in/bamboo/bamboomission.htm

In India, bamboo is mostly found in the forests. As per Forest Survey of India (1999) estimates, 9.6 million hectares forest area of the country contains bamboo amounting to 12.8% of the forest cover. India has the largest area under bamboo in the world, which is estimated around 11.36 million hectares. India is also very rich in bamboo diversity. It is the second richest country in the world in terms of genetic resources, after China.**** Sharma (1987) reported 136 species of bamboos, across 22 genera, occurring in India. Out of these, nineteen are indigenous and three are exotic. Naithani (1993) reported 124 indigenous and exotic species, under 23 genera, to be found naturally and/or under cultivation in India.

The distribution is, however, not uniform. The rich areas are confined to the North-Eastern parts of the country. The North-East is the richest source. Fifty-eight species of bamboo belonging to 10 genera are distributed in the North-Eastern States alone. Around twothirds of the growing stock or 66% of the growing stock of bamboo in India is found in the North- Eastern States, but with just 28% of the total area under bamboo in the country. Madhya Pradesh has the second highest area under bamboo, estimated at 20.3% of the area and with 12% of the growing stock. The details of the bamboo growing areas (in forests) and growing stock of major states is given in Table 1.

Table 1: Major States by Area under Bamboo.

State	Area (percentage)	Growing stock (percentage)
North East Region	28.0%	66%
Assam	7.54%	16.23%
Arunachal Pradesh	4.21%	11.91%
Mizoram	8.45%	13.18%
Manipur	3.39%	13.88%
Meghalaya	2.89%	5.34%
Nagaland	0.70%	4.43%
Tripura	0.86%	1.04%
Madhya Pradesh	20.3%	12%
Others	20.2%	5%

Source: Madhab Jayanta (2003) and the National Horticulture Mission at (http://agricoop.nic.in/AgriMinConf/National_hort_Mission.ppt.)

Clearly from the table above, states like Manipur and Arunachal Pradesh, within the North East and otherwise, have much higher productivity than rest of the states.

****China with 300 species is leading in genetic diversity of bamboo.

Productivity in India

The annual yield of bamboo per hectare varies around 2 tonnes per hectare per annum, depending upon the intensity of stocking and biotic interferences. It is however, known that yield in rain fed areas can be increased 4 to 5 times in five years if protection from grazing is ensured and proper management practices (soil working, fertilisation and thinning) are adopted (Lakshmana, 1994).
The yield per hectare is very low compared to other countries such as Japan, China, Taiwan and Malaysia. As compared to China and Taiwan, India's productivity is one fourth to one fifth. India has a long way to go on scientific cultivation of bamboo. Unfortunately, bamboo has no parent in the governmental set up. Only in the homesteads, farmers take care of bamboo. But the lack of scientific approach to cultivation prevents higher productivity.

With regard to the potential productivity of bamboo from forest areas in India, two observations can be made. Firstly, the present actual productivity is far less than the potential and in either case less than what is noticed in the homesteads. Moreover, even in the homesteads, bamboo cultivation is seldom accorded the attention and silvicultural requirements, which would come in when bamboo plantations are undertaken.

Traditionally the forest department's bamboo harvesting policy systematically maximizes dry bamboo output for paper mills rather than green bamboo output for artisans and mature bamboos (2-4 years old) for the industrial needs (apart from the paper industry). In fact, if bamboo forests are carefully worked and green bamboos/mature bamboos regularly harvested, bamboo output of an average clump would jump. Till date the management of state bamboo resources has many constraints with lack of post harvest treatment and technology for product development, inadequate trained manpower and inadequate infrastructure for large scale harvesting in the event of gregarious flowering.

In India bamboos have been primarily grown in forests, which are government owned land. The exceptions, as noted earlier, were Nagaland and Kerala. Although it is a well established fact that bamboos in India are primarily harvested for supplying to the paper and pulp industry as a raw material, and otherwise used by the rural communities for self consumption, it is very difficult to obtain even rough estimates of the consumption or utilisation pattern. Tiwari (1992) has done the only estimate on consumption pattern and this is given in the Table 2 below. There are two points to note in his consumption pattern outlined. First, the estimates of Tiwari (1992) do not include pre-fabricated houses using bamboo. In the housing sector, bamboo is used in different ways as a building material for roof structure in form of purlins, scaffolding, rafters, reapers, as reinforcement in foundations and in mud walls, flooring, doors/windows, walling, ceiling, water storage tanks, man-hole covers and even for roads in slushy areas. The other point to note is that the estimated percentage used in the paper and pulp industry was 35% in 1992. This fact looks quite circumspect.

In Assam, the overwhelming industrial use for bamboo is still for pulp and paper. The paper mills in the State have a capacity of 800,000 tonnes per annum, met largely from Assam, but to a lesser extent from the neighbouring States. Much of the bamboo utilized in these spheres comes from the forests through a system of contracts, leases and departmental operations. According to a survey report of the State Forest Department of Jharkhand for example, 75% of bamboo is used for pulp and paper, 23% for household and constructional needs, and 2% for bamboo based cottage industries.

Table 2: Consumption Pattern of Bamboos in North Eastern Region and India

Uses	**Percentage Consumption**
Pulp	35 %
Housing	20 %
Non-residential	5 %
Rural uses	20 %
Fuel (non – industrial)	8.5 %
Packing, including basket	5 %
Wood based Industries and Transport	2.5 %
Furniture	1 %
Others, including ladders, mats etc.	3 %
Total	**100 %**

Source: Tewari, D.N. (1992)

As noted before, the estimated annual harvest of bamboo in India is 13.47 million tonnes against the current domestic demand of 26.69 million tonnes. Therefore there is already a substantial shortfall in the supply of bamboos in India.

Regulating the Bamboo Sector

The Central laws pertain to forestland which is the property of the government. In other words, the central laws do not apply to private forests or private plantations. There are three central Acts that govern forest and forest produce. These are the Indian Forest Act 1927, the Forest Conservation Act 1980 and the Scheduled Tribes and Other Traditional Forest Dwellers (Recognition of Forest Rights) Act, 2006. Before proceeding to understand how these laws affect bamboo plantation, harvesting and transportation, it is imperative to outline the objectives that all these three laws purports to achieve. The Indian Forest Act 1927 is the single most important piece of legislation on forests.

This Act has only minor differences with the 1878 forest Act with the philosophy remaining the same.*****Two fundamental issues can clearly be identified in the Act. The first pertains to the establishment of absolute state property rights over forests. Towards this end, the classification of forests – into reserved forests, protected forests and village forests – and the legal separation of customary rights as well as the procedure for forest settlement in these was an administrative feature characterizing this Act. The second pertained to the control of timber and other forest produce in transit, the duty leviable on them and the collection of drift and stranded timber. The commercial motive and revenue generation remained the guiding principle. Of relevance to this study are the definitional aspects contained in Section 2 and chapter VII of the Act, which contains detailed and wide encompassing provisions empowering the government (more specifically the state governments) in the control of timber and other forest produce in transit by land or by water. The link between Section 2 and chapter VII lies in the fact that whatever got defined as a ‘forest produce’ could be controlled by the state governments through the rules framed by these various state governments in their respective states.

The Forest Conservation Act, 1980, deals with restriction on allotment of ‘forestland’ for nonforest purposes and de-reservation of reserved forests. The Act is a two-page document, consisting of only five sections. The Act clarifies that the term “non-forest purpose” means the breaking up of or clearing of any forest land for the cultivation of tea, coffee, spices, rubber, palms, oil-bearing plants, horticultural crops or medicinal plants, or nay purpose other than reforestation. The Act was a crisis driven response. The objective of enacting this Act was to empower the Central Government in directly managing India’s forests. The Act, is not really a substantive law, it is a delegated legislation, which empowers the Union Minister to make the decisions about how to use the forestlands. Further, this Act only forbids “reserve forests” from being de-notified by the states. The need to promulgate this Act was felt as remote sensing data of the 1970s showed the adverse consequences of large-scale diversion of forestlands to non-forestry purposes (which hit an astounding rate of 150,000 hectares per year prior to the 1980s). Again, after forests were transferred to the concurrent list by the Forty-Second Amendment Act of 1976and the Ministry of Environment and Forests (MoEF) was set up as a nodal central authority in 1980; the Union Government could now directly intervene.

*****The 1927 Act was promulgated to "consolidate the law relating to forests, the transit of forest produce and the duty leviable on timber and other forest produce". A brief genesis of the Act is in Supplementary Note 1

In particular there is no aspect of the Forest Conservation Act, 1980 that is of relevance to this study. However, the Supreme Court case - T. N. Godavarman Thirumulkpad vs. Union of India and others (Writ Petition No 202 of 1995) – was filed in contravention to this Act and this case has turned out to be a landmark one that has perhaps altered the way bamboo ought to be regulated in future. The other central law is the Scheduled Tribes and Other Traditional Forest Dwellers (Recognition of Forest Rights) Act, 2006, which was notified in the Gazette of India only on January 2, 2007. The rules under this Act are not yet notified. The Act seeks to undo the historical injustice done to forest dwelling communities and vests property rights on forestland in forest dwelling communities thereby addressing their long standing insecurity of tenure and access rights. The Act gives them access to minor forest produce (including rights to sell), and a stake in the preservation of open spaces. The Act provides heritable but non-transferable tenures if they have occupied the lands (up to a maximum of four hectares per family) for three generations from 1930, with December 13, 2005 as the cut-off date. The Act gives the right of jurisdiction of gram sabhas to settle tribal claims. Of relevance to this study is only the definition of bamboo.

There are two kinds of relevance vis-à-vis bamboo that the Central Acts deal with. The first is definitional, which defines bamboo as a forest produce by its origin. The second pertains specifically to the harvest and transit rules applicable to bamboo. The issue of trade regulation is contained in some of the State laws. The issue of harvest of bamboo from private lands or private cultivation is also contained in the State laws. Beginning with the second issue first, that is the harvest and transit in bamboo; it is primarily the provisions of the Indian Forest Act, 1927, that is of relevance.****** Specifically, by Section 26, removal of any forest produce (harvesting of bamboo)is prohibited in reserved forests, except by the forest department (usually in accordance with working plans). In protected forests, (Chapter IV) removal of timber or any other forest produce (including bamboo) is to be done with the written permission of the Forest Officer or in accordance with the rules framed by the State Governments. The rules so framed by the State governments can include among others, granting of licenses to persons felling or removing trees or timber or other forest-produce from such forests for the purposes of trade, and the examination of forest-produce passing out of such forests.

The provisions particularly related to transit are contained in Sections 41 and 42 of Chapters VII.*******Under clause (1) of Section 41, "the control of all timber and other forest-produce in transit by land or water is vested in the State Government, and it may make rules to regulate the transit of all timber and other forest-produce". The section is fairly detailed in its ambit, and gives the State Governments ample powers including the authority to frame rules for transit, control all river banks (as regards floating timber) and to make rules to prescribe the routes for import, export and other movements of timber or other forest produce from the State or within the State.

******According to the Scheduled Tribes and Other Traditional Forest Dwellers (Recognition of Forest Rights) Act, 2006, the forest dwellers have the right to "collect, use and dispose of minor forest produce" and which includes bamboo, but there is no explicit mention of trade or transit of either timber or any other forest produce. The word "dispose" is not assumed to mean either trade or transit.

*******Chapter VIII also contains certain related provisions. Chapter VII is titled "of the control of timber and other forest-produce in transit", while Chapter VIII of the Act deals with the "collection of drift and stranded timber". There was no particular need to have two different chapters on very similar aspects, and the former chapter was quite sufficient.

Thus the State rules regarding prohibition of such movements without pass, issuing of pass and prescribing fees in respect thereof becomes important and almost all states have laws/rules that guide movement of timber and other forest produce.

As mentioned before, the central laws on forests governed forestlands that were the property of the government. As regards the private forests or private plantations, the state laws, if any, governed the harvesting of bamboo. However, the transit rules applied to bamboo irrespective of its origin as the definition of trees in the Indian Forest Act 1927 makes bamboo a forest produce. Prior to the harvesting or felling of any tree from private lands, a certificate of origin is required from the state forest department, which is issued after due inspection and according to procedures laid out in the State laws that govern private forests for the respective states. Although the procedures vary the methodology follows this pattern. As seen in the following section, bamboo if included under the definition of a tree, and thus if treated as a forest produce even if its harvesting is from private lands would require a certificate of origin, and which would then form the basis of the issuance of the transit permit. So, section 41 and 42 of the Indian Forest Act 1927, and thereby all Rules framed on transit of forest produce by the States, will be applicable to bamboo as long as it is a forest produce.

Conclusion

Despite having fairly detailed estimates on the size and potential of the various market segments of the bamboo based industries or where bamboo is used, and despite they being estimates of a Planning Commission, Govt. of India Document, the appropriateness and reliability of the market potential, along with its availability and method of estimation is circumspect. As a result these estimates, duly quoted, are nevertheless questioned here. The process of consultation with the stakeholders - people associated with the resource use, including government officials and representatives from various bamboo based industry, along with the site visits to get a primary view of the process and the practical difficulties encountered helped us formulate the difficulties encountered.

The most important bottleneck was identified as the regulatory bottleneck, and as long as this was not meaningfully addressed, the sector cannot grow beyond a certain threshold level. In general, there seemed to be a strong promotional role of a governmental organisation, which would help generate awareness on bamboo products, run a nationalized campaign and help develop product market linkages, apart from handholding the sector in the initial stages. The government initiatives and agencies created for the development of the sector was described and although there seems to be overlapping of jurisdictions, the sector is presently at such a nascent stage of development that there cannot be shortages of initiatives. What perhaps is lacking is a more concerted effort and better planning, and we are of the opinion that either of the National Mission Bamboo Applications, National Bamboo Mission and perhaps the latter, should be converted into a permanent ‘Board’ for the development of the Bamboo sector in India, in lines of the ‘Coffee Board’, ‘Tea Board’ or than ‘Rubber Board’. This is especially called for because the report argues for bamboo cultivated in private plantations and it is hoped for that in future bamboo will be treated at par with other plantation crops once the viability of private plantations is demonstrated in different parts of the country.

References

Agarbatti Stick Production Under Andhra Pradesh Community Forest Management Project, INBAR-CIBART Documentation Centre, Bangalore, May 2006.

ASSOCHAM, (2007), "Replace Wood Products With Bamboo's To Help Govt. Save Rs. 7000 Cr. P.A", Mimeo, October 28, 2007.

Banik, R.L. (1986). Macro-propagation of Bamboos by Pre-rooted and Pre-rhizomed Branch Cutting, Bano Bigyan Patrika 13(1/2):67-73.

Basu, S.K., (1985), "The Present Status of Rattan Palms in India – An Overview", in K.M. Wong and N. Manokaran, (Eds.) "Proceeding of the Rattan Seminar", 77-90, FRI, Kepong, Malaysia.

Bhatt, K.M, (1992), "Changing Scenario of Rattan Trade in India", in S. Chand Basha and K.M. Bhatt (Eds.) "Rattan Management and Utilisation", Proceedings of the seminar held on 29-31, Jan., 1992 in Trichur, Kerala , pp. 335-339.

Cane & Bamboo News, Quality bulletin of CBTC, Vol. I. No. 4.

Champion H.G. and Seth, S.K. (1968). Revised Survey of the Forest Types of India 1-402, Manager, Publications, Delhi.

Cleuren, H. M., and A. B. Henkemans, (2003), "Development of the bamboo sector in Ecuador: harnessing the potential of Guadua angustifolia", Journal of Bamboo and Rattan, Volume 2, Number 2 / September, 2003

CRISIL (2006), "Demand Fundamentals Support Asset Mortgage Quality", Crisil Insight, January 2006.

FAO (1997), "Asia-Pacific Forestry Sector Outlook Study: Country Report – Malaysia", Working Paper No: APFSOS/WP/07. Forestry Department Headquarters, Peninsular Malaysia, Kuala Lumpur, Malaysia and Forestry Policy and Planning Division, Rome. Bangkok, FAO Regional Office for Asia and the Pacific.

FAO (2006), "Global Forest Resources Assessment 2005: India Country Report on Bamboo Resources", Working Paper No. 118, Forestry Department, FAO, Rome

Forest Survey of India, (1999), "State of Forest Report 1999", Forest Survey of India, Ministry of Environment and Forests, Dehra Dun.

Gadgil M., and R. Guha (1992), "This Fissured Land: An Ecological History of India", Oxford University Press, New Delhi.

Ganapathy, P. M.., (1997), "Sources of Non Wood Fibre for Paper, Board and Panels Production: Status, Trends and Prospects for India", Working Paper No: APFSOS/WP/10, Asia-Pacific Forestry Sector Outlook Study Working Paper Series, Asia-Pacific Forestry Commission, Rome.

Gangopadhyay, P. B., (2003), "Bamboo Resources as a Rural Livelihood Option in Madhya Pradesh, India", Paper submitted to XII World Forestry Congress, Quebec City, March 2003.

Guha, R., (1990), "An Early Environmental Debate: The Making of the 1878 Act", IESHR, 27, pp.65.

Guha, R., (1991), The Unquiet Woods: Ecological and Peasant Resistance in the Himalayas, Oxford University Press, New Delhi.

ICFRE. (1998). Timber/Bamboo Trade Bulletin. March 1998, No. 14. Directorate of Statistics, ICFRE, Dehra Dun. 31 pp.

Kumar, Arun and Cherla B. Sastry, (1999), "The International Network for Bamboo and Rattan", Unasylva, No. 198 on Non-wood Forest Products and Income Generation, FAO Lakshmana, A.C., (1994), "Rattans of South India", Evergreen Publishers, Bangalore.

Madhab, Jayanta, (2003), "The Green Gold: Under Exploited Wealth of the North East India", Dialogue, Volume 5, No. 2, October - December, 2003.

Naithani, H.B., (1993), Contributions to the Taxonomic Studies of Indian Bamboos. Ph.D. Thesis, Vol. I. H.N.B. Garhwal University, Srinagar, Garhwal. National Mission on Bamboo Applications, New Delhi, various documents.

Negi, S.S., (1996), "Bamboos and Canes", Bishen Singh Mahendra Pal Singh, Dehra Dun. Negi, S.S. and Naithani, H.B., (1994), Hand Book of Indian Bamboos, Oriental Enterprises, Dehra Dun.

Pabuayon, I.M. & Espanto, L.H., (1996), "The Philippine rattan sector: A case study of an extensive production system", Bamboo and Rattan Seminar/Workshop, 28 June 1996.

Planning Commission, (2003), "National Mission on Bamboo Technology and Trade Development" Government of India, Delhi

Press Information Bureau, (2004), "The Wonderful Natural Resource", Press Release, March 25, 2004.

Punhani, R.K.and Pruthi, K.S. (1991), "Substitution of Wood in Building some alternative Forest based Materials and their Technology", National Symposium on Substitution of Wood Building (SWOB) Roorkee.

Savur, Manorama, (2003), "And the Bamboo Flowers in the Indian Forests: What did the Pulp and the Paper Industry Do? Vol. I & II", Manohar Publications, Delhi

Shanmughavel, P.; Francis, K. and George, M. (1997), Plantation Bamboo, International Book Distributors, Dehra Dun.

Sharma, S.N., (1988), "Seasoning behaviour and related properties of some Indian species of bamboo", Indian Forester, 114(10): 613- 621.

Singhal, R.M. and Gangopadhyay, P.B., (1999), Bamboo and Its Database in India, ICFRE Publications.

Saxena, N.C., (1997), The Saga of Participatory Management in India, CIFOR Special Publication, Jakarta.

Singh, G., (1995), Environmental Law, Lawman (India) Pvt. Limited, New Delhi.

Singh, K., (1994), Managing Common Pool Resources, Oxford University Press, New Delhi.

Singh, C., (1986), Common Property and Common Poverty: India's Forest Dwellers and the Law, Oxford University Press, New Delhi.

Stebbing, E.P., (1922-27), The Forests of India, Vols. I - IV, John Lane, London. Subramaniam, K.N. (1998). Bamboo Genetic Resources in India. In : K. Vivekanandan, A.N. Rao and V. Ramanatha Rao (Eds.) : Bamboo and Rattan Genetic Resources in Asian Countries, IPGRI-APO, Serdang, Malaysia.

Tewari, D.N. (1992). A Monograph on bamboo. pp 1-498. International Book Distributors, Dehra Dun. Wagh, R. and Rajput, J.C. (1991). Comparative Performance of Bamboo with the Horticultural Crops in Konkan. In : Bamboo in Asia and Pacific. Proc. Ivth Intl. Bamboo Workshop, 27-30 Nov. 1991. Chiangmai, Thailand, FORSPA Publication-6. Canada. IDRC and FORSPA, Bangkok, Thailand, 1994 : 85-86.

Zhong Maogong and Liu Chang, (1999), "Retrospects and Prospects on Development of Bamboo Sector in China", in "Forestry Economy" 1999 No. 3, pp. 51-62.

Application of Recycled Polyethylene In Combination With Urea-Formaldehyde Resin To Produce Water Resistant Particleboard

A. Kargarfard *A. Jahan-Latibari*
Associate Prof., Wood and Forest Products Science Research Division,
Research Institute of Forests and Rangelands,Tehran, Iran
e-mail: a_kargarfard@yahoo.com
A. Jahan-Latibari
Associate Prof., Department of Wood and paper Science and Technology,
Karaj Branch, Islamic Azad University,
Karadj. IRAN

Abstract

Furniture grade particleboard always suffers from severe thickness swelling and water absorption which limits its utilization in humid places such as bathrooms, and those countries which do not produce water resistant panels are faced with this deficiency. To overcome such limitation, addition of recycled polyethylene (PE) in the surface layer of three layers particleboard was investigated. The content of UF resin used in the surface was 4% and one of the three levels (5, 10 and 15%) of recycled polyethylene and in the core layer 10% urea formaldehyde resin was applied. Three layers boards were produced applying press temperature of 185°C and 6 minutes pressing time. Boards were condition in a standard conditioning chamber, and then tested according to EN standard. When 5 recovered PE was added to surface layer, MOR and MOE were increased marginally, but at 15% addition of recovered PE to the surface layer, MOR was almost doubled and the MOE was increased by 50% compared to control boards. IB was improved as well and the value of 0.326 MPa. for control boards was raised to 0.537 and 0.466 MPa. for boards produced applying 10 or 15% PE and 4% UF resin respectively. As expected, both thickness swelling and water absorption were reduced to almost one third of the relevant values for control boards.

Keywords: Particleboard, Polyethylene, MOR, MOE, IB, thickness Swelling, Water Absorption

Introduction

Development, production and consumption of wood based panels initiated more than half a century ago and during this period, not only the production capacity was expanded, but in addition to particleboard which was the original product of this category. New products such as MDF, oriented Strand Board (OSB) and waferboard have been developed and presented to the consuming market. This wide range of products have provided the opportunity for the development of new consumer products as well as engineering products applications, thank to the sustainability of these products. However, an intensive competition exists among these products and products such as Medium Density Fiberboard (MDF) in furniture industry and OSB in construction field gained the upper hand (Regattieri and Bellomi 2009). Even though, particleboard had lost its initial fast growth, but it is still having a good share of the market, thanks to advances in production technology, utilization of wider range of raw material and cost saving.

During recent decades, new generation of composite material called WOOD Plastic Composite (WPC) combining wood and polymers as the main raw materials have been developed and used and this segment has witnessed a fast growth in wood based panel products (Youngquist 1995). Due to the presence of hydrophobic polymers, the dimensional stability of these products are superior. The application of recovered plastic in the production of wood plastic composite also helped to protect our environment. The research in this field points to the potential of this technology in the production of particleboard which usually uses larger size wood particles and employing the flat press technology (Borysiuk et al 2010, Hu et al. 2005). In this respect, waste thermoplastic are used as the binder (Borysiuk et al. 2011) which not only provides the chance of using waste material as a source of cheap binder but also reduces the environmental pollution by eliminating the plastic from the environment (Ayrilmis et al. 2008).

Lignocellulosic materials such as wood or other sources and the formaldehyde synthetic resins are the two main components in wood based panel production. Even though the swelling of resins is insignificant compared to lignocellulosic substances, but the content of resin is limited and does not play a major role in the swelling behavior of wood based panels (Medved et al. 2011). In addition, the concern on the formaldehyde emission for conventional wood based panels resin necessitated the development of the alternative bonding technology to easier bonding of wood particles without adverse affect of both quality of the final product and the cost (Jost and Sernek 2009).

Considering the fact that, to reduce the production cost, improve the quality of the particleboard product, and utilize the recovered waste thermoplastic in a value added product, the objective of our work is focused on the application of recovered waste polyethylene in the surface layer of three layer particleboard to reach better dimensional stability of the product, save the production cost and reduce the formaldehyde emission. The results are compared with normal furniture grade particleboard.

Experimental

Material

Eucalyptus cameldulensis wood was harvested from a plantation in the northern city of Gonbad, Iran and after felling, the bolts were transferred to Wood and Paper Laboratory for further processing. The bolts were first chipped using drum chipper (Pallmann PHT 120x430 and then flaked in a ring flaker (Pallmann PZ8) to be used in board making. Particles were dried using rotary drum dryer at 120°C to final moisture content of one percent. Dried particles were packed in polyethylene bags until used.

Urea-formaldehyde (UF) resin at 63% solid, specific gravity, viscosity, gel time and pH of 1.26 g/cm3, 69 seconds,81 seconds and 8.15 respectively was supplied by local resin manufacturing plant. Reagent grade ammonium chloride was used as harder. Waste polyethylene was purchased from local collection company and was first milled to 5 millimeter granules and then in a second grinder to the final size of about 50 microns.

Three layer boards were produced. The core layer was made applying 10% (based on the oven dry weight of the particles) UF resin and the surface layer with a combination of 4% (based on the oven dry weight of the particles) UF resin and one of the three dosages (5, 10 and 15% based on the dry weight of the particle) of polyethylene.

Board Making and Testing

Core layer particles were blended with UF resin and surface layer was also blended with UF resin utilizing rotary drum blender and spray nozzle and then the polyethylene particles were sprayed on the resin blended particles. Then core and surface layers particles were hand formed using wooden mold. Board target density and thickness was selected at 750 kg/cm^3 and 15 millimeters. Mats were pressed at 185°C for 6 minutes in a laboratory press (Buerkle L100) applying 30 bar specific pressure, five millimeters per seconds closing speed.
Three boards for each combination of variables and total of 27 boards were produced. Test samples were prepared from each board according to relevant EN standards. MOR and MOE was measured according to EN310/1996, Internal bonding (IB), EN319/1996 and dimensional changes, EN 317/1996 standards.

Results and Discussion

In recent decades, the concern on discharge of different plastic containing residues to our environment has been steadily increasing due to the expanding trend on the application and utilization of plastic packaging (Ayrilmis et al. 2008). Therefore, various research groups around the globe have been concentrating to find the application for waste plastics, among them using these plastic as partial substitute for conventional wood based panel synthetic resins. Wood plastic composites have been the first alternative for the utilization of waste plastic and particleboard production has also been investigated.

The results of strength and thickness swelling measurement on particleboard produced using different combinations of UF resin and recovered polyethylene are illustrated in Figures 1-3. Each value in Figures 1-3 is the average of 12 measurements (three replicate boards for each combination of variables and four sets of samples from each board). Similar properties of homogenous particleboard produced using 10% UF resin is also shown in Figures 1-3 for comparison.

Boards produced applying different dosages of recovered polyethylene exhibited higher flexural strength (Fig.1). Application of different content of polyethylene in the particleboard furnish also improved the IB of the boards compared with the control boards (Fig. 2).

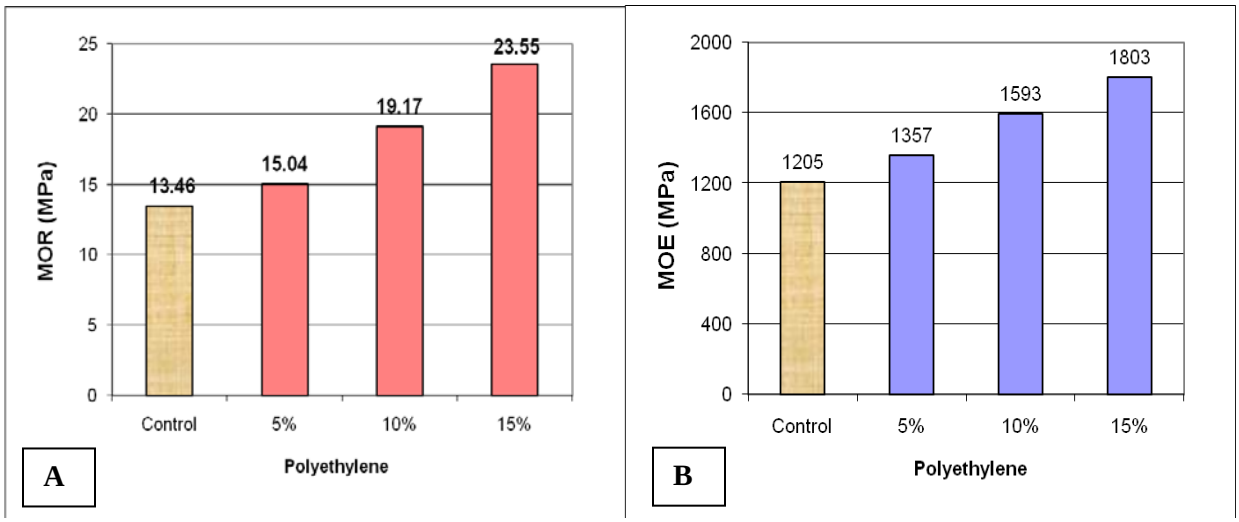

Figure 1- The influence of recovered PE dosage on MOR (A) and MOE (B) of particleboard

Both 2 and 24 hours thickness swelling and water absorption of the boards containing PE was lower than control boards, which indicate the potential of hydrophobic PE to impart water repellency (Figs. 3 and 4).

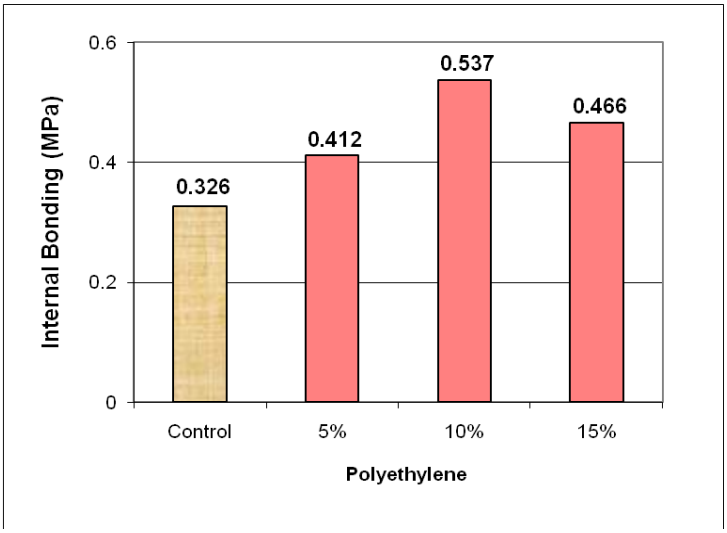

Figure 2- The influence of recovered PE dosage on the IB of particleboard

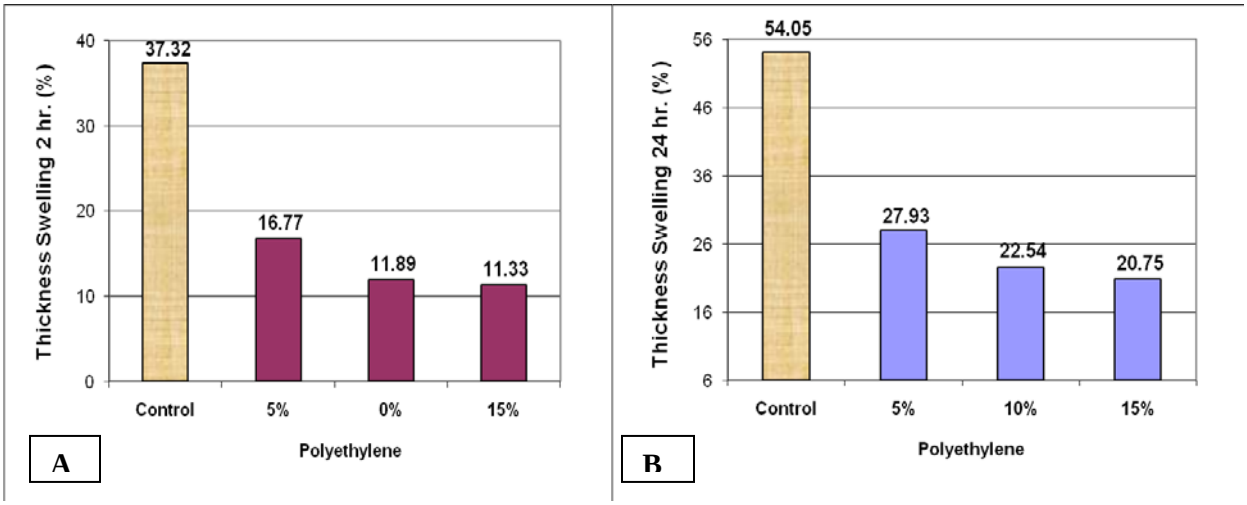

Figure 3- The influence of recovered PE dosage on 2 hr (A) and 24 hr. (B) thickness swelling of particleboard

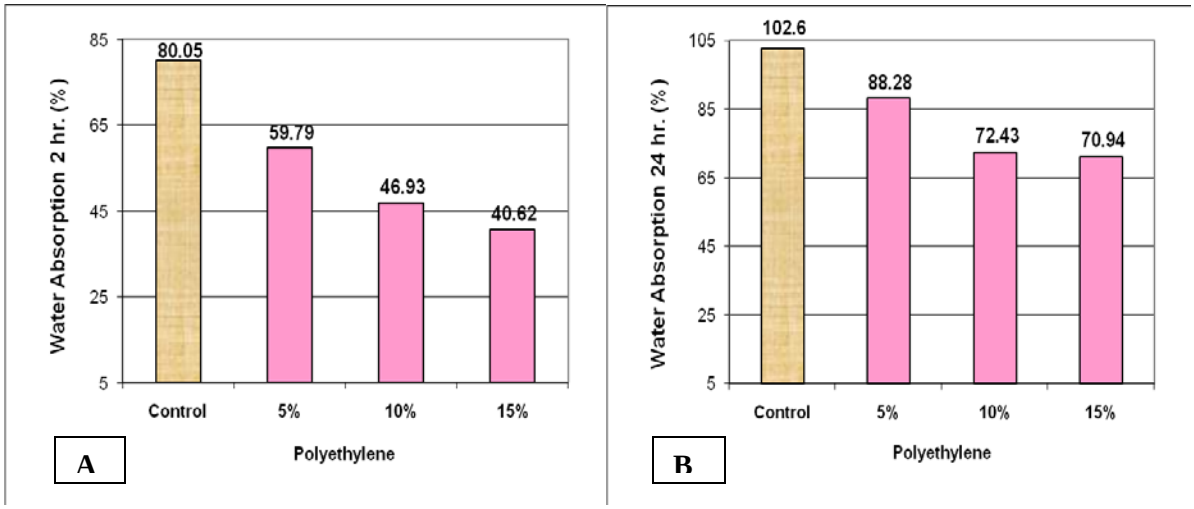

Figure 3- The influence of recovered PE dosage on 2 hr (A) and 24 hr. (B) water absorption of particleboard

We have investigated the application of recovered polyethylene as substitute for synthetic resin in the production particleboard to find the suitability of this material as a cheap source of binder and also to improve the performance of the product especially its water repellency. Conventional UF bonded panels are sensitive to moisture and therefore, its application is limited to dry climate. However, if the recovered PE is used in the surface layer of the boards, then the water repellency of the product will improve and lower thickness swelling and water absorption is reached. The flexural strength and modulus as well as the internal bonding of the panels not only deteriorated but were improved as well. This indicates that to reduce the cost of production and find new sources of raw material for an industry under pressure, waste materials such as recovered plastics can be viable material.

Conclusion

Particleboard production and marketing is under intense pressure from competitor both technologically and cost. Therefore, various measures have been undertaken to improve the performance of the particleboard in different applications and to reduce the production cost. One major limitation of conventional particleboard is it water absorbency with limits its application in humid locations. In this respect, utilization of hydrophobic materials such plastics will help to improve the water repellency of the final product. Application of different amount of recovered polyethylene in combination of lower amount of UF resin revealed that using even 5% recovered polyethylene in the surface layer will reduce both thickness swelling and water absorption of the particleboard.

Partial substitution of cheap source of recovered polyethylene in the production of particleboard will reduce the production cost and helps this panel to remain competitive in tense situation presently the type of panels are faced.

Utilizing recovered polyethylene in the surface layer not only do not scarify the strength properties of the final board, but also improve these properties.

References

Aryrilmis, N., Candan, Z., Hiziroglu, S., 2008. Physical and mechanical properties of Cardboard panels made from used bevearge carton with veneer overlay. Material and Design, 29:1897-1903.

Borysiuk, P., Maminski, M.L., Boruszewski, P., Grzeskiewicz, M., 2010. Application of polystyrene as binder for veneers bonding- the effect pf pressing parameters. European J. Wood and Wood Prod. 68:487-489.

Borysiuk, P., Zbiec, M., Boruszewski, P., Maminski, M., Grzeskiewicz, M., Jenczyk-Tolloczko, I.,2011. Flat pressed wood plastic composites- mechanical and physical properties and machining capacities. Proceeding International Panel and Panel Products Symposium 2011, p:227- 231.

European Standard EN 317. (1996). "Particleboards and fiberboards, determination of swelling in thickness after immersion," European Standardization Committee, Brussell.

European Standard EN 319. (1996.) "Wood based panels, determination of tensile strength perpendicular to plane of the board," European Standardization Committee, Brussell.

European Standard EN 326-1 (1993). "Wood based panels, Sampling, cutting and inspection. Sampling and cutting of test pieces and expression of test results." European Standardization Committee, Brussell.

European Standars EN 310. (1996). "Wood based panels, determination of modulus of elasticity in bending and bending strength," European Standardization Committee, Brussell.

European Standard EN 622-6 (1997). " Requirement for dry process boards (MDF)." European Standardization Committee, Brussell

Hu, Y., Nakao, T., Nakai, T., Gu, J., Wang, F., 2005. Vibrational properties of wood plastic plywood. J. Wood Sci. 51:13-17.

Jost, M., Sernek, M., 2009. Shear strength development of the phenol-formaldehyde adhesive bond during curing. Wood Sci Technol. 43:153-166.

Medved, S., Natasa, C., Kunaver, M., 2011. Sorption and moisture resistance of liquefied wood bonded particleboard. Proceeding International Panel and Panel Products Symposium 2011, p:129-138.

Regattieri, A., Bellomi, G., 2009. Innovative lay-up system in plywood manufacturing process. European J. wood and Wood Prod. 67(1):55-63.

Youngquist, J.A., 1995. Unlikely parameters? The marriage of wood and wood materials. Forest Prod. J. 45(10):25-30.

The Future Wood and Sustainable Materials Researcher

− The Society of Wood Science and Technology Student Membership

An Mao[1] – David Jones[2] - Weiqi Leng[3]*

[1] Research Assistant, Departament of Forest Products, College of Forest Resources - Mississippi State University, Mississippi State, MS, USA
amao@cfr.msstate.edu
[2] Assistant Extension Professor, Departament of Forest Products, College of Forest Resources - Mississippi State University, Mississippi State, MS, USA.
* *Corresponding author*
pdjones@ cfr.msstate.edu
[3] Research Assistant, Departament of Forest Products, College of Forest Resources - Mississippi State University, Mississippi State, MS, USA.
wleng@cfr.msstate.edu

Abstract

The Society of Wood Science and Technology is a professional organization of wood scientists, scholars, engineers, and other professionals who share an interest in wood and other sustainable materials. The purpose of Wood Science and Technology is to provide service to its members; to develop, promote, and advance the education and scientific research within the wood science profession; and to advocate the use of wood and other lignocellulosic products.
Student Membership of the Society of Wood Science and Technology is open to all students who are interested in furthering the purposes of the society and who are registered students from a college or university. Student members receive the following benefits:

1. A platform provided by the Society of Wood Science and Technology for sharing and exchanging of ideas, and communication between members from all over the world.
2. Free online access to the journal Wood & Fiber Science.
3. Discount on the Society of Wood Science and Technology annual international conference registration and publications.
4. Inclusion in the annual student poster contest.
5. Student travel grants to attend international conferences.

6. Thesis or dissertation title and graduation date printed in the journal Wood & Fiber Science to provide exposure to possible employers.
7. Career information such as job vacancies and resume posting.

***Keywords*:** Society of Wood Science and Technology, Wood and Fiber Science, Wood, Sustainable material, Student membership.

Introduction

Founded in 1958, the Society of Wood Science and Technology (SWST) (www.swst.org) is a professional organization of wood scientists, scholars, engineers, and other professionals who share an interest in wood and other lignocellulosic materials. The purpose of SWST is to provide service to its members; to develop, promote, and advance the education and scientific research within the wood science profession; and to advocate the use of wood and other lignocellulosic products.

Benefits of SWST Student Membership

As a professional society, SWST is encouraging students from all over the world to join the international family of wood science and sustainable materials professionals. Student Membership of SWST is open to all students who are interested in furthering the purposes of the society and who are registered students from a college or university and who are interested in wood science and sustainable materials. Student members receive the following benefits:

A platform provided by SWST for sharing and exchanging of ideas, and communication between members from all over the world.
SWST's annual meeting, forums, publications, and other events provide members opportunities to share and exchange ideas, to learn about each other's research, to look for cooperation in their research and work, and to promote the development of wood science and sustainable materials. Publications of SWST include bi-monthly published member newsletters, career and educational information related to wood science and technology, proceedings of annual conference or other meetings, and critical issues and position papers. Member newsletters cover society news, career information, announcements, and features of interest to members. Other information such as the annual membership directory and member handbook is available on the SWST website (www.swst.org).

Free online access to electronic version of Wood & Fiber Science (WFS) journal.

WFS is the official journal of the SWST. It is published four times a year and it publishes technical papers dealing with sustainable natural materials including contents of material science, product processing and manufacturing. The first issue was published in 1969, since then WFS has become a professional journal in the field of wood science and sustainable materials. The subscription price for the WFS is $250 per year for non-members. However, as a SWST student member, you will enjoy free access to all full-text electronic versions of current and past WFS issues (http://www.swst.org/members/login.html). Moreover, when considering publishing technical papers in WFS, the price for the members is $100 per page instead of $135 per page for the non-members.

Discount on SWST annual international conference registration and other publications.

Each year, SWST holds an annual conference. The conference is in North America in odd years and held outside North America in even years. The 2012 SWST annual conference is being held in Beijing, China. Each year's conference has a program topic. The program topic of this year's conference is "Sustainable Development of Wood and Biomass in Our New Global Economy". The annual conference is an opportunity for members to present their work, conduct business, meet old friends, make new friends, and discuss possible ways to improve the society. SWST student members receive discounts on conference registration fees and other publications from SWST.

Annual student poster awards.

Annual student poster awards are to encourage students' participation in the annual meeting and recognize their excellent research. Currently SWST is awarding $500 for the first place winner and $250 for the second place and $125 for the third place, plus a laser plaque to each winner.

Student travel grants to attend international conferences.

To offset some of the costs associated with attending an international conference, SWST provides funding to assist qualified students to attend the international conference. This encourages student's attendance to the international conference and helps support the exchange of knowledge.

Student members' thesis or dissertation titles and graduation dates printed in WFS.

As a professional journal in wood science field, WFS provides the opportunity for graduate student members who have completed their degree programs to submit thesis or dissertation titles to WFS for publication (www.swst.org/wfs/thesis.html). This informs SWST member's of your research and it also allows you to be aware of your peers progress in the field of wood science and sustainable materials. The latest titles were published in WFS volume 44 (2), 2012.

Improved curriculums, and career information such as job vacancies and resume posting.

To further the wood science and sustainable materials fields, SWST assists schools in providing better educational programs, industry in fundamental support and solution

finding, students in completing current education program and choosing future careers. SWST posts job vacancies for students who are seeking employment, and allows students to post their resumes online.

Mississippi State University Student Chapter of the Society of Wood Science and Technology (MSU-SWST) was officially formed in spring, 2012. It is also the first SWST student chapter in the world. The constitution of MSU-SWST was also approved by the university. Currently, MSU-SWST has 23 graduate and undergraduate student members. Besides the regular monthly meetings, MSU-SWST holds, co-hosts or participates in other activities, such as inviting guest speakers to the meetings, a yearly Mississippi Green Festival booth display, Wood Magic Science Fair volunteering and teaching, fund raising, and etc. These activities will provide student members more opportunities to cooperate with each other, to serve our community, to interact with industry, and to learn from the society.

There are many benefits for being a student member of SWST. So please consider joining our ever growing group of professionals.

For more information, please go to www.swst.org.

Biorefining of Bamboo Processing Residues

Han Li, Li Zhang, Xin Li, Qiang Yong

College of Chemical Engineering, Nanjing Forestry University

Nanjing, China

Abstract

Bamboo is known as China's second forest laudatory. Bamboo plants grow quickly, have the ability to propagate and are easy to update. Bamboo-cutting would result in a lot of leaves and sawdust residues. Comprehensive utilization of bamboo processing residues would improve resource utilization and economic benefits of bamboo. Due to the bamboo's nature and recalcitrant for fractionation, the bamboo processing residues were firstly pretreated by NaOH to remove hemicellulose fraction, which would be used for production of xylooligosaccharides. The left residues were enzymatically hydrolyzed to monosaccharides and further fermented to L-lactic acid by *Rhizopus oryzae*. In this article, hemicellulose fraction was extracted by NaOH varying concerntrations from 1% (w/v) to 10%(w/v) at 80℃,100℃,120℃, 7% (w/v) NaOH at 100℃was proved to be suitable for extraction of hemicellulosic fraction from bamboo processing residues and a higher xylan yield of 57.81% was achieved. The alkali-treated residues were rich in cellulose, which could be hydrolyzed to glucose by cellulase. The enzymatic hydrolysis yield at 7% (w/v) NaOH was 62.15%. Furthermore, glucose would be fermented to produce optical pure L-lactic acid by *Rhizopus oryzae*. The optimal lactic acid production condition was determined by the cellulose hydrolysis yield. Biorefining of bamboo processing residues is a promising alternative for the comprehensive utilization of bamboo processing residues.

Key words: Bamboo processing residues; Pretreatment; NaOH; xylooligosaccharides; L-lactic acid

1 Introduction

Bamboo is known as China's second forest laudatory. Bamboo plants grow quickly, have the ability to propagate and are easy to update. Bamboo-cutting would result in a lot of leaves and sawdust residues. Comprehensive utilization of bamboo processing residues would improve resource utilization and economic benefits of bamboo.

The chemical compositions of bamboo are similar to wood, including of cellulose, hemicellulose, lignin and a small amount of extract and ash. Physical, chemical or physico-chemical pretreatment is used t o break down the hemicellulose and lignin structure in order to improve the enzymatic hydrolysis rate (Zhang et al. 2007). The pretreatment approaches: steam explosion, dilute acid, and lime were discussed for enzymatic hydrolysis (Zhang et al. 2011). Binod et al. reported that sodium hydroxide pretreatment of cotton stalk was effective for deriving fermentable sugars (Binod et al. 2012). Lin Y.S. studied that production of xylooligosaccharides could use immobilized endo-xylanase of *Bacillus halodurans*(Lin Y.S. et al. 2011). The enzymatic production of xylooligosaccharides from alkali solubilized xylan of Sehima nervosum was economically feasible (Samanta et al.2012). Production of xylooligosaccharides from the steam explosion liquor of corncobs coupled with enzymatic hydrolysis using a thermostable xylanase has been reported(Teng et al. 2010).

Raw materials, starchy and cellulosic materials are currently receiving a great deal of attention to produce L-lactic acid, because they are cheap, abundant, and renewable (Hofvendahl et al. 2000). The utilization of waste office paper, fishmeal water has been reported as well(Park et al. 2004, Huang et al. 2007). In this paper, the bamboo processing residues were firstly pretreated by NaOH to remove hemicellulosic fraction, which would be used for production of xylooligosaccharides. The left residues were enzymatically hydrolyzed to monosaccharides and further fermented to L-lactic acid by *Rhizopus oryzae(R. oryzae)*. Biorefining of bamboo processing residues is a promising alternative for the comprehensive utilization of bamboo processing residues.

2 Materials and Methods

2.1 Pretreatment of bamboo processing residues

Bamboo processing residues were collected from Fujian province, which were the residues of bamboo processing. The bamboo processing residues were firstly pretreated by NaOH to remove hemicellulosic fraction at 80 ℃,100 ℃,120℃. The NaOH concentrations varied from 1 % to 10 %.

2.2 Enzymatic hydrolysis

The alkali-treated filtrate was hydrolysised by xylanase after ultrafiltration to obtain xylooligosaccharides. The alkali-treated residues was initiated by the addition of cellulose with 25 FPIU/g cellulose and cellobiase with 4 IU/g cellulose. Hydrolysis was carried out in a 250 ml Erlenmeyer flask, and cellulase and cellobiase were purchased from Sigma-Aldrich and used in the hydrolysis experiments. The reaction was performed at 50 °C for 48 h with pH adjusted to 4.5-5.0 by addition of 72 % (w/w) sulfuric acid. All the flask level experiments were carried out in duplicate and presented as an average.

2.3 Strain and spore culture medium

The microorganism was *R. oryzae* NLX-M-11 (Nanjing Forestry University). The fungus was first grown on potato-dextrose agar slants at 30 °C for 3-5 d. A spore solution of 10^7 spores/ml was precultured into 250 ml Erlenmeyer flasks containing 50 ml of the culture broth in flask cultivation with $CaCO_3$. The composition (g/l) of medium used in the preculture (g/l) consisted of 50 glucose, 3 $(NH_4)_2SO_4$, 0.75 $MgSO_4 \cdot 7H_2O$, 0.2 $ZnSO_4 \cdot 7H_2O$, and 0.30 KH_2PO_4. Preculture flasks were incubated at 30 °C with 170 r/min shake speed for 12 h.

2.4 Fermentation for lactic acid production

For the production of lactic acid, preculture was inoculated into 250 ml Erlenmeyer flasks containing 100 ml of fresh medium. The medium (g/l) consisted of enzymatic hydrolysate from bamboo processing residues, 2 $(NH_4)_2SO_4$, 0.75 $MgSO_4 \cdot 7H_2O$, 0.2 $ZnSO_4 \cdot 7H_2O$, and 0.3 KH_2PO_4. The culture temperature was maintained at 35 °C throughout the experiments. After the culture time of 12 h, 30 g/l $CaCO_3$ powder was added to avoid a decrease of pH. Culture was carried out 2-3d containing the bamboo processing residues hydrolysate. Lactic acid yield expressed as g lactic acid produced/g sugars consumed. Each experiment was done in duplicate and presented as an average.

2.5 Analytical methods

After sampling, the samples were capped tightly in the test tube and immersed in boiling water for 3 min to deactivate the hydrolytic enzyme, then the slurry was centrifuged and the supernatant kept for sugar assay. To determine the amounts of glucose, cellobiose and lactic acid produced, liquid fractions were analyzed by high performance liquid chromatography (HPLC) using an Aminex BioRad HPX-87H column, a mobile phase of H_2SO_4 (5 mmol/l) at a flow rate of 0.6 ml/min, and a column temperature of 55 °C.

3 Results and Discussion

3.1 Xylan extraction

Hemicellulose fraction was extracted by NaOH varying concentrations from 1 % (w/v) to 10 % (w/v) at 80 ℃, 100 ℃and 120 ℃; 7 %（w/v）NaOH at 100 ℃was proved to be suitable for extraction of hemicellulosic fraction from bamboo processing residues. The results of glucan yield of alkali-treated residues and xylan concentration of alkali-treated filtrate at different temperatures were shown in figure 1,2,3,4.

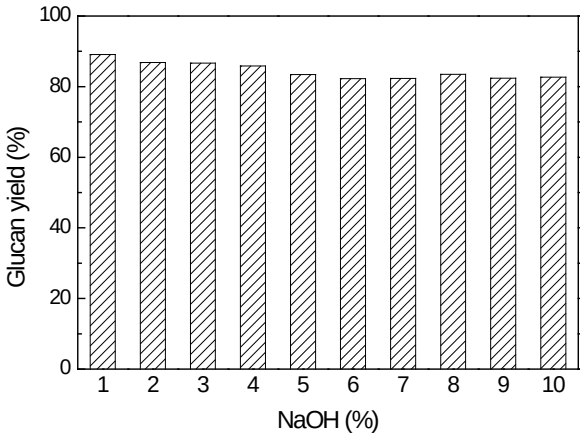

Fig. 1 The effect of different NaOH concentrations on glucan yield of bamboo processing residues at 80℃

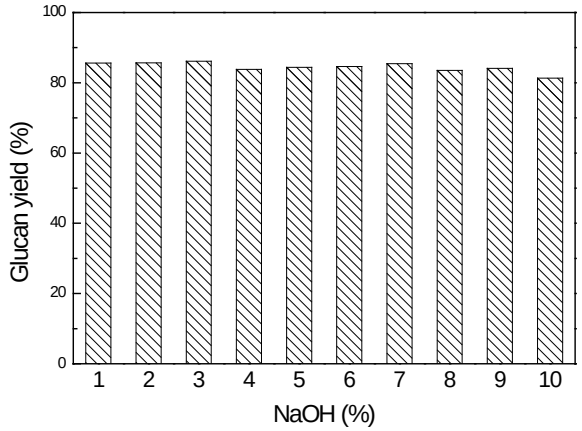

Fig. 2 The effect of different NaOH concentrations on glucan yield of bamboo processing residues 100℃

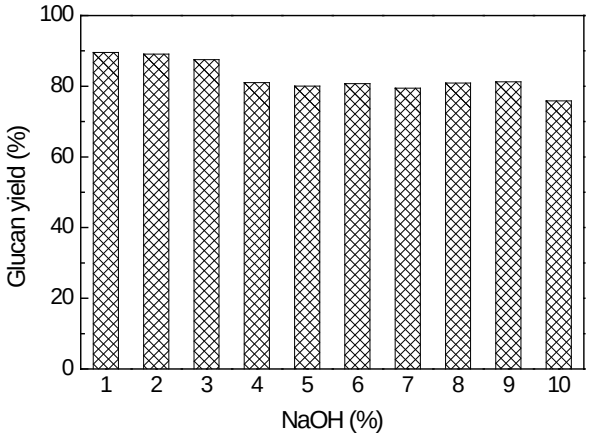

Fig. 3 The effect of different NaOH concentrations on glucan yield of bamboo processing residues 120℃

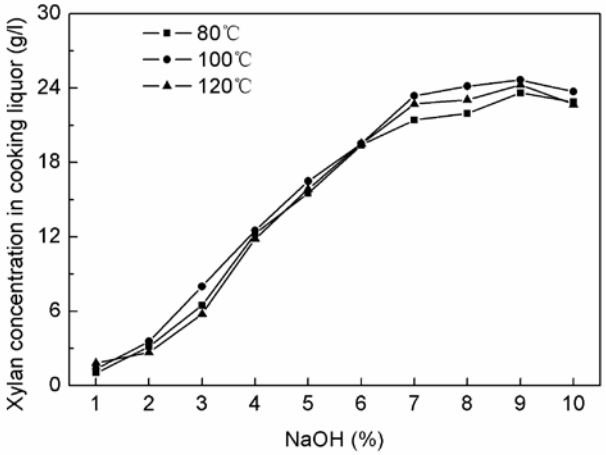

Fig. 4 The effect of different NaOH concentrations on xylan concentration of alkali-treated filtrate.

As shown in Figures 1,2,3, with the increase of NaOH concentration, the glucan yield declined. The temperature has little effect on glucan yield. According to Figure 4, xylan concentration in alkali-treated filtrate was the highest at 100℃.About 10% of material was removed as black liquor, a major portion of which include hemicellulosic sugars (Binod et al. 2012). The water-soluble materials contained various monosaccharides and oligosaccharidesthe (Asada et al. 2005). The xylan concentration increased along with the increase of NaOH concentration from 1% to 7%, not much have changed from 7% to 10%.

3.2 Production of Xylooligosaccharides

The bamboo processing residues were pretreated by NaOH to remove hemicellulosic fraction, which would be used for production of xylooligosaccharides.

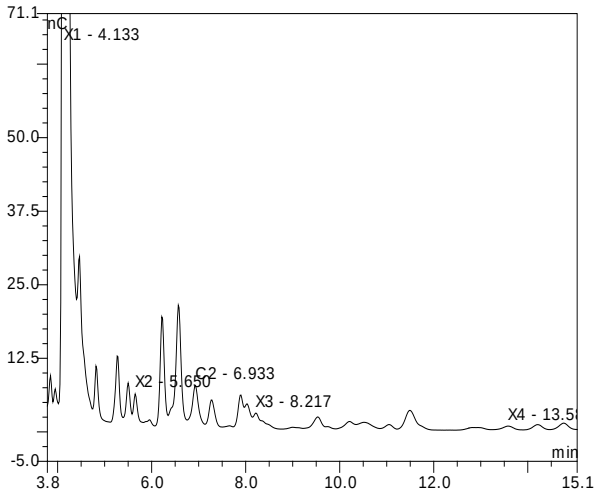

Fig. 5 Ion Chromatography analysis of the hydrolysate of alkali-treated filtrate.

Different degree of polymerization of the xylooligosaccharides could be detected by Ion Chromatography analysis.

3.3 Enzymatic hydrolysis

Enzymatic hydrolysis studies were carried out to investigate the effect of lignin and hemicellulose removal on hydrolysis yield (Öhgren et al. 2007).The alkali-treated residues were rich in cellulose, which could be hydrolyzed to glucose by cellulase. To investigate the influences of different NaOH concentrations on enzymatic hydrolysis, the results were as follows in figure 6.

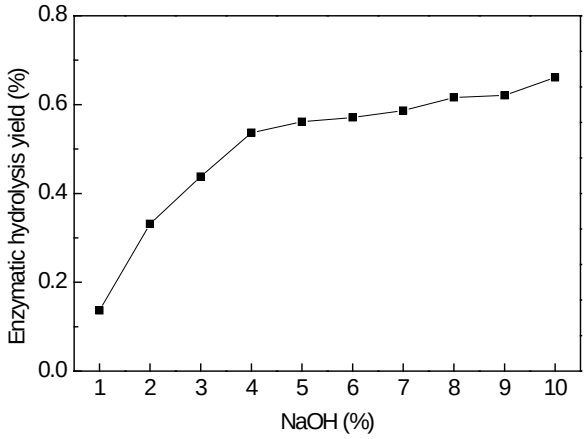

Fig.6 Enzymatic hydrolysis yield of alkali-treated residues with different NaOH concentrations.

The enzymatic hydrolysis yield were increasing sharply from 1% to 4% of NaOH concentrations, then the enzymatic hydrolysis yield were steady. The enzymatic hydrolysis yield at 7% NaOH was 62.15%, which could be promoted by different measures.

3.4 Production of L-lactic acid

Glucose would be fermented to produce optical pure L-lactic acid by *R. oryzae*. The optimal lactic acid production condition was determined by the cellulose hydrolysis yield.

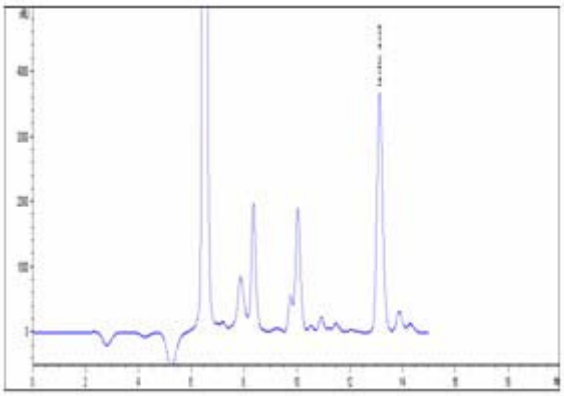

Fig. 7 HPLC analysis of the fermentation broth of alkali-treated residues hydrolysate.

L-lactic acid was detected by HPLC analysis. Lactic acid is currently considered as the most potential feedstock monomer for chemical conversions (Gao et al. 2011). Interest in L-lactic acid production has increased recently also due to its ability to serve as raw material for the manufacture of green solvent, such poly-L-lactic acid (PLLA), which are biodegradable and environmental friendly (Yu et al, 2007).

4 Conclusion

In the present study, the hemicellulose and cellulose of bamboo processing residues were utilized efficiently. Xylooligosaccharides and L-lactic acid were obtained from the two fractions respectively. In this artical, 7% (w/v) NaOH at 100℃was proved to be suitable for extraction of hemicellulosic fraction from bamboo processing residues and a higher xylan yield of 57.81% was achieved. The alkali-treated residues were rich in cellulose, which could be hydrolyzed to glucose by cellulase. Furthermore, glucose would be fermented to produce optical pure L-lactic acid by *R. oryzae*. Comprehensive utilization of bamboo processing residues would improve resource utilization and economic benefits of bamboo.

References

Asada C., Nakamura Y., Kobayashi F. 2005. Waste reduction system for production of useful materials from un-utilized bamboo using steam explosion followed by various conversion methods. Biochemical Engineering Journal. 23:131–137

Binod P., Kuttiraja M., Archana M., et al. 2012. High temperature pretreatment and hydrolysis of cotton stalk for producing sugars for bioethanol production.Fuel. 92:340-345.

Gao C, Ma CQ, Xu P, 2011. Biotechnological routes based on lactic acid production from biomass. Biotechnology Advances. 29: 930-939.

Hofvendahl K., Hahn-Hagerdal B.,2000. Factors affecting the fermentative lactic acid production from renewable resources. Enzyme and Microbial Technology. 26: 87–107.

Huang L.P., Dong T., Chen J.W., et al. 2007. Biotechnological production of lactic acid integrated with fishmeal residues water treatment by Rhizopus oryzae. Bioprocess and Biosystems Engineering .30: 135–140

Lin Y.S.,Tseng M.J.,Lee W.C.,2011. Production of xylooligosaccharides using immobilized endo-xylanase of Bacillus halodurans. Process Biochemistry. 46(11):2117-2121.

Öhgren K., Bura R., Saddler J., et al. 2007. Effect of hemicellulose and lignin removal on enzymatic hydrolysis of steam pretreated corn stover. Bioresource Technology.98:2503–2510.

Park E.Y., Anh P.N., Okuda N., 2004. Bioconversion of waste office paper to L (+)-lactic acid by the filamentous fungus Rhizopus oryzae. Bioresource Technology.93: 77-83.

Samanta A.K.,Jayapal N., Kolte A.P.,2012. Enzymatic production of xylooligosaccharides from alkali solubilized xylan of natural grass (Sehima nervosum). Bioresource Technology. 112:199-205.

Teng C., Yan Q., Jiang Z., 2010.Production of xylooligosaccharides from the steam explosion liquor of corncobs coupled with enzymatic hydrolysis using a thermostable xylanase. Bioresource Technology. 101(19):7679-7682.

Yu M.C., Wang R.C., Wang C.Y., et al. 2007. Enhanced production of L (+)-lactic acid by floc-form culture of Rhizopus oryzae. Journal of the Chinese Institute of Chemical Engineers.38: 223-228.

Zhang J., Ma X., Yu J., et al. 2011. The effects of four different pretreatments on enzymatic hydrolysis of sweet sorghum bagasse. Bioresource Technology. 102: 4585–4589.

Zhang X., Xu C., Wang H. 2007. Pretreatment of Bamboo Residues with Coriolus versicolor for Enzymatic Hydrolysis. Journal of Bioscience and Bioengineering. 104(2):149–151.

Acknowledgments

The authors wish to express thanks for the supports from Nanjing Forestry University.

Influence of Environmental Factors on Volatile Organic Compound（VOC）Emission from Plywood

Shuang Li[1] *– Jun Shen*[2*] *– Jingxian Wang*[3]

[1] College of Material Science and Engineering, Northeast Forestry University, NO.26, Hexing Rd, Harbin, PRC.
lishuang0413@126.com
[2] College of Material Science and Engineering, Northeast Forestry University, NO.26, Hexing Rd, Harbin, PRC.
* *Corresponding author*
shenjunr@126.com
[3] College of Material Science and Engineering, Northeast Forestry University, NO.26, Hexing Rd, Harbin, PRC.
wangjingxian_1985@163.com

Abstract

In this study, the impact of temperature (T=18℃, 23℃, and 28℃), relative humidity (RH=35%, 50%, 60%, and 75%), and air exchange rate (ACH=0.5/hr,1/hr, and 2/hr) on the Volatile Organic Compound(VOC) emission rate and concentration from plywood were investigated by small chamber testing for 5 days. Gas chromatography-mass spectrometer (GC/MS) was used to measure components of Total Volatile Organic Compound (TVOC). The aim of this study was to explore the properties of VOC emission from plywood in different environmental conditions. The experiment result showed that increasing temperature, relative humidity and air exchange rate accelerated VOC emission from plywood. The influence of environmental factors on VOC emission was only significant for initial emission. Few days later, the effect was not obvious. Arene compound were the main compounds of TVOC emission from plywood, and the content of alkane compounds were the second. Small amounts of alkene, esters and aldehydes compounds were emitted from plywood. The emission rate of arene compounds was higher than that of alkane compounds. Environmental factors affected arenas compounds emission rate more obviously than alkane compounds. Toluene emission rate was the highest, m,p-xylene was the second, and the ethylbenzene was third. The influence of environmental factors on these three compounds had no big differences.

Keywords: plywood； Volatile Organic Compound（VOC）；temperature； relative humidity； air exchange rate

Introduction

Many factors, such as hot-pressing process, secondary processing, and environmental conditions, affect Volatile Organic Compounds (VOC) emissions. Local and foreign researchers (Liu 2010, Zhang 2011, Kim et al 2010) had studied the influence of hot-pressing and secondary processing on VOC emissions from wood-based panels. Environmental factors, namely, temperature, relative humidity (RH), and air exchange rate (ACH), have a major influence on VOC emissions. Studies (Fang 1999, Wolkoff 1998) proved that the influence of environmental factors on VOC emissions depend on the type of materials and VOC.

This study used plywood that is widely used in indoor decorations. The influence of temperature (18 ºC, 23 ºC, and 28 ºC), RH (35%, 50%, 60%, and 75%), and ACH (0.5/hr, 1/hr, and 2/hr) on VOC emission rate and concentration from plywood were investigated using small chamber testing for five days. The study used a gas chromatography-mass spectrometer (GC/MS) to measure the components and quantities of TVOC.

Materials and Methods

Materials. The plywood came from a wood-based panel factory in Harbin. The plywood (1220 mm×2440 mm×9 mm) was cut into small pieces immediately after manufacture. The volume of the small chamber was 15 L. The loading rate was 1 $m^2 m^{-3}$, and the exposed area of the plywood was 0.015 m^2 (123 mm×123 mm). To prevent VOC emissions, the edges and other side of the plywood were wrapped with aluminum foil. After the edges and one side were wrapped, the plywood was wrapped with tin foil and polytetrafluoroethylene plastic. In the end, the plywoods were kept in the refrigerator at -30 ºC.

Equipments and methods. The volume of the environment chamber was 15 L. The background TVOC concentration of the chamber was less than 20 ug/m^3, and any individual compound concentration was less than 2 ug/m^3. These amounts corresponded with the *Technical requirement for environmental labeling products–Wood based panels and finishing products* (HJ 571-2010) .The parameters of 15L small chamber is showed in Table. 1.

Table.1. The parameters of 15L small chamber

Experiment parameters	15L small chamber		
	A	B	C
Volume(m^3)	0.015	0.015	0.015
Loading factor(m^2m^{-3})	1	1	1
Air exchange rate(hr^{-1})	1	1	0.5/1/2
Relative humidity (%)	35/50/60/75	50	50
Temperature (℃)	23	18/23/28	23
Chamber air flow(m^3h^{-1})	0.015	0.015	0.0075/0.015/0.03
Specific air flow rate ($m^3h^{-1}m^{-2}$)	1	1	0.5/1/2

The thermal desorption (TP-5000, China)-GC/MS (Thermo, DSQII) experiment parameters are as follows:
Thermal desorption: Carrier gas, helium; desorption temperature, 300 ºC; desorption time, 5 min; sample air entrance time, 1 min.
GC/MS: Chromatographic column (25m×0.25mm×0.25μm DB-5 silica capillary columns) was used. The temperature program started at 40 ºC, which was kept for 2 min. At 2 ºC/min, temperature rose to 50 ºC, which was maintained for 4 min. At 5 ºC/min, temperature rose to 150 ºC, which was maintained for 4 min. Finally, at 10 ºC/min, the temperature rose to 250 ºC and maintained for 8 min. The carrier inlet temperature was 250 ºC; the split flow rate was 30 l/min; the split flow ratio was 1:30. The electron impact ionization source (EI) was used. The ionization source temperature was 230 ºC, and auxiliary temperature was 270 ºC.

Results and discussions

The influence of environmental factors on TVOC emission. In this research, the TVOC is the sum of compounds within the retention time between the n-hexane and hexadecane. VOC emissions from plywood were tested in different environmental conditions. Air samples were collected in the Tenax tube using an air sample pump with electronic flow controller. A flow rate of 150 ml/min was used for sampling an air sample volume of 6 L. Then, the air sample was desorbed for 5 min and qualitatively analyzed with the GC-MS using the internal standard method (internal standard substance is toluene-d8). The emission rate or concentration/time profiles of TVOC emissions from plywood in different environmental conditions are shown in Figs. 1, 2 and 3.

Temperature

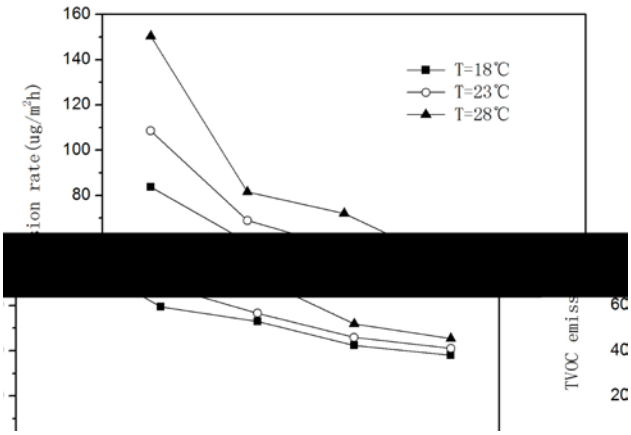

Fig. 1. TVOC rate/time profiles at different temperature

Fig. 1 shows that the increasing temperature accelerated the TVOC emission rate from the plywood. At higher temperatures, the TVOC emission rate decreased faster than that at lower temperatures. At the temperature of 28 ºC, the TVOC emission rate decreased 51.6% from the first day to the second day. On the first day, the TVOC emission rates at three different temperatures had the biggest differences. When temperature increased from 18 ºC to 28 ºC, the TVOC emission rate increased two times. With the emission of TVOC, no obvious difference was observed among emission rates, and the TVOC

emission rate gradually stabilized. This phenomenon showed that the effect was obvious only during short-term emissions; long-term emission levels were similar. The reason is that temperature can affect the vapor pressures and the diffusivities of VOC within the material. The temperature dependence of diffusivities D_a of VOC within materials can be expressed as the following equation (1):

$$D_a = D_{ref} Exp\left|-E\left|\frac{1}{T}-\frac{1}{296}\right|\right| \quad (1)$$

where D_a is the VOC diffusion coefficient within the material at the temperature of the environment (m^2/h), D_{ref} is the VOC diffusion coefficient within the material at 23 ºC (m^2/h), E is determined by experiment (with the general value at 9,000 K), and T is the absolute temperature (K). With the enhancement of temperature, the diffusion coefficient increases. According to the mass transfer theory, increasing the diffusion coefficient within the material can promote VOC emissions.

The temperature dependence of the vapor pressure of VOC can be expressed as follows equation (2):

$$\log p = a - \frac{b}{c+T} \quad (2)$$

where P is the vapor pressure of the compound within the material (atm), T is the absolute temperature (K), and a, b, and c are parameters greater than zero. According to this equation, enhancing the temperature can increase the compound vapor pressure within the material. Therefore, the vapor pressure gradient in the boundary layer between the surface of the material and the bulk phase of the air stream will become greater. A greater vapor pressure gradient will promote VOC emissions. Both diffusion control and vapor pressure control influence the VOC emission together for the initial emission (Fang 1999). However, the effect of vapor pressure on VOC emissions was not significant for long-term emission in his study. When the materials were ventilated for a long period, VOC emissions decreased to a low level, and the emissions became diffusion-controlled. In addition, the increasing diffusion coefficients of the emitted VOC within materials would be less than 10% for a temperature increased from 23 ºC to 35 ºC (Reid 1987). Therefore, the effect of temperature on VOC emissions is only obvious for initial emission.

Relative humidity

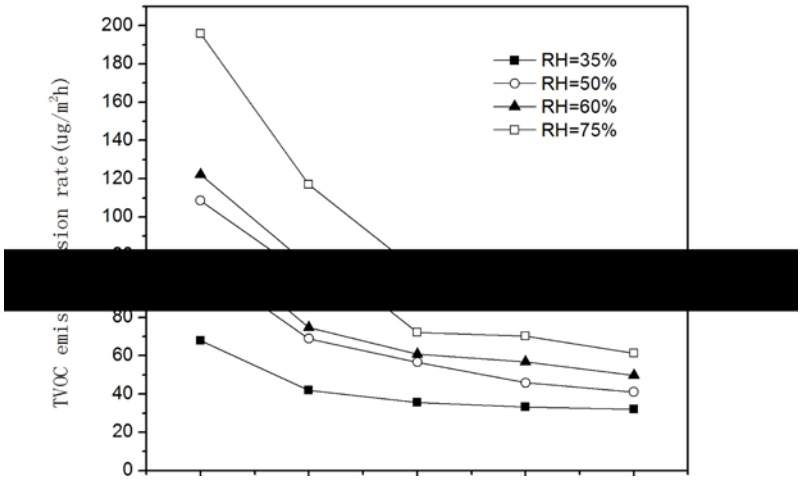

Fig. 2. TVOC rate/time profiles at different RH

As shown in Fig. 2, a higher RH resulted in a higher TVOC emission rate. At a higher RH, the TVOC emission rate decreased faster than that at a lower RH. On the first day, the TVOC emission rate had the biggest decrease. When the RH increased from 35% to 50%, from 35% to 60%, and from 35% to 75%, the TVOC emission rate increased 1.6, 1.8, and 2.9 times on the first day, respectively. For the emission of TVOC, no significant difference was observed among emission rates, and the TVOC emission gradually stabilized. This phenomenon showed that the influence of RH on VOC emissions for the initial emission was more significant than that on the long-term emission. The TVOC emission rate had the smallest change at the RH of 50% to 60%, and the biggest change at the RH was from 60% to 75%. The impact of RH on VOC is different in various RH ranges, which depend on the ranges of the RH. The enhancement effect of humidity on VOC emissions may result from the positive effect of humidity on the water vapor pressures of the external environment. Increasing the RH could improve the environment water vapor pressure, such that the evaporation rate of water vapor within the material becomes smaller. This process (evaporation of water) could absorb the heat of vaporization and retard VOC emissions. Under a lower RH, the retardation of VOC emissions was more significant than that under a higher RH (Lin 2009).

Air exchange rate

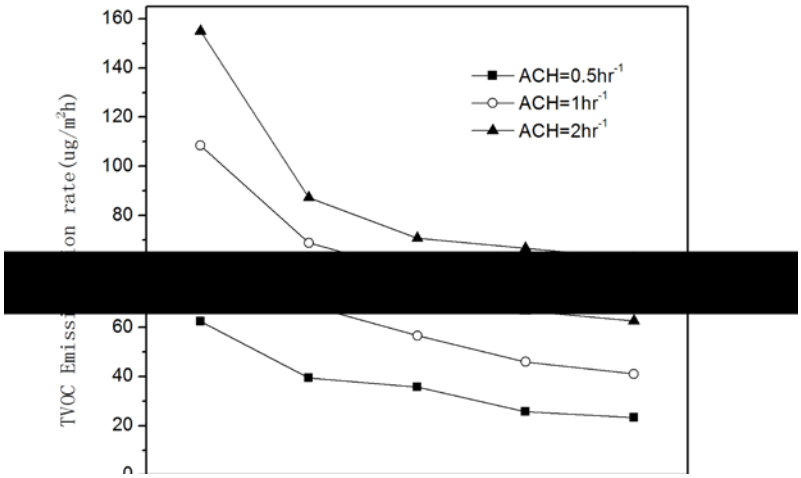

Fig. 3. TVOC rate/time profiles at different ACH

As shown in Fig.3, TVOC emission rates accelerated with the increase in the ACH, whereas TVOC concentration in the chamber decreased. Under a higher ACH, the TVOC emission rate decreased faster than that under a lower ACH. Under the ACH of 2 hr^{-1}, the TVOC emission rate decreased 43.7% from the first day to the second day. With increasing time, the TVOC emission gradually stabilized. Under the ACH of 0.5, 1, and 2 hr^{-1}, TVOC concentrations in the chamber were 46.68, 41.06, and 31.29 $ug \cdot m^{-3}$ on the fifth day, respectively. The reason in the increased VOC emission rate under a higher ACH is that the VOC concentration in the chamber decreased under the higher ACH. The decrease of VOC concentrations in the gaseous phase would result in the increasing concentration gradient in the boundary layer between the surface of the material and the bulk phase of the air stream. Therefore, VOC molecules were emitted into the air by the boundary layer faster.

The influence of environmental factors on individual components

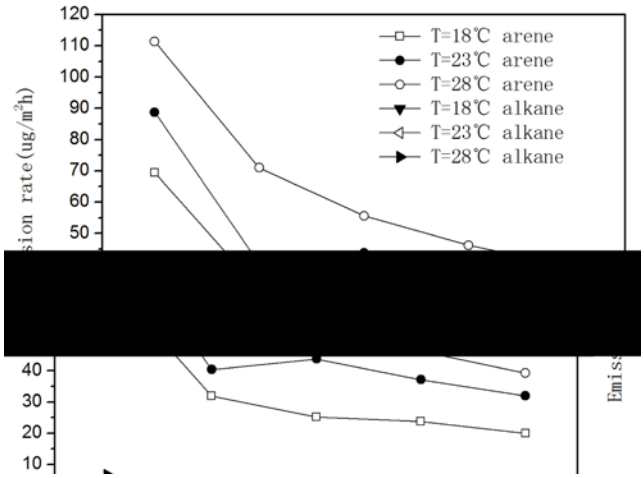

Fig. 4. Arenes and alkanes rate/time profiles at different temperature

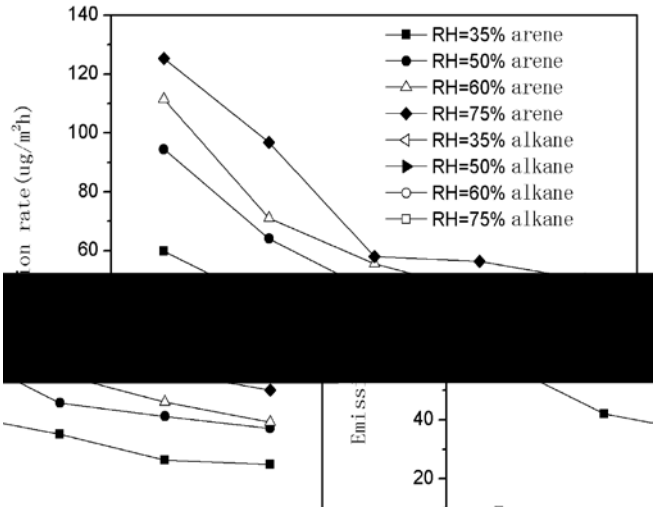

Fig. 5. Arenes and alkanes rate/time profiles at different RH

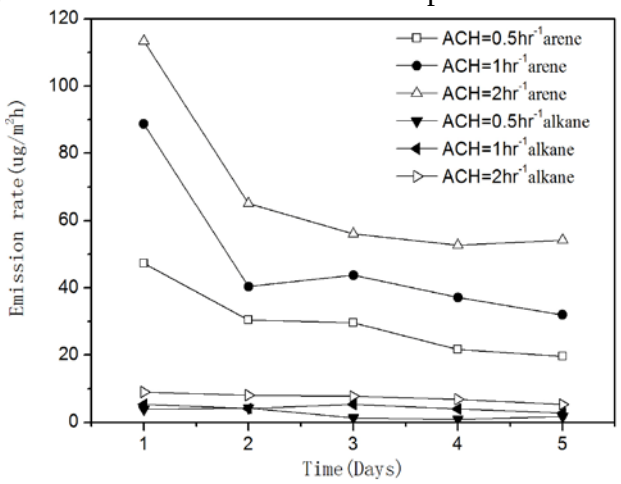

Fig. 6. Arenes and alkanes rate/time profiles at different ACH

As shown in Figs. 4, 5 and 6, the emission rate of arene compounds was higher than that of alkane compounds. In the early emission, arene compound emission rates declined rapidly; the rate declined about a third on the second day, and declined about one half on the third day. Finally, the emission rate gradually stabilized. However, there was no obvious characteristic that emission rates decreased rapidly during the emission process of the alkane compounds. The alkane compound emission rate was stable during the emission process.

The influences of temperature, RH, and ACH on arene compounds were more obvious than those on alkane compounds. The effect of temperature mainly depended on the VOC vapor pressure within the material affecting the VOC emission rate. The effect of temperature on the vapor pressure of alkane compounds within the material may be less obvious than that on arene compounds. The water vapor pressure was the dominant factor of RH affecting the VOC emission rate. For the low emission rate of alkane compounds, the retardation of alkane compound emission may be less significant than that of arene compounds. The effect of ACH mainly depended on VOC concentration in the chamber, which affected the VOC emission rate. The concentration of alkane compound in the

chamber was lower than that of arene compounds. The influence of ACH on the alkane concentration gradient in the boundary layer between the surface of the material and the bulk phase of the air stream may be less significant than that on arene compounds. Consequently, arene compounds emission rate was affected obviously by temperature, RH and ACH.

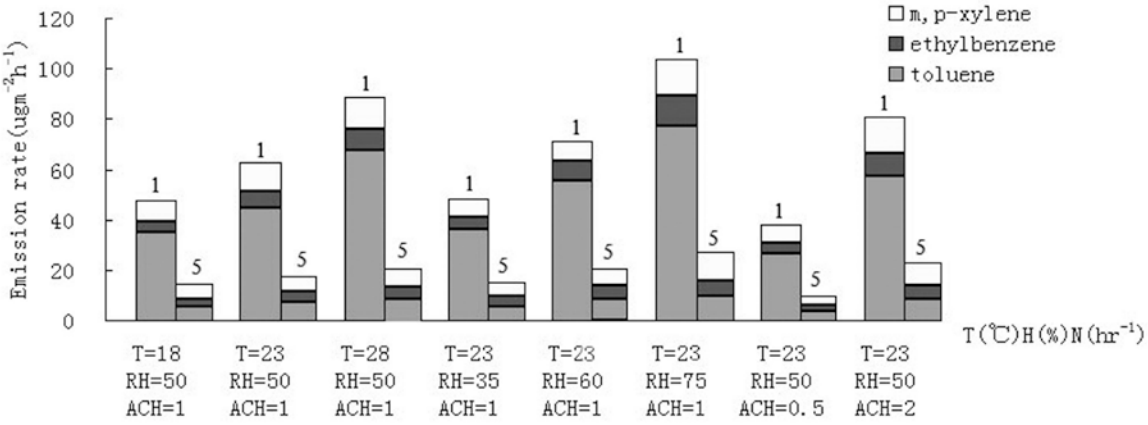

Fig. 7 Toluene, ethylbenzene and m,p-xylene emission rate on the first day and the fifth day

Toluene, ethylbenzene, and m,p-xylene were the main individual compounds of VOC emissions from the tested plywood. As shown in Fig. 7, the toluene emission rate was the highest, ethylbenzene was the second, and m,p-xylene was the lowest. The emission rates of ethylbenzene and m,p-xylene did not have a significant difference as both were lower than the emission rate of toluene. On the first day, the emission rates of the three compounds had the biggest difference in eight environmental conditions. With the emission of VOC, the emission rates of these three compounds had no significant difference. The emission properties of the three compounds were different. The toluene emission rate was higher for the initial emission than that for the later emission. The ethylbenzene and m,p-xylene emission rates were stable during the emission process. The effect of environmental factors on toluene, ethylbenzene, and m,p-xylene was more significant during the initial than the later emissions. The effects of the environmental factors did not differ significantly among these three compounds.

Conclusion

This study investigated the impact of RH, temperature, and ACH on VOC emission rates and concentrations from plywood using small chamber testing for five days. The VOC emission properties in different environmental conditions were analyzed.

With increasing temperature, RH, and ACH, the VOC emissions from plywood accelerated. The influence of environmental factors on VOC emissions was only significant during the initial emission. Arene compounds were the main compounds of TVOC emissions from plywood, and alkane compounds were the second. The influence of temperature, RH, and ACH on arene compounds was more significant than that on alkane compounds. The main VOCs emitted from plywood were toluene, ethylbenzene, and m,p-xylene. Toluene emission rate was the highest, m,p-xylene was the second, and

the ethylbenzene was the third. The effect of environmental factors on three individual VOCs had no major difference.

Acknowledgment

This research is supported by National Nature Research Fund Project (31070488), and Special Research Fund Project for Science and Technology Innovation Talent From Harbin Technology Division (2010RFXXS023).

References

Liu Yu. Control Technology and Comprehensive Evaluation of VOC Emissions from Particleboards. Northeast Forestry University 2010.

Zhang Wenchao. Research in Characteristics of VOC Release from Interior Overlaid Particleboard. Northeast Forestry University 2011.

Ki-Wook Kim, Sumin Kim, Hyun-Joong Kima, Jin Chul Park. Formaldehyde and TVOC emission behaviors according to finishing treatment with surface materials using 20 L chamber and FLEC. Journal of Hazardous Materials 2010; 177: 90–94.

L. Fang, G. Clausen, P. O. Fanger. Impact of Temperature and Humidity on Chemical and Sensory Emissions from Building Materials. Indoor Air 1999; 9: 193-201.

Wolkoff P. Impact of air velocity, temperature, humidity and air on long-term VOC emissions from building products. Atmospheric Environment 1998; 2659-2668.

Technical requirement for environmental labeling products- Wood based panels and finishing products. HJ 571-2010. 2010

Reid, R. C., Prausnitz. The Properties of Gases & Liquids. 1987.

Chi-Chi Lin, Kuo-Pin Yu, Ping Zhao, Grace Whei-May Lee. Evaluation of impact factors on VOC emissions and concentrations from wooden flooring based on chamber tests. Building and Environment 2009; 525-533.

Assessment of Carbon Emission and Balance from Hardwood Lumber Processing in Central Appalachia, USA

Wenshu Lin [1] *– Jingxin Wang*[2*] *– Pradip Saud*[3]

[1] Lecturer, College of Engineering and Technology, Northeast Forestry University, Harbin, China.
wenshu2009@gmail.com
[2] Professor, Division of Forestry and Natural Resources, West Virginia University, Morgantown WV, USA.
* *Corresponding author*
jxwang@wvu.edu
[3] Graduate Research Assistant, Division of Forestry and Natural Resources, West Virginia University, Morgantown WV, USA.
pradipsaud@yahoo.com

Abstract

This study assessed credit carbon emission and carbon balance from lumber processing of different size sawmills and its effect on the potential carbon offsetting capacity through wood product useful life. Data were obtained from a regional sawmill survey, public database and relevant publications. Credit carbon balance was statistically analyzed within the gate to gate life cycle inventory framework. Stochastic simulation of carbon emission and its impact on carbon balance and carbon flux from the lumber processing was carried out under different operational scenarios. The results showed that credit carbon balance from electricity consumption was significantly different among sawmills with different production levels and operation hours per week. Variation in carbon emission was also recognized due to different head saws, lighting types, and air compressors used at sawmills. Generated credit carbon balance in significant amount from energy consumption reduced carbon accountability of the lumber in useful life period at first order of decay of carbon. This credit carbon balance would also affect carbon disposition pattern in hardwood sawlogs. Substantial carbon flux occurred due to greater amount of energy consumption and exports of lumber would also reduce carbon accountability of lumber production. Carbon storage accountability of hardwood lumber and carbon flux during processing could be improved by using efficient equipment at sawmill and as well as appropriate mixture of electricity sources.

***Keywords*:** A. Carbon balance, B. Life cycle inventory, C. Sensitivity analysis, D. Energy consumption.

Introduction

Carbon (C) stocks of wood products are important in evaluating their potentials in greenhouse gas (GHG) mitigation (Brown et al. 1998, IPCC 2003). Carbon tracking in wood products requires knowledge of life cycle for realistic estimation and statistical representation of potential carbon contained in wood. Most estimates of C stocks and stock changes are based on indirect estimation models using hypothetical parameters (Harmon et al. 1994, Apps et al. 1999). One of the approaches to estimate C pools in wood products is accounting the amount of carbon expected to be stored in wood products and in landfills at the end of a 100-year period (Skog et al. 2004, Smith et al. 2006, Birdsey 2006). Estimation of C in wood products can start from the quantity of roundwood that is harvested, removed from the forest and available to primary processing for wood products in the mills (Birdsey 2006). Carbon emission estimation of wood products during their life time is affected by the decay rate and fraction of carbon allocated to long-lived products (Dias et al. 2005, Smith et al. 2006).

Lumber manufacturing involves different stage and different type of mechanical equipment that consume different energy sources. Mechanical equipment such as head saw and air compressors and sawmill management strategies such as production capacity and lighting bulbs, could have potential variation in carbon emission level from energy consumption. This type of variation in carbon emission "credit carbon" was overlooked in the previous studies of life cycle inventory (LCI) of wood product processing. Such carbon emission is also disregarded while accounting the carbon stored by the produced wood product in its useful life period. Therefore, it seems necessary to assess the carbon balance of hardwood lumber processing within the gate to gate life cycle inventory framework. The objectives of this study were to: (1) assess the carbon balance variation from energy consumption during hardwood lumber processing and (2) examine the effect of credit carbon in the carbon accountability of the product in its useful life period.

Methods

Methodological framework and system boundary. The debit and credit balance accounting principle was used to account carbon emission as greenhouse gas emission irrespective of other gaseous emission. The process of carbon storage begins with the green hardwood logs at log yard of sawmills and ends with the final product of planed dried sawn lumber within gate to gate life cycle inventory framework. The system boundary and the process unit were defined as described by the National Renewable Energy Laboratory Life Cycle Inventory (NREL 2010) database that covers the processing of green hardwood logs at sawmill, kiln drying of rough sawn hardwood lumber and planning of kiln dried sawn lumber. Data on lumber production, mill residue, energy consumption and energy efficiency practices in the Appalachian sawmills were obtained from a mail survey in 2010.

Carbon emission from energy sources. Carbon emission (Mg/TCM) from electricity consumption (MJ/TCM) was estimated using an average emission factor for mixed energy sources reported by the US Environment Protection Agency (USEPA 2010) on

emission and generation resource integrated database (eGrid) for the regions of RFC WEST (WV & OH), RFC EAST (PA) and NYUP (NY) in 2004, 2005, and 2007. Carbon emission from the mixed energy sources such as fossil fuel, coal, oil and gas was assumed as an average of 0.17 kg/MJ (USEPA 2010). Carbon generated from energy sources, such as natural gas, propane, fuel #1, fuel #4 and fuel #6 was estimated using the national average of carbon dioxide coefficient reported by USEIA (2011). Similarly, carbon from diesel and motor gasoline was estimated based on emission facts by USEPA (2005). Energy gained from wood source was excluded assuming that it was substituted by residue generated from lumber processing at sawmill and to avoid double quantification of carbon stock. Other related carbon emission from electricity consumption (*EC*) from offsite generation and onsite generation and all energy sources (*ES*) used in lumber processing was based on a report CORRIM (Bergman and Bowe 2008).

Carbon emissions (Mg/TCM) from electricity consumption in lumber processing of difference size sawmill were simulated using known variance (normal likelihood) and assuming conjugate normal prior mean for 1000 times to examine the uncertainty of carbon emissions through Markov-chain Monte Carlo (MCMC pack) simulation in R. Scenario analysis of carbon emission from electricity source in eGRid sub region was carried out assuming coal, gas, oil and other fossil fuel are major source of electricity generation. The electricity generation share percentage of these four energy sources were proportioned to the total electricity required for the hardwood lumber processing.

Carbon in lumber and mill residue. Wood loss occurred during lumber processing was accounted as a percentage of carbon loss from green log volume at sawmill yard. An average of 296 kg of carbon was contained in one cubic meter of logs for the central Appalachian mixed hardwood species (Saud 2011). A similar value of 307kg/m^3 was used for carbon in per unit of roundwood in the northeast region (Skog and Nicholson 1998). In hardwood lumber processing, volume shrinkage changed from 1.46 m^3 of green lumber to 1.37 m^3 of dried lumber (Bergman and Bowe 2008). Therefore, we assumed 315kg/m^3 carbon contained in per unit volume of planed dried lumber (Saud 2011, Bergman and Bowe 2008). Mill residues such as chips and sawdust reported in green tons were assumed to contain 50% moisture, and were then converted to dry tons (Siau 1984). Carbon content of mill residue was assumed to be similar to hardwood logs with mixed species (296 kg/m^3). Carbon emission from residue was termed as carbon emission with and without energy capture. Emitted with energy capture refers to carbon emission from wood in relation to energy generation and emitted without energy capture refers to carbon emission through combustion or decay without concomitant energy recapture.

Analysis of impact of carbon emission ($C_{emission}$) from electricity at sawmills and from other energy sources on the fraction of carbon (*j*) in lumber ($FC_{lum_{i,j}}$) from lumber production year (*i*) to over its useful life period of 100 years (*n*) was conducted. For this carbon pay off period (*PP*) (Eq. 1) was estimated, the pay off period starts at the time when the amount of carbon emitted/credit carbon balance from lumber processing equivalent to the fraction of carbon remained in lumber at year *i*. This payoff period was estimated under half-life scenario at first order of decay rate of carbon and the carbon

disposition rate based on hardwood lumber and industrial roundwood in the northeast region respectively (Smith et al. 2006). In the first year of lumber production year, i equal to 1 and j equals to zero because the fraction of carbon loss from produced lumber is zero (Smith et al. 2006). Similarly, carbon emission from an average of all energy consumption at sawmills was analyzed for the carbon disposition pattern in sawlogs for *n*-years period.

Carbon flux from lumber processing was also analyzed considering the carbon emission from energy consumption, export of lumber and carbon loss from mill residues at sawmill. Four different scenarios of carbon flux (*CF*) from energy ($CE_{enerery}$), export of lumber (CF_{export}) and lumber production FC_{lum}, for 100-year period (*n*) were analyzed. Cumulative carbon balance in lumber (CCB_{lumber}) (Eq. 2), cumulative carbon emission from energy (CCE_{energy}) (Eq. 3), cumulative carbon flux from export (CCF_{export}) (Eq. 4) were used to estimate cumulative carbon flux ratio (*CCFR*) (Eq. 5). The base case includes carbon flux from average energy consumption at sawmill and average export of the lumber from sawmill. Other scenario cases of carbon flux were (1) from export and all energy source consumption (2) from export and 25% reduction in carbon emission or in all energy source consumption, and (3) export and 50% reduction in carbon emission or all energy source consumption.

$$PP = C_{emission} = \sum_{i=1,\, j=0}^{n=100} FC_{lum_{i,\,j}} \tag{1}$$

$$CCB_{lumber} = \sum_{i=1,\, j=0}^{n=100} (FC_{lum_{i,\,j+n}} + FC_{lum_{i+1,\,j+n}} + \cdots\cdots\cdots + FC_{lum_{i+n,\,j+n}}) \tag{2}$$

$$CCE_{energy} = \sum_{i=1}^{n=100} CE_{energy_i} \tag{3}$$

$$CCF_{export} = \sum_{i=1}^{n=100} CF_{export_i} \tag{4}$$

$$CCFR = \frac{CCF_{export} + CCE_{energy}}{CCB_{lumber}} \tag{5}$$

Where, *PP* means carbon pay off period, $C_{emission}$ means carbon emission, $FC_{lum_{i,\,j}}$ means the fraction of carbon (*j*) in lumber from lumber production year (*i*); CCB_{lumber} means the cumulative carbon balance in lumber, *CF* means carbon flux, $CE_{enerery}$ means carbon flux from energy, means carbon flux from export of lumber, FC_{lum} carbon flux from lumber production; CCE_{energy} means cumulative carbon emission from energy, CE_{energy_i} means carbon flux from energy emission in year i; CCF_{export} means cumulative carbon flux from lumber export, CF_{export_i} means carbon flux from lumber export in year i; *CCFR* means cumulative carbon flux ratio.

Results and Discussion

Carbon emission from electricity consumption. Sawmills were operated with an average of 35, 40, 43 hours per week with one shift in small sawmills (SSM), medium sawmills (MSM) and large sawmills (LSM), respectively. Similarly, yearly operation weeks averaged 48 for SSM and 50 weeks for both MSM and LSM. The electricity consumption rate was different among sawmills with different production capacity (Table 1). The mean carbon emission from electricity consumption was 23.96, 11.03 and 0.87 Mg/month for LSM, MSM, and SSM, respectively. Therefore, carbon emission from lumber processing was 9.01, 17.51, and 9.40 Mg/TCM in LSM, MSM, and SSM, respectively. The lower carbon emission in LSM might attribute of the higher lumber production level with the use of efficient electric motor in the larger sawmills. Significant difference existed in carbon emission from electricity ($p=0.0047$, $F=6.6928$), among operating hours per week ($p=0.004523$, $F = 6.2198$), and among lumber production levels per week ($p=0.0001$, $F=125.44$) of different sawmills.

Table 1. *Descriptive statistics of lumber production and electricity consumption.*

Sawmill type	Lumber production (m^3/month)			Electricity (MJ/month)		
	Mean	Min	Max	Mean	Min	Max
SSM	152.16	4.72	377.56	18,943	1,800	79,200
MSM	822.29	424.75	1,415.84	318,337	5,796	1,025,640
LSM	2,624.03	2,123.76	3,539.61	584,431	400,000	1,168,358

Carbon emission and energy capture. To produce 1000 m^3 of lumber, a total of 2290 m^3 of green roundwood is required and almost 64% of the volume is turned into wood residues (NREL 2010, Bergman and Bowe 2008). From survey result, approximately, 316.5 out of 680.13 metric tons of wood carbon is deposited in major mill/wood residues such as sawdust, chips and slabs during lumber processing. Few sawmills produced slabs in each sawmill size group. An average of 637.5, 422.50, and 383.22 green Mg/TCM of chips and an average of 220.86, 262.50, and 232.71 green Mg/TCM of saw dust were generated in SSM, MSM, and LSM. It corresponds to an average of 212.5, 140.8, and 127.7 Mg/TCM of carbon from chips and 73.5, 87.5, and 77.6 Mg/TCM of carbon form sawdust in SSM, MSM, and LSM. Thus, an average of 286, 228.3, and 205.3 Mg/TCM of carbon were emitted with and without energy capture correspondingly from SSM, MSM, and LSM in the form of wood residue, respectively.

Onsite carbon emission due to energy capture was greater from the combustion of chips than sawdust (Fig. 1). Chips recaptured greater amount of carbon at sawmills when it was used either for heating or fueling purpose such as 91.1 Mg/TCM at SSM and 71 Mg/TCM at LSM, while carbon emission from sawdust was 18.4 Mg/TCM at SSM and 13.68 Mg/TCM at LSM, respectively. This recaptured carbon as energy source released into the atmosphere at year zero of the lumber production. In the study area, timber product output data of 2001 and 2006 showed that an average 92% of carbon is emitted from mill residue as energy source (USDA FS 2010). In addition, such energy captures could account to supply 1.5% of the total energy consumption in U.S. (Perlack et al. 2005).

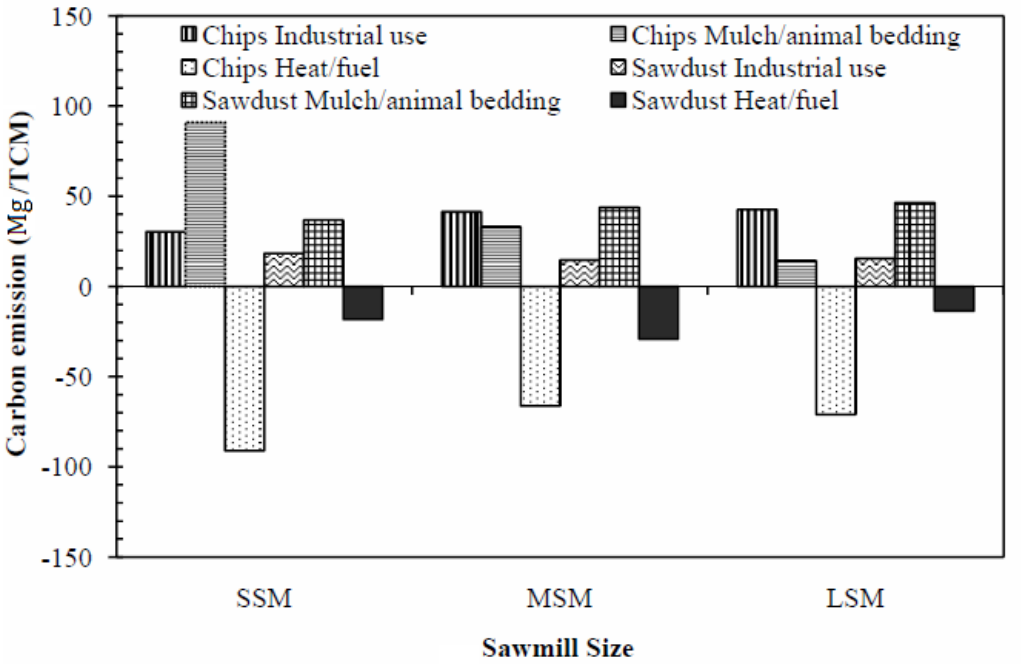

Figure 1. Carbon emissions with and without energy capture process from sawmill.

Industrial use of chips and sawdust was another source of carbon emission from energy capture process. Carbon emission from chips was greater in LSM and MSM while it was greater in SSM and LSM from sawdust. They were utilized either to generate heat or produce different short lived wood products, i.e. pulp and paper, pallets and barn that could lengthen carbon emission period. Carbon emission without energy captured from chips was significantly greater in SSM (91.1 Mg/TCM) and it was greater in LSM (46.54 Mg/TCM) from sawdust. Such carbon emission from the use of residue either for mulching purpose on the farm or for animal bedding lagged the carbon release time into the atmosphere than used for heat/fuel. This type of carbon emission, without energy capture, accounts for 8% of the total carbon from mill residues (USDA FS 2010). Mill residues used for industrial purpose or farm purpose would be supportive to lengthen wood carbon life and increase carbon stock, as wood product with short life does.

Energy efficient equipment. It was found based on our survey that MSM (13.9%) and LSM (8.3%) had upgraded efficient techniques to increase avoided carbon emission per unit of lumber production, but SSM didn't. However, every sawmill group had normally used efficient electric motor and had achieved usually 80-90% efficiency level (Table 2). The efficiency level was related to the use of different efficient techniques such as head saw, lighting bulb and air compressor. Sawing of logs was carried out from the use of head saw such as band (38.1%), circular saw (45.22%) and both saws (16.7%). Lighting used in sawmills varied from fluorescent bulb (53.8%), incandescent bulbs (17.9%) and both bulbs (28.2%). Similarly, sawmills used conventional air compressor (45.7%) and/or high efficiency screw drive air compressor (45.7%) and both compressors (8.6%).

Table 2. *Descriptive statistics of the efficient technique utilization in sawmill types.*

Efficient Techniques	SSM	MSM	LSM	Total
Upgraded for energy efficient	0.0%	13.9%	8.3%	22.2%
Efficient electric motor utilization	12.2%	36.6%	22.0%	70.80%
Efficiency level				
80-90%	13.6%	27.3%	9.1%	50.0%
91-94%	4.5%	13.6%	18.2%	36.4%
>94%	4.5%	4.5%	4.5%	13.6%

Carbon balance in lumber production. The credit carbon balance accounts for 2.9, 5.5, and 2.8% of the net debit carbon balance of lumber (316.5 Mg/TCM) at the zero year of lumber production in the SSM, MSM, and LSM, respectively. Effect of this credit carbon balance was not significant in the net debit carbon balance of lumber under half-life scenario up to 100 years (Fig. 2a). However, net debit carbon balance could be affected after the useful life period of 100 years, i.e. at beginning of the time period, and lumber would be discarded from their use purpose and disposed at landfills. The low credit carbon balance could be attributed to low electricity consumption by sawmills and it could be higher when other fossil fuels were consumed.

Estimated total carbon emission from electricity consumption (*EC*) was 28.5 Mg/TCM and it accounts for 9% of the carbon stored in the processed lumber. In 100 years of useful life period, it bisects at year 79 and becomes equivalent to the amount of carbon remained in lumber at first order of decay rate (Fig. 2b). The payoff period (*PP*) begins after year 79 and it reduced the carbon accountability period of lumber in its useful life by 21%. In addition, 35.91 Mg/TCM of credit carbon balance generated from all energy sources (*ES*) accounted for 11.35% of the carbon balance in lumber. It bisects at year 67 and shortens carbon accountable period of the lumber almost by 33% (Fig. 2b). Hence, carbon emitted from lumber after the bisected point year would be equivalent to the amount of carbon debt created by credit carbon balance from lumber processing. The higher the debt carbon balance is, the early *PP* and consequently lower the carbon accountability in useful life period of the lumber would be. This *PP* would vary depending on the hardwood tree species used for lumber processing because the carbon content value among tree species differs.

Lumber processing of 1000 m^3 sawlogs contains an average of 680 metric tons of carbon. This carbon disposition pattern of sawlogs was significantly affected by the generated credit carbon balance. An average credit carbon balance generated from all energy sources in lumber processing at sawmills only affected the carbon disposition pattern of sawlogs in landfills (Fig. 2c). The generated carbon credit balance from only *EC* affected the period of carbon disposition pattern of sawlogs and the *PP* begins for fraction of carbon in use either at later 11 years or for fraction of carbon in landfills at first 3 years (Fig. 2d).

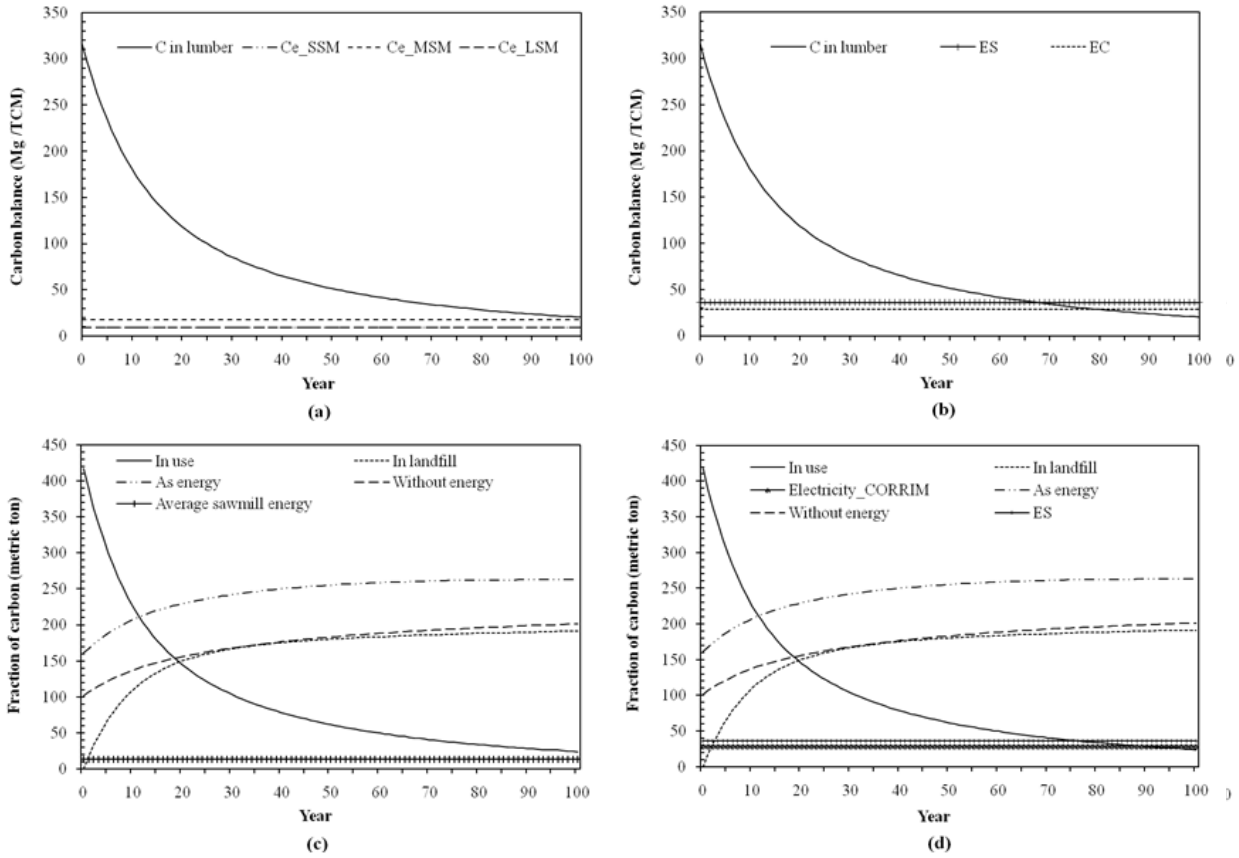

Figure 2. Effect of credit carbon balance in carbon balance of lumber and fraction of carbon disposition in sawlogs at 100 years period: (a) and (b) carbon balance by carbon emission level and energy consumption, (c) average sawmill energy consumption, and (d) electricity consumption (*EC*) all energy sources (*ES*).

Carbon flux from lumber processing. More carbon was emitted in the lumber processing mainly from the generated mill residues. Carbon flux from mill residues was 96.56 Mg/TCM as energy capture, 55.3 Mg/TCM as industrial use, 88.51 Mg/TCM as farm manure, and 123.8 Mg/TCM as others. The use and no use of mill residues increases the atmospheric carbon level from zero year of lumber production to 5 years depending on what purposes they are used for (Karjalainen et al. 2002, Skog 2008, Sharma 2010). Carbon flux was also instigated by export of the lumber. An average of 6.7% of lumber produced was exported and it reduced carbon stock of lumber production and place to 93.3% of available accountable wood carbon stock in the region.

The consequence of cumulative carbon emission from energy sources was observed in the cumulative carbon balance at the first order of carbon decay in the lumber production cycle of 100 years. In the base case, the CCF_{lumber} (21.1 Mg/TCM) was 57.2% higher than the cumulative carbon emission from electricity (13.1 Mg/TCM) at sawmills for 100 years of lumber production (Fig. 3a). However, the combined carbon flux from the electricity and export did not affect carbon stored in the produced lumber because the *CCFR* ranged from 0.12 to 0.42 from year zero to year 100.

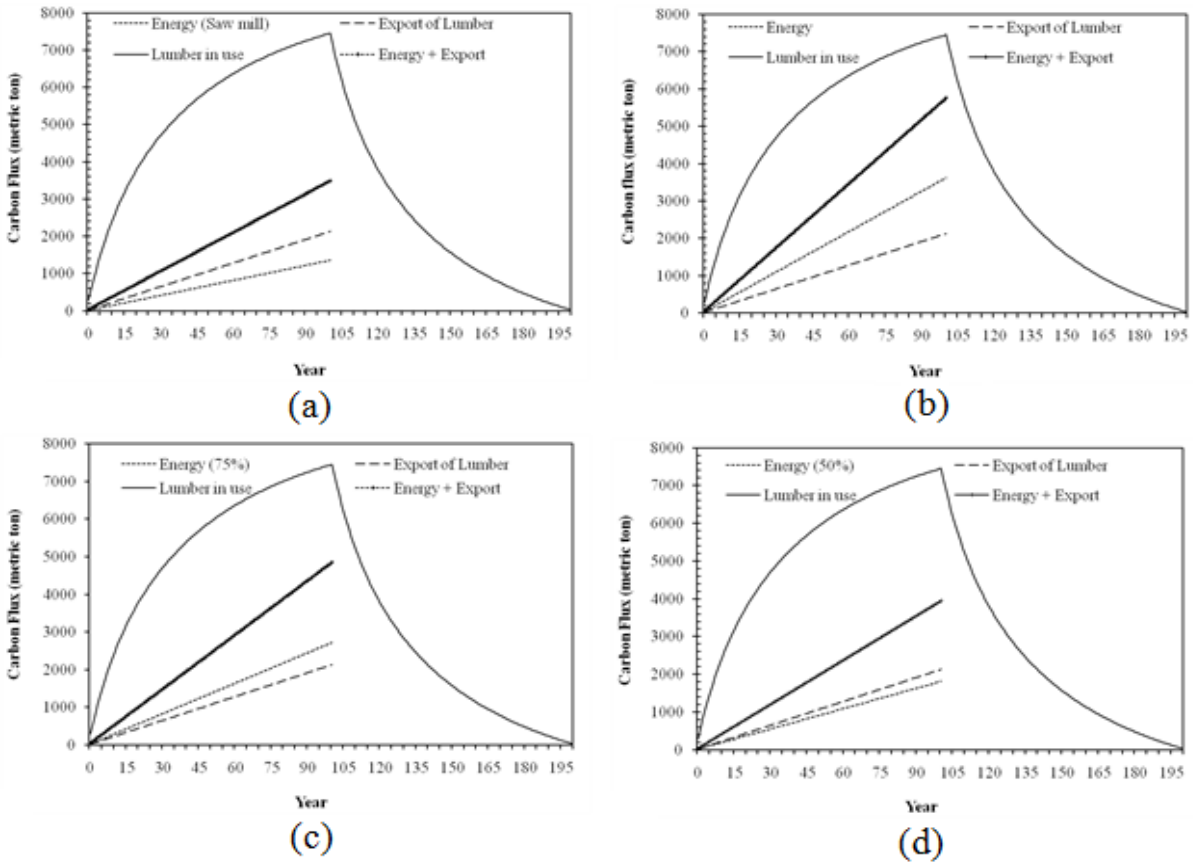

Figure 3. Atmospheric carbon fluxes from hardwood lumber processing in 100 years: (a) average electricity consumption at sawmills (b) all energy source consumption, (c) 25% reduction in all energy source consumption, and (d) 50% reduction in all energy source consumption.

The cumulative carbon emission from the total energy consumption and export of lumber could affect the cumulative carbon balance in lumber (Fig. 3b). In this case, the *CCFR* from the all CCE_{energy} energy source consumption (ES) (104.57 GJ/TCM) and CCF_{export} was 0.19 to 0.77 for the hardwood lumber production years of 0 to 100. Thus, at the end of 100 years of production period, only 23% of the CCB_{lumber} would be available to account as the net debit carbon balance. Therefore, a great amount of carbon emission would affect the CCB_{lumber} production period and it would also discount such credit carbon balance at later years of the wood product life.

When 25% of the carbon emission from all energy source consumption was reduced, the *CCFR* would range from 0.16 at zero years to 0.65 at 100 years (Fig. 3c). In this situation, 45% of the carbon in the lumber would be available to account as net CCB_{lumber} at 100 years. Similarly, if reducing 50% of carbon emission from all energy source consumption (Fig. 3d), it could have the similar effect as carbon flux created from electricity and export by sawmills.

Carbon emission under different energy sources. Since a great amount of electricity (607.2 GJ/TCM) is required for lumber processing (Bergman and Bowe 2008), it increases the atmospheric carbon level significantly. Generating such amount of electricity from natural gas would emit carbon equivalent to an average carbon emission level from the current electricity generation from the mixed energy sources in the Appalachian region. Estimated carbon emission amount was 39.2 Mg/TCM for other natural gas source, 32.8 Mg/TCM for coal source, 28.5 Mg/TCM for current mixed source, 25.6 Mg/TCM for natural gas, and 16.5 Mg/TCM for oil source (Fig. 4a). Carbon emission from single source of electricity generation such as fossil fuel would be greater followed by coal. Therefore, the electricity generated from an appropriate mixture of energy sources could help avoid certain amount of credit carbon balance. The base case represents electricity generation from the mixed energy sources in central Appalachian region, scenario 1 represents RFC WEST, and scenario 2 represents RFC EAST, and scenario 3 NYUP (Fig. 4b). The credit carbon balance was 30.9 Mg/TCM, 29.5 Mg/TCM, 27.2 Mg/TCM, and 32.8 Mg/TCM for the base case, scenario 1, scenario 2 and scenario 3, respectively.

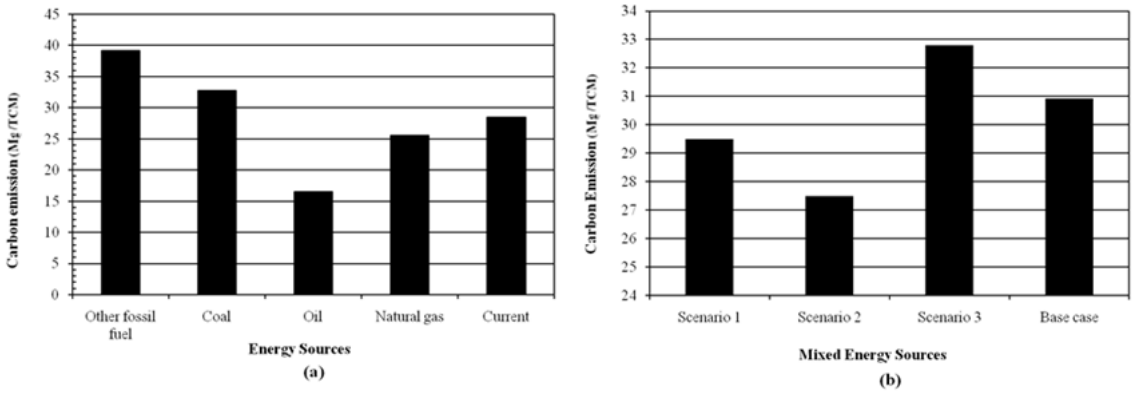

Figure 4. Carbon emissions from electricity generation during hardwood lumber processing using: (a) single energy sources and current average, and (b) mixed energy sources.

Conclusions

Carbon emission from electricity consumption during processing per unit of lumber varies depending on sawmill size. This variation would be coupled from electricity generation sources and available equipment at sawmills during processing per unit of lumber. The random mixed effect of the available equipment such as head saws types, lighting blubs types and air compressors types also influence the credit carbon balance of a sawmill. Such carbon emission could be avoided to some extent if using energy efficient motors and equipment at sawmill, which would be beneficial in abating carbon credit balance. Though carbon stored in produced lumber increases carbon stock of the wood carbon pool and magnifies humans' carbon mitigation efforts, carbon flux occurs due to significant wood loss during sawmill processing. Not all carbon loss from mill residues would be immediately recaptured as energy source and released into the atmosphere. Significant amount of mill residues would be help lengthen carbon release

time period from zero to 5 years through industrial use, or uses as mulching and farm bedding.

Carbon balance in lumber would be affected by the credit carbon generated during its processing. Carbon disposition pattern of sawlogs would also be affected greatly by this credit carbon balance. If accounted carbon emission that occurred from process of the wood product gain processing and product use such as: harvesting of timber, transportation of lumber and its uses in house construction or any other purposes, the debt carbon for lumber would attribute more. The potential measures to neutralize carbon debt could reforest the harvested area timely to pay off the carbon debt and it would also increase debit carbon balance benefit from wood. Carbon emission from electricity consumption could be minimized by using energy source that has lower carbon coefficient. Thus, appropriate mixed energy sources in the region would be helpful to minimize carbon emission from electricity consumption at sawmills. Carbon flux from export of lumber also decreases the carbon accountability of the cumulative lumber production in years. The greater the carbon flux ratio from energy and export is, the lower the carbon accountability of the produced lumber would be.

References

Apps M.J., Kurz W.A., Beukema S.J. and Bhatti J.S. 1999. Carbon budget of the Canadian forest product sector, Env. Sci. Policy. 2(1):25-41.

Bergman R.D. and Bowe S.C. 2008. Life-Cycle Inventory of Hardwood Lumber Manufacturing in the Northeast and North Central United States, CORRIM: Phase II Final Report Module C, 48p.

Birdsey R.A. 2006. Carbon accounting rules and guidelines for the United States Forest Sector. J. Environ. Qual. 35:1518-1524.

Brown S., Lim B. and Schlamadinger B. 1998. Evaluating approaches for estimating net emissions of carbon dioxide from forest harvesting and wood products. Meeting Report, IPCC/OECD/IEA Programme on National Greenhouse Gas Inventories, Dakar, Senegal, 5-7 May 1998.

Dias A.C., Louro M., Arroja L., and Capela I. 2005. The contribution of wood products to carbon sequestration in Portugal. Ann. For. Sci. 62 (8): 903-909.

Harmon M.E., Harmon J.E., Ferrell W.K. and Brooks D. 1994. Modeling carbon stores in Oregon and Washington forest products: 1900-1992. Climatic Change. 33(4):521-550.

Intergovernmental Panel on Climate Change (IPCC). 2003. Intergovernmental Panel on Climate Change Estimation, Reporting and accounting of harvested wood products – Technical Paper. UNFCCC paper. FCCC/TP/2003/7.
http://unfccc.int/resource/docs/tp/tp0307.pdf. accessed December 28, 2010.

Karjalainen T., Pussinen A., Liski J., Nabuurs G.J., Erhard M., Eggers T., Sonntag M. and Mohren F. 2002. An approach towards an estimate of the impact of forest management and climate change on the European forest sector budget: Germany as a case study. Forest Ecology and Management. 162:87-103.

National Renewable Energy Laboratory (NREL). 2010. Life cycle inventory database, http://www.nrel.gov/lci/database/, accessed December 20, 2010.

Perlack R.D., Wright L.L., Turhollow A.F., Graham R.L., Stokes B.J. and Erbach D.C. 2005. Biomass as feedstock for a bioenergy and bioproducts industry: The technical feasibility of a billion-ton annual supply. DOE/USDA Tech. Rep. DOE/GO-102005–2135. USDOE, Office of Scientific & Technical Information, Oak Ridge, TN, 78p.

Saud P. 2011. Analysis of forest carbon balance in central Appalachia region. Thesis, West Virginia University, Morgantown, WV. 91p.

Sharma B.D. 2010. Modeling of forest harvest scheduling and terrestrial carbon sequestration. Dissertation, West Virginia University, Morgantown, WV. 172p.

Siau J.F. 1984. Transport processes in wood. Springer-Verlag, NewYork. 245p.

Smith J.E., Heath L.S., Skog K.E. and Birdsey R.A. 2006. Methods for calculating forest ecosystem and harvested carbon with standard estimates for forest types of the United States. Gen. Tech. Rep. NE-343. Newtown Square, PA: U.S. Department of Agriculture, Forest Service, Northeastern Research Station. 216p.

Skog K.E., Pingoud K. and Smith J.E. 2004. A method country can use to estimate changes in carbon stored in harvested wood products and the uncertainty of such estimates. Environmental Management, 33(Suppl. 1):565-573.

Skog K.E. 2008. Sequestration of carbon in harvested wood products for the United States. Forest product journal. 58 (6):56-72.

USDA Forest Service. 2010. Timber Product Output (TPO) Reports November 04, 2010 http://srsfia2.fs.fed.us/php/tpo_2009/tpo_rpa_int2.php, accessed January 20, 2011.

US Energy Information Administration (USEIA). 2011. US Energy Information, Independent Statistics and Analysis, Voluntary reporting of greenhouse gases program fuel emission coefficients (http://www.eia.doe.gov/oiaf/1605/coefficients.html) accessed March 2, 2011.

US Environmental Protection Agency (USEPA). 2010. Environmental Protection Agency, Emissions & Generation Resource Integrated Database (eGRID) http://cfpub.epa.gov/egridweb/view.cfm, accessed December 28, 2010.

Proceedings of the 55th International Convention of Society of Wood Science and Technology
August 27-31, 2012 - Beijing, CHINA

Mild Pretreatment and Liquefaction of Cypress in Ethanol for Bio-oil Production

*Hua Min Liu[1]–Ming Fei Li[2]– Xue Fei Cao[1]–Run Cang Sun[1,2]**

[1] State Key Laboratory of Pulp and Paper Engineering, South China University of Technology, Guangzhou 510640, China
* *Corresponding author*
rcsun@scut.edu.cn
[2] The Institute of Biomass Chemistry and Technology, Beijing Forestry University, Beijing 100083, China
Rcsun3@bjfu.edu.cn

Abstract

Alkali pretreatment can decompose biomass and it is one of the most popular chemical agents because it is relatively inexpensive. In this study, cypress was pretreated with alkali and then was liquefied by sub/supercritical ethanol in a stainless steel reactor. The effect of temperature on the liquefaction of untreated and pretreated biomasses in sub- and super-critical ethanol was comparatively studied. The characteristics of pretreated and untreated cypresses were measured and compared to investigate the mechanism of the mild pretreatment and liquefaction cypress in ethanol by Thermo gravimetric analysis, Nitrogen Porosimetry, and Element analysis. Results showed that the pretreatment changed the main chemical components, physical structure and thermo-chemical character of cypress. The pretreated cypresses were less stable than the raw cypress. The mild alkali pretreatment increased surface area and pore volume of cypress, while it more effectively enhanced the bio-oil yield and decreased the temperature as compared to the untreated and stronger pretreated cypresses runs, in which the bio-oil yield increased from 15.5% to 23.5% and the optimum temperature decreased from 300 to 240 °C.

***Keywords*:** Liquefaction, Lump, Cypress; FT-IR, GC-MS.

Introduction

Among thermo-chemical conversion methods, liquefaction is the most widely used approach due to its relatively lower reaction temperature as compared to pyrolysis method (Fan et al. 2011). This can prevent the formation of char compounds owing to the cross-linking hydrocarbon and aromatics compounds (Liu et al. 2008). While approaches of converting biomass into sources of fuels are constantly improving, and are advancing towards low environmental impact, the search for high-yielding biomass with economical feasibility is also ongoing (Kreuger et al. 2011).

The physical pretreatment method generally uses mechanical comminution (including chipping, milling and griding) to make the biomass be exposed to high temperatures and this process is simple (Cadoche et al. 1989, Kumar et al. 2009). However, the higher energy consumption associated with it makes it not propitious to be implemented in a commercial scale production. Biological pretreatment method is associated with low hydrolysis rate which prolongs the pretreatment time of the process step (Harun et al. 2011). The chemicals commonly applied in the pretreatment process are either acid or alkali and the pretreatment has been successfully proven for biomass (Cheng et al. 2011, Rocha et al. 2011). The development of pretreatment approaches strong enough as to separate the cell wall arrangement and mild enough as to avoid a crucial chemical decomposing of biomass components is a challenge for today's chemical industry (Canettieri et al. 2007). For the novel pretreatment methods it is advisable to use cheap and easily recoverable chemicals and low-cost equipment. The use of environmentally friendly and low energy-intensive approaches is highly desired (Shuping et al. 2010). Alkali pretreatment can decompose biomass and it is one of the most popular chemical agents because it is relatively inexpensive.

In the previous papers (Liu et al. 2011a, Liu et al. 2011b), we first reported acid-chlorite pretreated and liquefied cornstalk in hot-compressed water and sub/supercritical ethanol for enhancing bio-oil production. The results showed that the shorter pretreatment times were more effective for enhancing the bio-oil yield and decreasing the optimum reaction temperature. In this work, the term 'mild pretreatment and liquefaction (MPL)' instead of 'liquefaction' was used to describe the thermo-chemical conversion of biomass, because the objective of this technology was to enhance the bio-oil yield and decrease the temperature in solvents liquefaction. However, the investigations can not evaluate systematically the chemical and physical characterization of biomass by pretreatment to study the mechanism of the MPL cypress in the present of ethanol.

In this study, cypress was pretreated with alkali and then was liquefied by sub/supercritical ethanol. The effect of temperature on the liquefaction of untreated and pretreated biomasses in ethanol was comparatively studied. The characteristics of pretreated and untreated cypresses were measured and compared to investigate the mechanism of the MPL cypress in ethanol by Thermo gravimetric analysis, Nitrogen Porosimetry, and Element analysis.

Materials and Methods

Materials. The cypress sample was collected from the city of Xuchang, Henan province in China. The feedstock was ground using a high-speed rotary cutting mill firstly, and then

sieved though 40 mesh. The cypress flour was extracted with water and ethanol to remove water-soluble compounds and polar organics, receptively, then dried at 105 °C for 24 h and kept in a desiccator at room temperature before used. The ash of cypress was determined by burning at 650 °C for 6 h.

Analysis. The element composition of solid residue was analyzed by CHNO Elemental Analyzer Vario EL (ELEMENTAR, Germany). The composition of oxygen (O) was estimated by difference. The higher heating values were obtained from calculation by Dulong's formula.

$$HHV(MJ/Kg) = 0.3383 \times C + 1.442 \times (H - O/8) \quad (1)$$

Where *C*, *H* and *O* are the weight percentages of carbon, hydrogen and oxygen, respectively.

Thermal analysis of the untreated and pretreated cypresses were carried out by thermo-gravimetric (TG) and differential thermo-gravimetric (DTG) analysis on a simultaneous thermal analyzer (SDT Q600, TA Instrument, Selb, Germany). The samples were weighed between 4 and 8 mg and the scans were carried out from room temperature to 600 °C at a rate of 10 °C per minute under nitrogen flow.Nitrogen Porosimetry (Micromeritics ASAP 2010, USA) was used to measure the surface area and pore volume of the cypress before and after pretreatment. The surface area was calculated using the Brunauer-Emmett-Teller (BET) model, and the pore volume was calculated using the Barrett-Joyner-Halenda (BJH) method.

Apparatus and experimental procedure. For the alkaline pretreatment, cypress (150.0 g) was incubated with 5% (w/v) NaOH at a solid-to-liquid ratio of 1: 6 (w/v) at 90 °C for 0.5 h, 1 h and 2 h, respectively. The pretreated materials were filtered through double layered muslin cloth and then washed extensively with water until neutral pH. To calculate its dried weight, the pretreated cypresses were dried at 105 °C for 24 h. The liquefaction experiments were carried out in a 1000 ml stainless steel reactor (Parr, USA) and the reactor can be worked at a maximum temperature of 350 °C and maximum pressure of 13 MPa. In a typical run, 10 g cypress powder and 100 ml ethanol were charged into the reactor. The air inside the autoclave was purged by nitrogen gas. Agitation was set at 150 rpm and kept constant for all tests. When the reactor was heated up to the setting temperature, the reactor was cooled down to room temperature by means of cooling coils, which was installed inside of the reactor. Briefly, the gas was removed from the autoclave after the reactor was cooled to room temperature and then the autoclave was opened. The solid and liquid mixture was removed from the autoclave for separation. After that, water and acetone were removed in a rotary evaporator and the corresponding fraction was weighed and designated as water-soluble oil (WSO) and heavy oil (HO). Solid residue was defined as the acetone insoluble fraction.All the experimental data were calculated on a dry-ash-free basis. Each test was performed twice and the reproducibility of the experimental data was shown to be within ± 6%.

Results and discussion

Elemental analysis of untreated and pretreated cypresses. The elemental composition of biomass is a key factor affecting efficiency of bio-oil production during conversion processes. Table 1 shows the elemental analysis of the untreated and pretreated cypresses. After alkali pretreatment, the C content of the cypress decreased, and the O content increased. The higher heating value (HHV) of the raw cypress was higher than that of the pretreated cypresses

because of the removal of the C content and the increasing of O content. In fact, the HHV of biomass represented the HHV mainly from lignin and partially from cellulose and hemicelluloses (Shi and He 2008). As reported in the paper that holocellulose (cellulose and hemicelluloses) had a HHV of 18.6 MJ/Kg, whereas lignin had the HHV of 23.26-26.58 MJ/Kg. Therefore, for production higher HHV of bio-oil, mild pretreatment would be favorable for liquefaction of cypress.

Table 1 Elemental analysis of untreated and pretreated cypresses.

Samples	Elemental components (wt %)				O/C	H/C	HHV (MJ/Kg)
	C	H	N	O			
Cypress	48.9	6.0	0.3	44.8	0.92	0.12	17.1
0.5 h	47.7	5.8	< 0.3	46.2	0.97	0.12	16.2
1 h	46.6	6.0	< 0.3	47.1	1.0	0.13	15.9
2 h	45.3	6.1	< 0.3	48.3	1.1	0.13	15.4

Thermo gravimetric analysis of untreated and pretreated cypresses. Thermogravimetric tests in inert nitrogen were achieved to evaluate the effect of alkali pretreatment on the pyrolytic behaviour of the cypress. The results obtained from the typical thermogravimetry and differential thermogravimetric curves of the untreated and pretreated cypresses are shown in Figure 1. The TG of the untreated and pretreated cypresses shows a two-step weight loss curve. The first one occurred between 50 °C and 100 °C and corresponded to the loss of water naturally trapped into the samples structure. This water represented about 3% of the samples initial weight, and the mainly weight loss of the samples occurred in the range 200 °C to 360 °C. Above 360 °C, an abrupt change in the slope of the TGA occurred leading to a slower weight loss in the temperature range 360 °C to 600 °C. In addition, as can be observed, the weight loss was 50.0% when the temperatures reached 345 °C (raw cypress), 335 °C (0.5 h), 338 °C (1 h) and 336 °C (2 h) for untreated cypress and pretreated cypresses. In the DTG curves, the exothermic peaks of the untreated and pretreated cypresses occurred around 354 °C (raw cypress), 339 °C (0.5 h), 342 °C (1 h), and 344 °C (2 h), respectively. These results indicated that the pretreated cypresses were less stable than the raw cypress. Therefore, the alkali pretreatment favored the thermal decomposition of cypress.

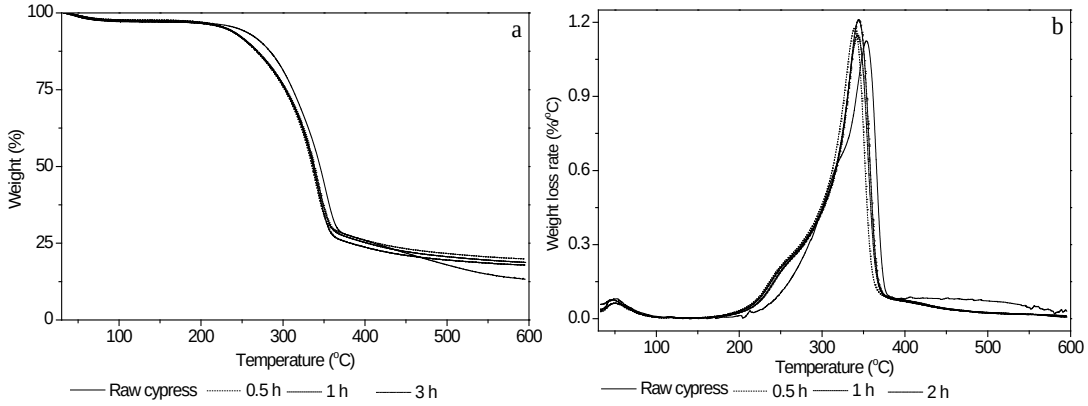

Figure 1. TG and DTG curves of the untreated and pretreated cypresses at 10 °C/min in nitrogen atmosphere.

Surface area and pore volume of cypresses before and after pretreatment. Nitrogen

porosimetry has been employed for the skin porous structure of cypresses before and after pretreatment. Figure 2 shows the adsorption isotherms for cypresses at three pretreatment times with untreated sample. The difference among the untreated cypress and the cypresses treated at 0.5 and 1 h is dramatic noticeable. Figure 2 shows a significant increase in the quantity of gas absorbed for the cypresses treated at 0.5 and 1 h, indicating a greater pore volume and a higher specific surface area. The results of surface area and pore volume are shown in Figure 2. Clearly, the shorter pretreatment times (0.5 and 1 h) resulted in bigger surface area and pore volume of cypress. For example, the surface area and pore volume of the pretreated cypress at 1 h increased by about 24.3% and 38.5%, respectively, as compared to the untreated sample. In addition, a reduction in surface area and pore volume of the pretreated cypress at 2 h also observed in Figure 2. This was mainly due to the degradation of micropores during the longer time alkali pretreatment process. Bigger surface area and pore volume could enhance the reaction rate of liquefaction process; therefore, the shorter pretreatment time was more favorable.

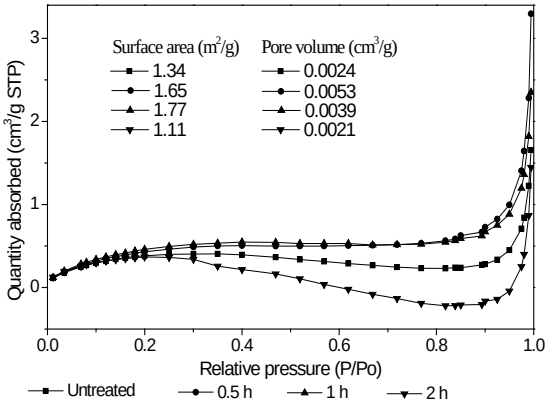

Figure 2. Nitrogen sorption isotherms for cypresses before and after pretreatment.

Liquefaction yields. The bio-oil yields from the liquefaction of the four samples at different final temperatures are shown in Figure 3. Obviously, as the temperature increased from 180 °C to 300 °C, the total conversion rate (100% - yield of solid residue) increased continually regardless of the untreated and pretreated cypresses liquefaction runs. It was worthy noting that all pretreatments increased the total conversion rate over the whole range of the temperatures tested as compared to the liquefaction of the untreated cypress. This might be due to the changes of the structure and chemical components, which made it easy for the liquefaction reagent to enter into the cypress. The increased in the total conversion rate with increasing temperature could either be owing to greater primarily decomposition of the cypresses at higher temperatures or via secondary decomposition of the solid residue.

As can be seen in Figure 3 (c), when the liquefaction temperature was increased from 180 °C to 300 °C the bio-oil obtained from raw cypress liquefaction showed an increase in the range 2.5% to 15.5 %. Comparatively, the pretreated cypresses conversion showed higher bio-oil yields and lower conversion temperatures as compared to that of the untreated cypress liquefaction run. The higher bio-oil yields obtained from the pretreated cypresses liquefaction were 20.0% (0.5 h), 23.4% (1 h) and 19.6% (2 h) at the reaction temperature of 240 °C, respectively. However, as the temperature was increased further, the bio-oil yields were decreased with the increase in temperature. Higher temperature was not usually suitable for production of liquid bio-oil. In general, there were two reasons for this result. Firstly the

secondary degradations reaction became active at higher temperatures, which led to the formation of gases (El-Rub et al. 2004). Secondly, the recombination of free radical reactions led to the tar formation due to their high amounts (Akhtar et al. 2011). These two mechanisms became dominant at higher temperatures, which reduced the production of bio-oil from cypress. As compared to the stronger pretreatment, the mild pretreatment were sufficient for the cypress form oily compounds, giving the higher bio-oil yields (23.4% and 20.0%). The higher temperature and stronger pretreatment resulted in a lower bio-oil yield and pretreatment yield, lower reaction temperature and mild pretreatment were more favorable. Therefore, operation the reactor system at the lower temperature and mild pretreatment were preferred because the bio-oil yield and pretreatment yield would be higher, and heat loss per unit mass of bio-oil produced was significantly lower, making the process more economical feasibility.

WSO mainly consisted of simple organic acids, furfural, sugars, etc., which are primarily formed from the conversion of holocelluloses through hydrolysis and de-polymerization reactions (Behreddt 2008, Xu et al. 2008). However, the HO primarily composed of phenolic compounds and phenols, results from the decomposition of lignin or from the dehydration of intermediate products derived from cellulose and hemicelluloses (Behreddt 2008, Xu et al. 2008). In addition, owing to various bio-oil formation temperatures for the different chemical components of biomass (i.e., cellulose, hemicelluloses and lignin), the optimum temperature for WSO and HO yields may depend on the relative abundance of chemical components in the raw material. Figure 3 (a) and (b) showed the effect of temperature on the WSO and HO yields obtained from untreated and pretreated cypresses liquefaction. Regardless of all the pretreated cypresses liquefaction runs, the WSO yields showed an identical trend, increasing after 180 °C, with a peak at 240 °C before decreasing. Possible reason to account for the level-off of the WSO yields at the higher temperatures would be cracking of the WSO products to HO. At the reaction temperature of 300 °C the HO yields obtained from raw cypress and stronger pretreated cypress liquefaction reached maximum of 10.2% and 10.4%, respectively. As compared with the untreated and stronger pretreated cypresses, the mild pretreated cypress liquefaction produced more HOs at the lower temperatures. For example, the maximum HO yields were 9.8% and 11.1% when the reaction temperature reached to 240 °C and 280 °C, respectively. This might be due to that the more lignin a biomass contains, the higher the reaction temperature should be (Yin et al. 2010).

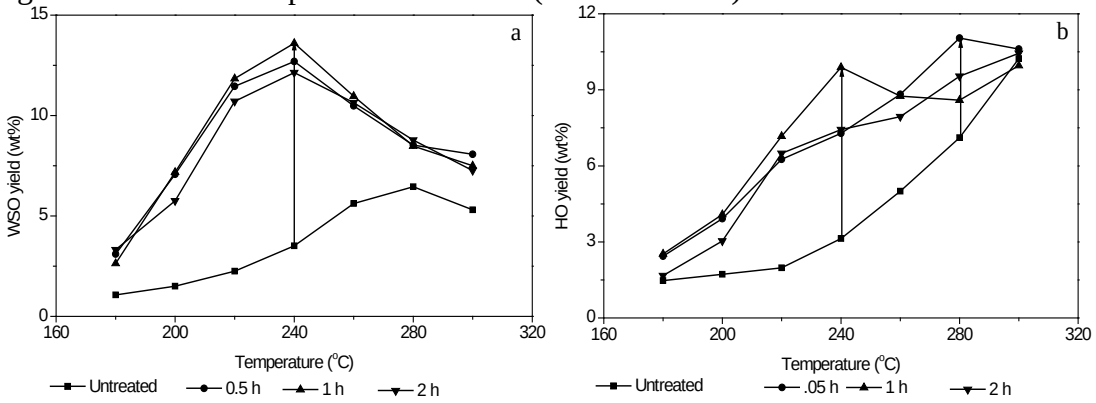

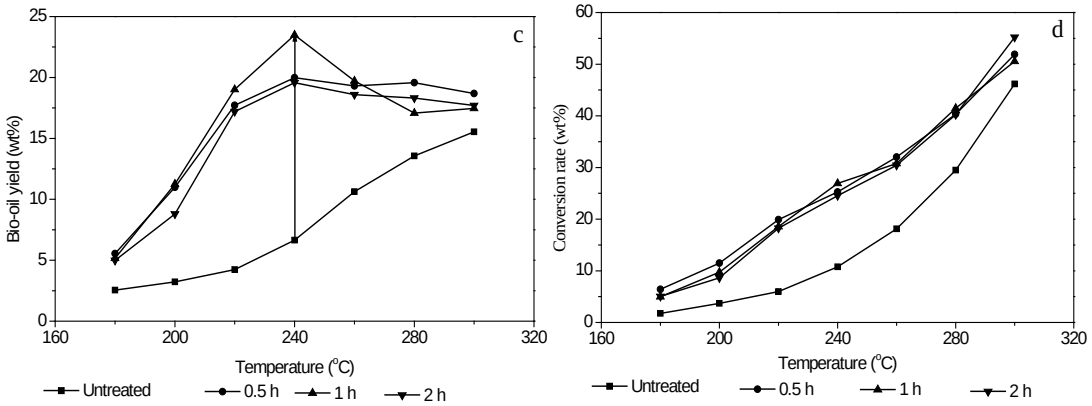

Figure 3. Effect of temperature on bio-oil yield, (a) WSO yield; (b) HO yield; (c) bio-oil yield; (d) conversion rate. (Conditions: 100 ml of ethanol, residence time of 0 min and 10 g of untreated or pretreated cypresses).

Conclusions

In this study, the cypress was subjected to alkali pretreatment and then liquefied in ethanol at different temperatures under a nitrogen atmosphere. The results showed that the pretreatment changed the main chemical components, physical structure and thermo-chemical character of cypress. The pretreated cypresses were less stable than the raw cypress. The mild alkali pretreatment increased surface area and pore volume of cypress, while it more effectively enhanced the bio-oil yield and decreased the temperature as compared to the untreated and stronger pretreated cypresses runs, in which the bio-oil yield increased from 15.5% to 23.5% and the optimum temperature decreased from 300 to 240 °C.

Acknowledgements

This study was support by the State Forestry Administration (201204803), the Major State Basic Research Projects of China (973-2010CB732204/1), National Natural Science Foundation of China (31110103902), and China Ministry of Education (111).

References

Akhtar, J. Amin, N.A.S. 2011. A review on process conditions for optimum bio-oil yield in hydrothermal liquefaction of biomass, Renew. Sust. Energy. Rev. 15: 1615-1624.

Behreddt, F. 2008. Direct liquefaction of biomass, Chem. Eng. Technol. 31: 667-677.

Cadoche, L. López, G.D. 1989. Assessment of size reduction as a preliminary step in the production of ethanol from lignocellulosic wastes, Biol. Waste. 30: 153-157.

Canettieri, E.V. Rocha, G.J.M. Jr, J.A.C. Silva, J.B.A. 2007. Optimization of acid hydrolysis from the hemicellulosic fraction of *Eucalyptus grandis* residue using response surface methodology, Bioresour. Technol. 98: 422-428.

Cheng, J. Su, H. Zhou, J.H. Song, W.L. Cen, K. 2011. Microwave-assisted alkali pretreatment of rice straw to promote enzymatic hydrolysis and hydrogen production in dark- and photo-fermentation, Int. J. Hydrogen Energ. 36: 2093-2101.

El-Rub, Z.A. Bramer, E.A. Brem, G. 2004. Review of Catalysts for Tar Elimination in Biomass Gasification Processes, Ind. Eng. Chem. Res. 43: 6911-6919.

Fan, S.P. Zakaria, S. Chia, C.H. Jamaluddin, F. Nabihah, S. Liew, T.K. Pua, F.L. 2011.

Comparative studies of products obtained from solvolysis liquefaction of oil palm empty fruit bunch fibres using different solvents, Bioresour. Technol. 102: 3521-3526.

Harun, R. Danquah, M.K. 2011. Influence of acid pre-treatment on microalgal biomass for bioethanol production, Process Biochem. 46: 304-309.

Kreuger, E. Sipos, B. Zacchi, G. Svensson, S.E. Björnsson, L. 2011. Bioconversion of industrial hemp to ethanol and methane: The benefits of steam pretreatment and co-production, Bioresour. Technol. 102: 3457-3465.

Kumar, R. Mago, G. Balan, V. Wyman, C.E. 2009. Physical and chemical characterizations of corn stover and poplar solids resulting from leading pretreatment technologies, Bioresour. Technol.100: 3948-3962.

Liu, H.M. Feng, B. Sun, R.C. 2011a. Acid-chlorite pretreatment and liquefaction of cornstalk in hot-compressed water for bio-oil production, J. Agr. Food Chem. 59: 10524-10531.

Liu, H.M. Feng, B. Sun, R.C. 2011b. Enhanced bio-oil yield from liquefaction of cornstalk in sub- and super-critical ethanol by acid-chlorite pretreatment, Ind. Eng. Chem. Res. 50:10928-10935.

Liu, Z.G. Zhang, F.S. 2008. Effects of various solvents on the liquefaction of biomass to produce fuels and chemical feedstocks, Energ. Convers. Manage. 49: 3498-3504.

Rocha, G.J.M. Martin, C. Soares, I.B. Maior, A.M.S. Baudel, H.M. Abreu, C.A.M. 2011. Dilute mixed-acid pretreatment of sugarcane bagasse for ethanol production, Biomass Bioenerg. 35: 663-670.

Shi, S.L. He, F.W. 2008. Analysis and measurement of Pulp and Paper; Chinese Light industry Press: Beijing, China.

Shuping, Z. Yulong, W. Mingde, Y. Kaleem, I. Chun, L. Tong, J. 2010. Production and characterization of bio-oil from hydrothermal liquefaction of microalgae *Dunaliella tertiolecta* cake, Energy 35: 5406-5411.

Xu, C.B. Lancaster, J. 2008. Conversion of secondary pulp/paper sludge powder to liquid oil products for energy recovery by direct liquefaction in hot-compressed water, Water Res. 42: 1571-1582.

Yin, S.D. Dolan, R. Harris, M. Tan, Z.C. 2010. Subcritical hydrothermal liquefaction of cattle manure to bio-oil: Effects of conversion parameters on bio-oil yield and characterization of bio-oil, Bioresour. Technol. 101: 3657-3664.

Preparation And Morphology Of Nanocrystalline Cellulose From Bamboo Pulp

Zhi-Ming Liu, Cheng Xie

(Key Laboratory of Bio-based Material Science and Technology of Ministry of Education, College of Material Science and Engineering, Northeast Forestry University, Harbin 150040, P. R. China)

ABSTRACT

The nanocrystalline cellulose (NCC) from bamboo pulp was prepared with two kinds of preparation conditions. Condition 1 is by using 55% of sulfuric acid mass fraction, 50℃ of reaction temperature and 4 h of hydrolysis time. Condition 2 is 55% of sulfuric acid mass fraction, 55℃ of reaction temperature and 3h of hydrolysis time. The morphology of NCC of bamboo pulp was characterized with Environmental Scanning Electron Microscope (SEM) and Transmission Electron Microscope (TEM), respectively. For the surface morphology of NCC from bamboo pulp, there is no significant difference between Condition 1 and Condition 2 by SEM. The surface morphology of rod-like NCC of bamboo pulp under preparation condition 1 forms a mesh under TEM.

Keywords: nanocrystalline cellulose, bamboo pulp, preparation; morphology

INTRODUCTION

Acid hydrolysis method is one of methods for nanocellulose preparation (Ye, 2007; Song et al. 2011; Satyamurthy et al. 2011; Bondeson et al. 2006). Nanocellulose can be prepared with different raw materials (Chen et al. 2012; Voronova et al. 2012; Peng et al. 2012; Lu et al. 2012; Dai, 2011;Liu et al. 2011). Green composites are prepared from sustainable nanocellulose with biodegradability of nanocellulose (Abdul khalil et al. 2012; Zhen et al. 2008; Yuan et al. 2010; Fan et al. 2010). Some researchers analyzed the morphology of nanocellulose (Liu et al. 2011; Tang et al. 2010; Krishnamachari et al. 2011). Bamboo pulp is a kind of raw materials for nanocellulose preparation. Nanocrystalline cellulose from bamboo pulp is prepared with sulfuric acid hydrolysis method and its morphology is analyzed by scanning electron microscope (SEM) and transmission electron microscope (TEM), respectively, for providing the basic data of green composites.

MATERIALS AND METHODS

Materials

Bamboo pulp, Guizhou Chitianhua Co., Ltd.; Sulfuric Acid (AR), Tianjin Kermel Chemical Reagent Development Center. Samples of bamboo pulp are listed in Fig. 1.


Fig. 1 Samples of bamboo pulp

Instruments

FZ102 Micro-plant shredders, 101-2A Drying oven, Tianjin Taisite Instrument Co., Ltd.; scientz-IID Ultrasonic cell crusher, Ningbo Xinzhi Biotechnology Co., Ltd.; FD-1A-50 Freeze-drying machine, Beijing Boyikang Experimental Instrument Co., Ltd.; H-7650 Transmission electron microscopy, Japan Hitachi Instrument Co., Ltd.

Determination of composition of bamboo pulp

Moisture content, ash content, SiO_2 in the ash content, lignin content , cellulose content of bamboo pulp were determined (Gao,2008; Nie,2008; Liu et al. 2011; Chen et al.1994; Xiao et al. 2009).

Preparation of nanocrystalline cellulose

2 g of bamboo pulp was placed into 100 mL reactor with mass fraction 55% sulfuric acid. Nanocrystalline cellulose (NCC) from bamboo pulp was prepared with two kinds of preparation conditions. Condition 1 is by using 55% of sulfuric acid mass fraction, 50℃ of reaction temperature and 4 h of hydrolysis time. Condition 2 is 55% of sulfuric acid mass fraction, 55℃ of reaction temperature and 3 h of hydrolysis time. The suspended solution was obtained respectively and centrifuged several times with $NaHCO_3$ neutralizing until the suspended solution is neutral, and then was placed in the ultrasonic cell disruption instruments for 10 min disruption, nanocrystalline cellulose colloid was obtained and freeze-dried.

RESULTS AND DISCUSSION

Composition of bamboo pulp

Composition of bamboo pulp is listed in table 1.

Table 1 Composition of bamboo pulp

Moisture content/%	Ash content/%	SiO_2 in the ash content /%	Lignin content/%	Cellulose content/%

5.15	4.25	0.11	5.43	88.96

SEM morphology analysis of bamboo pulp nanocrystalline cellulose

SEM morphology of bamboo pulp nanocrystalline cellulose is listed in Fig. 2.

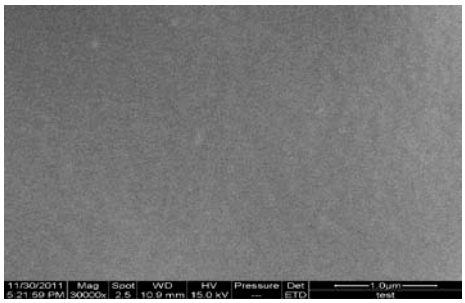

SEM of condition 1

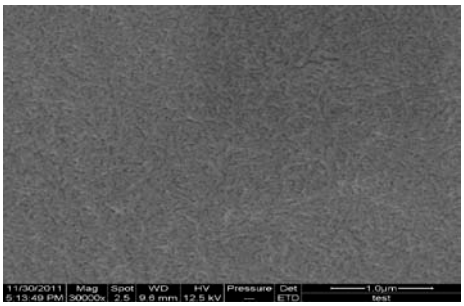

SEM of condition 2

Fig. 2 SEM of bamboo pulp nanocrystalline cellulose

For the surface morphology of nanocrystalline cellulose from bamboo pulp, there is no significant difference between Condition 1 and Condition 2 by SEM.

TEM morphology analysis of bamboo pulp nanocrystalline cellulose

TEM morphology of bamboo pulp nanocrystalline cellulose is listed in Fig. 3.

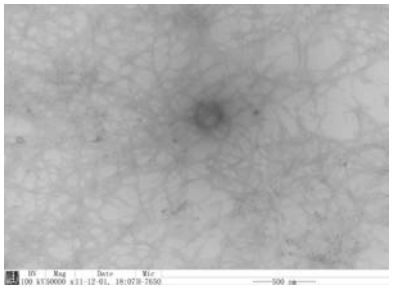

TEM of Condition 1

Fig. 3 TEM of bamboo pulp nanocrystalline cellulose

The surface morphology of rod-like nanocrystalline cellulose of bamboo pulp under preparation condition 1 forms a mesh under TEM.

Bamboo pulp nanocrystalline cellulose is prepared with 55% of sulfuric acid concentration, 22-min ultrasonic time, 49.5℃ofreaction temperature and 3.25 h of reaction time, TEM morphology of bamboo pulp nanocrystalline cellulose with ultrasonic-assisted acid hydrolysis method is listed in Fig. 4.

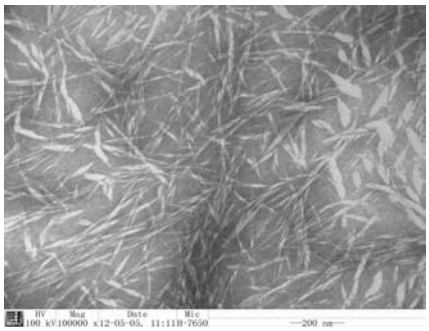

Fig. 4 TEM of bamboo pulp nanocrystalline cellulose with ultrasonic-assisted acid hydrolysis method

The surface morphology of rod-like nanocrystalline cellulose of bamboo pulp with ultrasonic-assisted acid hydrolysis method forms a mesh under TEM.

CONCLUSIONS

For the surface morphology of NCC from bamboo pulp, there is no significant difference between Condition 1 and Condition 2 by SEM. The surface morphology of rod-like NCC of bamboo pulp under preparation condition 1 and ultrasonic-assisted acid hydrolysis method forms a mesh under TEM.

ACKNOWLEDGEMENTS

The authors are grateful for Project 31070633 supported by National Natural Science Foundation of China, supported by “the Fundamental Research Funds for the Central Universities” (DL11EB01), Human Resources and Social Security Department of China Returned Overseas Students Science and Technology Merit-Based Funding Project(07041311401) for financial support.

REFERENCES

ABDUL KHALIL H.P.S.; BHAT, A.H.; IREANA YUSRA A.F. Green composites from sustainable cellulose nanofibrils: a review[J]. Carbohydrate Polymers, 2012, 87: 963-979.

BONDESON, D.; MATHEW, A.; OKSMAN, K. Optimization of the isolation of nanocrystals from microcrystalline cellulose by acid hydrolysis[J]. Cellulose, 2006, 13: 171-180.

CHEN, H.L.; GAO, T.M.; ZHENG, L.; et al. 2012. Preparation of nano-crystalline cellulose from pineapple leaf fiber. Chinese Journal of Tropical Crops, 33(1): 153-156. (in Chinese)

CHEN,Q.Z.; ZHU,Q.; ZHANG,G.L. 1994. GB/T 2677.8-1994. Beijing: Standards Press of China:1-3.(in Chinese)

DAI,D.S. 2011. Fabrication, characterization and application of nanocellulose from hemp fibres. Fuzhou: Fujian Agriculture and Forestry University, 1-120. (in Chinese)

GAO, J. 2008. GB/T 462-2008. Beijing: Standards Press of China:1-7. .(in Chinese)

GUO, N.W.; HE, J.X.; CUI, S.Z. 2012. Preparation of bamboo cellulose nanowhiskers. Journal of Cellulose Science and Technology, 20(1): 58-61.(in Chinese)

KRISHNAMACHARI, P.; HASHAIKEH, R.; TINER, M. Modified cellulose morphologies and its composites; SEM and TEM analysis[J]. Micron, 2011, 42: 751-761.

LIU, Z.M.; XIE, C.; FANG, G.Z.; et al. 2011. Morphology analysis of nano-microcrystalline cellulose from eucalyptus pulp and cotton nanocrystalline cellulose. Biomass Chemical Engineering, 45(2): 5-8. (in Chinese)

LIU, Z.M.; XIE, C.; FANG, G.Z.; et al. 2011. Preparation optimization and morphology analysis of nanocrystalline cellulose from reed pulp. Chemistry and Industry of Forest Products, 31(6): 87-90. (in Chinese)

LU,H.J.;WEN, H.L.; LIU, X. 2012. Study on preparation of nanocrystal cellulose by ultrasonic-assisted acid. Journal of the Chinese Cereals and Oils Association, 27(4): 96-100.(in Chinese)

NIE, J.H. 2008. GB/T 742-2008. Beijing: Standards Press of China:1-6.(in Chinese)
PENG, Y.C.; GARDNER, D.J.; HAN, Y. Drying cellulose nanofibrils: in search of a suitable method[J]. Cellulose, 2012, 19: 91-102.

SATYAMURTHY, P.; JAIN, P.; BALASUBRAMANYA, R.H.; et al. 2011. Preparation and characterization of cellulose nanowhiskers from cotton fibres by controlled microbial hydrolysis[J]. Carbohydrate Polymers, 83: 122-129.

SONG, X.Z.; WU, Q.L.; FU, F.; et al. 2011. Research progress of nanocrystalline cellulose prepared from crops and agricultural residues. Transactions of the Chinese Society for Agricultural Machinery, 42(11): 106-112. (in Chinese)

TANG, L.R.; HUANG, Biao; DAI, D.S.; et al. 2010. Optimum process conditions of nanocellulose crystal and morphology characterization. Journal of Fujian College of Forestry, 30(1): 88-91. (in Chinese)

VORONOVA, M.I.; ZAKHAROV, A.G.; KUZNETSOV, O.Y.; et al. The effect of drying technique of nanocellulose dispersions on properties of dried materials[J]. Materials letters, 2012, 68: 164-167.

XIAO,Q.; WAN, J.Q.; WANG, Y. 2009. CP/MAS ^{13}CNMR spectroscopy study of the ultrastructure of wood pulp fiber. Acta Chimica Sinica, 67(22): 2629-2634. (in Chinese)

YE, D.Y. 2007. Preparation of nanocellulose. Progress in Chemistry, 19(10): 1568-1575. (in Chinese)

YUAN, Y.; FAN, Z.Q.; SHEN, Q. 2010. Recent development in nanocellulose research and application Ⅰ. Polymer Bulletin, (2):75-79. (in Chinese)

FAN, Z.Q.; YUAN, Y.; SHEN, Q. 2010. Recent development in nanocellulose research and application Ⅱ.Polymer Bulletin, (3): 40-60. (in Chinese)

ZHEN, W.J.; SHAN, Z.H. 2008. Application of nanocellulose in green composites. Modern Chemical Industry, 28(6): 85-88. (in Chinese)

Variations in Topochemistry and Micromechanics between Opposite and Tension Wood Fiber from *Populus Nigra*

*Jian F. Ma[1] - Xia Zhou[1] – Zhi H. Zhang[1] - Feng Xu[1, 2, *]*

[1]Institute of Biomass Chemistry and Technology, Beijing Forestry University, Beijing 100083, China

[2]College of Light Industry and Textiles, Qiqihar University, Qiqihar 161006, China

**Corresponding author*

xfx315@bjfu.edu.cn

Abstract

Chemical imaging by confocal Raman microscopy has been used for the comparison of the topochemical distribution of cellulose and lignin, in particular with regard to coniferyl alcohol and coniferaldehyde (Lignin-CAA) between opposite wood (OW) and tension wood (TW) fiber. In the Raman image of the ratio of the 1655 cm^{-1} to the 1605 cm^{-1} band, the homogeneous distribution of Lignin-CAA was visualized both in OW and TW fiber S2. In situ Raman images also revealed that highest cellulose concentration was found in the OW fiber S2 and fewest in CC as well as CML. By comparison in TW fibers high cellulose concentration spots were confined mostly to fiber S2 and GL. Besides variation in chemical composition, OW and TW fiber also showed micromechanical differences reflected by the band shift at 1097 cm^{-1}. The band at 1097 cm^{-1} in OW fiber S2 shifted to 1095 cm^{-1} in TW fiber S2 and GL which demonstrated that TW fiber S2 as well as GL still loaded tensile strength even after the stress was released. The localization of lignin and cellulose together with the micromechanical variation at sub-cellular level will contribute to the further understanding of tensional stress origin in TW.

Keywords: *Populus nigra*, Opposite wood, Tension wood, Topochemistry, Micromechanics, Confocal Raman microscopy

Introduction

In response to mechanical stress such as wind and gravity the stems and branches of trees can bend or lean and the trees are able to progressively straighten their leaning trunks or branches by an active mechanical action driven by cambium, which produces a special type of wood, called reaction wood (Sinnot 1952). Reaction wood characteristics and location differ between angiosperm and gymnosperm trees. In gymnosperm trees, such as pine, the reaction wood is named compression wood (CW) and develops at the lower side of leaning stems and branches, whereas in angiosperm trees, such as poplar, it is named tension wood (TW) and occurs at the upper side. The morphology and chemical composition of reaction wood differ markedly from those of opposite wood (OW). In gymnosperms, CW fibers typically have a round shape, intercellular spaces and cracks in the cell wall (Timell 1986). Their wall is thick and heavily lignified, and the microfibrils are oriented at a wide angle with respect to the fiber axis. Among angiosperms, TW is commonly characterized by the presence of specialized G-fibers with a particular morphology, chemical composition and micromechanics due to the development of the so called gelatinous layer (GL). The GL has been variously described as filling the cell lumen, as being attached to the S3 layer (S1+S2+S3+GL), as replacing the S3-layer（S1+S2+GL）or partly or entirely substituting the S2 layer (S1+GL) (Dadwell and Wardrop 1955).

It has been reported that the GL is composed of axial orientated microfibrils and high crystallinity of cellulose (Norberg and Meier 1966, Pilate 2004). However, in addition to cellulose this layer also contains polysaccharides, including pectin and hemicelluloses. In sweetgum and hackberry TW, a number of antibodies that recognize arabinogalactan proteins and RG I-type pectin molecules bound to the GL (Bowling and Vaughn 2008). Using immunohistochemical method, (1, 4)-β-galactan in cell walls of poplar TW G-fibers was detected and found it to be mainly restricted to the interface between the GL and the adjacent secondary cell wall (Arend 2008). Evidence of xyloglucan and xyloglucan-synthesizing proteins in the GL has also been reported (Nishikubo et al. 2007). Furthermore, previous literatures have demonstrated the presence of aromatic compounds in the GL using different microscopic techniques (Gierlinger and Schwanninger 2006, Joseleau et al. 2004, Lehringer et al. 2008, Lehringer et al. 2009).

Although it has been well established that the GL with its microfibril angle parallel or nearly parallel to the longitudinal axis is the driving force of the tensile stress generated in TW (Fujita et al. 1974, Clair et al. 2011, Goswami et al. 2008, Chang et al. 2009, Clair and Thibaut 2005, Yoshida et al. 2002), the underlying mechanism at the origin of tensional stress in TW has been the subject of a lot of controversy. It has been proposed that it would be due to the swelling of the wood matrix substance during lignification, the angle of cellulose microfibrils controlling the anisotropy of the resulting stress (Yamamoto et al. 1990). Different hypotheses have been proposed to explain the mechanism, such as the contraction of amorphous zones within the cellulose microfibrils (Yamamoto 2004), the action of xyloglucans during the formation of microfibril aggregates, or the effect of changes in moisture content stimulated by pectin-like substances. However, no literature has focused on

the difference in micromechanics at the sub-cellular level using the confocal Raman microscopy.

Here, we use confocal Raman microscopy to acquire and compare chemical images between OW and TW fiber from *Populus nigra.* Differences in cellulose and lignin localization in the cell walls are visualized without staining of tissues. Furthermore, the miromechanical variations between and within cell wall layers were reflected by Raman band shift.

Material and methods

Plant material and preparation. An inclined 5-year-old *P. nigra* tree, which exhibited crooked growth in the lower parts of the stems, was provided by the arboretum of Northwest Agricultural and Forestry University, China. Specimens from fresh disks of inclined stem were collected. Without any embedding routine, 30-μm-thick cross-sections for chemical imaging were cut on a sliding microtome (Leica 2010R). For chemical imaging, samples were placed on a glass slide with a drop of D2O, covered by a coverslip (0.17 mm thickness) and sealed with nail-polish to prevent evaporation during measurement.

Confocal Raman microscopy. Raman spectra were acquired with a LabRam Xplora confocal Raman microscope. In order to achieve high spatial resolution, measurements were conducted with a high numerical aperture (NA) microscope objective from Olympus (100×, oil, NA=1.40) and a linear-polarized 532-nm laser excitation was focused with a diffraction-limited spot size (1.22λ/NA). The software (Labspect) was used for measurement setup and image processing.

Results

Variations in topochemistry between OW and TW fiber. The topochemical analysis of fibers in OW and TW reveals the distribution of cellulose and lignin within the morphologically distinct cell wall layers. The basic morphology of the measured cell walls in the OW (Fig. 1a) and TW (Fig. 1b) becomes apparent in the chemical images based on the C-H stretching bands (3000-2771 cm^{-1}), in which all cell wall polymers (cellulose, hemicellulose, pectin, lignin) contribute to the Raman signal (Atalla and Agarwal 1984, Wiley and Atalla 1987). In TW the GL was readily differentiated from the S2 and appeared as wavy structures with very irregular lumens. The formation of GL appeared to affect the development of S2 layer, which appears consistently thinner than that in OW.

Besides the cell wall structures, the distribution of cell components (cellulose and lignin) were also visualized. The characteristic cellulose vibrations can be seen in the region from 2900-2750 cm^{-1}, assigned to CH and CH2 stretching vibration (Agarwal and Ralph 1997, Agarwal 1999, Edwards et al. 1997). In OW fibers highest intensity was found in the secondary wall and fewest in the CC as well as CML and in TW fibers high cellulose concentration spots were confined mostly to S2 and GL (Figs. 1c and 1d).

The chemical image based on the O-D stretching band (integrating the intensity from 2775-2200 cm^{-1}) is shown for OW fiber (Fig. 1e). Highest intensity was found in the S2 followed by the CC and CML and the fewest in the S3. As expected, in TW fiber high intensity is observed in the GL. The O-D signal, albeit much weaker, is also observed in the S2 wall layer, the CC and in some parts of the CML (Fig. 1f). As a possible explanation, the higher concentration of D2O in the GL could have related to the porosity or the hydrophilicity of the various structures. As was reported earlier (Chang et al 2009), the results of adsorption-desorption isotherms revealed that the TW has much higher porosity and suggested that high porosity is an attribute of the GL itself.

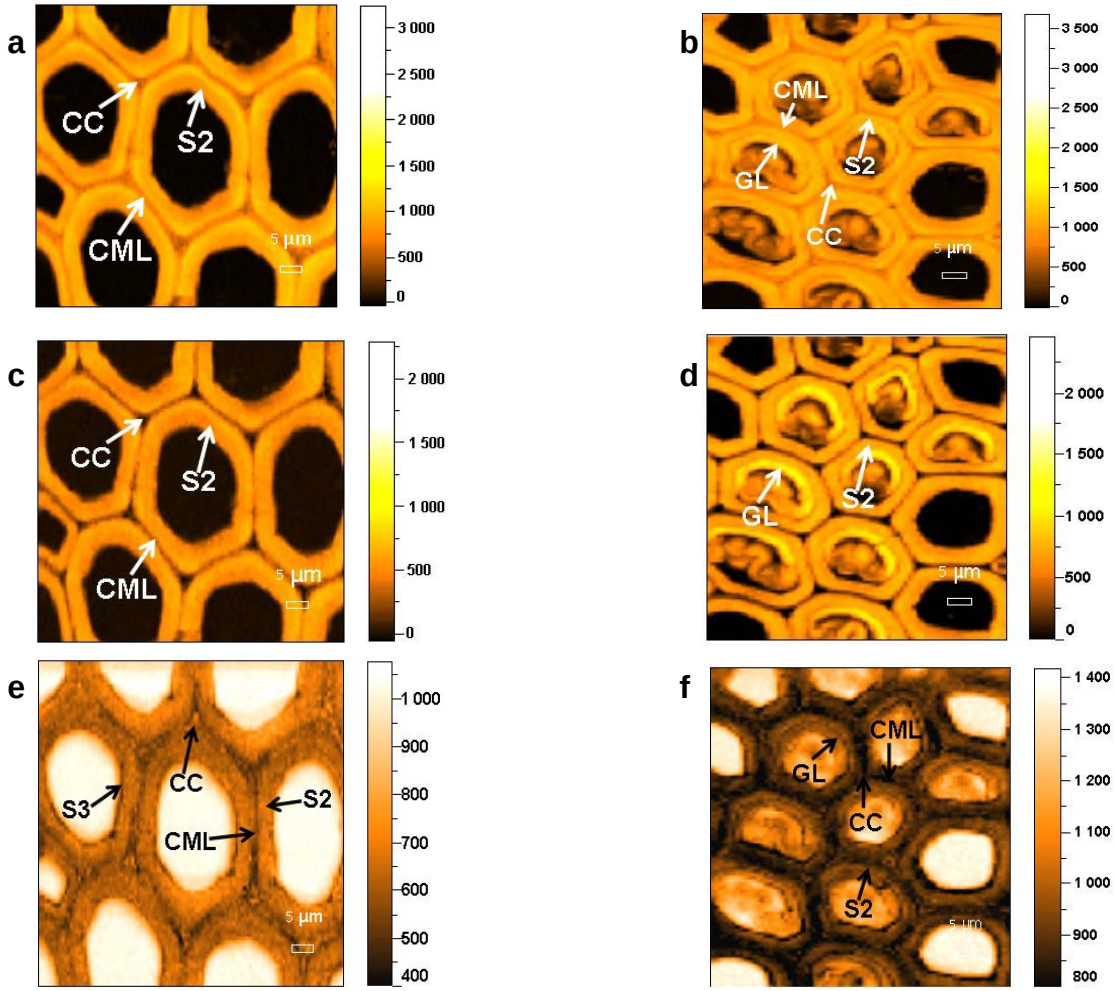

Figure 1. Raman images calculated by integrating over Raman bands attributed to different functional groups of cell wall polymers. The overall structures of OW (a) and TW (b) fiber, 3000-2771 cm^{-1}; The cellulose distribution of OW (c) and TW (d) fiber, 1150-1000 cm^{-1}. The D2O distribution of OW (e) and TW (f) fiber, 2775-2200 cm^{-1}.

Finally, lignin distribution was visualized by integrating over the 1600 cm^{-1} band, assigned to phenyl groups in lignin (Agarwal 2006, Agarwal and Ralph 2008). In OW fiber, there is strong contrast between morphologically distinct cell wall regions due to different lignin signal intensity (Fig. 2a). The higher lignin signal intensity was observed in the cell corner (CC) and somewhat lower in other regions of the compound middle lamella (CML). Within

the S2 wall layer of the fibers less, yet not insubstantial, amounts of lignin are observed. By contrast, there are marked differences for the TW fibers (Fig. 2b). While the relative lignin signal intensity is still higher in the CC and CML than in the S2 layer, there is a clear overall increase in the S2 layer of the fibers. This is further illustrated by semi-quantitative spectra analysis.

Owing to the in situ chemical sensitivity and the specific chemical attributions of the lignin bands, it is possible to further dissect the spatial lignin distribution both within and between samples. While the 1,605 cm^{-1}. band is due to aryl ring stretching and thus is a more general lignin marker, the 1665 cm^{-1}.band is indicative of coniferyl alcohol and coniferaldehyde. In order to gain more subtle differences, images for band ratios were obtained. In the OW and TW image for the ratio of the 1665 cm^{-1} to the 1605 cm^{-1} band (Figs. 2c and 2d), the intensity distribution of Lignin-CAA is homogeneous. The same results were also reported previously (Schmidt 2009), which presented that both in wild type and transgenic *Populus trichocarpa* the distribution of CAA was relatively even.

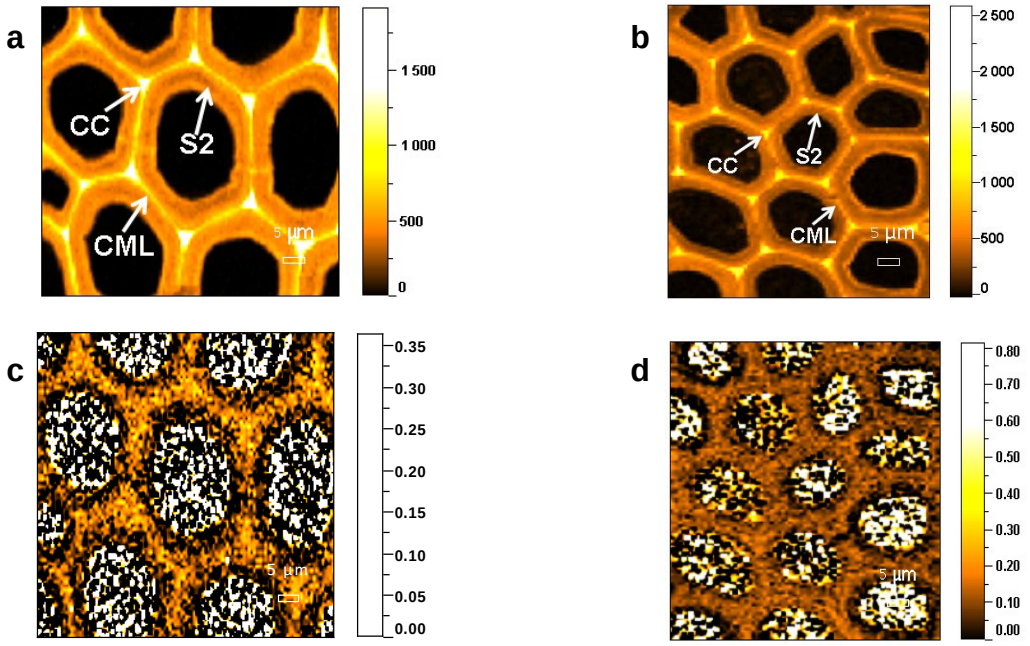

Figure 2. Raman images calculated by integrating over Raman bands attributed to different functional groups of cell wall polymers. The lignin distribution of OW (a) and TW (b) fiber, 1641-1546 cm^{-1}; The coniferyl alcohol and coniferaldehyde distribution of OW (c) and TW (d) fiber, 1670-1645 cm^{-1}.

Variations in micromechanics between OW and TW fiber. The mechanism for tree orientation in angiospems is based on the production of high tensile stress on the upper side of the inclined axis. In many species, the stress level has relations to the presence of the GL. In the TW the fibrils in the GL are parallel to the fiber axis, which enable them to deform approximately the same order of magnitude as the fiber.

When covalent bonds in a fibrous polymer are loaded in tension, their stretching vibrational bands in the infrared or Raman spectrum shift to lower frequency (Wool 1975). In order to

investigate the band shift at 1097 cm^{-1} attributed to C-C and C-O stretching of cellulose in TW fiber, the spectra range from 1250-1000 cm^{-1} was extracted. The resulting spectra were deconvoluted at the different frequency ranges. After the spectra fitting, we found besides changes in the overall Raman intensity, that some Raman bands showed obvious changes in band positions (Fig. 3). The band at 1097 cm^{-1} in the OW fiber S2 shifted to lower wavenumers in TW fiber S2 (1095 cm^{-1}) and GL (1095 cm^{-1}) (-2.0 cm^{-1} at its center). Negative band shifts are expected for covalent bonds aligned and stretched along the fiber axis. The same result was also reported that there exists a strong correlation between the shift of the band at 1097 cm^{-1} corresponding to the stretching of the cellulose ring structure and the applied strain (r=0.99). Along with increasing strain, the band at 1097 cm^{-1} shifted remarkably to lower wavenumbers (1091 cm^{-1}) (Gierlinger 2006). Thus, it is reasonable to assume that in comparison with OW and TW fiber S2 as well as GL still loaded tensile strength even after the stress was released.

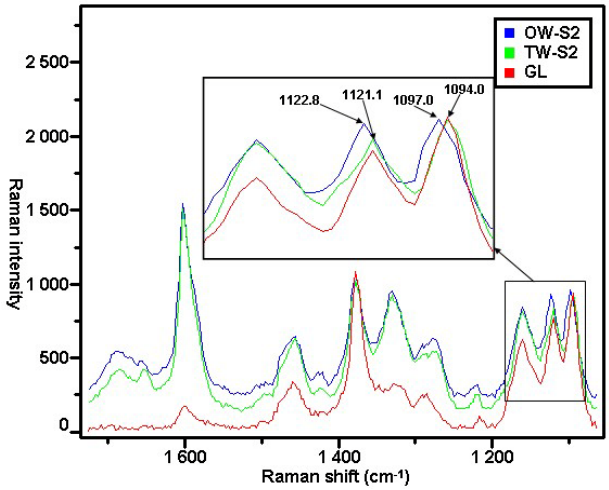

Figure 3. Average Raman spectra acquired from the OW fiber S2 (OW-S2), the TW fiber S2 (TW-S2) and the GL showing the bandshift of C-O-C.

The mechanism at the origin of tensile stress has been explored according to different hypothesis (Fujita et al. 1974, Clair et al. 2011, Goswami et al. 2008, Chang et al. 2009, Clair and Thibaut 2005, Yoshida et al. 2002). The G-layer swelling hypothesis proposed that the tensional deformation originates in the swelling of the GL and is transmitted to the adjacent secondary layers, where the larger MFAs allow an efficient conversion of lateral stress into axial tensile stress. Cellulose tension hypothesis postulated that tensional stress develops in the G-layer, which then drives shrinkage of the S-layer. Both hypothesis assumed that the generation of longitudinal shrinkage in the TW fiber S2 was induced by the GL. The negative band shift of TW fiber S2 and GL in our experiment revealed that after the fibers are transversally cut, the TW fiber S2 and GL kept the permanent tensional deformation. The tensional deformation of the TW fiber S2 may be due to its being in a state of tension during the TW formation. Thus, we can assume that the generation of longitudinal shrinkage in the TW fiber was the combination of S2 and GL.

Conclusion

High resolution confocal Raman microscopy proved to be a useful method for investigating topochemical and micromechanical characteristics of OW and TW fibers from *P. nigra*. In situ Raman images revealed that lignin-CAA was homogeneously distributed in OW and TW fiber S2. Furthermore, the Raman band shift reflected that the cellulose fibrils in TW fiber S2 and GL still loaded tensile strength even after the stress was released. The localization of lignin and cellulose together with the micromechanical variation at sub-cellular level will contribute to the further understanding of tensional stress origin in TW.

Acknowledgments

This work was supported by the Grants from State Forestry Administration of China (2010-4-16, 2010040706), Natural National Science Foundation of China (31070526), Doctoral Fund of Ministry of Education of China (20100014110005) and the Science Fund for Distinguished Young Scholars of Heilongjiang Province of China (JC200907).

References

Agarwal, U.P., Ralph, S.A. 1997. FT-Raman spectroscopy of wood: identifying contributions of lignin and carbohydrate polymers in the spectrum of black spruce (*Picea mariana*). Applied Spectroscopy. 51(11): 1648-1655.

Agarwal, U.P. 1999. An overview of Raman spectroscopy as applied to lignocellulosic materials. In: Argyropoulos E (ed) Advances in lignocellulosics characterization. TAPPI press, Atlanta, pp 201-225.

Agarwaln U.P. 2006. Raman imaging to investigate ultrastructure and composition of plant cell walls: distribution of lignin and cellulose in black spruce wood (*Picea mariana*). Planta 224(5):1141-1153

Agarwal, U.P., Ralph, S.A. 2008. Determination of ethylenic residues in wood and TMP of spruce by FT-Raman spectroscopy. Holzforschung 62(6): 667-675.

Arend, M. 2008 Immunolocalization of (1,4)-β-galactan in tension wood fibers of poplar. Tree Physiology. 28(8): 1263-1267.

Atalla, R.H., Agarwal, U.P. in Microbeam Analysis-1984, A.D. Roming and J.I. Gold stein, Eds. (San Francisco Press, San Francisco, 1984, pp. 125.

Bowling, A.J., Vaughn, K.C. 2008. Immunocytochemical characterization of tension wood: Gelatinous fibers contain more than just cellulose. American Journal Botanyt. 95(6): 655-663.

Clair, B., Gril, J., Baba, K., Thibaut, B., Sugiyama, J. 2005. Precautions for the structural analysis of the gelatinous layer in tension wood. IAWA Journal. 26(2): 189-195.

Chang, S.S., Clair, B., ,Ruelle, J., Beauchêne, J., Di Renzo, F., Quignard, F., Zhao, G.J., Yamamoto, H., Gril, J. 2009. Mesoporosity as a new parameter for understanding tension stress generation in trees. Journal of Experimental Botanay. 60(11): 3023-3030.

Clair, B., Thibaut, B. 2001. Shrinkage of the gelatinous layer of poplar and beech tension wood. IAWA Journal. 22(2): 121-131.

Clair, B., Alméras, T., Pilate, G., Jullien, D., Sugiyama, J., Riekel, C. 2011. Maturation stress

generation in poplar tension wood studied by synchrotron radiation microdiffraction. Plant physiology. 155(1): 562-570.

Côté, J.B., Day, A.C., Timell, T.E. 1969. A contribution to the ultrastructure of tension wood fibers. Wood Science and Technology. 3(4): 257-271.

Dadswell, H.E., Wardrop, A.B. 1955 The structure and properties of tension wood. Holzforschung 9 (4): 97-104.

Edwards, H.G., Farwell, M.D.W., Webster, D. 1997. FT-Raman microscopy of untreated natural plant fibers. Spectrochimica Acta , Part A. 53 (13): 2383-2392.

Fujita, M., Saiki, H., Harada, H. 1974. Electron microscopy of microtubules and cellulose microfibrils in secondary wall formation of poplar tension wood fibers (in Japanese). Mokuzai Gakkaishi. 20(4): 147-156.

Gierlinger, N., Schwanninger, M. 2006. Chemical imaging of poplar wood cell walls by confocal Raman microscopy. Plant Physiology. 140(4): 1246-1254.

Gierlinger, N., Schwanninger, M., Reinecke, A., Burgert, I. 2006. Molecular changes during tensile deformation of single wood fibers followed by Raman microscopy. Biomacromolecules 7(7): 2077-2081.

Goswami, L., Dunlop, J.W.C., Jungnikl, K., Eder, M., Gierlinger, N., Coutand, C., Jeronimidis, G., Fratzl, P., Burgert, I. 2008. Stress generation in the tension wood of poplar is based on the lateral swelling power of the G-layer. Plant Journal. 56(4): 531-538.

Joseleau, J.P., Imai, K., Kuroda, K., Ruel, K. 2004 Detection in situ and characterization of lignin in the G-layer of tension wood fibers of *Populus deltoides*. Planta 219(2): 338-345.

Lehringer, C., Gierlinger, N., Koch, G. 2008. Topochemical investigation on tension wood fibers of *Acer* spp., *Fagus sylvatica* L. and *Quercus robur* L. Holzforschung 62(3): 255-263.

Lehringer, C., Daniel, G., Schmitt, U. 2009. TEM/FE-SEM studies on tension wood fibers of *Acer* spp., *Fagus sylvatica* L. and *Quercus robur* L. Wood Science and Technology. 43(7-8): 691-702.

Nishikubo, N., Awano, T., Banasiak, A., Bourquin, B., Ibatullin, F., Funada, R., Brumer, H., Teeri, TT., Hayashi, T., Sundberg, B., Mellerowicz, E.J. 2007. Xyloglucan *endo-transglycosylase* (XET) functions in gelatinous layers of tension wood fibers in poplar-A glimpse into the mechanism of the balancing act of trees. Plant Cell Physiology. 48(6): 843-855.

Norberg, P.H. & Meier, H. 1966. Physical and chemical properties of the gelatinous layer in tension wood fiber of aspen (*Populus tremula L.*). Holzforschung 20(6): 174-178.

Pilate, G., Chabbert, B., Cathala, B., Yoshinaga, A., Leplé, J.C., Laurans, F., Lapierre, C., Ruel, K. 2004 Lignification and tension wood. Comptes Rendus Biologiesl. 327(9): 889-901.

Schmidt, M., Schwartzberg, A.M., Perera, P.N., Weber-Bargioni, A., Carroll, A., Sarkar, P., Bosnega, E., Urban, J.J., Song, J., Balakshin, M.Y., Capanema, E.A., Auer, M., Adams, P.D., Chiang, V.I., Schuck, P. 2009 Label-free in situ imaging of lignifications in the cell wall of low lignin transgenic *Populus trichocarpa*. Planta 230(3): 589-597.

Sinnott, E.W. 1952. Reaction wood and the regulation of tree form. American Journal of Botany. 39(1): 69-78.

Timell, T.E. 1986 Compression wood in gymnosperms. Springer, Heidelberg.

Yamamoto, H., Okuyama, T., Yoshida, M. 1995 Generation process of growth stresses in cell walls. Ⅵ. Analysis of growth stress generation by using a cell model having three layers (S1, S2, and I+P). Mokuzai Gakkaishi. 41(1): 1-8.

Yamamoto, H. 2004. Role of the gelatinous layer on the origin of the physical properties of the tension wood. Journal of wood Sciencei. 50(3): 197-208.

Yoshida, M., Ohta, H., Yamamoto, H., Okuyama, T. 2002. Tensile growth stress and lignin distribution in the cell walls of yellow poplar, *Liriodendron tulipifera* Linn. Trees 16(7): 457-464.

Wiley, J.H. & Atalla, R.H. 1987. Band assignment in the Raman spectra of celluloses. Carbohydrate Research. 160(15): 113-129.

Wool, R.P. 1975. Mechanisms of frequency shifting in the infrared spectrum of stressed polymer. Journal of Polymer. Science 13(9): 1795-1808.

Characterisation of Wheat Straw Using Dynamic Vapour Sorption Method

Peng Miao, Majid Naderi, Manaswini Acharya, Jiyi Khoo, Dan Burnett and Daryl Williams[#]

pmiao@smsuk.co.uk
Surface Measurement Systems Ltd
5 Wharfside, Rosemont Road, Alperton
London HA4 0PE, UK

[#] Department of Chemical Engineering
Imperial College
Kensington,
London SW7 2BY

Abstract

Wheat straw is an abundant and inexpensive natural biopolymer with 39% cellulose and 38.7% hemicelluloses [1]. Wheat straw has been used for a number of applications such as a bioabsorbent for waste water treatment [2, 3] and as a composite material reinforcement [4]. More recently, biofuel derived from wheat straw has been attracting more and more attention due to the future potential shortages of fossil fuel [5, 6]. One of the crucial steps of producing bio-ethanol from wheat straw is its pre-treatment which should facilitate the economic feasibility and yield efficient conversion into biofuel. This pre-treatment is expected to increase the accessible chemical sites of the straw, i.e. increase the fibre surface area as well as its hydrophilicity via the removal of waxes, also increase the total amorphous content and decrease the crystallinity of cellulose. This study highlights the important surface chemical information on wheat straw including BET surface area, water sorption kinetics and so on which may be obtained using the Dynamic Vapour Sorption (DVS) technique [7].

Key words: DVS, Sorption, Straw, Biofuel, Pre-treatment, Cellulose

Introduction

A common feature of the enzymatic hydrolysis step is the need for pre-treatment of the lignocellulosic biomass resulting in a more efficient reaction, which is a crucial step as it has direct impact on the subsequent yield of enzymatic hydrolysis to produce glucose and alcohol fermentation processes in the production of bio-fuel. This pre-treatment is intended to disrupt the crystalline structure of microfibrils to release the polymer chains of cellulose and hemicellulose, and modify amorphous content and open up pores in the biomass to increase accessible site of straw to enzymatic activity, which could be indicated by increase in sorption uptake, specific surface area and hydrophilicity etc. These surface modifications can be quantitatively characterised in terms of the sorption and desorption behaviour using Dynamic Vapour Sorption technique.

Pre-treatment and Experimental Conditions

Raw wheat straw (RWS) was pre-treated using a novel twin-strew extrusion technology by T.H Ng and co-workers at Brunel University, UK [5]. This technology was reported to have ability to provide high shear, rapid heat transfer, effective and rapid mixing and feasibility to combine with other pre-treatment – all in a continuous process [8, 9, 10, 11]. Detail of pre-treatment conditions and sample variation are summarised in Table 1.

Sample ID	**Pre-treatment conditions**
RWS	Wheat straw as received without pre-treatment
WCB10009	Extruded at 100 rpm and 50^{o}C with 4% NaOH (alkaline), Straw : H_2O = 1:2
WCB10009W	The same as WCB1009, but with H_2O wash after pre-treatment at 25^{o}C

Table 1 Pre-treatment conditions of wheat straw

Sample RWS is raw wheat straw without any pre-treatment. It is used for comparison with other pre-treated samples. Sample WCB10009 was extruded using a twin-screw technology with H_2O and alkaline (NaOH). The pre-treatment to sample WCB10009W is the same as that to sample WCB10009, but after pre-treatment, the sample was washed with water.

All water sorption measurements on the samples were performed using SMS dynamic vapour sorption instrument, DVS Advantage 1. During the measurements, the instrument was run in dm/dt mode (mass variation over time variation) to decide when equilibrium is reached. A fixed dm/dt value was selected at each RH segment. This criterion permits the DVS software to automatically determine when equilibrium has been reached and complete a step. When the rate of change of mass falls below this threshold over a determined period of time, the relative humidity set point will proceed to the next programmed level. All analyses were carried out using the SMS DVS Analysis

Suite version 6.1.1.2 and SMS DVS Analysis Suite version 6.1.1.2 (Advanced) macros.

Results and Discussions

Figure 1 shows the dynamic water sorption behaviour on raw wheat straw sample (RWS) at 25°C. It can seen that at lower relative humidity (RH < 50%), the uptake is low, but reaches equilibrium fast and at higher RH steps (> 50%), the uptake is relative high, but equilibrium has not reached. The low uptake at the lower RH is the contribution of suface sorption and the sorption is gradually developing from the surface into the bulk at higher RH, hence high uptake.

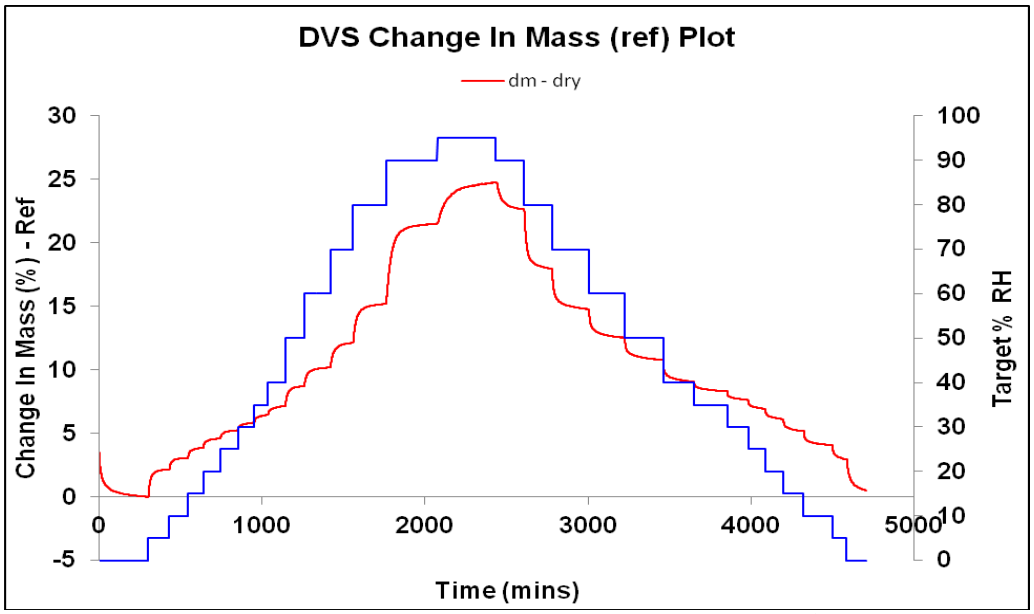

Figure 1 Dynamics of water sorption in raw wheat straw at 25°C

The corresponding isotherms plotted in Figure 2 show a mixed Type II/III behaviour, indicated by low initial sorption and substantial uptake at higher RH. The Type II behaviour indicates a more or less surface monolayer sorption mechanism which makes BET surface calculation feasible via the water sorption measurement (organic solvents, e.g. octane, are usually used for BET surface area measurements by DVS). Since biomass pre-treament is, generally speaking, an aqueous thermal process, water sorption is therefore preferable. The hysterisis of the desorption further verifies the bulk sorption. The BET plot is shown in Figure 3, which indicates a specific surface area of 1.734459 x 10^6 cm^2/g.

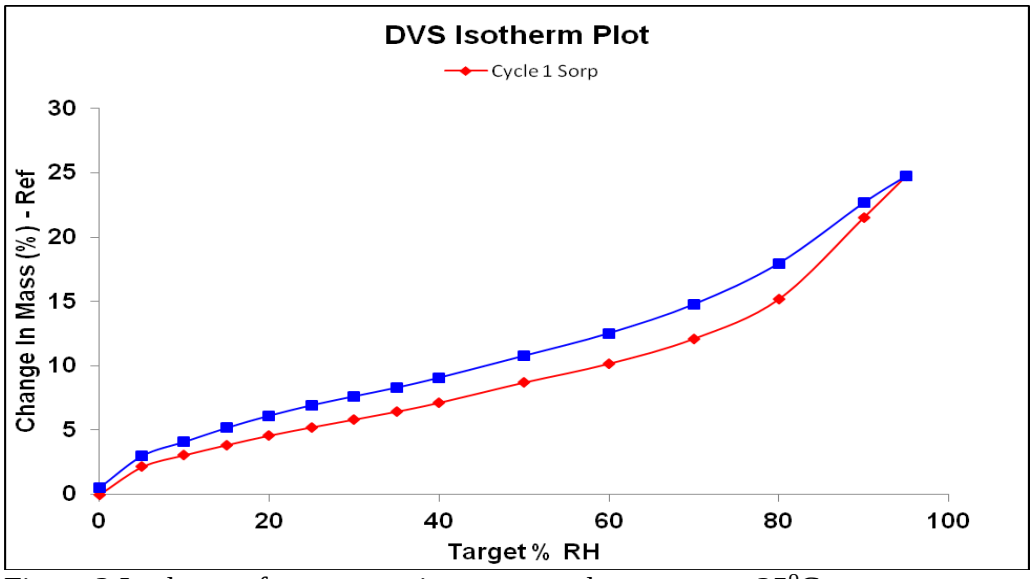

Figure 2 Isotherm of water sorption on raw wheat straw at 25°C

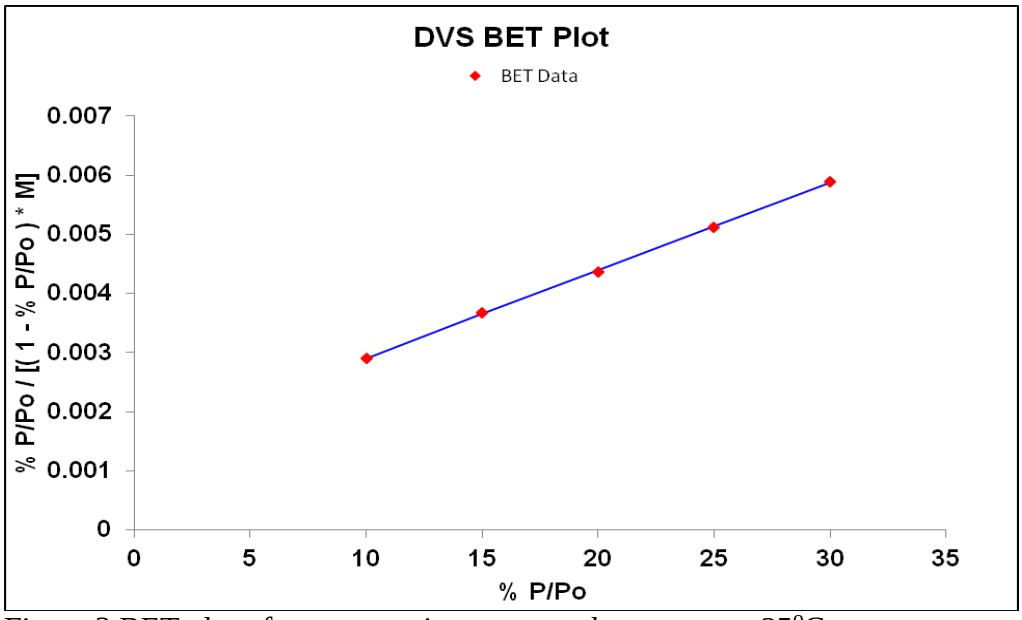

Figure 3 BET plot of water sorption on raw wheat straw at 25°C

The water sotption measurements were also performed on other two pre-treated samples (WCB10009 and WCB10009W) with the same experimental conditions. A superimposed plot of the isotherms of the three samples is shown in Figure 4. All isotherms show a similar mixed Type II/III behaviour, especially at lower RH (< 40%) where the suface sorption is dominant. This indicates that the surface hydrophilicity of wheat straw does not change significatly before and after the pre-treatment, which is a little bit out of expectation. In general, surface hydrophilcity should be improved due to the removal of the waxes on the straw surface during the pre-treatment and the isotherm shape should be more Type II like. However it cannot be concluded at this stage that the waxes were not

effienctly removed by the pre-treatment because the hydrophilicity is also dependent on the fibre type of the biomass. So a further investgation is needed.

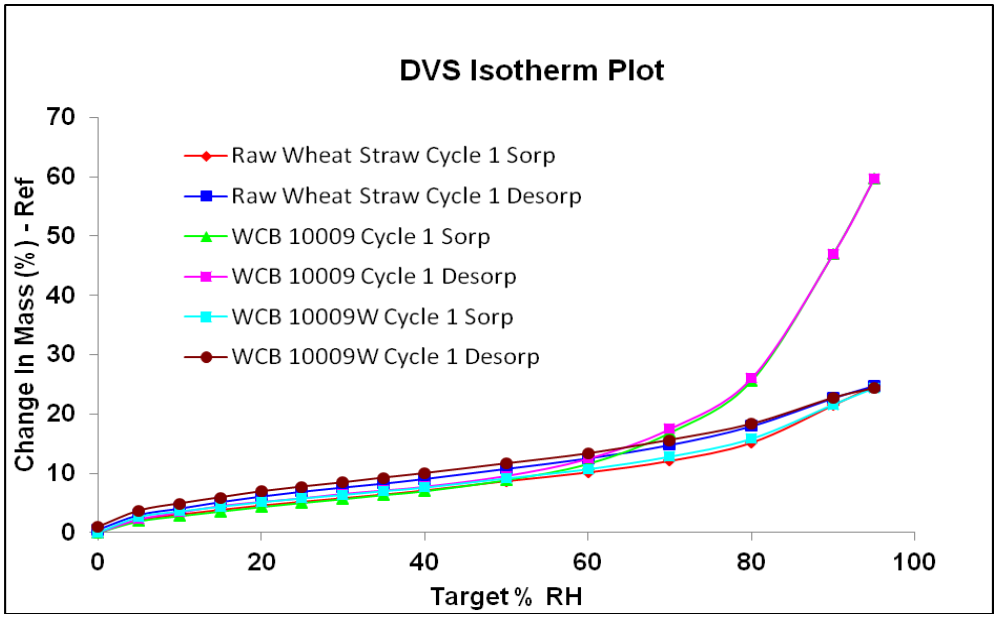

Figure 4 A superimposed plot of the isotherms of the three samples

In terms of total uptake at 95% RH, the pre-treated sample of WCB10009 has an uptake of 59.62% which is much higher than 24.76% of the untreated sample (RWS), indicating an open-up of more accessible sites to water molecules, which will be beneficial to subsquent hydrolysis process. One of the strategies employed in increasing enzymatic convertibility for fermentable sugars for bioethanol production is to decrease cellulose crystallinity [12] because amorphous region of the cellulose has faster hydrolysis rate than its crystalline region. Since most reactants, including water can mainly penetrate amorphous region and the surface of crystalline cellulose, so the uptake of water is also an indication of amorphous content of the biomass, i.e. the higher uptake, the higher amorphous content. Unlike other two samples, the water sorption behaviour on the pre-treated sample WCB10009 does not show hysteresis. This is probably due to the swelling of the pores in the material, hence less capillary force.

Comparing the isotherm of the raw wheat straw sample with that of the pre-treated sample WCB10009W, one can see that their isotherms are more or less identical and the total uptake at 95% RH is 24.76% and 24.33%, respectively. The low uptake of the pre-treated sample is likely due to the post pre-treatment wash with water, which removed most amorphous cellulose because it is much more soluble than crystalline cellulose. The similarity in hysteresis of the untreated sample (RWS) and the pre-treated sample (WCB1000W9) implies that the modification to pore size mainly takes place in the amorphous region of the cellulose.

The results of BET specific surface measurements on all three samples are summarised in Table 2. It can be seen clearly that the pre-treatment increases the specific surface area indeed, hence presents more accessible sites to hydrolytic

reaction. H.T Ng and co-workers found that after the pre-treatment, there is at least an increase by 30 times in the glucose recovery in the straw [5].

Sample ID	**BET specific surface are (cm^2/g)**
RWS	1.734459×10^6
WCB10009	1.747932×10^6
WCB10009W	1.775520×10^6

Table 2 Summary of BET specific surface area of the three samples

Conclusion

Three wheat straw samples were characterised with dynamic sorption technique using SMS DVS Advantage 1 instrument. Results showed that the uptake of the water sorption, specific surface area, amorphous content of the pre-treated samples are higher than those of the untreated raw wheat straw sample, indicating that the samples pre-treated with the twin screw extrusion technique have more accessible sites for subsequent enzymatic hydrolysis process. This has a crucial impact on the yield of the biofuel production. Further work is required to investigate the change in hydrophilicity of the wheat straw before and after pre-treatment, which was not observed as expected. This could be due to the fibre type of biomass.

Acknowledgements

Authors would like to thank T.H. Ng and co-workers at Brunel University UK for preparation of the wheat straw samples used for this study.

References

[1] F. Xu, C.F. Liu, Z.C. Geng, J.X. Sun, R.C. Sun, B.H. He, L. Lin, S.B. Wu, J. Je, Characterization of graded organosolv hemicelluloses from wheat straw, Polym. Degrad. Stab. 91 (2006) 1880–1886.

[2] Run-Cang Sun, Cereal Straw as a Resource for Sustainable Biomaterials and Biofuels, Elsevier, First edition 2010

[3] H.D. Doan, A. Lohi, V.B.H Dang, T. Dang-Vu, Removal of Zn+2 and Ni+2 by adsorption in a fixed bed of wheat straw, Process Saf. Environ. 86 (2008) 259–267.

[4] S. Panthapulakkal, A. Zereshkian, M. Sain, Preparation and characterization of wheat straw fibers for reinforcing application in injection molded thermoplastic composites, Bioresource Technology, Volume 97, Issue 2, January 2006, Pages 265-272

[5] Thian Hong Ng, Jim song, Karnik Tarverdi, Cereal straw pre-treatment for bio-fuel application: comparison between extrusion and conventional steam explosion, ResCon'11, 4th Annual Research Students Conference, School of Engineering & Design, Brunel University, 20 – 22 June 2011

[6] Jan B Kristensen**,** Lisbeth G Thygesen**,** Claus Felby**,** Henning Jørgensen and Thomas Elder, Cell-wall structural changes in wheat straw pretreated for bioethanol production, Biotechnol Biofuels. 2008 Apr 16; 1(1):5

[7] J.Y.Y. Heng, D.R. Williams "Vapour Sorption for Bulk and Surface Analysis", Solid State Characterization of Pharmaceuticals (Ed. R. Storey) Wiley-Blackwell, 2011, ISBN:9780470659359

[8] C. Karunanithy and K. Muthukumarappan, "Optimization of switchgrass and extruder parameters for enzymatic hydrolysis using response surface methodology," *Industrial Crops and Products,* vol. In Press, Corrected Proof,. ResCon'11, 4th Annual Research Student Conference, 20-22 June 2011 17

[9] S.-. Lee, Y. Teramoto and T. Endo, "Enhancement of enzymatic accessibility by fibrillation of woody biomass using batch-type kneader with twin-screw elements," *Bioresour. Technol.,* vol.101, pp.769-774, 2010

[10] C. Karunanithy and K. Muthukumarappan, "Combined effect of alkali soaking and extrusion conditions on fermentable sugar yields from switchgrass and prairie cord grass," in 2009, pp. 5165-5193.

[11] S. -. Lee, Y. Teramoto and T. Endo, "Enzymatic saccharification of woody biomass micro/nanofibrillated by continuous extrusion process I - Effect of additives with cellulose affinity," *Bioresour. Technol.,* vol.100, pp.275-279, 2009

[12] H. Jørgensen, JB. Kristensen, C. Felby. Enzymatic conversion of lignocellulose into fermentable sugars: challenges and opportunities. Biofpr. 2007;1:119–13

Proceedings of the 55th International Convention of Society of Wood Science and Technology
August 27-31, 2012 - Beijing, CHINA

Best Management Practices for Using Treated Wood in Aquatic Environments

Jeffrey J. MORRELL and Connie S. LOVE
Department of Wood Science and Engineering,
College of Forestry,
Oregon State University
Corvallis, OR 97331
United States of America
PH: +1-541-737-4222
FAX: +1-541-737-3385
jeff.morrell@oregonstate.edu

Preservative treatment of wood provides excellent protection against biological degradation, but the ability of these chemicals to migrate into the surrounding environment after installation has raised concerns about the potential risk of using treated wood in aquatic applications. Preliminary tests of utility pole sections and decking indicate that migration is greatest shortly after installation and then declines sharply to a background level. The behavior of treated wood migration suggests that steps to reduce surface deposits of chemical left after treatment might decrease chemical availability, thereby reducing the potential impacts. The potential for preservative migration from treated was assessed on penta and ACQ treated decking.

Key Words: Wood preservatives, pentachlorophenol, inorganic, aquatic risks, Best Management Practices.

Introduction

Preservative treatment has generally been viewed as an extremely beneficial method for extending the useful life of wood in extreme environments and these products can help reduce the need to harvest. However, preservatives are not without negative attributes. Most of these negatives occur when highly concentrated treatment solutions are applied to the wood in a treated facility and these risks are generally tightly controlled through worker safety regulations. Treated wood poses very little risk to the user when used properly, but one area of concern with these products is the risk of migration from the product into the surrounding environment.

Virtually all wood preservatives function by being slightly water soluble. The chemicals are present in the free water within the wood cell lumens where they are absorbed by and affect both fungi and insects that attack the wood. This water solubility is critical for function, but it also creates the potential for some of the chemical to move from wet wood and into the surrounding environment. These chemicals pose relatively little risk when released at low levels in the soil surrounding treated wood. In the case of metals, the low levels of migration are rapidly diluted with distance from the structure. Most studies find that metal levels fall to background levels within 300 mm of a treated wood structure. Organic preservatives such as pentachlorophenol or creosote can also migrate, but the components of these systems are rapidly degraded by the soil microflora.

The one area of concern with migration of preservatives from treated wood is in wood over or immersed in water. This is particularly important in water bodies with low rates of exchange. These risks have raised concerns with regulators, notably in situations where endangered or threatened species are present. This has led to restrictions and outright bans on the use of treated wood in these applications.

While preservatives have long been used to protect wood from biological degradation, there is surprisingly little information on the in-service mobility of these systems. This mostly reflects a tendency to concentrate on evaluating the effectiveness of a preservative against agents of decay. Over the past 15 years, the Pacific Northwest of the United States has been a focus of concern about preservative migration. The region is home to a number of native salmon species whose numbers have declined as result of a multitude of issues including hydroelectric dams, overfishing and changing climate conditions. The Federal government is charged with creating conditions that favor protection and recovery of endangered or threatened species. Among the steps taken has been to severely restrict the use of treated wood. These restrictions have encouraged producers of treated wood to explore a number of questions and to develop strategies for safely using treated wood in aquatic environments.

For decades, producers of treated wood contended that their chemicals did not move into the environment at appreciable levels and, when they did, were rapidly degraded. A thorough literature review and a recognition of facts indicated that this was not true. All of the preservatives in use have some degree of water solubility and can therefore move from the wood

into the surrounding environment. The rate of movement depends on the solubility of each component as well as the environment surrounding the wood. For example, studies of utility poles treated with pentachlorophenol, copper naphthenate or ammoniacal copper zinc arsenate that were exposed to natural rainfall showed that elevated chemical levels were present in the first rainwater runoff from these poles, but that this level declined sharply with continued rainfall (Figure 1). Chemical concentrations in runoff after the initial flush were similar regardless of the time interval between rainfall events, the volume of rainfall or a host of other factors. These findings indicate that chemical levels in runoff from treated wood are predictable based upon the amount of treated wood exposed to rainfall. This knowledge should allow for modeling to predict the amounts of chemical released when specific amounts of treated wood are employed in projects. Models developed by Brooks use this approach in conjunction with reported minimum effects levels to determine if projects have the potential to negatively impact the environment.

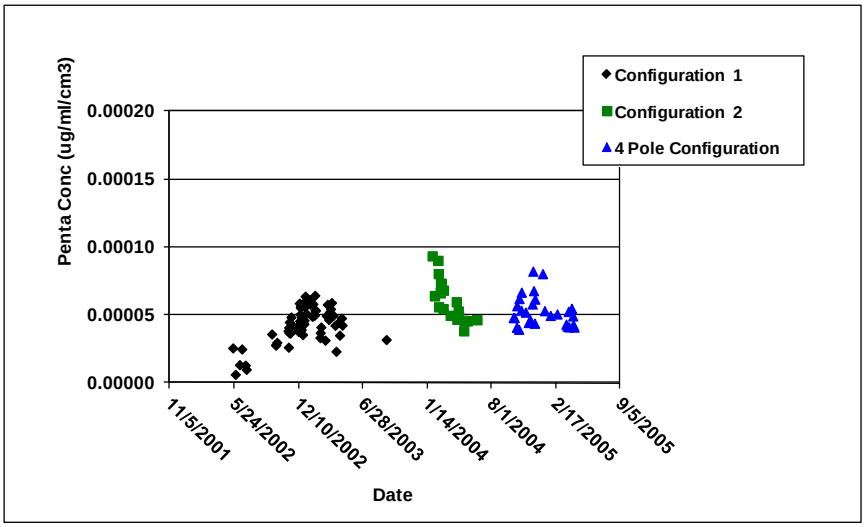

Figure 1. Example of penta levels in levels in rainwater runoff collected from beneath Douglas-fir poles treated with pentachlorophenol and exposed to natural rainfall for 4 years in Western Oregon. Groups of five poles were placed into two different configurations that exposed differing surface areas, while the final configuration exposed 4 poles in a straight line with no stacking.

The models show that effects are greatest in slow moving bodies of water. The models also showed that treated wood can be used in most environments with negligible effects; however, there have been significant debates about what constitutes an impact.

At the same time, it has become increasingly obvious that the greatest risk of using treated wood in aquatic environments occurs shortly after installation as any excess chemical on the wood surface is solubilized into the surrounding environment. Chemical levels then typically decline sharply to near background levels within 7 to 10 days. This process takes longer with wood exposed above the water and subjected to precipitation, but it follows the same basic form of a sharp increase in release following the first rainfall, then a sharp decline in preservative

concentration in the runoff in subsequent rainfall events. These trends suggested that it might be possible to modify the treatment processes to reduce the presence of surface deposits. These modifications evolved into a set of standards termed Best Management Practices or BMP's. Developed by the Western Wood Preservers' Institute, BMP's provide guidelines for treaters to use various treatment processes to reduce over-treatment of the wood, reduce the presence of excess preservative on the wood surface, and, where appropriate to ensure that preservatives are as fixed or immobilized as possible prior to leaving the treatment facility.

BMP's for oil-based preservative systems use combinations of heat and vacuum at the end of the treatment process to remove surface deposits of chemical and reduce any residual internal pressure. Internal pressure can lead to later bleeding of preservatives onto the wood surface. BMP's for water based materials primarily center around immobilizing the metals either by volatilization of the solvent or by reactions between the metals and the wood. This is most often accomplished using some form of heat, either steaming or kiln drying.

The BMP's also include simple recommendations for users of the treated product such as collecting all shavings and sawdust produced during field fabrication. Shavings and sawdust have extremely high surface areas and releasing them into the water beneath a structure and sharply increase the amount of preservative released after construction.

While BMP's should reduce the risk of releasing preservatives into the environment, there remains relatively little data on the effectiveness of these processes. In preliminary tests, Douglas-fir decking was pressure treated with either pentachlorophenol in oil (Penta) or ammoniacal copper quaternary (ACQ) compound to the above ground retention for each chemical (4.o kg/m^3). One half of the material from each treatment was then subjected to a BMP process. In the case of the penta, that involved steaming and vacuums to remove as much excess preservative as possible. In the case of the ACQ, the process involved a long vacuum to remove solvent. These materials were then used to construct small deck sections which were placed into containers that were placed outdoors in Western Oregon. The decks were subjected to natural rainfall and any water striking the decks fell into the containers where it could be collected for later analysis. Runoff was collected after any measurable rainfall event. Penta was extracted from the water column and analyzed by GC-MS, while ACQ runoff was acidified and analyzed by ion coupled plasma spectroscopy.

Penta concentrations in the runoff were slightly elevated shortly after installation then fell to approximately 1 ppm regardless of the volume of rainfall to which the materials were subjected (Figure 2). These tests only included BMP treated material. Conversely, metal levels in runoff from ACQ treated decks was initially much higher, and then dropped sharply with increasing rainfall (Figure 3). Once again, the metal levels fell rapidly to a background level. Analyses also showed a tendency for metal levels to be lower in runoff from BMP treated wood; however, these trends have been reversed in other tests of this chemical. In general, the results support the premise that the greatest risk of environmental impact occurs shortly after installation. They also showed differences in behavior with the two systems. Penta releases are much more limited, reflecting the low water solubility of this preservative. As a result, the initial spike in release is

relatively small. Copper has much higher water solubility and, as a result, the initial increase in metal levels is consistent with that enhanced solubility. In both cases, chemical levels rapidly declined to near background levels.

The lack of a consistent BMP effect was initially perplexing and suggested that BMP's might not be necessary; however, further discussion with several wood treaters revealed that many of the BMP practices have now become standard plant practice for all treated products. As a result, most of the material entering the market has already been subjected to some BMP treatment. Despite these practices, it seems prudent to continue to require BMP's for products destined for aquatic applications to ensure that the material is properly treated.

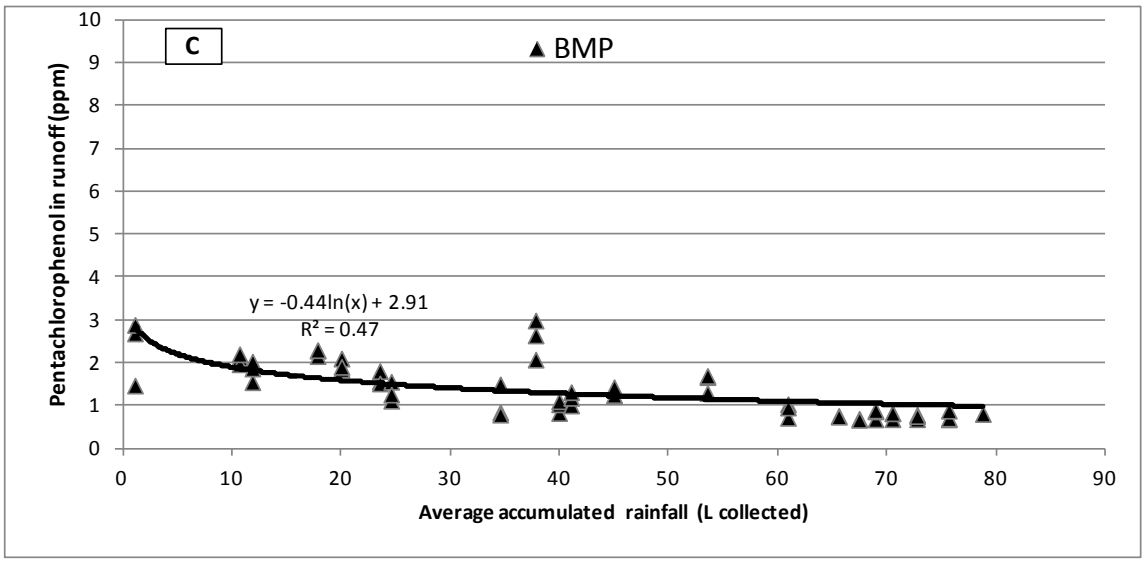

Figure 2. Concentrations of pentachlorophenol in runoff from penta treated decks subjected to natural rainfall.

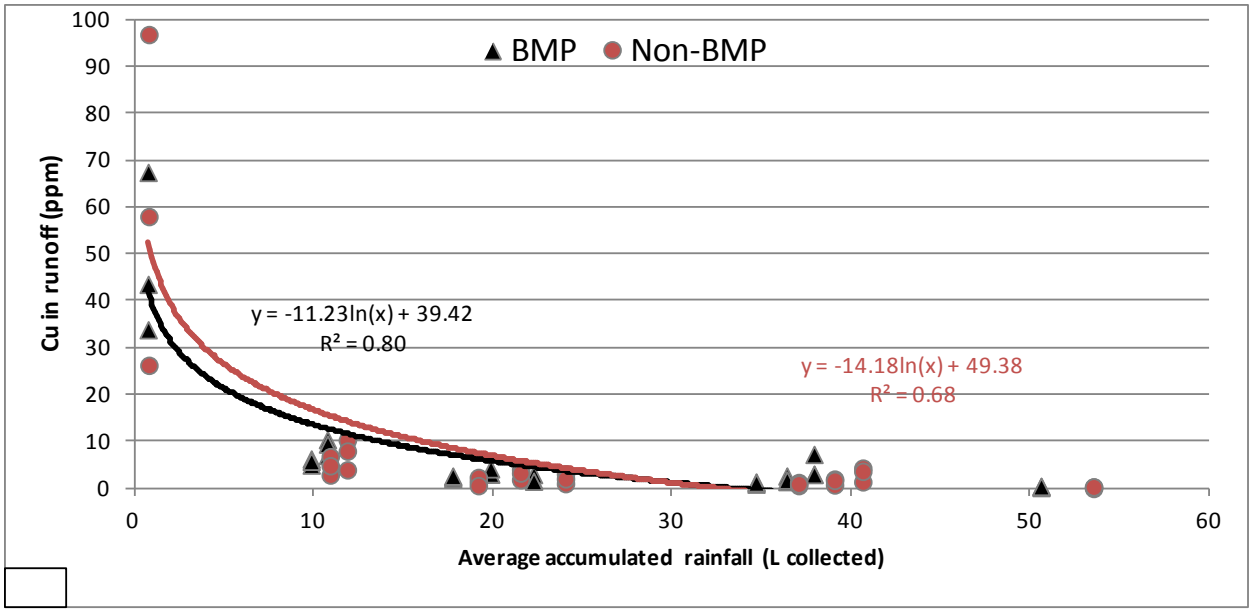

Figure 3. Concentrations of copper in runoff from ammoniacal copper quat (ACQ) treated decks subjected to natural rainfall. One half of the material was treated using Best Management Practices while the remainder was treated without supplemental practices to reduce migration.

Conclusions

While preservative treatment markedly extends the useful life of a variety of wood products, it also must be used properly to ensure that chemicals migrating from the material do not adversely affect the environment. One method for reducing the risk of impact is the use of Best Management Practices to reduce over-treatment and, as much as possible, immobilize chemical in the wood. Field trials suggest that properly treated wood poses the greatest risk shortly after installation and proper treatment coupled with careful installation can sharply reduce the impacts of using these products.

Influence of UF Resin on Characteristics and Bio-efficiency of Pyrolysis Liquids of Wood-based Panels

Jun Mu

Yongshun Feng

Shihua Chen

Sijin Li

College of Materials Science and Technology, Beijing Forestry University,

Beijing, China

Abstract

Pyrolysis is a promising method to reuse waste wood-based panels in the global sustainable development of forestry resources. Urea formaldehyde resin contained in these panels will largely affect the process and products of pyrolysis. By preparing particleboards with urea formaldehyde resin content of 6%, 9%, 12% and 15% respectively, experiments were carried out to clarify the influence of urea formaldehyde resin on the pyrolysis liquids of wood-based panels. Chemical components of pyrolysis liquids were analyzed by gas chromatography mass spectroscopy. Bio-efficiency was evaluated by examination the growth of white rot fungus *Coriolus versicolor* and brown rot fungus *Gloeophyllum trabeum*. Compared with solid wood, urea formaldehyde resin in the wood-based panels would make the pyrolysis liquids from acidic to alkaline. Components analysis showed that pyrolysis liquids of wood-based panels were greatly different from those of solid woods, especially for the nitric compounds. It was found that pyrolysis liquids of urea formaldehyde resin had strong inhibition effectiveness against fungi while pyrolysis liquids of wood-based panels also showed resistance against fungi, with inhibition rate of around 20%.Components degraded from urea formaldehyde resin contained in wood-based panels during the thermal process might contribute to the fungal inhibition of pyrolysis liquids of wood-based panels. Therefore pyrolysis liquids of wood-based panels have potentials to work as a component of preservatives for wood protection.

Keywords: bio-efficiency, GC-MS, pyrolysis, UF resin, wood-based panels

Introduction

Considering conventional fossil fuels are at the verge of getting extinct, bioresource and bio-energy have been widely studied and have already been used in practice in many countries. Pyrolysis as a kind of thermo-chemical conversion process shows great potentials in utilization of bioresources. Pyrolysis products include char, pyrolysis liquids and gases, which could be further upgraded into energy and high value-added chemical feedstocks. However the collection and logistics make the cost of biomass unacceptable in industrial production in some places. Every year in China, huge amounts of wood-based panels have been produced and consumed (Qian et al. 2010). As the civil rubbish, waste wood-based panels have very low cost but high content of lignocellulosic components, which could be used for energy recovery and materials reuse through thermo-chemical conversion. However the resins contained in wood-based panels accounting for around 10% would make pyrolysis characteristics of wood-based panels different from common biomass and the releasing nitric gases would do harm to the environment and human beings.

Study on the pyrolysis of urea formaldehyde (UF) resin and melamine formaldehyde (MF) resin suggested three reactions involved in the pyrolysis including initiation reactions, reactions splitting off volatile fragments and reactions forming stabilized structures. HCN yield was affected by temperature and air fed (Hirata et al. 1991). The pyrolysis study of UF resin by TG-FTIR also showed that the emissions of UF resin identified in the pyrolysis were CO_2, CO, HCN, HNCO and NH_3, with HCN as the most important nitrogen-containing gaseous products at low temperature. Therefore UF resin should be pyrolyzed at low temperature and burnt at high temperature for pollutant controlling (Jiang et al., 2010). For the wood-based panels containing UF resin, selective pyrolysis happened for UF resin and wood in waste wood board so that nitrogen could be effectively removed by low temperature pretreatment (Girods et al. 2008). There was still around 3% nitrogen in the char of waste wood board and if prepared into activated carbon, it could show excellence performance to acid gases and phenolic compounds due to the nitrogen-containing surface groups (Girods et al. 2009). Pyrolysis liquids were also different from wood vinegar with good inhibition ability to wood fungi (Mu et al. 2011, Nakai et al. 2007).

Apart from research works mentioned above, study of pyrolysis of waste wood-based panels is still lacking especially on the influence of UF resin contained in wood-based panels. In this paper, pyrolysis of particleboards with different UF resin content was done and characteristics of pyrolysis liquids together with their bio-efficiency were then analyzed.

Materials and Methods

Samples Preparation

The solid materials prepared for the experiment were wood, particleboard with 6% UF resin content (6%PB), particleboard with 9% UF resin content (9%PB), particleboard with 12% UF resin content (12%PB), particleboard with 15% UF resin content (15%PB) and UF resin. The molar ratio F/U of UF resin was 1.089. Pyrolysis liquids were obtained from pyrolysis of

different samples in the static batch bed. For each experiment around 500g samples were put in the reactor with the target temperature of 500℃ in 2h and hold at 500℃for 1h.

GC-MS Analysis of Pyrolysis Liquids

The chemical components of pyrolysis liquids were analyzed by GC-MS (Shimadzu 2010). A column (RTX-5) with the diameter of 0.32mm, the length of 30m and the thickness of film of 0.5μm was maintained at 50℃ for 2min. The temperature program was set at the heating rate of 10℃/min to 250℃and held at 250℃for 5min. The carrier gas was helium and the split mode was 30:1 with the injection temperature of 250℃. The ionization energy was 70eV in the mode of electron ionization (EI) and the scan range for m/z was 33-500.

Evaluation of Bio-Efficiency of Pyrolysis Liquids

The fungicidal effectiveness of pyrolysis liquids was tested against white rot fungus *Coriolus versicolor* and brown rot fungus *Gloeophyllum trabeum* in vitro. PDA medium was used with pyrolysis liquids diluted to a concentration of 0.5% to cultivate fungus. PDA medium was autoclaved at 121℃,0.1MPa for 20min. The PDA medium was poured into Petri dishes, which were then centrally inoculated with a 0.5mm plug of each fungi. The fungi was sub-cultured from the margins of actively growing cultures. Three replicates were set up for all test and controls which were with PDA medium only. All the cultures were developed in the incubator at 27℃ for 7 days when the growth of fungus in the controls reached the margin of Petri dishes. The colony diameter was screened and measured and the inhibition was calculated by the ratio of difference of colony diameter of controls and colony diameter of tested Petri dishes against colony diameter of controls. The effectiveness of pyrolysis liquids was then evaluated by the inhibition of fungal growth.

Results and Discussion

Influence of UF Resin on Characteristics of Pyrolysis Liquids

Pyrolysis products yield of different samples is shown in Figure 1. Gas yield is obtained by difference. It could be found that the yield of char from wood and PB is much stable from 21.6% (wood) to 25.7% (6%PB). The yields of pyrolysis liquids vary from 48.6% (15%PB) to 59.5% (12%PB). Although the char yield from pyrolysis of UF resin is the least and the liquid yield is the most among all the samples, pyrolysis products yields of wood-based panels with different UF resin content show no linear regulations. The influence of UF resin on the products yield of pyrolysis of wood-based panels is not significant with different resin content.

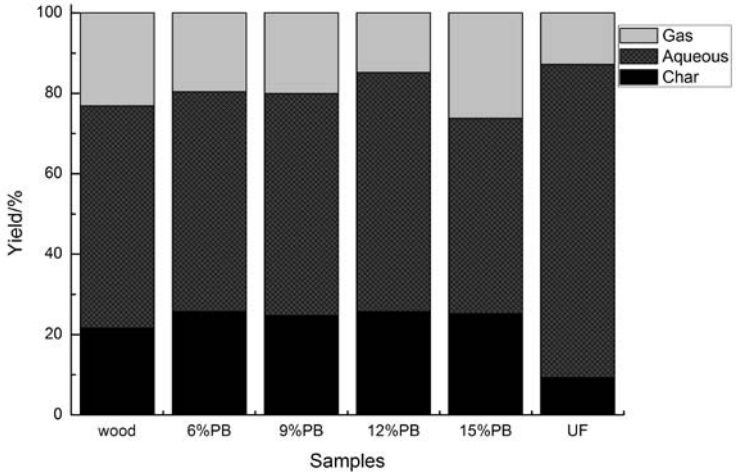

Figure 1 Pyrolysis products yield of different samples

Table 1 shows basic characteristics of pyrolysis liquids of different samples. It could be found that pyrolysis liquids contain large amount of water, as much as around 60%.

Table 1 Fundamental properties of pyrolysis liquids of different samples

Samples	**Moisture content/%**	**Water content/%**	**Density/(g/cm^3)**	**pH**
Wood	8.1	57.5	0.98	2.66
6%PB	7.0	60.5	0.98	5.50
9%PB	7.1	53.7	0.97	5.74
12%PB	7.6	63.8	0.97	6.01
15%PB	7.7	55.2	0.99	7.92
UF	0.8	53.5	1.06	9.82

Among the pyrolysis liquids of wood, PB with different UF resin content and UF resin, no significant regulations could be found in water content and density while pH of pyrolysis liquids from PB greatly changed because of UF resin. The presence of UF resin would make the pyrolysis liquids of wood-based panels from acidic to alkaline and pH value increases with the increase of UF resin content. Together with the results of products yield, it could be concluded that the influence of UF resin on the characteristics of pyrolysis liquids of wood-based panels is mainly on the chemical components rather than the products yields.

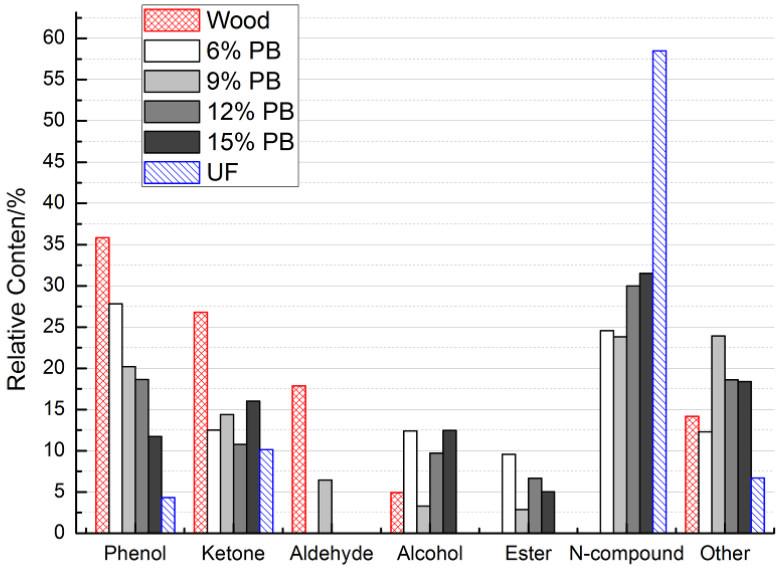

Figure 2 Relative contents of chemical components of pyrolysis liquids of different samples

In order to further make clear the influence of UF resin on the pyrolysis liquids of wood-based panels, chemical components were detected by GC-MS and the relative contents are listed in Figure 2. It could be found that phenol is the most important compound in wood but not in wood-based panels or UF resin. The transformation and fixation of nitrogen in UF resin is mainly on the nitrogen-containing compounds such as amides and ketones while the influence of UF resin on phenols, aldehydes, alcohols and etsters is not significant. Ketones are active compounds due to the double bonds, making concerted actions easier with nitrogen groups formed by the split of linear and net linkages in UF resin during pyrolysis. Component results indicate that the most two important compounds methyl-urea and N,N'-dimethyl-urea in pyrolysis liquid of UF resin are not detected in that of wood-based panels, which might be attributed to the reactions caused by acidic atmosphere introduced by pyrolysis of wood. Most of the compounds are aromatic so it could be concluded that the influence of UF resin is probably on the lignin constituent in wood.

Bio-Efficiency of Pyrolysis Liquids of Wood-based Panels

Figures 3 and 4 show the inhibition effect of pyrolysis liquids against white rot fungi and brown rot fungi. From the effectiveness it could be found that fungus in controls grew to the margin of the dishes while the growth of fungus in dishes with pyrolysis liquids was obviously inhibited.

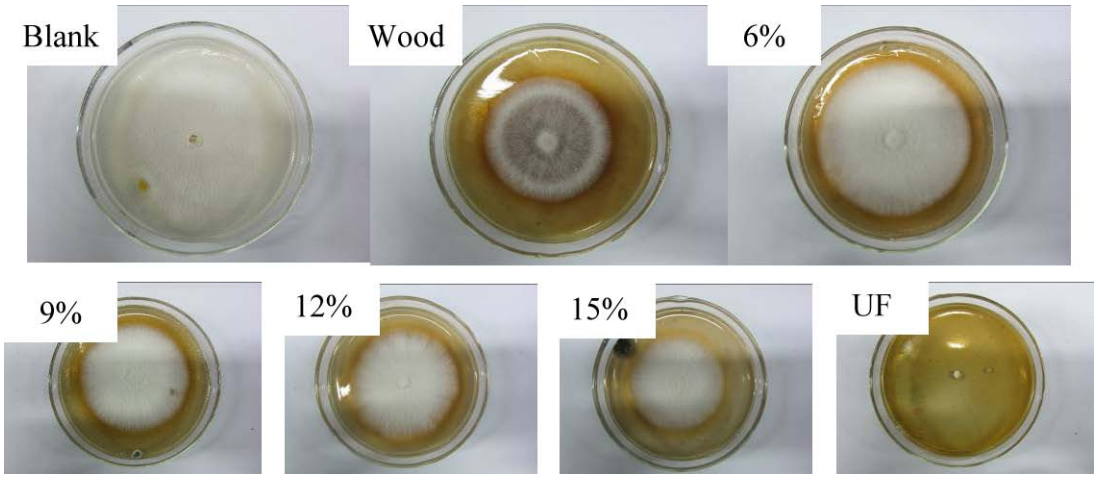

Figure 3 Inhibition effects of white rot fungi

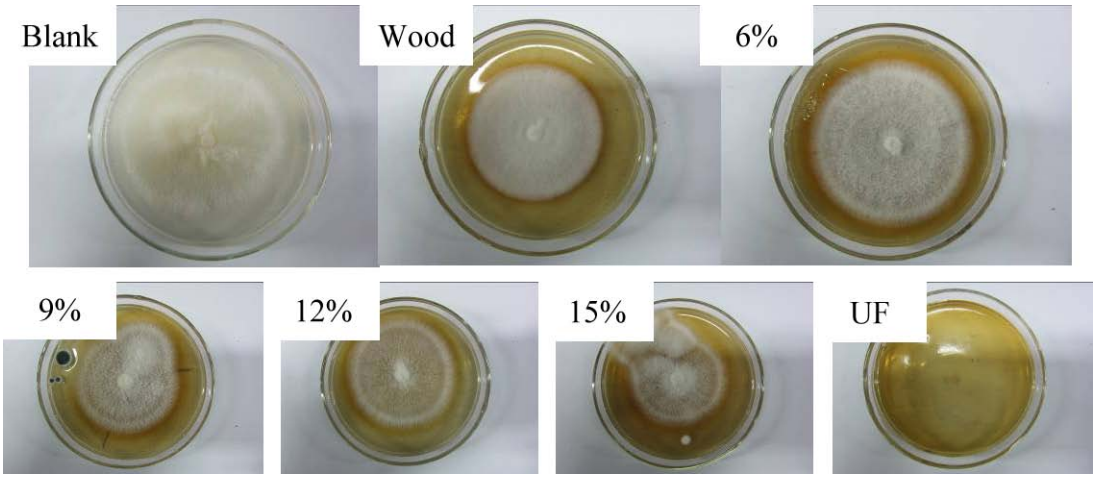

Figure 4 Inhibition effects of brown rot fungi

The inhibition rate of pyrolysis liquids of different samples against white rot fungi *Coriolus versicolor* and brown rot fungus *Gloeophyllum trabeum* are shown in Figure 5. It could be seen that pyrolysis liquids of UF resin has the strongest inhibition effect with inhibition rate of 100% against both fungus, which could be attributed the alkaline nitrogen-containing compounds. The inhibition effect of wood is better than that of wood-based panels with inhibition rate against white rot fungi to 38.7% and against brown rot fungi to 27.9%, which is in agreement with data from literatures (Nakai et al. 2007). From the results of GC-MS, phenol is the main component in pyrlysis liquids of wood but with less amount in wood-based panels and UF resin and phenol has strong antifungal activity, suggesting that valid antifungal components in pyrolysis liquids of wood are phenolic compounds while of wood-based panels are nitrogen-containing compounds. The inhibition rate of pyrolysis liquids of PB with different UF resin content varies from 8.7% to 25.7% and inhibition effectiveness constantly increases with the increase of UF resin content, which confirms former conclusions.

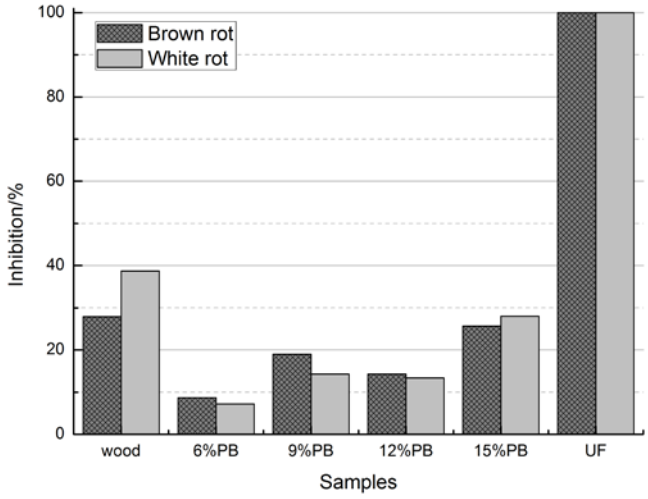

Figure 5 Inhibition rate of pyrolysis liquids of different samples

Nakai (2007) collected pyrolysis liquids of wood-based composites in different temperature ranges of room temperature-300℃, 300-400℃ and 400-500℃. Results show that pyrolysis liquids of wood-based composites obtained in low temperature range had much better inhibition effect to fungus compared with those obtained in high temperature ranges. Kartal (2004) showed that higher concentrations of the pyrolysis filtrates were critical to the inhibition against brown rot fungi. Experiments entail temperature ranges and concentrations of pyrolysis liquids of wood-based panels should therefore be further carried out.

Conclusions

The influence of UF resin on the pyrolysis liquids of wood-based panels was studied by the analysis of characteristics and components of pyrolysis liquids obtained from particleboards with different UF resin content. The main influence of UF resin is on the pH and components of the pyrolysis liquids. Nitrogen contained in UF resin is transformed mainly in the form of ketones and nitrogen-containing compounds such as amides in the pyrolysis liquids. The inhibition rate of pyrolysis liquids of wood-based panels is a little weaker than those of wood however the effectiveness increases with the increase of the UF resin content. The pyrolysis liquids have great potentials to be developed as new wood preservatives against fungal degradation. Further studies should be carried out on the specific components in pyrolysis liquids and concentrations of pyrolysis liquids should also be studied.

References

Girods, P., Dufour, A., Rogaume, Y., Rogaume, C., Zoulalian, A., 2008. Thermal removal of nitrogen species from wood waste containing urea formaldehyde and melamine formaldehyde resins. Journal of Hazardous Materials 159: 210-221.

Girods, P., Dufour, A., Fierro, V., Rogaume, Y., Rogaume, C., Zoulalian, A., Celzard, A. 2009. Activated carbons prepared from wood particleboard waste: Characterisation and phenol adsorption capacities. Journal of Hazardous Materials 166: 491-501.

Hirata, T., Kawamoto, S., Kouro, A., 1991. Pyrolysis of melamine-formaldehyde and urea-formaldehyde resins. Journal of Applied Polymer Science. 42: 3147-3163.

Kartal S.N., Imamura Y., Tsuchiya F., Ohsato K. 2004. Evaluation of fungicidal and termiticidal activities of hydrolysates from biomass slurry fuel production from wood. Bioresource Technology. 95: 41-47.

Mu, J., Yu, Z.M., Zhang, D.R., Jin, X.J. 2011. Pyrolysis characteristics of disused composite panels and properties of its products. Journal of Beijing Forestry University. 33(1): 125-128.

Nakai, T., Kartal, S.N., Hata, T., Imamura, Y., 2007. Chemical characterization of pyrolysis liquids of wood-based composites and evaluation of their bio-efficiency. Building and Environment. 42: 1236-1241.

Qian, X.Y., 2010. Current status and future challenges of wood-based panel industry in China. China Wood Industry. 4(1): 15-18.

Acknowledgements

This study was funded by National Natural Science Foundation of China (31170533).

Fixation of a Water-borne Copper Preservative in Wood by a Rosin Sizing Agent

Thi Thanh Hien Nguyen

*Shujun Li**

Jian Li

Key laboratory of bio-based material science and technology of Ministry of Education, Northeast Forestry University, China

Abstract

Samples of poplar wood (*Populus ussuriensis*) were treated with combinations of 3% $CuSO_4$ solution and 1.0%, 2.0%, or 4.0% rosin sizing agent. The fixation effect of copper preservative in wood and the efficacy of the preservatives against fungal decay was studied. The results showed that the treatment with only rosin sizing agent also had slight decay resistance. However, wood samples after being treated with the mixture of rosin sizing agent and $CuSO_4$ had good decay resistance. The average weight losses of the leached wood blocks samples degraded by both fungi *Trametes versicolor* and *Gloeophyllum trabeum* were less than 3%, were even lower than the non-leached samples. After leaching, the copper content in the leachates was analyzed by atomic absorption spectroscopy (AAS). Leaching copper from the samples treated with the copper-rosin solutions was only a half of those from the samples treated with copper alone. SEM-EDX analysis confirmed that the copper element was still in the cell lumens of leached wood blocks. This proved that the rosin sizing agent is very helpful to fix the copper preservative in wood. Therefore, the rosin sizing agent can reduce the hazard of the copper preservative leaching to the environment and help the wood treated with water-borne copper preservatives being used widely.

Keywords： rosin sizing agent, water-borne copper preservative, wood preservation, leaching resistant.

* Corresponding author: *lishujun_1999@yahoo.com*

Introduction

The efficacy of copper sulfate against wood decay due to fungi, insects, and marine borers was established in wood products from the 1970s and 1980s (Ngoc 2006). However, copper itself cannot ensure sufficient protection against wood destroying organisms because it is easily lost from treated wood (Ruddick 2000). In order to overcome this problem, copper was usually combined with other compounds such as sodium fluoride (NaF), sodium hydroxide (NaOH), arsenic (As), chromium (Cr), borate, *etc.* Among these compounds, chromate copper arsenate (CCA) has been used extensively for wood preservation for the longest. Nevertheless, recognition of the risks to human's health and potential environmental damage, CCA was completely banned in the European Union and limited to nonresidential uses in the United States (Townsend and Solo-Gabriele 2006).

Recently several methods have been researched to decrease copper leaching from wood, such as combined impregnation (Treu *et al.* 2011), incorporating additives into the preservative formulations (MitsuhashiGonzalez 2007), and combining copper with other co-biocides (Chen 2011; Humar et al. 2007). Some natural resources, such as enzymatic-hydrolyzed okara, soy protein products have been used to enhance the fixation of antifungal salts in wood structures (Ahn et al. 2010; Yang et al. 2006). Rosin, which comes from softwood, is abundant, natural, and renewable. It has a good hydrophobic and wood affinity. Over the years, its main widespread application has been in the paper industry as a sizing agent (Yao and Zheng 2000). Different chemical mechanisms between copper, rosin, and wood constituents have also been investigated (Pizzi 1993a). The copper-rosin soaps obtained when dissolved in a solvent (ethanol) have also been impregnated into wood (Pizzi 1993b). In another study, non-solvent rosin-copper formulations with double impregnation have been proposed (Roussel *et al.* 2000) and treated wood blocks have shown good performance when leached. In addition, earlier investigations showed that a rosin sizing agent can improve the moisture absorbing ability of wood and also help improve wood decay resistance (Li et al. 2011; Li et al. 2009). Therefore, the aim of this research work was to investigate the effect of rosin size on copper fixation to develop new formulations for wood preservation and determine the efficacy of copper-rosin preservatives against fungal decay.

Materials And Methods

Preparation Sample and Treating Solutions

Wood specimens measuring 20 x 20 x 20 mm were prepared from air-dried sapwood of poplar trees (*Populus ussuriensis* Komo). Feeder strips (22 x 22 x 3 mm (longitudinal direction)) were also prepared from poplar sapwood.

The analytical copper sulfate ($CuSO_4$: Cu) was used as preservative salts to protect wood against fungal decay at one concentration of 3%. The anion rosin scattered emulsion sizing agent (R) was an industrial product and was supplied by Guangxi Wuzhou Arakawa Chemical

Industries Co., Ltd. In this study, it was used to treat wood at three concentrations (1.0, 2.0, and 4.0%). All of the other chemical reagents used in this work were provided by Tianjin Kermel Chemical Reagent Co., Ltd. and were all pure grade reagents.

Treating and Leaching Procedures

The wood blocks were first vacuum-treated for 30 minutes under a vacuum of 0.01 MPa followed by injection of the preservative mixture and then brought back to atmospheric pressure. After the blocks were completely saturated, they were removed from the solution and immediately weighed to ascertain the retention of each block. Then the treated samples were air-dried for 48 hours, oven-dried at 103 °C overnight, and reweighed to determine actual retention of each sample.

Leaching test was determined according to the American Wood Preservers' Association E11-07. The treated blocks were immersed in beakers of distilled water over which a vacuum was applied for 30 min. After the vacuum was released, the wood blocks were kept in the distilled water. After 6, 24, and 48 h and thereafter at 48-h intervals, the leaching water was removed and replaced with an equal amount of fresh distilled water. Leaching was carried out for a total of 14 days. All leachates were kept to measure the contents of copper leached from the treated wood blocks by using an atomic absorption spectroscopy (AAS) analyzer.

Decay Test

Decay test was evaluated in accordance with Chinese standard LY/T 1283-1998. The white-rot fungi *Trametes versicolor* and brown-rot fungi *Gloeophyllum trabeum* were used as test fungi. Soil culture bottles with feeder strips on the soil surface were inoculated with fungus cultured on potato dextrose agar. After the feeder strips were covered with mycelium of the test fungi, sterilized wood blocks were placed onto the feeder strip. The soil-block culture was incubated in a temperature and humidity- controlled chamber at 28°C and 75% RH for 12 weeks. After exposure to the fungi, the blocks were removed from the decay bottles, brushed free of mycelium, dried at 103 °C overnight, and weighted to determine weight loss.

Microscopic Observation by SEM-EDX

After the decay test, the wood blocks were sliced into thin samples using a razor blade. The samples were mounted on a metal stub and were sputter-coated with a thin layer (approximately 20 nm thick) of gold. The specimens were then observed with a scanning electron microscope (SEM, FEI Quanta 200; USA). Random observations were made on different structures to identify the existence of copper in the anatomical structure of the specimens. The element composition was determined by regional analysis using an energy dispersive X-ray spectrometer (EDX) combined with the SEM.

Results And Discussion

Retention Results

Retention levels and percent actual retention of preservative formulations in wood blocks are recorded in Table 1. Total uptake of treating solutions in poplar wood, including both rosin alone and in combination with copper, were relatively uniform. The actual retentions of the copper-rosin preservatives were very close to theory retention, above 85%. Results indicated that the concentration of the solutions considered using the impregnation method described did not influence the penetration of the preservative complexes into the wood blocks.

Table 1 *Retention Levels and Treatability of Wood Samples Treated with Solutions*

Solution and Concentrations	Theory Retention (kg/m^3)	Actual Retention (kg/m^3)	Treatability[a] (%)
1.0% R + 3.0% Cu	33.95 (0.93)[b]	33.48 (1.66)	98.38 (2.32)
2.0% R + 3.0% Cu	41.61 (1.69)	39.30 (2.07)	94.41 (2.17)
4.0% R + 3.0% Cu	58.32 (1.68)	52.29 (1.97)	89.66 (2.52)
3.0% Cu	26.06 (1.26)	25.05 (2.14)	96.01 (4.49)
1.0% R	7.9 (0.32)	7.75 (0.52)	98.22 (6.34)
2.0% R	15.83 (0.94)	15.32 (1.32)	96.91 (7.34)
4.0% R	31.72 (0.39)	27.06 (1.34)	85.33 (6.23)

[a] Treatability refers to the percentage of actual preservative retention to the total retention.
[b] All results are means of 24 samples. Standard deviations are in brackets.

There were slight differences in the treatability of the three rosin formulations. The actual percent retention of preservative solution-containing rosin decreased from 98.22 to 85.33% with the increase in concentration of rosin from 1.0 to 4.0% in the impregnation solution. An explanation for this would be that when the concentration of rosin increases, the emulsion viscosity increases, which might be partially responsible for decreasing the actual retention of preservatives. However, this decrease was not significant and the highest retention was obtained with 1% rosin size and 3% added copper sulfate.

Copper Leaching

The analyzed results of copper ions released from blocks treated with the copper-rosin solutions and those treated with the copper sulfate alone taken at different time intervals is presented in Fig. 1. A significant reduction of copper ions leaching from wood samples treated with the copper-rosin solutions was observed. For all samples, the unfixed copper rapidly leached from wood during the first stages of the leaching process, and decreased significantly over time. However, the leaching of copper occurred much more slowly when wood samples were treated with rosin-copper solutions (Fig. 1). A large amount of copper ions was leached

out from wood samples treated with copper sulfate alone. After 9 leaching cycles, 715.49 mg of copper was leached out from the samples, which represented 69.3% of the copper impregnated in the wood blocks. However, the total amount of copper ions release from the samples treated with the copper-rosin solutions was 2 times less than those from the samples treated with only copper sulfate. The treatments with copper-rosin showed that content of Cu ions leaching slightly decreases with the increase of rosin concentration in the impregnation mixture. However, this difference was not significant and the results suggest that the rosin sizing agent in three concentrations had also a certain effect on the fixation of copper.

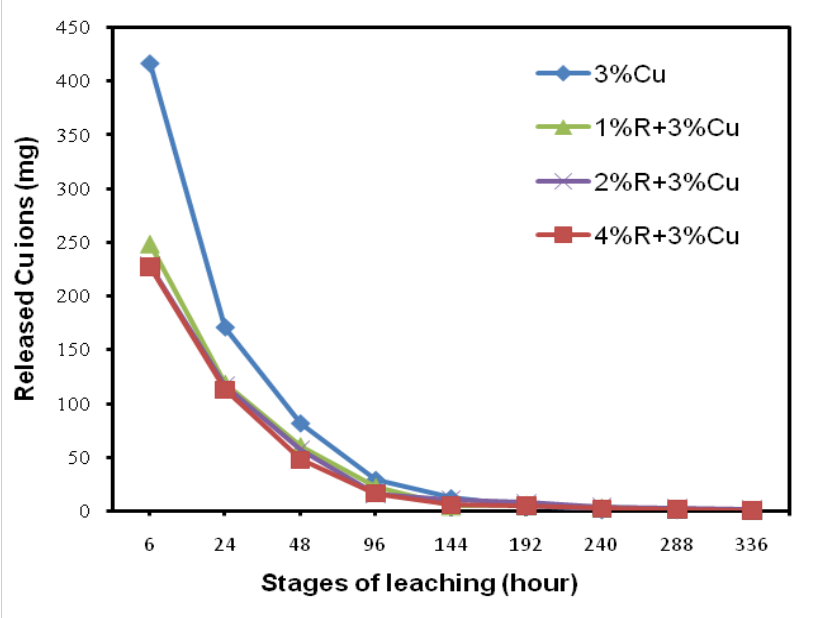

Figure 1. *Copper ions released from treated wood specimens at different time intervals.*

Decay Resistance

The results from the decay test are shown in Fig. 2. The weight losses of the control wood blocks against *Trametes versicolor* and *Gloeophyllum trabeum* were 70.45% and 61.84%, respectively. The unleached wood blocks treated with copper alone had approximately 4% or less weight loss for both test fungi. However, a severe weight loss (approximately 40%) was found for the leached wood samples treated with only copper.

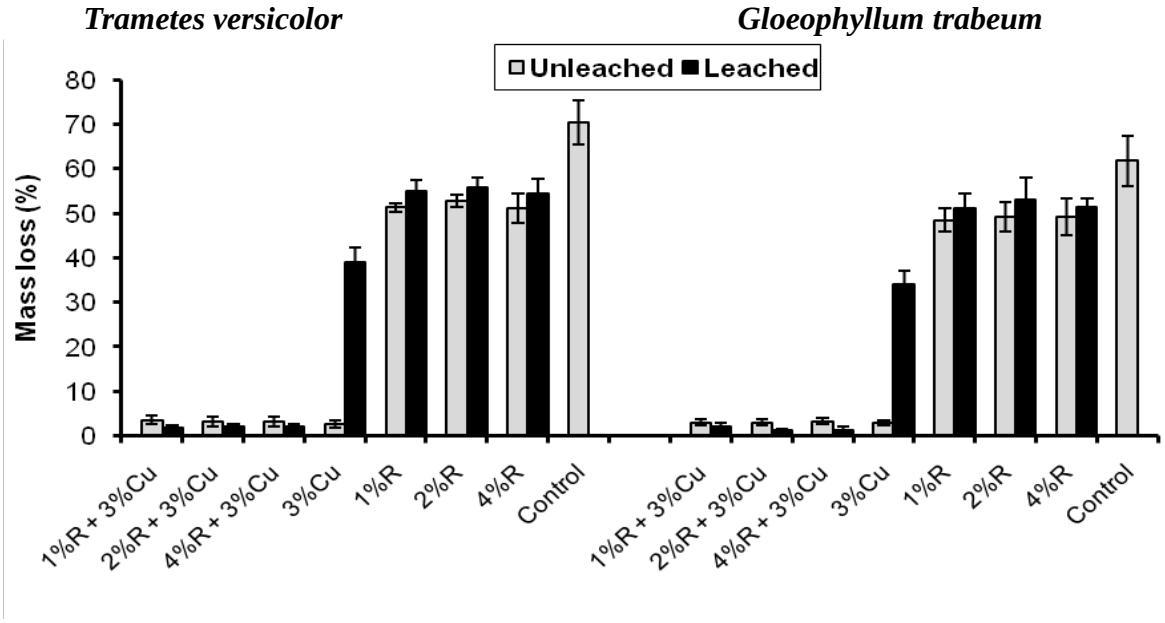

Figure 2. *Weight loss (%) of samples exposed to T. versicolor and G. trabeum attack.*

For the samples treated with only rosin sizing agents and leached had weight losses in the range of 48-55%, which was much lower than those of the untreated control samples. This signifies that the rosin sizing agent itself also has poor performance against fungal wood decay because of its water repellency and inherent decay resistance rather than general toxicity (Eberhardt et al. 1994). However, the samples treated with copper-rosin formulations showed good decay resistance against both *Trametes versicolor* and *Gloeophyllum trabeum*. After 12 weeks, the average weight loss of the samples degraded by fungi was approximately 4%. The leached wood blocks treated with copper-rosin formulations showed less than 3% weight loss and were not entirely covered by mycelium of both test fungi. Therefore, the use of rosin size as fixed agents may reduce environmental impact of wood treated with copper-based preservatives.

Microscopic Observation and Analysis

Figure 3 shows the SEM images of the control wood sample before and after the fungal exposure. It can be clearly seen that surface of wood cell wall of the control sample before the fungal exposure was extremely smooth (Fig. 3 left). After the fungal exposure, wood cell walls have been completely destroyed by the fungi (Fig. 3 right). When the wood blocks treated with copper sulfate alone and combination with rosin were observed, various crystal particles as well as spherical agglomerates were found in the cell lumens (Fig. 4).

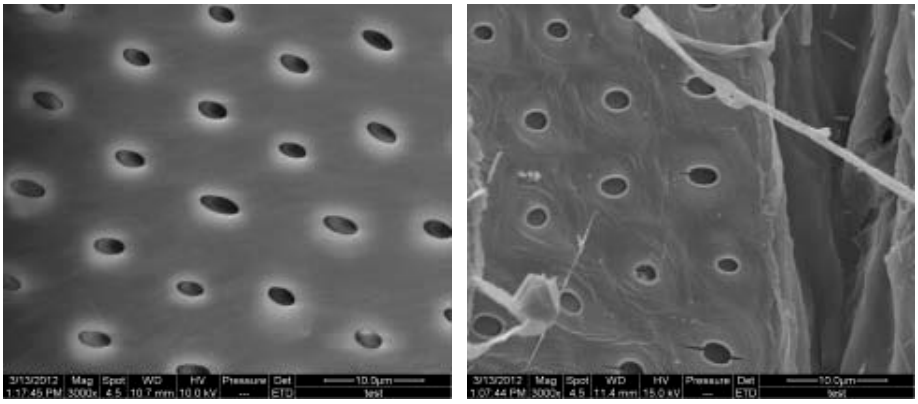

Figure 3. *Scanning electron microscopic images of control wood block before (left) and after (right) exposed to fungus.*

In the microscopic observation of the wood blocks treated with copper-rosin after leaching and decay, various spherical agglomerates were easily detected in the cell lumen (Fig. 5a,b). The spectrum obtained from the spot analysis confirmed that these agglomerates contained the element Cu (Fig. 5c,d). This signifies rosin interacted with copper and formed an adhesive film to cover the copper crystals. Therefore, Cu was fixed into the wood blocks. The SEM-EDX analysis results suggested that the presence of the preservative complexes containing Cu contributed to the good decay resistance of the leached wood blocks treated with the mixture of rosin size and copper sulfate.

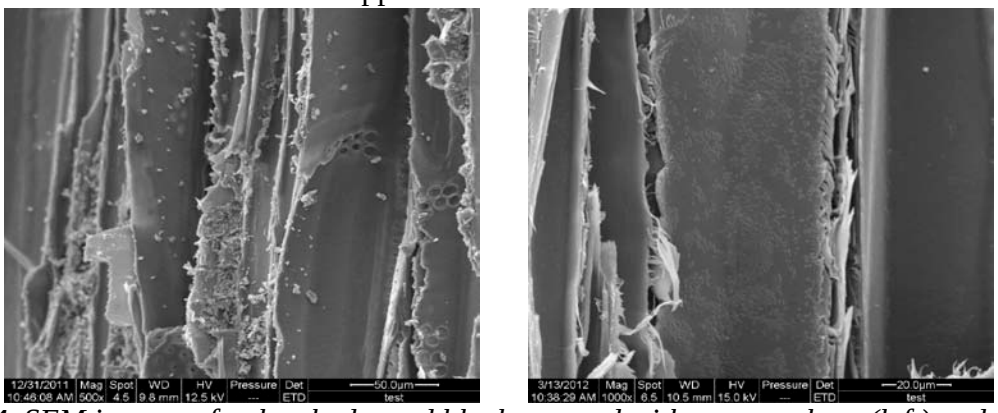

Figure 4. *SEM images of unleached wood blocks treated with copper alone (left) and with copper-rosin (right).*

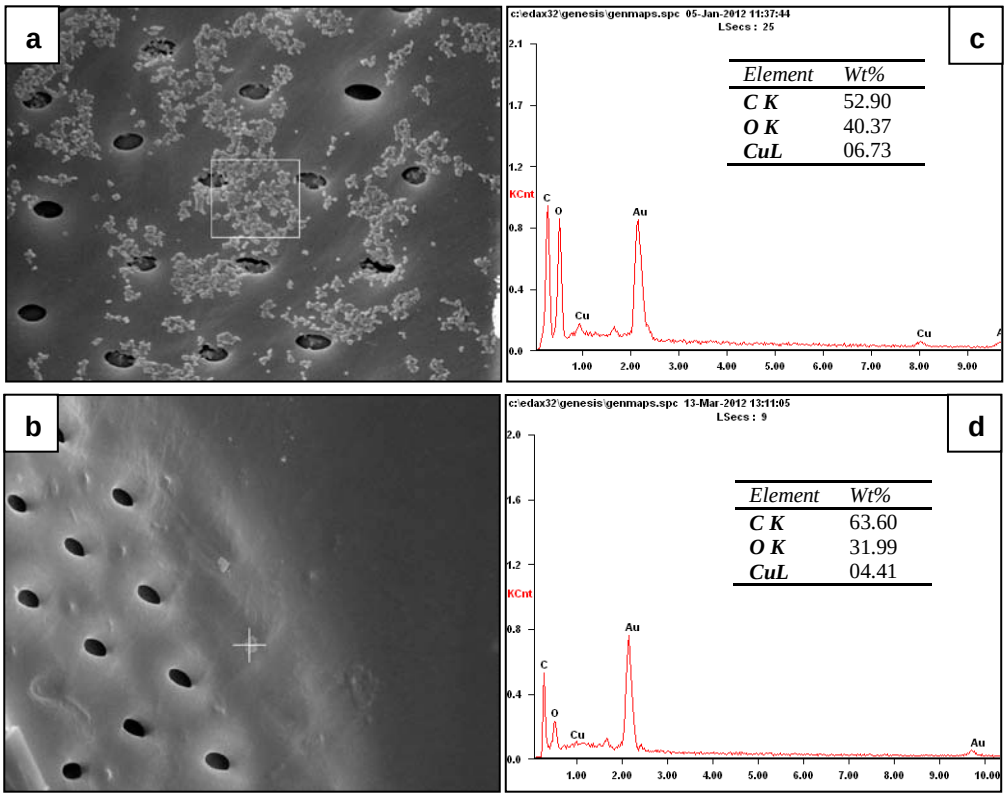

Figure 5. *SEM images (left side) and corresponding spectrum (right side) of wood blocks treated with copper-rosin: (a,c) after leached and (b,d) after leached and decayed.*

Conclusions

This study determined effect of rosin size on copper fixation and decay resistance of wood treated with copper sulfate and rosin sizing agent, separately or in combination, against white rot fungi *Trametes versicolor* and brown rot fungi *Gloeophyllum trabeum.* The results showed that, poplar wood after being treated with copper-rosin solutions were more effective against fungal wood decay than those impregnated with only copper after leaching. The average weight losses of the samples degraded by fungi were less than approximately 3%. The rosin size agents themselves also showed poor performance against wood decay fungi. The result of AAS analysis showed the amount of copper ions released from the samples treated with the copper-rosin solutions were 2 times less than those from the samples treated with copper alone. The SEM-EDX analysis of the wood blocks treated with copper-rosin confirmed that the element Cu existed in the cell lumens of leached and decayed wood blocks.

Acknowledgements

The authors are grateful for the support of the Vietnamese Government and the National Natural Science Foundation of China No. 31070487.

References

Ahn et al. 2010. Environmentally friendly wood preservatives formulated with enzymatic-hydrolyzed okara, copper and/or boron salts. Journal of Hazardous Materials. 178: 604-611.

Chen, G. 2011. Laboratory evaluation of borate:amine: copper derivatives in wood for fungal decay protection. Wood and Fiber Science. 43(3): 271-279.

Eberhardt, T. L., Han, J. S., Micales, J. A., and Young, R. A. 1994. Decay resistance in conifer seed cones: Role of resin acids as inhibitors of decomposition by white rot fungi. Holzforschung. 48(4): 278-284.

Humar, M., Žlindra, D., and Pohleven, F. 2007. Improvement of fungicidal properties and copper fixation of copper-ethanolamine wood preservatives using octanoic acid and boron compounds. Holz Roh Werkst. 65: 17-21.

Li, S., Thanh-Hien, N. T., Han, S., and Li, J. 2011. Application of Rosin in Wood Preservation. Chemistry and Industry of Forest Products. 31(5): 117-121.

Li, S., Wang, X., and Li, J. 2009. Effect of two water borne rosin on wood protection. Transaction of China pulp and paper, 24(supplement): 200-203.

Mitsuhashi Gonzalez, J. M. 2007. Limiting copper loss from treated wood in or near aquatic environments. Master's Thesis, Oregon State University, Corvallis, Oregon.

Ngoc, N. T. B. 2006. Wood preservation (in Vietnamese). Agriculture Press, Ha Noi.

Pizzi, A. 1993a. A new approach to nontoxic, wide-spectrum, ground-contact wood preservatives. 1. Approach and reaction mechanisms. Holzforschung. 47(3): 253-260.

Pizzi, A. 1993b. A new approach to nontoxic, wide-spectrum, ground-contact wood preservatives. 2. Accelerated and long-term field tests. Holzforschung. 47(4): 343-348.

Roussel, C., Haluk, J.-P., Pizzi, A., and Thévenon, M.-F. 2000. Copper based wood preservative: A new approach using fixation with resin acids of rosin. In: International Research Group on Wood Protectiont, Stockholm, Sweden.

Ruddick, J. N. R. 2000. The use of chemicals to prevent the degradation of wood. Uhlig's corrosion handbook, R. W. Revie, ed., John Wiley & Sons, Inc., Hoboken, New Jersey, Canada: 503-512.

Townsend, T., and Solo-Gabriele, H. 2006. Environmental impacts of treated wood. CRC, Boca Raton, Florida, USA.

Treu, A., Larnøy, E., and Militz, H. 2011. Process related copper leaching during a combined wood preservation process. Eur. J. Wood Prod. 69: 263-269.

Yang, I., Kuo, M., and Myers, D. J. 2006. Soy protein combined with copper and boron compounds for providing effective wood preservation. JAOCS. 83: 239-245.

Yao, X., and Zheng, L. 2000. Development potential of rosin sizing agent. Chemical Technology Market. 10: 21.

Tables Cited

Table 1. *Retention Levels and Treatability of Wood Samples Treated with Solutions*

Figure Cited

Figure 1. *Copper ions released from treated wood specimens at different time intervals*
Figure 2. *Weight loss (%) of samples exposed to T. versicolor and G. trabeum attack*
Figure 3. *Scanning electron microscopic images of control wood block before (left) and after (right) exposed to fungus*
Figure 4. *SEM images of unleached wood blocks treated with copper alone (left) and with copper-rosin (right)*
Figure 5. *SEM images (left side) and corresponding spectrum (right side) of wood blocks treated with copper-rosin: (a,c) after leached and (b,d) after leached and decayed*

Methods of Exterminating Biological Destructive Agents from Household Furniture in Jos Metropolis, Plateau State, Nigeria

Okwori, Ogbanje Robert Ph.D

Department of Industrial and Technology Education, Wood Technology Section

Federal University of Technology, Minna,

Niger State, Nigeria

Email: okworirobert@yahoo.com

Phone: +2348060996524

Abstract

This study identified methods of exterminating biological destructive agents from household furniture in Jos metropolis, Plateau State, Nigeria. It discovered types of biological destructive agents such as wood borers, ants and termites that infest household furniture in that area. The type of wood used for household furniture was also identified. Methods used in exterminating biological destructive agents were discussed. Three research questions were answered. A descriptive survey research design was adopted for the study. A structured questionnaire was used to gather data from one hundred and sixty-eight respondents. No sampling since the population wasn't much. Percentage and mean ratings were used for the analysis of data. Spearman Rank Order correlation Coefficient was used to determine the reliability of the instrument. The reliability coefficient of the instrument was found to be 0.82. The findings of the study revealed that majority of the cabinet makers used oil can to apply kerosene and use brush to apply creosote oil for exterminating biological destructive agents. The wood mostly used by cabinet makers for constructing household furniture was Achuwele (Hardwood). The biological agents that infest household furniture in that area were powder post beetles, ants and termites. It was recommended that baygun spray (insecticide) should be used since it is stronger, effective and faster in killing wood borers, hardwood such as Mahogany, Iroko and Agbuntu should be used for constructing household furniture. The wood to be used for furniture should be properly seasoned and the moisture content of such wood should not be more than twenty percent.

Key words: Biological agents, cabinet maker, Furniture, Insecticide, Preservative, termites, wood borer.

Introduction

Furniture are items such as tables, chairs, beds, cupboards and so on used in the houses offices, hospitals, schools, hotels and recreational areas for the comfort of man. Hornby (2000) defined furniture as moving articles such as tables, chairs or beds put into a house or an office to make it suitable for living or working. In the same opinion, Walton (1981) classified furniture as case furniture e.g wardrobes, wall cabinets and book cases; tables e.g tea, coffee or silver tables, beds and chairs. Walton further said that furniture can be made of metal or wood. Walton disclosed that the increase in domestic comfort especially in the palaces and houses led to the demand for more and better furniture expected to be constructed by cabinet makers.

Love (1979) identified wood used for furniture construction and these are softwood and hardwood. The softwood include yellow or red deal, (North or Scots pine) (Pinus sylverstris); douglas fir, sitka spruce; Larch and sequoia pine. Hardwood used for furniture are Amenican white wood, Ash Beech, Birch, Ecma, Greenheart, Jarrah, Lime, Mohagany, Maple Oak, Teak and walnut. The wood commonly available in west Africa includingNigeria are Agba, Ebony, Gaboon, Mohagony, Mansonia, Obeche and Sapele(Love,1979).

Biological destructive agents are the biological agents that infest household furniture. This includes Beetles, Insects, termites, fungi and so on. Household furniture can be infested due to several reasons such as high moisture content of the wood, failure to select the right wood for the furniture and also the workmanship.

Literature Review

The most common powder post beetles that infest furniture are Anobiid powder post beetles, Bostrichid powder post. Beetles and LyctidPowder post Beetle. The other wood infesting pests are old house borers and carpenter bees (Kochler & Oi, 2012). The Larvae of powder post beetles lived in and consumed dry seasoned wood. It was revealed that the Anobiid powder post beetle infest seasoned softwood and sapwood of seasoned hardwood. These Anobiid powder post beetles infest hardwood furniture, wall paneling, window, door mouldings. Woods such maple, beech, poplar and pine are susceptible to attack. The Bostrichid Powder post Beetles infest seasoned softwood and hardwood especially unfinished furniture while the Lyctids infest sapwoods of hardwoods mainly ash, oak and mahogany. It easily attack items made from wood that was improperly dried or stored (kochler& Oil,2012). Below are the biological agents that infest household furniture in Nigeria.

Courtesy:Carpenter, J(2012), Fig.1Anobiid Power Post Beetle

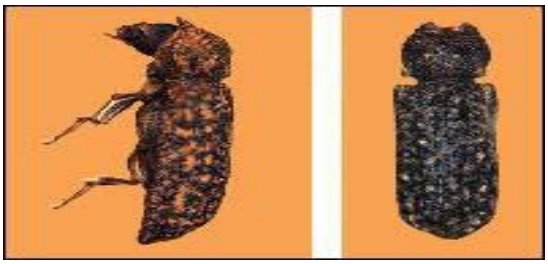

Fig.2 Bostrichid Power Post Beetle

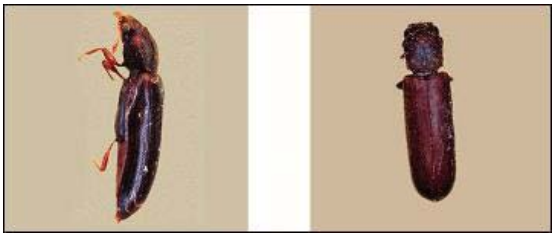

Fig.3 Lyctid Power post Beetle

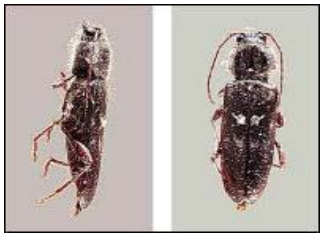

Fig.4 Old House Borer

The old house borer infests softwoods in Florida and also in Nigeria. They bore through the wood making irregular galleries. The Larvae damage both inside and surface of the wood and create tunnels. The carpenters bees cause damages to wood by creating tunnel on the wood. Koehier and Oi also described ants and termites as one of the biological agents that cause damages to furniture. Most ants and termites eat a variety of foods, although, some have specialized tastes such as fire ants feed on honeydew, sugars, proteins oils, seeds, plant and insects.

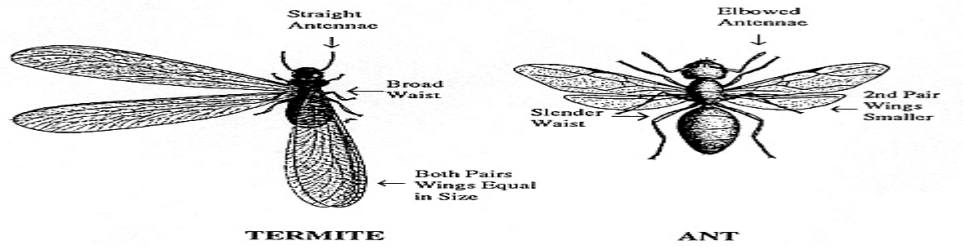

Ecosmart (2012) said that carpenter bees (Xylocopa latrecille) prefer to lay eggs in wood that are unpainted.It infest Furniture made of redwood, cedar, cypress and pine. Powder Pest Beetles Control Service (2012) disclosed that in India, the adult beetles are small ranging from 2-7mm in length, high sign of infestation is manifested by yellowish powder falling from furniture like an excreta of the organism. The Larvae eat hardwood and made tunnels in timbers. Ecosmart (2012) identified other wood borers to be shipworms (Bankia Setacea), Metallic wood Bores (Buprestidae Coleoptera), Horntails (Siricidae Tremex). The shipworms situate themselves on a wood source and begin their tunneling from there. They dwell in water and often attach themselves to vessels. Metallic wood borers are also called jewel beetles.

Poster and Reg (2006) discovered another wood destroying agent to be fungi. This could be non-rotting fungi and wood-rotting fungi. The non-rotting fungi (Sap stain) take their nourishment from the tree's food reserves left within sapwood of timber produced from softwood species and light coloured hardwoods. These fungi may attack softwood with distinct heart wood such as pines and larches, temperate hardwood e.g poplar, ash and tropical hardwoods e.g obeche, Jelutong, ramin and balsha wood.

In wood-rotting fungi, whenever the following conditions exist, one or more of these types of fungi will eventually establish. The types of fungus and its characteristics life style will be determined by the amount of moisture present in the wood. Fungi need the following to be established (a) food in form of cellulose from the wood tissue of sapwood and non-durable hardwood. (b)The wood must have moisture content above 20% (c) Temperature between 30^{o}c and 37^{o}c. Low temperature may reduce growth; high temperature will kill the fungi (d) There must be presence of air which is an essential requirement for growth and respiration of fungi.

Preventive Measures

Kochier and Oi (2012) Suggested the following preventive measures:

- Inspect wood to ensure that wood is not infested at the time of home construction.
- Beetles emerging from painted or varnished wood were either in the wood before finishing or were as a result of reinfestation by eggs that were laid in emergence holes of adult beetles. Sealing holes prevents reinfestation from eggs laid within the hole.
- spraying or brushing insecticide onto the infested holes on the wood can kill adult beetles as they chew the wood
- The infested furniture can be fumigated inside the fumigation chamber.
- Carpenter bees can be controlled by removing and replacing infested wood. Insecticides can be used to treat parts of wood where carpenter bees are active.

Ecosmart (2012) was of the view that pressure treated wood is less susptible to wood borer, therefore, wood should be subjected to the above process before usage. Spot treatment was also mentioned to control wood moisture by way of surface coverings.

Porter and Reg (2006) identified the following remedies for fungi (dry rot and wet rot).

Prevention of dry rot

- Eliminate all sources of dampness
- Remove all affested woodwork and fungus from the building.
- Surrounding walls and concrete floors etc may require sterilizing and treatment with fungicide
- All replacement timber should have moisture content less than 20% and be treated with preservative.

Prevention of Wet Rot

- Dry out the building and dampness should be avoided.
- Remove and safely dispose the effected timber
- suitable preservative should be applied to timber before use to avoid fungi
- All replacement timber must be dried and moisture content below 20% (Porter & Reg, 2006).

The development in technology in this modern society has led to increase in domestic comfort which has brought high demand for more better and sophiscated furniture in our homes. The destruction of household furniture by biological agents in Jos metropolis is at alarming rate which demands urgent attention. The researcher wonders whether this high rate of infestation of household furniture could be attributed to the type of wood used for the furniture construction or the inability of the cabinet makers to select the appropriate method of exterminating biological agents from household furniture. Kochler and Oi (2012) disclosed that Dealt Watch beetle (Anobiid) infest hardwood furniture and wall paneling. It was revealed by Kochler and Oi that this type of pest prefers to infest wood with high moisture content in poorly ventilated areas in crawl spaces of houses, utility rooms and garages.

Purpose of the Study

The purpose of the study is to determine methods of exterminating biological destructive agents from household furniture. Specifically, the study sought to:

1. Identify wood mostly used by cabinet makers for furniture construction in Jos.

2. Identify biological agents that infest household furniture in Jos metropolis.
3. Determine methods used by cabinet makers in exterminating biological agents that infest household furniture in Jos metropolis.

Research Questions

The following research questions were used for the study.

1. What type of wood Cabinet makers mostly use for furniture construction in Jos?
2. What kind of biological agent infest household furniture in Jos metropolis?
3. What are the methods used by cabinet makers in exterminating biological agents that infest household furniture in Jos metropolis?

Materials and Methods

The methodology adopted for the study is presented under the following subheadings: Research design, Area of the study, population of the study, sample and sampling procedure, instrument for data collection, validation of the instrument, method of data collection and method of data analysis.

Research Design

The study adopted survey research design based on the nature of the study.

Area of the Study

The study was carried out in Jos metropolis, Plateau State Nigeria.

Population of the Study

The population for the study was drawn from one hundred and eighty two cabinet makers and the information about the number of cabinet makers was obtained from wood workers trade union secretariat at Jos, Plateau State, Nigeria.

Simple and sampling Techniques

No sampling since all the cabinet makers were used for the study.

Instrument for Data Collection

A structure questionnaire was used for data collection. Section A sought for information on the type of wood used for furniture construction in Jos metropolis, section B sought for opinion of respondents on the type of biological agents that infest household furniture in Jo metropolis, section C sought for information on methods used by cabinet makers in exterminating biological agents that infest household furniture in Jos metropolis.

Validation of the Instrument

The instrument was subjected to face and content validation by four experts of wood technology. These experts were from Federal University of technology, Minna, Niger State, Nigeria. The recommendations of the experts were used to draft the final copy of the instrument. To check the reliability of the instrument, a piliot study was conducted using sixty cabinet makers in Minna City, Niger State, Nigeria. The researcher used test-retest to seek responses on methods of exterminating biological destructive agents from household furniture. The questionnaire was administered to the respondents at interval of two weeks. Spearman rank order correlation coefficient was used to determined the reliability of the instrument. The reliability coefficient of the instrument was found to be 0.86.

Method of Data Collection

The questionnaire was administered and collected by the researcher with two research assistants. Out of one hundred and eight two (182) questionnaire distributed, one hundred and sixty eight (168) were returned i.e 92.30% return rate.

Method of Data Analysis

Percentage and mean were used to answer the research questions. A five point likert scale was used for the study. Items having above 3.0 were accepted while those items having below 3.0 were rejected. Spearman rank order correlation coefficient was used to determine the reliability coefficient of the instrument.

Results and Discussion

Research Question 1

What type of wood Cabinet makers used for furniture construction in Jos metropolis? The data answering this research question is presented in Table 1.

Table 1

Percentage of responses of the respondents on the type of wood used for furniture construction in Jos metropolis.

S/NO	WOOD	NO	%
1.	Marobiya (Hardwood)	18	10.71
2.	Obeche (softwood)	12	8.33
3.	Agbuntu or Iron wood (Hardwood)	14	9.52
4.	Akpu (soft wood)	12	7.14
5.	Malina (Medium Hardwood)	10	5.14
6.	Akpo (Hardwood)	11	6.55
7.	Achuwele (Hardwood)	30	17.86
8.	Mahogany (Hardwood)	16	7.14
9	Abura (Hardwood)	7	4.17
11.	Iroko (hardwood)	7	4.17
12.	Afara (Hardwood)	8	4.76
13.	Mansonia (hardwood)	7	4.17
14.	Agba (Harwood)	6	3.57
15	Larch (softwood)	5	2.98

N= 168

The analysis of the result in Table 1 revealed that most cabinet makers used Achuwele, followed by marobiya and mahogany. They are all hardwood but Achuwele can easily be infested by wood borers if some parts of the timber contain sap while the other two can be infested by wood borers if they are not properly seasoned before usage. Achewele is cheaper in price when compared to Marobiya and Mahogany.

Research Question 2

What kind of biological agents infest household furniture in Jos metropolis? The result of the analysis is presented in Table 2.

Table 2

Mean of responses of the respondents on biological agents that infest household furniture in Jos metropolis.

S/NO	Biological Agent	Mean	Remark
1.	Anobiid powder post beetles	3.46	Accepted
2.	Bostrichid powder post beetles	3.35	Accepted
3.	Lyctid powder post beetles	4.08	Accepted
4.	Carpenter bees	2.92	Not Accepted
5.	Ants	3.23	Accepted
6.	Termites	3.00	Accepted
7.	Fungi	2.17	Not Accepted
8.	Wood wasp	2.58	Not Accepted

N = 168

With reference to Table 2, the respondents accepted items 1,2,3,5,6 and didn't accept items 4,7 and 8. This means household furniture were not infested by carpenter bees, fungi and wood wasp in Jos metropolis.

Research Question 3

What are the methods used for exterminating biological agents from household furniture? The response to research question 3 is presented in Table 3 below.

Table 3

Mean of responses of respondents on ways or methods cabinet makers used to exterminate biological agents from household furniture in Jos metropolis.

S/NO	Methods of exterminating biological agents	Mean	Remark
1.	Spraying Insecticides	2.38	Not Accepted
2.	Fumigation in the Chamber	1.93	Not Accepted
3.	Removing and replacing infested wood with another wood	3.81	Accepted
4.	Applying kerosene using eye dropper / oil can	4.91	Accepted
5.	Dry out the building and avoiding dampness	1.39	Not Accepted
6.	Use opaque and transparent finishes	2.92	Not Accepted
7.	Avoid using wood having moisture content above 20%	4.33	Accepted
8.	Apply creosote oil using brush	4.17	Accepted
9.	Methyl bromide	2.25	Not Accepted
10.	Mineral Turpentine	2.2	Not Accepted

N = 168

The data in table 3 showed that respondents accepted items 3,4,7,8 and didn't accept items 1,2,5,6,9 and 10. This means cabinet makers accepted using brush to apply creosote oil, applied kerosene using oil can, remove and replace infested wood with another wood and avoid using wood having moisture content above 20% for furniture construction.

Discussion

The infestation of furniture items by biological agents in Jos metropolis is so high which needs urgent attention. It was discovered from the study that cabinet makers used Achuwele (Hardwood) more than any other type of wood because it less expensive. Though, mahogany and Agbuntu are stronger and expensive than achuwele. Poster and Reg (2006) postulated that for wood to be free from wood borers and termites, the moisture content of the wood

should not be more than twenty percentage and durable wood should be selected for woodwork.

It was disclosed in the study that powder post beetles, ants and termites were the biological agents that infested household furniture in Jos metropolis. Biose (2005) explained that to prevent termite attack, termite resisting wood such as Iroko should be used and impregnate the timber with suitable preservative. To treat infested timber, the use of arsenic trioxide powder is essential. Biose reported that to prevent powder post beetles, the cabinet maker should avoid using untreated sapwood in construction work. Liquid insecticide can be forced into the tunnels with a syringe to penetrate the infested wood.

The study also revealed that use of brush to apply creosote oil, removing and replacing infested wood, use of oil can to apply kerosene and avoid using wood with moisture content above 20% were accepted by respondents. In the same opinion, love (1979) explained that much can be done to protect household furniture by sealing the open joints with wax or furniture cream and use of aromatic oil in some furniture also discourages beetles. Pest Control Service (PEPSOP) (2012) revealed that the treatment for powder post beetles is the use of oil based solution injected into the holes created then spray the holes and plug them with wood wax.

Conclusion

It is difficult to secure complete immunity from attack by biological agents such as wood borers, insects and termites. But when sound woods are selected for constructing household furniture and treated with preservative before usage, then, the rate of infestation will be reduced if not completely stopped. When household furniture is infested, it reduces the strength and durability of the furniture item. Therefore, serious attention should given to household furniture when infestation of furniture items by biological agents are noticed.

Recommendation

The following recommendations are hereby made.

1. Sound wood such as Mahogany, Agbuntu, Abura, Manosonia, iroko should be used for constructing household furniture irrespective of the price. Wood borers and termites hardly infest these woods if properly seasoned.
2. Woods should be properly seasoned at least not more than 20% moisture content before utilizing it for constructing household furniture. This will prevent or minimize attack by biological agents.
3. Household furniture should be renewed every three years by application of finishes. It can also assist in preventing wood borers, termites and ants from attacking furniture..
4. The infested part of the wood should be removed and replaced with another wood. The whole furniture piece should be protected with the application of preservatives e.g insecticide and finishes such as transparent or opaque finishes.
5. Insecticide such as baygun should be used to kill powder post beetles, ants and termites. This type of insecticide is very strong, poisonous and reliable.

References

Biose, C.A. 2005. Woodwork technology, Asaba: Otoba press Ltd.

Carpenter, J. 2012. Environmentally friendly press controls. Retrieved from http:www. biotechpestcontrols. com/html/wood-borers. html on the 18/5/2012.

Ecosmart Bug Spray. 2012. Organic Insecticides/Organic pesticides. Retrieved from http: // blog. ecosmart. Com/index. phy/2009/06/11 whats – a – wood – borers/on the 19/5/12.

Hornby, A.S. 2000. Oxford advance learners dictionary. Oxford: Oxford University Press.

Love, G. 1979. The Theory and practice of woodwork. Third Edition, Hong Kong: Wing King Tong Co. Ltd

Kochler, P.G. & Oi, F.M. 2012. Environmentally friendly press controls. Retrieved from http:www. biotechpestcontrols. com/html/wood-borers. html on the 18/5/2012.

Pest Control Service. 2012. Wood borers: Power pest beetles. Retrieved from http://www. pepsoppest Control. Com/pest – controls – services wood – borer. html on the 18/5/2012.

Porter, B & Reg, R. 2006. Carpentry and Joinery. Great Britain: Biddles Ltd.

Walton, J.A. 1981. Woodwork in theory and practice Australia: New Century Press.

Acknowledgements

I, Dr Robert Ogbanje Okwori thank the management of Federal University of Technology, Minna, Niger State for sponsoring me for this conference. I wish to extend my gratitude to those that I used their materials for this study. I also appreciate the efforts of Executive Director, Society of Wood Science and Technology for her hard work and for keeping me abreast of what is happening in the Association.

Fast Pyrolysis of Laurel (*Laurus Nobilis* L.) Seed in a Fixed-bed Tubular Reactor

Özlem ONAY
Anadolu University
Porsuk Vocational School
26470 Eskisehir, Turkey
oonay@anadolu.edu.tr

Abstract

The daphne seed can be utilized as a biomass feedstock for conversion to bio-oil with pyrolysis process. The samples were initially pyrolyzed on a lab-scale resistively heated fixed-bed pyrolysis system at different values in the ranges of 400-700 ^{0}C and 5-700^{0}Cmin^{-1} to determine the effects of operation temperature and heating rate on the yields on products, respectively. Then, the bio-oil in the highest yield (35.2%) which was obtained at pyrolysis final temperature (600^{0}C) temperature, heating rate (350^{0}Cmin$^-$1), and sweeping flow rate of 100 cm^{3}min^{-1} was characterized by Fourier Transform infra-red (FT-IR) spectroscopy, gas chromatography/mass spectrometry (GC-MS) and column chromatography. The characterization results revealed that the pyrolytic oils which were complex mixtures of C_{11}–C_{23} organic compounds. The elemental analysis and calorific value of the bio-oil were determined, the calorific value of 24.4 MJkg^{-1} and the empirical formula of $CH_{1.69}N_{0.04}O_{0.45}$. Based on the determined properties of the pyrolytic oil, it was decided that the use of pyrolytic oil derived from the daphne seed may possible be for the production of the alternative liquid fuels such as fuel for combustion systems in industry and finely chemicals after the necessary improvements.

Keywords

Laurel (*Laurus nobilis* L.); pyrolysis; biomass; synthetic fuels; renewable energy

Introduction

Biomass represents a renewable and alternative energy source, and due to the advantages of being CO_2 neutral, having low sulfur content, and being easy to transport, will become more important in the future. Biomass material can be converted to the many useful products such as charcoal, liquid fuels, gas fuel, etc. with suitable conversion process such as pyrolysis (slow, fast, flash and vacuum), gasification, liquefaction, hydrothermal upgrading (in water or solvent) and combustion, etc. Among these processes, pyrolysis is the most widely used thermochemical conversion process which is the chemical decomposition of organic material by heating in the absence of oxygen. The product distributions from the pyrolysis of biomass depend on pyrolysis parameters; pyrolysis reactor design, reaction parameters (temperature, heating rate, residence time, pressure, reaction atmosphere, i.e. N_2, H_2 or steam and catalyst), and biomass type and characteristics;particle size, shape, and structure (Murata et al.2012, Duman et al. 2011, Ucar et al. 2011). Slow pyrolysis conditions (long residence times at slow heating rates) at low temperature produce mainly charcoal, and high temperatures mainly produce gaseous products. On the other hand, fast heating rates at short residence times, and moderate temperatures favor a high yield of bio-oil (Huber et al. 2006). Bio-oil is a dark-brown organic liquid and also it includes a lot of the organic compounds like phenols, alcohols, ketones, esters, aldehydes, oxygenated hydrocarbons, etc. (Czernik et al. 2004, Goyal et al. 2008). Bio-oil can be readily stored, transported, and used as chemical feedstock for the production of various industrialized chemicals and also, it can be burned directly, co-fired and upgraded to other fuels (Mckendry 2002).

Turkey has considerable sources of renewable energy which include hydropower, wind, solar, geothermal and biomass. Among these energy sources, biomass will become precious sources of energy in the future since Turkey is an agricultural country and has abundant biomass sources. (Ogulata 2002). Sunflower, cotton, rape, safflower and euphorbia species are among the most promising renewable sources that have already been studied from the pyrolysis parameters and fuel properties. As an addition to biomass diversity of Turkey a wild growing evergreen tree Laurel is focused for possible use as a renewable fuel source. Laurel *(Laurus nobilis* L.), belongs to the family Lauraceae growing in most of the Mediterranean countries. Italy, former Yugoslavia and Turkey are among the most important producers of the botanical raw material. The tree is utilized mainly for its leaf for spice and essential oil industry and for its wood, which is very suitable for fence posts or supporters of wine plants. On the other hand Laurel berry contains, substantial amounts of fixed oil consisting mainly of odorless lauric acid, myristic acid and related compounds. From this point of view, laurel seed is of importance as a very important candidate of potential source of renewable fuels and chemical feedstock in Turkey.

In the present study, this is the first time that fast pyrolysis of daphne seeds was investigated in a well swept resistively heated fixed-bed pyrolysis reactor. The yield and characterization of the pyrolysis oils was investigated using some chromatographic and spectroscopic techniques, such as gas chromatography–mass spectrometry (GC–MS), and elemental analysis.

Methods

Materials. The samples of daphne seed (*Laurus nobilis* L.) were obtained from the town of Silifke, located in the Mediterranean region of Turkey. Prior to use, the sample was air-dried,

grounded in a high-speed rotary cutting mill and then screened to give a particle size between 0.6-0.85 mm. Proximate analyses of the sample were performed according to The Standard Methods of the American Society for Testing and Materials (ASTM) procedure. Ultimate analyses were performed on safflower seed to determine the elemental composition LECO TruSpec CHN Elemental Analyzer was used to determine the weight fractions of carbon, hydrogen and nitrogen, and the weight fraction of oxygen was calculated by difference. Cellulose, oil and protein, being the main constituents of daphne seed, were also determined (Table 1).

Table 1. Main characteristic of the daphne seed

Proximate analysis(wt.%,as received)			
Moisture	6.6	H/C molar ratio	1.68
Volatile	85.8	O/C molar ratio	0.49
Fixed C	5.8	Empirical formula	$CH_{1.68}N_{0.04}O_{0.49}$
Ash	1.8	Calorific value (MJ/kg)	22.9
Elemental analysis (wt%, daf.basis)		Protein	16.4
C	54.2	Cellulose	4.9
H	7.6	Oil	21.8
N	2.7		
O(by difference)	35.5		

Pyrolysis. The fixed-bed pyrolysis experiments were conducted in a well-swept resistively heated fixed-bed reactor (8 mm i.d., 90 cm long). To determine the effect of pyrolysis temperature and heating rate on the pyrolysis yields, 3 g of air-dried sample, sieved to in the particle size range of 0.6-0.85 mm was placed in the reactor and a sweep gas velocity of 100 cm^3 min^{-1} was controlled and measured with a rotameter. The sample was heated at a heating rate of either 30, 100, 350 or 700°C min^{-1} to the final pyrolysis temperature of either 400, 500, 550, 600 or 700°C and held at that temperature for 30 min or until no further significant release of gas was observed. Heating rate and pyrolysis temperature were controlled by a PID controller. The flow of the gas released was measured, using a soap film meter, for the duration of the experiments. The liquid phase was collected in a glass liner located in a cold trap maintained at about 0°C. Particularly, water was determined by refluxing the toluene solutions in a Dean&Stark apparatus. After pyrolysis, char yield was determined from the overall weight losses of the reactor tube. The gas yield was then calculated by difference.

Characterization. The oil analyzed was obtained under the experimental conditions giving the maximum oil yield (pyrolysis temperature of 600°C and heating rate of 350°Cmin^{-1}). The elemental composition and calorific value of the well-swept fixed-bed reactor oil were determined. The ^1H NMR of the oil was obtained at an H frequency of 90 MHz using a Jeol EX 90 A instrument. The sample was dissolved in chloroform-d. The I.R. spectrum of the oil was recorded using a Jasco FT: IR-300 E Fourier transform infrared spectrophotometer. The chemical class composition of the oil was determined by a liquid column chromatographic technique. The oils were separated into two fractions as *n*-pentane soluble and insoluble compounds (asphaltenes) by using *n*-pentane. The *n*-pentane soluble material was further separated on activated silica-gel (70-230 mesh). The column was eluted successively with *n*-pentane, toluene and methanol to produce aliphatic, aromatic and polar fractions, respectively. The GC-MS analyses of the *n*-pentane fractions was performed on an Agilent HP 6890N gas chromatography equipped with an Agilent HP 5973N mass selective detector (GC/MS) and a 30 m × 0.25 mm i.d.; 0.25 μm film thickness, HP-5MS column. Helium was the carrier gas at a flow rate of 0.8 ml/min. The column temperature was programmed from 50°C (kept for 2 min) to 280°C at 10°C min^{-1}. The final temperature was held at 280°C for 5 min. Typical

operating conditions were: ionization energy 70 eV; ion source temperature 230°C; scan per s over mass range electron (m/z) = 40-500.

Results and discussion

Product yields. The product yields were discussed for effect of pyrolysis temperature and heating rate. First, to determine the effect of pyrolysis temperature on the pyrolysis product yields, experiments were conducted with final pyrolysis temperatures of either 400, 500, 550, 600 or 700°C at the heating rate of 350 ^{0}Cmin^{-1}. The product yields of the fast pyrolysis in relation to pyrolysis temperature are given in Fig. 1. As shown in Figs. 1, the char yield significantly decreased as the final pyrolysis temperature was a raised from 400 to 700°C. In other words, the pyrolysis conversion increased. As the pyrolysis temperature increased to a level of 600°C the liquid product yield reached the highest value of 35.2%, but further increasing the temperature to 700°C, the conversion increased to a level of 83.6%, but in contrast liquid product yields go down to 30.2%, however, brought an increase in the total pyrolysis conversion, resulting in an increase in gas product yield only. This result is in agreement with the literature (Ates et al. 2009, Gonzalez, et al. 2005).

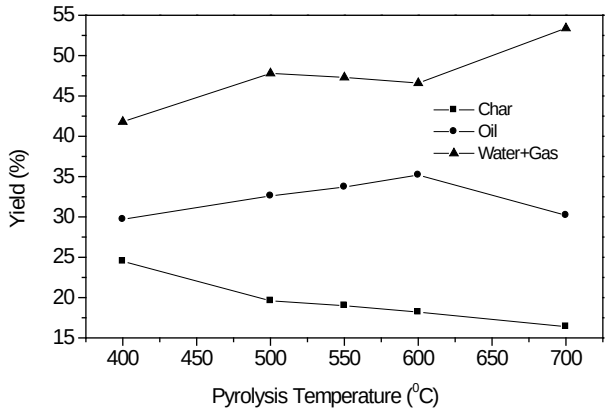

Fig. 1. Influence of temperature on product yield distributions.

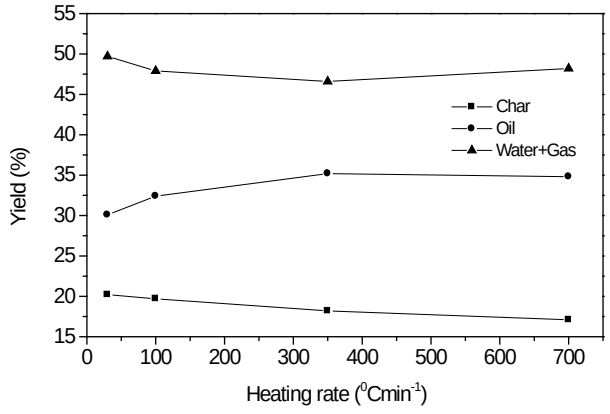

Fig. 2. Influence of heating rate on product yield distributions.

In order to determine the effect of heating rate on pyrolysis yields, experiments have been conducted at heating rates of either 30, 100, 350 or 700^{0}C min^{-1} (Figure 2). The maximum oil yield of 35.2% was obtained at pyrolysis temperature of 600^{0}C and a heating rate of 350^{0}C

min^{-1}. Fig. 2 shows that at the higher heating rate of 350°C min^{-1} the overall conversion of the pyrolysis was only about 2.5% higher than that of the lower heating rate of 30°C min^{-1}. However, the oil yield was about 16.9% higher than that of 30°C min^{-1}. As can be seen, employing the higher heating rate of 350°C min^{-1} breaks the heat and mass transfer limitation in the pyrolysis, resulting in the maximum oil yield. Above this heating rate increase in the oil yield is negligible, remaining constant at the maximum level of 35%.

Table 2. The elemental compositions and calorific values of pyrolysis oils

Elemental analysis [a]	Oil
C	56.2
H	7.9
N	2.4
O[b]	33.5
H/C molar ratio	1.69
Calorific value ($MJkg^{-1}$)	24.4

[a] Weight percentage on dry ash free basis
[b] By difference

Product characterization. The elemental composition of the sample of the oil characterized and the calorific values are listed in Table 2. The average chemical composition of the oil analyzed is $CH_{1.69}N_{0.04}O_{0.45}$. Further comparison of H/C ratio with conventional fuels indicates that the H/C ratios of the oil obtained in this study (1.69) were very similar to that between light and heavy petroleum products. Also, calorific value indicates that the energy content of the oil is very close to that of petroleum. The IR spectrum of the oil is given in Figure 3. The O–H stretching vibrations between 3200 and 3400 cm^{-1} indicate the presence of phenols and alcohols. The C–H stretching vibrations between 2800 and 3000 cm^{-1} and C–H deformation vibrations between 1350 and 1475 cm^{-1} indicate the presence of alkanes. The C=O stretching vibrations with absorbance between 1650 and 1750 cm^{-1} indicate the presence of ketones and aldehydes. The absorbance peaks between 1575 and 1675 cm^{-1} represent C=C stretching vibrations indicative of alkenes and aromatics.

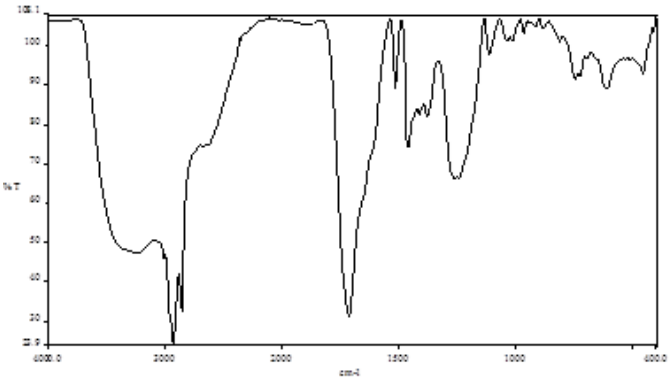

Fig. 3. The IR spectra of the pyrolysis oil

The GC chromatogram of the oil is given in Figure 4. The straight chain alkanes range from C_{11} to C_{23}, and distribution of straight chain alkanes exhibit a maximum in the range of C_{13} to C_{19} in the oil. At the same time, the compounds recognized in this fraction were listed in Table 5. Moreover, it was determined that oil contains mostly paraffinic and olefinic hydrocarbons.

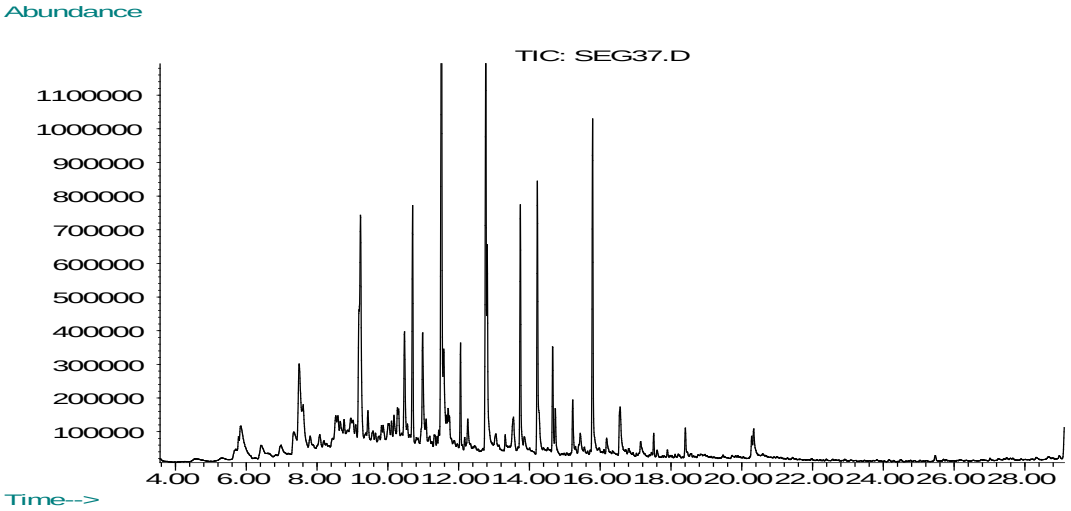

Fig. 4. The GC-MS chromatogram of the pyrolytic oil

Conclusion

Fixed-bed pyrolysis of daphne seed has shown significant recoveries of liquid hydrocarbon. The pyrolysis conversion increased with a final pyrolysis temperature up to 700^0C, but the oil yield increased with temperature up to 600^0C, after which there was a significant decrease in the oil yield. As a result of breaking heat and mass transfer limitations in the pyrolysis of daphne seed by increasing the heating rate from 30^0C min^{-1} to 700^0C min^{-1}, there was a significant change in the oil yield. As a result, the final pyrolysis temperature of 600°C temperature, heating rate of 350°Cmin^{-1} and sweeping gas flow rate of 100 cm^3min^{-1} were more suitable for high-quality bio-oil production.

References

1. Murata, K., Liu, Y., Inaba, M., Takahara, I. 2012. Catalytic fast pyrolysis of jatropha wastes. Journal of Analytical and Applied Pyrolysis. 94:75–82.
2. Duman, G., Okutucu, Ç., Ucar, S., Stahl, R., Yanik, J. 2011.The slow and fast pyrolysis of cherry seed. Bioresource Technology. 102:1869–1878.
3. Uçar, S., Karagöz, S. 2011. The slow pyrolysis of pomegranate seeds: The effect of temperature on the product yields and bio-oil properties. Biomass and Bioenergy. 3 5: 4297-4304.
4. Huber, G.W., Iborra, S., Corma, A. 2006. Synthesis of transportation fuels from biomass: chemistry, catalysts, and engineering. Chem. Rev. 106:4044–4098.
5. Czernik, S., Bridgwater, A.V. 2004. Overview of applications of biomass fast pyrolysis oil. Energ and Fuel. 18:590-598.
6. Goyal, H.B., Seal, D., Saxen, R.C. 2008. Bio-fuels from thermochemical conversion of renewable resources: a review. Renew Sust Energ Rev. 12:5004-5017.
7. Mckendry, P. 2002. Energy production from biomass (part 2): conversion technologies. Bioresour Technol. 83:47-54.
8. Ogulata, R.T. 2002. Energy from Renewable Sources in Turkey: Status and Future Direction. Renew. Sustain. Energy Rev. 6: 471.
9. Ateş ,F., Isıkdag, M.A., 2009. Influence of temperature and alumina catalyst on pyrolysis of corncob. Fuel .88: 1991–1997.

10. Gonzalez, J.F., Ramiro, A., Gonzalez-Garcia, C.M., Ganan, J., Encinar, J.M., Sabio, E., Rubiales, J. 2005. Pyrolysis of almond shells. Energy applications of fractions. Ind. Eng. Chem. Res. 44:3003–3012.

Fire-resistant Property of Poplar Treated with BL Fire Retardant by Microwave and Ultrasonic Wave Method

Jing PAN

Jun MU

College of Materials Science and Technology, Beijing Forestry University

Beijing, China

Abstract

Poplar is playing an important role as a kind of building materials. To reduce the flammability of *Poplar*, fire-retardants are used during its processing so that it can acquire better flame retardant effects. As to it, flame retardant impregnation process is the key step. In this study, BL flame retardant prepared by Beijing Forestry University，which is efficient and environmental，is used to treat *Poplar*. The samples were impregnated by four fire-retardant treatment methods which include impregnation at atmosphere and high temperature, impregnation at atmospheric vacuum pressure, impregnation at atmosphere after treated by microwave and impregnation under ultrasonic wave after treated by microwave. According to drug-loading ratios and Limiting-oxygen Index (LOI), the optimum process was explored. Throughout the experiment，it is discovered that *Poplar*'s permeability could be significantly improved after treated by microwave and strong cavitation effect of ultrasonic could make flame retardants efficiently dip into *Poplar*. From experimental results, samples treated by impregnation at ultrasonic wave after treated by microwave had the highest drug-loading ratios and LOI. The optimum process for fire-retardant treatment of *Poplar* using BL fire retardant was: microwave heating 2 min, ultrasonic wave dipping 30 min at 40 ℃，the concentration of the flame retardant solution was 15%，the liquor ratio of the flame retardant solution to *Poplar* was 10:1. Drug-loading ratios of fire-retardant *Poplar* could reach to 26.4%, while LOI could be up to 62.2%. CONE results showed the optimum process with BL fire retardant could greatly improve fire-resistant property of *Poplar*.

Key words：*Poplar*；microwave and ultrasonic wave methods；fire-resistant property；BL fire retardant；LOI；CONE

Introduction

Poplar, which is an important tree species for fast-growing and high yield in the north of China, is commonly used as building materials. Because of small density, stable processing properties and cheap price, it is widely used to manufacture furniture, core board and the backplane of solid wood composite floor boards. To some degree， its flame retardant performance is taken seriously.

The application of fire retardant agents as a method for fire prevention is extremely significant for fire safety of buildings. They can improve considerably fire parameters of materials as: rate of combustion, flame spread and heat release. At the same time, they can also increase fire resistance and reduce the spread of fire (Wojciech 2012).

In general, the types of compounds used for fire-retardant wood mainly include phosphorus-based compounds, boron-containing compounds, carbonate and sulphate compounds (Qu et al. 2011). BL flame retardant used in this study is phosphorus-nitrogen flame retardant agent produced by College of Materials Science and Technology, Beijing Forestry University. BL-environmental flame retardant belongs to N-P flame retardant series, and its main raw materials are phosphoric acid and urea, which is the same as ammonium polyphosphate (APP) (Li et al. 2006). It has such advantages as environmental protection, non-toxic, cost inexpensive and efficiency. However, its high absorption properties should be improved according to various processing methods or additive components (Wang et al. 2010).

Nowadays, there are three main methods for applying flame retardants to wood and to products made from wood: impregnation with a flame-retardant solution, incorporation of flame retardants into the glue system, and surface treatment of the product (Qu et al. 2011). It is indicated in previous research that microwave and ultrasonic could improve wood's permeability (Zhu et al. 2009), but studies about combined treatment for fire-retardant wood and flammability evaluation were rare.
In this research, treatment method of impregnation under ultrasonic wave after treated by microwave for *Poplar* with BL fire retardant would be studied and LOI with CONE would be used to evaluate the fire resistant property of treated *Poplar*.

Experimental

Raw material

Samples of *Poplar* (North of China) with density in the range of 540–550 kg/m^3 were gained from Beijing Dong Ba Lumber Market. Test materials were separated from heartwood and sapwood. The moisture content of heartwood was 10.97% and that of sapwood was 9.50%. Sizes (L×W×T) were 100 mm×6 mm×3 mm for *LOI* test and Sizes (L×W×T) were 100 mm×100 mm×10 mm for CONE test. Specimens should be oven dried in 103±2℃before

treatment. BL environmental protection flame retardant powders were taken from Beijing Shengda Huayuan Technology Co., Ltd.

Treatment

The oven dried specimens of heartwood and sapwood were respectively divided into five groups， each group including five CONE test samples and six *LOI* test samples. BL flame retardant fluid 15% was prepared to treat samples. Microwave power was 850 W and the ultrasonic power output was 0.4 W/cm^2. The five treatment groups are as follows：

I. untreated wood;

II. wood treated by impregnation at atmosphere and high temperature for 3h;

III. wood treated by impregnation at vacuum pressure：a vacuum of 0.9MPa for 30min and pressure of 1.4 MPa for 150min；

IV. wood treated by impregnation at atmosphere for 24h after treated by microwave;

V. wood treated by impregnation under ultrasonic wave after treated by microwave;

Detailed experimental conditions are in Table 1.

Table 1 Experiment conditions

Treatment group	Treatment condition			
	the ratio of solid to liquid [a]	microwave	ultrasonic wave	temperature
I	-	-	-	-
II	10:1	-	-	85±2℃
III	10:1	-	-	atmosphere
IV	10:1	high intensity 2min	-	atmosphere
V	10:1	high intensity 2min	30min	40℃

[a] the ratio of solid to liquid is the volume ratio of *Poplar* to BL flame retardant fluid

Limiting-oxygen-index *(LOI)*

LOI values were determined in accordance with GB/T 2406.2-2009 by means of a General Model LFY-605 apparatus (Shandong Spinning Science and Instrument Research Institute).

Cone Calorimeter (CONE) Tests

The tests were carried out with a cone calorimeter C3 (TOYO SEIKI SEISAKU-SHO., LTD). Cone values were determined in accordance with GB/T16172-2007/ISO5660-1：2002. Horizontal samples were subjected to a heat flux of 50kW/m^2, which correspond to a heater temperature about 780℃.The samples were wrapped in aluminium foil, with the upper face exposed, and the tests were done using spontaneous ignition as the endpoint. Flammability investigations were carried out on at least two samples for each variant with dimensions 100mm×100mm×10mm thick (Wojciech 2012). The time for combustion test was about 10min. According to the standard cone calorimeter software, the following fire properties were examined: heat release rate (HRR), mass loss rate (MLR), total heat released (THR), effective heat of combustion (HOC), specific extinction area (SEA), time to ignition T_{ign}. The investigations involved the determination of the fire properties, which characterize wood treated with BL flame retardant by optimum process. Following this standard, the results

obtained for the treated wood are compared with the results of investigations for natural wood.

Results And Discussions

Average Drug-Loading Ratios Analysis

Wood's uptake of flame retardants has close relationship with permeability of wood. Heartwood of *Poplar* contains more extracts than sapwood and internal pipeline structure of *Poplar* is complex that all of them made it difficult for flame retardant liquid into *Poplar* internal (P. Rousset et al. 2004). Average drug-loading ratios of all samples were listed in Table 2. From the data in Table 2, average drug-loading ratios of V are about twice as much as that of III. It was observed that average drug-loading ratios of samples significantly increased after microwave treatment, high temperature bath in II couldn't highly improve *Poplar*'s permeability. But there was no obvious rule between treated sapwood and treated heartwood after impregnation. For microwave, several experimental studies have shown that it could make pit membranes which are on wood cell wall burst and it makes extracts inside wood separated or distributed, then it could accelerate the mass loss of wood (Zhu et al. 2009). Ultrasonic's strong cavitation effect could significantly shorten dipping time and increase active components loading (Li et al. 2006). Combined action of microwave and ultrasonic wave in V proved previous conclusions. Microwave combined with ultrasonic wave could greatly increase the drug-loading ratios.

Table 2. LOI and drug-loading ratios of samples

Treatment group	Average LOI %	Average drug-loading ratios %
I sapwood	20.9	-
I heartwood	20.9	-
II sapwood	55.6	3.2
II heartwood	58.8	4.3
III sapwood	55.9	13.8
III heartwood	52.1	13.4
IV sapwood	60.7	7.4
IV heartwood	55.3	17.3
V sapwood	62.9	27.0
V heartwood	61.5	25.9

Limiting-Oxygen-Index *(LOI)* Analysis

The LOI value is the minimum amount of oxygen in oxygen–nitrogen mixture required to support complete combustion of a vertically held sample that burns downward from the top. It was known that the higher the LOI value is, the more effective the flame-retardant treatment is (Gao et al. 2004). Average LOI of all samples were shown in Table 2. According to GB 8624-2006, B1 level flame retardant materials should be tested in national designated testing center. Due to the limited conditions, in this study, we use LOI which has a better comparison with B1 level test (Fang et al. 2000) to discuss fire-retardant effect of

impregnation methods. With LOI reaching more than 50%, materials could be achieved through B1 level detection. From II to V, all LOI values were more than 50%, it indicated that all treated samples could be B1 level flame retardant materials. However, impregnation at atmosphere and high temperature in II would decrease wood processing performance and mechanical strength, its low drug-loading ratios would make fire-retardant inside have a loss at high absorption property. For impregnation at vacuum pressure in III, we discovered that once the pressure removes, flame retardant liquid could spill from the surface to contaminated surfaces and reduce drug-loading ratios. As to impregnation at atmosphere after treated by microwave in IV, it could reach high LOI, but the treated time was too long to be used in industrialization. Above all, impregnation under ultrasonic wave after treated by microwave in V had short treatment time, high LOI and average drug-loading ratios. Defined as the optimum process, microwave and ultrasonic wave method could further improve the fire resistance (Li et al. 2006). In addition, BL flame retardants could be efficient at low concentrations. However, from the results, no obvious linear relationship between LOI and average drug-loading ratios was discovered.

Cone Calorimeter (CONE) Analysis

The investigation of flammability by CONE is a widely accepted standard method of analyzing the rate of heat release, mass loss rate, total heat release and smoke generation emitted from materials. The results of measurements of HRR (Figure 1), THR (Figures 2) during the exposure of crude *Poplar* and samples treated with BL fire retardants by microwave and ultrasonic wave method are now discussed. In addition, fire properties of samples such as T_{ign}, HOC, HRR in different periods, MLR, SEA, THR, HRR_{max} and the time until the occurrence of HRR_{max} were compared in Table 3.

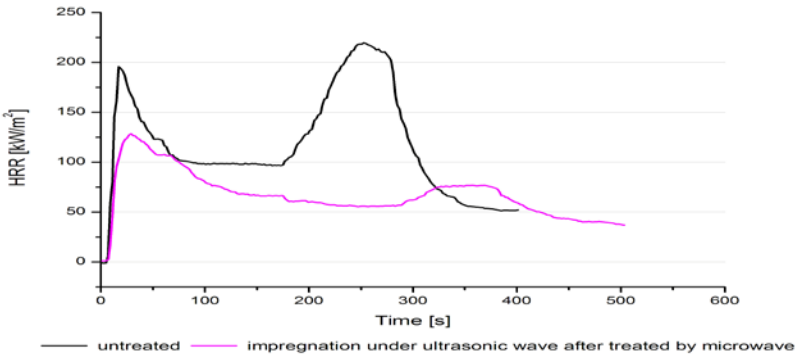

Figure 1 HRR curve of Sapwood impregnation under ultrasonic wave after treated by microwave

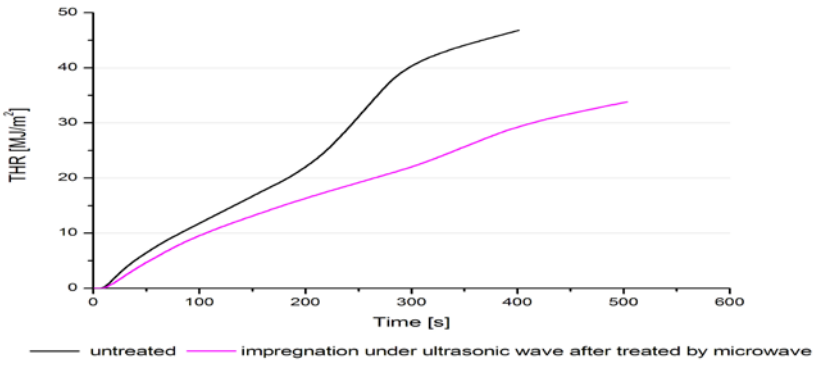

Figure 2 THR curve of Sapwood impregnation under ultrasonic wave after treated by microwave

In HRR curve, though wood heating time of the treated samples was a little bit in advance, it didn't have impacts upon fire resistance. After ignition, the first sharp peak of treated samples is a little later than untreated samples and two peak values are sharply lower. Time to appearance of second peak of treated samples is almost twice as long as untreated samples. Due to the optimum process, a significant reduction in THR is observed on THR curve (Figure 2). THR curve corresponds to the HRR curve.

From data in Table 3, compared to untreated sapwood, there is a 41% decrease in HRR_{max} of treated samples. A 38% decrease in MLR, a 16% decrease in HOC, a 46% decrease in THR and a 82% decrease in SEA were calculated according to data in Table 3. Wojciech (Wojciech 2012) had studied the effect of 20% potassium carbonate and urea (referred to as WM mixture) on pine wood and gained a 38% decrease in THR. Qingwen Wang (Wang et al. 2004) treated wood with FRW flame retardant and got a 48% decrease in $HRR_{max.}$ Compared with them, the optimum process with BL fire retardant is more efficient for short treatment time.

Table 3. Intervals and mean values from cone calorimeter.

Flammability traits	Untreated sapwood	Treated sapwood [a]
Time to ignition (s)	16.3	15.6
Heat release rate in 60 s (kW/m^2)	139.68	113.81
Heat release rate in 180 s (kW/m^2)	113.69	86.19
Heat release rate in 300 s (kW/m^2)	136.05	75.15
Heat release rate maximum (kW/m^2)	219.58	128.53
Mass loss rate (g/s·m^2)	11.945	7.411
Effective heat of combustion (MJ/kg)	11.31	9.46
SEA(m^2/kg)	80.29	14.21
Total heat released(MJ/m^2)	41.01	22.11
Time to heat release rate maximum (s)	252.90	29.00

[a] impregnation under ultrasonic wave after treated by microwave

As to BL fire retardant, it is composed of phosphoric acid, urea and catalyst. Large amounts of incombustible gas (ammonia and water vapor) released in combustion of *Poplar* (Hu et al. 2000). The polycondensation of BL fire retardant generated ammonium polyphosphate (APP) which is a good flame retardant itself. With its strong dehydration catalysis for carbon-forming, BL fire retardant greatly postpone the combustion of wood (Li et al. 2006). Significantly, impregnation under ultrasonic wave after treated by microwave would be greatly combined with BL flame retardants and all of that could gain outstanding treatment results.

Conclusions

• Flame resistance of all samples treated by BL flame retardants greatly increased and got high *LOI* values. It is evident that BL flame retardants could be efficient at low concentration.
• The optimum process for fire-retardancy of *Poplar* is: microwave heating 2 min, ultrasonic wave dipping 30 min at 40 ℃， the concentration of the flame retardant solution is 15%， the liquor ratio of the flame retardant solution to *poplar* is 10:1.The drug-loading ratios of fire-retardant *poplar* can reach to 26.4%, while the *LOI* value could be up to 62.2%.
• For the optimum process of impregnation under ultrasonic wave after treated by microwave, when introduced into wood, it could increase fire-resistant performance of *Poplar*, as evidenced by greatly decreasing HOC, THR, MLR, HRR_{max}, SEA and the heat of combustion of treated samples.

References

Gao, M., Sun, C.Y, Zhu, K. 2004. Thermal degradation of wood treated with guanidine compounds in air flammability study. Journal of Thermal Analysis and Calorimetry 75: 221–232.

Qu, H.Q., Wu, W.H., Wu, H.J., Jiao, Y.H., Xu, J.ZH. 2011. Thermal degradation and fire performance of wood treated with various inorganic salts. FIRE AND MATERIALS 35:569–576.

Hu, Y.CH., Zhou, P.J., Qu, S.SH. 2000. TG-DTA studies on wood treated with flame-retardants. Holz als Roh- und Werkstoff 58: 35-38.

Wang, M., Hu, Y.CH. 2010. Research progress in fire-retardant of wood and wood plastic composites. Plastics Science and Technology 38(3): 104-109

Wojciech Łukasz Grze´skowiak. 2012. Evaluation of the effectiveness of the fire retardant mixture containing potassium carbonate using a cone calorimeter. FIRE AND MATERIALS 36:75–83.

Zhu, CH.Q., Zhang, J., Zhuang, Q.Y., Li, Q., Yang, W.M. 2009. Study on the Effect of

Technological Conditions on Permeability of Microwave Treated Fir. FORESTRY MACHINERY & WOODWORKING EQUIPMENT 37(11):18-25.

P. Rousset, P. Perré , P. Girard. 2004. Modification of mass transfer properties in *Poplar* wood (P. robusta) by a thermal treatment at high temperature. European Journal of Wood and Wood Products 62:113-119

Li, X.D., Hao, W. X., Qi, X.Y. 2006. Application of ultrasonic wave in impregnation methods of wood treated with fire retardants. Journal of Fujian Forestry science and Technology 33(1):64-66

Wang, Q.W., Li, J., Jerrold E. Winandy. 2004. Chemical mechanism of fire retardance of boric acid on wood. Wood Science Technology 38:375–389

Li, G.P., Yu, L.P., Liu, Y. 2006. BL-environmental friendly flame retardant. Fine and Specialty Chemicals 14(18):9-10

Fang, G.ZH., Pang, J.Y., Ai, M.Y., Li, SH.J. 2000. Dimensional stability and painting performance of modified wood with Fire Retardant WFRJ1. CHINA WOOD INDUSTRY 14(5):13-15

Acknowledgments

This study was funded by Forestry Public Welfare Project Foundation of China (201204704).

Evaluation of Hygroscopic Property of Thermally Treated Yellow Poplar (*Liriodendron tulipifera*) Wood

Yoon-Seong Chang[1] , *Jun-Ho Park*[2] , *Yonggun Park*[3] , *Ju-Hee Lee*[4], *Hwanmyeong Yeo*[5*]

[1,2,3,4] Graduate Research Assistant, Departament of Forest Science, College of Agriculture, Seoul National University, Seoul, South Korea.
Jang646@snu.ac.kr
[5] Associate Professor, Research Institute for Agriculture and Life Sciences, Departament of Forest Science, College of Agriculture, Seoul National University, Seoul, South Korea.
**Corresponding author*
hyeo@snu.ac.kr

Abstract

For modern people who spend most of their time indoor temperature and humidity to be controlled by electrical appliances have a great effect on the emotion and health of human. However, inappropriate operation of the artificial facilities frequently creates substances to be harmful to our body and causes asthma, allergic rhinitis. Because of those, the importance of natural humidity control performance of interior materials is being emphasized. This study was carried out for quantifying the hygroscopic property of some interior finishing wooden materials. Dried and heat treated yellow poplar (*Liriodendron tulipifera*) lumbers, OSB, and plywood were selected for this experiment. Moisture adsorption and desorption rates of wooden materials were measured (ISO 24353). Also, effects of morphological, physical and chemical factors, like surface microstructure, density, and functional groups, on the hygroscopicity were analyzed. It is expected that the results from this study can contribute to establish a system for evaluating and controlling the hygroscopic property of wooden building.

***Keywords*:** Hygroscopic, Heat-treated wood, FE-SEM, FT-IR, Roughness

Introduction

As indoor environments of building comprise a large proportion of those living in modern people, there are many efforts to improve it. Because of indoor environments of building are affected not only people but also energy efficiency, it needed a multilateral effort into indoor environmental improvement. Especially, one of factors with influenced indoor environments in building, indoor relative humidity (RH) is reported the primary cause of condensation and biological pollutions such as mold. (Cho and Kim, 1990). However, inappropriate operation of the artificial facilities frequently creates substances to be harmful to our body and causes asthma, allergic rhinitis. Because of those, the importance of natural humidity control performance of interior materials is being emphasized. Wood, controlled humidity in residential space by moisture ad/desorption as humidity of the atmosphere; is used to interior materials in buildings. Humidity change of indoor buildings which is composed wood is low deviation than other materials. Therefore, the more wood exposure, the less humidity changes in indoor building.

These hygroscopic properties of wood are affected by changing moisture content and morphological difference. The anatomical structures were examined the heat treatment process by using scanning electron microscope (SEM) (Awoyemi and Jones 2011). And ^{2}H NMR relaxation measurements methods are used to measure the response of liquid confined in porous materials. These methods were used to study on moisture transfer and changes in structure of thermally modified Scots pine wood (Hietala et al 2002). The relation between surface roughness values and drying speed was searched using correlation analysis. It was determined that there was no effect of surface roughness on drying speed wood veneer in radial cut (Gungor et al 2010). Also, to evaluate the interior decorative value of small diameter larch which has low utilization, the study methods of timber are evaluated by the physical characters of it are evaluated by density, swelling, hygroscopicity, hardness, surface roughness, etc. (Park et al. 2010). This study was carried out for quantifying the hygroscopic property of some interior finishing wooden materials. And it is expected that the results from this study could contribute to improve the supplying wooden building.

Materials and Methods

Materials Yellow poplar (*Liriodendron tulipifera*) logs from 25-30 year-old trees, Seoul national university forest, Suwon-si, Gyungki-do, Korea were obtained for this study. Sawn dimensional stock of 50mm (T) x 150mm (W) x 1000 mm (L) were prepared for air-drying(AD), kiln-drying(KD) and high temperature heat-treatment(HT).

AD from green condition (with initial moisture content at an average of 68%) was conducted for three months. And KD was conducted by FPL scheduled which is drying condition runs at initial dry bulb temperature (DBT) 60°C, relative humidity (RH) 87% and final DBT 82°C, RH 26%. And, using high temperature oven, HT runs at DBT 200°C condition for six hours.

Ad/Desorption on wood Yellow poplar sawn lumbers thickness of 10mm, 30mm and vertical, width of 100mm x 100mm, 150mm x 150mm for air-drying(AD), kiln-drying(KD) and high temperature heat-treatment(HT). Except for surface area of

measurement, all the section was sealed by aluminum tape. Using temperature & humidity chamber, the mass of wood at each state measured to mass change for 24hr less than 0.01g. Since then, to raise the RH, adsorption process for 12hr was calculated mass of specimen and dropped the RH, desorption process for 12hr was same way.

And following formula, moisture ad/desorption contents and rates of moisture ad/desorption after 12hr were calculated at each state. Except for moisture ad/desorption by humidity condition, surface roughness, microstructure and functional group were conducted by medium humidity condition.

$$\rho_{A,a} = \frac{w_a - w_o}{A} \qquad \rho_{A,d} = \frac{w_a - w_d}{A} \qquad G_n = \frac{w_n - w_{n-1}}{A \cdot \Delta t} \qquad \text{(Eq.1)}$$

$\rho_{A.a}$ = Moisture adsorption content(kg/m^2), $\rho_{A.d}$ = Moisture desorption content(kg/m^2), G_n = Rate of ad/desorption at state(kg/(m^2·h)), w_0 = Weight of final state at equilibrium(kg), w_a = Weight of final state at absorption(kg, after 12hr), w_d = Weight of final state at desorption(kg, after 12hr), A = Surface area(m^2), t = Time(hr)

Table 1. Humidity conditions for testing specimens

Humidity Conditions (Temp. 23℃)	Relative Humidity(%)	
	Adsorption(12hr)	Desorption(12hr)
Low (Equilibrated at 30%RH)	55	30
Medium (Equilibrated at 50%RH)	75	50
High (Equilibrated at 70%RH)	95	70

Functional group FT-IR spectrum analysis on wood was conducted for changing functional group by heat-treatment. Using ball miller (pulverisette 23, Fritsch), specimens were milling of the 100mesh. The FT-IR spectra were recorded on a FT-IR-6100 spectrometer, operating in the spectral range 650-4000 cm^{-1} with a resolution of 8 cm^{-1}.

Microstructure Field-emission scanning electron microscopy (FE-SEM, SUPRA 55VP, Carl Zeiss, Germany) was used to image the changing microstructure of wood by heat treatment. The cross, radial, tangential section of wood were prepared using a microtome with 100㎛ in thickness.

Roughness The surface section of KD wood was ground by 180, 1000 grit sandpaper and measured rate of adsorption. The quantitative analysis of surface roughness of wood was conducted by using surface roughness measurement device (TR-200, Time High Tech.)

Results and Discussions

Ad/Desorption Figure 1 shows that moisture ad/desorption contents after 12hr was calculated at each condition. In case of relative humidity, high moisture ad/desorption contents on high humidity condition than others, it related to sorption property of bound water on wood by multilayer adsorption on high relative humidity. And then moisture ad/desorption contents weren't a distinct difference by surface area and thickness

These results were similarly changing humidity conditions in indoor building during the day. It is used base data to calculated appropriate area and thickness of wooden interior

materials with concerning size of space and changing humidity conditions in indoor building.

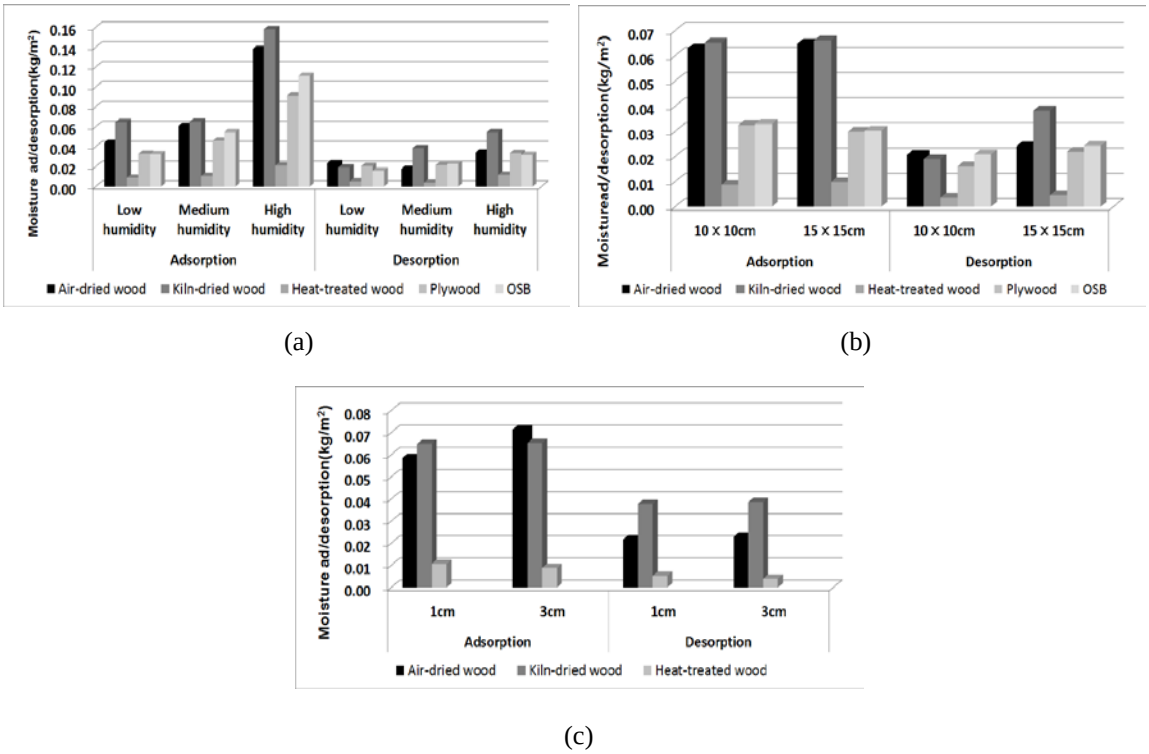

(a) (b)

(c)

Fig 1. Quantity of Moisture in wood after 12hr adsorption and desorption at different conditions ((a): Relative Humidity, (b): surface area, (c): thickness)

But, these data which calculated by a cycle of 12hr weren`t knew when and how much to attain moisture ad/desorption contents, it was needed to measure those per hour. The results of rates of moisture ad/desorption at each material, all specimen were high ad/desorption rates for 2hr and gradually convergent trend. The rates of moisture ad/desorption is a degree of moisture ad/desorption of materials per unit surface area and time, its high value means efficiently responds to rapid change in humidity. As compared with other specimens, HT wood was certainly lower in those. It is due to hydrophobicity of wood surface that hard to adsorption of water molecule. Also, rates of moisture ad/desorption on KD wood is higher than that of AD wood. Vapor and moisture transfer on KD wood easier than that of AD wood because KD wood increase of inner opening on wood with volatilization of wood extractives by heat treatment.

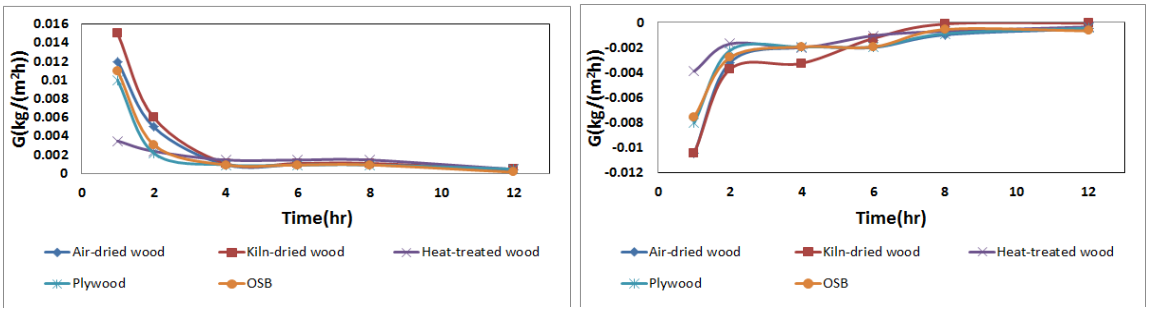

Fig 2. Moisture adsorption and desorption rate of air-dried, kiln-dried and heat-treated *Liriodendron tulipifera* wood

FT-IR Figure 3 shows FT-IR spectra at AD/KD/HT yellow poplar wood. Moisture adsorption point of wood is OH group from cellulose and hemicellulose. It was related to hygroscopic property of wood. And the more high temperature treatment, the lower peaks at around 3400 cm^{-1} represents OH group and 2900 cm^{-1} represents the C-H group a symmetric stretching in aliphatic methyl. It means that combinations of alkyl group, aromatic compound, carboxylic acid were broken on the dehydration by heat treatment.

A band at approximately 1650 cm-1 is characteristic to C=C stretching vibration in aromatic skeletal of lignin. This peak`s decrease occurred in wood with volatilization of wood extractives by heat treatment. In a KD wood, beside AD wood, was lower peaks at around 3400 cm^{-1} because it occurred water molecule loss and combination between the cellulose, which ester linkages simultaneously by heat treatment and decreased the ratio of hemicellulose which has many OH groups. But, rates of moisture ad/desorption of KD wood higher than AD wood, vapor and moisture transfer were easier because KD wood increase of micro pore on wood cell wall with volatilization of wood extractive by heat treatment.

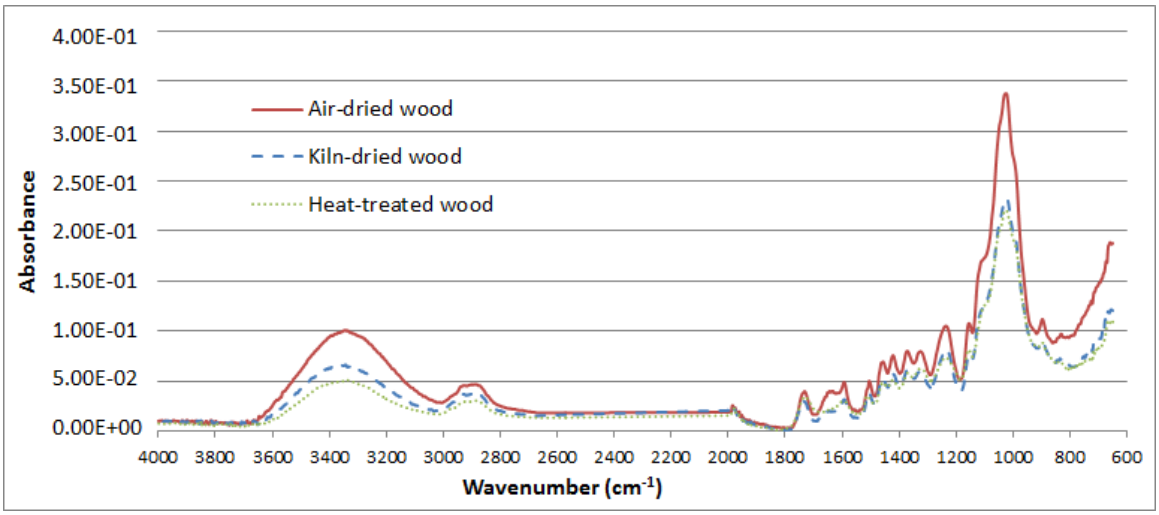

Fig 3. FT-IR spectrum of air-dried, kiln-dried and heat-treated *Liriodendron tulipifera* wood

FE-SEM In a HT wood, many micro cracks, shrinkage of cell wall and collapsed wood cell as sharply water loss were found on the cross section of wood. And rise of surface roughness and expansion of micro movement path were increased the speed of ad/desorption by

reduced the vapor diffusion resistance. But these effects of structure change lesser than those of chemical change such as hydrophobicity, rates of moisture ad/desorption were lower than others.

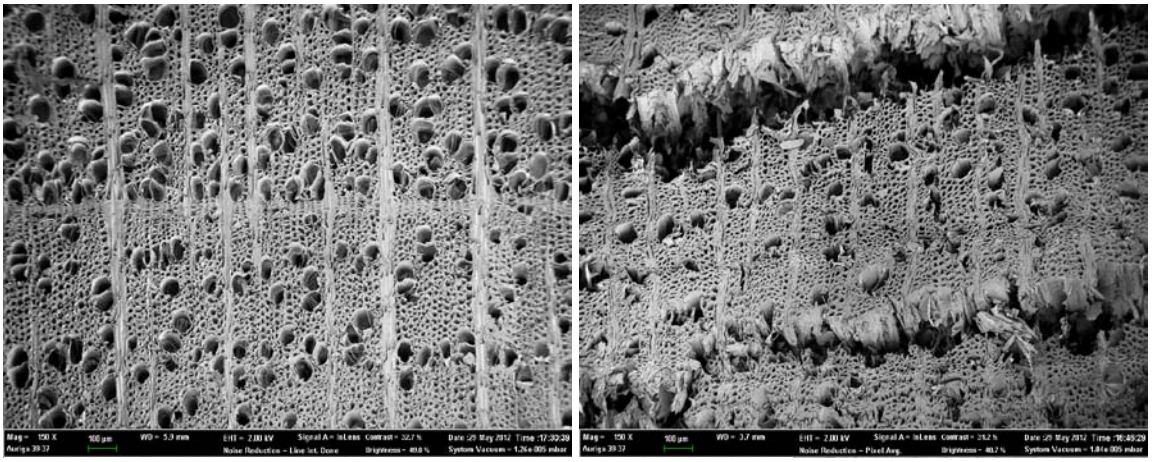

Fig 4. Cross-sectional view of air-dried(left), heat-treated wood(right)

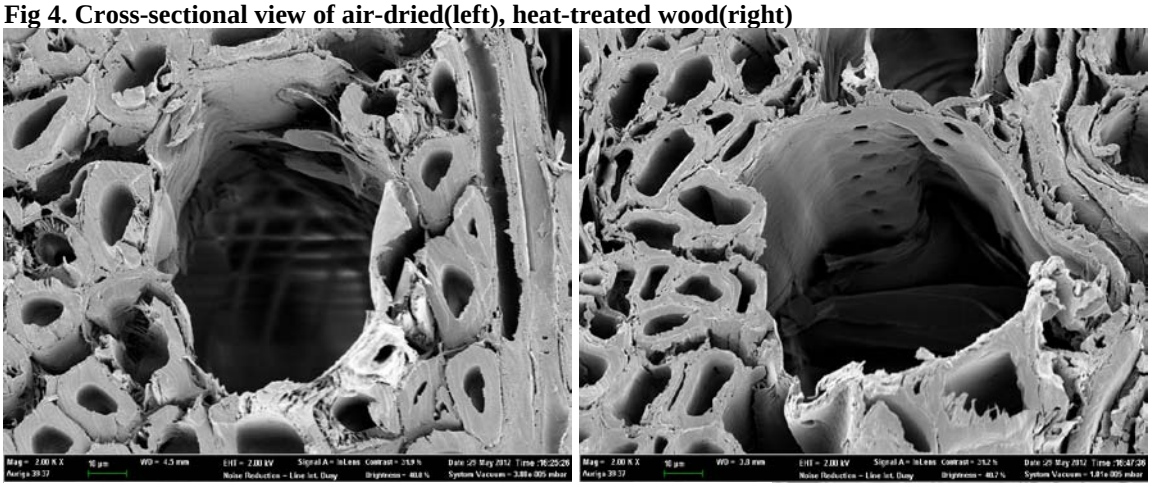

Fig 5. Cell wall of air-dried wood(left) and heat-treated wood(right)

Roughness As the effect of hydrophobicity by heat treatment, AD wood was conducted to measure rate of adsorption by each surface roughness because it wasn`t clearly found the relation between the speed of adsorption and surface roughness. Four main roughness parameters, mean arithmetic deviation of profile (R_a), root mean square roughness (R_q), maximum roughness (R_t) and mean peak-to-valley height (R_z), obtained from the surface of wood were used to evaluate the effect of heat treatment on the surface roughness of the specimens.

Table 2. surface roughnesses of specimens abraded with 180-grit and 1000-grit sandpaper

Material	Roughness(㎛)			
	R_a	R_q	R_t	R_z
180grit (air dried wood)	8.09	11.83	45.85	31.95
1000grit (air dried wood)	3.6	5.366	41.1	28.2

In a grinded AD wood by sandpaper, it shows distinctly difference that R_a: 8㎛, R_q: 12 ㎛ at 180-grit and 4㎛, R_q: 5㎛ at 1000-grit. As moisture adsorption rate, 180-grit is higher than 1000-grit and these results were interpreted to high roughness was increased contact surface between water molecule and wood surface. The gap between 180-grit sandpaper's adsorption rate and that of 1000-grit sandpaper was about 5 g/m^{2}h at initial time, the gap was gradually decreasing. In the initial adsorption, surface roughness was major factor of adsorption because water molecule was absorbed surface of wood. But, it was lesser because water molecule diffused wood cell wall as time went on.

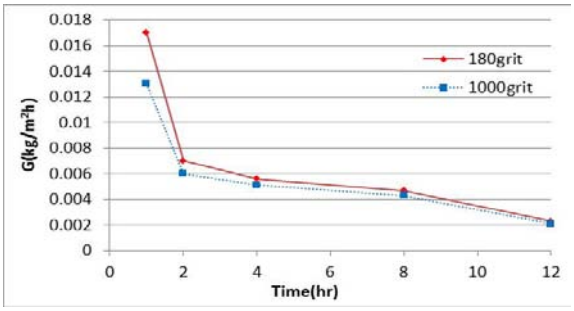

Fig 6. Moisture adsorption rate by surface roughness in wood

Conclusion

This study was carried out for changing the hygroscopic property of yellow poplar by heat treatment. In the moisture ad/desorption contents, KD wood was higher than AD wood. And these results were interpreted by changing microstructure, surface roughness and functional group. Surface roughness was considered major factor of initial ad/desorption. Also, KD wood is highest rate of ad/desorption value, it means that appropriate hygroscopic performance with severe changing humidity condition. And heat treatment with appropriate temperature will contributed to enhanced hygroscopic performance of wood. And, HT wood had a lower hygroscopic property. But, it has an advantage of high dimensional stability and decay resistance which using products.

Therefore, it used to interior material in space of continuous high RH condition. Also, It is possible that substance of outstanding hygroscopic property was injected into extended inner openings of HT wood to enhance hygroscopic performance. This study was expected to base data for quantifying the hygroscopic property of residential space on wooden house.

Acknowledgement

This research was supported by the Basic Science Research Program through the National Research Foundation of Korea (NRF) funded by the Ministry of Education, Science and Technology(2011-0003453).

Reference

Avramidis, St. and J. F. Siau. 1987. An investigation of the external and internal resistance to moisture diffusion in wood. Wood Sci Technol 21: 249~256.

Awoyemi, L and I. P. Jones. 2011. Anatomical explanations for the changes in properties of western red cedar (*Thuja plicata*) wood during heat treatment. Wood Sci Technol 45: 261~267.

Cho, S. H. and H. Kim. 1990. A review of health effects of relative humidity in office building. The Korean Journal of Occupational Medicine. 2(2): 123~133.

Gungor, N. M. et al. 2010. Effect of surface roughness on drying speed of drying lamellas in veneer roller dryer. African Journal of Biotechnology 9(25): 3840~3846.

Hietala, S. et al. 2002. Structure of thermally modified wood studied by liquid state NMR measurements. Holzforschung 56: 522~528.

Kang, C. W. et al. 2008. Wood physics & mechanics. Hwangmoonsa pp.338

Park, B. H. et al. 2010. A Development of Interior Decoration Timber thorough Evaluation of the Quality with Domestic *Larix Kaempferi.* Journal of the Korean Society of Design Culture 16(4): 248~262.

Siau, J. F. 1995. Wood: Influence of Moisture on Physical Properties, Department of Wood Science and Forest Products, Virginia Tech pp.227

Sik, H., K. Choo, S. Zakaria, S. Ahmad, M. Yusoff, C. Chia. The Influence of Drying Temperature on the Hygroscopicity of Rubberwood (*Hevea Brasiliensis*). Journal of Agricultural Science 2(1): 48~58.

Straže, A., S. Pervan, Ž. Gorišek. 2010. Impact of various conventional drying conditions on drying rate and on moisture content gradient during early stage of beechwood drying. Proceeding of Conference COST Action E53 “The Future of Quality Control for Wood & Wood Products.” NO.56 paper.

Isolation and Characterization of Acetyl and Non-acetyl Hemicelluloses of *Arundo donax*

Feng Peng[1] -Bian jing[1]- Pai Peng[2]- Feng Xu[1] – Runcang Sun[1,2]*

[1] Lecturer, Institute of Biomass Chemistry and Technology, Beijing Forestry University, Beijing, China.
* *Corresponding author*
fengpeng@bjfu.edu.cn
[2] Professor, State Key Laboratory of Pulp and Paper Engineering, South China University of Technology, Guangzhou, China
rcsun@scut.edu.cn

Abstract

Delignified *Arundo donaxl* was sequentially extracted with DMSO, saturated barium hydroxide and 1.0 M aqueous NaOH solution. The yields of the soluble fractions were 10.2, 6.7 and 10.0% (w/w), respectively, of the dry *Arundo donaxl* materials. The DMSO-, $Ba(OH)_2$- and NaOH-soluble hemicellulosic fractions were further fractionated into two subfractions by gradient 50% and 80% saturation ammonium sulphate precipitation, respectively. Monosaccharide, molecular weight, FT-IR, 1D (^1H and ^{13}C) and 2D (HSQC) NMR analysis revealed the differences in structural characteristics and physicochemical properties among the subfractions. The subfractions precipitated with 50% saturation ammonium sulphate had lower arabinose/xylose and glucuronic acid/xylose ratios, but had higher molecular weight than those of the subfractions precipitated by 80% saturation ammonium sulphate. FT-IR and NMR analysis revealed that the highly acetylated DMSO-soluble hemicellulosic subfraction (H_{D50}) could be precipitated with a relatively lower concentration of 50% saturated ammonium sulphate, and thus the gradient ammonium sulphate precipitation technique could discriminate acetyl and non-acetyl hemicelluloses. It was found that the DMSO-soluble subfraction H_{D50} precipitated by 50% saturated ammonium sulphate mainly consisted of lowly substituted *O*-acetyl arabino-4-*O*-methylglucurono xylan with terminal units of arabinose linked on position 3 of xylose, 4-*O*-methylglucuronic acid residues linked on position 2 of the xylan bone, and the acetyl groups (degree of acetylation, 37%) linked on position 2 or 3. The DMSO-soluble subfraction H_{D80} precipitated by 80% saturated ammonium sulphate was mainly composed of highly substituted arabino-4-*O*-methylglucurono xylan and β-D-glucan.

***Keywords*:** *Arundo donax,* Hemicelluloses, Gradient ammonium sulphate fractionation, Characteristics.

Introduction

Arundo donax is a fast growing perennial grass, native to East Asia, and widespread throughout the Mediterranean area, which has been highlighted as one of the most promising crops in terms of energy production in southern Europe (Angelini et al. 2009). Hemicelluloses are non-cellulosic and short-branched chain hetero-polysaccharides consisting of various different sugar units, which are arranged in various proportions and substituents. Hemicelluloses generally display a high degree of polydispersity in their molecular size and chemical structure, and exhibit variations in proportions of sugar constituents, linkage type, functional groups (i.e. OH groups, acetoxy groups, carboxyl groups, methoxyl groups, etc.), or degree and arrangement of branching. Due to their different chemical and molecular structure, hemicelluloses represent a different type of polysaccharide that behaves differently with cellulose and starch. Relatively small differences in the structure of polysaccharides may give rise to substantial variations in their physicochemical properties and applications. Therefore, it is sometimes necessary, when examining their molecular structures or structure property relationships, to fractionate them into structural1y more homogeneous material. In recent years, much attention has been paid to developing effective isolation and purification methods to obtain homogeneous hemicelluloses with both high purity and yield. Salting-out procedures, such as ammonium sulphate precipitation, commonly utilized in isolation and fractionation of proteins (Stec et al. 2004), have received less attention in the area of isolation and fractionation of polysaccharides. In the current work, the hemicellulosic fractions were prepared by stepwise extraction of *Arundo donax* samples with DMSO, saturated $Ba(OH)_2$ and aqueous 1.0 M NaOH, followed by subfractionation through precipitation with gradient ammonium sulphate. Moreover, the structural characterization of each subfraction was investigated by high performance anion exchange chromatography (HPAEC), Fourier transform infrared spectra (FT-IR), gel permeation chromatography (GPC), and nuclear magnetic resonance (NMR) spectra.

Materials and Methods

Materials. *Arundo donaxl* was harvested in January 2011 in Sichuan Province, China. After removal of leaves, the trunks were chipped into small pieces.The powder was dewaxed with 2:1 (v/v) toluene-ethanol in a Soxhlet apparatus for 6 h. The dewaxed sample was further dried in a cabinet oven with air circulation at 60 ^{o}C for 16 h. The components (%, w/w) of the *Arundo donaxl* were holocellulose 66.1%, pentosans 25.4%, Klason lignin 19.9%, extractives 1.5%, and ash 3.9%, which were determined according to Tappi standards (Tappi 2002) for measuring the chemical composition. All standard chemicals were analytical grade, purchased from Sigma Chemical Company (Beijing).

Extraction and Fractionation. The fractional isolation of hemicelluloses from *Arundo donaxl* is illustrated in Fig. 1. The dewaxed powder was delignified with 6% sodium chlorite at pH 3.6-3.8, adjusted with 10% acetic acid, at 75 ^{o}C for 2 h. Then the holocellulose (25.0 g) was successively extracted by dimethyl sulfoxide (DMSO), saturated $Ba(OH)_2$, and 1.0 M aqueous NaOH. The filtrate obtained by the DMSO treatment was concentrated, and then mixed with three volumes of ethanol. The

precipitate was then redissolved in water, and ammonium sulphate was added slowly up to 50% saturation**.** The precipitated hemicelluloses were collected by centrifugation (3500 g, 15 min), redissolved in distilled H_2O, and dialyzed, freeze-dried, and designated as H_{D50}. Then the saturation level of $(NH_4)_2SO_4$ in the remaining filtrate was subsequently adjusted to 80%. The corresponding precipitated hemicelluloses were labeled as H_{D80}. The filtrates obtained by the treatment of saturated $Ba(OH)_2$, and 1.0 M NaOH were adjusted to pH at 6.0 with 6.0 M HCl, concentrated, dialyzed until free of $BaCl_2$ or NaCl, and obtained saturated $Ba(OH)_2$ and 1.0 M NaOH extracts, which were further fractionated by ammonium sulphate precipitation in a similar manner mentioned above. Four subfractions were obtained from each extract: H_{B50}, H_{N50}, H_{B80}, and H_{N80}.

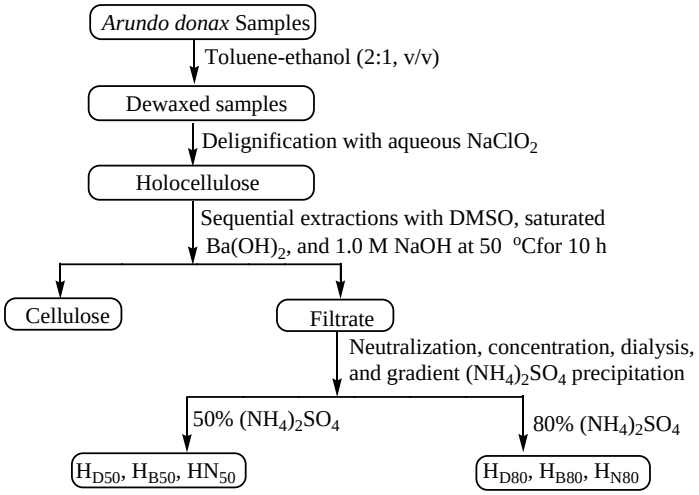

Figure 1. Scheme for fractional isolation of hemicelluloses from *Arundo donaxl.*

Analytical Methods. The composition of neutral sugars, uronic acids and the molecular weights of the hemicellulosic samples were determined according to the literature (Peng et al. 2010). FT-IR experiments were conducted using a Thermo Scientific Nicolet iN 10 FT-IR Microscopy (Thermo Nicolet Corporation, Madison, WI) equipped with a liquid nitrogen cooled MCT detector. The solution-state ^{1}H-NMR spectra were recorded on a Bruker NMR spectrometer at 400 MHz. The degree of acetylation (DS_{AC}) was determined from the relative intensities of signals of acetyl group at 2.1 ppm and those of all carbohydrate signals in ^{1}H-NMR spectra. The following equation was used:

$$DS_{AC} = \frac{(\text{Sum of integrals for acetyl groups at 2.1 ppm})/3}{(\text{Sum of integrals for carbohydrate signals at 3.0-5.5 ppm})/6}.$$

The ^{13}C-NMR spectra were recorded at 25 °C after 30 000 scans. The proton-detected heteronuclear single quantum correlation (HSQC) spectra were acquired by HSQCGE experiment mode, over a t_1 spectral width of 10,000 Hz and a t_2 width of 1800 Hz, and the acquired time (AQ) was 0.1163 s.

Results And Discussion

Yield and Composition. The sugar components of the six subfractions are presented in Table 1. All the hemicellulosic subfractions were composed mainly of xylose (49.8-87.3%), arabinose (4.9-19.0%), and glucuronic acid (4.8-12.7%). Small amounts of

glucose and galactose were also detected. The data above suggested that a substantial proportion of the polysaccharide in the cell walls of *Arundo donax* consists of glucuronoarabinoxylans. It should be noted that in H_{D50} and H_{D80} obtained from the DMSO-soluble hemicelluloses, xylose decreased from 87.3% (H_{D50}) to 60.2% (H_{D80}), whereas arabinose increased from 4.9% to 6.5%, and glucuronic acid (GlcA) from 2.7% to 11.1%. The ratios of arabinose to xylose (Ara/Xyl) and glucuronic acid to xylose (Glc*p*A/Xyl) are indicative of the degree of linearity or branching of hemicelluloses (Chaikumpollert et al. 2004). The ratios of Ara/Xyl and Glc*p*A/Xyl increased from 0.06 to 0.11 and from 0.06 to 0.18, respectively, with increasing concentrations of saturated ammonium sulphate from 50% to 80%.These results suggested that the hemicellulosic subfractions precipitated at the lower saturation level of ammonium sulphate (50%) had a lesser substituted xylan backbone as compared with those subfractions at a higher salt concentration (80%), which were consistent with the results found for arabinoxylans of wheat endosperm and wheat flour by graded ethanol or ammonium sulfate precipitation techniques (Izydorczyk et al. 1994, Hoffmann et al. 1991). The results of the present study indicated that the less-branched hemicelluloses backbone were more likely to aggregate, force out of the solution, and precipitated at relative low levels of saturation $(NH_4)_2SO_4$.

Table 1. Yield and Composition of Hemicellulosic Subfractions from *Arundo donaxl*

subfraction[a]	yield[b] (%)	molar composition[c] (mol %)					molar ratio	
		Ara	Gal	Glc	Xyl	GlcA	GlcA/Xyl	Ara/Xyl
H_{D50}	8.13	4.91	0.19	4.98	87.27	2.65	0.03	0.06
H_{D80}	1.15	6.53	5.22	17.03	60.15	11.08	0.18	0.11
H_{B50}	3.80	9.60	0.83	3.16	78.60	7.81	0.10	0.12
H_{B80}	1.39	15.82	3.68	6.45	61.33	12.72	0.21	0.25
H_{N50}	6.17	8.11	0.07	0.48	86.49	4.84	0.06	0.09
H_{N80}	2.15	18.96	11.80	10.11	49.79	9.34	0.19	0.38

[a] H_{D50} and $H_{D80,}$ H_{B50} and $H_{B80,}$ and H_{N50} and H_{N80} represent the subfractions precipitated at 50% and 80% $(NH_4)_2SO_4$ from DMSO-, $Ba(OH)_2$-, and NaOH-soluble hemicelluloses, respectively. [b] Based on dry starting materials (w/w). [c] Expressed in relative molar percentages.

Molecular Weight. As can be seen from Table 2, the M_w of hemicelluloses followed this order: DMSO-soluble hemicelluloses (H_{D50} and H_{D80}) > saturated $Ba(OH)_2$-soluble hemicelluloses (H_{B50} and H_{B80}) > 1.0 M KOH-soluble hemicelluloses (H_{N50} and H_{N80}). In addition, HD_{50} obtained by precipitation with 50% saturated ammonium sulphate had a higher M_w of 38 100 g mol^{-1} than H_{D80} (M_w=18 350 g mol^{-1}) precipitated with 80% saturated ammonium sulphate. These trends were also observed in other four subfractions (H_{B50} and H_{B80}, H_{N50} and H_{N80}), which suggested that subfractions exhibiting higher molecular weight were precipitated with the lower concentration of saturated ammonium sulphate than those precipitated with the higher concentration of $(NH_4)_2SO_4$. Based on this observation and the Glc*p*A/Xyl and Ara/Xyl ratios, it could be concluded that the less-branched hemicelluloses with a high molecular weight were precipitated in lower ammonium sulphate percentages, while with increasing ammonium sulphate

concentrations, more branched hemicelluloses with low molecular weights were obtained, which were in a good agreement with the result of other study on alkali-extracted arabinoxylans (Izydorczyk et al. 1992).

Table 2. Weight-average(M_w) and number-average (M_n) molecular weights (g/mol) and polydispersity (M_w/M_n) of the hemicellulosic subfractions

	hemicellulosic subfractions[a]					
	H_{D50}	H_{D80}	H_{B50}	H_{B80}	H_{N50}	H_{N80}
M_w	38100	18350	28650	13570	19190	11560
M_n	12400	3220	6820	2220	3990	1650
M_w/M_n	3.1	5.7	4.2	6.1	4.8	7.0

[a] Corresponding to the hemicellulosic subfractions in **Table 1**.

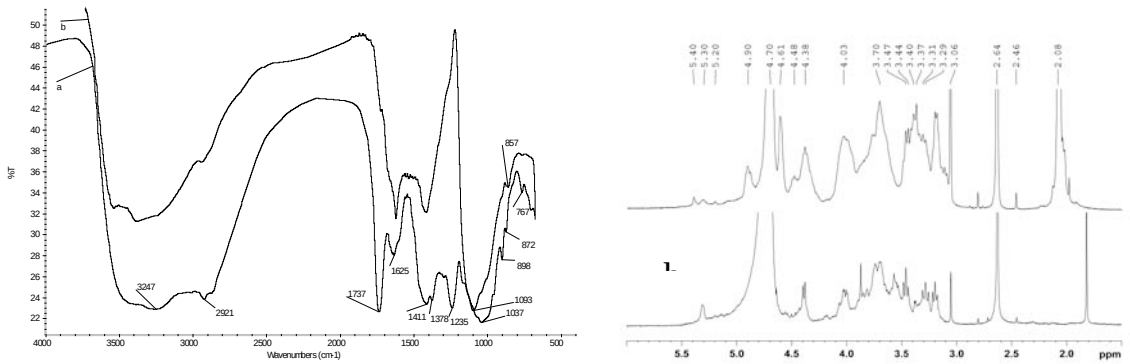

Figure 2. FT-IR spectra of DMSO-soluble hemicellulosic subfractions H_{D50} (spectrum a) and H_{D80} (spectrum b).

Figure 3. ^{1}H NMR spectra of hemicellulosic subfractions H_{D50} (spectrum a) and H_{D80} (spectrum b).

FT-IR Spectra. The FT-IR spectra of DMSO-soluble subfractions H_{D50} (spectrum a) and H_{D80} (spectrum b) precipitated by 50% and 80% saturated ammonium sulphate are shown in Fig. 2. The sharp signal at 1737 cm^{-1}, attributed to C=O stretching of carbonyl and acetyl groups in the hemicelluloses, is present in H_{D50} (spectrum a) obtained at 50% saturated ammonium sulphate, which indicates that under the treatment of dimethyl sulfoxide, the most common neutral (non-destructive) solvent, the hemicelluloses can be extracted without cleaving the acetyl ester groups. The acetyl group is believed to be mostly associated either with xylose or uronic acid residues of hemicelluloses, and easily cleaved by alkali (Sjöström 1981). However, the absence of a signal at 1737 cm^{-1} in H_{D80} (spectrum b) implied that the graded ammonium sulphate technique can discriminate acetyl and non-acetyl hemicelluloses. Evidently, the major bands at 1037 and 1093 cm^{-1} are assigned to the C-OH bending mode. The small band at 1162 cm^{-1} (spectrum a, data not shown) is assigned to the C-O stretching in C-O-C glycosidic linkages, and contribution of C-OH bending from arabinoxylans, and the variation of the signal intensity reflect the degree of substitution by arabinose residues (Mathew et al. 1987). The absorbance at 896 cm^{-1} (spectrum a), the carbohydrate C_1-H deformation and ring-stretching frequency, is characteristic of dominant β-glycosidic linkages between the

sugar units in the subfractions. The signals at 857 and 767 cm^{-1} are indicative of α-glycosidic linkages, which indicate that the arabinose, glucose, glucuroninc acid are probably linked by α-glycosidic linkages. In addition, two bands at 1625 and 1411 cm^{-1} are assigned to the $–COO^-$ antisymmetric and symmetric stretching of glucuronic acid or glucuronic acid carboxylate, respectively (Marchessault et al.1962).

Table 3. ^1H and ^{13}C chemical shift (ppm) assignments for hemicellulosic subfractions H_{D50} and H_{D80}

sugar residue	chemical shift (ppm) H/C							
	1	2	3	4	5ax[a]	5eq[b]	6	OCH_3
H_{D50}								
→4)-β-Xyl*p*(1→	4.38 101.6	3.19 72.7	3.46 73.5	3.70 76.3	3.31 62.9	4.03 62.9		
α-GlcA*p*-(1→2	5.32 99.8	3.38 70.9	3.71 71.3	3.13 82.3	4.15 71.2		173.2	3.37 59.9
α-Ara*f*-(1→3	5.40 107.3	4.08 80.4	3.90 76.1	4.23 84.7	3.73 60.5	3.76 60.5		
→4)-β-Xyl*p*(1→, 3-*O*-Ac	4.48		4.61					
	101.5		73.2					
→4)-β-Xyl*p*(1→, 2-*O*-Ac	4.61	4.90						
	100.0	74.9						
H_{D80}								
→4)-β-Xyl*p*(1→	4.39 101.6	3.19 72.7	3.46 73.6	3.29 76.3	3.28 62.9	4.03 62.9		
α-GlcA*p*-(1→2	5.31 99.6	3.52 71.5	3.73 71.2	3.15 82.4	4.19 71.9		171.1	3.38 59.9
α-Ara*f*-(1→3	5.31 107.6	4.07 80.8	3.85 77.1	4.20 84.7	3.72 60.5	3.76 60.5		

[a] ax, axial, [b]eq, equatorial.

NMR Spectra. ^1H NMR spectra of H_{D50} (spectrum a) and H_{D80} (spectrum b) are shown in Fig. 3. As can be seen, the relevant signals occurred in two regions, namely, the anomeric region (4.3-4.9 ppm for β-anomers and 4.9-5.6 ppm for α-anomers) and the ring proton region (4.3-3.0 ppm). From the anomeric region, the spectra of the two subfractions revealed the DMSO-soluble hemicelluloses are mainly composed of three populations. The signals at 4.38 ppm are assigned to the anomeric protons of (1→4)-linked β-D-Xyl*p*. The signal at 5.4 ppm is originated from anomeric protons of terminal Ara*f* linked to *O*-3 of Xyl*p*. An anomeric proton at 5.3 ppm is characteristic of 4-*O*-methylglucuronic acid attached via α-(1→2) linkage to xylose (Ohkoshi et al. 1997). A strong resonance at 5.3 ppm found in H_{D80} (spectrum b) precipitated by 80% saturated ammonium sulphate indicated that a majority of the branching sites were represented by single substituted Xyl*p*. These results were in agreement with the results of sugar analysis (**Table 1**). The signal at 2.1 ppm indicated that the hemicellulosic subfraction H_{D50} precipitated by 50% saturated ammonium sulphate was highly acetylated. The degree of acetyl substitution

(DS_{AC}) of the hemicellulosic subfraction H_{D50} was 0.37, which was determined by integration of the signals of acetyl groups at 2.1 ppm and those of all carbohydrate signals (Teleman et al. 2000). However, the signal at 2.08 ppm was absent in the subfraction H_{D80} (Fig. 3b), which suggested that the highly acetylated hemicelluloses were precipitated at the relatively lower concentration of saturated ammonium sulphate, corresponding to the results obtained by FT-IR. The ^{13}C NMR spectra of H_{D50} (spectrum a) and H_{D80} (spectrum b) also suggested that the presence of *O*-acetyl groups in the hemicellulosic subfraction (H_{D50}), but these signals for *O*-acetyl groups were absent in H_{D80}, which were in accordance with the results of FT-IR and ^{1}H NMR.

As can been seen from Fig. 6 and Table 3, the HSQC NMR analysis revealed three important groups: Ara*f* residues, 4-*O*-Me-α-D-Glc*p*A-(1→2) units, and (1→4)-β-D-Xyl*p*. In addition, a low amount of β-D-glucans (103.3/4.55 ppm) was also observed (*51*). Other signals of β-D-glucans are overlapped with those of xylan-type hemicelluloses. The reason for low intensity of signals from β-D-glucans was probably due to the low solubility in D_2O at ambient temperature (20 ^{o}C) (Wen et al. 2010). Some acetate was detected at 23.3/1.82 ppm in the H_{D80} NMR spectrum (data not shown), which was unclear whether this was originated from the liberation of *O*-acetyl groups (Teleman et al. 2000). Therefore, it was concluded that H_{D80} was mainly composed of arabino-4-*O*-methylglucurono xylan and β-D-glucan.

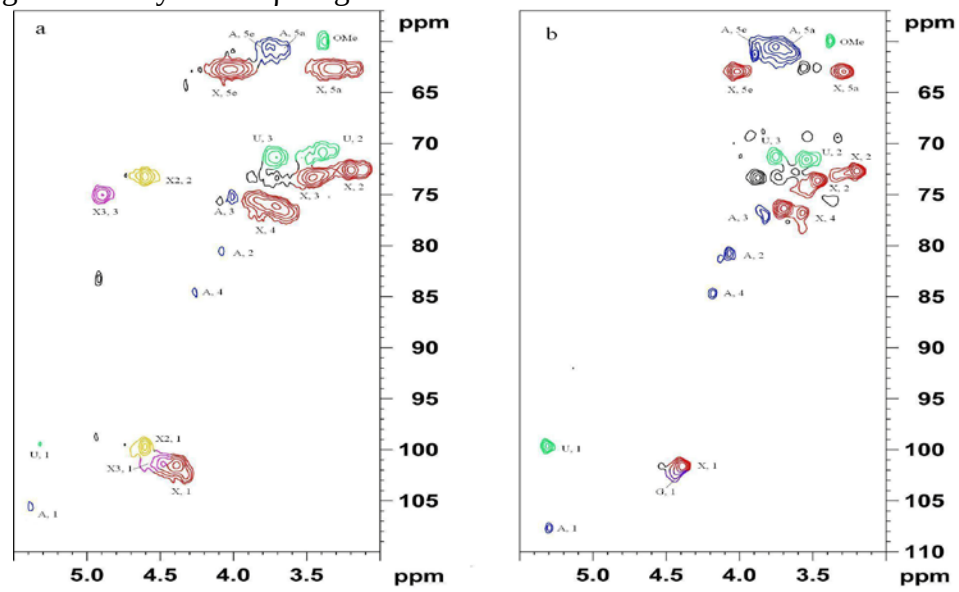

Figure 6. HSQC spectra of hemicellulosic subfractions H_{D50} (spectrum a) and H_{D80} (spectrum b). Designations are follows: X, Xyl*p*; A, Ara*f*; U, 4-*O*-Me-α-Glc*p*A; X2, 2-*O*-acetylated Xyl*p*; X3, 3-*O*-acetylated Xyl*p*; G, Glc*p*.

Conclusions

The present study was aimed at obtaining detailed structural characteristics of hemicelluloses extracted successively with dimethyl sulfoxide (DMSO), saturated $Ba(OH)_2$, and 1.0 M aqueous NaOH from *Arundo donax*, and fractionated with gradient ammonium sulphate technique. The sugar analysis indicated that the hemicellulosic

subfractions precipitated at the lower saturation level of ammonium sulphate (50%) were lesser substituted hemicelluloses as compared with those subfractions obtained at a higher salt concentration (80%).With increasing ammonium sulphate concentrations, the average molecular weights of the hemicellulosic subfractions decreased. FT-IR and NMR analysis indicated the gradient ammonium sulphate technique could discriminate acetyl and non-acetyl hemicelluloses. The DMSO-soluble hemicelllosic subfraction H_{D50} precipitated mainly consists of low substituted *O*-acetyl arabino-4-*O*-methylglucurono-(1→4)-β-D-xylan, in which 4-*O*-Me-α-D-GlcpA-(1→2) units was linked at position *O*-2, Ara*f* residues at *O*-3, and *O*-acetyl groups at *O*-2 or *O*-3. The H_{D80} is mainly composed of highly substituted arabino-4-*O*-methylglucuronoxylan and β-D-glucan.

Acknowledgements

This work was supported by the grants from Beijing Forestry University Young Scientist Fund (2010BLX04), Ministry of Science and Technology (973 project, 2010CB732204), the Natural Science Foundation of China (No. 30930073).

Reference

Angelini, L. G.; Ceccarini, L.; Nassi, N.; et al. Comparison of *Arundo donax* L. and *Miscanthus x giganteus* in a long-term field experiment in Central Italy: analysis of productive characteristics and energy balance. *Biomass Bioenerg.* **2009**, *33*, 635-643.
Hoffmann, R. A.; Roza, M.; Maat, J. Structural characteristics of the cold-water-soluble arabinoxylans from the wheat flour of the soft wheat variety kadet. *Carbohyd. Polym.* **1991**, *15*, 415-430.
Izydorczyk, M. S.; Biliaderis, C. G. Influence of structure on the physicochemical properties of wheat arabinoxylan. *Carbohyd. Polym.* **1992**, *17*, 237-247.
Izydorczyk, M. S.; Biliaderis, C. G. Studies on the structure of wheat-endosperm arabinoxylans. *Carbohyd. Polym.* **1994**, *24*, 61-71.
Mathew, M. D.; Jain, A. K.; Ray, P. K. Infrared-spectra of Jute. *Cell Chem. Technol.* **1987,** *21*, 17-29.
Marchessault, R. H.; Liang, C. Y. The infrared spectra of crystalline polysaccharides. VIII. Xylans. *J. Polym. Sci.* **1962**, *59*, 357-378.
Ohkoshi, M.; Kato, A.; Hayashi, N. C-13-NMR analysis of acetyl groups in acetylated wood. 1. Acetyl groups in cellulose and hemicellulose. *Mokuzai Gakkaishi* **1997**, *43*, 327-336.
Peng, F.; Ren, J. L.; Xu, F.; Bian, J.; Peng, P.; Sun, R. C. Fractionation of alkali-solubilized hemicelluloses from delignified *Populus gansuensis*: structure and properties. *J. Agric. Food Chem.* **2010**, *58*, 5743-5750.
Sjöström E. Wood polysaccharides. In *Wood chemistry, fundamentals and applications*; Sjöström E., Ed.; Academic Press: New York, 1981; pp 61-67.
Stec, J.; Bicka, L.; Kuzmak, J. Isolation and purification of polyclonal IgG antibodies from bovine serum by high performance liquid chromatography. *Bull. Vet. Inst. Pulawy.* **2004**, *48*, 321-327.
Teleman, A.; Lundquvist, J.; Tjerneld, F.; Stalbrand, H.; Dahlman, O. Characterization of acetylated 4-*O*-methylglucuronoxylan isolated from aspen employing ^{1}H and ^{13}C NMR

spectroscopy. *Carbohyd. Res.* **2000**, *329*, 807-815.
Wen, J. L.; Sun, Y. C.; Xu, F.; Sun, R. C. Fractional isolation and chemical structure of hemicellulosic polymer obtained from *Bambusa rigida* species. *J. Agric. Food Chem.* **2010**, *58*, 11372-11383.

Proceedings of the 55th International Convention of Society of Wood Science and Technology
August 27-31, 2012 - Beijing, CHINA

Eco Audit BBSS-EVO and other Guadua Bamboo Structural Systems using Ashby Methodologies and Cambridge Material Selector Software

José Luis REQUE CAMPERO

BOLBAMBÚ Program Coordinator, Research Institute of Architecture. Doctoral Fellow in Energy and Development, Universidad Mayor de San Simon, UMSS. Cochabamba, BOLIVIA
jlreque21@gmail.com Tel. Fax + 591 - 4 - 4255731

Abstract

Green design in architecture and structural systems has many aspects, one of which is the evaluation and selection of materials. The materials are energy intensive, with high embodied energy and associated carbon footprint. Not only is the choice of materials and their impact on manufacturing, but which affects the weight of the product and its thermal and electrical characteristics and therefore the energy consumed during use, and influences the potential for recycling or recovery energy at the end of its life cycle.

The research attention has focused on some materials such as bamboo, which has found application in preindustrial times. At first glance, the use of this material appears to be satisfactory. One examines the causes of its rapid implementation and observes the scientific discoveries in the last three decades, the balance is very positive.

The unprecedented structural system Bamboo-EVO Bolivia Spatial Structures (BBSS-EVO) provides technologically advanced mechanical connections for active form and active vector form structure systems. Currently, initial stage research continues under the guidelines of the Doctoral Program in Energy and Development. Within a global context, the research develops academic and scientific activities that identify the most promising of Guadua bamboo structural systems, with special interest in BBSS- EVO. Systems will be evaluated by Ashby methodologies and the Cambridge Materials Selector software (CMS) by means of Eco-Audit in order to identify life-cycle, embodied energy, and carbon footprint, determinations of balance, and eco-design options.

Keywords: Bamboo, Structural System, Eco Audit

The Problem

Natural and created complex systems often interact. When two complex systems tend to develop without interacting with each other, the consequences are unpredictable. While we have achieved development and welfare in many aspects of life, we have impoverished nature, and as we proceed with this developmentalist, polluting, and predatory endeavor, nature and the environment set limits which we are increasingly unaware because we have lost the perception of life.

Negative impacts on environment and ecosystems were shown since industrial revolution, when hydrocarbons as an energy source began extensively to be part of the materials production chains. There were corrective actions with as limited success as many other "eco-concerns" rose from the ways we use energy and materials. Unfortunately, we have no global understanding of these problems until now. If we understand the origins and potential effects of materials, we will be able to choose them carefully and by that mean to contribute to alleviate those negative impacts.

Only industrial materials needed in construction mobilize massive financial resources. Energy-intensive production requires focused and linear processes. Precisely because they are linear, these processes are facing a vast crisis, since they cannot operate indefinitely on a finite planet. Materials research today is based mainly on the need to find new, non-polluting, light weight material technologies, able to consume small amounts of energy, and with good thermal and electrical characteristics.

Several research efforts have focused on Guadua Bamboo as locally produced material with high ecological qualities, low-cost and low power consumption in its production, and able to prevent the outflow of currency for raw materials. Eco-Cost of Bamboo is the lowest, if we focus on the production of a material that resists 1 N/mm^2, since it requires less energy. Wood and concrete Eco-Costs are following, and steel is the most expensive, since requires an amount of energy 50 times greater than which is used by bamboo (Table 1).

Material	*Bamboo*	*Wood*	*Concrete*	*Steel*
$MJ/M^3/MPA$	30	80	240	1500

Table 1. Ratio of Energy Production Per Unit Voltage (Source: Ghavami, 2002)

Purpose

Main Goals

The main goal of this research is by means of Ashby methodologies and Cambridge Materials Selector (CMS) software, to execute Eco-Audits on research proposals about Guadua bamboo structural systems in a global context, and particularly, on "Bamboo Bolivia Spatial Structures, BBSS-EVO" Structural System, in order to establish the validity of eco-design options (Fig. 1).

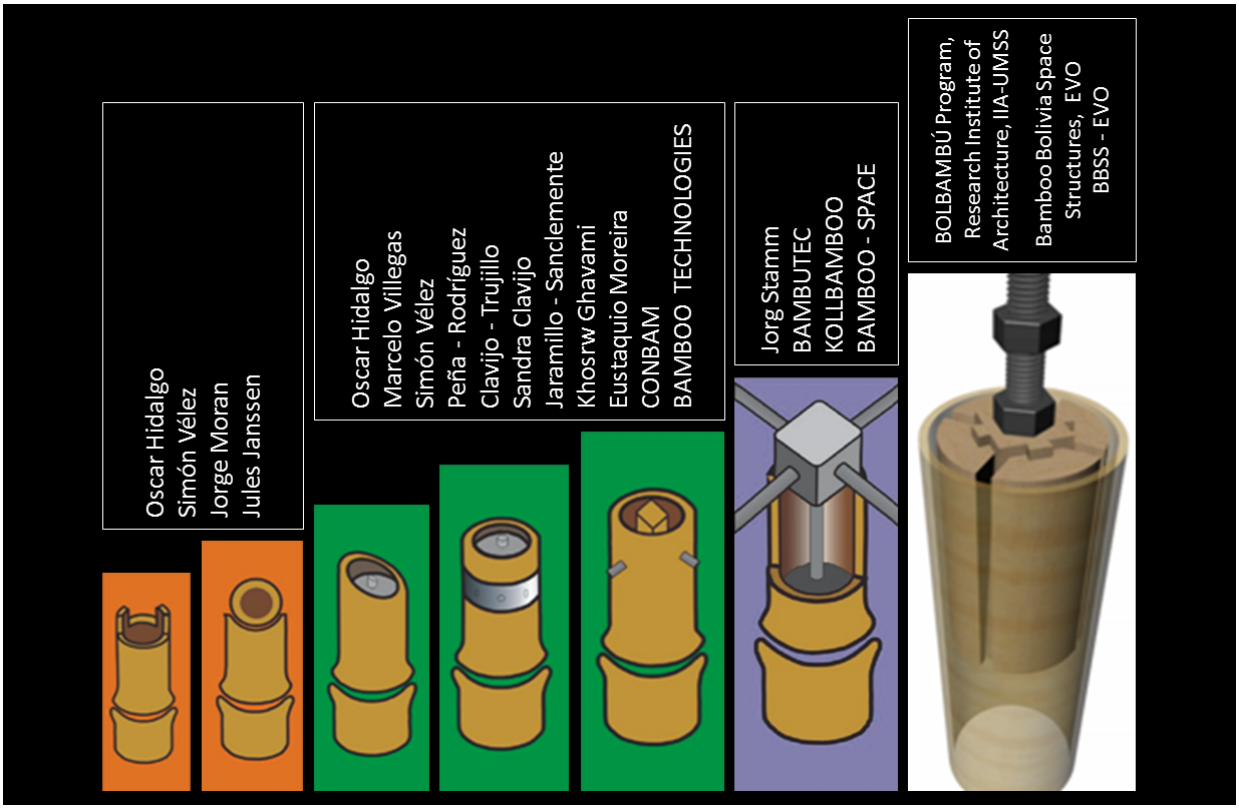

Fig. 1. Structural Systems in the World developed by people and institutions, in Bolivia: BBSS - EVO. (Source: Reque, 2012)

Specific Goals

- To identify life cycles.
- To identify the energy that is incorporated.

- To identify carbon footprints.
- To explain eco-structural systems.

Theoretical Background

Research brought about in the Faculty of Civil Engineering at the University PUC-Rio showed that the main advantages of bamboo are low energy per tension unit and high resistance to traction stresses. The use of bamboo as a building and structural material has motivated the interest of an increasing number of research endeavors on a global level, such as those developed at the University of Cambridge, demonstrating their superior structural efficiency compared with other natural materials and industrial products known in the materials engineering. For this purpose we used the Cambridge Materials Selector —CMS software—, which, in other settings, uses a merit index including the elasticity module, the strength and the density of the material.

Methodologies developed by Ashby,[1] along with the CMS software, showed their validity in to explaining how we depend on materials and their uses, and aiming to overcome certain simplifications and misinformation that took place in public debates on environment. Ashby introduced methods to think and design with materials. One of the main objectives is to minimize the environmental impact (a goal that is often in conflict with others, in particular with the minimization of costs, where bamboo once more has advantages over other materials). Ashby methodologies do not offer "the latest solutions." They rather provide a new background perspective, methods and data to induce researchers to make their own judgments regarding one of the central issues of environmental concerns: the fact that the use of materials also provides essential background for a rigorous approach to address environmental concerns, providing an essential basis for the study of broader issues. Among these are the issues of sustainability and possibilities of future (an attempt to anticipate future problems and possible solutions). These methodologies also present (in the CMS software) a set of engineering data sheets for metals, polymers, ceramics, compounds, and of course, the hybrid materials such as bamboo. Each datum has a description and a picture, a table of mechanical, thermal, and electrical properties, and a table of properties related to environmental issues—extremely important for the purpose of this research.

From Ashby's and other researchers' vantage point, all materials have a life cycle, with a series of stages, beginning with the extraction of raw materials, continuing with the manufacturing, transport, and use processes, and at the end of their lives, with the delivery to a landfill or to recycling centers. Ordinary people have usually an approach to this reality. The great contribution of Ashby is to have established clear rules in the analysis, showing that, almost always, there is a stage of a life cycle, in which the consumption of resources, energy and the generation of emissions are greater than those of all the other stages put together. One of the

[1] Since 1973 member of the University of Cambridge, Department of Engineering, where he is currently Professor of the Royal Society Research.

main goals of this research is to identify the stage in which the consumption of energy and resources is the greatest. Life cycle assessment, LCA, attempts to do this by focusing on these major elements: resource (bamboo and other materials), energy, and CO_2 emissions.

Every material carries an energy content (the energy needed to create it) and a carbon footprint (CO_2 that is emitted in this creation process). So do the stages of the life cycle in which the heating, cooling and transport (Fig. 2), for example, are among the most energy-intensive. However, the correct choice of materials can reduce this indicator, especially if one uses the bamboo in its natural state. From this point spring the design decisions that minimize or eliminate adverse eco-impacts. The duly informed selection of materials is a central aspect of this task, along with the information needs of the material attributes that most directly affect environment. Some, such as embodied energy and carbon footprint, recycling of the fraction and toxicity, have obvious eco-connections. However, more often mechanical, thermal, and electrical properties are the most important in the design to minimize environmental impact.

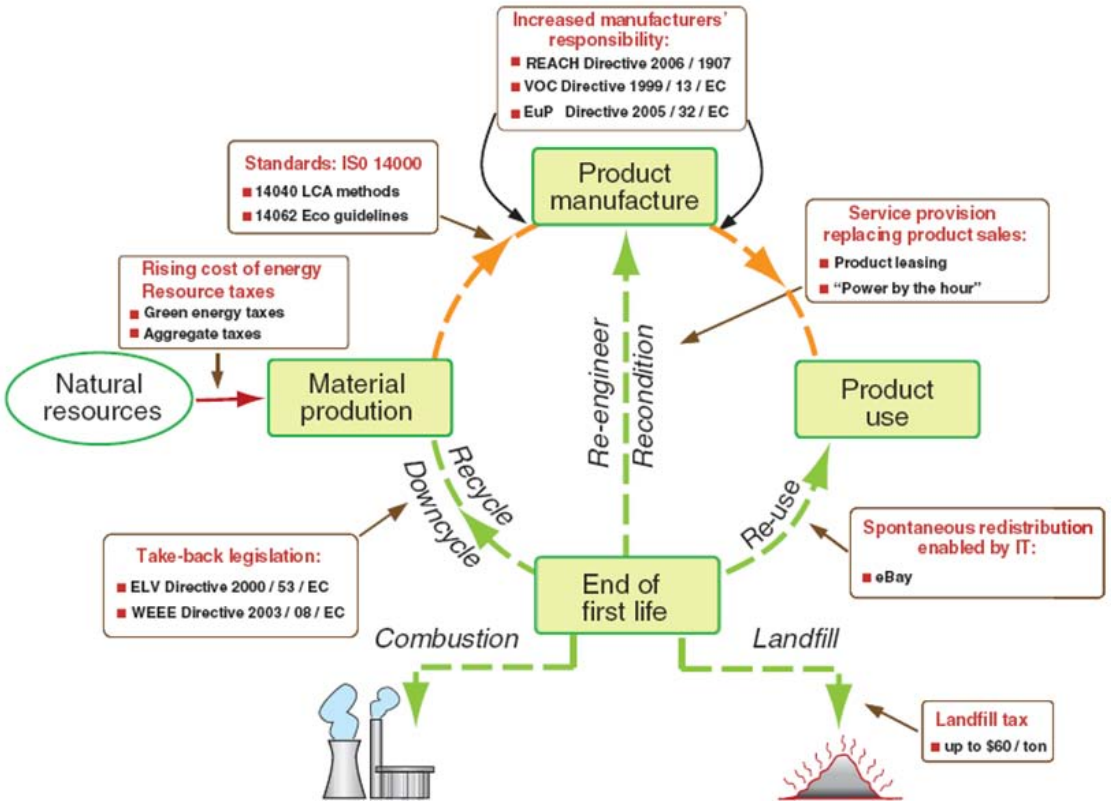

Fig. 2. The life cycle of a material.
Raw materials are extracted and processed to produce a material with interventions and other mechanisms that influence the flow of life cycles. The material is a manufactured product used and the end of his life is discarded, recycled, or, less commonly, renewed or reused. Energy and materials consumed in each phase generate waste heat and solid, liquid and gaseous emissions. (Source: Asbhy, 2009)

Methodological Scheme

The research consists of three parts and eight chapters, namely: Part I, Research and Design (two chapters), Part II, Evaluation and Results (five chapters), Part III Conclusions and Recommendations (one chapter). The following is the conceptual map of the methodology (Fig.3).

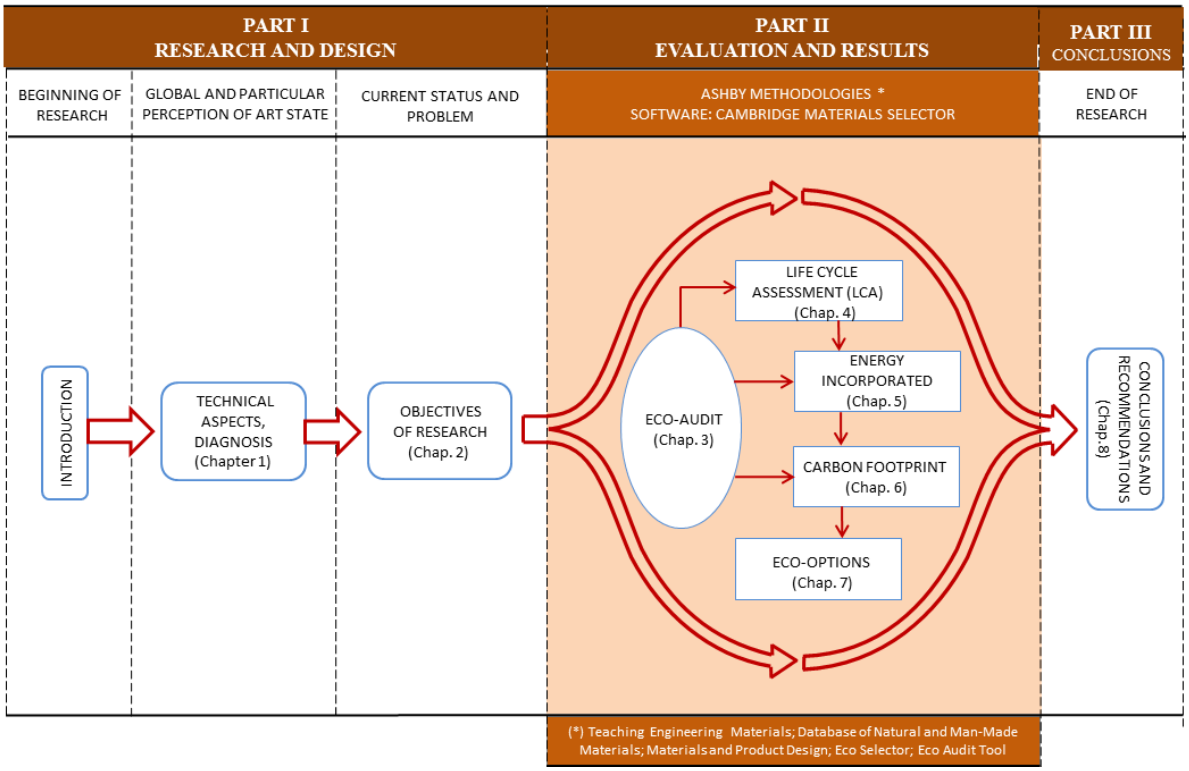

Fig. 3. Methodological scheme (Source: Reque, 2012)

Part I *(Research and Design)* is the analysis of the problems that lead to the main purpose of research as a central issue rose in the Introduction and the structure of the research. The diagnosis of Bamboo intervention in architectural design and structural (mechanical joints), under a global perception and particularly the state of art in an international context, and, endogenously, BBSS-EVO, in Chapter 1; then in Chapter 2, particularize the current state of the problem with main mechanic junctures.

Part II *(Evaluation and Results)* is structured on the basis of the main element of action research:

methodologies and software, Asbhy CMS, the fundamental bases of analysis and discussion. The Eco-Audit in Chapter 3, (graphically detailed below) and that under the "circle evaluator" is related to three other themes: Life Cycle Assessment (Chapter 4), Energy Incorporated (Chapter 5) Carbon Footprint (Chapter 6.) Finally and as a result of this, we present the Eco-Options for Structural Systems (Chapter 7).

The design of BBSS-EVO structural model, and its analysis and verification, the differences between it and the conventional knowledge and the basic structural models are considered in Chapter 3 under the optics of Eco-Audit (Fig. 4). In Chapter 4 the lifecycle stages are evaluated. We devote Chapters 5 and 6 to check what stage embodies the greatest consumption of energy and resources. In Chapter 7, a balance is established on the eco-options in structural design with Guadua Bamboo.

Finally, there is an evaluation of the intervention itself, based upon relevant indicators emerging from the "assessing circle" in Part II. The audit process is carefully analyzed, trying to answer the question: "What happened in the assessment circle?" It provides the overall balance of Eco-audit of Structural Systems with Bamboo and recommendations to expand or improve the intervention in the future. Those aspects are considered in Part III *(Conclusions and Recommendations)* of Chapter 8.

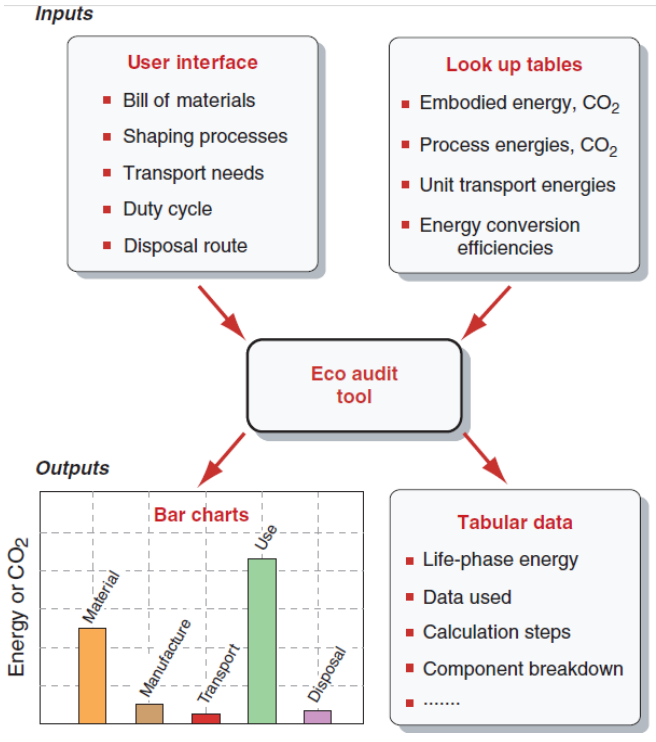

Fig 4. The method of energy audit. (Source: Ashby, 2009)

References

Asbhy, Michael F., *Materials and the Environment. Eco-Informed Material Choice*, Elsevier, 2009.

Acknowledgements

My appreciation for Mr. PhD. Robert Hukai, professor at the Institute of Electrical Engineering, University of Sao Paulo, Brazil.

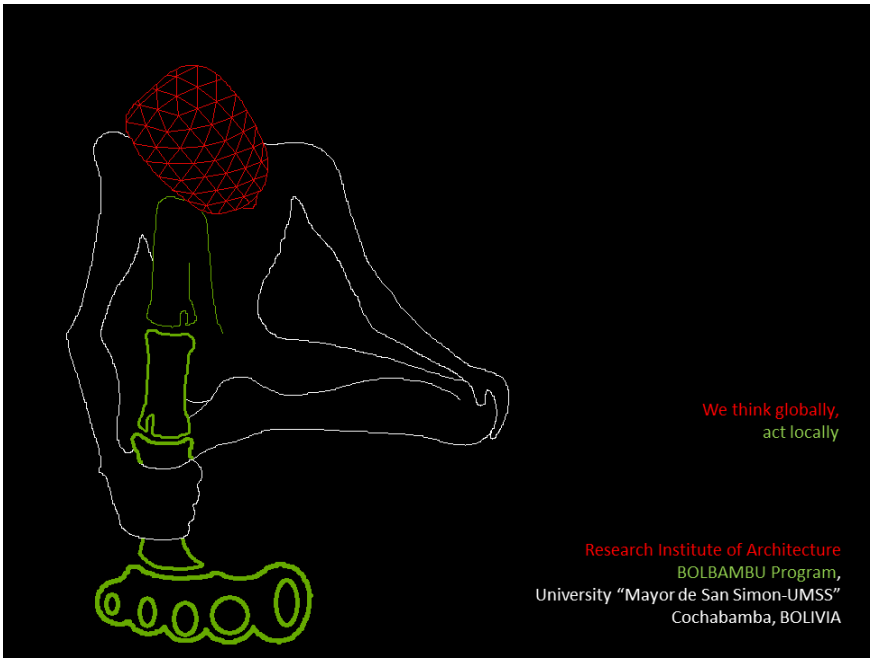

A Novel Ca^{2+} Binding of Highly Thermostable Xylanase from *Thermotoga thermarum*: Cloning, Expression and Characterization

Hao SHI, Xun LI, Huaxiang GU, Liangliang WANG, Ye WANG, Huaihai DING,

Yinjun HUANG, Fei WANG[*]

China College of Chemical Engineering, Nanjing Forestry University,

Nanjing 210037, China

Jiangsu Key Lab of Biomass-Based Green Fuels and Chemicals,

Nanjing 210037, China

Abstract

A xylanase gene (*Tth xyn10A*) of 3474 bp was cloned from the extremely thermophilic bacterium *Thermotoga thermarum* that encodes a protein containing 1158 amino acid residues. Based on amino acid sequence homology, hydrophobic cluster, and three dimensional structure analyses, this xylanase belongs to the glycoside hydrolase families (GHF) 10 with five carbohydrate binding domains. When the xylanase gene was cloned and expressed in *Escherichia coli* BL21 (DE3), the activity of xylanase produced by the recombinant strain was up to 136 U/mg. The xylanase is optimally active at 95^{o}C and pH 7.0 with a high thermostability over broad range of pH 4-8.5 and temperature 55-90^{o}C by the addition of 5 mM Ca^{2+}. It is confirmed by Ion Chromatography System (ICS) analysis that the end products of the hydrolysis of beechwood xylan are xylose, xylobiose, xylotriose, xylotetraose, xylopentaose and xylohexaose. The xylanase from *T. thermarum* is one of the hyperthermophilic xylanases that exhibits high temperature stability, and thus, it is a suitable candidate for generating xylooligosaccharides from cellulosic materials like agriculture residues and forestry residues for the uses as prebiotics and precursor for yielding furfural or other chemicals.

Key words: xylanase, xylan, thermostability, beech wood, oat spelt, birch wood

Introduction

Xylanases (EC 3.2.1.8) have been shown important role in industrial processes, and they are used as additives to enhance the quality of baked goods and animal feeds and to bleach kraft pulp (Fuzi et al. 2011). The xylanases are also the crucial enzymes for depolymerization and randomly hydrolyze the β-1,4-glycosidic bonds of xylan to produce xylooligomers with different lengths, and they have immense commercial value. Compare to other renewable resources, hemicelluloses are the second most abundant resource in the world, only are fewer than cellulose (Jiang et al. 2010, Khandeparker et al. 2011). Because of the diversity in chemical structure of xylans derived from woods, cereal or other plant materials, a large quantity of xylanases with various catalytic properties and molecular structures are known (Weng and Sun 2010). On the basis of amino acid sequence homology, hydrophobic cluster, and three dimensional structural analysis (3D), xylanases are maily classified into two glycoside hydrolase families (GHF), 10 and 11, yet enzymes with activity are also found in GHF 5, 7, 8, 16, 26, 43, 52 and 62 (Collins et al. 2005, Khandeparker et al. 2011, Ruller et al. 2008). GHF10 comprises enzymes with a number of known activities; xylanase (EC 3.2.1.8); endo-1,3-beta-xylanase (EC 3.2.1.32); cellobiohydrolase (EC:3.2.1.91). Compared to GHF11, GHF10 xylanases have better thermostability and binding of cellulose, as they have several cellulose binding domain.

Recent years, more and more genomes have been sequenced from hyperthermophilic bacteria and archaea (Angelov et al. 2010, Baba et al. 2008, Chen et al. 2005, Göker et al. 2010, Guo et al. 2011, Liolios et al. 2010, Liu et al. 2011, Mardanov et al. 2011, Mardanov et al. 2010), so there are so many sequences we can obtain from the database (http://www.ncbi.nlm.nih.gov/). *T. thermarum* DSM 5069, which was isolated from continental solfataric springs at Lac Abbe (Djibouti, Africa) (Windberger et al. 1989) was also reported its genome last year (GenBank accession number: CP002351). Currently, no information is available about the cloning and molecular characterization of the xylanases encoding genes from *T. thermarum*.

In this paper, we described the cloning, expression and functional characterization of the *Tth xyn10A* gene encoding for Tth Xyn10A, a xylanase from *T. thermarum* belonging to GHF10.

Results

Cloning and sequence analysis of *Tth xyn10A*

By analysis of the genome sequence of *T. thermarum* DSM 5069, a protein defined as xylanase consists of a 3,531 bp fragment encoding 1,171 amino acids, which belonged to GHF10. It shares the highest sequence similarity of 51% with the xylanase from *Thermotoga petrophila* RKU-1 (Genbank No. YP_001244458), *Thermotoga naphthophila* RKU-10 (Genbank No. YP_003346200) and *Thermotoga sp*. RQ2 (Genbank No. YP_001738920), which were sequenced but has not been biochemically characterized. Through blast of the catalytic domain (CD) of Tth xyn10A on GenBank, it shares the highest similarity of 78%

with another xylanase in *T. thermarum* DSM 5069 (Genbank No. YP_004660782). There is a signal peptide sequence (32 amino acids, 94 bp) in Tth xyn10A by using SignalP 4.0 Server (http://www.cbs.dtu.dk/services/SignalP/), so only the DNA fragment of a protein (*Tth xyn10A*) gene (3, 474 bp) was amplified from the synthesized fragment with optimal codons in *E. coli*, and ligated to pET-20b at *Nde* I and *Xho* I sites to generate plasmid pET-20b-*Tth xyn10A*.

Expression and purification of recombinant Tth xyn10A

The ORF region of the *Tth xyn10A* gene was expressed in *E. coli* BL21(DE3), harboring the construct Tth xyn10A, for functional analysis of the recombinant protein. In comparison to non-induced cells, the heterologous protein was expressed at high levels by induced cells with 0.5 mM IPTG. The recombinant protein was purified through a heat treatment and a Ni-NTA affinity. SDS-PAGE analysis of extracts from the bacteria harboring the construct Tth xyn10A revealed a band of approximately 130 kDa (Fig. 1). The MW of Tth xyn10A conforms to the theoretical molecular weight of the mature protein (130,949 Da), without the signal peptide.

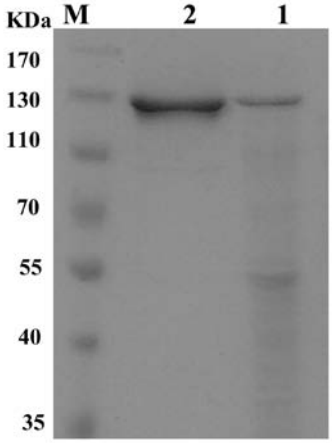

Figure 1 SDS–PAGE of Tth xyn10A. Lane M, MW standards; lane 1, crude lysate; lane 2, protein purified by Ni–NTA.

The purified Tth xyn10A was most active at pH 7.0 (Fig. 2A, B), and the xylanase activity was higher than 40% of the maximum activity at the pH range from 5.5 to 8.5 (Fig. 2B). The xylanase exhibited its optimal activity at 95^{o}C (Fig. 2C), and it retained nearly 100% of its activity at 55^{o}C-85^{o}C for 2 h when tested at pH 7.0 (Fig. 2D) (the temperature under 85^{o}C not shown). It retained more than 80% of its activity up to 90^{o}C for 30 min, and under this temperature, the enzyme had a half-life for approximately 1 h. The chemical reactions about the thermostability of temperature and pH above need 5 mM concentration of Ca^{2+}. The residual activity at 85^{o}C at pH 7.0 in the absence of the Ca^{2+} is less than 20% of that addition of 5 mM concentration of Ca^{2+} (data not shown).

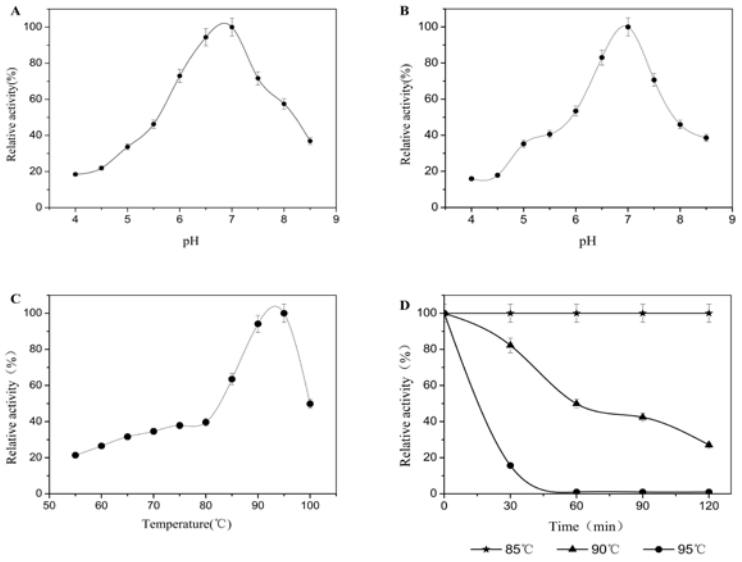

Figure 2 Effects of temperature and pH on Tth xyn10A activity and stability. (A) Determination of xylanase activity at various pHs at 85^{o}C for 10 min, using beech wood xylan as a substrate (same to the B, C, and D). The highest activity at pH 7.0 was defined as 100% level. (B) Determination of the effects of pH on xylanase stability by incubating the purified enzyme at various pHs for up to 2 h and measuring the remaining activity. The original enzyme activity before treatment was defined as 100%. (C) Determination of xylanase activity at various temperatures at pH 7.0 for 10 min. The highest activity at 95^{0}C was defined as 100% level. (D) Determination of the effects of temperature on xylanase stability by incubating the purified enzyme at various temperatures for up to 2 h and measuring the remaining activity. The original enzyme activity before treatment was defined as 100%.

The effects of metal ions and chemicals on the enzyme activity were shown in (Fig. 3). In various assays, the enzyme activity was significantly enhanced by Ca^{2+}, Mn^{2+}, Co^{2+}, Al^{3+} and SDS, and completely inactivated by Cu^{2+}. The effects other metal ions and chemicals on the enzyme activity were not so significant. The K_m and V_{max} of recombinant xylanase for oat spelt xylan as the substrate were 2.57 mg ml^{-1} and 325.32 μmol mg^{-1} min^{-1}, respectively (Table 1).

Table 1 The characteristics of recombinant xylanases of T. thermarum

Property	The recombinant Tth xyn10A
Specific enzyme activity	145.81 U mg^{-1}
Molecular weight	131 KDa
K_m	2.57 mg ml^{-1}
V_{max}	325.32 μmol mg^{-1} min^{-1}

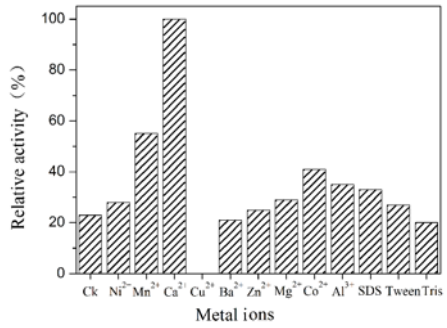

Figure 3 Effects of metal ions and reagents on purified Tth xyn10A activity. Final concentration, 1 mM metal ions or 0.1% chemical reagents.

Analysis of xylan degradation

Compared to beech wood xylan, birch wood xylan and oat spelt xylan, the maximum activity on birch wood xylan followed by beech wood xylan and oat spelt xylan was shown in Tth xyn10A xylanase, this result is similar to the xylanse from *Geobacillus Thermoleovorans* (Verma and Satyanarayana 2012) and there is almost no activity on CMC-Na. When xylan from oat spelt, birch wood and beech wood were hydrolyzed using the recombinant xylanase, xylose, xylobiose, xylotriose, xylotetraose, xylopentaose and xylohexaose were detected by ICS (data not shown).

Analyses of phylogeny and catalytic amino acid residues

To gain insights into the classified status of Tth xyn10A among xylanases, the phylogenetic trees of 22 candidate amino acid sequences were constructed using he NJ method and the MP method respectively, both supporting by almost the same topology, and three well-supported clades were detected (Fig. 4A, B). Clade I was hyperthermophilic xylanases from genus *Thermotoga*, Clade II was other xyalnases from other mesothermal and hyperthermophilic bacteria and Clade II was hyperthermophilic xylanases from archaea. It can be concluded that there exits a monophyletic group in Clade I, Tth xyn10A xylanase from *T. thermarum* (GenBank No: AEH51685) sited in boundary of Clade I shows a good relationship with the xylanase from *P. mobilis* in Clade II (GenBank No: YP_001567298).

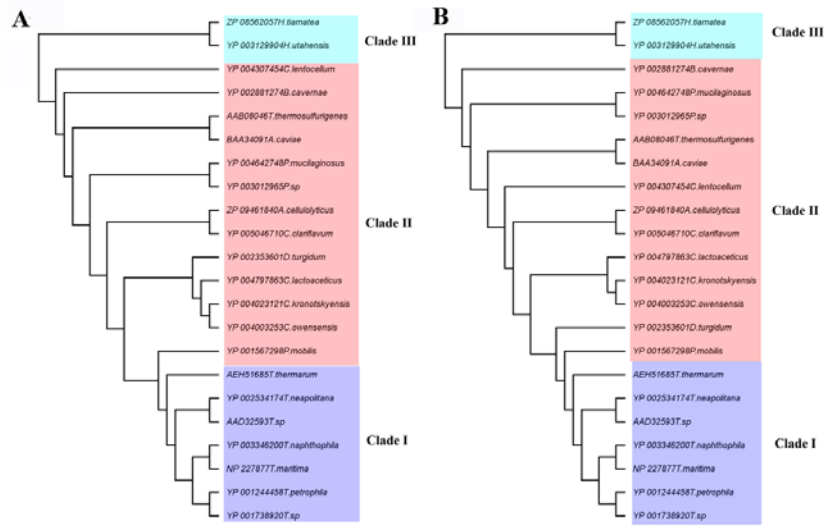

Figure 4 The Neighbor-Joining (NJ) (A) and Maximum-Parsimony (MP) (B) trees results from analysis of xylanase of 22 amino acid sequences.

After homology modeling, the 3D structure of CD of the Tth xyn10A was obtained (shown in Fig. 5)**.** Two glutamic acid residues are the catalytic nucleophile and proton donor of that Tth xyn10A, and this is same to other xylanases (Derewenda et al. 1994, Verma and Satyanarayana 2012). The amino acid sequences of Clade I and that of *P. mobilis* were aligned once again. Glu525 and Glu726 might be the catalytic nucleophile and proton donor, respectively (Fig. 5).

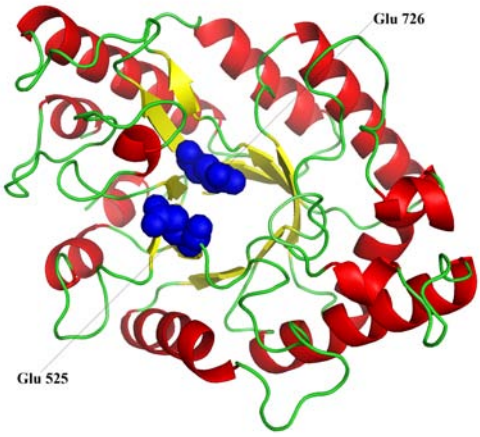

Figure 5 Structure modeling of the protein Tth xyn10A. Glu525 and Glu726 were marked with blue.

Discussion

Enzymatic hydrolysis of hemi-cellulose is a complex process, needing a few enzymes among them xylanase is a key enzyme. Members of the genus *thermotoga* including *T. thermarum*, which may produce a number of thermostable enzymes including xylanases, have been isolated from the terrestrial and marine hydrothermal areas. The recently released genome sequence of *T. thermarum* DSM 5069 revealed the presence of a GHF10 protein. A protein BLAST search in the GenBank database and the phylogenetic analysis (similar to Fig. 4a, b) showed that other proteins closely related to this protein were xylanases of GHF10, and therefore we thought this putative protein might be a xylanase of GHF10. Moreover, it shared only the 51% similarity with the *Thermotoga petrophila* RKU-1 (Genbank No. YP_001244458) and *Thermotoga sp*. RQ2 (Genbank No. YP_001738920), both of the two bacteria belong to the genus *Thermotoga*. The phylogenetic analysis showed that the Tth xyn10A was distant with the xylanases from archaea (Fig. 4A, B), and it had six domains that were different from the xylanases of the same genus. The results indicated that a new thermostable xylanase via genetic engineering technology was obtained and it could have some different properties. Significant amounts of the hydroxyl amino acids, Glu and Asp with about 15% amount, were seen to be present in Tth xyn10A, and it has been reported for other heat-tolerant xylanases of the same genus *Thermotoga* (Nelson et al. 1999, Swithers et al.

2011, Zhaxybayeva et al. 2009, Zverlov et al. 1996). They are presumed to provide catalytic performance in the structure of polysaccharide hydrolases. There are almost no Cys detected in those xylanases and this is vital to their thermostability.

The xylanase enzyme from *T. thermarum* DSM 5069 had a pH optimum of 7.0 and a temperature optimum of 95^{o}C (Fig. 2C). Enzyme activity was mainly inhibited by Cu^{2+}, this result is same to the xylanase from *Bacillus subtilis* cho40 (Khandeparker et al. 2011). However, the xylanase activity was greatly stimulated by Ca^{2+}, Mn^{2+} and Co^{2+}, and nearly 400% was enhanced by 1 mM concentration of Ca^{2+} (Fig. 3). It was implied that a few metal ions especially that Ca^{2+} is required for maintaining the structure stability, as there are probably two CBMs with Ca^{2+}. These results showed that Tth xyn10A differs from the other bacteria xylanases (Khandeparker et al. 2011, Ko et al. 2010, Verma and Satyanarayana 2012) except for the xylanases from genus *Thermotoga*, and the major difference is that Ca^{2+} show significant effects. As the longer active life means the less consumption of the enzyme, the high thermostability of the enzyme is desired in industrial production. The Tth xyn10A residual activity was almost 100% after being incubated at 85^{o}C for 2 h with the addition of 5 mM concentration of Ca^{2+}(Fig. 4D), and it exhibited high activity in broad temperature from 55 to 90^{o}C at pH 7.0.

Acknowledgements

This work was financially supported by the National Natural Science Foundation of China (No. 31170537), Jiangsu Provincial Government (CXZZ11_0526), Doctorate Fellowship Foundation of Nanjing Forestry University, as well as A Project Funded by the Priority Academic Program Development of Jiangsu Higher Education Institutions (PAPD).

Reference

Angelov, A., Liebl, S., Ballschmiter, M., et al. 2010. Genome sequence of the polysaccharide-degrading, thermophilic anaerobe *Spirochaeta thermophila* DSM 6192. Journal of Bacteriology. 192(24): 6492-6493.

Baba, T., Kuwahara-Arai, K., Uchiyama, I., et al. 2008. Complete genome sequence of *Macrococcus caseolyticus* strain JSCS5402, reflecting the ancestral genome of the human-pathogenic staphylococci. Journal of Bacteriology. 191(4): 1180-1190.

Chen, L.M., Brugger, K., Skovgaard, M., et al. 2005. The genome of *Sulfolobus acidocaldarius*, a model organism of the Crenarchaeota. Journal of Bacteriology. 187(14): 4992-4999.

Collins, T., Gerday, C. and Feller, G. 2005. Xylanases, xylanase families and extremophilic xylanases. FEMS microbiology reviews. 29(1): 3-23.

Derewenda, U., Swenson, L., Green, R., et al. 1994. Crystal structure, at 2.6-A resolution, of the *Streptomyces lividans* xylanase A, a member of the F family of beta-1,4-D-glycanases. The Journal of biological chemistry. 269(33): 20811-20814.

Fuzi, S.F.Z.M., Mahadi, N.M., Jahim, J.M., et al. 2011. Development and validation of a medium for recombinant endo-β-1,4-xylanase production by *Kluyveromyces lactis* using a statistical experimental design. Annals of Microbiology. 62(1): 283-292.

Göker, M., Held, B., Lapidus, A., et al. 2010. Complete genome sequence of *Ignisphaera aggregans* type strain (AQ1.S1T). Standards in Genomic Sciences. 3(1): 66-75.

Guo, L., Brugger, K., Liu, C., et al. 2011. Genome analyses of icelandic strains of *Sulfolobus islandicus*, model organisms for genetic and virus-host interaction studies. Journal of Bacteriology. 193(7): 1672-1680.

Jiang, Z., Cong, Q., Yan, Q., et al. 2010. Characterisation of a thermostable xylanase from *Chaetomium sp*. and its application in Chinese steamed bread. Food Chemistry. 120(2): 457-462.

Khandeparker, R., Verma, P. and Deobagkar, D. 2011. A novel halotolerant xylanase from marine isolate *Bacillus subtilis* cho40: gene cloning and sequencing. New Biotechnology. 28(6): 814-821.

Ko, C.-H., Tsai, C.-H., Tu, J., et al. 2010. Molecular cloning and characterization of a novel thermostable xylanase from *Paenibacillus campinasensis* BL11. Process Biochemistry. 45(10): 1638-1644.

Liolios, K., Sikorski, J., Jando, M., et al. 2010. Complete genome sequence of *Thermobispora bispora* type strain (R51(T)). Standards in Genomic Sciences. 2(3): 318-326.

Liu, L.-J., You, X.-Y., Zheng, H., et al. 2011. Complete genome sequence of *Metallosphaera cuprina*, a metal sulfide-oxidizing archaeon from a Hot Spring. Journal of Bacteriology. 193(13): 3387-3388.

Mardanov, A.V., Gumerov, V.M., Beletsky, A.V., et al. 2011. Complete genome sequence of the thermoacidophilic crenarchaeon *thermoproteus uzoniensis* 768-20. Journal of Bacteriology. 193(12): 3156-3157.

Mardanov, A.V., Svetlitchnyi, V.A., Beletsky, A.V., et al. 2010. The genome sequence of the crenarchaeon *acidilobus saccharovorans* supports a new order, Acidilobales, and suggests an important ecological role in terrestrial acidic hot springs. Applied and Environmental Microbiology. 76(16): 5652-5657.

Nelson, K.E., Clayton, R.A., Gill, S.R., et al. 1999. Evidence for lateral gene transfer between archaea and bacteria from genome sequence of *Thermotoga maritima*. Nature. 399(6734): 323-329.

Ruller, R., Deliberto, L., Ferreira, T.L., et al. 2008. Thermostable variants of the recombinant xylanase A from *Bacillus subtilis* produced by directed evolution show reduced heat capacity changes. Proteins-Structure Function and Bioinformatics. 70(4): 1280-1293.

Swithers, K.S., DiPippo, J.L., Bruce, D.C., et al. 2011. Genome sequence of *Thermotoga sp* strain RQ2, a hyperthermophilic bacterium isolated from a geothermally heated region of the seafloor near ribeira quente, the azores. Journal of Bacteriology. 193(20): 5869-5870.

Verma, D. and Satyanarayana, T. 2012. Cloning, expression and applicability of thermo-alkali-stable xylanase of *Geobacillus thermoleovorans* in generating xylooligosaccharides from agro-residues. Bioresource Technology. 107: 333-338.

Weng, X.Y. and Sun, J.Y. 2010. Hydrolysis of xylans by a thermostable hybrid xylanase expressed in *Escherichia coli*. Applied Biochemistry and Microbiology. 46(5): 511-514.

Windberger, E., Huber, R., Trincone, A., et al. 1989. *Thermotoga thermarum* sp-nov and *Thermotoga neapolitana* occurring in african continental solfataric springs. Archives of Microbiology. 151(6): 506-512.

Zhaxybayeva, O., Swithers, K.S., Lapierre, P., et al. 2009. On the chimeric nature, thermophilic origin, and phylogenetic placement of the Thermotogales. Proceedings of the National Academy of Sciences of the United States of America. 106(14): 5865-5870.

Zverlov, V., Piotukh, K., Dakhova, O., et al. 1996. The multidomain xylanase A of the hyperthermophilic bacterium Thermotoga neapolitana is extremely thermoresistant. Applied Microbiology and Biotechnology. 45(1-2): 245-247.

Proceedings of the 55th International Convention of Society of Wood Science and Technology
August 27-31, 2012 - Beijing, CHINA

Influence of Thermo-modification on the Color of Cylicodiscus spp Heartwood

QiangShi[1,a] FuchengBao[2,b] JianxiongLu[3,c]

[1,2,3] Wood Industry Research Institute, Chinese Academy of Forestry, China

[a] shiqiangok2008@yah00.cn
[b] fucheng.bao@caf.ac.cn
[c] jianxiong@caf.ac.cn

Abstract

In this study the effect of high temperature on color change of okan wood was investigated. Wood specimens were subjected to heat treatment at 160℃,180℃,200℃,220℃for 2, 4, 6, 8 hours with the superheated steam as a heating medium and a shielding gas. Color changes were measured in the Minolta Croma-Meter CR-300 color system. The color parameters *L**, *a**, *b** were determined by the CIE*L*a*b** method on the surface of untreated and treated wood, and their variation with regard to the treatment ($\Delta L^*, \Delta a^*, \Delta b^*$) were calculated. It was found that heat treatment resulted in a darkening of wood tissues, Color became dark with the temperature increases. The darkening accelerated when treatment temperature exceeded approximately 200℃. We found that heat treatment temperature were substantially important regarding the color responses. Strong correlations between total color difference and the treatment temperature were found. The effect of treatment temperature on color change in sapwood is more obvious than that in heartwood, the color of sapwood and heartwood tended to be more uniform when the temperature reaches more than 200.

Keywords: *Cylicodiscus* spp; heat treatment; wood color

Introduction

Among the construction materials which are used by people, wood holds a special place because of its impressive range of attractive properties [1]. Among these properties color is of considerable importance in wood species which are used for decorative purposes [2]. Color is a very important wood property for the final consumer and, in some cases it is the determining factor for the selection of a specific wood since the visual decorative point of view is often prevailing [3]. In species with pale colored wood which are usually considered less appellative, the darkening would be an important advantage of the heat treatment giving the wood a “tropical flavor ” that is valued in many countries.

Today there is a common trend towards high-temperature drying of wood, which is mainly motivated by shorter processing times, lower energy consumption and probably fewer deformations. Wood can undergo changes in color, during heat-treatment processing [4]. Color changes often occur and its relation to aesthetic appearance is an important issue. It is also of interest to know more about these color changes, since they imply alteration of wood components, which can have an affect on wood properties [5]. A heat-treatment process with controlled color change is therefore desired.

Materials and Methods

Green okan (*Cylicodiscus* spp) wood log was chosen for test materials, with the length of three meters, the diameter of one meter, which were taken from Africa tropical rainforest. All test specimens originated from the same log. This was intended, since the presentation of color responses versus heat-treatment temperature was the focus of this work. Okan heartwood is yellow color. The log was sawn to pieces of boards, then these boards were made test specimens, separated heartwood with dimensions 500×120×25mm in longitudinal, tangential and radial directions respectively were used, and all test specimens were kiln dried for one month, to its moisture content at 10% before heat-treating and testing.

Heat-treatment Test

The specimens were divided into sets of 30 specimens for each material, totaling 240 specimens, only specimens of clear wood were selected, avoiding drying defects. There are heartwood sets for the different temperatures and different duration. The specimens were placed orderly in the drying machine, there were division bar between the two specimens layers.

The equipment for the wood heat-treatment test was the wood drying machine (Lignomat, made in German). The heat treatments were carried out with superheated steam in the absence of air. The treatment started at ambient temperature with a raising heat time of about 4~5 hours. Four treatment temperature(160℃,180℃200℃220℃)and2h, 4h, 6h, 8h treatment duration were applied. The temperature was kept constant, when the temperature inside the drying machine reached the setting temperature. After treatment, the specimens were cooled down to 60℃, then were taken out of the equipment.

Measurement of Color

It is known that when wood is used for joinery, furniture or panels, it is often planed 2-3mm. Therefore all specimens in this investigation were planed approximately 3mm before measuring the wood surface color. The color measurements of all specimens were recorded on the surface of wood specimens before and after heat treatment with a colorimeter Minolta Croma-Meter CR-300 (made in Japan), The sensor head was 6mm in diameter. Measurements were made using a D_{65} illuminant and 10-degree standard observer. Percentage of reflectance, collected at 10nm intervals over the visible spectrum (from 400 to 700nm) was converted into the CIE*L*a*b** color system, where *L** describes the lightness, *a** and *b** describe the chromatic coordinates on the green-red

and blue-yellow axis, respectively. From the $L^*a^*b^*$ values, the difference in the lightness(ΔL^*)and chromatic coordinates(Δa^{**}*and* Δb^*), and total color difference ($\triangle E$) were calculated using the following formulae:

$$\Delta L^* = L^* - L_0^* \quad (1)$$

$$\Delta a^* = a^* - a_0^* \quad (2)$$

$$\Delta b^* = b^* - b_0^* \quad (3)$$

$$\Delta E = [(\Delta L^*)^2 + (\Delta a^*)^2 + (\Delta b^*)^2]^{1/2} \quad (4)$$

Where, L^*, a^*, $b^*$are the final color coordinate, L_0^*, a_0^*, $b_0^*$are the initial color coordinate, ΔL^*, Δa^*, $\Delta b^*$are the color coordinate change.

Results and Discussion

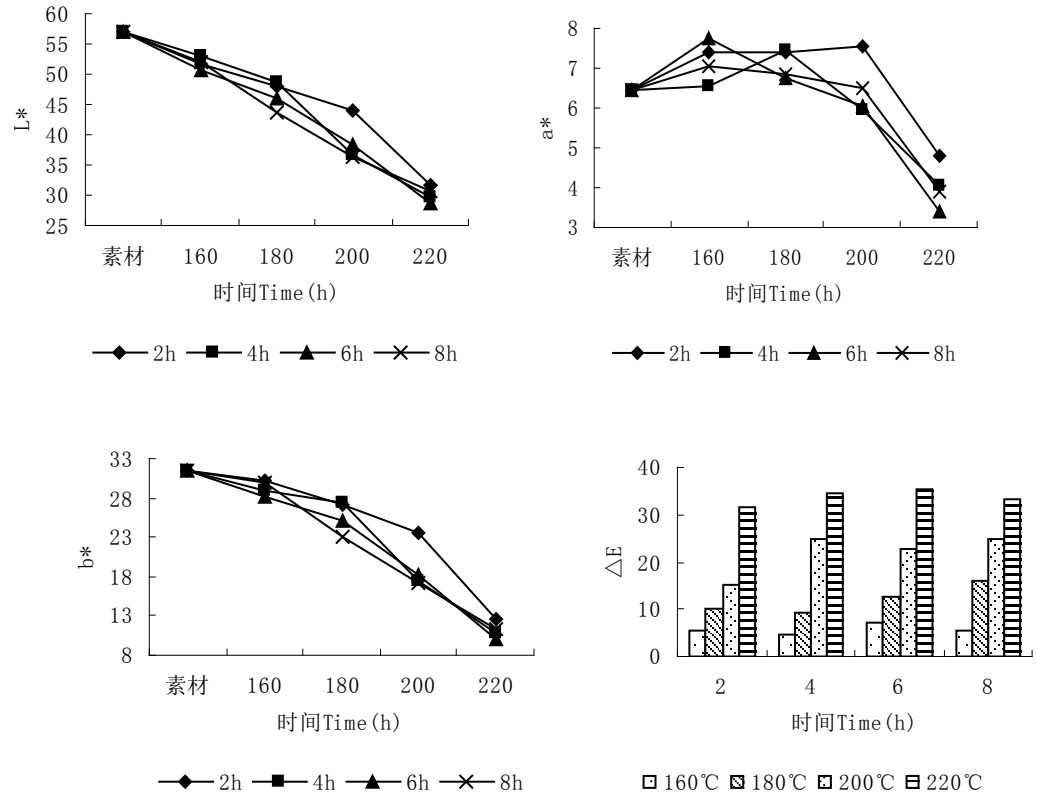

Fig.1. Change in the color parameters of okan heartwood with different technological conditions

Fig.2. The color of heat treatment and control test specimen

Fig.1 shows the color parameter *L** value, *a** value, *b** value at different heat treatment temperatures and durations. Fig.2 shows the effect of heat treatment temperature on okan wood color.

As shows in the Fig.1 and Fig.2, when we focused on color parameters including the color parameter *L**, *a**, *b*, we found that color changes were drastic after heat treatment. *L** value, *a** value, *b**value tends to decrease, with the increase in heat treatment temperature. Lightness *L** value and *b**value start to decrease over 160℃ and significantly decreases at 200℃, while *a** value reaches a minimum value at 200℃, and afterwards begin to increase. The effect of temperature on the total color difference $\triangle E$ is shown. With temperature increasing from 160 to 200， the total color difference increased.

As to okan heartwood, lightness *L** decreased from 56.91 to 30.59, the loss of lightness was approximately 46.25% at 220℃ heat treatment, decreasing 26.32 units compared with 56.91 units for unheated wood. The *a** value decreased during the 160~200℃ heat treatment, and thereafter increased at 220℃. Thus, wood changed color to green and after that color changed towards red. The *b** value decreased from 31.56 to 11.23, the loss of The *b** value was 64.42% at 220℃ heat treatment, decreasing 20.33 units compared with 31.56 units for unheated wood. This testifies that color changed towards blue during the 160~220℃ heat treatment. The total color difference increased from 5.5 to 35.52 during heat treatment.

In general, the contribution of lightness *L** is the most, the *b**is the second, and the *a** is the least to the total color difference during all heat treatment process.

The high temperature heat treatment has a significant influence on the discoloration of the okan wood. Heat treatment at 200~220℃ induced extensive darkening and reddening of okan wood.

In color changes studies, Bourgios et al. [6] showed that the decrease in lightness and the increa se in the color difference of wood under heat treatment at 240-310℃ are caused by a decrease in hemi-cellulose content, especially pentosan. For a chemical explanation of wood color changes, Chen and Workman [7] and Kubinsky and Geza[8] studied the influence of steaming on the color of press-extracted wood fluids, regarding extractives in wood fluids as the main wood pigments.

Relationships between wood color and phenolic content are discussed in the study of Burtin et al. [9]. Authors indicated that new technological processes of steaming or artificial coloring with natural phenolic compounds could be developed.

Conclusions

As regards color, the heat treatment temperature showed an interesting potential to obtain the controlled color of the wood surface. With heat treatment, the color of wood is modified acquiring a darker tonality. Darkening increased with treatment is in agreement with earlier findings.

Acknowledgment

This research was supported by the CAFINT2009K04 Program in 2009 of the Wood Industry Research Institute, Chinese Academy of Forestry.

References

[1]P. Bekhta, P. Niemz. Effect of high temperature on the change in color, dimensional stalility and mechanical properties of spruce wood. Holzforschung. 57(5): 539-546(2003).

[2]P. J. Bourgois, G. Janin, R. Guyonnet. The color measurement: A fast method to study and to optimize the chemical transformations undergone in the thermally treated wood. Holzforschung. 45(4): 377-382(1991) .

[3]B. Sundqvist. Color changes and acid formation in wood during heating. Doctoral Thesis, Lulea University of Technology, (2001).

[4]B. Sundqvist. Color changes and acid formation in wood during heating. Doctoral Thesis, Lulea University of Technology, (2001).

[5]Sehistedt-Persson. Color respinses to heat treatment of extractives and sap from pine and spruce. In: 8th International IUFRO wood drying conference, Brasov, 459-464(2003).

[6]Borugois, P.J., G.Janin and R.Guyonnet. 1991. La mesure decouleur. Une methode detude et doptimisation des transformations chimiques du bois thermolyse. Holzforschung 45,3 77-382.

[7]Burtin, P., C. Jay-Allemand, J.-P. Charpentier and G. Janin. 2000. Modifications of hybrid walnut(*Juglans nigra 23xJuglans regia)* wood color and phenolic composition under various steaming conditions. Holzforschung54, 33-38.

[8]Chen,P.Y.S.and E.C.Workman Jr. 1980. Effect of steaming on some physical and chemical properties of black walnut heartwood. Wood and Fiber 11(4), 218-227.

[9] Kubinsky, E. and I. Geza. 1973. Influence of steaming on the properties of red oak. Part I. Structural and chemical changes. Wood Sci. 6(1),87-94.

Comparative Life-cycle Assessment of Sheet Molding Compound Reinforced by Natural Fiber vs. Glass Fiber

Jinwu Wang[1], Sheldon Q. Shi[2], and Kaiwen Liang[2]

1 Assistant Research Professor, Washington State University, Composite Materials and Engineering Center, P.O. Box 641806, Pullman, Washington, 99164-1806
jinwuwang@wsu.edu

2 Associate Professor and Assistant Research Professor, Department of Mechanical and Energy Engineering, University of North Texas, 3940 North Elm St., Denton, Texas 76207
Sheldon.shi@unt.edu, Kaiwen.liang@unt.edu

Abstract

The investigation is on comparative life-cycle assessments of three fiber-reinforced sheet molding compound (SMC) made from kenaf fiber, glass fiber and soy-based resin, respectively. SMCs for automotive applications are typically made of unsaturated polyesters and glass fibers. Using kenaf fiber and soy-based resin to partially replace the glass fiber and polyester resin is driven by their potential environmental benefits. A soy-based resin, maleatedacrylatedepoxidized soy oil (MAESO), was synthesized from refined soybean oil. SMC1 composite was made from kenaf fiber and polyester resin while SMC2 composite fromkenaf fiber and a resin blend of 20 % MASEO and 80% unsaturated polyester. SMC1 and SMC2 have both achieved substantial physical and mechanical properties, but were not yet comparable to a glass fiber reinforced polyester SMC in strength property (Springer, 1983, J. Reinforced Plastics Composites, 2(2):70-89). Thus, functional unit was defined as a mass to achieve the equal stiffness and stability when used to make interior parts for automobiles. The life-cycle assessments were conducted for three composites: SMC1, SMC2 and the glass fiber reinforced SMC. The materials and energy input/output of producing one functional unit of three composites were collected from lab experiments and literature. The key environmental measures were computed with SimaPro software. The results show that both kenaf fiber reinforced SMCs perform better than glass fiber SMC in every environmental category. The global warming potential of kenaf fiber SMC (SMC1) and kenaf soy resin based SMC (SMC2) were only about 45% and 58% of that for glass fiber SMC, respectively. This preliminary result has demonstrated that using soy-based resin and natural fiber for SMC would have a great ecological benefit.

Key words: Natural fiber; reinforced composites; sheet molding compound; life-cycle assessment.

Introduction

Sheet molding compound (SMC) is a mixture of molding resin, fibers, fillers, and additives. The traditional SMC molding resins for automotive applications are various unsaturated polyester resins (UPR) and vinyl ester. The reinforcementsareusually chopped short fiberglass and carbon fibers. Bast fibers such as kenaf have a similar morphology compared to the glass fibers, and their tensile strength and modulus are very attractive. Scientists are trying to find answers if these natural renewable fibers could replace the non-renewable glass fibers and plastic fibers. Various natural fiber reinforced polymer composites have been investigated using natural fibers such as kenaf, hemp, jute, and coir and commodity polymers such as polyethylene, polypropylene and unsaturated polyester resins (Holbery and Houston 2006; Kalia et al. 2011). However, no natural fiber reinforced composites achieved comparable physical and mechanical properties to glass fiber reinforced composites even in the laboratory with controlled process parameters. Especially, water resistance and impact toughness of natural fiber reinforced composites are far inferior to glass fiber composites (John and Anandjiwala 2008). The hydrophilic and intra-tangle characteristics of the natural fiber present challenges to disperse the fibers uniformly into the resin matrices in a scalable production. Although there is a need to improve current technology enabling natural fiber reinforced composites, this paper focuses on environmental impacts of the current technology of natural fiber reinforced composites.

The natural fiber reinforced composites have been generally perceived as renewable, biodegradable and environmentally friendly products. It is obvious that a technology utilizing the natural fibers to make composite materials reduces the global dependency on petroleum, however, quantitatively measurements of their environmentally friendliness are not fully conducted. It is not self-evident that it helps reduce the global carbon dioxide emissions since agriculture itself generates greenhouse gases due to the use of fertilizers, herbicides and pesticides and land clearing. While there is often an intuitively appealing or claims about renewability, biodegradability, and environmental friendliness of a product, process or service, the claims do not always stand up to an objective analysis. In addition, there is very little relevant data about what will happen at the end of life for these bio-based materials. If placed in a landfill, for example, off-gas is the natural by-product of the decomposition of solid waste in landfills and is comprised primarily of carbon dioxide and methane. Methane is a greenhouse gas and also an important energy source. When the conventional plastics are placed in a landfill, excavation data shows that they degrade very slowly with a time frame of 100 years. While this is not positive from a landfill capacity perspective, it does mean that carbon is sequestered and air and water pollution is minimized. In this sense, biodegradability is not a desirable feature of the product.

If landfill, however, installs a landfill gas collection system to collect and use landfill gas as a green energy source, generating electricity on-site which is then connected to the municipal utilities electric grid, biodegradability of materials will be beneficial to society. For example, the capacity of the electric generator fueled with the landfill gas in Denton, TX with a population of 113,383 in 2010 was 1.6 megawatts, powering the equivalent of approximately 1,600 homes per year (www.cityofdenton.com). In this sense, biodegradability and their rate of degradation are relevant to methane gas production rate and landfill capacity recovery. This unique effort to utilize methane emissions from landfill provides significant energy, economic and environmental benefits and justify biodegradable a desire feature for products.

Life-cycle assessment (LCA) is a standardized process for quantifying the life-cycle environmental impacts of materials, processes or services in terms of environmental impact indicators like global warming potential, embodied energy and embodied water. It consists of goal definition and scoping which defines the product, process or activity; inventory analysis which identifies material usage and environmental releases; impact analysis which assesses the human and ecological effects of energy, water and material usage; and last interpretation, which evaluates the results of each analysis. Integration of life-cycle analysis elements into early stages of materials development, product and construction designs will avoid short-lived, costly, and resource-intensive structures that generate negative environmental impacts. With a clear understanding of the most dominating causes of the environmental load in various life-cycle stages, it becomes easy to set priorities in the process or product improvement.

The overall goal of the project is to substitute of natural fiber reinforcement for glass fiber in thermoplastic or thermoset composites to achieve cost and weight savings without sacrificing the mechanical property requirements. This report investigates its environmental impacts, concentrating on the comparison of kenafbast fiber versus glass fiber as reinforcement in sheet molding composites (SMC),specifically,to determine if the use of kenaf fiber to replace glass fiber as reinforcement and the use of 20% soybean oil modified resin in fabricating SMC are advantageous from an ecological point of view.

Methods

A series of kenaf fiber reinforced SMCs have been fabricated in the laboratory for scoping and optimization. The life-cycle assessment was conducted on three product scenarios: Formulation SMC1 (kenaf fiber SMC), Formulation SMC2 (kenaf fiber 20 % soy resin SMC, blending 20% modified soybean oil with unsaturated polyester resin), and conventional glass fiber SMC. The life-cycle assessment of SMCs was assessed in two steps: (i) collecting life-cycle inventory (LCI) for material and energy inputs and emissions from SMC production processes, (ii) using an SimaPro model to perform environmental impact assessment for the emissions tabulated in (i). The LCA data for soybean oil resin and kenaf fiber reinforced composites were collected from lab syntheses. Actual industrial practices are expected to be much more energy- and material-efficient both currently and in potential future scale-up. The data for unsaturated polyester resin and glass fiber SMC were collected from literature(Liang and Shi 2010; Springer 1983). Other LCA data related with manufacturing raw materialswere collected from SimaPro software database (US LCI database andEcoInvent database). Catalysts and additives were not included as these materials represent less than 1% of the total material and negligible environmental impact. These data include energy and materials balances for manufacturing 1 kg raw materials, intermediates, and products, as well as emissions to air, discharges to water, and solid wastes to land. These data were then entered into the LCA software SimaPro V7.3. Environmental performances were measured by a set of environmental impact indexes came up with by NIST Building for Environmental and Economic Sustainability (BEES), cumulative energy demand and a weighted environmental burden.

Environmental Impact Assessment

Life-cycle impact assessment methods describe environmental impacts in terms of characterization factors. For a wide assessment of the environmental impact, the Building for Environmental and Economic Sustainability (BEES) set of impacts and Eco-indicator 99 were used. LCI results for the product comparisons are classified into impact categories, that is, categories in which a set of related flows may contribute to impacts on human or environmental health. Three types of environmental damages were considered: human health, ecosystem quality and resources. These damages are quantified by damage models. The Eco-indicator 99 Points were calculated by normalization and weighting of the damage factors. Ecoindicator single score is a tool to be used in the search for more environmentally friendly design alternatives and is intended for internal use. The scale is chosen in such a way the value of 1 Pt is representative for one thousandth of the yearly environmental load of one average European inhabitant (Goedkoop et al. 1999). The energy resource efficiency was assessed by the cumulated energy demand. The cumulated energy demand considered the entire demand of primary energy which flowed into the product system per functional unit (VDI 1997).

BEES has a recognized and accepted methodology to ensure a level playing field in terms of its methodological approach. All midpoint scores are expressed in units of a reference substance and related to the four damage categories human health, ecosystem quality, climate change, and resources as shown in Table 1(Lippiatt 2007). The global warming potentials (GWP) used by BEES were developed in 2001 by the International Panel of Climate Change. The 100 year GWP used are as follows: fossil carbon dioxide 1, methane 23, nitrous oxide 296, CFC/HCFCs 1700, methylene chlorine 10, HCFC22 1700. Biogenic CO_2 uptake is considered to be negative impact.

Table 1 Environmental impact indices

	Impact Category	Units
1	Global Warming	CO2 equivalents
2	Acidification	H+ equivalents
4	Human Health – Cancer	C6H6 equivalents
5	Human Health – NonCancer	C7H7 equivalents
6	HH Criteria Air Pollutants	microDALYs
7	Eutrophication	N equivalents
8	Ecological Toxicity	2,4-D equivalents
9	Smog	NOx equivalents
10	Natural Resource Depletion	MJ surplus energy
11	Indoor Air Quality	TVOC equivalents
12	Habitat Alteration	T & E count
13	Water Intake	liters of water
14	Ozone Depletion	CFC-11 equivalents

Results & Discussion

The LCA from cradle to gate for fibers and resins as well as comparative LCA of SMCs are summarized. The product with the highest impact is shown as representing 100%, while the impact of the other products is shown as a percentage of that value.

Fiber LCA

Fig. 1 indicates that kenaf fiber has less negative environmental impacts than glass fiber in stages from raw materials extraction to fiber manufacturing (cradle to gate). Fig. 2 shows that bast fibers (jute and kenaf) consume less energy than other fibers in manufacturing 1-kg fibers; most of consumed energy is renewable energy. Method to calculate the Cumulative Energy Demand (CED) was based on the method published by Ecoinvent version 2.0 and expanded by PRé Consultants for raw materials available in the SimaPro 7 database. CED has been the most important aggregated result of the inventory used for comparisons of product-related systems. The CED is the most meaningful parameter in judging the energy efficiency of systems since losses due to transformation and transport are fully taken into account. In addition to the cumulative process and transportation energy, it also contains the "feedstock energy", i.e. the primary energy equivalent of the materials produced from oil, coal, wood, etc

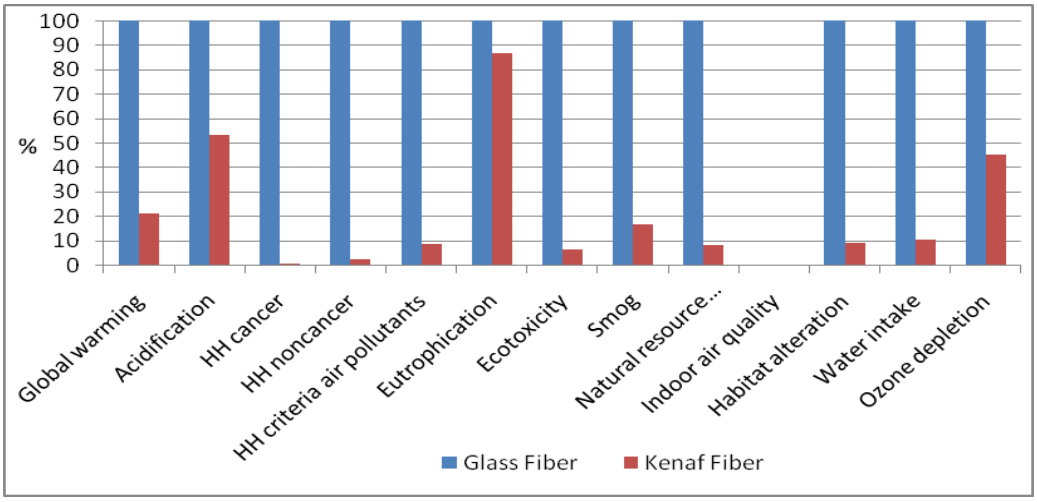

Figure 1 Comparison of environmental impacts of glass and kenaf fibers in BEES impact indices. Functional Unit: 1 kg fiber, Cradle to gate. Data: Kenaf Fiber, India; Glass Fiber, Europe.

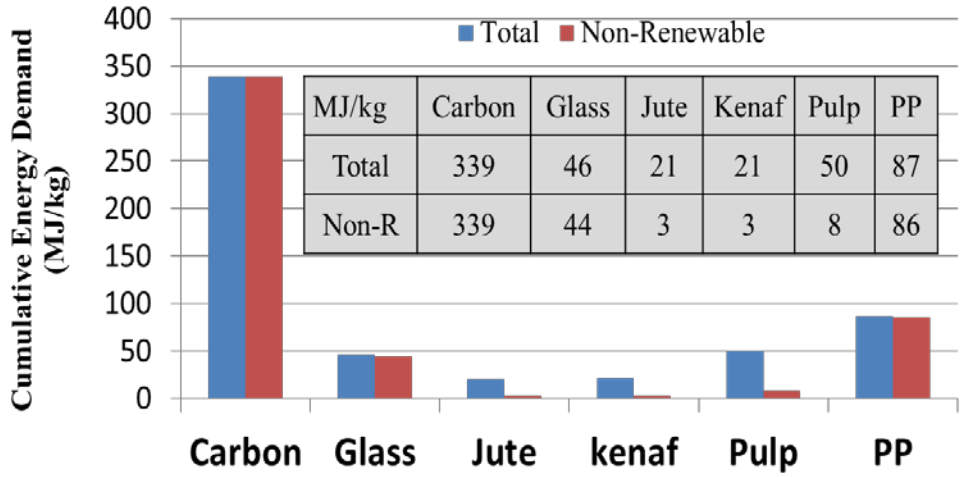

MJ/kg	Carbon	Glass	Jute	Kenaf	Pulp	PP
Total	339	46	21	21	50	87
Non-R	339	44	3	3	8	86

Figure 2 the cumulative (primary) energy demand (CED) per 1-kg fiber.

Figure 3 indicates environmental burdons of different fibers from cradle to gate. One Pt represents one thousandth of the yearly environmental load of one average European inhabitant. Overall, fibers has a greater environmental impact in the category corresponding to its effects on respiration, mainly due to the releasing substances of an inorganic source such as particle matter, sulphites and nitrates. Another aspect worthy of mention is the consumption of fossile fuels for the petroleum-based fibers. Glass fiber has a substantial effect of carcinogens. Land use contributes substantial portions for agri-fibers. Fig. 3 demonstrates that natural fibers achieve overall lower environmental burdens. Land uses contributed substantial portions for agri-fibers (jute and kenaf).

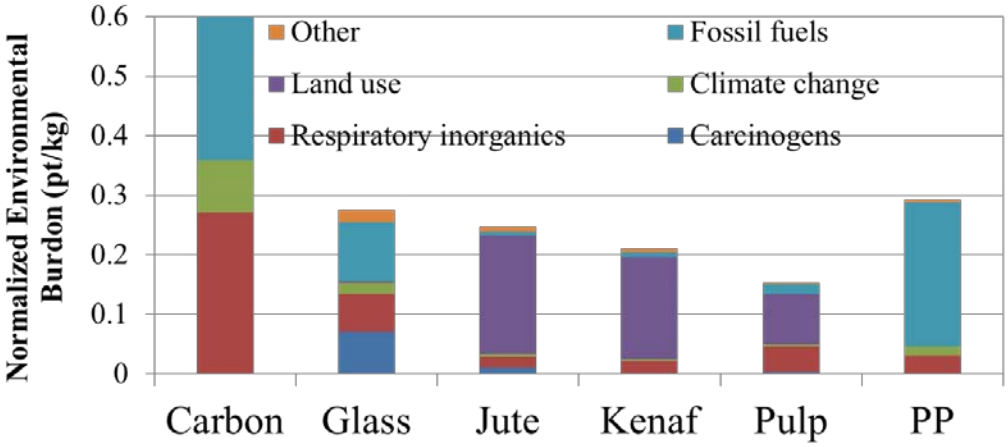

Figure 3 Comparison of environmental impacts of fibers in Eco-indicator 99 Points per 1-kg fiber.

Resin LCA

Figures 4,5 & 6 show comparisons of three resins in commulative energy demand, BEES emvironmental impact indices and Eco-indicator 99 Points. The use of fossil fuel in manufacturing resins contributes a large portion of environmental impacts.

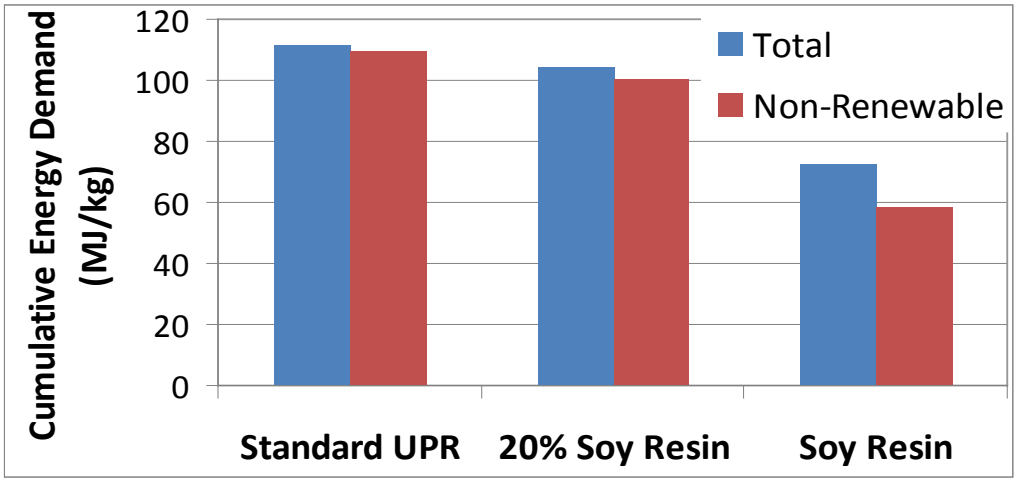

Figure 4 the cumulative (primary) energy demand (CED) of resins per 1-kg resin.

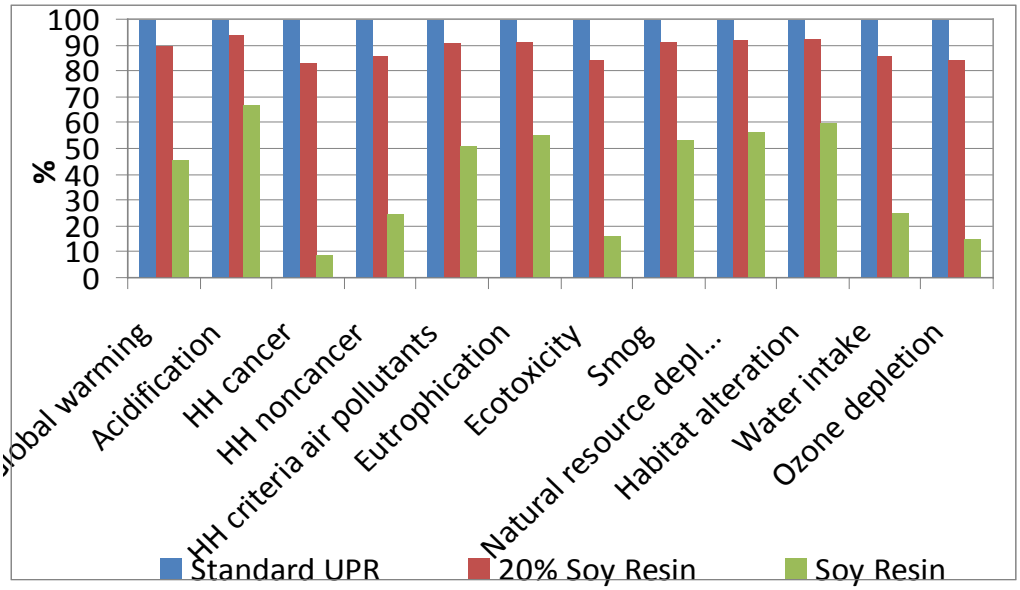

Figure 5 Comparison of environmental impacts of three resins in BEES impact indices.

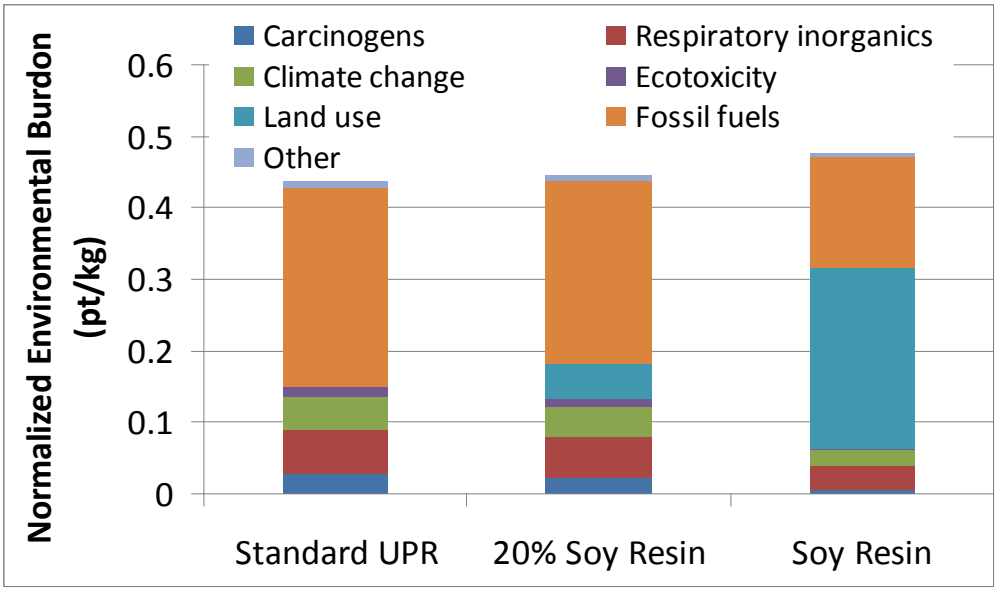

Figure 6 Comparison of environmental impacts of resins in Eco-indicator 99 Points per 1-kg resin.

LCA of SMC

The key environmental measures for three product scenarios were computed withSimaPro software and are shown as in Fig. 7. Both kenaf-fiber reinforced SMCs perform better than glass fiber SMC in every environmental category. The global warming potential of the kenaf fiber SMC (SMC1) could be only about 45% of that for the glass fiber SMC. The global warming potential of the kenaf fiber soy-resin composites (SMC2) is slightly higher than that of kenaf fiber SMC due to the agricultural production of soybeans.

Negative means carbon credit, i.e. saving non-renewable resources otherwise being used due to the energy recovery at the end-of-life disposal. Overall, the inclination at the end of the life of the kenaf and soy resin contained composites generates additional energy. In SimaPro program, this additional energy is treated as a substitute of fossil resources to significantly reduce the impact associated with the categories of acidification, air pollutants, and smog. Furthermore, using resources beyond their rate of replacement is considered to be resource depletion. Kenaf and soy are annual crops, if coming from sustainable farming, which does not contribute to natural resources depletion.

Conclusions

This preliminary result has demonstrated that the use of modified soybean oil and natural fiber to make sheet molding compound had a great potential from an ecological point of view. LCA is an effective tool to analyze environmental impact of the developed materials and products. Life-cycle thinking and assessment can be a great educational tool to promote renewable bioproducts.

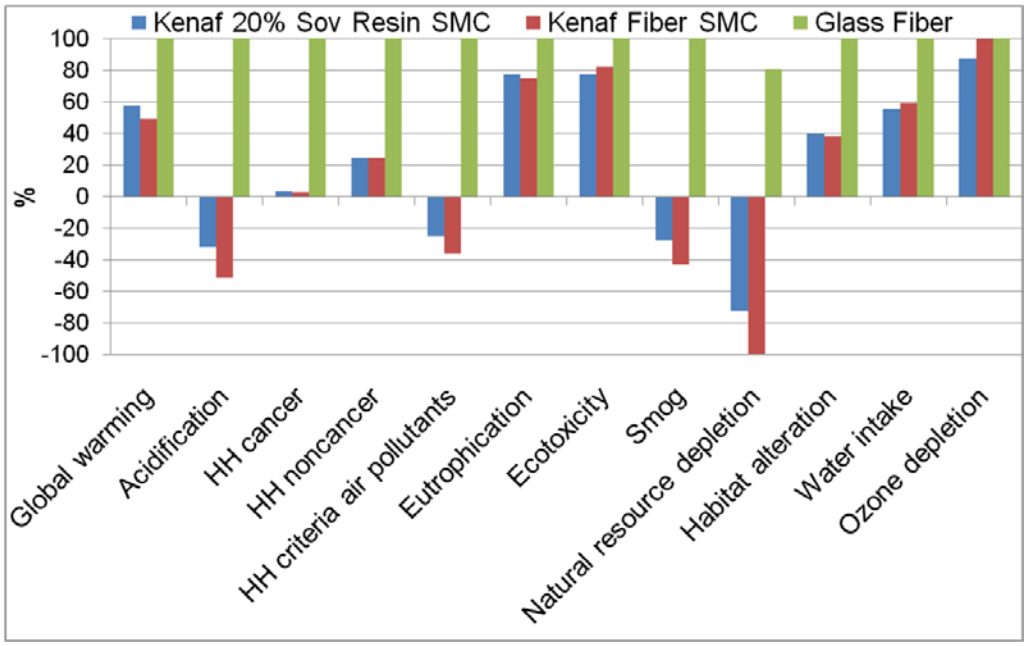

Figure 7 Relative Contribution of three SMCs per 1 functional unit

Acknowledgement

The research work was supported by Department of Energy (DOE), funding # 362000-060803 through Center for Advanced Vehicular System (CAVs) at Mississippi State University. Acknowledges are given to Dr. Philip Steele and Dr. Jerome Cooper for providing the LCA SimaPro software.

Reference

Goedkoop, M., Spriensma, R., van Volkshuisvesting, M., en Milieubeheer, R. O., and Communicatie, C. D. (1999). "The Eco-indicator 99: A damage oriented method for life cycle impact assessment." Ministerie van Volkshuisvesting, Ruimtleijke Ordening en Milieubeheer.

Holbery, J., and Houston, D. (2006). "Natural-fiber-reinforced polymer composites applications in automotive." *Jom*, 58(11), 80-86.

John, M. J., and Anandjiwala, R. D. (2008). "Recent developments in chemical modification and characterization f natural fiberΓÇÉreinforced composites." *Polymer composites*, 29(2), 187-207.

Kalia, S., Dufresne, A., Cherian, B. M., Kaith, B. S., Averous, L., and Njuguna, J. (2011). "Cellulose based bio and nanocomposites: a review.".

Liang, K., and Shi, S. Q. Resins from soybean oil-based additives for natural-fiber sheet molding compound (SMC) composites: Synthesis and characterization. Pages 91-96 in Proceedings, 2009 International Conference on Wood Adhesives. 2010.
Ref Type: Generic

Lippiatt, B. C. (2007). "BEESRG 4.0: Building for Environmental and Economic Sustainability Technical Manual and User Guide.".

Springer, G. S. (1983). "Effects of Temperature and Moisture on Sheet Molding Compounds." *Journal of Reinforced Plastics and Composites*, 2(2), 70.

VDI, V. D. I. Richtlinie 4600: 1997-06: Kumulierter Energieaufwand-Begriffe, Definitionen, Berechnungsmethoden (VDI guideline 4600: 1997-06: Cumulated energy demand-Terms, definitions, calculation methods). 1997. 1997. VDI Verlag: D++sseldorf.
Ref Type: Generic

Basic Research on the World's Largest Bamboo Species (*Dendrocalamus Sinicus*): Isolation and Characterization of Hemicelluloses

*Zheng-jun Shi[1] – Ling-ping Xiao[2] – Jia Deng[3] – Feng Xu[4] – Run-cang Sun [5]**

[1] PHD student, Institute of Biomass Chemistry and Technology- Beijing Forest University, Beijing, China
shizhengjun1979@163.com
[2] PHD student, Institute of Biomass Chemistry and Technology- Beijing Forest University, Beijing, China
lingpingxiao@163.com
[3] PHD student, Institute of Biomass Chemistry and Technology- Beijing Forest University, Beijing, China
dengjia1983@163.com
[4] Professor, Institute of Biomass Chemistry and Technology- Beijing Forest University, Beijing, China
xfx315@163.com
[5] Professor and director, Institute of Biomass Chemistry and Technology- Beijing Forest University, Beijing, China
rcsun3@bjfu.edu.cn
* *Corresponding author*

Abstract

Dendrocalamus sinicus, which is the largest bamboo species in the world, has broad prospects in biomass-energy and biorefinery applications. In this study, five soluble hemicelluloses fractions were sequentially isolated with 80% ethanol (containing 0.025 M HCl, 0.50% NaOH, respectively), and alkaline aqueous solution (containing 2.00, 5.00, and 8.00% NaOH, respectively) at 75 °C for 4 h from dewaxed *D. sinicus*, and their structural properties were examined. Gel permeation chromatography (GPC) revealed that the hemicelluloses isolated from *D. sinicus* show a wide distribution of molecular weights. The hemicelluloses isolated by ethanol had lower weight-average molecular weights (ranging from 17380 to 19620 g/mol), while the hemicelluloses isolated by alkaline aqueous solution had relatively higher weight-average molecular weights (ranging from 22510 to 42150 g/mol). Neutral sugar analysis indicated that the soluble hemicelluloses were mainly composed of arabinoglucuronoxylans, followed by minor amount of β-glucan and starch. Spectroscopic analyses suggested that the isolated arabinoglucuronoxylans from bamboo (*D. sinicus*) could be defined as a linear (1→4)-β-linked-xylopyranosyl backbone to which α-L-arabinofuranose units and/or short chains of 4-O-methyl-glucuronic acid were attached as side residues via α-(1→3) and/or α-(1→2) linkages. The results obtained from the research provide basic and necessary scientific information for conversion of bamboo biomass to biorefinery.
***Key words*:** *Dendrocalamus sinicus*, Biorefinery, Hemicelluloses, Isolation, Characterization

Introduction

With the inevitable depletion of the world's fossil fuels supply, there has been an increasing worldwide interest in exploring alternative, renewable resources to support future industry (Fitzpatrick et al. 2.10, Hallac et al. 2009). Bamboo species *D. sinicus*, is the world's largest bamboo species, belonging to *Bambusoideae* of *Gramineae*, and has strong, woody stems (maximum diameter 30 cm, maximum height 33 m), is mainly distributed in the southwest region of China (Ohrnberger, 1999). Due to its easy propagation, fast growth, and high productivity, *D. sinicus* is considered as a potential renewable non-woody forestry feedstock for the production of value-added products from its lignocellulosic components, such as hemicelluloses. However, as far as we know, the detailed physicochemical properties of hemicelluloses present in the largest bamboo species have not been reported in the previous literatures. Hence, the present work aims at isolation and characterization of hemicelluloses from the cell wall of the bamboo (*D. sinicus*).

Materials and Method

Materials. Bamboo (*D. sinicus*), 3 years old, was obtained from Yunnan Province, China. It was first dried in sunlight and then chipped into small pieces. The air-dried pieces of bamboo were ground and screened to obtain a 40-60 mesh fraction. This fraction was subjected to extraction with toluene/ethanol (2:1, v/v) in a Soxhlet apparatus for 6 h, and then the dewaxed powder was further dried in an oven under circulated air at 60 °C for 16 h before use. All standard chemicals, such as monosaccharide and chromatographic reagents, were purchased from Sigma Chemical Company (Beijing, China).

Isolation of hemicelluloses fractions. The dewaxed bamboo sample (15.00 g) was sequentially extracted with 80% ethanol containing 0.025 M HCl (H_1), 80% ethanol containing 0.50% NaOH (H_2), and 2.00, 5.00, and 8.00% NaOH alkaline aqueous solution (H_3, H_4, H_5, respectively) at 75°C for 4 h with a solid to liquid ratio of 1:25 (g/mL). The extracted solutions were filtrated through filter paper using vacuum filtration. After filtration, the filtrate was neutralized to pH 5.5 (acidic ethanol-extractable solution was neutralized with 0.025 M NaOH and all other solutions were neutralized with 6 M hydrochloric acid), and then concentrated to less than 30 mL with a rotary evaporator under reduced pressure. After concentration of the filtrate, each concentrated filtrate was slowly poured into three volumes of ethanol with continuous stirring, and precipitation occurred. The precipitated hemicelluloses fractions were centrifuged and washed with 70% ethanol at room temperature prior to freeze-drying in water. All the experiments were performed at least in duplicate. Yields of the hemicelluloses fractions were calculated on dry weight basis related to the dewaxed bamboo samples. The relative standard deviation was observed to be lower than 4.60%.

Characterization of the hemicelluloses fractions. Sugar composition and molecular weights of the hemicellulosic fractions were determined as described in previous reports (Shi et al. 2011). ^{1}H and ^{13}C-NMR experiments were performed on samples in D_2O (20 and 80 mg/ml, respectively) at 25 °C, using a Bruker AVIII 400 MHz instrument. Two-dimensional NMR (HSQC) experiments were performed according to standard pulse sequences available in the Bruker software.

Results and Discussion

Fractional yield and composition of hemicelluloses

Table 1. *Yield and chemical composition of hemicelluloses fractions from D. sinicus*

Fraction	Yield (%)	Composition (%)						
		Ara	Gal	Glu	Xyl	Uronic acid	Xyl/Ara	Xyl/Uronic acid
H_1	2.10	20.16	9.01	29.65	34.72	4.46	1.72	7.78
H_2	0.40	16.56	7.97	32.28	38.96	4.22	2.35	9.23
H_3	4.90	8.57	2.43	1.81	85.85	1.33	10.02	64.55
H_4	9.80	8.14	0.47	0.75	87.87	2.76	10.79	31.84
H_5	7.20	7.20	0.68	2.28	87.55	2.30	12.16	38.07

As shown in Table 1, the yields of the hemicelluloses fractions were 2.10%, 0.40%, 4.90%, 9.80%, and 7.20% of the initial amount of dewaxed bamboo (*D. sinicus*), for H_1, H_2, H_3, H_4, and H_5, respectively. The total yield of the five soluble hemicelluloses fractions was 24.60% of the initial dry weight. The results revealed that the sequential treatments of the bamboo (*D. sinicus*) with ethanol and alkaline solutions were very effective to separate hemicellulosic polysaccharides.

The neutral sugar analysis results showed that the major sugar components of the ethanol-soluble hemicelluloses fractions H_1 and H_2 were xylose (34.72-38.96%), glucose (29.65-32.28%), and arabinose (16.56-20.16%). Uronic acid (4.22-4.46%), mainly glucuronic acid (GlcpA) or 4-O-methyl-glucuronic acid, was present as a minor amount. However, xylose was the absolutely dominant components (85.85-87.87%) in the alkaline aqueous solution solubilized hemicelluloses fractions (H_3, H_4, and H_5), and only small amounts of arabinose (7.20-8.57%) and uronic acid (1.33-2.76%) were observed from these hemicelluloses fractions. These analysis results implied that the ethanol soluble hemicelluloses (H_1, H_2) probably contained arabinoglucuronoxylans, β-glucan, and starch, while the alkaline aqueous solution soluble hemicelluloses (H_3, H_4, and H_5) probably contained significantly amount of arabinoglucuronoxylans, which was in agreement with those findings in other bamboo species (Fengel and Shao 1984, Meakawa 1976, Peng et al. 2011).

Molecular weight distribution

Table 2. *Weight-average (M_w) and number-average (M_n) molecular weights and polydispersity (M_w/M_n) of the hemicelluloses fractions isolated from bamboo (D. sinicus).*

	Hemicelluloses fractions [a]				
	H_1	H_2	H_3	H_4	H_5
M_w	17380	19620	22510	42150	41260
M_n	8670	15650	16750	25640	37320
M_w/M_n	2.00	1.25	1.34	1.64	1.11

The molecular weight distribution analysis results are listed in Table 2. It was found that the initial two stages of treatment of dewaxed bamboo sample with weakly acidic ethanol followed by weakly alkaline ethanol resulted in dissolution of hemicellulosic polysaccharides with lower average molecular weights (ranging from 17380 to 19620 g/mol). The subsequent three stages of treatment of bamboo residue with alkaline aqueous solutions containing different concentrations of NaOH led to release of hemicellulosic polysaccharides with relatively higher molecular weights (ranging from 22510 to 42150 g/mol). These results

suggested that the ethanol solution only released low molecular weight hemicelluloses, while the strong alkali can dissolve the higher molecular weight hemicelluloses.

1D and 2D NMR spectra

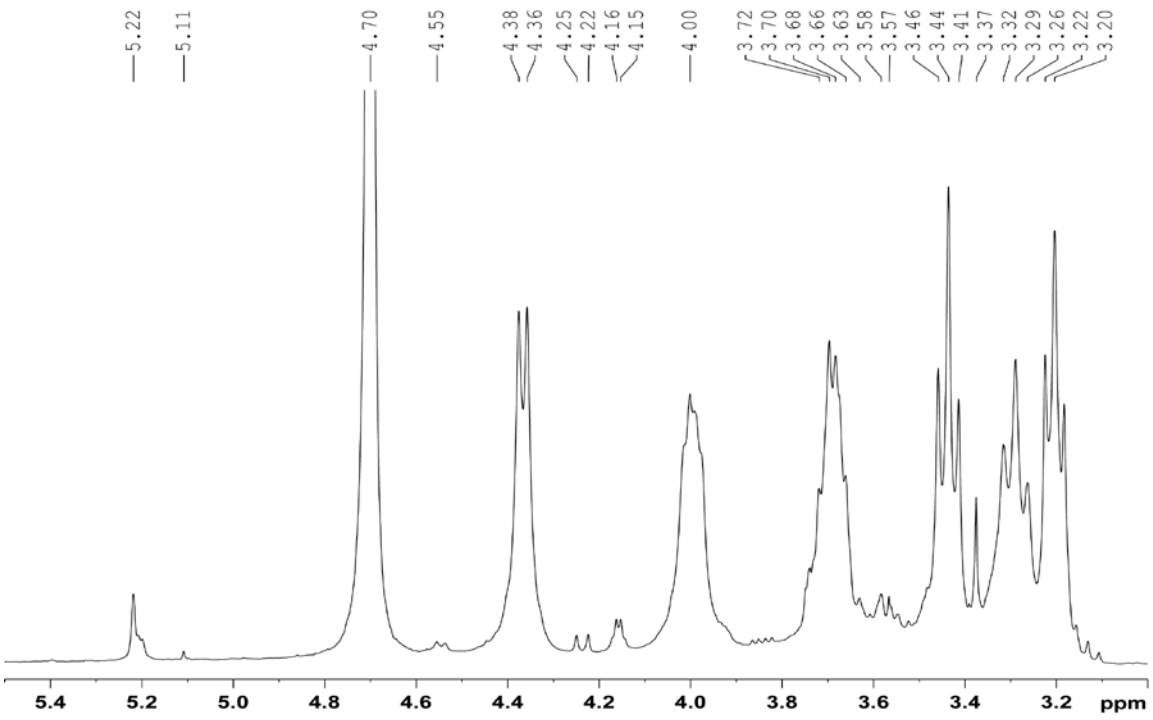

Fig. 1. *^{1}H-NMR spectrum (in D_2O) of the hemicelluloses fraction H_4 isolated with 2.00% NaOH solution.*

Examination of the proton spectrum of 2.00% NaOH-soluble hemicelluloses fraction H_4 (Figure 1) showed the relative simplicity of the structure. This was exhibited by major signals corresponding to non-substituted β-D-xylose residues, minor signals originating from α-L-arabinfuranosyl residues, and weak signals corresponding to 4-O-methyl-α-D-glucuronic acid residues. Strong signals at 4.36, 4.00, 3.72, 3.44, 3.29, 3.20 ppm, correspond to H-1, H-5eq, H-4, H-3, H-5ax, and H-2 of non-substituted β-D-xylose residues, respectively. Minor signals at 5.22 (H-1), 4.16 (H-4), 4.00 (H-2), 3.70 (H-3), 3.66 (H-5) ppm, originate from α-L-arabinfuranosyl residues. Weak signals at 5.22, 4.22, 3.63, 3.57, 3.13 ppm, correspond to H-1, H-5, H-3, H-2, and H-4 of 4-O-methyl-α-D-glucuronic acid residues, respectively (Vignon and Gey 1998).

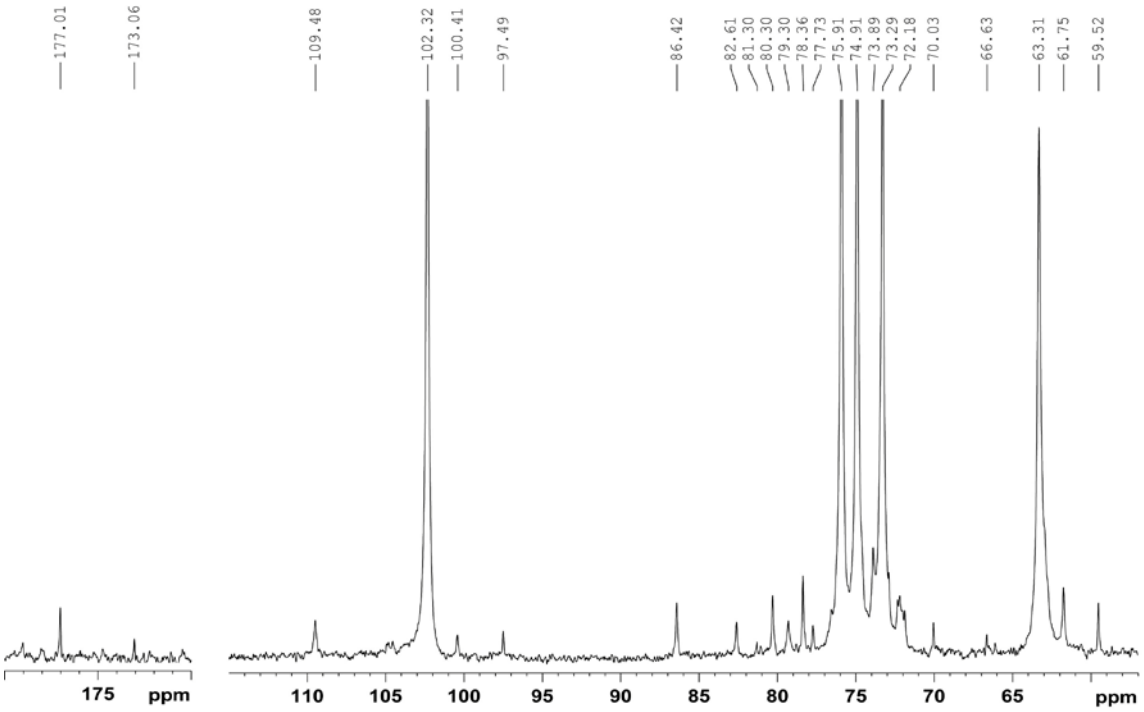

Fig. 2. *^{13}C-NMR spectrum (in D_2O) of the hemicelluloses fraction H_4 isolated with 2.00% NaOH solution.*

The ^{13}C NMR spectrum (Figure 2) of H_4 exhibits five major signals corresponding to those of (1→4)-linked-β-D-xylan. The signal at 102.32 ppm corresponds to the anomeric region in a β-configuration, while the signals at 75.91, 74.91, 73.29, and 63.31 ppm correspond to C-4, C-3, C-2, and C-5 of (1→4)-linked-β-D-xylopyranosyl units, respectively. The signals at 177.01, 97.49, 82.61, 79.30, 72.18, and 70.03 ppm, arise from C-6, C-1, C-4, C-3, C-5, and C-2 of 4-O-methyl-α-D-glucuronic acid, respectively. Other signals at 109.48, 86.42, 80.30, 78.36, and 61.75 ppm correspond to C-1, C-4, C-2, C-3, and C-5 of α-L-arabinfuranosyl residues, respectively (Chaikumpollert et al. 2004).

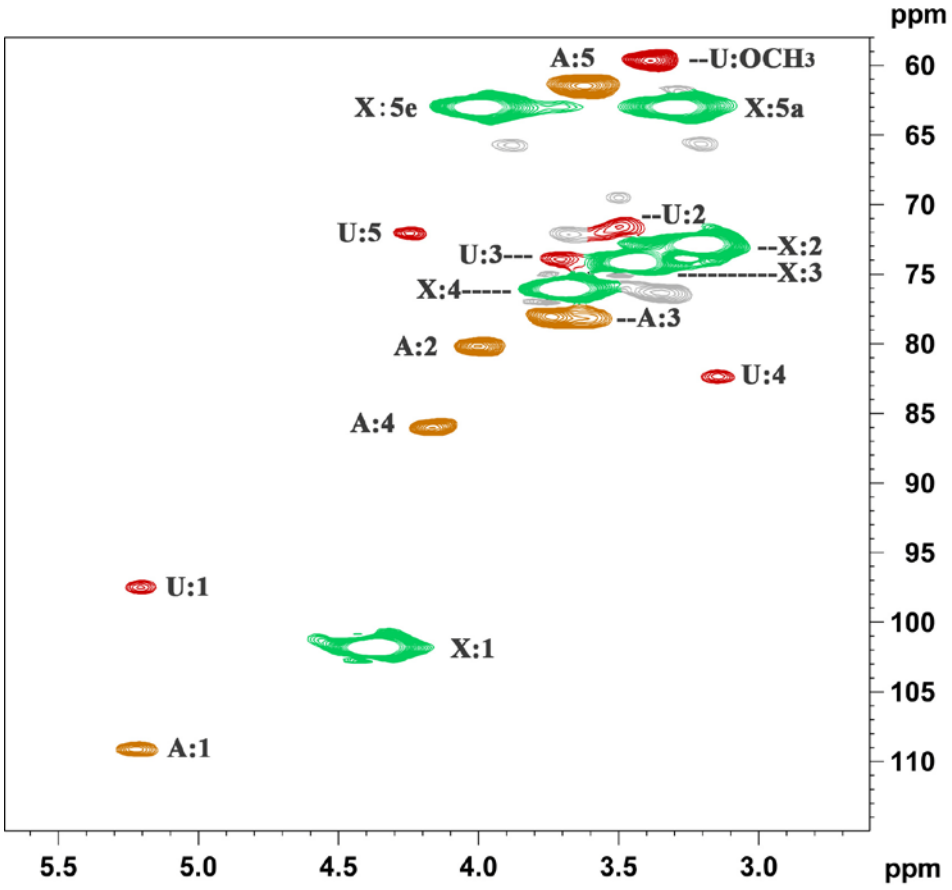

Fig. 3. *$^{1}H/^{13}C$ NMR (HSQC) of the hemicelluloses fraction H_4 isolated with 2.00% NaOH solution.*

Table 3. *Assignment of $^{1}H/^{13}C$ cross-signals in the HSQC spectrum of the hemicelluloses fraction H_4 isolated with 2.00% NaOH solution.*

Saccharide	NMR	Chemical shift (ppm)							
		1	2	3	4	5eq [a]	5ax [b]	6	OCH_3
X [c]	^{13}C	102.32	73.29	74.91	75.91	63.31	63.31	-	-
	^{1}H	4.36	3.20	3.44	3.72	4.00	3.29	-	-
A [d]	^{13}C	109.48	80.30	78.36	86.42	61.75	61.75	-	-
	^{1}H	5.22	4.00	3.70	4.16	3.66	-	-	-
U [e]	^{13}C	97.49	70.03	79.30	82.61	72.18	-	177.01	59.52
	^{1}H	5.22	3.57	3.63	3.13	4.22	-	8.40	3.46

[a] eq, equatorial; [b] ax, axial; [c] X, (1→4)-β-D-Xylp; [d] A, α-Araf residues; [e] U, Uronic acid

From the HSQC spectrum of H_4 (Figure 3), the dominant five cross-peaks could be expressly identified at 102.32/4.36, 75.91/3.72, 74.91/3.44, 73.29/3.20, 63.31/4.00 and 3.29 ppm, which were assigned to C_1-H_1, C_4-H_4, C_3-H_3, C_2-H_2, and C_5-H_5 of the (1→4)-linked-β-D-xylopyranosyl units, respectively (Xu et al. 2007). The HSQC spectrum also provided the additional evidences for the presence of 4-O-methyl-D-glucuronic acid and α-L-arabinose. For full details of the chemical shifts assignments of the 2D NMR of hemicelluloses fraction H_4 refer to Table 3.

Based on the above analysis results and the existing literature about the structural properties of bamboo hemicelluloses (Wilkie and Woo 1976, Wilkie and Woo 1977), it could be concluded that the polysaccharide fractions isolated from the bamboo (*D. sinicus*) were mainly composed of arabinoglucuronoxylans, together with small amounts of β-glucan and starch. The structure of the isolated arabinoglucuronoxylans from bamboo (*D. sinicus*) was defined as having a linear (1→4)-linked-β-xylopyranosyl backbone to which α-L-arabinofuranose units and/or short chains of 4-O-methyl-D-glucuronic acid were attached as side residues via α-(1→3) and/or α-(1→2) linkages, with a ratio of uronic acid/arabinose/xylose of 1:3:32. Therefore, the potential structures of L-arabino-(4-O-methyl-D-glucurono)-D-xylan isolated from bamboo species *D. sinicus* with alkaline aqueous ethanol could be illustrated as Figure 4.

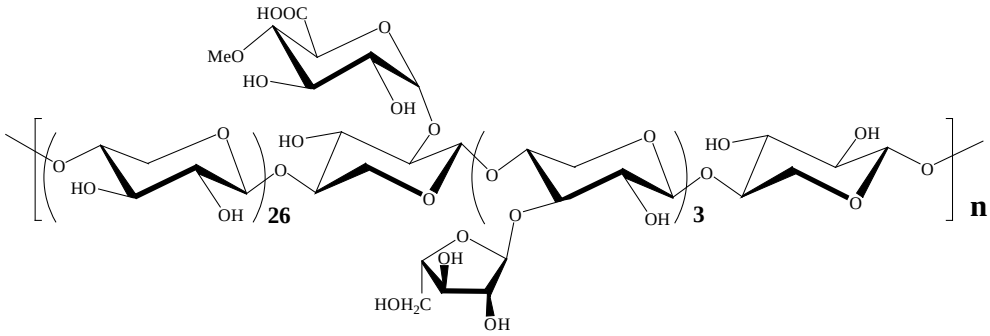

Fig. 4. *Potential structures of arabinoglucuronoxylans isolated from bamboo D. sinicus*

Conclusions

The sequential treatments of dewaxed bamboo (*D. sinicus*) samples with 80% ethanol containing 0.025 M HCl, 80% ethanol containing 0.50% NaOH, and alkaline aqueous solution (containing 2.00, 5.00, and 8.00% NaOH) at 75°C for 4 h with a solid to liquid ratio of 1:25 (g/mL) yielded 24.60% soluble hemicelluloses. The dominant components of the soluble hemicelluloses from bamboo (*D. sinicus*) were arabinoglucuronoxylans. The isolated arabinoglucuronoxylans was defined as having a linear (1→4)-β-linked-xylopyranosyl backbone to which α-L-arabinofuranose units and/or short chains of 4-O-methyl-glucuronic acid were attached as side residues via α-(1→3) and/or α-(1→2) linkages.

Acknowledgements

The authors are grateful for the financial support from State Forestry Administration (200804015), Major State Basic Research Projects of China (973-2010CB732204), National Natural Science Foundation of China (30930073, 30710103906), China Ministry of Education (111), Education Department of Yunnan Province, China (2011Z040), and Southwest Forestry University Scientific Research Fund Project, China.

References

Chaikumpollert, O., Methacanon, P., Suchiva, K. 2004. Structural elucidation of hemicelluloses from Vetiver grass. *Carbohydrate Polymer*. 57(2): 191-196.

Fengel, D., Shao, X. 1984. A chemical and ultrastructural study of the bamboo species *Phyllostachys makinoi* Hay. *Wood Science and Technology.* 18(2): 103-112.

Fitzpatrick, M., Champagne, P., Cunningham, M. F., Whitney, R. A. 2010. A biorefinery processing perspective: treatment of lignocellulosic materials for the production of value-added products. *Bioresource Technology*. 101(23): 8915-8922.

Hallac, B. B., Sannigrahi, P., Pu, Y.Q., Ray, M., Murphy, R. J., Ragauskas, A. J. 2009. Biomass characterization of *Buddleja davidii*: a potential feedstock for biofuel production. *Journal of Agricultural and Food Chemistry*. 57(4): 1275-1281.

Meakawa, E. 1976. Studies on hemicelluloses of bamboo. *Wood Research.* 59/60: 153-179.

Ohrnberger, D. 1999. The Bamboos of the World: Annotated Nomenclature and Literature of the Species and the Higher and Lower Taxa. Amsterdam, New York: Elsevier.

Peng, P., Peng, F., Bian, J., Xu, F., Sun, R. C. 2011. Studies on the starch and hemicelluloses fractionated by graded ethanol precipitation from bamboo *Phyllostachys bambusoides* f. shouzhu Yi. *Journal of Agricultural and Food Chemistry.* 59(6): 2680-2688.

Shi Z. J., Xiao L. P., Deng J., Sun R. C. 2011. Isolation and characterization of soluble polysaccharides of *Dendrocalamus brandisii*: a high-yielding bamboo species. *BioResources*. 6(4): 5151-5166.

Vignon, M. R., Gey, C. 1998. Isolation, ^{1}H and ^{13}C NMR studies of (4-O-methyl-D-glucurono)-D-xylans from luffa fruit fibres, jute bast fibres and mucilage of quince tree seeds. *Carbohydrate Research.* 307(1-2): 107-111.

Wilkie, K. C. B., Woo, S. L. 1977. A heteroxylan and hemicellulosic materials from bamboo leaves, and a reconsideration of the general nature of commonly occurring xylans and other hemicelluloses. *Carbohydrate Research.* 57: 145-162.

Wilkie, K. C. B., Woo, S. L. 1976. Non-cellulosic β-D-glucans from bamboo, and interpretative problems in the study of all Hemicelluloses. *Carbohydrate Research.* 49: 399-409.

Xu, F., Sun, J. X., Geng, Z. C., Liu, C. F., Ren, J. L., Sun, R. C., Fowler, P., Baird, M. S. 2007. Comparative study of water-soluble and alkali-soluble hemicelluloses from perennial ryegrass leaves (*Lolium peree*). *Carbohydrate Polymer.* 67(1): 56-65.

Proceeding of the 55th International Convention of Society of Wood Science and Technology
August 27-31, 2012 – Beijing, CHINA

A Spectroscopic Study on the Fuel Value of Softwoods in Relation to Chemical Composition

Chi-Leung So[1] – Thomas L. Eberhardt[2] – Leslie H. Groom[3] – Todd F. Shupe[4]*

[1] Assistant Professor, School of Renewable Natural Resources, Louisiana State University Agricultural Center, Baton Rouge, LA, USA
* *Corresponding author*
cso@agcenter.lsu.edu
[2] Research Scientist, USDA Forest Service, Southern Research Station, Utilization of Southern Forest Resources, Pineville, LA, USA
[3] Project Leader, USDA Forest Service, Southern Research Station, Utilization of Southern Forest Resources, Pineville, LA, USA
[4] Professor, School of Renewable Natural Resources, Louisiana State University Agricultural Center, Baton Rouge, LA, USA

Abstract

The recent focus on bioenergy has led to interest in developing alternative technologies for assessing the fuel value of available biomass resources. In this study, both near- and mid-infrared spectroscopic datawere used to predict fuel value in relation to extractives and lignin contents for longleaf pine wood. Samples were analyzed both before and after extraction.Using both near- and mid-infrared spectroscopy, strong correlations were found between fuel value and extractives content for the unextracted wood samples, with the mid-IR models providing better correlations while using less factors. These findings were further evident in the plots of the regression coefficients for fuel value and extractives content. Although, total lignin content does impact total fuel value, the predictive ability for both mid-infrared and near-infrareddata were similarly poor for the extractive-free wood samples. The use of these techniques provides further spectroscopic support for the relationships mentioned previously.

Keywords: fuel value, extractives content, lignin content, longleaf pine, near-infrared spectroscopy, mid-infrared spectroscopy.

Introduction

Gross calorific value (GCV)is a measure of fuel valueandis synonymous with higher heating value (HHV) and gross heat of combustion (GHC). Several studies have attempted to relate these fuelvalues to specific chemical constituents comprising different types of biomass. For example, White (1987) used linear regression to show that HHV values from several softwoods and hardwoods could be correlated with lignin content alone ($R^2 = 0.70$) or by including a factor for extractives content ($R^2 = 0.76$). Analysis of extractive-free samples gave a higher correlation ($R^2 = 0.97$) with lignin content. Demirbas (2001) was also able to relateHHV to lignin content using a variety of extractive-free biomasssamples that provideda wide range of lignin values (15.01-55.29%); in a subsequent study, HHV was also related to extractives content (Demirbas 2003).

\The application of near-infrared (NIR) spectroscopy, coupled with multivariate analysis, allows for predictions of values for fuel value.For example, Lestander and Rhen (2005) used this technique to determine the calorific content of Norway spruce samples. However, for determinations of calorific value for poplar samples, the accuracies of the calibration models were limited (Maranan and Laborie 2007). Gillon et al. (1997) found this technique to be half as accurate as the direct determinations. Recently, NIR-based models were successfully used to predict GCV in longleaf pine wood samples(So and Eberhardt 2010). Unlike prior studies, here the GCV models were driven by the extractives, and not the lignin content.Alternatively, mid-IR spectroscopic data can be used to build models. The added benefit to mid-IR spectroscopy is that it allows clearer spectral investigations to determine those chemical features imparting the greatest effect. Only recently, Zhou et al. (2011), used mid-IR spectroscopic data coupled with multivariate analysis, to predict both the calorific value and lignin content for a single species ofhybrid poplar wood, and concluded that calorific value was unrelated to lignin content. In the current study, the impact of both extractives and lignin content on GCV for longleaf pine wood was investigated using both NIR and mid-IR spectroscopic techniques. Building upon prior work (So and Eberhardt 2010), the multivariate analyses were carried using the same sampling populations allowing direct comparisons between the two techniques.

Materials And Methods

Materials. Forty longleaf pine (*Pinuspalustris*) wood sampleswere obtained following a harvest from the Kisatchie National Forest, Louisiana, USA. A strip of wood, from each of 40 tree section disks collected, was reduced in size to allow grinding in a large Wiley mill equipped with a 2 mm mesh sieve plate.

Extractives, lignin and GCV determinations. Milled wood samples were extracted with acetone using a Soxhlet apparatus. Extracts were dried *in vacuo*and weighed. Extractive-free milled wood samples were further ground in a small Wiley mill equipped with a 40-mesh screen. Lignin content was determined using the acetyl bromide method (Morrison 1972) using an absorptivity value of 23.30 g^{-1} L cm^{-1} (Johnson et al. 1961). Moisture contents, determined bydrying samples in an oven (102 ± 3 ºC), were used to adjust values for extractives and lignin

contents to a dry-weight basis.Values for GCV were determined in triplicate using a Parr oxygen bomb calorimeter 6100 per the manufacturer's operating instructions(Parr Instruments 2006).

Mid-IR and NIR spectroscopy. Mid-IR spectra were collected using a ThermonicoletNexus Model 670 FTIR spectrometer equipped with a Golden Gate MKII Single Reflection ATR accessory. Samples were applied directly to the diamond window. Spectra were collected at wavenumbers between 650-4000 cm^{-1}.NIR spectra were collected using an ASD Field Spec spectrometer with a fiber optic probe oriented perpendicular to the sample surface. The samples were illuminated with a DC lamp oriented at 30° above the sample surface, and rotated at 45 rpm to minimize specular interference and surface heterogeneity. Spectra were collected at wavelengths between 350-2500 nm. For both spectroscopic techniques, three spectra were collected from each sample.

Multivariate analysis. Data analyses were performed using the Unscrambler (version 8.0) software. The spectroscopic data were first averaged to one spectrum per sample. The full range was utilized for the mid-IR spectra, while the NIR region was narrowed down to 1100-2400 nm for analysis. Principal component analysis (PCA) was performed on the spectral data to observe any clustering between the samples. Partial least squares (PLS) regression was used to predict GCV, extractives content, and lignin content for the samples. Calibration and test sets were randomly created for the analyses with 30 and 10 samples, respectively. The models were assessed using several common measures of calibration performance, including the correlation coefficient (R^2), the standard error of cross validation (SECV) and the standard error of prediction (SEP), and the ratio of performance to deviation (RPD).

Results And Discussion

Extractives, lignin, and GCV. The extractives content for the 40 longleaf pine wood samples varied between 0.0 to 20.6%, which is smaller than that reported by Via et al. (2007) with values as high as 33%. The mean GCV for the samples, prior to extraction, ranged from 20.2 to 23.6 $MJkg^{-1}$. The relationship between GCV and extractives content was investigated by applying a standard linear regression to the data and a strong correlation ($R^2 = 0.91$; p-value < 0.0001) was found. The lignin content was determined from the extracted samples and the values ranged between 26.6 to 31.5% similar to those previously reported (Via et al. 2007). The GCV range was lower and narrower following extraction (19.5-20.6 $MJkg^{-1}$). The relationship between lignin and GCV (extracted) was much poorer ($R^2 = 0.12$; p-value < 0.0266) than that obtained using extractives content.

Mid-IR and NIR spectra. An averaged mid-IR spectrum of all 40 unextracted longleaf pine wood is shown in Figure 1(a), exhibiting the commonly observed bands about 1000-1150 (C-O stretch), 1700-1750 (C=O stretch), 2800-3000 (C-H stretch), and 3100-3600 (O-H stretch) cm^{-1}. Peaks at 1689, 2865and 2925 cm^{-1}, typical of the pine resin components, were greatly reduced following extraction as shown in the spectrum of the corresponding extracted sample in Figure 1(b). Although this not clearly observed in Figure 1 due to scaling, a difference spectrum (Figure 1 (c)) was calculated from these two averaged spectra showing well resolved peaks at the

aforementioned wavenumbers. This mid-IR difference spectrum is very similar to a difference spectrum between resinous and non-resinous Scots pine heartwood (Nuopponen et al. 2003). This was repeated with the NIR data with Figures 2(a) and (b) displaying the unextracted and extracted spectra, respectively. Differences were not readily observable as seen in Figure 1 with the mid-IR spectra.

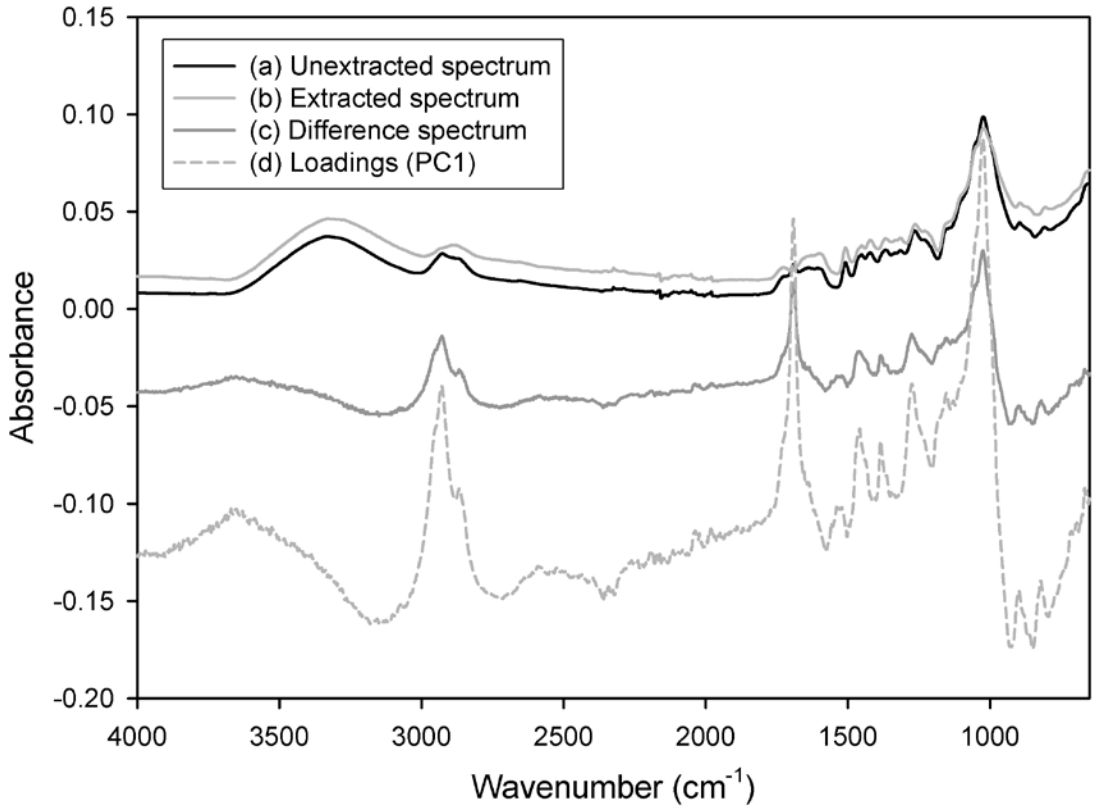

Figure 1*.Averaged mid-IR spectra for the (a) unextractedand (b) extracted samples, as well as the resulting (c) difference spectrum, and (d)loadings plot (PC1). The spectra are not to scale.*

PCA of unextracted wood samples. PCAwas performed on the mid-IR spectra and the resultant scores plot provided separated clustersof the unextracted and extracted wood samples (plot not shown). Theloadings plot for PC1 (Figure 1(d)), explaining 91% of the variation, exhibited some clearly defined bands at: 1014, 1271, 1389, 1461, 1689, 2865 and 2925 cm^{-1}. These peaks match very closely with the difference spectrum in Figure 1(c). The same analysis with the NIR spectra produced similar results with separation between the extracted and unextracted samples. Figure 2(d) shows the loadings plot for PC1 with broad bands at: 1205, 1455, 1725, 1945 and 2305 nm, matching those observed in the NIR difference spectrum (Figure 2(c)).

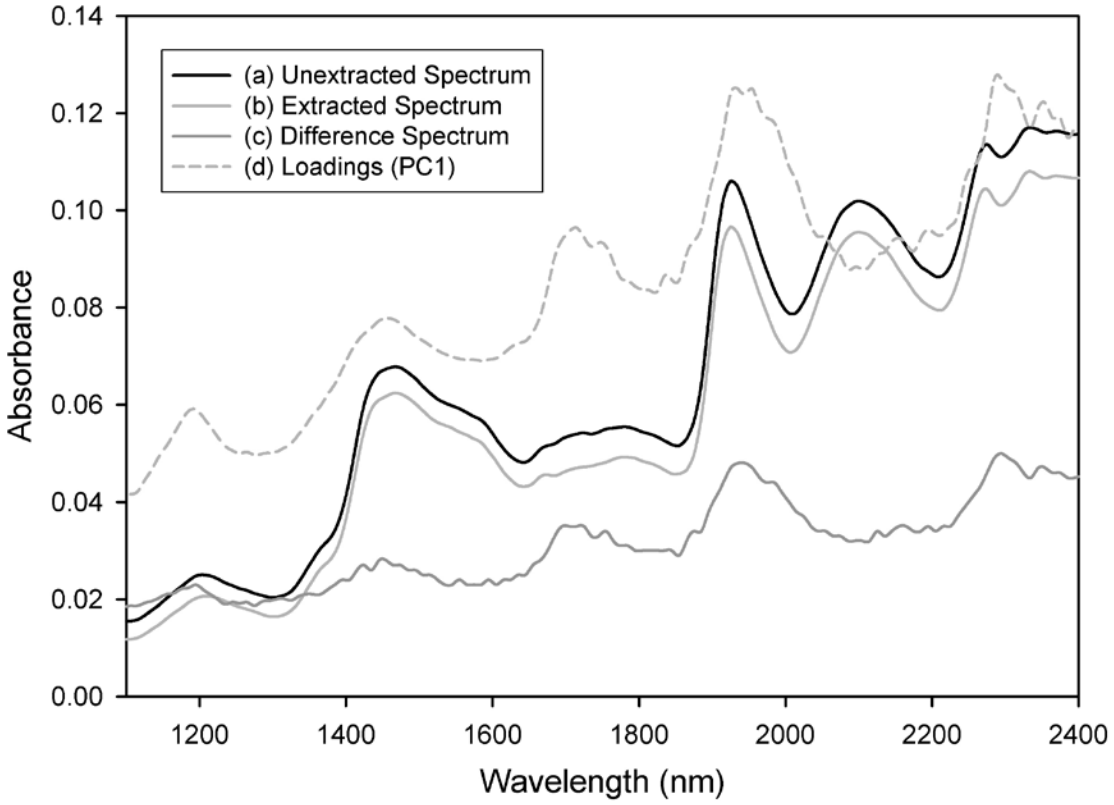

Figure 2*. Averaged NIR spectra for the (a) unextractedand (b) extracted samples, as well as the resulting (c) difference spectrum, and (d) loadings plot (PC1).The spectra are not to scale.*

PLS of unextracted wood samples. Calibration models for extractives content provided strong calibration statistics (R^2 = 0.94 and 0.93; SECV = 1.46% and 1.78%, RPD = 3.68 and 3.01 for mid-IR and NIR, respectively) with the mid-IR model providing a better RPD while using less factors (Table 1). RPDis a statistical parameter that accounts for the various properties and their ranges. A RPD value of 2.5 is considered satisfactory for screening, while 1.5 may be acceptable for preliminary use (Williams and Sobering 1993).The same trend was noted with the models for GCV. However, these were not as strong as those for extractives content providing lower RPD values (3.09 and 2.39 for mid-IR and NIR, respectively). The predictive ability of the extractives content was very strong for the mid-IR data with a RPD (3.63) very similar to that of the calibration model, but it was notably poorer for the NIR data (1.22) from the same test samples. The predictive ability for GCV was much poorer for both mid-IR and NIR analyses (Table 2) with much lower RPD values (2.14 and 1.31, respectively) than for the calibration models, and also poorer than the predictive ability for extractives.

PLS of extracted wood samples. Models were built for lignin content and GCV using the extracted samples and the results listed in Table 2. The correlations obtained from the mid-IR

data were poor for both lignin (R^2 = 0.61; SECV = 0.89%; RPD = 1.01) and GCV (R^2 = 0.58; SECV = 0.23 $MJkg^{-1}$; RPD = 1.06). No improvement was observed when using a reduced wavenumber range (650-1800 cm^{-1}). The use of NIR data led to a slight improvement for the lignin model (R^2 = 0.65; SECV = 0.80%; RPD = 1.10) but was poorer for the GCV model (R^2 = 0.30; SECV = 0.24 $MJkg^{-1}$; RPD = 1.03). The predictive ability for both mid-IR and NIR data were similarly poor compared to that obtained from the calibration models (Table 2). It was clearly observed that the models obtained with the extracted samples were much poorer than those from the unextracted samples in Table 1. However, in previous studies, strong correlations for GCV have been obtained from extractive-free hybrid poplar samples (Zhou et al. 2011). R^2 values ranged from 0.86-0.90 in the mid-IR range using a variety of preprocessing methods. Nevertheless, these models did require between 10-12 factors.

Table 1*. PLS model statistics obtained fromunextracted samples.*

Method	Sample	Property	SD	No. of Factors	R^2	SECV/P	RPD
Mid-IR	Calib	GCV	0.85	2	0.91	0.28	3.09
		Extractives	5.36	2	0.94	1.46	3.68
	Test	GCV	0.59	2	0.78	0.28	2.14
		Extractives	4.07	2	0.94	1.12	3.63
NIR	Calib	GCV	0.85	2	0.86	0.36	2.39
		Extractives	5.36	3	0.93	1.78	3.01
	Test	GCV	0.59	2	0.54	0.45	1.31
		Extractives	4.07	3	0.45	3.33	1.22

The units for SECV/P are expressed in GCV ($MJkg^{-1}$) and extractives (%), respectively.

Table 2*. PLS model statistics obtained from extracted samples.*

Method	Sample	Property	SD	No. of Factors	R^2	SECV/P	RPD
Mid-IR	Calib	GCV	0.24	3	0.58	0.23	1.06
		Lignin	0.90	4	0.61	0.89	1.01
	Test	GCV	0.30	3	0.33	0.25	1.18
		Lignin	1.43	4	0.54	1.03	1.38
NIR	Calib	GCV	0.24	2	0.30	0.24	1.03
		Lignin	0.90	4	0.65	0.80	1.10
	Test	GCV	0.30	2	0.31	0.25	1.17
		Lignin	1.43	4	0.68	0.80	1.79

The units for SECV/P are expressed in GCV ($MJkg^{-1}$) and lignin (%), respectively.

Regression coefficients. The regression coefficients provide information about the models built in the PLS analyses and are plotted in Figure 3 for the extractives content and GCV models based on the mid-IR data. The plots appear to be very similar, indicating that the strong calibration models for extractives content and GCV were based on the same chemical features. Furthermore, these plots exhibit the same peaks as observed in the loadings plot and the difference spectrum (Figure 1), with particularly strong peaks at 1689, 2865 and 2925 cm^{-1},in

addition to peaks at1271, 1389 and 1461 cm^{-1}. The models were negatively correlated with 1014 cm^{-1}(C-O stretch) peak.

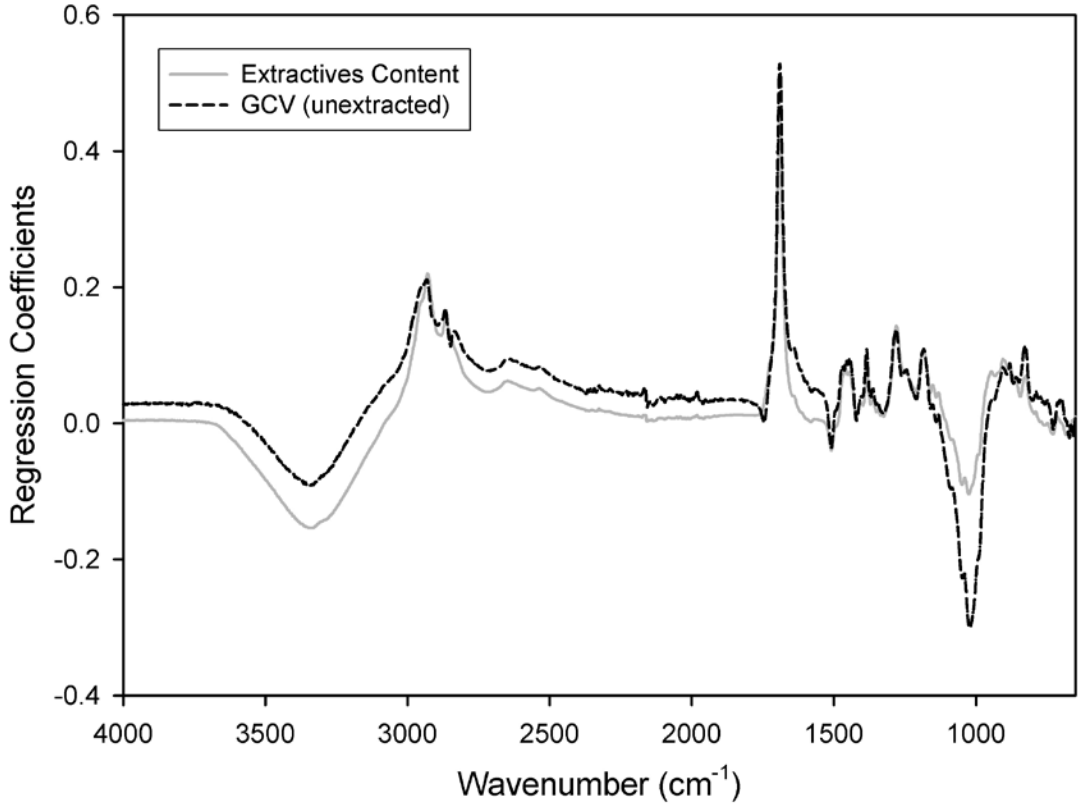

Figure 3*.Regression coefficients for the extractives content and GCV models based on the mid-IR data from the unextracted samples.*

The analyses using the models based on NIR data are plotted in Figure 4. The plots of regression coefficients for extractives content and GCV were again similar with several bands of interest at: 1205, 1725 and 2305 nm. Thepeaks centered near 1705 nm correspond to the 1st overtone of aliphatic and aromatic CH stretching in CH_2 groups present in both lignin and extractives. The other major peak at 2295 nm is due to OH and C-O stretching (Michell and Schimleck, 1996). Similar high regression coefficients for the prediction of GCV, from hybrid poplars, were reported at 1725 and 2270 nm (Maranan and Laborie, 2007). However, unlike the mid-IR results, high regression coefficients are not clearly attributable to the extracts and not lignin.

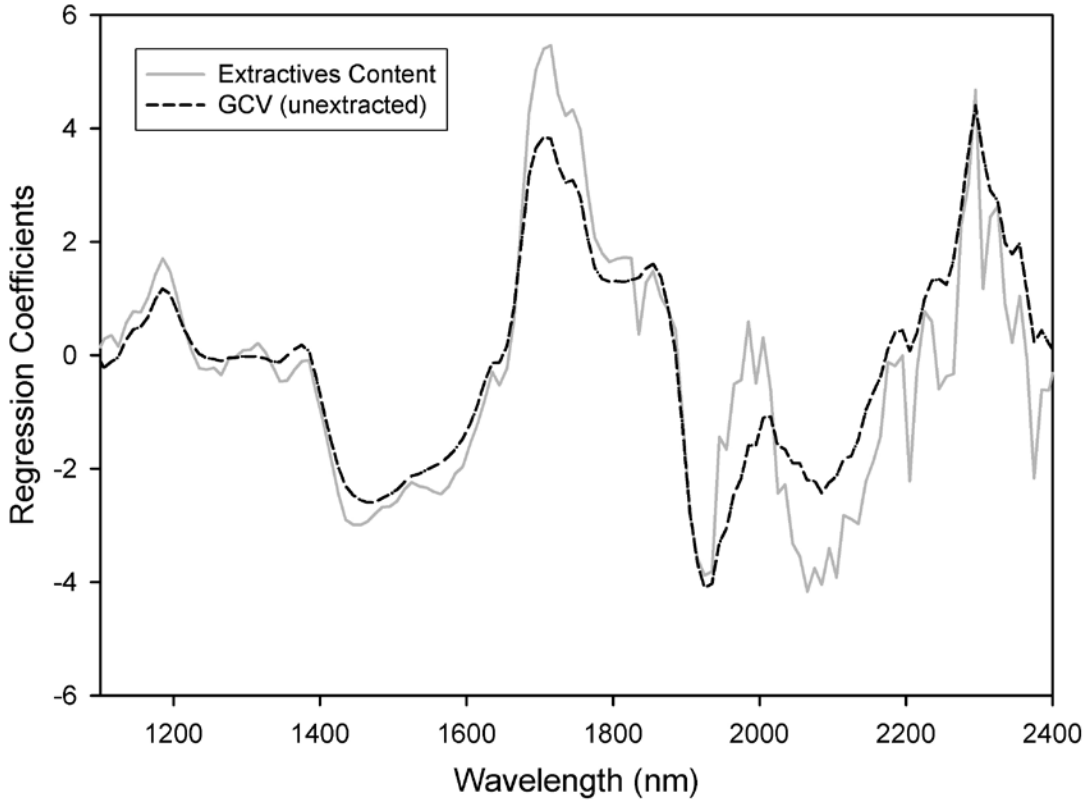

Figure 4*.Regression coefficients for the extractives content and GCV models based on the NIR data from the unextracted samples.*

Conclusions

Strong relationships were apparent between the variation in GCV and variation in extractives content using both mid-IR and NIR spectroscopic data. Plotting the regression coefficients for GCV and extractives content showed that the same bands were responsible for these strong models. Although, total lignin content does impact total GCV, no correlation was found between the variation in GCV with lignin content for the extractive-free wood samples.

Acknowledgements The authors are grateful to Karen Reed and Donna Edwards for sample preparation and collection. Additional thanks go to Jim Scarborough and Jacob Floyd for sample collection.

References

Demirbas, A. 2001.Relationships between lignin contents and heating values of biomass.Energy Convers. Manage. 42:183-188.

Demirbas, A. 2003.Fuelwood characteristics of six indigenous wood species from the Eastern Black Sea Region. Energy Source 25:309-316.

Gillon, D., Hernando, C., Valette, J.and Joffre, R. 1997. Fast estimation of the calorific values of forest fuels by near-infrared reflectance spectroscopy. Can. J. Forest Res. 27:760-765.

Johnson, D.B., Moore, W.E. andZank, L.C. 1961.The spectrophotometric determination of lignin in small wood samples.Tappi J. 44:793-798.

Lestander, T.A. andRhen, C. 2005. Multivariate NIR spectroscopy models for moisture, ash and calorific content in biofuels using bi-orthogonal partial least squares regression. Analyst 130:1182-1189.

Maranan, M.C. and Laborie, M.P.G. 2007. Analysis of energy traits of Populus spp. clones by near-infrared spectroscopy. J. Biobased Mater. Bioenergy 1:155-162.

Michell, A.J. and Schimleck, L.R. 1996. NIR spectroscopy of woods from Eucalyptus globulus.Appita J. 49, 23.

Morrison, I.M. 1972.A semi-micro method for the determination of lignin and its use in predicting the digestibility of forage crops. J. Sci. Food Agric. 23:455-463.

Nuopponen, M., Vuorinen, T., Jamsa, S. andViitaniemi, P. 2003.The effects of a heat treatment on the behavior of extractives in softwood studied by FTIR spectroscopic methods. Wood Sci. Technol. 37:109-115.

Parr Instruments. 2006. Parr 6100 Operating Manual, version date 9-6-06. Parr Instruments, Moine, IL.

So, C.L. and Eberhardt, T.L. 2010.Chemical and calorific characterization of longleaf pine using near infrared spectroscopy. J. Near Infrared Spectrosc. 18:417-423.

Via, B.K., So, C.L., Groom, L.H., Shupe, T.F., Stine, M. andWikaira, J. 2007. Within tree variation of lignin, extractives, and microfibril angle coupled with the theoretical and near infrared modeling of microfibril angle. IAWA J. 28:189-209.

White, R.H. 1987.Effect of lignin content and extractives on the higher heating value of wood. Wood Fiber Sci. 19:446-452.

Zhou, G., Taylor, G. and Polle, A. 2011. FTIR-ATR-based prediction and modeling of lignin and energy contents reveals independent intra-specific variation of these traits in bioenergy poplars. Plant Methods 7:9.

Proceedings of the 55th International Convention of Society of Wood Science and Technology
August 27-31, 2012 - Beijing, CHINA

New Bio-composites Containing Industrial Lignins

Nicolas Mariotti[1] – Lei Hu[2] – Diane Schorr[3] – Tatjana Stevanovic[4] – Denis Rodrigue[5] – Xiang-Ming Wang[6] – Papa Niokhor Diouf[7] – Daniel Grenier[8]*

[1] PhD student and SWST member, Département des sciences du bois et de la forêt, Université Laval, Québec, QC, G1V0A6, Canada.
[2] PhD student, Département de génie chimique, Université Laval, Québec, QC, G1V0A6, Canada.
[3] PhD student, Département des sciences du bois et de la forêt, Université Laval, Québec, QC, G1V0A6, Canada.
[4] Professor, Département des sciences du bois et de la forêt, Université Laval, Québec, QC, G1V0A6, Canada.
* Corresponding and presenting author
Tatjana.Stevanovic@sbf.ulaval.ca
[5] Professor, Département de génie chimique, Université Laval, Québec, QC, G1V0A6, Canada.
[6] Principal scientist and group leader, FPInnovations, Québec, QC, G1P 4R4, Canada.
[7] Researcher, SEREX, Amqui, QC, G5J1K3, Canada.
[8] Researcher, CRIQ, Québec, QC, G1P4P3, Canada.

Abstract

An important decrease in demand for the pulp and paper products in the last decade has caused the shift of this industry towards the integration of biorefinery concept into existing mills. The valorization of industrial lignins is one of such solutions. In this research we have explored the application of Kraft lignins in two types of bio-composites based on high density polyethylene (HDPE): one with esterified lignin, coupling agent and HDPE and another with HDPE, lignin or coupling agent and bark fibers (extracted or not). Tensile properties of the produced composites were determined by standard tests. The results of these tests indicated the positive effect of utilization of coupling agents along with lignins on good mixing and homogeneity of HDPE based composites. The production of such composites could contribute to the sequestration of CO_2 on several levels: by replacement of synthetic polymers by renewable lignins and bark fibers and through the process of lignin precipitation from black liquor itself (with CO_2 provided from Kraft pulping plant). The pre-extraction of the bark fiber was determined not to cause any deterioration of tensile properties of the bio-composites containing them, and the integration of extraction step could therefore yield interesting co-products with high added value (pharmaceutical, cosmeceutical, nutraceutical), transforming this process into real biorefinery.

***Keywords*:**
Kraft lignins, esterified lignin, chemical properties, thermal properties, HDPE, composites, bark fibers (extracted or not), tensile properties, sequestration of CO_2.

Introduction

Lignins are renewable and natural polymers the structure of which varies depending on plant origin and process of isolation. They are the most abundant aromatic polymers on earth and second only after cellulose. Lignin content varies from 20% to 35% depending on the plant origin [1]. Lignins are the main components of residual liquors from chemical pulping, notably black liquor from the Kraft process. It is estimated that in Quebec, 130,000 tons of black liquor containing lignin could be used for lignin precipitation annually, without disturbing the mill production [2]. In this investigation, two lignins were precipitated from black liquor obtained from two Quebec pulp and paper mills (*Domtar Windsor* and *Kruger Wayagamack*), following a procedure inspired by LignoBoost protocol, using carbon dioxide to decrease the pH. A comparison of these Kraft lignins with a commercially available Kraft lignin (IndulinAT) was performed. Kraft lignins were modified by esterification in order to improve their compatibility with a polymer matrix (HDPE) and consequently the tensile properties of the bio-composites produced from that materials. In the second application, the use of non-modified and esterified lignins as coupling agent between HDPE and yellow birch (*Betula alleghaniensis*) or black spruce (*Picea mariana*) bark fibers was examined.

Materials and Methods

Materials. Two Kraft black liquors from Quebec pulp and paper industry (*Kruger Wayagamack* and *Domtar Windsor*) were used to precipitate Kraft lignin. A commercial Kraft lignin (IndulinAT) was received from *Westvaco Corporation*. The high density polyethylene (HDPE) from *Exxon Chemicals* used in this study has a melt index of 5 g/10 min [3] and a density of 948 kg/m^3. Maleic anhydride grafted to polyethylene (MAPE) was used as a coupling agent for the manufacture of composites based on polyethylene (PE). The Epolene C-26 (MAPE) used here was gratefully donated by *Westlake Chemicals Corporation*. Yellow birch (*Betula alleghaniensis*) bark splinters were obtained directly after the rosser-head debarker, from the sawmill *Bois Poulin North Inc.*, St-Jacques de Leeds, Quebec, Canada. The bark was air dried at ambient temperature until reaching constant moisture content (9%) and stored adequately. Size separation was carried out by sieving after drying. Fibers of black spruce (*Picea mariana*) bark were obtained by refining at the pilot plant of *FP Innovations* installations in Quebec, QC, Canada. The weight and moisture of this bark were measured (above 5% moisture content) and stored properly.

Precipitation of industrial lignins. Carbon dioxide was used to precipitate lignin by decreasing the pH of black liquor (*Kruger Wayagamack* and *Domtar Windsor*) from the initial pH 13-14 to 8-9 following the procedure inspired by LignoBoost process [4-5]. A purification step consisted of washing lignins with sulfuric acid and distilled water. These precipitation and purification protocols are designed to contribute to greenhouse gas sequestration (CO_2) and sustainable chemistry.

Characterization of lignins. Klason lignin and ash content were analyzed in order to determine the purity of lignin samples [6-7-8-9-10]. The spectral characteristics of lignin

samples were analyzed by Fourier Transform Infrared (ATR-FT-IR/FT-NIR Perkin Elmer Spectrum 400) both for non-modified and esterified lignins. The thermal properties were studied by thermogravimetric analysis (TGA/DTA 851e METTLER TOLEDO), differential scanning calorimetry (DSC 822e METTLER TOLEDO) [11] and thermo-mechanical analysis (TMA/SDTA 640 METTLER TOLEDO).

Esterifications of lignins with butyric anhydride. The commercial Kraft lignin (Indulin AT) was dried in an oven at 80°C overnight. Various amounts of butyric anhydride were added to the reaction system to obtain a desired substitution degree. 1, 4-dioxane and 1-methylimidazole were used as solvent and catalyst, respectively. The reaction was conducted at 60°C for two hours. The product was precipitated by adding distilled water to the solution and then washed with 0.5 M solution of $NaHCO_3$ and distilled water. The esterified lignins were dried at 60°C under reduced pressure overnight.

Esterifications of lignins with stearoyl chloride. Esterification applied acid chloride rather than the anhydride and the reaction time was extended to 5 hours at a temperature of 70°C [12]. By the end of reaction, 100 ml of hexane were added to the system and the precipitated esterified lignin was repeatedly washed with a total of 220 ml of hexane and 220 ml of distilled water. The product was finally dried at 60°C under reduced pressure overnight.

Water extraction of barks. The black spruce bark fibers (obtained from disk-refiners) and the yellow birch bark particles were each extracted with boiling distilled water (30 g oven dry bark with 1L distilled water) for two hours. The objective of extraction was to determine its impact on the properties of the bio-composites. The hypothesis was that the removal of hydrophilic extractives would increase the hydrophobicity of the bark fibers and thus improve their compatibility with hydrophobic polyethylene matrix.

Manufacturing process of bio-composites. Modified, non-modified lignins and bark fibers were previously dried at 80°C overnight. In order to study the effect of esterification on compatibility of lignins with HDPE, a comparison with a commercial coupling agent, polyethylene-graft-maleic anhydride (MAPE), was made. Blends of HDPE with lignin were prepared in various proportions by melt-processing using a twin-screw extruder (Haake TW-100). The temperature was set between 150°C (at the supply) and 165°C (at the output of the extruder) with a screw speed of 40 rpm. The amount of MAPE in the blends was selected to be similar to the lignins content. An internal mixer (Haake Buchler Rheomix) at temperature fixed at 165°C for10 minutes was used to prepare the bio-composites containing black spruce bark fibers (30%) or the yellow birch particles (50%) to prepare the HDPE-lignin bio-composites. All blends were pelletized and compression molded at 160°C for 5 minutes under 3 tons pressure.

Tensile characterization of bio-composites. From the plates produced, dumbbell shaped specimens (type V) were cut following ASTM D-638 [13]. Tensile properties of the bio-composites HDPE - lignins specimens were investigated using an Instron 5565 universal tester without extensometer at room temperature with a crosshead speed was 5 mm/min. For the bio-composites HDPE - coupling agent – barks, an MTS Qtest/5 was used at

regulated temperature and humidity with an extensometer MTS 634.11F-24, with a crosshead speed of 1 mm/min as specified in ASTM D-638 [13]. Young's modulus and yield stress were obtained from the stress-strain curves.

Experimental Results

Characterization of non-modified lignin: Purity of the Kraft lignins (Wayagamack, Windsor and Indulin AT). The purity of Kraft lignins was higher than 96% [10], in agreement the results obtained by El Mansouri (2006 [6], 2007 [7]). Both lignins precipitated (Wayagamack and Windsor) in our laboratory have low ash content (less than 1%). These results suggest that the precipitation and purification protocols were well defined. The commercial Kraft lignin samples, Indulin AT had somewhat higher ash content (above 3%) than the lab precipitated lignins.

Thermal analyses of non-modified lignin: Thermogravimetric analysis (TGA-DTG). The lignin degradation was observed under nitrogen in a large range of temperature (150-700°C). The degradation of Kraft lignins started at temperatures higher than 260°C. At 700°C under nitrogen atmosphere, lignins were not completely decomposed but remain in form of highly condensed char-like structures (27-45% of initial mass). These results confirm the strong reticulation and good thermal properties of Kraft lignin [10].

Thermal analyses of non-modified lignin: Differential scanning calorimetry (DSC) versus thermomechanical analysis (TMA). The melting temperatures (T_m) were determined by DSC and TMA (Fig. 1). The differences between these results reflect the differences of principles of measurements by these two analytical methods. For DSC the measurement principle is calorimetric while it is physical for TMA. The comparable Tm values were obtained for all Kraft lignins.

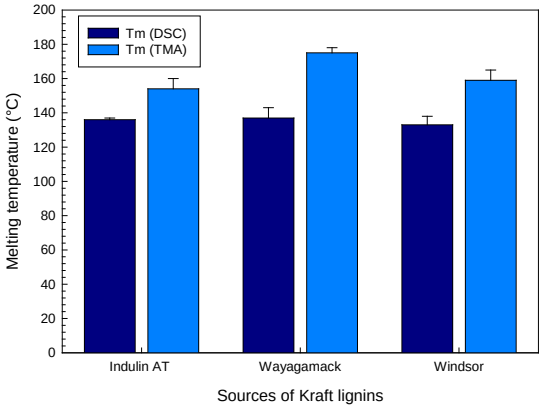

Figure 1: Comparisons of two techniques (DSC versus TMA) used to determining the melting temperature of different sources of Kraft lignins.

Esterification of IndulinAT lignin. The extent of esterification with butyric and stearic anhydride was analyzed by ATR FT-IR spectroscopy. The decrease in O-H stretching bands (3400-3500 cm^{-1}), C-H stretching band (2850-2950 cm^{-1}) and C-O bending band (1030 cm^{-1}) of primary alcohol group and the increase in the bands attributable to ester

groups (absorption at 1730 cm^{-1} assigned to C=O bond in the ester group) were taken as indication of good esterification [13].

Characterization of HDPE-MAPE-lignins blends. The addition of lignins into HDPE had an effect on the increase of the Young's modulus of the composite, while the addition of esterified lignin had slightly less effect on the modulus (Fig. 2). Compared to HDPE alone, the addition of esterified lignin did not seem to be beneficial to tensile strength properties. The tensile strength increased however significantly with the addition of 6 wt% MAPE, especially high tensile strength being determined for the composite containing 40% Lignin – 6% MAPE – 54% HDPE which is now comparable to that of neat HDPE. Luo et al. (2009, [14]) have already observed a high increase in tensile strength with MAPE addition. These results showed that lignin compatibility with HDPE was improved by MAPE addition.

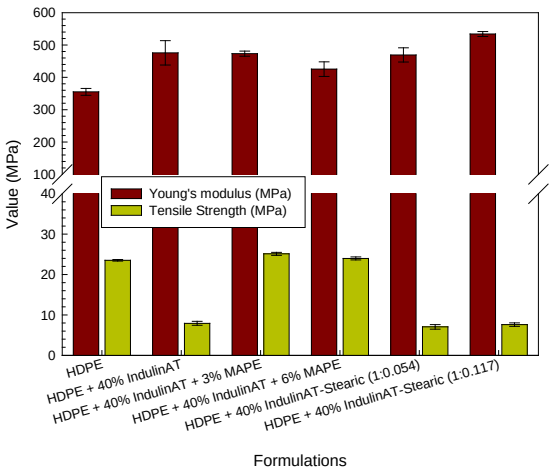

Figure 2: Tensile properties of lignin based composites (Young's modulus calculated without extensometer [crosshead], gage length of 7.62mm [13]).

Characterization of blends HDPE-coupling agent-bark fibers: Bio-composite made by black spruce fibers bark (~30%) with different refining conditions, HDPE (~70%) and coupling agents (~5% w/w of barks). No significant differences of mechanical properties were observed for bio-composites made with black spruce bark fibers from four different refining conditions (GreenBark, rotation rate = 2200rpm, time =10.1min, p=12Bar, distance between discs= 3.5mm; PreExtracted Bark; rotation rate = 2200rpm, 13,5 min, 12Bar, 0.1mm; 12Bar = dry bark, 2200rpm, time- 13.5min, p= 12 Bar, distance between discs =0.5mm; 8Bar = dry bark, 2200rpm, 13.5min, 8Bar, 0.1mm) (Fig. 3a). Two refining conditions parameters seemed however to be slightly more favorable (8 Bar and green bark conditions). The bark extraction that carried out for 2 hours in boiling water had no significant effect on the tensile properties (Fig. 3b). This observation allows us to envisage the use of extracts of bark for other applications with added value. Three options have been considered for improving composite properties by using the coupling agent versus, without (without coupling agent), lignin indulinAT and MAPE (Fig. 3c). The MAPE could improve the bio-composite properties as observed by Yemele et al 2009 [15], but unmodified lignin indulinAT was not an effective coupling

agent. The Young's modulus calculated from the extensometer (gage length 12.5 mm corresponds to the dimension of extensometer]) is systematically higher than that calculated from the crosshead movement (gage length 24.5 mm equal to the distance between grips [13]), but the tendencies are similar. This difference can be explained by the fact that the crosshead integrates the phenomena of slip in the grips and other mechanical noise associated to this test. With the extensometer, the strain measured solely from the area solicited by the tensile test is without errors implicated in the previous technique. The accuracy and sensitivity of the extensometer is designed to gather the intrinsic value of the test material.

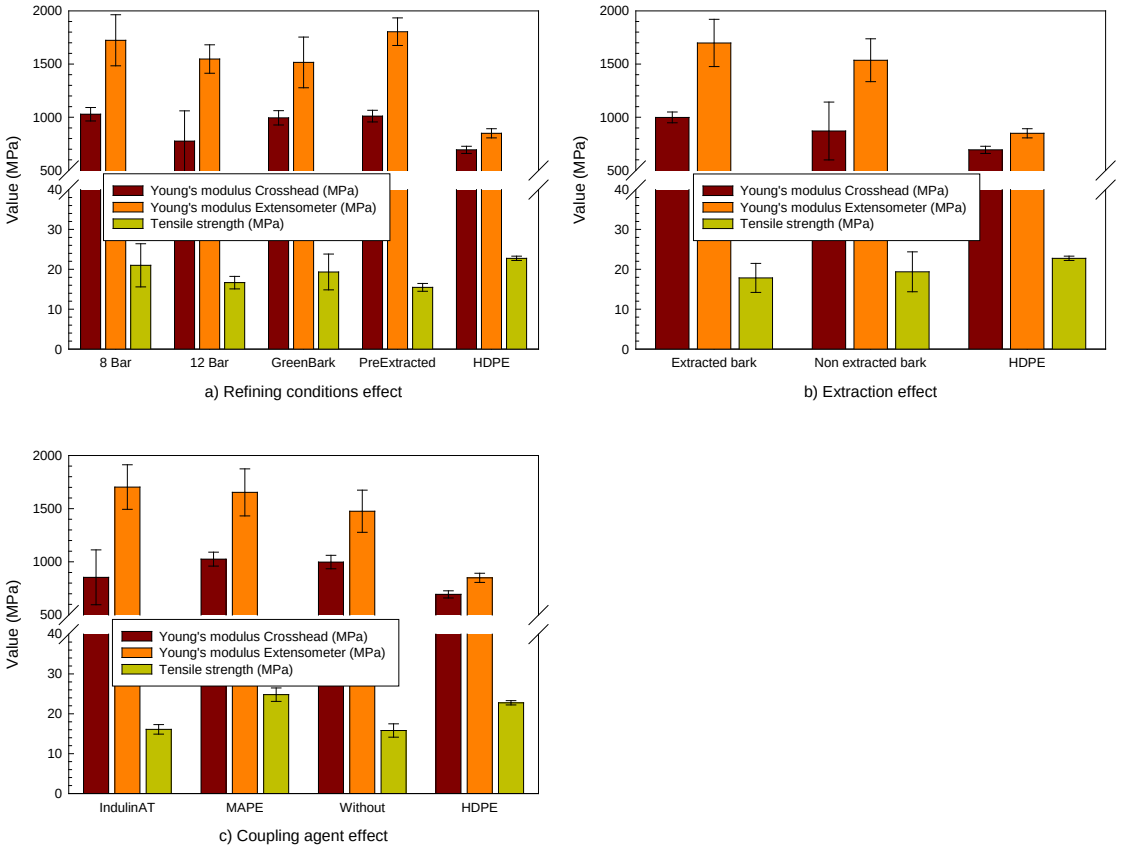

Figure 3: Analysis of simple effects on bio-composites for black spruce bark fibers; a) refining conditions effect, b) extraction effect, c) coupling agent effect.

Characterization of blends HDPE-coupling agent-bark fibers: Black spruce barks fibers (~30%) versus yellow birch bark particles (~30%) with HDPE (~70%) and coupling agents (5% w/w of barks). Better composites properties have been determined for composites containing black spruce bark than for those with yellow birch bark particles (Fig. 4). The addition of the non-modified indulinAT, or of IndulinAT esterified with butyric anhydride or stearoyl chloride did not bring any improvements of the bio-composites properties. The properties of the bio-composites containing MAPE have, however, been determined to be significantly improved [15]. Young's modulus calculated from the extensometer is higher than the crosshead. An estimate of measurement errors

associated to both techniques (crosshead versus extensometer) will be carried out in future work.

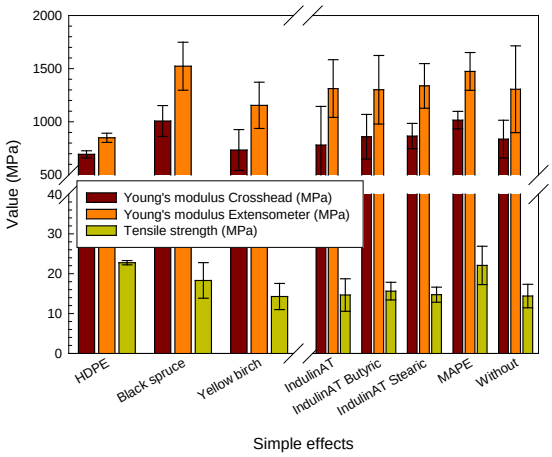

Figure 4: Analysis of simple effects; left: the species bark effect; right: different coupling agent effect.

Characterization of blends HDPE-coupling agent-bark fibers: Bio-composite made with yellow birch barks particles (~50%) with HDPE (~50%) and coupling agents (~5% w/w barks). The influence of particle sizes of yellow birch bark on the composite properties were measured and there was no significant difference, so the results are not presented here Two extrusion temperatures were analyzed and there were not to be significant impact on the tensile properties (and other measured properties, not shown here). As observed for black spruce, the extracted bark had no significant effect on the tensile properties (Fig. 5a). As compared to the non-extracted bark, allowing the potential use of extractives for other value added products. IndulinAT lignin was demonstrated to be inefficient as coupling agent, since the properties of the composite based on HDPE and bark fibers did not improve upon its addition (Fig. 5b). Contrary to the observation by Sewda and Maiti (2007 [16]), we observed an improvement of the modulus with addition of bark but a decrease of tensile for these composites. MAPE was determined to be a good coupling agent for this type of material [15].

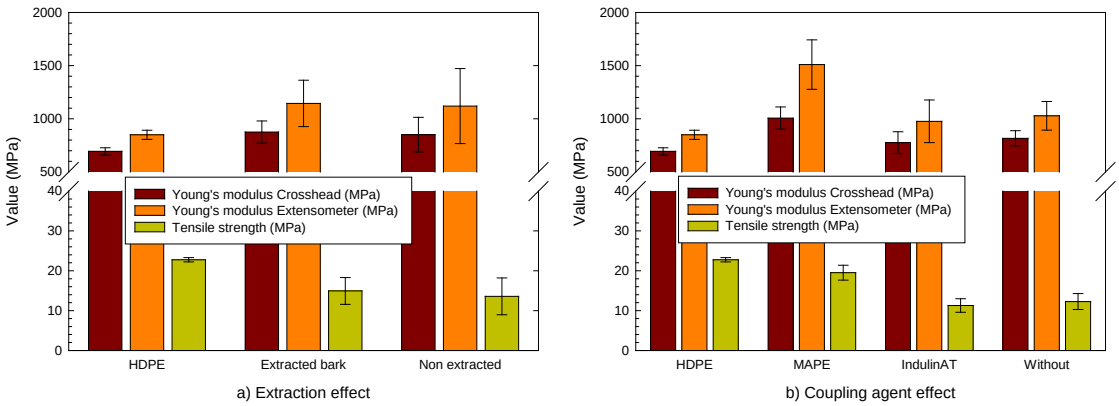

Figure 5: Analysis of simple effects on bio-composites for yellow birch bark particles; a) extraction effect, b) coupling agent effect.

Conclusion

Two Kraft lignins have been precipitated by carbon dioxide from the black liquor provided by Domtar–Windsor and Kruger-Wayagamack pulp and paper mills in Quebec. The purification protocol was confirmed by their high purity and low ash contents. Esterification reactions were performed on IndulinAT with butyric anhydride and stearoyl chloride to improve lignin compatibility with HDPE but proved to be insufficient. Stearate lignin was incorporated into HDPE matrix by melt blending. However, the tensile properties of blends were not improved by incorporation of esterified lignins only, but were possible with the standard compatibilizer (MAPE).
For blends produced with HDPE –Indulin AT lignin (esterified with butyric anhydride or or stearoyl chloride and non-modified) no improvements of mechanical properties of the composites have been observed, which indicated that lignins esterified as mentioned were inefficient as coupling agents. The commercial coupling agent, MAPE, was however determined to be a good compatibilizer for this kind of material. The composites made with black spruce bark fibers have been determined to have superior properties to those determined for the composites produced with yellow birch bark particles. The water extraction of the bark fibers prior to their incorporation was determined not to have significant impact on the tensile properties of the bio-composites produced with them. The pre-extraction of the bark fibers was determined not to cause any deterioration of tensile properties of the bio-composites containing them.
Therefore the integration of extraction step could yield interesting co-products with high added value (pharmaceutical, cosmeceutical, nutraceutical), completing thus the biorefinery concept studied here. Other acid anhydrides will be tested for lignin esterification, the cyclic anhydrides, maleic and succinic, in order to examine thus modified lignins as coupling agents in manufacturing the HDPE-bark fibers blends and their properties.

Acknowledgments

The authors are grateful to the *Fonds Québécois de la Recherche sur la Nature et les Technologies* (FQRNT) for financial support, *Kruger-Wayagamack* and *Domtar-Windsor* for black liquors and *FPInnovations* and *Les bois Poulin Inc* for bark fibers supply. David Lagueux, Flavien Mattesi, Yann Giroux, and Yves Bédard are gratefully acknowledged for their technical support.

References

[1] Stevanovic, T. and Perrin, D. 2009. La chimie du bois, Presse Polytech. Universitaire et Romande, pp 145-177.
[2] FP Innovations, Ressource Naturelle et faune du Québec, (2009) Guide de développement Le bioraffinage forestiers : possibilités pour les entreprises Québécoise de pâte et papier.
[3] ASTM Standard "D 1238 Standard Test Method for Melt Flow Rates of Thermoplastics by Extrusion Plastometer." 1-15.

[4] Öhman, F., Theliander, H., Tomani, P. and Axegard, P. 2006. Method for separating lignin from black liquor, Patent, Application publication, Stfipackforsk ab, Stockholm, Pub n° WO 2006/031175 A1, (March, 23rd, 2006).

[5] Öhman, F. and Theliander, H. 2007. Filtration properties of lignin precipitated from black liquor, TAPPI J., Vol 6, N°7 (July, 2007) pp 3-9.

[6] El Mansouri, N.-E. and Salvadó, J. 2006. "Structural characterization of technical lignins for the production of adhesives: Application to lignosulfonate, kraft, soda-anthraquinone, organosolv and ethanol process lignins." Industrial Crops and Products 24(1): 8-16.

[7] El Mansouri, N.-E. and Salvadó, J. 2007. "Analytical methods for determining functional groups in various technical lignins." Industrial Crops and Products 26(2): 116-124.

[8] ASTM Standard "D 1102: Standard Test Method for Ash in Wood" 1-2.

[9] Faix O. 1992. Chap 4.1 Fourier Transform Infrared spectroscopy, in Methods in Lignin Chemistry by Lin, Y. S. and Dence, C. W., Springer Verlag, pp 83-121.

[10] Stevanovic, T., Rodrigue, D., Diouf P., Schorr, D. and Hu L. 2012. "Characterization of modified and non-modified industrial lignins for biocomposites production." Conference presented at the *66th international convention of the Forest Products Society* Washington, DC, United States, 3 to 5 June 2012.

[11] ASTM Standard "D 3418 Standard Test Method for Transition Temperatures of Polymers by Differential Scanning Calorimetry." 1-7.

[12] Adamopoulos, L. 2006. Understanding the Formation of Sugar Fatty Acid Esters. Master thesis, North Carolina State University, pp 34

[13] ASTM Standard. "D 638 Standard Test Method for Tensile Properties of Plastics." 1-15.

[14] Luo, F., Ning, N. Y., Chen, L., Su, R., Cao, J., Zhang, Q., Fu, Q. 2009. Effects of compatibilizers on the mechanical properties of low density polyethylene/lignin blends, Chinese J. Polym. Sci., Vol 6: 833-842.

[15] Yemele, M. C. N., Koubaa, A., Cloutier, A., Souounganga P. and Wolcott, M. 2010. "Effect of bark fiber content and size on the mechanical properties of bark/HDPE composites." Composites Part A: Applied Science and Manufacturing 41(1): 131-137.

[16] Sewda, K. et Maiti, S. N. 2007. "Mechanical properties of HDPE/bark flour composites." Journal of Applied Polymer Science 105(5): 2598-2604.

Porous Woodceramics Prepared form Liquefied Corncob and Poplar Powder

Sun Delin
Professor
Liu Wenjin
Professor
College of Furniture and Art Design, Central South University of Forestry and Technology, ChangSha, Hunan, P. R. China;
Yu Xianchun
Associate professor
Basis Department, Yue Yang Vocational & Technical College, YueYang, Hunan, P. R. China

Abstract. A porous woodceramics makes from liquefied corncob and poplar powder, its basic property closely connects with the carbonization temperature and liquefied corncob content. Thermo gravimetric analysis shows that higher liquefied corncob content has benefit to decrease the weight loss. Scanning electron microscopy observation indicates that the porous structure presents three-dimensional network, its pores range from 5 to 20 *u*m which partly keep the native characteristics of the wood suggesting poplar powder is as a natural plant template. The apparent density increases as carbonization temperature before about 1100°C, and then decreases as temperature rises further, whereas the apparent porosity increases continuous; bending strength increases from 8.3 MPa to 13.8 MPa when the liquefied corncob content raises 50%-150%. Meanwhile, the fraction coefficient of the sample obtained at 800 °C is almost 1.8 times of the sample at 1700 °C.

Key words: Porous woodceramics, basic property, liquefied corncob, poplar powder.

1 Introduction

Woodceramics is a new porous carbonic material which can partly keep the microstructure of biomaterial (Hirose et al. 2002). It has a lot of advantages, such as low weight, high specific strength, excellent thermal stability and good friction properties, its application prospect is becoming widely (Kano et al. 1997; Izuka et al. 1999; Suda et al. 1999; Sun et al. 2009). At present, the typical method of making woodceramics is to impregnate wooden material with phenol-formaldehyde (or epoxy) resin and then carbonize at high temperature (Li and Li 2006; Qian et al. 2004a), which consumes a lots of industrial chemicals.

Corncob is agriculture residue, a lot of corncobs are discarded in the field or as fuel in north China, this not only pollute the environment, but also waste biomass resources. Currently, there is no report about the preparation of woodceramics from liquified corncob. Liquefaction corncob (LC) is used to instead phenol-formaldehyde resin and poplar powder is as biomaterials to prepare woodceramics in this study. The preparation, thermo gravimetric analysis (TGA), microstructure characterization, and mechanical property have discussed in the following sections.

2 Materials and Methods

2.1 Material Preparation

Discarded corncob is dried at 5% moisture content and smashed into granules of 0.5 mm, the LC is obtained while 1 parts of phenol is mixed with 2 part of the corncob powder and suitable water which stir at 140 °C for 2 hours while the 98% sulfuric acid is as catalyst. Different rates of poplar power is mixed with the liquefied material and stir for 3 hours, after the mixture is dried at 70 °C for 24 hours, it is hot-pressed into corncob composites under the pressure of 8 MPa at temperature of 160 °C for 8 min. Finally, the composites are put into a high temperature sintering furnace to carbonize according the method described in the reference (Sun et al. 2010), the porous woodceramics is obtained.

2.2 Characterization

A thermo gravimetric analyzer (TGA, PerkinElmer Pryis6, USA) is employed to record and analyze the weight loss of woodceramics, and the morphology is investigated by scanning electron microscopy (SEM, JSM-35C, Japan) operated at 20 kV and 20 mA. Archimedes' measurements and a density tester (MDMDY-300, China) are employed to tested the apparent density and apparent porosity. The bending and compressive strength are measured with mechanical testing machine (Instron 8802, USA) according with SENB method, and wear-resisting property is tested with a friction testing machine (UMT-3, USA).

3 Results and Discussion

3.1 Thermo Gravimetric Analysis

During carbonization process, poplar powder is transformed into amorphous carbon, whereas LC becomes a glassy carbon (Akagaki et al. 1999). The TGA curve can describe the weight loss processing of organics effectively (Hirose et al. 2002). Figure 1 shows the TGA curves of

three sample with different LC content. Before 100 °C, it is dry stage, free water in the composite is evaporated and the curves are very similar. 100 °C to 300 °C is slowly thermolysis stage, cellulose, hemicellulose, lignin and LC begin to dehydrate and decompose, pyrolysis gases such as H_2O, CH_4, H_2, CO, CO_2, et al begin to escape. The TGA curves present difference due to the different LC conents. During the stage of 300 °C to 550 °C, fiere thermal pyrolysis take place, C-O and C-C bond in the wood and LC are broken as well as the condensation reaction continue to occur between hydroxy and methylene, and to form aromatic ring structure (Rhim et al. 2010). Meanwhile, there are a lots of pyrolysis gases escepe, which lead to reduce the weight greater and leave pores. So, the weight loss yield is large in this stage, moreover, the lower LC content sample presents larger value. After 550 °C, the fiercest thermolysis almost end, but the remainder hydrogen is deprived continuous untill to form stable structure.

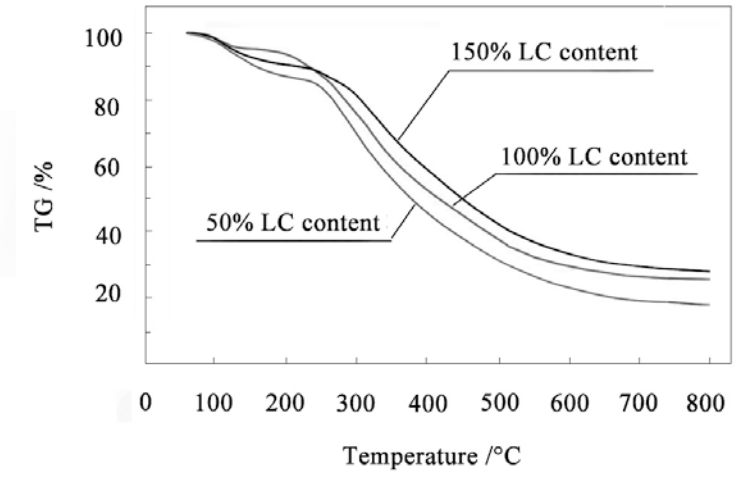

Figure 1 Thermo gravimetric curve

Compare with the three TAG curves in Figure 1, the TG value is 53.6% at 400 °C of the sample which has 150% LC content, but other one is 29.4% which only has 50% LC content, this suggest the LC content has benefit to increase carbon yield.

3.2 Pore structure

SEM can observe the microstructure of woodceramics (Treusch O et al. 2004). Figure 2a shows the micrograph which obtain at LC content of 50% and carbon temperature of 1 100 °C, a lots of pores and cracks with regular and irregular shapes are found in this material with sizes ranging from 5 μm to 20 μm. The micropores structure can observe clearly in the enlarged micrograph, which partly keep poplar's structure obviously, suggesting poplar is as a natural plant template and the characteristic biological of wood can be inherited.

Figure 2b is the micrograph of woodceramics with 150% LC content, the surface is covered with glassy carbon and present translucency state with specially gloss, suggesting more LC content has more glassy carbon.

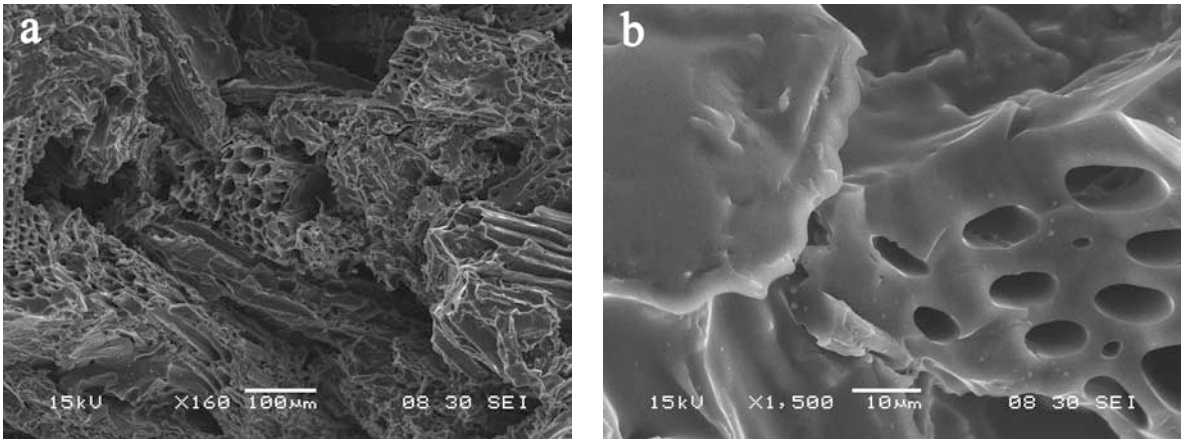

Figure 2 Microstructure of woodceramics

3.3 Apparent porosity and apparent density

Apparent density and apparent porosity are the important parameters of woodceramics (Zhao et al 2002), it closely connect with carbonization temperature and LC content. The relationship between carbonization temperature, LC content and apparent density are showing in Figur 3: as carbonization temperature increases from 500 °C to 1 700 °C, apparent porosity rises quickly at first, and decreases over 1 100 °C, but the tendences become slowly as the temperature gets higher. This probably because of the pyrolysis gases release as wood powder and LC are pyrolysed in the initial stage, and the gasification and contraction of carbon increase at higher temperature. It can also find in Fig.3 that morer LC content, higher apparent density.

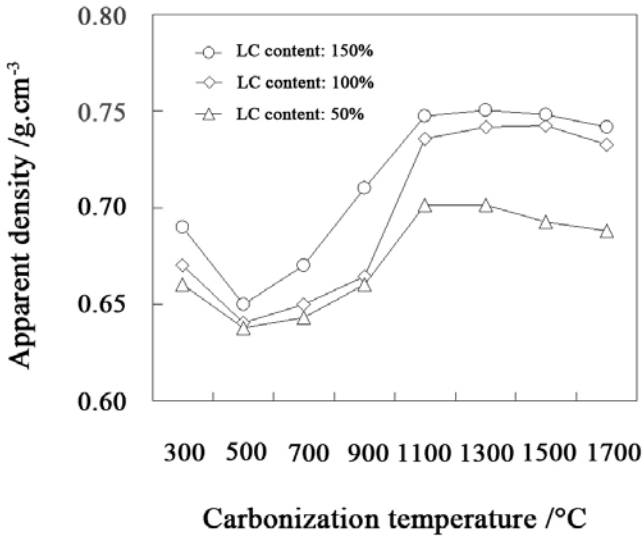

Figure 3 Effects of carbonization temperature on apparent density

Figure 4 shows the effects of carbonization temperature and LC content on the apparent porosity: higher carbonization temperature results in highter apparent porosity since the pyrolysis gases release and gasification increases in this stage. But higher LC content sample has lower apparent porosity for there are more aromatic ring in LC leading to high carbon yield.

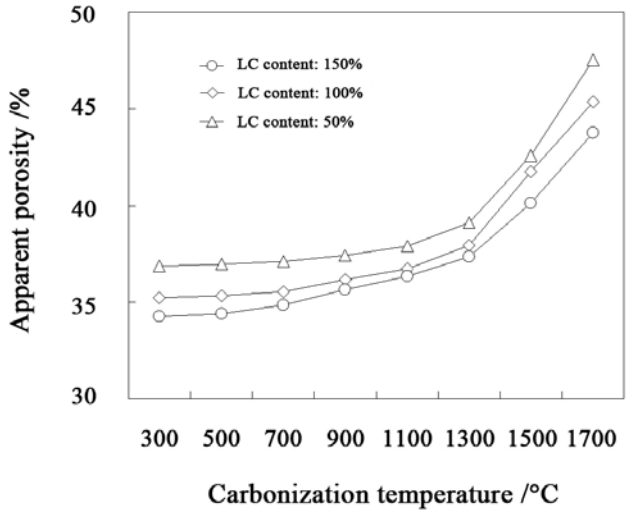

Figure 4 Effects of carbonization temperature on apparent porosity

3.5 Bending and wear-resisting property

Bending strength with different LC content of woodceramics at different carbonization temperature shows in Figure 5. Bending strength increases rapidly as the temperature and LC content increase, but decreases at high temperature. It seems to be only at 8.3 MPa when the LC content is 50%, but increases quickly to 13.8 MPa as LC content become 150% at the temperature of 1 100 °C, suggesting the LC has great benefit to improve bending strength, which correspond with the changes of apparent density.

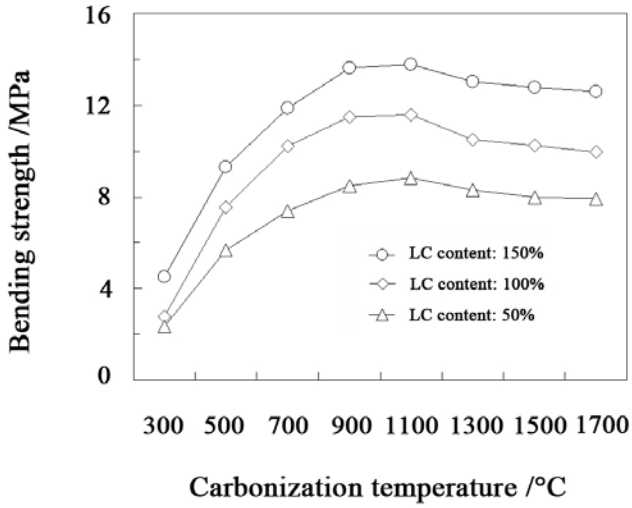

Figure 5 Relationship between carbonization temperature and bending strength

This can explain that glassy carbon has a higher strength than amorphous carbon (Qian et al. 2004b). Higher LC content lead to more glassy carbon, which can elevate woodceramics' density, reduce porosity, and enhance mechanical strength. Meanwhile, the higher carbonization temperature can promote glassy carbon and amorphous carbon to fuse and join tighter together. Along with the elevation of carbonization temperture, a three dimensional network structure has formed, and the strength has been improved. But the gasification of

woodceramics increases also at higher temperature, which increases porosity and decreases density, as a result, the mechanical strength declines.

Figure 6 shows the abrasion loss of woodceramics obtained at different carbonization temperature. About sample of LC content of 150%, its abrasion loss decreases from 0.0075 g to 0.0043 g as the temperature increases from 500 °C to 1 100 °C, presents sharply down tendency, and almost reaches the lowest value (about 0.004 g), and then, the down tendency becomes slowly.

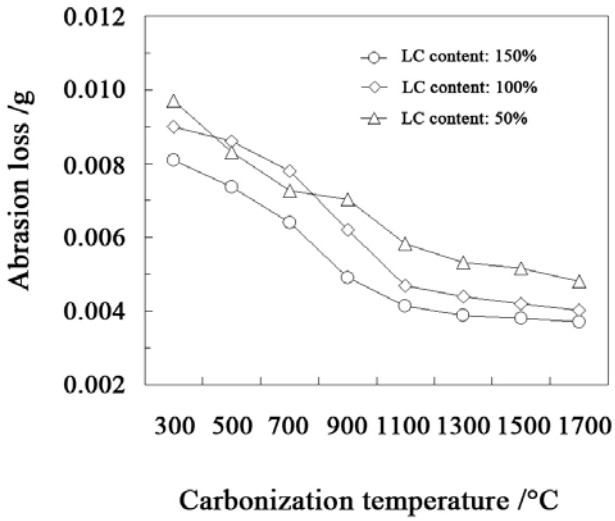

Figure 6 Effect of carbonization temperature on the abrasion loss

This is because, on the one hand, the dehydrogenation, deoxidization and the condensation aromatic polynuclear structure almost finish and form complete ring-like carbon structure until the temperature reaches about 800 °C (Li and Li 2006; Kim et al 2004). On the other hand, higher temperature can lead to increase the compactness and the graphitization degree (Zhang et al. 2008) (although woodceramics cann't graphitization completely), which is a good lubricant and has self-lubricating. In addition, the pore of woodceramics obtained in the higher temperature is more developed due to the gasification, that is mean more pores can keep more abrasive dust on the friction surface, in other word, the amount of lubricant has increased, hence, the abrasion loss reduces.

But higher temperature leads to increase the pores and cracks, and decrease the apparent density, which has harmful to the strength and increase the abrasion loss. Thus, the wear-resisting property can adjust with the appropriate carbonization temperature and LC content.

Figure 7 shows the relationship between carbonization temperature and friction factor, the average value of friction factor is 0.23 as the carbonization temperature is 800 °C, but it decreases to 0.13 when the temperature rises to 1 700 °C, it is almost 1.7 times. That is because that the graphitization degree of woodceramics obtained at lower temperature is lower, the amount of graphite microcrystalline is less, the pore structure is underdevelopment and the carbon structure is imperfect, but this have greatly improved at higher temperature, so the friction and friction factor decrease rapidly.

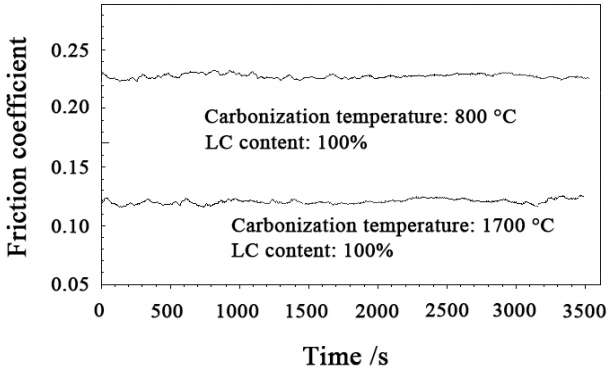

Figure 7 Relationship between carbonization temperature and friction factor

4 Conclusions

Porous woodceramics prepared from LC and polpar powder can partly keeps the biological structures of wood. Carbonization temperature and LC content act an important role, and the basic property of this materials can improve with it. Along with the carbonization temperature elevate, the apparent density, porosity, compress and bending strength increase about before 1 100°C, and then slowly decrease as the temperature rise, as well as the apparent porosity still shows the increasing tendence. But the wera-resisting and friction factor present continuous reducing as temperature and LC content rise. Higher LC content lead to morer glassy carbon which can enhance the mechanical property.

Acknowledgements

The authors wish to acknowledge the fund of Hunan Provincial Education Department (No. 10c1329) and Introduction of Talent Foundation of Central South University of Forestry and Technology (No. 104-0109).

References

Akagaki, T., Hokkirigawa, K., Okabe, T., Saito, K. 1999. Friction and wear of woodceramics under oil and water lubricated sliding contacts. Journal of Porous Materials. 6(3): 197-204.
Hirose T., Fan T.X., Okabe T., Yoshimura M. 2002. Effect of carbonizing speed on the property changes of woodceramics impregnated with liquefacient wood. Materials Letters 52: 229-233.
Izuka, H., Fushitani, M., Okabe, T. 1999. Mechanical Properties of Woodceramics: A Porous Carbon Material. Journal of Porous Materials. 6(3): 175-184.
Kano, M., Momota, M., Okabe, T., Saito, K. 1997. Specific heat capacity of new porous carbon materials: woodceramics. Thermochim Acta. 292: 175-177.
Kim, Y.J., Kim, M.L., Yun, C.H., Ji, Y.C, Chong R.P., Michio I. 2004. Comparative study of carbon dioxide and nitrogen atmospheric effects on the chemical structure changes during pyrolysis of phenol-formaldehyde spheres. Journal of Colloid and Interface Science. 274(2): 555-562.
Li, J., Li, S.J. 2006. Pyrolysis of medium density fiberboard impregnated with phenol-formaldehyde resin. Journal of Wood Science. 52(4): 331-336.
Qian, J.M., Jin, Z.H., Wang, J.P. 2004a. Structure and basic properties of woodceramics made

from phenolic resin–basswood powder composite. Mater. Sci. Eng. 368(1-2): 71-79.
Qian, J.M., Jin, Z.H., Wang, J.P. 2004b. Study on structural changes during preparing wood-ceramics from phenolics resin/basswood powder composite. Acta Material composite Sinica. 21(4): 18-23.
Rhim, Y.R., Zhang, D., Rooney, M., Nagle, D.C., Fairbrother, D.H., Herman, C., Drewry III, D.G. 2010. Changes in the thermophysical properties of microcrystalline cellulose as function of carbonization temperature. Carbon 48(1): 31-40.
Suda, T., Kondo, N., Okabe, T., Saito, K. 1999. Electrical properties of woodceramics. Journal of Porous Materials. 6(3): 255-258.
Sun, D.L, Yu, X.C., Liu, W.J., Sun, D.B, Liu, D.T. 2009. Effects of sintering conditions on microstructure changes of wood-ceramics impregnated with low-molecular phenol-formaldehyde resin. Wood and Fiber Science. 41(4): 433–439.
Sun, D.L., Yu ,X.C., Liu, W.J., Sun, D.B. 2010. Laminated wood–ceramics prepared from beech veneer and phenol formaldehyde resin. Wood and Fiber Science. 42(4): 474-479.
Treusch, O., Hofenauer, A. , Tröger, F., Fromm, J., Wegener, G. 2004. Basic properties of specific wood-based materials carbonised in a nitrogen atmosphere. Wood Science and Technology. 38(5): 323-333.
Zhang, L.B, Li, W., Peng, J.H., Li, N., Pu J.Z., Zhang, S.M, Guo, S.H. 2008. Raman spectroscopic investigation of the woodceramics derived from carbonized tobacco stems/phenolic resin composite. Material and Design 29(1): 2066-2071.
Zhao, B.Y., Hirose, T., Okabe, T., Zhang, D., Fan, T.X., Hu, K.A. 2002. Woodceramics prepared from wood powder/phenolated wood composite. Journal of Porous Materials. 9(3): 195-201.

Selective Separation and Recovery of the Lignin from Lignocellulosic Biomass Using Ionic Liquid

Yong-Chang Sun[1], Ji-Kun Xu[1], Bo Wang[1], Feng Xu[1,], Run-Cang Sun[1,2]*

[1] Institute of Biomass Chemistry and Technology, Beijing Forestry University, Beijing 100083, China

* Corresponding author: xfx315@bjfu.edu.cn (F. Xu)

[2] State Key Laboratory of Pulp and Paper Engineering, South China University of Technology, Guangzhou 510640, China

Abstract

Lignocellulosic biomass represents a potentially key and sustainable source for transformation into biofuels and other commodity chemicals. However, efficient means of separating and depolymerising the hard components are required. The use of ionic liquids (ILs) in biomass pretreatment has attracted significant attention as promising green solvents for its effectiveness at decreasing biomass recalcitrance. In this study, an efficient pretreatment method using the low-cost IL 1-butyl-3-methylimidazolium acesulfamate [BMIM]Ace and organic solvents for the extraction of lignin and recovery of carbohydrate-enriched materials (CEMs) from Eucalyptus. The lignin was recovered from the IL by precipitation with acetone, allowing the IL to be recycled. The results showed a synergy effect with exceeding 89.6% of the CEMs recovery and 14.1% of the lignin obtained. It was found that the presence of some organic solvents have affected the extraction efficiency, probably due to the difference of dielectric constants of the organic solvents. The regenerated ionic liquid showed good retention of structure and properties. The purity of the lignin fractions were characterized by high-performance anion exchange chromatography (HPAEC). Moreover, the lignin fractions were characterized with Fourier transform infrared (FT-IR). The recovered CEMs can be serving as a valuable source for enzymatic saccharification. These results indicates a potential approach in further optimization of the choice of low-cost ILs and organic solvents systems for the efficient utilization of the lignocellulosic biomass, and all constituents can be fully recovered and further processed.

Keywords: Lignocellulosic biomass; Lignin; Ionic liquid; Organic solvents; Extraction

Introduction

The depletion of the world's petroleum supply and environmental issues associated with crude oil usage increase a demand for developing alternative, environmental friendly, and non-petroleum dependent energy sources [1]. An alternative and sustainable source for chemicals, materials, and fuels is lignocellulosic biomass. However, the structure of the lignocellulosic biomass is very complex; the rigid structure makes it highly resistant to biological and chemical degradation [2]. Lignocellulosic biomass consists mainly of cellulose (35-50%), hemicelluloses (20-35%), and lignin (5-30%) [3]. Cellulose is a linear polymer of β-1,4-linked D-glucopyranose monomers, and there are large amount of intra- and inter molecular hydrogen bonds in the cell walls [4]. However, cellulose is traditionally material used as a raw material for the production of paper, paperboard, fiberboard, and other similar products. Hemicelluloses are consisted of different five or six sugars, which can be further produced of xylitol and furfural. Hemicelluloses can also be hydrolyzed and used for fermentation, but the usage is more complicated due to the fact that xylose, which is the dominating monosaccharide released, is difficult to ferment [5]. Lignin is a stubborn polymer, which formed covalent bond with hemicelluloses. Lignin is a three dimensional network, and the complex structure is difficult for chemicals and microbial attack. All these factors make lignocellulosic biomass usage limitation. Recently, ionic liquid (IL) has received growing interest as green solvents for lignocellulosic biomass pretreatment [6]. IL is salts that melting point blow 100°C, and can be design for different cation and anion. It has several advantages, such as neligible volatility, wide liquid range, and relatively high thermal stability as well as ability to solubilize organic, inorganic, or polymeric substances [7,8] In this paper, the ball-milled wood was dissolved in a new IL named 1-butyl-3-methylimidazolium acesulfamate [BMIM]Ace to extract lignin. Organic solvents were firstly added in this IL solution. The lignin obtained was characterized by high-performance anion exchange chromatography (HPAEC) and Fourier transform infrared (FT-IR).

Methods

Materials and Reagents. Eucalyptus was received from Guangdong province, China, Leaves and bark were removed, and the stems were chipped into small pieces (1-3 cm). After drying at 60°C for 16 h in an oven, the chips were ground using a mortar and sieved through a 40-60 mm mesh. The sawdust was milled for 3 h. The content of acid-insoluble lignin was 30.1% according the procedure of the National Renewable Energy Laboratory (NREL/TP-510-42618, TP-510-42622). The ionic liquid [BMIM]Ace was synthesized according to the literature [9]. The chemicals used were of analytical or reagent grade.

Wood Dissolution and Regeneration. 2.0 g of ground wood was added to 30 g of [Bmim]Ace, and 10mL of DMSO, dimethylacetamide (DMAc), dioxane, and methanol were added in the mixture, respectively. The mixture was mechanically stirred at 120°C for 3 h in an oil bath in open atmosphere. After that, the wood was regenerated in hot water, and the solution was added into acetone to precipitate lignin after remove water. Lignin was separated

by filtration. The acetone was evaporated for the recycle use of IL.

Sugar Analysis. The sugar content of the lignin fractions were detected by high-performance anion exchange chromatography (HPAEC). A 4-6 mg sample was hydrolyzed with 1.475 mL of 10% H_2SO_4 for 2.5 h at 105°C. The mixture was filtered and diluted. The sample was injected into the HPAEC system. L-arebinose, D-glucose, D-xylose, D-rhamnose, D-mannose, D-galactose, uronic acids were detected. All experiments were performed at least in duplicate, and the average values calculated for all of the lignin fractions.

FT-IR Analysis. The Fourier-transform infra-red (FT-IR) spectra of the samples were recorded using a Thermo Scientific Nicolet iN10-MX FT-IR chemical imaging microscope (Thermo Scientific, America) fitted with a narrow-band liquid nitrogen cooled MCT detector. Spectra were recorded with 64 scans at a resolution of 4 cm^{-1} between the wave numbers of 4000 and 700 cm^{-1}.

Results and Discussion

Yield of Lignin. The yield of the lignin was showed in Table 1. Interestingly, different organic solvents resulted in different yields. The dioxane + IL mixture released a higher content of lignin (14.1%), while the methanol + IL mixture yield 3.0% of lignin. The neat IL extraction resulted in 11.5% of lignin released. The results indicated that some organic solvents such as dioxane can increase the lignin extraction efficiency, while DMSO, DMAc, and methanol will decrease it. This results probably due to the difference of dielectric constants of the organic solvents [10]. Meanwhile, adding of organic solvents is that the anions become more delocalized and the strength of the interaction with lignin decreases with increasing the polarity parameter.

Tbale 1. Yield of lignin (% Klason lignin) released in different solvents systems.

Solvent	DMSO+IL	DMAc+IL	Dioxane+IL	Methanol+IL	Neat IL
Yield[a] (%)	8.6	11.8	14.1	3.0	11.5

[a] The yield was based on the Klason lignin

Purity Analysis. To characterize composition of the IL/IL+ organic solvents systems, the five lignin preparations were prepared for determination of their carbohydrate content, and the results are given in Fig. 1. As can be seen, all lignin fractions contained different amount of sugars. The total content of sugars detected in the lignin fractions were in the order of the extraction systems of methanol+IL>dioxane+IL>neat IL>DMSO+IL>DMAc+IL, indicating that IL+methanol mixture result in a high content of carbohydrate loss. The DMAc +IL system has a weak effect on the hemicelluloses moiety in the wood cell. Glucose and xylose were the mainly sugars detected in the five lignin fractions. Moreover, we should note that neat IL extraction released more xylose (7.6%) than glucose (2.8%). Therefore, the results suggest that the hemicellulosic polymers in the cell walls might be degraded during the treatments with different organic solvents combined with IL under the conditions given.

FT-IR Analysis. To identify the isolated extracts as lignin, the IR spectra of the five extracts obtained were analyzed (Fig. 2). As can be see from the spectra, all the five spectra have typical bands at 1572, 1509, and 1431 cm^{-1}, corresponding to aromatic skeletal vibrations. The band at 2961, 2874, and 1462 cm^{-1} arise from the C-H stretching and asymmertric vibrations of CH_3 and CH_2, respectively [11]. The wide absorption band at 3395 cm^{-1} originated from the O-H stretching vibration in aromatic and aliphatic OH groups. However, the bands at 1648 and1738 cm^{-1} are assigned to the presence of conjugated and nonconjugated carbonyl groups in the lignin structure. The ILL (extracted with neat IL) spectra has a strong absorption band at 1738 cm^{-1}, indicating that more C=O groups present in the lignin fraction, adding organic solvents in IL could decrease the C=O group. Syringyl and condensed guaiacyl absorptions are obviously observed at 1313 cm^{-1}, whereas guaiacyl ring breathing with C=O stretching appears at 1265 cm^{-1}. The absorption at 1055 cm^{-1} is owing to the C-H in-plane deformation. In addition, aromatic C-H out of plane bending appears at 938 and 853 cm^{-1}.

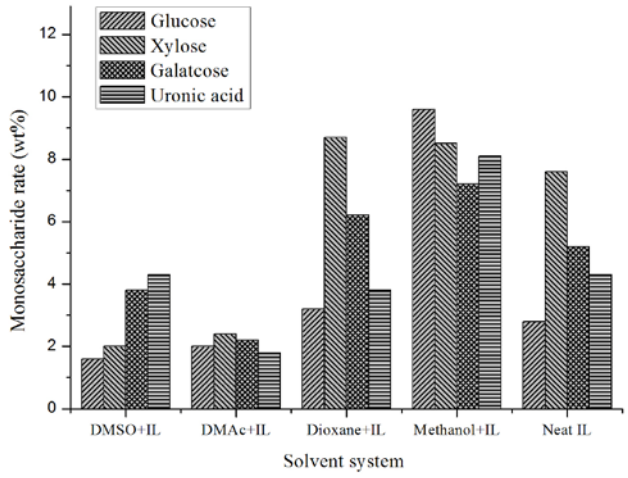

Fig. 1. The monosaccharide rare (wt%) of the different extraction systems.

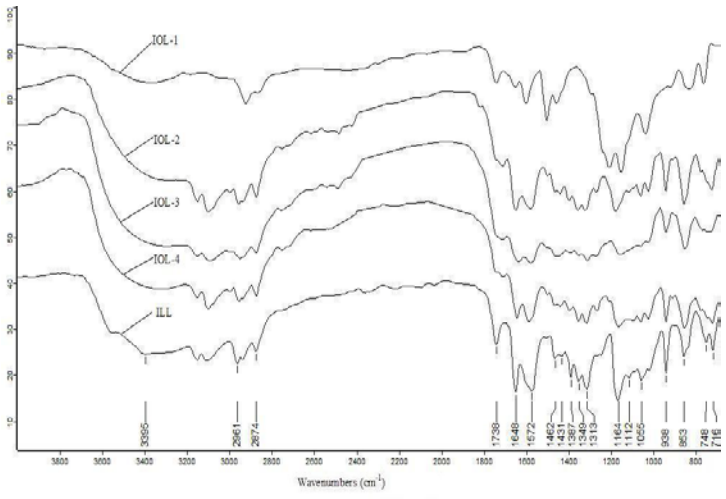

Fig. 2. The FT-IR spectra of the extracted lignin: IOL-1, ionic liquid+methanol extracted lignin; IOL-2, ionic liquid+DMSO extracted lignin; IOL-3, ionic liquid+DMAc extracted lignin; IOL-4, ionic liquid+Dioxane extracted lignin; ILL, neat ionic liquid extracted lignin.

Conclusion

It was proved that imidazolium acesulfamate ILs has the ability to dissolved wood lignin in an open atmosphere. Different organic solvents+IL systems released different content of lignin from the lignocellulosic biomass. This was probably due to the difference dielectric constants of the organic solvents. The IL+methanol system resulted in a relatively high content of carbohydrate loss. The recovered carbohydrate-enriched materials (CEMs) can be used as a valuable source for enzymatic saccharification. These results indicated a potential approach in further optimization of the choice of low-cost ILs and organic solvents for the efficient utilization of the lignocellulosic biomass.

Acknowledgements

The authors are grateful for the financial support of this research from the Specific Programs in Graduate Science and Technology Innovation of Beijing Forestry University (No. BLYJ201213).

References

[1] Farrell, A.E. Plevin, R.J. Turner, B.T. Jones, A.D. O'Hare, M. Kammen, D.M. 2006. Ethanol can contribute to energy and environmental goals. Science 311, 506-508.
[2] Yang, B. Wyman, C.E. 2008. Pretreatment: the key to unlocking low-cost cellulosic ethanol. Biofuels Bioprod. Bioref. 2, 26-40.
[3] Lynd, L.R. Weimer, P.J. van Zyl, W.H. Pretorius, I.S. 2002. Microbial cellulose utilization: fundamentals and biotechnology. Microbiol. Mol. Biol. Rev. 66 (3), 506-577.
[4] Zhbankov, R.G. 1992. Hydrogen-bonds and structure of carbohydrates. J. Mol. Structure 270, 523-539.
[5] Garde, A. Jonsson, G. Schmidt, A.S. Ahring, B.K. 2002. Lactic acid production from

wheat straw hemicellulose hydrolysate by Laceobacillus pentosus and Lactobacillus brevis. Bioresour. Technol. 81 (3), 217-223.
[6] Simmons, B.A. Singh, S. Holmes, B.M. Blanch, H.W. 2010. Ionic liquid pretreatment. Chem. Eng. Prog. 106 (3), 50-55.
[7] Macfarlane, D.R. Seddon, K.R. 2007. Ionic liquid-progress on the fundamental issues. Aust. J. Chem. 60, 3-5.
[8] Seddon, K.R. 1997. Ionic liquids for clean technology. J. Chem. Tcehnol. Biotechnol. 68, 351-356.
[9] Pinkert, A. Goeke, D.F. Marsh, K.N. Pang, S.S. 2011. Extracting wood lignin without dissolving or degrading cellulose: investigations on the use of food additive-derived ionic liquids. Green Chem. 13, 3124-3136.
[10] Li, W.J. Zhang, Z.F. Zhang, J.L. Han, B.X. Wang, B. Hou, M.Q. Xie, Y. 2006. Fluid Phase Equilibria 248, 211-216.
[11] Tejado, A. Pena, C. Labidi, J. Echeverria, J.M. Mondragon, I. 2007. Physico-chemical characterization of lignins from different sources for use in phenol-formaldehyde ersin synthesis. Bioresour. Technol. 98, 1655-1663.

Deriving Wood Quality Properties Through Their Links With Tree And Stand Attributes

Chhun-Huor UNG[1] - Bastien FERLAND-RAYMOND[2] - Xiao Dong WANG[3] - Isabelle DUCHESNE[1] - D. Edwin SWIFT[1]*

1 Natural Resources Canada, Canadian Wood Fibre Centre, Canada
**Correspondant author*
chhun-huor.ung@nrcan-rncan.gc.ca
2 Minsitère des ressources naturelles et de la faune du Québec, Canada
3 Luleå University of Technology, Sweden

Abstract

One of the important Canadian Wood Fibre Centre's mandates is to develop methods to facilitate the flow of information on the wood quality and quantity along the chain of forest values. Among its research projects, one entitled Enhanced Forest Inventory aims to produce tools to map the wood attributes in terms of physico-mechanical properties by using prediction models based on the attributes of the forest tree and stand. The main inputs of these models come from non-destructive measurements on standing trees (acoustic probe, resistograph, terrestrial lidar) and from spatial data (aerial lidar). Among the obtained results, the correlations are significant between acoustic velocity, drill resistance, and tree and stand attributes. These results open the prospect of using the data of non destructive measurements such as acoustic probe and resistograph as complementary input with tree and stand attributes (dbh, crown, and competition index) for prescribing the intensity of thinning to a desired level of wood density.

Key words: non-destructive measurements, tree and stand attributes, acoustic velocity, resistograph, wood density

Introduction

The forest is currently subject to diverse and growing expectations for resources (timber production, carbon sinks, biodiversity, recreation, landscape, and hunting). To date, wood sale is the main financial resource of the forest and contributes, thereby ensuring the integrity of the forest and the ecological and social functions it fulfills in North America. However, in recent years, the profitability of timber production has declined significantly. It was therefore necessary to consider more efficient silvicultural methods and more innovative timber processing. Among all the solutions considered, the tree silviculture (irregular silviculture, tree-target silviculture) appears as a way to ensure profitability while preserving the forest ecological and social issues of the forest. These diverse and high unit value woods require marketing methods highlighting their own unique qualities. These changes were implemented and led the whole wood forest chain (from producers to processors) to adapt. For answering to these changes, we proposed to produce tools to map the quantity and quality of forest wood using predictive models based on nondestructive evaluation of mechanical wood traits and on tree and stand attributes. Here we present the preliminary results of two objectives:
1.Predicting the acoustic velocity from the standing tree attributes
2.Quantifying the correlations between drill resistance profiles, acoustic velocity data, tree attributes, and inter tree competition.

Objective 1. Predicting the acoustic velocity from the standing tree attributes

Context. Theoretically, acoustic velocity is related to wood density and dynamic modulus of elasticity as following:

$$v = \sqrt{\frac{MoE}{\rho}} \qquad [1]$$

where v is the acoustic velocity (km/s), MoE is the modulus of elasticity or wood stiffness (N/m^2), and ρ is the wood density (kg/m^3). Thus, the more accurate is the measurement of v by non-destructive device ST300 (http://www.fibre-gen.com/st300.html) or by the destructive device HM200 (http://www.fibre.gen.com/hm200.html), the more promising the derivation of ρ or MoE from Eq. 1 will be. Indeed, Auty and Achim (2008) demonstrated that v and ρ can be used to predict MoE and particularly that v can be used for sorting logs in the sawmill yard. Also, Jones and Emms (2010) showed that there are strong associations between the log acoustic velocity and branch size variables, the number of branches and whorls. Obtaining the earliest possible assessment of wood quality is primordial to the efficiency and the sustainability of the wood value-chain i.e. for assessing and tracing wood properties from the standing tree to the end-product. Then, it becomes relevant to assess the reliability of v to obtain an early assessment of wood quality on logs (destructive velocity) and especially on standing tree (non-destructive velocity). In addition, as destructive velocity might be more expensive than the non-destructive velocity because it requires harvest, it is justified to quantify the gain in accuracy of the destructive velocity on logs, compared with the non-destructive velocity on trees.

Material. Non-destructive acoustic velocity was measured on 40 sugar maple (*Acer saccharinum* L.) trees and 24 yellow birch (*Betula alleghaniensis* Britton) trees sampled from sixteen 400-m^2 circular plots. Plots were distributed across two forest eco regions in New Brunswick, Canada. The measured tree attributes were stem diameter at 1.30 m (dbh), total height, and crown variables (Fig. 1). These crown variables allowed computing light crown area especially. Two types of tree defects were measured. First, the stem deformation (curvature and elbow) is quantified by the ratio depth/length. Second tree defect was recorded as either, hole, split, wound, or stump swelling and these variables were estimated by their area (width x length). Each of the 64 trees was bucked, and destructive velocity was measured on each sawlogs produced. The destructive velocity in the tree is the mean velocity in logs weighted by the log volumes; each log was assumed to be a truncated cone. Table 1 summarises the obtained data.

Table 1 Data summary: tree, stand, non-destructive velocity and destructive velocity

Variable	**Sugar maple n=40**				**Yellow birch n=24**			
	Min	**Max**	**Mean**	**Std**	**Min**	**Max**	**Mean**	**Std**
Stand basal area m^2/ha	14.00	33.00	25.18	5.86	14.00	33.00	23.96	4.94
Stand height m	17.65	24.50	21.06	2.11	17.40	21.42	18.85	1.29
Dbh cm	24.00	48.00	33.40	6.93	24.00	50.00	33.42	7.06
Crown width dm	15.333	39.67	28.47	6.01	17.67	45.33	31.91	6.03
Total crown area m^2	163.28	673.14	384.97	106.18	171.54	714.00	399.89	123.97
Light crown area m^2	130.55	646.57	342.67	116.09	155.11	638.86	327.85	113.34
Non-destructive velocity km/s	2.94	4.08	3.58	0.27	3.37	4.30	3.88	0.23
Destructive velocity km/s	3.25	4.69	4.07	0.26	3.82	4.71	4.30	0.23

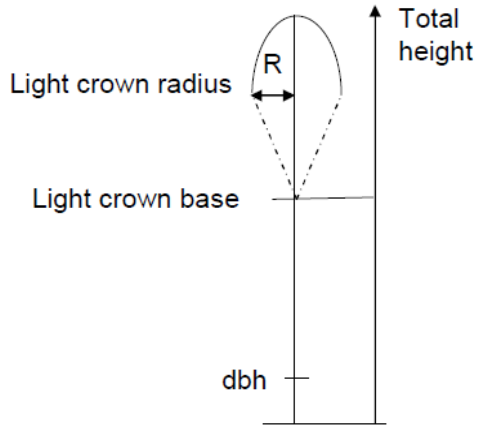

Figure 1. Tree parameters

Method. The following linear regression was used for addressing the prediction of velocity by tree attributes:

$$v_{ij} = \mu + S_j + T_{ij} + e_{ij} \qquad [2]$$

with v_{ij} acoustic velocity of tree i in plot j, μ the overall population mean, S_j the fixed effects of stand attributes, T_{ij} the fixed effects of tree i attributes in plot j, and e_{ij} random error of tree i in plot j. The mixed model procedure was used for separating the fixed effects of tree and stand attributes from the random effect.

Results and discussion. Tree species effect was significant on non-destructive and destructive velocity (Table 2). Stand attributes represented by stand basal area and stand height were not significant on both velocities and for both species (Table 3). The insignificant impact of stand attributes should be caused by the relatively narrow range of the observed stand basal and stand height. None of the considered tree defects had significant effect on both velocities and for both species (tests not shown). Apparently, this lack of correlation seems to contradict Sandoz and Lorin (1996) who advocated the use of acoustic velocity for detecting gross defects on standing trees (cavity, advanced decay or soft rot). However, in reality, this lack of correlation in our data simply means that the observed defects are not quite as advanced as the defects considered by Sandoz and Lorin (1996). It is clear that tree dbh, tree crown width, and light crown area explain significantly both velocities and for both species.

Table 2 Tree species effect on non-destructive and destructive velocity

Numerator degree of freedom=1 Denominator degree of freedom=62	Effect	F value	Pr >F
Non-destructive velocity	Tree species	12.72	0.0007
Destructive velocity* (avg. per tree)	Tree species	19.54	<0.0001

(*on sawlogs only)

Table 3 Effects of dbh, tree height, tree crown, stand basal area and stand height on non-destructive and destructive velocity

Sugar maple: numerator degree of freedom=1; denominator degree of freedom=29				
	Non-destructive velocity		**Destructive velocity**	
Effect	**F value**	**Pr >F**	**F value**	**Pr >F**
Dbh	37.96	<.0001	3.09	0.0893
Tree height	2.37	0.1343	4.17	0.0503
Crown length 1	8.69	0.0063	0.02	0.8940
Crown length 2	7.24	0.0117	0.00	0.9593
Crown width	0.92	0.3447	0.11	0.7429
Crown length 1x Crown width	11.49	0.0020	0.01	0.9090
Crown length 2x Crown width	9.95	0.0037	0.07	0.7896
Stand basal area	4.35	0.0459	0.71	0.4064
Stand heigth	0.28	0.6025	1.66	0.2083

Yellow birch: numerator degree of freedom=1; denominator degree of freedom=13				
	Non-destructive velocity		**Destructive velocity**	
Effect	**F value**	**Pr >F**	**F value**	**Pr >F**

Dbh	3.61	0.0798	5.24	0.0395
Tree height	0.70	0.4193	4.87	0.0459
Crown length 1	0.16	0.6968	0.50	0.4903
Crown length 2	7.24	0.0117	1.34	0.2683
Crown width	0.08	0.7781	0.48	0.4999
Crown length 1x Crown width	0.00	0.9449	0.28	0.6063
Crown length 2x Crown width	0.25	0.6242	1.35	0.2669
Stand basal area	0.64	0.4377	1.31	0.2728
Stand heigth	0.72	0.4127	0.99	0.3371

Objective 2.Quantifying the correlations between wood density based on drilling resistance profiles, acoustic velocity, tree attributes, and inter tree competition.

Context. In addition to the acoustic probe, the drilling resistance device provides additional option for indirect field measurement of wood properties. The literature suggests that the mean value of resistance profiles are correlated with wood density in standing trees (Isik and Li 2003, Eckard et al 2008). Thus, we proposed to build a model of cause and effect between these two types of measurements on the one hand, and the attributes of the tree and stand on the other hand.

Material. For each of the 27 sugar maple and 23 yellow birch sampled in the same forest stands of objective 1, three types of data were collected: competition, resistograph and acoustic probe. The competition data were obtained by dividing the field into six equal areas around each of the 50 trees. For each area, the measurement on the nearest competitor tree was taken and included the distance from the nearest neighbor tree and the central tree, neighbor tree dbh, neighbor tree height, central tree crown with its neighbor crown. The second type of data available is represented by resistograph data. These data were obtained for each tree by drilling the tree at breast height from bark to pit using the IML Resistograph F400. Resistance profile data contained percent amplitude measurements at each 0.1 mm increment of drilling. Basic data such as tree species, dbh, height and crown were collected also. The third type of collected data on 50 trees was the acoustic velocity data using the ST300 probe previously mentionned in objective 1.

Method. Correlations between the three types of data were quantified using the structural equation modeling (Shipley 2002). This modeling allowed verifying the following hypothesis: competition affects tree growth and thus its size; tree size affects the velocity, which subsequently affects tree resistance. The proposed model consists of four latent variables: tree size, acoustic velocity, competition, and drill resistance (Fig. 2). The Size variable is composed of tree dbh, height and crown base. The Velocity variable consists of four successive measurements performed on each tree. Competition and Resistance variables are described below.

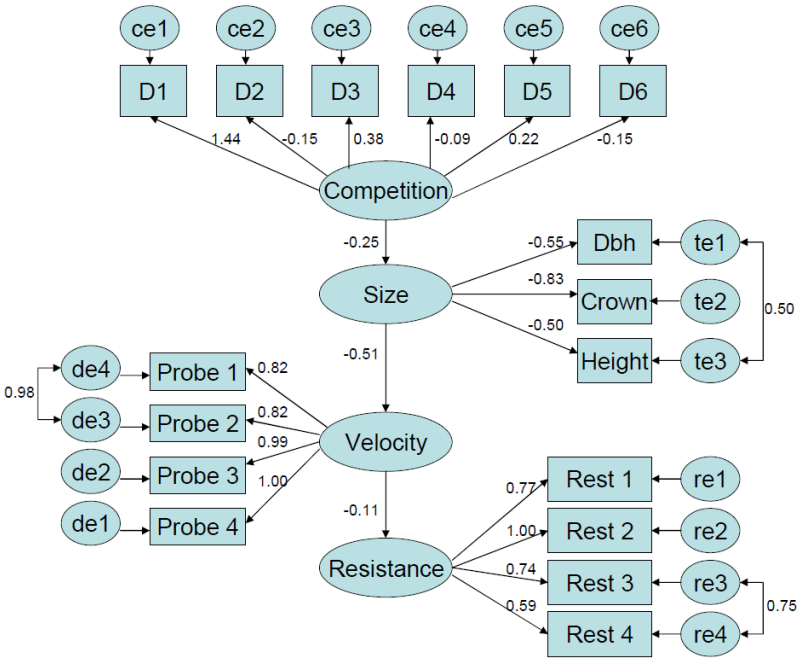

Figure 2. Structural equation model with standardized estimators. n=50, chisq=141.76, df=113, p=0.035

Competition

It is usually required to have at least four measured variables for each latent variable. For competition, it was possible to consider each area around the tree as a measured variable of competition. A total of six variables (areas) were used to estimate the competition variable. Also, tree dbh, tree height and distances between central tree and its neighbours are available. A competition index was used for integrating all these data to be entered directly into the model. The competition index is actually the product of two components of tree competition: height difference and crown radius ratio.

Height difference can be formulated as follow:

$$A = \frac{\pi}{2} - \arctan\left(\frac{h_a - h_v}{d}\right) \qquad [3]$$

where *A* is the angle of height difference in radians, h_a central tree height, h_v neighbor tree height and *d* the distance between the central tree and its neighbor. A low angle implies that the central tree "looks" at its neighbor and then it is dominant (Fig. 3). Conversely, a high angle, or more than 90 °, implies that the central tree is dominated by its neighbor. A nearby tree taller than the central tree will have a smaller angle if it lies at a great distance.

Crown radius ratio is represented by:

$$E = \frac{r_v}{r_a} \times \frac{(r_a + r_v)}{d} \qquad [4]$$

where E is the crown invasion, r_a the crown radius of the central tree and r_v the crown radius of the neighbor tree. E has a high score if the neighbor tree has a crown radius larger than the central tree and if the two crowns are touching.

Then, the competition index is:

$DI=A\times E$ [5]

This index has a minimum of zero corresponding to no competition. An index of one indicates that both trees have a similar dominance. An index greater than one indicates that the central tree is dominated.

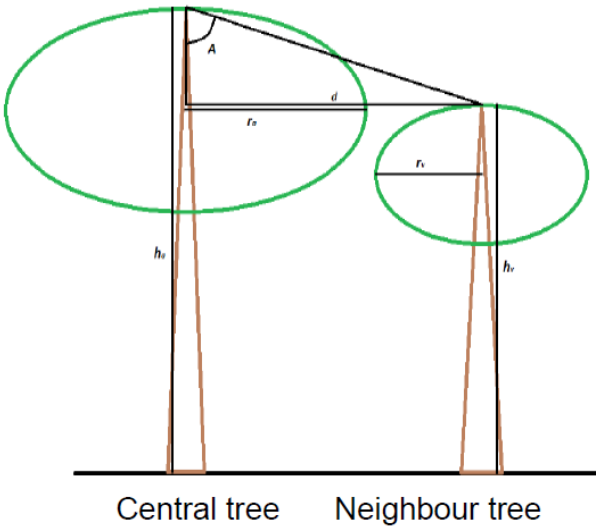

Figure 3. Trees attributes used for computing the competition index

Resistance

The resistance data are longitudinal as a vector of resistance values is produced for each sampled tree (Fig. 4). Therefore, they need to be transformed data to create the Resistance variable for the structural equation model. The transformation consists to create four variables from the mean values of resistance by quartiles.

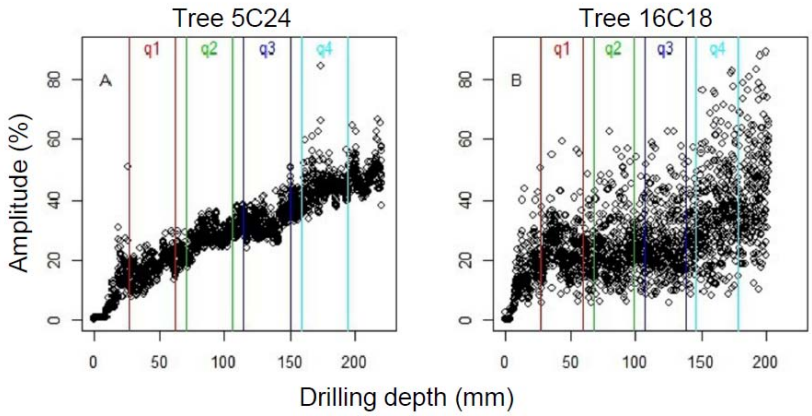

Figure 4. Examples of resistograph amplitude profile. The color bands represent the quartiles used in the structural equation model

Result and discussion

The component Competition of the structural equation model is significant with p = 0.365 (must be greater than 0.05). However, its parameters are still difficult to interpret. The component Resistance has the p value of 0.085. It is interesting to note that the interpretation of the estimators is very natural in this case. Indeed, there is an increase of resistance with the quantile. The quantile 4 is lower than the percentile 3, which is partly explained by the frequent presence of heart rot.

The complete structural equation model (Fig. 2) has the p value of 0.035, very close to 0.05. From the obtained results, Competition has a negative effect on Size, which subsequently negatively affects the stand density. Finally, a high stand density has the effect of causing a greater resistance to drilling. The negative relationship between Competition and Size seems appropriate. However, it is important to note that Size variable is difficult to interpret since the relationship between height and dbh does not have the same sign as that between crown area and height. Another problem of Size variable is that it represents the current state of the tree. However, competition does not affect tree size directly, but its growth (Dutilleul et al 1998). It is therefore necessary to complement the Size variable by a variable that measures growth e.g. radial increment in recent years of the life of the tree. Then, strong competition would tend to reduce growth and vice versa. The low sample size is another important gap that could explain the weak obtained results. According to Shipley (2002, p. 177), the sample size should be five times higher than the number of free parameters. Since the model contains 40 free parameters, a minimum sample size of 200 is needed to ensure the validity of the chi-square approximation.

Conclusion

Correlations were low between acoustic velocity, drill resistance, tree attributes and competition iondex. Although these correlations are still weak, they open the prospect of using the data of non destructive measurements such as acoustic probe and resistograph as complementary input with tree and stand attributes (dbh, crown, and competition index) for prescribing the intensity of thinning to a desired level of wood density. Such statistical models will greatly improve forest inventory by offering the possibility to assess the quality of individual trees. Thus, they will contribute to realize the full economic potential of the tree.

Acknowledgement

We thank Mr. Roger Gagné and Mr André Beaumont (Canadian Wood Fibre Centre) for completing the collection of all field data. Dr. Gary Warren (Canadian Wood Fibre Centre) and Mr Gaétan Numainville (Minsitère des ressources naturelles et de la faune du Québec) are thanked for their assistance in the use of resistograph. Finally, we thank Professor Alexis Achim and his student Mr Normand Paradis (Université Laval) for their assistance in the use of the acoustic probe.

References

Auty, D. and A. Achim. 2008. The relationship between standing tree acoustic assessment and timber quality in Scots pine and the practical implications for assessing timber quality from naturally regenerated stands. Forestry 81(4): 475-487.

Dutilleul, P., M. Herman, and T. Avella-Shaw. 1998. Growth rate effects on correlations among ring width, wood density, and mean tracheid length in Norway spruce (*Picea abies*). Can. J. For. Res. 28:56–68.

Eckard, J. T., F. Isik, B. Bullock, B. Li, and M. Gumpertz. 2008. Selection efficiency for solid wood traits in Pinus taeda using time-of-flight acoustic and micro-drill resistance methods. For. Sci. 56(3): 233-241.

Isik, F., and B. Li. 2003. Rapid assessment of wood density of live trees using the resistograph for selection in tree improvement programs. Can. J. For. Res. 33(12): 2426-2435.

Jones, T G and G W Emms 2010. Influence of acoustic velocity, density, and knots on the stiffness grade outturn of radiata pine logs. Wood and Fiber Science 42(1): 1-9.

Sandoz, J-L and P. Lorin. 1996. Tares internes de bois sur pied: détection par ultrasons. Rev. For. Fr. 48(3): 231-240.

Shipley, B. (2002). Cause and Correlation in Biology: A User's Guide to Path Analysis, Structural Equations and Causal Inference. 2nd Edition. Cambridge University Press: Cambridge UK.

Wood Construction Under Cold Climate Part One: Shear Tests Of Glued Wood Joints Under Cold Temperatures

Xiaodong (Alice) WANG - Niclas BJORNGRIM - Victoria KRASNOSHLYK- Olle HAGMAN

Assistant professor - Ph. D student - Ph. D student - Professor
Wood Products Engineering, Luleå tekniska universitet, Sweden
* *Corresponding author*
alice.wang@ltu.se

Abstract

As wood constructions increasingly use engineered wood world wide, concerns arise about the integrity of the wood and adhesives system. The glueline stability is a crucial issue for engineered wood. Many researchers have worked on the performance of glueline at elevated temperatures. How will glue act under cold conditions? It is important in cold regions such as Scandinavia, Canada, Alaska, Russia, and North Japan etc. The engineered wood constructions in these areas will be exposed to low temperature in a quite long period each year. Normally glue is considered to be more brittle under certain temperatures. The objective of this project is to determine how engineered wood behaves when exposed to temperatures between 20 °C to -60 °C. There are four steps to reach the main objective. Here it is the first step: Study the influence of cold temperatures on the shear strength of small samples of glued Norway Spruce (*Picea abies*) joints (150mm x 20mm x 10mm). Total 375 specimens with four different commercially available adhesives (PUR, PVAc, EPI and MUF) plus solid wood, at five different temperatures (T = 20, -20, -40, -50 and -60 °C) were investigated in this paper. With decreasing temperature, the shear strength of solid wood and glued wood joints decreased. There were significant differences in shear strength and wood failure behavior between the adhesives. PVAc bonds showed the best results at all temperatures among all types of adhesives used here, even compared to the average wood strength, and the wood failure percentage was comparatively low. MUF demonstrated the lowest shear strength among all, regardless the temperature changes. The significant lower shear strength was found at -40°C or -50°C depending the adhesive type.

Keywords: Engineered wood, Glueline stability, Cold climate, Shear strength, Wood failure.

Introduction

The wood constructions are increasingly using engineered wood products (such as glued-laminated timber (glulam), laminated veneer lumber (LVL), structural-composite lumber (SCL), or cross laminate timber (CLT)) [1]. Adhesives are the key part of these engineered wood products and play an important role in the performance of engineered wood products. The response of glue line to temperature changes and extreme temperatures as regularly occurs in normal use raise some concerns on the integrity of wood structure. It is believed that the most commercial wood adhesives are vulnerable to the extreme temperatures and temperatures changes. The concern is stronger in the regions having extreme weather like Scandinavia, Canada, Alaska, Russia, and North Japan etc. Wood constructions in these areas are exposed to low temperatures during a quite long period each year. Despite this, thermal effects are usually not a consideration in the design of wood constructions. Wood and adhesives are very different in terms of swelling and shrinkage coefficients. Glue line of most adhesives is also more brittle than wood. If not compensated for, any differential between wood and adhesives thermal properties can lead to performance problems when the construction is exposed to large temperature changes. In these cases, the design needs to compensate for differential movement of components while preserving structural integrity. The performance of glue line at elevated temperatures is well documented [2, 3, 4], but not much information is available on the stability of glue line at low temperatures and especially under extremely cold temperatures, although some studies worked on timber bridges in cold climates [5, 6, 7].

Materials and Methods

The main objective of this project is to determine how engineered wood behaves when exposed to temperatures between 20 °C to -60 °C. There are four parts to reach this goal. In this study (Part one), we just investigated the influence of cold temperatures (T=20 °C to -60 °C) on the shear strength of small samples of glued wood joints (according to EN 302-1).

All bonding were carried out with Norway Spruce (*Picea abies*). For testing the glue-line stability of glued wood joints under cold temperatures, different commercially available adhesives from different producers were used (PUR, PVAc, EPI and MUF). These adhesives vary in their chemical composition. All of them are certified according to EN 301-302 [8, 9, 10] standards and are primarily used in the field of engineered wood. With decreasing of temperature, the shear strength of solid wood and glued wood joints were tested. The failure behavior of wood and adhesives were observed. SAS paired test has been used for statistical analysis of shear strength and wood failure.

Materials.

1. Wood

All bondings were carried out with Norway Spruce with average density 500 kg/m^3 and EMC of 12%. The growth ring angle (angle between growth rings and glued surface of the specimen) of the wood was between 30 and 90°.

2. Adhesives

For testing the glueline stability, commercially available adhesives from different producers were used. There were:

- One-component polyurethane (PUR)
- Polyvinyl acetate (PVAc)
- Emulsion-polymer-isocyanate (EPI)
- Melamine-urea-formaldehyde resin (MUF)

These adhesives are commonly used for bonded wood components (such as engineered wood) for construction proposes. Table 1 demonstrates the bonding parameters for each adhesive as they are recommended by the manufacturers.

Table 1 Adhesives and their bonding properties

Adhesive	Adhesive-Hardener ratio	EN301 certification	EMC (%)	Pressure (MPa)	Pressing time (Minute)	Temperature (^{0}C)	Application	Spread per side (g/m^2)
PUR	--	√	≥8	0.3	30	20	One side	200
PVAc	--	--	NA	0.3	30	20	One side	200
EPI	100:15	√	6-15	0.3	30	20	One side	200
MUF	100:20	√	≈12	0.3	15	80	One side	200

3. Production of the specimens

According to EN 302-1, the prefabricated boards were stored under standard climatic conditions (20°C, 65% RH) until the equilibrium wood moisture was reached. Before the bonding process, the boards were planed to the necessary thickness of (5±0.1) mm to exclude aging effects on the wood surface. The adhesives were bonded with close contact bond line (≈0.1mm) at room temperature. The pressure for all adhesive bonds was 0.3 MPa. After seven days storage under standard climatic conditions, the adhesive bonds were cut into specimens according to EN 302-1: 150 mm x 20mm x 10mm.

4. Testing procedure

The shear strength was determined according to EN 302-1. To investigate the influence of the temperatures on shear strength, 15 specimens of each group were tempered in a special climate chamber (from company Adopticum in Skellefteå) for 12h at -20, -40, -50 and -60°C, respectively. The tests were executed at a universal testing machine (Fig. 1). The testing room of machine was 20°C, thus the specimens' temperature was increased when tested. The tests were performed position-controlled with a feed speed of 2 mm/min. After measuring the shear strength, the wood failure percentage was estimated visually in 10%-steps, as recommended in EN 302-1. Then the specimens were weighed and the wood moisture content was determined.

Fig. 1 Machine and test specimens according to EN302-1

Results and Discussions

Solid wood specimens

To obtain a reference value for the strength of the glued specimens, non-glued solid wood specimens were tested in addition. These specimens were designed according to the geometry requirements of shear specimens in EN 302-1.
The shear strength of tested solid wood specimens decreased with decreasing temperature (Fig. 2, Table 2). There are significant differences between 20°C, -20°C with -50°C and -60°C (Table 3). That means when environment temperature dropped lower than -50°C, the Norway Spruce solid wood get weaker for supporting shear load.

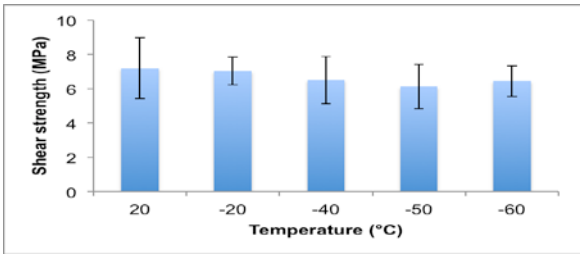

Fig. 2 Shear strength of Norway Spruce solid wood against temperature

Table 2 Shear strengths of wood and adhesive bonds at different temperatures

Temperature (°C)	Shear strength (MPa)					
		Spruce	PUR	PVAc	EPI	MUF
20	Mean	7.19	5.98	7.03	6.32	5.09
	Std. Dev.	1.78	0.95	0.63	0.99	1.41
-20	Mean	7.04	5.85	6.82	6.07	4.87
	Std. Dev.	0.81	1.41	1.51	1.00	1.03
-40	Mean	6.51	5.42	6.25	5.84	5.12
	Std. Dev.	1.37	0.93	1.41	1.64	1.01
-50	Mean	6.13	5.35	5.61	5.27	4.58
	Std. Dev.	1.29	1.74	1.69	1.43	1.15
-60	Mean	6.45	5.04	6.09	5.78	4.89
	Std. Dev.	0.88	1.77	1.87	0.85	1.52

Table 3 Paired t-tests results for shear strengths at different temperatures

Glue type	Variable1	Variable2	Difference	tValue	DF[1]	P Value[2]
Wood	20°C	-50°C	20°C vs. -50°C	2.458	15	0.03
Wood	-20°C	-50°C	-20°C vs. -50°C	3.206	15	0.01
Wood	-20°C	-60°C	-20°C vs. -60°C	2.099	14	0.05
PUR	20°C	-40°C	20°C vs. -40°C	2.708	15	0.04
PVAc	20°C	-40°C	20°C vs. -40°C	1.854	14	0.05
PVAc	-20°C	-50°C	-20°C vs. -50°C	2.003	15	0.05
PVAc	-20°C	-60°C	-20°C vs. -60°C	1.867	14	0.04
EPI	-20°C	-50°C	-20°C vs. -50°C	1.918	15	0.05

DF[1]: Degree of freedom; P Value[2]: Probability value which is significant at level of 0.05.

Glued wood specimens

Shear strength of the tested adhesive bonds at different temperatures were demonstrated in Table 2, Figs. 3 and 4. At standard condition (room temperature 20°C), the PUR and MUF showed already much lower shear strength than solid wood and PVAc. There is no significant different between 20°C and -20°C for all type of adhesives bonds tested (PUR, PVAc, EPI and MUF). The PVAc bonds were in the range of solid wood strength and the wood failure percentage was comparatively low (Table 4). No matter of the temperatures changed, MUF showed lowest shear strength among all. There is no significant different between 20, -20, -40, -50 and -60°C for MUF bonds.

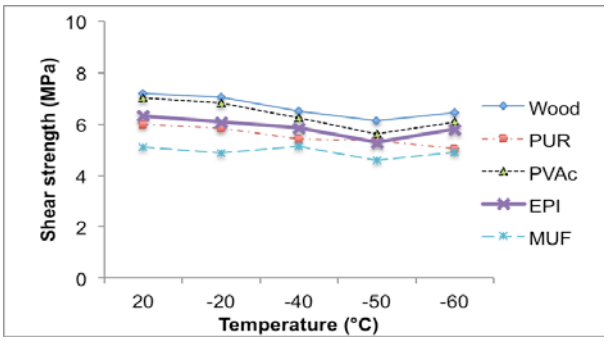

Fig. 3 Shear strength of all tested specimens against temperature

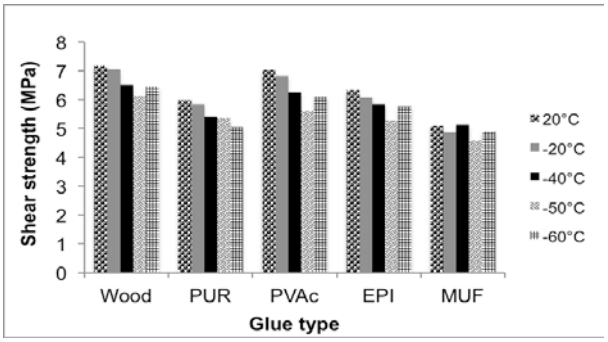

Fig. 4 Comparison of shear strength of wood and adhesive bonds at different temperature

Table 4 Wood failure percentages of adhesive bonds at different temperatures

Temperature (°C)	Wood failure percentages (%)				
		PUR	PVAc	EPI	MUF
20	Mean	63.6	40.7	49.6	80.4
	Std. Dev.	37.5	28.2	25.8	21.6
-20	Mean	60.7	57.3	54.6	56.9
	Std. Dev.	37.9	31.1	29.9	33.8
-40	Mean	53.3	38.2	37.7	37.5
	Std. Dev.	35.3	31.6	34	29.6
-50	Mean	39.1	39.2	41.8	35
	Std. Dev.	38.6	30	30	24.7
-60	Mean	32	44	53.3	57.7
	Std. Dev.	37.8	29.1	29.6	32.4

PUR

As shown in Fig. 5, the shear strength of PUR bonds was decreased when temperature dropped. But there is no significant difference between all temperatures except 20°C with -40°C (P = 0.04) (Table 3). The similar trend is for wood failure percentage (Table 4). There is a significant difference between 20°C with -40°C and -60°C (Table5).

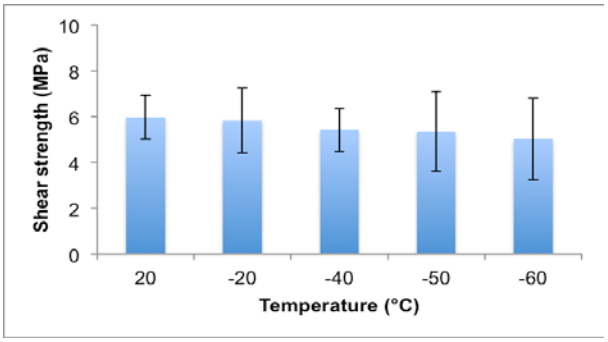

Fig. 5 Shear strength of PUR bonds against temperature

Table 5 Paired t-tests results for wood failure percentage at different temperatures

Glue type	Variable1	Variable2	Difference	tValue	DF[1]	P Value[2]
PUR	20°C	-40°C	20°C vs. -40°C	1.952	15	0.05
PUR	-40°C	-60°C	-40°C vs. -60°C	1.829	13	0.05
PVAc	20°C	-20°C	20°C vs. -20°C	-2.276	15	0.04
PVAc	-20°C	-50°C	-20°C vs. -50°C	2.157	15	0.05
EPI	20°C	-40°C	20°C vs. -40°C	2.567	15	0.03
MUF	20°C	-40°C	20°C vs. -40°C	4.861	15	0.00
MUF	20°C	-50°C	20°C vs. -50°C	3.648	15	0.00
MUF	-20°C	-40°C	-20°C vs. -40°C	1.964	14	0.05
MUF	-20°C	-50°C	-20°C vs. -50°C	1.827	15	0.05
MUF	-50°C	-60°C	-50°C vs. -60°C	-2.136	15	0.04

DF[1]: Degree of freedom; P Value[2]: Probability value which is significant at level of 0.05.

PVAc

The shear strength of PVAc bonds was also decreased when temperature decreased (Fig. 6, Table 2). There are significant differences between 20°C, -20°C with -40°C, -50°C and -60°C (Table 3). For the wood failure percentage (Table 4), there are significant differences (lower) between 20°C, -20°C with -50°C (Table 5).

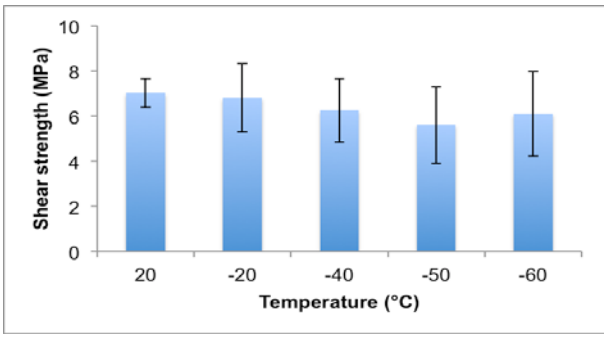

Fig. 6 Shear strength of PVAc bonds against temperature

EPI

Till -40°C the shear strength of EPI bonds showed a good stability (Fig. 7, Table 2). There is a significant different between -20°C with -50°C (Table 3). The relatively low wood failure percentage demonstrated in all temperature tested (Table 4). Still there is a significant different between 20°C with -40°C (Table 5).

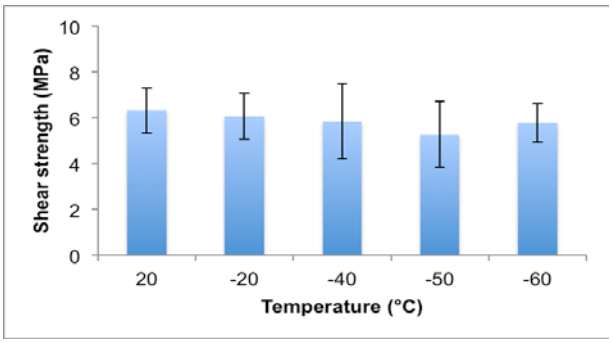

Fig. 7 Shear strength of EPI bonds against temperature

MUF

The tested shear strength of MUF bonds were weak, but no significant different had found through all temperatures (Fig. 8, Table 2 and 3). The wood failure percentage dropped fast from 20°C and -20°C to -40°C and -50°C (Table 4 and 5).

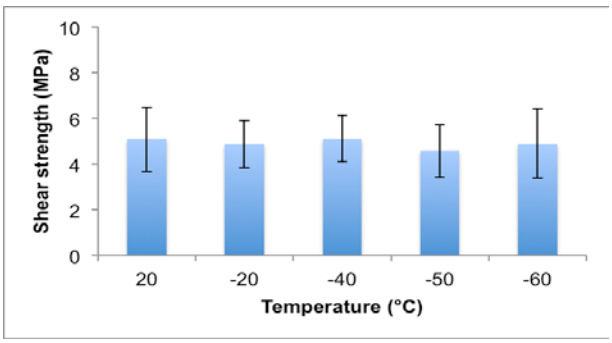

Fig. 8 Shear strength of MUF bonds against temperature

Conclusions And Recommendations

The shear strength of wood (Norway Spruce) and adhesive (PUR, PVAc, EPI and MUF) bonds at different temperatures (20, -20, -40, -50 and -60°C) were tested. PVAc bonds at all temperatures achieved the best results compared to the average wood strength, and the wood failure percentage was comparatively low. MUF reached the lowest shear strength among all, regardless the temperature changes. Till -20°C, all bonds showed good stability. The significant lower shear strength demonstrated at -40°C or -50°C depending the adhesive type. Here it must be pointed out that temperature lower than -20°C is normally not in a range of practical relevance, but it is still important in the cold regions. For further investigation, -30°C should be added to the testing in order to further define the point where the strength drops significantly. More important changes in the future work are two points: 1) Subject the samples to cycling temperature changes in order to create a more realistic test. For example -40°C for 12 hours, follow by -20°C for 12 hours, then -40°C again for 12 hours for about 5 cycles. 2) From statistic point of view, the sample size should be increased to 30 specimens of each type of adhesives and temperatures, instead of the current 15 specimens.

References

[1] J. L. Howard.: U. S. Timber Production, Trade, Consumption, and Price Statistics 1965 to 2005.

[2] Clauss S., Joscak M., Niemz P. Thermal stability of glued wood joints measured by shear tests. European Journal of Wood and Wood Products 69(2011): 101-111.

[3] Falkner H, Teutsch M (2006) Load-carrying capacity of glued laminated wood girders under temperature influence. Bautechnik 83(6): 391-393.

[4] Frangi A, Fontana A, Mischler A (2004) Shear behavior of bond lines in glued laminated timber beams at high temperatures. Wood Sci. Technol 38(2): 119-126.

[5] Kainz J, Ritter M (1998) Effect of cold temperatures on stress-laminated timber bridge deck. Proceedings of the 5th World Conference on Timber Engineering, 1998, Montreux, Switzerland. WCTE, August 17-20,, 1998 Swiss federal institute of Technology Lausanne Switzerland Montreux. Eds.., Natterer, J. and Sandoz, J. L. Vol. 2: 42-49.

[6] Wacker J.P. (2003) Cold temperature effects on stress-laminated timber bridges-A laboratory study. Res. Pap. FPL-RP-605. Madison, WI: U.S. Department of Agriculture, Forest Service, Forest Products Laboratory. 22p.

[7] Wacker J. P. (2009) Performance of stress-laminated timber highway bridges in cold climates. P. E. M. ASCE. Copyright ASCE 2009. Cold Regions Engineering 2009.

[8] EN 301: adhesives, phenolic and aminoplastic, for load bearing timer structures-Classification and performance requirements (2006).

[9] EN 302-1: Adhesives for load-bearing timber structures – Test methods – Part 1: Determination of longitudinal tensile shear strength (2011).

[10] EN 302-2: Adhesives for load-bearing timber structures – Test methods – Part 2: Determination of resistance to delamination (2011).

Sensitivity of Several Selected Mechanical Properties of Moso Bamboo to Moisture Content Change Under Fiber Saturation Point

Zehui Jiang, Hankun Wang, Genlin Tian, Xing'e Liu, Yan Yu*

The moisture dependence of different mechanical properties of bamboo was not fully understood. In the paper, longitudinal tensile modulus, bending modulus, compressive strength and shearing strength parallel to grain of bamboo with 0.5, 1.5, 2.5 and 4.5 years old were tested under different moisture content (MC) to elucidate the sensitivity of different mechanical properties of bamboo to MC change. The results showed that the four mechanical properties of bamboo respond differently to MC change. Compressive and shearing strength parallel to gain were most sensitive to MC change, then was longitudinal tensile modulus and followed by bending modulus, which can be partially explained by the different response of the three main components in the plant cell wall to MC change. For tensile modulus and bending modulus, the effect of bamboo ages on the sensitivity to MC change was insignificant while young bamboo (0.5 years old) was more sensitive to MC change for shear strength and less sensitive for compression strength than the older ones.

Key words: bamboo; mechanical properties; moisture dependence; specific density

Contact information: Department of Biomaterials, International Center for Bamboo and Rattan, State Forestry Administration of China No.8 Futong Dong Dajie, Wangjing Area, Chaoyang District, Beijing 100102， China
** Corresponding author: Yan Yu, Doctor, Associate researcher, Email: yuyan9812@icbr.ac.cn; Tel: 86-10-84789812; Fax: 86-10-84238052*

Introduction

Water exists in plant material during its entire life cycle from growth, processing to application. For wood and wood-based products, the relationship between mechanical properties and moisture content (MC) is rather important for quality control and product application. For the past decades, considerable researches have been performed on water in wood and its relevance to mechanical properties (Green et al. 1986; Kretschmann and Green, 1996; Wang et al. 1999; Kojima and Yamamoto, 2004; Liu and Zhao, 2004; Green et al. 2007). At MC from oven-dry to the so called fiber saturation point (FSP), bound or adsorbed water accumulates in the wood cell wall. Above the FSP, free water accumulates in the cell cavity. It is well known the change of moisture content below FSP significantly influences the mechanical properties of wood, whereas affects very little above FSP. Furthermore, it has been further revealed different mechanical properties of wood showed different sensitivity to the change of MC (Green et al. 1999; Ishimaru et al. 2001; Sudijono et al. 2004). Specifically, the data in United States wood handbook has declared the longitudinal tensile strength of wood decreased 16.7% from air-dried state (MC 12%) to saturated state, followed by bending modulus (23.7%), shearing strength parallel to gain (30.0%) and compressive strength parallel to gain (42.5%).

Bamboo is one of the most important non-wood forest resources in the world, growing faster than almost all the trees on earth. As a plant material, bamboo is also hygroscopic, gaining or losing water to equilibrate with its environment (Hui and Yang, 1998). Although the effect of MC on the mechanical properties of bamboo might be similar to wood in general (Zhou, 1998), specific relationship might be somewhat different, since significant difference exists in chemical composition and microstructure between bamboo and wood. This study is part of a program aimed to gain a better understanding of the effect of MC on the mechanical properties of bamboo. In this paper, the effect of MC from oven dry to FSP on four selected mechanical properties (namely longitudinal tensile modulus, bending modulus of elasticity, shear strength parallel to gain and longitudinal compression strength) of bamboo with ages of 0.5, 1.5, 2.5 and 4.5 years was investigated in order to reveal the different sensitivity to MC change of the selected mechanical properties of bamboo with different ages under FSP.

Materials And Methods

Sample preparation

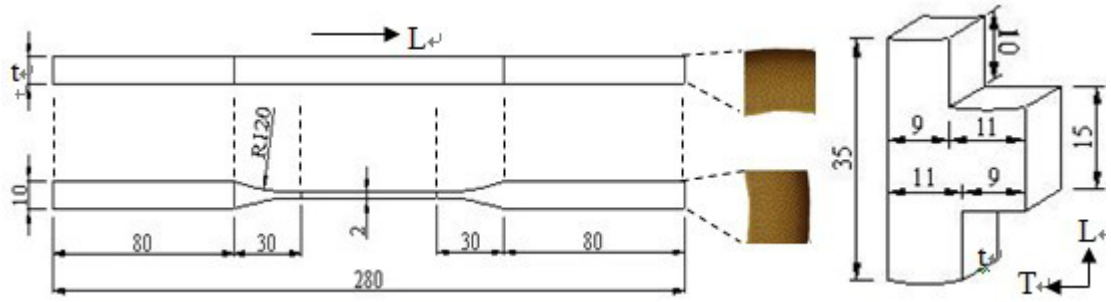

Figure 1. The specific shape and size of those two kind of samples
Longitudinal tensile (Left); Shear strength parallel to gain (Right)

Moso bamboo (Phyllostachys pubescens Mazei ex H.de Lebaie) aging with 0.5, 1.5, 2.5 and 4.5 years was taken from a bamboo plantation located in Zhejiang Province, China. 32 bamboo culms were cut down in total with 8 culms for one age. All the samples for mechanical testing were cut from 15-25 internodes and prepared according to a Chinese national standard for bamboo (GB/T 15780-1995). The specific dimensions of the samples were as follows: 20 (L)×20 (T)×t (Thickness of bamboo culm wall) for compression strength parallel to grain; 160 (L)×10 (T)×t (Thickness of culm wall) for three point bending modulus. The specific shape and size of samples for longitudinal tensile modulus and shear strength parallel to grain gain were showed in Figure 1. All the samples were air-dried in the lab environment for more than six months before moisture conditioning.

Moisture conditioning

All the air-dried mechanical samples were randomly divided into 9 groups for moisture conditioning. Each group contained 20 samples for compressive strength, 16 samples for longitudinal tensile modulus, 16 samples for bending modulus, and 12 samples for shear strength with each bamboo age. The samples with MC under FSP were conditioned in desiccators containing different aqueous saturated sale solution listed in Table 1.

Table 1. Relative humidity (RH) levels in the experiments and the corresponding equilibrium moisture contents (EMC).

NO.	RH, Average (%)	EMC, Average (%)	Chemicals for conditioning
A	2.9	0.5	Silica Gel
B	12.5	4.7	LiCl
C	37.1	5.5	MgCl2
D	53.9	7.1	K2CO3
E	68.7	11.8	NaBr
F	74.1	12.5	NaCl
G	88.9	16.3	KCl
H	100	30.5	Water soaking
I	100	50.9	Water soaking

The desiccators were put in the lab with a constant temperature of 20 ℃ for at least one month. Relative humidity (RH) in the desiccators was measured with a hygrothermograph (TESTO 608-H1) placed in the containers. The actual EMC of each sample was measured by weighing after conditioning. The EMC above FSP were achieved by water soaking.

Measurement of mechanical properties

Mechanical testing was conducted according to a Chinese National Standard for bamboo (GB/T 15780-1995). A universal mechanical tester (5582, Instron Co. USA) was used for both three point bending and tensile testing. The span for bending test is 120 mm and the loading speed is 4 mm/min . A noncontact video extensometer was used for measuring tensile strain during tensile test. The tensile speed was set at 1.5 mm/min. Compressive strength parallel to grain and shear strength parallel to grain were tested by another mechanical tester (WDW-E100D, JINANSHIJIN Co. China) because the 5582 mechanical tester is not equipped with the standard grips we needed.

Results And Discussion

Mechanical properties of bamboo under different MC

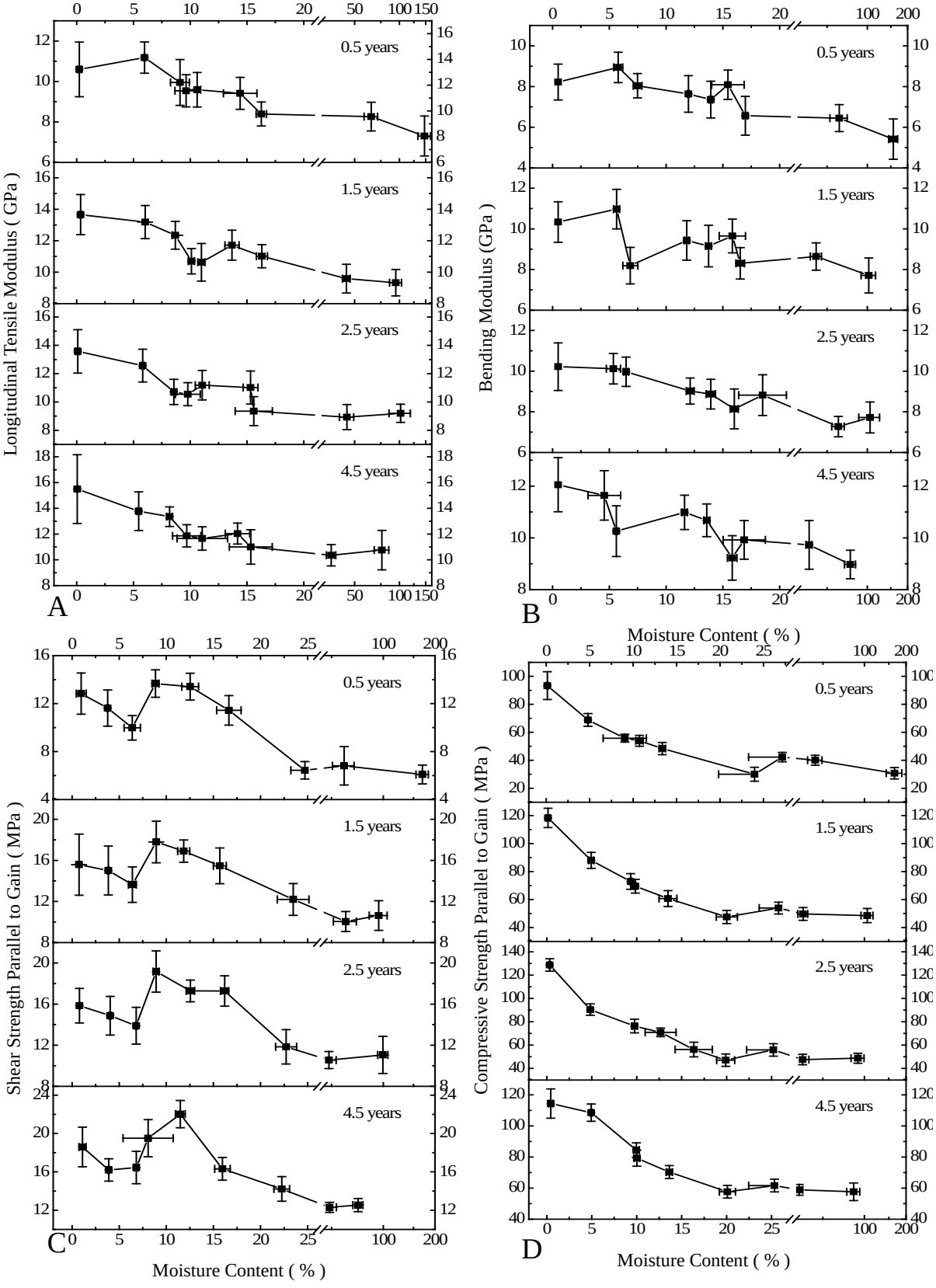

Figure 2A:Longitudinal tensile modulus of four ages bamboo measured under different RH

and in wate;
Figure 2B: Bending modulus of four ages bamboo measured under different RH and in wate;
Figure 2C: Shear strength parallel to gain of four ages bamboo measured under different RH and in wate;
Figure 2D: Compressive strength parallel to gain of four ages bamboo measured under different RH and in wate;

Although the general relationship between MC and mechanical properties of bamboo should be similar to that of wood to a large extent, some specific differences still exist since the structure and chemical compositions were different. Tensile modulus, bending modulus, shear strength parallel to grain and compression strength parallel to grain of bamboo plotted against MC are respectively shown in Figure 2A-D. Figure 2A showed the effect of MC on the longitudinal tensile modulus of bamboo with different ages (0.5, 1.5, 2.5, 4.5 years). A general decrease trend with the increase of MC can be easily observed. However, there seemed to have a plateau from MC 10% to 15%, followed by a continuing decrease with rising MC until FSP. For bending modulus, a general decrease trend with MC rising from nearly zero to water saturation was also observed (Figure 2B). However, the bending modulus of 0.5 and 1.5 years bamboo at MC 5%-6% was abnormally higher than the value measured at nearly zero MC, which might be attributed to the inherent sample variation between groups since the bamboo with 2.5 and 4.5 years old did not show similar behavior. The relationship between MC and shear strength parallel to gain of the four ages bamboo are shown in Figure 2C. An initial reduction at the early stage of moisture increasing can be observed, followed by a rising to the maximum value at MC 8%-9%. The shear strength then decreased again with increasing MC to FSP. For compressive strength parallel to gain (Figure 2D), a stable and more linear decrease trend was obtained with MC increasing to 20% for the bamboo of 1.5, 2.5 and 4.5 years old, and 25% for the bamboo of 0.5 years old. However, an unexpected, small but stable increase when MC was about 25% or more was repeatedly observed for the bamboo of all the ages, which has not been reported before and no explanations could be proposed presently.

Sensitivity to MC change of different mechanical properties of bamboo

In order to get a quantitative relationship between the four mechanical properties of bamboo and MC for practical application, a linear fitting was performed on the data involving all the four ages (Figure 3). The value of mechanical properties at FSP is actually the average of the two values measured at water saturation presented in Figure 2. Here oven dry has not been selected as the start point of low MC only because such low MC was seldom to be encountered in the practical application. Therefore, the variation scope of MC of longitudinal tensile modulus, bending modulus, shear strength parallel to gain and compressive strength parallel to gain of bamboo was 5.5%~FSP, 5.5%~FSP, 8%~FSP, 5%~FSP, respectively. In a previous study, we have found the FSP of Moso bamboo was related to its ages (Wang et al. 2010). For the young bamboo with only 0.5 years old, the FSP was about 28%, while the bamboo aging 1.5, 2.5 and 4.5 years has nearly the same FSP 23%. From the obtained four linear equations, it can be inferred per 1% MC change would result in a increase or decrease of 0.21 GPa for tensile modulus, 0.10 GPa for bending modulus, 0.52 MPa for shear strength

and 2.50 MPa for compression strength. In order to further compare the sensitivity of the four properties to MC change, a reference value must be obtained in advance. Here, the properties at MC 12% were selected as the reference value, which can be calculated according to the above four equations. Then the moisture sensitivity K, namely the change rate of the properties per 1% MC change, can be defined by the ratio between the scopes of the linear equations and the properties at 12% MC (P12)according to formulae (1). The calculation result was showed in Figure 4.

$$K = 100\% \times \frac{Scope}{P_{12}} \qquad (1)$$

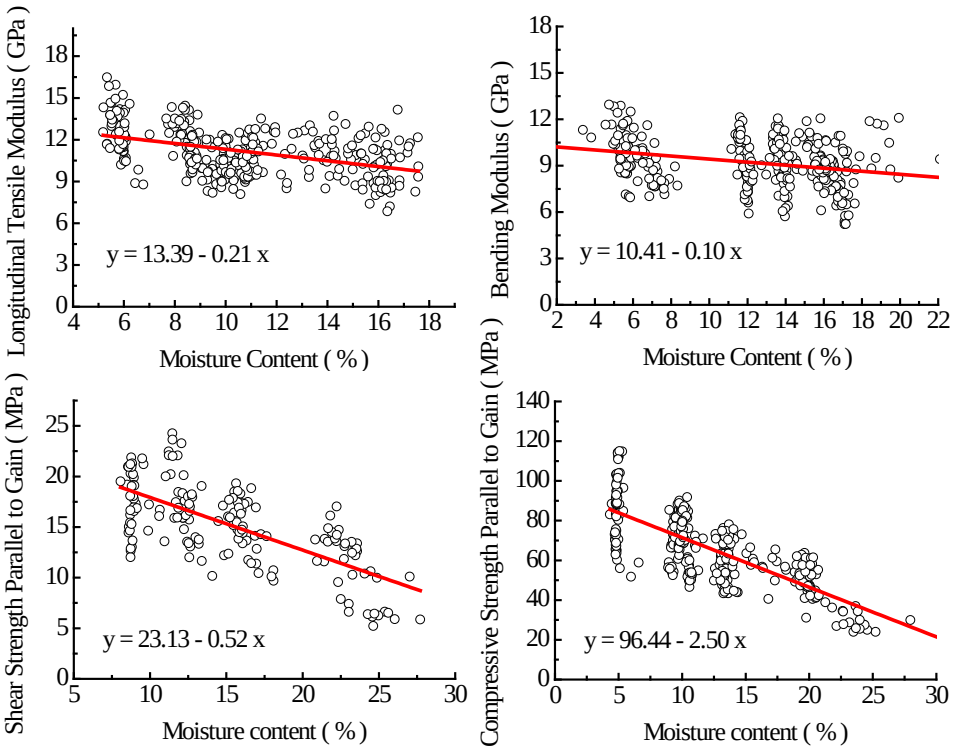

Figure 3 The Relation Model of Moisture Content and Mechanical Properties

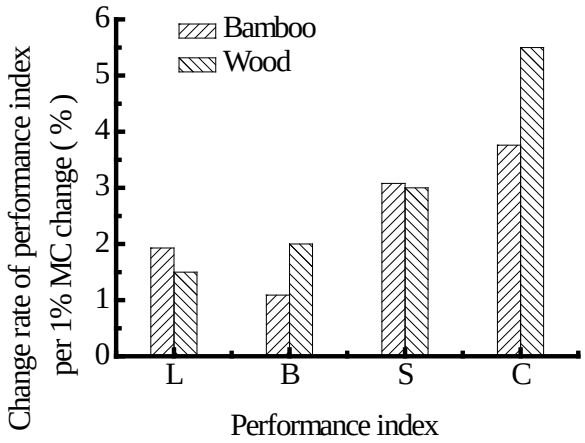

Figure 4 The change rate of mechanical properties per 1% MC change
L: Longitudinal tensile modulus; B: Bending modulus; S: Shear strength parallel to gain; C: Compression strength parallel to gain

Figure 4 indicates bending modulus exhibits the smallest sensitivity to MC change by a K value of 1.09%, followed by 1.93% for longitudinal tensile modulus, 3.08% for shear strength parallel to gain and 3.76% for compression strength parallel to gain. Bending modulus and tensile modulus showed much less sensitivity to MC change than shear strength and compression strength, which can be partially explained by the different response to MC change of the three main components (cellulose, hemicelluloses and lignin) in the plant cell wall. The mechanical properties of lignin/hemicelluloses matrix have been experimentally (Cousins, 1976, 1978) and theoretically (Sakurada et al. 1962; Koponen et al. 1989) proved to be much more sensitive to MC change than cellulose. In the process of shear and compression testing, hemicellulose/lignin matrix gives considerable contribution to the final failure, while for the stiffness measurement both in the tensile and bending modes, cellulose undoubtedly dominates the whole process. Although bamboo also belongs to lignocellulosic materials, their mechanical responses to MC change show some differences from wood. The sensitivity of bending modulus to MC change of bamboo is significantly less than that of tensile modulus, while the former is higher than the latter for wood. That seems to be incapable of being explained by the chemical differences between them, while should be more attributable to the two phase composite structure of bamboo with much softer parenchymal cells embedded in much stiffer fiber bundles. We assumed the MC increase tended to weaken the interfacial bonding between parenchymal cells and fibers, resulting in extra internal slipping and reduced stiffness. Compared with wood, bamboo was lower sensitive to MC change than wood in bending modulus and compression strength, but had higher sensitivity in tensile modulus and comparable sensitivity in shear strength. This suggests that some mechanical properties of bamboo are better than wood in resisting the change of environment humidity.

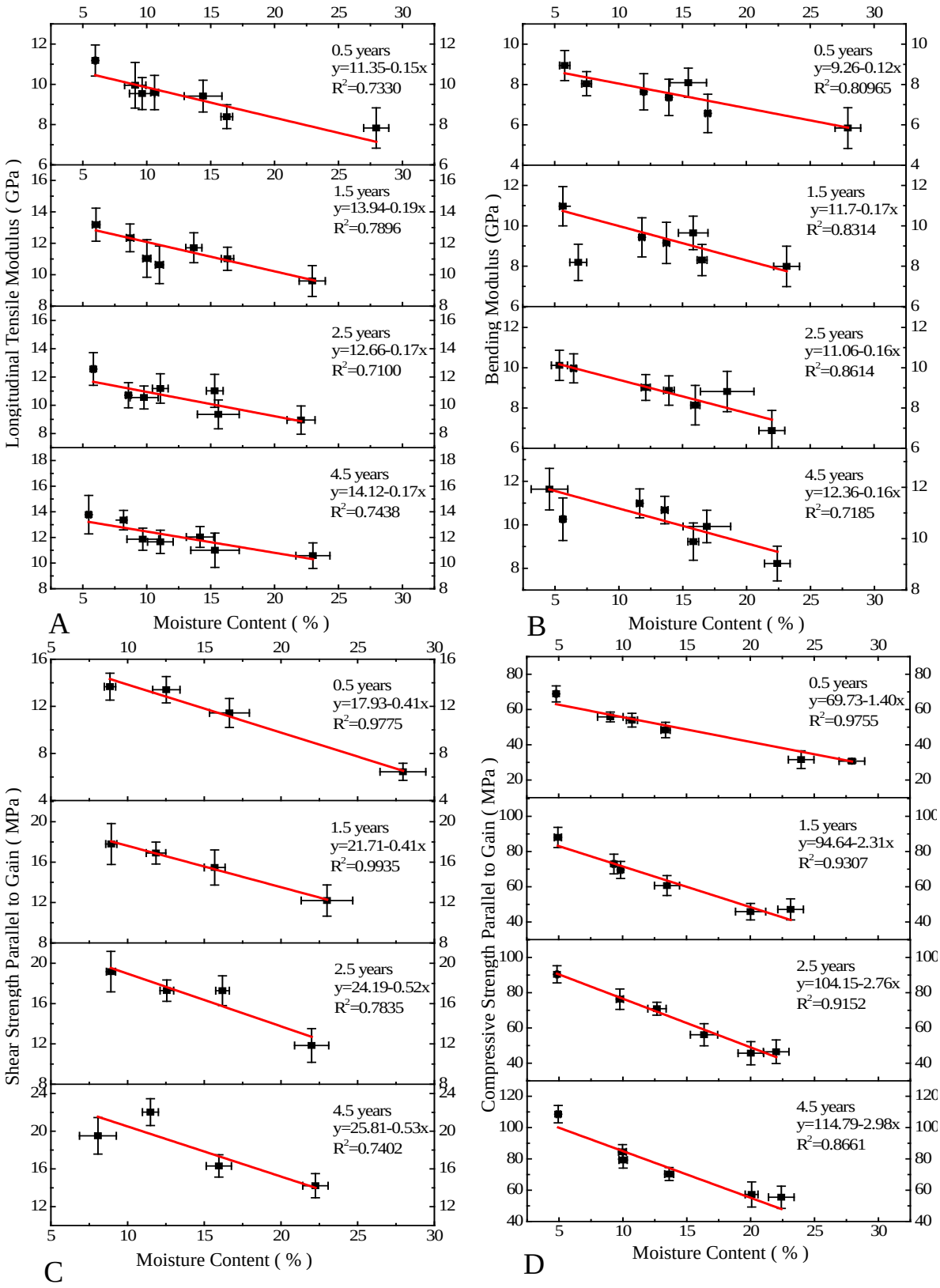

Figure 5 Correlation between the four mechanical properties and moisture content.
A: longitudinal tensile modulus; B: bending modulus; C: shear strength; D: compressive strength.

The effect of ages on the sensitivity to MC change of different mechanical properties of bamboo

In order to further investigate the effect of ages on the moisture dependence of different mechanical properties of bamboo, a linear fitting was performed for the range from MC 5.5% (or 8% for shear strength) to FSP (Figure 5). From the obtained linear equations, it could be inferred the mechanical properties of bamboo with 0.5 years old normally changed smaller in absolute value than that with older ages for per 1% MC change. However, no significant difference was found among the bamboo with 1.5, 2.5 and 4.5 years old in general. Similarly, for further comparing the different sensitivity to MC change of bamboo with different ages, the K value of bamboo with different ages was calculated according to the approach adopted in the last section. The results were plotted in Figure 6.

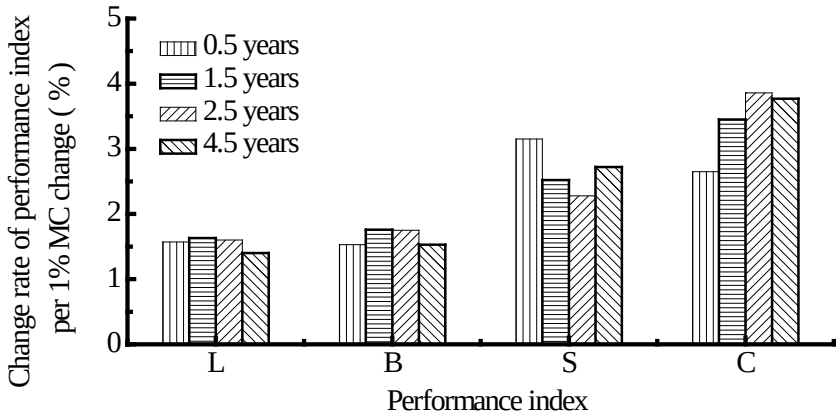

Figure 6. The change rate of different mechanical properties per 1% MC change under different ages
L: Longitudinal tensile modulus; B: Bending modulus; S: Shear strength parallel to gain; C: Compression strength parallel to gain

It seemed bamboo ages affected little on the K value of tensile modulus and bending modulus. However, the K value of shear strength of bamboo with 0.5 years old was a little higher than that of mature bamboo with 1.5 to 4.5 years old, which means young bamboo may be more sensitive to MC change in shear strength. For compression strength, the K value of bamboo with 0.5 years old was significantly lower than that of bamboo with 1.5 to 4.5 years old, which indicates young bamboo may be less sensitive to MC change in compression strength. Why different mechanical properties of bamboo with different ages responded differently to MC change need to be further explored from both microstructure and chemical compositions.

Conclusions

The results of combined investigation of four mechanical properties of bamboo under different MC permit the following conclusions:
Four mechanical properties of bamboo exhibited different sensitivity to MC change. Compressive and shearing strength parallel to gain were most significantly affected by MC, then was longitudinal tensile modulus and followed by bending modulus. The sensitivity of

tensile modulus and bending modulus was little affected by bamboo ages, while young bamboo was more sensitive to MC change than mature one in shear strength parallel to grain and less sensitive in compression strength parallel to grain.

Acknowledgement

We are grateful to the National Natural and Science Foundation of China (31070491) and National Natural and Science Foundation of China (30730076) for financial support.

References Cited

Cousins, W.J. (1976) Elastic modulus of lignin as related to moisture content. Wood Sci. Technol. 10:9–17.

Cousins, W.J. (1978) Young's modulus of hemicelluloses as related to moisture content. Wood Sci. Technol. 12:161–167.

Green D W , Link C L, DeBonis A L, et al. (1986) Predicting the effect of moisture content on the flexural properties of southern pine dimension lumber. Wood Fiber Sci. 18(1) : 134-156

Green D W , Winandy J E , Kretschmann D E. Mechanical Properties of Wood in Wood Handbook. Forest Products Laboratory, Forest Service, USDA : 1999.

Green D W , Evans J W , Barrett J D, et al. (2007) Predicting The Effect of Moisture Content On The Flexural Properties of Douglas-Fir Dimension Lumber. Wood Fiber Sci. 20(1) : 107-131

Hui C M, Yang Y M.Editor-in-Chief. Bamboo timber resources, industrial use. Yunnan Science and Technology Publishing House. Kunming. 1998.

Ishimaru Y, Arai K, Mizutani M, et al. (2001) Physical and mechanical properties of wood after moisture conditioning. J Wood Sci. 47:185-191

Kojima Y, Yamamoto H. (2004) Properties of the cell wall constituents in relationto the longitudinal elasticity of wood. Wood Sci Technol. 37: 427–434

Koponen, S., Toratti, T., Kanerva, P., Koponen, S., Toratti, T., Kanerva, P. (1989) Modelling longitudinal elasticity and shrinkage properties of wood. Wood Sci. Technol. 23:55–63.

Kretschmann, D.E. and Green, D.W. (1996) Modeling Moisture Content-Mechanical Property Relationships for Clear Southern Pine, Wood and Fiber Science. 28(3) : 320-337

Liu Y X, Zhao G J. Wood resource materials. China Forestry Publishing House. Beijing. 2004.

Wang H K, Yu Y, Yu Y S, et al. (2010) Moisture Dependence of Different Mechanical Properties of Bamboo. Journal of Cen tral South Un ivers ity of Forestry & Technology. 32(2): 112-115

Wang S Y, Wang H L. (1999) Effects of moisture content and specific gravity on static bending properties and hardness of six wood species. Wood Sci Technol. 45:127-133

Sakurada, I., Nukushima, Y., Ito, T. (1962) Experimental determination of the elastic modulus of crystalline regions in oriented polymers. J. Polym. Sci. 57:651–660.

Sudijono , Dwianto W, Yusuf S, et al. (2004) Characterization of major, unused, and unvalued Indonesian wood species I. Dependencies of mechanical properties in transverse direction on the changes of moisture content and/or temperature. J Wood Sci. 50:371–374

Zhou F C. Bamboo cultivation school. China Forestry Publishing House. Beijing. 1998.

Synthesis and Characterization of Nanoscale CuO Powders

Jiahe Wang [1] –Fengzhu Li [2] - Min Xu [3]*

[1] Graduate, Key Laboratory of Bio-based Material Science and Technology of Ministry of Education, Northeast Forestry University, Harbin,China.
myted@126.com
[2] Graduate, Key Laboratory of Bio-based Material Science and Technology of Ministry of Education, Northeast Forestry University, Harbin,China.
[3] Professor, Key Laboratory of Bio-based Material Science and Technology of Ministry of Education, Northeast Forestry University, Harbin,China..
xumin1963@126.com
** Corresponding author*

Abstract

Cu(OH)2 precursor was synthesized by direct precipitation method and CuSO4 and NaOH were used as raw materials. Then, Cu(OH)2 precursor was calcined in muffle furnace at 400℃ for 2h in order that CuO particle was obtained. Through the analysis of the factors affecting the CuO, the paper determined the optimum conditions for the synthesis of nano-CuO with the direct-precipitation method. Then the paper analyzed phase composition and crystal structure of samples using X-Ray Diffraction ,according to CuO (111) crystal plane corresponding to the width at half maximum, using Scherrer formula $D = K\lambda / \beta\cos\theta$ calculations, the average grain size of the sample prepared in the optimum conditions is 18nm, we also observed and analyzed by Transmission Electron Microscope to characterize the morphology and particle size of samples, the results showed that The particle size of the sample, synthesized in the optimum conditions was distributed in the 14nm ~ 20nm, which are consistent of the results of Scherrer formula. These nano-powders have uniform particle size and distribution and narrow distribution range. Also these results showed that the development of nano-particles is normal and the preparation conditions is reasonable. The optimum precipitation conditions are as follows: when the precipitation agent is 3.2:1, reaction time 40min and precipitant concentration 0.6mol.L-1. The average size of CuO particle prepared under the conditions is 18nm and the yield is 96%..

***Keywords*:** nano-copper oxide; direct precipitation method; copper yield; Particle size; optimum conditions.

Introduction

Nano-CuO is a versatile nanomaterial. Due to the surface effect, quantum size effect and Kubo effect, the electric, it has broad application prospects in magnetic, catalytic and other areas, particularly in the field of catalytic (Frietsch M et al.2000, Kounmoto K et al.2001). It has a good catalyst in the field of removal of hydrogen sulfide, ammonium perchlorate decomposition and complete oxidation of carbon monoxide, ethanol, ethyl acetate and toluene and other volatile organic compounds, so it has unique excellent performance in sewage treatment, air purification, etc. (Larsson P O and Andersson A,1998). And then it has great significance in the field of production safety, environmental protection and others. Therefore, Preparation of nano-CuO and applied research, in recent year, caused widespread concern (Cui Baochen et al.2004). According to the literature, there are lots of methods to synthesize nano-CuO such as spray method (Zhang Rubing et al.2000), precipitation method (Li Dongmei and Xia xi 2001, Luo Yuanxiang, 2002), and solid-phase synthesis method (YU Jian-qun et al.2000) and so on. Spray method need complicate operation, and solid-phase method is simple, but in the preparation process, it's easy for the introduction of impurities and particles are distributed unevenly. The direct precipitation method has much advantage such as simple operation, less demanding on the equipment, high purity products, and lower cost and facilitating the actual production and other characteristics, so it is the most capable of industrial prospect. Therefore, in this article nano-CuO was synthesized by direct-precipitation method, and then through analyzing the factors affecting the yield of copper, the paper determined the optimum precipitation conditions to synthesize nano-CuO.

Materials and Methods

Methods. In this study, we select main factors affecting nano-CuO field in reaction process as the research object for experimental analysis, which include that: Precipitant dosage, precipitant concentration, reaction time for the preparation of nano-CuO.

Materials. Reagents: Anhydrous copper sulfate, sodium hydroxide, anhydrous ethanol (all analytically pure).Equipment: HH-S-type constant temperature water bath pot, JJ-1-type force increasing timing electric agitator, TM-06120-type muffle furnace, SHZ-D (Ⅲ)-type circulating water pump, 101-2A-type Blast Oven, D/MAX2000 X-ray diffractometer, H-7650 type transmission electron microscope.

Proceedings of the 55th International Convention of Society of Wood Science and Technology
August 27-31, 2012 - Beijing, CHINA

Copper leached from Micronized Copper Quaternary (MCQ) Treated Wood: Influence of the Amount of Copper in the Formulations

Lei Wang and Pascal Kamdem

School of Packaging/ Department of Forestry, Michigan State University, East Lansing, MI, USA 48823

Abstract

The objectives of this study was to evaluate the influence of the amount of copper uptake in the amount of copper leached from Micronized copper quat treated wood at target retention of 3.60 kg/m3. Red pine (*pinusresinosa*) and southern pine were used as softwood reference species. Leaching protocol described in AWPA standard E11 was used. The amount of copper leached from treated wood was proportional to the amount of copper uptake during the treatment in good agreement with data published in the literature for ACQ and MCQ.

The percentage of Cu leached increases with the increase of quatin the formulation suggesting competed reactions between copper and quat for the available interactions sites in wood. This competition between copper and quat made the ratio of CuO to quat in the preservative formulation an important factor to be investigated on the long term efficacy of MCQ treated wood. No considerable difference was observed for red or southern pine.

Key word: ratio of CuO to DDAC, leaching, competition, wood preservative

Introduction

Alkaline copper quat (ACQ) and micronized copper quat (MCQ) are emerging commercial copper based wood preservatives used to replace arsenic and chromium containing formulations to protect wood used for residential and commercial applications where decay and insects are known to be a considerable menace. This emerging formulation contains two major ingredients known to be effective against decay and insects destroying wood for centuries: copper and quaternary ammonium salt. One of the major obstacles of copper based formulations used to treated wood has been the bioavailability of copper versus the migration in the surrounding environment that may create issues on the prediction of their long term efficacy. To alleviate the problem, micronized basic copper carbonate with low water solubility and reduced migration has been proposed in the formulations of copper based preservatives formulations (Zhang and Leach, 2005). However, limited information is available on the migration of the ingredients from treated wood to the surrounding environment, mostly the influence of the amount of quat on the migration/fixation of copper from micronized copper quat treated wood.

It has been proposed andassumed that positively charged copper ions or copper complexes chemically or/and physically interact with the negatively charged phenolate/carboxylate groups of lignin/hemicellulose/cellulose/extractives present in wood to limit the migration of copper in copper preservatives treated wood (Rennie et al. 1987; Cooper 1991; Thomason and Pasek 1997; Kamdem et al. 2001; Ruddicket al. 2001; Cooper and Lee, 2010). The interaction of other positively charges moieties in the formulations such as quaternary ammonium, monoethanolamine (MEA)werereported for the ACQ soluble copper based preservative system by several authors (Tascioglu et al. 2005; Lee and Cooper 2011;Pankras and Cooper 2012).They suggest the existence of competition between copper and other positively charged moieties for the negatively interaction sites in wood.Data for solid copper particulate with low water solubility but dispersed in water formulations containing quat and dispersant are not available in the open literature.

Understanding the interaction of copper and quaternary ammonium salt and wood substrate is useful to predict the long term efficacy of this type of wood preservatives. The objective of this study was to evaluate the amount of copper leached from red pine and southern pine wood treated with formulations of MCQcontaining various proportion of copper oxide toquat using AWPA protocol (AWPA 2009).

Material And Methods

Micronized copper and quaternary salts were obtained graciously from Osmose INC and used as received without further analysis in our formulations. A series of formulations were made using the CuO to quat following ratios: 3:1, 2:1, 1:1, 1:2, and 1:3. A 1% formulation was made afterwards by adding water.

Defect free kiln dried sapwood of red pine and southern pine were selected and used to 19mm cubes with no visible defect. They were placed in a chamber conditioned at 20 °C and 70% to a

constant weight before further testing. Conditioned blocks were selected based on similar density and used for treatments following AWPA E11 (2009).

Copper content in the treating solutions, leachates and treated wood were analyzed by atomic absorption spectroscopy (AAS) following standard protocol listed in AWPA A 11-93 (2007).

Results And Discussion

Tables 1 and 2 listed the copper oxide content in MCQ treating solutions used and the total copper in mg leached from 6 cubes after the leaching periods (2 weeks) for SP and RP, respectively. The copper contents in treating solutions for RP and SP vary from 0.85 to 0.26%, and almost similar for each target concentrations levels.

The total amount of copper leached from treated SYP and RP samples increased with the increase of ratio of CuO toquat in the MCQ formulation. This indicated that more copper leached from high copper retention in good agreement with previous studies on alkali water soluble copper based wood preservatives (Lebow et al 2006). The total amount of copper leached from MCQ treated wood vary with initial copper uptake for wood treated with formulation in the range of CuO to quat ratio used in this study.

Table 3 contains the total copper and the percentage of copper leached from MCQ treated wood at various CuO to quat ratios. This clearly shows that less copper is leached from MCQ treated wood in comparison of alkali water soluble systems published in the literature. A maximum of less than 10% level was observed for the worst case scenario for both species treated with MCQ.At CuO to quat ratio of 2:1, about 4% copper was leached from MCQ treated wood. The Ratio of 2:1 is the ratio commercially used for treatment.

The percentage of copper leached increased with the decrease of ratio of CuO to quat in the preservative formulation. Even though less copper amount contained in the lower ratio of CuO to quat preservative formulation, high percentage of copper leached from the treated both SYP and RP. This strongly suggested that quat competed with the limited available sites in wood with copper. In formulation with low ratio of CuO to quat preservative formulation, more quat is present in the formulation and can compete with copper resulting in less copper interacting with the available sites in wood to form a less mobile/leachable copper.

The pH values of the leachate measured vary from 5.6 to 6.0. Even though the 1% MCQ treating solution used to treat wood was alkaline and ranged from 8.9 to 9.7, the leachate was not influenced that much. The pH values of leaching at less than 6 confirm that leaching was conducted in an acidic environment.The different ratio of CuO to quat used did not influence the pH of leachate too much; therefore pH did not play a major role on the leaching of copper. Low value of copper migration from MCQ treated wood observed here in comparison of water soluble copper based wood preservatives formulations was attributed to the low water solubility of copper used in the formulations of MCQ in good agreement with the previous researches (Cooper and Ung 2009; Wang and Kamdem 2011).

Conclusion

Higher value of copper were leached from RP and SP wood treated with 1% MCQ preservative formulation containing higher levels of CuO and low levels of Quat. However, the value of the percentage of copper leached calculated as the amount of copper leached divided by total copper retention was lower for formulation containing high levels of copper/low quat.

This result strongly suggested that quat competes with copper for the same limited available sites in wood during the treatment. At concentration of MCQ 1%, copper had low leaching resistance when MCQ contained copper less than quat.

References

Cooper, P.A. 1991.Cation exchange adsorption of copper on wood.Wood Protect. 1:9–14.

Cooper, P. A. andUng, Y. T. 2009.Component leaching from CCA, ACQ and a micronized copper quat (MCQ) system as affected by leaching protocol. IRG/WP 09-50261. International research group on wood protection.IRG, Stockholm, Sweden.

Kamdem, D.P., Zhang, J., andAdnot, A. 2001.Identification of cupric and cuprous copper in copper naphthenate-treated wood by X-ray photoelectron spectroscopy.Holzforschung 55:16–20.

Lebow, P., Ziobro, R., Sites, L., Schultz, T., Pettry, D., Nicholas, D., Lebow, S., Kamdem, D. P., Fox, R. and D. Crawford. 2006. Statistical analysis of influence of soil source on leaching of arsenic and copper from CCA-C treated wood. Wood and Fiber Science 38(3): 439-449.

Lee, M. J. and Cooper P. 2010. Copper monoethanolamine adsorption in wood and its relation with cation exchange capacity (CEC). Holzforschung. 64: 653–658.

Lee, M. J. and Cooper P. 2011. Effects of ionic strength, monoethanolamine, copper, and pH on adsorption of alkyl dimethyl benzyl ammonium chloride in wood.Holzforschung. 65: 421–427.

Rennie, P.M.S., Gray, S.M., and Dickinson, D.J. 1987. Copper basedwaterborne preservatives: copper adsorption in relation to performance against soft rot. IRG/WP 87-3452. International

Research Group on Wood Protection. Stockholm, Sweden.

Ruddick, J.N.R., Xie, C., and Herring, F.G. 2001. Fixation of amine copper preservatives: Part 1. Reaction of vanillin, a lignin model compound with monoethanolamine copper sulphate solution.

Holzforschung 55:585–589.

SedricPankras and Paul A. Cooper. 2012. Effect of ammonia addition to alkaline copper quaternary wood preservative solution on the distribution of copper complexes and leaching.Holzforschung. 66: 397–406.

Tascioglu, C., Copper, P. and Ung, T. 2005. Rate and extent of adsorption of ACQ preservative components in wood.Holzforschung. 59: 574-580.

Thomason, S.M. and Pasek, E.A. 1997. Amine copper reaction with wood components: acidity versus copper adsorption. IRG/WP 97-30161.International Research Group on Wood Protection.

Stockholm, Sweden.

Wang, L. and Kamdem, D. P. 2011. Copper Migration from Micronized Copper Preservatives Treated Wood in soil contact: Effect of soil pH. IRG/WP 11-50280. International research group on wood protection. Stockholm, Sweden.

Zhang, J. and Leach, R. M. 2005.Non-alkaline micronized wood preservative formulations.United States Patent Application 200060086284.

Acknowledgement

We would like to acknowledge Osmose, Inc. (Griffin, GA), Michigan State University and China Scholarship Council (CSC).

Table 1 CuO concentration in MCQ treating solution

	MCQ for SP	MCQ for RP
Target CuO concentration (%)	AAS analyzed CuO concentration (%)	AAS analyzed CuO concentration (%)
0.75%	0.85%	0.80%
0.66%	0.70%	0.71%
0.50%	0.51%	0.53%
0.33%	0.35%	0.34%
0.25%	0.26%	0.26%

Table 2 Total Cu amount leached out from six 19 mm treated cubes (mg)

Ratio CuO:Quat	SP	RP
3:1	3.27	3.69
2:1	3.15	3.96
1:1	3.09	3.69
1:2	2.74	3.17
1:3	2.34	2.65

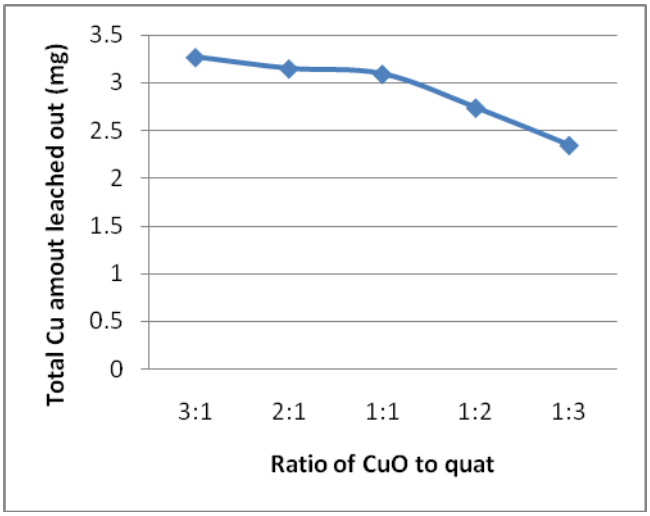

Figure 1 Total Cu amount leached out from treated SP VS ratio of CuO to quat

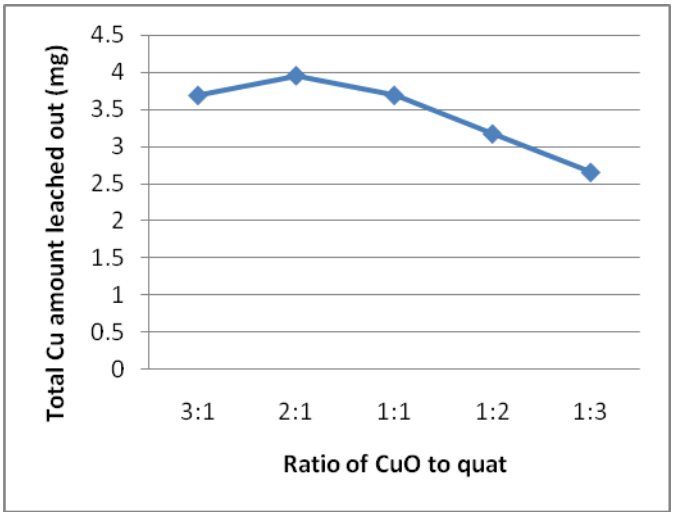

Figure 2 Total Cu amount leached out from treated RP VS ratio of CuO to quat

Table 3Percentage of Cu leached out VS ratio of CuO to quat

SP			
Ratio of CuO to quat	Total Cu amount leached out(mg)	Initial Cu amount (mg)	Percentage of Cu leached out (%)
3:1	3.27	84.96	3.85%
2:1	3.15	81.70	3.85%
1:1	3.09	61.15	5.06%
1:2	2.74	35.87	7.63%
1:3	2.34	26.28	8.91%
RP			
Ratio of CuO to quat	Total Cu amount leached out (mg)	Initial Cu amount (mg)	Percentage of Cu leached out (%)
3:1	3.69	88.82	4.16%
2:1	3.96	78.87	5.02%
1:1	3.69	60.44	6.11%
1:2	3.17	37.29	8.51%
1:3	2.65	29.05	9.13%

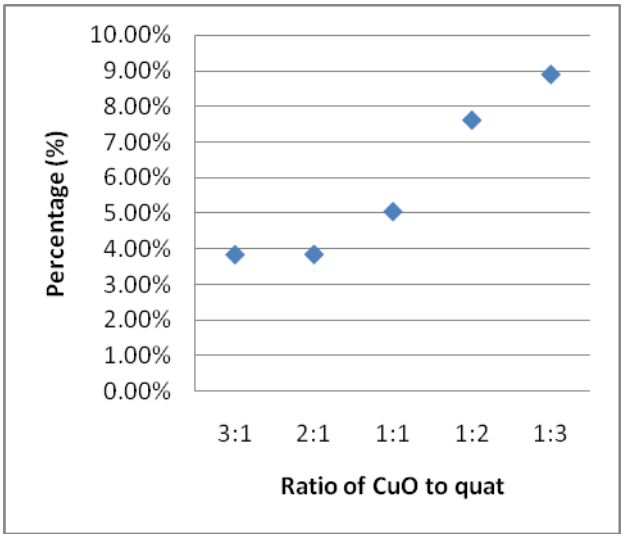

Figure 3 Percentage of Cu leached out from treated SP

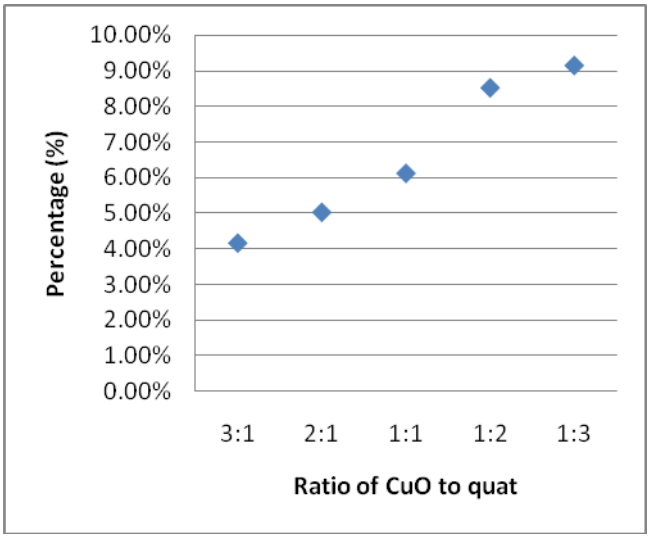

Figure 4 Percentage of Cu leached out from treated RP

Table 4 pH of treating solution

Ratio of CuO to quat	pH of solution for treating SP	pHof solution for treating RP
3:1	9.51	9.53
2:1	9.56	8.87
1:1	9.43	9.71
1:2	9.34	9.45
1:3	9.40	9.49

Table 5 pH of leachate during two weeks leaching process

SP	
Ratio of CuO to	Duration (hour)

quat											
	0 hour	6 hrs	24 hrs	48 hrs	72 hrs	96 hrs	144 hrs	192 hrs	240 hrs	288 hrs	336 hrs
3:1	5.62	5.96	5.98	5.84	5.84	5.93	5.9	5.83	5.97	5.73	5.79
2:1	5.72	5.8	6.00	5.91	6.04	5.91	5.81	5.92	5.93	5.74	5.87
1:1	5.75	5.81	5.97	5.90	5.87	5.96	5.92	5.85	5.86	5.79	5.75
1:2	5.71	5.73	5.9	5.87	5.81	5.84	5.79	5.86	5.77	5.73	5.69
1:3	5.64	5.67	5.87	5.85	5.73	5.8	5.76	5.86	5.74	5.74	5.7
RP											
Ratio of CuO to quat	Duration (hour)										
	0 hour	6 hrs	24 hrs	48 hrs	72 hrs	96 hrs	144 hrs	192 hrs	240 hrs	288 hrs	336 hrs
3:1	5.67	5.73	5.87	5.85	5.82	5.79	5.9	5.79	5.77	5.67	5.77
2:1	5.63	5.68	5.88	5.86	5.85	5.78	5.83	5.72	5.75	5.65	5.72
1:1	5.58	5.63	5.77	5.82	5.84	5.73	5.69	5.63	5.77	5.60	5.67
1:2	5.60	5.76	5.9	5.72	5.78	5.68	5.74	5.65	5.74	5.63	5.6
1:3	5.59	5.63	5.76	5.76	5.8	5.64	5.61	5.57	5.78	5.58	5.64

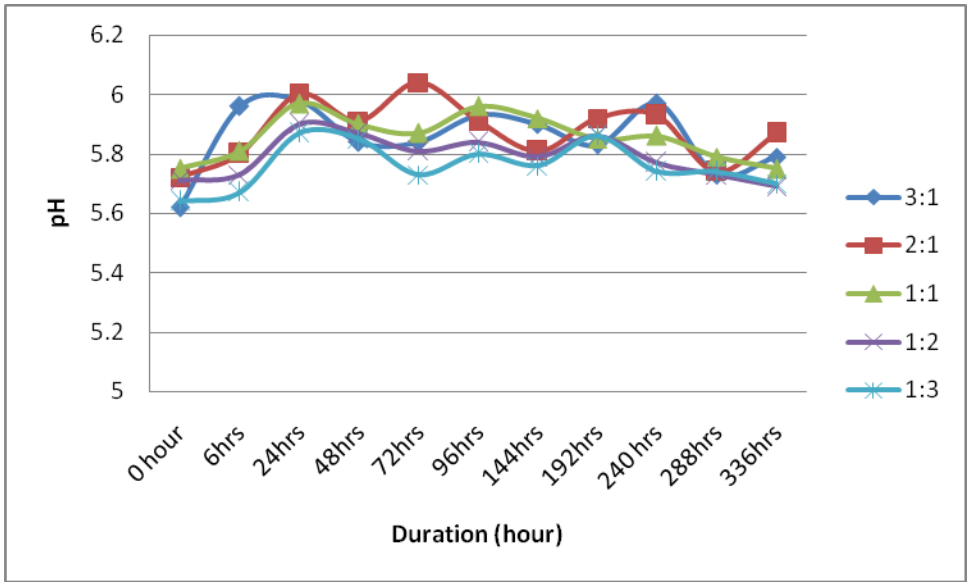

Figure 5 pH of leachate from SP

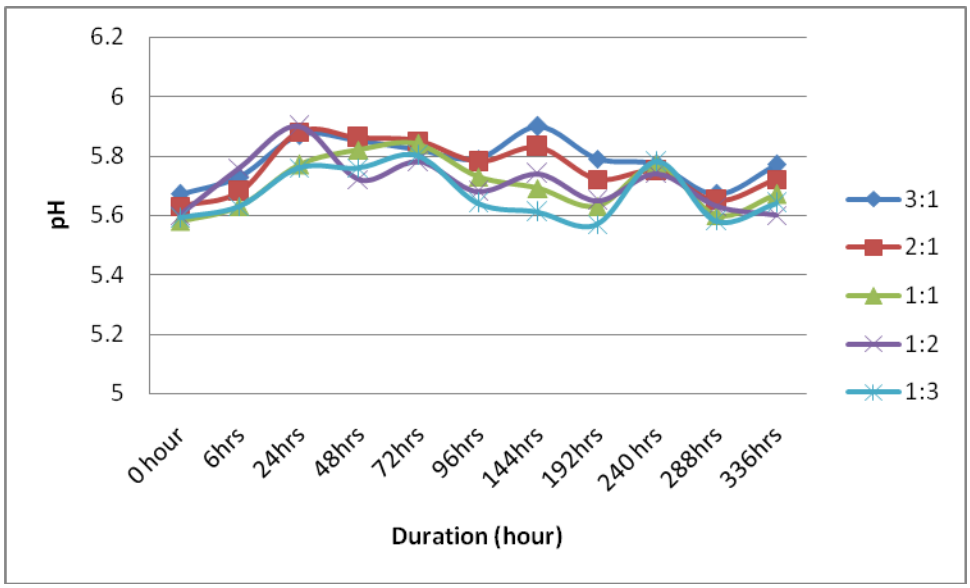

Figure 6 pH of leachate from RP

Influence of Veneers' Lathe Checks on Strain Distribution at Wood-adhesive Interphase Measured by Electronic Speckle Pattern Interferometry (ESPI)

Lu Wang[1] *- Mingjie Guan*[2*] *- Mingming Zhou*[3]

[1] Master Candidate, College of Wood Science and Technology, Nanjing Forestry University, Nanjing Jiangsu, China.

nfuwanglu@hotmail.com

[2] Associate Professor, Ph.D, Bamboo Engineering Research Center, Nanjing Forestry University, Nanjing Jiangsu, China.

**Corresponding author*

mingjieguan@hotmail.com

[3] Master Candidate, College of Wood Science and Technology, Nanjing Forestry University, Nanjing Jiangsu, China.

Zhoumingming2011@hotmail.com

Abstract

When lathe checks exist in veneers, adhesive will penetrate excessively along them into wood substrate causing strain alteration at bonding interphase under loads, which affects the overall bonding strength of board. We plan to apply ESPI (Electronic Speckle Pattern Interferometry) to study the effect of lathe checks on the strain distribution at wood-adhesive interphase and to find a solution against the lathe checks. A sealing treatment is supposed to be figured out to improve the low bonding strength of board due to over-penetration of adhesive without adding more adhesive to veneers.

Keywords: veneers' lathe checks, sealing treatment, bonding interphase, ESPI, strain distributio

Introduction

With growing attention on global ecological changes and environmental problems, more rational and effective use of forest resources has been emphasized. From this point, wood adhesives and adhesion will be the significantly important factor. For peeling veneers, adhesive will penetrate along lathe checks into deep part of wood substrates and affect the geometry of interphase, which would ultimately have a significant impact on the performance of the bond (Kamke 2007). Thus, it is critical to investigate the influence of checks on the geometry and bond performance of wood components.

Fluorescence microscopy was found superior to other optical techniques for observing adhesive distribution among interphase where there is poor color contrast (Kamke 2007). Electronic speckle pattern interferometry (ESPI) is an optical 3D gauging technique which has been demonstrated by a few authors that this new technique is applicable to wood surfaces and allows analysis of multiaxial sample deformation (Dumail 2000 and Jernkvist 2001). For example, the strain distribution along wood bond lines of lap joint specimen was studied (Muller et al. 2005), the measurements showed that a very small volume of material close to the ends of the overlapping area was highly strained.

In the present work, we characterized the influences of lathe checks on the geometry of interphase by fluorescence microscopy, as well as the strain distribution at the interphase of phenol formaldehyde resin (PF) glued components using ESPI to understand the effect of lathe checks on wood-adhesive interphase.

Materials and Methods

Materials. Peeling and planing veneers of poplar (*Populus Euramevicana Cv.*) with dimensions of 400mm×400mm×3mm and 180mm×70mm×5mm respectively were both from South Wood Technology Ltd. (Lian Yungang, China). The process of self-made phenol formaldehyde resin was as follows: phenol, water and sodium hydroxide were added to reactor and stirred at a temperature range of 40-45℃. The first part of formaldehyde (80% of total amount) was added and the liquid in the reactor was heated up to 80-85℃. After reaction for 45min, the water was warmed up to boiling for 10min. Then the liquid was cooled to 40-45℃to accept the left formaldehyde. The total solution was reacted at 85-90℃for 80min. Finally, the reaction mixture was cooled down to room temperature and poured out. The formula and property of adhesive can be found on Table1. The process of self-made soy adhesive was as follows: defatted soy flour was added to water slowly and stirred for 15min until no massive substance was observed. Then sodium hydroxide (concentration of 30%) was put in the suspension and stirred until it became sticky. The mass ratio of components was soy flour: sodium hydroxide: water=100:15:400.

Table1 Formula and property of PF adhesive

Resin	F：P Ratio	NaOH （%）	Solid content （%）	Viscosity （mPa.s）
PF adhesive	1.5	8.8	46.3	36

Sealing treatment on interface between wood and adhesive. Ordinary soybean adhesive was chosen as sealant and spread on the surface of veneers having checks prior and laid aside for 30min. Then PF adhesive covered the sealed the surfaces of veneers which were laid up parallel to longitude with the checks on both sides facing each other. The assembly was pre-loaded for 30min before hot-press. Double-side glue application of soy adhesive was 150 g/m^2, single-side glue application of PF adhesive was 150 g/m^2. The parameters of hot-press were 140℃1min/mm, 2.6MPa.

Characterization of adhesive penetration into wood. Slices of 20μm were achieved with microtome (YAMATO TU-213). The slices were stained for 30min with toludine blue water solution with a concentration of 0.5%. Finally, sections were observed under microscopy (Olympus BX51). The optical filter set used consisted of a 450-480nm excitation filter, 575nm dichromatic mirror and a 500nm emission filter. Specific process can be obtained via reference (Kamke 1992).

Strain distribution measurement along wood bondline. The basic principle of the ESPI technique can be explained by the example of a Michelson interferometer (Gerthsen et al. 1986 and Muller et al. 2005). The specimens were sawed according to the dimension in Figure 1. Tensile tests were performed on lap shear samples as shown in Figure 2 using a manually loading device combined with a TS-SI-1XP ESPI (Suzhou, China). Since the available device here can only detect the displacement of one dimension, in order to achieve the shear strain, measurements parallel and vertical to bondline were conducted respectively. The size of the field of view observed with ESPI was 45 mm by 36 mm. A pre-tension of 15 N were imposed on specimens and 8 steps of strain with an increment of 2 N. Thus, total load of 31N were applied to specimens, which ensured only elastic deformation of the samples. A speckle image of the field of view was taken at each displacement step. The displacement maps were calculated by summing up information from all 8 displacement steps. The stack of speckle images obtained was stored on computer and used for deformation calculation after the mechanical experiments. Post-processing of the speckle images was performed with Matlab software. The strain components, i.e., axial strain ε_x, ε_y, γ_{xy} can be calculated from the 2D deformation field according to equations (Eqs.(1), (2) and (3)).

$$\varepsilon_x = \frac{\partial u}{\partial x}, \quad (1)$$

$$\varepsilon_y = \frac{\partial v}{\partial y}, \quad (2)$$

$$\gamma_{xy} = \frac{1}{2}\left(\frac{\partial v}{\partial x} + \frac{\partial u}{\partial y}\right), \quad (3)$$

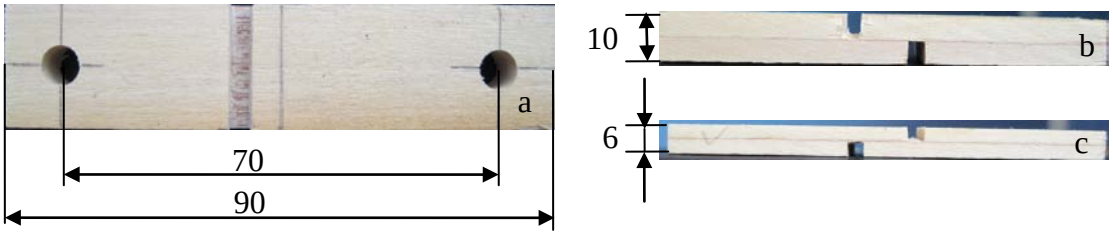

Fig. 1 Dimensions (mm) of shear samples from planing veneers (a, b) and peeling veneers (c).

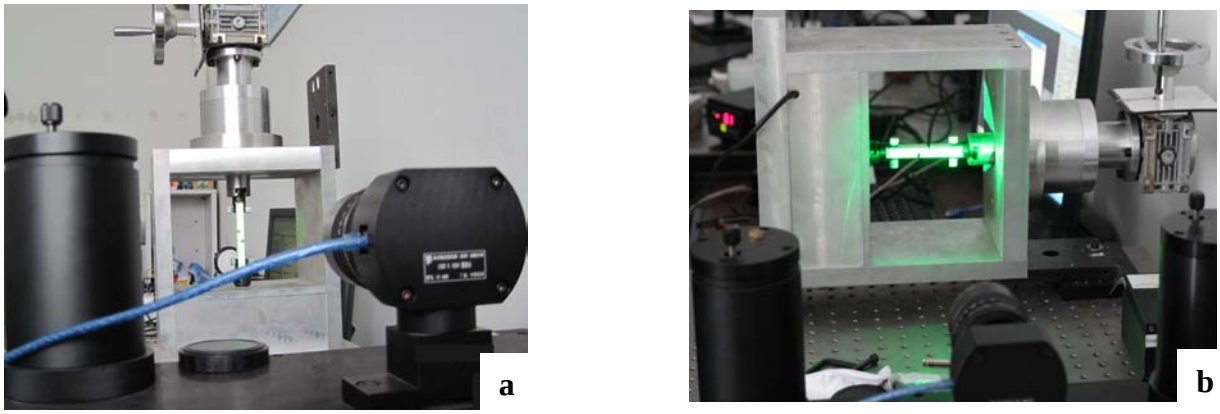

Fig. 2 Tensile shear experiments on samples by ESPI vertical (a) and parallel (b) to bondline.

Results and Analysis

Influence of sealing treatment of veneer surface on PF penetration into poplar. The images of sections were processed by ImageJ image analysis software (http://rsb.info.nih.gov/ij/) and performance index of penetration were shown on Table 2. The EP is the total area of adhesive detected in the interphase region of the bondline divided by the width of the bondline. The MP is the average distance of penetration of the five most distant adhesive objects detected within the field of view. Specific process of measurements can be achieved via reference (Sernek 1999).

Table2 Performance index of PF penetration into wood

Material type	Soy adhesive consumption g/m^2	MP μm	EP μm	Adhesive penetration area（%）
Planing veneer	0	596	44	3.5
Peeling veneer	0	921	113	7.1
	75	756	98	5.8

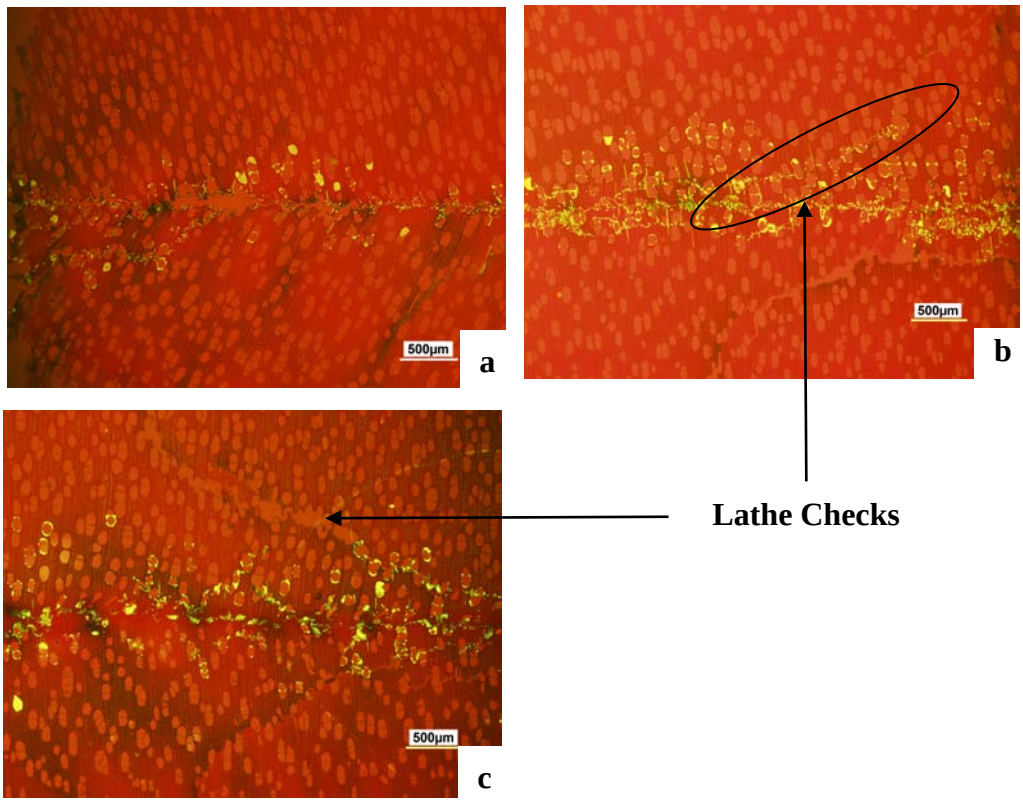

Fig. 3 Fluorescent graphs of planing-veneer based sample (a) and peeling-veneer based sample without (b) and with (c) sealing treatment.

It can be informed from Figure 3 and Table 2 that due to the lathe checks, the EP and MP of PF into peeling veneer were much more than those of planing veneer, because checks provide accessible paths for adhesive into deep part of wood. Then, spreading soy adhesive on veneer surfaces before applying PF adhesive could efficiently prevent adhesive from over-penetration into wood. The MP descended by 18%, EP decreased by 13%. The reason might be that soy adhesive fills the macro gaps such as checks and cell lumen, thus channels for adhesive into wood substrates are reduced. Moreover, soy with modified protein and existence of soluble carbohydrates can absorb moisture (Hunt et al. 2010) from PF adhesive, increasing the viscosity of adhesive.

Strain distribution at wood-adhesive interphase. Figure 4 showed that compared to planing-veneer based sample, peeling-veneer based sample had higher strain as a whole. Besides, the former owned higher strain at interphase than at wood substrate, while the latter's strain tended to be homogeneous. Because PF penetrated into deep part of wood substrates, which could dissipate the shear stress from bulk adhesive into softer substrates, creating greater strain at these areas.

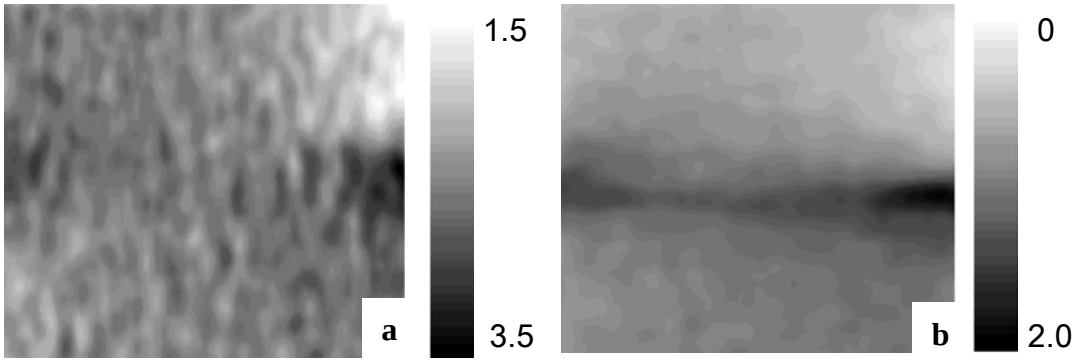

Fig. 4 Shear strain of peeling-veneer based sample (a) and planing-veneer based sample (b). Scale bars indicate strains multiplied by 10^{-3}.

As indicated in Figure 5, these two kinds of samples had high strain concertration at both ends of the overlapping area along the bondline. However, peeling-veneer based sample had higher strain (2.8×10^{-3}) than planing-veneer based sample (1.2×10^{-3}) did. Due to the over-penetration of PF into veneer, the bulk adhesive does not have enough adhesive left in the bondline to form a strong bridge between the substrate (Frihart 2005), leading to generate higher strain under load.

Ground on the results of Figure 6, sample with sealing treatment owned less strain (1.8×10^{-3}) compared to that (2.8×10^{-3}) without treatment did, owing to effective blocking of PF over-penetration, as a result, stress from bulk adhesive couldnot be transferred to deep substrate. Meanwhile, the bulk adhesive strain of the former(2.0×10^{-3}) was less than that of the latter (2.9×10^{-3}) as a result of enhancement on mechanical srength of bulk adhesive with sealing treatement withstanding over-penetration. It should be mention that the strain of sample with treatment still tended to be homogeneous. Maybe two-lay peeling-veneer LVL has thin thickness and low mechanical strength, reulting in deformating easily under load.

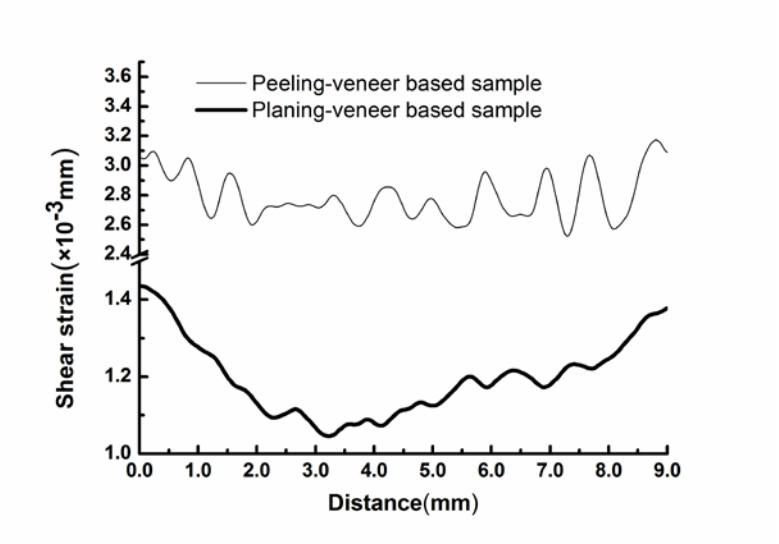

Fig. 5 Shear strain distribution along the bondline of peeling-veneer based sample and planing-veneer based sample.

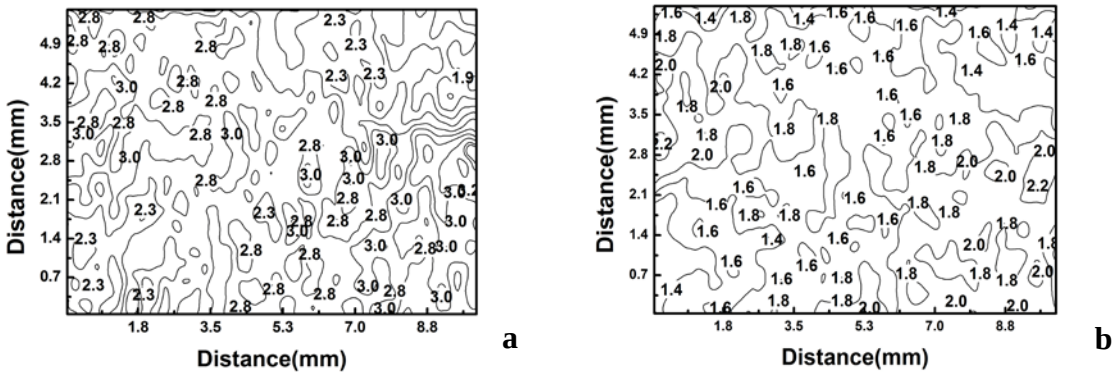

Fig. 6 Shear strain distribution on the observed field of peeling-veneer based samples without (a) and with (b) sealing treatment.

Conclusions

Fluorescence microscopy analysis showed that spreading soy adhesive on peeling veneer surfaces before applying PF adhesive can efficiently prevent adhesive from over-penetration into wood. As indicated in the ESPI test, as a whole, planing-veneer LVLs owned less strain than peeling-veneer LVLs did. Peeling-veneer LVLs with sealing treatment had lower strain than that without treatment did. Thus, sealing treatment can decrease the interphase strain of peeling-veneer based LVL. .

Acknowledgement

This research is from Jiangsu State Nature Science Foundation of China (BK2011822) and Science & Technology Specific Project for Enriching People and Strengthening County

Economy of China (BN 2010207).

References

Dumail, J.-F., Kenneth, O., Salmen. L. 2000. An analysis of rolling shear of spruce wood by the Iosipescu method. Holzforschung. 54: 420-426.

Frihart, C.R. 2005. Utility of Horioka's and Marra's models for adhesive failure. In: Wood Adhesives 2005; 2005 November; San Diego, CA. Forest Products Society, Madison, WI, pp. 233-238.

Gerthsen, C., Kneser, H.O., Vogel, H. 1986. Physik. Springer-Verlag, Berlin, Heidelberg, New York, Tokyo. 504–508 pp.

Hunt, C., Wescott, J., Lorenz, L. 2010. Soy Adhesive-Moisture Interactions. In: Wood Adhesives 2009. South Lake Tahoe, CA, Forest Products Society, Madison, WI, pp. 280-284.

Jernkvist, L.O., Thuvander, F. 2001. Experimental determination of stiffness variation across growth rings in *Picea abies*. Holzforschung. 55: 309-317.

Kamke, F.A., Johnson, S.E. 1992. Quantitative analysis of gross adhesive penetration in wood using fluorescence microscopy. J. Adhesive, 40:47-61.

Kamke, F.A., Jong, N.L. 2007. Adhesive penetration in wood-A review. Wood and Fiber Science. 39(2): 205-220.

Muller, U., Sretenovic, A., Vincenti, A., Gindl, W. 2005. Direct measurement of strain distribution along a wood bond line–Part I: shear strain concentration in a lap joint specimen by means of electronic speckle pattern interferometry. Holzforschung. 59: 300-306.

Sernek, M.J., Resnik, Kamke, F.A. 1999. Penetration of liquid urea formaldehyde adhesive into beech wood. Wood Fiber Sci. 31(1):41–48.

Selected Properties Of Bamboo Scrimber Flooring Made Of India Melocanna Baccifera

Mingjie Guan[1] - Cheng Yong[2] - Lu Wang [3] - Qisheng Zhang[4]*

[1] Ph.D, Associate Professor, Bamboo Engineering and Research Center, Nanjing Forestry University, Nanjing, Jiangsu, China
* *Corresponding author*
mingjieguan@hotmail.com
[2] Master Candidate, College of Wood Science and Technology, Nanjing Forestry University, Nanjing, Jiangsu, China
yongcheng0520@hotmail.com
[3] Master Candidate, College of Wood Science and Technology, Nanjing Forestry Univesity, Nanjing, Jiangsu, China
nfuwanglu@hotmail.com
[4] Professor, Bamboo Engineering and Research Center, Nanjing Forestry University, Nanjing, Jiangsu, China
Zhang-qs@njfu.com.cn

Abstract

Melocanna baccifera (Muli) is difficult to be used for common flooring material for its small-diameter, thin culm wall. To understand technique feasibility to produce bamboo scimber flooring from *Melocanna baccifera* rolled bundles, we produced three types of the bamboo scimber flooring, that is, Muli-nature, Muli-carbonized, and Muli-mixed together and properties were tested and compared with those of Moso-nature. The results showed that Muli scrimber flooring had better performance than Moso-nature bamboo scrimber flooring in China. The order of MOR was Muli-nature>Muli-carbonized> Muli-Mixed>Moso-nature and MOE trend was similar. It is supposed that Muli bamboo can be processed into not only scrimber flooring to replace the high-value hardwood flooring, but also other special engineered composite with its high-strength.

Key words: bamboo, scrimber, flooring, rolled bundles

Introduction

Bamboo industry has developed many engineered bamboo based composites such as plybamboo, woven bamboo plywood, bamboo flooring and so on in the world (Liese W. 1987) , especially many bamboo-based engineered products with Moso bamboo in China (Qisheng Zhang et al. 2002). In recent two decades, bamboo scrimber has become poplar as a new composite flooring with high density and hardness like hard wood such as teak and oak. Bamboo scrimber is also called recombination or reconstructed lumber in China (Qin.Li et al. 2000**),** "zephyr board " in Japan (Naresworo Nugroho. Naoto Ando.2000, 2001) whose relevant researches emerged at the beginning of 1990's, aiming at using the small-diameter bamboo culms as the raw material to make the reconstructed structure material by the method of wood scrimber (Hutchings BF, Leicester RH. 1988, Jordan BA .1989). By now, Moso bamboo scrimber has been a substitute for solid wood-based material in furniture industry in China with its good properties (Guan M.J and al. 2009, Zhang B.Y. 2008).

In northeast of India, there are so large natural forest of *Melocanna baccifera(*Muli bamboo) distributing in Mizoram, Tripura and other states. Muli bamboo is 3-5mm in thickness of culm wall and 4-8cm in diameter, much thinner than those of Moso bamboo in China. Therefore，it is difficult to be used for common bamboo flooring with strip as unit for its small-diameter and thin wall. Local farmer and government are eager to find a way to use Muli bamboo as raw material for industry product to benefit the local farmer and economy development.

Therefore, this research aims to study the technology feasibility of Muli bamboo being used as raw material of bamboo scrimber flooring by using Chinese Moso bamboo scimber process and equipment to understand properties of Muli bamboo products totally.

Materials and Methods

Materials

Muli bamboo(*Melocanna baccifera***)** sliver was processed in Tripura of India and transported into appointed testing factory in Zhejiang Province, China, cooperating with Bamboo Engineering and Research Center, Nanjing Forestry University.

Muli bamboo sliver：9 **~** 15mm×2 **~** 3mm×2400mm(width×thickness×length)

weight, 700kg; moisture content, 9-12%; bamboo age, 2-2.5 years. Half of Muli bamboo slivers were carbonized and dried together with nature slivers. Then slivers were processed by roll machine into net-like bundles and impregnated with phenol formaldehyde resin(solid content is about 23%) for 15min and drained. Then the glued muli bamboo bundles were dried to 12-15% moisture content to prepare for forming and hotpress.

The slivers were divided into three color, nature, carbonized, mixed(nature and carbonized. See Fig.1) to form three color board in 12mm×1.22m×2.2m.

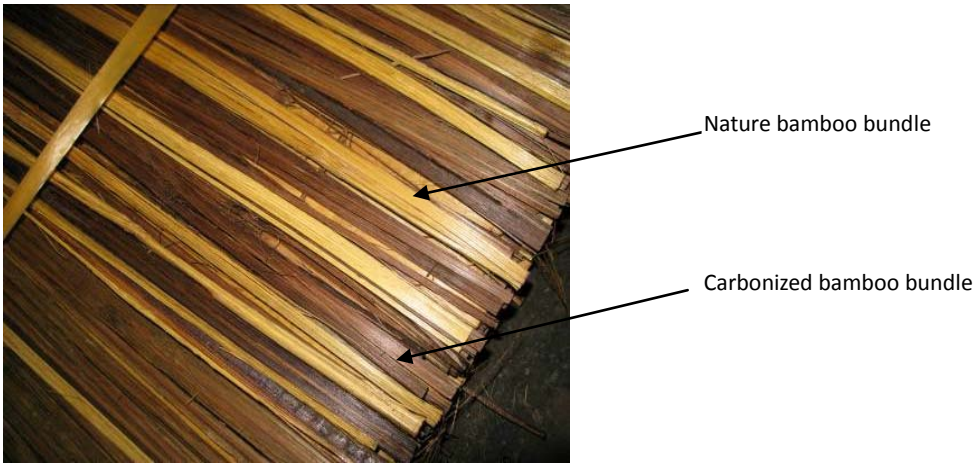

Fig1. Mixed color mat with nature and carbonized bamboo bundles

Hotpress parameters: Temperature, 135℃; Pressure, 60MPa; Press type, cold-hot-cold; Time, 20min. The boards were sawed into 12mm×100mm×2.2m and conditioned +for 21 day to balance the moisture and inner stress and then were processed into the flooring in size of 10mm×1.0m×96mm without paint on the surface by planing and sand machine.

Methods

Basic properties test

Test of Muli bamboo scimber flooring was mainly based on the method of Chinese national standard, GB/T 17657—1999. The testing items included density, moisture content, modulus of rupture (MOR), modulus of elasticity(MOE) of bamboo scrimber flooring. Ten specimens were prepared for each test.Sizes of samples for density, MC, water absorption were 50mm by 50mm by 10mm, and those of MOR and MOE were 50mm by 220mm by10mm. During statistic bending test, the span was 200mm, load speed was 6mm/min and loading/supporting blocks' diameter were 30mm. In order to compare with Moso scrimber flooring, nature Moso bamboo scrimber (hereinafter Moso nature) was also tested here.

Hardness test

Muli bamboo scribmer flooring without paint was test by modified Janka ball test as described by ASTM D1037. Each specimen was 75mm in width and 75 mm in length. Because the scrimber board was 10mm in thickness, less than 25mm, three specimen were glued together to achieve the required thickness for hardness test. Ball diameter was 11mm and penetrated into half of it diameter. Speed of test was 6mm/min and maximum load required to embed the "ball" to half of its diameter was recorded. The hardness of all specimens were tested after reaching EMC at 65% RH. In addition, other properties of the materials such as density, MC, and MOR, MOE were also measured under this condition.

Results And Discussion

Density, MC and water absorption

The mean density, MC, and water absoption of Muli bamboo scrimber flooring and Moso scimber flooring without paint are summarized in Table 1.

Table 1 Density, MC and 24h cold water absorption

Materials	Density(g/cm^3)	MC(%)	24h cold water absorption (%)
Muli-Nature	1.24(0.02)	9.63(0.24)	4.28(0.16)
Muli-Carbonized	1.35(0.01)	7.13(0.9)	3.38 (0.31)
Muli-Mixed	1.29(0.01)	7.72(0.18)	3.27 (0.56)
Moso-nature	1.09(0.05)	8.32(0.21)	3.67(1.36)

Each value is the average of 10 specimens and numbers in parentheses are standard deviation

Dimensional swelling

Fig. 2 showed the results of grain, cross, thickness swelling of Muli bamboo scrimber and Moso nature scrimber flooring. As it showed, the thickness swelling in bamboo scrimber flooring was greater than grain swelling and cross swelling with maximum value is below 5%. Muli-nature had the highest swelling among the four kinds of bamboo scrimber. Carbonized Muli bamboo showed the reduced swelling in cross and thickness direction compared to nature, which indicated the carbonized treatment had certain effect on improving the dimension stability of bamboo scrimber flooring, though grain swelling was a little higher. Three Muli bamboo scrimber showed higher swelling value than that of Moso bamboo scrimber in China, maybe because Muli scrimber has higher density than Moso bamboo does. Muli bamboo is thin in culm wall with higher distribution of vascular bundles than Moso bamboo, which can cause the higher density and higher dimension swelling. After painting on the surface, Muli and Moso bamboo scrimber should have lower dimension swelling.

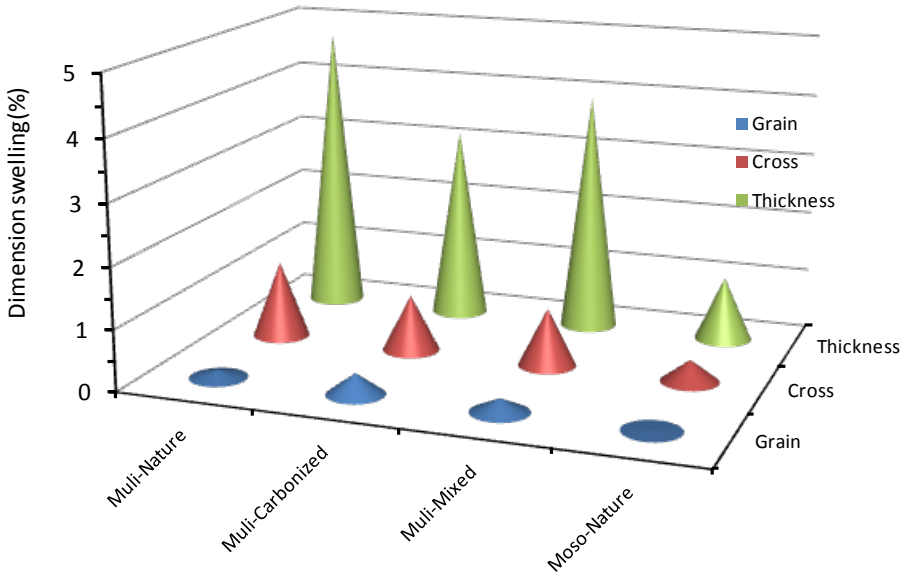

Fig.2 Dimension swelling of Muli bamboo scrimber and Moso scrimber flooring

Static bending property and hardness

Table 2 showed the results of static bending properties and hardness of Muli and Moso bamoo scrimber. As a whole, the static bending properties and hardness of Muli bamboo scimber were higher than those of Moso-nature bamboo scimber flooring, partly because the density of Muli-based scribmer is higher than that of Moso bamboo. MOE and MOR decreased accordingly from Muli-nature, carbonized, mixed to Moso-nature. Therefore, carbonized treatment not only changed the nature bamboo to dark coffee-like color, but also reduced its static bending properties. As far as hardness is concerned, carbonized Muli bamboo scrimber flooring performed the maximum value. Static bending properties of Muli bamboo scrimber were about 10% higher than those of Moso bamboo scrimber flooring.

Table 2 Static bending properties and hardness of Muli and Moso bamboo scrimber flooring

Materials	MOR(MPa)	MOE(MPa)	Hardness(KN)
Muli-Nature	265.88(12.66)	15218 (313)	22.8(1.96)
Muli-Carbonized	257.73(7.71)	14085 (136)	24.27(2.85)
Muli-Mixed	229.65(17.19)	13080 (109)	22.57(2.31)
Moso-Nature	202.73(7.66)	11433 (454)	16.06(2.76)

Each value is the average of 10 specimens and numbers in parentheses are standard deviation

Conclusions

Based on the results of the above study, the following conclusions about Muli bamboo scrimber flooring without paint can be drawn. Muli bamboo scrimber flooring showed much higher density, above 1.2g/cm^3, and their dimension swelling values were higher than those of Moso nature bamboo scrimber floring. Static bending properties and hardness were about 10% higher than those of Moso nature bamboo scrimber flooring. The order of MOR and MOE was Muli-nature>Muli-carbonized>Muli-Mixed>Moso-nature. In the same manufacturing process parameters of Moso bamboo scrimber, Muli bamboo had very high performance except for dimension swelling values. With so exciting results of Muli bamboo scrimber, it is supposed to be used not only as flooring but as a new high strength engineered composite in future.

Acknowledgement

This research is from Jiangsu State Nature Science Foundation(BK2011822) and Chinese and India cooperation project(Tripura 220476). A Project Funded by the Priority Academic Program Development of Jiangsu Higher Education Institutions, PAPD also support this work. The research was also supported by the Scientific Research Foundation for Postgraduat e of the Higher Education Institutions of Jiangsu Province, China (CXLX11_0537).

References

Liese W. 1987.Reseach on bamboo . Wood Science Technology.21:180-209

Zhang,Q.S, Jiang, Sh.X. Tang,Y.Y., 2002. Industrial utilization on bamboo, Technical Report No.26, International Network for Bamboo and Rattan

Hutchings BF, Leicester RH. 1988. Scrimber. In: Proceedings of the 1988 international conference on timber engineering. Vol 2, pp 525-533

Jordan BA .1989.Scrimber: the leading edge of timber technology. In: Proceedings of 2 n~ pacific timber engineering conference, Vol 2: 13-15

Li, Q. Wang,K.H. Hua,X.Q. Weng,P.J. He.Q.J. 2002. Experimental research on recombination bamboo timber made from small-sized sundry bamboo timber(In Chinese). Journal of Bamboo Research. 21(3):33-36

Naresworo Nugroho. Naoto Ando. 2001. Development of structural composite products made from bambooII: fundamental properties of bamboo zephyr board. Journal of Wood Science,; 47:237--242

Naresworo Nugroho. Naoto Ando. Development of structural composite products made from bamboo I: fundamental properties of bamboo zephyr board. Journal of Wood Science, 2000;46:68-74

Guan M J, Lin Zh.M, Zhu, Y.X; 2009. Shrinkage and swelling properties of

recombinant bamboo (In Chinese). Journal of Bamboo Research. 28(3):38-41

Zhang B.Y. 2008. Recombined bamboo, a new sustainable development material for good quality furniture (In Chinese). Furniture, No.164 /3:64-65

Aguilera A, Martin P. 2001.Machining qualification of solid wood of Fagus silvática L. and Picea exelsa L.: cutting forces, power requirements and surface roughness. Holz Roh-Werkst; 59(6):483

GB 17657-1999.Test methods of evaluating the properties of wood-based panels and surface decorated wood-based panels. General administration of quality supervision, inspection and quarantine of the People's Republic of China

Unveiling the Structural Heterogeneity of Bamboo Lignin by in-situ HSQC NMR Technique

Jia-Long Wen[1] – Bai-Liang Xue[2] – Feng Xu[3]–Run-Cang Sun[4]*
[1] PHD student, Institute of Biomass Chemistry and Technology- Beijing Forest University, Beijing, China
wenjialonghello@126.com
[2] Master student, Institute of Biomass Chemistry and Technology- Beijing Forest University, Beijing, China
xuebailiang67@163.com
[3] Professor, Institute of Biomass Chemistry and Technology- Beijing Forest University, Beijing, China
xfx315@163.com
[4] Professor and director, Institute of Biomass Chemistry and Technology- Beijing Forest University, Beijing, China
rcsun3@bjfu.edu.cn
* *Corresponding author*

Abstract

One of the primary challenges for efficient utilization of lignocellulosic biomass is to clarify the complicated structure of lignin. In this study, in-situ HSQC-NMR characterization of the structural heterogeneity of lignin polymers during successively treated bamboo was emphatically performed without componential separation. Specially, the NMR spectra were successfully obtained by dissolving the acetylated and non-acetylated bamboo samples in appropriate deuterated solvent ($CDCl_3$ and DMSO-d_6). The heterogeneous lignin polymers in bamboo samples were demonstrated to be HGS-type and partially acylated at the γ-carbon of the side chain by p-coumarate and acetate groups. The major lignin linkages (β-O-4, β-β, and β-5, etc.) were assigned and the frequencies of the major lignin linkages were quantitatively obtained. In particular, the residual enzyme lignin (REL) contained a higher amount of syringyl units and less condensed units as compared to other samples. Inspiringly, the method gives us a vision to track the structural changes of plant cell wall (e.g. lignin polymers) during the different pretreatments.

***Keywords*:** Pretreatment · Bamboo lignin · *in-situ* NMR technique · S/G ratios · β-O-4 linkage · DMSO/NMI

Introduction

With the inevitable decrease in supply of petroleum-based resources and mitigate the pressure of greenhouse gas, lignocelluloses, such as agricultural and forest residues, have been viewed as sustainable alterative resources for producing energy and chemical feedstock because of their huge abundance and sustainability [1]. However, one of the primary challenges for efficient utilization of lignocellulosic biomass is to clarify their complicated structure. In the past, researchers have focused on characterization of the chemical structures of various components in the plant cell walls (cellulose, hemicelluloses and lignin). In general, waxed-free kibbling samples or ball-milling preparations are required for common isolation and spectroscopic analysis of its components. The methods have played a very significant role in plant chemistry; however, they only focus on one component of cell-wall, could not provide panoramic structural features or changes of the whole cell-wall components *via* an un-isolated approach, i.e. *in-situ* approach. Ideally, the chemical structure of the cell wall and its components should be identified in intact samples containing the native cell wall [1]. Thanks to the advanced NMR techniques, the *in-situ* characterization of plant cell wall has been primitively achieved [2]. This developed method can be used in tracing the structural changes of biomass during fungal treatments [3]. In consideration of the fact that current conversion of biomass to biofuels is detrimentally impacted by its native recalcitrance [4, 5], such as the adverse impact of lignin and hemicelluloses, the method of *in-situ* characterization gives us enlightenment to track the structural changes of plant cell wall during the continuous pretreatments, especially the evolution of lignin structure during successive treatments.

In the present study, in-situ solution-state 2D-HSQC NMR technique was applied to investigate the structural inhomogeneity of lignin polymers (acetylated samples) in the bamboo during sequential treatments (regeneration and enzymatic hydrolysis treatment). In addition, the enzymatic hydrolysis bamboo (EB and REB, non-acetylated), which could be used as a raw material for developing lignin-based products, were subjected to in-situ analysis to track the structural changes of lignin polymers and the lignin-carbohydrate complex (LCC) during the enzymatic treatment. Furthermore, the ball-milled bamboo undergone consecutive treatments were also analyzed by GPC to estimate the possible changes of the corresponding molecular weight distributions during the successive treatments.

Materials and Methods

Materials. Solvents (Dimethylsulfoxide and *N*-methylimidazole, DMSO and NMI) used were AR grade and supplied by Beijing chemical company, Beijing, China. Deuterated chloroform was purchased from Sigma Chemical Co. (Beijing, China).
The cellulolytic enzyme used in this study was Celluclast 1.5 L, kindly supplied by Novozymes, China. It had a filter paper activity of 70 FPU/g.

Bamboo, *Bambusa rigida sp.* was obtained from Sichuan, China. The bamboo culms were dried in an oven at 50 °C, followed by grinding to obtain particles with a size

distribution between 450-900 μm (20-40 mesh). The subsequent treatment with a mixture of toluene/ethanol (2:1, v/v) in a Soxhlet extractor for 12 h removed most extractives. Klason lignin in the de-waxed bamboo was determined to be 23% via NREL method (Determination of Acid-Insoluble Lignin in Biomass). The de-waxed sample was then dried at 60 °C in an oven for 16 h prior to ball milling with a planetary ball mill (FritschGMBH, Idar-Oberstein, Germany) for 5 h. The milling bowl was composed of zirconium dioxide (500 ml) and contained 25 zirconium dioxide balls (1 cm diameter). The milling was conducted at room temperature under N_2 atmosphere with a milling frequency of 500 rpm. To prevent overheating, 10 min breaks followed by 10 min of ball-milling. MWL, which represents the native lignin released by aqueous dioxane (96%, v/v), was prepared according to the classical procedure.

Dissolution and Acetylation of Bamboo Meal in DMSO/NMI. Dissolution and acetylation of bamboo cell walls was conducted according to a previous paper [6].

Successive Treatments of Ball-milled Bamboo. The detailed procedures for handling the ball-milled bamboo are shown in Figure 1. In this section, the successively acetylated samples (Ac-EB, AC-REB, Ac-CEL, Ac-RCEL, Ac-REL, and Ac-RREL) were obtained.

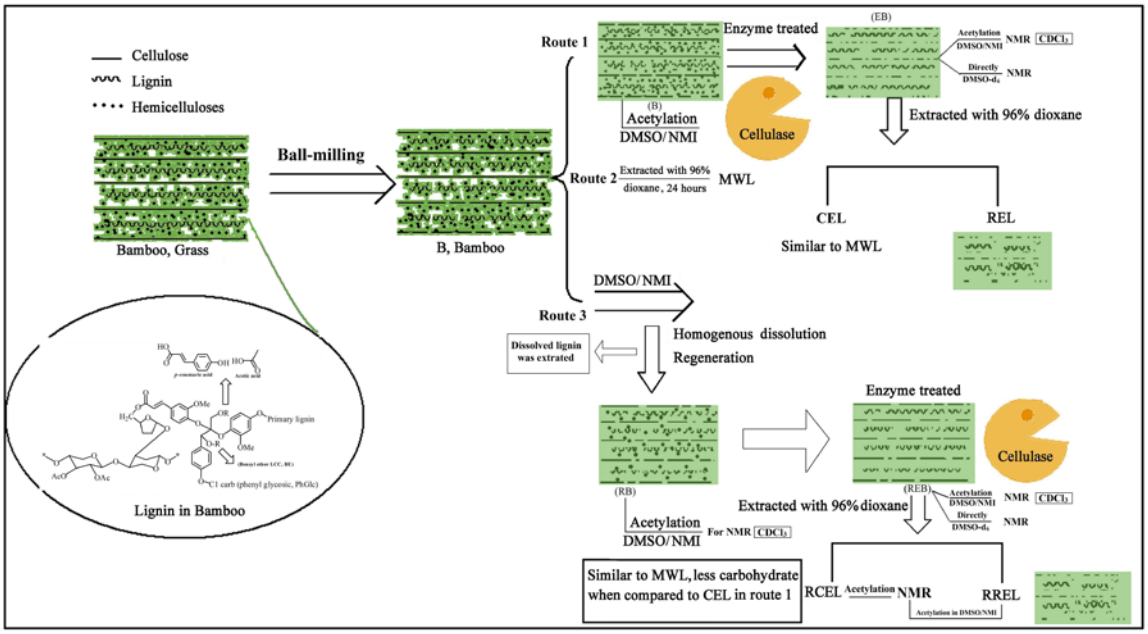

Figure 1. Scheme for *in-situ* characterization of bamboo during successively treatments

NMR Spectra of acetylated and non-acetylated Bamboo Samples. Quantitative Heteronuclear Single Quantum Coherence (Q-HSQC) NMR spectra were recorded on a 400MHz NMR spectrometer (Avance III, Bruker, Germany) with a 5 mm BBO probe at 300 K according to the literature with minor modifications [7].

Results and Discussion

The schematic diagram of successive treatments is illustrated in Figure 1. The purpose of this work was to unmask the structural changes of lignin polymer in biomass (grass, bamboo) during the regeneration and enzymatic hydrolysis. During the processes, lignin-rich residues were obtained. Whether the structural features of lignin changed in the residues prompt us to investigate the inhomogeneity of the lignin polymer in the residue. More importantly, in the current bio-ethanol production, the structural features of enzymatic hydrolysis residue (EB and REB) should be clarified prior to subsequent utilization.

Structural Analysis of Lignin in the acetylated Bamboo Samples during various Treatments. 2D ^{1}H-^{13}C HSQC NMR spectra were used to track the structure heterogeneity of the lignin in the treated bamboo samples by simple acetylation in DMSO/NMI mixture in this study. Figure 2 shows the HSQC spectra (side-chain region) of the acetylated bamboo samples (RB, REB, RREL, and RCEL). The HSQC spectra of acetylated cell walls (softwood and hardwood) have been obtained by the equal dissolved system [6]. However, only the signals for cellulose and aromatic region of lignin polymer were obviously distinguished. The side-chain region of lignin was still overlapped with numerous signals of carbohydrate, which was deemed to impede the in-situ characterization of lignin by NMR techniques. In this study, the successively treated samples were used to unmask the structural heterogeneity of lignin in bamboo *via in-situ* method. It was found that the samples (B and RB) show distinct signals for β-O-4 (**A**) and methoxy group (**OMe**). However, other inter-linkages signals, such as β-β (**B**), β-5 (**C**), and β-1 (**D**) are overlapped with other signals for carbohydrates. After enzymatic hydrolysis, REB shows the unequivocal signals of lignin, especially the distinguishable side-chain of spectra as compared to that of RB (Figure 2). However, the spectra of EB and REB were found to be similar except for different abundances. The CEL preparations extracted from the original and regenerated ball-milled bamboo were also used for characterization of lignin polymer. However, the CEL obtained based on DMSO/NMI regenerated system (i.e. RCEL) was only used for structural analysis since a previous study has demonstrated that the CEL from original and regenerated ball-milled wood presented a similar structure feature, just differed in the yield [8]. In addition, the final residue REL (i.e. RREL) after RCEL extraction, which rarely be used for structural analysis of lignin *via* liquid NMR technique due to its limited solubility, was also investigated by 2D-HSQC NMR *via* acetylating the residue in DMSO/NMI dissolving system. Furthermore, more distinct signals for lignin polymer were found in the order of RB < REB < RCEL. However, RREL was observed to contain less lignin polymer since the lignin exposed after enzymatic hydrolysis was mostly separated as RCEL by 96% aqueous dioxane.

The distinguishability of the spectra was significantly improved after enzymatic hydrolysis of RB. It was found that REB shows a similar spectrum to that of RCEL (Figure 2). Therefore, the REB was selected to illustrate the lignin structure in this study. The C-H correlations from all major lignin substructures (β-O-4, β-β, β-5, and β-1), can be readily assigned. The prominent correlating signals observed are the methoxyl groups (**OMe**, δ_C/δ_H 55.6/3.76 ppm) and β-O-4 aryl ether linkages. The C_α–H_α correlation in β-

O-4 substructures (**A**) was observed at δ_C/δ_H 74.1/6.02 ppm. The signals located at δ_C/δ_H 76.6/5.07 and 80.3/4.59 ppm are attributed to the **G**-type and **S**-type of β-O-4 (β-position), respectively [8]. The C_γ–H_γ correlation of β-O-4 structure was probably at about δ_C/δ_H 61.0-63.0/4.19-4.4 ppm, which is seriously overlapped with **Glc6** correlating signals. In addition, the C_γ–H_γ of acylated β-O-4 was not clearly observed. The C_α–H_α, C_β–H_β, and C_γ–H_γ correlations of the resinol **B** (β-β) substructures appeared at δ_C/δ_H 85.6/4.70, 71.7/3.92-4.28, 54.3/3.08 ppm, respectively [16]. The correlations at δ_C/δ_H 88.2/5.49, 50.2/3.77 ppm are originated from the C_α–H_α, C_β–H_β of the phenylcoumaran **C** (β-5) structures. However, their C_γ–H_γ correlations were overlapped with other signals. In addition to these linkages, the C_α–H_α, C_β–H_β, and C_γ–H_γ correlations (δ_C/δ_H 133.0/6.60, 123.0/6.30, and 64.2/4.7 ppm) in *p*-hydroxycinnamyl alcohol end groups (**F**) and the C_β-H_β correlation (δ_C/δ_H 57.5/2.98 ppm) of spirodienone substructure (**D**), was also tentatively assigned [9]. Even in the residue (RREL), the main substructures, such as β-O-4, β-β, β-5, and *p*-hydroxycinnamyl alcohol end groups could also be assigned (**A**, **B**, **C** and **F** unit, depicted in Figure 5). Therefore, the data presented in the spectra suggest that the structure of RREL was similar to those of native lignin. However, the RREL was not easily dissolved in DMSO due to the association with carbohydrates, which was agreement with a previous study [10].

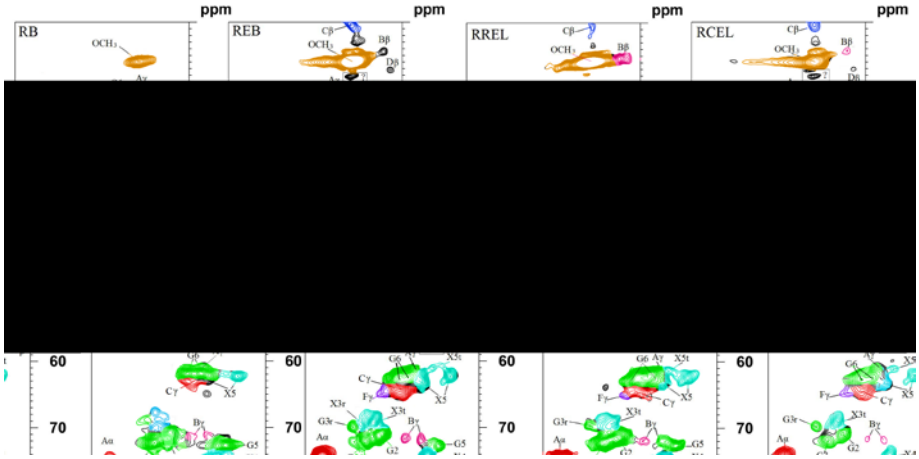

Figure 2. The side-chain region of HSQC spectra of the treated bamboo samples (acetylated)

In the aromatic regions of the HSQC spectra of different acetylated bamboo samples (B, RB, EB, REB, RREL, and RCEL, shown in Figure 3), cross-signals from syringyl (**S**), guaiacyl (**G**), and *p*-hydroxyphenyl (**H**) lignin units could be distinctly observed. The **S**-type lignin units showed a prominent signal for the $C_{2,6}$–$H_{2,6}$ correlations at δ_C/δ_H 104.1/6.59 ppm whereas the **G**-type lignin showed different correlations for C_2–H_2, C_5–H_5, and C_6–H_6 at δ_C/δ_H 110.7/6.96, 116.0/6.80, and 120.1/6.87 ppm, respectively. Signals corresponding to $C_{2,6}$–$H_{2,6}$ correlations in C_α-oxidized **S** units (δ_C/δ_H 105.7/7.17 and 106.1/7.47 ppm) are presented in the HSQC spectra (B, EB, REB, and RCEL), but were not found in the spectra of RB and RREL. This fact suggested that the oxidized lignin fractions derived from ball-milling was extracted in the initial regeneration process (Figure 3, Route 3). However, some oxidized lignin fractions probably released after enzymatic hydrolysis process, as shown in REB and RCEL (Figure 4). The correlations for the C_6–H_6 in oxidized α-ketone structures **G'** was tentatively assigned in the spectrum

of RCEL. Furthermore, the $C_{2,6}$–$H_{2,6}$ aromatic correlating signals from **H** units were clearly observed at δ_C/δ_H 128.8/7.05 ppm.

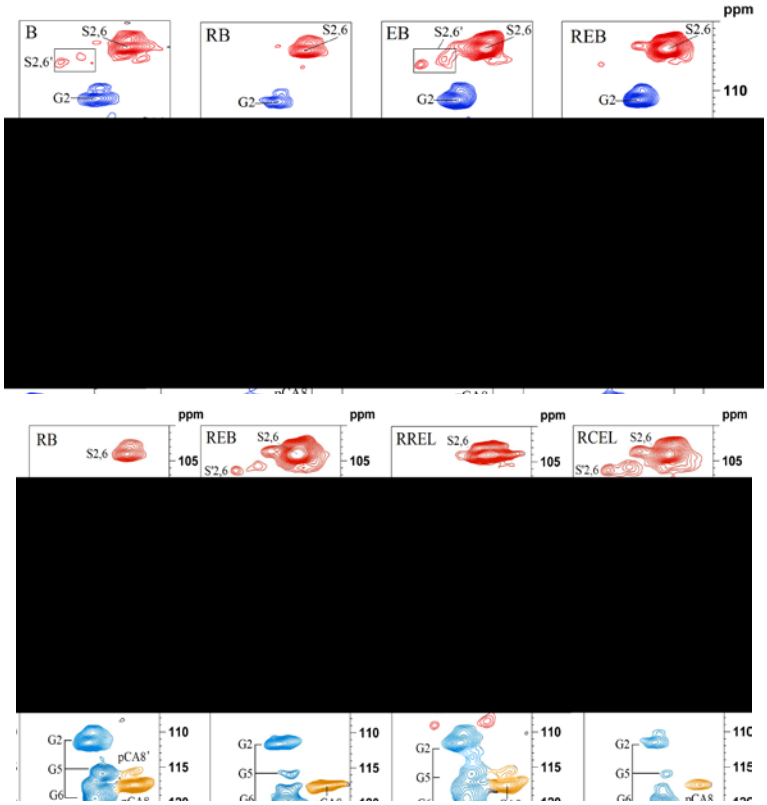

Figure 3. The aromatic regions of HSQC spectra of the acetylated samples

A previous report indicated that *p*-coumaric acid (***p*CA**) is acylated at C-γ of lignin side chain in grass species [11]. To clarify the existence of the acylated ***p*CA** in the bamboo samples, the HSQC spectra of *in-vitro* acetylated bamboo samples were detailedly investigated. The $\boldsymbol{pCA_{2/6}}$ correlations in the acetylated bamboo samples are found at δ_C/δ_H 129.3/7.48 ppm, and $\boldsymbol{pCA}_{3,5}$ correlations at δ_C/δ_H 122.0/7.08 ppm. However, the $\boldsymbol{pCA_{3/5}}$ and $\boldsymbol{pCA_{2/6}}$-correlations were found at δ_C/δ_H 115.8/6.83 and 130.2/7.48 ppm in non-acetylated bamboo cell walls. The $\boldsymbol{pCA_8}$ gave a correlation at δ_C/δ_H 117.4/6.33 ppm, while the corresponding signal in the non-acetylated samples was found at δ_C/δ_H 113.9/6.29 ppm [2]. In consideration of the migration of chemical shifts value (δ) of the correlative signals of $\boldsymbol{p\text{-}CA_{3/5}}$ and $\boldsymbol{p\text{-}CA_8}$ to low field (high δ value) after acetylation, therefore, the *in vitro* acetylation was demonstrated to occur at C-4 of ***p*-CA**. Besides, the question that whether the ***p*-CA** acylated at C-γ of lignin still remain uncertain from the spectra. Adding the accessional evidence of the subsequent HSQC spectra of non-acetylated bamboo samples, the analysis suggested that the *in-vitro* acetylation was occurred at C-4 (phenolic hydroxyl group) of ***p*-CA**. In addition, ***p*-CA** was esterified to the C-γ of the side-chain of lignin in the evolutionary process of the bamboo.

Structural Analysis of Lignin in the non-acetylated Bamboo Samples during various Treatments. Chemical modification of the cell wall, even simple derivatization, leads to

the loss of some information. For example, natural acetylation in the wall is masked when the sample is per-acetylated. To detect the possible changes of the bamboo samples after *in vitro* acetylation with acetic anhydride in DMSO/NMI system, the enzymatic treated bamboo samples (EB and REB) were subsequently examined by NMR without derivatization. Fortunately, the EB and REB were found to be entirely dissolved in DMSO-d_6 under ordinary ultrasonic bath for a few hours. Figure 4 shows the HSQC spectra of the RB and REB as well as MWL.

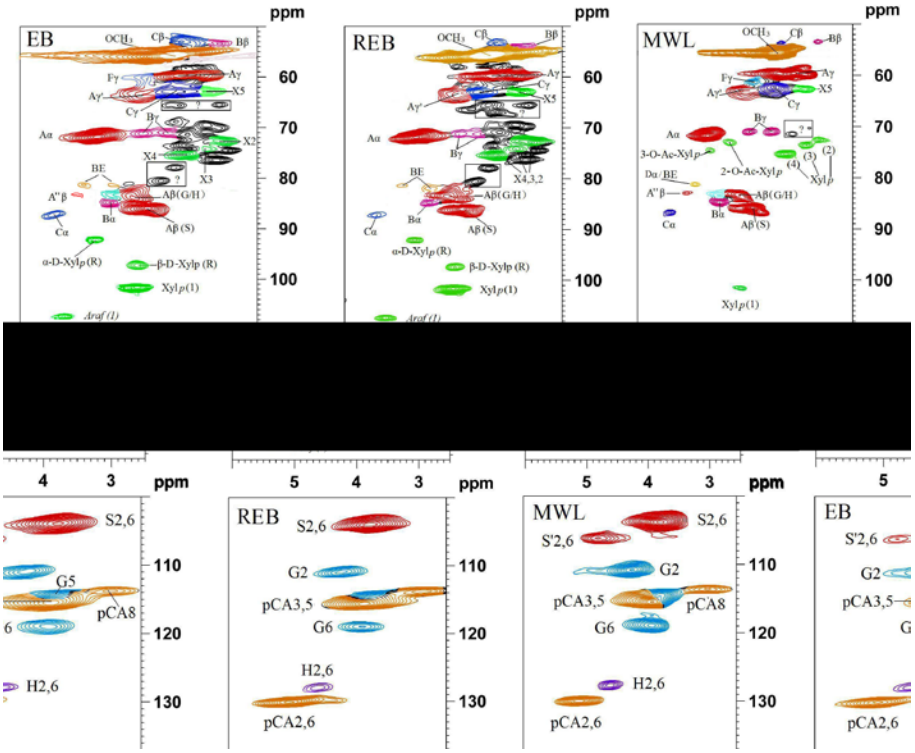

Figure 4. HSQC spectra of EB, REB, and MWL (non-acetylated)

Lignin Side-Chain Regions. In this section, the two non-acetylated samples (EB and REB) and MWL were directly dissolved in DMSO-d_6 to investigate the structural features of lignin polymers. It was found that they provide remarkably well resolved spectra that can be compared to that of MWL in the present study (Figure 4). The important correlations, such as those from substructures of β-ether (β-O-4) **A**, resinol (β-β) **B**, and phenylcoumaran (β-5) **C** can be readily assigned according to the recent literatures [2]. Interestingly, oxidized substructure β-ether (β-O-4) A" were also found in the spectra of MWL and EB rather than REB according to previous reports [12]. The fact that oxidized substructures appeared in the initial extraction and treated sample were in agreement with the acetylated samples that discussed aforementioned.

The question that whether the ***p*CA** acylated to C-γ of lignin in the enzymatic treated bamboo samples were clarified by the chemical shifts of ***p*CA$_8$** in the non-acetylated bamboo samples (EB, REB and MWL). It was observed that the ***p*CA$_8$** correlations are located at δ_C/δ_H 113.9/6.29 ppm in these samples. In addition, the ***p*CA$_{2/6}$** correlations are at δ_C/δ_H 130.2/7.48 ppm, and their 3, 5-correlations at δ_C/δ_H 115.8/6.83 ppm are overlapped with those from guaiacyl units in these non-acetylated bamboo samples. The ***p*CA$_7$** correlation (δ_C/δ_H 144.8/7.51) is also noted. The signals observed are highly

consistent with the reported NMR data for *p*-coumarate units [2]. In addition to the obvious signals of *p*-coumarate units, minor signals for ferulate (**FA**), which is believed to be responsible for cell wall cross-linking in grasses, are also well resolved. The $\mathbf{FA_2}$ and $\mathbf{FA_6}$ correlations were observed at δ_C/δ_H 110.7/7.35 and 123.1/7.17 ppm (not displayed in the current contour level), respectively. Moreover, $\mathbf{FA_7}$ correlation coincides with that of *p*CA7 at δ_C/δ_H 144.8/7.51 ppm.

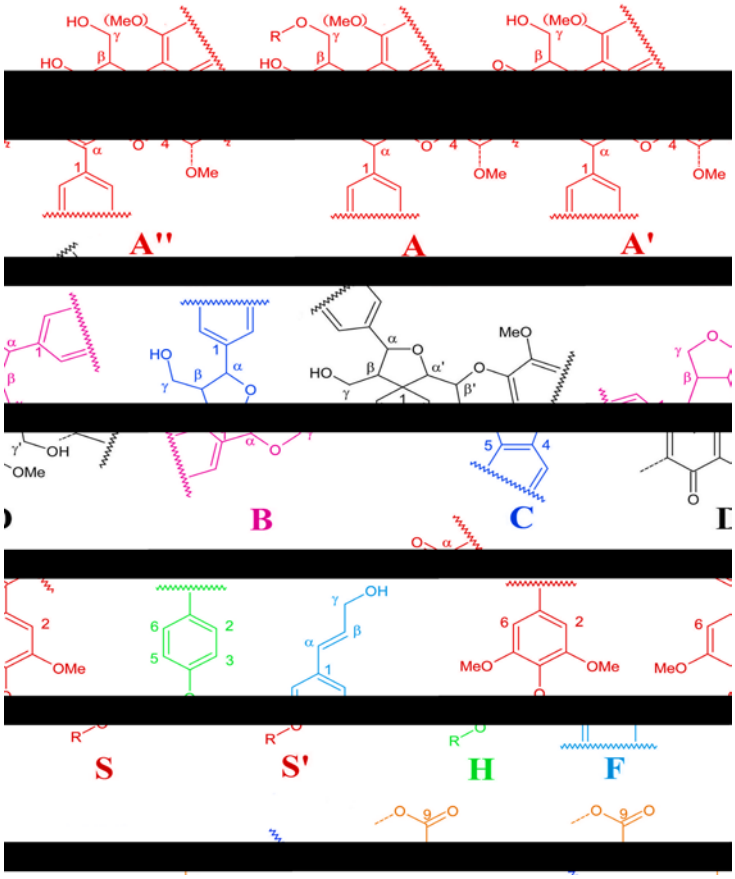

Figure 5. Main lignin substructures in the treated bamboo samples (A) β-O-4 linkages; (A') acylated β-O-4 substructures; (A") Cα-oxidized β-O-4 linkages substructures (B) resinol structures formed by β-β/α-O-γ/γ-O-α linkages; (C) phenylcoumarane structures formed by β-5/α-O-4 linkages; (D) spirodienone structures formed by β-1 linkages; (S) syringyl unit; (S') oxidized syringyl unit linked a carbonyl or carboxyl group at Cα (phenolic); (H) p-hydroxyphenyl units; (F) *p*-hydroxycinnamyl alcohol end groups; (G) guaiacyl unit; (G') oxidized guaiacyl units with a Cα ketone; (FA) ferulate; (*p*-CA) *p*-coumarate.

Quantitative Analysis of Lignin Structures in the Bamboo Samples during various Treatments. In order to maximize the utilization of enzymatic hydrolysis residue, the quantitative information of its structural features should be investigated. A recent published 2D-HSQC NMR quantitative method was applied to estimate the lignin coupling bond in hardwood and softwood samples [13].

According to the methods, it was found that the frequencies of β-O-4 coupling bonds in all the samples are ranged from 47.53-54.55/100Ar. The amounts of β-O-4 linkage were observed to be high in Ac-RB and Ac-REB as compared to that of Ac-B and Ac-EB. This suggests that Ac-B and Ac-EB are more degraded preparations whereas Ac-RB

and Ac-REB undergone less degradation from the bamboo samples studied. As expected, the content of β-O-4 in Ac-REB was between that of Ac-RCEL and Ac-RREL because that REB was fractionated into RCEL and RREL. Moreover, the content of β-O-4 linkage in REB, RCEL, and RREL was decreased in the order of Ac-RCEL > Ac-REB > Ac-RREL (Table 1).

Table 1. Quantitative characteristics of the lignin in the treated bamboo samples by *in-situ* NMR technique

Sample	*β-O-4* [a]	*β-β* [a]	*β-5* [a]	***S/G*** [b]
Ac-B	51.11	0.95	ND	1.42
Ac-RB	48.95	0.81	0.45	1.36
Ac-EB	54.55	5.48	3.45	1.35
Ac-REB	50.97	2.78	1.67	1.61
Ac-RCEL	52.50	2.02	0.88	1.71
Ac-RREL	47.96	1.12	ND	1.80
EB	47.68	6.60	2.65	1.37
REB	47.53	5.33	3.58	1.60
MWL	49.01	7.07	2.17	1.77

[a] results express per 100 Ar based on quantitative 2D NMR (eq 1)
[b] S/G ratio obtained by the this equation: S/G ratio $=IS_{2,6}/2/IG_2$
ND, not detected

The different **S/G** (syringyl to guaiacyl) ratios in the samples studied (Table 1) are caused by fractionation during different handling processes [14]. It is worth estimating the **S/G** ratio of the different bamboo samples during the regenerated and enzymatic process. It was estimated that the **S/G** ratios for B and RB were 1.63 and 1.46, respectively. The lower **S/G** ratio of RB was probably due to the removal of a small lignin fragment rich in **S** units during the regenerated process. Similar result indicated that **S**-rich lignin fragments were firstly released during the delignification process [15]. However, after enzymatic treatment, the **S/G** ratios for acetylated EB and REB were estimated to be 1.37 and 1.61, respectively. Similar **S/G** ratios were observed in the non-acetylated bamboo samples (EB and REB, Table 3). In addition, the **S/G** ratios of RCEL and RREL (from REB) were calculated to be 1.71 and 1.80, respectively. Interestingly, it was found that the residue RREL was abundant with **S** units in this study. This was in agreement with a recent report [16]. They also found that ASAM residual lignin from beech wood was rich in syringyl units. On the basis of higher **S/G** ratio and non-detectable amount of condensed unit β-5 (REL), a likely speculate is that RREL contained less condensed units than those of RCEL and REB. Furthermore, the different chemical reactivities between syringyl and guaiacyl units ($R_S < R_G$) also added some clues to such low amount of condensed units. Coincidentally, a previous report also indicated that REL is less condensed units than that of MWL [10].

Conclusion

The chemical composition changes of bamboo during successively treatments were characterized by *in-situ* HSQC NMR technique without component isolation. The regenerated cell wall showed higher enzymatic efficiency than the original bamboo. However, the obstinate cellulose still remained in the RREL, suggesting that the cellulose was not easily degraded even after regeneration process. In addition, the fact that the

acetyl groups linked to xylans were cleaved during the treatment with cellulase suggested that the esterifiable acetyl groups were sensitive to cellulase (celluclast 1.5 L) and the cellulase preparation probably possess esterase activity.

Another important objective, unveiling the structural heterogeneity of lignin during enzymatic treatment by *in-situ* NMR (HSQC) techniques (acetylated and non-acetylated samples) was also successfully performed. The major lignin substructures (β-O-4, β-β, and β-5, etc.) and various LCC linkages (benzyl ether and phenyl glycosidic linkages) were assigned in the successively treated samples. In addition, the various frequencies of β-O-4, β-β, and β-5 linkages and **S/G** ratios in all the samples were quantitatively obtained *via in-situ* HSQC NMR spectra. Furthermore, the RREL contained a larger amount of syringyl units and less condensed units as compared to those of RCEL and REB. Therefore, *in-situ* characterization by HSQC NMR analysis is a beneficial structural analysis methodology in the emerging biomass research field for the characterization of pretreated biomass and enzymatic hydrolysis lignin.

Reference

1. Lu, F.C., Ralph, J. 2011. Solution-state NMR of lignocellulosic biomass. Journal of Biobased Materials and Bioenergy. 5:169–180
2. Kim, H., Ralph, J. 2010. Solution-state 2D NMR of ball-milled plant cell wall gels in DMSO-d_6/pyridine-d_5. Organic & Biomolecular Chemistry. 8:576–591
3. Martínez1, A.T., Rencoret, J., Nieto, L., Jiménez-Barbero, J., Gutiérrez, A., del Río, J.C.2011. Selective lignin and polysaccharide removal in natural fungal decay of wood as evidenced by in situ structural analyses. Environmental Microbiology.13:96–107
4. Samuel, R., Foston, M., Jaing, N., Allison, L., Ragauskasa, A.J. 2011. Structural changes in switchgrass lignin and hemicelluloses during pretreatments by NMR analysis. Polymer Degradation and Stability. 96:2002–2009
5. Samuel, R., Foston, M., Jaing, N., Allison, L., Cao, S.L., Allison, L,, Studer, M., Wymanc, C., Ragauskas, A.J. 2011. HSQC (heteronuclear single quantum coherence) ^{13}C–^{1}H correlation spectra of whole biomass in perdeuterated pyridinium chloride–DMSO system: An effective tool for evaluating pretreatment. Fuel. 90:2836–2842
6. Lu, F.C., Ralph, J. 2003. Non-degradative dissolution and acetylation of ball-milled plant cell walls: high-resolution solution-state NMR. Plant Journal. 35:535–544
7. Heikkinen, S., Toikka, M.M., Karhunen, P.T., Kilpelainen, I.A. 2003. Quantitative 2D HSQC (Q-HSQC) via suppression of *J*-Dependence of polarization transfer in NMR spectroscopy: application to wood lignin. Journal of the American Chemical Society. 125:4362–4367
8. Zhang, A.P., Lu, F.C., Sun, R.C., Ralph, J. 2010. Isolation of cellulolytic enzyme lignin from wood preswollen/dissolved in dimethyl sulfoxide/*N*-methylimidazole. Journal of Agricultural and Food Chemistry. 58:3446–3450
9. Qu, C., Kishimoto, T., Kishino, M., Hamada, M., Nakajima, N. 2011. Heteronuclear single-quantum coherence nuclear magnetic resonance (HSQC NMR) characterization of acetylated Fir (*Abies sachallnensis MAST*) wood regenerated from ionic liquid. Journal of Agricultural and Food Chemistry. 59:5382–5389

10. Holtman, K.M., Chang, H.M., Kadla, J.F. 2007. An NMR comparison of the whole lignin from milled wood, MWL, and REL dissolved by the DMSO/NMI Procedure. Journal of Wood Chemistry and Technology. 27:179–200
11. Lu, F.C., Ralph, J. 1999. Detection and determination of *p*-Coumaroylated units in lignins. Journal of Agricultural and Food Chemistry. 47:1988–1992
12. Zhang, A.P., Lu, F.C., Liu, C.F., Sun, R.C. 2010. Isolation and characterization of lignins from *Eucalyptus tereticornis* (12ABL). Journal of Agricultural and Food Chemistry. 58:11287–11293
13. Sette, M., Wechselberger, R., Crestini, C. 2011. Elucidation of lignin structure by quantitative 2D NMR. Chemistry - A European Journal. 17:9529–9535
14. Balakshin, M., Capanema, E., Gracz, H., Chang, H.M., Jameel, H. 2011. Quantification of lignin–carbohydrate linkages with high-resolution NMR spectroscopy. Planta. 233:1097–1110
15. Wen, J.L., Sun, Z.J., Sun, Y.C., Sun, S.N., Xu, F., Sun, R.C. 2010. Structural characterization of alkali-extractable lignin fractions from bamboo. Journal of Biobased Materials and Bioenergy. 4:408–425
16. Choi, J.W., Faix, O. 2011. NMR study on residual lignins isolated from chemical pulps of beech wood by enzymatic hydrolysis. Journal of Industrial and Engineering Chemistry.17:25–28

The Properties of Torrefied Biomass from Six Major Bamboos in Taiwan

Chun-Te Wu[1] *– Far-Ching Lin*[2*]

[1] Graduate Student, School of Forestry and Resource Conservation - National Taiwan University, Taipei 10617, TAIWAN
r99625045@ntu.edu.tw
[2] Assistant professor, School of Forestry and Resource Conservation - National Taiwan University. Taipei 10617, TAIWAN.
* Corresponding author
farching@ntu.edu.tw

Abstract

Torrefaction is a kind of thermal treatment process that carried out at temperatures ranging from 200 to 300 ^{o}C to improve its heat value and grindability for substitution of coal. In this process the biomass hemicellulose is degraded, maintaining its cellulose and lignin content. Six kind of major bamboos including Moso bamboo, Makino bamboo, Ma bamboo, Green bamboo, Thorny bamboo, and Long shoot bamboo were torrefied in the study. First, bamboos were dried and heated to 250, 270, and 290 ^{o}C with 60, 75, and 90 minutes duration. Then the torrefied mass was carried basic property testing including proximate analysis, ultimate analysis, TGA, and heat value in order to understand the difference between raw material and its torrefied products.

Results show that the color of biomass will turn to brown or dark brown as increasing of torrefied temperature and time duration. So does the carbon content of torrefied mass. Ultimate analysis shows that oxygen element was reduction while hydrogen and carbon content increased with the temperature increasing. Therefore, torrefaction process results in reduction in O/C ratio which essentially contributes to increase in heat value. The results of the proximate analysis also shown as increasing of terrified temperature, volatile fraction was reduced while fixed carbon was increased. Raw bamboos were about 80-89% of volatiles and 3-14% of fixed carbon, however, volatiles reduced to 73-76% and fixed carbon increased to 17-24% after torrefaction. Ash content of raw bamboos were about 1-2% and increased to about 3.5-4.5% of torrefied bamboo at 290 °C.

Generally, heat value of torrefied bamboos are 6-16% higher than that of raw material except Moso bamboo. Most of bamboo kept about 70-80% of original weight after torrefaction while heat value kept higher percentage than that of weight. This indicates that bamboo is a suitable biomass source for torrefaction process.

Key Words: A. Bamboo, B. Torrefaction, C. Biomass, D. Biofuel, E. Energy

Introduction

Because the fossil fuel resources are depleted, the international crude oil prices increases year after year. Moreover, over consumptions of the fossil fuel also makes the environmental problem like climate change and the global warming, therefore, many countries are actively looking for alternative energy resources. Biomass is good alternative that could reduce the impaction of energy crisis and environmental problem. Because carbon dioxide (CO_2) released during the utilization is an integral part of the carbon cycle, it is considered as a kind of carbon neutral fuel. However, in general, raw biomass is hygroscopic and high moisture contained so that it cannot be stored for a long time. Whereas the energy density and utilization efficiency of raw biomass is also lower than that of fossil fuels, th results reveal that the applications of raw biomass in industry are restricted.

Torrefaction is a kind of thermal treatment process that carried out at temperatures ranging from 200 to 300 ^{o}C to improve its heat value and to reduce hygroscopic for substitution of coal. In this process, hemi-cellulose of biomass is degraded and most of its cellulose and lignin content are maintained. In recent years, torrefaction of lignocellulosic biomass has been studied for potential applications.

Bamboo is a fast-growing plant and it is the plenteous resource in Taiwan. It is the versatile material being used for building materials, as food source, industrial material, even as energy production. Torrefaction of bamboo is an approach to energy densification and makes the product stable. Six kind of major bamboos in Taiwan including Moso bamboo, Makino bamboo, Ma bamboo, Green bamboo, Thorny bamboo, and Long shoot bamboo were torrefied in the study. Then the torrefied mass was carried out basic properties tests including proximate analysis, ultimate analysis, thermogravimetric analysis, and heat value in order to understand the difference between raw material and its torrefied products.

Materials and Methods

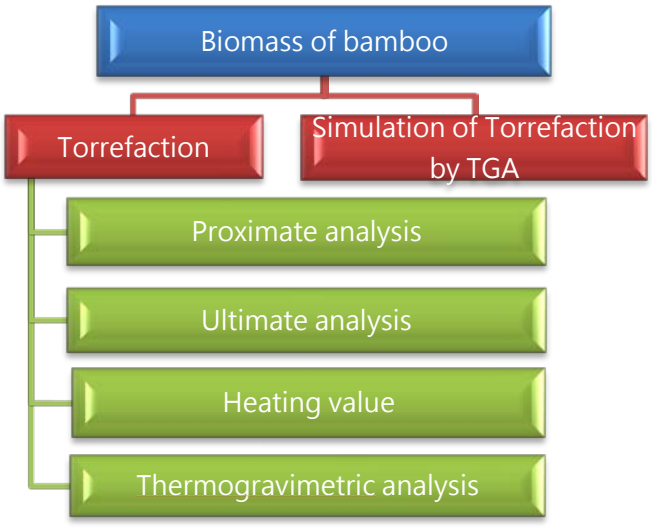

Fig 1. Research structure of torrefaction

Materials. Materials were cut on Oct. 2010 at 3 years that from the 7th compartment, Shuei Li Tract, The Experimental Forest, College of Bio-Resources and Agriculture,

National Taiwan University. The six major bamboos in Taiwan are:

Moso bamboo；*Phyllostachys pubescens*
Makino bamboo；*Phyllostachys makinoi*
Ma bamboo；*Dendrocalamus latiflorus*
Green bamboo；*Bambusa oldhamii*
Thorny bamboo；*Acanthophyllum pungens*
Long shoot bamboo；*Bambusa dolichoclada*

Experimental. First, bamboos were dried and heated to 250, 270, and 290 ^{o}C with 60, 75, and 90 minutes duration. Then the torrefied mass was carried out basic propertiey tests including proximate analysis, ultimate analysis, thermogravimetric analysis, and heat value in order to understand the difference between raw material and its torrefied products, shown in Fig 1.

Torrefaction. Torrefaction consists of thermally treating the biomass at temperatures between 200 and 300^{o}C under a non-oxidizing environment. In this process, hemicellulose of biomass is degraded and most of its cellulose and lignin content are maintained. Under this condition, biomass were converted into a more stable product with higher energy denity. First, raw bamboos were grinded and sieved to the maximum particle size of 40 mesh (i.e. particle size $\leqq$ 0.42 mm), then dried in an oven at the temperature of 105^{o}C for 24 hours . The 15g material powder of each bamboo were put into terrified reactor (Fig 2) with increasing temperature at 6-8 ^{o}C/min to 250, 270, and 290 ^{o}C with 60, 75, and 90 minutes duration under a nonoxidizing environment. After the torrefaction procedure, the torrefied bamboos were placed in plastic bags and stored in a desiccator at room temperature until the analyses were carried out.

Fig 2. Reactor for torrefaction

Results And Discussions

Fig. 3 show the result of bamboo torrefied biomass at 250, 270, 290 ^{o}C. The color of biomass will turn to brown or dark brown as increasing of torrefied temperature and time duration.

Fig 3. Torrefied biomass of bamboo

Table 1 Ultmate analysis of six bamboos and torrefied bamboos at 290°C

Sample	Ultimate analysis (wt.% daf)				
	N(%)	C(%)	S(%)	H(%)	O(%)
F-Makino-raw	0.37	48.43	0.03	6.06	45.11
F-Makino 290-90	0.47	50.90	0.00	5.34	43.29
F-Moso-raw	0.13	47.67	0.00	6.30	45.89
F-Moso 290-90	0.20	49.39	0.00	6.22	44.18
F-Ma-raw	0.20	44.59	0.47	6.04	48.69
F-Ma 290-90	0.21	50.31	0.29	5.55	43.65
F-Green-raw	0.21	46.30	0.06	5.91	47.52
F-Green 290-90	0.25	50.31	0.00	5.59	43.85
F-Thorny-raw	0.18	45.33	0.63	6.31	47.55
F-Throny 290-90	0.23	50.61	0.37	5.81	42.99
F-Long-branch-raw	0.25	46.98	0.40	6.05	46.32
F-Long 290-90	0.33	52.21	0.22	5.44	41.79

daf: dry ash free basis

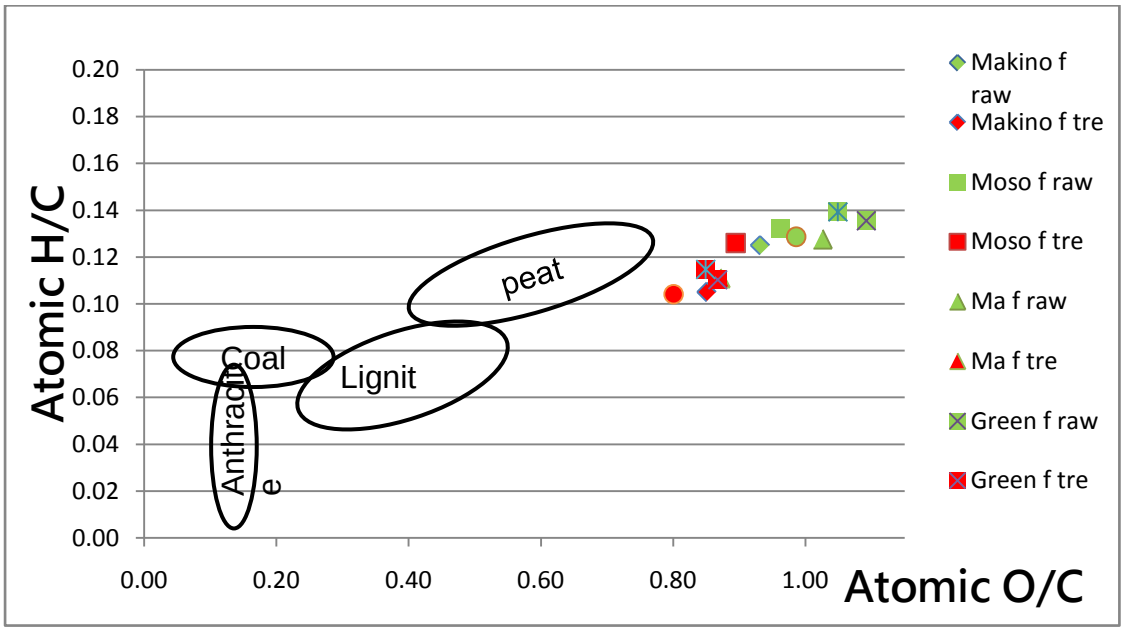

Fig 4. Van Krevelen diagram for bamboo and torrefied biomass

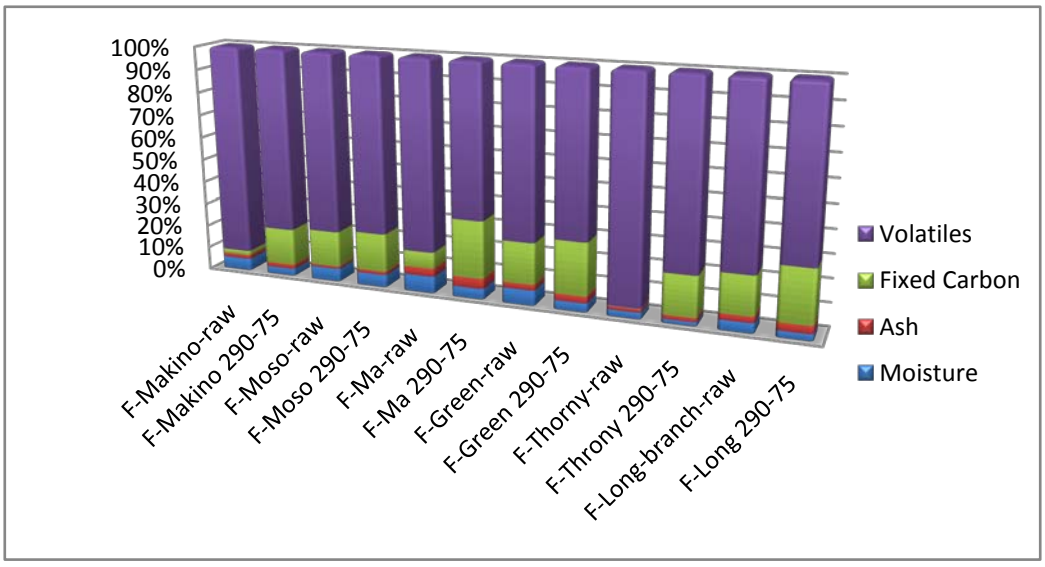

Fig 5. Proximate analysis for bamboo and torrefied biomass

Ultimate analysis. Table 1 shows the ultmate analysis of six bamboos and torrefied bamboos at 290^{o}C. There is a reduction in oxygen element and correspondingly increase 18% in the carbon content through torrefaction at 290^{o}C. In addition, Sulfur element is a tiny bit content in the bamboos and torrefied bamboos, wherein it in Ma and Thorny bamboo is less than 1%. Therefore torrefaction process results in reduction in O/C ratio which essentially contributes to increase in heat value.Further, the result of ultimate analysis that the elemental constituents like C, H and O are drawn into a Van Krevelen diagram by ratio O/C and H/C as shown in Fig 4. Finally, the diagram indicates that the chemical composition of bamboo biomass will tend to be the peat coal through torrefaction.

Proximate analysis. The results of the proximate analysis of six bamboo and torrefied bamboo on moisture, ash, volatiles and fixed carbon are shown in Fig. 5. The raw bamboo has about 80-89% volatiles and 3-14% fixed carbon is transformed to contain about 73-76% volatiles and 17-24% fixed carbon after torrefaction process under 290 °C. It is evident that as the torrefy temperature increasing, the volatiles will reduce while the fixed carbon is increased. Especially, fixed carbon of Ma bamboo and Thorny bamboo are increased about 18% significantly through torrefaction. The ash content of raw bamboos are about 1.03-2.00% and increased to about 3.5-4.5% of torrefied bamboo at 290 °C that is slightly higher than that of woody torrefied biomass. The highest ash content was ma bamboo. The moisture content is from 5-7 % to 1-2% of torrefied bamboo, and it is slightly lower than that of woody torrefied biomass. In short, the moisture content in the biomass is substantially reduced and the volatiles are liberated through torrefaction. Consequently, hydrophobic solids with higher content of fixed carbon are produced. It is the positive meaning to enhance the heating value and the properties of fuel.

Heating value and energy density. The results of high heating value (HHV) of six bamboos and torrefied bamboos are show in Fig.6. The heating value of torrefied bamboo torrefied under 290 °C were increased 6%, 16%, 11%, 13%, and 8% for Makino bamboo, Ma bamboo, Green bamboo, Thorny bamboo, Long-shoot bamboo, respectively. However, the heating value of Moso bamboo is the highest, it is not

increased significantly after torrefaction. Overall, the HHV of torrefied bamboo at 290 °C were increased 6-16% (from 4,200-4,400 to 4,800-5,000 kcal/kg on dry basis) higher than that of raw material except Moso bamboo.

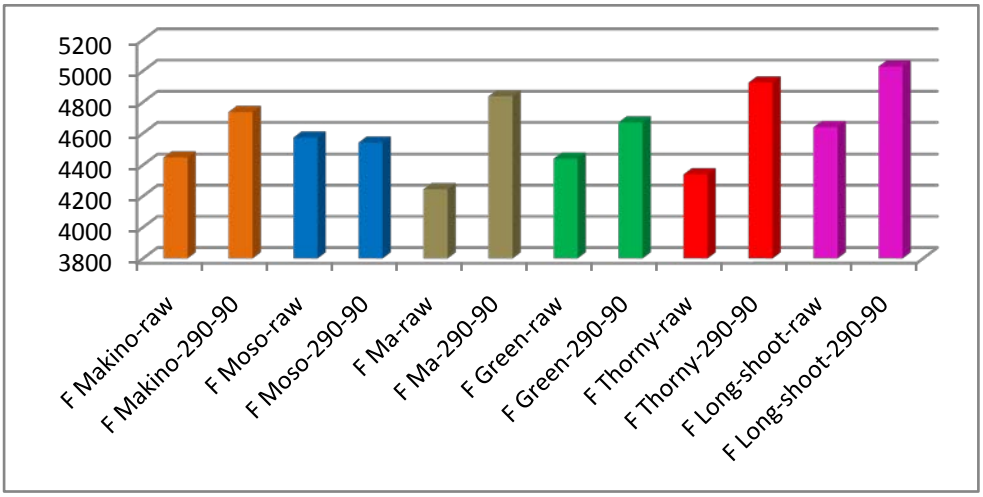

Fig 6. HHV for bamboo and torrefied biomass

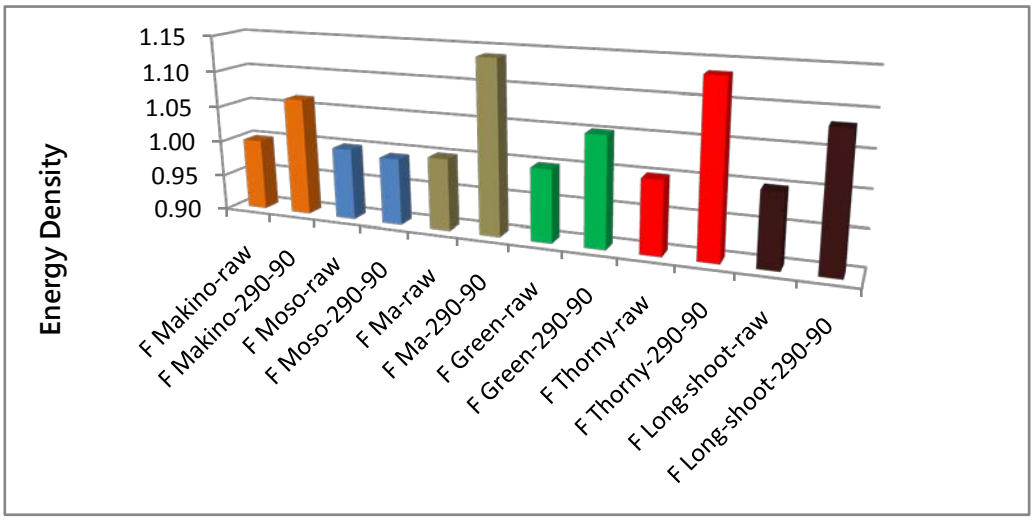

Fig 7. Energy Density for bamboo and torrefied biomass

Energy density of the torrefied bamboo compared to raw bamboo was shown in Fig 7. It was calculated as heating value divided weight of yield and heating value of raw material. Most of bamboo kept about 70-80% of original weight after torrefaction while heat value kept higher percentage than that of weight. As a result, the energy density of torrefied bamboo are higher than that of raw bamboo except Moso bamboo. Ma bamboo and Thorny bamboo were significantly increased.

Thermogravimetric analysis (TGA) for raw biomass and torrefied biomass. The pyrolysis and torrefaction characteristics of the six bamboo materials were analyzed by using a thermogravimetry. A crucible loaded with biomass particles was placed inside the thermogravimetry where the weight was constantly measured. The function of the thermogravimetry is to measure and record the dynamics of biomass weight loss as increasing temperature and time. [2]

From the recorded distribution of the weight loss, one was able to obtain the thermogravimetric analysis (TGA) and derivative thermogravimetric (DTG) analysis. In the past studies, it has been recognized that the lignocellulosic structure of biomass can be qualitatively identified by means of DTG. In other words, because of intrinsic difference in the structures of hemicellulose, cellulose and lignin contained in biomass, as stated above, they may be distinguished from the distributions of weight loss intensity of biomass. [2]

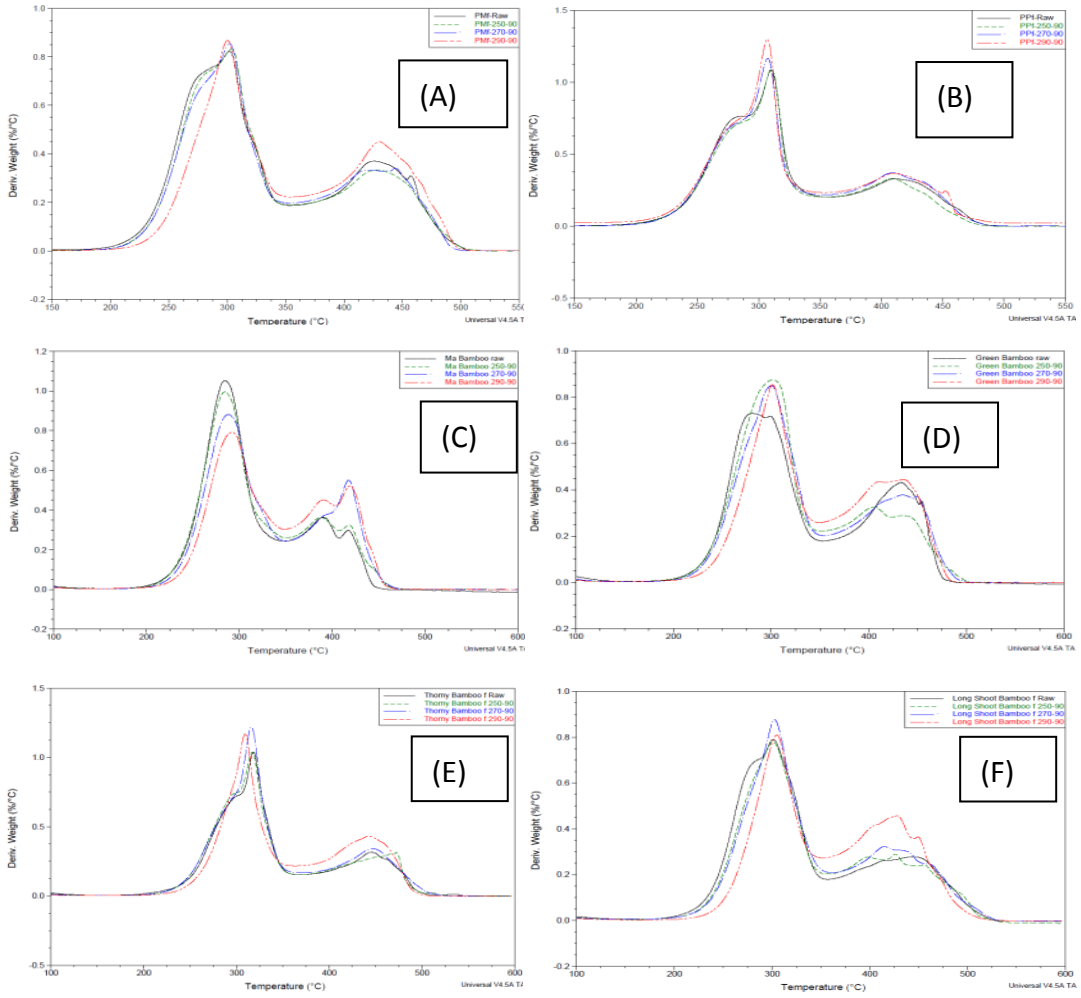

Fig 8. DTG curves of 250°C , 270°C and 290°C torrefied bamboo biomass at 90 min (A) Makino (B)Moso (C)Ma (D) Green (E) Thorny (F)Long-Shoot

The distributions of DTG of the six bamboos and their torrefied biomass are shown in Fig. 8. (A), (B), (C), (D), (E), and (F) are Makino bamboo, Moso bamboo, Ma bamboo, Green bamboo, Thorny bamboo, and Long-shoot bamboo, respectively. The black curve in Fig 8 indicates the DTG of raw biomass; the green, blue, and red are the DTG of torrefied bioma under 250°C, 270°C, and 290°C, respectively. First, the black curve in Fig 8-(A), (B), (D), (E), (F) presents a shoulder and two well-defined peaks, especially the shoulder in Fig 8-(D) is obvious. Generally, the shoulder exhibited at around 275°C means the thermal decomposition of hemicellulose, because it decomposed temperatures is ranged from 150 to 250 °C. The , the first peak is for decomposition of cellulose occurs at temperatures ranged from 275 to 350 °C; and the second peak is the decomposition of lignin at the

temperatures between 250 and 500 ^{o}C.
Nevertheless, the black curve of Ma bamboo in Fig 8-(C) did not show the hemicelluose shoulder, only one peak is exhibited. The peak developed at 284 ^{o}C from the thermal decomposition of cellulose and the curve of hemicellulose is almost merged by that of cellulose. Next, in comparison to the green, blue and red curves, it depicts that the peaks become sharper than black one, the shoulder for hemicellulose is disappeared, especially in the Green bamboo, Thorny bamboo and Long-shoot bamboo. It follows that the torrefaction has a tremendous impact on hemicellulose. Even so, the influence of the torrefaction on cellulose and lignin is slight. Furthermore, for the Moso bamboo, the red curves is not complete disappeared that could be the reason why its heating value was not increased significantly.
In brief, when the torrefaction was performed, the results indicated that the hemicellulose contained in the biomass was degraded significantly, whereas cellulose and lignin were slightly affected.
Summarizing the observations in Fig 8, two groups of the bamboo biomass materials can be catagorized. Specifically, leptomorph system bamboo like Moso bamboo can be classified into the relatively inactive species, resulting from not obviously improved in character of fuel after torrefaction; pachymorph rhizome system bamboo like Green bamboo are the active species, they are obviously improved in character of fuel after torrefaction.

Conclusion

Results show that the color of biomass will turn to brown or dark brown as increasing of torrefied temperature and time duration. So does the carbon content of torrefied mass. Ultimate analysis shows that oxygen element was reduction while hydrogen and carbon content increased with the temperature increasing. Therefore, torrefaction process results in reduction in O/C ratio which essentially contributes to increase in heat value. The results of the proximate analysis also shown as increasing of terrified temperature, volatile fraction was reduced while fixed carbon was increased. Raw bamboos were about 80-89% of volatiles and 3-14% of fixed carbon, however, volatiles reduced to 73-76% and fixed carbon increased to 17-24% after torrefaction. Ash content of raw bamboos were about 1-2% and increased to about 3.5-4.5% of torrefied bamboo at 290 °C.
Generally, heat value of torrefied bamboos are 6-16% higher than that of raw material except Moso bamboo. Most of bamboo kept about 70-80% of original weight after torrefaction while heat value kept higher percentage than that of weight. This indicates that bamboo is a suitable biomass source for torrefaction process.

Reference

[1] Sridhar G. *et al* (2007) Torrefaction of bamboo. 15th European Biomass Conference & Exhibition. Berlin, Germany. pp532-535
[2] Chen, W. H. and P. C. Kuo (2010) A study on torrefaction of various biomass materials and its impact on lignocellulosic structure simulated by a thermogravimetry. Energy 35:2580-2586

Effects of Treatments With Alcohols and N-hydroxymethyl Compound on the Mechanical Properties of Wood

*Qiliang Fu - Qingwen Wang - Haigang Wang -Yanjun Xie**

Key Laboratory of Bio-based Material Science and Technology (Ministry of Education), College of Material Science and Engineering, Northeast Forestry University, Harbin, PR China
* *Corresponding author*
yanjunxiecn@hotmail.com

Abstract

Both alcohols (ethylene glycol and 1,2-propylene glycol) were respectively incorporated with 1,3-dimethylol-4,5-dihydroxyethylene urea (DMDHEU) to treat poplar wood and the modifying effects on several mechanical properties of wood were investigated. Compared to the untreated controls, the treated wood obtained an increased weight percent gain (WPG) but reduced moisture content with increasing concentration of the treating solutions. Wood treated with the mixture of DMDHEU and MgCl2 exhibited a reduction in impact strength and modulus of rupture in bending (MOR) up to 34.2 and 29.2%, respectively; at a comparable DMDHEU concentration, incorporation of the alcohols caused a reduction in impact strength and MOR of 14.4 and 14.9%. The less reduction due to addition of alcohols may be attributed to the extension of DMDHEU molecule chains thereby making the network established between DMDHEU and wood polymers more flexible. Modification of wood with DMDHEU and alcohols led to an increase in modulus of elasticity (MOE) in bending ranging from 6.0 to 32.7% compared to the untreated controls. In addition, the hardness and compression strengthen of wood in longitudinal, radial, and tangential directions were enhanced probably due to an increased density. This study demonstrates that incorporation of low molecular weight alcohols can inhibit the loss in impact strength caused from DMDHEU treatments.

Keywords: Wood chemical modification, N-hydroxymethyl, alcohols, ethylene glycol, mechanical properties.

Introduction

Wood as a nature material has been widely used by mankind for millennia because of its excellent material properties. However, there are some defects that such as dimensional unstability, cracking and degradation by UV/sunlight or fungi, thus, both methods of heat treatment and chemical modification to modify wood are employed and developed.
Heat-treatment is a type of techniques treating wood at high temperatures (typically 150-230°C) in the shield media such as steaming, nitrogen gas, and vegetable oils (Militz 2002). Chemical modification is that a kind of the methods impregnated reagent into wood, subsequently reacting with the cell wall caused permanent cell wall bulking (Hill 2006). Treatment of wood with DMDHEU, a kind of chemical modification wood, which had been reported about improving dimensional stability, decay resistance, surface coating, and mechanical properties. Xie (2007) showed that the zero and final span tensile strength of thin veneer lossed up to 40%. Bollums (2010) demonstrated that MOR and bending strength had same degree loss, especially the impact strength was significant reduced. Dieste (2008) pointed out DMDHEU treatment had slightly negative influence on the MOR of 5-layer plywood.
Polyethylene glycol (PEG) modification wood improved its dimensional stability, absorption vapor, and surface stability (Jeremic et al. 2007b, Wallström and Lindberg 1995). The low molecular weight of PEG (100 to 1000) easily made it to impregnate into cell wall (Jeremic et al. 2007a, Jeremic et al. 2007b), and to bulk the cell wall (Jeremic and Cooper 2009). However, large molecular weight (range from 1000 to 8000) filled in cell lumen (Jermic et al. 2009).
Zeronian (2009) reported that tensile strength of DMDHEU treated cotton fiber was reduced. Kang (1998) and Yang (2003) demonstrated that increasing the brittleness of treated cellulose-based materials was increased might due to bulking and cross-linking with the cell walls. Combination ethylene glycol or 1,2-propylene glycol with DMDHEU to treat wood is very seldom. Only one literature reported about this, Simonsen (1998) showed that treated wood with polyglycol and DMDHEU had a lack of dimensional stability. Some mechanical properties of treated wood were increased, such as compression strength, hardness and MOE. However, to some degree, the compact strength and/or MOR were decreased.
The objective of this paper is that used both alcohols and DMDHEU to modify wood, and improved its mechanical properties compared to the traditional method of treatment wood with DMDHEU treated only.

Materials and Methods

Original materials: Poplar wood boards were purchased in China (Yicun, Harbin) measuring 1000mm×60mm×60mm (L×T×R), which cut into blocks according to China National Standard-Testing Methods. All chemicals (DMDHEU, ethylene glycol, 1,2-propylene glycol and $MgCl_2$) were purchased in China.
Impregnation and preparation of modified wood: The impregnation parameters of solution concentration are showed in Table 1. Prior to treatment all of the prepared samples were dried at 103±2℃for 24h before impregnation, then, with a vacuum of -0.1MPa for 6h and a subsequent at pressure of 0.6MPa for 6h, finally applying a vacuum of -0.05MPa for 30min to remove excrescent solution. After the impregnation processing, the treated samples were displayed at room temperature for 72h, then dried at the conditions of 40℃for 4h, 60℃for 4h and 80℃for 4h, finally at the curing temperature of 120℃for 24h.

Table1 1 *Solution concentration parameters of the untreated and treated samples used in this study.*

Sample NO.	Solution concentration (w, %)	Mole ratio (DMDHEU/ Ethylene glycol)	Mole ratio (DMDHEU/1,2-propylene glycol)	Magnesium chloride (w, %)
1	0	—	—	0
2	30	Only DMDHEU	—	0
3	10	Only DMDHEU	—	1.5
4	20	Only DMDHEU	—	1.5
5	30	Only DMDHEU	—	1.5
6	30	1:1	—	1.5
7	30	—	1:1	1.5

Note: — expression does not addition this regent

Physical properties calculation: Weight percent gain (WPG) of treated samples was calculated using the following equation (1):

$$WPG\ (\%) = \frac{W_t - W_c}{W_c} \times 100\% \qquad (1)$$

where W_t is the oven-dry weight of treated sample, and W_c is the oven-dry weight of untreated sample.

Leaching ratio evaluate the property of chemicals curing in wood after 3 repeat deionized water leaching test, which was calculated by the following equation (2):

$$\text{Leaching ratio}\ (\%) = \frac{W_t - W_l}{W_t - W_c} \times 100\% \qquad (2)$$

where W_t is the oven-dry weight of treated sample, W_l is the oven-dry mass of after leaching test, and W_c is the oven-dry weight of untreated sample.

Moisture content (MC) is the moisture adsorption of treated sample, MC was calculated as (3):

$$MC\ (\%) = \frac{W_{ta} - W_t}{W_t} \times 100\% \qquad (3)$$

where W_t is the oven-dry weight of treated sample, W_{ta} is the mass of treated sample at atmosphere ambient.

Mechanical properties test: The dimensions and mechanical properties of the samples size ware prepared according to China National Standard-Testing Methods for Wood Physical and Mechanical properties.

Results and Discussion

Weight percent gain, leaching test and moisture content: The results of WPG were increased with solution concentration increasing, whether added alcohols into the DMDHEU solution or not (Fig. 1 a). The WPG of samples NO.5, 6 and 7 were higher than only 30% DMDHEU without catalyst treated sample (NO.2), and the WPG of both alcohols combination with DMDHEU samples (NO.6 and 7) were 67.15% and 68.48%, respectively. Leaching ratio of all the treated samples had slight changing, the ratio range from 6.21% to 9.94%. The moisture contents (MC) of treated sample were a little reduction compared to the untreated sample (Fig. 1 b). The MC of 30% solution concentration treated samples (NO.5, 6 and 7) were less than that of the untreated and low concentration samples (NO.3 and 4).

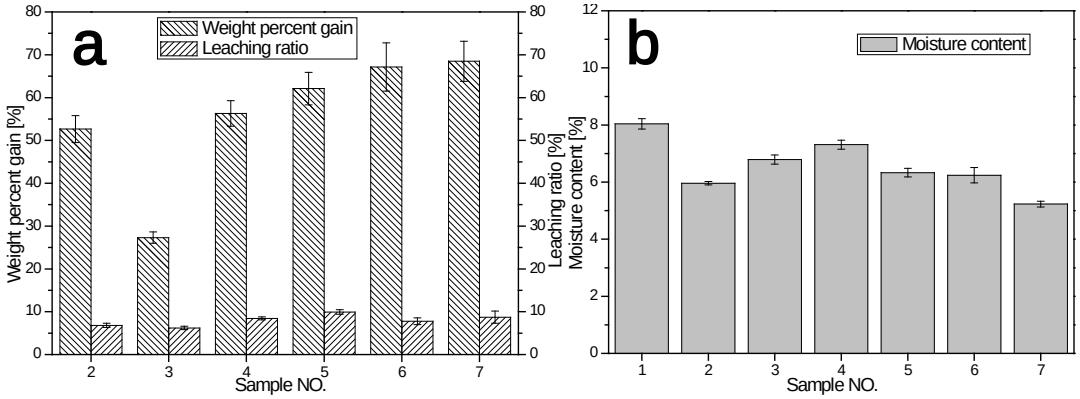

Figure 1 *The weight percent gain, leaching ratio (a) and moisture content (b) of untreated (NO.1) and treated (NO.2~7) samples*

Impact strength, MOE and MOR: The impact strength of all treated sample were declined (Fig. 2), this might be due to acid hydrolysis and cross-linking with the cellulose (Xie et al. 2007). Treated samples with alcohols and DMDHEU samples reduction 20.24% and 16.93% (Fig. 2 b) compared to the untreated sample, however, the impact strength was enhanced 14% and 17.31% compared to the NO.5 sample, respectively.

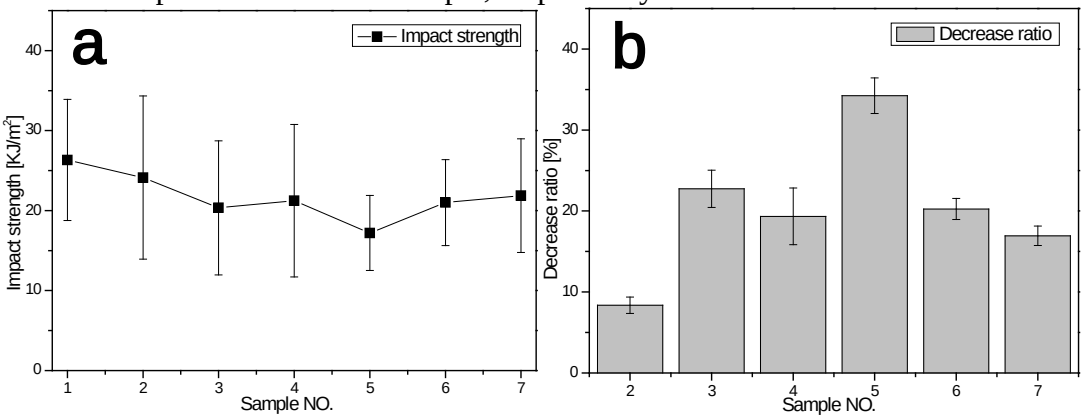

Figure 2 *The impact strength of the untreated and treated samples (a), and decrease ration of the impact strength (b).*

Several literatures had been reported that the alcohols (PEG, EG or PG) could soften nature cellulose-based materials (El-Sayed Mohamed et al. 2009, Yang and Chen 1999, Zeronian et al. 1989). Kang (1998) investigated the effects of mechanical properties of cotton fabrics on treated with DMDHEU, and the reduction tensile strength attributed to acid-catalyzed depolymerization and cross-linking cellulose molecules. Beside, the pre-curing cellulose treatment also caused a much higher loose than that of tensile strength (Yang et al. 2003).

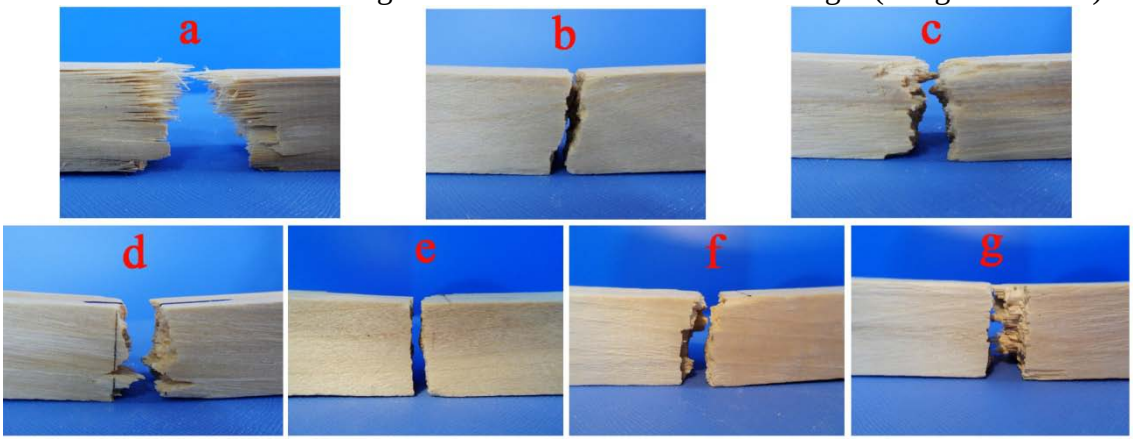

Figure 3 *The impact fractures of (a) the untreated sample, and (b, c, d, e, f and g) treated*

samples NO. 2 to 7, respectively.

Treatment of wood veneer with DMDHEU and magnesium chloride caused a reduction of z- and f-span tensile strength due to Lewis acid depolymerization polysaccharide (Xie et al. 2007) which indicated that the treated samples were embrittlement. The Figure 3 illustrated that the fractures of treated samples were linear smoothing, while the untreated one was zigzag, the fractures samples of Figures 3 g and f were great more roughness than the without alcohols sample (Fig. 3 e). Bollums (2010) reported that the tensile and compact strength of Beech wood modified with DMDHEU reduction 38.8% and 79.3% compared to the control sample, respectively.

Both alcohols incorporated with DMDHEU samples loss impact strength, but enhancement the impact strength (Fig. 2) compared to the treated samples of treating with DMDHEU, which might due to be extension of DMDHEU molecule chains thereby making the network established between DMDHEU and wood polymers more flexible. When the treated wood subjected to a load could distribution power to the long molecule.

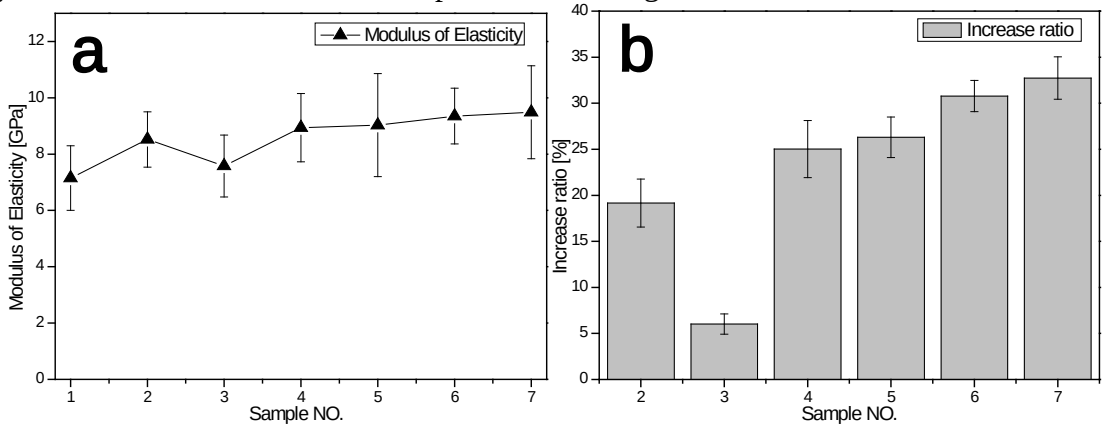

Figure 4 *The MOE of the untreated and treated samples (a), and decrease ration of the MOE (b).*

Modulus of elasticity (MOE) and modulus of rupture (MOR) datum were presented in Figures 4 and 5, the MOE increased with the concentration of alcohols and/or DMDHEU solution increased (Fig. 4 a). The MOE of treated samples ethylene glycol or 1,2-propylene glycol went up 30.78% and 32.73% (Fig. 4 b), respectively. Moreover, those two samples were higher 5% and 6.42% than the 30% DMDHEU concentration sample (NO.5). We found that the MOR reduced with the concentration of DMDHEU increasing (Fig. 5 a), however, the MOR of the samples treated with alcohols (ethylene glycol and 1,2-propylene glycol) and DMDHEU were enhanced 14.9% and 15.6% compared to sample NO.5 (Fig. 5 b), respectively.

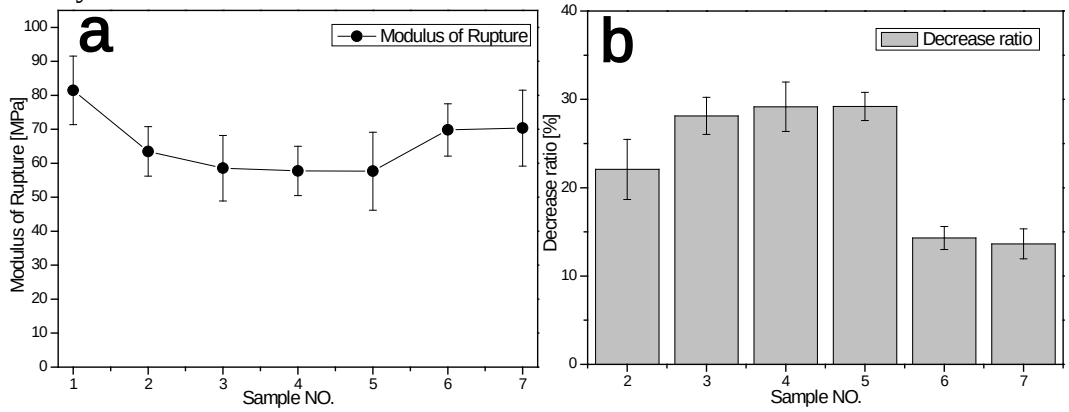

Figure 5 *The MOR of the untreated and treated samples (a), and decrease ration of the MOR (b).*

Bollums (2010) demonstrated that the bending strength reduced 19.3% for 1.3M DMDHEU concentration, while the MOE rosed 24.3%. Dieste (2008) founded that MOE and bending strength of 5-layer plywood were slightly effected by the treatment with DMDHEU, because the orientation of 5-layer plywood grain was significant. With N-methyl-melamine and aluminium salt as catalyst treated 5-layer beech veneers, the treated plywood sample exhibited increase in MOE and MOR (Trinh et al. 2012). DMDHEU modified wood caused acid-depolymerization cellulose, when every two orthogonal veneers fold up together and then manufacturing 5-layer plywood could enhancement the MOE and MOR, while the MOR was negatived influenced by using solid wood treatment. The MOE was enhanced, but the MOR was reduced, DMDHEU treatment samples decreased the compact strength and increased the brittleness. However, the alcohols addition exhibited some extent improving modified wood mechanical properties of the modified wood compared to without alcohols samples.

Hardness and compression strength: The hardness and compression strength increased with the solution concentration increasing (Fig. 6). Moreover, the value of hardness of longitudinal direction was twice as the other directions (Fig. 6 a), and the compression strength of longitudinal direction was dramatic more than the other directions (Fig. 6 b), which was connected with wood species and grain direction.

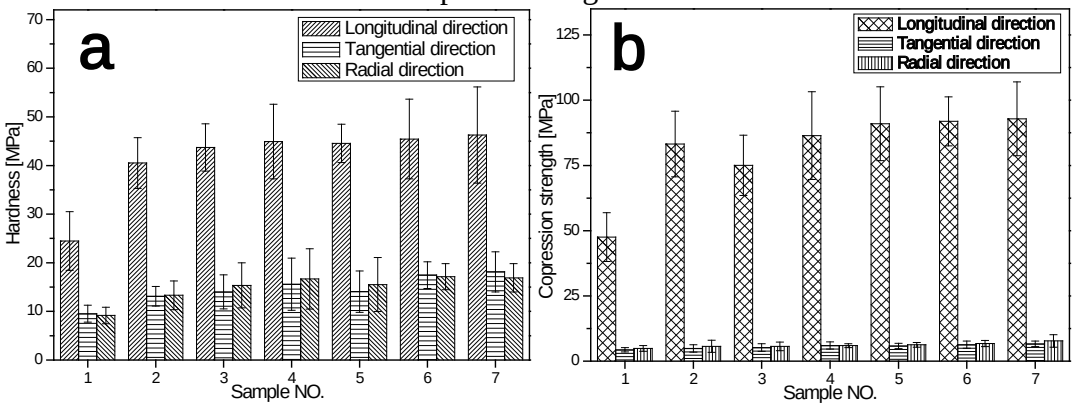

Figure 6 *Three directions hardness (a) and compression strength (b) of untreated and treated samples.*

The examination of hardness of Poplar wood at longitudinal direction was 24.5MPa (Fig. 6 a). Dieste (2008) reported the Brinell hardness of modified layer wood improving 46~108%, the higher DMHEUE concentration the higher hardness, which was the same to our research. Bollums (2010) demonstrated that hardness and compression strength increasing 82.1% and 65.1% treatment by 2.3M DMDHEU concentration, respectively. Table 2 shows the results of increase ratio hardness and compression strength of modified wood, we observed that the increasing ratio 37.78~90.24% for hardness, and 12.47~93.33% for compression strength. Moreover, the treated samples of addition alcohols were higher than other modified samples (Table 2).

Table 2 *The increase ratio of hardness and compression strength of treated samples.*

Sample NO.	Increase ratio of hardness (%)			Increase ratio of compression strength (%)		
	Longitudinal	Tangential	Radial	Longitudinal	Tangential	Radial
2	65.62	37.78	45.41	75.05	12.47	16.84
3	78.70	47.01	67.58	57.89	20.09	16.22
4	83.61	63.59	81.99	81.85	38.57	22.18
5	82.05	47.64	69.32	91.44	33.49	28.34
6	85.81	83.32	87.01	93.33	45.50	39.01

7	89.17	90.24	84.61	95.41	52.89	59.34

Conclusions

The results showed that the mechanical properties of hardness, compression and MOE were increase, but compact strength and MOR of treated wood decreased compared to the untreated wood. Mechanical properties of both two alcohols (ethylene glycol and 1,2-propylene glycol) respectively combination with DMDHEU treated wood were increased compared to the samples of DMDHEU treated only, especially the compact strength and MOR were enhanced, which might due to the addition of alcohols, and attributed to extension of DMDHEU molecule chains thereby making the network established between DMDHEU and wood polymers more flexible.

References

Bollmus, S., P. Rademacher, Krause, A., and Militz, H. 2010. Material evaluation and product performances of Beech wood modified with 1,3-dimethylol-4,5-dihydroxyethyleneurea (DMDHEU). European Conference on Wood Modification 2010.

Dieste, A., Krause, A., Bollmus, S., and Militz, H. 2008. Physical and mechanical properties of plywood produced with 1.3-dimethylol-4.5-dihydroxyethyleneurea (DMDHEU)-modified veneers of Betula sp. and Fagus sylvatica. European Journal of Wood and Wood Products. 66:281-287.

El-Sayed Mohamed, Z., Abo-Shosha, M., and Ibrahim, N. 2009. Preparation of polyethylene glycol/polyacrylamide adduct and utilization in cotton finishing. Carbohydrate Polymers. 75:479-483.

Hill, C. 2006. Wood modification: chemical, thermal and other processes. Recherche 67:02.

Jeremic, D., Cooper, P., and Brodersen, P. 2007a. Penetration of poly (ethylene glycol) into wood cell walls of red pine. Holzforschung. 61:272-278.

Jeremic, D., Cooper, P., and Heyd, D. 2007b. PEG bulking of wood cell walls as affected by moisture content and nature of solvent. Wood Science and Technology. 41:597-606.

Jeremic, D., Quijano-Solis, C., and Cooper, P. 2009. Diffusion rate of polyethylene glycol into cell walls of red pine following vacuum impregnation. Cellulose. 16:339-348.

Kang, I.S., Yang, C.Q., Wei, W., and Lickfield, G.C. 1998. Mechanical strength of durable press finished cotton fabrics. TextileResearch Journal. 68:865-870.

Militz, H. 2002. Thermal treatment of wood: European processes and their background. IRG/WP 40241.

Simonsen, J. 1998. Lack of dimensional stability in cross-linked wood-polymer composites. Holzforschung. 52: 102-104.

Trinh, H.M., Militz, H., and Mai, C. 2012. Modification of beech veneers with N-methylol-melamine compounds for the production of plywood. European Journal of Wood and Wood Products. 70:421-432.

Xie, Y., Krause, A., Militz, H., Turkulin, H., Richter, K., and Mai, C. 2007. Effect of treatments with 1, 3-dimethylol-4, 5-dihydroxy-ethyleneurea (DMDHEU) on the tensile properties of wood. Holzforschung 61:43-50.

Zeronian, S., Bertoniere, N., Alger, K., Duffin, J., Kim, M., Dubuque, L., Collins, M., and Xie, C. 1989. Effect of Dimethyloldihydroxyethyleneurea on the Properties of Cellulosic Fibers. Textile Research Journal. 59:484-492.

Yang, C.Q., and W. Chen. 1999. Investigation of Flexible Crosslinking Systems for the

Retention of Mechanical Strength and Abrasion Resistance in Durable Press Cotton Fabrics. National Textile Center Annual Report. C 97:1.

Yang, C.Q., W. Zhou, G.C. Lickfield, and K. Parachura. 2003. Cellulase treatment of durable press finished cotton fabric: Effects on fabric strength, abrasion resistance, and handle. Textile Research Journal. 73:1062-1065.

Successive Solvent Fractionation of Bamboo Formic Acid Lignin for Value-Added Application

Ming-Fei LI [1], Shao-Ni SUN [1], Feng XU [1,], Run-Cang SUN [1,2,*]*

[1] Institute of Biomass Chemistry and Technology, Beijing Forestry University, 100083, Beijing, China

Corresponding author. Tel./fax: +86 10 62336972

E-mail address: xfx315@bjfu.edu.cn (Feng Xu); rcsun3@bjfu.edu.cn (Run-Cang Sun).

[2] State Key Laboratory of Pulp and Paper Engineering, South China University of Technology, 510640, Guangzhou, China

Abstract

Formic acid delignification process is a promising organosolv technique, which is used to separate lignocelluloses for the production of bioethanol as well as cellulose-based materials. To achieve a full volatilization of lignocelluloses in the concept of biorefinery, the dissolved lignin, a major by-product in the process, should be fully exploited and utilized. However, the value-added utilization of lignin is strongly affected by its heterogeneous nature. In this case, bamboo formic acid lignin was successively fractionated with organic solvents of increasing dissolving capacity (i.e., ether, ethyl acetate, methanol, acetone, and dioxane/water) to obtain homogeneous preparations. The starting lignin and the fractions obtained were compared in terms of molecular weight and functional groups by a set of chemistry and spectroscopy technologies. It was found that the yield of the five fractions obtained was 2.80, 39.85, 18.64, 23.38, and 13.30%, respectively. The lignin fraction extracted with ethyl acetate contained homogeneous materials of low molecular weight whereas the lignin fraction extracted with acetone was composed of a mixture of medium and high molecular weight materials. As evidenced by sugar analysis, there was strong association between hemicelluloses and lignin in the preparations with different molecular weights. Spectroscopy analysis indicates that with increasing the dissolving capacity of solvent, the contents of methoxyl, phenolic, and aliphatic hydroxyl groups in the extracted lignin fractions were decreased. The lignin fraction extracted with ethyl acetate, having a high radical scavenging index (RSI), will be a good feedstock as stabilizer. The results above suggest that the sequential solvent fractionation provides a promising way to prepare lignin with homogeneous structure and good functional properties for potential application.

Keywords: Bamboo, Formic acid lignin, Solvent fractionation, Antioxidant capacity

Introduction

The value-added utilization of lignin is strongly affected by its heterogeneous nature. Lignin shows different physicochemical properties depending on the sources, processing as well as post-treatments [1, 2]. Due to the heterogeneous feature of lignin, it is very difficult to control and standardize the properties and qualities of the derived products from lignin; thus, several techniques have been developed to homogenize the macromolecule. Lignin can be fractionated into sub-fractions by gel permeation chromatography [3], ultrafiltration [4, 5], selective precipitation [6], etc. However, these methods have high cost in large scales [7]. Recently, increasing attention has been attracted in fractionation lignin into homogeneous preparations with organic solvents in a successive manner. Successive fractionation of lignin with increasing hydrogen-bonding solvents is mainly based on the pioneering work of Schuech [8], who found that the salvation power of solvent depended on both the cohesive energy and hydrogen-bonding capacity of the solvent. Sun et al. [9] fractionated soda-anthraquinone (AQ) lignin from oil palm empty fruit bunch by successive extractions and found that the high molecular weight fraction had a high thermal stability. Similar conclusions have also been drawn in the subsequent fractionation investigation, in which kraft-AQ lignin from *Eucalyptus pellita* was sequentially extracted with different solvents [10, 11]. In addition, fractionation provides an attractive approach to refine lignin for a variety of potential applications. For instance, commercial Alcell lignin, birch organosolv lignin, as well as steam-exploded pine and eucalypt lignins were sequentially fractionated with organic solvents, and the obtained fractions with high homogeneity were further modified by laccases via polymerization [12]. The phenoxyl radicals obtained can be used for further enzymatic or chemical functionalization. Lignin-starch composites were prepared by casting fractionated preparations from pine kraft lignin with starch, in which the low molecular weight fractions of lignin seemed to be principally involved in plasticization or compatibilization [13]. Several solvent fractionated preparations from Alcell lignin were applied to manufacture matrix granules with bromacil as a model compound through a melt process [14]. It was speculated that the heterogeneity of lignin played an important part in altering the release rate of the active ingredient for the matrix granules.

In this case, the organosolv lignin from bamboo was successively fractionated by organic solvents with increasing dissolving capacity for lignin, and the starting lignin and its sub-fractions were compared in terms of yield, molecular weight distribution, and functional groups. Additionally, their antioxidant activity and thermostability were also investigated owning to the importance for value-added application.

Materials and Methods

Raw material and preparation of organosolv lignin. Air-dried Bamboo (*Phyllostachys sulphurea*) (70 g) together with formic acid was placed in a 1L flask equipped with a condenser, and delignified by using formic acid with a concentration of 88%, a temperature of 100.5 °C, a cooking time of 120 min and a liquid to solid ratio of 10 mL/g. Subsequently, the cellulosic pulp was filtered and washed with 88% formic acid followed by water and then dried. The filtrate and washing liquor (88% formic acid-soluble) were combined and concentrated under reduced pressure. After 10 volumes of water was added into the concentrated liquor, the solid material was recovered by filtration and washed thoroughly with water. Subsequently, it was freeze-dried and extracted with pentane in a Soxhlet

apparatus to remove extractives. The specimen was dried and noted as crude bamboo organosolv lignin.

Solvent fractionation of crude lignin. The crude lignin was sequentially fractionated with ether, ethyl acetate, methanol, acetone, and dioxane/water (9/1, v/v). 8 g lignin was suspended in 160 mL specified solvent in a 250 mL volumetric flask. After that, the mixture was agitated for 2 h using a magnetic stirrer at room temperature. The undissolved material was filtered over a filter paper. Subsequently, the solid fraction was suspended for an identical extraction until filtrates were colorless. Then the filtrates were combined and evaporated under reduced pressure to obtain lignin fractions. The lignin fractions were suspended in water and then freezing-dried to ensure complete removal of the rest of the solvents. The lignin fractions extracted with ether, ethyl acetate, methanol, acetone, and dioxane/water (9/1, v/v) were noted as F0, F1, F2, F3, and F4, respectively.

Component analysis, structural characterization and antioxidant activity determination were conducted according to a previous report [15].

Results And Discussion

Fractionation of organosolv lignin. The organosolv lignin prepared from bamboo was sequentially extracted with five organic solvents with increasing dissolving capacity for lignin according to our preliminary experiments, i.e., ether, ethyl acetate, methanol, acetone, and dioxane/water (9/1, v/v); and the yields of the five fractions obtained were 2.80, 39.85, 18.64, 23.38, and 13.30%, respectively (**Table 1**). The ether-soluble fraction of organosolv lignin was a sticky residue, rather than free-flowing powders in the case of the other fractions. In addition, the FTIR spectroscopy analysis in a preliminary investigation indicates that it was extractives (such as fatty acids and resinous materials). For this reason, together with its low yield (2.80%), this preparation was discarded as unmeaning fraction and further analyses were focused on the fractions extracted with ethyl acetate (F1), methanol (F2), acetone (F3), and dioxane/water (F4).

Table 1

Yield, weight-average ($\overline{M}_w$) and number-average ($\overline{M}_n$) molecular weights and polydispersity ($\overline{M}_w / \overline{M}_n$) of bamboo organosolv lignin and fractionated lignins (%).

Lignin sample [a]	Yield	$\overline{M}_w$ (g/mol)	$\overline{M}_n$ (g/mol)	$\overline{M}_w / \overline{M}_n$
FL	-	8280	4360	1.90
F1	39.85	3870	2930	1.32
F2	18.64	5760	4120	1.40
F3	23.38	13160	7950	1.66
F4	13.30	11820	6800	1.74

[a] FL represents the starting lignin; F1, F2, F3, and F4 represent lignin preparations extracted with ethyl acetate, methanol, acetone, and dioxane/water, respectively.

To investigate the effect of solvent extraction on the molecular weight of the lignin, the samples were investigated with GPC. The weight-average and number-average molecular weights and polydispersity of the lignin specimens, calculated based on the curves of GPC, are listed in **Table 1**. From F1 to F3, a steady increase of both the molecular weight and polydispersity strongly suggests that F1 contained materials of relatively homogeneous low molecular weight whereas F3 was composed of a mixture of medium and high molecular

weight materials. With respect to F1, a significantly high amount of low molecular weight lignin in organosolv lignin (FL) was extracted with ethyl acetate. In addition, F2 was a medium molecular weight material, basically depleting of materials with low and high molecular weights. Overall, the solvents used in the present study showed good selectivity for fractionation organosolv lignin, evidenced by the increasing molecular weight from F1 to F3.

Sugar analysis. Sugar content of lignin and its sub-fractions is listed in **Table 2**. Overall, the bound sugar contents were below 4.0%, indicating that the organosolv lignin separated by formic acid delignification technology produced lignin by-products with a relatively low amount of impurities. Clearly, there were no marked differences among the sugar contents of the fractionated specimens and the starting material. This suggests that the strong association between hemicelluloses and lignin existed in the organosolv lignin samples with different molecular weights. For all preparations, xylose was the predominate sugar followed by arabinose and glucose. This was in well agreement with the fact that arabinoxylan was the main sugar impurity in lignin being linked with arabinose side chains of xylan via ether/ester bonds in grass [16].

Table 2
Sugar analysis of bamboo organosolv lignin and fractionated lignins (%).

Lignin sample [a]	Total	Arabinose	Galactose	Glucose	Xylose	Glucuronic acid
FL	3.26	1.03	0.07	0.53	1.33	0.30
F1	3.43	0.99	0.11	0.55	1.44	0.35
F2	2.12	0.78	0.05	0.12	0.93	0.24
F3	2.15	0.70	0.03	0.21	1.02	0.19
F4	3.35	0.61	0.15	1.01	1.28	0.30

[a] Corresponding to the lignin samples in Table 1.

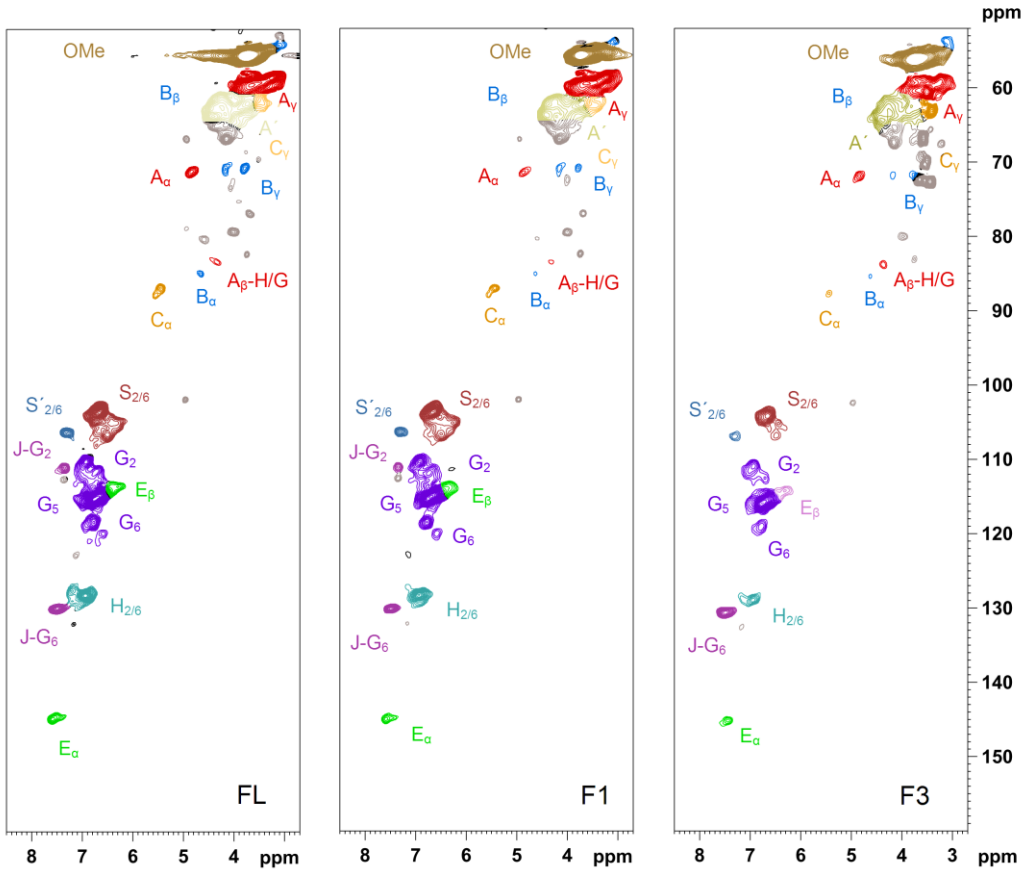

Fig. 1 HSQC spectra of bamboo organosolv lignin (FL) and fractionated lignins (F1 and F3). See Fig. 2 for the main lignin substructures.

Spectral analysis. The HSQC spectra of bamboo organosolv lignin (FL) and the lignin fractions were recorded and typical spectra of lignin samples (FL, F1, and F3) are illustrated in **Fig. 1**. and the main substructures identified are shown in **Fig. 2**. The signal assignments of HSQC spectra are shown as follows. In the side religion, the prominent correlation signals corresponding to *β-O*-4' substructures (A) were observed for *α*- and *γ*-C positions at δ_C/δ_H 71.2/4.83 and 59.6/3.25—3.85, and for *β*-C positions at δ_C/δ_H 83.4/4.32 in G and H type lignins. γ-Acylated *β*-O-4' aryl ether linkages (A') were observed with their correlations at δ_C/δ_H 61.9/3.55—3.95 for the γ-C-position. Additionally, signals corresponding to other linkages were also observed. Strong signals for resinol structures (*β-β´/α-O-γ´/γ-O-α´* linkages, B) were observed with their C-H correlations for *α*-, *β*-, and *γ*-C positions at δ_C/δ_H 84.6/4.65, 53.4/3.07, and 70.9/3.80, 70.9/4.16. Phenyl coumaran substructures (C) were observed by C-H correlations for *α*- and *γ*-C positions at δ_C/δ_H 86.8/5.46 and 62.2/3.75. Cinnamate units (E) were characterized by their C_α-H_α correlations at δ_C/δ_H 145.0/7.58 and C_β-H_β correlations at δ_C/δ_H 114.4/6.30, due to *p*-coumarate and ferulate [17]. In the aromatic region, signals from G S H units were clearly observed. The S units showed a prominent signal for the $C_{2,6}$-$H_{2,6}$ units at δ_C/δ_H 104.0/6.68, whereas the G units showed different correlations for C_2-H_2 (δ_C/δ_H 110.3/6.92), C_6-H_6 (δ_C/δ_H 118.5/6.77), and C_5 (δ_C/δ_H 115.0/6.80). In addition, signals from the oxidized (α-ketone) structure of syringyl lignin (S') were presented at δ_C/δ_H 106.2/7.30 [18]. A high amount of *p*-hydroxyphenyl (H) units was identified by the correlations at δ_C/δ_H 127.8/7.21.

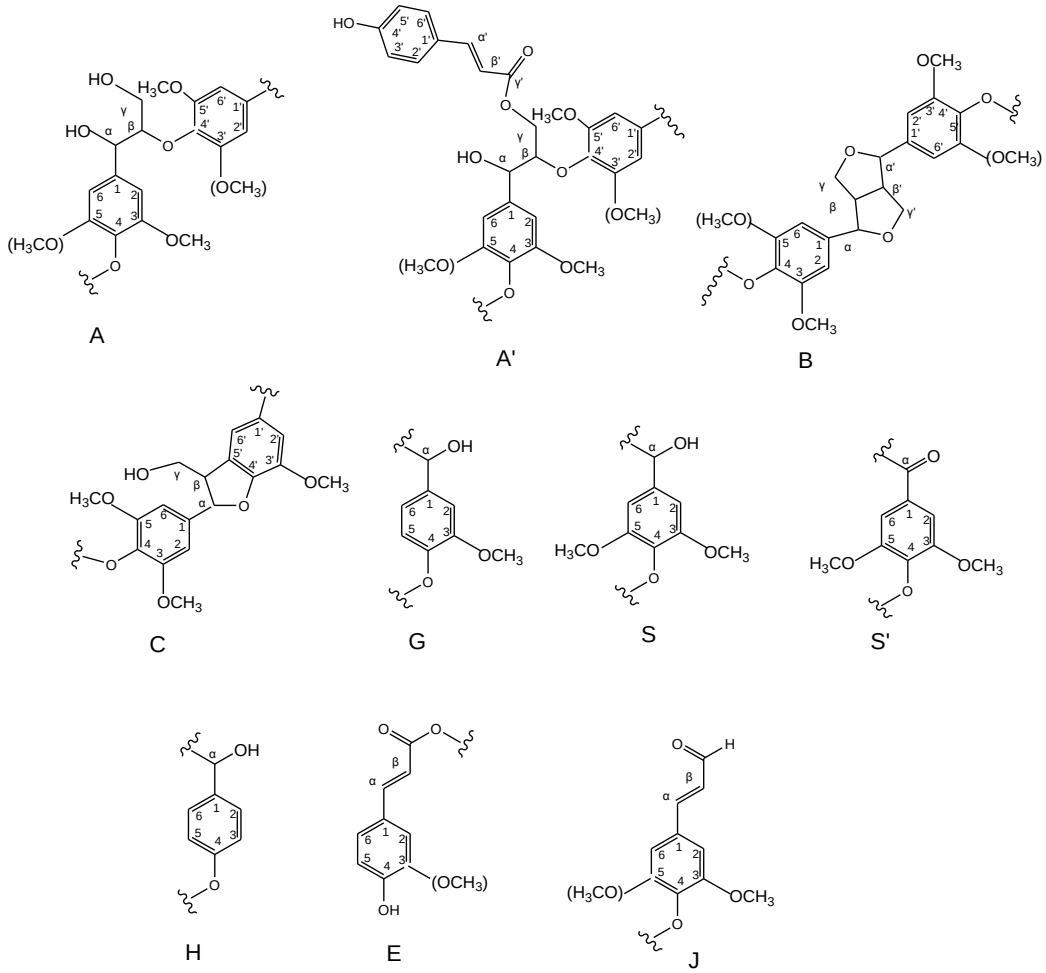

Fig. 2 Main substructures of bamboo organosolv lignin involving different side-chain linkages and aromatic units identified by HSQC.

The functional groups in lignin were determined by ^{1}H NMR spectroscopy, and the data are presented in **Fig. 3**. A decrease of the contents of methoxyl, phenolic and aliphatic hydroxyl groups in the lignin fraction was observed from F1 to F4. Generally, a higher phenolic hydroxyl content indicates more serious degradation of the lignin macromolecule. Among these fractions, the highest content of phenolic hydroxyl group in F1 was in well agreement with its low molecular weight due to the serious degradation. For the preparation of novel materials, the most important functional group in lignin structure is free phenolic group, which is preferentially attacked by chemicals. The highest phenolic hydroxyl group in F1 suggested that it had the greatest potential to react with oxyalkylating reagents (i.e., ethylene oxide and propylene oxide). The compatibility between lignin and polyolefins would be greatly improved and the lignin would disperse more homogeneously [19]. The high content of phenolic hydroxyl group in F1, suggesting its good reactivity with formalde.

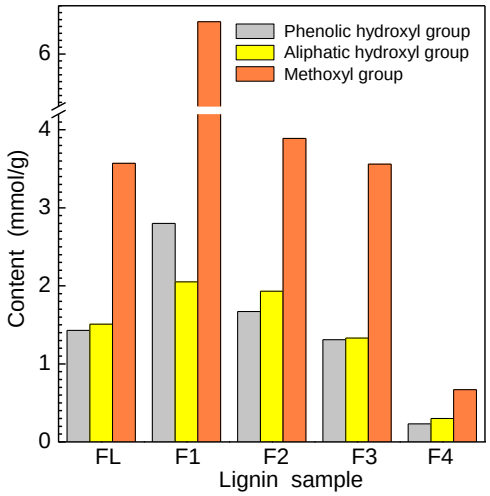

Fig. 3 Contents of phenolic and aliphatic hydroxyl groups in bamboo organosolv lignin and fractionated lignins.

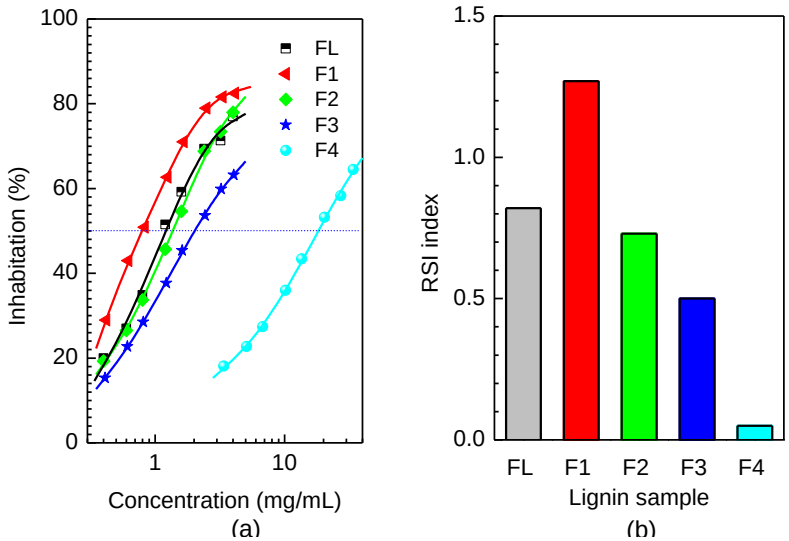

Fig. 4 Antioxidant activity against DPPH of bamboo organosolv lignin and fractionated lignins. (a) DPPH inhibitory effect; and (b) RSI value.

Antioxidant capacity. Many studies have demonstrated that the extracts from lignocelluloses, mainly composed of phenolic structures, have antioxidant and antimicrobial capacity [20, 21]. To investigate the effect of the fractionation on the antioxidant capacity of lignin, the samples were tested against DPPH since oxidation is usually occurred resulted from free radical attack. The profiles of DPPH inhibitory effects of the lignin fractions are illustrated in **Fig. 4a** and the corresponding radical scavenging index (RSI) values are calculated as shown in **Fig. 4b**. From **Fig. 4a**, the inhibitory effect increased with increasing the concentration of lignin for all samples. The calculated RSI values were 1.27, 0.73, 0.50, and 0.05 for F1, F2, F3, and F4, respectively, as compared to 0.82 for FL. Obviously, the antioxidant capacity of the lignin fraction showed a decreasing trend with increasing the dissolving capacity of solvent. The antioxidant ability of lignin is mainly contributed by the free phenolic hydroxyl group content. In addition, other groups, such as aliphatic hydroxyl group and methoxyl group, also showed effects on the antioxidant ability. The most powerful radical scavenger of F1 may be explained as follows. The high content of phenolic hydroxyl

group was essential for the formation of large amounts of phenoxyl radicals (i.e., hydrogen atom abstraction) [22]. The high amount of the methoxyl group in the lignin largely stabilized the phenoxyl radicals formed. The lignin fraction F1 with the highest high RSI value would be a promising material as stabilizer to prevent polymer aging [23].

Conclusions

Bamboo organosolv lignin (FL) was fractionated into five preparations by sequential solvent extractions with ether (F0), ethyl acetate (F1), methanol (F2), acetone (F3), and dioxane/water (F4). A significantly high amount (39.85%) of low molecular weight fraction in organosolv lignin was extracted with ethyl acetate. Sugar analysis suggests that the strong association between hemicelluloses and lignin existed in the organosolv lignin samples with different molecular weights. The contents of methoxyl, phenolic， and aliphatic hydroxyl groups in the lignin fractions were decreased from F1 to F4. The antioxidant capacity of the lignin fractions showed a decreasing trend with increasing the dissolving capacity of solvent. The lignin fraction extracted with ethyl acetate, having a high RSI value, would be a promising material as stabilizer to prevent polymer aging.

References

[1] S. Sahoo, M.O. Seydibeyoglu, A.K. Mohanty, M. Misra, Characterization of industrial lignins for their utilization in future value added applications, Biomass Bioenerg. 35 (2011) 4230–4237.
[2] A. Casas, M. Oliet, M.V. Alonso, F. Rodríguez, Dissolution of *Pinus radiata* and *Eucalyptus globulus* woods in ionic liquids under microwave radiation: Lignin regeneration and characterization, Sep. Purif. Technol. doi:10.1016/j.seppur.2011.1012.1032.
[3] T.K. Kirk, W. Brown, E.B. Cowling, Preparative fractionation of lignin by gel-permeation chromatography, Biopolymers. 7 (1969) 135–153.
[4] A. Toledano, A. Garcia, I. Mondragon, J. Labidi, Lignin separation and fractionation by ultrafiltration, Sep. Purif. Technol. 71 (2010) 38–43.
[5] C. Bhattacharjee, P.K. Bhattacharya, Ultrafiltration of black liquor using rotating disk membrane module, Sep. Purif. Technol. 49 (2006) 281–290.
[6] A. Garcia, A. Toledano, L. Serrano, I. Egues, M. Gonzalez, F. Marin, J. Labidi, Characterization of lignins obtained by selective precipitation, Sep. Purif. Technol. 68 (2009) 193–198.
[7] R.W. Thring, M.N. Vanderlaan, S.L. Griffin, Fractionation of Alcell ^{R} lignin by sequential solvent extraction, J. Wood Chem. Technol. 16 (1996) 139–154.
[8] C. Schuerch, The solvent properties of liquids and their relation to the solubility, swelling, isolation and fractionation of lignin, J. Am. Chem. Soc. 74 (1952) 5061–5067.
[9] R.C. Sun, J. Tomkinson, S. Griffiths, Fractional and physico-chemical analysis of soda-AQ lignin by successive extraction with organic solvents from oil palm EFB fiber, Int. J. Polym. Anal. Ch. 5 (2000) 531–547.
[10] K. Wang, F. Xu, R. Sun, Molecular characteristics of Kraft-AQ pulping lignin fractionated by sequential organic solvent extraction, Int. J. Mol. Sci. 11 (2010) 2988–3001.
[11] T.Q. Yuan, J. He, F. Xu, R.C. Sun, Fractionation and physico-chemical analysis of degraded lignins from the black liquor of Eucalyptus pellita KP-AQ pulping, Polym. Degrad. Stabil. 94 (2009) 1142–1150.

[12] D. van de Pas, A. Hickson, L. Donaldson, G. Lloyd-Jones, T. Tamminen, A. Fernyhough, M.L. Mattinen, Characterization of fractionated lignins polymerized by fungal laccases, Bioresources 6 (2011) 1105–1121.
[13] S. Baumberger, C. Lapierre, B. Monties, Utilization of pine kraft lignin in starch composites: Impact of structural heterogeneity, J. Agric. Food Chem. 46 (1998) 2234–2240.
[14] R.M. Wilkins, J. Zhao, Controlled release of a herbicide from matrix granules based on solvent-fractionated organosolv lignins, J. Agric. Food Chem. 48 (2000) 3651–3661.
[15] M.F. Li, S.N. Sun, F. Xu, R.C. Sun, Mild acetosolv process to fractionate bamboo for the biorefinery: Structural and antioxidant properties of the dissolved lignin, J. Agric. Food Chem. 60 (2012) 17303–17312.
[16] A.U. Buranov, G. Mazza, Lignin in straw of herbaceous crops, Ind. Crop. Prod. 28 (2008) 237–259.
[17] H. Kim, J. Ralph, Solution-state 2D NMR of ball-milled plant cell wall gels in DMSO-d_6/pyridine-d_5, Org. Biomol. Chem. 8 (2010) 576–591.
[18] D. Ibarra, M.I. Chavez, J. Rencoret, J.C. del Rio, A. Gutierrez, J. Romero, S. Camarero, M.J. Martinez, J. Jimenez-Barbero, A.T. Martinez, Structural modification of Eucalypt pulp lignin in a totally chlorine-free bleaching sequence including a laccase-mediator stage, Holzforschung 61 (2007) 634–646.
[19] P. Mousavioun, W.O.S. Doherty, Chemical and thermal properties of fractionated bagasse soda lignin, Ind. Crop. Prod. 31 (2010) 52–58.
[20] S. Dudonne, X. Vitrac, P. Coutiere, M. Woillez, J.M. Merillon, Comparative study of antioxidant properties and total phenolic content of 30 plant extracts of industrial interest using DPPH, ABTS, FRAP, SOD, and ORAC Assays, J. Agric. Food Chem. 57 (2009) 1768–1774.
[21] J.M. Cruz, J.M. Dominguez, H. Dominguez, J.C. Parajo, Antioxidant and antimicrobial effects of extracts from hydrolysates of lignocellulosic materials, J. Agric. Food Chem. 49 (2001) 2459–2464.
[22] L.R.C. Barclay, F. Xi, J.Q. Norris, Antioxidant properties of phenolic lignin model compounds, J. Wood Chem. Technol. 17 (1997) 73 – 90.
[23] A. Gregorova, B. Kosikova, A. Stasko, Radical scavenging capacity of lignin and its effect on processing stabilization of virgin and recycled polypropylene, J. Appl. Polym. Sci. 106 (2007) 1626–1631.

Composition Changes and Enzymatic Hydrolysis Property of *Tamarix* under Various Factors of Steam Explosion

Hong Xu, Qiang Yong, Shiyuan Yu

College of Chemical Engineering, Nanjing Forestry University,

Nanjing, China

Yong Xu[*]

College of Chemical Engineering, Nanjing Forestry University,

Nanjing, China

Jiangsu Key Laboratory of Biomass-based Green fuels & Chemicals, Nanjing,

China

Abstract

It's essential and important to carry out research on the *tamarix* high-valued biorefining for promoting national land afforestation, ecological construction and agricultural income as *tamarix* is a kind of abundant lignocellulosic resources in western China. Few reports about *tamarix* have been found now. In this study, effects of residence time, explosion temperature and severity factor (lg *R*) on the composition and cellulose enzymatic hydrolysis performance of *tamarix* were presented during steam explosion pretreatment (SEP). The result showed that SEP hardly changed the contents of cellulose and sulfuric acid insoluble lignin in *tamarix*; however, it could break effectively the native structure of *tamarix* and promote most xylan to degrade into xylose by its auto-hydrolysis, in which some small molecule derivates came together, such as acetic acid, formic acid and furfural and so on. In view of the recovery ratio and the enzyme hydrolysis yield of cellulose in *tamarix*, maximum glucose yields upon enzymatic hydrolysis were obtained after pretreatment at 210℃ for 10 min. Based on the cellulose recovery rate and the cellulose hydrolysis yield, the optimum steam explosion pretreatment conditions for *tamarix* biorefinery was at the lg *R* value of 4.239(Steam explosion temperature was 210℃, residence time was 10 min). And in the steam-exploded *tamarix* the cellulose content changed little, it's all around 42%, while the residual hemicellulose was only 1.65%, and generated 0.28% formic acid and 2.18% acetic acid. The enzymatic hydrolysis yield of cellulose in the steam exploded *tamarix* raised to 86% from 15.5% of the native material at lg *R* = 4.239 with the cellulase loading of 20.0 FPIU/ (g

cellulose) after reaction for 48 h. Overall, this study shows that steam explosion without an acid catalysis is a good pretreatment method for saccharification of *tamarix*. Optimal steam explosion conditions need to be a compromise between sugar accessibility and sugar degradation.
Key words: *Tamarix*; steam explosion pretreatment; severity factor; cellulose enzymatic

1 Introduction

In recent years, our society is developing in a high speed with the consumption of gas, oil and coal. Because of greenhouse gas emissions and because fnite resources are being depleted, it's problematic of the scale and intensity of the use of these fossil fuels. Increasing concern on global climate change and energy security coupled with diminishing fossil fuel resources have spurred a renaissance of interest in the development of alternative forms of fuel and materials from renewable resources (Poulomi, 2010). Lignocellulosic biomass is a renewable resource, which can be converted to liquid transportation fuels as well as used as a plat form to produce bio-based materials (Hendriksa, 2009). The most dominant biofuel produced today is bioethanol with a global production of 85.8 billion liters in 2010, mainly produced from sugar and starch based biomass (Johansson, 2010). The currently dominating crops and the land on which they are produced are also potential resources for food production, and it is well recognized that the use of edible crops for biofuel production may threaten food security (Svetlana, 2009). In order to avoid the occurrence of these potential threats, biofuel production should be based on the use of non-edible biomass fractions (Sims, 2010).

In our country, the most abundant non-edible biomass resource is lignocellulosic biomass, of which large amounts are produced in the agriculture and forest sectors (Lin, 2006; Lal, 2005). *Tamarix* is a typical kind of plant in plateau, which is rich in western China. Every year, it can produce up to one million tons of the abandoned branches. At present, the branches are used to burning, which is a waste of resource (Shizhong Li, 2011). So it's essential to carry out research on the *tamarix* high-valued biorefining for promoting national land afforestation, ecological construction and agricultural income. Successful exploitation of this and other lignocellulosic waste biomass for bio-based product is quiet interesting (Chandra, 2007).

The biorefinery of lignocellulosic often has three steps: pretreatment, enzymatic hydrolysis and fermentation (Michael, 2010). The pretreatment aims to improve the rate of production as well as the total yield of liberated sugars in hydrolysis step. The overall efficiency of the pretreatment process is correlated to a good balance between low inhibitors formation and high substrate digestibility (Carolina, 2011; Mirjam, 2007). Steam explosion is one of the most efficient pretreatment methods for lignocellulosic biomass (Chandra, 2007). It involves heating biomass at relatively high pressure, followed by a mechanical disruption of the fibers by a rapid pressure drop (explosion). The main factors of steam explosion are explosion temperature, residence time and type of material and so on. The explosion temperature and residence time can be combined into a single "reaction ordinate"(R) often reported as the "severity factor" lg *R* (Wyman, 2005). In this study, steam explosion without an acid catalysis were used for pretreatment of *tamrix*. We have carried out a systematic study of the effect of various steam explosion conditions. The effects of the pretreatment conditions were evaluated by studying composition changes and enzymatic hydrolysis yield.

2 Materials And Methods

2.1 Raw material

Dry *tamarix* was provided by Yongjing, Gansu province. The raw tamrix was cut to 6-8cm and stored at room temperature before use.

2.2 Steam explosion pretreatment (SEP)

The steam explosion unit (Nanjing Forestry University) consists of a 3.0L pressure vessel and a flash tank with a removable bucket to collect the pretreated material. The steam is generated by a electric steam boiler.

200g dry matter (DM) of cut *tamarix* was added to pressure vessel in each treatment. SEP of *Tamarix* was carried out using 9 different steam explosion conditions with temperatures ranging from 180 – 220℃ and residence times ranging from 5 – 15min. The temperature and residence time variables can be combined into a single "reaction ordinate" (R) often reported as the "severity factor" lg *R*. The severity factor in this pretreatment screening set up varied from 3.355 – 4.533(see Table 1). After each SEP the unit was cleaned by running 2 steam explosions with only steam for 60sec and then flushing the flash tank and bucket with water. The pretreatment fractions were stored at -20℃ before composition analysis and enzymatic hydrolysis.

Table1 Pretreatment conditions and the corresponding strength factor

explosion temperature/℃	residence time/s	severity factor (lg *R*)
210	300	3.938
210	480	4.142
210	600	4.239
210	720	4.318
210	900	4.415
180	600	3.355
190	600	3.650
200	600	3.944
220	600	4.533

2.3 Hydrolysis

Hydrolysis was carried out in 125 mL Erlenmeyer flask using 50 g reaction system that was horizontally shaken at 150 rpm, 50℃. The pH in the hydrolysis reactions was adjusted by adding 1.0M lemon acid buffer, pH 4.5, to the final pH 4.8. The substrate concentration in the flasks was 50 g DM L^{-1} substrate and the dosage of cellulase was 20 FPIU/ (g cellulose).

2.4 Analysis

Analysis of the carbohydrate and lignin content in tamarix samples before and after steam explosion were carried out using the method of NREL. The sugar compositions were determined by NREL, too. Dry

matter (DM) was determined by drying the samples at 105℃ for more than 6 hours.

HPLC analysis of reaction mixtures were run in house using Aiglent 1260 (USA) set up with combined refractive index (for cellobiose, glucose, xylose, arabinose, acetic acid, HMF, formic acid and ethanol and so on determination) . The HPLC samples were prepared by diluting samples from the reactions within the standard square by deionized water followed by centrifugation and filtration (0.22μm Sarsted Filtropur S). 10 μL samples were applied to a Bio-Rad HPX-87H column conditioned at 55 ℃ with 0.6 mL min^{-1}, 5mM H_2SO_4.

3 Results And Discussion

3.1 Steam explosion

Pretreatment of *tamarix* was carried out using different steam explosion conditions showed in table 1. The severity factor was combined with explosion temperature and residence time by the formula of lg *R*= lg {t ×exp [(T-100)/14.75]}（Wyman, 2005）. Generally, more harsh pretreatment conditions led to a darker brown colored biomass with less visible residual fiber structure. At the higher temperatures, the pretreatment led to a relative increase in content of cellulose and lignin, and a relative reduction in the hemicellulose content.

3.1.1 Physical structure before and after SEP

SEP can effectively change the physical structure of lignocellulosic *tamarix*. Along with the SEP intensity coefficients improve, the color of the mixture (tamarix after SEP) transited from brown to black gradually. The shape of them was fibrous or muddy. Also the SEP can destroy the internal structure, which can be found by the SEM as Figure 1.

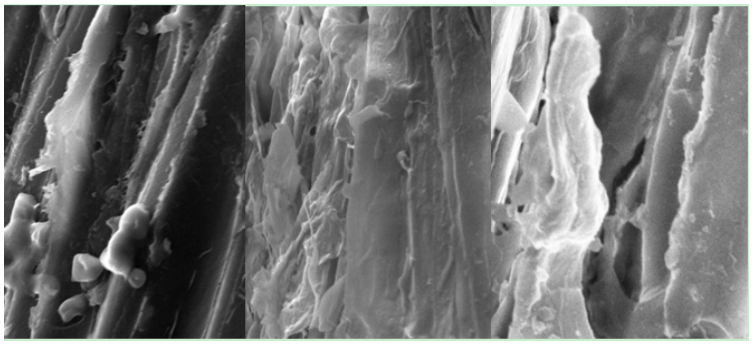

(a) (b) (c)

Fig.1 SEM photos of *tamarix* before and after SEP

PS: All of the magnification is 2400. (a) before SEP(b) after SEP, lg *R*=4.239 (c) after SEP, lg *R*=4.415

Figure 1 shows that the *tamarix* fiber surface before SEP is smooth. And the fiber arranged in a rule and close together. After SEP, the organizations of tamarix become loose and cavity increasing. The fiber surface appeared a lot of crack and lobes that was very helpful in improving the enzymatic hydrolysis. So SEP really can destroy the structure of *tamarix*, what were very important in the next process.

3.1.2 Dissolution content after SEP

In the process of SEP, the xylan, glucan and others were degraded to monosaccharide and other small molecules, such as acetic acid, formic acid, HMF, etc. These are all water-soluble, so they were in the

liquid (see Table 2).

Table 2 Dissolution content in the liquid after SEP (100g DM)

explosion temperature/℃	residence time/s	Glucose /g	Xylose /g	Arabinose /g	Formic acid/g	Acetic acid/g	HMF /g	Furfural /g	Total /g
210	300	0.334	0.768	0.000	0.383	0.665	0.388	0.675	3.212
210	480	0.378	0.301	0.002	0.243	1.724	0.187	0.483	3.318
210	600	0.105	0.382	0.009	0.275	2.176	0.218	0.572	3.736
210	720	0.116	0.419	0.005	0.416	3.332	0.409	0.722	5.418
210	900	0.129	0.413	0.006	0.403	3.357	0.378	0.796	5.516
180	600	0.113	0.653	0.054	0.287	1.233	0.141	0.368	2.849
190	600	0.249	0.987	0.111	0.399	1.899	0.221	0.527	4.394
200	600	0.345	0.925	0.014	0.427	2.814	0.378	0.796	5.698
220	600	0.064	0.261	0.002	0.283	2.366	0.229	0.384	3.587

Although the variation of the various substances is not very obvious in Table 2, but from based on the total content, it still can be found that, with the increase in explosion temperature or residence time, would lead to more degradation of polysaccharides and lignin. At the higher temperature, more volatile substance may be produced, so the total content declined.

3.1.3 Composition changes before and after SEP

In the process of SEP, most of the cellulose and lignin are in the solid, including little of hemicellulose. The residue content of cellulose, lignin and hemicellulose after SEP will directly influence the follow-up of enzymatic hydrolysis. The composition changes of the solid before and after SEP were shown in Figure 2.

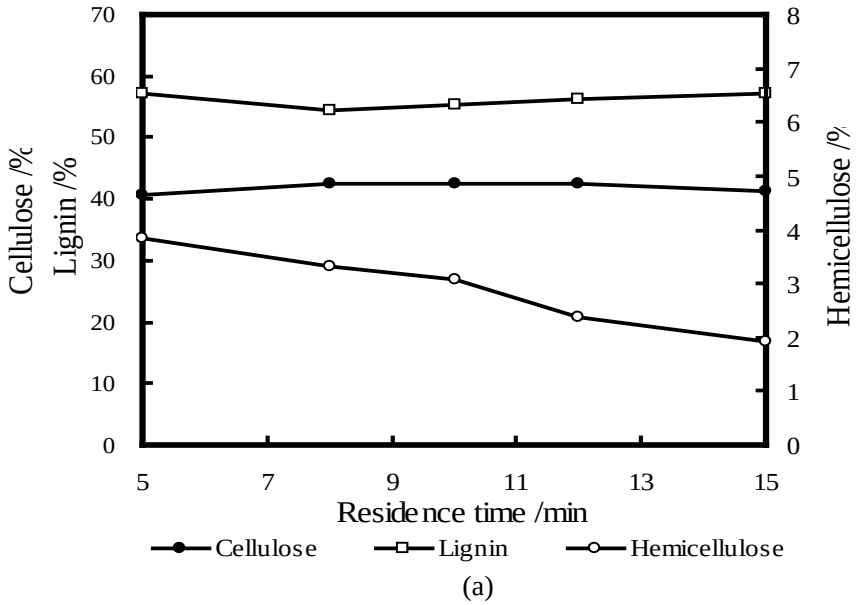

(a)

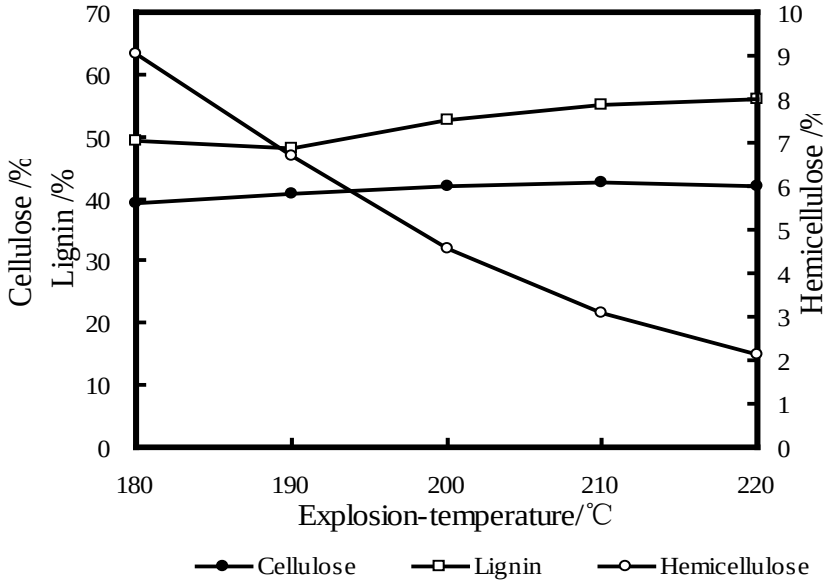

(b)

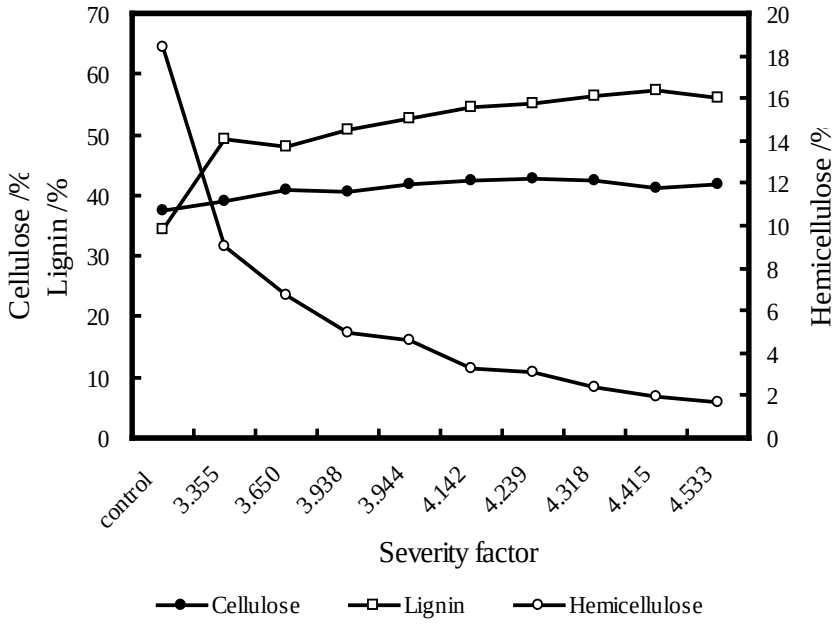

(c)

Fig.2 Composition changes of *tamarix* before and after SEP

(a) The influence of residence time on composition changes

(b) The influence of explosion temperature on composition changes

(c) The influence of severity factor on composition changes

The sample labeled "control" contained untreated *tamarix*.

The Figure 2 shows that SEP can effectively make the hemicellulose degraded. The composition changes were prominent compared before and after SEP, especially the content of hemicellulose. Before SEP, it

consisted of 38% cellulose, 18% hemicellulose and 37% lignin and others. Whereas after SEP, it made up of 39% cellulose, 9% hemicellulose and 49% lignin at lowest severity factor 3.355. With the severity factor increasing, changes of cellulose and lignin were not obvious. At the higher temperatures, the pretreatment led to a relative increase in content of cellulose and lignin, and a relative reduction in the hemicellulose. At the same residence time, with the explosion temperature increasing, more and more of the hemicellulose was degraded to xylose and other small molecules, such as acetic acid, formic acid and HMF and so on(Figure 2 & Table 2). From the Figure 2, just thinking of composition, we can know that the hasher the condition is, the greater the changes. But with the severity factor of SEP improving, more energy was consumed. Importantly, high temperature led the lignin to melt and cover the cellulose, which would make the hydrolysis were difficult. In addition, the requirements of equipment were increased. This is a typical effect of steam explosion (Ballesteros, 2004; Horn, 2010) caused by degradation of hemicellulose sugars and loss of volatile compounds in the outlet steam. Optimal steam explosion conditions need to be a compromise between sugar accessibility and sugar degradation.

3.2 Enzymatic hydrolysis

To evaluate the effect of the different thermal pretreatment, the 9 different samples of steam treated *tamarix* were hydrolyzed using commercial cellulase preparations at substrate concentration of 50 g DM L^{-1} and 100 g DM L^{-1}. The steam treat material was used directly after solid-liquid separation, i.e. without washing. Figure 3 shows that the enzymatic hydrolysis yield based on released glucose after 24 h at substrate concentration of 50 g DM L^{-1} and 100 g DM L^{-1}. The data show that steam explosion conditions of 210 ℃ and 10 min residence time (severity factor 4.239) yield maximum glucose release, so the enzymatic hydrolysis yield is highest, which is 86%(50 g DM L^{-1}) and 66%(100 g DM L^{-1}). The data further suggest that at severity factor 4.239 is preferable; above or below the severity factor yielded somewhat lower glucose concentration. Compared with the control (untreated *tamarix*), the enzymatic hydrolysis yields of materials after SEP had greatly improved, from 15% to 41-86%, which indicated that SEP is a effective method for *tamarix* treatment. Clearly, from the Figure 3, the enzymatic hydrolysis yield of 50 g DM L^{-1} is higher than 100 g DM L^{-1}. That because substrate concentration would influence the mass transfer and the enzyme may be uneven distribution, and then the enzyme can't effectively combine of the substrate. At the hasher conditions, the enzymatic hydrolysis yield decreased that because at higher temperature the lignin began to melt and cover the cellulose. Moreover, the hasher conditions will damage the cellulose of non-crystalline which is easily hydrolyzed, thereby affecting the enzymatic hydrolysis yield (Hodge, 2008).

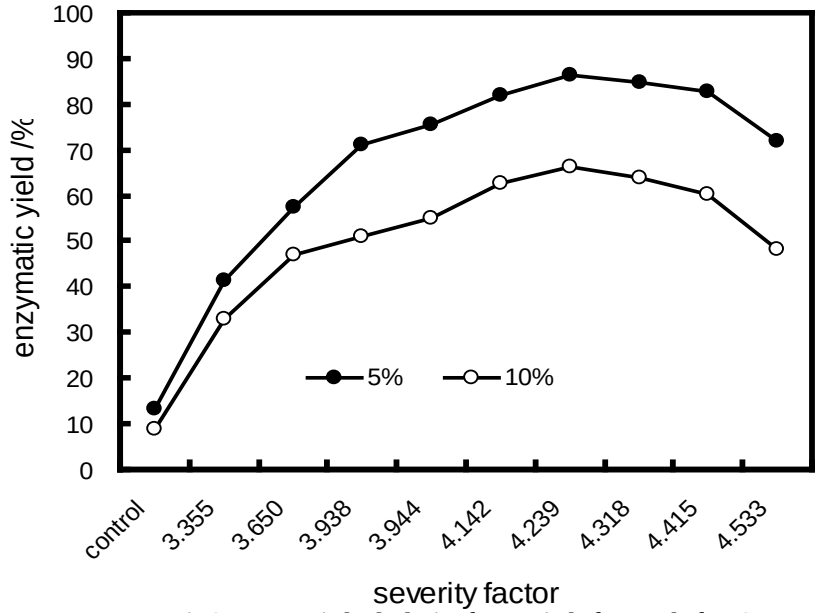

Fig.3 Enzymatic hydrolysis of tamarix before and after SEP

The reactions were carried out at pH 4.8 and 50 ℃with 50 g DM L^{-1} and 100 g DM L^{-1}. The sample labeled "control" contained untreated *tamarix*. The theoretical maximum enzymatic hydrolysis yield for the material pretreated for 10 min at 210 ℃(severity factor (lg R) 4.239) is 86%.

4 Conclusions

This study has shown that steam explosion is an effective pretreatment method for hemicellulose degradation and saccharification of *tamarix,* even without any additional treatments such as acid impregnation and washing steps. At optimum pretreatment condition enzymatic hydrolysis yield based on released glucose was in the order of 86% of the theoretical maximum, indicating excellent cellulose availability after the steam explosion step.

The main purpose of this study was to see whether the *tamarix* is a potential and excellent raw material for biorefinery and how variation in steam explosion pretreatment parameters affects the enzymatic digestibility of *tamarix*. The enzymatic hydrolysis was mainly used to screen for the effect of steam explosion. To develop an industrial process these steps also have to be developed and optimized (e.g. lower enzyme dosages, higher DM content) and they are indeed subject to intensive and successful research. So far there are little reports about *tamarix* biorefinery.

References

Ballesteros M., 2004. Ethanol from lignocellulosic materials by a simultaneous saccharification and fermentation process (SFS) with *kluyveromyces marxianus* CECT 10875. Process Biochem. 39:1843-1848.

Carolina B., 2011. Effect of inhibitors formed during wheat straw pretreatment on ethanol fermentation by *Pichia stipitis*. Bioresource Technology. 102: 10868-10874.

Chandra R., 2007. Substrate pretreatment: the key to effective enzymatic hydrolysis of lignocellulosic. Adv Biochem Eng/ Biotechnol. 108:67-93.

Hendriksa TW M., 2007. Pretreatment to enhance the digestibility of lignocellulosic biomass. Bioresource Technology. 100(1):10-18.

Hodge DB, 2008. Soluble and insoluble solids contributions to high-solids enzymatic hydrolysis of lignocellulose. Bioresource Technology. 99: 8940-8948.

Horn SJ, 2010. Enzymatic hydrolysis of steam-exploded hardwood using short processing times. Biosci Biotechnol Biochem. 74:1157-1163.

Johansson K, 2010. Agriculture as provider of both food and fuel. Ambio. 39:91-96.

Lal R, 2005. World crop residues production and implications of its use as a biofuel. Bioresource Technology. 31: 575-584.

Lin Y, 2006. Ethanol fermentation from biomass resources: current state and prospective. Appl Microbiol Biotechnol. 69:627-642.

Michael, 2010. A biorefinery processing perspective: treatment of lignocellulosic materials for the production of valued-added products. Bioresource Technology. 101:8915-8922.

Mirjam A., 2007. Effect of pretreatment severity on xylan solubility and enzymatic break down of the remaining cellulose from wheat straw. Bioresource Technology. 98:2034-2042.

Poulomi S., 2010. Cellulosic biorefinery - unleashing lignin opportunities. Current Opinion in Environment Sustainability. 2:383-393.

Sassner P., 2005. Steam pretreatment of Salix with and without SO_2 impregnation for production of Bioethanol. Appl Biochem Biotechnol. 121:1101-1117.

Sims REH, 2010. An overview of second generation biofuel technologies. Bioresource Technology. 101: 1570-1580.

Shizhong Li, 2011. Study on the Necessity and Feasibility of Tamarix Development in Yongjing Country. Jilin Agriculture.4: 234.

Svetlana N, 2009. Bioethanol production from corn meal by simultaneous enzymatic saccharification and fermentation with immobilized cells of *Saccharomyces cerevisiae var.* ellipsoideus. Fuel.88:1602-1607.

Wyman CE., 2005. Coordinated development of leading biomass pretreatment technologies. Bioresource Technology. 96:1959-1966.

Acknowledgments

This study was funded by Government Public Industry Research Special Funds for Projects (Grant No.201004001), National Natural Science Foundation of China (Grant No.31070514), the Technology Innovation Team of Jiangsu Higher Education Institutions and the Priority Academic Program Development of Jiangsu Higher Education Institutions. We thank the people who help us in the experiment process.

Polyols Production by Chemical Modification of Autocatalyzed Ethanol-Water Lignin From *Betula Alnoides*

Bai-Liang Xue[1] *–Jia-Long Wen*[2] *– Feng Xu*[3] *–Run-Cang Sun*[4*]

[1] Master student, Institute of Biomass Chemistry and Technology- Beijing Forest University, Beijing, China
xuebailiang67@163.com
[2] PHD student, Institute of Biomass Chemistry and Technology- Beijing Forest University, Beijing, China
wenjialonghello@126.com
[3] Professor, Institute of Biomass Chemistry and Technology- Beijing Forest University, Beijing, China
xfx315@163.com
[4] Professor and director, Institute of Biomass Chemistry and Technology- Beijing Forest University, Beijing, China
rcsun3@bjfu.edu.cn
* *Corresponding author*

Abstract

Betula alnoides lignin, recovered as a byproduct in auto-catalyzed ethanol-water pulping process, was converted into viscous polyols through oxypropylation and liquefaction methods, with the aim of valorising this byproduct. The oxypropylation reaction was performed by reacting auto-catalyzed ethanol-water lignin (AEL) with propylene oxide under acidic and alkaline conditions at room temperature respectively, whereas the liquefaction reaction was carried out using the mixed solvents of polyethylene glycol and glycerol at 160 ºC with sulfuric acid as a catalyst. The resulting polyol products from each method were characterized by FT-IR, ^{1}H and ^{31}P NMR spectroscopy, gel permeation chromatography (GPC). The results showed that the aliphatic hydroxyl groups and molecular weights of the polyols all increased significantly after oxypropylation and liquefaction reaction as compared to original AEL. These polyols used as precursors in polyurethane synthesis gave promising results.

***Keywords*:** lignin, oxypropylation, liquefaction, polyol, NMR

Introduction

In recent years, the exploitation and utilization of lignocellulosic biomass for chemicals and materials has been attracting considerable attention, mainly due to the economical and environmental problems accompanied with the use of fossil resources. Lignin is the second most abundant components of lignocellulosic materials in plant cell walls after cellulose, corresponding to an annual production of 5×10^7 tons [1]. Organosolv pretreatment is considered as an environmental and promising biomass pretreatment technology for biofuels, enormous amounts of auto-catalyzed ethanol-water lignin (AEL) are produced by treatment of biomass with ethanol [2]. AEL is a usually high-purity and sulfur-free lignin, which has less condensed structure and narrower molecular weight distribution than lignin obtained from other methods [3]. AEL was utilized as a sole precursor in the synthesis of prepared polyols and their subsequent incorporation into polyurethane, two alternative approaches have been put forward: (i) oxypropylation of lignin with propylene oxide (PO), (ii) liquefying lignin with polyethyleneglycol (PEG) and glycerol [4, 5].

In this work, the aim was to establish the feasibility of converting AEL from *Betula alnoides* using both oxypropylation and liquefaction methods into the polyols. The generating bio-based polyol products obtained under optimized condition can be used directly for the preparation of polyurethane foams without any additional treatment. The resulting polyols were characterized by using spectroscopic techniques such as Fourier transform infrared spectroscopy (FT-IR), nuclear magnetic resonance (NMR), and their thermal stability were studied in terms of thermogravimetric analysis.

Materials and Methods

Materials. Birch (*Betula alnoides*) was obtained from Yunnan Province, China. All chemical reagents used were analytical grade.

AEL preparation. The lignin preparation was carried out using a 1.0 L stainless steel reactor (Parr, America). The reactor was loaded with material (20-40 mesh) and 60% ethanol solution with a solid to liquid ratio of 1:10 (g/mL), and then heated up to at 200 ºC for 2 h. After treatment, the reactor was cooled down rapidly, the pulp was removed to filtrate using a nylon cloth and washed repeatedly by 60% aqueous ethanol. The filtrate and washings were collected and poured into a three volume of water to precipitate lignin. The resulting lignin precipitate was filtrated to through filter paper, and then freeze dried. The crude lignin obtained was purified by dissolving it into 1, 4-dioxane and filtrated, and then the lignin preparation obtained was freeze-dried for further analysis.

Oxypropylation and liquefaction of AEL. Oxypropylation reactions were conducted according to Ahvazi et al. with slight modifications [6]. Briefly, AEL (200 mg) and 100 mL of 37 % PO were mixed in a 250 mL beaker under constant magnetic stirring for 30 min. Two different batches were carried out at room temperature under constant agitation for five days, 5 mL of 0.1 N NaOH under alkaline and 5 mL of 1 M H_2SO_4 under acidic conditions were added as the catalyst, respectively. After the reaction completed, excess

PO was removed under reduced pressure. The product was oven dried at 105 ºC to a constant weight before further analysis. Liquefaction experiment was performed according to the published literatures [7, 8], the optimal liquefaction conditions (liquefying solvents by weight ratio of PEG-400: glycerol: sulfuric acid of 90:10:3; reaction temperature: 160 ºC; reaction time: 60 min) were chosen. Liquefying solvents were added into a three-necked glass flask (250 mL) immersed in an oil bath and heated, which was equipped with reflux condenser and thermometer under constant magnetic stirring at nitrogen atmosphere. When the temperature reached at 160 ºC, a specific quantity of AEL was added gradually, and the liquefaction reaction was carried out for 1 h to obtain a homogeneous liquefied product. After the reaction time, the flask was cooled down rapidly in ice-bath, the liquefied products were oven dried at 105 ºC to a constant weight before further analysis.

Measurement of reaction extent. Reaction extent from oxypropylated and liquefied products was determined as following: 1g of the product was weighed and diluted with 20 mL 1, 4-dioxane-water mixture (80/20, w/w), the dilution was adequately stirred over 2 h and filtered with filter paper, and then oven dried the filter residue at 105 ºC to a constant weight and calculated the residue content.

Yield=$[1–M/M_0] \times 100\%$

where M_0 is the mass of AEL and M is the mass of the residue content in 1, 4-dioxane obtained after oxypropylation or liquefaction reaction.

FT-IR analysis. FT-IR spectra were performed using a Thermo Scientific Nicolet iN10 FT-IR Microscope (Thermo Nicolet Corporation, Madison, WI) equipped with a liquid nitrogen cooled MCT detector.

^{1}H, HSQC and ^{31}P NMR analysis. ^{1}H NMR spectra was performed after 128 scans. Samples (20 mg) were dissolved in 1 mL of deuterated dimethylsulfoxide (DMSO-d_6, 99.8% D). A repetition time of 3.98 s for acquisition time and 1 s for relaxation time were used. ^{1}H-^{13}C correlation 2D (HSQC) NMR spectrum was recorded with a z-gradient double resonance probe. Sample (25 mg) was dissolved in 1 mL of deuterated dimethylsulfoxide (DMSO-d_6, 99.8% D). The spectral widths were 8000 and 20,000 Hz for the ^{1}H- and ^{13}C- dimensions, respectively. ^{31}P NMR spectra were recorded with 32768 data points and a spectral width of 60606.06 Hz. A relaxation delay of 5 s was used, and the number of scans was 512. Samples (30mg) were weighted into 2mL a volumetric flask, 500 μL of a solvent mixture containing anhydrous pyridine and deuterated chloroform (1.6:1, v/v) were added. This was followed by the addition of 100 μL of cyclohexanol (10.85 mg/mL), as an internal standard, and 50 μL of chromium (III) acetylacetonate solution (5.6 mg/mL in anhydrous pyridine and deuterated chloroform 1.6:1, v/v), as a relaxation reagent. Finally, the mixture was treated with 100 μL of phosphitylating reagent (2-chloro-1, 3, 2-dioxaphospholane) and then transferred into a 5 mm tube for subsequent NMR analysis. All NMR experiments were carried out a Bruker AV III NMR spectrometer at 400 MHz at 25 ºC. Spectra were processed and analyzed using the Bruker Topspin 1.3 software package.

GPC analysis. Gel permeation chromatography (GPC, Agilent 1200, USA) was carried out on a PL-gel 10 µm mixed-B 7.5 mm ID column. Detection was achieved with a Knauer differential refractometer. The column was eluted with tetrahydrofuran at the flow rate of 1.0 mL/min. Samples (4 mg) were dissolved with 2 mL tetrahydrofuran. Monodisperse polystyrene was used as the standard for the molecular weight of samples.

Results and Discussion

AEL based polyol products were conducted through oxypropylation and liquefaction method in the synthesis of preparing polyurethane foams. With comparison of two distinct processes, an appropriate and reasonable suggestion on converting AEL into polyol products was offered. The content of both oxypropylation and liquefaction reactions was high as expressed by the amount of unreacted lignin residue that was barely present in the polyol products. The oxypropylated product yield of 93% was obtained at AEL: PO ratio of 2 (mg/ml) by using 37% PO at room temperature for five days under alkaline condition, whereas the corresponding yield of 80% under acidic condition. In the case of the liquefaction process, a yield of 97% was obtained at AEL: liquefying solvent ratio of 0.2 at 160 ºC for 1h. Consequently, the results indicated that the efficiency of liquefaction reaction was higher than oxypropylation method for conversion of AEL into polyols, although a small amount of residue was present in the liquefied solution.

FT-IR analysis. The spectroscopy of the lignin and its derivatives were shown in **Figure 1**, the peaks at about 3600-3100 cm^{-1} were attributed to OH groups stretching absorption, 2939-2847, 1458 and 1370 cm^{-1} were assigned to CH_3, CH_2 and CH aliphatic groups, respectively. The bands at 1593, 1508, 1458 and 1421 cm^{-1} were due to aromatic skeletal vibrations of sample (a). Furthermore, the syringyl absorption around 1323 cm^{-1}, weak band at 1262 cm^{-1}, strong band near 1215 cm^{-1}, and its maximum absorbance at 1119 cm^{-1} were attributed to sample (a). Sample (b) exhibited more increase in the peak intensity of OH groups than the corresponding OH groups from sample (c), indicating that the oxypropylation reaction between AEL and PO had indeed occurred. Moreover, this phenomenon suggested that AEL was more liable to oxypropylation under alkaline condition than their counterparts under acidic condition, which were well in agreement with the previous published results [4, 6]. Sample (d) showed the absorption intensity of OH and methyl groups increased significantly, which might be due to the structure of PEG and glycerol. Additionally, according to Jin, et al., the increase in the peak intensity of methyl groups was probably due to two reasons, one reason was that the bonds between the coupling of benzene ring units ruptured and smaller benzene ring units formed, the other was that the alkylation reaction of the phenol hydroxyl units of the lignin occurred [8]. All the above results indicated that oxypropylation and liquefaction processes induced a successful chain extension reaction for the conversion of AEL into polyols.

Figure 1. FT-IR spectra of (a) AEL, (b) oxypropylated lignin with PO under alkaline condition, (c) oxypropylated lignin with PO under acidic condition, (d) liquefied lignin with glycerol and PEG.

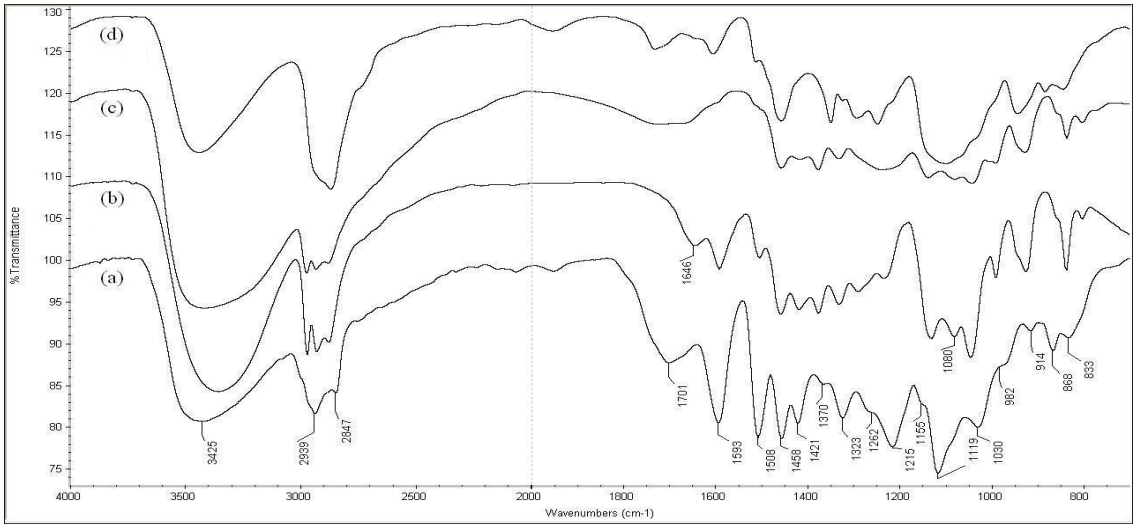

^{1}H NMR analysis. ^{1}H NMR spectra of different samples were shown in **Figure 2**, most of the peak features were consistently similar, apart from some different signals. The peaks at around 3.8, 3.5 and 1.1 ppm were attributed to CH_3, CH_2 and CH groups of PO homopolymer of sample (b) and (c), respectively. Furthermore, it should be noted that the doublet in the case of the methyl signal of PO can not be observed probably due to the broadening effect of the PO homopolymer chains [4]. In addition, strong peaks in the region of 6.5-7.5 ppm were assigned to aromatic ring of sample (a) whereas these peaks in other samples (b-d) were quite diluted. Moreover, the peak intensity of the hydroxyl groups of sample (b) and (c) compared with sample (a) increased remarkably. All these signals indicated that polyols were indeed prepared through two methods.

Figure 2. ^{1}H NMR analysis of (a) AEL, (b) oxypropylated lignin with PO under alkaline condition, (c) oxypropylated lignin with PO under acidic condition, (d) liquefied lignin with glycerol and PEG.

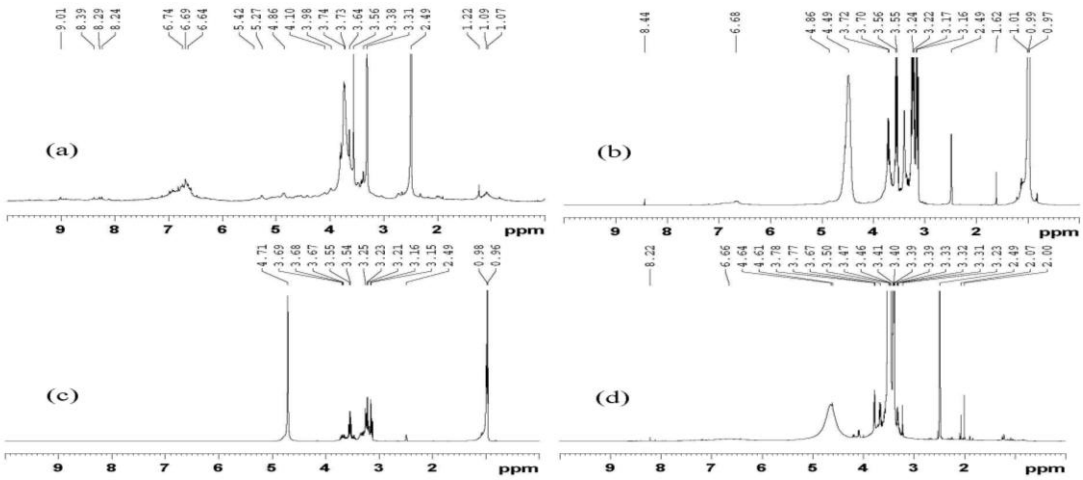

^{31}P NMR analysis. ^{31}P NMR spectroscopy was used to identify and quantify several different classes of hydroxyl groups in lignin and its derivatives. The distinction between

primary and secondary aliphatic hydroxyl groups was examined by integration of ^{31}P NMR spectra (**Table 1**). The spectral regions were identified as follows: erythro (136.7-134.5 ppm), threo (134.5-133.8 ppm), primary hydroxyl units (133.5-132.5 ppm), syringyl phenolic units (132.0-131.4 ppm), guaiacyl phenolic units (129.7-129.5 ppm), *p*-hydroxyphenyl phenolic units (128.0-127.0 ppm), and carboxylic acids (126.8-126.6 ppm) [6]. As seen from the spectra (**Figure 3**), sample (a) showed typical features for a hardwood lignin, which mainly included syringyl and guaiacyl units, meanwhile, minor amount of *p*-hydroxyphenyl units was existed. These above signals were in accordance with the aforementioned results of NMR and FT-IR analysis. Comparison of sample (b) and (c), it can be found that large amounts of aliphatic hydroxyl groups changed obviously during the oxypropylation reaction, the secondary hydroxyl groups of sample (b) increased to 2.016 mmol/g whereas the primary hydroxyl groups of sample (c) added up to 2.194 mmol/g. Faix, et al.showed that the signals of secondary hydroxyl groups were probably assigned to the *erythro* and *threo* configurations of the *β-O*-aryl ether structures in lignin [9]. Argyropoulos demonstrated that the formation of predominantly secondary alcohols probably occurred at Cα-aryl structure [10]. Furthermore, according to Pandey, et al., PO is probably attacked at the sterically less hindered CH_2 carbon in lignin under alkaline condition, resulting in the formation of secondary hydroxyl groups, in contrast, more primary than secondary hydroxyl groups were detected under acidic condition [11]. With regard to the liquefaction process, the content of primary hydroxyl groups significantly increased from 1.113 to 4.296 mmol/g, indicating that the bio-based polyols were formed by the introduction of PEG and glycerol chains into the lignin structure. However, the interesting phenomenon is that the content of secondary hydroxyl groups became zero. Based on the conclusion of Jasiukaityte, et al., the increased amount of primary hydroxyl groups were probably due to the introduction of PEG and glycerol molecule at Cα position of lignin [12]. As for the results of secondary hydroxyl groups, the reason may be interpreted in terms of lignin self-polymerization. Accordingly, the higher primary hydroxyl groups were obtained in the liquefaction process, in contrast, more secondary hydroxyl groups were found during alkaline oxypropylation reaction.

Figure 3. ^{31}P NMR analysis of (a) AEL, (b) oxypropylated lignin with PO under alkaline condition, (c) oxypropylated lignin with PO under acidic condition, (d) liquefied lignin with glycerol and PEG.

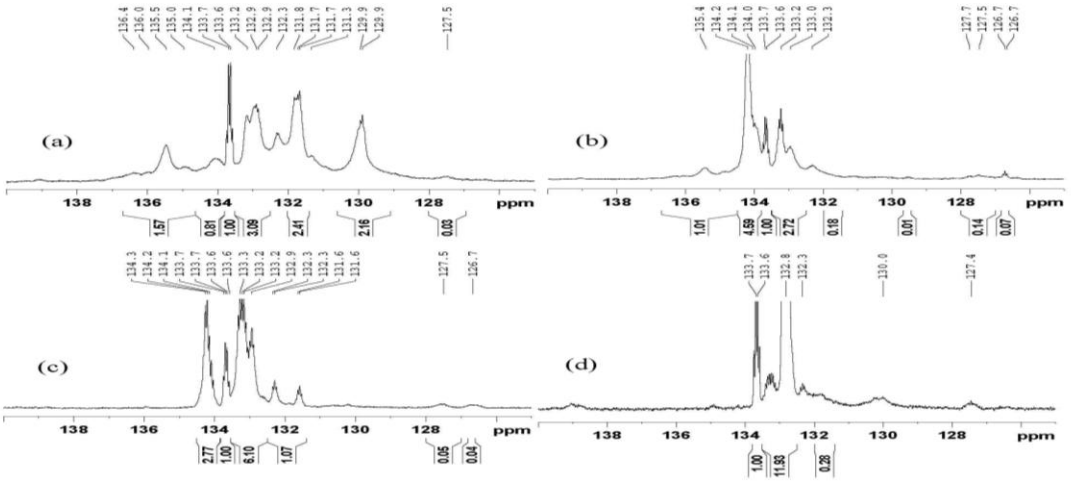

Table 1 ^{31}P NMR spectroscopy analysis of (a) AEL, (b) oxypropylated lignin with PO under alkaline condition, (c) oxypropylated lignin with PO under acidic condition, (d) liquefied lignin with glycerol and PEG. (mmol/g)

parameter	(a)	(b)	(c)	(d)
COOH		0.026	0.013	
G	0.778	0.003		
S	0.909	0.067	0.16	0.101
H	0.012	0.052		
aliphatic-OH				
primary	1.113	0.98	2.194	4.296
secondary (erythro and threo)	0.859	2.016	0.997	
total-OH	3.671	3.144	3.364	4.397

GPC analysis. Weight-average (*Mw*) and number-average (*Mn*) molecular weights and polydispersity (*Mw/Mn*) of the samples for GPC analysis were shown in **Table 2**. Compared with the sample (a) (*Mw* 2560 g/mol, *Mn* 1530 g/mol), the growth of *Mw* and *Mn* after oxypropylation reaction occurred under alkaline condition (*Mw* 3130g/mol, *Mn* 2080 g/mol), more importantly, the obvious increase of *Mw* and *Mn* was observed after liquefaction reaction (*Mw* 4990g/mol, *Mn* 4630 g/mol). The products obtained showed increased molar masses, indicating that the condensation reactions between the lignin and multifunctional alcohols occurred, moreover, the molecular weights of simple (d) had more intensively increase than simple (b) and (c). Lai, et al. have reported that residual lignin self-polymerization reaction occurred during the liquefaction reaction of the dissolved lignin by glycerol and diethylene glycol moieties [13]. Jasiukaityte, et al. have suggested that the high molecular weight of simple (d) was mainly due to the condensed structures formed by the incorporation of the aliphatic glycerol and DEG moieties into the lignin structure [12]. Furthermore, it should be noted that the molecular weights of the simple (b) was not increased remarkably, indicating that lignin was less prone to oxypropylation under acidic condition than corresponding alkaline condition, these results were well in agreement with the results of FT-IR and NMR analysis. In addition, a similar low value of polydispersity for (*Mw/Mn* 1.08-1.67) indicated that all the samples had a narrow molecular weight distribution.

Table 2 Molecular weight analysis of (a) AEL, (b) oxypropylated lignin with PO under alkaline condition, (c) oxypropylated lignin with PO under acidic condition, (d) liquefied lignin with glycerol and PEG

parameter	(a)	(b)	(c)	(d)
M_w	2560	3130	2960	4990
M_n	1530	2080	1860	4630
M_w/M_n	1.67	1.51	1.59	1.08

Conclusions

Oxypropylation and liquefaction techniques have been used as possible ways of utilizing the AEL from the autocatalyzed ethanol-water pulping process. The polyols obtained from two methods would be used directly in manufacturing polyurethane without any additional treatment. In future works, the research of preparing polyurethane with the polyols generated from oxypropylation and liquefaction products will be further illustrated.

References

1. Klemm, D., Heublein, B., Fink, H.P., Bohn, A., 2005. Cellulose: fascinating biopolymer and sustainable raw material. Angewandte Chemie International Edition. 44: 3358–3393.
2. Pan, X.J., Kadla, J.F., Ehara, K., Gilkes, N., Saddler, J.N., 2006. Organosolv ethanol lignin from Hybrid Poplar as a radical scavenger: relationship between lignin structure, extraction conditions, and antioxidant activity. Journal of Agricultural and Food Chemistry. 54: 5806–5813.
3. Sannigrahi, P., Ragauskas, A.J, Miller, S.J., 2010. Lignin structural modifications resulting from ethanol organosolv treatment of loblolly pine. Energy Fuel. 24: 683–689.
4. Nadji, H., Bruzzése, C., Belgacem, M.N., Benaboura, A., Gandini, A., 2005. Oxypropylation of lignins and preparation of rigid polyurethane foams from the ensuing polyol. Macromolecular Materials Engineering. 290: 1009–1016.
5. Cateto, C.A., Barreiro, M.F., Rodrigues, A.E., Belgacem, M.N., 2009. Optimization study of lignin oxypropylation in view of the preparation of polyurethane rigid foams. Industrial & Engineering Chemistry Research. 48: 2583–2589.
6. Ahvazi, B., Wojciechowicz O., Ton-That T.M., Hawari J., 2011. Preparation of Lignopolyols from Wheat Straw Soda Lignin. Journal of Agricultural and Food Chemistry. 59: 10505–10516.
7. Briones, R., Serrano, L., Younes, R.B., Mondragon, I., Labidi, J., 2011. Polyol production by chemical modification of date seeds. Industrial Crops and Products. 34: 1035–1040.
8. Jin, Y.Q, Ruan, X.M, Cheng, X.S, Lu, Q.F., 2011. Liquefaction of lignin by polyethyleneglycol and glycerol. Bioresource Technology. 102: 3581–3583.
9. Faix, O., 1994. Determination of hydroxyl groups in lignins. Holzforschung. 48: 387–394.
10. Argyropoulos, D.S., 1995. ^{31}P NMR in wood chemistry: a review of recent progress. Research on Chemical Intermediates. 21: 373–395.
11. Pandey, K.K., Vuorinen, T., 2008. Study of kinetics of reaction of lignin model compounds with propylene oxide. Holzforschung. 62: 169–175.
12. Jasiukaityte, E., Kunaver, M., Crestin, C., 2010. Lignin behaviour during wood liquefaction—Characterization by quantitative ^{31}P, ^{13}C NMR and size-exclusion chromatography. Catalysis Today. 156: 23–30.

13. Lai, Y.Z., Sarkanen, K.V. Isolation and structural studies, in: Y.Z. Lai, K.V. Sarkanen (Eds.), Lignins Occurrence, Formation, Structure and Reactions, Wiley-Intersciense, New York, 1971; pp 165–240.

Analysis of the Required Energy for Wood Heat Treatment Processes Using Superheated Steam

Yonggun Park[1]-Yeonjung Han[1] - Jun-Ho Park[1] - Yoon-Seong Jang[1] - Sang-Yun YANG[1] - Hwanmyeong YEO[2]*

[1]Dept. of Forest Sciences, CALS, Seoul National University,
599 Gwanak-ro, Gwanak-gu, Seoul – South Korea.
[2]Research Institute for Agriculture and Life Sciences,
Dept. of Forest Sciences, CALS, Seoul National University,
599 Gwanak-ro, Gwanak-gu, Seoul – South Korea.
hyeo@snu.ac.kr
** Corresponding author*

Abstract

The Heat Treatment (HT) is a method to change the physio/bio-chemical properties of wood to be better to human by heating at high temperature(150-300℃), which can modify its composition. Wood increases in hydrophobicity and dimensional stability, its inhomogeneous surface color becomes homogeneous, and its decay-resistance is improved due to HT. On the contrary, because of HT, wood tends to decrease in strength due to the development of many internal checks.And when it has not been adequately dried before HT, more defects such as checks, warping, and fractures occur during oven HT. In addition, there also exists the danger of fire during the oven HT process because wood can catch fire due to the effect of the high temperature. Consequently, this study seeks to develop an HT method, which uses superheated steam as a medium of HT for reducing fire hazard. By simultaneously drying green wood and exposing it to HT, controlling the process, analyzing the energy required for the entire process, and evaluating the energy efficiency, usability of superheated steam was evaluated in view of its significant for safety and energy efficiency. Generally, the thermodynamic energy required for eliminating moisture from wood in drying process can be classified into the heat energy (H_1) for increasing the temperature of wood, heat energy (H_2) for overcoming absorptive power, heat energy (H_3) to heat the residual moisture in wood, and heat energy (H_4) for heating and evaporating the moisture to be eliminated from wood. After calculating the total required energy (H_{Total}) including the for producing and handling the superheated steam (H_5), through comparing the totally required energy with the energy actually consumed in the superheated steam drying-HT process, the amount of lost energy and the energy efficiency of the process were evaluated. Through the results of this study, the eco-friendly effect of superheated steam HT method was proved quantitatively.

***Keywords*:**Superheated steam, drying, heat treatment, required energy, efficiency, water movement, defect-free

Introduction

Wood has contributed to survival of humanity and civilization and developed variously from simple living tools of primitive man to engineering wood of civil man. By being interested in the safety of residential living and environmental conditions and preferring eco-friendly materials, the demand of wood has been increased. Wood is regarded as eco-friendly material which can enhance the living standards.

The wood has not only aesthetic benefits as materials that are consistent with people's emotions like a variety of colors and patterns, smooth touchand visual sensation that cannot expected in other materials, and but also physical benefits like great strength and stiffness per unit weight and, good thermal and electrical insulation, and the various extractives in the wood can be used as raw materials for chemical products and drugs. But, the wood has some disadvantages like uneven dimensional stability and durability by each water sorption state. To overcome and/or minimize these disadvantages some treatments like heating, compressing and injecting chemical agents have been used.

The Heat Treatment (HT) is a method to change the physio/bio-chemical properties of wood to be better to human by heating at high temperature (150-300℃), whichcan modify its composition. Because of increasing the concerns about environmental pollution of chemical preservativeinsecticide and its health hazard,the method is attracting attentions as artificial preservative-free treating technique. Militz (2002) had compared some HT processes each other and evaluated the effects of Finland (Thermo Wood process), Netherlands (Plato process), France (Rectification process and Boisperdure process) and Germany (OHT-Oil Heat Treatment process).And he reported that increasing dimensional stability and durability is possible if the processes control properly depending on species in the temperature range of 160 ~ 260℃. Kamdem (2002) reported that French HT (for Pine, Fir and Beech) improves durability of wood but decreases its bending strength. Also, Esteves et al. (2007) reported that dimensional stability of Eucalyptus was enhanced but its strength was decreased by mass loss and equilibrium moisture content decreased after heat treatment at 170~200℃

On the other hand, it has been reported that the heat treatment without pre-drying causes serious cracks. Also, Conventional oven HT process is known to have a higher risk of fire. The cautions on the risk are needed.

Superheated Steam, steam with a temperature above the boiling point, began to be used at the drying in the early 1900 and was used at the drying industry in Germany in the 1930s (Mujumdar, 1990). Drying method by superheated steam has many advantages. The method can save net energy because it is easy to condense the used vapor and recover energy. Andthe method can diminish amount of hazard substances emitting to the outside and have additional effects on the sterilization and deodorization. Also, the method is safe, because there is no oxidation or combustion reaction, and its drying rate can be higher than kiln drying rate. In this study, green lumber was dried and heat-treated with superheated steam for preventing the occurrence of drying check and diminish the fire risk. And energy efficiency of the treatment was evaluated.

Materials and Methods

Materials.
Pitch Pine (*Pinusrigida*) tree produced in Korea was cut and it was sawed and planned.Lumbers with dimension of 150mm (width) × 50mm (thickness) × 600mm (length) were prepared.

Superheated steam heat treatment (SHS HT)
Superheated steam HT was performed in the following order. A green lumber was put into reactor and 150mL water was supplied into the reactor.The reactor was sealedtightly. (The water which is poured into reactor is changed to superheated steam rapidly and helps a fast heat transfer from steam to wood at initial stage of drying process.)Next, the air in sealed reactor was drawn off with vacuum pump, then control temperature (about 255℃), inner surface of reactor, was adjusted to heat to target temperature (220℃). Water in reactor was evaporated;the reactor became filled up with superheated steam. Asliquid water in reactor and water in wood being evaporated, vapor pressure in reactor increased. If vapor pressure in reactor reached target pressure, pressure controller was operated to maintain target pressure.

Normal heat treatment.
Normal oven HT was performed as a control to compare its required energy and its energy efficiency with those of superheated steam HT. Target temperature and processing time were same as superheated HT, butinitial moisture content of lumber was different. Pre-dried specimen of about 8% MC was used. Reactor was not sealed and air in reactor was heated at atmospheric pressure.

Evaluation of water movement in wood during superheated steam HT process.
To evaluatemoisture movement in wood during superheated steam HT, the average moisture content (MC) of lumber and sectional specimen's MCs along longitudinal and transverse direction after 4, 6, 8, 10 and 12hour treatments. Figure 1 shows the specimenswhich were classified to 3 parts - End, Quarter, and Middle. Left and right three parts in figure were specimens for evaluating moisture distribution along longitudinal direction and transverse direction, respectively. Each specimen of transverse direction was cut [illegible]2).

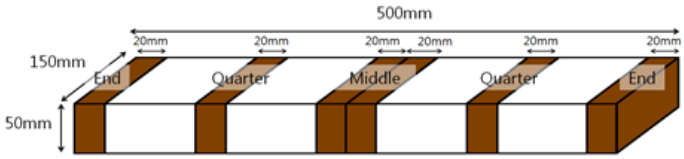

Figure1.Location of specimens prepared for evaluating moisture distribution along longitudinal and transversal direction during SHS heat treatment process

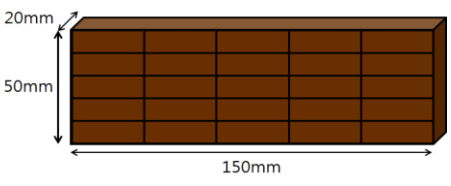

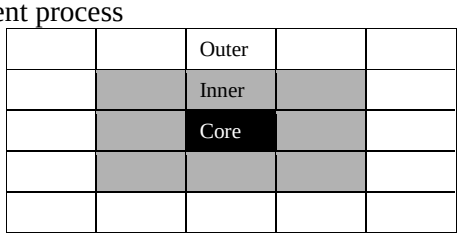

Figure2. Sectioning specimen to evaluatemoisture distribution along transverse direction

Evaluation of required energy and energy efficiency.

Generally, the thermodynamic energy required for eliminating moisture from wood in drying process can be classified into the heat energy (H_1) for increasing the temperature of wood, heat energy (H_2) for overcoming absorptive power, heat energy (H_3) for heating the residual moisture in wood, and heat energy (H_4) for heating and evaporating the moisture to be eliminated from wood. This classification can be applied to evaluate the energy consumption in heat treatment process. Heat energy (H5) for generating superheated steam (forsuperheated steam HT),and heating air in reactor (fornormal HT) could be added to the above 4 kinds of heats. Table 1 summarizes the equations for calculating each heat-energy. The energy efficiency was defined as the ratio of entire required energy to actual amount of energy used in each process.

Table 1. Summary for equations calculating each heat-energy

Heat energy for rising wood temperature (H_1)	$W_0 C_{wood}(T_1 - T_0)$
Heat energy for overcoming hygroscopic force (H_2)	$W_0 H_{de}$
Heat energy for heating remaining water in wood (H_3)	$W_0 M_R (T_2 - T_0) C_{water}$
Heat energy for heating and evaporating water removed from wood (H_4)	$W_0 \Delta mc(\Delta T c_{water} + h_{water})$
Heat energy for generating superheated steam or heating air in reactor (H_5)	

W_0 = oven-dry weight of wood (g)
C_{wood} = specific heat of wood(=$\frac{m+0.29}{1+m}$cal/g ・℃)
C_{water} = specific heat of water(=1cal/g ・℃)
T_0 = initial temperature of wood before heating (℃)
T_1 = final temperature of wood after heating (℃)
T_2 = temperature of wood when dry (℃)
H_{de} = heat of desorption per unit weight of wood(=$10^{1.2335-5.408M_R}$) (cal/g)
M_R = residual moisture content (fraction)
Δmc = changes of moisture content (fraction)
ΔT = difference temperature between vapor(air) and outer air when oven-dry (℃)
h_{water} = Latent heat of vaporization(=$598.25 - 0.6T$) (cal/g)

Results And Discussion

Evaluation of water movement during superheated steam HT.

Table 2 showsthe moisture content before and after superheated steam HT at each processing times.

Table 2.Moisture content before and after superheated steam HT at each processing times

Processing Time (hour)	Initial Moisture Content (%)	Final Moisture Content (%)
4	63.50	32.58
6	45.83	7.28
8	31.80	0.00
10	39.71	0.00
12	45.08	0.00

After 4 hours, average moisture content (AMC) of wood was dropped to half of initial moisture content.After 6 hours, AMC was dropped to below 10% MC. Although there is a little time variation depending on the initial moisture content, wood became completely dried (oven-dried) after 8hours treatment. Figure 3showsthe changes of the temperature of wood and the temperature and pressure of vapor during 8hours, 10hours and 12hours treatments respectively. 3 graphs in the Figure 3 show the temperature rise of wood at between 6hours and 8hours. The temperature rise time could be determined to the time to reach oven-dry state of wood.

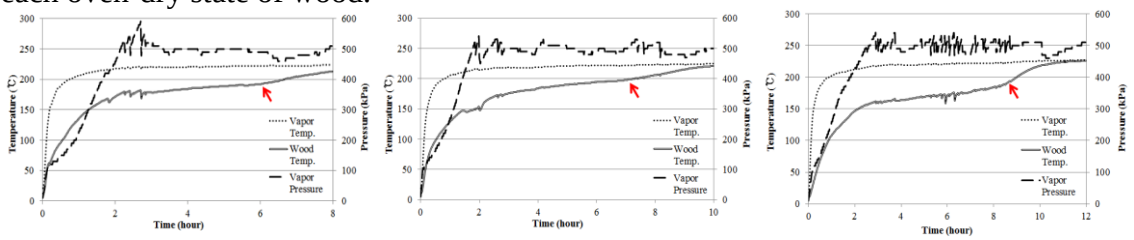

Figure3. Graph of changes of temperature in wood and temperature, pressure of vapor and power with processing time (left: 8 hours, center: 10 hours, right: 12 hours)

Figure 4 shows the distribution of moisture content in lumber along longitudinal direction. After 8hour superheated steam HT, the wood became oven-dry, all parts of End, Quarter and End are almost 0% MC. At the case of superheated steam HT for 6hours difference between End part and Middle part is about 5%;it means that moisture gradient in longitudinal direction is very small.

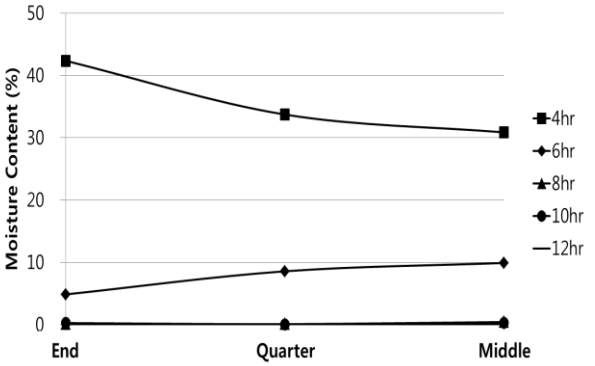

Figure4. Distribution of moisture content along longitudinal direction in lumber after 4, 6, 8, 10 and 12hour SHS HT

Figure5shows moisture contentsof outer part and core part in lumber after 4 hours (left) and 6 hours (right) SHS HT. In both case, moisture content of Outer part is lower than Core part. In case of 4 hours, the graph shows that MC difference between Core and Outer is 40%MC.It looks very large. But MC of Outer part is greater than 10%. It is a relatively high MC value at high temperature drying and HT process.This relatively high MC of outer part seems to prevent drying check occurrence during SHS HT. In case of 6 hours the MC difference between Outer and Core, is about 10%MC. This figure shows that moisture content gradient was small enough and time to dry was short enough to prevent a drying check occurrence.

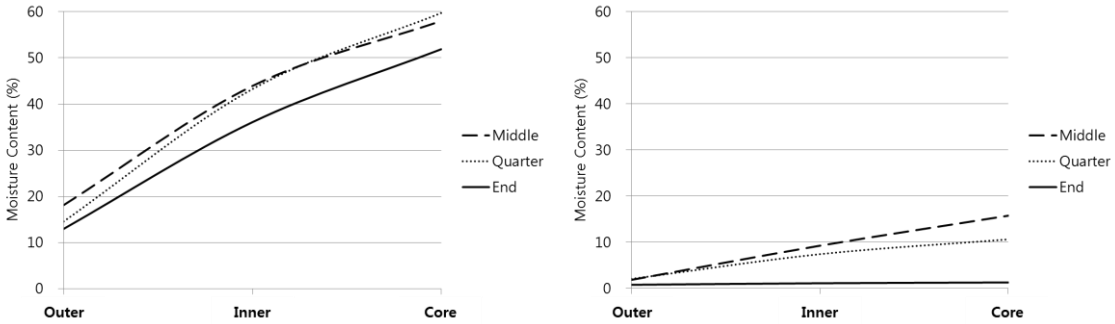

Figure 5. Moisture content of outer and core parts in lumber during SHS HT (left: 4hours, right: 6hours)

Evaluation required energy and energy efficient.
The followings are the steps for calculating required energy and energy efficiency of superheated steam HT (0.5MPa, 220℃).

a. Heat energy for rising wood temperature (H_1)
The oven-dry weight of wood was 2075.19g.Average specific heat of wood, depending on moisture content of wood, was calculated 0.40cal/g℃ with equation in the Table 1. Initial temperature of wood before heating was 11℃, and final temperature of wood was 226℃. So, heat energy for rising wood temperature was 178.54kcal.

b. Heat energy for overcoming hygroscopic force (H_2)
The heat of desorption per unit weight of wood from above fiber saturation point to oven-dry depends on residual moisture content (M_R). After superheated steam HT, wood became oven-dry, so the heat of desorption per unit weight of wood was 17.12cal/g. And heat energy for overcoming hygroscopic force was 35.53kcal.

c. Heat energy for heating remaining water in wood (H_3)
After superheated steam HT, the wood became oven-dry. So, the residual moisture content was 0. Therefore, heat energy for heating remaining water in wood was 0kcal.

d. Heat energy for heating and evaporating water removed from wood (H_4)
Fig. 6shows the changes of temperature of wood, vapor's temperature and pressure and the power used at the processing time. As mentioned above, after around 8 hourssuperheated steam HT, the wood specimen became completely dried. In case of superheated steam HT at 0.5MPa and 220℃target conditions, the real temperature of vapor, the temperature of outer air and the latent heat for vaporization of water were 227℃, 25℃ and 465.05cal/g respectively. Therefore heat energy for heating and evaporating water removed from wood was calculated to 618.25kcal.

e. Heat energy for generating superheated steam (H_5)
The process of 'water of 0.1MPa, 20℃ → superheated steam of 0.5MPa, 227℃' can be classified and analyzed to 'water of 0.1MPa, 20℃ → water of 0.1MPa, 100℃ → saturated vapor of 0.1MPa, 100℃ → superheated steam of 0.5MPa, 227℃'. Required

energy at the process of 'water of 0.1MPa, 20℃ → water of 0.1MPa, 100℃' is calculated to 12kcal by the equation of $Q = c_{water} \times m_{water} \times \Delta T$ and required energy at the process of 'water of 0.1MPa, 100℃ → saturated vapor of 0.1MPa, 100℃' is calculated to 80.74kcal by equation for latent heat of vaporization of water in Table 1. The enthalpy of saturated water at 0.1MPa, 100℃ conditions is 2674.90J/g and the enthalpy of superheated steam at 0.5MPa, 227℃ conditions is 2912.71J/g. So, the difference of two conditions is 237.81J/g. The Volume of reactor is 15L and the specific volume of superheated steam at 0.5MPa, 227℃ conditions is 0.45L/g. So, the weight of superheated steam in reactor when the process is over is 33.21g. Therefore required energy at the process of 'saturated vapor of 0.1MPa, 100℃ → superheated steam of 0.5MPa, 227℃' is calculated to 1.89kcal. As a result, heat energy for generating superheated steam was calculated to 94.62kcal.

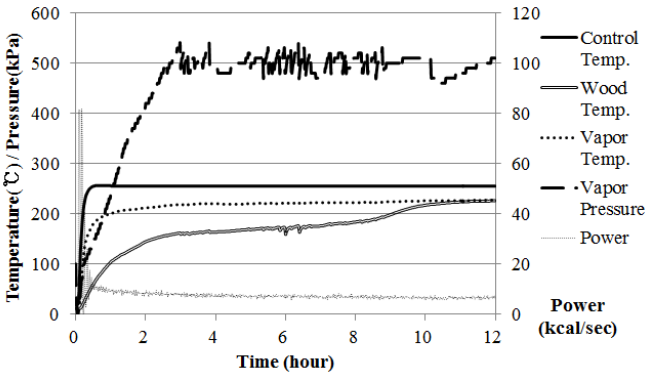

Figure6.Wood temperature in wood, Vapor's temperature and pressure and the power used at processing time

f. Energy efficiency

The actual amount of used power was monitored and recorded by and/or in a data acquisitioncomputer system connecting to reactor.The total amount of energy consumed during superheated steam HT was 1364.35kcal. And the total heat energy required for HT is 928.81kcal. Therefore the energy efficiency of superheated steam HT is calculated to 68.08%.

The required energy and the energy efficiency of normal HT were calculated in the same way and shownin Table 3.

Table 3. Required energy and energy efficiency for normal and superheated steam HT

	Required Energy (kcal)						**Actual Energy Consumption (kcal)**	Lost Energy (kcal)	**Energy Efficiency (%)**
	H_1	H_2	H_3	H_4	H_5	**H_{Total}**			
Normal HT	109.50	27.87	0.00	160.51	0.85	**298.73**	**1087.77**	789.03	**27.46**
SHS HT	178.54	35.53	0.00	620.11	94.62	**928.81**	**1364.35**	435.54	**68.08**

The energy efficiency of superheated steam HT was higher than the efficiency of normal HT. In case of normal HT, Lostenergy was much higher than superheated steam HT because high temperature air in reactor leaks free.

Conclusion

Bythe 4 hour heat treatment with 0.5MPaand 220℃superheated steam, moisture content of 50mm thick green lumber was dropped down to a half of the initial MC of the lumber (63.50%MC to 32.58%MC).And within only 8 hours the lumberreached oven-dry state. During superheated steam HT moisture gradient along the longitudinal direction was maintained small. Moisture content gradient was small enough and time to dry was short enough to prevent a drying check occurrence. Also, the energy efficiency of superheated steam HT (68.08%) was much higher than normal HT (27.46%). The defects-free superheated steam heat treatment process developed in this study would be very useful for treating green wood without pre-drying with high energy efficiency.

References

Cooper, P. 2009. High Temperature Treated Wood. Value to Wood Research Program Poster Presentation.

Deventer, H. C., 2004. Industrial Superheated Steam Drying,TNO-report, R 2004/239.

Esteves, B., I. Domingos and H. Pereira. 2007. Improvement of technological quality of eucalyt wood by heat treatment in air at 170 ~ 200℃. Forest Products Journal 57(1/2): 47-52.

Kamdem, D.P., A. Pizzi and A. Jermannaud. 2002. Durability of heat-treated wood. HolzalsRoh- und Werkstoff 60(1) : 1-6.

Militz, H. 2002. Heat treatment technologies in Europe: Scientific background and technological stateof art. Conference on Enhancing the durability of Lumber and Engineered Wood Products, Forest Products Society, Madison, USA.

Mujumdar, A. S.. 1990. CEA Report. 816 U 671. Montreal. Canada.

Og Sin Kim, Dong Hyun Lee and Won Pyo Chun. 2008. Eco-Friendly Drying Technology using Superheated Steam. Korean Chemistry Engineering Research, 46(2): 258-273.

NIR Spectroscopic Wood Surface Moisture Content Distribution Image Construction using Computerized Numerical Control System

Sang-Yun ***YANG***[1]**,** *Yeonjung* ***HAN***[1]**,** *Yoon-Seong* ***CHANG***[1]**,** *Juhee* ***LEE***[1]**,** *Hwanmyeong* ***YEO***[1.2*]

[1] Dept. of Forest Sciences, CALS, Seoul National University,
599 Gwanak-ro, Gwanak-gu, Seoul – South Korea
[2] Research Institute for Agriculture and Life Sciences,
Dept. of Forest Sciences, CALS, Seoul National University,
599 Gwanak-ro, Gwanak-gu, Seoul – South Korea
hyeo@snu.ac.kr

Abstract

Near infrared (NIR) spectroscopic image construction using computerized numerical control system (CNC) for nondestructively monitoring and analyzing the surface moisture content distribution of Korean pine (*Pinus koraiensis*) lumbers was performed in this study.

It is highly emphasized that a proper moisture content control is essential in using and/or processing hygroscopic material such as wood. Surface stress and internal stress occurred in wood by severe moisture gradient could lead to unexpected deformations of fiber in a smaller scale and defects of lumber in a larger scale. To prevent the occurrence of harmful defects, an appropriate moisture content monitoring is essentially needed. NIR spectroscopy was employed for constructing surface moisture content distribution image in this study.

Before constructing the image, we had developed moisture content regression model of Korean pine (below fiber saturation point at 25℃) using 1000nm ~ 2400nm band. R^2 and RMSEP value of regression model were 0.97 and 1.08 respectively. In order to acquire the signal relevant to moisture content distribution on the surface of wood, optical fibers, which send a ray source and receive a reflected ray, are installed to CNC machine. NIR reflectance spectra of specimen were acquired in discrete location by the optical fibers which moved following the programmed grid by CNC machine. The acquired reflectance spectra were used as the independent variables in the previously developed regression model and transformed to two-dimensional surface moisture content matrix for constructing the moisture content distribution image of lumber.

Key words*:* Near Infrared spectroscopy, moisture content, nondestructive test, image construction.

Introduction

Because moisture gradient in wood induced by external moisture environment makes various drying defects e.g. collapse, failure, surface and internal check, optimization of drying process is essential for using wood reasonably. It is necessary to measure the amount of water in wood for controlling the manufacturing process and the product quality efficiently. Oven drying method which is absolute moisture content measurement criterion has disadvantage taking a lot of time and damaging to wood. There are several wood moisture content measurement devices based on electrical properties of wood which are direct current resistant and dielectric methods (Skaar, 1988). These methods also have adverseness such as not fully nondestructive because pin electrode makes crack on test surface, reliance problem based on various chemical composition of wood or narrow moisture content measurement range (Tiitta, 1999).

Near infrared (NIR) spectroscopic analysis might overcome preceding adverseness. NIR is electromagnetic wave within wavelength range in 780 nm to 2500 nm. NIR spectroscopy is generally applied to analyze the chemical composition and evaluates the physical properties of the materials such as wood and wood composites recently (Tsuchikawa, 2007). The research to predict moisture content of wood was performed successfully (Hoffmeyer, 1995, Tsuchikawa, 1996). Because NIR frequency contains water vibration band (Maeda 1995), the highly reliable regression model for measuring the moisture content of wood using the spectra of the ray reflected from wood. The NIR technique, which is an on-line nondestructive method, lets us seize information relevant to moisture content on the surface of wood.

In the case of industrial application, detecting and monitoring the moisture content on the entire surface of product are required for its quality control. To fill the requirement, an optical fiber mode NIR spectrometer and a computerized numerical control (CNC) system, which can trace up a numerical coordinate exactly, was used for constructing surface moisture content distribution image in this study.

Materials and Methods

In this study, NIR reflectance spectra of various moisture-content wood specimens were acquired and moisture content prediction model was developed by partial least squares (PLS) analysis. Using the prediction model and the optical fiber mode NIR spectrometer loaded on CNC system which traces up square grids, two dimensional surface MC profile image of wood was constructed

Materials.

Korean pine (*Pinus koraiensis*) tress was cut in Gangwon-do, Korea. 10 disk- shape sapwood specimens with a dimension of 30 (diameter) x 5 (thickness in longitudinal direction) mm were prepared to evaluate moisture content of Korean pine.

For constructing surface moisture content image, 90 x 90 x 8 (longitudinal x tangential x radial length) mm Korean pine specimen was prepared.

Near Infrared Spectroscopic Moisture Content Regression Model Development.

The NIR reflectance spectra were acquired using optical probe type NIR spectrometer (NIR Quest 256-2.5, Ocean Optics) at wavelength between 870 - 2510 nm. The NIR spectrometer used 20W tungsten-halogen lamp as a light source. The optical probe is composed of 6 circular optical fibers that emit light from the light source to sample and 1 circular optical fiber that collects diffuse-reflected light from the sample to detector (Fig. 1). The samples were illuminated at 45°. Before sample measurement, diffuse reflectance calibration was performed using white reflectance standard (WS-1-SL, labsphere).

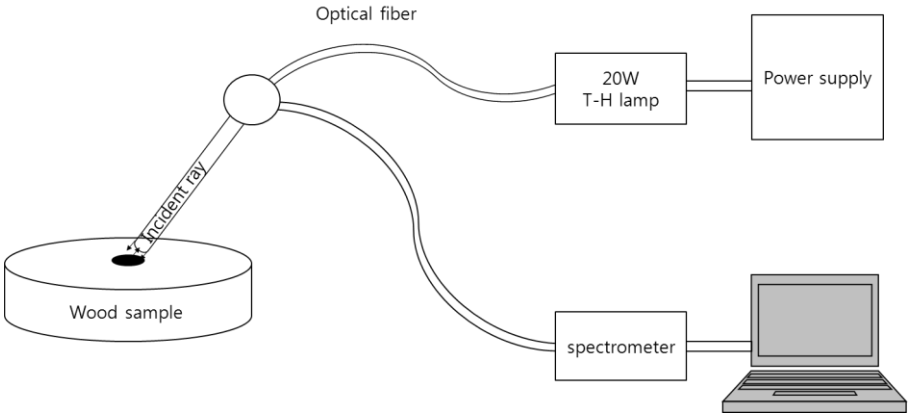

Figure 1. Schematic diagram of NIR infrared spectroscopic measurement

Small disk-shape wood specimens were humidified at each of 6 different relative humidity levels at ranging from near fiber saturation point state to low RH. NIR reflectance spectra of the humidified wood were acquired at 25℃ isothermal desorption process as shown in Table 1. For each sample, 3 scans were performed and the three times scanning signals was averaged into single reflectance spectrum. The reflectance spectra were extracted from 1000 nm to 2400 nm because electrical error affects to end spectral region. After acquiring the reflection spectra of specimens at each equilibrium condition, spectral preprocessing techniques were applied. In this study, when Norris 2nd derivative (gap size=1) after 3 point moving average was applied, because this procedure shows the most effective validation of moisture content prediction in many procedures which we tried in this study. PLS regression analysis using the Unscrambler (CAMO Inc., USA) software was applied to describe the relationship between the NIR spectra and the moisture content of specimen. PLS evaluation was performed with external validation based on two subsets (calibration set and validation set) divided into 20 segments. The sample selection of each subset was randomized.

Table 1. Environmental conditions for humidifying wood specimen under fiber saturation point

Temperature(℃)	RH(%)	Target EMC*(%)	Average MC(%)	Standard deviation of MC	Facility
25	99	25.77	25.18	0.63	Temperature & humidity chamber
	95	23.28	18.20	0.39	
	80	16.40	15.30	0.51	
	65	11.95	12.90	0.41	
	50	9.06	9.70	0.30	

	25	5.47	7.64	0.36

*Equilibrium moisture content

Moisture Content (MC) Distribution Image Construction using the Computerized Numerical Control System.

To construct surface moisture content distribution image, CNC machine was used. The specimen's surface which was tested for image construction was sealed by aluminum tape except the target surface for measuring the NIR reflectance. It was the reason of specimen sealing to restrain an excessive moisture transfer to external environment. Specimen was humidified in hygrostat at 25℃ and 95% RH, and was confirmed to reach equilibrium state. The humidified specimen was carried outside, where is relative dry (40% RH), and was scanned by optical probe attached to CNC machine.

Geometrical information of specimen was input to Auto CAD and two dimensional rectangular grids were designed. Since grid scale of abscissa and ordinate was 5 mm each, 18 x 18 pixels image of surface moisture content profile could be constructed. After coordinate design, trace and order of scanning was set on Lazy CAM.

Optical probe acquired reflectance spectra 5mm away from specimen surface at each grid. Reflectance spectra corresponding to specific coordinate were input to the previously developed MC prediction model, and moisture content matrix was constructed. The matrix was transformed to two-dimensional MC distribution image by contour plotting in Origin Pro 8.

Result and Discussion

Evaluation of Near Infrared Spectroscopic Moisture Content Regression Model.

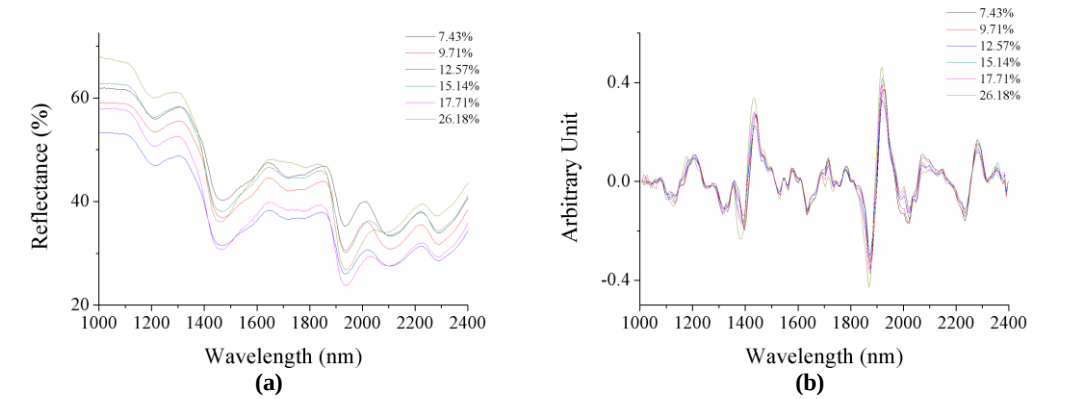

Figure 2. Near infrared spectra of each representative moisture content (a) raw reflectance spectra and (b) mathematical preprocessed spectra

As it is known that 1190, 1450 and 1940 nm regions are water absorption bands (Maeda 1995), Figure 2 (a) shows the specific absorption bands at each wavelength. In reflectance spectra, absorption bands of 2nd derivative appear positive peaks, contrary to absorbance spectra (Fig. 2 b). As moisture content increased, Norris 2nd derivative value also shows increment tendency.

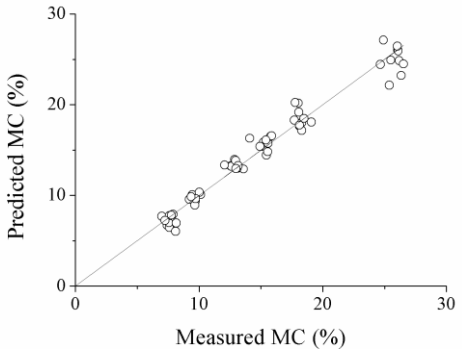

Figure 3. Relationship between NIR predicted MC versus measured moisture content (%)

Figure 3 describes the validation of PLS regression analysis on the NIR reflectance spectra of Korean pine wood. This means that the MC predicted by NIR spectroscopic prediction model and MC measured by oven-drying method are quite close. The coefficient of determination (R^2) of regression model was 0.98 and root mean square error of prediction (RMSEP) was 0.97. Since the number of Principal component of model was 2 of 20, the developed regression model could be used for measuring surface MC of other Korean pine wood with high reliability.

Moisture Content Distribution Image Construction using Computerized Numerical Control System.

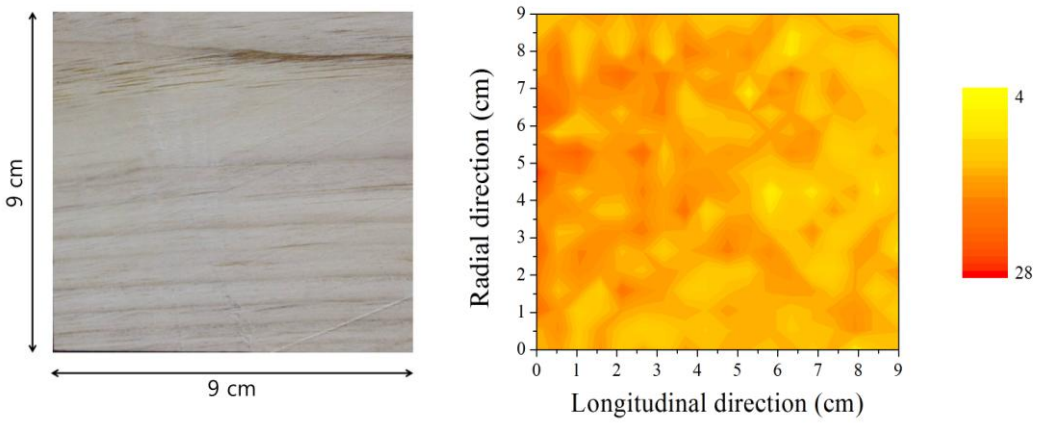

Figure 4. Photograph of test panel (a) and its moisture content distribution image (b)

Dot-scanned sample of korean pine panel (Fig. 4 a) shows no visual distribution of moisture content. There were a gradient of moisture content at transformed image by prediction model. As scanning trace followed 18 point of radial direction with every 5 mm interval at fixed abscissa then moved 5mm toward longitudinal direction, the optical fiber's movement to x axis was relatively slow. So, some time-delay (43 minute) for moving from (0, 0) to (9,9) occurred. Although the panel was humidified in hygrostat at 25℃ 95% RH, surface moisture of wood panel was emitting actively outside during

measurement because of the surrounding air around CNC machine was relative dry condition (28℃ 40% RH). It is concluded that moisture content gradient had occurred because moisture emission on surface to external circumstance was faster than internal moisture diffusion. It is a reason that moisture contents of left side wood are higher than MC of right side wood.

NIR spectra interact with about 1 mm (Tsuchikawa, 1996) depth from surface, spectral information could be considered to reflect surface of wood. However, it should be improved to acquire reflectance spectra correctly during CNC machine operation. Although moisture emission occurred excessively, it is reasonable that there were not able to dry 4% moisture content. This phenomenon might be resulted from synchronization problem. Because reflectance spectra acquisition of spectrometer from optical fiber was manual, on the contrary, CNC machine operated automatically, erroneous reflectance might be acquired.

Conclusion

In this study, the regression model for detecting moisture content of Korean pine wood was created successfully using NIR spectra and PLS analysis. The coefficient of determination of regression model was 0.98 and RMSEP was 0.97. Using the model and NIR spectrometer loaded to CNC system, MC distribution image construction system was developed and its usability was confirmed with high reliability.

This system has a possibility to construct other chemical composition and/or wood cell structure image with moisture image simultaneously, if the numerical model for other characteristics could be developed.

However the system, which took a relatively long time for constructing MC image, could not carry out the real-time image construction, because this application was proto type adopting the manually controlled spectra acquisition method. Efforts for the program synchronization between CNC system and NIR spectrometer are needed to diminish the time for constructing MC image

References

Skaar, C. 1988. Wood-Water Relations. New York, NY: Springer-Verlag

Marra, G. 1979. Overview of wood as material. Journal of Educational Modules for Materials Science and Engineering. 1(4): 699–710.

Tiitta, M., Savolainen, T., Olkkonen, H., Kanko, T. 1999. Wood moisture gradient analysis by electrical impedance spectroscopy. Holzforsching. 53(1): 68-76.

Tsuchikawa, S. 2007. A review of recent near infrared research for wood and paper. Applied Spectroscopy. 42(1): 43-71.

Hoffmeter, P., Pedersen, J.G. 1995. Evaluation of density and strength of Norway spruce wood by near infrared reflectance spectroscopy. Holz als Roh- und Werkstoff. 53(3): 165-170.

Tsuchikawa, S. 1996. Application of near infrared spectrophotometry to wood IV. Calibration equations for moisture content. Journal of the Japan Wood Research Society. 42(8) : 743-754.

Maeda, H., Ozaki, Y., Tanaka, M., Nobuyuki, H., Kojima, T., 1995. Near infrared spectroscopy and chemometrics studies of temperature-dependent spectral variations of water: relationship between spectral changes and hydrogen bonds. Journal of near infrared spectroscopy. 3(4): 191-201.

Effect of Cross-Kerfing Nonslip Process on the Friction Performance of Deck

Yeonjung Han[1] – Ju-Hee Lee[1] – Yonggun Park[1]– Hwanmyeong Yeo[2]*

[1] Research Associate, College of Agriculture and Life Science, Seoul National University, Seoul, Korea.
[2] Associate Professor, Department of Forest Sciences, College of Agriculture and Life Science, Seoul National University, Seoul, Korea. Research Institute for Agriculture and Life Sciences in Seoul National University, Seoul, Korea.
* *Corresponding author*
hyeo@snu.ac.kr

Abstract

The installation of deck has been popularized in creating Cultured and Eco City in Korea, recently. However, there is a relatively lack of research on the basic physical properties and safety of deck. The major factor affecting maneuverability of a pedestrian is a frictional force caused between and outsole of shoe and surface of deck. The magnitude of frictional force is influenced by a number of factors including the kinds of deck material, the shape of deck surface, moist conditions on deck surface, and the shape of shoe outsole. This study focused on the effect of various patterns of deck on the frictional force and evaluated the coefficient of friction(COF).
In this study, decks were manufactured with two types of materials, natural wood and wood plastic composite. Decks were processed for nonslip with five type patterns (longitudinal kerf, grid pattern A, grid pattern B, riffle pattern, clover picture). Longitudinal kerf deck was manufactured by the groove treatment on the surface of deck along the longitudinal direction. In order to manufacture other pattern decks additional groove treatments along transverse direction were carried out after longitudinal kerf process. To analyze the effect of free water and bound water in the shell of deck on the friction, friction tests were carried out with specimens whose surface moisture was controlled. After surveying outsole pattern of sports shoes in markets, three different outsole patterns, straight line, rectangle shape and W shape, as primary outsole patterns of sports shoe were chosen for the test.
Corresponding to those patterns and design parameters, various patterns specimens are prepared for fictional experiments. After performing frictional tests with those specimens, coefficient of friction are collected and analyzed.

***Keywords*:** deck; wood plastic composites; coefficient of friction; patterns of deck; shoe outsole; kerf; nonslip

Introduction

Friction is the force resisting the relative motion of solid surfaces, fluid layers, and material elements sliding against each other. The coefficient of friction(COF) is a dimensionless scalar value which describes the ratio of the force of friction between two bodies and the force pressing them together.
Static friction is friction between two or more solid objects that are not moving relative to each other. And kinetic(or dynamic) friction occurs when two objects are moving relative to each other and rub together. The coefficient of static friction is usually higher than the coefficient of kinetic friction(Sheppard 2005, Meriam and Kraigh 2002).

The elementary properties of sliding(kinetic) friction were discovered by experiment in the 15^{th} to 18^{th} centuries and were expressed as three empirical laws: 1)Amontons' first law- The force of friction is directly proportional to the applied load, 2)Amontons' second law- The force of friction is independent of the apparent area of contact, 3) Coulomb's law of friction- Kinetic friction is independent of the sliding velocity.

The coefficient of friction for wood is related to various factors including tree species, slope of grain, moisture content, temperature, coarseness of contacting surface, and loading speed(McKenzie and Karpovic 1968). McKenzie and Karpovic investigated the relationship between the coefficient of friction and species of tree, coarseness of contact surfaces, and load speed. The study shows that coefficient of friction ranges from 0.1 to 0.65 and it differs according to the species of tree and roughness of contact surfaces. And the coefficient of friction for western hemlock was measured at 0.58 by Murase(1984). But these studies were concerned about friction resistance between wood and metal. Grönqvist et al(1990) assessed the slipperiness of typical deck and other commonly used underfoot surface in ships and showed that the measured average coefficients of kinetic friction were in a range of 0.05 to 0.64.

Recently, installation of deck continues its upward trend in Korea. But it is insufficient to study on the stability and physical performance of deck during human activity and exercise on it. The friction between shoe and deck has an effect on mobility of pedestrian. It is influenced by many factors like kinds of flooring, flooring conditions and forms of outsole. This study was carried out to measure the difference in friction by patterns of deck and the degree of sliding for safe working with two kinds of deck material, wood and wood plastic composite (WPC), which have five different surface patterns at two different surface moist condition; dry and wet.

Materials and Methods

Materials. In this study, solid wood and wood plastic composite (WPC) decks were used to assess coefficient of friction. The species of tree used for manufacturing the solid wood deck were merbau(*Intsia palembanica*) and ipe(*Tabebuia upo Standle*). WPC deck samples were manufactured using mixture of wood fiber and polymer (Polyethylene (PE), Polypropylene (PP), polyvinyl chloride (PVC)). Specimens were processed for enhancing nonslip performance with five type patterns (longitudinal kerf, grid pattern A, grid pattern

B, riffle pattern, clover picture, Fig. 1). Longitudinal kerf deck was manufactured by the groove treatment on the surface of deck along the longitudinal direction. In order to manufacture other pattern decks additional groove treatments along transverse direction were carried out after longitudinal kerf process

Solid wood deck specimens with surface area of 375mm (length) x 90mm (width) and WPC specimens with surface area of 375mm (length) x 150mm (width)were prepared. Because temperature and humidity affect the results of friction tests, all specimens were stored and tested at 24°C and 65% RH. Specific gravity and moisture content of all wood deck specimens were assessed. The average values were 0.49 and 12% MC, respectively. These equilibrated specimens were used for "dry" friction test. Specimens which were soaked in water for 10minutes were used for "wet" friction test.

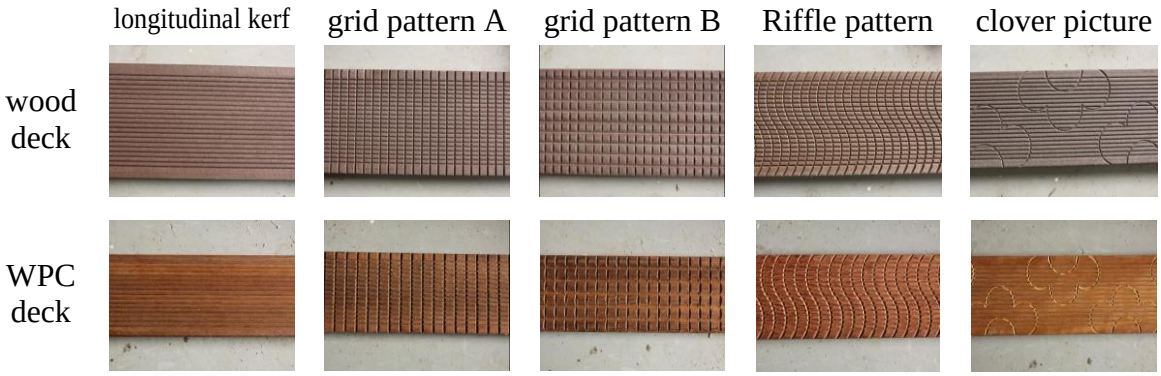

Figure 1 Surface patterns of decks machine-processed for enhancing the nonslip performance

The frictional force is produced between shoe and floor when pedestrian walk, varied depending on patterns and materials outsole(Nigg 1987). In this study, sports shoe, which is typically used in walking on deck, was chosen as the reference shoes for the assessments (Fig. 2 and Table 1).

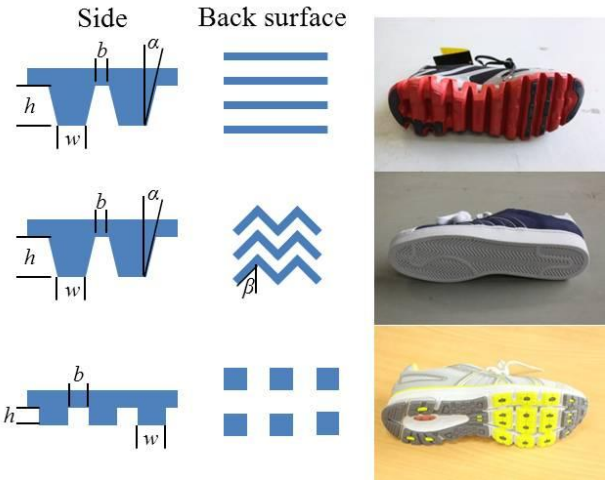

Figure 2 Outsole type of reference footwear

Table 1 Dimension of outsole

Type of outsole	*b*(mm)	*w*(mm)	*α*(deg)	*β*(deg)	*h*(mm)
Straight line	13.5	13.0	22.0	-	15.4
W shape	4.5	1.5	0.5	20	3.5
Rectangle shape	7.8	8.5	-	-	6.2

Methods. Test assembly for determining the coefficient of friction for deck, American Society of Testing Materials(ASTM) D2394-05, 'Standard Test Method for Simulated Service Testing of Wood and Wood-Based Finish Flooring', and ASTM G115-10, 'Standard Guide for measuring and Reporting Friction Coefficients' were used to analyze results of friction test. The equipment used for these experiments is illustrated in Fig. 3. As shown in Fig. 3, using pulley and tension cable which is connected to Universal Testing Machine(UTM, Zwick, Capacity: 10 ton), shoe was loaded by the UTM at the speed of 3mm/min. Change of the load and head travel were monitored and recorded by UTM during test.. After test, maximum static friction force were evaluated, when steady normal force(30kgf and 70kgf) was maintained between shoe and deck.

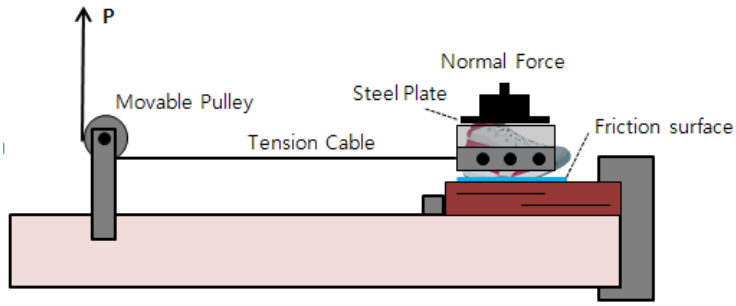

Figure 3 Simplified diagram of the friction testing device

Results and Discussion

Coefficients of friction. Maximum static friction force was estimated when test samples started to move. The coefficient of friction was calculated as follows.

$$F = \mu N \qquad (1)$$

where, F = friction force
μ = coefficient of friction
N = normal force

Coefficient of static friction was evaluated with variation of normal force, water condition of deck surface, outsole patterns of shoe, and surface pattern of deck, as shown in Table 2. The average of coefficients of static friction of solid wood and WPC decks were 0.579 and, 0.485, respectively. It means that human who is walking on solid wood deck feels less slippery compared to man on WPC deck.
Solid wood's COFs measured after soaking in water are especially higher than WPC's those. It seems that because physiomechanical property of wood cell was changed by

water adsorption and it increases the specific contact area between wood deck and shoe console, COF of solid wood was very increased with water adsorption.
However, WPC's COFs measured after soaking in water do not show this trend. These results indicate that wood deck has biological material. Because the biological material is transformed into small pressure, contact area is changed and adhesion phenomenon is occurred of surface in wet condition. Then frictional force is increased and frictional properties of material are changed(Kim et al 2006).

Table 2 Coefficient of friction

Normal Force	Outsole Type	Water Condition	Longitudinal kerf		Grid pattern A		Grid pattern B		Riffle pattern		Clover picture	
			WPC	Wood	WPC	Wood	WPC	Wood	WPC	Wood	WPC	Wood
30kgf	Straight line	Dry	0.528 (0.057)*	0.475 (0.023)	0.523 (0.056)	0.607 (0.064)	0.628 (0.012)	0.666 (0.021)	0.520 (0.039)	0.601 (0.039)	0.514 (0.018)	0.519 (0.032)
		Adsorbed water	0.494 (0.029)	0.609 (0.016)	0.559 (0.042)	0.670 (0.017)	0.685 (0.020)	0.750 (0.022)	0.523 (0.016)	0.639 (0.026)	0.512 (0.015)	0.616 (0.005)
	W shape	Dry	0.457 (0.034)	0.424 (0.025)	0.326 (0.057)	0.469 (0.026)	0.451 (0.039)	0.439 (0.030)	0.284 (0.026)	0.479 (0.018)	0.408 (0.060)	0.436 (0.016)
		Adsorbed water	0.478 (0.022)	0.494 (0.016)	0.335 (0.026)	0.594 (0.028)	0.457 (0.019)	0.535 (0.013)	0.317 (0.029)	0.540 (0.009)	0.444 (0.038)	0.536 (0.013)
	Rectangle shape	Dry	0.537 (0.087)	0.606 (0.019)	0.393 (0.003)	0.584 (0.025)	0.537 (0.027)	0.625 (0.065)	0.360 (0.016)	0.586 (0.016)	0.570 (0.017)	0.633 (0.043)
		Adsorbed water	0.530 (0.019)	0.611 (0.017)	0.468 (0.010)	0.678 (0.038)	0.558 (0.014)	0.692 (0.002)	0.468 (0.024)	0.636 (0.019)	0.570 (0.006)	0.685 (0.012)
70kgf	Straight line	Dry	0.540 (0.015)	0.487 (0.020)	0.530 (0.038)	0.564 (0.037)	0.679 (0.017)	0.594 (0.034)	0.535 (0.012)	0.560 (0.022)	0.536 (0.017)	0.518 (0.026)
		Adsorbed water	0.499 (0.048)	0.569 (0.015)	0.541 (0.023)	0.617 (0.058)	0.629 (0.049)	0.643 (0.032)	0.545 (0.022)	0.587 (0.025)	0.489 (0.034)	0.619 (0.016)
	W shape	Dry	0.430 (0.020)	0.442 (0.009)	0.294 (0.024)	0.448 (0.026)	0.447 (0.021)	0.451 (0.025)	0.302 (0.023)	0.452 (0.004)	0.383 (0.034)	0.463 (0.005)
		Adsorbed water	0.443 (0.003)	0.476 (0.008)	0.325 (0.006)	0.525 (0.012)	0.429 (0.014)	0.534 (0.029)	0.322 (0.011)	0.522 (0.024)	0.442 (0.007)	0.570 (0.006)
	Rectangle shape	Dry	0.539 (0.044)	0.590 (0.039)	0.450 (0.014)	0.680 (0.020)	0.611 (0.028)	0.691 (0.051)	0.391 (0.010)	0.629 (0.026)	0.568 (0.010)	0.646 (0.017)
		Adsorbed water	0.596 (0.007)	0.604 (0.006)	0.494 (0.008)	0.719 (0.004)	0.596 (0.015)	0.717 (0.015)	0.468 (0.006)	0.656 (0.008)	0.586 (0.019)	0.708 (0.026)

* Standard deviation

Frictional variable. In this study, COFs according to normal forces(30kgf, and 70kgf) were measured to evaluate of pedestrian safety. 30kg, and 70kg were based on the average weight of child and adult, respectively. As shown in Table 2, COF of 30kgf normal force were higher than 70kgf. But the difference of COF due to normal force was insignificant.

English(1995) reported that the minimum of coefficient of static friction is 0.5 for safety of pedestrian. According to five types of outsole of shoe, COFs measured in Grid pattern B were higher than other type of processed deck surface. COFs measured in Grid pattern A and Riffle pattern were relatively low value except in the Straight line of outsole pattern. In case of Grid pattern B, the gap between longitudinal grooves was increased by eliminating the groove of longitudinal kerf. Grid pattern A and Riffle pattern were processed by additional groove treatment (straight and curve line, respectively) to the transverse direction. To analyze the difference according to groove treatment, contact area between deck surface and outsole of shoe using image analysis. The outsole type of

W shape was excepted because depth of outsole(*h* in Table 1) was low and COF was relatively lower than other types. Table 3 shows that contact area at two types of outsole patterns in 30kgf normal force.

Table 3 Contact area of outsole patterns of shoe

Normal Forcke	Outsole Type		Longitudinal kerf		Grid pattern A		Grid pattern B		Riffle pattern		Clover picture	
			WPC	Wood	WPC	Wood	WPC	Wood	WPC	Wood	WPC	Wood
30kgf	Straight line	Contact area(㎟)	1251	1026	821	1350	1289	1213	1084	1209	1152	1266
		Friction coefficient	0.528	0.475	0.523	0.607	0.628	0.666	0.520	0.601	0.514	0.519
	Rectangle shape	Contact area(㎟)	1019	1401	813	993	1155	1455	897	1277	1182	1429
		Friction coefficient	0.537	0.606	0.393	0.584	0.537	0.625	0.360	0.586	0.570	0.633

The contact area is generally proportional to the normal force. In this study, 30kgf normal force was used to compare with COF according to contact area. As shown in Table, the contact area is not necessarily fully correlated with the COF. But, the contact area in Rectangle shape of outsole in Table 3 shows the relationship between the contact area and COF.

As mentioned above, COFs measured in Grid pattern B were higher than other surface type of deck . The big variation of load that was developed between the groove of deck and the rough outsole of shoe during friction test seems to make the resilts. The big load was found when straight line of outsole was inserted into the additional straight groove treated along the transverse direction on deck surface.

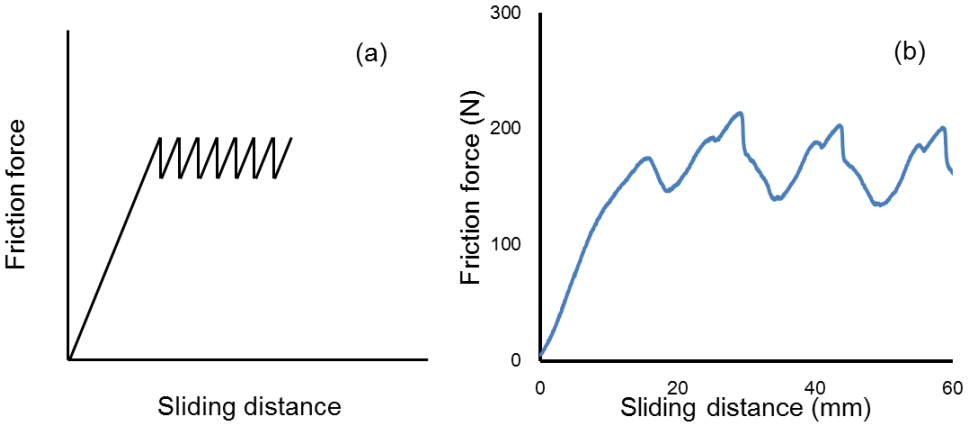

Figure 4 (a) Common friction curve, (b) friction force between straight line outsole and Grid pattern B deck surface

The maximum static friction and kinetic friction force showed difference according to friction force - sliding distance curve patterns. Fig. 4(a) and (b) show the common

friction curve and friction curve for straight line of outsole at Grid pattern B, respectively. In Fig. (b), the maximum static friction force remained unclear. And the distance of each peck was approximately 16.0mm that is similar to gap of straight line outsole. The high value of COF between straight line outsole and Grid pattern B deck surface seems to be from the phenomenon of being caught between each groove.
Solid wood deck feels less slippery compared to man on WPC deck.
Solid wood's COFs measured after soaking in water are especially higher than WPC's those. It seems that because physiomechanical property of wood cell was changed by water adsorption and it increases the specific contact area between wood deck and shoe console, COF of solid wood was increased with water adsorption.

Conclusions

One of the major factors affecting maneuverability of a pedestrian is frictional force caused between an outsole of shoe and surface of deck. The magnitude of frictional force is influenced by a number of factors including kinds and patterns of deck, conditions on deck surface, and outsole patterns of shoe. This study focused on the effect of various patterns of deck on the frictional force and evaluated the coefficient of friction.

Results of this study which was conducted on friction generated between deck surfaces and outsole of shoe were as follows. – There is no change of friction coefficient according to normal force. – COFs of deck without transverse groove were proportional to the contact area. – In deck with transverse groove, it was considered the phenomenon of being caught between each groove.

References

Sheppard SD (2005) Statics: Analysis and Design of System in Equilibrium. Wiley and Sons. 618pp.
Meriam JL, Kraige LG (2002) Engineering Mechanics: Statics. Wiley and Sons. 330pp.
McKenzie WM, Karpovic H (1968) Frictional behavior of wood. Wood Sci Technol 2: 138-152.
Murase Y (1984) Friction of wood sliding on various materials. J Fac Agric Kyushu Univ 28: 147-160.
Grönqvist R, Roine J, Korhonen E, Rahikainen A (1990) Slip resistance versus surface roughness of deck and other underfoot surface in ships. J Occupational Accidents 13: 291-302.
Nigg BM Bahlsen HA, Luethi SM, Stokes S (1987) The influence of running velocity and midsole hardness on external impact forces in heel-toe running. J Biomechanics 20: 951-959.
Kim MS, Kum DH, Kim KB, Kim MH, Noh SH, Cho YJ, Cho KG. (2006) Physical and Engineering Properties of Biological Materials. Munundang. Seoul. 461pp .
English W (1995) Ten myths concerning slip-resistance measurement. American Society of Safety Engineers. p35-38.

American Society of Testing and Materials (2005) Standard test methods for simulated service testing of wood and wood-base finish flooring. West Chnshohocken. PA. ASTM D 2394-05.

American Society of Testing and Materials (2004)Standard guide for measuring and reporting friction coefficients. West Chnshohocken. PA. ASTM G 115-04.

Mechanical Function of Lignin and Hemicelluloses in Wood Cell Wall Revealed with Microtension of Single Wood Fiber

Shuangyan Zhang [1] *–Benhua Fei* [2*] *– Yan Yu* [3] *Haitao Cheng* [4]
Chuangui Wang [5] *–Genlin Tian* [6]

[1] School of Forestry and Landscape Architecture, Anhui Agricultural University, Hefei
zsyhj_2006@163.com
[2] Deputy Director General, International Centre for Bamboo and Rattan, Beijing
* *Corresponding author*
feibenhua@icbr.ac.cn
[3] International Centre for Bamboo and Rattan, Beijing
[4] International Centre for Bamboo and Rattan, Beijing
[5] Associate Professor, School of Forestry and Landscape Architecture, Anhui Agricultural University, Hefei
[6] International Centre for Bamboo and Rattan, Beijing

Abstract

The mechanical properties of wood are highly dependent on the structural arrangement and properties of the polymers in the wood cell wall. To improve utilization and manufacture of wood materials, there is an increasing need for a more detailed knowledge regarding structure/property relations at cellular level. In this study, Fourier-Transform Infrared (FT-IR) spectrometer and microtension technique were jointly adopted to track both changes in the chemical structure and cell wall mechanical properties of single tracheid fibers of Chinese Fir, which had been subjected to extraction treatments with sodium chlorite ($NaClO_2$) for delignification, as well as with sodium hydroxide (NaOH) at different concentrations for extraction of hemicelluloses. Measurements with FT-IR spectroscopy provided information about the chemical changes in cell wall during the extraction process, while the microtension experiments gave qualitative information about the micromechanical properties of the extracted cell wall. The micromechanical data indicated that lignin had little impact on air-dried tensile elastic modulus and strength of cell wall, while hemicelluloses affected these properties significantly. Our results underlined the key role of hemicelluloses to maintain the integrity of wood cell wall.

***Keywords*:** hemicelluloses, lignin, cell wall, mechanical properties, microtension.

Introduction

Wood cell wall is a highly organized composite that may contain many different polysaccharides, proteins, and aromatic substances. Recent scientific and technological advances offer new possibilities to using plant cell walls in the production of cost-effective biofuels (Michael et al. 2007, Pu et al. 2011). However, the key obstacle for transitioning from plant cell wall to biofuels is the complicated structure of the cell wall, which is, by nature, resistant to breakdown-the recalcitrance problem. In view of this, fundamental understanding of structure and chemical components properties of cell wall is of great importance.

Cellulose, hemicelluloses and lignin are the main components of wood cell wall. The arrangement of chemical components, their interactions and their mechanical properties result in mechanical properties of the cell wall which finally affect the macroscopic properties of wood. Mechanical investigations of the wood polymers show that there are strong interactions between the hemicelluloses, xylan and glucomannan, and the other wood polymers, cellulose and lignin. Studies of the softening behavior of glucomannan and xylan suggest that xylan is more associated with lignin while the glucomannan is more associated with cellulose (Salmén and Olsson 1998, Åkerholm and Salmén 2001, Stevanic and Salmén 2009). However, most previous work of wood polymers in cell wall had been carried out by spectroscopic studies.

Microtension of single fibers belongs to a powerful tool for mechanical characterization of plant fibers. In this context, Jayne (1959) was one of the first who performed tensile experiments on single pulp fibers. Since then, mechanical properties of different kinds of plant fibers were tested. At the same time, sample preparation, alignment of fibers to tensile direction and cell wall area determination of this method were improved (Burgert et al. 2002, Yu Y et al. 2010, 2011).

This study used single-fiber-test technology to investigate the effects of chemical components on mechanical properties of single fibers. The techniques for isolating fibers mechanically and extraction treatments were introduced. FT-IR microscopy was applied to track the chemical changes in cell wall. A further aim was to gain insight into the arrangement of the polymer network from mechanical point.

Materials and Methods

Materials. Material was taken from the adult wood of a 42-year-old Chinese Fir (*Cunninghamia lancolata* (Lamb.) Hook) grown in Anhui Province, China. Tangential slices of 100-μm-thick were cut with a microtome from never dried adult latewood. Some tangential slices were fixed under a light microscope and single fibers were isolated using very fine tweezers (Burgert et al. 2002). Others were treated with extraction methods which were $NaClO_2$ for delignification and NaOH at different concentrations for extraction of hemicelluloses. For delignification, three kinds of chemical solutions were chosen to delignify wood cell wall with different extent: A) an aqueous solution of 0.3% $NaClO_2$ buffered with glacial acetic acid at pH 4.4~4.8 for 4h at 80℃; B) an aqueous solution of 0.3% $NaClO_2$ buffered with glacial acetic acid at pH 4.4~4.8 for 8h at 80℃; C) an aqueous solution of 150ml distilled water, 1.0g $NaClO_2$ and 2.0ml glacial acetic acid for 8h at 80℃. On the delignified samples, a successive extraction of hemicelluloses

which allowed a reasonably specific degradation of hemicelluloses (Nelson 1961) was carried out by a treatment with (i) 6% NaOH, (ii) 6 and 8% NaOH and (iii) 6, 8 and 10% NaOH at 60℃ for 2h each. Subsequently, fibers were washed carefully in deionized water several times and dried on glass slides at room temperature (25℃).

FT-IR Spectroscopy. FT-IR spectra of the treated and control samples were collected using a Nexus 670 spectrometer equipped with a MCT/A detector. Each spectrum was recorded over the 4000 to 400cm^{-1} range, with a resolution of 4 cm^{-1}, and derived from the average of 200 scans. The range from 800 to 1800cm^{-1} was selected as reference for the normalization using OMINIC software version 7.1.
To investigate the effect of treatments on the chemical components of cell wall, specific wavenumbers of cell wall polymer absorption bands of cellulose, hemicelluloses, that is, xylan and glucomannan, and lignin were examined in the area from 800 to 1800cm^{-1}. Three vibration bands of cellulose, that is, the C-H deformation at 898cm^{-1}, the C-H bending vibrations at 1368cm^{-1} and the CH_2 wagging vibration at 1316cm^{-1} were used (Stevanic 2009, Åkerholm and Salmén 2001). For hemicelluloses, two bands of xylan, namely, the C=O stretching vibration at 1734 and 1600cm^{-1} were used. For glucomannan, the band at 810cm^{-1} (Marchessault 1962), attributed to vibrations caused by equatorially aligned hydrogen on the C_2 atom in the mannose unit, was observed. The band of aromatic skeletal vibrations in lignin at 1508cm^{-1} (Schwanninger et al. 2004) and the vibration of the guaiacyl ring, together with the C=O stretch at 1264cm^{-1} (Åkerholm and Salmén 2003) were observed.

Microtensile Tests.

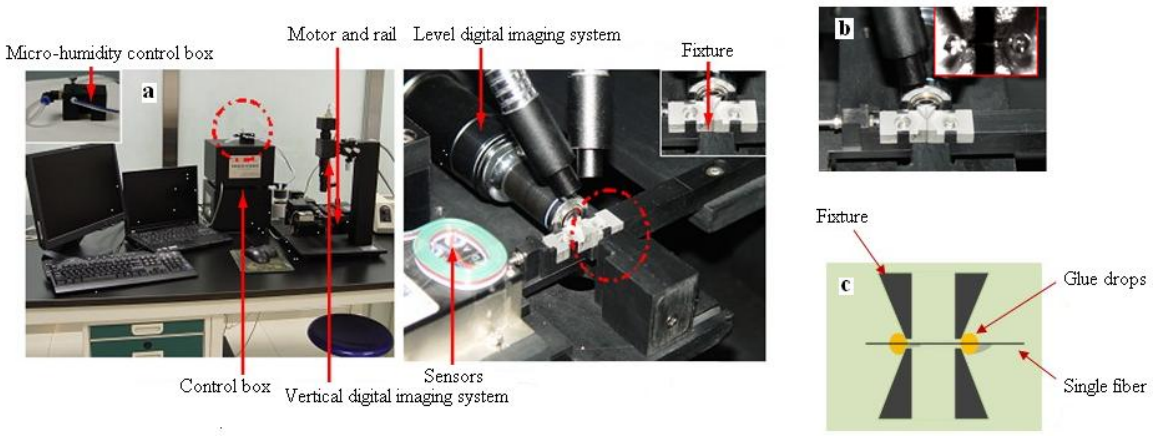

Fig. 1 Microtensile testing system.
SF-Microtester I (a), "ball and socket" type fiber clamping (b, c).

Tensile tests on single fibers were performed with a custom-built microtension tester (SF-Microtester I) (Figure 1, a). "Ball and socket" type fiber gripping was adopted for microtensile testing (Figure 1b, c). Two resin droplets (cold-curing adhesive, HY-914) approximately 200μm in diameter were placed in the center portion of each fiber via a fine tweezers. The capacity of load cell used was 5N. The tensile speed was 0.8μms^{-1}. Tensile testing of the dried fibers was carried out in an environment of 20±5℃ and

20±5% RH. The cell wall cross-sections of every broken fiber were measured with a confocal scanning laser microscope (Meta 510 CSLM, Zeiss) (Yan Yu et al, 2010, 2011). In total, 54 mechanically isolated fibers and 50-60 fibers for each chemical treatment were analyzed.

Lignin Quantification. The lignin contents of native and chemically altered fibers were determined by acid-insoluble lignin (GB/T 2677.8-94).

Results and Discussion

Selective Removal of Lignin and Hemicelluloses. The FT-IR measurements were used to assess the effectiveness of the treatments on the samples which provide a reliable characterization for the semiquantitative interpretation of cell wall chemical components. FT-IR spectra of native and treated fibers were analyzed, see Figure 2. Only changes in the relative intensities of specific bands were evaluated.
The 1508cm^{-1} peak is often taken as a reference for lignin since it results purely from an aromatic skeletal vibration (C=C) in lignin. With the removal of lignin by $NaClO_2$/glacial acetic acid, a significant reduction of the peak at 1508cm^{-1} can be observed. The relative intensity of the lignin band at 1508cm^{-1} showed decreased obviously with the decrease of lignin content. And the peak at 1508cm^{-1} nearly disappeared when the lignin content decreased to 0.4% after the delignified treatment of method C (Table 1). The same change of relative intensity of lignin band at 1264cm^{-1} was also observed.

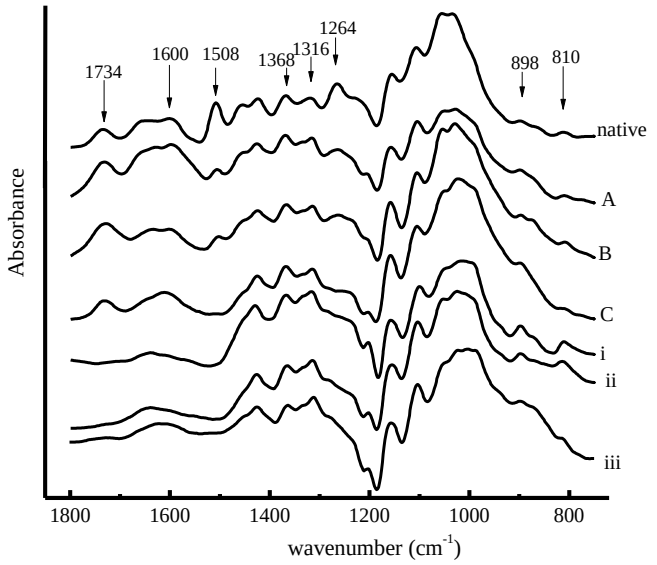

Fig. 2 IR-Spectra of different treatments

Table 1 Lignin content after delignified treatments

Sample	Lignin content (%)
Native sample	33.61
A	29.76
B	25.37
C	0.40

The relative intensity of hemicelluloses (xylan and glucomannan) bands at 1734, 1600 and 810cm^{-1} showed little changes due to delignification. After a successive treatment with 6% NaOH on delignified samples, the bands at 1734 and 1600cm^{-1} disappeared (Figure 2i). This indicated that xylan was almost removed. The intensity of glucomannan band at 810cm^{-1} showed minor change after successive treatments with 6% and 6%+8% NaOH (Figure 2i, ii). However, the peak at 810cm^{-1} nearly disappeared after treatment with 10% NaOH, which implied glucomannan was almost removed (Figure 2iii).

The small variations of the absorption spectra bands at 1368 and 1316cm^{-1} for native and treated fibers indicated that the cellulose underwent least change during the process of lignin and hemicelluloses extraction.

Stress-strain curves. The typical stress-strain curves of single fibers after different treatments were presented in Figure 3. All the fibers tested showed a linear stress-strain behavior to failure, which indicated that chemical components changes did not affect the tensile behavior of single fibers. Groom (2002a) found the shape of the stress-strain curve of softwood fibers depended on microfibrillar angle (MFA) that Individual fibers with MFAs less than 20° appeared to be full linear during the test. In this study, the MFAs of wood fibers were around 10°, explained why all the wood fibers display linear stress-strain behavior.

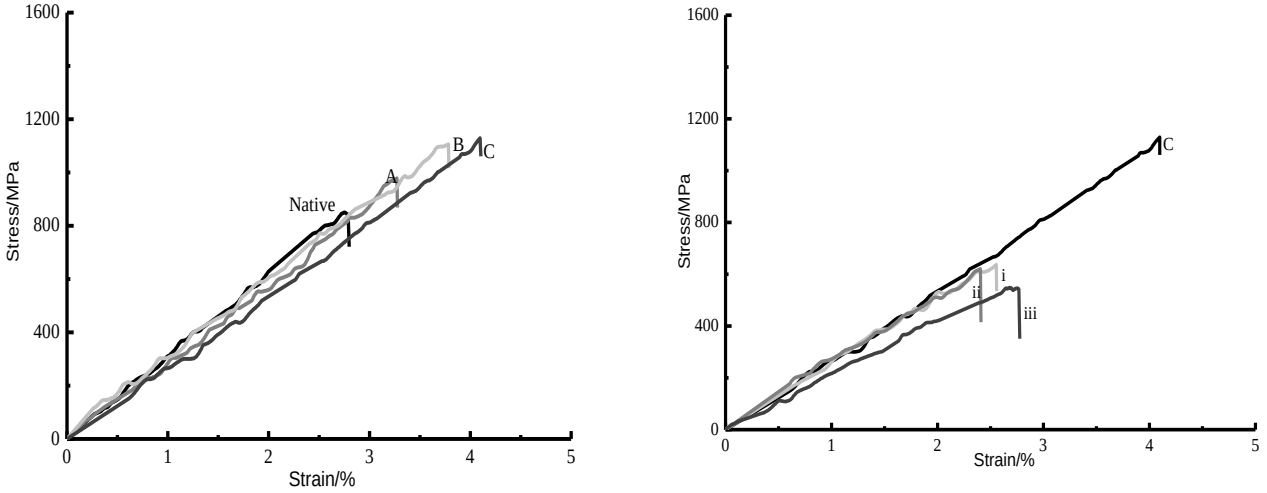

(a) delignified treatments (b) hemicelluloses-extracted treatments

Fig. 3 Typical stress-strain curves of single fibers after different treatments

Mechanical Function of Lignin in Cell Wall. Figure 4 and Figure 5 showed the effect of lignin on the tensile modulus and strength of fiber cell wall. The tensile modulus was reduced by 1.96%, 4.74%, and 5.10% with lignin content decreasing by 11%, 25%, and 99%, respectively (Figure 4). However, the average tensile strength of single fibers showed an increasing trend when there was a decrease in the lignin content (Figure 5). That was increased by 26.28%, 34.22%, and 41.18% for delignification reduced by 11%, 25%, and 99%, respectively.

In the cell wall of softwood tracheids, cellulose is the main structural component working as a framework substance. Since the stiffness of cellulose (167.5GPa) is more than 80 times that of lignin (2.0GPa), even a twofold increase of the lignin content should not noticeably alter the stiffness of the composite cell wall. And the results were consistent with the measurements made by Duchesne (2001) on kraft pulp fibers by FE-SEM and CP/MAS 13C-NMR.

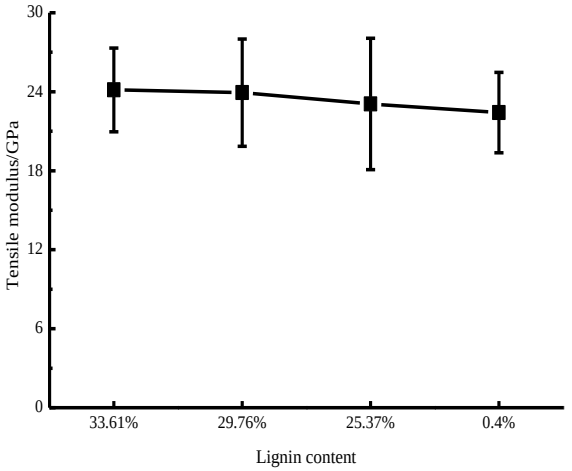

Fig. 4 Tensile modulus of single fiber with delignified treatments

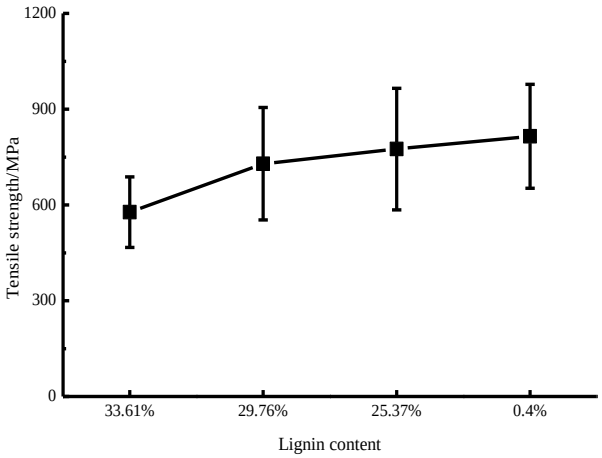

Fig. 5 Tensile strength of single fiber with delignifed treatments

Mechanical Function of Hemicelluloses in Cell Wall.

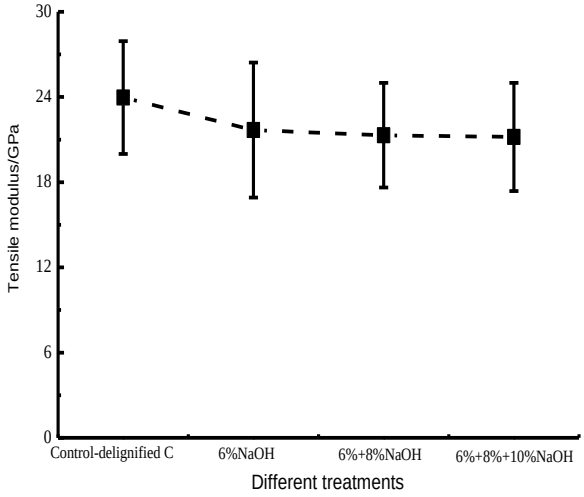

Fig. 6 Tensile modulus of single fiber with hemicelluloses-extracted treatments

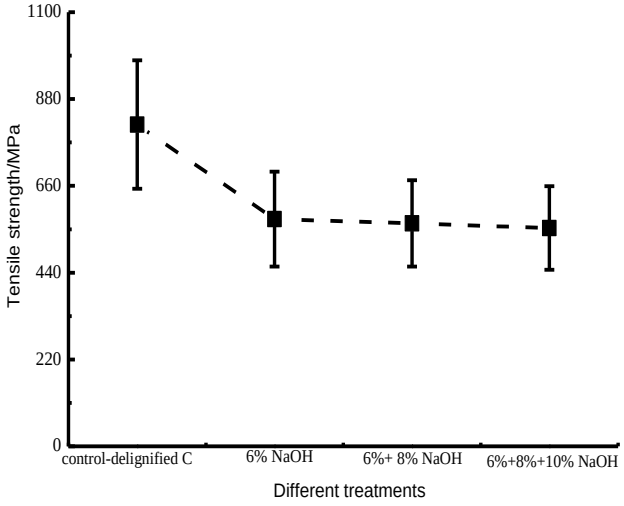

Fig. 7 Tensile strength of single fiber with hemicelluloses-extracted treatments

The effect of successive extractions of hemicelluloses on the tensile modulus and strength of fiber cell wall were presented in Figure 6 and Figure 7. The tensile modulus and strength of delignified fibers treated with increasing concentration NaOH showed an obvious decreasing. The tensile modulus was reduced by 9.55%, 11.08%, and 11.57%, while the tensile strength of single fibers was reduced by 29.36%, 30.71%, and 32.15% for hemicelluloses-extracted at 6% NaOH, 6+8% NaOH, and 6+8+10% NaOH, respectively. Compared to lignin, the effect of hemicelluloses on tensile modulus was more significant than that of lignin in dry condition.

Xylan and glucomannan are the two main kinds of hemicelluloses in the cell wall of softwood tracheids. Glucomannan is more closely associated with cellulose as it is more difficult to separate from cellulose than xylan. Extraction treatments on delignified samples with NaOH allow degradation of xylan firstly (Figure 2i). In cell wall,

hemicelluloses act as an interfacial coupling agent between the highly ordered cellulose of the microfibrils and lignin. And hemicelluloses play an essential role in the maintenance of the cell wall assembly. Therefore, the removal of hemicelluloses would destroy the integrity of cell wall. This may have been the cause of the obvious decrease in tensile modulus and strength when there was a degradation of hemicelluloses.

A Modified Cell Wall Model. The tensile properties of single fibers are highly dependent on the structural arrangement of the polymers in the fiber cell wall. As the results above, we established a new cell wall model, see Figure 8. It showed that cellulose was the main structural component in cell wall, the source of cell wall strength. Hemicelluloses (xylan and glucomannan) connected with the highly ordered cellulose of the microfibrils and lignin, and most of xylan contacted with glucomannan and lignin. Glucomannan and cellulose in close contact within the cell wall, and the force between xylan and glucomannan was less than that between glucomannan and cellulose. Xylan acted as an interfacial coupling agent between highly ordered cellulose of the microfibrils and lignin, which was important to maintain the integrity of cell wall mechanics. Lignin linked to xylan, but the connection was easy to destroy. To a certain extent, its existence enhanced the mechanical properties of cell wall.

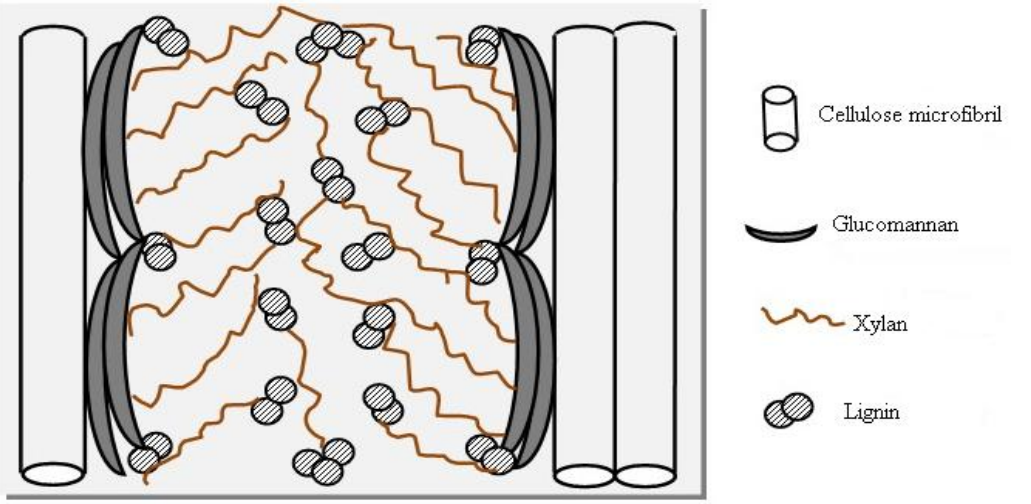

Fig. 8 Schematic diagram of interaction between chemical components in cell wall

Conclusions

The nanostructural organisation of wood cell wall after established extraction treatments method was studied by microtension experiments in combination with FT-IR spectroscopy. Different degrees of structural degradation were observed upon delignification and subsequent treatment with increasing concentrations of NaOH. The chemical changes might have reduced linkages between polymers in the cell wall. These chemical components changes could account fully for the changes observed in tensile properties of single fibers. The obvious decreasing tensile modulus and tensile strength in fibers treated with sodium hydroxide (NaOH) at concentrations of 6% were consistent with the xylan degradation. The findings suggest that xylan may contact with glucomannan and lignin in cell wall, and is important to maintain the integrity of cell wall mechanics.

References

Åkerholm, M. and Salmén, L. 2001. Interactions between wood polymers studied by dynamic FT-IR spectroscopy. Polymer. 42:963-969.
Åkerholm, M.and Salmén, L. 2003. The oriented structure of lignin and its viscoelastic properties studied by static and dynamic FT-IR spectroscopy. Holzforschung. 57:459-465.
Burgert,I.; Keckes, J.; Frühmann, K.; et al. 2002. A comparison of two techniques for wood fiber isolation evaluation by tensile tests of single fibres with different microfibril angle. Plant Biology. 4:9-12.
Duchesne, I.; Hult E-L; Molin, U.; et al. 2001. The influence of hemicellulose on fibril aggregation of kraft pulp fibres as revealed by FE-SEM and CP/MAS 13C-NMR. Cellulose. 8(2):103-111.
Groom, L.H.; Mott, L.; Shaler, S.M. 2002a. Mechanical properties of individual southern pine fibers. Part I: determination and variability of stress-strain curves with respect to tree height and juvenility. Wood Fiber Sci. 34:14-27.
Himmel, M.E.; Ding, S.Y.; Johnson, D.K.; et al. 2007. Biomass Recalcitrance: Engineering Plants and Enzymes for Biofuels Production. Science. 315(5813):804-807.
Jayne, B.A. 1959. Mechanical properties of wood fibers. Tappi. 42:461-467.
Marchessault, R.H. 1962. Applications of infrared spectroscopy to the study of wood polysaccharides. Spectrochim Acta. 18:876-876.
Nelson, R. 1961. The use of holocellulose to study of cellulose supermolecular structure. J. Polym. Sci. 51:27-58.
Pu, Y.Q.; Kosa, M.; Kalluri, U.C.; et al. 2011. Challenges of the utilization of wood polymers: how can they be overcome? Applied microbiology and biotechnology. 91(6):1525-1536.
Salmén, L. and Olsson, A.M. 1998. Interaction between hemicelluloses, lignin and cellulose: structure-property relationships. Journal of Pulp and Paper Science. 24:99-10.
Stevanic, J.S. and Salmén, L. 2009. Orientation of the wood polymers in the cell wall of spruce wood fibres. Holzforschung. 63:497-503.
Schwanninger, M.; Rodrigues, J.C.; Pereira, H.; et al. 2004. Effects of short-time vibratory ball milling on the shape of FT-IR spectra of wood and cellulose. Vibrational Spectroscopy. 36:23-40.
Yu, Y.; Jiang, Z.H.; Fei, B.H.; et al. 2010. An improved microtensile technique for mechanical characterization of short plant fibres: a case study on bamboo fibres. Journal of Material Science. 46:739-746.
Yu, Y.; Tian, G.L.; Wang, H.K.; et al. 2011. Mechanical characterization of single bamboo fibers with nanodentation and microtensile technique. Holzforschung. 65:113-119.

Acknowledgements

This study was sponsored by Department of Biomaterials of International Center for Bamboo and Rattan, Beijing, China, would like to gratefully acknowledge the financial support from the Chinese National Natural Science Foundation (No. 30730076).

The Optimum Process of Wheat-straw Fiber Treated By Enzyme

LIU Cong[1] *- ZHANG Yang*[2*] *-Su Yong*[3]

[1] Phd student, College of Wood Industry , Nanjing Forestry University, CHINA

spriteno1@126.com

[2] Professor and Research Director, Wood Materials & Engineering Laboratory, Nanjing Forestry University, CHINA

** Corresponding author*

yangzhang31@126.com

[3] Master Degree Candidate, College of Wood Industry , Nanjing Forestry University, CHINA

Abstract

It was investigated that the optimum process of wheat-straw fiber treated by enzyme. Being boiled with12% NaOH in 150℃for 4h and bleached with 5% H_20_2 in 70℃for 6 h, the wheat-straw material used for enzyme treatment was composed of 88.32% cellulose，1.43% hemicellulose and 2.53% lignin..From the glucose amount and enzyme dose of different samples, enzyme activity mesuration formula was attained, and the filter paper enzyme activity and corresponding solid enzyme vitality was got: 0.2969 IU/mL of 2g/L liquid enzyme fibrils and 148.45IU/g. Single-factor experiment was applied in order to get the optimum enzyme treatment condition: water bath in the oscillation trough at the frequency of 80 in 50℃ with enzyme usage 35IU/g for 48h. The wheat-straw micro/nano fibrils suspension was got with disposal to mixture system of enzyme decomposing production after enzyme treatment.

Keywords: enzyme treatment; wheat-straw; micro/nano fibrils

Introduction

China is lack of forestry resources, with percentage of forest cover 20.36%, taking up 67% or so of world forest acreage. And forest cover possession per capita is 0.145hm^2, not reaching to 1/4 of world possession per capita, while forest cumulation per capita 10.151m^3, only 14.3% of world cumulation per capita[1]. Therefore, making full use of non-wooden materials is a effective way to make up for the shortage of wood resources in China.
Wheat-straw is a kind of price moderate, fast grown and rich raw material, which can also be applied in wood-based panel[2-4]. It contains about 65-68% holocellulose and 20-21% acid-insoluble lignin[5].

Cellulose micro/nano fibrils has many advantages, promising a broad future in application. At present, there are three ways to prepare cellulose micro/nano fibrils[6], chemical, mechanical and biological methods. Preparing cellulose micro/nano fibrils with enzyme treatment is placid and concentrated, but has a special requirement to enzyme and reaction process[7]. The aim of the paper is to investigate the optimum preparation process of the micro/nano fibrils from the wheat-straw treated by enzyme.

Materials and Methods

Materials. Wheat-straw material, being boiled with 12% NaOH in 150℃ for 4h and bleached with 5% H_20_2 in 70℃ for 6 h[8]; composed of 88.32% cellulose，1.43% hemicelluloses and 2.53% lignin.

Enzyme treatment process

Enzyme activity measuration

According to the standard measuration commented by International Union of Pure and Applied Chemistry (IUPAC)，an international unit (FPU) of filter paper enzyme energy equals to the enzyme amount that created 1 mol glucose in standard condition in one minute, as following:
(1) In 5 of the 6 cuvettes, add 50 mg rotary filter paper (1×6 cm） to each cuvette and dilute enzyme liquor relevantly. Manipulate as table 1. (No.5 with substrate without enzyme, No.6 with enzyme without substrate)

Tab. 1 different adding amount of diluted enzyme and 0.05M citric acid buffer solution

Sample No.	1	2	3	4	5	6

Adding amount of diluted enzyme（ml）	0.2	0.3	0.4	0.5	0	0.5
Adding amount of 0.05M citric acid buffer solution（ml）	1.3	1.2	1.1	1.0	1.5	1.0

(2) Seal the cuvettes with plastic cloth and tie with elastics. Bathe in water in 50℃at the frequency of 80 for 60 minutes. Add 3 ml DNS solution rapidly after taking it out and boil it in 100 ℃for 5 minutes. Afterwards, cool it down in ice water and make it constant volume 50 ml. Shake up and measure absorbency OD in 550 nm, and get the glucose amount in reaction according to the glucose standard curve.

(3) Chart the glucose amount produced by 0.2、0.3、0.4、0.5 ml enzyme separately as abscissa, and the logarithm of enzyme dose as ordinate. The enzyme needed to product 2 mg glucose was attained from the chart, and then the filter paper enzyme energy of sample can be calculated with formula.

Optimum enzyme amount

(1)To ensure reaction process equally in the water bath oscillation trough, control the buffer solution volume 25ml and substrate quality 0.5g on the basis of reaction container. Mark 5、15、25、35、50 IU/g substrate separately with sample number 1-5 to ascertain the enzyme amount(the substrate is production apart from the hemicelluloses and lignin which contains 88.32% cellulose), as tab. 2.

Tab. 2 enzyme amount test with different enzyme usage

Sample No.	Substrate quality（g）	Enzyme usage（IU/g substrate）	Enzyme quality needed（mg）	Buffer solution volume（mL）
1	0.5	5	16.84	25
2	0.5	15	50.52	25
3	0.5	25	84.20	25
4	0.5	35	117.88	25
5	0.5	50	168.41	25

(2) Decompose the samples in water bath oscillation trough at the frequency of 80 times each minute in 50℃. After centrifuge treatment, take clear solution of the enzyme decomposing production to measure the glucose concentration with DNS method.

Optimum enzyme decomposing time

Choose enzyme usage as 35IU/g, and enzyme decompose in 50℃in water bath oscillation trough at the frequency of 80 for 12h、24h、48h、72h separately. After centrifuge treatment, take clear solution of the enzyme decomposing production to measure the glucose

concentration with DNS method.

Disposal to mixture system of enzyme decomposing production

(1) To release the enzyme activity, cook the flask of mixture with enzyme decomposing production in boiling water for 5 min.
(2) Wash in centrifuge to wipe out the soluble materials of the mixture system such as glucose, and repeat it 3 to 5 times.
(3) After centrifuge washing, disperse the fibrils with trifle enzyme in distilled water. Add disperse system and chloroform in a cuvette in 1:4 volume proportion. Shake up and then keep static for 30min±5min. Finally, the mixture system was delaminated. The upper-layer was chloroform, under-layer water, and the middle-layer was fibrils and deposition which was denaturalized protein in chloroform.
(4) In the cuvette, protein deposited in the bottom of water while the fibrils suspension separated out. Extracting the upper suspension with tubularis, and fibrils without protein was attained. In avoid of protein, 5-6 cm bottom of water cannot be extracted.

Results And Discussion

Enzyme activity mesuration

The absorbency of sample is listed in tab. 3:

Tab. 3 the absorbency of sample

Sample No.	1	2	3	4	5	6
absorbency	0.432	0.537	0.601	0.685	0.055	0.204

Substitute the absorbency to the standard curve formula y=12.85x-0.0377, the glucose amount of sample 1-4 was attained, as in tab. 4:

Tab. 4 the glucose enzyme of sample production

Sample No.	1	2	3	4
Glucose amount（mg）	0.820	1.228	1.477	1.804
logarithm of enzyme dose	-0.6990	-0.5229	-0.3979	-0.3010

Charting the glucose amount as abscissa, and the logarithm of enzyme dose as ordinate, the enzyme activity formula can be attained: y=0.412x-1.029（R^2=0.991）, as fig. 1 shows.

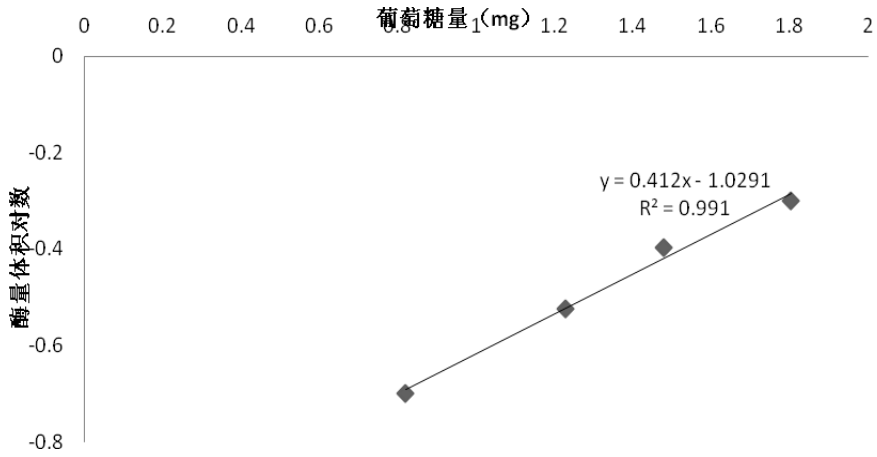

Fig. 1 the enzyme activity mesuration formula

According to the above formula, the enzyme needed to produce 2ml glucose is 0.6237mL. Choosing the testing liquor concentration as 2g/L，then calculate the enzyme activity with the formula:

Filter paper enzyme activity=

$$\frac{2mg\ glu\cos e}{60\min\times 0.18(mg/\mu mol)\times the\ enzyme\ needed\ to\ produce\ 2mg\ glu\cos e\ (\mathrm{mL})}$$

So the filter paper enzyme activity of 2g/L liquid enzyme fibrils is 0.2969 IU/mL, and its corresponding solid enzyme vitality is 148.45IU/g.

Optimum enzyme amount

Tab. 5 the glucose concentration after 24h and 72h enzyme decomposing

Sample No.	1	2	3	4	5
Glucose concentration after 24h enzyme decomposing（g/L）	0.107	0.200	0.249	0.320	0.324
Glucose concentration after 72h enzyme decomposing（g/L）	0.215	0.388	0.454	0.481	0.492

From tab. 5 we can conclude that productions of sample 4 and 5 contained highest glucose amount. In the view of economy, choose sample 4 as the optimum enzyme amount, namely the enzyme usage is 35IU/g.

Optimum enzyme decomposing time

Tab. 6 the glucose concentration of different decomposing time

Enzyme decomposing time（h）	12	24	48	72
Glucose concentration（g/L）	0.222	0.323	0.450	0.481

From tab.6 we can choose 48h as optimum decomposing time, with the glucose concentration 0.45 g/L, as decomposing efficiency decreased with time increasing.

Conclusions

The filter paper enzyme activity of 2g/L liquid enzyme fibrils is 0.2969 IU/mL, and its corresponding solid enzyme vitality is 148.45IU/g. The optimum enzyme treatment condition was water bath in the oscillation trough at the frequency of 80 in 50℃ with enzyme usage 35IU/g for 48h. With enzyme treatment above, micro/nano fibrils can be attained from wheat-straw fiber. Preparing micro/nano fibrils with enzyme is complicated to control the reaction, so it's still called for further research before put into manufacturing.

Acknowledgements

This work was supported by the National Natural Science Foundation of China (NSFC31070492).

References

1. Dingguo Zhou and Changtong Mei, J. Journal of Nanjing Forestry University. 5 (2000)
2. Dingguo Zhou, J. Forestry Industry. 2 (2002)
3. Xuhe Chen, J. International Wood Industry. 4 (2002)
4. Ping Yi and Shaoqun Tang, J. Wood-based Panel communication. 11 (2001)
5. Hailan Lian, Dingguo Zhou and Jixue You, J. Wood Chemistry and Industry. 25, 1 (2005)
6. Qing-zheng Cheng, Si-qun Wang , Ding-guo Zhou , RIAL S Tim , Yang Zhang, J. Journal of Nanjing Forestry University (Natural Sciences Edition). 31,4 (2007)
7. Guimin Luo, Editor, Enzyme Engineer, Chemistry industry Publishers, Beijing (2002)
8.Ogren K, Bura R, Saddler J, et al. J. Bioresource Technology. 98(2007)

Mechanical Properties of Parenchymal Ground Tissues from Moso Bamboo

AN Xiao-jing, YU Yan, WANG Han-kun, TIAN Gen-lin*

Department of Biomaterials. International Center for Bamboo and Rattan. No.8, Fu tong Eastern Street, Wang jing Area, Chao-yang District. Beijing, China, 100102

* *Corresponding author*
yuyan9812@icbr.ac.cn

Abstract

Increasing attentions are being paid to bamboo because of its unique biological structure and mechanical performance. The main component units of bamboo are parenchymal ground tissues (PGT) and fiber bundles, which respectively functions as matrix and reinforcement in the composite. The mechanical properties of bamboo fiber have been well measured and established but no experimental data have been reported for PGT as far as we know. That is mainly due to the difficulty in the preparation of a PGT tensile sample. In this paper, the tensile modulus and strength of pure PGT with two different sizes were experimentally measured for the first time. The result shows sample size significantly affects the mechanical properties of PGT. The smaller group has an average tensile modulus 0.17 GPa and a ultimate strength 2.14 MPa respectively, much smaller than the corresponding value 1.70 GPa and 40.02 MPa for the bigger one. This can be explained by the higher ratio of damaged cells to the intact ones. Our experimental data demonstrates the unreliability of deriving the tensile modulus and strength of PGT using the classic mixture law of composites, which is normally valid for bamboo fibers.

Keywords: bamboo, parenchymal ground tissues, fibers bundles, mechanical properties.

Introduction

In recent years there has been increasing interest in biomaterials , which could be used as a reference in the biomimetic design of advanced composites. Bamboo has been applied in many aspects, not only because of its renewability, easy availability, low cost and friendliness to environment, but also its remarkable mechanical properties. Bamboo is a complicated hierarchical natural fiber reinforced composites with PGT and fiber bundles respectively functioning as matrix and reinforcement phase (Fig. 1).

Many studies on mechanical properties of bamboo fibers have been reported. Shao et al (2009) reported the tensile modulus and strength of bamboo fibers are 482.2 MPa and 33.9 GPa respectively. Shang (2011) measured to be 778.63 MPa and 50.02 GPa for the same bamboo species. Though Amada et al (2001) calculated the tensile modulus and strength of PGT of bamboo to be 2 GPa and 50 MPa respectively, no experimental data have been reported as far as we know.

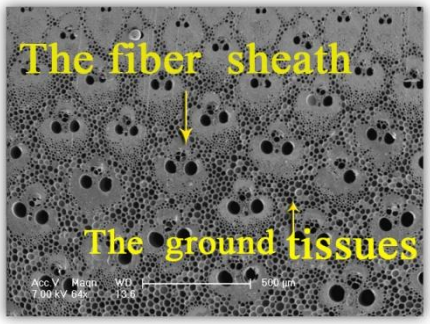

Fig 1 The two phase composite structure of bamboo

In this paper, we proposed the methodology of developing tensile samples of pure PGT with different sizes from bamboo under the aid of a light microscope. A microtensile tester was employed for obtaining the tensile mechanical properties of PGT. Meanwhile, the microfibrilar angle of these samples was obtained with X-ray diffraction technique. Our aim is to experimentally identify the tensile modulus and strength of PGT from bamboo. For comparison, the tensile modulus and strength of PGT are also calculated based on composite mixture law and the tensile results of bamboo sheets.

Materials and Methods

Materials. Moso bamboo （*phyllostachys edulis*）with 4 years old was selected for the present study. Bamboo blocks with the size 10 mm (R) *10 mm (T) *40 (L) were saturated in water before sample preparation.

Methods. The process of preparing tensile samples of bamboo fiber bundles and PGT (smaller size) are shown in Fig. 2. Microtomed bamboo section with thickness 70-100 μm were sliced along the radio direction using a sliding microtome, from which the pure PGT were carefully

separated with a very sharp knife under a stereo light microscope. However, only the samples with invisible damage and regular dimensions were selected for testing. The sectional area of the samples ranges from 0.087 to 0.157 mm^2. The fiber bundles were prepared with similar approach. The length of these samples is about 40 mm.

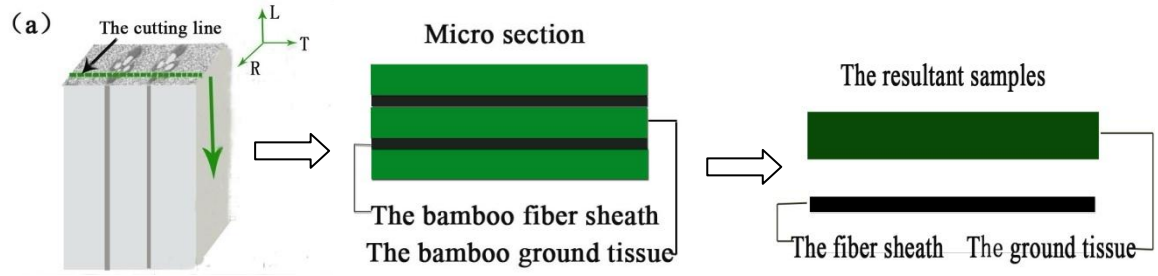

Fig 2 Schematic diagram showing the procedure of preparing the tensile samples of bamboo fiber bundles and PGT with 70-100 μm thickness.

The progress of preparing irregular tensile samples of PGT with bigger size is shown in Figure 3. First, a target PGT area close to the inner part of a bamboo culm was selected under a microscope. The fibers component in the selected area was then carefully removed by a sharp knife and the pure PGT was left. The cross sectional area of this bigger sample is from 0.6 mm^2 to 1.6 mm^2.

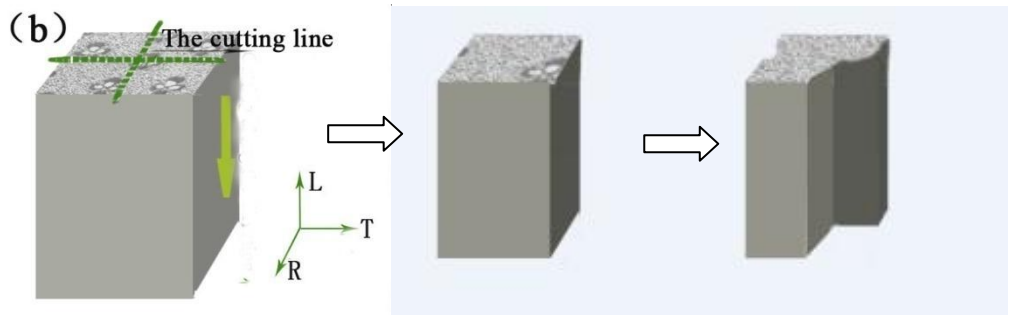

Fig 3 Schematic diagram showing the process of preparing a big PGT tensile sample from bamboo

Tensile tests on fibre bundles and PGT with different sizes

Before testing, the prepared samples were dried between two glass slides for more than 5 h to keep them straight. The fiber bundles or PFT samples were all glue between two Poplar wood veneers with a thickness of about 1mm as shown in Figure 4.

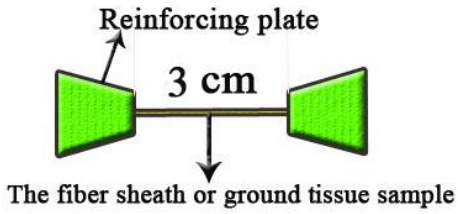

Fig 4 Schematic diagram showing the state of fiber sheath before testing

Measurement is performed with a high resolution microtester (5848, Instron, USA). The load sensor is 50 N and the tensile rate of the crosshead is 1.5 mm/min. Video extensometer is applied for strain measurement. It was tested under controlled environment at 24.7 ℃and 64% relative humidity. The sectional area of all the broken samples was measured with a scanning electron microscope (ESEM XL-30, FEI).

For comparison, the tensile modulus and strength of more than 50 bamboo sheets with different fiber contents were measured with a common mechanical test (5832, Instron, USA). The elastic modulus and strength of pure PGT could be calculated using the well known mixture law of composites.

Results And Discussion

The validity of methodology for PGT tensile samples development

Fig. 5 shows the cross section of PGT samples with different sizes. A regular cross section was found for the smaller PGT that contains about 3- 4 rows of parenchymal cells at the thickness direction. The cross section of the bigger PGT is relatively irregular and contains much more cells than the small one.

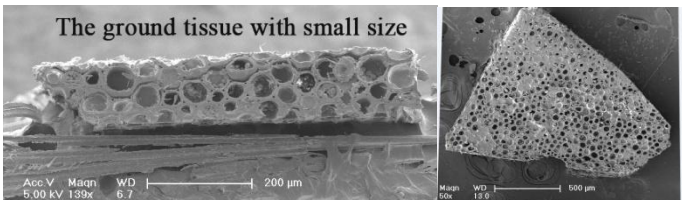

Fig 5 SEM Photographs showing the sectional area of PGT with different sizes

The sectional area variation along the length of PGT tensile samples was shown in the Fig 6. Little variation was found for the both types of samples, which demonstrates the validity of the prepared PCT tensile samples.

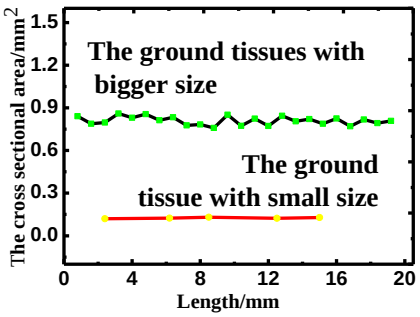

Fig 6 The sectional area variation along the length direction of PGT tensile samples

The stress-strain curves

Fig. 7 shows the typical stress-strain curves of bamboo fiber bundles and PGT with different size. For the fiber bundles, the portion from the beginning of loading to the breaking point was entirely linear due to its small microfibrillar angle (less than 10 degree). High rupture

strength and high MOE were observed. For the bigger PGT samples, a small linear portion was firstly observed followed by obvious yield until failure. The extensibility of PGT was found to be significant higher than that of bamboo fiber bundles, which could be explained by its high microfibrillar angles (about 40 degrees). However, a short curve with much smaller slope was found for the PGT with small size, which indicates the distinct pre-mature failure caused by the high ratio of damaged cells located on the surface of samples.

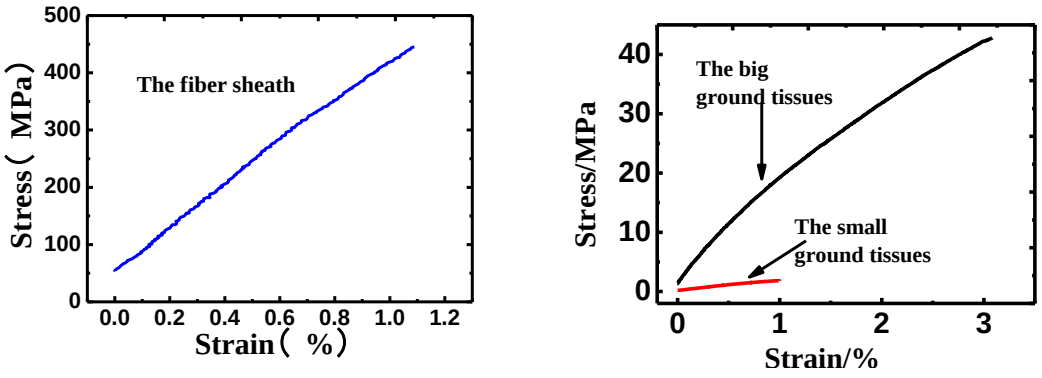

Fig 7 Stress-strain curves of fiber bundles and PGT with different sizes

Comparison in the tensile modulus and strength of PGT

Table1 The tensile strength and modulus of PGT and fiber bundles of bamboo

	MOE(GPa)	Tensile strength （MPa）	The strain of samples (%)	Coefficient of variatio	The Number of samples
The smaller ground tissues	0.17	2.14	0.7	0.28	18
The bigger ground tissues	1.70	40.02	2.8	0.15	18
Fiber sheath	42.73	728.99			8
Calculated	-1.07	83.42			
Amada(2001)	2.0	50			
Shao(2009)	0.22	19.04			

The tensile strength and modulus of the fiber bundles and PGT with different sizes are given in Tab.1. The tensile modulus of the bigger PCT is more than 8 times of the small one. This discrepancy reaches about 20 times for the tensile strength. It can be concluded that sample size significantly affects the mechanical properties of PGT, especially at micron scale. At this scale, the ratio of damaged parenchymal cells to intact cells was exceptionally high, resulting in significant reduction both in stiffness and strength. This so called size effect of mechanical

performances was also observed for other porous biomaterials, such as wood (Yu et al, 2009). Some publications reported the calculated value of PGT of bamboo in both tensile modulus and strength. Amada et al (2001) calculated the tensile modulus and strength of PCT from Moso bamboo to be 2.0 GPa and 50 MPa respectively (Amada et al, 2001), which seems to agree well with our experimental results. However, our own calculation obtained with similar approach produce -1.07 GPa for tensile modulus and 83.42 MPa for tensile strength. The results reported by Shao et al (2009) to be 0.22 GPa and 19.04 MPa respectively. From the previous studies, it can be found the calculation result of PGT of bamboo is highly variable, which can be explained as follows.

From the classic mixture law of composites, we can get：

$$E=E_f V_f+E_m(1-V_f) \quad (1)$$
$$E_f=nE_m \quad (2)$$
$$Em= E/((n-1) V_f+1) \quad (3)$$

Here, E is the modulus of the bamboo sheet; V_f is the fiber content in volume. E_m and E_f is the modulus of PGT and bamboo fiber bundles respectively. n is the ratio between E_f and $E_{m.}$ From formula (3), it can be found the error in V_f can be magnified by (n-1) times when calculating E_m. n might be 20 or higher based on our experimental results (Tab.1). Therefore, a measurement error of 5% in V_f might lead to 100% error for E_m. On the contrary, the effect on E_f will be much smaller.

Conclusion

1. The tensile modulus and strength of PGT are significantly correlated to sample size. The smaller ones are measured to be 0.17 GPa for tensile modulus and 2.14 MPa for strength, significantly less than the value 1.7 GPa and 40.02 MPa for the bigger ones.

2. PGT shows significant difference in stress-strain curves from fiber bundles, which can be explained by its high microfibrillar angles.

3. The tensile modulus and strength of PGT calculated based on mixture law of composites are highly variable and unreliable because the error in fiber content measurement would be significantly magnified during the calculation.

Acknowledgement

We would like to thank National Natural and Science Foundation of China (31070491) for financial support.

References

Amada S, Untao S, et al. 2001. Fracture properties of bamboo.Composites: Part B. 32:451-459

Eiichi Obataya, Peter Kitin, Hidefumi Yamauchi. 2007. Bending characteristics of bamboo (Phyllostachys pubescens) with respect to its fiber–foam composite structure. Wood Sci Technol. 41:385–400

Kohler L, Spatz H C.2002. Micromechanics of plant tissues beyond the linear-elastic range. Platna.215:33-40.
Shang L L.2011. The research of Morphology and Tensile mechanical properties of MOSO bamboo vascular bundle. International Center of Bamboo and Rattan:Master degree thesis.
Shao Z.P , Fang C.H, Huang S.X et al. 2009. Tensile properties of Moso bamboo and its components with respect to its fiber-reinforced composite structure. Wood Sci Technol
Y. Yan, Jiang Z.H, Tian G.L. 2009. Size effect on longitudinal MOE of microtomed wood sections and relevant theoretical explanation. For. Stud.11(4): 243–248.

Development of Low Formaldehyde-Emitting Laminate Flooring by Nanomaterial Reinforcement

Zeki Candan [1*] *– Turgay Akbulut* [1]

[1] Department of Forest Products Engineering, Faculty of Forestry
Istanbul University, Sariyer, 34473, Istanbul, TURKEY.
* *Corresponding author*
forestproductsengineer@yahoo.com

Abstract

Nanoscience and nanotechnology have numerous advantages for wood or composite materials. Formaldehyde emission from laminate flooring is of great importance on human health. Developing low formaldehyde-emitting laminate flooring as an environmentally friendly material by nanotechnology application was aimed in this study. Formaldehyde based resin used to produce laminate flooring was reinforced with different nanomaterials. The overlay papers were impregnated with the nanomodified resin. The papers were used to manufacture the flooring materials. Formaldehyde emission analysis was carried out according to EN standard. The results obtained in this study showed that some nanomaterials significantly decreased formaldehyde emission of the laminate flooring materials. Using nanotechnology, it is possible to produce low formaldehyde-emitting laminate flooring.

***Keywords*:** A. Nanotechnology, B. Nanomaterial reinforcement, C. Formaldehyde emission, D. Laminate flooring.

Introduction

Laminate flooring is among composite wood products. Laminate flooring having sufficient surface performance is widely used as flooring materials in both residential and nonresidential applications. Laminate flooring materials are shown in Figure1 (Candan, 2012). Laminate flooring was found in 1977 by Pergo (Sweden). The first products were started to sell in Europe in 1984 while in the US in 1994 (WFCA, 2012).

Fig. 1 Laminate Flooring

Production capacity and using area of these composite materials are increasing year by year. Formaldehyde emission is disadvantage in applications and is a crucial performance property for laminate flooring. Nanotechnology has been identified as a technological revolution by scientists from all over the world. Nanoscience and nanotechnology have numerous advantages also for composite materials (Ciraci, 2005; Jones et al. 2005; Roughley, 2005). To overcome this disadvantageous, use of nanomaterials in manufacture of laminate flooring is of a great importance and novelty (Candan, 2012). In this study, development of low formaldehyde-emitting laminate flooring materials by nanotechnology was objected.

Materials and Methods

Materials

Kraft paper, HDF panels, decorative paper, and overlay paper were used to produce laminate flooring. The resin was melamine formaldehyde. Silica, alumina, and zinc oxide nanoparticles were used to reinforce laminate flooring.

Laminate Flooring Manufacturing

The papers were impregnated with melamine formaldehyde resin in a commercial impregnation line. After that the impregnated kraft paper was used as a balance paper in the bottom layer of the laminate flooring. HDF panel was placed on the kraft paper. Then, the impregnated decorative paper and overlay paper were placed over it, respectively, and then it was hot pressed in the short-cycle press line (Kastamonu Integrated Wood

Industry and Trade Inc., Kastamonu, Turkey). Manufacturing of the laminate flooring is shown in Figure 2.

Fig. 2 Manufacturing of Laminate Flooring (Photo: Candan)

The loading levels of the nanomaterials were 1% and 3%. The control laminate flooring material was also produced for the comparison. The panels were cut into the test samples. The experimental set-up of the formaldehyde emission test is shown in Figure 3.

Fig. 3 Formaldehyde Emission Test Set-up (Photo: Candan)

Formaldehyde emission tests on the laminate floorings were conducted according to TS 4894 EN 120 (1999) standard. Perforator and spectrophotometer were used to determine the formaldehyde emission properties of the nanomaterial reinforced laminate flooring in this study.

Statistical Analyze

To evaluate formaldehyde emission properties of the laminate flooring materials reinforced with nanomaterials, all multiple comparisons were first tested using an analysis of variance (two-way ANOVA) at $p<0.05$. Significant differences between the mean values of treated and untreated groups were determined using Duncan's multiple range test.

Results and Discussion

Formaldehyde emission results of the nanomaterials reinforced laminate flooring were shown in Figure 4.

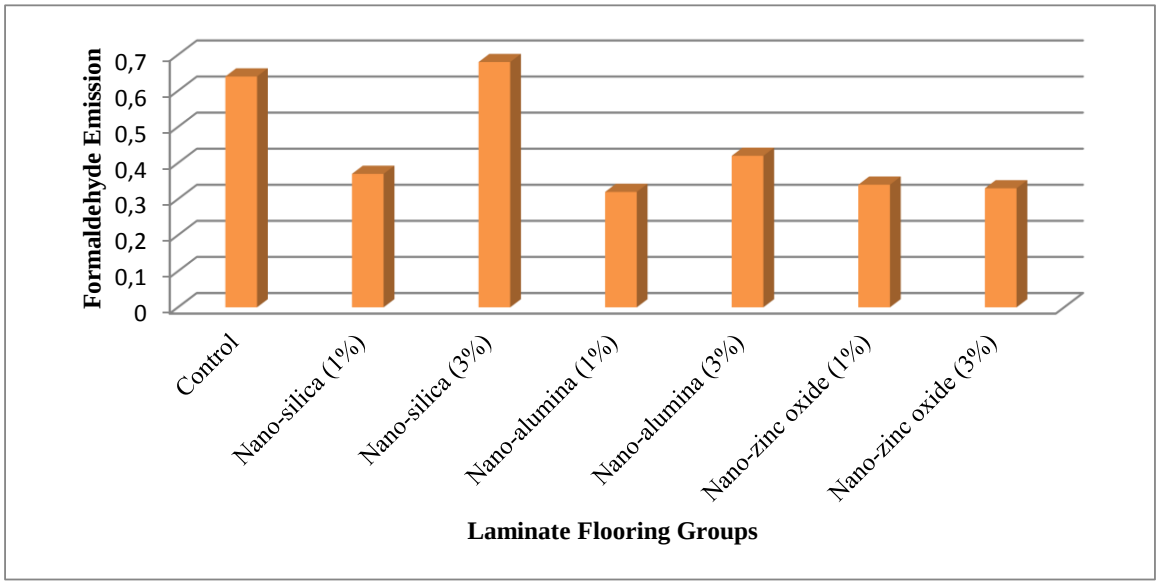

Fig. 4 Test Results of the Laminate Flooring Reinforced with Nanomaterials

The results indicate that the nanomaterials significantly affected the formaldehyde emission of the laminate flooring. All the laminate flooring groups reinforced with nanomaterials had lower average formaldehyde emission values than those of the control group's values, except nanosilica (3%) which was slightly higher than the control group.

The lowest formaldehyde emission value was determined in the laminate flooring reinforced with nano-alumina (1%). The formaldehyde emission values increased with increasing the nanomaterial levels for nano-silica and nano-alumina. There was no important change for nano-zinc oxide. The formaldehyde emission values of the laminate flooring with nano-silica (1%) were decreased by 50%.

Conclusions

Formaldehyde emission property is of a great important for laminate flooring materials because it could affect human health. The nanomaterial type and nanomaterial loading level significantly affected the formaldehyde emission values of the laminate flooring. The formaldehyde emission values could be decreased with using proper nanomaterial type or loading level. The result of this research indicates that nanoscience and nanotechnology could be used to develop laminate flooring materials having an enhanced property.

References

Candan, Z., 2012, Nanoparticles use in manufacture of wood-based sandwich panels and laminate flooring and its effects on technological properties, Ph.D. Thesis, 289 pp., Istanbul University, Istanbul, Turkey.

Ciraci, S., 2005, Science and technology at one of a billionth of a meter, Science and Technique, Tubitak, Ankara, Turkey.

Jones, P., Wegner, T. et al. 2005, In: Nanotechnology for the forest products industry – Vision and technology roadmap, Based on the Results of the Nanotechnology for the Forest Products Industry Workshop, Landsdowne, Virginia, USA, October 17 – 19, 2004. Atlanta: TAPPI Press, p. 92.

Roughley, D.J., 2005, Nanotechnology: implications for the wood products industry, p. 73, Forintek Canada Corporation, Canada.

TS 4894 EN 120, 1999, Wood based panels – Determination of formaldehyde content – Extraction method called the perforator method, Turkish Standard Institute (TSE), Ankara, Turkey.

World Floor Covering Association (WFCA), 2012, Laminate flooring buying guide, www.wfca.org [Visiting Date: 04.09.2012].

Acknowledgements

The authors thank Istanbul University Research Fund for its financial support in this study (Project No: 4806, Project No: 19515, and Project No: UDP – 26015). The author also would like to express their appreciation for the assistance provided by Kastamonu Integrated Wood Industry and Trade Inc., Kastamonu, Turkey.

Proceedings of the 55th International Convention of Society of Wood Science and Technology
August 27-31, 2012 - Beijing, CHINA

A Novel Energy Saving Wood Product with Phase Change Materials

Fang Chen [1], Amanda Kessel [2], Michael Wolcott [3]*

[1] PhD student, Composite materials and engineering center (CMEC), Washington State University, Pullman, WA, 99163, USA.
[2] Summer REU student in CMEC, Washington State University (2011).
[3] Professor and Research Director, Composite materials and engineering center (CMEC), Washington State University, Pullman, WA, 99163, USA.
* Corresponding author
wolcott@wsu.edu

Abstract

Phase change materials (PCM) are utilized for thermal energy storage. Structure and properties of PCM have been studied extensively in the past because they are highly correlated to materials' energy saving ability and application. However, with the quickly growing requirement of PCM application in buildings, to reduce our reliance on air conditioning and heating through solar energy storage, the problem of PCM leakage must be solved first. This study is focusing on verification of the feasibility of manufacturing a novel energy saving wood product with PCM, using wood as a low cost porous structure material for PCM instead of the porous materials that are widely studied. Scanning electron microscope (SEM) imaging was carried on to investigate the possibility of paraffin to get into lumen of wood chips. The ability of wood flour to absorb paraffin is calculated. PCM and wood flours were compounded utilizing a parallel co-rotating twin screw extruder. Melting and crystallization behavior of the blends were investigated by differential scanning calorimeter (DSC). Based on the hypothesis that wood encapsulation and polymer sealing can help to restrict leakage of PCM, a novel energy saving wood product with PCM by using wood lumen as containers of PCM is possible to be made.

Keywords: Phase change materials, wood product, energy saving, composites, paraffin

INTRODUCTION

Thermal energy can be stored in several ways, sensible heat, thermochemical, and latent heat. Phase change materials possess high energy storage density and isothermal operating characteristics making them very efficient materials for utilizing latent heat in application [1-3]. Many researchers are focusing on organic PCM, inorganic PCM, and eutectics[4] for passive solar energy storage, all very promising areas for energy saving in buildings. Phase change materials can be implemented in the walls of buildings. When absorbing energy instead of the interior of buildings, the phase of PCM can be changed from solid to liquid. When the ambient temperature drops, PCM begins to solidify, releasing stored thermal energy to the building and stabilizing the interior temperature. The temperature of PCM will be maintained closer to the desired temperature during each phase transition period for a long period of time until the phase change is complete. In this way, PCM can be used to increase human comfort by decreasing swings in internal air temperature[5]. Energy conservation is achieved through this reversible and repeatable phase change.

The primary phase change of interest in the proposed work is the solid-liquid change in PCM. Other types of phase change store and release latent heat energy during transition, but they are impractical for most energy storage applications. In solid-liquid PCM, exudation occurs after the PCM absorbs enough energy to complete the phase change to liquid, undermining its application value. Controlling this leakage is the current major obstacle to the use of PCM in the thermal envelopes of buildings. Encapsulation is widely applied to contain PCM to prevent leakage. But this method comes with some issues, such as low flame retardancy and thermal conductivity with the core-shell structure, low chemical and thermal stability, and high cost[6, 7]. To use porous structure materials, such as expanded perlite (EP), diatom earth (DE), expanded graphite[8-10], concrete[11], porous metallic foams[12] and so on, instead of conventional encapsulation method is a promising way to capture PCM and protect it from leakage when melting.

For a mature cell in wood in which there is no protoplast, the open portion of the cell is known as the lumen. Most wood cells in wood have two domains which are the cell wall and the cell lumen[13]. The cell lumens are connected by pits by which cell walls are modified to allow communication between the cells in the living plant[13]. The objective of this study is to verify the feasibility of manufacturing a novel energy saving wood product with phase change materials, using wood as a low cost porous structure material for PCM instead of other porous materials which have already been widely studied.

MATERIALS AND METHODS

Materials. The materials used are paraffin (Technical Octadecane) from Roper Thermals, Ponderosa pine flour from American wood fibers, and maple chips.

SEM. The maple chips are soaked in melt paraffin for 10 min followed by SEM imaging.

Extrusion. Paraffin and WF (40, 60, 80 mesh) mixtures in 60/40, 70/30, and 80/20 (wt%) ratios were prepared, respectively, and blended in a co-rotating twin screw extruder (Leistritz ZSE-18HP) at 50°C.

DSC. The melting temperature and crystallization temperature of paraffin in composites were determined using a deferential scanning calorimeter (DSC) in the range from 0 to 75°C. The scanning rate was 10°C/min.

RESULTS AND DISCUSSION

Wood is a natural structural material with a honeycomb-like microstructure. Fig.1 shows a SEM image of paraffin infiltration into maple lumen. The lumen size may influence paraffin infiltration. If sealing a layer of plastic on the external surface of wood, we can achieve a good encapsulation of PCM in wood composites.

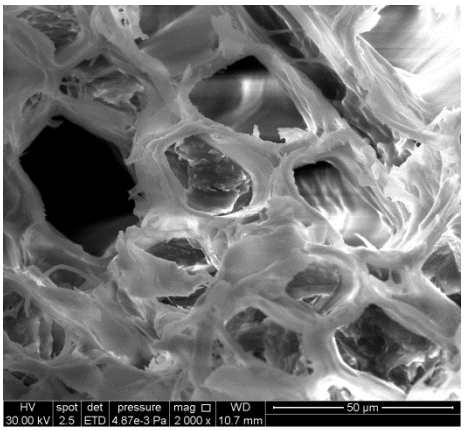

Figure 1. Paraffin infiltration into maple lumen

The result above shows that it is possible to encapsulate PCM into wood. In addition, how much PCM could be encapsulated? To estimate how much PCM could be penetrated into wood, the density values in table 1 are used.

Species	Density (g/cc)
Ponderosa Pine	0.35
Paraffin	0.65
Wood cell wall	1.5

Table 1 Density

Wood porosity (Φ) is calculated as follows.

$$\phi = 1 - \frac{1/\rho_{cellwall}}{1/\rho_f} = 0.77$$

Assuming that paraffin fills wood lumen completely, we calculate the maximum paraffin weight fraction in the mixture as follows.

$$W_p = \frac{\rho_p \phi}{\rho_p \phi + \rho_{cellwall}(1-\phi)} = 0.59$$

In the equations above, ρ is density, f represents fiber, and p represents paraffin.

DSC results in figure 2 show that after blending with wood flour, paraffin maintains its phase change and its energy saving ability is not removed. Besides, based on our study on miscibility of polyethylene (PE)/Paraffin blends, after blending with PE, paraffin functions well, too. Further, with the help of plastic, good encapsulation of PCM is expected to be achieved. Thus, it is possible to make a novel energy saving wood product with phase change material (paraffin) and polyethylene

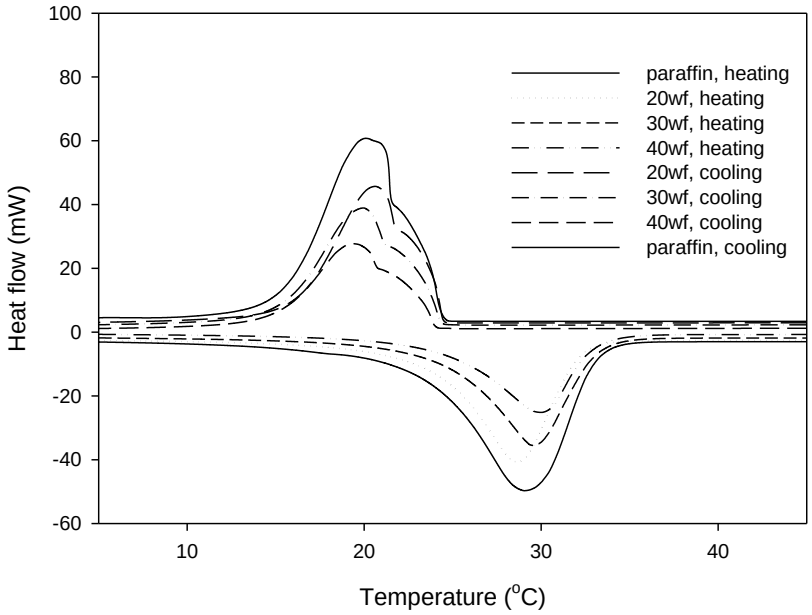

Figure 2. Influence of wood flour content on melting and crystallization of paraffin

CONCLUSIONS

It is possible to make a novel wood product with PCM by using wood lumen as containers of PCM for efficient energy saving. The encapsulation of paraffin with wood flour and plastic combined together needs to be studied. Composites formulation and wood lumen size need to be considered as well.

References

1. Wang, W., et al., *Preparation and performance of form-stable polyethylene glycol/silicon dioxide composites as solid-liquid phase change materials.* Applied Energy, 2009. **86**(2): p. 170-174.
2. Olabisi, O., Robeson, L.M. and Shaw, M.T., *Polymer-polymer miscibility.* 1979.
3. Edwards, R.T., *Crystal Habit of Paraffin Wax.* Industrial & Engineering Chemistry, 1957. **49**(4): p. 750-757.
4. Pasupathy, A., R. Velraj, and R.V. Seeniraj, *Phase change material-based building architecture for thermal management in residential and commercial establishments.* Renewable and Sustainable Energy Reviews, 2008. **12**(1): p. 39-64.
5. Khudhair, A.M. and M.M. Farid, *A review on energy conservation in building applications with thermal storage by latent heat using phase change materials.* Energy Conversion and Management, 2004. **45**(2): p. 263-275.
6. Carpenter, J.A., *The Physical and Chemical Properties of Paraffin Wax, Particularly in the Solid State.* Inst. Pet. Tech, 1926. **12**: p. 288.
7. Katz, E., J. Inst. Petroleum, 1930. **16**: p. 870.
8. Zhang, Z. and X. Fang, *Study on paraffin/expanded graphite composite phase change thermal energy storage material.* Energy Conversion and Management, 2006. **47**(3): p. 303-310.
9. SarI, A. and A. Karaipekli, *Thermal conductivity and latent heat thermal energy storage characteristics of paraffin/expanded graphite composite as phase change material.* Applied Thermal Engineering, 2007. **27**(8-9): p. 1271-1277.
10. Py, X., R. Olives, and S. Mauran, *Paraffin/porous-graphite-matrix composite as a high and constant power thermal storage material.* International Journal of Heat and Mass Transfer, 2001. **44**(14): p. 2727-2737.
11. Hawes, D.W. and D. Feldman, *Absorption of phase change materials in concrete.* Solar Energy Materials and Solar Cells, 1992. **27**(2): p. 91-101.
12. Yang, Z. and S.V. Garimella, *Melting of Phase Change Materials With Volume Change in Metal Foams.* Journal of Heat Transfer, 2010. **132**(6): p. 062301.
13. Miller, A.C.W.a.R.B., *Structure and Function of Wood.* 2005.

Acknowledgments

I'm grateful to my professor Dr. Michael Wolcott's advice, encouragement and patience. Useful discussions with Dr. Bo Liu are greatly appreciated.

Mechanical Properties of Ramie Fiber Woven Composites under Biaxial Tensile Loadings

Zehui Jiang, Fuming Chen, Ge Wang, Hai-tao Chen and xing'e Liu

International Centre for Bamboo and Rattan, Beijing, China, 100102

Sheldon Q. Shi

Mechanical and Energy Engineering, University of North Texas,

Denton,TX76203-1277,USA

Abstract

The objective of this work was to use a novel 3-D test analysis system for evaluating the mechanical properties of the natural fiber fabric composites under biaxial loads. Composites with three resin matrices (water-based epoxy resin, isocyanate resin, phenolic resin) were investigated, and strain-filed were characterized by using the digital speckle correlation (DSCM). The water-based epoxy resin plate and isocyanate resin plate demonstrated a characteristic of orthotropy and elastoplasticity, while the phenolic resin board revealed linear elastic and brittle-fracture simultaneously at X,Y-axial. Dissimilarities of biaxial load value were related to the orthotropy of composite structure, and load changes in fracture direction had a negative effect on the other directions at breaking moment. The degrees of dropping presented a positive correlation with the load values at rift direction. Under the linear elastic stage, the value of load and average strain at Y-direction were larger than that under X-direction within the same testing area. The strain-filed at X/Y-direction provided by isocyanate and phenolic resin plates illustrated a more smooth change than that of the water-based epoxy resin plate.

Keywords: Ramie, Natural Fiber Fabric Composite, Biaxial tension, Digital Spackle Correlation Method, Strain Filed

Introduction

Natural fibers, offered a renewable resource and a lower cost feedstock, have been extensively used for composite manufacturing. In addition, the fibers' high specific strength and stiffness, damage tolerance, and eco-friendly characteristics make them desirable for utilization (Xu *et al* 2008). These composite products suffer from uniaxial stress in practical engineering applications, but they also develop biaxial or even multi-axial stress states, in many situations, such as wind or seismic effects (Hu *et al* 2004, Luo *et al* 2008). This brings about considerable difficulty to evaluate its mechanical properties objectively. Investigating and simulating the non-liner response characteristics of stress-strain due to the complex stress state and material anisotropy have became a key part for structural design successfully or not. Experimental techniques and different kinds of material cruciform-specimens have been used to produce biaxial stress states, such as soft textile composites, notched composite and sheet molding laminates as well as fiber reinforced laminates (Arnold *et al* 1995, Smits *et al* 2006, Virginio *et al* 2008).

.

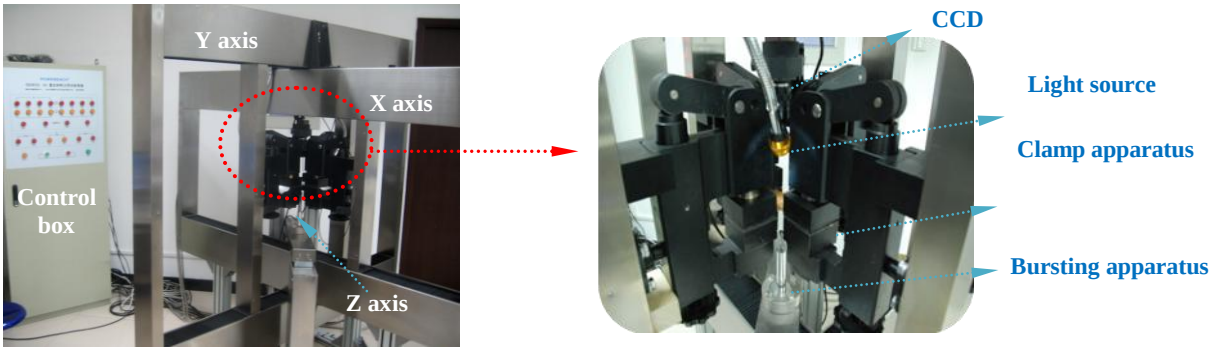

Fig. 1 3-D loading test device for composite material analysis system

In order to successfully model and simulate the behavior of materials for optimal use in structural applications, a novel testing device, the 3-D Composite Material Analysis System (Fig. 1) was developed at the International Center for Bamboo and Rattan (ICBR) in Beijing, China. The overall objective of this research was to investigate the mechanical properties of natural fiber woven composites based on three thermosetting resins under biaxial tensile loading. Meanwhile, the strain-fields were characterized by digital speckle correlation method (DSCM) during the stretching process(Chen *et al* 2009,Wang *et al* 2010).

Sample preparation

Balanced plain woven ramie fabrics were supplied by the company Hua Sheng. The basic parameters were: surface density- 244.8 g/m2, yarn linear density- 74.1 tex, thickness- 0.4 mm, warp density 184 roots/10 cm, and weft density- 137 roots/10 cm. Resin types: water-based epoxy resin (epoxide equivalent: 1,200-1,850g/eq), phenolic resin(Solids content: 47%) and isocyanate resin (supplied by Huntsman Corporation). Firstly, ramie woven is soaked in water-based epoxy resin, phenolic resin and isocyanate resin respectively. Then, putting them in an oven (65°,3-hours) can reserve for compressing composites. Molding technological conditions: hot-pressing pressure, time and temperature are 2MPa,5min and 120°,and paving way：$[(0/90)]_5$。

Equipment

The 3-D Composite Material Analysis System (Fig.1) can evaluate materials not only for tension or compression in the X and Y axial directions, but also bursting at the Z axis simultaneously.There are

two sensors for measuring the forces in x, y direction and each direction has two clamps. Sensor accuracy is 1.0 N， maximum load value is 5.0 kN， and drawing speed is 0.013-1.066 mm/s. The system is equipped with Digital Speckle Correlation Method Analysis System software**(DSCM)**.

Biaxial Testing and Digital Speckle Correlation Methods

Fillet cruciform specimens were cut to shape with a laser to a total length of 300.0 mm with each arm measuring 50.0 mm wide. In order to form a uniform and randomly distributed speckle image, the surface of each cruciform specimen was sprayed with a layer of black glass bead paint layer for image enhancement. Biaxial tensile tests were conducted at stretching rates of 0.033 mm/s in each direction. The biaxial tensile test was conducted with the modulated speckle image captured by a high speed charge-coupled device (CCD) camera for description of the microscopic changes occurring on the surface. The pictures were saved in a file for analysis of the strain field. The observed speckle pattern included information on the object's surface height with the different degrees of gray reflecting the different stress-strain states of the specimens. The data were smoothed 3 pixels in both the X and Y directions. Ten samples were tested. The size of measured surface area of fabric was: 60 x 60 pixle, and the accuracy of measurement is about 0.01pixel theoretically.

Results and Discussion

Biaxial tension experiment.

Fig.2 illustrates: (1)mechanical properties at X-direction are different from Y-direction for all three types composites， namely X-direction fracture load value are smaller at than Y. This dissimilarity are linked with fiber volume fraction in X/Y-direction. Under the paving way of $[(0/90)]_5$, there are two warp-layers and three weft-layers in X-direction, while Y-direction has three warp-layers and two weft-layers. Warp yarns are fabricated to a higher density than those for weft（Y-direction）as yarns in the warp direction（X-direction）, resulting fiber volume fraction in X are less than Y-direction.

(2)Composites demonstrated variable characteristics of stress-strain behavior under biaxial tensile loads. Orthotropy and elastoplasticity were showed by water-based epoxy resin plate and isocyanate resin plate (Fig.2a,b), while phenolic resin board revealed a high-quality linear elastic in Load-Time curve and simultaneous brittle-fracture properties in X,Y-direction(Fig.2c) .

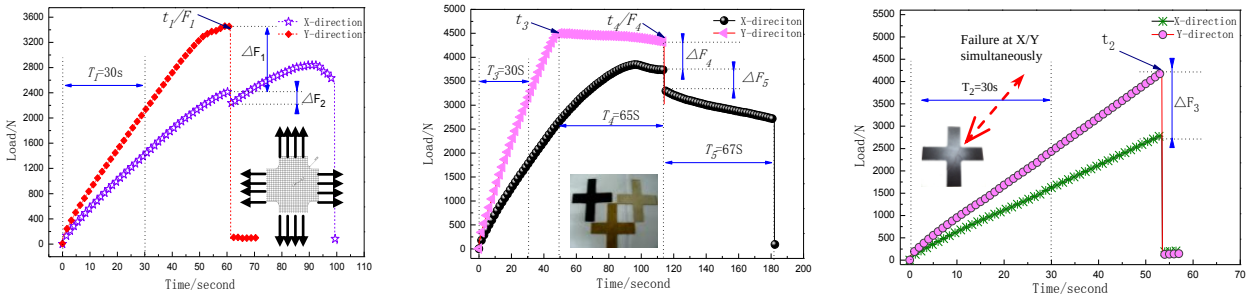

(a) (b) (c)

Fig.2 Time-load curves under biaxial loads for composites:（a）water-based epoxy resin plate; （b）isocyanate resin plate;（c）phenolic resin plate.

(3) Water-based epoxy resin composites'Y-directional failure occurred firstly at the moment of t_1, load difference value between X and Y-direction was $\triangle F_1$=875.92N. As Y-direction load became disappearance suddenly, stress state transformed from biaxial loadings (both X and Y tensile) into a

unaixal (only X-axial tension). The instant change of suffering loading way has a decreasing effect on the value of load in X-direction, and the X-load dropping value was $\triangle F_2$=210.12N(Fig.2a) .

Ahead of t_3, isocyanate resin plate showed a generally linear variation curve of load-time under biaxial tension. However, plastic deformation began at t_3 and formed necking down gradually after the moment of t_3,the lasting time was T_4=65S,the loading value reduced to F_4= 4322 N, $F_4 > F_1$. At the moment of t_4, Y-direction failure happened and load difference value between X and Y-direction was $\triangle F_4$=588.59 N,with $\triangle F_1 > \triangle F_4$; the X-load dropping value was $\triangle F_5$=309.48 N (Fig.2b) . These analysis above indicates that the load instant variation at breaking-direction has a negative effect on the other directions' load values, and the dropping degrees were linked with breaking load as well as load difference value between X and Y-direction.

Strain-filed by DSCM.

We can see in Fig .2 the curves of time-load represent a high quality linear during 0-30seconds in biaxial tensile process, so their linear variation stage are correctly selected for investigating information of strain-filed(Fig. 3) by using DSCM.

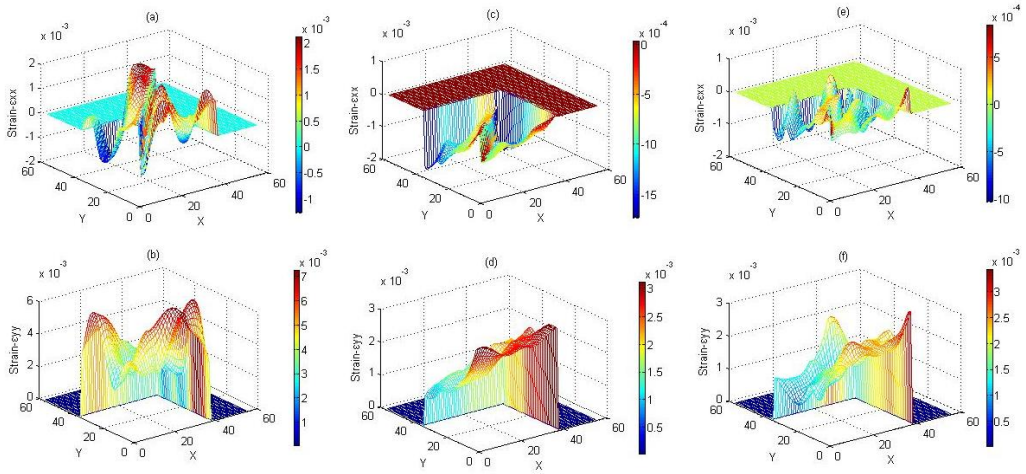

Fig. 3 Strain-fields for composites during 0-30seconds under biaxial tensile loads: a),b) for X ,Y-direction of water-based epoxy resin plate; c),d) for X ,Y- direction of isocyanate resin plate; e),f) for X and Y- direction of phenolic resin plate.

Values of field-strains revealed for Figure 3 shows: $\varepsilon_{yy} > \varepsilon_{xx}$,and X,Y-directions' strain mean value of water-based epoxy resin plate, phenolic resin and isocyanate resin plate are respectively e_{xx}=0.67，-0.86，-0.15, and e_{yy}=4.42，2.08，1.82(unit-10-3) during T1,T2,T3.The loads for 0-30seconds are within the limit in the elastic proportion and the value of loads in Y-direction are larger than X-direction, therefore the strain in Y-direction are larger than X-direction for elastic modulus unchanged and the same testing cross sectional area.

Fig. 3a and 3b show that the values of water-based epoxy resin plate' strain has a larger fluctuating range with a distribution range of -1.38 to -2.03 in X-direction and 0 to 7.13 in Y-direction, while strain-filed for phenolic resin plate and isocyanate resin plate are comparatively gently, with a distribution range of -1.81～0.01 and 0～3.21 in X-direction, and -1.01～0.92,0～3.52 in Y-direction respectively,Figures 3c,d,e,f. Analysis of the strain-field accounted for characteristics of orthogonal anisotropy of water-based epoxy resin plate.

Results and Discussion

1) Under thebiaxial tensile loads, the mechanical behavior for the composites from three resin matrices have different properties. The water-based epoxy resin plate and isocyanate resin plate represented orthogonal anisotropy and elastoplasticity, while phenolic resin board revealed a high-quality linear elastic and simultaneous brittle-fracture properties at X,Y-direction. Instant load change at the breaking-direction had a negative effect on the other direction. The dropping degrees were positively related to breaking load as well as load difference value between X and Y-direction.

2) Within the limit in the elastic proportion of biaxial tension, the mean value of strain-field are larger in Y-direction than X because of material anisotropy. Variation of strain-filed for phenolic resin plate and isocyanate resin plate are moderately gently and smoothly, while water-based epoxy resin plate' strain fluctuation are comparatively large.

Acknowledgement

We are grateful to the National High Technology Research and Development Program of China (863 Program,2010AA101701) financially supporting this project.

References

[1] Arnold, W. S., Robb, M. D., and Marshall, I. H. 1995. Failure Envelopes for Notched CSM Laminates Under Biaxial Loading, *J*. Composites. 26, 739-747.

[2] Chen Fuming, Wang Ge, Cheng Haitao, et al. 2009.Study on the Factors Influencing the Mechanical Properties of Natural Fiber Fabrics Under Biaxial Tensile Load, J. Forestry Machinery & Woodworking Equipment. 38(4),17-19.

[3] Kong, H., Mouritz, A. P., and Paton, R.2004.Tensile Extension Properties and Deformation

Mechanisms of Multiaxial Non-crimp Fabrics, J. Composite Structures. 66, 249-259.

[4] Luo, Y. X., Hu, H., and Fangueiro, R. 2008. Tensile and Tearing Properties of PVC Coated Biaxial Warp Knitted Fabrics Under Biaxial Loads, J. India Journal of Fiber & Textile Research. 33(2), 146-150.

[5]Smits, A., Hemelrijck, D. V., Philippidis, T. P., and Cardon. A. 2006.Design of A Cruciform Specimen for Biaxial Testing of Fibre Reinforced Composite Laminates, J. Composites Science and Technology. 66, 964-975.

[6] Virginio, Q., Carola, C., and Carlo, P. 2008. Experimental Characterization of Orthotropic Technical Textiles Under Uniaxial and Biaxial Loading, *J*. Composites Part A: Applied Science and Manufacturing. 39, 1331-1342.

[7] Wang Ge, Chen Fuming, Cheng Haitao, et al. 2010.Mechanical Properties of Natural Fiber Textiles Laminate With Hole, J. Acta Materiae Compositae Sinica. 27(4), 45-49.

[8] Xu, X., Jayaraman, K., Morin, C., and Pecqueux, N. 2008. Life Cycle Assessment of Wood-fibre Reinforced Polypropylene Composites, *J*. Journal of Materials Processing Technology. 198, 168-177.

Bamboo Bundle Composite Laminated Composites Part I. 3-Dimesional Stability in Response to Corrugating Effect

Fuming Chen, Zehui Jiang, Ge Wang, Hai-tao Chen and xing'e Liu

International Centre for Bamboo and Rattan, Beijing, China, 100102

Sheldon Q. Shi

Mechanical and Energy Engineering, University of North Texas,

Denton,TX76203-1277,USA

Abstract

A novel bamboo bundle laminated composite with a corrugated structure, called BCLC was developed. This series of publications is related to the design, processing, and physical and mechanical properties of the BCLC. The objective of this part of the work was to investigate how the 3-D shrinkage and swelling properties are affected by the shape of the composites. Three types of stacking sequences were designed and their shrinkage and swelling performances were compared. A shaped parameter, K, was used to quantify the corrugated effect on the shrinkage or swelling in three directions. The shrinkage ratio, difference in shrinkage (D),drying coefficient (DC), swelling ratio, difference in swelling(S), apparent density(AD),porosity ratio(PR), and water absorption(WA) were determined. It was found that the dimensional stability of the BCLC was significantly different among the 3directions of the composites, and it was affected by the stacking sequence of the bamboo bundles. Shrinkage ratio, swelling ratio, and drying coefficient were significantly greater in the thickness direction compared to those in the length or width directions. The shape parameter was largest in the length direction and the smallest in the thickness direction, $K_L > K_W > K_T$. The corrugated effect of BCLC was more pronounced with swelling than with shrinkage. The correlations of PR vs. AD was determined as r=-0.930, and that of WA vs. AD was determined as r = -0.940, with both being negative. The correlation of WA vs. PR was positive (r=0.997). The synergistic effect of staking sequence accounted for 11.3%,9.2%,and0.6% of the total correlation above. A good linear relationship was found between WA and AD, and between WA and AD.

Key words: Bamboo, Corrugated structure, 3-D Shrinkage and Swelling, Shaped Parameters, Synergistic Effect

Introduction

Plant based fibers are renewable, biodegradable, and environmental friendly(John and Thomas 2008; Wang *et al.* 2011). Bamboo has provided abundant and high-quality cellulose fibers for centuries, becoming a primary feedstock for the weaving, pulp and paper, and fiber-based composite industries in China (Scurlocka 2000; Chen *et al.* 2011). Bamboo presents excellent mechanical properties, *e.g*. the tension module of an individual bamboo fiber is 26GPa (Wang *et al.* 2011; Yu*et al.* 2011). During the past 20 years, research activities concerning bamboo fiber-reinforced composites(BFRC) have been dedicated to developing economical and lightweight composites for structural applications (Shin and Yipp 1989; Jain *et al.* 1993; Okubo *et al* 2009).

Product performance is not only related to the material properties themselves, but also to the structure design of the composites. Corrugated structure has long been valued as a good engineering design that can be tailed to a variety of applications, such as shipping containers transported by rail, truck, sea, or air (Briassoulis1986; Thorpe and Choi 1992; Duong *et al.* 2010). The advantages of a corrugation structure design include: 1) high energy absorption at impact (Torre and Kenny 2000); 2) anisotropic nature, which is flexible in the corrugation direction and stiff in the transverse direction (Yokozeki *et al.* 2006); and 3) light-weight (Guo *et al.* 2010, 2011).

Renewable biomass, *e.g.* wood, bamboo, and rattan, are typically heterogeneous, anisotropic, viscoelastic, and hydrophilic, and are considerably sensitive to ambient moisture and temperature. The properties of the corrugated composite structure are basically homogeneous along the thickness direction, but vary for the corrugated laminates in 3-D. The shape of the corrugated design of the composites may increase the anisotropic nature compared to that of planar composites (Kress and Winkler 2011). Furthermore, the hygroscopic characteristics of cellulosic fibers from bamboo used for the BCLC will lead to dimensional instability, such as swelling and shrinkage, which will reduce the mechanical properties of the composites. (Moe and Kin 2002; Moe and Kin 2003; Hyo and Do 2006).

Currently, limited published experimental data is available on the manufacturing of bamboo fiber-enhanced composites with a corrugatedstructure. Cruz (2007) fabricated corrugated roof panels using high-density polyethylene (HDPE) reinforced with wood fibers prepared from urban waste materials and found that with a60% wood fiber content, the mechanical properties decrease as the particle size is reduced, additionally, more processing conditions and rheological tests were required to obtain the best processing conditions to reach a high mechanical performance. Hunt (2007) used the finite element analysis (FEA) method to investigate the constitutive behaviors of 3D engineered fiberboard, and indicated that linear-elastic isotropic material properties in combination with simplified engineering equations could be used for an initial evaluation of corrugated panels. As a structure’s geometry becomes complicated, however, it becomes necessary to use more sophisticated

models to handle more detailed constitutive properties of the material.
The overall goal of this project was to investigate the feasibility of manufacturing BCLC from bamboo bundles and UF resin, and to evaluate the 3-D shrinkage and swelling properties as affected by the shape of the composite structure.

The specific objectives were: 1. To explore the technical feasibility of manufacturing BCLC; 2. To investigate the 3-D shrinkage and swelling behaviors of BCLC; 3. To develop an empirical shaped parameter K used for shrinkage and swelling processes from which the parameter can be used to quantify the corrugated effect in 3-D; and 4. To quantitatively evaluate the synergistic effect of stacking sequence on the correlation of apparent density(AD),porosity ratio(PR), and water absorption(WA).

Materials And Methods

Preparation of Bamboo Bundle

Three-year-old Cizhu bamboo (*Neosinocalamus affinis*) was obtained from Changning, Yibin, Sichuan Province, China. The bamboo material had an initial moisture content (MC) of about 65%. For the material preparation, the bamboo tubes were first split into four pieces of approximately the same size. The bamboo joints were removed using a hatchet. An untwining machine was designed for brooming and rolling the bamboo.

The untwining machine was made up of three main sections: a drive unit(to provide power), idler wheels(to broom the bamboo), and an adjustment device(to regulate the pressure between the idler wheels).The idler wheel was 16cm in diameter with halve-trapezoid shaped cutter teeth. The length, width, inter-tooth spacing, and inclination angle of the teeth were designed as 1, 1.5, 2.3,mm and 45°, respectively. By adjusting the distance of the upper and lower pressure rollers, the teeth could realize different brooming and discongesting effects during the bamboo feeding process. The schematic for the brooming, rolling, and compression processes are shown in Fig. 1.

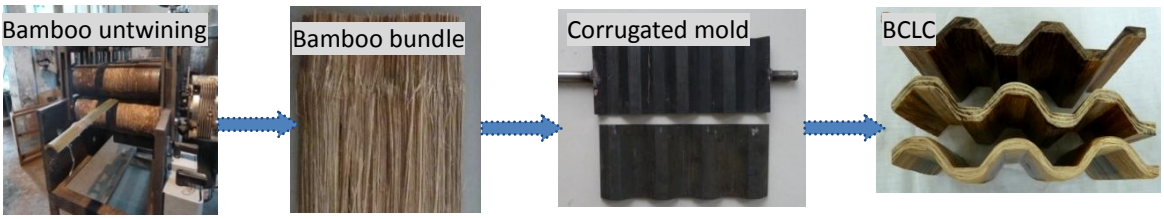

Fig. 1. Brooming, rolling, and compression process

Because of the high MC of the inner portion of bamboo, the bamboo bundles were easily tangled up on rollers due to the high plasticity of the material. At a low MC (<10%),the bamboo joint becomes too brittle which may lead to the separation of the bamboo bundle sheet. Based on the results of the initial testing, an ideal brooming effect was found when the MC of the bamboo was controlled between 24 and 30%.

During the brooming process, the bamboo chips were first flattened using a relatively greater gap between the upper and lower rollers: 3 to 4mm for the 1st roller set,2.5 to 3.5mm for the 2nd, 2 to2.7mm for the 3rd, and 2 to 2.7mm for the 4th. For the subsequent brooming process, the gap for the third and fourth roller sets was reduced to 0.75 to 1mm. After repeating the process five times, the bamboo strips were rolled, knead, and flattened into a loosely laminated reticulate sheet. The laminated sheet was cross linked together in the width direction with no fracture along the length direction, and was nearly uniform in thickness, maintaining the original bamboo fiber arrangement. The bamboo bundle sheets were finally cut into pieces of 300 mm in length, and then air-dried to a MC between 8 to 12%. This brooming process produces greater than a 90% bamboo yield.

Preparation of BCLC

A commercial phenol formaldehyde (PF) resin obtained from Taier Corporation (4 West Road, Dahongmeng, Fengtai District, Beijing, China) was used for the composites fabrication. The PF resin was diluted with water to a solid content of 15%. The bamboo bundles were immersed in the PF resin for 8 minutes and then dried to a MC between 10% and12% under an ambient environment. A 300 mm×300 mm CARVER Auto M-3895 hot press with a Press MAN control system (Carver Inc. USA) and a custom designed corrugated mold was used to press the BCLC at a platen temperature of 160^{o}C. The dimensions of the BCLCwere300 mm (length) by 150 mm (width) by 8 mm (thickness). The target density was set as 0.88 g/cm^{3}.The "cold-cold" process was used to ensure a complete curing of the resin. The hot press time was 30 minutes (10 minutes for press closing, 10 minutes for the pressure maintained at the target thickness, and 10 minutes for press opening). Three types of stacking sequences were designed: 1) bamboo fibers were aligned along the corrugated wave direction (I-type), 2) bamboo fibers were aligned perpendicular to the corrugated wave direction (II-type), and 3) bamboo fibers were cross laminated [0/90/0] (III-type). Composites with ramie woven fabrics bonded with the MDI resin were also fabricated and used as controls. Three replicates were made for each condition.

Methods

3-Dimensional shrinkage and swelling testing

The following properties of the BCLC were tested in accordance with the standard procedures described in GBT 7019(1997), China: Shrinkage ratios (β_L,β_W,β_T),shrinkage difference (D), drying coefficient(DC), swelling ratios(γ_L,γ_W, and γ_T),swelling difference (S), apparent density (AD), porosity ratio (PR), and water absorption (WA). The WA and swelling ratio were measured after a 24-h immersion in distilled water at 20^{o}C. Two types of shrinkage and swelling were designed to analyze the 3-D changes of BCLC: 1) Shrinkage: air dry to oven dry, air dry to saturation then to oven dry; 2) Swelling: air dry to saturation, oven dry to saturation.

(1) The shrinkage ratio and swelling ratio, the percent of hygroscopic dimensional change or volume change, were calculated using the following equations:

$$\beta = \frac{l_A - l_0}{l_A} \times 100\% \quad , \quad \gamma = \frac{l_W - l_1}{l_1} \times 100\% \qquad \text{——(1)}$$

where β is the shrinkage ratio (%) and γ is the swelling ratio (%); l_A and l_0 are the specimen sizes (mm) in an air-dry state and an oven dry at 60°C, respectively; l_w and l_1 are the specimen dimensions (mm) after the water immersion at 5°C for 24 h and after oven drying at 103 °C for 24 h, respectively.

(2) The shrinkage difference (and swelling difference) represents the ratio of a tangential shrinkage(or swelling)of wood to its radial shrinkage (or swelling). Different shrinkage /swelling ratios are used to describe the dimensional stability of wood.
Shrinkage/swelling ratio differences were calculated based on the following equations (Guan *et al.* 2009):

$$\mathrm{D} = \frac{\beta_T}{\beta_W} \quad , \quad S = \frac{\gamma_T}{\gamma_W} \; . \qquad \text{——(2)}$$

where β_T and γ_T are the shrinkage ratio and swelling ratio along the thickness direction, respectively, and β_w and γ_w are the shrinkage ratio and swelling ratio in the width direction, respectively.

(3) The drying coefficient is the shrinkage ratio after 1% change in MC and calculated using the following equation

$$\mathrm{K_{L,W,T}} = \beta / (\mathrm{W_1 - W_2}) \qquad \text{——(3)}$$

where $K_{L,W,T}$ represents the drying coefficient in length, width, and thickness respectively; and W_1 and W_2 are the initial and final MC,%.

(4) The shaped parameter was calculated in order to quantify the corrugation effect on the shrinkage or swelling in 3 directions. The shaped factor was determined by subtracting the shrinkage ratio or swelling ratio from the shrinkage ratio or swelling ratio along the corrugated direction(having the material and shaped combining effect) from that perpendicular to corrugation(with the material effect only). The following formulae were used to estimate the actual efficiency of corrugated structure for shrinkage or swelling in 3-D:

$$K_L = \beta_L(\text{I-type}) - \beta_w(\text{II-type}) \quad \text{or} \quad \gamma_L(\text{I-type}) - \gamma_w(\text{II-type}) \qquad \text{——(4)}$$

$$K_W = \beta_L(\text{II-type}) - \beta_w(\text{I-type}) \quad \text{or} \quad \gamma_W(\text{II-type}) - \gamma_w(\text{I-type}) \qquad \text{——(5)}$$

$$K_T = \beta_T(\text{II-type}) - \beta_T(\text{I-type}) \quad \text{or} \quad \gamma_T(\text{II-type}) - \gamma_T(\text{I-type}) \qquad \text{——(6)}$$

where K_L, K_W, K_T are the factors for length, width, and thickness, respectively after air dry to oven dry or air dry to saturation.

Water Absorption Measurements

The water absorption rate (WA), apparent density (AD), and porosity ratio(PR)of BCLC can be determined using the following equations:

$$WA(\%) = \frac{m_3 - m_1}{m_1} \times 100 \quad \text{——(7)}$$

$$AD = \frac{m_1 \times p_o}{m_3 - m_1} \quad \text{——(8)}$$

$$PR(\%) = \frac{m_3 - m_1}{m_3 - m_2} \times 100 \quad \text{——(9)}$$

where m_1 is the weight of the oven dry specimen (g), $m_2$isthe wet specimen weight in water after immersed in water for 24h (g), $m_3$isthe wet specimen weight in air after immersed in water for 24h(g), and p_o is the water density (g/cm^3).

Three replicates were used. SPSS 12.0 and Origin 8.0 were used for the statistical analysis with a significance level of alpha=0.05.

Results And Discussion

3-D Shrinkage and Swelling

The effects of thecorrugated structure on the3-D shrinkage and swelling properties of BCLC are shown in Tables 1 and 2. Figure 2 reveals the 3-D drying coefficient (DC) from air dried to oven dried process.

Table 1. Shrinkage Ratio and Shrinkage Difference of BCLC，the Parameters of a and b Indicate the Significant Difference inmean by SPSS at a Significance Level of 0.05

Item	Air dry-absolute dry				Air dry-Saturation-absolute dry			
	β (%)	β_W (%)	β_T (%)	*D*	β_L (%)	β_W (%)	β_T (%)	*D*
I-type	0.38a	0.91a	1.67b	1.84	0.41a	1.64a	1.07b	0.66
II-type	0.98a	0.20a	1.74b	8.92	2.26a	0.20a	1.69b	8.24
III-type	1.50a	0.32a	1.51b	4.69	1.67a	0.21a	2.39b	22.13
Control	0.27a	0.22a	1.12b	5.12	0.27a	0.82a	1.15b	1.40

Table2. Swelling Ratio and Swelling Difference of BCLC, the Parameters of c andd Indicate the Significant Difference inmean by SPSS at a Significance Level of 0.05

Item	Air dry-Saturation				Absolute dry-Saturation			
	γ_L (%)	γ_W (%)	γ_T (%)	S	γ_L (%)	γ_W (%)	γ_T (%)	S
I-type	0.84c	1.29c	3.78d	2.93	1.26c	2.53c	4.30d	1.70
II-type	1.43c	0.25c	3.82d	15.25	2.95c	0.39c	6.25d	15.95
III- type	1.37c	0.26c	4.10d	15.90	3.55c	0.32c	6.24d	19.69
Control	0.50c	0.22c	1.94d	8.81	0.78c	1.05c	4.14d	3.94

In general, the shrinkage and swelling properties of 3-D. shrinkage ratio (β_T), swelling ratio (γ_T), and DC were significantly greater along the thickness direction than in the length and

width directions. The ANOVA test also confirms the observation at the95% confidential level (Tables 1 and 2 and Fig. 2). Bamboo is a viscoelastic material having both elastic and plastic behaviors. During hot-pressing, bamboo bundles were bent passively by the combined effects of pressure, temperature, and corrugated molding. During the initial stage of hot-pressing, the temperature was much higher at the surface than that at the core; therefore, the surface bundles softened, leading to a greater compression rate. As the resin continued to cure, the bamboo initially began to experience plastic deformation and become consolidated. The core layer was therefore not easily compressed resulting in a lower compression rate, which caused an uneven density distribution along the thickness direction and a high inter-laminar stress in the composites. In addition, the corrugated structure accelerated the fiber deformation or fracture under the effect of the bending wave. These deformed fibers that arranged along the corrugated wave direction will have a trend towards recovering their original shape when absorbing water; however, bamboo bundles can't stretch freely due to the limitation of their corrugated shape. Under the hydrothermal effects, partial stresses will be released from other unconstrained directions leading to a much higher degree of variation in 3-D.

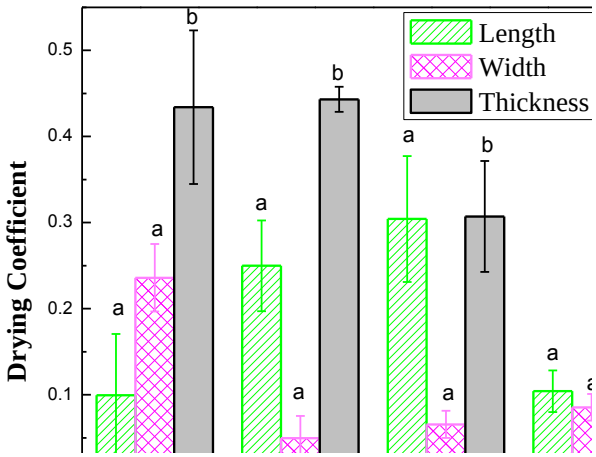

Fig. 2. Drying coefficient in 3-D of BCLC for different stacking sequences

As shown in Tables 1 and 2, the3-D shrinkage and swelling performance of BCLC were quite different for different stacking sequences. For theI-type stacking sequence, the shrinkage ratio (β_L), DC, and swelling ratio (γ_L) were lower in the length direction, but higher in the width direction than that for the II-type and III-type. Additionally, the D and S for the I-type were also the lowest compared with that for the II-type and III-type. These results indicated that the I-type composites had a relatively better stability in the direction parallel to the corrugated wave compared with that of the II-type and III-type composites, whereas it has an inferior resistance against shrinkage or swelling in the transverse direction to the corrugation. Contrarily, the II-type composites (bamboo fiber orientation vertical to the corrugation direction) represented an overall stability along the transverse direction of the corrugated wave as compared to that in the parallel direction. As shown in Tables 1 and 2 and Fig. 2, lower values of shrinkage ratio (β_w), DC, and swelling ratio (γ_w) were observed in the width direction than that in the length direction. III-type BCLC showed intermediate values of

shrinkage ratio ($\beta_L$andβ_w) and swelling ratio (γ_L and γ_w) in the length and width directions. The stacking sequence showed no effect on shrinkage and swelling behaviors along the thickness direction. Modified by the stacking sequence, the variability of BCLC for 3-D stability could be mainly due to the difference in bamboo fibers' shrinkage or swelling properties in 3-D. The shrinkage or swelling in the length direction of the fiber is much smaller compared to that in the transverse direction. As a result, the dimensional stability in the length direction (corrugated wave direction)showed a better performance than that in the width direction when the fiber's direction is parallel to the corrugated wave(I-type).Bamboo bundles, however, arranged along the transverse direction to corrugation (II-type), BCLC exhibited an optimum dimensional stability in the width direction(vertical direction to corrugated wave).

In comparison with the ramie woven control specimen, a lower dimensional stability was observed for BCLC, where the values of shrinkage ratio, shrinkage difference, swelling ratio, and swelling difference were generally larger than those of the control specimen. A better dimensional stability of ramie woven corrugated panel could be mainly contributed to the interweave structure. Further study would need to be conducted to optimize the untwining degree of the bamboo bundle sheet, and to modify the hot-pressing parameters and the corrugated structure in order to improve the performance of BCLC.

Shaped effect in 3-D

As mentioned in the previous section, the corrugated shape has a certain effect on the shrinkage and swelling properties in 3-D. The degree of shaped effect in regard to the corrugated structure could be quantitatively characterized by subtracting the value of shrinkage ratio or swelling ratio in the direction parallel to the corrugation of I-type(with both material and structure effect)from that perpendicular tothe corrugation of II-type(only material effect),as shown in Equation(4)-(6).

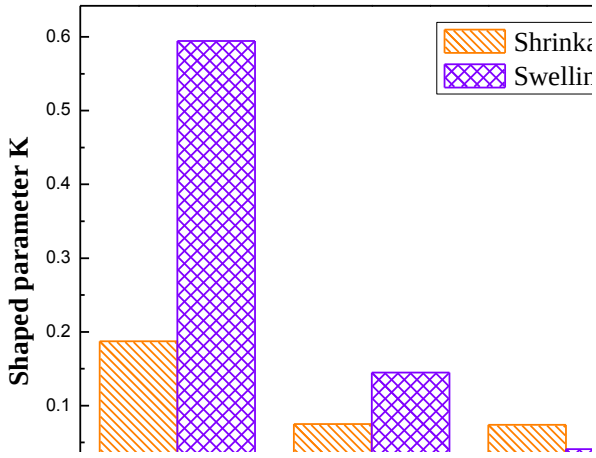

Fig. 3. Shaped parameter K of corrugated effect in 3-D

Figure 3 shows the shaped parameter *K*. *K* in 3-D was 0.187, 0.075, and0.074for shrinkage

and 0.595, 0.145, and0.041 for swelling. It is seen that $K_L > K_W > K_T$, where K_L, K_W, and K_T are the shaped parameter for the length, width, and thickness directions. This result indicates that the largest shaped effect for both shrinkage and swelling was in the length direction, followed by width and then thickness. The dimensional variability was probably due to the biggest deformation along the bamboo fiber's direction caused by the effects of bending, compressing, and folding during hot-pressing to form the corrugated shape. The following order regarding shape changes were transverse direction of the bamboo bundle. In addition, the sum of K_L, K_W, and K_T calculated for swelling (0.780) was greatly higher than that for shrinkage (0.336), demonstrating that a shaped effect in response to swelling was much larger than that for shrinkage. When the BCLC is in contact with water, the hydrophilic groups of the bamboo fibers will attract the water molecules. Then, water molecules continually step into a micro capillary system, filling the gaps between the fibers and the matrix resulting in cell wall swelling and localized yielding along with micro crack growth (Sandeep and Lopez-Anido 2011). As a result, the interfacial bonding strength of BCLC decreases, leading to reduced dimensional stability as compared to shrinkage.

Correlation of Physical Properties to Water Absorption

BCLC is a porous material with diverse mechanical properties for different AD or PR. In order to quantitatively investigate the linear relationship between AD and WA and between PR and WA with the synergistic effect of stacking sequence, Pearson correlation analysis was performed. A partial correlation analysis was also conducted for different stacking sequences.

Table 3. Bivariate and Partial Correlation Analysis by SPASS

Variable		Apparent Density	Porosity Factor	Water Absorption
Apparent density	Correlation Coefficient	1	-0.926**(-0.863)	-0.936**(-0.885**)
	Significance(2-tailed)		<0.001(0.01)	<0.001(<0.001)
	Degree of Freedom	0	10(9)	10(9)
Porosity ratio	Pearson Correlation	-0.926**(-0.863)	1	0.997**(0.994**)
	Significance(2-tailed)	<0.001(0.01)		<0.001(<0.001)
	Degree of Freedom	10(9)	0	10(9)
Water absorption	Pearson Correlation	-0.936**(-0.885**)	0.997**(0.994**)	1
	Significance(2-tailed)	<0.001 (<0.001)	<0.001(<0.001)	
	Degree of Freedom	10(9)	10(9)	0

Notes: **correlation is significant at the 0.01 level (2-tailded), and the numbers in parentheses represent the partial correlation analysis' results.

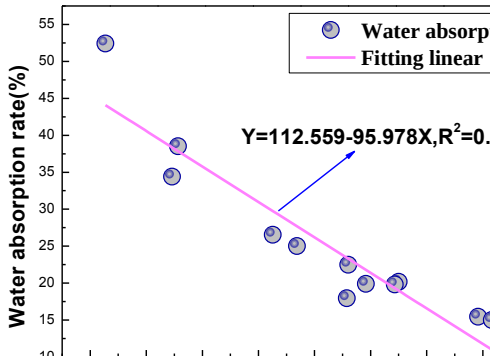

Fig. 4. Water absorption*vs*.apparentdensity

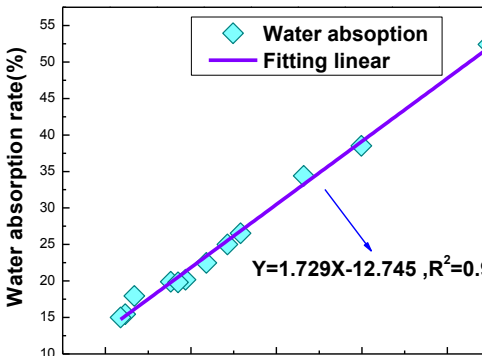

Fig. 5. Water absorption *vs*.porosity ratio

The Pearson's correlation coefficients between AD and WA, and between PR and WA were -0.936 and 0.997 ($p<0.01$), respectively while the corresponding slopes were-95.978 (decreasing) and 1.729 (increasing) when not controlled for stacking sequence, as shown in Table 3 and Figs. 4 and 5. When controlled for stacking sequence, the Pearson's correlation coefficients between AD and WA, and between PR and WA decreased to -0.863 and 0.997 ($p<0.01$), respectively, as shown in Table 3. There were 9.287%and 0.597% degree of linear correlations between AD and WA, and between PR and WA, respectively, during the water absorption process, which was determined by synergism of the stacking sequence. Unexpectedly, the synergistic effect of the stacking sequence for the linear relationship between AD and PR was the largest at11.271%.Calculations of the degree of linear correlation for the water adsorption process are shown below.

between AD and WA:9.287% = $(-0.9360)^2 – (-0.885)^2$, between PR and WA: 0.597% = $(0.997)^2 – (0.994)^2$, and between AD and PR: 11.271% = $(-0.926)^2 – (-0.863)^2$

AD and PR are key parameters in characterizing the physical properties of corrugated composites so therefore, AD and PR were used to describe how the physical properties affect the water absorption(see Figs. 4 and 5).It is shown in Figs.4 and 5 that linear relationships exist between AD and WA, and between PA and WA. The relationships were established as:

WA=112.56-95.98AD, R^2=0.87; WA=-12.75+1.73PR,R^2=0.99.

Conclusions

1. Shrinkage and swelling properties were significantly different in 3-D. The shrinkage ratio, swell ratio, and DC were greatest in the thickness direction. The I-type stacking sequence exhibited a better dimensional stability in the direction parallel to the corrugated wave, while the II-type represented an optimized stability along the transverse direction of the corrugation.

2. The shaped parameter *K* provided a quantitative characterization for the corrugated effect on shrinkage and swelling in 3-D. For both shrinkage and swelling, it showed that $K_L > K_W > K_T$. The corrugated effect in response to swelling was larger than that of shrinkage.
3. Strong linear relationships were found between AD and WA, and between PA and WA. The degrees of linear correlation determined by synergism of stacking sequence were 9.29% and0.60%, respectively.

Acknowledgements

The authors are grateful for the financial support of the National Forestry Public Welfare Scientific Research Program (201204701)and the Forestry Science and Technology Promotion Program (2010-20).

References

Briassoulis D. 1986.Equivalent orthotropic properties of corrugated sheets. Comput Struct 23(2):129-38.
Chen H, Cheng H, Wang G.2011. Properties of single bamboo fibers isolated by different chemical methods.Wood Fiber Sci 43(2):1-10.
Cruz R.H., Canche G., Herrera P.J., Gonzalez P.I., Martinez G.E., Duarte S., May A. and Martín C. 2007. Wood-Plastic Composites Based on Recycled Urban Materials as an Alternative for Roofing. Advanced Biomass Science and Technology for Bio-Based Products, Bejing. 391-397 PP.
Duong V. H. , Yusuke N. , Fumihiko T. , Daisuke H., Toshitaka U.2010. Preserving the strength of corrugated cardboard under high humidity condition using nano-sized mists. Composites Science and Technology 70:2123–2127.
Guo Y , Wang X , Zhang Q.2010. Design Methods and experimental study on the stability behavior of trapered beam-columns with sinusoidal corrugated web. Engineering Mechanics 27(9):139-146.
Guo Y. Wang X, Zhang Q, Jiang Z .2011. Design theory and application of steel structures of light- weight buildings. Building Structure 41(4):11-19.
Hyo J.K. and Do W. S. 2006. Effect of water absorption fatigue on mechanical properties of sisal textile-reinforced composites. International Journal of Fatigue 28:1307-1314.
Jain S, Jindal U.C., Kumar R.1993.Development and fracture mechanism of the bamboo/polyester resin composite. J Mater Sci Lett 12:558–60.
John F. H.2007.Measurement of Orthotropic Fiberboard Properties for Use in Finite Element Analysis of 3D Engineered Fiberboard. Advanced Biomass Science and Technology for Bio-Based Products, Beijing.326-339 PP.
Kazuya O., Toru F., Erik T.T.2009.Multi-scale hybrid biocomposite: Processing and mechanical characterization of bamboo fiber reinforced PLA with microfibrillated cellulose. Composites: Part A 40 :469-475.

Kress G. and Winkler M. 2011.Corrugated laminate analysis: A generalized plane-strain problem. Composite Structures 93 : 1493–1504.
Moe M. T. and Kin L.2002. Effects of environmental aging on the mechanical properties of bamboo-glass fiber reinforced polymer matrix hybrid composites. Composites: Part A 33:43-52.
Moe M. T. and Kin L.2003. Durability of bamboo-glass fiber reinforced polymer matrix hybrid composites. Composites Science and Technology 63:375-387.
Sandeep T. and Roberto A. L. 2011.Water absorption of wood polypropylene composite sheet piles and its influence on mechanical properties. Construction and Building Materials 25 :3977–3988.
Scurlocka J.M.O., Dayton D.C., Hames B. 2000. Bamboo: an overlooked biomass resource? Biomass Bioenergy 19:229-44.
Shin F.G., Yipp M.W. 1989. Analysis of the mechanical properties and microstructure of bamboo-epoxy composites. J Mater Sci 24:3483–90.
Thorpe J. L. and Choi D. 1992.Corrugated container failure Part 2-Strain measurements laboratory compression tests. Tappi Journal 7:155-161.
Tomohiro Y., Shin-ichi T., Toshio O., Takashi I.2006. Mechanical properties of corrugated composites for candidate materials of flexible wing structures. Composites: Part A 37: 1578–1586.
Torre L., Kenny J.M. 2000. Impact testing and simulation of composite sandwich structures for civil transportation civil transportation. Composite Structures 50:257-267
Wang G, Yu Y, Shi S.Q., Wang J. W.，Cao S.P.，Cheng H.T.2011.Microtension test method for measuring tensile properties of individual cellulosic fibers. Wood Fiber Sci 43(3):251-256.
Yu Y, Jiang Z.H., Fei B.H., Wang G., Wang H.K.2011.An improved microtensile technique for mechanical characterization of short plant fibers: a case study on bamboo fibers. J Mater Sci 46:739-746.

Contact Angles of Single Fibers Measured in Different Temperature and Related Humidity

Hong CHEN, Benhua FEI, Ge WANG, Haitao CHENG

International Center for Bamboo and Rattan, Beijing, 100102, China

Abstract

Studying single fiber wettability plays an important part in many areas, such as textile, paper treatment, and material-selection procedures of fiber-reinforced composite. Contact angles, which provide useful information about wettability, are needed in the modification of fiber surfaces or adjustment of rheological properties of the wetting prepolymer of polymer melts. Meanwhile, the contact angle measured in different environment is probably different. Knowing the changing of contact angles caused by various environment factors, such as temperature and humidity, is also important. So the contact angle of single bamboo fibers and terylene fibers in different temperatures and humidities were further studied. The results showed that when the temperature went up and related humidity kept in constant, contact angles of bamboo fibers decreased, whereas that of terylene fibers increased. However, contact angles of the two fiber types changed in the same trend that both increased with the increasing humidity and constant temperature. And the contact angle of bamboo fiber increased significantly, while that of terylene fibers ascended a little. These findings will aid researchers in better understanding the requirements needed for consideration of measuring the contact angle of different fiber types.

Key words: single fibers, contact angles, temperature, humidity

Introduction

Mounting concerns for the environment have sparked renewed interest in the development of biodegradable, mechanical bio-composite in which the natural fibers serve as a reinforcement by enhancing the strength and stiffness to the resulting composite (A. K. Mohanty, 2000; Alexis Pietak, 2007). Due to low density, high mechanical performance and problem-free disposal, natural fibers derived from plant offer a good promising alternative to other technological reinforcing fibers presently available (A. K. Mohanty, 2000; Ibon, 2003). For better utilization of natural fibers as reinforcements in composites, it is essential to know information on the wettability of the natural fibers and the interrelationships between wettability and measurement environment conditions. Contact angles provide useful information about wettability, and the degree to which liquids wet a fiber determines how easily the liquid can penetrate fiber assemblages (Ibon, 2003). Contact angle measurement is probably the most common method of wettability measurement. One of the most frequently used methods of contact angle assessment is the sessile drop technique (M. Amaral, 2002). However, detailed knowledge about whether the contact angle are affected by the measurement conditions is still lacking. As attempt has therefore been made, to investigate the change occurring in contact angle of single bamboo fiber due to different temperature and humidity of environment, and single terylene fibers were measured as control samples to find how the environment conditions affect the contact angles of different fiber types (natural plant fibers and chemical synthetic fibers).

Materials and Methods

Material was taken from 2-yr-old Cizhu bamboo (*Neosinocalamus affinis*) grown in Qionglai, Chendu, Sichuan Province, China. The bamboo was cut into strips (20 mm longitudinally and 2×2 mm in cross-section), then the strips were immersed in the chemical solution (one part H_2O_2, four parts distilled water, and five parts HAc) kept at 60℃ for 42 h to separate. And the bamboo fibers were washed to neutrality and air-dried to a constant weight before being kept in humidity chamber. The terylene fibers were provided by Ningbo Shuaibang Chemical Fiber Company Limited.The terylene fibers were washed in the distilled water and acetone in turn to get rid of dust and grease, if there are any.

Contact angle testing of distilled water on single fibers was conducted with Kruss DSA 100 equipped with an environmental chambers assisting of a temperature chamber and a humidity chamber. The given temperature and humidity limits was 160 ℃ or -30 ℃ and 0 or 100%. Single fibers were obtained using fine-tipped tweezers and mounted on a slatted platform with double-sided tape. Then the platform was put in the environmental chambers and moved into position using CCD cameras in the x, y, and z directions. First of all, the humidity in the environment chamber was kept at 30%, but the temperature was changed from 20 ℃ to 70 ℃. And then the temperature in the environment chamber was kept at 20 ℃ while the humidity

was changed from 10% to 80%. The temperature and the humidity in the environment chamber were kept 5 min after being adjusted to target value. The CCD cameras recorded the process of the water droplet dropping on the single fiber until disappearing gradually. The baseline for a sessile drop static contact angle measurement was made at the liquid-solid interphase with droplet size held to a contant10 uL. Contact angle were calculated using the ellipse method in the DSA 3 software (Fig. 1). Six samples were tested for each fiber type.

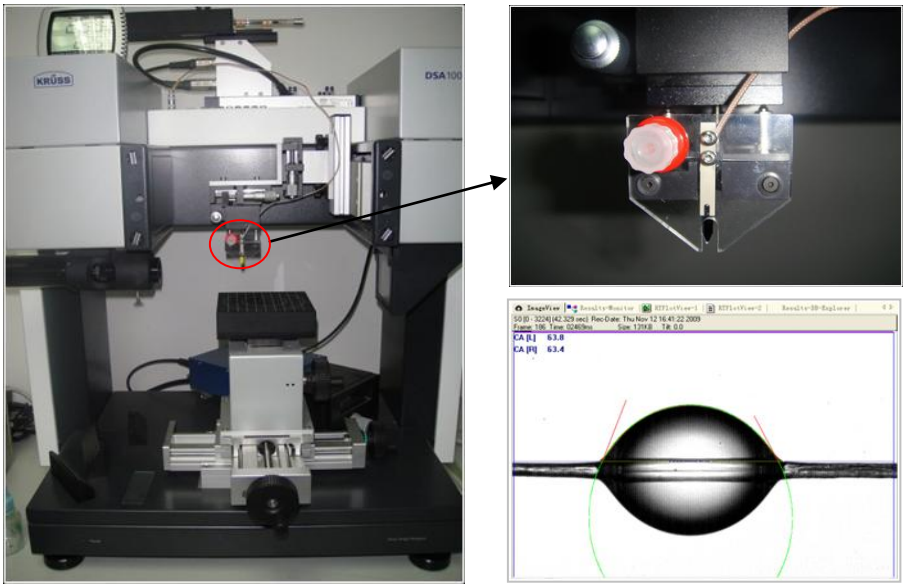

Figure 1 Contact angle measured by Kruss 100 and calculated by DSA 3 software.

Results and Discussion

Contact angle of single fibers measured in different temperature

Figure 2 Contact angle measured in different temperature

When the humidity in the environment chamber was kept at 30%, the contact angle of single

bamboo fiber decreased with the increasing temperature, but the contact angle of single terylene fiber increased, (Fig. 2). Meanwhile, the contact angle of single bamboo fiber changed a little when the temperature changed between 20℃ and 40℃, whereas that decreased significantly when the temperature increased above 40℃.

The single bamboo fiber is a kind of complicated and unstable natural plant fiber and is mainly made up of cellulose, hemicellulose and lignin which are easily affected by the environment conditions, especially the hemicellulose (Mohanty, 2000). The changing of temperature lead to changing of water in the fiber which makes the ability of fiber for adsorbing water change. What is observed macroscopically is the contact angle of single fibers change differently (Prasad, 2004; Pietak, 2007). With the increasing temperature, the single fiber loses water, and the ability for absorbing water is increasing, which lead to higher contact angle. Moreover, the trend of changing about contact angle is more distinct when the temperature is higher and higher, which also can be observed in Figure 1. However, single terylene fiber, consisting of polyethylene terephthalate, is a kind of chemical synthetic fibers and the component of which is simplex and stable. Therefore, the single terylene fiber is scarcely influenced by the environment conditions. The contact angle of single terylene fiber may be affected mainly by the surface tension of water. As known, there are three-phase equilibrium in the sessile drop experiment. The interfacial tensions tensions of the solid-vapour, liquid-vapour, solid-liquid interface, and the contact angle are related through Young's Equation (Adamson, 1990): $\cos\theta = \frac{\gamma_{sv} - \gamma_{sl}}{\gamma_{lv}}$. θ is the contact angle. γ_{sv} and γ_{lv} represent, respectively, the interfacial tension of the solid and the liquid in equilibrium with liquid vapour. γ_{sl} is the interfacial tension between the solid and the liquid. When the temperature increased, the surface tension of water increased, but not significantly (Mei, 2008), namely γ_{sl} and γ_{lv} increased a little, from the equation, it can be deduced the contact angle of the single terylene fiber increased a little, because it is mainly determined by the change of surface tension of water. However, for single bamboo fiber, the change caused by the fiber itself is much more significantly than that caused by surface tension of water so that the change caused by surface tension of water can be ignored.

Contact angle of single fibers measured in different humidity

Figure 3 Contact angle measured in different humidity

As shown in Figure 3, the contact angle of both single bamboo fiber and single terylene fiber increased when the humidity increased, while the former increased much more significantly than the latter. Besides, when humidity changed between 20%-30%, contact angle of single bamboo fiber increased little, and yet it increased significantly when humidity changed above 30%. There were a large number hydrophilic radical in single bamboo fibers (Bismarck, 2002), which may be responsible for increase of contact angle when humidity increased. The bamboo fiber attract moisture through hydrogen bonding because because the cell wall polymers contain hydroxyl and other oxygen-containing groups (R. M. Rowell, 1985). The hemicelluloses are mainly responsible for moisture sorption, but the accessible cellulose, noncrystalline cellulose, lignin, and surface of crystalline cellulose also play major roles (A. K. Mohanty, 2000). However, the single terylene fiber, lacking hydrophilic radical, was a kind of chemical synthetic fibers. So the contact angle of single terylene fiber almost did not change with increasing humidity.

Conclusions

The contact angle of natural plant fibers, such as single bamboo fibers, changed significantly when environmental temperature and humidity changed, especially humidity. The contact angle of chemical synthetic fibers, single terylene fiber for example, changed a little with changed temperature and almost kept the same when humidity changed. Therefore, it is necessary to confirm the environment temperature and humidity before measuring the contact angle of natural plant fibers. However, measuring the contact angle of chemical synthetic fibers only need to consider temperature of environment.

References

Adamson A W.1990. Physical chemistry of surface. 5th ed. New York: wiley.

Aranberri-Askargorta I, Lampke T, Bismarck A. et al. 2003. Wetting behavior of flax fibers as reinforcement for polyprophylene. Journal of Colloid and Interface Science. 263 (2) : 580–589.

Bismarck A, Aranberri-Askargorta I, Springer J. 2002. Surface characterization of flax, hemp and cellulose fiber; surface properties and the water uptake behavior. Polymer Composites. 23 (5): 872-894.

Mei C X, Wang G P, Liu Y. 2008. The relationship between surface tension coefficient of liquid and temperature and consistency. Journal of Xianyang Normal University. 23 (6): 21-22.

Mohanty K, Misra M, Hinrichsen G. 2000. Biofibres, biodegradable polymers and biocomposites: A overiview. Macromolecular Material and Engineering. 276/277: 1-24.

Pietak A, Korte S, Tan E, Alison Downard, et al. 2007. Atomic force microscopy characterization of the surface wettability of natural fibres. Applied Surface Science. 253: 3627-3635.

Prasad B, Sain M, Roy D. 2004. Structure property correlation of thermally treated hemp fiber. Macromolecular Materials and Engineering. 289 (6): 581-592.

Rowell R M, Banks W B, Gen. Tech. Rep. FPL-GTR-50; USDA Forest Service, Forest Products Laboratory, Madison, WI, 1985, 24 pp.

Acknowledgment

This work is funded by the Project of Manufacturing Technology of Bamboo High Value-added Building Products (201004005).

Effects of In Situ Deposited Calcium Carbonate Nanoparticles on Tensile Performance of Single Bamboo Fibers and Their Composites

Gao Jie[1], *Wang Ge*[*1], *Cheng Hai-tao*[1], *Sheldon Q. Shi*[2]

[1] International Centre for Bamboo and Rattan, Beijing, P.R. CHINA

[2] University of North Texas, Department of Mechanical and Energy Engineering,

Denton, Texas, USA

Abstract

This article applied an ironic solution reaction to in situ deposit calcium carbonate particles onto bamboo fibers at 5°C, 15°C, 25°C, 45°C and 65°C respectively. The fibers were then vacuum filtered to handsheets and hot compressed into thermoplastic composites with alternatively laminated polypropolene films(1 : 3 by weight). Surface features of individual bamboo fibers and tensile properties of fibers and their composites were investigated.

The results show that nanoparticles and submicron particles grew into the wrinkles and micropores of fibers, the size, morphology and adsorbance of which were distinctively varied at different temperatures. The highest calcium carbonate adsorbance (2.34% of fibers' weigt) was obtained at 25°C. The **precipitating** treatment is a useful method to densify and hydrophobize bamboo fibers and heal the cell wall defects. The mean values of contact angles increased and the variations within group were reduced as the loading percentage of particles rose, which might be due to reduced hydrophilic groups and lumen space for water after coatings of calcium carbonate particles. Besides, tensile properties of all the treated individual bamboo fibers were enhanced. Comparing to the average tensile strengh and modulus of elasticity of the untreated, those of the treated bamboo fibers with the biggest calcium carbonate loading were higher by 30.50% and 32.71% respectively. What's more, the treatments were approved to enhance the compatibility of bamboo fibers and polypropylene, comparing to tensile strengh and modulus of elasticity of the untreated composites, those of the treated bamboo fiber composites with the biggest calcium carbonate loading were higher by 14.6% and 19.6% respectively.

Keywords: In situ precipitated calcium carbonate, Bamboo fiber, Surface modification, Microtensile testing, Wettability, Interfacial compatibility

[*] Corresponding author. Tel: +86 010-84789751; Email address: wangge@icbr.ac.cn.
Contract grant sponsor: National Nature Science Foundation of China;
Contract grant Number: 31170525.

Introduction

Bamboo, as a durable, sustainable, environment friendly and affordable building material, is one of the tranditional construction materials for permanent housing, public structures and temporary shelters all around southern China[1]. It had been estimated that more than 5 million ha. of bamboo were planted all around China and the output of bamboo products was over 82.1 billion yuan in 2010[2].

In recent years, the composite field shows great passion to exploring natural fibers to manufacture low-weight, environmentally friendly products, for their combination of desirable properties, including renewable resources, low cost, relatively high strength-weight ratio[3,4]. Bamboo fiber, with abundant availability, high strengh and length/diameter ratio, is one of the best candidates[5,6]. However, bad interfacial adhesion of hydrophilic cellulosic fibers and hydrophobic polymer matrix, which is responsible for mechanical properties, dimensional stability and life circle of goods under indoor and outdoor situations, has set constraints on the enhanced utilization of bamboo fibers in thermoplastic composites[7]. Therefore, a lot of treatments were employed to improve the compatibility between natural fibers and the matrix in previous studies[8]. Inorganic nanoparticles as cell wall fillers were used for improvements of physical and mechanical properties of paper and fiber reinforced plastic composites, for the reason of its huge specific surface area, to better fiber wetting in the molten polymer matrix and initiate the polymer's crystalline orientation [9-11].

The understanding of properties, especially mechanical behavior of single bamboo fibers, as the load-bearing constituent of bamboo, could provide the valuable engineering mechanical data for the optimal design for utilization of bamboo and bamboo fibers-based products, such as pulp and paper, fiberboards, textile and fiber reinforced plastic composites. The study of mechanical behavior of individual plant fibers has gained momentum in recent years, to establish a direct correlation between fiber mechanical properties with plant cell wall microstructure and chemical compositions[12-14]. It is particularly important in biomaterials science to learn from the hierarchically organized structure and from specific molecular mechanistic phenomena at the cell wall level. Fiber defects, like pits and micropores after retting in the cell wall, have been proven to influence mechanical properties and failure mechanisms of natural fibers[12,15].

The objectives of the current study involve in situ depositing treatments of calcium carbonate ($CaCO_3$) particles onto bamboo fibers through the ionic reaction of sodium carbonate (Na_2CO_3) and calcium chloride ($CaCl_2$) aqueous solution, their impacts on surface features, wettability and tensile properties of single bamboo fibers and mechanical properties of laminated thermoplastic composites reinforced by modified fibers.

Materials and Methods

Sample preparation

All fibers were extracted with the blended chemical solutions of hydrogen peroxide and glacial acetic acid from the outer-chipped 3-year bamboo sticks (*Neosinoealamus affinis*, Changning County, Sichuan Province). The detailed preparation method was described by Leslie H. Groom [16]. Na_2CO_3 and $CaCl_2$ (Regent grade, Sinopharm Chemical Reagent Beijing Co., Ltd) were digested into 0.1 mol/l aqueous solution with distilled water. Ethylenediamine tetraacetic acid disodium (EDTA-2Na) applied as crystalline control agent, was provided by Sinopharm Chemical Reagent Beijing Co., Ltd, too. Air-dried bamboo fibers and 300ml 0.1 mol/l $CaCl_2$ aqueous solution(1:50 g/ml) were mixed by mechanical stirring at 5°C, 15°C, 25°C, 45°C and 65°C separately for 20 minutes, then the chemical additive was added, following 300ml 0.1 mol/l Na_2CO_3 aqueous solution at the rate of 25 ml/min. The whole together were blended for another 25 minutes. Excess $CaCO_3$ particles between fibers and other by-products were removed under running water. Afterwards, the retted fibers as control samples and the treated fibers were air-dried and stored in a constant temperature and humidity chamber, at 20°C, with the relative humidity(RH) of 65%.

The retted fibers as control samples and the treated fibers were made into circle handsheets with a diameter of 100 mm, and dried in a circulation oven at 103°C for 20 min, then stored in sealed plastic bags. Afterwards, the mats were laminated by fiber handsheets and polypropylene (PP) films alternatively, with the ratio of 1:3 by weight, and put into platens that preheated to 100°C. It took about 12min to raise the temperature between platens up to 180°C, then a pressure of 2MPa was applied to the mat constantly for 2min, and the platens were not open until cooled to 40°C. Three panels were obtained for each level and the control.

Physical and Mechenical Properties of Bamboo Fibers

Surface morphology of fibers and element analysis of particles were conducted by field emission scanning electron microscopy(FESEM XL30, FEI Incorporated, Holand). Fibers were coated with 15nm thick carbon film to avoid electron charging effect. The microscopy was operated at 5kv in a high vacuum environment， no higher than 5×10^{-5} Pa.

The fibers' ash contents were under test according to GB-T 742-2008. The $CaCO_3$ loading percentages were calculated by the difference of ash contents between the treated and the control fibers. Two duplicates were measured for each level, with a maximum error of 0.2%.

Dynamic contact angles of bamboo fibers, were obtained by the optical contact angle measuring device (Kruss DSA100, Germany) at (25 ± 2) °C, (50 ± 5) %RH, with distilled water droplets as the test liquid. The testing process and the calculating method were depicted by Chen Hong et al. in detail[17]. 15 specimens were test for each level.

The tensile tests were conducted by the microtester (Instron 5848, USA) at room environment

(23°C, 40%RH) with a loading rate of 0.048mm/min, 30 replicates for each treating level. The cell wall area of every broken fiber was determined with a confocal scanning laser microscope (CSLM Meta510, Zeiss, Germany).The mean values as well as standard deviations of tensile strength and modulus of elasticity were calculated from the stress-strain curves. The testing process were conducted as the same as Yu Yan et al[18].

Tensile Test of Bamboo Fiber Reinforced PP Composites

The specimens were cut into dog-bone shape using a laser cutting machine(CMA-1610TF, Yue Ming Laser Science Co., Ltd, Guangdong), half sized referring to GB1040.3-2006-T, 5 replicates for each panel. They were kept in a desiccator for 2 days at least prior to testing. The tensile tests were conducted by Instron 5848 at room environment with a strain rate of 2mm/min. The mean values and standard deviations of tensile strength and modulus of elasticity were calculated from the stress-strain curves.

Results and Discussion

In situ $CaCO_3$ Growth on the Treated Bamboo Fibers' Surface

Surface morphologies of bamboo fibers were shown in Figure 1. Figure 1(A) represented the untreated fiber surfaces, with visible micropores, such as pits, lognitudinal wrinkles formed during air-drying and pores emerged where lignin and hemicelluloses were removed. These micropores could benefit the impregnation of ionic solutions along the fibers and provide sites for $CaCO_3$ crystals' deposition. There were a few nanoparticles in the pores of bamboo fibers at 5°C, and the crystals appeared single, irregularly tetrahedral. As the temperature ascended, Figure 1(C) displayed that the sizes and amounts of $CaCO_3$ particles got larger, and more pits and wrinkles were filled. Since Ca^{2+}、CO_3^{2-} ions moved faster and the solubility of $CaCO_3$ went down, more $CaCO_3$ crystals were ready to form[19]. As $CaCO_3$ particles continued to grow, they could not fit the pores anymore, more likely to be removed during washing, as shown in Figure 1(E,F).

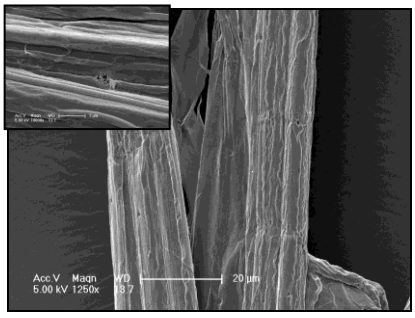

(a) The untreated

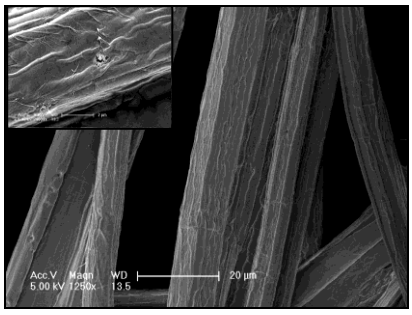

(b) 5℃

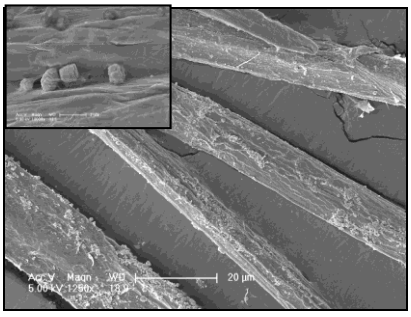

(c) 15℃

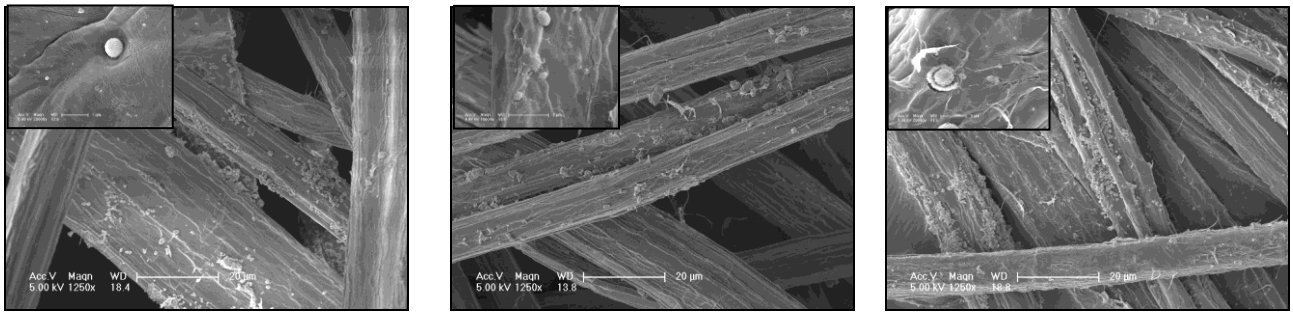

(d) 25℃ (e) 45℃ (f) 65℃

Fig.1 Surface morphologies of bamboo fibers

Effects of $CaCO_3$ Precipitation on Contact Angles of Bamboo Fibers

Table 1 displayed that $CaCO_3$ loadings went up at first, then declined slightly when the temperature rose, as the similar trend with contact angles. Fibers treated at 25°C had the highest adsorbance. Although the differences of $CaCO_3$ loadings among the variables were no more than 1% fibers' oven dried weight, the particles filled and grew from micropores of fibers, the surface roughness of which may change consequently. The mean contact angle values of bamboo fibers changed within 2°. But it shouldn't be neglected that the mean values of fibers modified at 15 °C and 25°C did get an increment and the standard deviations of contact angles declined at the same time. The coating of $CaCO_3$ nanoparticles may result in a smoother surface and reduced hydrophilic groups. As the particle sizes grew larger, combined with decreased $CaCO_3$ loading percentages, particles couldnot be well-distributed on the fibers. Therefore, the surfaces were rough again, and the mean values of contact angles decreased while the standard deviations got increments. These might influence interlacements of fibers and interfacial adhesion between fibers and polymer matrix.

Table 1 $CaCO_3$ Adsorbance and Static Contact Angles of Single Bamboo Fibers

The Treated Conditions （℃）	$CaCO_3$ adsorbance （%）	Static Contact Angle （°）		
		The Average	The Minimum	The Maxmum
The untreated	-	65.75	63.1	69.1
5	1.01	68.07	65.6	72.0
15	1.57	69.63	66.9	72.6
25	2.34	70.91	68.1	72.4
45	1.49	68.91	64.4	73.5
65	1.61	69.56	66.6	75.2

Tensile Properties of Individual Bamboo Fibers

Table 2 show that tensile properties of all the treated individual bamboo fibers were enhanced, with the peak of a 30.50% increase in tensile strength (from 1035.87MPa to 1383.99MPa) and a 32.71% increase in modulus of elasticity (from 27.36GPa to 36.30GPa) was obtained for the fibers treated at 25°C, and then decreased a bit when the temperature rose, as the same trend of $CaCO_3$ adsorptions. Analysis of variances present that tensile strength and modulus of elasticity had distinct differences among groups and no significant variance within groups. These might be explained by the fact that $CaCO_3$ nanoparticles filled fiber defects, like pits, where large microfibril angles were around and plastic deformation occurred first[15]. The improvement in the tensile properties should also be attributed to the impregnation of $CaCO_3$ particles in fiber cell wall, which increases the density of the fibers[20]. For the modified fiber, during the tensile process, the stress around the pits could be passed to the fillers, thus the rapid deformation and rupture of pits might be effectively prevented.

Table 2 Tensile properties of single bamboo fibers modified under different temperatures

The treated conditions （°C）	Tensile strength （MPa）	Modulus of elasticity （GPa）	Elongation at break （%）
The untreated	1035.87(280.37)	27.36(6.88)	4.21(1.42)
5	1136.64(286.82)	29.80(6.90)	4.09(0.95)
15	1237.71(406.61)	30.70(8.55)	4.33(0.90)
25	1383.99(413.50) *	36.30(8.92) *	3.89(0.52)
45	1176.71(261.80)	31.50(6.71)	3.97(0.66)
65	1167.18(265.89)	29.43(8.00)	4.34(0.91)

In the parentheses are the standard deviations. * was significantly different at $\alpha = 0.05$ according to results of multiple comparison with Fisher's Least Square method.

Tensile Properties of Bamboo Fiber Reinforced PP Composites

For all the treatment conditions in Table 3, the bamboo fibers reinforced PP composites showed improvement in both tensile strength and tensile modulus.The composites' tensile strength and modulus of elasticity increased firstly, then decreased a bit as the temperature rose, and they had distinct differences among groups and no significant variance within groups. Furthermore, multiple comparison demonstrated that tensile properties of the composites were remarkably enhanced when $CaCO_3$ nanoparticles in situ deposited in micropores of bamboo fibers at 15°C and 25°C as shown in Table 3. The composites reinforced with the fibers treated at 25°C gave the highest tensile strength and modulus, which were 14.6%, 19.6% separately higher than those reinforced with untreated fibers, which might be explained by the fact that $CaCO_3$ nanoparticles played a role of heterogeneous nucleation in PP crystallization, the degree of PP crystallization increased while the crystal size became smaller, so that the mechanical properties of PP composites got reinforced[20]. On the other hand, the wettability of fibers had a significant improvement at the same level. In summary, $CaCO_3$ nanoparticles contributed to the progress in compatibility of bamboo fibers and PP

matrix to a dramatic extent.

Table 3 **Tensile strength and modulus of elasticity of bamboo fibers/PP composites**

The treated conditions （℃）	Tensile strength （MPa）	Modulus of elasticity （GPa）
The untreated	48.91（6.32）	1.78（0.27）
5	51.27（7.37）	1.90（0.27）
15	54.49（4.21）*	1.96（0.22）*
25	56.04（4.79）**	2.13（0.14）**
45	50.73（5.20）	1.86（0.20）
65	52.27（5.95）	1.88（0.28）

Standard deviations are in the parentheses. * and ** were significantly different at α= 0.05 and 0.01 respectively according to results of multiple comparison with Fisher's Least Square method.

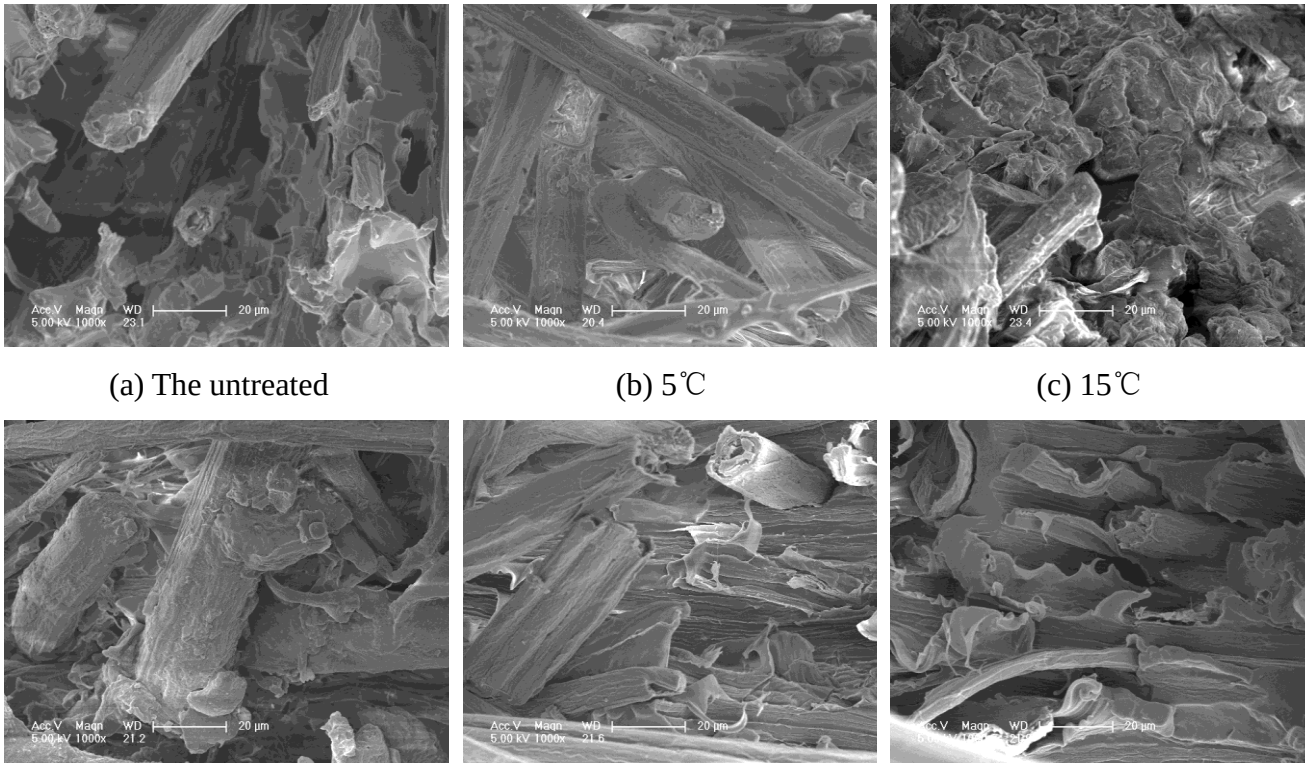

(a) The untreated (b) 5℃ (c) 15℃

(d) 25℃ (e) 45℃ (f) 65℃

Fig. 4 Fracture surface of composites reinforeced by bamboo fibers modified under different temperatures

Conclusions

$CaCO_3$ nanoparticles and submicron particles in situ grew into micropores of bamboo fibers. Although the loading percentages of $CaCO_3$ were small, distinct improvements of surface wettability and mechanical properties of fibers and modified fibers/PP composites appeared.

Optimal temperature for $CaCO_3$ nanoparticles treated bamboo fibers was 25°C, the $CaCO_3$ adsorbance and contact angle of fibers were 2.34%, 70.9°; the average tensile strength and modulus of elasticity of modified fibers reached 1.35GPa and 36.3 GPa, 30.50% and 32.71% higher than those of the unteated respectively. The average tensile strength and modulus of elasticity of modified fibers reinforced composites arrived at 56.04 MPa and 2.13 GPa, higher by 14.6%, 19.6% separately, comparing to those of the unteated.

Acknowledgements.

We would like to thank National Natural and Science Foundation of China (31170525) for financial support. Dr. Yu Yan is greatly appreciated for the help in the explainations for microtensile fracture mechanism of single fibers.

References

[1] Jiang Zehui. 2002, Bamboo and rattan in the world. LiaoNing: LiaoNing Science and Technology Publishing House.
[2] http://www.chinairn.com/news/20111020/381618.html.
[3] T. Shito, K. Okubo, and T. Fujii. 2002, Development of eco-composites using natural bamboo fibers and their mechanical properties, High Performance Structures and Composites, 4: 175-182.
[4] Xiao Jia-yu, et al. 2000, Status of research and development for the natural high performance fiber reinforced composite and its product. Fiber reinforced plastics/composites, 2: 38-43.
[5] Ge Wang, et al. 2011, Tensile properties of four types of individual cellulosic fibers. Wood and Fiber Science, 43(4): 353-364.
[6] Zhou Xiao. Xing, Lin Q., Chen L.. 2011, Mechanical properties and rheological behavior of injection moulded foaming bamboo powder-polypropylene composites. Advanced Material Research, (287-290): 1980-1986.
[7] G. Han, et al. 2008, Bamboo–fiber filled high density polyethylene composites: effect of coupling treatment and nanoclay. J Polym Environ, 16: 123–130.
[8] Yanjun Xie, et al. 2010, Silane coupling agents used for natural fiber/polymer composites: A review. Composites: Part A, 41: 806–819.
[9] Jiang Feng, Qin Te-fu. 2007, Research on toughening of wood-plastic composites. China plastics industry, 35(6): 137-140.
[10] S. Lee, S. Q. Shi. 2007, Multifunctional nanoparticles at the hydrophilic and hydrophobic interface. Proceedings of Advanced Biomass Science and Technology for Bio-based Products, Beijing, 173-181.
[11] Chen Zai-liang, Wang chuan-yang. 2007, Fabrication and characterization of nano $CaCO_3$ / polyproperlene foam sheets. Journal of Wuhan University of Technology(Mater. Sci. Ed), 22(4): 607-611.
[12] I. Burgert, N. Gierlinger, T. Zimmermann. 2005, Properties of Chemically and Mechanically Isolated Fibres of Spruce (*Picea abies [L.] Karst.*). Part 3: Mechanical Characterisation. Holzforschung, 59(2): 354-357.
[13] J. D. Boyd. 1982, An anatomical explanation for visco-elastic and mechanosorptive creep in

wood, and effects of loading rate on strength. In: New Perspective in Wood Anatomy. Ed. Baas, P. Martinus Nijhoff/Dr. W Junk Publishing, La Hague, 171-222.
[14] A. Bergander, L. Salmen. 2000, The transverse elastic modulus of the native wood fiber wall. Journal of Pulp and Paper Science, 26(6): 234-238.
[15] L. Mott, S.M. Shaler, L. H. Groom. 1996, A technique to measure strain distributions in single wood pulp fibers, Wood Fiber and Science, 28: 429-437.
[16] L.H. Groom, L.Mott, S.M. Shaler. 2002, Mechanical properties of individual southern pine fibers. Part I: determination and variability of stress-strain curves with respect to tree height and juvenility, Wood Fiber and Science, 34: 14-27.
[17] Chen Hong, Wang Ge, Cheng Hai-Tao. 2011, Properties of single bamboo fibers isolated by different chemical methods, Wood and Fiber Science, 43: 111-120.
[18] Yu Yan, et al. 2011, An improved microtensile technique for mechanical characterization of short plant fibers: a case study on bamboo fibers, J Mater Sci, 46: 739-746.
[19] A. W. Rudie, A. Ball, N. Patel. 2006, Ion exchange of H+, Na+, Mg2+, Ca2+, Mn2+, and Ba2+ on wood pulp. Journal of Wood Chem. and Tech., (26)：255-272.
[20] **Shi Jinshu**，et al. 2011，Kenaf bast fibers-Part II: Inorganic nanoparticle impregnation for polymer composites. International Journal of Polymer Science，2011 (736474)：1-7.

Chemical Composition of Some Commercial Tannins Produced in Turkey

Oktay GONULTAS [1*] *– Mualla BALABAN UCAR* [1]

[1] Department of Forest Products Engineering, Faculty of Forestry
Istanbul University, Sariyer, 34473, Istanbul, TURKEY
* *Corresponding author*
o_gonultas@hotmail.com

Abstract

This study was aimed to investigate the chemical composition of commercial tannins produced in Turkey mostly used by leatherworking. Tannin samples from pine bark, valonia, and gall nuts as well as ground sumac leaves were provided from the plant. It is well known that valonia, gall nuts, and sumac tannins compose of hydrolysable tannin whereas pine bark tannin consists of condensed tannins. Therefore methods of hydrolyzed and condensed tannins were applied in commercial samples. The methanol-water solubility of tannin samples was determined, after that total phenol content was assayed by spectrometrically in aqueous phase and ether phase. Amount of condensed tannin in the samples was determined by spectroscopical acid-butanol methods as well as stiasny number method gravimetrically. Content of gallotannin in samples was determined with Rhodanine Method; amount of ellagtannins was assayed with Nitrous Acid method. Functional group analysis of the tannin samples were investigated by FTIR instrument after compressing KBr pellets.

***Keywords*:** Tannin, Pine bark, Valonia, Turkish galls, Sumac, FTIR

Introduction

Tannin is commonly used in the leather industry as tanning material since the past. During tanning, these compounds that interact with proteins in animal skin for precipitate protein in the skin to provide make stabilized against the effect of bacterial degradation and gives flexibility. Also traditionally they are used for the needs of the local people as herbal drug. Furthermore tannins have been used as raw materials in medicine and pharmacology due to their antiviral, antimicrobial and anticancer effects. In addition, these compounds have used to clarify wine and beer, chemical and paint industry. Polyphenols are the most important secondary biomass in the non-wood forest products. However, nowadays, natural and renewable biomass sources especially in the chemical industry are more important with the increasing use and popularity. Many studies were aimed to use of plant tannins as natural phenolic compounds more area and efficient rather than petroleum-derived raw materials especially after the 1970s oil crisis in the world. Tannins were produced in commercially as preparation of low formaldehyde emission adhesives, ink production, dyeing of textile products and corrosion inhibitor (Bisanda, 2003)

Chemical structure of tannins are consist multiple adjacent polyhydroxyphenyl groups. This structure of tannins gives opportunity to bond with macromolecular compounds such as proteins, metal ions and polysaccharides (especially glucose) (Ozacar et. al., 2006).

There are two main groups based on constituent of tannins, these are hydrolysable and condensed tannins. Hydrolysable tannins are esters of formed by glucose with gallic acid and ellagic acid. It is easy soluble in water. Condensed tannins (proanthocyanidins) are polymers formed by condensation of flavanoid units. Main component of the condensed tannin is catechin and anthocyanindin. Although the tannins are natural condensed compounds, they are still having capable of condensation reaction with various chemicals as formaldehyde. Rigid carbon-carbon bond of condensed tannin possess cannot cleavage by hydrolysis (Bisanda et al., 2003).

According to Pizzi (2006) 200.000 tones of commercial tannins are produced worldwide each year and condensed tannins constitute more than 90% of the total world production. Species, trade names, and origin of commercial tannins of produced in the world are given in Table 1.

Table 1. Commercial Tannins in the World

Scientific Name	Trade Name	Origin	References
Schinopsis balance	Quebracho Tannin	Argentine	Mosiewicki et al.,(2004)
Acacia mearnsii	Mimosa Tannin	South Africa	
Acacia mearnsii	Mimosa Tannin	Brazil	
Acacia sp.	Mimosa Tannin	Italy	Zhao et al., (2010)
Quercus sp.	---	Tanzania	Bisanda et al., (2003)
Acacia sp.	Wattle Tannin	Chili	
Eucalyptus sp.	---	Brazil	
Salix caprea	Willow		
Acacia sp.	Wattle Tannin	Tanzania	Ndazi et al., (2006)
Acacia mangium	Mimosa Tannin	Malaysia	Hoong et al.,(2010)
Carya illinoensis	Pecan Nut Tannin		
Tsuga heterophylla	Hemlock bark extract	North America Canada	Franklin, (1980)
Castanea sativa	Chesnutt extract	Italy	http://en.silvateam.com/
Schinopsis balansae	Quebracho	South America	
Schinopsis lorentzii	Tannin	Argentine Paraguay	
Caesalpinia spinosa	Tara Tannin	Peru South America Northern Africa	
Uncaria gambir	Gambier extract	China, India Malaysia, Indonesia	
Terminalia chebula	Myrobalan extracts	East Indies	
Rhizophara sp.	Mangrove tannin	Nigeria	Sowunmi et al.,(1996)
Rhus sp.	Sumac extracts	Southern Europe	Pizzi., (2006)
Pinus sp.	Pine bark extract		
Vitis vinifera	Grape seed tannin	France	Ping et al., (2011)

The aim of this research was to investigate chemical composition with emphasis to phenolic compounds of pine bark tannin, valonia tannin, Turkish gall tannin, and sumac leaf from industrially produced in Turkey.

Materials and Methods

The tannin samples used in this study were supplied from Balaban Valeks Inc., Manisa, Turkey.

Determination of Phenolics

Methanol:water extraction of wood samples was performed as described previously (Balaban and Ucar, 2001). The Stiasny number reaction was used to determine the polyphenol content of extracts according to Yazaki and Hillis (1977). Total phenol content was determined by the Folin–Ciocalteu method (Singleton and Rossi, 1965). Gallotannins were hydrolysed with 1 M sulphuric acid, and gallic acid was then assayed using the Rhodanin reagent according to the method of Inoue and Hagerman (1988).

Gallic acid was used as the standard and assays were carried out in triplicate. The amount of ellagic tannin was determined with acidic sodium nitrite method by spectroscopically (Bate-Smith, 1972). The determination of proanthocyanidin was carried out as described by Govindarajan and Mathew (1965) and the results were expressed as cyanidin equivalents per amount of extracted wood (ε = 43.700; Fuleki and Francis, 1968).

FTIR Spectroscopy

Spectroscopic measurements were performed in a Bio-Rad Excalibur series FTS 3000 spectrophotometer using the standard KBr method (300 mg KBr plus 1 mg tannin; resolution: 4 cm^{-1}; 64 scans). The spectra were base line corrected at 3,700, 1,850 and 700 cm^{-1} and normalized to the highest band at 1,510 cm^{-1}.

Results and Discussions

Table 2 shows that the methanol-water solubility and total phenol content of commercial tannins. Pine tannin has high methanol-water solubility than other samples. Total phenol content of samples was determined ether and aqueous phases. Results of aqueous phase were similar while Turkish gall tannin had the highest value of ether phase.

Table 2. Methanol-Water Solubilities and Total Phenol Content of Commercial Tannins

Sample	Methanol-Water Solubility (%)	Total Phenol Content (mg g^{-1})	
		Ether Phase	Aqueous Phase
Pine Tannin	94.71	44.01	100.53
Valonia Tannin	82.93	26.60	104.45
Turkish Gall Tannin	67.61	53.72	102.44
Sumac Leaves	44.27	52.97	100.96

The stiasny number, proanthocyanidins, and pH in samples can be seen in Table 3. According to the results, pine tannin contains condensed tannins while other tannin samples contain hydrolysable tannins. Ozdemir (2010) reported the proanthocyanidin content for quebracho and mimosa tannins, respectively, 119.26 and 103.25. As can be seen from fourth column of the table, pH of pine tannin solution was higher. Valonia, Turkish gall tannin, and Sumac leaves had lower pH values due to hydrolysable tannins including gallic and ellagic acid.

Table 3.Condensed Tannin Amount and pH of Commercial Tannins

Sample	Stiasny Number	Proanthocyanidins (mg g^{-1})	pH
Pine Tannin	70.77	148.55	4.76
Valonia Tannin	nd.	2.03	3.81
Turkish Gall Tannin	nd.	nd.	4.24
Sumac Leaves	nd.	nd.	4.62

Sumac leaves include only gallotannin while valonia and Turkish gall tannin contain both of hydrolysable tannins, it was indicated in Table 4. Pizzi et al. (2009) had similar results for commercial hydrolysable tannins. It was stated that sumac leaves and Turkish gall tannin were occurred by mainly polygallic oligomers.

Table 4. Hydrolyzable Tannin Content

Sample	Hydrolyzable Tannins (mg g^{-1})	
	Gallotannin	Ellagic Tannin
Pine Tannin	15.12	nd.
Valonia Tannin	50.77	75.35
Turkish Gall Tannin	26.35	21.95
Sumac Leaves	30.79	nd.

The wide peak in the region 3550–3100 cm^{-1} is characteristic of the OH stretching vibration of benzene nucleus and methylol group of tannin (Ping et al. 2012; Ooa et al. 2009; Jianzhong et al. 2009; Puica et al. 2006; Kim and Joongkim, 2003; Ozacar et al. 2006). Small peak around 2900 cm^{-1} are due to aromatic CH stretching vibration of both methyl and methylene groups (Ping et al. 2012; Kim and Joongkim, 2003; Ozacar et al. 2006). The peaks pronounced at 1619-1450 cm^{-1} shows presence of aromatic rings (Ping et al. 2012; Ooa et al. 2009; Puica et al. 2006; Kim and Joongkim, 2003, Laghi et al. 2010, Ozacar et al. 2006). The region of peaks 1500-950 cm^{-1} are called fingerprint region for FTIR spectra of tannins.

The peak at 1285 cm^{-1} in the spectrum of pine tannin is a characteristic feature for the flavonoid based tannins (Edelmann et al. 2002). It was determined that the peak only for the pine tannin spectra (see Fig 1). According to Laghi (2010), oak tannins have characterized by bands at1324 and 1037 cm^{-1} due to symmetrical and asymmetrical C–O valence vibration. There is a peak at 1324 cm^{-1} in spectra's of valonia, Turkish gall, and sumac leaves. The carboxyl-carbonyl group appears at 1732 cm^{-1} in the spectrum of valonia tannin according to Ozacar (2006). The peaks around 910-740 cm^{-1} in all spectra's are deformation vibrations of the C-H bond in the benzene rings (Ping et al. 2012; Kim and Joongkim, 2003; Ozacar et al. 2006, Ozacar et al. 2008).

Figure 1. FTIR Spectra of Pine Tannin

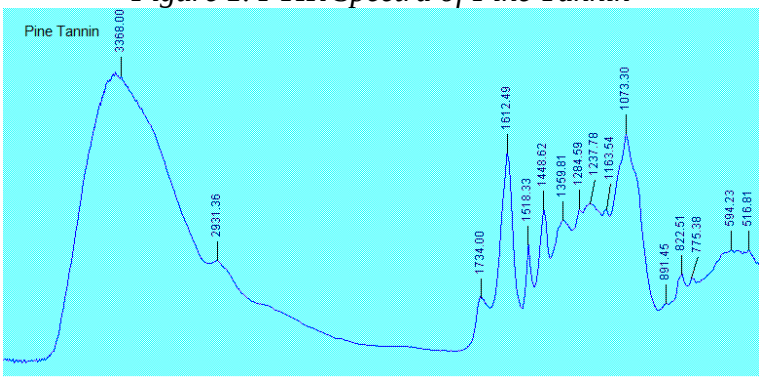

Figure 2. FTIR Spectra of Valonia Tannin

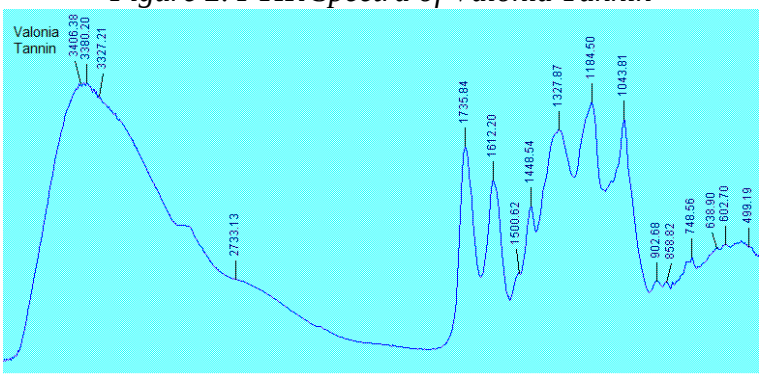

Figure 3. FTIR Spectra of Turkish Gall Tannin

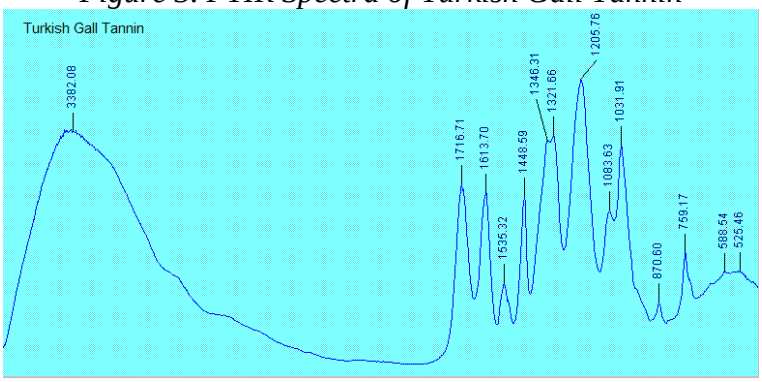

Figure 4. FTIR Spectra of Sumac Leaves

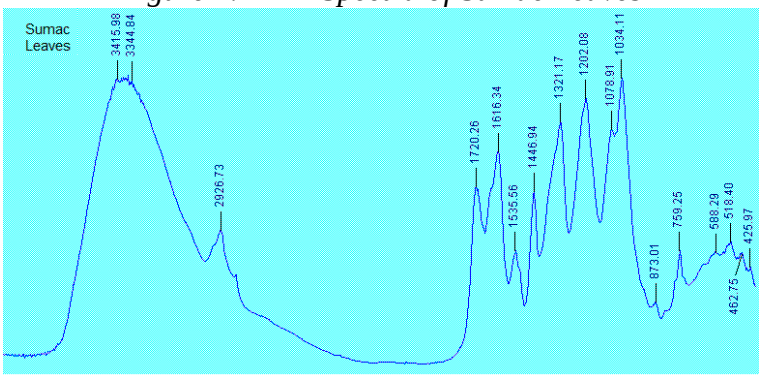

Conclusions

The results obtained in this study indicated that proanthocyanidisns is main constituent of pine tannins while gallo tannins for sumac leaves, gallo, and ellagic tannins for valonia and Turkish gall tannin. Based on the stiasny number analysis, pine tannins can be used in synthesis of tannin based bio-adhesives. The different functional groups were identified by FTIR investigation in this present study.

Acknowledgments

This work was supported by the Research Fund of the Istanbul University (Project Number: 22881). The authors would like to thank Istanbul University for its financial support in this project.

References

Balaban, M. 2003. Forest Products Chemistry, Class notes, Department of Forest Products Engineering, Faculty of Forestry, Istanbul University, Istanbul.

Balaban, M. Ucar, G. 2001. Extractives and tructural components in wood and bark of endemic oak Quercus vulcanica Boiss. Holzforschung. 55: 478–486.

Bate-Smith, E.C. 1972. Detection and determination of ellagitannins. Phytochemistry. 11: 1153-1156

Bisanda, E.T.N. Ogola, W.O. Tesha, J.V. 2003. Characterization of tannin resin blends for particle board applications. Cement & Concrete Composites. 25: 593–598

Edelmann, A. and Lendl, B. 2002. Toward the optical tongue: flow-through sensing of tannin-protein interactions based on FTIR spectroscopy. J. AM. CHEM. SOC. 124: 14741-14747

Franklin, W.H., 1980. Chemistry and utilization of western hemlock bark extractives. J. Agric. Food Chern. 28: 228-237

Fuleki, T. Francis, F.J. 1968. Quantitative methods for anthocyanidins. 1- extraction and determination of total anthocyanidins in cranberries. J Food Sci 33: 72–77.

Govindarajan, V.S. Matherw, A.G. 1965. Anthocyanidins from leucoanthocyanidins. Phytochemistry. 4: 985-988

Hoong, Y.B. Pizzi, A. Paridah, M.D. Tahir, C. Pasch, H. 2010. Characterization of Acacia mangium polyflavonoid tannins by MALDI-TOF mass spectrometry and CP-MAS ^{13}C NMR. European Polymer Journal. 46: 1268–1277

Inoue and Hagerman. 1988. Gallotannin determination with rhodanine. Anal. Biochemistry. 169: 363-369

Jianzhong, M.A. Yun L. Bin, L. Dangge, G. and Likun, W. 2009. Synthesis and properties of tannin/ vinyl polymer tanning agents. Accessed 24 March 2011 from http://www.aaqtic.org.ar/congresos/china2009/download/2-4/2-128.pdf

Kim, S. and Joongkim, H. 2003. Curing behavior and viscoelastic properties of pine and wattle tannin-based adhesives studied by dynamic mechanical thermal analysis and FT-IR-ATR spectroscopy. J. Adhesion Sci. Technol. Vol. 17, No. 10: 1369–1383

Mosiewicki, M. Aranguren, M.I. Borrajo, J. 2004. Thermal and mechanical properties of woodflour/tannin adhesive composites. Journal of Applied Polymer Science. Vol. 91: 3074–3082

Ndazi, B. Tesha, J.V. Karlsson, S. Bisanda, E.T.N. 2006. Production of rice husks composites with Acacia mimosa tannin-based resin. Journal Mater Science. 41: 6978–6983

Ooa, C.W. Kassima, M.J. Pizzi, A. 2009. Characterization and performance of Rhizophora apiculata mangrove polyflavonoid tannins in the adsorption of copper (II) and lead (II). Industrial Crops and Products. 30: 152–161

Ozacar, M. Soykan, C. Sengil, I.A. 2006. Studies on synthesis, characterization, and metal adsorption of mimosa and valonia tannin resins. Journal of Applied Polymer Science. Vol. 102: 786–797

Ozacar, M. Ayhan, I. Engil, S. Turkmenler, H. 2008. Equilibrium and kinetic data, and adsorption mechanism for adsorption of lead onto valonia tannin resin. Chemical Engineering Journal. 143: 32–42

Ozdemir, H. 2010. Bark tannins from commercially important Turkish conifer trees and their use as adhesive in fiberboard. PhD Thesis. Institute of Natural Science. Istanbul University. 154p.

Ping, L. Bronsse, N. Chrusciel, L. Navartete, P. Pizzi. A. 2011. Extraction of condensed tannins from grape pomace for use as wood adhesives. Industrial Crops and Products. 33: 253–257

Ping, L. Pizzi, A. Guo, Z.D. Brosse, N. 2012. Condensed tannins from grape pomace: Characterization by FTIR and MALDI TOF and production of environment friendly wood adhesive. Industrial Crops and Products. 40: 13– 20
Pizzi, A. 2006. Recent developments in eco-efficient bio-based adhesives for wood bonding: opportunities and issues. J. Adhesion Sci. Technol. 20. 8: 829-846

Pizzi, A. Pasch, H. Rode, K. Giovando, S. 2009. Polymer structure of commercial hydrolyzable tannins by matrix-assisted laser desorption/ionization-time-of-flight mass spectrometry. J. Appl. Polym. Sci. 113: 3847–3859.

Puica, N.M. Pui, A. and Florescu, M. 2006. FTIR spectroscopy for the analysis of vegetable tanned ancient leather. European Journal of Science and Theology, 2(4):49-53.

Silvateam S.p.a.Via Torre, 7 12080 San Michele M.vì (CN) Italy. Accessed 19 March 2012 < http://en.silvateam.com/ >

Singleton, V.L. Rossi, J.A. 1965. Colorimetry of total phenolics with phosphomolybdicphosphotungstic acid reagents. Am. J. Enol. Vitic. 16: 144-158

Sowunmi, S. Ebewele, R.O. Conner, A.H. River, B.H. 1996. Fortified mangrove tannin-based plywood adhesive. Journal of Applied Polymer Science. 62: 577-584

Yazaki, Y. Hillis, W.E. 1977. Polyphenolic extractives of Pinus radiata bark. Holzforschung. 31: (1) 20-25

Zhao, W. Fierro, V. Pizzi, A. Celzard, A. 2010. Bimodal cellular activated carbons derived from tannins. J Mater Sci. 45: 5778–5785

From a Production Orientation to a Stakeholder Orientation: The Evolution of Marketing Sophistication in Private, Multi-site U.S. Sawmills

Xiaoou Han
Ph. D Candidate
Department of Wood Science and Engineering
College of Forestry
Oregon State University
Corvallis, OR 97331
xiaoou.han@oregonstate.edu

Eric Hansen
Professor
Department of Wood Science and Engineering
College of Forestry
Oregon State University
Corvallis, OR 97331
eric.hansen2@oregonstate.edu

Abstract

Marketing can be thought of as a means of satisfying stakeholder needs in a social context. The role of marketing within a firm and the way it is conducted serve as indications of the sophistication of a firm. When marketing is purely a selling function, the company is likely production oriented. Conversely, marketing as an integrator or relationship-builder implies a more sophisticated market-orientation. Based on previous research, it is clear that marketing is changing over time. This study is focused on the "real" marketing sophistication and practice present in the US sawmilling sector. Here, marketing sophistication is used to mean the "degree of market orientation." It also explores the evolution of marketing sophistication in the sawmilling sector during the past years and the direction towards which marketing will develop. Finally, it investigates the interface between marketing and sales departments which can have essential impacts on marketing sophistication.

Key words: marketing sophistication, evolution, recession, customer, stakeholder

Introduction

During the early years when demand was high and customer needs were relatively unified, companies were mainly focused on producing large volumes of commodity products and would rely on a sales force to sell those products to customers. As the marketplace changes over time, especially with respect to customer needs and competitors, companies must become more sophisticated in their marketing approach to remain competitive. Instead of focusing only on production, companies should put more efforts to satisfy customers and other stakeholders.According to Narver and Slater (1990), a market orientation is a focus on customers and competitors and an ability to bring information about each back into the organization and effectively integrate it into operations (Narver and Slater 1990). This perspective is broadened by adding the idea of "stakeholder orientation" (Ferrell et al. 2010).

The forest industry is traditionally production-oriented and competes on low cost. Marketing is implemented as a sales-tool. However, the marketplace has evolved and become much more sophisticated. Marketing has to keep up with the change, especially during recession and times when the companies are facing severe challenges. Therefore, the understanding and approach of marketing must be improved to provide forest product companies with continuous competitive advantages. Hence, the objectives of this study, in the context of private-owned, multi-site, medium-sized U.S. sawmills are the following:

1) To learn the current situation of marketing sophistication

2) To investigate the evolution of a marketing sophistication

3) To assess the role ofmarketing departments in sawmilling companies

Theoretical background

Market orientationconceptualization

Lear's (1963) work is the earliest literature that can be found discussing market orientation and it can be considered quite similar to customer orientation. However, after decades of development, market orientation has turned into a rich concept including multiple dimensions. It is considered as the actual implementation or interpretation of the marketing concept (Kohli and Jaworski 1990).Narver and Slater (1990) and Kohli and Jaworski (1990) are the two well-know "camps" regarding market orientation. Narver and Slater (1990) consider market orientation as an organizational culture consisting of three components, namely, customer orientation, competitor orientation and interfunctional coordination. However, Kohli and Jaworski (1990) understand market orientation as a behavioral process of intelligence generation, intelligence dissemination and responsiveness. They provide two perspectives to approach market orientation with the same focus - the customers. The two perspectives are different but can be integrated as a whole.

From the cultural perspective, market orientation could be understood as attitudes and values that are shared by the people in the organization. It is like "an invisible hand" guiding individuals' behavior (Lichtenthal and Wilson 1992). The behavioral view of market orientation provides a

framework of implementation of market orientation (Vazquez et al 2001). Cadogan and Diamantopoulos (1995) synthesize these two perspectives and suggest a reconstruction of market orientation (Figure 1).

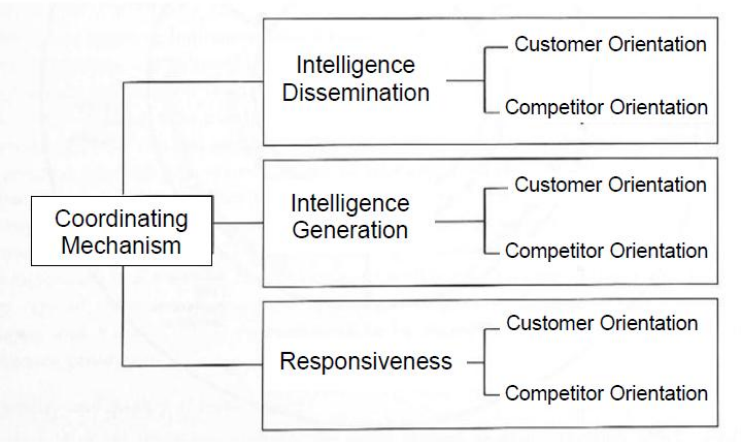

Figure 1: An integrated model of market orientation (adapted from Cadogan and Diamantopoulos, 1995)

In this integrated construct of market orientation, the three behavioral components- intelligence generation, intelligence dissemination and responsiveness-are led by customer orientation and competitor orientations. The coordinating mechanism dictates the manner in which these three behaviors are performed. That is to say, the activities associated with a market orientation take place following the process of intelligence generation, intelligence dissemination and responsiveness. The activities and the process that take place are oriented towards customers and competitors. Also, a coordinating mechanism steers the entire process to make sure things can be done effectively and efficiently. It focuses on the communication within a functional group as well as on the interaction among different functional groups.

The scope of a market orientation has expanded to include other stakeholders.Besides customers and competitors, other factors such as suppliers and communities could each highly influence companies (Lusch and Laczniak 1987). Taking such factors into consideration, the idea of stakeholder orientation is suggested(Maignan and Ferrell 2004, Ferrell et al. 2010). A stakeholder orientation emphasizes the importance of all individuals and organizations that have a "stake" in the company. It is suggested to be an extension of a market orientation, broadening the focus of the concept from just customers and competitors to all stakeholders.

As mentioned earlier, the stakeholder perspective is proposed and it enriches the concept of marketing. From the stakeholder perspective, marketing not only focuses on customers but also takes employees, suppliers, communities, etc. into consideration. Ferrell et al. (2010) proposes the definition of a stakeholder orientation as "the organizational culture and behaviors that induce organizational members to be continuously aware of and proactively act on a variety of

stakeholder issues." A stakeholder orientation has concerns for a variety of parties rather than being centered on any specific group. On the contrary, a traditional market orientation identifies customers and competitors as the key focus while paying little attention to other stakeholders. Although a stakeholder orientation does not put more importance on any specific group than the others, neither does it consider them equal. Different stakeholder groups may be prioritized depending on the issue. Bringing this idea together with the integrated construct of market orientation, the focus of each behavioral component can possibly be expanded from a customer and competitor orientation to a stakeholder orientation (Figure 2).

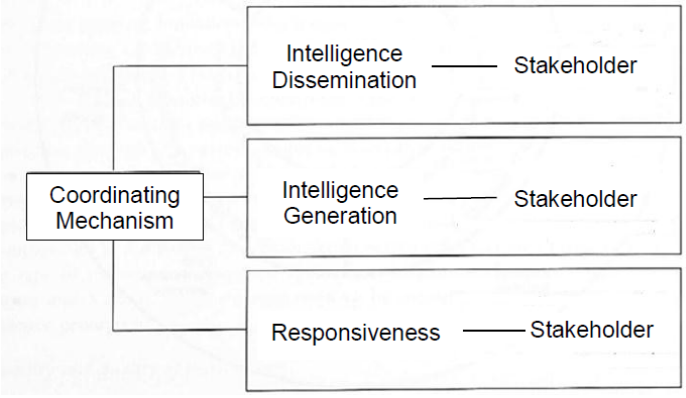

Figure 2: An integrated model of market orientation, from a stakeholder view

Marketing and sales

The distinction between the marketing department and the sales department is receiving increasing attention in the generic marketing literature, although in the past they were not well distinguished. In some research, sales is considered a subunit under the marketing department managed by the marketing executive (Dashpande and Webster 1989; Ruekert et al. 1985), while some authors only talk about the marketing department and don't even mention the sales department (Dastmalchian and Boag 1990). In fact, sales and marketing are two different concepts with different mind-sets or thought worlds behind them.

The role of either a sales department or a marketing department can differ between companies, thus, the distinction of these two departments can vary from one company to another. However, there are some perspectives regarding sales-marketing distinction that can fit the situations of most companies. An example would be that sales is suggested to be short-term oriented and marketing is long-term oriented (Homburg et al.2008; Rouziès 2005). Sales people are normally motivated by month-to-month or quarter-to-quarter goals while marketers often aim for sustainable competitive advantages which may take years to achieve. Also, sales is considered people-oriented (or individual-oriented), for the salespeople often focus on building relationships with the individual customers whom they directly deal with, while marketing has its focus more on analysis of the customer group and market research, in order to get higher level knowledge and better understanding of a larger scope.

It becomes more complicated when scholars try to differentiate sales and marketing using the notion of product-orientation vs. customer-orientation. According to Rouziès et al. (2005), sales is customer-oriented, for the salespeople normally work with a certain group of customers. They promote various products and services to their customers and make efforts to build good relationships with them. Different from sales, marketing mainly focuses on a certain product or product line. This aligns with Cespedes (1994) and Homburg and Jensen (2007) that sales is customer-oriented while marketing is product-oriented. However, Lear (1963) considers sales as product-oriented and marketing as customer-oriented.According to Lear (1963), a product-oriented firm is likely to have a sales department in which people focus more on products, while in a market-oriented company, there will be a marketing department focusing on the market. Another important aspect regarding marketing and sales department is the marketing and sales interface. As two different but closely connected departments in one company, the marketing department and sales department interact and collaborate in a number of ways. Simply speaking, the marketing department can lead, follow or be independent from the sales department (Day 1999; Kotler et al. 2006). However, the actual situation of marketing and sales configuration is rather complicated. Homburg et al. (2008) creates five categories with each category representing one type of marketing and sales configuration. In each category, the marketing department maintains a different level of knowledge, ranging from low to high, regarding products and marketing and so is the sales department. Also, the marketing department can be either short-term focused or long-term focused and the situation of the sales department is similar. The collaboration and communication between the marketing department and the sales department varies among categories.

Marketing sophistication in the forest sector

The term ‘marketing sophistication’ means the degree of market orientation in an organization.Traditionally, marketing in the forestry sector is largely production-oriented. Take sawmills for example. During the “good old days”, sawmills would just produce as much as they could. Production was their major focus and lumber they produced could be sold very quickly. However, the market is changing. Sawmills in the U.S. are facing increasing competition from other parts of the world. Hansen et al. (2002) suggest that the lumber from European countries is gaining market share in the U.S. market, although it was just a temporal phenomenon. Also, market needs to become more diversified with the growing sophistication of customers with more specific demands. The traditional commodity strategies can no longer satisfy the customers. In addition, the recession that started in 2008 brings more challenge to the industry. Many sawmills shut down during the recession. Some other sawmills are suffering from low profit and high inventories. There are calls for a development of marketing sophistication in the industry and at this point they seem especially urgent. Recent work focusing on marketing in the forest industry companies provides some evidence of increased marketing sophistication (Tibbets 2009, Juslin and Hansen 2003, Hansen et al. 2002). On the other hand, other results show that marketing in forest industry companies is not well implemented (Hansen 2006). Despite the evidence in both directions, there is limited understanding regarding the “real” marketing sophistication and practice in the forest industry.

Methods

Data wascollected throughin-person interviews. A semi-structural interview protocol was created and pre-tested on individuals in both academia and industry. The pre-tests were conducted following the same procedures as the actual interviews. Marketing managers and CEO/president of the private, multi-site, medium-sized, US sawmilling companies were the targets for interviews. They were sampled from the softwood and hardwood sawmills located in different regions of the U.S. In total, 19 interviews were conducted with 14 sawmills. The interviews were verbally transcribed and analyzed using the qualitative software NVIVO. Themes and important information were identified to address the objectives outlined in the beginning of this paper.

Results

We found that in most of the sawmills studied sales plays a larger role than marketing. The sales/marketing department in these sawmills largely operates focusing on sales. The major function of the department includes making phone calls to current/potential customers, establishing and maintaining relationships and then selling products. Marketing tends to be interpreted as advertising and promotion, which in general are led bythe sales department and are not really important to most of the sawmills. Although the overall marketing sophistication (market orientation) in the sawmills is still relatively low, there are evidences indicating that it has evolved from the traditional production orientation towards a market orientation and a stakeholder orientation. We learned that instead of being production-oriented and concentrating on mass production at low costs, the sawmills now put more effort into understanding the market environment and demands, and then implement strategies and activities accordingly. The analysis is still on-going, but some patterns already emerged from the interview data.

Companies now pay more attention to the stakeholders relevant to their business, including customers, competitors, community, environmental world, etc. as external stakeholders. Customer seems like the most important stakeholder group for the companies. Customer wants and needs become essential to the sawmills. To retain current customers and gain potential customers, the sawmills need to be more customer-oriented-to identify what they want and provide the products and services wanted. This was not considered an important issue years ago when market demand was quite high. During the recession time when market demand was relatively low, sawmills became more proactive in terms of satisfying their customers. Although the major focus of most sawmills interviews is still on the domestic market, the oversea customers are of growing importance nowadays due to the shrinkage of the U.S. market. Developing countries such as China and India still maintain a relatively high demand for lumbers and other forest products. They can be a good potential market for U.S. sawmills.

Also, the environmental world is of a great importance to the sawmills.Sawmills are expected to be environmentally responsible with its operations.One way the companies address it is to provide third-party certified products. They also promote the fact that they manage their forest land in a sustainable manner to build a positive public image. Furthermore, some sawmills actively participate in national programs and industry associations in order to promote the forest sector as a whole.

Overall, the evolution of marketing sophistication gains a firm better understanding of the customers and the market environment. It also helps a firm to better respond to various demands from customer and other stakeholders and thus enhances firm competitiveness within the forest sector. Eventually, it may increase the competitiveness of the forest sector.

References

American Marketing Association.1948. Report of the Definitions Committee. Journal of Marketing 13(2):202-217.

Bartels, R. 1962. The Development of Marketing Thoughts. Richard D. Irwin, Inc, Homewood, IL.

Berg, B. L. 2009 Qualitative Research Methods. Pearson education, Inc. Boston.

Cadogan, J. W. and A. Diamantopoulos. 1995. Narver and Slater, Kohli and Jaworski and the market orientation construct: integration and internationalization. Journal of Strategic Marketing. 3(1):41-60.

Cespedes, F. V. 1994. Industrial marketing: managing new requirements. Sloan Management Review. 35(3):45-60.

Day, G. 1999. Aligning organizational structure to the market. Business Strategy Review. 10(3): 33-46.

Hansen, E., J. Seppälä, and H. Juslin. 2002. Marketing Strategies in the Western Softwood Sawmill Industry. Forest Products Journal. 52(10):19-25.

Dastmalchian, Aand D. A. Boag. 1990. Environmental dependence and departmental structure: case of the marketing function. Human Relations. 43 (12): 1257–1276.

Deshpandé, R and F. E. Webster. 1989. Organizational Culture and Marketing: Defining the Research Agenda. Journal of Marketing. 53 (1): 3–15.

Deshpande, R and G. Zaitman. 1982. Factors affecting the use of market research information: a path analysis. Journal of Marketing Research, 19 (1): 14-31.

Fern, E. F. 1982. The use of focus groups for idea generation: the effects of group size, acquaintanceship, and moderator on a response quality and quantity. Journal of Marketing Research. 19, 1-13.

Ferrell, O. C., T. L. Gonzalez-Padron., G. T. M. Hult and I. Maignan. 2010. From market orientation of stakeholder orientation. Journal of Public Policy and Marketing. 29 (1): 93-96.

Hibbard, B.H and A. Hobson. 1916. Marketing farm product by parcel post and express. American Economic Review. 6 (3): 589-608..

Homburg, C and O. Jensen. 2007. The thought worlds of marketing and sales: which differences make a difference?. Journal of marketing. 71(3):124-142.

Homburg, C., J. P. Workman and H. Krohmer. 1999. Marketing's influence within the firm. Journal of Marketing. 63 (2): 1-17.

Homburg, C., O. Jensen and H. Krohmer. 2008. Configurations of marketing and sales: a taxonomy. Journal of Marketing. 72 (2): 133-154.

Hunt, Shelby D. 2007. A Responsibilities Framework for Marketing as a Professional Discipline," Journal of Public Policy &Marketing, 26 (Fall), 277–83.

Juslin, H. and E. Hansen. 2003. Strategic Marketing in the Global Forest Industries. Author's Academic Press. Corvallis, Oregon. 610 pp.

Kohli, A.K. and B.J. Jaworski. (1990). Market Orientation: The Construct, Research Propositions, and Managerial Implications. Journal of Marketing. 54(2):1-18.

Kotler, P. 2003. A Framework for Marketing Management. Pearson Education, Inc, Upper Saddle River, NJ.

Kotler, P., N. Rackham and S. Krishnaswamy. 2006. Ending the war between sales & Marketing. Harvard Business Review. 84 (7-8): 68-78.

Kotler, Phillip. 1977. From Sales Obsession to Marketing Effectiveness. Harvard Business Review. 55(6): 67-75.

Lichtenthal, J. D and D. T. 1992. Becoming market oriented. Journal of Business Research. 24 (3)3: 191-207.

Lusch, R. F. and G. R. Lazniak. 1987. The Evolving Marketing Concept, Competitive Intensity, and Organizational Performance. Journal of the Academy of Marketing Science. 15 (3): 1-11.

Lear, R.W. 1963. No Easy Road to Market Orientation. Harvard Business Review 41(5):53-60.

Maignan, I. and O.C. Ferrell. 2004, Corporate social responsibility and marketing: an integrative framework, The Journal of the Academy of MarketingScience. 32 (1): 3-19.

Narver, J.C. and S.F. Slater. 1990. The Effect of a Market Orientation on Business Profitability. Journal of Marketing. 54(4):20-35.

Powell, F.W. 1910. Co-operative Marketing of California Fresh Fruit. Quarterly Journal of Economics 24(2):392-418.

Tadajewski, M. 2009. Eventalizing the marketing concept. Journal of Marketing Management 25(1/2):191-217.

Tibbetts, A. 2009. A Qualitative Benchmark Study of the Evolution of Oregon's Forest Products Industry's Emphasis on Marketing. Senior Thesis. Wood Science and Engineering. Oregon State University. Corvallis, Oregon.

Rouziès, D., E. Anderson., A. K. Kohli., R. E. Michaels., B. A. Weitz and A. A. Zoltners. 2005. Sales and marketing integration: a proposed framework. Journal of personal selling and sales management. 25(2): 113-122.

Ruekert, R. W., O C Walker Jr., and K. J. Roering. 1985. The Organization of Marketing Activities: A Contingency Theory of Structure and Performance. Journal ofMarketing. 49(1): 13-25.

Vázquez, R.; M. L. Santos and L. I. Álvarez.2001. Market orientation, innovation and competitive strategies in industrial firms. Journal of Strategic Marketing. 9 (1):69-90.

Weld, L.D.H. 1915. Marketing Distribution: The University of Minnesota. American Economic Review 5:125.

Weld, L.D.H. 1917. Marketing Agencies between Manufacture and Jobber. Quarterly Journal of Economics 31(4):571-599.

Proceedings of the 55th International Convention of Society of Wood Science and Technology
August 27-31, 2012 - Beijing, CHINA

Comparison of Properties of Pine Scrim Lumber Made From Modified Scrim[1]

Weiqi Leng [1] *– H. Michael Barnes*[2*]

[1] Forest Products Department, Mississippi State University, Mississippi State, MS, USA.
wleng@cfr.msstate.edu

[2] Forest Products Department, Mississippi State University, Mississippi State, MS, USA.
mbarnes@cfr.msstate.edu
* *Corresponding author*

Abstract

In this study scrim from small-diameter southern pine bolts was treated with melamine formaldehyde (MF), phenolic formaldehyde (PF), and furfuryl alcohol (FA) at different loadings and formed into 25-mm thick pine scrim lumber (PSL) panels. Modulus of elasticity (MOE), modulus of rupture (MOR), work to maximum load, internal bond, toughness, water absorption, thickness swelling, dynamic swelling, and termite resistance performances were evaluated.

Results showed that samples treated with 5% MF resin had the highest MOE, MOR and work to maximum load values (15.3 GPa, 54.2 MPa and 25.4 KJ/m3, respectively), while those treated with 10% MF resin had the highest internal bond (IB) and edgewise toughness values of 390 kPa and 12 N•m, respectively. With respect to dimensional stability, samples treated with 20% FA had the lowest swelling values after 24 h submersion in water (ASE = 36.8%), and the lowest water absorption value (27.5%). Five hour dynamic swelling test revealed much higher dimensional stability for furfurylated samples (ASE > 45%). As for termite resistance, both untreated and treated PSL had little weight loss (1.10% to 1.56%), high visual rating (8 to 9.3/10), and high mortality (100%) in laboratory tests. MF and FA impregnation appeared to be feasible modification methods in this study.

[1] This paper is approved as Journal Article FP656 of the Forest & Wildlife Research Center. Mississippi State University

***Keywords*:** Pine Scrim Lumber, Phenol formaldehyde, Melamine formaldehyde, Furfuryl alcohol, Mechanical properties, Dimensional properties, Termite resistance.

Introduction

Chemical modification of wood can be defined as a process of bonding a reactive simple chemical to a reactive part of a cell wall polymer, with or without catalyst, to form a covalent bond between the two (Rowell 2006), which results in lowering of the cell-wall water holding capacity and the fiber saturation point (Kumar et al. 1991; Militz 1991; Codd et al. 1992). The essential requirement is that the reacting chemical should penetrate into the cell wall and react with the available hydroxyl groups of the cell-wall polymer, preferably in neutral or mild alkaline conditions at temperatures below 120 ºC. The major types of linkages formed by reaction with wood are ether, acetal, ester, etc., of which ester bonds are the weakest and are liable to acid or base attack (Kumar 1994).

Impregnation with phenol formaldehyde (PF) resin was first introduced in the 1930s (Stamm and Seborg 1939). Hygroscopicity, shrinking and swelling, and susceptibility to biodeterioration were all reduced (Stamm and Baechler 1960). High mechanical strength was obtained (Stamm and Seborg 1939). PF resin was located mainly in the cell wall (Kumar 1994). A good decay resistance was reported at about 10% polymer loading in the cell wall (Furuno et al. 1992). In further study researchers found that average molecule weight of PF resin affected the performance of impregnation (Ryu et al. 1993). Low molecular weight (LMW) PF resin could easily penetrate into the cell wall, playing a vital role in dimensional stability and decay resistance; while medium and high molecular weight resin could only partially penetrate with most depositing within the cell lumen, resulting in negligible contribution to dimensional stability and decay resistance (Furuno et al. 2004). Ryu et al. (1993) pointed out that molecular weight distribution and pH of the resin also contributed to the decay resistance. PF resin consisted exclusively of monomeric phenol alcohols with two or three reactive alcohol groups and that had lower alkalinities was less apt to decay. Similar to PF resin, water soluble melamine formaldehyde (MF) resin could be utilized to impregnate wood (Gindl et al. 2003). The MF resin could penetrate into wood cell wall (Rapp et al. 1999) and amorphous region of cellulose fibrils (Hua et al. 1987a, b), forming covalent bonds with cellulose and lignin (Troughton 1969; Troughton and Chow 1968). Decreased hygroscopicity and bio-deterioration were reported (Minato et al. 1993). Improved surface hardness and MOE of wood products could also be obtained when impregnated with LMW MF resin (Gindl et al. 2003). With the development of the adhesive industry, furfuryl alcohol (FA) was recognized as a substitute for PF resin, and furfurylation of wood was then introduced in the early 1950s. FA has a low molecular weight, which is preferable to penetrate into wood cell wall (Baysal and Osaki 2004). At that time, researchers' main interests were in durability towards acids and alkali, improved mechanical properties, dimensional stability, and biological durability (Dunlop and Peters 1953). PF, MF, and FA impregnation did not decrease the mechanical properties of wood, which were crucial for structural material. No research has been done to evaluate the performance of chemically modified pine scrim lumber (PSL). In this study, mechanical, dimensional, and biological properties of PSL were tested, and possible mechanisms are discussed.

Materials and Methods

In this study, pine scrim was chemically treated and made into panels, followed by the evaluation of mechanical, dimensional, and biological durability properties.

Small diameter southern pine bolts (<205 mm) were crushed then processed through a scrim line to produce scrim. The scrimming process has been described earlier (Barnes et al. 2010; Linton et al. 2008; Linton et al. 2010). Treating solutions of 5, 10, 15% PF (Arclin, Springfield), and MF solutions (INEOS Melamines LLC, Springfield), and solutions of 20, 30, 40% FA solutions (Fisher Scientific) were utilized for chemical treatment. Citric acid (1% wt/wt, Fisher Scientific) was used as a catalyst for furfurylation. After the treatment, the scrim was made into panels (810mm x 810mm x 25mm) using the Dieffenbacher one meter laboratory press with Pressman controls. The whole process is shown in Figure 1.

Panels were then put into the conditioning chamber at 20 ºC and 65% relative humidity until the moisture content was constant. Then mechanical, dimensional, and biological properties were evaluated according to ASTM standards D4761 (2005), D1037 (2006), D143 (2007), and AWPA E1-09 (2010).

Results and Discussion

Mechanical Properties

Bending Properties

As shown in Table 1, samples treated with all three levels of MF and 30% FA have significantly higher MOE values than the control group (significance level is α=0.05 here and in the whole study), while the MOE for samples treated with other levels of chemicals are not significantly different from the control group. For MOR, Only samples treated with 5% MF, and 20%, 30% FA are significantly better than the control group. Work to maximum load in bending (WML) is an ability to absorb shock with some permanent deformation and more or less injury to a specimen (FPL 2010). As shown in Table 1, groups treated with 5%, 10% MF and 30% FA have significantly higher WML values than controls. It is obvious that samples treated with 5% MF perform the best with respect to MOE, MOR, and WML.

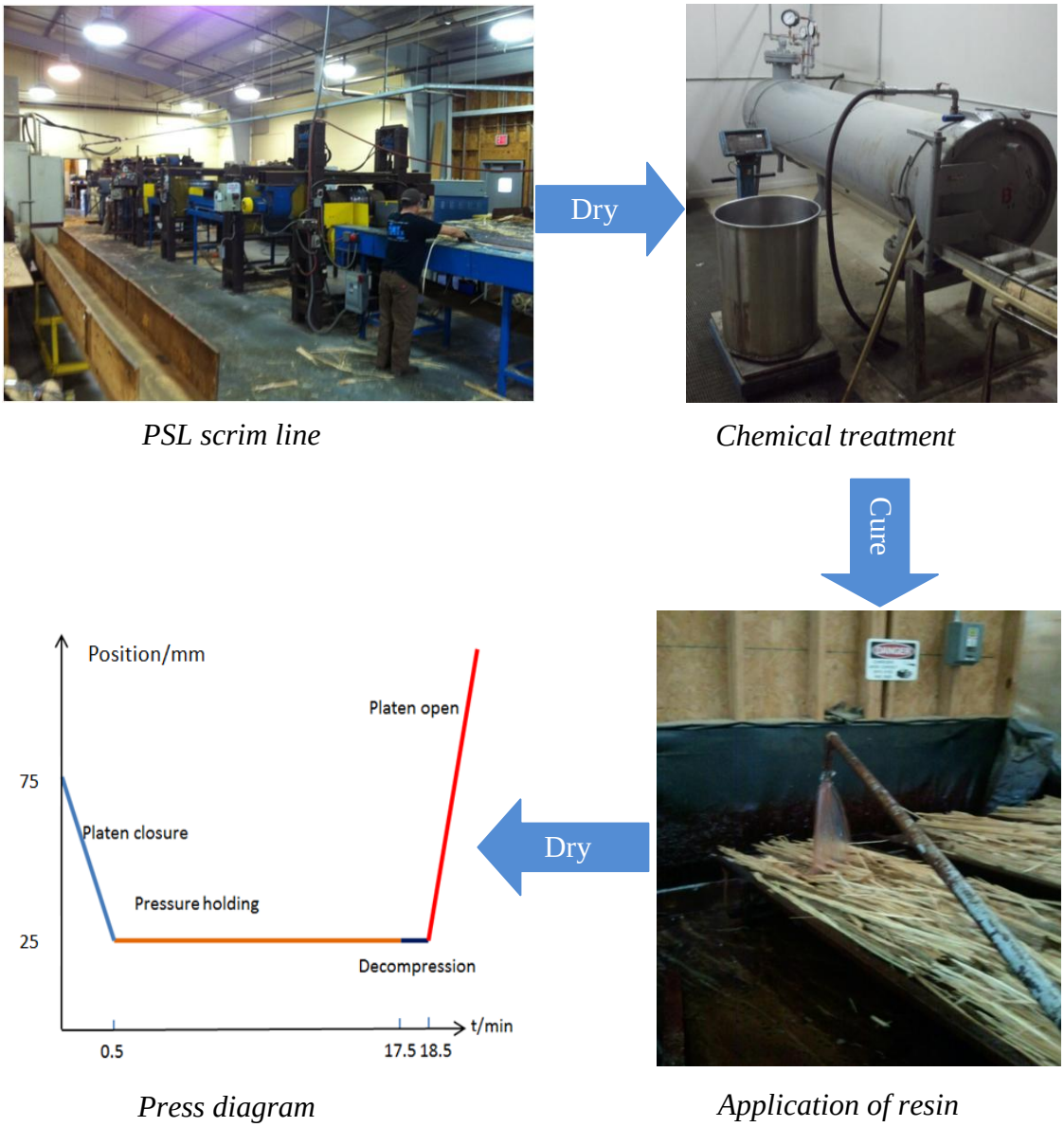

PSL scrim line *Chemical treatment*

Press diagram *Application of resin*

Figure 1. Preparation of pine scrim lumber

According to Stamm and Seborg (1939), PF treated wood should have improved bending properties, while in this study, opposite results are observed. The molecular weight of the resin might be a possible reason. As pointed out by Furuno et al. (2004), lower concentrations of lower molecular weight PF resin could easily and fully penetrated into cell wall and form wall polymers. With an increase in molecular weight and solids content, increased fractions of PF resin were found deposited in cell lumen. The PF resin used in this research has a molecular weight of 1300-1400, much higher compared with 350 and 451, which were studied by Wan and Kim (2008). In this study, since densities of all panels are not significantly different, more resin may deposit in the cell lumen, which means a lower proportion in the cell wall, resulting in weaker bending properties. Another reason for the weaker strength might be the effect of curing thermal treatment on the scrim.

Results obtained for MF impregnation and furfurylation are as expected. It is possible that the molecular weight of both of MF and FA is so low that the chemicals could easily access into the cell wall, thus improving the strength of the products (Gindl et al. 2003; Baysal and Osaki 2004). A detailed microscopic study should be conducted to investigate the mechanism of improved properties.

Table 1 Mean bending properties for both treated and control groups

Variable	WPG %	MOE MPa	COV %	MOR MPa	COV %	Work To Max Load KJ/m^3	COV %
M5	7.94	15321 A[1]	25	54 A	32	25.5A	35
F30	7.70	15146 A	24	48 AB	28	17.6B	41
M15	19.04	13785AB	21	38 BCD	31	14.2BCD	39
M10	15.15	13657AB	32	39 BCD	43	17.3BC	59
F40	8.18	12783ABC	26	33 CDE	38	11.4BCD	51
P15	23.48	11263BC	27	27 E	36	10.7BCD	40
F20	6.35	10905C	39	40 BC	45	15. 6BCD	56
Control	0.00	107178C	26	30 DE	27	9.6D	41
P5	7.88	10381C	26	29 E	40	13.4BCD	49
P10	17.72	10331C	20	27 E	41	10.4CD	50

[1]Means not followed by a common letter are significantly different at $\alpha = 0.05$.

Internal Bond and Density Profile

As shown in Figure 2, all treated samples have significantly higher IB values than controls except for those treated with 10 and 15% PF solutions. IB is related to resin type/content, sample density and element geometry (Dai et al. 2007). In this research, resin type/content, and pressing parameters are the same for each panel. Element geometry and density could not be controlled to be the same because of the variation in scrim size and geometry. According to the output from QMS density profile system (Figure 3), the density profile of controls varies significantly through thickness direction. The loss of bonding strength could start from the weakest point, which would be the lowest density region. Thus, the control group has the lowest mean IB value although the average density is in the medium range. It is unexpected that IB strength for panels treated with 10% and 15% PF solutions are not significantly higher than that of controls. The density profiles for both of them are smoother through thickness direction, and average densities are much higher than those treated with 5% PF solution. Possible reasons could be the scrim size and geometry with larger scrim size leading to less interfacial contact surfaces and many more voids among the scrim, thus lower IB strength is obtained. In order to find detailed reasons for this phenomenon, microscopic techniques should be applied to determine if rupture was due to resin failure. An analysis comparing the pressing parameters and density profiles with IB values and failure modes could be useful.

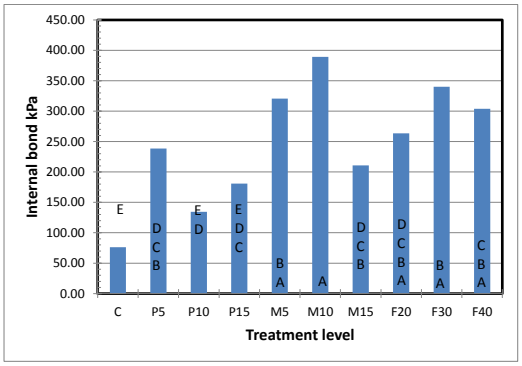

Figure 2 Internal bond (Means without a common letter are significantly different one from another at α = 0.05)

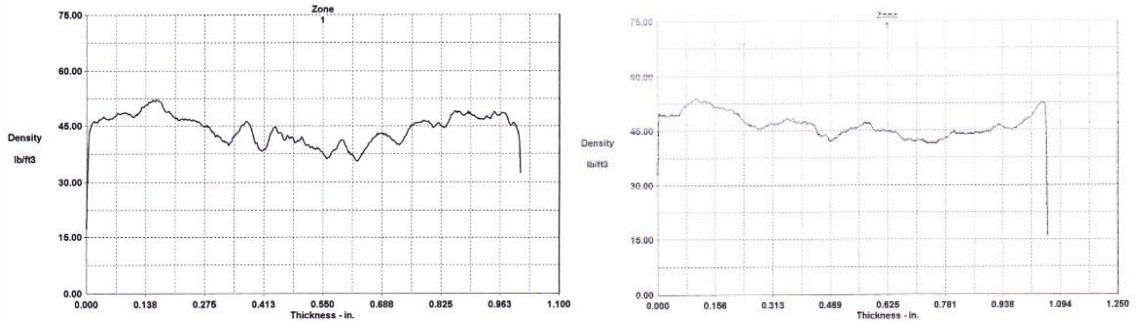

Figure 3 QMS density profile for the control (left) and PF-treated samples (right)

Toughness

There is randomness in toughness in both force directions within each group (Table 2). The large variation of toughness was also reported by Gerhards (1968) and in the Wood Handbook (FPL 2010), with a coefficient of variation (COV) around 30%. Toughness is the most sensitive mechanical property, which can vary sample by sample because of uneven density distributions, differences in resin coverage, annual rings, and moisture content.

Table 2 Mean toughness properties for treated and control groups

Variable	Force direction parallel to the panel surface		Force direction perpendicular to the panel surface	
	Mean N·m	COV %	Mean N·m	COV %
M10	12.0 A	45	9.0AB	32
P5	11.2AB	28	10.5A	24
P15	9.5ABC	25	7.2BCD	23
F30	9.0ABC	24	7.6BCD	29
M5	8.6BC	42	9.1AB	33
C	8.4BC	21.	5.8CD	30
F20	7.9C	13	5.7D	25
M15	6.9C	35	7.1BCD	25
P10	6.8C	21	8.3ABC	21
F40	6.7C	24	7.0BCD	20

Physical Properties

Water Absorption, Tangential Swelling, and Thickness Swelling

Results for water absorption, tangential swelling (swelling across the grain of the scrim), and thickness swelling are illustrated in Table 3. None of the treatments included wax to retard water movement. Samples treated with FA solution have smaller water absorption, tangential swelling, thickness swelling and lower MC values than the others. For water absorption, samples treated with 5% PF solution perform significantly worse than controls, while those treated with 10 and 15% PF solution and 5 and 15% MF solution have no significant difference from controls. This result means that impregnation of MF and PF does not prevent samples from absorbing water when submerged under water for 24h, while FA solution does. It is possible that the PF and MF resin do not efficiently occupy the water absorption sites.

Table 3 Summary statistics for swelling tests of treated and control groups

Variable	WA[2]	Tangential swelling	Thickness swelling	MC
	%			
P5	60.40 A	7.49 A	20.07 A	6.91 AB
P10	53.15 B	5.93 AB	15.33 B	7.76 A
P15	51.39 B	6.44 AB	14.76 B	6.48 ABCD
M5	50.73 B	5.49 BC	12.66 BC	6.40 ABCD
Control	48.92 BC	5.49 BC	15.50 B	7.48 A
M15	44.64 CD	4.18 CD	8.11 D	7.68 A
M10	41.88 D	4.24 CD	9.47 CD	6.54 ABC
F20	34.15 E	3.49 D	8.23 D	5.36 CD
F40	36.08 E	3.75 D	6.17 D	5.63 BCD
F30	27.46 F	3.47 D	7.15 D	5.00 D

[2]WA-water absorption.

Anti-swelling efficiency (ASE) for thickness swelling is shown in Figure 4. The ASE values within each group are proportional to the concentration of chemicals used. It is obvious that PF impregnation in this study has little positive, sometimes even adverse effect on dimensional stability of PSL. However, according to Wan and Kim (2006), ASE values for PF impregnated oriented strand board (OSB) were up to 26 and 45%, respectively, for 1.0 and 5.0% resin solids content. Probable reasons for the different results are the geometry of raw material, molecular weight of resin. For OSB, there are larger interfaces between flakes, thus yielding stronger internal bond, while for PSL, there are less interfaces between scrim as a result of the geometry of scrim. The molecular weight of PF resin used in OSB treatment is 310-451, much lower than that used in this study, which is about 1300. Higher molecular weight of PF resin impedes penetration of resin into cell wall, thus could not interlock wood polymers effectively. Larger amount of PF resin deposited in the cell lumen could have a negative effect on gluing. All these reasons could render a weak internal bonding strength of PF treated samples, which is proved by the fact that the PF impregnated PSL are loose, some of them even falls apart, after submerging under water for 24 h. When samples are loose, more voids are created, resulting in larger water absorption and less ASE. Low molecular weight of PF resin should be studied in the future.

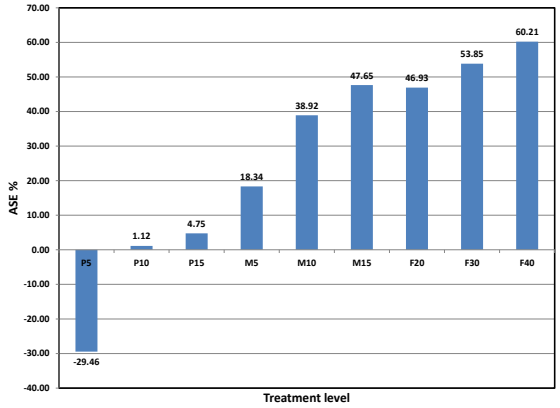

Figure 4 ASE for thickness swelling

Dynamic Swelling

Dynamic swelling for all treatment fits a logarithmic regression function, with the r^2 illustrated in Figure 5. Similar to the thickness swelling, the 5h dynamic swelling for both PF and FA treated samples are inversely related to the concentration of chemicals impregnated. However, for MF treated samples, there is a decrease in 5h dynamic swelling and then an increase as the concentration increases.

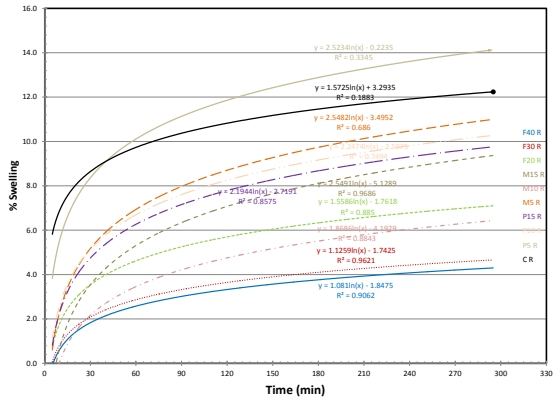

Figure 5 Dynamic swelling for PSL through thickness direction

Termite Resistance

Results of termite resistance for both treated and controls are shown in Figure 6. Visual appearance of the blocks after exposure to termites is shown in Figures 7 and 8. For southern pine positive controls, the average weight loss is 28.4% and the AWPA rating 4 (very severe attack), with no mortality. These results confirm the validity of the termite test. On the other hand, for both untreated and treated PSL tested, the average weight loss ranges from 1.10% to 1.56%, and the AWPA rating from 8 to 9.3 (moderate to trace attack), with 100% mortality. This means both untreated and treated PSL are termite resistant. For both untreated and treated PSL, termites were all dead after three weeks in the cabinet, which means that termites does not feed on PSL, whether chemically treated or not. PF resin applied for gluing might prevent the termites from eating the PSL.

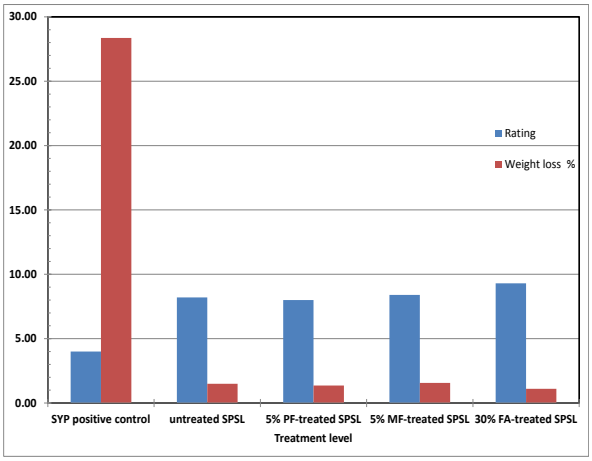

Figure 6 Comparison of visual rating and weight loss

Figure 7 Block appearance for southern pine positive control after 28-day termite test

Figure 8 Block appearance for untreated and treated PSL after 28-day termite test

Summary and Conclusions

Data collected from bending test demonstrate that PF impregnation is not successful in this study, while MF impregnation and furfurylation show satisfactory results, with the lowest level of MF and medium level of FA performing the best with respect to MOE, MOR, and WML. Statistically, low level of chemicals is preferable to improve the internal bond property. Data from 24h thickness swelling test show that samples treated

with MF and FA are significantly better than the controls. Results from 5h dynamic swelling of PSL show similar trends to the 24h thickness swelling tests. Evaluation of termite resistance shows that both untreated and treated PSL are termite resistant in laboratory scale.

References

ASTM 2005 D 4761-05. Standard Test Methods for Mechanical Properties of Lumber and Wood-Base Structural Material. American Society for Testing and Materials. West Conshohocken, PA.

ASTM 2006 D 1037-06a. Standard Test Methods for Evaluating Properties of Wood-Base Scrim and Particle Panel Materials. American Society for Testing and Materials. West Conshohocken, PA.

ASTM 2007 D 143-94. Standard Methods for Testing Small Clear Specimens of Timber. American Society for Testing and Materials. West Conshohocken, PA.

AWPA 2010 E1-09. Standard Method for Laboratory Evaluation to Determine Resistance to Subterranean Termites. American Wood Protection Association. Woodstock, MD.

Barnes, H.M. Seale, R.D. Linton, J.M. 2010. Steam-pressed scrim lumber (SPSL). In: Proceedings of the 53rd International Convention of the Society of Wood Science & Technology, October 11-15, 2010, Geneva, Switzerland, 8 pp.

Baysal, E. Osaki, S.K. 2004. Dimensional stability of wood treated with furfuryl alcohol catalysed by borates. Wood Science and Technology. 38: 405-415.

Codd, P. Banks, W.B. Cornfield, J.A. Williams, G.R. 1992. The biological effectiveness of wood modified with heptadecenylsuccinic anhydride against two brown rot fungi: Coniofora puteana and Gloephyllum trabeum. International Research Group on Wood Preservation. Doc. No. IRG/WP 3705.

Dai, C.P. Yu, C.M. Zhou, C. 2007. Theoretical modeling of bonding characteristics and performance of wood composite. Wood and Fiber Science. 39(1): 48-55.

Dunlop, A.P. Peters, F.N. 1953. The Furans. New York: Reinhold Publishing Corp.

FPL (2010) Wood Handbook - Wood as an engineering material. Gen Tech Rep FPLGTR-190. USDA Forest Service Forest Products Laboratory, Madison, WI. 509 pp.

Furuno, T. Imamura, Y. Kajita, H. 2004. The modification of wood by treatment with low molecular weight phenol-formaldehyde resin: a properties enhancement with neutralized phenol-resin and resin penetration into wood cell walls. Wood Science and Technology. 37: 349-361.

Furuno, T. Ueharaa, T. Jodai, S. 1992. The role of wall polymer in decay durability of wood-polymer composites. Mokuzai Gakkaishi. 38(3): 285-293.

Gehards, C.C. 1968. Effects of type of testing equipment and specimen size on toughness of wood. USDA Forest Service Research Paper. FPL 97.

Gindl, W. Zargar-Yaghubi, F. Wimmer, R. 2003. Impregnation of softwood cell walls with melamine-formaldehyde resin. Bioresource Technology. 87: 325-330.

Hua, L. Flodin, P. Ronnhult, T. 1987a. Cellulose scrim-polyester composites with reduced water sensitivity (2)-Surface analysis. Polymer Composite. 8: 203-207.

Hua, L. Zadorecki, P. Flodin, P. 1987b. Cellulose scrim-polyester composites with reduced water sensitivity (1)-Chemical treatment and mechanical properties. Polymer Composite. 8: 199-202.

Kumar, S. 1994. Chemical modification of wood. Wood and Fiber Science. 26(2):270-280.

Kumar, S. Indradev, Singh, S.P. 1991. Hygroscopicity and dimensional stability of wood acetylated with thioacetic acid and acetyl chloride. Journal of the Timber Development Association of India. 37(1):25-32.

Linton, J.M. Barnes, H.M. Seale, R.D. 2008. Effect of species-type on properties of steam pressed scrim lumber (SPSL). In: Proceedings, 51st Annual Meeting, Society of Wood Science & Technology, Concepción, Chile, November 10, 2008, paper WS-32, 8 pp.

Linton, J.M. Barnes, H.M. Seale, R.D. Jones, P.D. Lowell, E.C. Hummel, S.S. 2010. Suitability of live and fire-killed small diameter ponderosa and lodgepole pine trees for manufacturing a new structural wood composite. Bioresource Technology. 101(15): 6242-6247.

Militz, H. 1991. Improvement of shrinking and swelling behavior and durability of wood by treatment with noncatalyzed acetic anhydride. Holz Roh Werkst. 49(4):147-152.

Minato, K. Yusuf, S. Imamura, Y. Takahashi, M. 1993. Hygroscopic, vibrational, and biodeterioration characteristics of medium-density scrimboard treated with formaldehyde. Mokuzai Gakkaishi. 39(2): 190-197.

Rapp, A.O. Bestgen, H. Adams, W. Peek, R.D. 1999. Electron loss spectroscopy (EELS) for quantification of cell-wall penetration of a melamine resin. Holzforschung. 53: 111-117.

Rowell, R.M. 2006. Acetylation of wood journey from analytical technique to commercial reality. Forest Products Journal. 56(9): 4-12.

Ryu, J.Y. Imamura, Y. Takahashi, M. Kajita, H. 1993. Effects of molecular weight and some other properties of resins on the biological resistance of phenolic resin treated wood. Mokuzai Gakkaishi. 39(4): 486-492.

Stamm, A.J. Baechler, R.H. 1960. Decay resistance and dimensional stability of five modified woods. Forest Products Journal. 10: 22-26.

Stamm, A.J. Seborg, R.M. 1939. Resin-treated plywood. Industrial & Engineering Chemistry Research. 31(7): 897-902.

Troughton, G.E. 1969. Accelerated aging of glue-wood bonds. Journal of Wood Science. 1: 172-176.

Troughton, G.E. Chow, S.Z. 1968. Evidence for covalent bonding between melamine formaldehyde glue and wood. Part I-Bond degradation. Journal of the Institute of Wood Science. 21: 29-33.

Wan, H. Kim, M.G. 2006. Impregnation of southern pine wood and strands with low molecular weight phenol-formaldehyde resins for stabilization of oriented strandboard. Wood and Fiber Science. 38(2): 314-324.

Wan, H. Kim, M.G. 2008. Distribution of phenol-formaldehyde resin in impregnated southern pine and effects on stabilization. Wood and Fiber Science. 40(2): 181-189.

Proceedings of the 55th International Convention of Society of Wood Science and Technology
August 27-31, 2012 - Beijing, CHINA

Finite Element Analysis on the Shape Change of a Two-Layer Laminated Wood Product Subjected to Moisture Change

Ling Li[1], Meng Gong[2], Y.H. Chui[3], Marc Schneider[4]*

[1] Ph.D. Student, Faculty of Forestry and Environmental Management, University of New Brunswick, Fredericton, New Brunswick, CANADA

* *Corresponding author*
ling.li@unb.ca

[2] Research Scientist, Wood Science and Technology Centre, University of New Brunswick, Fredericton, New Brunswick, CANADA

mgong@unb.ca

[3] Professor, Faculty of Forestry and Environmental Management, University of New Brunswick, Fredericton, New Brunswick, CANADA

yhc@unb.ca

[4] Professor, Faculty of Forestry and Environmental Management, University of New Brunswick, Fredericton, New Brunswick, CANADA

mhs@unb.ca

Abstract

A two-layer laminated wood productcomprising of densified wood as surface reinforced material is an option forusing the underutilized softwood. Due to the improvedbending strength and surface hardness of densified wood, this type of laminated wood product could be used as flooring. However, its shape will change if the relative humidity (RH) and temperature of surroundings are variable. The shape change cannot be totally eliminatedbut could bediminished to a minimum by designing an appropriatethe thickness ratio of the densified and untreated wood layer. This study was aimed at developing a finite element (FE) model to predict the shape change of a two-layer laminated wood product subjected toa six-week treatment of RH and temperature. Balsam fir (*Abiesbalsamea (L.) Mill.*) was used to make densified and untreated wood. The dimensions of each specimen were 19mm (thick) by 52mm (width) by 280mm (length). Two thickness ratios ofdensifed and untreated wood were 3/16 and 7/12. All specimens were treated in a conditioning chamber of 80% RH and 20ºC for one week and then moved to another chamber of10% RH and 60ºC for another week. This procedure was repeated three times over six weeks. A FE model first simulated the transient

moisture movement with increasing time and then calculated the moisture induced deformation of the two-layer wood product. The cupping values were directly measured using a caliper. The results indicated that the FE model developed couldpredict the shape change of the two-layer laminated wood product.

***Keywords*:**Densified wood,Finite element,Shape change, Transient moisture diffusion, Two-layer laminated wood.

Introduction

Laminated wood products manufactured by adhesively bonding different types of wood strips togetherwith a designed configuration, such as sandwich configuration, have displayed a great benefit insavinghigh quality hardwood resources (Blanchet et al 2005).Meanwhile, to better utilizelow density softwood available in Canada, previous study by Lamason and Gong (2007) has shown that thermal-mechanical densification technology can assist in improving some mechanical properties of low-density softwood, e.g. balsam fir (*Abiesbalsamea (L.)* Mill.) and eastern white pine (*Pinusstrobus L.*) and they found the modulus of elasticity and surface hardness of densified balsam fir could be comparable with those of sugar maple (*Acer saccharum Marsh*). Therefore, the densified softwood shows a great potential as a substitute for hardwood to make laminated wood products. Furthermore, in order to decrease the production cost of laminated wood products due to use of densified wood, a two-layer laminated wood product made of densified wood as surface reinforced layer and untreated wood as substrate becomesanoptional approach, which may be used as flooring.

However, one critical issue about the dimensional stability of this two-layer laminated wood product should be considered. When the relative humidity (RH) and/or temperature of surroundingschange, the moisture movement in wood undergoes transient moisture diffusion resulting in moisture gradient varying with time until reaches moisture equilibrium. The moisture gradient can cause wood swelling or shrinkage to some degree. Thus, the shape changes, such as cupping, twisting, distorting, and crooking, etc.,may be generateddue to the difference of swelling/shrinkage coefficient among densified and untreated wood and adhesive.Asevere shape change will decrease thequality of final wood products.

The transient moisture diffusion movement in wood has been studied well, whichis usually applied in wood drying process (Avramidisand Siau 1987, Gui et al 1994). Comparing to some analytical approachesused for steady state moisture and/or temperature movement problems, a finite element (FE) analysis can solve some complicated problems. Gui et al (1994) developed a nonlinear FE model with the consideration of density variation along the growth rings to analyze the unsteady-state heat and moisture transfer in wood. The dynamic moisture and temperature profile with the increase of drying time simulated by FE model matched well with the experimental results. They also pointed out the reasonably accurate solution obtained by FE model can be incorporated into mechanical models to analyze drying-induced stress and strain distributions.

This study was aimed at developing a finite element (FE) model to predict the shape change of a two-layer laminated wood product subjected toa six-week treatment of RH and temperature. To reach this goal, moisture diffusion equations were solved as a first step. From the solutions to the diffusion equationsdescribingthe moisture profile as a function of time, the moisture induced deformation distributionsin this laminated wood productcould be calculated based on the classical linear elastic mechanical theory.

Materials and Methods

Materials.Balsam fir (*Abiesbalsamea (L.)*Mill.) was used to make densified wood and untreated wood. Plane sawn clear wood had an average oven-dried density of about 375±25kg/m^3 and the initial moisture content (MC) of about 12%. The optimal compression parameters were adopted from the research done by Li et al (2009), i.e. a pressing temperature of 230°C, pressure holding time of 20 minutes and a 60%compression ratio (CR) defined as the ratio of thickness reduction to initial thickness. A two-layer laminated wood product was fabricated by bonding densified woodand untreated wood together using one component polyurethane (PUR) adhesive along the parallel-to-grain direction. The nominaldimensions were 19mm-thick by 52mm-width and 280mm-length. Two thickness ratiosof densified wood to untreated wood were 3/16 and 7/12. The thickness of PUR adhesive was approximately specified as 0.5mm. There were three (3) replicates in each group. All specimens were placed, after fabrication, in a conditioning chamber at about 60±5% RH and 20±2ºC until the MC of densified and untreated wood stabilized at about 5% and 12%, respectively.

Methods. In order to activate the shape change, all specimenssubjected to a six-week treatment of RH and temperature. All specimens were first placed in a conditioning chamber of about 80% RH and 20ºC for one week and then transferred into another chamber of about 10% RH and 60ºC for another week.This procedure was repeated three times over six weeks. The corresponding equilibrium MCs (EMCs) of densified and untreated wood were about 7% and 15% at 80% RH and 20ºC, and about 2% and 5% at 10% RH and 60ºC. Considering the water resistance of cured PUR adhesive, the initial MC of PUR adhesive was assumed as *zero*. The effect of temperature on shape change wasneglected in this study.

Table 1 Mechanical and physical properties of material components used in FE analysis

	Parameters		Densified wood	Untreated wood	PUR adhesive
Mechanicalproperties (12% MC)	Elastic modulus (MPa)	E_R	1311 [a]	577 [a]	480 [d]
		E_T	2002 [a]	235 [a]	
	Poisson's ratio(μ)	μ_{TR}	0.64 [a]	0.15 [a]	0.03 [d]
	Shear modulus (MPa)	G_{RT}	255 [b]	152 [c]	
Physical properties	Swelling/Shrinkage coefficient (β)(mm^{-1} %$^{-1}$)	β_R	1.9^{-3} [a]	1.7^{-3} [a]	1.0^{-4} [d]
		β_T	1.8^{-3} [a]	4.2^{-3} [a]	
	Moisture diffusion coefficient (D) (m^{2}s^{-1})	D_T	1.8×10^{-11}	4×10^{-11}	0
		D_R	1.8×10^{-11}	4×10^{-11}	
	Convective mass transfer	h	3.2×10^{-4}	3.2×10^{-4}	3.2×10^{-4}

	coefficient (h) ($kgm^{-2}s^{-1}\%^{-1}$)				

Note: [a]. Directly measured by the authors; [b]. Adopted from Kitamori et al.(2008); [c]. Adopted from Wood Handbook (FPL 2010); d. Adopted from Sheffler et al. (2007).

Finite element (FE) model.A 2D FE model was developed to analyze the shape change of a two-layer laminated wood in *T-R*planevia ABAQUS (ABAQUS 6.6). The effects of MC change on the mechanical properties of densified wood andcurvature on mechanical properties of untreated wood in *T-R* section were ignored in this present study.The relationship of mechanical properties of untreated wood and MC changes below fiber saturated point (FSP) was assumed to follow the exponential law mentioned (FPL 2010).The mechanical and physical properties of densified and untreated wood used in FE analysis are given in Table 1, in which some were directly measured by the authors and others were obtained from literature. The FE model first simulated theunsteady state moisture diffusion movement with increasing time. TheMCgradient profile, as input data, was then incorporated in the calculation of the elastic stress field induced by MC changes. The detailed information regarding the unsteady state moisture movement and the linear elastic hygro-mechanical stress-strain relationships used in FE model was reported elsewhere. The principal material directions of wood are assumed perfectly oriented with the strip and a Cartesian coordinate system was used in the FE model. Eight-node plane strain thermally coupled quadrilateral, biquadratic displacement elements were chosen.The elements near two free edges of the bond line of the specimen were refined with the size of 0.01mm by 0.01mm. The size of elements in the rest part was 0.05mm by 0.05mm in order to save the computing time. The boundary conditions were shown in Fig.1.

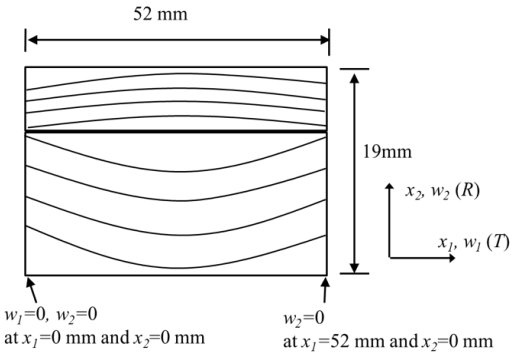

Fig.1Boundary conditions used in FE model

Results and Discussion

The transient moisture diffusion movementwith increasing time for two types of laminated wood specimens was simulated by ABAQUS. Two typical moisture profiles after the six-week treatment are shown in Fig. 3, respectively. According to the experimental design, the moisture adsorption occurred in the first, third and fifth week treatment, while the moisture desorption appeared in thesecond, fourth and sixth week treatment. Due to the axial symmetric structure of a specimen in the vertical direction (i.e. *y* axial), only the moisture profiles of a half specimen are displayed. The moisture profiles of two types of specimens showed that the significant moisture gradient mainly distributed at a finite area

next to the free edge.Meanwhile, the moisture gradient distribution of the specimen varies with the change of thicknesses of densified wood and untreated wood. Since the moisture diffusion coefficient in PUR adhesive layer was assumed to be *zero* in Table 1,the change of moisture was ignored in the PUR adhesive layer after treatment. The moisture gradient induced shape changes of two specimens predicted by FE model were displayed in Fig 4. Cupping of two specimens could be observed at the centre of the bottom and labelled by red color. FE results reveal that the cupping values oftwo types of specimens with thickness ratios of 3/16 and 7/12are about 0.24mm and 0.27mm, respectively.

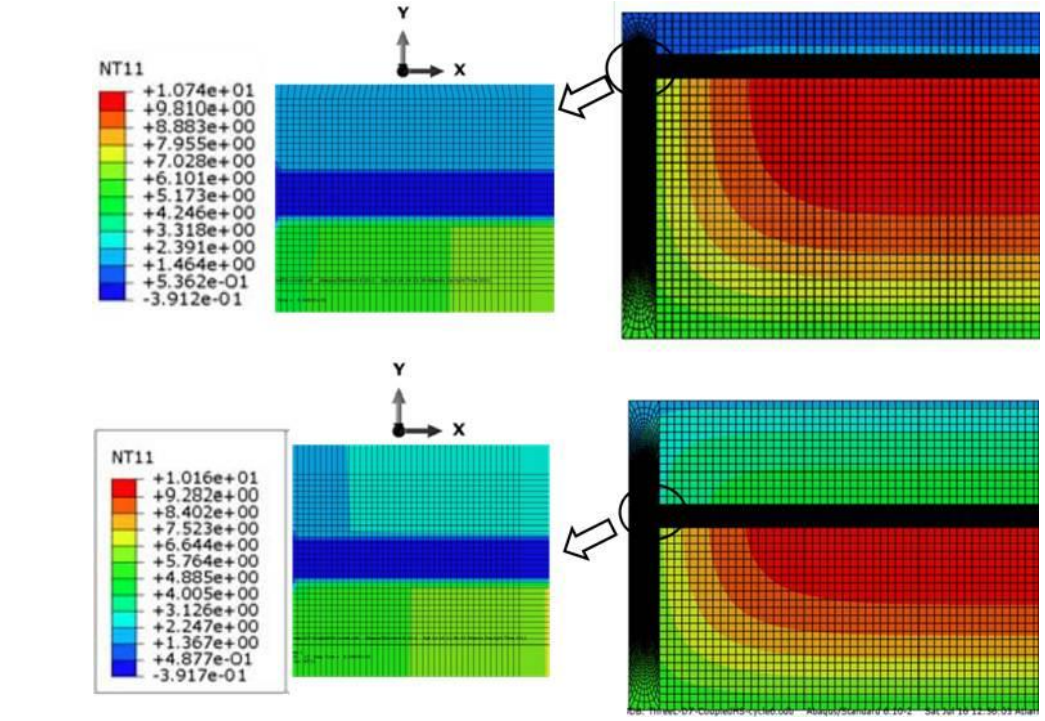

Fig.3 MC profiles of two specimens with thickness ratio of 3/16 (top) and 7/12 (bottom) after six-week treatment

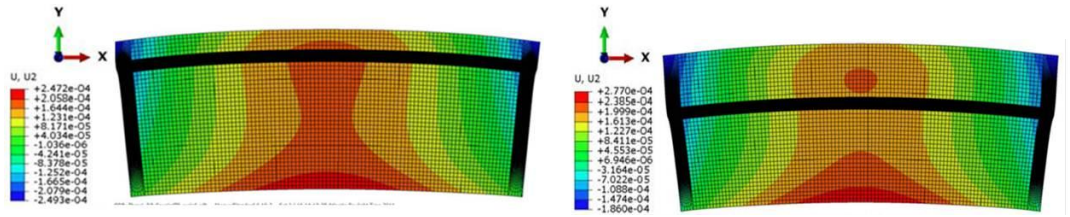

Fig. 4 Theshape changes of two specimens with thickness ratio of 3/16 (left) and 7/12 (right) after six-week treatment

The measurement of cupping of two types of specimens were performed using a caliper, which having a measurementaccuracy of 0.01mm. Two ends of each specimen were measured, giving a total of six values for each type of specimens (i.e. three replicates). The measured results show that the mean values of two types of specimens having 3/16 and 7/12 thickness ratios are 0.23mm and 0.36mm, respectively.

The comparison of FE results with experimental results is shown in Fig.6. It is seen thatthe cupping values obtained from the FE modelfortwo types of specimensof thickness ratiosof 3/16 and 7/12,were about 6% larger and 21% smaller than the average experimental values, respectively. The variation (standard deviation bar in Fig. 6) suggests that the accuracy of prediction to D-3mm specimens of a thickness ratio of 3/16 was higher than that of D-7mm ones of a thickness ratio of 7/12. However, it was observed that the cupping values were relatively small (only 0.23mm and 0.36mm for two types of specimens) when MC of densified wood and untreated wood varied in the range from 2% to 7% and 5% to 15% during the six-week treatment,

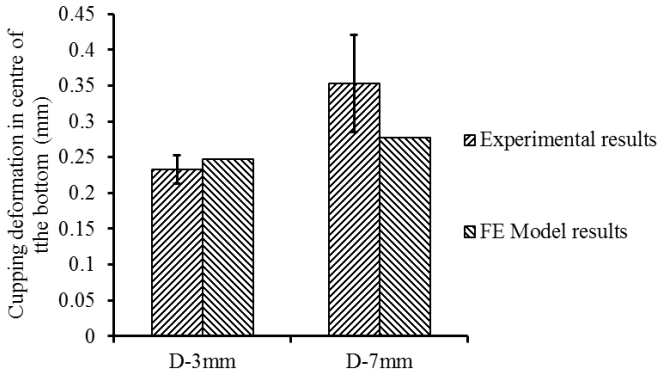

Fig. 6 Comparison of FE results and experimental results

Concluding Remarks

In this study, a 2D FE model was developed to explore its reliability on the simulation of the moisture induced shape change of a two-layer laminated wood product. By comparing the shape changes predicted by FE model with experimental results, the FE model developed in this study appeared to be a reliable approach to provide reasonable results.It could be concluded that 1) The moisture profiles of two types of specimens showed that the significant moisture gradient mainly distributed at a finite area next to the free edge; and 2) The cupping values obtained from the FE modelfor the specimensof thickness ratiosof 3/16 and 7/12 were about 6% larger and 21% smaller than the experimental values, respectively.

Acknowledgements

This study was supported Natural Sciences and Engineering Research Council of Canada (RGPIN 311808-05).

References

ABAQUS version 6.6 manual. ABAQUS Inc., 2006.

Avramidis, St. and Siau, J.F. 1987. An investigation of the external and internal resistance to moisture diffusion in wood.Wood science and technology. 21: 249-256.

Blanchet, P., Cloutier, A., Gendron, G. and Beauregard, R. 2005.Engineered wood flooring design using the finite element method. Journal of Forest Products, 56(5): 59-65.

Forest Products Laboratory (FPL).2010. Wood handbook-Wood as an engineering material. Gen. Tech. Rep. FPL–GTR–113. Madison, WI: U.S. Department of Agriculture, Forest Service, Forest Products Laboratory. 463 p.

Gui, Y.Q., Jones, E.W., Taylor, F.W., and Issa, C.A. 1994. An application of finite element analysis to wood drying.Wood Fiber and Science. 26(2):281-293.

Kitamori, A., Jung, K., Mori, T. and Komatsu, K. 2008.The evaluation on mechanical properties of compressed wood in accordance with the compression rate.Proceedings of the International Conference on Forest Products. Harbin, China. On Proceedings CD. pp. 233-234.

Lamason, C. and Gong, M. 2007. Optimization of pressing parameters for mechanically surface-densified aspen.Journal of Forest Products.57(10):64-68.

Li, L., Gong, M., Li, K. and Li, D.G. 2009. Evaluation of bonding quality between densified and virgin wood laminates in terms of Mode I fracture energy. Proceedings of the 12th International Conference on Fracture, Ottawa, ON. Paper: T47003.

Scheffler, M., Weber, T., Niemz, P. and Hardtke, H.J. 2007. Determination of residual stress in bonded wood components. Holzforschung.61: 285-290.

Proceedings of the 55th International Convention of Society of Wood Science and Technology
August 27-31, 2012 - Beijing, CHINA

Drying Cellulose Nanofibrils: Morphology Characterization

Yucheng Peng, Douglas J. Gardner, and Yousoo Han

University of Maine

AEWC Advanced Structures and Composites Center

Orono, Maine 04469

Abstract

Increasing research activity on cellulose nanofibril-based materials provides great opportunities for novel, scalable manufacturing approaches. Cellulose nanofibrils (CNFs) are typically processed as aqueous suspensions because of their hydrophilic nature. One of the major manufacturing challenges is to obtain dry CNFs while maintaining their nano-scale dimensions. Five methods were examined to dry cellulose nanocrystal (CNC) and nanofibrillated cellulose (NFC) suspensions: (1) oven drying, (2) air drying, (3) freeze drying (FD), (4) critical-point drying (CPD), and (5) spray-drying (SD). Morphologies of the dried CNFs were studied using scanning electron microscopy (SEM). Oven drying and air drying were deemed to be not suitable for obtaining nano-scale cellulose fibrils. Critical-point drying was found to preserve the nano-scale of the CNFs. Freeze drying formed ribbon-like structures of the CNFs. Spray-drying was found to provide a potentially scalable manufacturing process to preserve the nano-scale size of the cellulose fibrils. From the point view of obtaining a dry form of CNFs for manufacturing nanocomposites, spray-drying is proposed as a method to dry aqueous CNF suspensions.
Keywords: cellulose nanofibril, drying, freeze drying, critical-point drying, spray-drying

Introduction

The application of cellulosic nanofibrils (CNFs) as a reinforcing phase in composites has gained increasing attention (Siro and Plackett 2010, Siqueira et al. 2010, Klemm et al. 2011, Moon et al. 2011). With the size decrease from bulk wood cells to nanofibrils, the elastic modulus of cellulose is reported to increase from about 10 GPa to 70 GPa (Jeronimidis 1980), which would result in significant mechanical property improvement for cellulose nanofibril-reinforced polymer composites. Besides, biodegradability, low density, worldwide availability, low price and modifiable surface properties provide potential opportunities to develop a new generation of composites based on natural fibers. However, compared with conventional reinforcements of glass fibers or inorganic fillers, CNFs are not currently used in industrial practice, especially in the field of extrusion or similar thermal melting processes. During thermal melting processes, water is not tolerated. CNFs are typically produced as aqueous suspensions because of their hydrophilic nature. Therefore, drying of aqueous suspensions of CNFs and understanding the drying process are necessary to use them in developing polymer composites.

The objective of the present study is to investigate the effect of different drying methods on the material properties of dried CNF and to find a suitable method to obtain a scalable manufacturing method to produce commercially viable amounts of CNFs. Different CNF suspensions were studied including nanofibrillated cellulose (NFC) suspensions and cellulose nanocrystal (CNC) suspensions. Each suspension was dried using five methods: (1) air drying, (2) oven drying, (3) freeze drying, (4) critical-point drying, and (5) a novel spray-drying method. The morphologies and size of the dried products were examined using scanning electron microscopy (SEM).

Experimental

Suspension preparations: Two CNF suspensions were involved: (1) 6.49 wt. % of cellulose nanocrystal suspension (CNC) from the Forest Product Laboratory in Madison, Wisconsin, and (2) a commercial product of nanofibrillated cellulose (NFC) suspension ARBOCEL MF 40-10 in 10 wt. % from J. RETTENMAIER & SOHNE GMBH+CO.KG, Germany. Before drying, distilled water was added into the original suspensions and mixed using a Speed Mixer® for 4 minutes at 2000 rpm to obtain final weight concentrations of CNC and NFC at 2 %. The stability of diluted suspensions was examined for a period of several weeks.

Suspension drying: Air drying (AD) of the suspensions was conducted at room temperature with 65±5 % RH for 48 hours by settling the suspensions in plastic containers. Oven drying (OD) was performed at 105 °C for 24 hours in glass beakers. Prior to freeze drying (FD), CNF suspensions (about 20 ml) were frozen in vials at a temperature of -80 °C for 24 hours. Frozen suspensions were then transferred to a Virtis Freezemobile 25 SL freeze dryer, which has a condenser temperature of -80 °C and a vacuum of 11 mTorr. Lyophilization was allowed to continue for 72 hours. Critical-point drying of the prepared suspension was conducted on the

Tousimis Samdri PVT-3 Critical-Point dryer. A graded series of ethanol concentrations (50%, 75%, 95%, and 100%) was used to chemically dehydrate the samples before drying. A novel spray-drying method was conducted using Mini Spray Dryer B-290 (Buchi, Switzerland) Details of the spray drying process are the subject of a provisional patent application.

Morphology examination: Scanning electron microscopy (SEM) studies on the morphologies of dried samples were carried out using an AMR 1000 (AMRay Co.) scanning electron microscope. All samples were sputter-coated with gold before the microscopic observations were obtained. SEM images were taken at an accelerating voltage of 10 kV at various magnifications.

Results and Discussions

The morphologies of air-dried CNC and NFC are shown in Figure 1. Air drying of the two suspensions formed bulk materials with different surface roughness and fracture surfaces. In removing water from the suspensions, the distance between the cellulose nanofibrils or nanocrystals becomes smaller and the molecular contact is finally reached because of the capillary forces and diffusion forces. Under this situation, strong intermolecular hydrogen bonds were developed to form solid bulk materials. Air-dried NFC exhibits a smoother top surface (Figure 1A) than the bottom surface (Figure 1B). Settling of the prepared NFC suspensions at room temperature precipitated the large particles on the bottom, indicating that the NFC suspension is not thermally stable. Parts of the fibers in the original suspension are short in length and large in diameter (Figure 1A and B). At the same time, deposition of small scale cellulose nanofibrils was observed on the top surface while not on the bottom. The surfaces of dried CNC are much smoother than those of NFC, indicating a denser packing for CNC. This might be caused by the much smaller size of cellulose nanocrystals in the suspensions (Figure 1C and F). The morphologies of oven-dried samples are similar to the air-dried samples and are not shown in this paper.

The morphologies of freeze-dried NFC and CNC are shown in Figure 2. The dried samples from the two suspensions formed similar plate materials with different sizes (Figures 3A and D), differing from AD or OD samples. Large size in length and width is caused by the lateral agglomeration of cellulose nanofibrils or nanocrystals. This lateral fibril aggregation has been demonstrated by Hult et al. (2001). The thickness of these plate materials can reach to the sub-micrometer size range. The close-up evaluation on the surface morphologies shows that the FD samples are similar to those dried in air or the oven. For the CNC, much smoother surfaces were obtained for freeze-dried samples compared with those air or oven-dried (Figure 2F versus 1F). During the freeze drying process, the capillary forces are minimized (Lyne and Gallay 1954) and no bulk material was formed. However, the lateral agglomeration still occurred which may indicate that capillary forces are mainly responsible for the formation of bulk material in air or oven drying processes. The lateral aggregation may be driven by diffusion forces or perhaps

hydrogen bonding. This may further indicate that the cellulose nanofibrils or nanocrystals in the suspension just align laterally with many layers and each layer has different amounts of nanofibrils or nanocrystals laterally bonded together. Elazzouzi-Hafraoui et al. (2008) demonstrated that CNC consisting of several laterally parallel crystallites has the dimensions of a nanofibril. Considering the sheet structure of cellulose, the proposed weak hydrogen bonds (Nishiyama et al. 2003) or hydrophobic bonds (Jarvis 2003) between different sheets of cellulose fibrils are more easily broken than the lateral hydrogen bonds (Klemm et al. 1998).

The morphologies of critical-point dried samples from NFC suspensions are shown in Figure 3. During the dehydration CNC suspensions, water in the suspension cannot be replaced by ethanol. CPD cannot be applied to CNC suspensions and no dry form of CNC was obtained from the CPD method. The reason for the observation may be the strong three-dimensional hydrogen bonding formed between water molecules and cellulose nanocrystals. From the micrographs in Figure 3, nano-scale cellulose nanofibrils were observed. CPD is the best drying method from the point view of obtaining nano-scale CNFs. However, even using the CPD method, nanofibril aggregates were also observed during dehydration using ethanol (Thimm et al. 2000). The nanofibril size in the original suspensions may be smaller than these shown in the micrographs. In addition, these micrographs have also demonstrated that large diameter and short fibrils existed in the NFC suspension.

The morphologies of the spray-dried samples are shown in Figure 4. These micrographs show that SD of cellulose suspensions formed particles with different morphologies. The common dimensions are in micrometers. Many particles with nano-scale dimensions were also observed. Drying of the CNC suspension formed spherical particles with different sizes while drying of NFC formed irregular shaped particles. Spherical CNC material may be related to the agglomeration of small nanofibrils while the NFC particles may be partially related to the original configuration of CNFs in the suspensions.

Conclusions

The effect of various drying methods on the morphologies of CNFs was investigated for CNC and NFC by direct comparison using SEM. Different drying techniques and different sources of CNF suspensions provide different morphologies after drying. Air drying and oven drying were deemed to be not suitable for obtaining nano-scale cellulose fibrils. Critical-point drying was found to preserve the nano-scale of the CNFs. Freeze drying formed ribbon-like structures of the CNF. Spray-drying was found to provide a potentially scalable manufacturing process to obtain cellulose fibrils on the nano-scale. For obtaining nano-scale cellulose fibrils, CPD is the best technique to preserve the nano-dimensions. However, CPD is appropriate for drying small amounts of nanofibrils and may not be suitable for commercial scale-up. From the point view of obtaining a dry form of CNFs for manufacturing nanocomposites, spray-drying is proposed as a method to dry aqueous cellulose nanofibril suspensions.

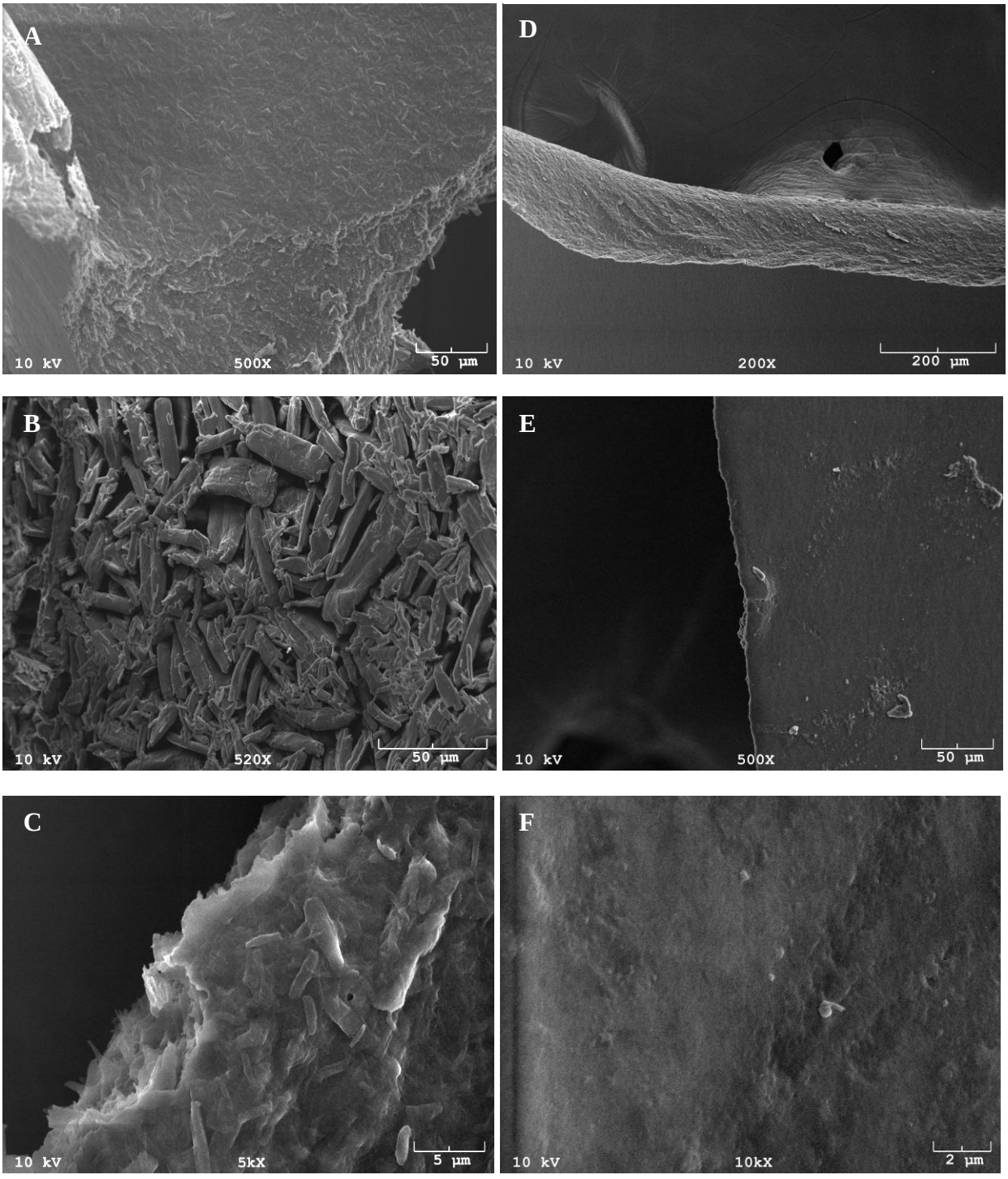

Figure 1. Morphologies of air-dried NFC: (A) (B) (C) and CNC: (D) (E) (F).

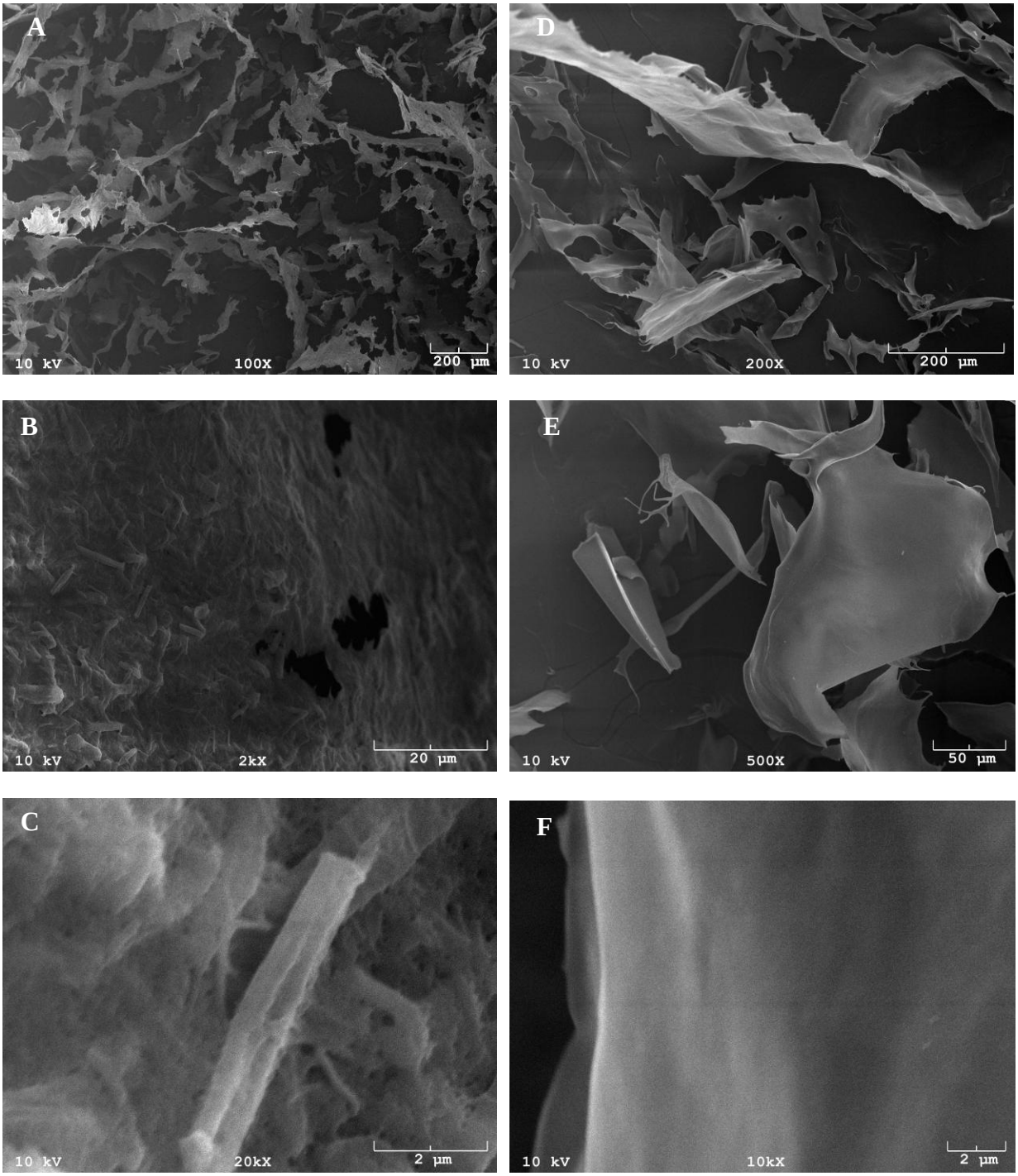

Figure 2. Morphologies of freeze dried NFC: (A)(B)(C) and CNC: (D)(E)(F).

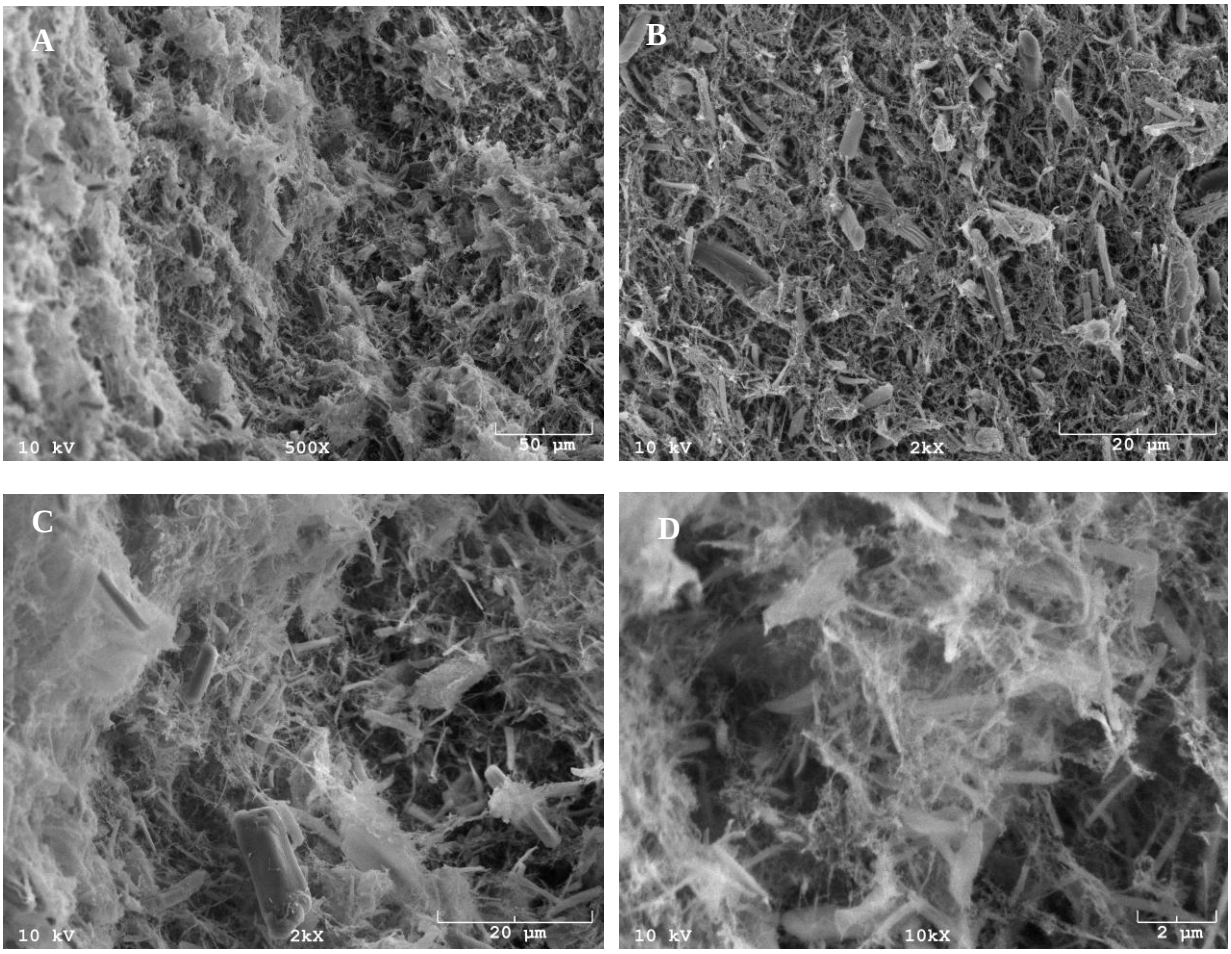

Figure 3. Morphologies of critical-point dried NFC at various magnifications: (A) (B) (C) (D).

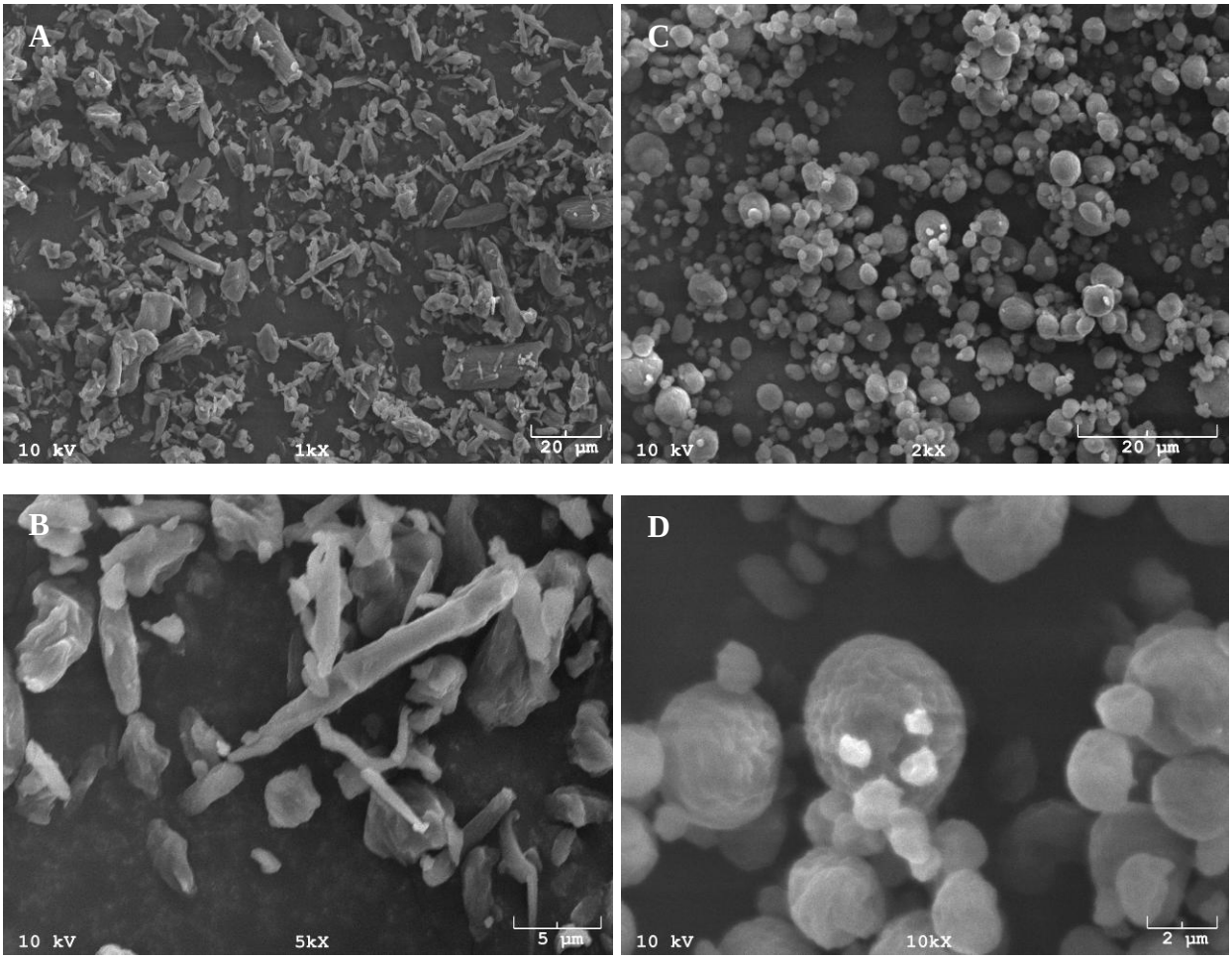

Figure 4. Morphologies of a novel spray dried NFC: (A) (B) and CNC: (C) (D).

References

Elazzouzi-Hafraoui S., Nishiyama Y., Putaux J. L., Heux L., Dubreuil F. and Rochas C. 2008. The shape and size distribution of crystalline nanoparticles prepared by acid hydrolysis of native cellulose. Biomacromolecules 9: 57-65.

Hult E. L., Larsson P. T. and Iversen T. 2001. Cellulose fibrils aggregation – an inherent property of kraft pulps. Polymer 42: 3309-3314.

Jarvis M. 2003. Cellulose stacks up. Nature 426: 611-612.

Jeronimidis G. 1980. Wood, One of Nature's Challenging Composites. In: The Mechanical Properties of Biological Materials, Eds. Vincent J. F. V. and Currey J. D., Cambridge University Press, Cambridge 169-182.

Klemm D., Philipp B., Heinze T., Heinze U. and Wagenknecht W. 1998. Comprehensive Cellulose Chemistry. Volume 1, Fundamentals and Analytical Methods. Weinheim, New York, Chichester, Brisbane, Singapore, Toronto: Wiley-VCH VerlagGmbH, Weinheim 1.

Klemm D, Kramer F, Moritz S, Lindstrom T, Ankerfors M, Gray D, Dorris A (2011) Nanocelluloses: a new family of nature-based materials. Angew. Chem. Int. Ed. 50: 5438-5466

Lyne L. M. and Galay W. 1954. Studies in the fundamentals of wet web strength. Tappi 37(12): 698-704.

Moon RJ, Marini A, Nairn J, Simonsen J, Youngblood J (2011) Cellulose nanomaterials review: structure, properties and nanocomposites. Chem. Soc. Rev. 40: 3941-3994.

Nishiyama Y., Sugiyama J., Chanzy H. and Langan P. 2003. Crystal structure and hydrogen bonding system in cellulose I alpha from synchrotron X-ray and neutron fiber diffraction. Journal of American Chemical Society 125: 14300-14306. Siqueira G, Bras J, Dufresne A (2010) Cellulosic bionanocomposites: a review of preparation, properties and applications. Polymers 2: 728-765.

Siro I. and Plackett D. 2010. Microfibrillated cellulose and new nanocomposite materials: a review. Cellulose 17: 459-494.

Thimm J. C., Burritt D. J., Ducker W. A. and Melton L. D. 2000. Celery (Apium graveolens L.) parenchyma cell walls examined by atomic force microscopy: effect of dehydration on cellulose microfibrils. Planta 212: 25-32.

The Effects of International Trade Show Marketing Strategies on Trade Show Performance: A Preliminary Analysis

Wenping Shi [1] – Paul M. Smith[2] - Shuangbao Zhang[3]*
[1] Graduate Research Assistant, Dept. of Agricultural and Biological Engineering,
The Pennsylvania State University, University Park PA, USA
** Corresponding author*
wxs191@psu.edu
[2] Professor, Dept. of Agricultural and Biological Engineering, The Pennsylvania State University, University Park PA, USA
pms6@psu.edu
[3] Professor, College of Material Science and Technology,
Beijing Forestry University, Beijing, China
shuangbaozhang@tom.com

Abstract

International trade shows are important venues where international marketing opportunities occur. Exhibiting at an international trade show is increasingly being viewed by firms as a cost-effective and efficient way to improve export performance and penetrate global markets. This study targets exhibitors at the largest international furniture supply trade show in China to examine their trade show strategies and trade show performance. A four-dimension framework of trade show performance is presented relevant to this particular market setting (i.e., sales-relational, psychological-related, market-exploring, and competitive-intelligence). And the differential effects of six trade show marketing strategies (i.e., visitor-attraction techniques, number of exhibited product, booth size, booth staff number, booth staff training, and follow-up contacts) on these four performance dimensions is examined. Marketing executives tasked with trade show planning, in particular, from furniture supplying industries and are considering exhibiting in China, may use the results from this study to more effectively implement trade show strategies to enhance specific dimension(s) of trade show performance.

***Keywords*:** International trade show, trade show marketing strategies, trade shows performance, China, furniture supply trade show

Introduction

Companies who conduct their marketing activities must decide where to best apply their resources for these business elements. In terms of marketing efforts, trade shows (TSs) are growing in importance as viable promotional and selling strategies (Smith et al. 2003). With the acceleration of globalization, international trade shows (ITSs) have increasingly represented a cost efficient and quick way to promote exports and to gain valuable information for market entry (Shoham 1999, Motwani et al. 1992, Rice 1992). These venues require a considerable expenditure for participants. TSs represent a significant line item in the business marketing budget, accounting for 10-15 percent of the business marketing communications budgets of U.S. firms (Dekimpe et al. 1997, Smith et al. 2003, Harriette et al. 2010), and more than 20 percent of the budget for European firms (Skallerud 2010, Sandler 1994).

To rationalize high TS exhibitor expenditures, researchers have focused on understanding the TS strategic factors (e.g., visitor-attraction techniques, booth size, booth staff number, and booth staff training) affecting TS performance to help TS practitioners develop effective strategies for successful TS exhibits (Li 2008, Smith et al. 2004, Dekimpe et al. 1997, Gopalakrishna et al. 1995, Li 2007). However, many of these studies examined the effects of TS strategies on single performance measures, such as booth-attraction effectiveness (Dekimpe et al. 1997), sales leads generated during the show (Gopalakrishna and Lilien 1995), and Return On Trade Show Investment (ROTSI) (Smith et al. 1999). Recent studies have reached a consensus that TSs represent a multi-dimensional marketing tool (Tafesse and Korneliussen 2011, Lee and Kim 2008, Hansen 2004) and exhibitors tend to have multiple TS objectives. Thus, a better understanding of specific TS strategy factors on each dimension of TS performance can aid marketing executives tasked with TS planning of effective implementation of TS strategies.

Opportunities in Emerging Markets

The global TS industry has grown dramatically. China's TS exhibition industry has experienced rapid advancement with the boom of the country's economy over the past several decades (Jin et al. 2010). According to the Global Association of the Exhibition Industry (UFI), China's indoor exhibition space totaled approximately 4.7 million square meters in 2011, accounting for 15% of the world's total after the U.S. with share of 21% (UFI 2011).

Within the forest products industry, one type of typical horizontal TSs, "International Furniture Supply Trade Shows" (IFS-TSs), feature furniture supplying industries such as wood raw materials, woodworking machinery, hardware and other furniture accessories. These IFS-TSs have long served as an important venue for suppliers in these industries to communicate with target customers worldwide. As a result of Chinese market liberation and the subsequent rapid growth of the Chinese furniture industry, IFS-TSs in China have grown in international importance and prestige, attracting increasing numbers of exhibitors and attendees from around the world. The top 3 major IFS-TSs identified by Shi and Smith (2011) attracted approximate 116,000 attendees and 2,270 exhibitors

worldwide in 2010, and these numbers are still growing annually. This indicates how suppliers in this industry value TSs as an important marketing and selling strategy.

Despite the increasing popularity of TSs in China, inquiry into the dimensionality of TS performance and the affecting TS strategies in this market is lacking. Although there are a few limited research efforts in emerging markets (Tafesse and Korneliussen 2011, Li 2008), none of these studies examine the different effects of TS strategies on multi-dimensional TS performance. Several researchers have noted that TS strategies and TS performance evaluation may differ across countries and/or industries (Dekimpe et al. 1997, Hansen 2004, Tafesse and Korneliussen 2011). These differences imply that TS performance dimensions and the relationship between TS strategy and TS performance developed in the extant literature may not be generalizable to other TS contexts.

Therefore, this study contributes to the limited emerging market research by investigating the multi-dimensionality of TS performance through an ITS-FS venue in China. Further, this study extends research on the effects of TS strategies on relevant TS performance dimensions to IFS-TSs; thus providing additional empirical evidence regarding these relationships.

Study framework

TS performance has typically been evaluated based on exhibiting firm's ability to enhance key TS activities set by senior marketing managers such as lead generation, customer relations-building, competitor intelligence gathering, image building, and sales team training (Bonoma 1983, Bello 1992, Kijewski et al. 1993, Hansen 2004, Kerin and Cron 1987). This study applied the sixteen TS activities validated in previous literature to measure exhibitors' TS performance; and the six TS marketing strategies from earlier studies to examine their effects on exhibiting firms' TS performance. The framework is presented in Fig. 1.

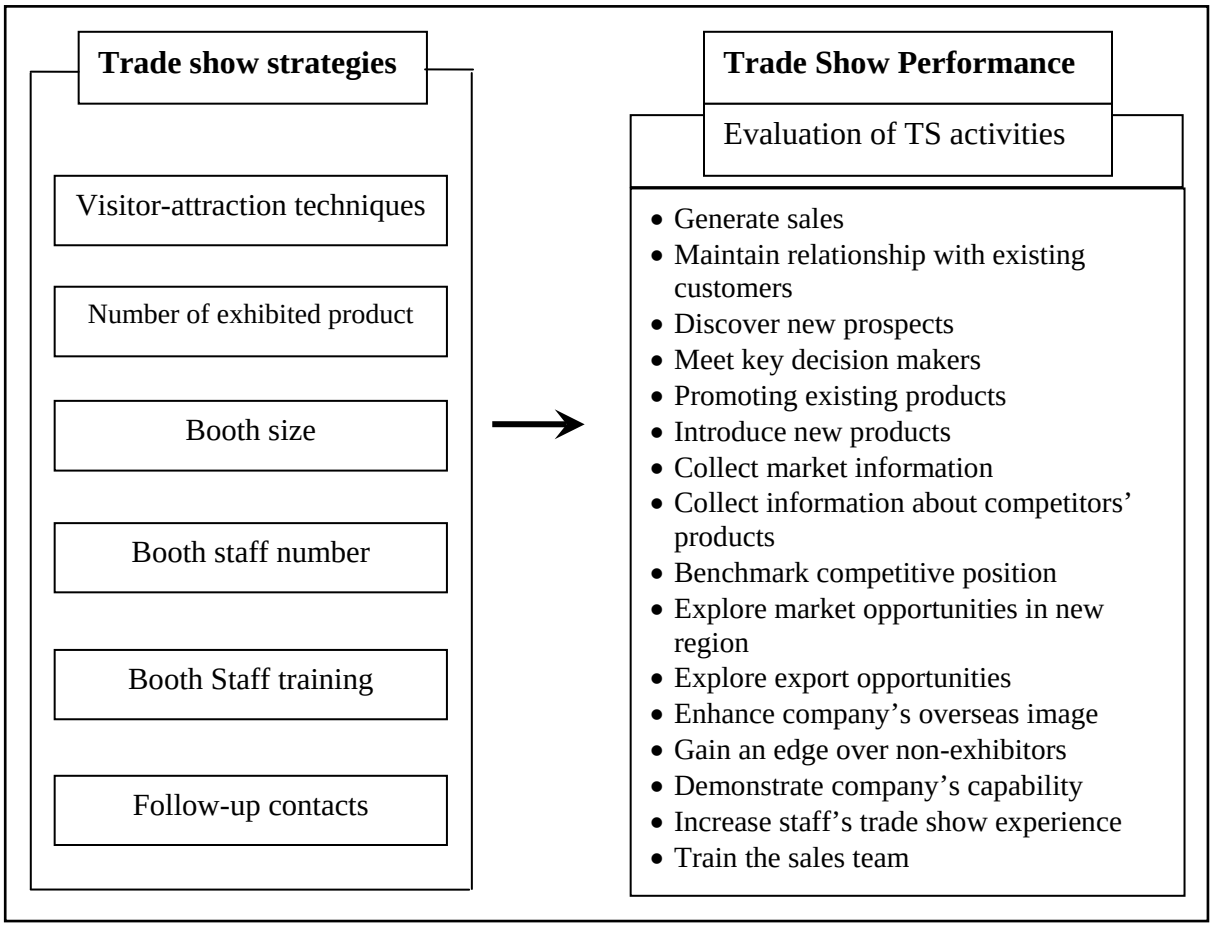

Figure 1. Framework of Trade Show Strategies and Trade Show Performance

Research Methodology

Data collection

This study defines the population as all exhibiting firms at the largest IFS-TS in China, the Chinese International Woodworking Machinery and Furniture Raw Material Fair in 2011 (CIFM'11). The official directory of exhibitors through the CIFM exhibition organizer, Koelnmesse Co., Ltd. was used as sample frame and a census was conducted to ensure adequate responses for further analysis and inferences. Online surveys were developed in two languages (English and Chinese) using SurveyMonkey. To establish translation equivalence, the original English-version instrument was translated into Chinese by a bilingual person and re-checked by another bilingual person. Observed discrepancies were addressed and resolved.

Before administering the survey, pretesting was performed with both an expert panel and an industry panel drawn from the database of exhibitors at CIFM'11 to assess the applicability of the online instrument and the precision of language translation and interpretation. The finalized surveys were sent to all exhibitors at CIFM'11 (n=970) with a customized message. Delivery failures and/or bounced email addresses reduced the total population to 940. After one week, a second survey was sent to non-respondents.

Two weeks after the initial online surveys, a systematic random sample of 160 non-respondents received follow-up phone calls, which further increased the number of respondents by 61 while also providing an opportunity to examine non-response bias.

A total of 300 responses were obtained, of which 267 respondents completed all questionnaire items related to trade show strategies and performance. Non-response bias check was performed on key demographic variables and selected TS performance and strategy variables resulting in no significant differences (at the p=.05 level) between respondents and non-respondents. Characteristics of respondents were categorized according to nationality of exhibitor (international/domestic), industry sector, and size of company (number of employees) (Table 1).

Table 1. Respondent Profile

Category	N	%
Nationality		
International	99	33.0
Domestic	201	67.0
Industry sector		
Woodworking machinery	57	19.0
Raw material and components	168	56.0
Hardware and other	75	25.0
Number of employees		
1-99	99	33.0
100-299	156	52.0
300-599	34	11.3
Over 600	11	3.7

Measurements

TS strategy variables from previous studies were used and included visitor-attraction techniques, number of exhibited products, follow-up contacts, booth size, number of booth staff, and booth staff training (Table 2). TS performance was measured via a 7-point scale on the 16 trade show activities validated in earlier studies.

Table 2. Description of measurement variable used in this study

Measure	Scale description	Source
Trade Show Strategy		
Visitor-attraction techniques	Total number of techniques used	Seringhaus and Rosson (2001)
Number of exhibited products	Number of displayed product at the booth	Kerin and Cron (1987)
Booth size	Booth space used in square meter	Dekimpe et al. (1997)
Booth staff number	Number of booth staff used	Gopalakrishna and Lilien (1995)
Booth staff training	Degree of systematic training received (5-point scale)	Gopalakrishna and Lilien (1995)

Follow-up contacts	Total number of contact tools used	Seringhaus and Rosson (2001)
Trade show performance	Performance on 16 identified international trade show activities (7-point scale)	Kerion and Cron (1987); Hansen (2004); Lee and Kim (2008); Tafesse and Korneliussen (2011)

Research Results

Multi-Dimensions of Trade Show Performance

To develop the multi-dimensional constructs of TS performance evaluated by TS activities, principal component analysis (PCA) was performed on the identified 16 TS activities using SPSS 20.0. PCA is a multivariate technique which determines the structure of measured variables by specifying condensed sets of dimensions with minimal loss of information (Fabrigar et al. 1999, Hair et al. 2010). The factorability of the performance variables was tested by using Kaiser-Meyer-Olkin (KMO) test to measure sampling adequacy and Bartlett's test for sphericity. A KMO value of 0.743 and significant (0.000) for Bartlett's test ensures the adequacy.

PCA analysis resulted in a reduction of the 16 TS activities into four components, suggesting the multi-dimensionality of TS performance. The four components explained 66 percent of the total variance in the data. The variability of the components was evaluated using Cronbach's alpha coefficient. Each component attained Cronbach's alpha greater than 0.7 (0.815, 0.842, 0.832, and 0.92) indicating satisfactory level of reliability. Based on the previous studies and the nature of the 16 TS activities in this study, we assigned these labels to the four components from PCA as our four TS performance dimensions: sales-relational, psychological-related, market-exploring, and competitive-intelligence[1].

Multiple Regression Analysis Results

Effects of TS Strategies on Sales-Relational Dimension

Visitor-attraction techniques, booth size, booth staff number and follow-up contacts were found to have a significant positive effect on the sales-relational performance dimension (Table 3). Unlike results from previous studies (Gopalakrishna and Lilien 1995, Li 2007, Lee and Kim 2008), booth staff training was not found to be significantly related to sales-relational performance dimension. Our study measured booth staff training by asking exhibitors to evaluate the level of systematic TS training booth staff received in preparation for CIFM'11, without asking for information on the detailed content of the actual training and ignoring the possibilities that the booth staff could be well-trained and experience prior to this particular show. Therefore, future studies may consider a better design of this variable for clearer interpretation.

[1] Due to the page limit, the PCA results are not presented in this paper.

Compared to visitor-attraction techniques, follow-up contacts were found to have a strong influence on sales-relational performance (beta coefficient: 0.254 vs. 0.134). At TSs, the interaction and buying process are often complex and may require months to complete. Sales leads generated at these shows may lead to actual contracts through follow-up contact activities. This could explain the strong impact of follow-up contacts on sales-relationship performance.

Table 3. Multiple Regression Analysis of TS Strategies Effects on TS Performance Dimensions

Independent variables	**Trade show performance dimensions**			
	Sales-Relational	Psychological-Related	Market-Exploring	Competitive-Intelligence
	----------Standardized regression coefficient (beta) [1]----------			
Visitor-attraction techniques	0.134*[2]	0.083	0.058	0.024
Number of exhibited products	0.041	0.091	-0.174**	-0.045
Booth size	0.253***	0.112*	-0.014	0.022
Booth staff number	0.179***	0.187**	0.136**	0.2**
Booth staff training	0.096	0.075	0.377***	0.238**
Follow-up contacts	0.254***	0.178**	0.12*	0.039
R square [3]	0.350	0.165	0.345	0.166
Adjust R square [4]	0.335	0.145	0.330	0.146

1. Standardized regression coefficient (beta) refers to how many standard deviations a dependent variable will change, per standard deviation increase in the independent variable, while controlling for other independent variables;
2. This is 2-tailed p-values associated with testing whether a given beta coefficient is significantly different from zero. * Significant at 0.10 level; ** significant at 0.05 level; *** significant at 0.001 level;
3. R square tells the proportion of variance in the dependent variable (TS performance dimension) which can be explained by the independent variables (TS strategies);
4. Adjust R square is intended to control for overestimates of the R square resulting from small samples, high collinearity or small subject/variable ratio.

Effects of TS Strategies on Psychological-Related Dimension

Booth size, booth staff number and follow-up contacts were found to be significantly positively related to psychological-related performance. This is in line with existing literature. A sizable booth and sufficient booth staff numbers attract more attendees to the booth so that booth staff has a greater chance to communicate directly with attendees. And the more booth staff engages in follow-up contacts, the more opportunities they have to interact with existing and/or potential customers. Through these communications and interactions, booth staff may enhance the corporate image and gain more experience.

Effects of TS Strategies on Market-Exploring Dimension

Booth staff number, booth staff training and follow-up contacts were found to have a significant positive impact on the market-exploring dimension. The number of exhibited products was found to be significantly negatively related to exhibiting firm's market-exploring performance. Since the CIFM'11 is a horizontal show, how exhibitors from different industry sectors interpret the number of exhibited products might be different.

For instance, hardwood lumber exhibitors may view the number of exhibited products as one for lumber instead of counting different species. Therefore, the interpretation of these results should be taken with caution.

Booth staff training was found to have a stronger influence on market-exploring performance than other variables (beta coefficient 0.377). It has been shown that better-trained booth staff can make more contacts with attendees and interact with prospects in an efficient way (Gopalakrishna and Lilien 1995, Li 2008). In this international TS venue (CIFM'11), well-trained booth staff were found to be more important to help a company identify prospective markets and evaluate threats and opportunities in these markets.

Effects of TS Strategies on Competitive-Intelligence Dimension

Booth staff number and booth staff training were found to have a significant positive impact on competitive-intelligence performance. Booth staffs are the personnel who identify potential prospects' needs and collect information on competitors' products, prices and strategies. Sufficient trained booth staff may help exhibiting company to collect, synthesize, and analyze competition and external environment that can affect company's plans, decisions and operations. These competitive-intelligence gathered by booth staff could lead to more insightful market-based actions.

Implications and Future Activities

China is the largest furniture producer and exporter in the world and demand for various raw materials, components, and hardware (furniture supplies) has grown dramatically. Chinese IFS-TSs provide a great opportunity for furniture supplying firms to sell products, network with hard to reach customers, build their reputation, collect foreign market information, and perform a variety of important sales and promotional activities in a cost-effective venue. This preliminary analysis of the effects of different TS strategies on each dimension of TS performance could help marketing executives tasked with TS planning decisions such as booth staffing practices, and appropriate follow-up contacts. Booth staffing may include sufficient and well-trained personnel to strengthen market research and competitive intelligence gathering. Follow-up efforts may be designed to improve relational and psychological-related performance (i.e., image building and experience gaining).

More analysis on how different TS strategies impact each dimension of TS performance will be carried out in future work to provide additional marketing insights and applications for TS decision markers and, in particular, those from furniture supplying industries.

Literature Cited

Bello, D. C. 1992. Industrial Buyer Behavior at Trade Shows. Journal of Business Research, (25): 59-80.

Bonoma, T. V. 1983. Get More Out of Your Trade Shows. Harvard Business Review, Jaunuary-February: 75-83.

Dekimpe, M. G., François, P., Gopalakrishna, S., Lilien, G. L., and Bulte, C. v. d. 1997. Generalizing about Trade Show Effectiveness: A Cross-National Comparison. Journal of Marketing, 61(4): 55-64.

Fabrigar, L. R., Wegener, D. T., MacCallum, R. C., and Strahan, E. J. 1999. Evaluating the Use of Exploratory Factor Analysis in Psychological Research. Psychological Methods, 4(3): 272-99.

Gopalakrishna, S. and Lilien, G. L. 1995. A three-stage model of industrial trade show performance. Marketing Science, 14(1): 22-43.

Gopalakrishna, S., Lilien, G. L., Williams, J. D., and Sequeira, I. K. 1995. Do Trade Shows Pay Off? Journal of Marketing, 59(July 1995): 75-83.

Hair, J. F., Black, B., Babin, B. J., and Anderson, R. E. 2010. Multivariate Data Analysis: A Global Perspective. Uper Saddle River, NJ: Prentice Hall.

Hansen, K. 2004. Measuring Performance at Trade Shows Scale Developement and Validation. Journal of Business Research, 57(1): 1-13.

Harriette, B.-O., Cromartie, J. S., Johnston, W. J., and Borders, A. L. 2010. The Return on Trade Show Information (RTSI): A Conceptual Analysis Journal of Business & Industrial Marketing, 25(4): 268-71.

Jin, X., Weber, K., and Bauer, T. 2010. The State of the Exhibition Industry in China. Journal of Convention & Event Tourism, 11(1): 2-17.

Kerin, R. A. and Cron, W. L. 1987. Assessing trade show functions and performance: an exploratory study. The Journal of Marketing, 51(3): 87-94.

Kijewski, V., Yoon, E., and Young, G. 1993. How exhibitors select trade shows. Industrial Marketing Management, 22(4): 287-98.

Lee, C. H. and Kim, S. Y. 2008. Differential Effects of Determinants on Multi-dimensions of Trade Shows Performance: By Three Stages of Pre-show, At-show, and Post-show activities. Industrial Marketing Management, 37(7): 784-96.

Li, L.-y. 2007. Marketing Resources and Performance of Exhibitor Firms in Trade Shows: A Contigent Resource Perspective. Industrial Marketing Management, 36: 360-70.

--- 2008. The effects of firm resources on trade show performance: how do trade show marketing processes matter? Journal of Business & Industrial Marketing, 23(1): 35-47.

Motwani, J., Rice, G., and Mahmoud, E. 1992. Promoting Exports Through International Trade Shows:A Dual Perspective. Review of Business, 13(4): 38-42.

Rice, G. 1992. Using the interaction approach to understand international trade shows. International Marketing Review, 9(4): 32-45.

Sandler, G. 1994. "Fair Dealing". The Journal of European Business, 4(Mar/Apr): 46-48, 52.

Seringhaus, F. H. R. and Rosson, P. J. 2001. Firm Experience and International Trade Fairs. Journal of Marketing Management, 17: 877-901.

Shi, W. and Smith, P. M. 2011. Exploring opportunities for U.S. hardwoods via international furniture supply trade shows in China. Presentation on International Scientific Conference on Hardwood Processing, October 16-18, 2011 Blacksburg, VA.

Shoham, A. 1999. Performance in Trade Shows and Exhibitions:A Synthesis and Directions for Future Research. Journal of Global Marketing, 12(3): 41-57.

Skallerud, K. 2010. Structure, Strategy and Performance of Exhibitors at Individual Booths versus Joint Booths. Journal of Business & Industrial Marketing, 25(4): 259-67.

Smith, T. M., Gopalakrishna, S., and Smith, P. M. 1999. 'Trade Show Synergy: Enhancing Sales Force Efficiency.' in Trade Show Synergy: Enhancing Sales Force Efficiency, 1-38. University Park, PA: Institute for the Study of Business Markets, The Pennsylvania State University.

--- 2004. The complementary effect of trade shows on personal selling. International Journal of Research in Marketing, 21(1): 61-76.

Smith, T. M., Hama, K., and Smith, P. M. 2003. The effect of successful trade show attendance on future show interest: exploring Japanese attendee perspectives of domestic and offshore international events. Journal of Business & Industrial Marketing, 18(4/5): 403-18.

Tafesse, W. and Korneliussen, T. 2011. The Dimensionality of Trade Show Performance in an Emerging Market. International Journal of Emerging Markets, 6(1): 38-49.

UFI 2011. Global exhibition industry statistics. Global Association of the Exhibition Industry: 31.

Controlled Growth and Properties of TiO_2 Coating onto Wood Surface Using a Low-Temperature-Cosolvent Hydrothermal Method

QingfengSun[1] - Yun Lu[1] - Jian Li[1] - Haipeng Yu[1] - Yixing Liu[1]**
[1] Key laboratory of Bio-based Material Science and Technology, Ministry of Education, Northeast Forestry University
* *Corresponding author*
yxliu@nefu.edu.cn and qfsun@nefu.edu.cn

Abstract

Growth of TiO_2 inorganic coating onto the wood surface has great research values and practical significance to the persistent, functional and high value-added utilization of wood materials. In the present paper, TiO_2 coating with controlled morphologies, sizes, and crystalline type was successfully grown onto the wood surface using a low-temperature-cosolvent hydrothermal method. SEM, EDS, FTIR, and XRD techniques were employed to characterize the as-prepared wood sample. Dimensional stability, UV-resistance, wettability, antibacterial property, and photocatalytic activities of the prepared wood sample were also measured. The morphologies, sizes, and crystalline type of TiO_2 grown onto the wood surface could be controlled through the regulations of the reaction parameters. Compared with the control wood, water absorption of TiO_2-coated wood decreased by 11 times after 90-days cold water immersion and the dimensions had no obvious change under different relative humidity (20%~90%). Rutile TiO_2-coated wood exhibited significant UV-resistance after 1200-hour UV irradiation due to high UV light absorption capability, superior light scattering property and high recombination of the photogenerated electron and hole of the deposited rutile TiO_2 on the wood surface. With further modification of the hydrothermal grown TiO_2, the hydrophilic wood surface presented the superhydrophobicity with WCA of 154°. Meanwhile, anatase TiO_2-coated wood revealed favorable antibacterial property and photcatalytic degradation of gas formaldehyde, the bactericidal rates of *E.coli* and *S. auresus* aureus were 94.7% and 92.6%, respectively; and the degradation rate of gas formaldehyde was about 98.7%. This paper potentially provided a feasible pathway for fabrication of inorganic/wood, fiber, or bamboo composites.

***Keywords*:** Low-temperature-cosolvent hydrothermal method, TiO_2, superhydrophobicity, photocatalysis, UV-resistance, wood.

Introduction

Wood continues to be used for wide applications (Fig. 1) because of its many excellent material properties (such as a good strength to weight ratio, aesthetic appearance etc.). However, it also suffers from a number of disadvantages which are presented in Fig. 2. Dimensional changes in response to altering atmospheric conditions, susceptibility to biological attack and changes in appearance when wood exposed to weathering place restrictions on the potential end-uses of wood.

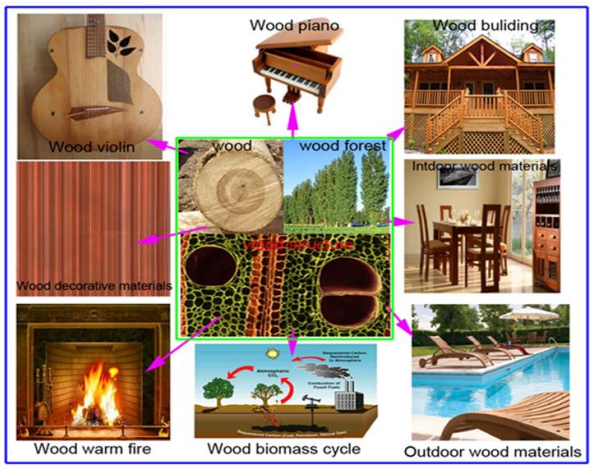

Fig. 1 Wide applications of wood

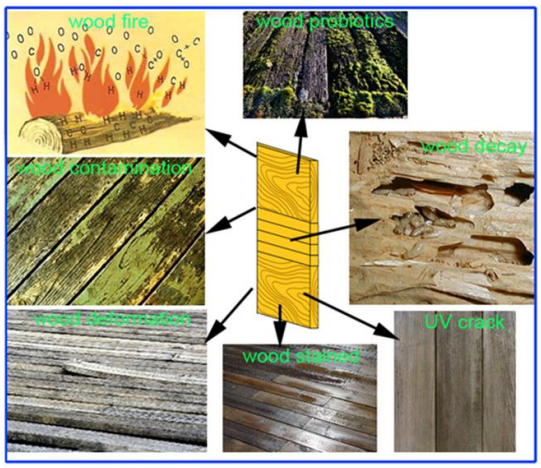

Fig. 2 Disadvantages of wood

Wood surface modification can overcome these wood disadvantages and grant some other unique characteristics such as superhydrophobicity, antibacterial property and so on. But conventional surface modification like mechanical brush or direct immersion can result in uneven dispersion and negative bonding which are illustrated in Fig. 3. The currently most method for surface modification methods are summarized as painting, sol-gel method, plasma or corona discharge etc. However, most of the above processes require expensive equipment or reagents, which suggest that they are unlikely to be used on a large scale in the foreseeable future. Therefore, how to develop a facile method for surface modification is a hot tissue in wood science and technology.

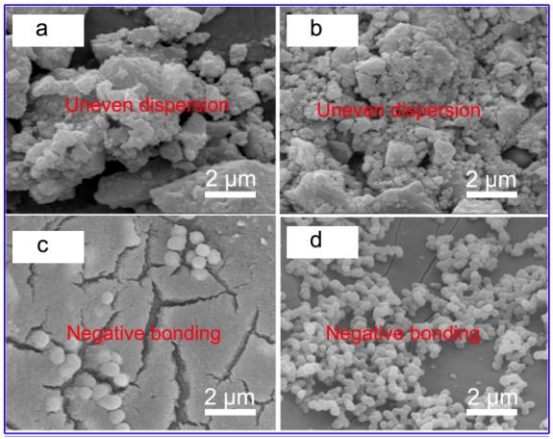

Fig.3 Disadvantages of conventional wood surface modification

As one of the most promising functional materials, titanium dioxide (TiO_2) has been extensively used in photocatalysis , solar cells and paints because of its superior chemical stability and nontoxicity. TiO_2 exists mainly in four polymorphs in nature, namely, anatase (tetragonal, space group $I4_1/amd$), rutile (tetragonal, space group $P4_2/mnm$), brookite (orthorhombic, space group P*bca*), and TiO_2 (B) (monoclinic, space group $C2/m$) (Fig. 4). Because of instability and scarcity of the latter two, the former two are often employed and studied in many fields.

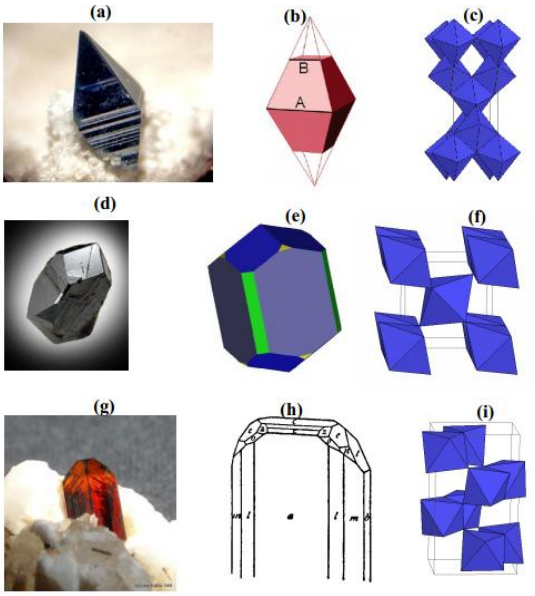

Fig. 4 Anatase, rutile and brookite TiO_2 single crystals in nature (a, d, g) and their crystal structure (b, e, h); unit cells (c, f, i) of anatase, rutile and brookite TiO_2

In the present paper, TiO_2 nanomaterials were grown onto the woo surface through LTCHM. The inherent properties of wood have been greatly improved and some new special characteristics were also granted by the thin grown inorganic TiO_2 layer.

Materials and Methods

Low-temperature-cosolvent hydrothermal method (LTCHM) is a new method proposed by our research group. Wood materials are set in the solution or colloid containing inorganic free ions or colloidal particles, which will grow into nanometer materials with the hydrothermal energy effect. The groups generated on the surface react with hydroxide radical on the wood surface and forms hydrogen bond, in this way to be connected on the wood surface and further generate the inorganic nanometer crystal layer on the wood surface. Finally, the wood properties are improved and new special properties are derived.

The possible mechanism of LTCHM is presented in Fig. 5.

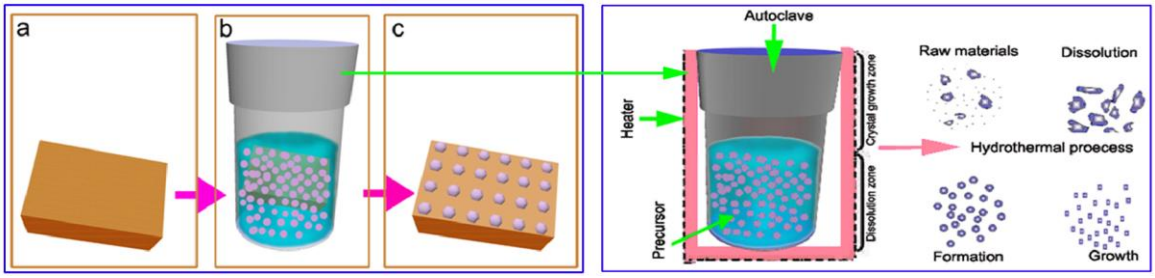

Fig. 5 Schematic illustration of the mechanism of LTCHM

Results and Discussion

Water resistance and dimensional stability Moisture absorption and dimensional distortion are the major drawbacks of wood utilization as building material. In this study, poplar wood coated with a thin layer of titanium dioxide (TiO_2) was prepared by LTCHM. Afterwards, its moisture absorption and dimensional stability were examined. SEM images revealed that the wood substrate was closely and entirely covered with the TiO_2 coat and micro-scale features were visible despite masking of the ultrastructural features of the cell wall (Fig. 6). To explore the effects of TiO_2 coating on the water-repellency and dimensional stability of wood, a 90-day water immersion test was carried out. Results show that water absorption and thickness swelling of TiO_2-coated wood increase very slowly and minimally. Weight change after 90 days of water immersion was reduced to 20.5%, nearly one-tenth of untreated control wood, and that maximum cross-sectional relative swelling was only 1.2% (Fig. 7). Specimens were conditioned for 3 months at different relative humidity (RH, 20%~90%) to determine the effects of RH on moisture absorption and dimensional swelling of TiO_2-coated wood. There was no change in weight after 3 months of being exposed to humidity conditions below 60% while there was linear weight increase above 60% RH, but the maximum change was less than 6%. Cross-sectional relative swelling was less than 0.3% below 60% RH but increased as RH exceeded 60%. The maximum change was approximately 3%. Anisotropic thickness swelling of wood was almost eliminated after coating. The corresponding graph data were shown in Fig. 8 and 9. It is obvious that TiO_2 coating can act as a moisture barrier for wood and is an exceptionally strong water vapor-inhibiting shield under very humid conditions.

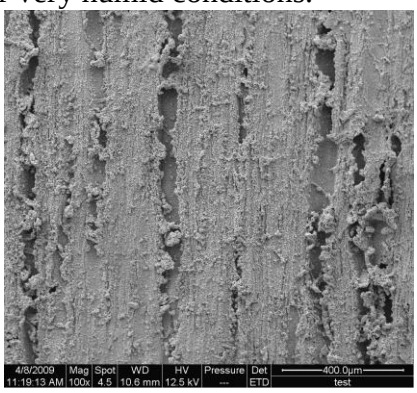

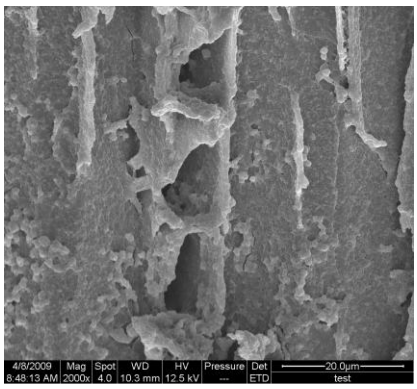

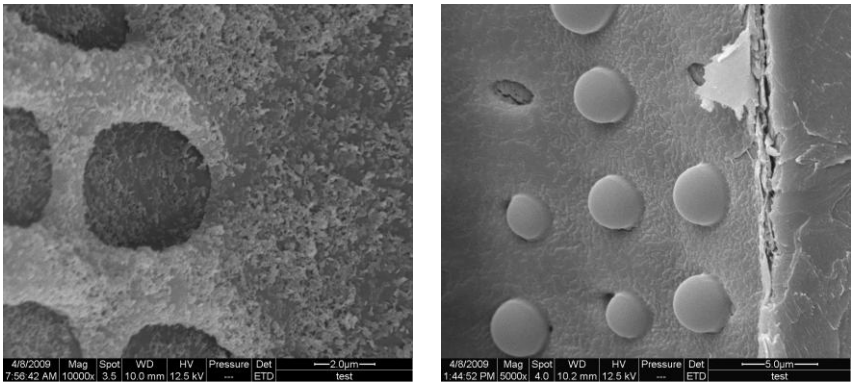

Fig. 6 SEM images of the TiO_2-coated wood at low (100×, scale bar 400 μm) and high (2 000×, scale bar 20 μm; 5 000×, scale bar 5 μm; 10 000×, scale bar 2 μm) magnification. Low-magnification image (a) shows the TiO_2 coat on the cut cellular nature of wood with its micro-scale features. High-magnification image (b) shows the changes in the lumen surface and ray cells with the film masking the exposed surfaces. (c) shows the vessel-ray cross-field pits in radial section and (d) shows the intervessel pits in tangential section.

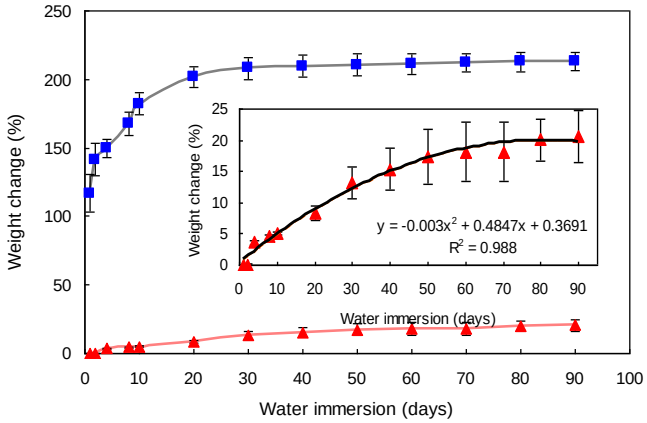

Fig. 7 the weight percentage change of untreated control wood (square symbols) and TiO_2-coated wood (triangle symbols) during ninety days of water immersion test

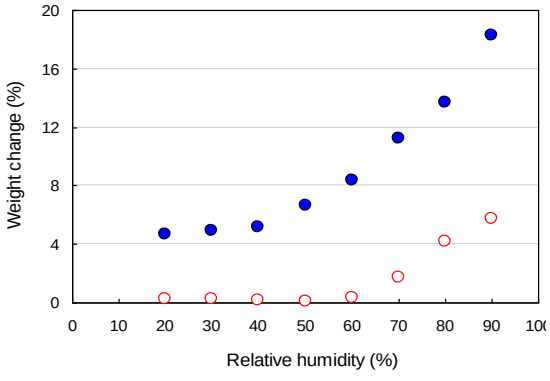

Fig. 8 the weight percentage change of untreated control wood (solid circle symbols) and TiO_2-coated wood (open circle symbols) due to water vapor absorption as different RH conditions for a period of three months

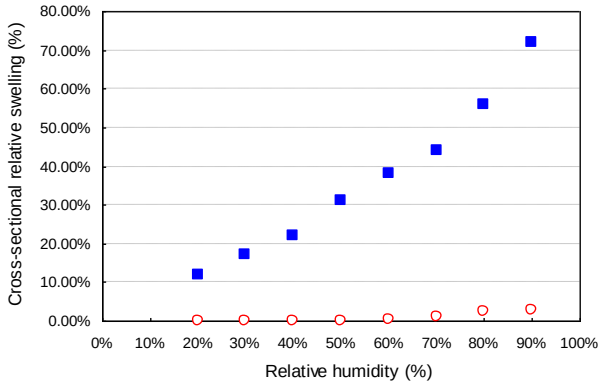

Fig. 9 Difference in cross-sectional relative swelling between the untreated control wood (solid square symbols) and TiO_2-coated wood (open circle symbols) due to water vapor absorption in different relative humidity conditions

UV-resistance Wood with UV-resistant ability was successfully prepared by depositing submicrometer-sized rutile TiO_2 spheres on wood surface using LTCHM. Meanwhile, anatase TiO_2 coated-wood was also fabricated using the LTCHM. SEM images showed the diameters of anatase and rutile TiO_2 were about 150 nm and 200 nm, respectively (Fig. 10). XRD and ATR-FTIR spectra demonstrated that firmly chemical bonds were formed at the interfaces between rutile TiO_2 and wood owing to the presence of hydroxyl groups, the schematic illustration was also proposed (Fig. 11 and 12). Accelerated aging test was used to measure the UV resistance of the original wood (OW), anatase TiO_2/wood (ATW) and rutile TiO_2/wood (RTW). Comparison with OW and ATW samples, RTW exhibited more superior UV-resistant ability due to high UV light absorption capability, superior light scattering property and high recombination of the photogenerated electron and hole of the submicrometer-sized rutile TiO_2 spheres on the wood surface (Fig. 13 and 14).

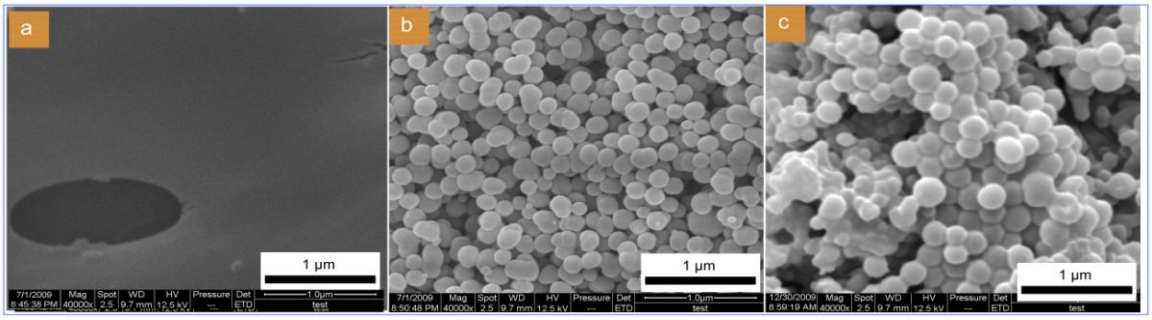

Fig. 10 SEM images of the (a) OW, (b) ATW and (c) RTW, respectively

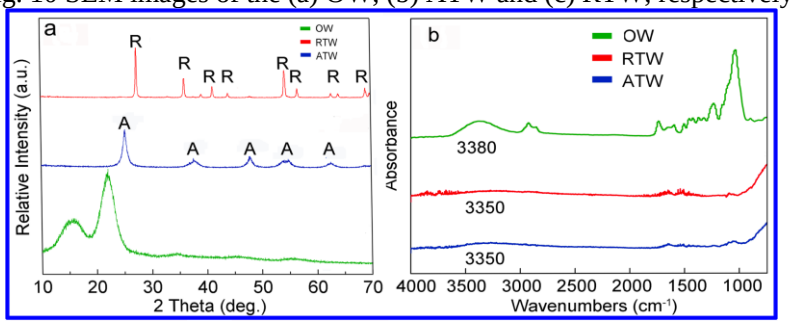

Fig. 11 XRD patterns (a) and ATR-FTIR spectra (b) of the OW, ATW and RTW, respectively

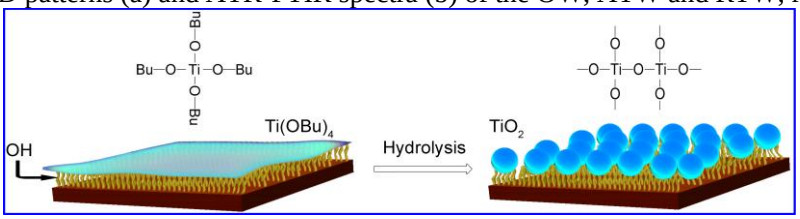

Fig. 12 Schematic illustration of the hydrothermal deposition of submicrometer-sized TiO_2 spheres on wood surface. Bu: C_4H_9

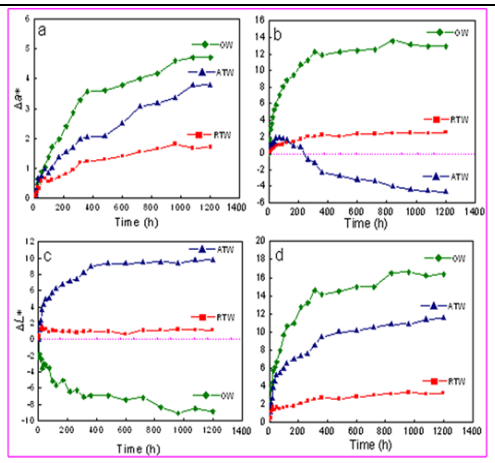

Fig. 13 Change tendency of Δ*a**, Δ*b**, Δ*L**, and Δ*E** of the OW, ATW and RTW, respectively

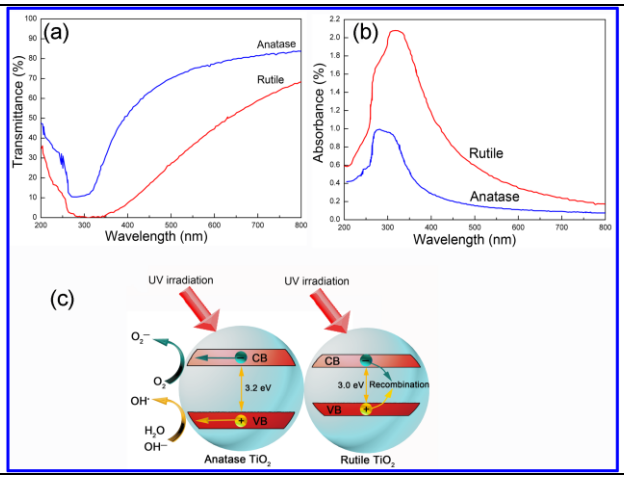

Fig. 14 (a) UV-vis transmittance spectra, (b) UV-vis absorbance spectra of ATW and RTW samples and (c) Photocatalytic reaction behaviors of anatase and rutile TiO_2 under UV irradiation

Wettability Inspired by surface topography-induced superhydrophobicity of lotus leaves and water strider's legs, a barrier TiO_2 coating could also be grown on wood surface to exhibit hydrophobic properties for meeting higher water repellent requirements. Hydrophobic $TiO_2$was grown onto the wood surface using LTCHM. XRD and FTIR proved that anatase TiO_2 chemically bonded to the wood surface through the combination of hydrogen groups during the hydrothermal process (Fig. 15 and 16). The values of WCAs manifested that the hydrophobicity of the treated wood was mainly dependent on specific reaction conditions, especially on reaction pH value and hydrothermal temperature. The highest WCA reached 154° when the hydrothermal temperature was 130 °C, the schematic illustrations for fabricating the hydrophobic wood were also described in the text. (Fig. 17 and 18).

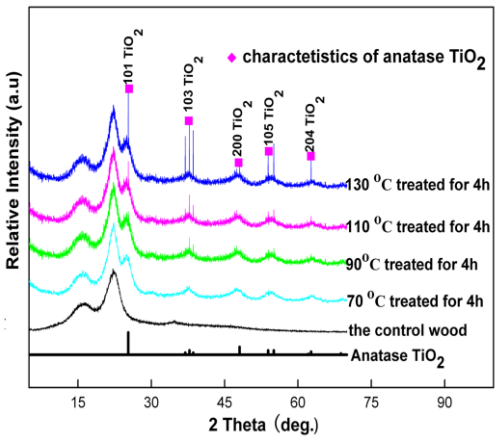

Fig. 15 XRD patterns of the control and treated wood at different temperatures

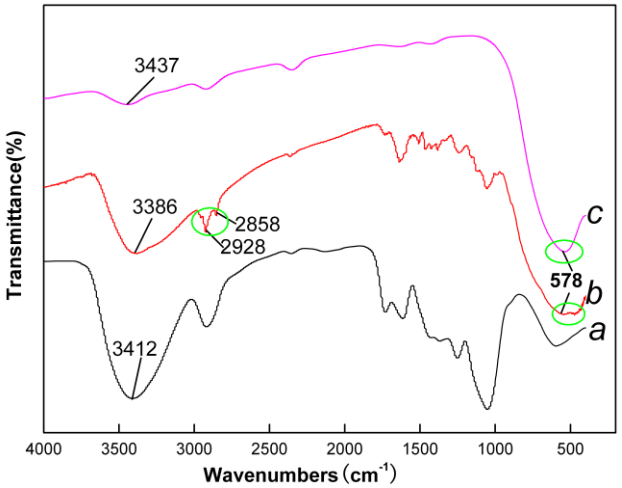

Fig. 16 FT-TR spectra of (a) the treated wood, (b) the control wood, and (c) nano-TiO_2

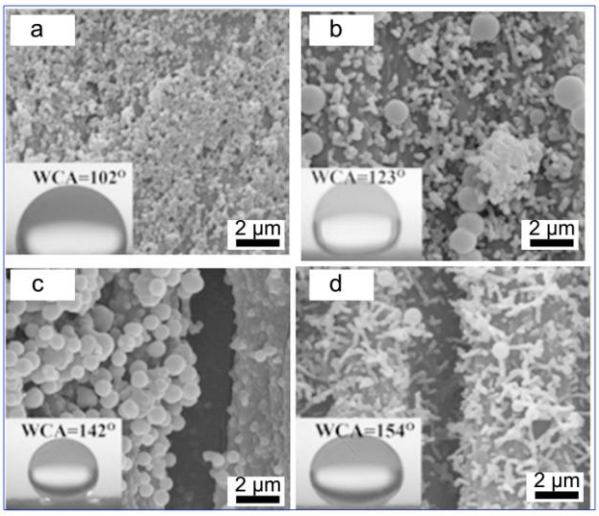

Fig. 17 WCA values of hydrophobic TiO_2-coated wood

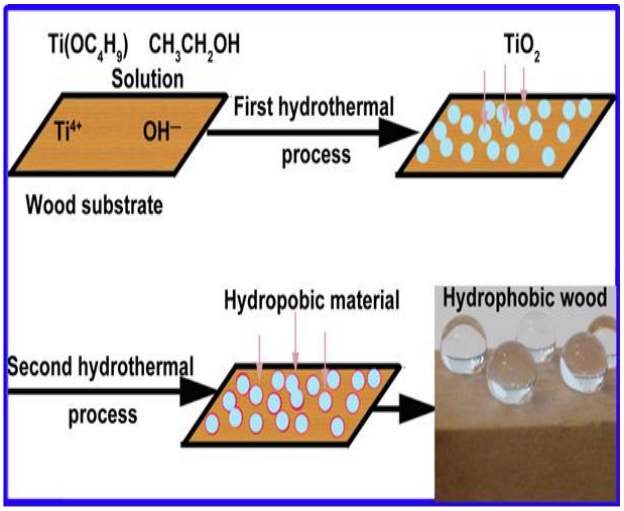

Fig. 18 Schematic illustrations for fabricating the hydrophobic wood using the hydrothermal method

Antibacterial property and degradation of formaldehyde Antibacterial property and the degradation ratio of anatase TiO_2 coated- wood were measured, respectively. From SEM images observation and XRD analysis, the wood surface was totally covered by smooth anatase TiO2 with the diameter of about 80~200 nm and AFM image revealed the thickness is about 1.2 μm (Fig. 19). The anatase TiO_2/wood has good antibacterial property and photcatalytic degradation of gas formaldehyde; the sterilization rates of *escherichia coli* and *staphylococcus aureus* are 94.7% and 92.6%, respectively under ultraviolet light (Fig. 20). The degradation rate of gas formaldehyde can amount to 98.7% in 168 hours at room temperature (Fig. 21). The mechanism of anatase TiO_2/wood can be ascribed to anatase TiO_2 grown onto the wood surface. Under the UV light, the electrons (e−) in the conduction band and positive holes (h+) in the valence band of TiO_2 were formed. Excited state electrons and holes can recombine and then dissipate the input energy as heat, get trapped in metastable surface states, and react with electro n donors/acceptors. If a suitable reductant (electron donor) or oxidant (electron acceptor) is available to trap the hole or electron, recombination is prevented and subsequent photocatalytic reactions may occur efficiently on the semiconductor surface. Actually, photocatalytic reactions may occur by either directly via the valence-band hole or indirect oxidation via the surface-bound hydroxyl radicals (i.e., a trapped hole at the particle surface reacts with HO or H_2O to be transformed into •OH). The •OH radicals produced by TiO_2 are one of the most powerful oxidizing species with an oxidation potential. Unlike other radicals, hydroxyl radicals are non-selective and thus readily attack a large group of organic chemicals to be hydroxylated or form partially oxidized intermediates. At sufficient contact time and proper operation conditions, it is practically possible to mineralize the target pollutants to CO_2 and H_2O (Fig. 22).

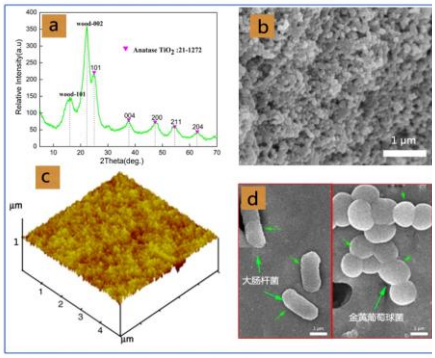

Fig.19 (a) XRD patterns, (b) SEM images, and (c) AFM imaged of treated wood, (d) SEM images of *E. coli* and *S. aureus*

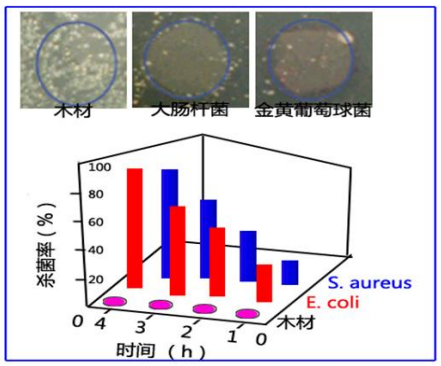

Fig. 20 Percent reduction of *E.coli* and *S. auresus* by the control wood and TiO_2-coated wood

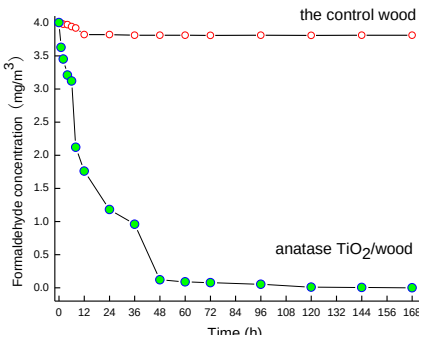

Fig. 21 Formaldehyde adsorption and degradation curve of control wood and TiO_2-coated wood

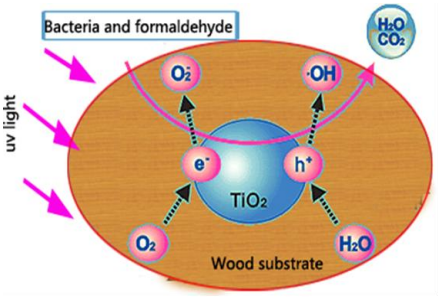

Fig. 22 Mechanism illustration of TiO_2-coated wood for antibacterial and photodegradative activities

Flame retardacy Using the cone calorimetry technique, the significant difference in combustion parameters between the untreated and the TiO_2 coated wood was observed. In comparison to the untreated wood, the burning time of TiO_2 coated wood was doubled (Fig. 23) and the initial yield of CO2 and CO was almost zero (Fig. 24). As a result, the TiO_2 coating can effectively act as a protective layer for wood and convert wood from a flammable material into a fireproof material.

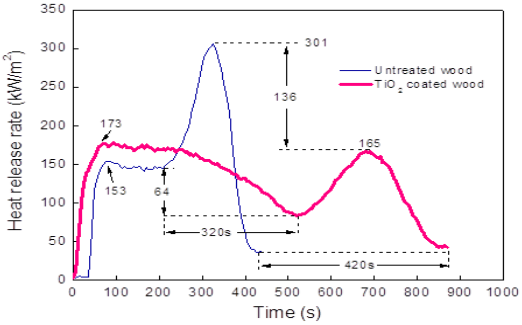

Fig. 23. HRR patterns of the untreated and TiO_2 coated wood

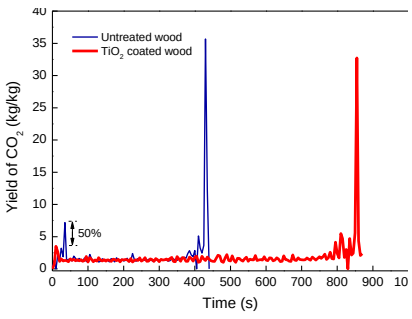

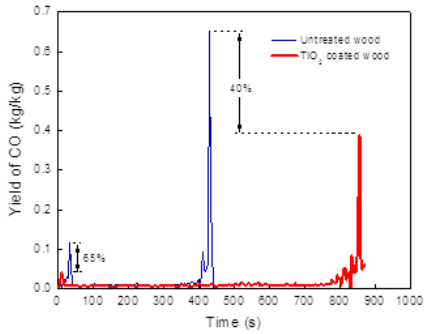

Fig. 24 CO2Y and COY patterns of untreated and TiO_2 coated wood

Conclusions

(1) Low-temperature-cosolvent hydrothermal method is a feasible method for growing inorganic TiO_2 onto the wood surface.
(2) With the combination of wood and the grown TiO_2, the intrinsic properties of wood can be improved and some special properties were also granted.
(3) This paper potentially also provides a feasible pathway for synthesis of inorganic nanomaterials/wood, fiber, or bamboo hybrid composites.

Acknowledgement

This work was supported by the Breeding Plan of Excellent Doctoral Dissertation of Northeast Forestry University (GRAP09), the Programme of Introducing Talents of Discipline to Universities of China (B08016) and National Natural Science Foundation of China (Grant No. 31170523).

References

H. Miyafuji,S. Saka. 1997. Fire-resisting properties in several TiO_2 wood-inorganic composites and their topochemistry. Wood Science and Technology. 31 (6): 449-455
C. Mai,H. Militz. 2004. Modification of wood with silicon compounds. Treatment systems based on organic silicon compounds — a review. Wood Science and Technology. 37 (6): 453-461
M. Tshabalala,L.-P. Sung: 'Wood surface modification by in-situ sol-gel deposition of hybrid inorganic–organic thin films', Journal of Coatings Technology and Research, 2007, 4, (4), 483-490
J. Li, H. Yu, Q. Sun, Y. Liu, Y. Cui and Y. Lu: 'Growth of TiO2 coating on wood surface using controlled hydrothermal method at low temperatures', Appl Surf Sci, 2010, 256, (16), 5046-5050
Q Sun, H Yu, Y Liu, J Li, Y Cui, Y Lu. 2010. Prolonging the combustion duration of wood by TiO2 coating synthesized using cosolvent-controlled hydrothermal method. Journal of Materials Science 45: 6661-6667
Q Sun, H Yu, Y Liu, J Li, Y Lu, JF Hunt. 2010. Improvement of Water Resistance and Dimensional Stability of Wood through Titanium Dioxide Coating, Holzforschung. 64: 757–761.
Q. Sun, Y Lu, Y Liu. 2011. Growth of hydrophobic TiO_2 on wood surface using a hydrothermal method. Journal of Materials Science. 46: 7706-7712.
Q Sun, Y Lu, H Zhang, H Zhao, H Yu, J Xu, Y Fu, D Yang, Y Liu. 2012. Hydrothermal fabrication of rutile TiO2 submicrospheres on wood surface: an efficient method to prepare UV-protective wood. Materials Physics and Chemistry. 133： 253-258

Hydrothermal Carbonization of Lignocellulosic biomass: Chemical and Structural Properties of the Carbonized Products

Ling-Ping Xiao[1] - *Zheng-Jun Shi*[1] - *Feng Xu*[2] - Run-Cang Sun[2,3*]

[1] Ph.D. Candidate, Institute of Biomass Chemistry and Technology, Beijing Forestry University, Beijing, China
[2] Professor, Institute of Biomass Chemistry and Technology, Beijing Forestry University, Beijing, China
* *Corresponding author*
rcsun3@bjfu.edu.cn
[3] Professor and Director, State Key Laboratory of Pulp and Paper Engineering, South China University of Technology, Guangzhou, Guangdong, China

Abstract

Hydrothermal carbonization (HTC) is a novel thermochemical conversion process to convert lignocellulosic biomass into value-added products. In this work, two different biomass materials: corn stalk and *Tamarix ramosissima* were used as feedstock. HTC processes were performed at the temperature of 250 °C for 4 h, using a batch reactor system. Chemical and structural characterization of the solid materials was carried out by elemental analysis, nitrogen adsorption, scanning electron microscopy, X-ray diffraction, and spectroscopic techniques including Fourier transform infrared, X-ray photoelectron, and Raman. The results indicated HTC treatment brought an increase of the higher heating value up to 29.2 and 28.4 MJ/Kg for corn stalk and *T. ramosissima*, respectively, corresponding to an increase of 66.8% and 58.3% as compared to the natural biomass. The surface area determined by Brunauer–Emmett–Teller analyses was 10.8 and 11.3 m^2/g, which was 4.8 and 10.9 fold for the hyrochars of corn stalk and *T. ramosissima*, respectively. Additionally, liquid products extracted with ethyl acetate were analyzed by gas chromatography–mass spectrometry. The identified compounds were phenolic and furan derivatives, confirming the mechanisms of dehydration, decarboxylation, and demethanation reactions during the carbonization processes. Based on these results, HTC is considered to be a potential treatment in a lignocellulosic biomass refinery.

***Keywords*:** Hydrothermal carbonization, biomass, SEM, FT-IR, raman, XPS, GC–MS

Introduction

Hydrothermal carbonization (HTC) is a novel thermochemcial conversion process to convert lignocellulosic biomass into value-added products. Recently, HTC method has attracted a great deal of attention because it uses water which is inherently present in green biomass, non-toxic, environmentally benign, and inexpensive medium (Libra et al. 2011). Typical HTC of biomass is achieved in water at elevated temperatures (180–250 °C) under saturated pressures (2–10 MPa) for several hours (Funke and Ziegler 2010, Mumme et al. 2011). Some publications have reported on the chemical transformations of model compounds under pressure in HTC processes, particularly cellulose, pentoses/hexoses (glucose and xylose), starch, and phenolic compounds (Titirici et al. 2008, Sevilla and Fuertes 2009, Ryu et al. 2010). However, the majority focused on model compounds and establishing the reaction kinetics and reaction pathways of such compounds in hydrothermal medium. So far, literature on the hydrothermal treatment of real complex biomass provides a rather inconsistent picture, and only few reports have provided a detailed description on the chemical composition of the reaction products. Therefore, the main objective of this work was to gain insights into the underlying mechanisms during HTC. This study focused on the reaction of natural complex biomass, their chemical and structural properties of carbonaceous solids (hydrochars) as well as the degradation products.

Materials and Methods

Materials. The dried raw materials were firstly ground to pass a 40-mesh screen and Soxhlet-extracted with ethanol/benzene (1:2, v/v) for 8 h. The extractive-free samples were oven-dried at 60 °C for 16 h and stored in a desiccator for use. All chemicals used were of analytical grade purchased from Sigma-Aldrich Company (Beijing).

Experimental procedure. The hydrothermal processes were carried out using 10 g feedstock dispersed in 100 mL of distilled water in a 1-L Parr stirred pressure reactor (Parr Instrument Company, Moline, Illinois) which was heated up to 250 °C at a heating rate of around 4 °C min^{-1} (pressure at 250 °C of around 580 psi). The reactor was maintained at this temperature for 4 h with an agitation speed of 150 rpm. The reaction mixture, consisting of a liquid solution and solid phase (hydrochar) was collected in a glass beaker for separation by filtration and the solid was washed thoroughly with hot distilled water and then dried in an oven at 60 °C overnight. The hydrochar samples obtained from the feedstocks of CS and TR were denoted as CS250 and TR250, respectively.

Characterization of the hydrochars and liquors. The chemical compositions of the untreated and HTC treated biomass were determined using two-step acid hydrolysis and given in detail elsewhere (Xiao et al. 2011). Elemental analysis (C, H, N, and S; O content by difference) of the samples was performed in a vario MACRO cube (Elementar Analysensysteme GmbH, Germany). The surface area of the hydrochar sample was estimated by the standard Brunauer–Emmett–Teller (BET) method (nitrogen absorption isotherms). FT-IR spectra were recorded on an FT-IR spectrophotometer. Raman spectra

were recorded at ambient temperature on a Renishaw RM 2000 microspectrometer. Scanning electron microscopy (SEM) images were obtained with a Quanta 200F equipment (FEI, USA). X-ray photoelectron spectroscopy (XPS) were recorded performed using a Thermo Scientific Escalab 250Xi instrument equipped with Al K_α radiation ($h\nu$ = 1486.6 eV). Binding energies for the high-resolution spectra were calibrated by setting C 1s at 284.8 eV. The degradation products in the liquor fractions were analyzed by gas chromatography–mass spectrometry (GC–MS) (GC: GC 7890A; MS: Agilent MS 5975C). Agilent HP-5MS capillary column (30 m × 0.25 mm × 0.25 μm) column and the NIST mass spectral library were used for the identification of compounds.

Results and Discussion

Yield and chemical characteristics of the hydrochars

The solid yield of biomass after HTC and its composition are presented in Table 1. As expected, the yields of hydrochars after the treatment were 35.5% and 38.1% for CS and TR, respectively, due to the high solubilization of components in hydrolysis liquors. On the other hand, the coal-like solid products were mainly composed of lignin, suggesting that there was a nearly complete hydrolysis of hemicelluloses and cellulose. Additionally, the fixed carbon contents in the both hydrochars were similar, ranging from 54.2% to 58.6%, indicating that a large fraction of the carbon in the lignocellulosic biomass was stored. The rest of the carbon (~41.4–45.8%) was mainly contained in the organic compounds that were dispersed in the aqueous phase, which will be discussed afterwards.

The elemental composition (C, O, and H) of the solid materials changed markedly as the result of HTC. The carbon content increased from 46.8% to 48.0% in the raw material to 71.4–72.1% in the hydrochar samples. Simultaneously, a reduction in the oxygen and hydrogen contents indicated that the hydrochar samples were less condensed (higher O/C and H/C atomic ratios). This was verified by the van Krevelen diagram (van Krevelen 1950) as illustrated in Figure 1, which allows for delineation of reaction pathways. In this diagram, the straight lines represent the dehydration, decarboxylation, and demethanation processes. The H/C–O/C atomic ratios for other substances (wood, cellulose, lignin, lignite coal, and bituminous coal) reported previously are also plotted in the same figure for comparison. The position of the hydrochars on this plot was similar to those associated with bituminous and lignite coals. Moreover, the energy contents of the raw materials and the corresponding hydrochars were also calculated and listed in Table 1. HTC processes brought an increase in the higher heating value (HHV) of the hydrochars up to 29.2 and 28.4 MJ/kg for CS and TR, respectively, which corresponded to an increase of 1.67- and 1.58-fold when compared with the raw materials.

The quantitative summary of surface area and pore volume is also listed in Table 1. A significant increase in the quantity of adsorbed nitrogen gas was observed for the carbonaceous hydrochars, indicating a higher specific surface area and a greater pore volume. The BET surface area increased from 2.3 to 10.8 m^2/g and from 1.0 to 11.3 m^2/g, which was 4.8 times and 10.9 times greater for the hyrochars of CS250 and TR250, respectively. Additionally, there was a 5.3-fold and 11.6-fold increase in the measured pore volume after HTC.

Table 1 Chemical characteristics and product yields of the raw materials and the hydrochars prepared from the HTC of CS and TA.

Sample	Elemental composition (%)			Atomic ratio		Yield (%)	Fixed carbon yield (%)	Klason lignin (%)	HHV (MJ/kg)[a]	BET surface area (m^2/g)	BJH pore volume (cm^3/g)
	C	H	O	O/C	H/C						
CS	46.84	6.26	40.70	0.652	1.591	–	–	20.96	17.51	2.26	0.01
CS250	71.36	5.60	16.27	0.171	0.935	35.48	54.21	96.50	29.21	10.79	0.03
TR	47.95	6.62	43.37	0.679	1.646	–	–	15.69	17.93	1.03	0.01
TR250	72.08	5.42	20.87	0.217	0.896	38.10	58.55	94.65	28.38	11.33	0.02

[a] HHV, higher heating value. Evaluated using the Dulong's Formula: HHV = 0.3383 × C + 1.422 × (H – O/8).

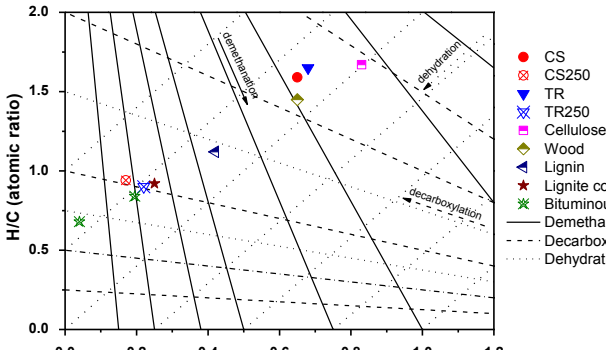

Figure 1. Atomic H/C versus O/C ratios (van Krevelen diagram) of the feedstocks and hydrochars prepared from the HTC of CS and TR. The atomic ratios of bituminous (two data points representing a range of H/C and O/C ratios), wood, cellulose, lignin, and lignite coals are included for comparison. The lines represent demethanation, dehydration, and decarboxylation pathways.

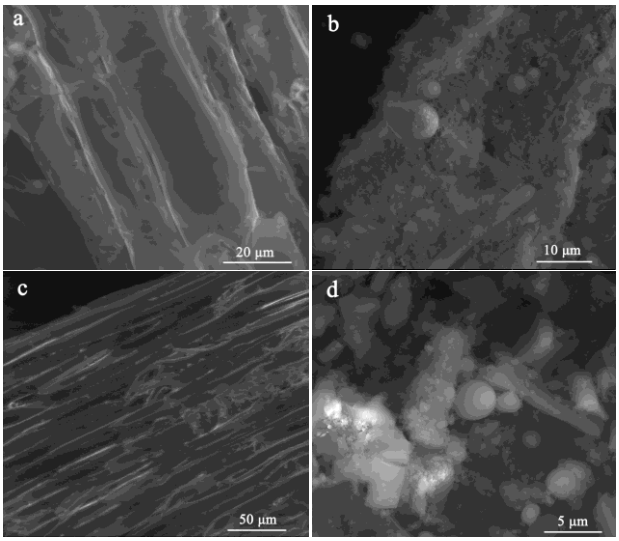

Figure 2. SEM images of CS (a) and the corresponding hydrochar CS250 (b); TR (c) and the corresponding hydrochar TR250 (d).

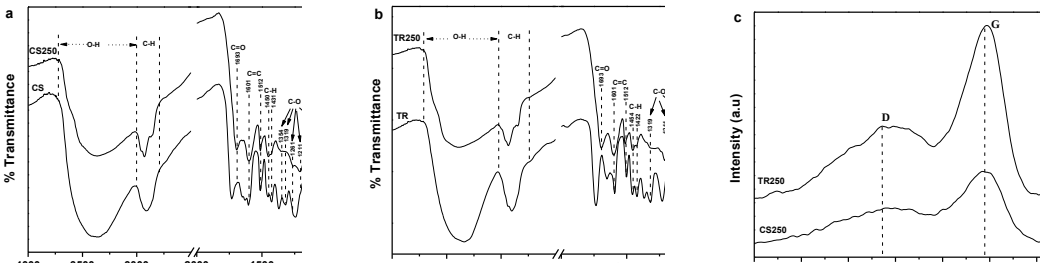

Figure 3. FT-IR and Raman spectra of feedstocks and hydrochars prepared by HTC at 250 °C for 4 h. (a) FT-IR spectra of CS and the corresponding hydrochar CS250; (b) FT-IR spectra of TR and the corresponding hydrochar TR250; (c) Raman spectra of hydrochars CS250 and TR250.

Structural prosperities of the carbonized hydrochars.

SEM images of the raw materials and the corresponding hydrochars are illustrated in Figure 2. A prominent change in the hydrochars was a more uneven and rougher surface morphology when compared to the pristine biomass.

Figure 3a and b shows the FT-IR spectra of the feedstocks and the corresponding hydrochars prepared by HTC at 250 °C for 4 h. The remarkable changes of the transmittance peaks mainly appeared in the range of 1800–750 cm^{-1}. It can be seen that the peaks at 1736 (C=O stretching), 1160 (C–O–C asymmetry stretching), and 899 cm^{-1} (C–O–C stretching at β-glycosidic linkages) in the untreated feedstock spectra were absent in the hydrochar spectra, revealing that cellulose and hemicelluloses were thermally decomposed. Lignin, unlike cellulose and hemicelluloses, is aromatic and possesses olefinic carbon–carbon double bonds in cyclic structures and side chains. The peaks at 1512, 1427, and 1601 cm^{-1} were well represented, suggesting that the aromatic nuclei of lignin were almost stable during the hydrothermal treatment. This result confirmed that the compact matrix of lignocellulosic material was significantly decomposed, and the remaining solid product was mainly composed of lignin, corroborating the aforementioned composition analyses in Table 1. Moreover, a new vibration band at 1693 cm^{-1}, corresponding to C=O groups, appears in the hydrochar material, indicating the aromatization of the samples. The intensities of the peaks at 1512, 1450, 1422, and 1261 cm^{-1} were slightly decreased, suggesting the degradation of organic matter to some degree. In addition, an absorption band at 837 cm^{-1} (aromatic out-of-plane C–H deformation and bending) was observed, which is attributed to the existence of phenolic compounds in the carbonaceous products, in accordance with the results reported by Ryu et al. (2010). A comparative analysis of the FT-IR spectra of the hydrochars and those of the raw materials of CS and TR suggested that dehydration and aromatization processes occurred during the HTC treatment, confirming the results deduced from the evolution of the O/C–H/C atomic ratios in the van Krevelen diagram (see Fig. 1).

The Raman spectra of the carbonaceous samples in the range of 1100–1800 cm^{-1} with λ_0 = 514.5 nm are presented in Figure 3c. All the curves exhibit two broad and overlapping peaks with intensity maximas at ~1370 and ~1590 cm^{-1}, which correspond to the D and G bands of the disordered graphite, respectively (Cuesta et al. 1994). The vibration mode of the D peak is assigned to ring-breathing vibrations in benzene or condensed benzene rings in amorphous carbon films, whereas for the G peak involves the in-plane bond-stretching motion of pairs of C sp^2 atoms both in aromatic and olefin molecules. The G and D bands observed in the carbonaceous materials were relatively broad, indicating that the crystallite size of the carbon in the hydrochar samples was small. Therefore, both peaks revealed the presence of small aromatic clusters in the carbonaceous materials, corroborating the aromatization of the materials observed by FT-IR spectroscopy.

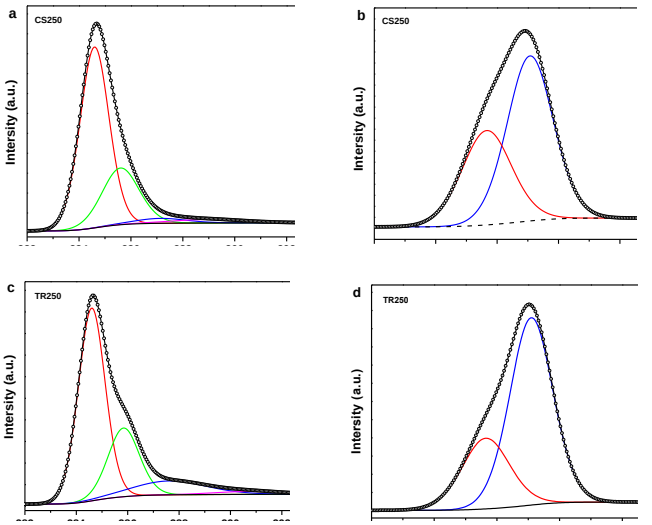

Figure 4. XPS spectra of C 1s (a: CS250, c: TR250) and O 1s (b: CS250, d: TR250) core-level spectra of the hydrochar samples.

XPS was used to characterize the oxygen functional groups at the outer surface of the hydrochar particles. The C 1s core level spectra obtained for the hydrochar samples, together with the peak-fitting of its envelope, are deposited in Figure 4. Each spectrum was resolved into four individual component peaks, namely: (1) aliphatic or aromatic carbon group (CH_x, C–C/C=C; BE = 284.6 eV); (2) sp^3 hybridized carbon atoms (BE = 285.6 eV); (3) carbonyl groups (>C=O; BE = 287.6 eV); (4) carboxylic groups, esters or lactones (>COOR; BE = 290.7 eV) (Sevilla et al. 2011). On the other hand, the O 1s region in the XPS spectra of hydrochar materials exhibited two deconvoluted peaks at 533.1 and 531.7 eV, representing C=O and C–OH/C–O–C groups, respectively. These results indicated that the hydrochars obtained were enriched in oxygen-containing groups. Meanwhile, a comparison of the (O/C) atomic ratios determined by elemental analysis (see Table 1) with those calculated by XPS (0.169 and 0.230 for CS250 and TR250, respectively) confirmed that the (O/C) atomic ratios in the core and in the shell of the particles were quite similar, further demonstrating that there was also a high concentration of oxygen in the inner part of the hydrochar materials (Sevilla and Fuertes 2009).

Composition of hydrothermal liquors.

Figure 5 shows the results of GC–MS analysis of the ethyl acetate extracts of liquors from the HTC of CS and TR, respectively. The GC–MS analysis of the liquid products revealed that the main sugar-derived products were furfural, 2-ethyl-5-methyl-furan, and 2-hydroxy-3-methyl-2-cyclopenten-1-one. The amounts of these sugar-derived products from CS were lower than those of TR. It was found that the main phenol monomers of the ethyl acetate extracts from CS consisted mainly of 2,6-dimethoxyl, butyl 2-methylpropyl ester-1,2-benzenedicarboxylic acid, and 4-ethoxy-2,5-dimethoxybenzaldehyde. The results showed that these organic molecules ranged from C_8 to C_{16}. On the other hand, the major hydrocarbons of the lignin-derived compounds of TR were 2,6-dimethoxyphenol, 3-methoxy-1,2-benzenediol, *p*-xylene, and phenol, which were in the range of C_6–C_8. Compared to CS, TR produced more benzenediol and phenol derivatives. Additionally, the identified compounds were phenolic compounds and furan derivatives, confirming the mechanism of dehydration, decarboxylation, and demethanation reactions during the carbonization process, in well agreement with the results in the van Krevelen diagram aforementioned. Moreover, phenolic compounds from plant biomass are attractive renewable feedstock to produce phenolic precursors, polymer substitution, carbon fibers, and natural antioxidants as well as green aromatic-based compounds (Lavoie et al. 2011).

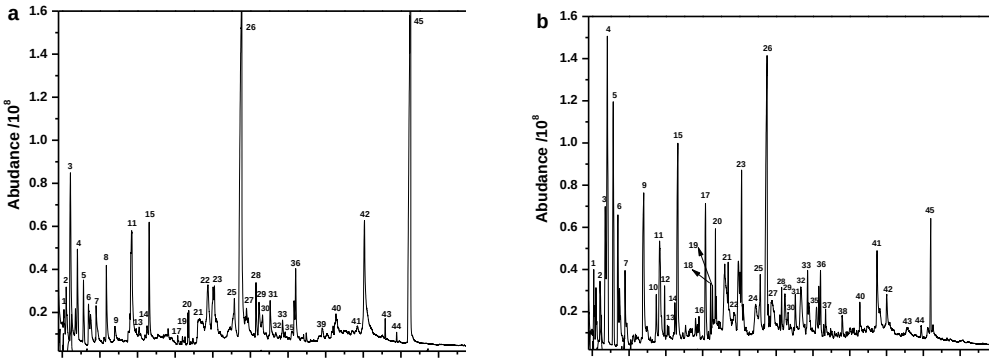

Figure 5. GC–MS chromatograms of the ethyl acetate extracts of the hydrolysates obtained by HTC of CS (a) and TR (b) with internal tetracosane standard (100 μg/mL).

Conclusions

Hydrothermal carbonization of lignocellulosic biomass completely broke down the plant cell wall and allowed rapid conversion of biomass into a carbon-rich and lignite-like product (hydrochar). The carbonized products were composed of water-soluble compounds and solid residues. The aqueous phase contained sugar and lignin derived compounds, which may be desirable feedstocks for biodiesel and chemical production. The resulting solid products consisted mainly of lignin with a high degree of aromatization and a large amount of oxygen-containing groups. Moreover, the hydrochar had a considerably higher heating value than that of the raw material. At last, we proposed a schematic representation of the possible formation process of hydrochars from lignocellulosic biomass via hydrothermal carbonization as shown below:

Acknowledgements

The authors are grateful for the financial support from the Major State Basic Research Projects of China (973-2010CB732204), National Natural Science Foundation of China (31110103902), and China Ministry of Education (111).

References

Cuesta, A. Dhamelincourt, P. Laureyns, J. Martinez-Alonso, A. Tascón, J.M.D. 1994. Raman microprobe studies on carbon materials. Carbon 32(8): 1523–1532.

Funke, A. Ziegler, F. 2010. Hydrothermal carbonization of biomass: a summary and discussion of chemical mechanisms for process engineering. Biofuel. Bioprod. Bior. 4(2): 160–177.

Lavoie, J.M. Baré, W. Bilodeau, M. 2011. Depolymerization of steam-treated lignin for the production of green chemicals. Bioresour. Technol. 102(7): 4917–4920.

Libra, J.A. Ro, K.S. Kammann, C. Funke, A. Berge, N.D. Neubauer, Y. Titirici, M.M. Fühner, C. Bens, O. Kern, J. Emmerich, K.H. 2011. Hydrothermal carbonization of biomass residuals: a comparative review of the chemistry, processes and applications of wet and dry pyrolysis. Biofuels 2(1): 71–106.

Mumme, J. Eckervogt, L. Pielert, J. Diakité, M. Rupp, F. Kern, J. 2011. Hydrothermal carbonization of anaerobically digested maize silage. Bioresour. Technol. 102(19): 9255–9560.

Ryu, J. Suh, Y.W. Suh, D.J. Ahn, D.J. 2010. Hydrothermal preparation of carbon microspheres from mono-saccharides and phenolic compounds. Carbon 48(7): 1990–1998.

Sevilla, M. Fuertes, A.B. 2009. The production of carbon materials by hydrothermal carbonization of cellulose. Carbon 47(9): 2281–2289.

Sevilla, M. Maciá-Agulló, J.A. Fuertes, A.B. 2011. Hydrothermal carbonization of biomass as a route for the sequestration of CO_2: chemical and structural properties of the carbonized products. Biomass Bioenergy 35(7): 3152–3159.

Titirici, M.M. Antonietti, M. Baccile, N. 2008. Hydrothermal carbon from biomass: a comparison of the local structure from poly- to monosaccharides and pentoses/hexoses. Green Chem. 10(11): 1204–1212.

van Krevelen, D.W. 1950. Graphical-statistical method for the study of structure and reaction processes of coal. Fuel 29(12): 269–284.

Xiao, L.P. Sun, Z.J. Shi, Z.J. Xu, F. Sun, R.C. 2011. Impact of hot compressed water pretreatment on the structural changes of woody biomass for bioethanol production. BioResources 6(2): 1576–1598.

Optimal Percentage of Pulp and Paper Mill Secondary Sludge Incorporated in particleboard

Suying Xing[1]-Bernard Riedl[2] – Ahmed Koubaa[3] –James Deng[4]*

[1]PhD Student, Centre de Recherche sur le Bois, Université Laval, Québec, 2425 rue de la Terrasse, Québec QC, G1V 0A6, Canada
suying.xing.1@ulaval.ca
[2]Professor, Centre de Recherche sur le Bois, Université Laval, Québec, 2425 rue de la Terrasse, Québec QC, G1V 0A6, Canada
* *Corresponding author*
Bernard.Riedl@sbf.ulaval.ca
[3] Professor, Université du Québec en Abitibi-Témiscamingue, 445 boul. de l'Université, Rouyn-Noranda QC, J9X 5E4, Canada
Ahmed.Koubaa@uqat.ca
[4] Scientist and group leader, FPInnovations-Forintek Division, 319 rue Franquet, Québec QC, G1P, 4R4, Canada
James.Deng@Fpinnovations.ca

Abstract

The pulp and paper mill produce a considerable amount of sludge. Their composition mainly depends on the type of paper produced and the origin of cellulose fibres. In this work, the secondary sludge (SS) from three conventional pulping processes (thermomechanical pulp (TMP), chemical-thermomechanical pulp (CTMP) and Kraft pulp (Kraft)) was collected from three mills. The buffering capacity and pH of SS and particle of SPF (spruce, pine and fir) were measured. The dry SS as co-adhesive was added in the formulation of particleboard manufacturing. The urea-formaldehyde (UF) content is 7% (dry weight of resin per dry weight of particle), and the different percentages of secondary sludge (dry weight of SS per dry weight of particle) were added in the particleboards. Each combination of urea-formaldehyde--secondary sludge type--secondary sludge content was considered as a different formulation, with 3 replications for each one. The internal bond strength (IB) was measured. Results indicated that secondary sludge can be used in particleboard manufacturing and there is an optimal percentage for each SS type, whereas the value of percentage depends on the type of SS and paper mill.

***Keywords*:** Particleboard, Secondary sludge, Urea-formaldehyde, Internal bond, optimal percentage.

Introduction

Wastewater treatment processes in pulp and paper mills generate large amounts of solid residues known as pulp and paper sludge. Sludge production accounted for about 4.8% of mill production in 2009 (MDDEP 2009). Similarly, sludge generated by the European pulp and paper industry accounts for about 4.3% of final mill production (Ochoa de Alda 2008). This huge quantity of waste biomass has posed serious changes for the paper industry, requiring extra economic resources to deal with disposal and environmental issues. The water treatment process typically includes primary treatment followed by secondary treatment (Smook 2002). Primary treatment removes suspended solids from wastes. The solid residue obtained after thickening is called primary sludge (PS). Waste waters from primary treatment go to secondary treatment, also called biological treatment, and the solid residue obtained after thickening is called secondary sludge (SS). The main organic components of SS are microbial extracellular polymeric substances (EPS), non-biodegraded materials, and microbial cells (Bitton 2005).

Currently, the most common sludge disposal methods are landfilling, incineration for power production, and land application for soil amendment (Mahmood and Elliott 2006; Smook 2002). However, current disposal alternatives suffer from shrinking space, public opposition, stricter regulatory pressures, and above all, poor economics (Mahmood and Elliott 2006). Recent studies showed that sludge could be used for medium density fiberboard (MDF) and particleboard manufacturing with and without resins (Geng and Zhang 2007; Migneault et al 2010; Migneault et al 2011a; Taramian et al 2007). The use of sludge was beneficial for improving the internal bond strength mainly due to the bonding potential of SS. The use of sludge in MDF manufacturing also contributed to formaldehyde reduction (Migneault et al 2011b).

In recent years, interest in bio-based adhesives has increased. Bio-based adhesives are derived from natural materials such as proteins, carbohydrates and lignin (Pizzi 2006; Rowell 2005). Secondary sludge from paper mill contains some of these substances, and already showed good bonding ability (Geng et al 2007; Zerhouni et al 2009).

Considering the bonding ability of SS, and the substantial amount of resin used by the wood composites industry, the use of SS as co-adhesive with urea-formaldehyde resin (UF) is an interesting option for recycling SS in particleboard manufacturing. The main objective of this study was to find the optimal percentage of SS from three pulping processes as co-adhesive in particleboard manufacturing.

Materials and Methods

Sludge Collection, Drying and Grinding. SS from thermomechanical pulp (TMP) was collected from the Stadacona White Birch Pulp and Paper Mill in Québec City (Quebec, Canada). Kraft SS was collected from the SFK Pulp Fund commercial pulp mill in Saint-Félicien (Quebec, Canada). CTMP SS was sampled from the Abitibi-Bowater pulp and paper mill in Dolbeau–Mistassini (Quebec, Canada). Samples were refrigerated at 4°C, squeezed and dried at 60°C for one week to avoid protein deterioration. The dried SS

samples were ground in a roller mill. The milled material was further screened with a 30 mesh sieve (600 µm) and the fraction was collected. The collected materials were used to manufacture the particleboard. The milled materials between 40 mesh -60 mesh was then placed in an airtight container to homogenize moisture content for subsequent chemical analysis.

Particle Preparation. The particleboard was manufactured with spruce, pine, and fir (SPF) particles ranging from 1–5 mm in size and at 2–4% moisture content. The wood particles were obtained from Tafisa (Quebec, Canada).

Particle and Secondary Sludge Characterization. Buffering capacity and pH were measured according to the previous authers (Johns and Niazi 1980; Migneault et al 2010; Xing et al 2006). An aqueous extract was prepared by refluxing 25 g of dry furnish in 250 ml distilled water for 20 min. Extract solution was then passed through a filter paper using a vacuum, cooled at room temperature before titrating. Two extract solutions were prepared for each furnish type. The extract (50 ml) was titrated to a pH of 3 using 0.025-N H_2SO_4 solution for alkaline buffering capacity or to a pH of 8 using 0.025-N NaOH solution for acid buffering capacity. Two titrations were conducted for each titration solution. Thus, the initial pH value for each sample is the average of eight measurements, while each buffering capacity value (mmol/100g oven-dry mass) is the mean of four determinations.

Cellulose content was determined by Kürschner and Hoffer's nitric acid method (Browning 1967). Pentosans content was obtained according to TAPPI T 223 cm-84. Total lignin content was determined by the Klason method according to TAPPI T 222 om-98 (acid-insoluble lignin) and quantified by absorption spectroscopy at 205 nm according to TAPPI useful method UM-250 (acid-soluble lignin). Total extractive content was determined by successive extractions with an organic solvent mixture (ethanol/toluene) followed by hot water according to TAPPI T 204 cm-97 and T 207 om-93, respectively. Ash content was determined by combustion in a muffle furnace at 525^{o}C according to TAPPI T 211 om-93. Two replicates were conducted for chemical analysis.

Panel Manufacturing and Testing. Particleboards were made using a) 7% urea-formaldehyde resin (UF, UL 232, Arclin Canada, Sainte-Thérèse, Quebec, Canada, b) three type SS from three pulping processes (TMP, CTMP and Kraft) and c) different SS percent (dry weight of SS per dry weight of particle). Three particleboard panels were made for each experimental condition (three repetitions). Three control panels were also made. The panels target density was 690 kg/m^3, pressing temperature was 210 ^{o}C, and pressing cycle was 7.5 min (including closing and opening time). The target thickness was 11 mm. For each formulation, 0.5% dry weight of emulsion wax (EW58A, Hexion Canada, Lévis) per dry weight of particles and 0.20% dry weight of ammonium chloride (as a catalyst) per dry weight of resin were mixed and diluted to the appropriate consistency to reduce viscosity. First, dry SS was added to the particles in a conventional rotary drum blender mounted with a spray nozzle. Then, the mixture of UF, water, wax, and ammonium chloride was then added to the blender through the spray nozzle. Total

furnish MC was 12%. Mats were hand-formed in a 250 mm x 350 mm mold and pressed in a Dieffenbacher hydraulic press with a 1000 mm x 1000 mm plate.

All panels were conditioned at 20 ± 3°C and 65% relative humidity (RH) until equilibrium moisture content was reached. Fifteen 25 mm x 25 mm IB samples were cut from the panel.The internal bond (IB) were measured according to ASTM D 1037-2006a (ASTM 2006) method and compared with ANSI A 208.1-2009 standard (ANSI 2009). Density profiles of each IB specimen after sanding were measured with a QMS density profile system, version 1.25. An analysis of variance (ANOVA) with multiple comparisons (contrasts) was conducted using SAS 9.2 (SAS Institute, Cary, NC, USA). To include control panels in the statistical analysis, a Waller-Duncan multiple comparison test (5% significance level) was conducted.

Results and Discussion

Secondary Sludge and Particle Properties.

Chemical Composition. Chemical composition of SS is presented in table 1. Of the SS resource, the TMP SS is the best candidate for panel manufacturing in term of protein, and the Kraft SS is the worst. The positive effect of protein on internal bond strength, was shown by the use of proteins in wood adhesive formulations ((Pizzi and Mittal 2003; Rowell 2005). The negative effect of extractives on panel manufacturing is, a) low the curing of adhesive, b) a decrease in the resistance to moist conditions, and c) delamination, etc. So in term of low extractives content, the CTMP SS (1.7%) is the best candidate, and the TMP SS (21.5%) in the worst. The ash (ash test) is inorganic since the carbohydrates are broken down during combustion (Edalatmanesh et al 2010; Méndez et al 2009). The ash content is proportional with some chemical, mineral and metal content. The SS from the kraft process is richer in ash (41.3%), because of the use of chemicals during bleaching (Zerhouni 2010). The sludge contains several metals at low concentrations (Davis et al 2003; Edalatmanesh et al 2010; Méndez et al 2009; Zerhouni 2010), however the metals and minerals are generally unfavorable components in panel manufacturing. Therefore, in term of ash, the Kraft SS is the worst candidate. Since the SS consists of favorable and unfavorable components, so we must consider a variety of factors to determine it's good or bad.

Table 1 *Chemical composition of secondary sludge (SS) from the three pulping processes (adapted from Migneault et al 2011a).*

Pulping process	Ash (%)	Extractives (%)	Cellulose (%)	Lignin (%)	Pentosan (%)	Nitrogen (%)
TMP(Stadacona)	12.0 (0.1)	21.5 (0.6)	19.7 (0.2)	50.2 (0.5)	3.0 (0.1)	7.7 (0.0)
CTMP (Bowater)	18.0 (0.2)	1.7 (2.2)	26.6 (0.0)	50.0 (1.1)	2.2 (0.0)	5.4 (0.1)
Kraft (SFK)	41.3 (1.4)	7.9 (0.0)	18.9 (0.4)	36.4 (1.0)	3.4 (0.0)	1.3 (0.0)

The numbers in parentheses are standard deviation.

Buffering Capacity and pH Value of SS and Particle. The buffering capacity and pH value of SS and particle are presented in table 2. The pH value of particle is 4.5, a pH

value is about 4-5 or lower is recommended for UF resin to obtain a reasonable pressing time (Maloney 1993; Rowell 2005).The acid buffering capacity is 0.50 NaOH mmol/100 g oven-dry mass, the alkaline buffering capacity is 0.34 H_2SO_4 mmol/100g oven-dry mass. The pH value of TMP SS is 6.10, whereas the CTMP SS is 7.05 and the Kraft SS is 6.76, in term of pH, thus the TMP SS is the best candidate, and the CTMP SS is the worst. A resin catalyst (such as ammonium chloride) can decrease the furnish pH, but a low alkaline buffering capacity is preferable. In terms of buffering capacity, Kraft sludge is the best candidate for panel manufacturing and TMP the worst.

Table 2 Buffering capacity and pH value of SS and particle

	Particles	TMP	CTMP	Kraft
pH	4.50	6.10	7.05	6.76
Acid buffering capacity (mmol /100 g oven-dry-mass)	0.50	3.16	1.31	0.32
Alkaline buffering capacity (mmol / 100 g oven-dry mass)	0.34	4.83	3.78	0.56

Internal Bond Strength (IB). The IB results are shown in Figures.1-3. IB of panels made with TMP SS as co-adhesive (Fig.1) did not meet the requirements of M-2 particleboard grade for interior use (0.40 MPa) according to ANSI A 208.1-2009 except a case of added 0,35% SS. When the quantity of SS added was low, IB of mixed panels increased compared to that of control panels, and with the SS content increased, the IB decreased, but when the SS content increased to 8.75%, the IB of mixed panels increased and equaled to that of control panels. Furthermore, while the SS content continued to increase, the IB of mixed panels decreased definitively compared to that of control panels. This phenomenon showed that IB did not decrease linearly with added SS; instead, it showed a U-shaped profile. This result departs from previous reports. Although the mechanism is not fully understood, this discrepancy could be attributed to a stoichiometric UF–SS ratio giving best properties due to a chemical crosslinking between UF and SS.

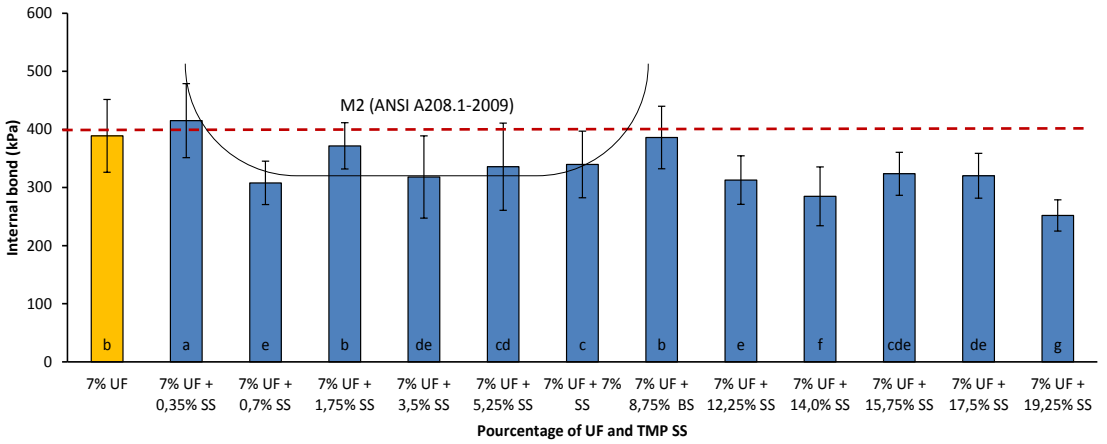

Figure 1 Internal bond strength of particleboard at 7% UF and different TMP SS as co-adhesive. Means with the same letter are not significantly different at the 5% probability level.

Most IB values of the panels made with Kraft SS as co-adhesive (Fig.2) did not meet the requirements of M-2 particleboard grade for interior use, except the panels added 3,5% and 5,25% SS. With the SS added to panels, the IB of mixed panels decreased compared to that of control panels, but when the SS content was increased to 3.5% and 5.25%, the IB of mixed panels increased and exceeded or equaled to that of control panels. However after 5.25%, IB of mixed panels decreased definitively with the SS content increasing. Here, IB values showed again a U-shaped profile.

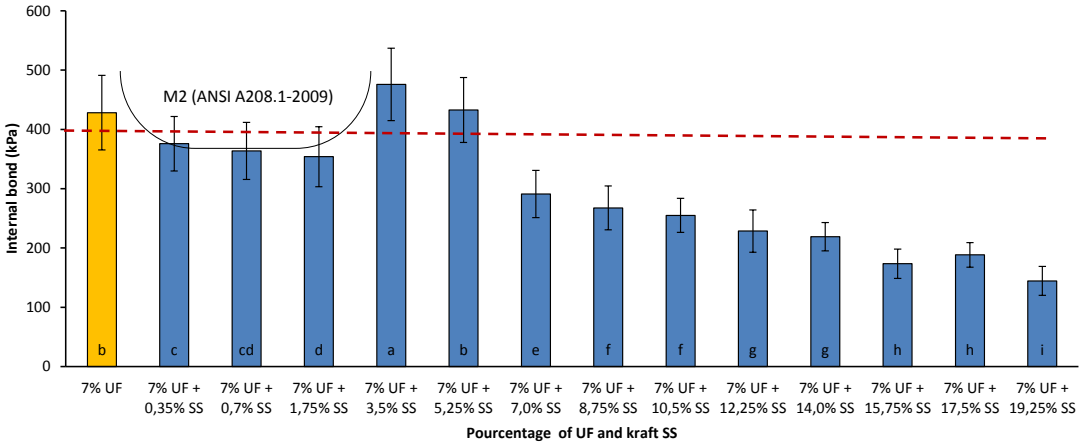

Figure 2 Internal bond strength of particleboard at 7% UF and different Kraft SS as co-adhesive. Means with the same letter are not significantly different at the 5% probability level.

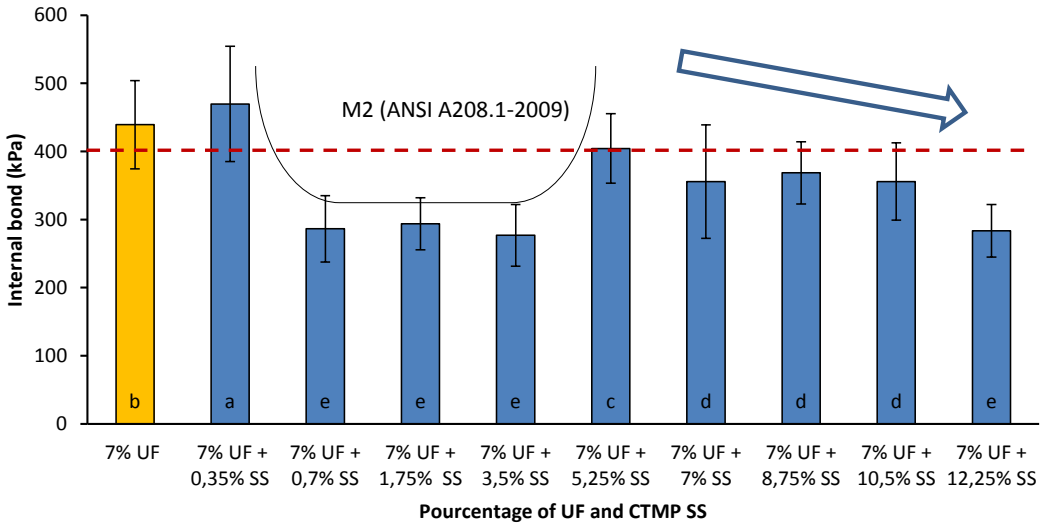

Figure 3 Internal bond strength of particleboard at 7% UF and different CTMP SS as co-adhesive. Means with the same letter are not significantly different at the 5% probability level.

For the panels made with CTMP SS as co-adhesive (Fig.3), IB of panels made with CTMP SS as co-adhesive did not meet the requirements of M-2 particleboard grade for interior use (0.40 MPa) according to ANSI A 208.1-2009 except two cases of added 0,35% and 5.25% SS. When the quantity of SS was few little (0.35%), IB of mixed panels increased compared to that of control panels, and with the SS content increased, the IB decreased, but when the SS content increased to 5.25%, the IB of mixed panels increased and equaled to that of control panels. Furthermore, with the SS content continued to increase, the IB of mixed panels decreased definitively compared to that of control panels. This phenomenon is exactly like that for the first two cases.

In a word, there is an optimal percentage of added SS, which can be incorporated in particleboards. However, the percentage varies with pulp process, with pulp mill and the time also, since the chemical composition, buffering capacity and pH value of SS vary with pulp processes, pulp mill and the time.

Conclusions

Results from this work indicated that the use of SS from three different pulping processes as a co-adhesive in panels is feasible, however the SS content incorporated in particleboards should be correctly selected. The optimal percentage varies with pulping processes and pulp mill. These results show beneficial environmental impacts of the valuing sludge in such application including recycling of pulp and paper residues, reducing the use of synthetic resins known by their harmful emissions.

Acknowledgements

The authors acknowledge the financial support of the Natural Sciences and Engineering Research Council of Canada (NSERC) and FPInnovations, Forintek and Paprican Divisions. The authors are also grateful to White Birch Paper, Stadacona Division in Quebec City (Quebec Canada), the SFK Pulp Fund in Saint-Félicien (Quebec, Canada) and Abitibi-Bowater pulp and paper mill in Dolbeau–Mistassini (Quebec, Canada) for supplying materials and sampling assistance.

References

ANSI (2009) American national stadanard particleboard ansi a 208.1-2009 American National Standards Institute, Composite Panel Association, 19465 Deerfield Avenue, Suite 306, Leesburg, VA 20176.

ASTM (2006) Standard test methods for evaluating properties of wood-base fiber and particle panel materials astm d1037 – 06a. American Society for Testing and Materials, 100 Barr Harbor Drive, PO Box C700, West Conshohocken, PA 19428-2959, United States.

Bitton G. (2005) Wastewater microbiology Wiley-Liss, John Wiley & Sons, Hoboken, N.J. pp.

Davis E, Shaler SM, Goodell B. (2003) The incorporation of paper deinking sludge into fiberboard. Forest Prod J 53(11-12):46-54.

Edalatmanesh M, Sain M, Liss SN. (2010) Cellular biopolymers and molecular structure of a secondary pulp and paper mill sludge verified by spectroscopy and chemical extraction techniques. Water Sci Technol 62(12):2846-2853.

Geng X, Deng J, Zhang SY. (2007) Paper mill sludge as a component of wood adhesive formulation. Holzforschung 61(6):688-692.

Geng XL, Zhang SY. (2007) Characteristics of paper mill sludge and its utilization for the manufacture of medium density fiberboard. Wood Fiber Sci 39(2):345-351.

Johns WE, Niazi KA. (1980) Effect of ph and buffering capacity of wood on the gelation time of urea-formaldehyde resin. Wood and Fiber 12(4):9.

Mahmood T, Elliott A. (2006) A review of secondary sludge reduction technologies for the pulp and paper industry. Water Res 40(11):2093-2112.

Maloney TM. (1993) Modern particleboard and dry-process fiberboard manufacturing. Miller-Freeman, San Francisco, CA. 688 pp.

MDDEP (2009) Bilan annuel de conformité environnementale--secteur pâte et papiers 2009. Ministère du dévelopement durable, de l'environnement et des parcs du Québec, Canada.

Méndez A, Fidalgo JM, Guerrero F, Gascó G. (2009) Characterization and pyrolysis behaviour of different paper mill waste materials. Journal of Analytical and Applied Pyrolysis 86(1):66-73.

Migneault S, Koubaa A, Nadji H, Riedl B, Zhang SY, Deng J. (2010) Medium-density fiberboard produced using pulp and paper sludge from different pulping processes. Wood Fiber Sci 42(3):292-303.

Migneault S, Koubaa A, Riedl B, Nadji H, Deng J, Zhang SY. (2011a) Binderless fiberboard made from primary and secondary pulp and paper sludge. Wood Fiber Sci 43(2):180-193.

Migneault S, Koubaa A, Riedl B, Nadji H, Deng J, Zhang T. (2011b) Potential of pulp and paper sludge as a formaldehyde scavenger agent in mdf resins. Holzforschung 65(3):403-409.

Ochoa de Alda JAG. (2008) Feasibility of recycling pulp and paper mill sludge in the paper and board industries. Resources, Conservation and Recycling 52(7):965-972.

Pizzi A. (2006) Recent developments in eco-efficient bio-based adhesives for wood bonding: Opportunities and issues. J. Adhes. Sci. Technol. 20(8):829-846.

Pizzi A, Mittal KL. (2003) Handbook of adhesive technology. Marcel Dekker, New York, NY. 672 pp.

Rowell RM. (2005) Handbook of chemistry and wood composites. CRC Press, Boca Raton, FL, USA pp.

Smook GA. (2002) Handbook for pulp & paper technologists. Angus Wilde Publications, Vancouver, Canada. 425 pp.

Taramian A, Doosthoseini K, Mirshokraii SA, Faezipour M. (2007) Particleboard manufacturing: An innovative way to recycle paper sludge. Waste Manage 27(12):1739-1746.

Xing C, Zhang SY, Deng J, Riedl B, Cloutier A. (2006) Medium-density fiberboard performance as affected by wood fiber acidity, bulk density, and size distribution. Wood Sci Technol 40(8):637-646.

Zerhouni A. (2010) Caractérisation des propriétés physico-chimiques des boues issues des principaux procédés papetiers. mémoire, Université du Québec en Abitibi-Témiscamingue. 102 pp.

Zerhouni A, Mahmood T, Koubaa A. (2009) The use of paper mill biotreatment residue as furnish or as a bonding agent in the manufacture of fiber-based boards. pages 475-480, PAPTAC Annual Meeting, Pulp and paper technical assoaition of Canada, Montreal Canada.

Study on Compressive and Tensile Properties of Recombinant Bamboo

*ZHANG Junzhen[1] - ZHOU Xianwu[2] - REN Haiqing[3] - ZHAO Rongjun[4]**

[1,2] Student, Research Institute of Wood Industry, Chinese Academy of Forestry, Beijing 100091
junzhenzhang@126.com
[3] Professor, Research Institute of Wood Industry, Chinese Academy of Forestry, Beijing 100091
renhq@caf.ac.cn
[4] Associate Professor, Research Institute of Wood Industry, Chinese Academy of Forestry, Beijing 100091
* *Corresponding author*
rongjun@caf.ac.cn

Abstract

By taking recombinant bamboo made of *Bambusa emeiensis* as the research object, the tensile and compressive properties of recombinant bamboo was studied and the results were compared with those of larix and other wood species. The results showed that tension strength parallel to grain and compressive strength parallel to gain of recombinant bamboo were 248.15MPa and 129.17MPa respectively, and the properties of which were stable. 1) The compression strength perpendicular to grain, tensile strength parallel to grain and compressive strength parallel to gain of recombinant bamboo were higher than three kinds of wood including larix, while difference between transverse and longitudinal was much smaller. E_L/E_T was smaller than wood, and the Poisson's ratio of μ_{LR} and μ_{TR} were higher than wood, but μ_{LT} was lower, however μ_{TL} was among these three kinds of wood. 2) The curve of compressing perpendicular to grain was divided into three parts(elastic stage, plastic stage and failure stage), and the graph turned from linear relationship to non-linear relationship, then failed at last, also the plastic deformation increased, so the recombinant bamboo showed good ductility and was plastic failure in the end.

***Keywords*:** recombinant bamboo, *Bambusa emeiensis*, compression strength, tension strength, elastic modulus, Pisson's ratio, strength weight ratio.

Introduction

The characteristics of bamboo are fast growth rate, early mature and high yield etc, and bamboo resources and quality in China occupy the first place in the world, so there is a great potential to develop (The 33rd order of the Ministry of Land and Resources in The People's Republic of China 2006, LIU Yixing and ZHAO Guangjie 2004, SHAN Wei, LI Yu-shun 2008, LI Ming and ZHENG Liang 2011). With the rising of wood structure in china, the demand of structural timber is increasing. While the structural wood materials in China is relatively deficient, bamboo timber can replace part of wood in building structure. In the past, bamboo timber was mainly used for furniture and packaging material etc(LI Ming and ZHENG Liang 2011). Wu Yan etc (2008) investigated the application of modified bamboo in decoration, component, furniture, package and transportation etc. According to the problem in the application status, they made some suggestions for the development of modified bamboo so as to extend its application. Guan Mingjie etc (2009) studied the shrinkage and bulking of recombinant bamboo used in furniture manufacturing. They found that with the same density, the shrinkage coefficient of recombinant bamboo was smaller than that of several common wood such as *Quercus acutissima* Carr., which indicated that recombinant bamboo is suitable for manufacturing furniture. Chinese scholars have carried out some research in manufacturing technology of recombinant bamboo (WANG Sunguo and HUA Yukun 1991, LI Qin et al.2003, LIU Baiping et al. 2009, CHENG Liang et al. 2009, WANG Sunguo and HUA Yukun 1994, YE Liangming 1996). Also there are some researchers who have studied the physical and mechanical properties of recombinant bamboo. Meng Fandan etc (2011) introduced the preparation method of basicunits, utilization rate of bamboo, manufacturing processes and methods. Mechanical properties of laminated bamboo veneer lumber, bamboo glulam, laminated bamboo strip lumber and bamboo restructuring were compared. The results showed that all mechanical properties of laminated bamboo veneer lumber are excellent, and it is a new material for sustainable development. Guan Mingjie etc (2006) tested the modulus of elasticity (M0E)and modulus of rupture (M0R)of poplar scrimber and bamboo scrimber. They found that a new low density-high strength material (bamboo-wood composite scrimber) could be produced by combining higher MOE of bamboo scrimber at lower densities with higher MOR of poplar scrimber. Density, temperature and light etc effect the physical and mechanical property of recombinant bamboo heavily. With density grows, the mechanical property of recombinant bamboo increases. In the mean while, water absorption decreases. The color of the surface changes greatly with light, but the elastic modulus doesn't change much with the variation of the conditions ZHU Rong-xian and YU Wenji 2011, Qin L. and YU W.J. 2009).

In summary, researches about recombinant bamboo in china focus on the manufacturing coefficient, property and comparison. There is a lack of systematic studies in compressive and tensile properties of recombinant bamboo. With the improvement of manufacturing progress and technology of recombinant bamboo, the mechanical properties of which have increased sharply. Nowadays the recombinant bamboo is mainly used in non-structural level. Judged from this, this paper chose *Bambusa emeiensis* as the main material. The author carried out comparative research about the tensile and compressive

property of recombinant bamboo. The purpose of this paper is to provide scientific basis for the application of recombinant bamboo in building structure.

Materials and Methods

Materials. In the test, recombinant bamboo is made in Hongya Bamboo Era Science and Technology Co.,Ltd.. *Bambusa emeiensis* was used as the research object, and the moisture content of which is about 10%. During the compression strength perpendicular to the grain test, there are four tests including compressing all parts of the samples and partial of the samples in radial and tangential direction. There are 15 samples in each test, the size of which are 30mm×20mm×20mm. And there are 25 samples for tension strength parallel to grains, the size are 370mm×20 mm×20mm. In addition there are 4 groups of samples for the compressive elastic modulus perpendicular to grain and Poission's ratio, 3 samples each. the size of the samples are 60mm×20mm×20mm.

Methods. Because there are not relevant standards and code testing mechanical property of recombinant bamboo in China, the methods testing physical and mechanical property of wood was used in this paper in order to make comparison with wood. Compression strength perpendicular to the recombinant bamboo grain was tested by GB/T1939-2009; tension strength parallel to grain was tested according to GB/T1938-2009;compression strength parallel to grain was in accordance with GB/T 1935-2009. Compressive elastic modulus perpendicular to grain and Poission's ratio were tested using pasting gauges according to GB/T 1943-2009, namely 1/4 bridge method. Both ends of the sample should be smooth, when pasting gauges, and the gauges should be perpendicular to the edge of the sample. Also the gauges should be attached to 20mm from both ends at the centre of the radial section or tangential section .The main equipments are Instron(10t) mechanical testing machine and TDS-530 static data acquisition system.

Result and Discussion

Compression and Tension Strength

Compression Strength Perpendicular to Grain.

Test results of compression strength perpendicular to grain are in table 1. Variation coefficient of compression strength in both directions are less than 10%, which indicates the property is good. When both directions are loaded, compression strength of compressing part of the sample is obviously higher than compressing all part of the sample. Comparing the compression strength in radial direction with tangential direction, compression strength in radial by compressing all part of the sample is 1.12 times that of tangential direction. Compression strength by compressing part of the sample is 1.09 times that of tangential direction. It can be concluded that the property of recombinant bamboo in radial direction is better than tangential direction.

Table 1 Compression strength perpendicular to grain of recombinant bamboo MPa

Item	compressing all part of radial direction	compressing part of radial direction	compressing all part of tangential direction	compressing part of tangential direction

	PL	CS	PL	CS	PL	CS	PL	CS
Average	34.61	45.50	59.61	93.10	28.15	40.19	44.05	85.59
Standard deviation	2.000	3.468	3.069	8.986	2.452	4.298	2.254	6.086
Coefficient of variation	0.058	0.076	0.051	0.097	0.087	0.107	0.051	0.071

Note: PL is short for proportional limit, CS is short for compression strength

By comparing the compression strength perpendicular to grain of recombinant bamboo with that of wood(CHENG Junqing 1985)(table 2), recombinant bamboo is 3-19 times higher than spruce etc; compression strength by compressing part of the sample in radial direction is 5-26 times higher; compression strength in tangential direction is almost 6 to even more than 20 times higher. The difference of recombinant bamboo between parallel and perpendicular to grain is much smaller than *Larix gmelini* etc. *L. gmelini* etc are anisotropic materials, compression strength parallel to grain is 3-21 times that perpendicular to grain. However, the value for recombinant bamboo is 1-3, which suggests that recombinant bamboo is more suitable to be used in loaded in both directions.

Table 2 Comparison of mechanical properties between recombinant bamboo and wood

	elastic modulus /GPa			compression strength perpendicular to grain/MPa				tension strength parallel to grain /MPa	compression strength perpendicular to grain/MPa	density Kg/m^3
	Compress parallel to grain	Compress in tangential direction	Compress in radial direction	All in radial direction	Part in radial direction	All in tangential direction	Part in tangential direction			
1	37.73	2.27	32.84	45.50	93.10	40.19	85.59	248.15	129.17	1 159.66
2	--	--	--	2.25	3.72	2.16	3.82	70.95	37.24	306
3	--	--	--	2.74	3.33	2.84	4.41	92.12	37.83	459
4	--	--	--	4.21	5.68	4.61	7.06	128.78	51.65	528
5	--	--	--	2.06	3.92	3.04	6.47	102.80	43.51	519
6	--	--	--	4.61	7.25	6.08	8.92	129.65	48.80	509
7	--	--	--	10.68	14.99	7.45	10.34	137.20	54.00	709

Note:1 recombinant bamboo, 2 Cunninghamia lanceolata Hook., 3 Picea asperata Mast.,4 Larix gmelini, 5 Pinus massoniana Lamb., 6 Fraxinus. mandshurica Rupt., 7 Acer. mono maxim.

The fitting curves for compressing perpendicular to grain of recombinant bamboo and wood are shown in Figure 1 . By comparison, the curves are obviously different. There are three stages in the curves for compressing perpendicular to grain of recombinant bamboo(elastic stage, plastic stage and failure stage). At elastic stage, the cells of recombinant bamboo and glue layer deformed slightly. And displacement was proportional to load, which caused elastic deformation. With load growing, the cells of recombinant bamboo was being compressed to damage, while the deformation of glue line continued growing. The curve turned from elastic relationship to non-elastic. At failure stage, the glue line couldn’ t withstand the growing load, and were damaged. Brittle failure occured in the end. Then the composites in the cell of recombinant bamboo were compressed, causing growing plastic deformation. It showed good ductility. During the compressing stage, there was some sound from tearing. When sound turned loud, the sample was damaged. While the load descended slowly, and that was plastic failure in the

end. When wood are compressed perpendicular to grain: ①The cell deformed slightly, and displacement was proportional to load, which caused elastic deformation;②After the yield point, the cells were compressed to broken gradually. Cell wall collapsed to cell lumen and were compressed to deformation. In this field the deformation increased sharply while the load increased slightly;③After cell lumen were fully filled, the composite began to be compressed. With the increasing displacement, load increased sharply. After that, load increased sharply with displacement. But wood was not damaged totally, the composites of the cell wall started to be compressed (LIU Yixing and ZHAO Guangjie 2004).

The ability of compressing resistance of recombinant bamboo is good, also the property of which is superior. The reason is that fibrous bundles of *Bambusa emeiensis* are bonded together, so the curing of glue increase the compressive resistant ability perpendicular to grain. Fitting curves for compressing perpendicular to grain of recombinant bamboo and wood are both divided into three stages. But in the latter two stages, the curves and the cause of which are obviously different due to the difference in anatomy.

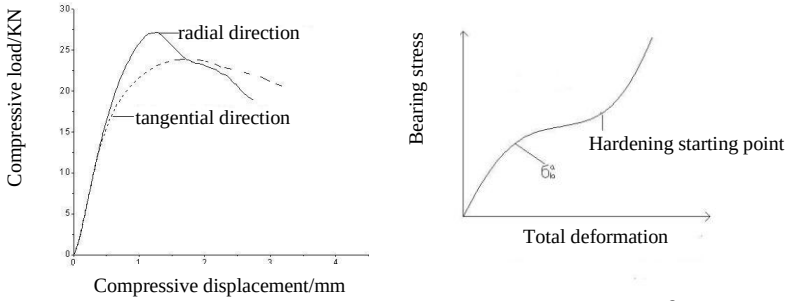

Figure 1 Fitting curves for compressing perpendicular to grain of recombinant bamboo and wood(PAN Jinglong and ZHU Enchun 2009)

Compression and Tension Strength Parallel to Grain

According to the tests, the compression strength parallel to grain of recombinant bamboo is 248.15 MPa, and the variation coefficient is 13.8%. Tension strength parallel to grain is 129.17 MPa, and the variation coefficient is 1.9%. Compression strength parallel to grain is almost 2 times of tension strength, and the variation coefficient of the former is higher than the latter.

From table 2, tension strength parallel to grain of recombinant bamboo is 1.5～3.8 times higher than *C. lanceolala* Hook. etc. Compression strength is almost two times of other six wood species. In conclusion, the compressive and tensile properties of recombinant bamboo are both much better than wood.

Elastic Modulus and Poisson's Ratio

The elastic modulus and Poisson's ratio were tested by means of pasting gauges, the results are in table 3. The variation coefficients of elastic modulus and Poisson's ratio are

all below 10%. The variation coefficient of elastic modulus in compression parallel to grain and that in tangential direction is lower, which indicated the properties in parallel to grain and tangential direction were much stable. The value of elastic modulus in compression parallel to grain divided by that in tangential direction(E_L/E_T)is 16.6, but this values for hard wood and softwood are 18.5 and 24(YIN Sici 1996)separately. By comparison, the value of E_L/E_T for recombinant bamboo is smaller than wood, the difference of deformation resistance parallel to grain from tangential direction is much smaller.

Table 3 Modulus of elasticity and Poisson's ratio for recombinant bamboo

	modulus of elasticity			Poisson's ratio			
	E_L/GPa	E_T/GPa	$E_L^{'}$/GPa	μ_{LR}	μ_{LT}	μ_{TR}	μ_{TL}
Average	37.73	2.27	32.84	0.588 5	0.474 1	0.417 5	0.028 7
Standard deviation	2.674	0.186	2.48	0.032	0.065	0.017	0.002
variation coefficient	0.071	0.082	0.076	0.054	0.138	0.042	0.067

Note: E_L compressing elastic modulus parallel to grain, E_T elastic modulus in tangential direction, $E_L^{'}$ tensile elastic modulus parallel to grain; In Poisson's ratio, L,R,T are short for longitudinal shrinkage, radial shrinkage and tangential shrinkage; μ_{LR} is radial shrinkage/ longitudinal shrinkage.

The variation coefficients of Poisson's ratio in all directions are within 10%, which is more stable. The order of Poisson's ratio in all directions is $\mu_{LR}>\mu_{LT}>\mu_{TR}>\mu_{TL}$. Poisson's ratio of recombinant bamboo is quite different from wood(YIN Sici 1996)(table 4), μ_{LR} and μ_{TR} of recombinant bamboo are higher than *P. asperata* mast., *Fagus longipetiolata* seem and *Swietenia mahagoni* jacq.. While μ_{LT} is lower, μ_{TL} is among the three species. It indicated that the ability of deformation resistance varied in directions, by comparing with wood in the same direction.

Table 4 Comparison in Poisson's ratio between recombinant bamboo and wood

	μ_{LR}	μ_{LT}	μ_{TR}	μ_{TL}
Recombinant bamboo	0.588 5	0.474 1	0.417 5	0.028 7
P. asperata mast.	0.23	0.49	0.24	0.009
F. longipetiolata seem	0.45	0.51	0.36	0.044
S. mahagoni jacq.	0.31	0.55	0.41	0.022

Strength Weight Ratio

The strength weight ratio of recombinant bamboo and *C. lanceolata* Hook. etc are listed in table5(CHENG Junqing 1985). By comparison, the strength weight ratio of recombinant bamboo compressing all and part in radial direction are 2.6～9.9 times and 3.8～11.1 times of *C. lanceolata* Hook. etc. The differences in strength weight ratio are smaller than in compression strength. It is the same in tangential direction. It indicates that the ability of compression resistance per unit mass of recombinant bamboo is stronger than that of wood. The reason is that the curing glue improved the compression resistance ability. In radial direction, the strength weight ratio was among the six wood species. So the recombinant bamboo can partly replace wood in building construction.

Table 5 Comparison in strength weight ratio between recombinant bamboo and wood

wood species	Strength weight ratio/$(N\cdot m\cdot g^{-1})$

	Compress perpendicular				Tension parallel to grain	Compress perpendicular to grain
	All in radial direction	Part in radial direction	All in tangential direction	Part in tangential direction		
Recombinant bamboo	39.24	80.28	34.66	73.81	213.99	111.39
C. lanceolata Hook.	7.35	12.16	7.06	12.48	231.86	121.70
P. asperata Mast.	5.97	7.25	6.19	9.61	200.70	82.42
L. gmelini	7.97	10.76	8.73	13.37	243.90	97.82
P. massoniana Lamb.	3.97	7.55	5.84	12.47	198.07	83.83
F. mandshurica Rupt.	9.06	14.24	11.94	17.52	254.72	95.87
A. mono maxim.	15.06	21.14	10.51	14.65	193.51	76.16

Conclusion

The tension and compression strength parallel to grain are 248.15 MPa and 129.17 MPa respectively. In compression strength perpendicular to grain, all compression strength and part compression strength are 85.59 MPa and 40.19 MPa respectively. The strength of recombinant bamboo in all directions are high, and the property is excellent.

The compression strength perpendicular to grain, compression and tension strength parallel to grain of recombinant bamboo are higher than *L. gmelini* etc. The difference of compression strength between parallel and perpendicular to grain is smaller than *L. gmelini* etc, which indicates recombinant bamboo is more suitable to be used in occasions loaded in both directions. The E_L/E_T value of recombinant bamboo is smaller than wood, and the difference of deformation resistance parallel to grain from tangential direction is much smaller. The Poisson's ratio of recombinant bamboo is quite different from wood. μ_{LR} and μ_{TR} of recombinant bamboo are bigger than *P. asperata* mast., *F. longipetiolata* seem *and S. mahagoni* jacq.. while μ_{LT} is lower, and μ_{TL} is among the three species. The strength ratio of recombinant bamboo perpendicular to grain is higher than *C. lanceolata* Hook. etc. But the strength weight ratio parallel to grain is among the six wood species.

The curve of compressing perpendicular to grain is divided into three parts(elastic stage, plastic stage and failure stage). The graph turned from linear relationship to non-linear relationship, then failed at last. In the meanwhile, the plastic deformation increased, so the recombinant bamboo showed excellent ductility and was plastic failure in the end.

References

The 33rd order of the Ministry of Land and Resources in The People's Republic of China 2006. The policy of "equalizing cultivated land occupied for construction use with compensation in same amount and quality".National land ＆Resources Information (13):9-10. (in Chinese)

LIU Yi-xing, ZHAO Guang-jie 2004. Material science of wood resources. Beijing: China Forestry Publishing House. (in Chinese)

SHAN Wei, LI Yu-shun 2008. Application prospect of bamboo utilization in building structures. Forest Engineering ,24(2):62-65. (in Chinese)

LI Ming, ZHENG Liang 2011. Application of bamboo in building engineering, Guangdong Building Materials, (2):23-26. (in Chinese)

WU Yan, LI Yu-shun, GE Bei-de, et al. 2008. Application and prospect of modified bamboo. Forest Engineering, 24(6):68-71. (in Chinese)

GUAN Ming-jie, LIN Ju-mei, ZHU Yi-xin 2009. Shrinkage and swelling properties of recombinant bamboo. Journal of Bamboo Research,28(3):38-41. (in Chinese)

WANG Sun-guo, HUA Yu-kun 1991. A study on the manufacturing process of reconsolidated bamboo. China Wood Industry,5(2):14-18. (in Chinese)

LI Qin, WANG Kui-hong, YANG Wei-ming,et al. 2003. Research on technology of remaking bamboo glued board. Journal of Bamboo Research,22(4):56-60. (in Chinese)

LIU Bai-ping, CHENG Wan-li, ZHOU Jian-bo, et al.2009. A preliminary study on manufacturing technology of bamboo engineering panel from laminated circular arc. Wood Processing Machinery, 20(6):31-34. (in Chinese)

CHENG Liang, WANG Xi-ming, YU Yang-lun 2009. Effect of glue immersion parameters on performance of reconstituted dendrocalamopsis oldhami Lumber China Wood Industry,23(3):16-19. (in Chinese)

WANG Sun-guo, HUA Yu-kun 1994. Effect of softening process variables on reconsolidated bamboo and bamboo itself properties. Journal of Nanjing Forestry University,18(1):57-62. (in Chinese)

YE Liang-ming, YE Yian-hua, JIANG Zhi-hong, et al. 1996. Studies on the board of reconsolidated bamboo. Journal of Bamboo Research,15(1):58-65. (in Chinese)

MENG Fan-dan, YU Wen-jiz, CHEN Guang-sheng 2011. Processing and properties comparison between four kinds of bamboo-based panel. Wood Processing Machinery,22(1):32-35. (in Chinese)

GUAN Ming-jie,ZHU Yi-xin,ZHANG Xin-an 2006. Comparison of bending properties of scrimber and bamboo scrimber. Journal of Northeast Forestry University,34(4):7-7,21. (in Chinese)

ZHU Rong-xian,YU Wen-ji 2011.Effect of density on physical and mechanical properties of reconstituted small-sized bamboo fibrous sheet composite. Advanced Materials Research,150-151:634-639.

Qin L., YU W.J. 2009. Research on surface color, properties of thermo-treated reconstituted bamboo lumber after artificial weathering test. Advanced Materials Research,79-82:1395-1398.

CHENG Jun-qing 1985. Wood science. Beijing: China Forestry Publishing House. (in Chinese)

PAN Jin-long, ZHU En-chun 2009.Design principle of wood structure.Beijing: China Building Industry Publishing House. (in Chinese)

YIN Si-ci 1996. Wood science. Beijing: China Forestry Publishing House. (in Chinese)